



NUREG/CR-6980

RBHT Reflood Heat Transfer Experiments Data and Analysis

Office of Nuclear Regulatory Research

**AVAILABILITY OF REFERENCE MATERIALS
IN NRC PUBLICATIONS**

NRC Reference Material

As of November 1999, you may electronically access NUREG-series publications and other NRC records at NRC's Public Electronic Reading Room at <http://www.nrc.gov/reading-rm.html>. Publicly released records include, to name a few, NUREG-series publications; *Federal Register* notices; applicant, licensee, and vendor documents and correspondence; NRC correspondence and internal memoranda; bulletins and information notices; inspection and investigative reports; licensee event reports; and Commission papers and their attachments.

NRC publications in the NUREG series, NRC regulations, and *Title 10, Energy*, in the Code of *Federal Regulations* may also be purchased from one of these two sources.

1. The Superintendent of Documents
U.S. Government Printing Office
Mail Stop SSOP
Washington, DC 20402-0001
Internet: bookstore.gpo.gov
Telephone: 202-512-1800
Fax: 202-512-2250
2. The National Technical Information Service
Springfield, VA 22161-0002
www.ntis.gov
1-800-553-6847 or, locally, 703-605-6000

A single copy of each NRC draft report for comment is available free, to the extent of supply, upon written request as follows:

Address: U.S. Nuclear Regulatory Commission
Office of Administration
Publications Branch
Washington, DC 20555-0001
E-mail: DISTRIBUTION.RESOURCE@NRC.GOV
Facsimile: 301-415-2289

Some publications in the NUREG series that are posted at NRC's Web site address <http://www.nrc.gov/reading-rm/doc-collections/nuregs> are updated periodically and may differ from the last printed version. Although references to material found on a Web site bear the date the material was accessed, the material available on the date cited may subsequently be removed from the site.

Non-NRC Reference Material

Documents available from public and special technical libraries include all open literature items, such as books, journal articles, and transactions, *Federal Register* notices, Federal and State legislation, and congressional reports. Such documents as theses, dissertations, foreign reports and translations, and non-NRC conference proceedings may be purchased from their sponsoring organization.

Copies of industry codes and standards used in a substantive manner in the NRC regulatory process are maintained at—

The NRC Technical Library
Two White Flint North
11545 Rockville Pike
Rockville, MD 20852-2738

These standards are available in the library for reference use by the public. Codes and standards are usually copyrighted and may be purchased from the originating organization or, if they are American National Standards, from—

American National Standards Institute
11 West 42nd Street
New York, NY 10036-8002
www.ansi.org
212-642-4900

Legally binding regulatory requirements are stated only in laws; NRC regulations; licenses, including technical specifications; or orders, not in NUREG-series publications. The views expressed in contractor-prepared publications in this series are not necessarily those of the NRC.

The NUREG series comprises (1) technical and administrative reports and books prepared by the staff (NUREG-XXXX) or agency contractors (NUREG/CR-XXXX), (2) proceedings of conferences (NUREG/CP-XXXX), (3) reports resulting from international agreements (NUREG/IA-XXXX), (4) brochures (NUREG/BR-XXXX), and (5) compilations of legal decisions and orders of the Commission and Atomic and Safety Licensing Boards and of Directors' decisions under Section 2.206 of NRC's regulations (NUREG-0750).

DISCLAIMER: This report was prepared as an account of work sponsored by an agency of the U.S. Government. Neither the U.S. Government nor any agency thereof, nor any employee, makes any warranty, expressed or implied, or assumes any legal liability or responsibility for any third party's use, or the results of such use, of any information, apparatus, product, or process disclosed in this publication, or represents that its use by such third party would not infringe privately owned rights.

RBHT Reflood Heat Transfer Experiments Data and Analysis

Manuscript Completed: January 2011
Date Published: April 2012

Prepared by:
L. E. Hochreiter
Fan-Bill Cheung
T. F. Lin
J. P. Spring
S. Ergun
A. Sridharan
A. Ireland
E. R. Rosal (Applied Research Laboratory)

The Pennsylvania State University
University Park, PA 16802

K. Tien, NRC Project Manager

NRC Job Code N6154

Office of Nuclear Regulatory Research

ABSTRACT

A total of 25 valid bottom reflood heat transfer experiments have been performed in the Pennsylvania State University/U.S. Nuclear Regulatory Commission Rod Bundle Heat Transfer (RBHT) Test Facility to examine the effects of both dispersed flow film boiling and inverted annular film boiling in rod bundle geometry. The RBHT Test Facility had a full length, 3.66 m (12 ft), 7x7 rod array with typical pressurized water reactor rod diameters of 9.49 mm (0.374 in) and a rod pitch of 12.59 mm (0.496 in). The heater rods had a top skewed power shape with a peak to average power of 1.5 at the 2.77 m (9.08 ft) elevation. The ranges of conditions for the experiments were pressures from 138 to 414 kPa (20 to 60 psia), flooding rates from 0.0254 to 0.1524 m/s (1 to 6 in/s), and initial peak clad temperatures from 1033 to 1144 degrees K (1400 to 1600 degrees F), inlet subcooling from 11 to 83 degrees K (20 to 150 degrees F), and peak powers of 1.32 to 2.31 kW/m (0.4 to 0.7 kW/ft). The experiments were performed using a constant power rather than simulating the reactor decay power. The use of a constant bundle power extended the reflood transient several hundred seconds and resulted in quasi-steady film boiling over the majority of the bundle length. There were approximately 500 channels of transient data recorded for each test including the bundle power, heater rod temperatures, upper plenum pressure, inlet flow rate, inlet water subcooling, superheated vapor temperatures in the bundle, spacer grid temperatures, liquid carryover of the bundle, and the detailed axial bundle pressure drop. Transient mass balances were typically within five percent for the low flooding rate experiments, and larger for the higher flooding rate experiments. The experimental data has been qualified and submitted to the U.S. Nuclear Regulatory Commission data bank for analysis and computer code validation.

FOREWORD

Reflood thermal-hydraulics represents an important set of phenomena during a hypothetical large break loss-of-coolant-accident (LOCA). These phenomena must be accurately simulated by systems codes in determining plant response to a LOCA. In spite of significant research into reflood thermal-hydraulics, there still exists a large uncertainty in these calculations. As a result, the Nuclear Regulatory Commission (NRC) conducts experimental investigations of reflood thermal-hydraulics in order to provide data for model development and to more thoroughly assess its systems codes.

The NRC is currently assessing and improving the TRAC/RELAP Computational Engine (TRACE) code for best estimate analysis of light water reactors. While calculation of reflood by TRACE appears to be reasonable, higher accuracy is needed as the code is applied to power uprates and new plant designs to ensure acceptable margin between expected plant performance and the regulatory limits. Accurate prediction of the consequences of a large break LOCA is important because it is one of the postulated accident scenarios that determine the licensed core power and several other operational parameters. As the NRC places greater emphasis on risk-informed regulation, a more accurate and reliable systems code is needed to obtain realistic rather than conservative predictions.

To acquire detailed, fundamental data for use in developing models for an LBLOCA, the NRC sponsored the design and construction of a Rod Bundle Heat Transfer (RBHT) Test Facility. Some of these detailed data have only recently become possible because of recent advances in instrumentation technology for two-phase flow measurements.

This report presents the results of reflood heat transfer tests. The data from these tests will be used to develop and assess a reflood model for the TRACE code. The results of other test series will be reported in separate reports. Additional information about the RBHT Test Program is provided in two previously published reports: NUREG/CR-6975, "Rod Bundle Heat Transfer Test Facility Test Plan and Design," and, NUREG/CR-6976, "Rod Bundle Heat Transfer Test Facility Description."

With improved data and code models for an LBLOCA, we can more accurately predict the consequences of LBLOCA accidents and provide better technical bases for regulations associated with such accidents. As a result, this study will help to achieve the NRC's strategic performance goals of making the agency's regulations more effective, efficient, and realistic.

CONTENTS

	<u>Page</u>
ABSTRACT	iii
FOREWORD	v
EXECUTIVE SUMMARY	xiii
ABBREVIATIONS	xv
1. INTRODUCTION	1
1.1 Rod Bundle Heat Transfer Program Reflood Heat Transfer Test Matrix	3
1.2 References	3
2. TEST FACILITY DESCRIPTION FOR REFLOOD EXPERIMENTS	7
2.1 General Facility Description	7
2.1.1 Test Section	9
2.1.2 Lower Plenum	16
2.1.3 Upper Plenum	16
2.1.4 Large and Small Carryover Tanks	18
2.1.5 Steam Separator and Collection Tank	21
2.1.6 Pressure Oscillation Damping Tank	22
2.1.7 Exhaust Piping	24
2.1.8 Injection Water Supply Tank	25
2.2 Facility Improvements Over Previous Tests	26
2.3 Instrumentation and Data Acquisition System	26
2.3.1 Loop Instrumentation and Controls	27
2.3.2 Test Section Instrumentation	29
2.3.3 Data Acquisition System	38
3. CALCULATIONAL METHODS USED FOR THE RBHT REFLOOD HEAT TRANSFER EXPERIMENTS	40
3.1 Transient Heat Transfer Coefficient Calculation (DATARH)	40
3.1.1 Introduction	40
3.1.2 Mathematical Model	40
3.1.3 Structure of the source program DATARH.F	45
3.1.4 RBHT Rod Geometry and Materials	47
3.1.5 Input File Required for Executing the Current Version of the Program	48
3.1.6 Calculation of the Power Factor at Each Thermocouple Location	51
3.2 Quench Front Determination	57
3.3 RBHT Mass Balance	65
3.3.1 Introduction	65
3.3.2 Methodology	65
3.3.3 Summary of Mass Imbalances	67
3.3.4 Transient Mass Balance	68
3.3.5 Mass Storage in the Bundle	70
3.4 Droplet Measurements	73
3.4.1 Droplet Measurement Instrumentation	73
3.4.2 Droplet Size Measurements	75

3.4.3 Droplet Size and Elevation	75
3.4.4 Droplet Velocity	82
3.4.5 Calculation of Interfacial Area from Droplet Distribution Data	83
3.4.6 Droplet Measurement Data for Individual Experiments	85
3.5 References	86
4. CONCLUSIONS	88
APPENDIX A. TEST RESULTS	A-1
APPENDIX B. UNCERTAINTIES	B-1
B.1 Measurement Errors	B-1
B.2 Heat Transfer Coefficient Uncertainty Analysis	B-8
B.3 References	B-24

FIGURES

		<u>Page</u>
1.1	Reflood Flow Regimes for High and Low Reflood Rates	2
2.1	RBHT Test Facility Schematic	8
2.2	Test Facility Isometric View	8
2.3	Test Section Isometric View	11
2.4	Rod Bundle Cross Section View	12
2.5	Heater Rod Schematic	13
2.6	Heater Rod Axial Power Profile	14
2.7	Mixing Vane Grid	14
2.8	Low Melt Reservoir	15
2.9	Housing Window	15
2.10	Lower Plenum	17
2.11	Upper Plenum	17
2.12	Exhaust Line Baffle	18
2.13	Small Carryover Tank	19
2.14	Large Carryover Tank	20
2.15	Steam Separator	21
2.16	Steam Separator Collection Tank	22
2.17	Pressure Oscillation Damping Tank	23
2.18	Exhaust Piping	24
2.19	Injection Water Supply Tank	25
2.20	Loop Instrumentation Schematic	28
2.21	Rod Bundle and Housing Instrumentation Axial Locations	30
2.22	Instrumented Heater Rod Radial Locations	31
2.23	Mixing Vane Grid Instrumentation	31
2.24	Grid No. 2 Instrumentation	32
2.25	Grid No. 3 Instrumentation	32
2.26	Grid No. 4 Instrumentation	33
2.27	Grid No. 5 Instrumentation	33
2.28	Grid No. 6 Instrumentation	34
2.29	Grid No. 7 Instrumentation	34
2.30	Traversing Steam Probe Rake Schematic	36
2.31	Laser Illuminated Digital Camera System Setup	37
3.1	RBHT Test Facility, Heater Rod Locations (Looking Down from Top)	51
3.2	Axial Power Ratio for Rod F4	52
3.3	Power Factor as a Function of Length (Beginning of Heated Length to PCT)	54
3.4	Power Factor as a Function of Length (From PCT to End of Heated Length)	54
3.5	Clad Temperature at 2.24 m, Experiment 1096	57
3.6	Temperature and First Derivative of Temperature at 2.24 m Elevation	59
3.7	Temperature and First Derivative of Temperature Curve at 2.42 m Elevation	60
3.8	Temperature and First Derivative of Temperature Curve at 2.42 m Elevation	61
3.9	Quench Temperature at Different Quench Locations, Experiment 1096	62
3.10	Quench Temperature at Different Quench Locations, Experiment 1383	63
3.11	Housing Quench Front, Experiment 1096	63
3.12	Housing Quench Front, Experiment 1383	64
3.13	Rod and Housing Quench Front, Experiment 1096	64
3.14	Rod and Housing Quench Front, Experiment 1383	65

3.15	Summary of Mass Imbalances	68
3.16	Supply Tank Cross-Sectional Area	69
3.17	Mass Balance Plot for Experiment 1383	72
3.18	General Schematic of the Imaging System	74
3.19	Typical VisiSizer Image Through the Rod Bundle (No Droplets Present)	74
3.20	Normalized Droplet Distributions Upstream and Downstream Grid	76
3.21	Probability Distribution Log-Normal Curve Fits Upstream and Downstream Grid	77
3.22	Drop Breakup Data as a Function of Droplet Impact Weber Number	78
3.23	Comparison of Droplet Diameters	79
3.24	Comparison of Droplet Diameters	80
3.25	Comparison of Droplet Diameters	81
3.26	Size and Velocity Distribution Downstream of the Spacer Grid	82
3.27	Sauter Mean Diameter Time History for Experiment 1383	84
3.28	Liquid Flow rate for Experiment 1383	85
3.29	Rate of Interfacial Area for Experiment 1383	86

TABLES

	<u>Page</u>
1.1 Reflood Heat Transfer Test Log	4
3.1 Geometry and Dimensions of RBHT Heater Rod	47
3.2 Heater Number 1	51
3.3 Sample Power Factor Calculation for One Heater Rod	53
3.4 Axial Power Factors for the RBHT Heater Rods	55
3.5 Supply Tank Parameters	68

EXECUTIVE SUMMARY

As part of the U.S. Nuclear Regulatory Commission's safety analysis computer code development efforts, the Rod Bundle Heat Transfer (RBHT) Test Facility has been designed and constructed at The Pennsylvania State University. The RBHT Test Facility is a full length simulation of a portion of a pressurized water reactor (PWR) fuel assembly. The bundle is a 7x7 rod array with four unheated corner rods and 45 heated electrical rod which simulate a 17x17 PWR fuel assembly. The RBHT Test Facility has a heated length of 3.66 m (12 ft), with typical PWR rod diameters of 9.49 mm (0.374 in) and a rod pitch of 12.6 mm (0.496 in). The heater rods have a top skewed power shape with a peak to average power of 1.5 at the 2.77 m (9.08 ft) elevation. The ranges of conditions for the experiments are pressures from 138 to 414 kPa (20 to 60 psia), flooding rates from 0.0254 to 0.1524 m/s (1 to 6 in/s), and initial temperatures from 1033 to 1144 degrees K (1400 to 1600 degrees F), inlet subcooling from 11 to 83 degrees K (20 to 150 degrees F), and peak powers of 1.32 to 2.31 kW/m (0.4 to 0.7 kW/ft). Typical PWR mixing vane spacer grids were simulated in the RBHT bundle.

There are approximately 500 channels of transient data recorded for each test including the bundle power, heater rod temperatures, upper plenum pressure, inlet flow rate, inlet water temperature, superheated vapor temperatures in the bundle, spacer grid temperatures, liquid carryout of the bundle, and the detailed axial bundle pressure drop. Transient mass balances were typically within five percent for the low flooding rate experiments, and larger for the higher flooding rate experiments. There are a total of 25 valid experiments performed and reported to the U.S. Nuclear Regulatory Commission. The data from these experiments were qualified and submitted to the U.S. Nuclear Regulatory Commission's data bank for analysis and code validation purposes.

There are several unique features of the RBHT program which are not found in other rod bundle reflood heat transfer experiments. The RBHT experiments are performed using constant power rather than simulating decay power as in previous rod bundle experiments. The use of constant power results in a quasi-steady dispersed flow film boiling regime in the bundle and extends the reflood transient. The longer experimental time allows a more detailed examination of the dispersed flow film boiling heat transfer models in the analysis codes without the additional complication of a rapidly moving quench front up the bundle. There are traversing miniature steam probes in the bundle at several elevations which measured the superheated steam temperature in the presence of saturated entrained droplets. The steam probes are located up- and downstream of the spacer grids and can indicate the effects of the spacer grids on the two-phase droplet flow. There is also a laser illuminated high resolution digital camera and associated software which can measure the entrained droplet size within the bundle at different elevations relative to the spacer grids. There are a large number of very sensitive differential pressure cells along the bundle. The mixing vane grids are also instrumented with several miniature thermocouples such that spacer grid temperature behavior can also be characterized in addition to the heater rod and vapor temperature measurements. The RBHT Test Facility reflood heat transfer experiments have provided integrated detailed data that can be used for advanced safety analysis computer code assessment for dispersed flow film boiling and inverted annular film boiling in a prototypical rod bundle geometry.

ABBREVIATIONS

DATARH	Data Reduction and Heat Transfer Computer Program
ECC	Emergency Core Cooling
FLECHT	Full-Length Emergency Core Heat Transfer
FLECHT-SEASET	Full-Length Emergency Core heat Transfer – Separate Effects and System Effects Tests
HP	Hewlett-Packard
IEEE	Institute of Electrical and Electronics Engineers
INEEL	Idaho National Engineering and Environmental Laboratory
LBLOCA	Large-Break Loss of Coolant Accident
LIDCS	Laser Illuminated Digital Camera System
NRC	U.S. Nuclear Regulatory Commission
PWR	Pressurized Water Reactor
TC	Thermocouple
RBHT	Rod Bundle Heat Transfer
SMD	Sauter Mean Diameter
STP	Standard Temperature and Pressure Conditions

INTRODUCTION

The objective of the Rod Bundle Heat Transfer (RBHT) Program is to provide high quality experimental data for computer code model development and validation. As part of this program, a series of experiments are performed to examine reflood thermal/hydraulic behavior over a wide range of conditions.

A series of reflood experiments are performed in the (RBHT) facility over a range of pressures, flow rates, inlet temperatures and simulated powers. The experiments are run using constant power, which is different from the previously performed FLECHT (Refs. 1 and 2) and FLECHT-SEASET (Ref. 3) experiments such that the reflooding behavior is quasi-steady for much longer periods of time. It is believed that the quasi-steady behavior of the RBHT experiments will make model development and validation easier since the film boiling portions of the experiments are extended in time. Also, the specific instrumentation which was added to the RBHT for improved understanding of the reflooding process will provide new and improved data for the quasi-steady reflood experiments. Specifically, subchannel vapor measurements using miniature thermocouples on traversing steam probe rakes yield vapor superheat for extended times as the quench front advances up the heater rods.

There are two basic flow regimes for reflooding in a rod bundle. For high flooding rates, typically, 0.1524 m/s (6 in/s) or higher, the dominant flow regime for the post-CHF regions in the bundle is an inverted annular regime in which a thin layer of vapor separates the heated wall from the subcooled liquid flow which nearly fills the channel. Since the inlet flow is larger than the quench rate of the fuel rods, a long region of inverted film boiling can exist above the quench front. As one proceeds upward along the bundle, liquid becomes saturated and begins to break into chunks or liquid slugs. The length of the inverted annular and the liquid chunk regimes depends on the flooding rate into the heated bundle, initial subcooling of the liquid, system pressure, and the rod bundle initial temperature and power level. The heat transfer in this regime is high and results in immediate clad temperature turnover such that lower peak cladding temperatures are calculated for this reflood regime. Figure 0.1 shows an example of both the high and low flooding rate reflood heat transfer and flow regimes.

For low flooding rates, there is no subcooled inverted annular film boiling region. Because of the low injection flow rate, the liquid quickly reaches saturation and there is bulk boiling of the fluid below the quench front. In the quench front region, and above the quench front, there is a froth region which has a medium range void fraction which transitions between a low void fraction, below the quench front, to the much higher void fraction in the dispersed flow regions above the quench front. This behavior is shown in Figure 0.1. The heat transfer in this region occurs between the heated wall and the superheated steam. Liquid droplets in the superheated steam evaporate reducing the steam temperature as well as increasing the flow rate of the steam. As a result, the calculated peak cladding temperature usually occurs in this region. In most reactor reflood calculations, after the initial surge into the core, the flooding rates are very low, typically 0.0254 m/s (1 in/s) or less such that the dispersed flow film boiling region is the dominant flow regime of interest and is the heat transfer regime in which the peak cladding temperature occurs.

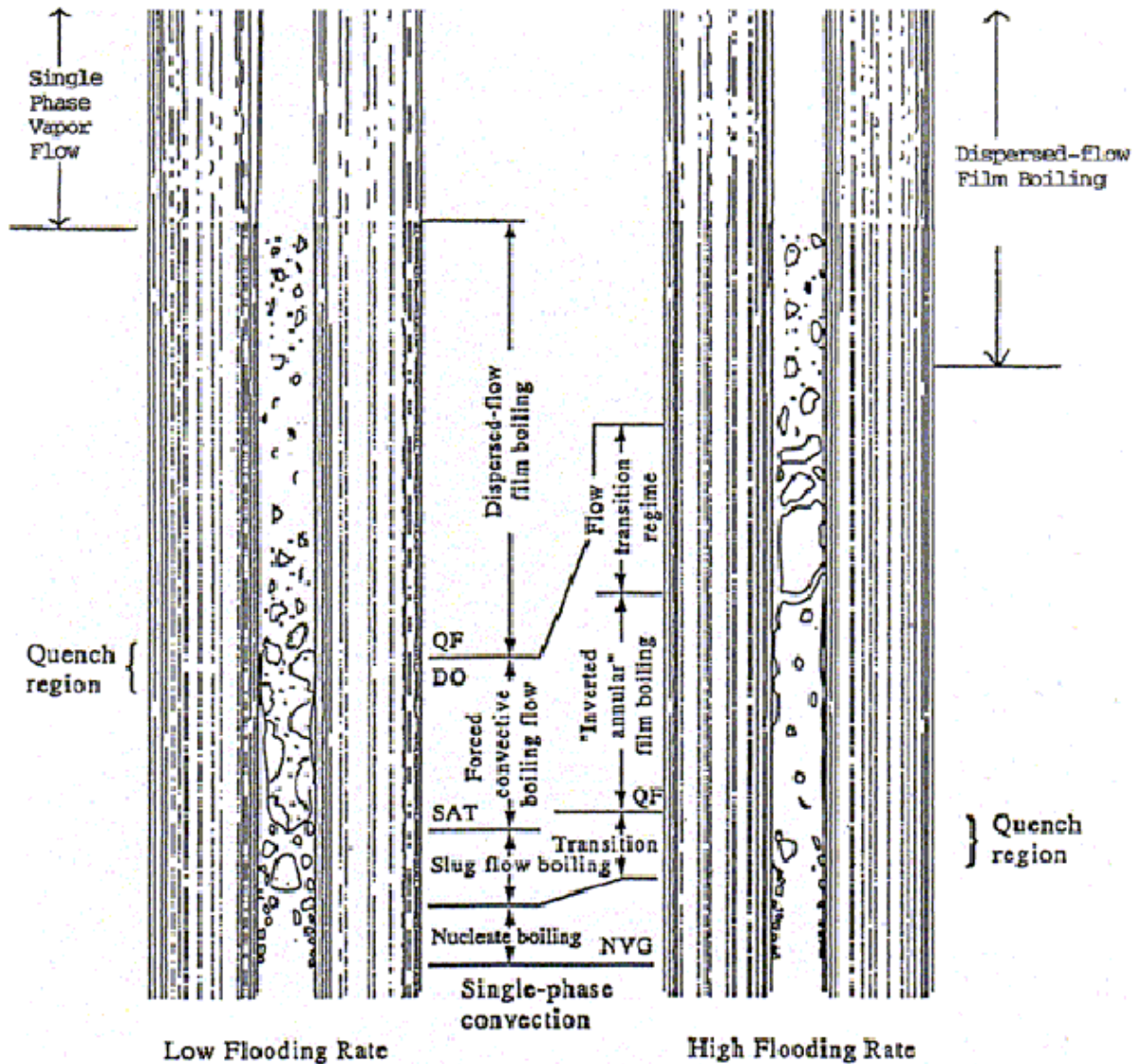


Figure 0.1 Reflood Flow Regimes for High and Low Reflood Rates.

The RBHT instrumentation strategy is primarily designed to obtain detailed information for the low flooding rate experiments. The low flooding rate conditions are more limiting for postulated accident conditions, and the phenomena associated with the low flooding rate behavior are more difficult to predict with accuracy.

This report provides a summary of the data obtained, the data reduction methods and assumptions used in reducing the data as well as the uncertainty in the experimental data and derived quantities from the data. A full set of the experimental data was transmitted to the NRC data bank.

1.1 Rod Bundle Heat Transfer Program Reflood Heat Transfer Test Matrix

A series of reflood heat transfer experiments are performed to provide data for dispersed flow film boiling in rod bundles as well as for the inverted annular flow film boiling heat transfer regime. The range of pressures expected during a PWR LBLOCA was examined as well as the inlet subcooling of the Emergency Core Cooling (ECC) flow into the test bundle. The initial temperatures are selected to represent a Best-Estimate peak cladding temperature at the beginning of the reflood portion of the LOCA transient. Most of the experiments use a peak cladding temperature of 1033 to 1144 degrees K (approximately 1400 degrees F). The flooding rates vary from 0.0254 to 0.1524 m/s (1 to 6 in/s).

There are a number of repeat experiments in which the laser illuminated digital camera system is moved to different axial positions in the rod bundle. The strategy is to obtain drop size information at different elevations, relative to the quench front, for the same system conditions such that the evolution of the entrained flow can be determined by super-positioning the data gathered in different experimental runs.

While there is a learning curve in performing the experiments, the test repeatability, mass balances, and test performance continued to improve over the testing period. The most significant problem encountered in the reflood test series is pressure oscillations which occurred due to the control logic for the exhaust control valve. Pressure variations in the test section were usually small, but there are several experiments in which pressure oscillations could not be damped and the experimental runs are considered invalid. The reflood heat transfer test log is given in Table 1.1 for the different experiments performed and there is a Quick Look Report (QLR) written for each valid experiment which contains a mass balance calculation. The data from these experiments has been sent to the NRC's data bank in electronic format.

1.2 References

1. Rosal, E. R., Hochreiter, L. E., McGuire, M. F., Krepinevich, M. C., "FLECHT Low Flooding Rate Cosine Test Series Data Report," WCAP-8651, December (1975).
2. Rosal, E. R., Conway, C. E., Krepinevich, M. C., "FLECHT Low Flooding Rate Skewed Test Series Data Report," WCAP-9108, May (1977).
3. Lee, N., Wong, S., Yeh, H.C., and Hochreiter, L.E., "PWR FLECHT-SEASET Unblocked Bundle, Forced and Gravity Reflood Task Data Evaluation & Analysis Report," NRC/EPRI/Westinghouse Report No. 10, WCAP-9891, NUREG/CR-2256, EPRI NP-2013, November (1981).

Table 1.1 Reflood Heat Transfer Test Log

RBHT Run # NRC Test #	Test Conditions									Validity	Comments
	Pressure kPa (psia)	Flooding Rate m/sec (in/sec)	Peak Power kW/m (kW/ft)	Initial Temp. K (°F)	Inlet Subcooling K (°F)	Steam Probe Info.	Laser Camera Elevation m (in.)	Start Time sec	End Time sec		
937 1a	138 (20)	0.0254 (1)	1.31 (0.4)	1033 (1400)	11 (20)	Rakes 1, 2, 4, 6, 7, 9, 10, 11, 13 in center		301.3	1362	Valid	No droplet data
945 2a	276 (40)	0.0254 (1)	1.31 (0.4)	1033 (1400)	11 (20)	Rakes 1, 2, 4, 6, 7, 9, 10, 11, 13 in center		1709	2490	Valid	No droplet data
973 2b	276 (40)	0.0254 (1)	1.31 (0.4)	1033 (1400)	11 (20)	Rakes 1, 2, 4, 6, 7, 9, 10, 11, 13 in gap	2.86 (112.5) downstream of grid #6	400	1233.5	Valid	
1088 2c	276 (40)	0.0254 (1)	1.31 (0.4)	1033 (1400)	11 (20)	Rakes 3, 4, 5, 6, 7, 9, 10, 11, 12, 13, in center	2.74 (108) upstream of grid #6	162.5	368.5	Valid	Test terminated early, valid to end time
1096 1b	138 (20)	0.0254 (1)	1.31 (0.4)	1033 (1400)	11 (20)	Rakes 3, 4, 5, 6, 7, 9, 10, 11, 12, 13, in center	2.36 (93) downstream of grid #5	227.4	1916	Valid	
1103 4a	138 (20)	0.0254 (1)	1.31 (0.4)	1033 (1400)	11 (20)	Rakes 3, 4, 5, 6, 7, 9, 10, 11, 12, 13, in center				Invalid	Pressure, therefore temperature oscillations
1108 4b	138 (20)	0.0254 (1)	1.31 (0.4)	1033 (1400)	83 (150)	Rakes 3, 4, 5, 6, 7, 9, 10, 11, 12, 13, in center	2.36 (93) upstream of grid #5	110.6	1492.5	Valid	
1132 5a	138 (20)	0.1524 (6)	2.3 (0.7)	1144 (1600)	83 (150)	Rakes 3, 4, 5, 6, 7, 9, 10, 11, 12, 13, in center	2.21 (87) upstream of grid #5			Invalid	Inlet flow oscillations
1143 5a	138 (20)	0.1524 (6)	2.3 (0.7)	1144 (1600)	83 (150)	Rakes 3, 4, 5, 6, 7, 9, 10, 11, 12, 13, in center	2.36 (93) downstream of grid #5	740.3	1022.5	Valid	
1155 5b	138 (20)	0.1524 (6)	2.3 (0.7)	1144 (1600)	11 (20)	Rakes 3, 4, 5, 6, 7, 9, 10, 11, 12, 13, in center		369	774	Valid	Test terminated early, valid to end time. No droplet data
1160 6	276 (40)	0.127 (5)	2.3 (0.7)	1144 (1600)	83 (150)	Rakes 3, 4, 5, 6, 7, 9, 10, 11, 12, in center	2.36 (93) downstream of grid #5	129.5	504.6	Valid	
1170 10	276 (40)	0.1524 (6)	2.3 (0.7)	1144 (1600)	11 (20)	Rakes 3, 4, 5, 6, 7, 9, 10, 11, 12, in center		298	771.8	Valid	No droplet data
1178 8	276 (40)	0.1524 (6)	2.3 (0.7)	1144 (1600)	53 (96)	Rakes 3, 4, 5, 6, 7, 9, 10, 11, 12, in center				Invalid	Scrammed, DAS not synchronized
1183 8	276 (40)	0.1524 (6)	2.3 (0.7)	1144 (1600)	53 (96)	Rakes 3, 4, 5, 6, 7, 9, 10, 11, 12, in center				Invalid	Insufficient nitrogen for flow control
1196 8	276 (40)	0.1524 (6)	2.3 (0.7)	1144 (1600)	53 (96)	Rakes 3, 4, 5, 6, 7, 9, 10, 11, 12, in center	2.36 (93) downstream of grid #5	226.6	718.7	Valid	No droplet data
1202 9	276 (40)	0.1524 (6)	2.3 (0.7)	1144 (1600)	23 (42)	Rakes 3, 4, 5, 6, 7, 9, 10, 11, 12, in center		258.5	801.7	Valid	No droplet data

Table 1.1 Reflood Heat Transfer Test Log (Cont)

RBHT Run # NRC Test #	Test Conditions									Validity	Comments
	Pressure kPa (psia)	Flooding Rate m/sec (in/sec)	Peak Power kW/m (kW/ft)	Initial Temp. K (°F)	Inlet Subcooling K (°F)	Steam Probe Info.	Laser Camera Elevation m (in.)	Start Time sec	End Time sec		
1223 10	276 (40)	0.1524 (6)	2.3 (0.7)	1144 (1600)	11 (20)	Rakes 3, 4, 5, 6, 7, 9, 10, 11, 12, in center		135.2	788.6	Valid	No droplet data
1228 11	138 (20)	0.1524 (6)	2.3 (0.7)	1144 (1600)	23 (42)	Rakes 3, 4, 5, 6, 7, 9, 10, 11, 12, in center		120.5	1112.5	Valid	No droplet data
1248										Invalid	Scrammed prior to reflood
1252 6	276 (40)	0.1524 (6)	2.3 (0.7)	1144 (1600)	83 (150)	Rakes 3, 4, 5, 6, 7, 9, 10, 11, 12, in center				Invalid	Large inlet flow conditions
1280 5a	138 (20)	0.1524 (6)	2.3 (0.7)	1144 (1600)	83 (150)	Rakes 3, 4, 5, 6, 7, 9, 10, 11, 12, in center		173.2	506.2	Valid	No droplet data
1285 6	276 (40)	0.1524 (6)	2.3 (0.7)	1144 (1600)	83 (150)	Rakes 3, 4, 5, 6, 7, 9, 10, 11, 12, in center		115.8	418.5	Valid	No droplet data
1291 7	414 (60)	0.1524 (6)	2.3 (0.7)	1144 (1600)	83 (150)	Rakes 3, 4, 5, 6, 7, 9, 10, 11, 12, in center		122.9	366.6	Valid	No droplet data
1295 12	414 (60)	0.1524 (6)	2.3 (0.7)	1144 (1600)	23 (42)	Rakes 3, 4, 5, 6, 7, 9, 10, 11, 12, in center		114	451.2	Valid	No droplet data
1300 13	276 (40)	0.1524 (6)	2.3 (0.7)	1144 (1600)	76 (136)	Rakes 3, 4, 5, 6, 7, 9, 10, 11, 12, in center		141.2	727.5	Valid	No droplet data
1310 1c	138 (20)	0.0147 (0.58)	1.31 (0.4)	1033 (1400)	11 (20)	Rakes 3, 4, 5, 6, 7, 9, 10, 11, 12, in center	1.84 (72.5) downstream of grid #4	185	785	Valid	Power turned off at 449.7 sec.
1319 2d	276 (40)	0.0149 (0.59)	1.31 (0.4)	1033 (1400)	11 (20)	Rakes 3, 4, 5, 6, 7, 9, 10, 11, 12, in center	1.84 (72.5) downstream of grid #5	844.7	1289	Valid	Power turned off at 1010.5 sec.
1340 1c	138 (20)	0.0254 (1)	1.31 (0.4)	1033 (1400)	11 (20)	Rakes 3, 4, 5, 6, 7, 9, 10, 11, 12, in center				Invalid	Pressure, therefore temperature oscillations
1346 2d	276 (40)	0.0254 (1)	1.31 (0.4)	1033 (1400)	11 (20)	Rakes 3, 4, 5, 6, 7, 9, 10, 11, 12, in center				Invalid	Pressure, therefore temperature oscillations
1351 2e	276 (40)	0.0254 (1)	1.31 (0.4)	1033 (1400)	11 (20)	Rakes 3, 4, 5, 6, 7, 9, 10, 11, 12, in center				Invalid	Pressure, therefore temperature oscillations
1356 1d	138 (20)	0.0254 (1)	1.31 (0.4)	1033 (1400)	11 (20)	Rakes 3, 4, 5, 6, 7, 9, 10, 11, 12, in center				Invalid	Pressure, therefore temperature oscillations
1361 1a	138 (20)	0.0254 (1)	1.31 (0.4)	1033 (1400)	11 (20)	Rakes 3, 4, 5, 6, 7, 9, 10, 11, 12, in center				Invalid	Pressure, therefore temperature oscillations

Table 1.1 Reflood Heat Transfer Test Log (Cont)

RBHT Run # NRC Test #	Test Conditions									Validity	Comments
	Pressure kPa (psia)	Flooding Rate m/sec (in/sec)	Peak Power kW/m (kW/ft)	Initial Temp. K (°F)	Inlet Subcooling K (°F)	Steam Probe Info.	Laser Camera Elevation m (in.)	Start Time sec	End Time sec		
1378 2a	276 (40)	0.0254 (1)	1.31 (0.4)	1033 (1400)	11 (20)	Rakes 3, 4, 5, 6, 7, 9, 10, 11, 12, in center				Invalid	Pressure, therefore temperature oscillations
1383 2a	276 (40)	0.0254 (1)	1.31 (0.4)	1033 (1400)	11 (20)	Rakes 3, 4, 5, 6, 7, 9, 10, 11, 12, in center	2.86 (112.5) downstream of grid #6	313.2	1202	Valid	
1389 2d	276 (40)	0.0254 (1)	1.31 (0.4)	1033 (1400)	11 (20)	Rakes 3, 4, 5, 6, 7, 9, 10, 11, 12, in center	1.84 (72.5) downstream of grid #4	139.6	1529	Valid	
1402 2e	276 (40)	0.0254 (1)	1.31 (0.4)	1033 (1400)	11 (20)	Rakes 3, 4, 5, 6, 7, 9, 10, 11, 12, in center	1.32 (52.5) downstream of grid #3	465.2	2440	Valid	
1407 15	276 (40)	0.0762 (3)	2.3 (0.7)	1144 (1600)	23 (41)	Rakes 3, 4, 5, 6, 7, 9, 10, 11, 12, in center	2.86 (112.5) downstream of grid #6	126.3	2030	Valid	

2. TEST FACILITY DESCRIPTION FOR REFLOOD EXPERIMENTS

The RBHT Test Facility was developed by The Pennsylvania State University and the United States Nuclear Regulatory Commission. The facility is designed to conduct systematic separate effects tests under well-controlled laboratory conditions in order to generate fundamental rod bundle heat transfer data from: two-phase level swell tests, steam flow tests with and without droplet injection, inverted annular film boiling reflow tests, and dispersed flow film boiling reflow heat transfer tests. The facility is capable of operating in steady-state forced and variable reflow modes covering a wide range of flows and heat transfer conditions at pressures from 1.0 (14.5 psia) to 4.2 bars (60 psia).

2.1 General Facility Description

The test facility consists of the following major components shown schematically in Figure 2.1, and in an isometric view in Figure 2.2:

- A test section consisting of a lower plenum, a low-mass housing containing the heater rod bundle, and upper plenum.
- Coolant injection and steam injection systems.
- Closely coupled phase separation and liquid collection systems.
- An injection system.
- A pressure fluctuation damping tank and steam exhaust piping.

The test facility is a once-through flow facility in which either water or steam can enter the lower plenum and flow upward through the rod bundle. The lower plenum is attached to the bottom of the flow housing and is used as a reservoir for the coolant prior to injection into the rod bundle during reflow. The upper plenum serves as the first stage for phase separation and liquid collection of the two-phase effluent exiting the rod bundle. The liquid phase separates from the flow due to the sudden expansion from the bundle to the larger plenum flow area.

The facility has a large and small liquid carryover tank provided to collect the liquid carryover in order to measure the amount of entrainment in the flow. The de-entrained liquid from the upper plenum drains into the top of a 25.6 mm tube, which extends inside the small carryover tank. When the small carryover tank fills, it overflows into the large carryover tank. A centrifugal two-phase separator is located downstream of the upper plenum and acts to separate out the remaining liquid flow from the vapor such that the vortex meter at the exit of the steam pipe will measure single phase vapor flow only. There is a third liquid collection tank on the phase separator, which collects the separated liquid.

A pressure-damping tank located before the vortex flow meter and pressure control valve acts to damp out any pressure oscillations to maintain tight pressure control on the facility. Separating the exit flows from the bundle provides a means of calculating a transient mass balance as well as an energy balance on the facility.

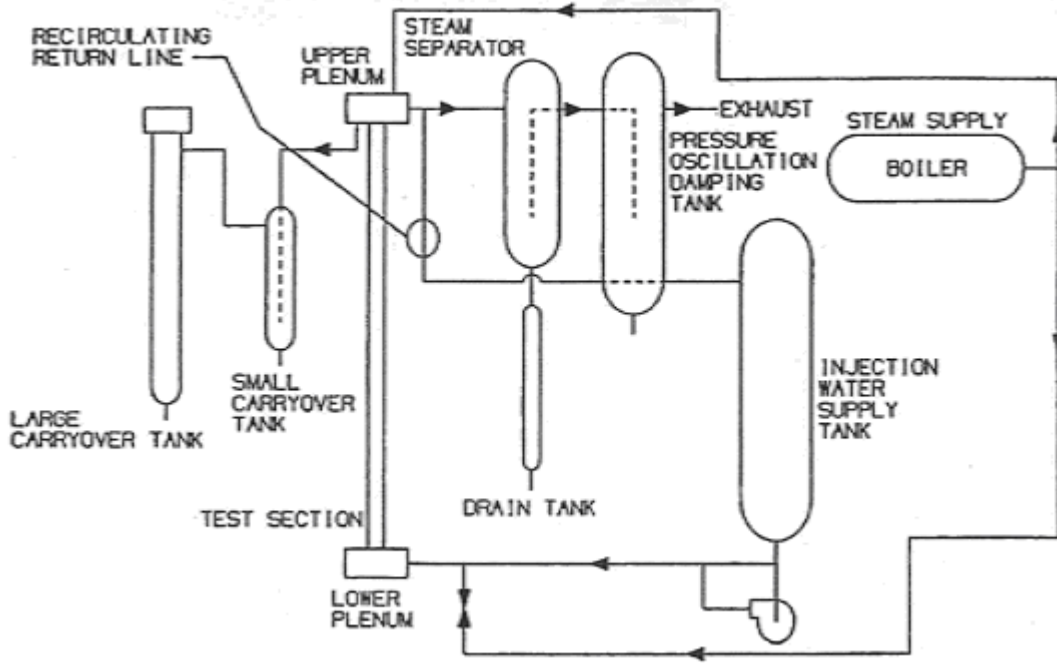


Figure 2.1 RBHT Test Facility Schematic.

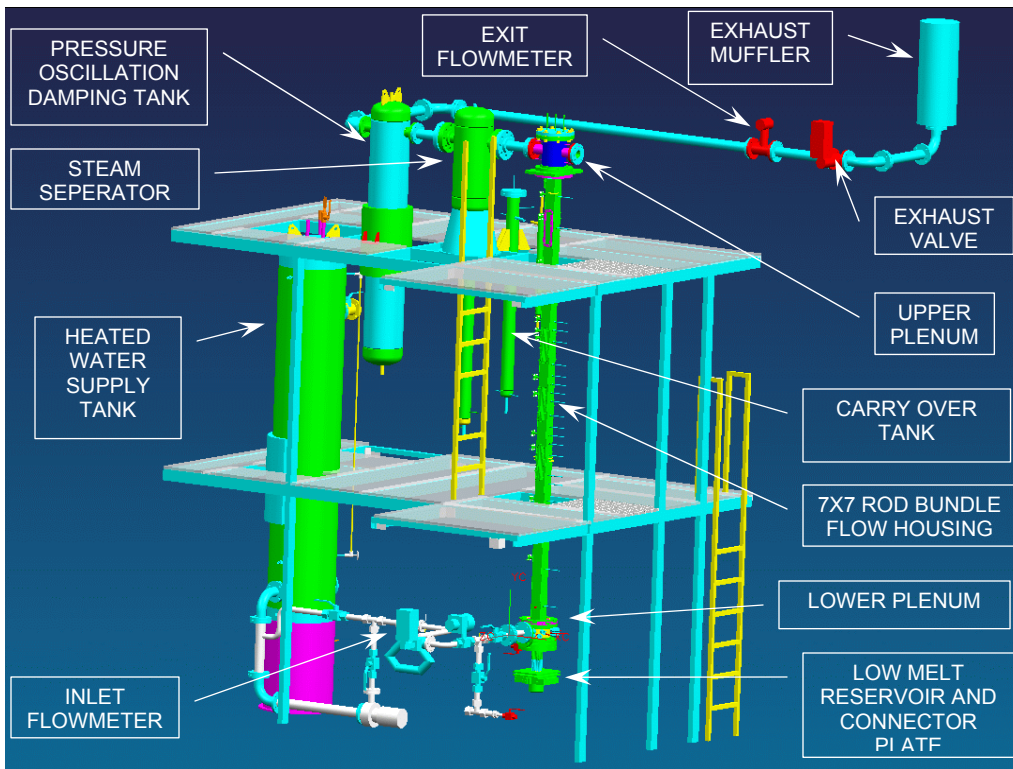


Figure 2.2 Test Facility Isometric View.

2.1.1 Test Section

The test section consists of the heated rod bundle, flow housing, and the lower and upper plenums, as shown in Figure 2.3. The heater rod bundle simulates a small portion of a 17x17 PWR reactor fuel assembly. The electrically powered heater rods have a diameter of 9.5 mm (0.374 in) arranged in a 7x7 array with a 12.6 mm (0.496 in) pitch, as shown in Figure 2.4. The bundle has 45 heater rods and 4 unheated corner rods. The corner rods are used to provide structural support for the bundle and provide exit points for thermocouple leads. The support rods are made from Inconel 600 tubing having a diameter 9.525 mm (0.37 in), a wall thickness of 2.108 mm (0.083 in), and a total length of 3.96 m (156 in). The heater rods are single ended and consist of a Monel 500 electrical resistance heating element surrounded by hot pressed boron nitride (BN) insulation and enclosed in a Inconel 600 cladding, as shown in Figure 2.5. Since it is desired to re-use the heater rods for multiple experiments, the cladding material was chosen for its high strength and low thermal expansion coefficient at high temperatures, which minimizes rod bowing and failure at high temperature operating conditions. The heater rods have a 3.66 m (12 ft) heated length with a skewed axial power profile, as shown in Figure 2.6, with the peak power located at the 2.74 m (9 ft) elevation. The maximum-to-average power ratio (P_{max}/P_{avg}) is 1.5 at the peak power location and 0.5 at both ends of the heated length. The bundle has a uniform radial power distribution.

Power to each rod is provided by a 60 volt, 12,600 amp, 750 kW DC power supply. Each rod is rated for 10 kW, and designed to operate at 13.8 bars (200 psig) at a maximum temperature of 1477 degrees K (2200 degrees F), but because of its solid construction it can be operated up to 103.4 bars (1500 psig). Rods marked with an "I" in Figure 2.4 are instrumented with eight 0.508 mm (0.02 in) diameter ungrounded thermocouples attached to the inside surface of the Inconel sheath at various locations. Rods marked with a "U" are not instrumented. All of the thermocouple leads exit at the heater rod bottom end. The Inconel 600 thermocouple sheath is compatible with the heater rod cladding and housing material to reduce differential thermal expansion and minimize the possibility of causing thermocouple failure during the thermo-cycling operations.

The rod bundle has seven mixing vane grids shown in Figure 2.7. These grids are similar in design of a PWR 17x17 fuel assembly, but instead of having dimples and springs, these grids have only dimples which provide a cold clearance of 0.127 mm (0.005 in) around each heater rod in order to prevent bowing when the heater rods are linearly expanding at high temperatures. The grids straps are made out of Inconel 600 alloy sheets which are 0.51 mm (0.020 in) thick and are 44.5 mm (1.75 in) in height including the mixing vanes. The grids are located 522 mm (20.55 in) apart except for the spacing between the first and second grid, which is 588 mm (23.26 in) apart. The first grid is located 102 mm (4.01 in) above the bottom of the heater length. The grids in conjunction with the corner rods form the heater rod bundle support structure. The grid locations are similar to the ones found in a 17x17 PWR fuel assembly. The heater rod top extensions are attached to the 25.4 mm (1 in) thick nickel ground plate by means of a Morse taper that provides a good electrical contact. The heater rod bottom extension and copper electrode extend through the lower plenum O-ring pressure seal plate.

The copper electrodes, which are 5.84 mm (0.023 in) in diameter and 203 mm (8 in) long, extend through holes drilled in the low-melt reservoir shown in Figure 2.8. This reservoir serves as the electrical power supply positive connection. It contains a low temperature melting alloy at about 344 degrees K (160 degrees F) which is an excellent conductor, thus providing a good

electrical contact and mechanical cushion allowing for rod thermal expansion to each heater rod.

The flow housing provides the pressure and flow boundary for the heater rod bundle. It has a square geometry. Its inside dimensions are 90.2 x 90.2 mm (3.55 x 3.55 in), and wall thickness 6.4 mm (0.25 in) as shown in Figure 2.4. The housing is made out of Inconel 600, the same material used for the heater rod cladding and thermocouple sheaths. As pointed out previously, the high strength of Inconel 600 at elevated temperatures will minimize housing distortion during testing. The 6.4 mm (0.25 in) wall thickness is the minimum allowable for operating at 4.2 bars (60 psig) and 811 degrees K (1000 degrees F) taking into consideration the cutouts to accommodate the large windows and numerous pressure and temperature penetrations through the walls, as shown in Figure 2.3. The empty housing has a flow area of 83.4 cm² (12.9 in²). With the rod bundle in place the flow area is 48.6 cm² (7.5 in²). This area is 7.21 percent larger than the ideal flow area of a 7x7 rod bundle configuration. The excess flow area is due to the flow housing inside dimensional tolerance and the space needed to insert the rod bundle in the housing. The gap between the outer rods and the flow housing inner wall is 2.5 mm (0.1 in) wide.

The flow housing has six pairs of windows. Each window provides a 50.8 x 292 mm (2.0 x 11.5 in) viewing area. Each pair of windows is placed 180 degrees apart and located axially at elevations overlapping rod bundle spacer grids, thus providing a viewing area about 88.9 mm (3.5 in) below and 152 mm (6 in) above the corresponding space grids. The windows will facilitate the measurement of droplet size and velocity using a Laser Illuminated Digital Camera System (LIDCS). In addition, high speed movies using diffused back lighting can be taken during the experiments for visualization and flow regime information. The windows are made out of optical grade fused quartz and are mounted on the housing by means of a bolted flange and Kemprofile high temperature gasket material, as shown in Figure 2.9.

The flow housing is supported from the nickel plate and upper plenum, allowing it to freely expand downward, thus minimizing thermal buckling and distortion. The two-phase void fraction will be measured using sensitive differential pressure cells. The flow housing has 23 pressure taps located at various elevations, as shown in Figure 2.3. The pressure taps are connected to sensitive differential pressure (DP) cells providing measurements to calculate single-phase friction losses for determining base rod bundle and grid loss coefficients. Sixteen of these pressure taps are located about 76.2 to 127 mm (3 to 5 in) apart to provide detailed void fraction measurements in the froth region above the quench front.

The flow housing also has thirteen stand-off penetrations at various elevations for the traversing steam probe rakes which measure the superheated steam temperatures in the dispersed flow regime.

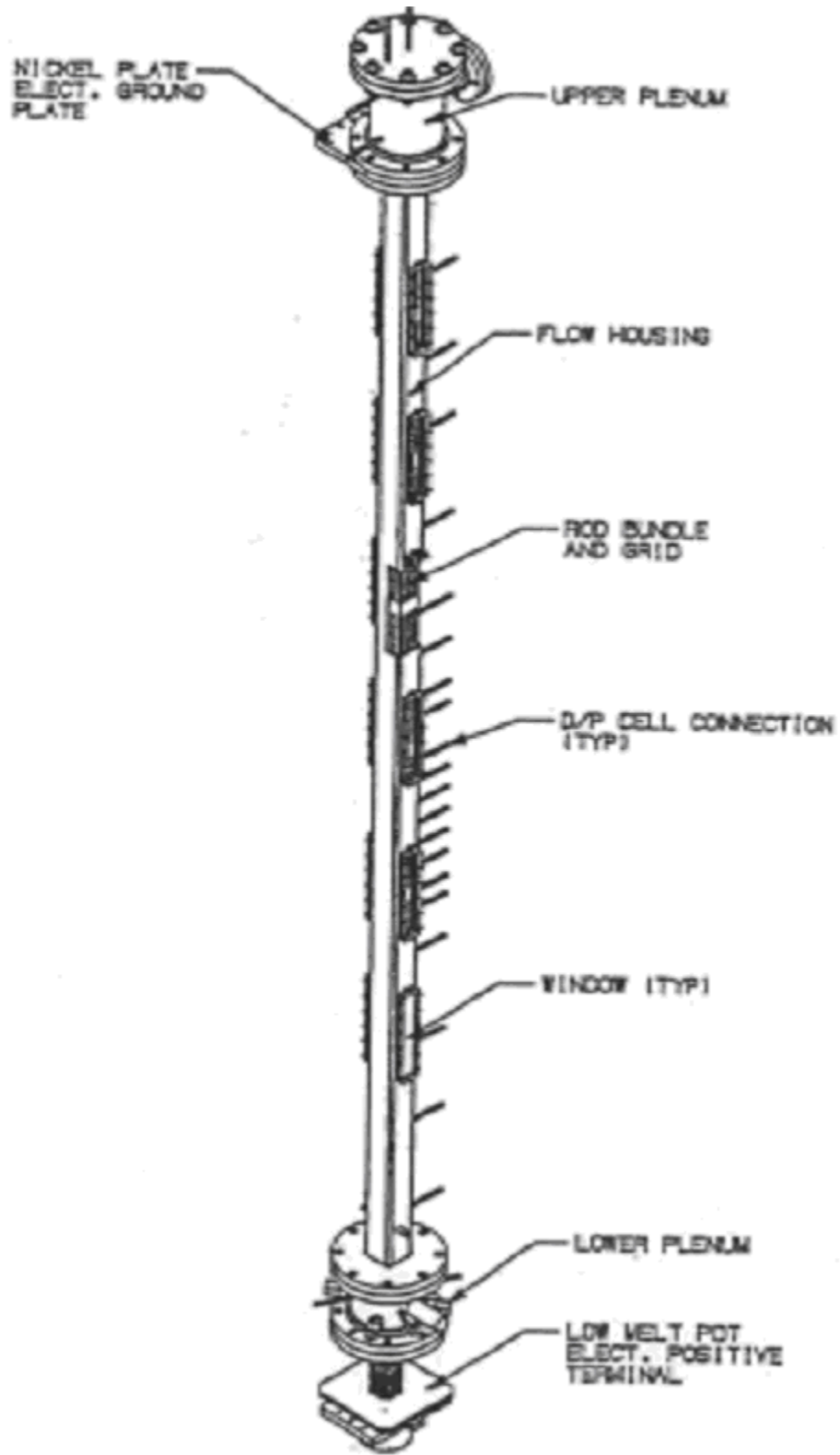


Figure 2.3 Test Section Isometric View.

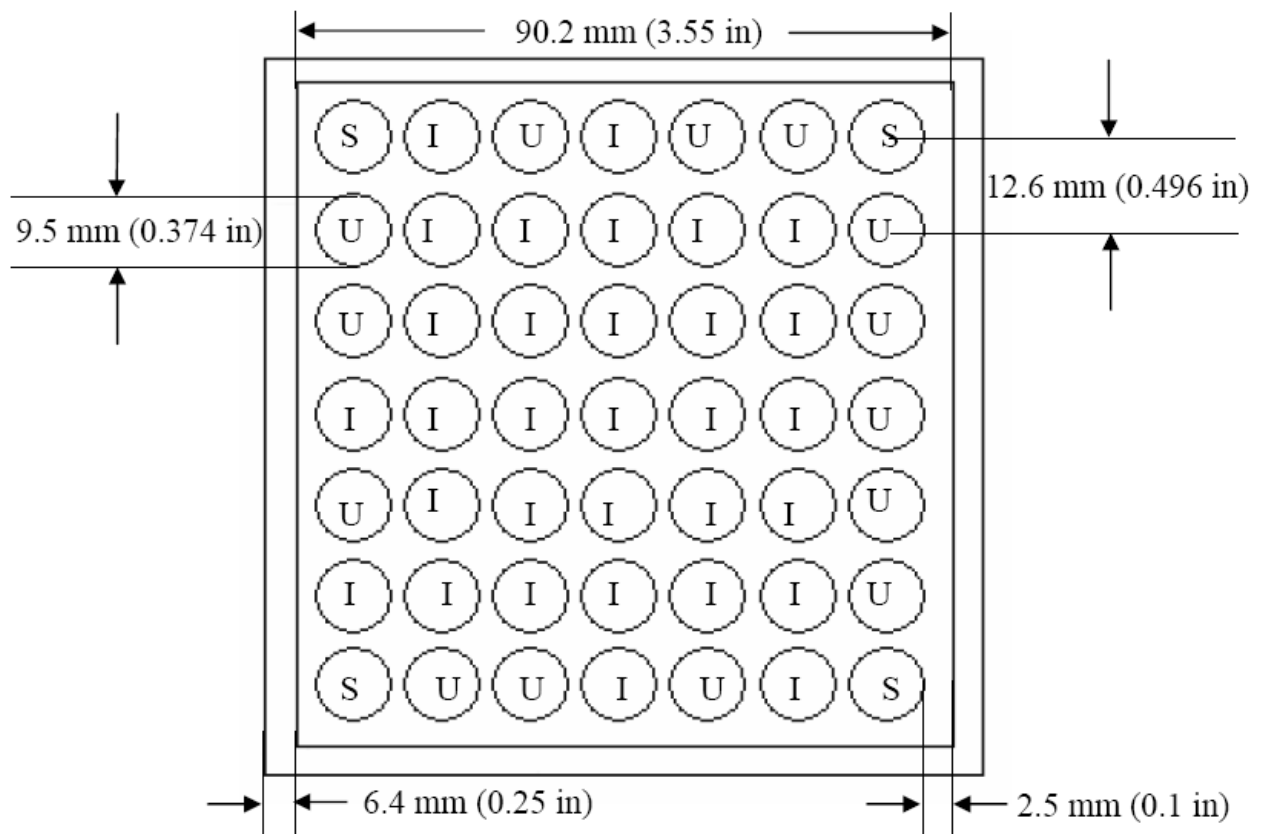
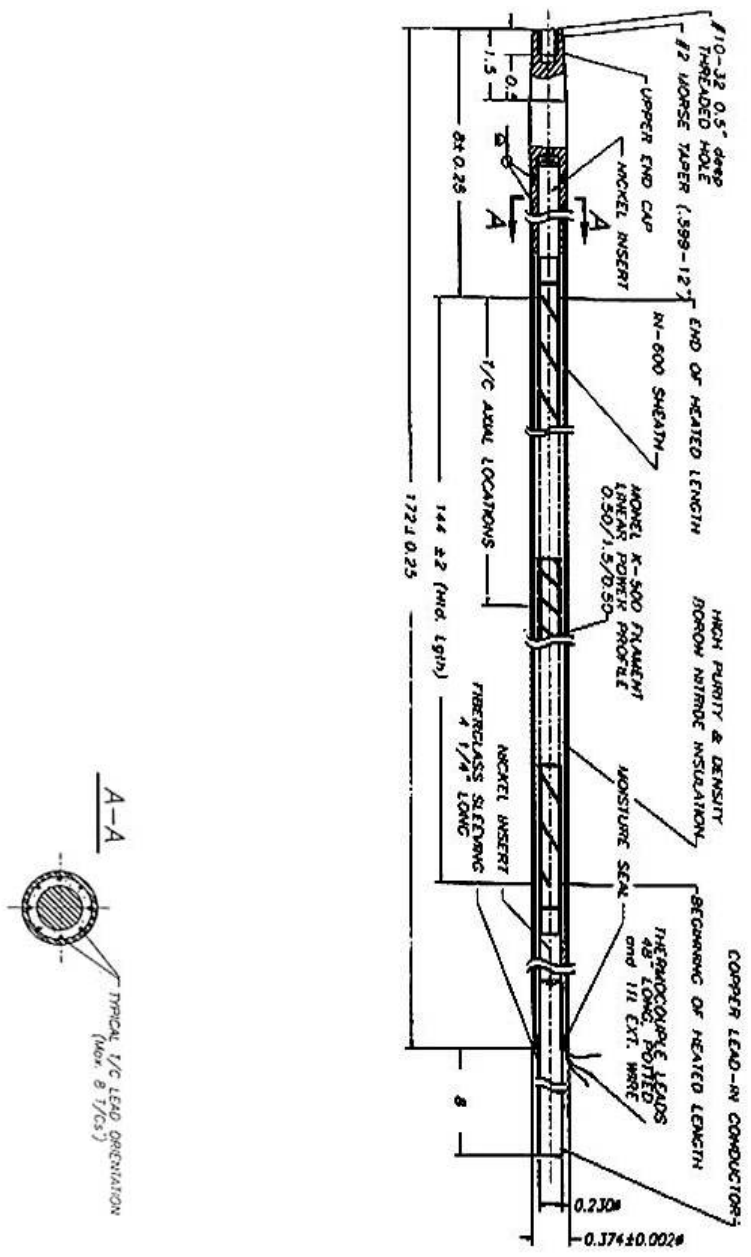


Figure 2.4 Rod Bundle Cross Section View.



NOTES:
 1. All dimensions in inches.

Figure 2.5 Heater Rod Schematic.

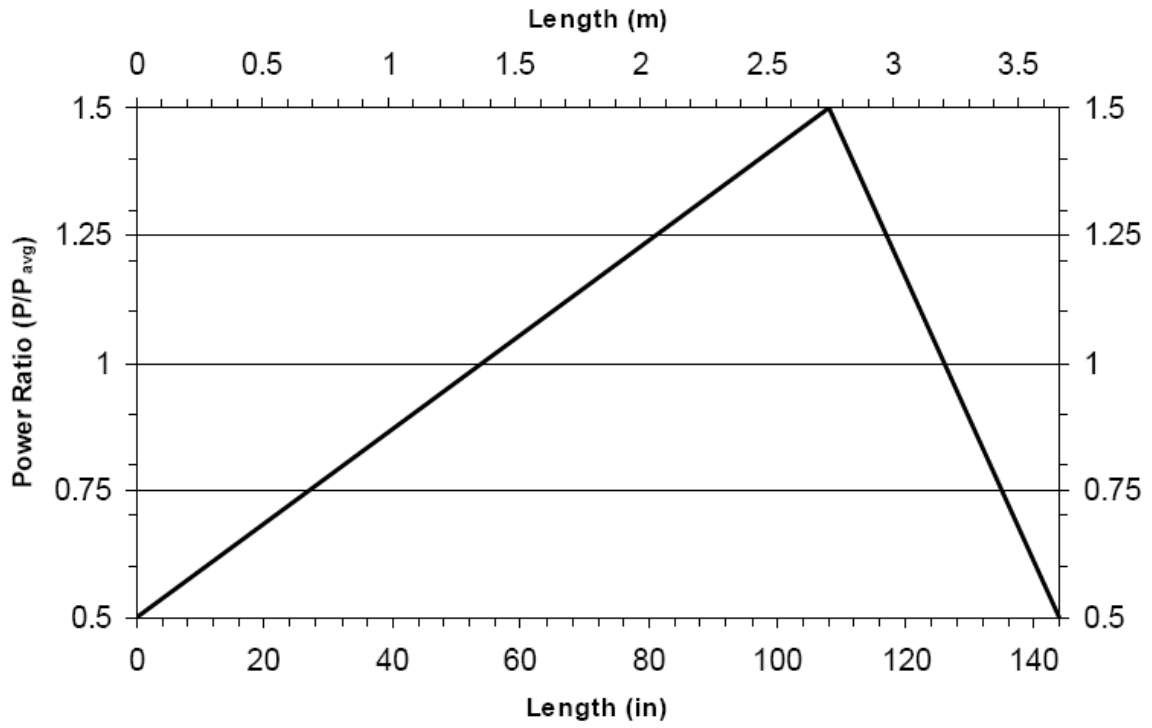


Figure 2.6 Heater Rod Axial Power Profile.

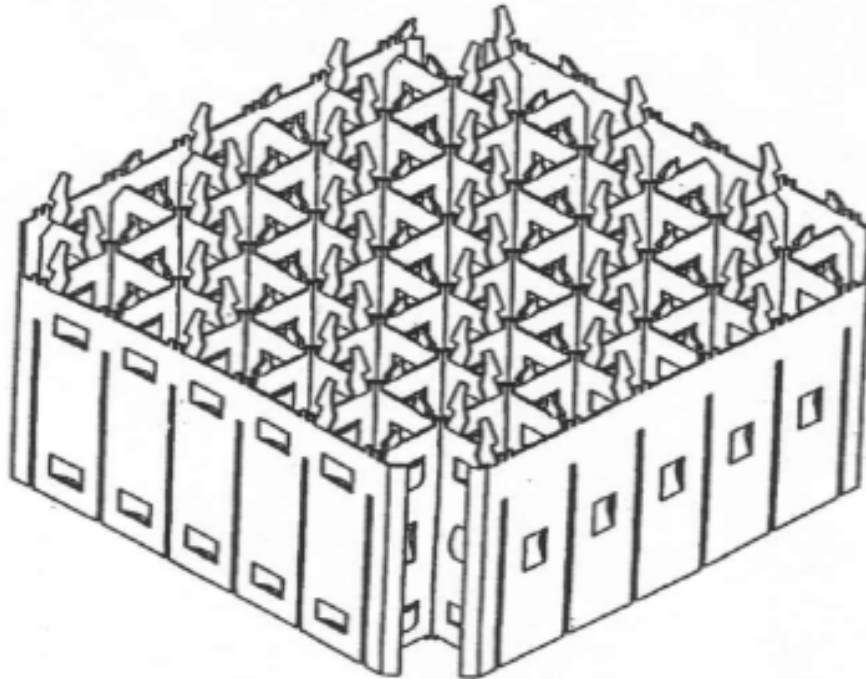


Figure 2.7 Mixing Vane Grid.

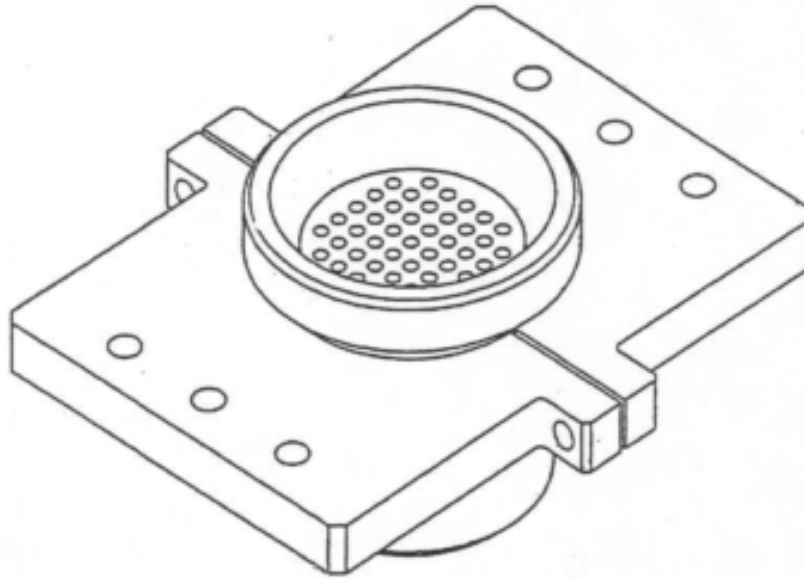


Figure 2.8 Low Melt Reservoir.

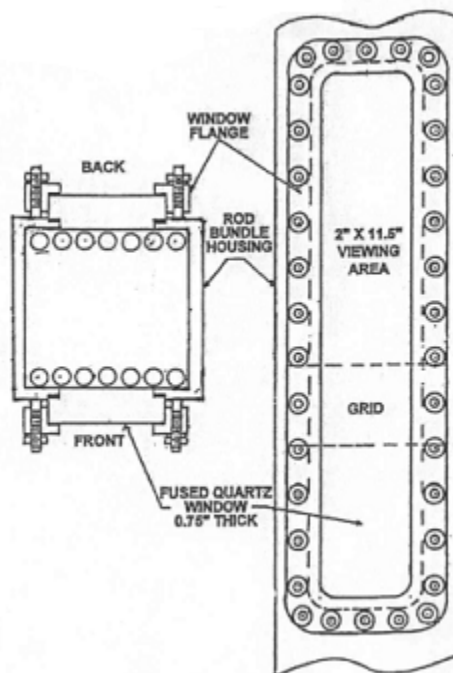


Figure 2.9 Housing Window.

2.1.2 Lower Plenum

The lower plenum is attached to the bottom of the flow housing. The lower plenum is made out of nominal 203 mm (8 in) schedule 40, 304 stainless steel pipe with an inside diameter of 202 mm (7.94 in), a height of 203 mm (8 in), and a volume of 6570 cm³ (0.232 ft³), as shown in Figure 2.10. The lower plenum is used as a reservoir for the coolant prior to injection into the rod bundle during reflood. It connects to the injection water line and steam cooling line. It has two penetrations for thermocouples monitoring the coolant temperature prior and during reflood, and pressure taps for static and differential pressure measurements.

The lower plenum also has four Conax fittings with multiple probes sealing glands for the bundle grid, steam probes and support rod wall thermocouple extensions that are routed through the bottom of the rod bundle. It contains a flow baffle, which is attached to the flow housing bottom flange. The flow baffle has a square geometry, similar to the holes that act as a flow distributor and flow straightener to provide and even flow distribution into the rod bundle.

2.1.3 Upper Plenum

The upper plenum serves as the first stage for phase separation and liquid collection of the two-phase effluent exiting the rod bundle. The liquid phase separates due to the sudden expansion from the bundle to the larger plenum flow area. The de-entrained liquid is collected around the flow housing extension in the upper plenum. The extension acts as a weir preventing the separated liquid from falling back into the heater rod bundle. The upper plenum vessel configuration is shown in Figure 2.11. The vessel is made from a 203 mm (8 in) 204 stainless steel pipe with an inside diameter of 202 mm (7.94 in) and a height of 305 mm (12 in). It has a volume of 9873 cm³ (0.347 ft³). The plenum has a 76.2 mm (3 in) pipe flange connection to the steam separator and two penetrations for fluid thermocouples. It is covered with a 203 mm (8 in) 304 stainless steel blind flange. This flange has a 25.4 mm (1 in) penetration for steam injection, venting, and connecting the safety relief valve and rupture disc assembly. It also has a pressure tap penetration for static and differential pressure measurements. In addition, the upper plenum contains an exhaust line baffle shown in Figure 2.12. The baffle is used to further de-entrain water from the steam and prevents water dripping from the upper plenum cover flange to be carried out by the exhaust steam. The baffle has a 76.2 mm (3 in) flange connection at one end. It is inserted through the upper plenum exit nozzle, and it is bolted between the nozzle flange and the flange of the pipe going to the steam separator.

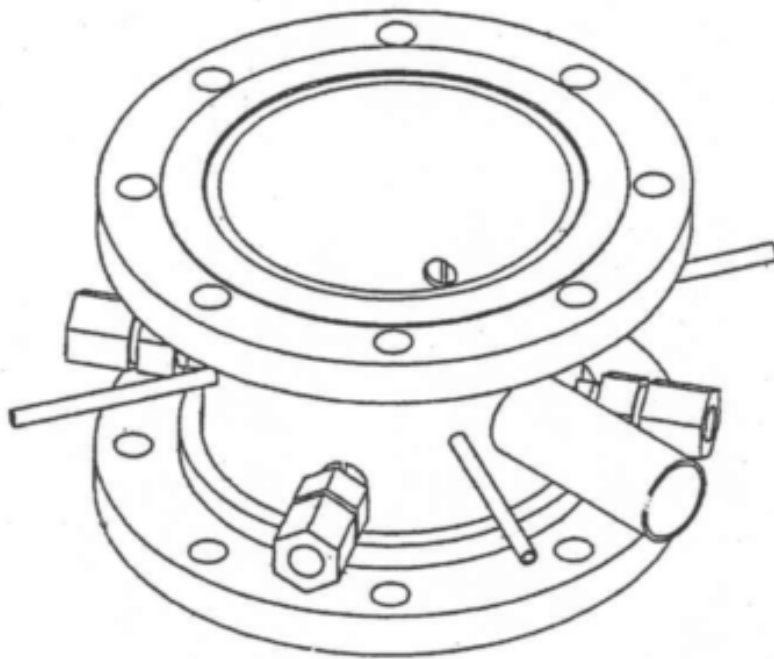


Figure 2.10 Lower Plenum.

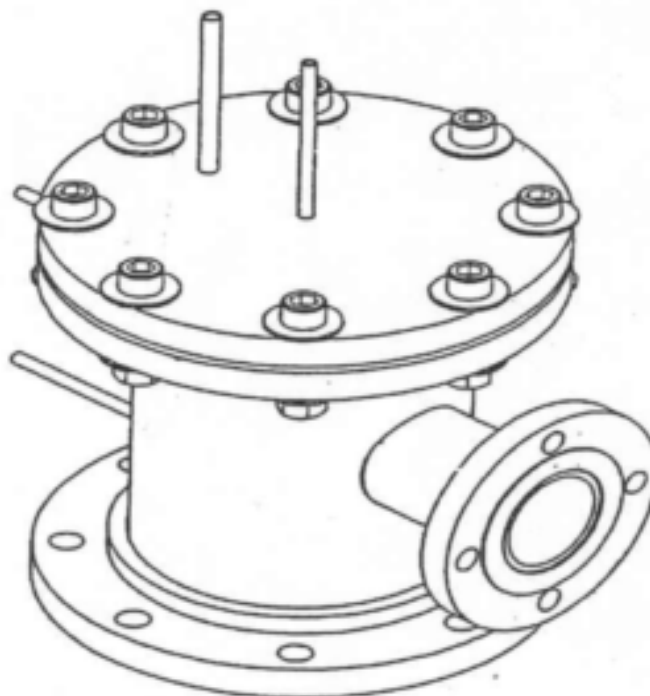


Figure 2.11 Upper Plenum.

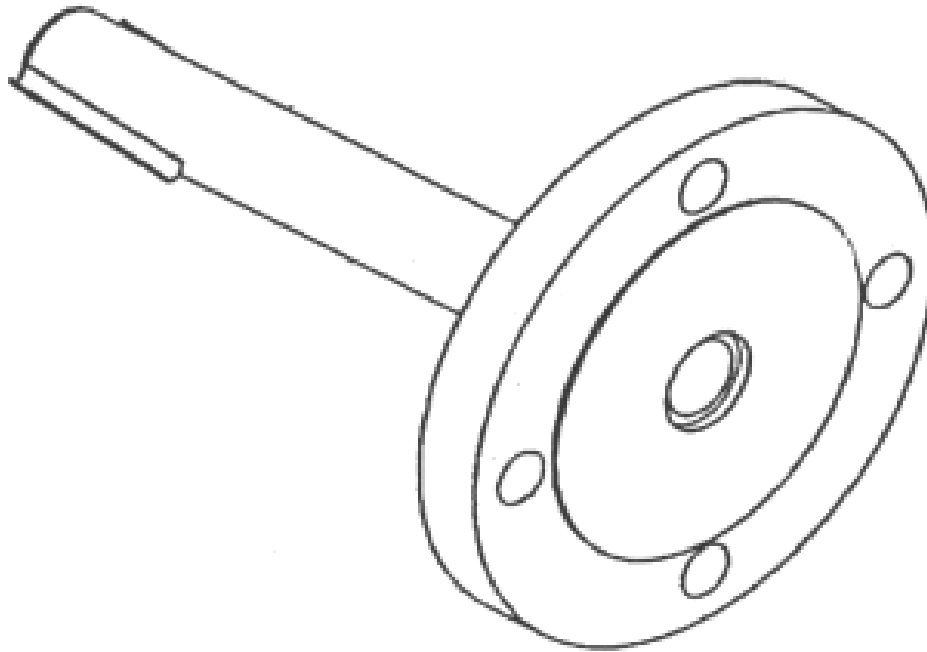


Figure 2.12 Exhaust Line Baffle.

2.1.4 Large and Small Carryover Tanks

The de-entrained liquid from the upper plenum drains into the top of a 25.4 mm (1 in) tube which extends inside a small carryover tank to detect and measure the carryover liquid as soon as possible. This tank, shown in Figure 2.13, is close-coupled in series with a larger carryover tank, shown in Figure 2.14, which collects and measures and the amount of liquid overflow from the smaller carryover tank. The small carryover tank has a volume of about 1388 cm³ (0.049 ft³), and is used to more accurately measure the initial water being collected as a function of time. The smaller carry over tank is made from 50.8 mm (2 in) schedule 80 pipe having an overall length of 914 mm (36 in) including the end caps. The large carryover tank is made from a 102 mm (4 in) schedule 40 pipe with a bottom end cap and top flanges having an overall length of 183 cm (6 ft) and a capacity of 15917 cm³ (0.562 ft³). Each tank is connected with 25.4 mm (1 in) flexible hose, and has a 25.4 mm (1 in) drain tube, and 9.5 mm (0.375 in) wall penetrations for installing fluid instrumentation and level indicators.

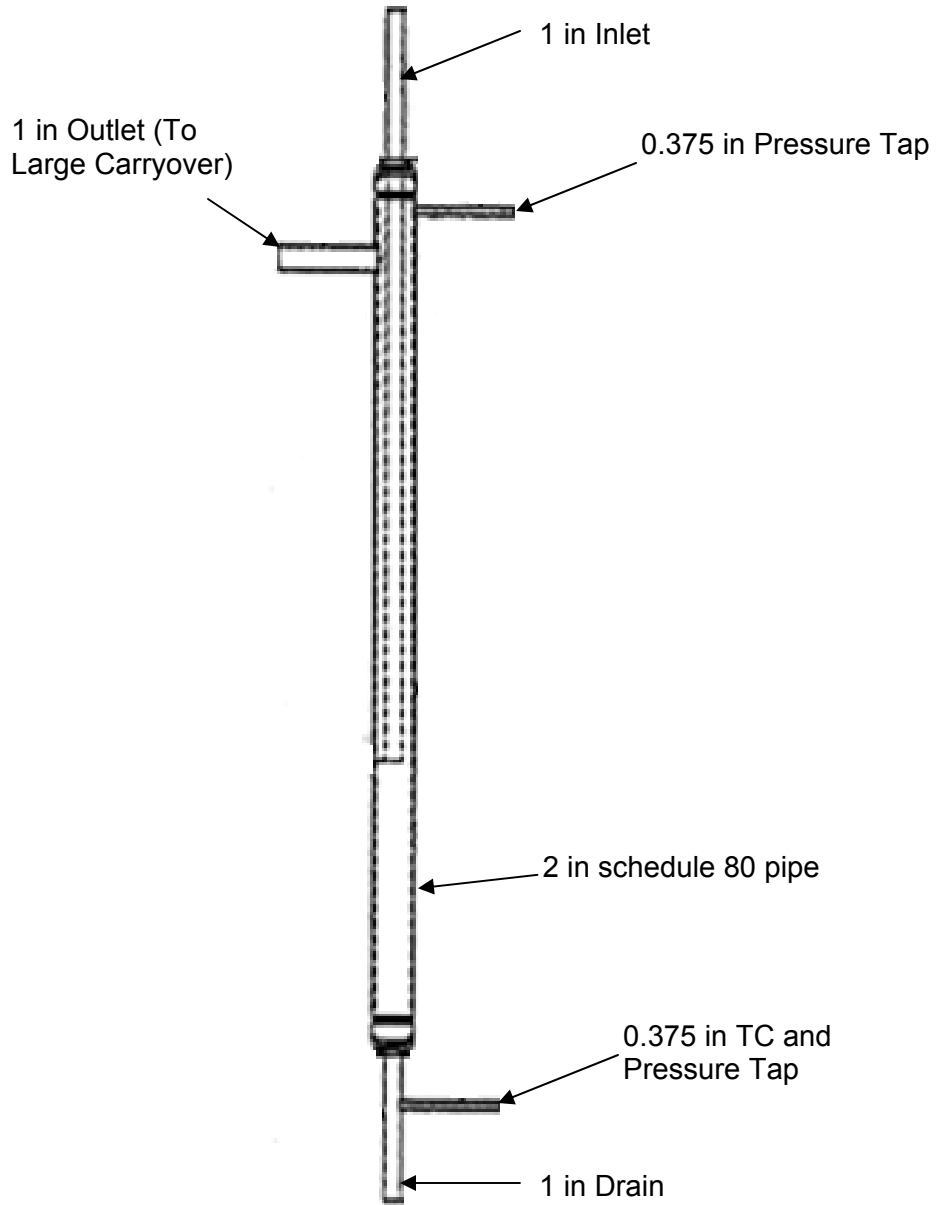


Figure 2.13 Small Carryover Tank.

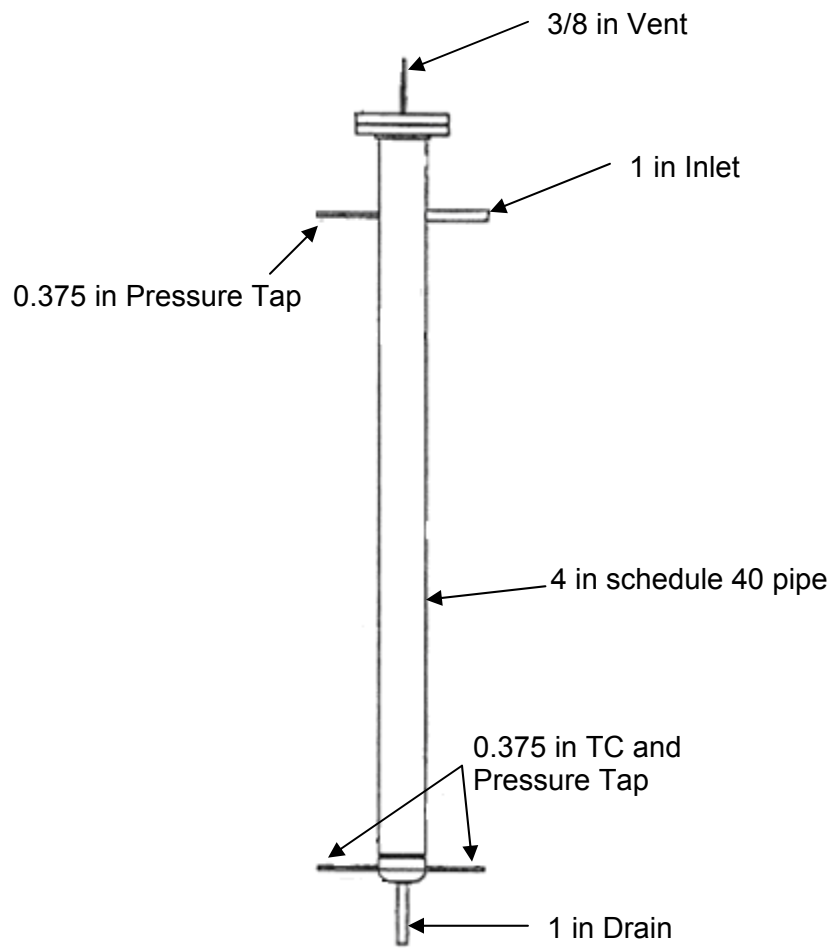


Figure 2.14 Large Carryover Tank.

2.1.5 Steam Separator and Collection Tank

The wet steam exhausted from the upper plenum flows through a steam separator (or dryer), shown in Figure 2.15, where carryover liquid droplets are further separated from the steam and collected in a small collection tank, shown in Figure 2.16, attached to the bottom of the steam separator. The steam separator relies on centrifugal force action to provide 99 percent dry steam. The separated liquid is drained into a collection tank where a differential pressure cell is used as a level meter to measure liquid accumulation. The steam separator is fabricated from a 356 mm (14 in) diameter 316 stainless steel pipe and is 914 mm (36 in) long. It has 50.8 mm (2 in) connecting nozzles, a 25.4 mm (1 in) drain, and a 12.7 mm (0.5 in) top vent. It also has two pressure taps for liquid level measurements and two 38.1 mm (1.5 in) side nozzle connections. The drain tank is a small vessel with a capacity of 11329 cm³ (0.4 ft³). It is made from a 102 mm (4 in) schedule 80 pipe with an overall length of 1.78 m (70 in), including both end caps. It has a 25.4 mm (1 in) drain nozzle, a 25.4 mm (1 in) top pipe connection to the steam separator, pressure taps and fluid thermocouple connections.

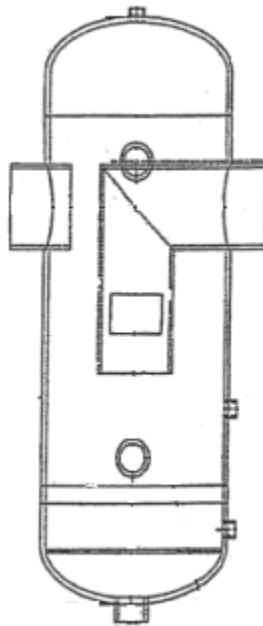


Figure 2.15 Steam Separator.

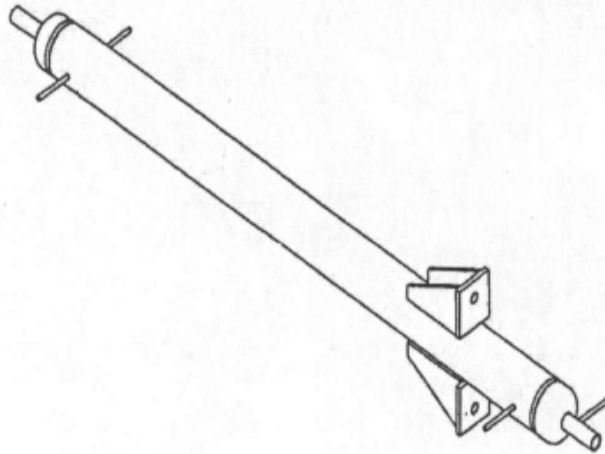


Figure 2.16 Steam Separator Collection Tank.

2.1.6 Pressure Oscillation Damping Tank

The dry steam from the steam separator flows into a pressure oscillation-damping tank. As its name implies, it is used to dampen pressure oscillations at the upper plenum caused by rapidly oscillating steam generation rates in the heater rod bundle during reflood. This effect is coupled to the characteristics of the pressure control valve, which is located downstream in the steam exhaust line. It is desirable to have a smooth pressure control in order to minimize uncertainties when calculating mass balances, steam generation rates, and heat transfer coefficients in the heater rod bundle, and avoid the pressure control valve causing oscillations in the bundle as it cycles. The tank has a volume of 0.209 m^3 (7.38 ft^3), which is approximately equal to the total volume of the rest of the test facility. The pressure tank is fabricated from 356 mm (14 in) diameter, 304 stainless steel standard schedule pipe and is 2.59 m (102 in) long, as shown in Figure 2.17. Inside the tank is a 76.2 mm (3 in) schedule 40, 304 stainless steel pipe that provides a tortuous path for the steam flow to expand into a large volume, thus damping pressure oscillations. The inlet and outlet nozzles are 76.2 mm (3 in) in diameter with flanges. The vent and drain lines are made of 25.4 mm (1 in) stainless steel pipe. There are 9.53 mm (0.375 in) tube penetrations for a fluid thermocouple and two static pressure taps. The tank walls are heated with clamp-on-strip heaters up to about 11 degrees K (20 degrees F) above saturation temperatures to prevent steam condensation.

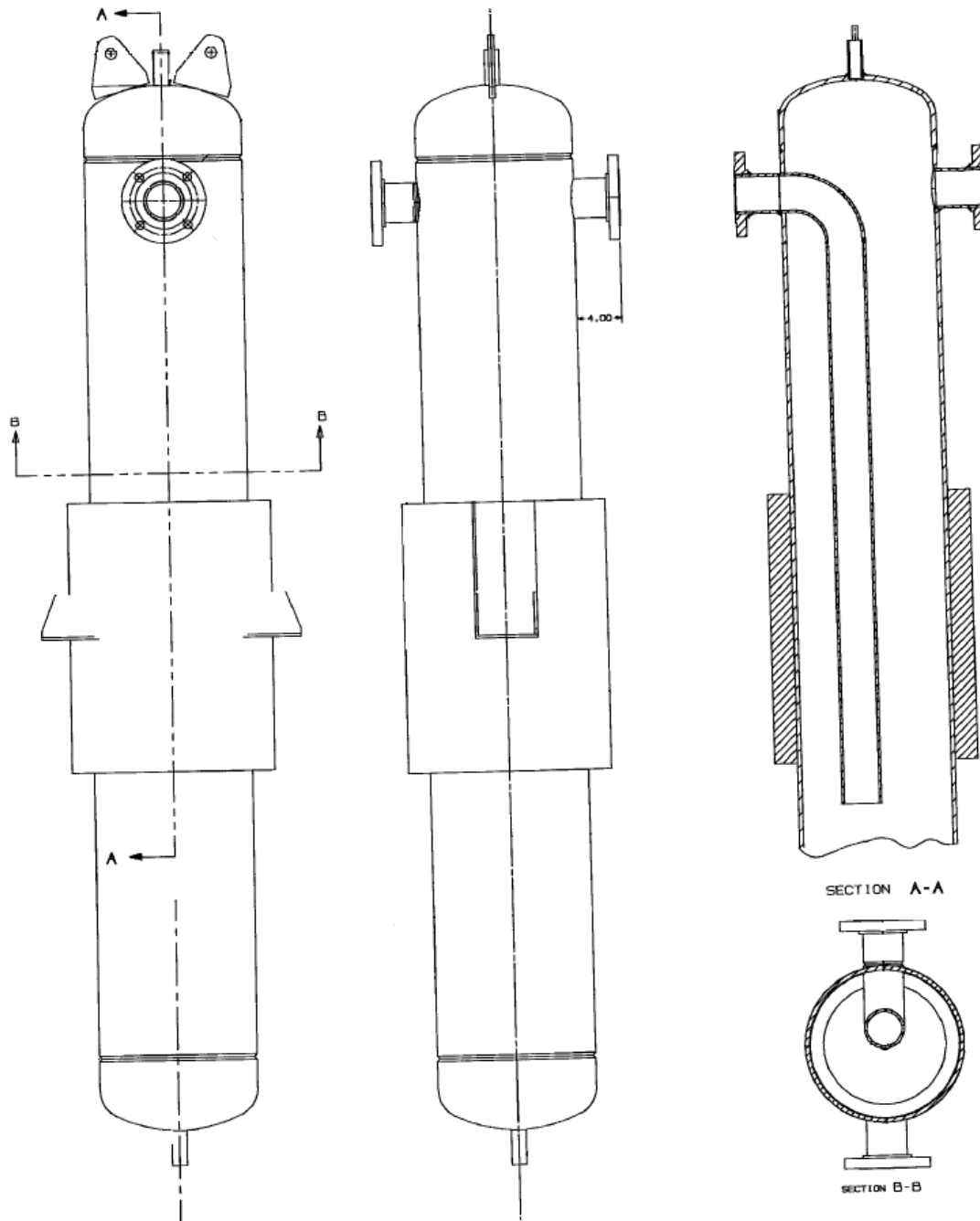


Figure 2.17 Pressure Oscillation Damping Tank.

2.1.7 Exhaust Piping

The steam flows out of the pressure oscillation-damping tank through a 76.2 mm (3 in) schedule 40, 304 stainless steel pipe shown schematically in Figure 2.18. The exhaust line has a Vortex flow meter, a 76.2 mm (3 in) V-Ball pressure control valve, and a muffler at the exit to minimize the noise caused by steam blowing into the atmosphere. The pressure control valve is activated by a signal from a static pressure transmitter located on the upper plenum. The line is also instrumented with a static pressure transmitter, fluid thermocouples, and outer wall thermocouples. The 76.2 mm (3 in) line has flow-straightening vanes which reduce the pipe length requirements upstream of the Vortex flow meter in order to obtain accurate flow measurements. This line has strapped-on electrical heaters to keep the wall temperatures about 11 degrees K (20 degrees F) above saturation to insure that single-phase steam flow measurements are made by the Vortex flow meter.

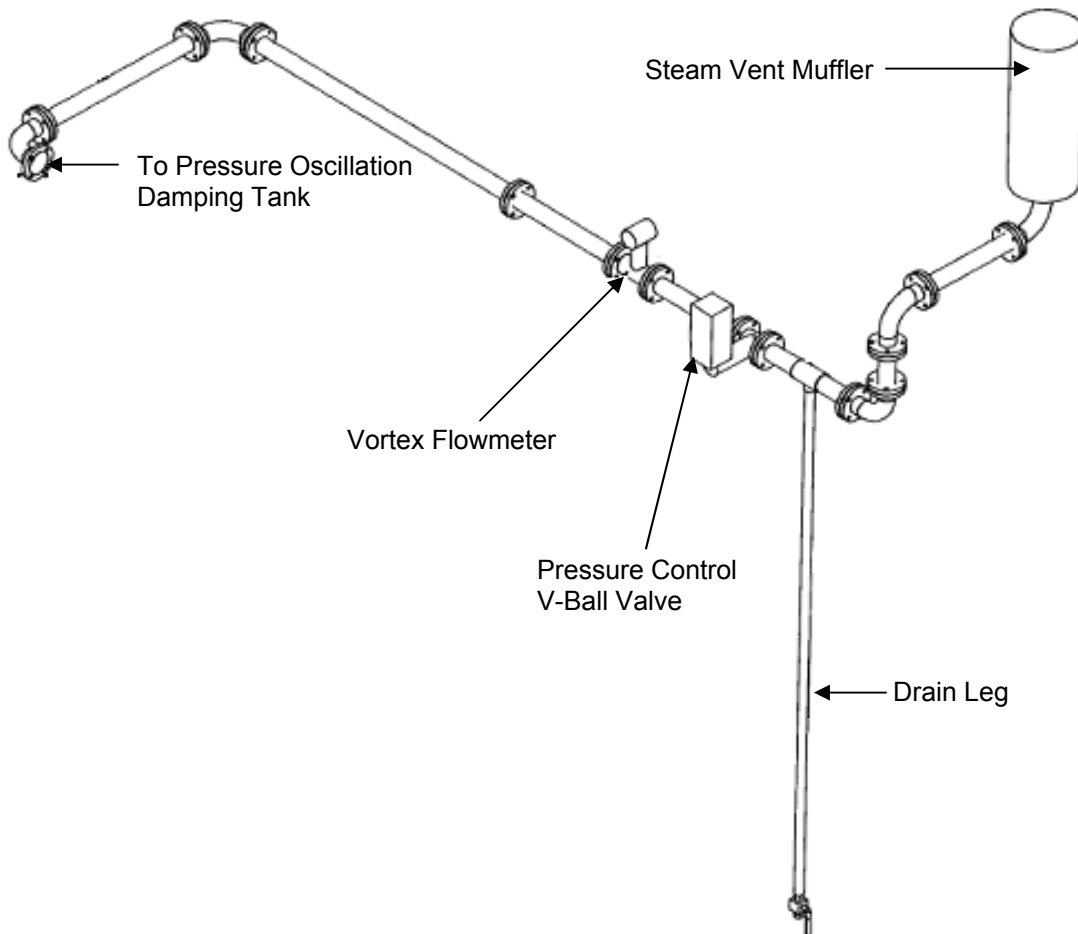


Figure 2.18 Exhaust Piping.

2.1.8 Injection Water Supply Tank

The injection water system consists of a water supply tank, a circulation pump, and interconnecting lines to the test section lower plenum. The water supply tank shown in Figure 2.19, has a capacity of 0.953 m³ (251.75 gal). It is designed for 4.14 bars (60 psig) and 427 degrees K (310 degrees F). The tank is equipped with a submersible electrical heater to heat the injection water to specified test temperatures. The tank is pressurized by a nitrogen supply system, which regulates the over-pressure needed for the forced flooding injection tests. The tank has inlet and outlet nozzles, pressure taps for level measurements, fluid and wall thermocouples. Water from the tank can be circulated through the test section by a centrifugal pump with a capacity up to 0.946 m³/min (250 gpm), which is needed to perform liquid single-phase flow tests.

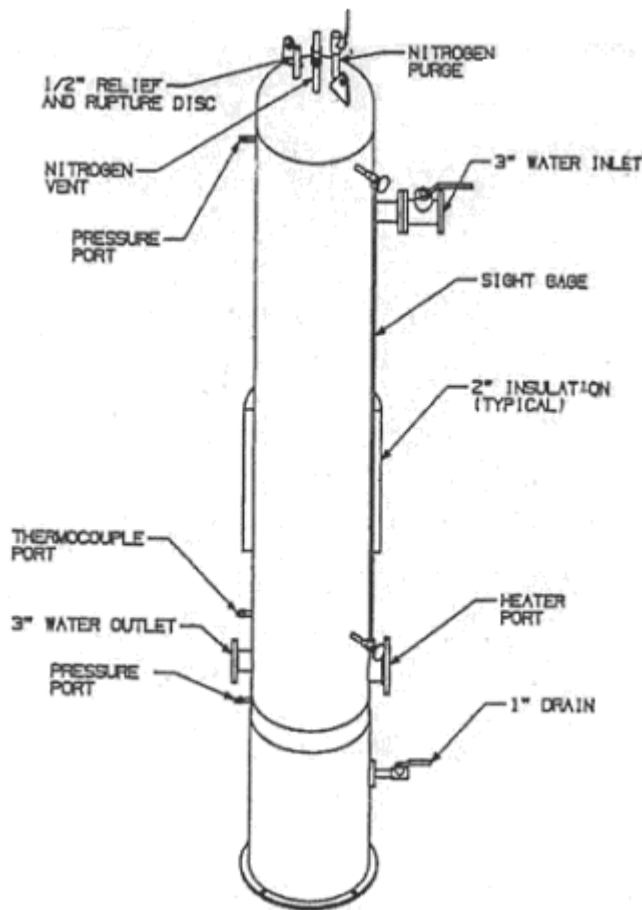


Figure 2.19 Injection Water Supply Tank.

2.2 Facility Improvements Over Previous Tests

Significant improvements related to other heater rod bundle testing programs, listed in Section 3.0 Literature Review of the RBHT Test Facility Test Plan and Design Report (NUREG/CR-6975), have been incorporated in the RBHT Test Facility. These improvements include:

- A low mass square flow housing design which better fits a square rod bundle array and minimized the housing mass and excess rod bundle flow area.
- The six pairs of windows which provide large viewing areas below and above grid locations, making it possible to observe and make void fraction and droplet measurements during reflood testing.
- The use of a laser illuminated Digital Camera system to measure entrained water droplets sizes, distribution, and velocities in the transition and disperse flow regions.
- The use of a traversing steam probe rake to measure simultaneously steam temperatures in the flow subchannel and in the rod-to-rod gap. They are specially designed such that they would not stay wet after having contacted by liquid droplets.
- Differential pressure transmitters axially located 76.2 to 127 mm (3 to 5 in) apart in conjunction with heater rod and flow housing wall thermocouples to obtain detailed void fraction and heat transfer information.
- Water droplet injection system in conjunction with steam injection to study the droplet-steam cooling effects on heat transfer and grids.
- Addition of a large pressure oscillation-damping tank to minimize test section oscillations observed in the FLECHT and FLECHT-SEASET tests.
- The incorporation of close coupled entrained liquid collection tanks and piping to reduce delay times for liquid collection.

2.3 Instrumentation and Data Acquisition System

The test instrumentation is designed to measure temperatures, power, flows, liquid levels, pressures, void fractions, droplet sizes, distributions, and droplet velocities. The vapor velocity cannot be directly measured in a two-phase dispersed flow, but it can be calculated at different axial positions from the data. Overall the transient mass and energy balances, mass inventories, carryover liquid and steam flow can be calculated as functions of time. Heater rod power, heat rod temperature, and fluid temperature are used to calculate heat fluxes and heat transfer coefficients, quench times, rod bundle energy losses, convective and radiation heat transfer to steam, droplets, grids, support rods, and housing. Effects of grids, support rods and housing behavior during reflood can be determined. Void fraction measurements below the quench front and in the froth level above the quench front, in conjunction with the laser illuminated digital camera measurements are used to determine droplet entrainment behavior, droplet effects on heat transfer, and steam desuperheating. The laser illuminated digital camera system measurements provide droplet size distribution and velocities during reflood.

2.3.1 Loop Instrumentation and Controls

Loop instrumentation is shown schematically in Figure 2.20. There are 123 instrumentation channels assigned to the collection of electrical power, fluid and wall temperatures, levels, flow differential pressures, and static pressure measurements. The injection water supply tank has three fluid and three wall thermocouples to monitor water and wall temperatures during heat-up prior to testing. It has a differential pressure transmitter used as a level meter to determine water mass in the tank and mass depletion during reflood testing. It also has a static pressure transmitter that monitors the nitrogen over pressure and controls the nitrogen flow needed to maintain a constant pressure during forced injection reflood tests. The water injection line is equipped with a Coriolis Effect Micromotion flow meter that directly measures mass flows up to 454 kg/min (1000 lbs/min) with an accuracy of plus or minus eleven hundredths of a percent (± 0.11 percent) of rate. The steam line has a Rosemount Vortex shedding flow meter to measure flow up to 7.08 m³/min (250 ft³/min) with an accuracy of plus or minus 65 hundredths of a percent (± 0.65 percent) of rate. Each flow meter is connected through a pneumatic controller to a V-ball flow control valve. Each line has a fluid thermocouple to measure water or steam temperature during heat-up and forced injection testing. They also have a static pressure transmitter which in conjunction with the thermocouples can determine the thermodynamic properties of the fluid. The injection line has three wall thermocouples to monitor wall temperatures during heat-up and during testing. One of these thermocouples in conjunction with a temperature controller regulates the power to an electrical heating cable wrapped around the injection line. The heating cable is used to heat-up the injection line wall and to maintain the injection water at the required injection temperature.

The small carryover tank has one fluid and two wall thermocouples. The large carryover tank instrumentation consists of one fluid thermocouple, three wall thermocouples. Both tanks have a liquid level meter, which measures the amount of carryover liquid being collected during testing. In addition, a differential pressure transmitter is connected from the top of the carryover tank to the upper plenum to determine the static pressure in the carryover tank.

The steam separator is instrumented with one fluid and two wall thermocouples. The drain tank is instrumented with two fluid and two wall thermocouples. The fluid thermocouple measures the de-entrained water temperature during testing. The wall thermocouples monitor wall temperatures during heat-up. The volume of de-entrained water is measured with a level meter connected across the drain tank.

The pressure oscillation damping tank has two fluid and three wall thermocouples which are used to monitor vessel walls during heat-up, and to insure that the vessel wall is at a temperature above saturation to prevent condensation. One wall thermocouple in conjunction with a temperature controller monitors the power applied to clamp-on heaters that heat up the tank to the desired wall temperature.

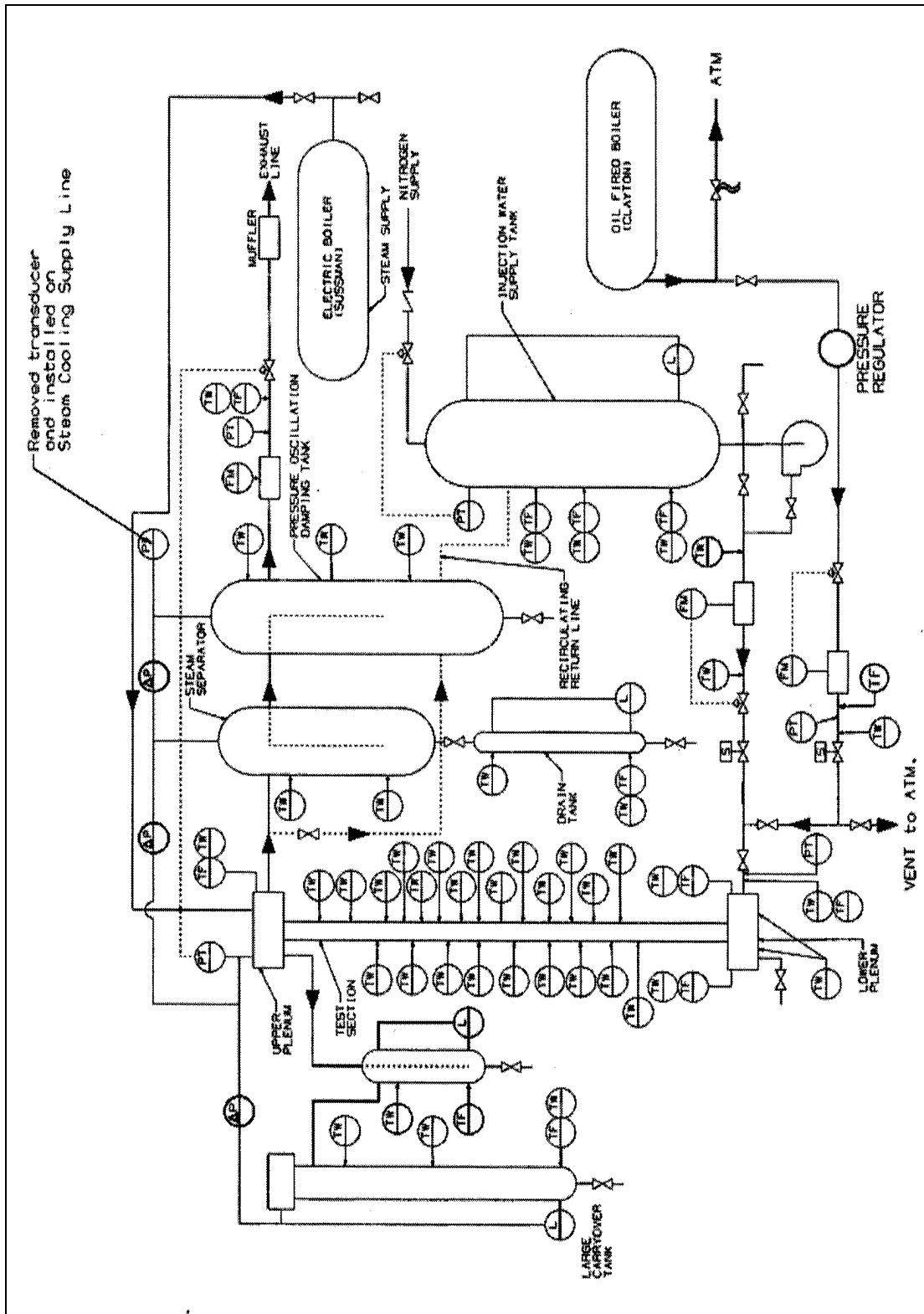


Figure 2.20 Loop Instrumentation Schematic.

The exhaust line is equipped with a Vortex flow meter which, in conjunction with a static pressure transmitter and fluid thermocouple measurements, is used to calculate steam volumetric flows up to 7.08 m³/min (250 ft³/min). The flow meter has an accuracy of plus or minus 65 hundredths of a percent (± 0.65 percent) of the rate. The exhaust line also has three wall thermocouples to measure pipe wall temperatures. One wall thermocouple in conjunction with a temperature control regulates the power going to clamp-on-heaters which are used for heating the pipe walls up to a temperature of about 11 degrees K (20 degrees F) above saturation to prevent steam condensation and to insure accurate single phase steam flow measurements. The exhaust line has a V-ball pressure control valve. This valve is controlled by a static pressure transmitter through a pneumatic controller connected to the top of the upper plenum in order to maintain constant test section pressure during testing.

2.3.2 Test Section Instrumentation

The test section instrumentation consists of the heater rod bundle and flow housing, the low plenum, and the upper plenum groups. The heater rod bundle and flow housing instrumentation is shown schematically in Figure 2.21. This figure shows the instrumentation axial locations in relation to heater rod heated length, grids, steam probe rakes, housing pressure taps and windows.

Six grids have thermocouples attached to their surfaces in order to determine quenching behavior during reflood shown in Figure 2.23 through Figure 2.29. Grid and steam probe axial locations are shown schematically in Figure 2.21. Eight groups of heater rods have thermocouples at different elevations to cover, as much as possible, the entire rod bundle heated length. The radial location of each heater rod group is shown in Figure 2.22. The radial locations of instrumentation rods were chosen in order to be able to characterize heat transfer of hot rods simulated by the center rods, rod-to-rod and rod-to-housing radiation heat transfer. For this purpose, heater rod thermocouples, steam probes, and housing wall thermocouples are located at the same elevations. In addition, symmetrical location of the same group of instrumented heater rods will help in the data analysis and will determine any anomalies in the radial flow distribution through the heater rod bundle. Heater rod thermocouples are also placed at varying distances downstream from a grid to determine the decreasing heat transfer gradient between grid spans. The steam probes or fluid thermocouples are located at short distances upstream and downstream of a grid to determine the effect of water droplets being shattered by the grids on droplet size and distribution, and the desuperheating effect on the steam temperatures in the disperses flow regime.

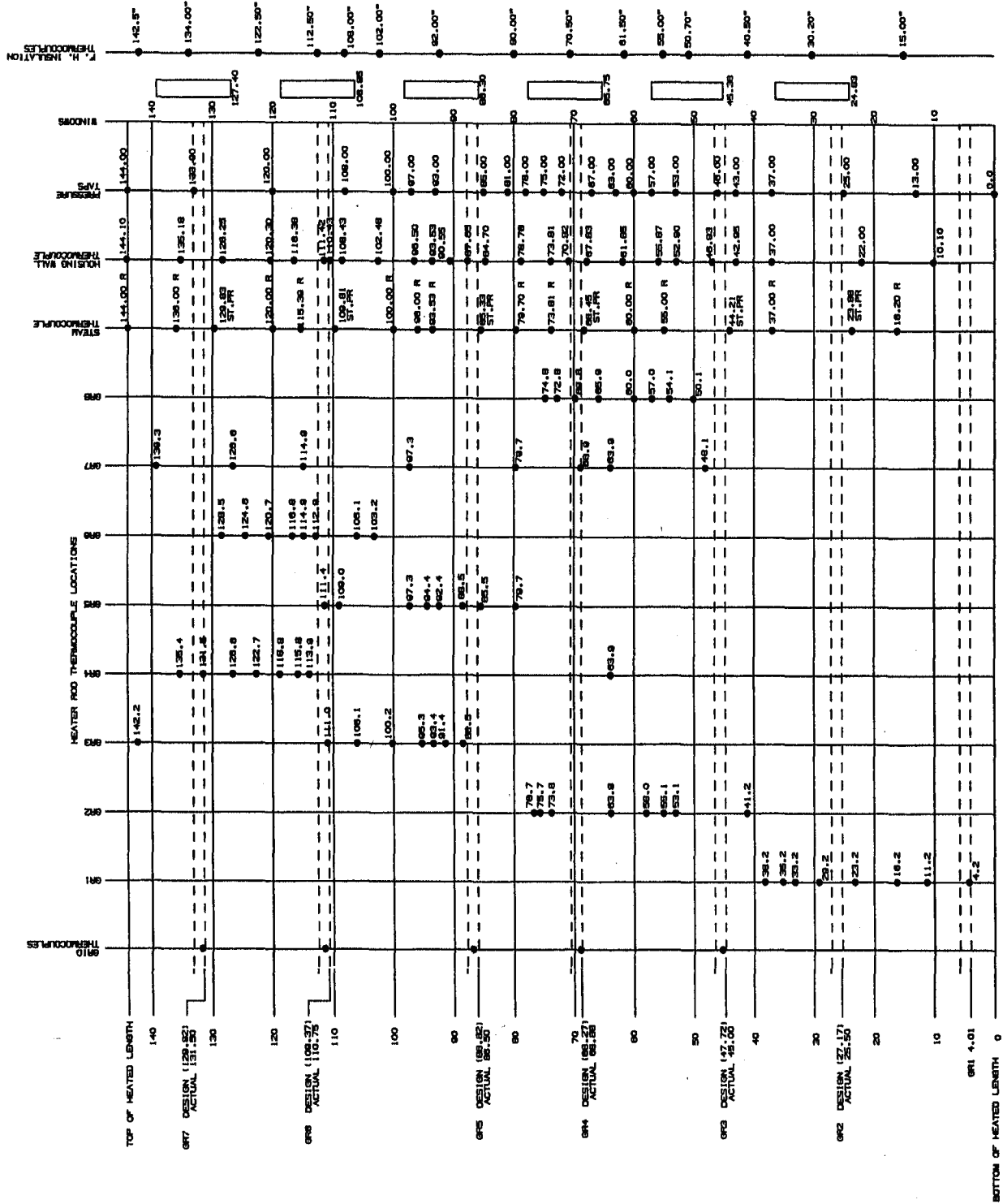


Figure 2.21 Rod Bundle and Housing Instrumentation Axial Locations.

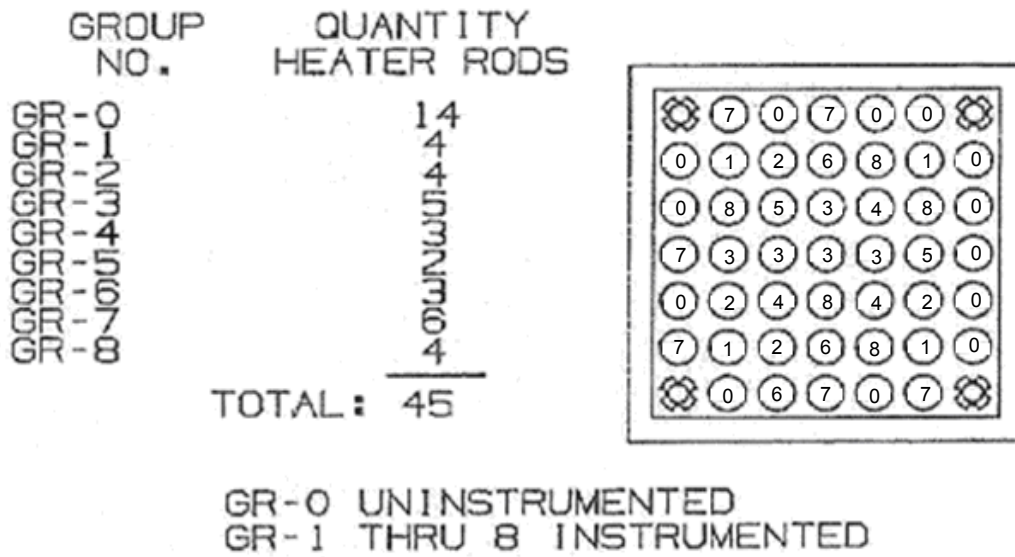


Figure 2.22 Instrumented Heater Rod Radial Locations.

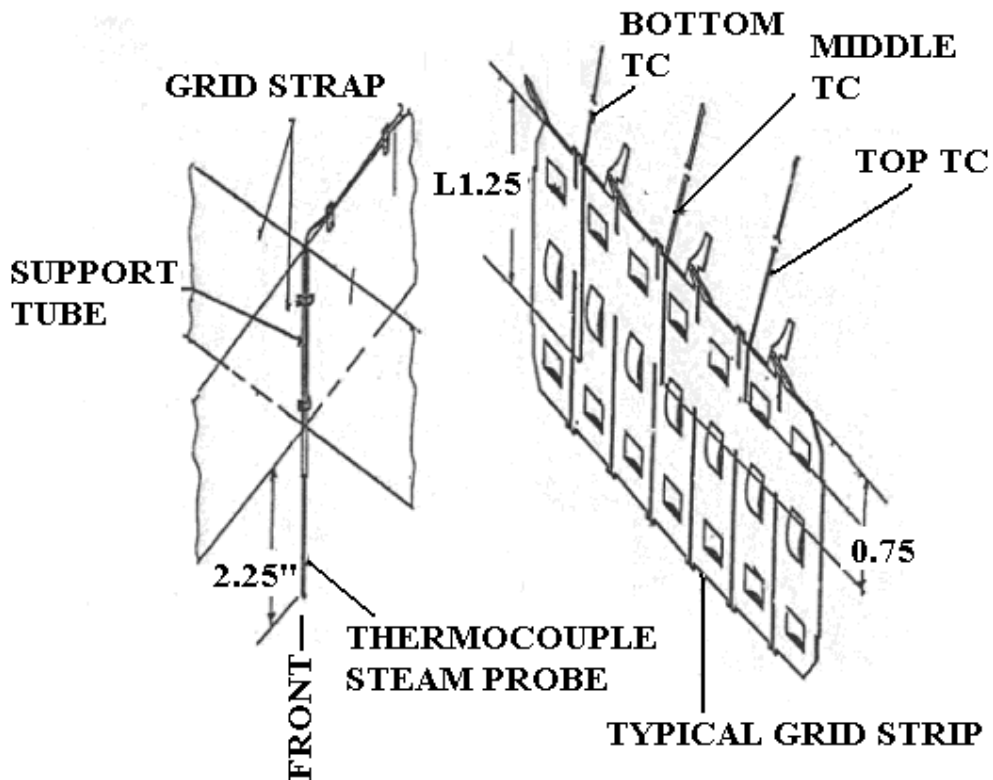


Figure 2.23 Mixing Vane Grid Instrumentation.

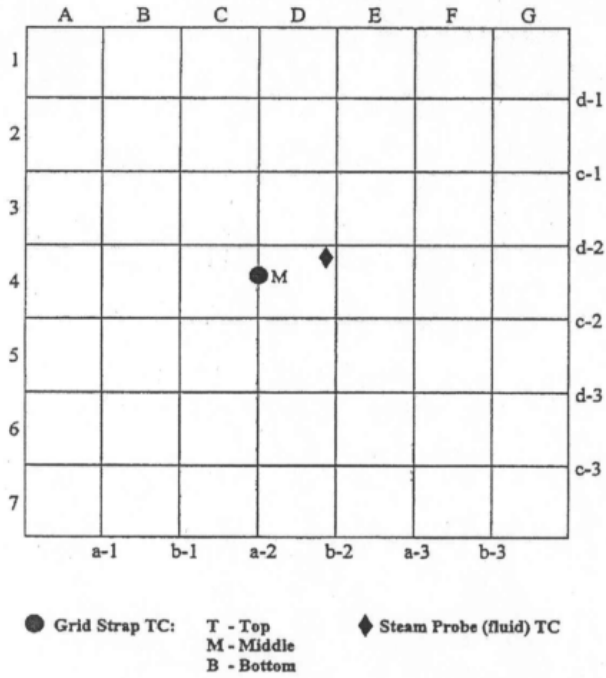


Figure 2.24 Grid No. 2 Instrumentation.

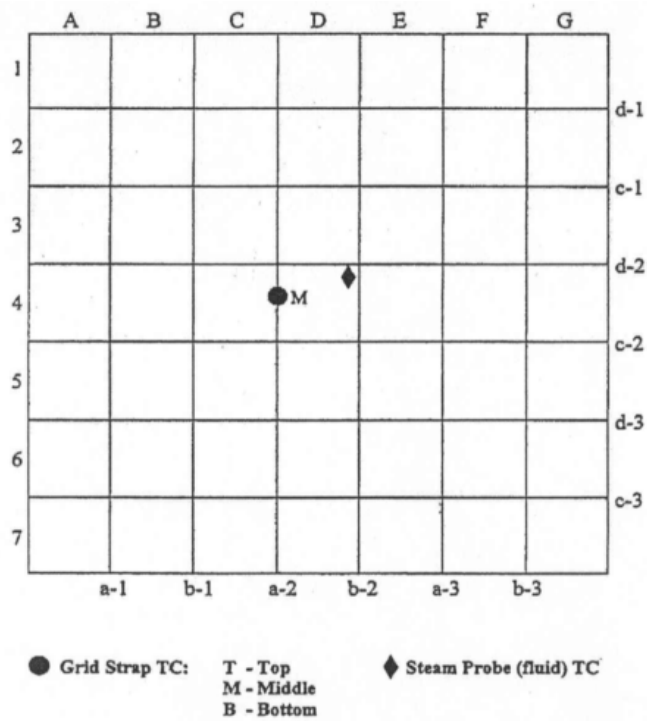


Figure 2.25 Grid No. 3 Instrumentation.

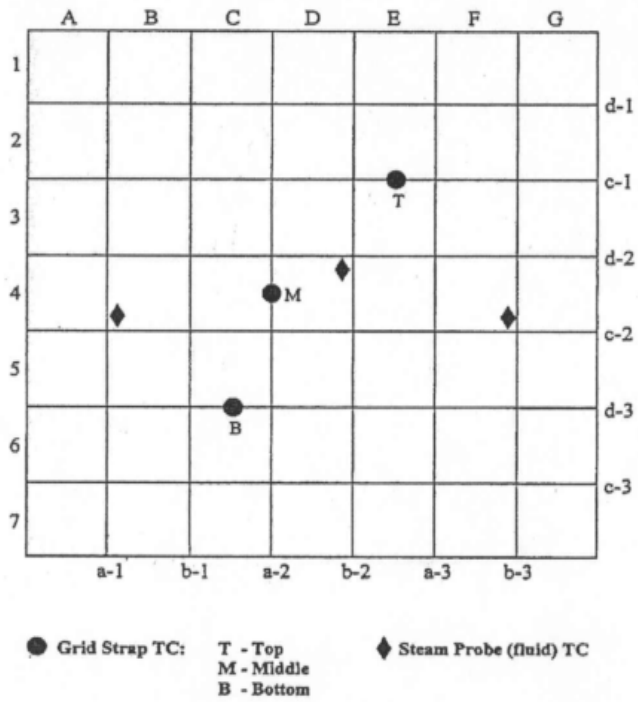


Figure 2.26 Grid No. 4 Instrumentation.

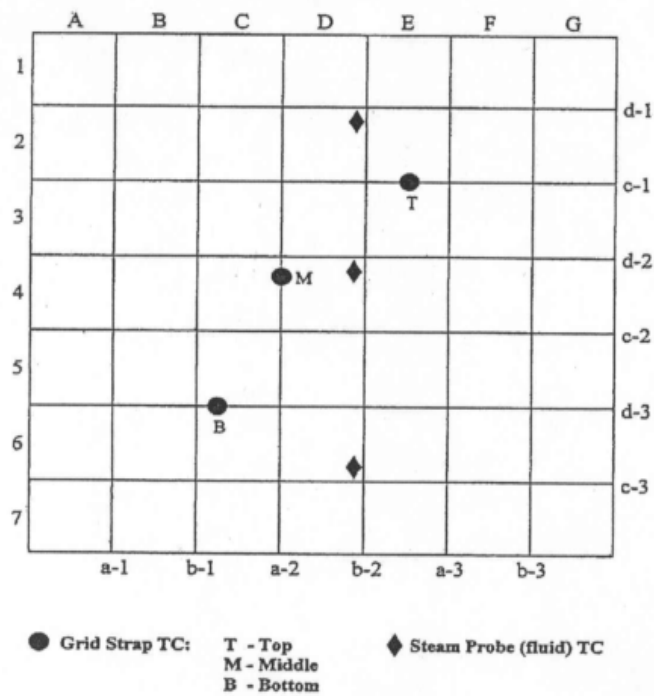


Figure 2.27 Grid No. 5 Instrumentation.

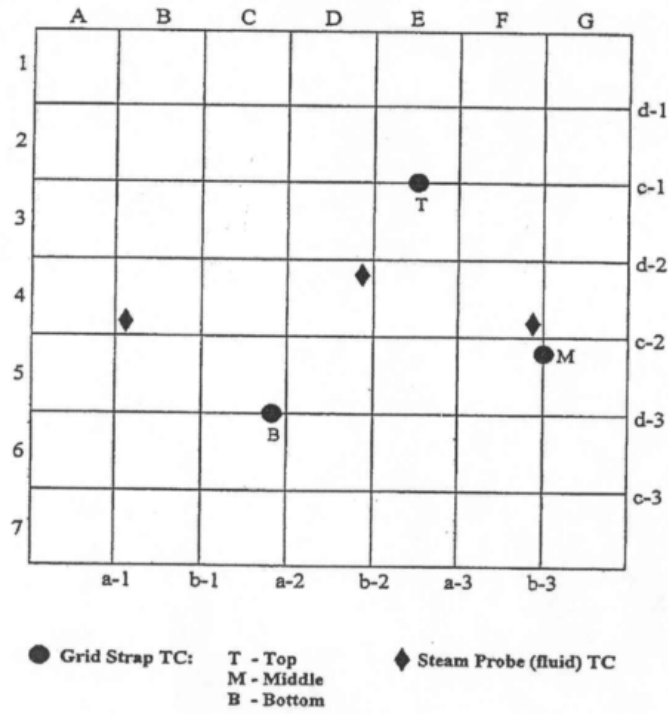


Figure 2.28 Grid No. 6 Instrumentation.

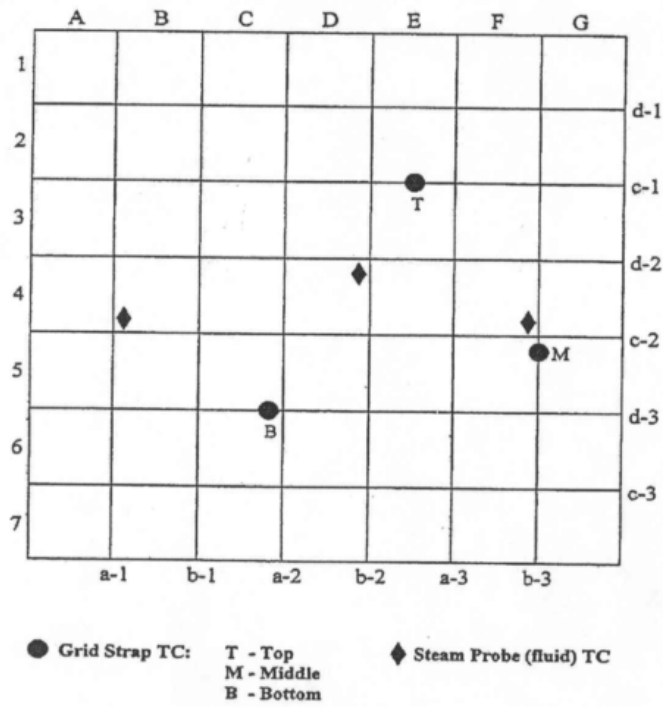


Figure 2.29 Grid No. 7 Instrumentation.

The vapor or steam temperature will be measured using miniature thermocouples having a diameter of 0.813 mm (0.032 in) which are attached to the spacer grids, as well as the traversing steam probe rakes having a diameter of 0.381 mm (0.015 in). These are very small diameter thermocouples that have a fast response time such that they can follow the vapor temperature accurately in a dispersed, non-equilibrium, two-phase flow. As the froth front approaches, the number and sizes of the droplets increase which can lead to wetting of these thermocouples. Experiments performed as part of the FLECHT-SEASET program indicated that very small thermocouples would provide reliable vapor superheat ready for the longest time period until they quench as the froth region approaches. While the Lehigh vapor probe was considered, it is too large and causes a flow distribution effect which is not typical of the bundle. The Lehigh probe would block 68 percent of the gap between adjacent heat rods. The effect of the probe would be to distort the data downstream of the sensing location. Such flow distribution effects were observed in the Lehigh data as well as the INEEL single tube data which used these probes.

The traversing steam probe rakes are located at the spans between the grids at the upper heater rod bundle elevations, as shown schematically in Figure 2.30. The traversing steam probes rakes will measure steam temperatures in the heater rod bundle flow subchannels and the gaps between the heater rods during the dispersed flow regime. Each rake consists of three 0.381 mm (0.015 in) diameter ungrounded thermocouples mounted on a 0.356 mm (0.014 in) thick by 6.35 mm (0.25 in) wide Inconel strip. The thermocouples are spaced 12.6 mm (0.496 in) apart which correspond to the heater rod spacing in the bundle. The thermocouple tips are located facing the steam flow. A 2.39 mm (0.094 in) diameter tube attached to the strip is used to traverse the steam probe rake across the rod bundle. This tube also carries the thermocouples leads outside the flow housing through a pressure seal. The tube is attached to an automated sliding mechanism. It consists of a sliding bar, a 24 DCV motor with a ball drive shaft, and a linear potentiometer provides a voltage input to the Data Acquisition which determines the rake thermocouple location and travel distances across the heater rod bundle.

Two fluid thermocouples are placed 24.5 mm (1 in) below the bottom of the bundle heated length such that injection water temperatures are monitored prior to and when reflood is started. There are 23 differential pressure transmitters connected to the housing wall pressure taps providing measurements to calculate single phase flow bundle and grid friction losses, bundle mass inventory, and void fraction during reflood. There are nine differential pressure cells connected to pressure taps located 76.2 mm to 127 mm (3 to 5 in) apart to provide detailed mass inventory, and void fraction data in the froth region above the quench front. In addition, heater rod and housing wall thermocouples are placed at these pressure tap mid span locations to determine convective and radiant heat transfer coefficients in the froth region where the differential pressure cells will give the average void fraction.

The flow housing has six pairs of windows at the following elevations: 61.4 cm (37.2 in), 114 cm (44.7 in), 166 cm (65.3 in), 218 cm (85.8 in), 270 cm (106.4 in), and 322 cm (126.9 in). Each pair of windows are 180 degrees apart. The window lenses are made from optical grade fused quartz and provide a viewing area of about 10.2 cm (4 in) below and 15.2 cm (6 in) above grids two through seven. The windows are preheated to minimize wetting during reflood using infrared heaters on each window and by pulsing the heater rod bundle when preheating the flow housing walls. The infrared heaters are removed just before a test is started. Droplet measurements above and below a grid can be made through the windows.

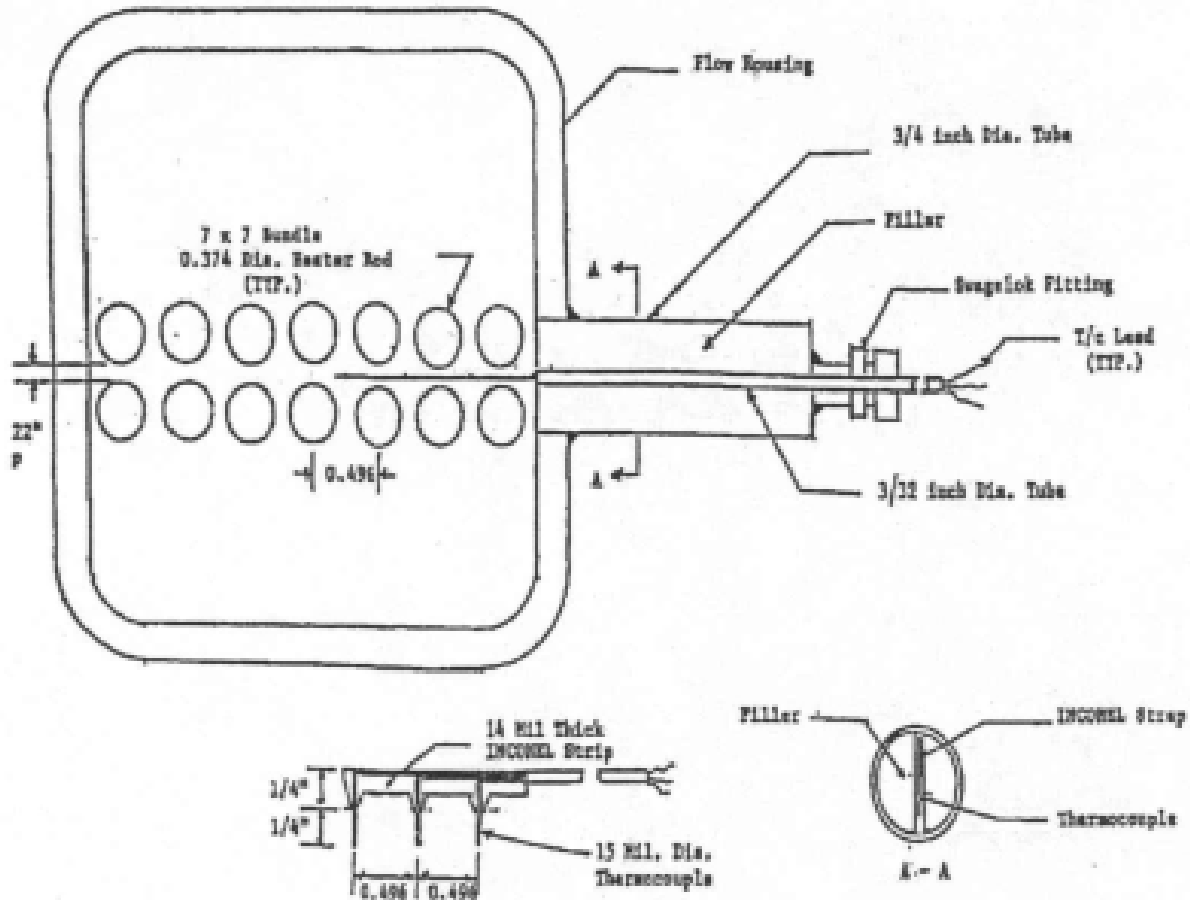


Figure 2.30 Traversing Steam Probe Rake Schematic.

A droplet imaging system known as VisiSizer was developed in conjunction with Oxford Lasers to measure the size and velocity of water droplets entrained in the steam flow of the RBHT test section shown schematically in Figure 2.31. VisiSizer uses a pulsed infrared laser to image water droplets on a 1000x1000 pixel high-resolution black and white digital camera through a set of windows in the bundle housing. A digital system such as VisiSizer was chosen over conventional high-speed cameras which are capable of only a few seconds of imaging and have lower data acquisition speeds. Further, each frame from a standard imaging technique would need to be analyzed by hand. The VisiSizer system is capable of analyzing 12 to 13 frames per second for an indefinite period of time. Film from the FLECHT-SEASET tests show poorer image quality than images taken with VisiSizer in the RBHT experiments. However, VisiSizer is incapable of measuring anything other than complete droplets. This makes it an inadequate tool for gathering information about the entrainment front where there are ligaments and other unusual water behavior.

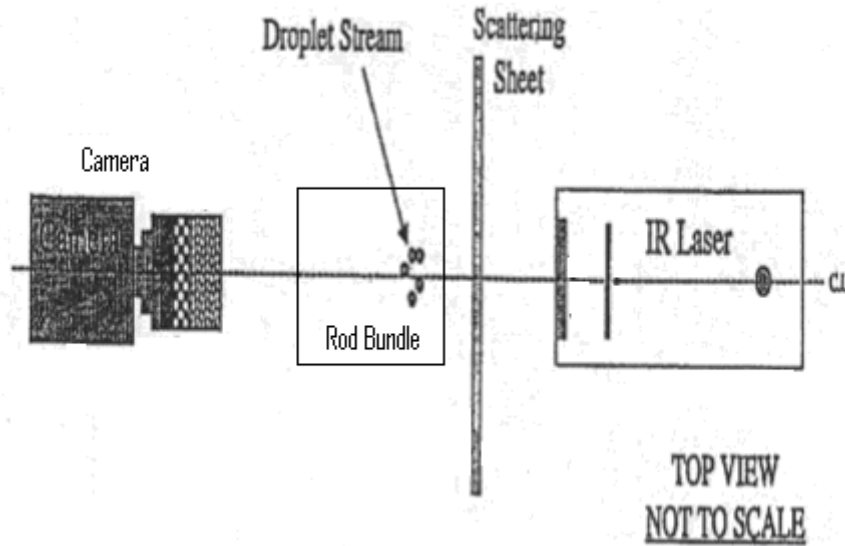


Figure 2.31 Laser Illuminated Digital Camera System Setup.

An infrared laser is used with the system because it is capable of passing through the quartz viewing windows and being absorbed by the water droplets entrained in the steam flow. Because the infrared rays are absorbed by the water droplets, the resulting droplet shadows can be recorded by the digital camera. So far, there has been no effect of laser light scattering from rods to droplets. Pictures taken in and out of the rod bundle have the same imaging characteristics, droplet analyzing capability and clarity. A band pass laser light filter is placed in front of the digital camera to eliminate non-infrared light from other sources and an anti-glare attachment is used to eliminate any illumination interference from outside the viewing area. In addition, rod bundle geometry has little effect in the measurement of droplet distributions and velocities.

The frames captured by the camera are fed back to a PC at approximately 12 to 13 frames per second. The software can analyze each frame for droplet size and velocity and write the recorded data to a size and velocity data array. The software program determines droplet sizes by determining the area of black vs. white pixels in each droplet image. Once the droplet area is determined, the program calculates the perimeter of the droplet image to determine the sphericity of the droplet. The VisiSizer system is capable of determining the surface area based on diameter of any and all droplets.

Operating the laser in a double pulse mode enables the VisiSizer system to measure both droplet diameter and velocity for a particular probe volume. The laser pulses twice with a known pulse delay (on the order of 1 ms) while the camera shutter remains open, creating two images in the same frame for each droplet. The distance between images is then determined and the velocity calculated. These velocity characteristics are enough to characterize the behavior of the flow despite the fact that the droplets are only captured in a single frame.

The local distribution of droplets can be determined for a known probe volume governed by the software settings. Droplets that lie out of this probe volume on either side of the line of sight will

be rejected based on focus. The opposite sides of the probe volume will be set by the spacing of the rods in the bundle. Each droplet is recorded in a two-dimensional array according to size and velocity. The droplet sizes are recorded in lognormal bins while the velocity bin size is user defined. Data for the transient reflood experiments is recorded in user defined quasi-steady state time periods. At the end of each time period the data is saved and a new array is opened.

The VisiSizer enable the experimenters to collect a vast amount of information about the droplet flow in the test section. The information will be collected in an easy to handle data array and all information will be written to a CD-ROM to ensure the information will be available for later use.

The four corner support rods are unheated, they are used to support the bundle grids and to support grid and steam probes thermocouple leads going out of the bundle. These rods are instrumented with eight thermocouples attached at various elevations corresponding to heater rods and housing wall thermocouples. The purpose of this arrangement is to quantify radiation heat transfer losses to unheated surfaces and determine their behavior during reflood.

The DC power supply can be controlled by regulating the voltage, current, or total power output. The voltage drop across the heater rod bundle is measured by a voltmeter connected to voltage taps at the Low-Melt pot and the Nickel Ground Plate. The electrical current is measured by a copper shunt calibrated for 15,000 amps proportional to an output signal of 0-50 millivolts.

The lower plenum is instrumented with two fluid and two wall thermocouples. The fluid thermocouples monitor the injection water temperature prior and during testing. The wall thermocouples measure the vessel wall during heat-up and testing. One of the wall thermocouples in conjunction with a temperature controller regulates electrical power to clamp-on-heater rods to maintain the vessel wall at inlet temperatures.

The upper plenum is also instrumented with two fluid thermocouples and two wall thermocouples. The fluid thermocouples measure steam and carryover liquid during testing. The wall thermocouples monitor vessel wall temperatures during heat-up and testing. The Upper Plenum is also instrumented with a static pressure transmitter which measures and controls the test section pressure during testing.

2.3.3 Data Acquisition System

The control and data acquisition system provides control functions and data collection functions for the RBHT Test Facility. This system consists of two parts: the computer and display terminals residing in the control room and the VXI mainframe and terminal panels residing in the test facility. The two parts are connected via an industry standing IEEE 1394 (Firewire) serial control and data interface.

The computer provides the display, control, and data storage functions. It has the capability of displaying control function set points and process variables, and critical operating parameters during tests, along with selected variables such as various rod temperatures displayed in real-times during the experiment. This system will provide dial, meter, and strip-chart functions as required. The computer collects and saves data from the various instruments, such as voltage, current, pressure, level flow and temperature; and provides control functions such as heater rod power, injection water pressure, upper and low plenum temperatures, etc.

The instrumentation part of this system, residing in the test facility, consists of an industry standard VXI mainframe (Vme bus with extensions for Instrumentation) from Hewlett-Packard (HP-E8401AA), and a set of terminal panels (HP E1586A). The VXI mainframe contains a firewire controller card (HPE8491A) and several (currently seven) state-of-the art data acquisition and control cards (HP E1419A). The terminal panels provide the isothermal reference junctions needed for the thermocouples, as well as the voltage and current-loop input/output (i/o) interface to the RBHT Test Facility. These terminal panels are connected to the HP E1419A cards with SCSI cables. Seven cards yield a capability of 448 I/O. The VXI mainframe can hold up to twelve cards, and the firewire interface can support up to sixteen mainframes.

Each E1419A card can support up to eight signal conditioning plug-ons (scp's), conditioning eight channels each. Each E1509A scp contains low-pass anti-aliasing filters, fixed at 7 Hz. Because of this, the scan rate for each channel must be greater than or equal to the Nyquist rate of 14 Hz. The maximum a/d conversion rate on each HP E1419A card is nominally 100kHz, but is controlled to rate the user requires. The seven cards can be synchronized to perform the scans simultaneously. The theoretical maximum scan rate for each channel (on any individual card) is $100,000/64 = 1,56235$ Hz, if all 64 channels are scanned. (Note, the actual scan rate would be less because of multiplexer switching, amplifier settling times due to gain changes, etc. There are different scp's available from HP providing different filter values to scan at these rates.) The normal data-scanning rate will be 2 Hz during the majority of the tests, but this rate can be increased to 10 Hz for specific times during testing.

3. CALCULATIONAL METHODS USED FOR THE RBHT REFLOOD HEAT TRANSFER EXPERIMENTS

3.1 Transient Heat Transfer Coefficient Calculation (DATARH)

3.1.1 Introduction

The DATARH program is used to calculate the transient heater rod outside surface temperature, the total surface heat flux and a FLECHT type heat transfer coefficient defined as

$$h_{FLECHT} = \frac{q_w''}{(T_w - T_{sat})} \quad (3-1)$$

which is referenced to the saturation temperature in the test bundle. Both the surface heat flux q_w'' and the FLECHT heat transfer coefficient represent a total heat transfer from the heater rod surface and would include radiation heat transfer as well as convection and flow boiling.

Program DATARH.F contains the source code to perform an inverse heat conduction calculation in an electrically heated rod, in which internal cladding thermocouples exist.

The purpose of the code is to calculate the surface temperature, the surface heat flux and the FLECHT type transient heat transfer coefficient for heater rods. The program uses experimental data and heater rod dimensions to perform calculations. The mathematical model for the calculations is described in Section 3.1.2 below.

The program described herein has been modified for the RBHT experiments from the DATARH.F program used for the FLECHT-SEASET experiments. Differences between heater rods used in the FLECHT-SEASET experiments and the RBHT experiments (e.g., rod dimensions, differences in rod internal materials) have been accounted for in this version of the program.

The sections that follow describe the structure of the DATARH program, RBHT rod geometry, heater rod materials, and the input files required for executing the current version of the program.

3.1.2 Mathematical Model

A heat conduction problem is termed an "Inverse Heat Conduction Problem" if at least one spatial condition is specified at an interior point of a heat conducting body. Because of this unorthodox condition, the solution to an inverse problem is more complicated. Even if the governing equations are linear, classical methods such as Fourier analysis and Laplace transformation would fail to yield a solution. For the Fourier method, the eigenvalues are not readily obtainable from the resulting Sturm-Liouville system of equations; hence, Fourier series representation of the solution cannot be determined. Transformation techniques lead to a solution in Laplace variable space which defines an inverse transform into the real time space. Although the numerical method is not without difficulty, meaningful results can be obtained if due care is exercised.

The finite difference approximation in implicit form of a one-dimensional heat conduction equation in cylindrical coordinates is typically

$$B(n)T(n-1) + A(n)T(n) + C(n)T(n+1) = T'(n) - Q(n); 1 \leq n \leq N \quad (3-2)$$

where

$$B(n) = \frac{\Delta\theta}{(\Delta\theta)^2} \frac{r(n-1/2)}{r(n)} \cdot \frac{k(n-1/2)}{\rho(n)c(n)} \quad (3-3)$$

$$C(n) = \frac{\Delta\theta}{(\Delta\theta)^2} \frac{r(n+1/2)}{r(n)} \cdot \frac{k(n+1/2)}{\rho(n)c(n)} \quad (3-4)$$

$$A(n) = B(n) - C(n) - 1 \quad (3-5)$$

$$Q(n) = \frac{q(n)\Delta\theta}{\rho(n)c(n)} \quad (3-6)$$

and $T(n)$ the unknown temperature node at point n , $T'(n)$ the known temperature at node point n (This is also the "initial value"), r the spatial variable, Δr the spatial increment, and $\Delta\theta$ the time increment.

k , ρ , c are the thermal conductivity, density and heat capacity, respectively. Their numerical values are computed at T' . If values at half intervals are required, they are evaluated at the average of two adjacent temperatures. q is the volumetric heat generation rate. N is the number of internals. Hence, there are $N+1$ node points.

For $n = 1$, the node point is at the center of the rod, $T(n-1) = T(n+1)$, since at this point the symmetry requires the flux be zero. At the point $n-M$, $T(n)$ is the known measured temperature and finally, at the outer boundary point, $n = N$, $T(n+1)$ is the desired wall temperature. If the heat conducting body is made up by composite material, the temperature at the interface can be handled by usual means; i.e., both the temperature and flux must be continuous. However, in this case, the spatial interval size, Δr , would vary from region to region such that particular node points coincide with the material interfaces and $T(M)$.

Apply Equation (3-2) to node points $n = 1, 2, \dots, N$ and combining the boundary condition $T(0) = T(2)$ with the finite difference equation at $n = 1$ to eliminate $T(0)$, we have a set of N linear simultaneous equations with N unknown temperatures, $T(n)$; $n = 1, \dots, N+1$, $n \neq M$. The solution of this set of equations defines the temperature field at a given time step, θ . The transient solution can thus be obtained by repeating the same procedure with successive increments of $\Delta\theta$.

The method outlined above is simple-minded in principle and straightforward in practice. Because of the implicit finite difference scheme, the stability of the computation is guaranteed. As long as reasonable increment sizes, Δr and $\Delta\theta$, are chosen, acceptable numerical accuracy is expected.

It is noticed that if $M = N+1$, the inverse heat conduction problem is reduced to a more conventional type with a flux condition specified on one boundary (centerline) and a temperature condition specified on the other (wall). In this case, the coefficient matrix for the linear equations, as defined by Equation (3-2), is tri-diagonal. However, the presence of a known temperature, $T(M)$ at $M \neq N+1$, in the linear set to replace the wall temperature, $T(N+1)$, destroys the tri-diagonality and consequently complicates the solution procedure since for linear equations with a tri-diagonal coefficient matrix, the solution can be obtained by a time saving matrix resolution technique which is not applicable to any other form of matrix.

Let us, for the time being, ignore the fact that $T(M)$ is known and assume that $T(N+1)$ is known instead. The linear equation, written in the usual manner is:

$$[J]\vec{T} = \vec{F} - C(N)T(N+1)\vec{G} \quad (3-7)$$

where $[J]$ is the tri-diagonal coefficient matrix defined by Equations (3-2) and (3-3), \vec{T} the solution vector with N components, \vec{F} the "source" vector with the components defined by the quantities on the left-hand side of Equation (3-2), \vec{G} the vector with first $N-1$ components equal to zero and the N -th component equal to one (i.e., $q(i)=C$, $i \neq N$, $q(i)=1$, $i=N$).

If \vec{X} and \vec{Y} are, respectively, solutions of

$$[J]\vec{X} = \vec{F} \quad (3-8)$$

$$[J]\vec{Y} = -\vec{G} \quad (3-9)$$

The linearity of Equation (3-7) leads to

$$\vec{T} = \vec{X} + C(N)T(N+1)\vec{Y} \quad (3-10)$$

Equation (3-10), in scalar form for $n = M$, gives

$$T(M) = X(M) + C(N)T(N+1)Y(M) \quad (3-11)$$

or

$$T(N+1) = \frac{T(M) - X(M)}{C(N)Y(M)}, Y(M) \neq 0 \quad (3-12)$$

Since all the quantities on the right hand side of Equation (3-11) are known, the wall temperature $T(N+1)$, can be computed. The remaining temperature field can be obtained by repeated application of Equation (3-10).

If the transient temperature measurement $T(M)$ is both accurate and frequent enough, the method outlined above will produce acceptable results. In practice, however, such accuracy and frequency as demanded by the numerical method is almost impossible to achieve. Any

error in T(M), either due to instruments or due to interpretation, would be amplified in this numerical process. An error is usually propagative and oscillatory and results from a successive over and under correction of the heat balance as demanded by the governing heat conduction equation. A small error in T(M) often renders the calculations for wall temperature and wall flux useless since their error is amplified as the calculation steps through time.

Therefore, it is desirable to devise a numerical method such that the input error of T(M) could be damped during the subsequent computation steps. One such method is programmed in DATARH. It must be stressed that damping of input error can only improve the accuracy of the computed results by reducing the input error amplification. The inheritant error due to inaccurate input data still remains.

The basic principle of the method is to utilize the information of T(M) available over an open time span when the computation is just entering this time span. Let the parenthesized superscript denote a relative time step, then the computation of $\bar{T}^{(1)}$ would not only involve an initial value $\bar{T}^{(0)}$, but also $\bar{T}^{(2)}(M), \bar{T}^{(23)}(M), \dots$. This calculation is followed by an optimization process to minimize the error amplification. This optimization can be accomplished in, although not restricted to, a least-squared sense.

Following Equation (3-2) and the subscript notation defined above, we have:

$$B(n)T^{(1)}(n-1) + A(n)T^{(1)}(n) + C(n)T^{(1)}(n+1) = -Q(n) - T^{(0)}(n) \quad (3-13)$$

$$B(N)T^{(1)}(N-1) + A(N)T^{(1)}(N) = -Q(N) - T^{(0)}(N) - C(N)T(N+1) \quad (3-14)$$

The solution using Equation (3-10) is;

$$\bar{T}^{(1)} = \bar{X}^{(1)} + C(N)T(N+1)\bar{Y}^{(1)} \quad (3-15)$$

In the above equation, all of the components in $\bar{X}^{(1)}$ and $\bar{Y}^{(1)}$ are known. $\bar{T}^{(1)}$ is not known since the wall temperature T(N+1) needs to be determined.

The computation can be carried out for one more time step as:

$$\begin{aligned} & B(n)T^{(2)}(n-1) + A(n)T^{(2)}(n) + C(n)T^{(2)}(n+1) \\ & = -Q(n) - T^{(2)}(n) \\ & = -Q(n) - \bar{X}^{(1)}(n) - C(N)T(N+1)\bar{Y}^{(1)} \end{aligned} \quad (3-16)$$

$$\begin{aligned} & B(N)T^{(2)}(N-1) + A(N)T^{(2)}(N) \\ & = -Q(N) - T^{(1)}(N) - C(N)T(N+1) \\ & = -Q(N) - X^{(1)}(N) - C(N)T(N+1)Y^{(1)}(N) - C(N)T(N+1) \\ & = -Q(N) - X^{(1)}(N) - C(N)T(N+1)\{Y^{(1)}(N) + 1\} \end{aligned} \quad (3-17)$$

The above equations form a linear system which is in the same form as that defined in Equation (3-7) provided that the vectors \vec{F} and \vec{G} are suitably modified. The linear set has the solution of the form of Equation (3-10)

$$\vec{T}^{(2)} = \vec{X}^{(2)} + C(N)T(N+1)\vec{Y}^{(2)} \quad (3-18)$$

For the other time steps, similar equations can be written:

$$\vec{T}^{(3)} = \vec{X}^{(3)} + C(N)T(N+1)\vec{Y}^{(3)} \quad (3-19)$$

$$\vec{T}^{(j)} = \vec{X}^{(j)} + C(N)T(N+1)\vec{Y}^{(j)}; j = 1, 2, \dots, J \quad (3-20)$$

In the above equations, the vectors $\vec{X}^{(j)}$ and $\vec{Y}^{(j)}$ are known for all j and time steps. The computation can terminate at any value of J . This set of equations are optimized to obtain the value of $T(N+1)$.

At a location where the measurements are recorded for $T^{(j)}(M)$, Equations (3-19) and (3-20) give

$$T^{(j)}(M) = X^{(j)}(M) + C(N)T(N+1)Y^{(j)}(M) \quad (3-21)$$

The measured temperatures $u^{(j)}$ are known for all values of j . The error between the computed and measured temperature is given as

$$\begin{aligned} \theta(j) &= T^{(j)}(M) - u^{(j)} \\ &= X^{(j)}(M) + C(N)T(N+1)Y^{(j)}(M) - u^{(j)}; j = 1, 2, \dots, J \end{aligned} \quad (3-22)$$

The problem is now reduced to finding a $T(N+1)$ such that θ is at a minimum. This can be accomplished by a least-squares method

$$\theta^2 = \sum_j \{E^{(j)}\}^2 = \sum_j \{X^{(j)}(M) + C(N)T(N+1)Y^{(j)}(M) - u^{(j)}\}^2 \quad (3-23)$$

$$dT(N+1) \Rightarrow 0 \quad (3-24)$$

$$\sum_j \frac{X^{(j)}(M) - u^{(j)}}{Y^{(j)}(M)} + C(N)T(N+1) = 0 \quad (3-25)$$

$$T(N+1) = \frac{1}{C(N)} \sum_j \frac{u^{(j)} - X^{(j)}(M)}{Y^{(j)}(M)} \quad (3-26)$$

Therefore, the desired temperature field can be calculated by

$$\vec{T}^{(1)} = \vec{X} + C(N)T(N+1)\vec{Y}^{(1)} \quad (3-27)$$

Equation (3-27) defines the initial values for the computations of the subsequent time step. The computation can be carried out repeatedly for each advance of time increment.

3.1.3 Structure of the source program DATARH.F

This section briefly describes the structure of the source program. Detailed comments may be found within the body of the source program as well. The reader is advised that it will be helpful if a listing of the program DATARH.F is referenced as the remainder of this section is being read, since this will enhance the reader's understanding of the description of the program structure that follows.

All real variables used in the program have been declared double precision numbers, as indicated by the use of the implicit double precision (a-h, o-z) statement. The program reads two character variables, title1 and rloc, that may each be up to 15 alphanumeric characters in length. These are intended to be identifiers of a test case. No intermediate spaces may be present within each set of alphanumeric characters. However, each identifier may be of length less than 15 alphanumeric characters if desired.

The program utilizes a number of data arrays, which may be identified by examining the dimension statements within the main program and sub-programs. It is important to note that some of these arrays have been declared to be of length 20000, while others have been declared to be of length 10 or 50. There are several arrays that have multiple dimensions; e.g., array t_i is seen to be of dimension 10x10. These numerical figures are indicative of limits built into the program.

The length 20000 indicates that the current version of the program is capable of reading in up to a maximum of 20000 sets of input data, each comprising time, clad temperature and power to the rod being analyzed (See input file described below). It also indicates that the maximum number of points in time for which the program is capable of computing heat flux and heat transfer coefficient values is limited to 20000.

The length 10 indicates that the region between two adjacent conduction nodes may be divided into a maximum of 10 sub-regions. As seen by the data (r(i), i = 1,5) statement, the program is capable of handling five outer conduction nodes and one implied conduction node at the rod-center, and hence five regions. Thus, the length 50 arises from the fact that the total number of sub-regions that may be handled by this version of the program is 10x5. The radial distance from the center of a heater rod to each outer conduction node is initialized by the data (r(i), i = 1,5) statement.

The program reads input data via an input file. The file name is "datarhin.dat" and the file must exist at the time the executable is run. The required content of this file is described in a section that follows. The program will write output data to a file by the name of out1.dat. This file will be created by the executable during a run, and a file by this name must not be present in the working directory at run-time. If the output file from a previous run exists, it must either be deleted, or be renamed.

Initializing the number of sub-regions within the region between a given pair of conduction nodes is accomplished by the array $intv(i)$, $i = 1$ through 5. As discussed above, the maximum number of sub-regions within any region is limited to 10. The heater rod length is set to be 3.66 m (12 ft) by means of variable $tlength$.

After all input data has been read, and once the initialization of the conduction region dimensions and heater rod length has been completed, the program will write a summary of the input data to the output file. It is after this that the computational procedures begin.

The first step is to convert the input time scale (array $timer$) so that the time of reflood is treated as zero-time. This is accomplished by a do loop that causes the time of reflood, $tflood$, to be subtracted from each time value (array $timer$) that was read by the program. Next, the number of data points that would be output by the program, $jtime$, is computed using the last value of input time, $timer(nscan)$, the first value of input time, $timer(1)$, and the value of dt (which is the time interval between results computed by the program). Note that $nscan$ is the number of sets of input data points. Now, an array of time values at which results will be output, array $time$, is computed. This too is accomplished by a do loop, and is performed by first setting $time(1)$ equal to $timer(1)$, and then successively adding the value of dt to the current value of time to get the next time value.

The next step is to compute an array of sink temperatures, T_{sink} . This array will have $nscan$ number of values. It should be noted that the current version of the program treats the saturation temperature corresponding to the operating pressure as the sink temperature throughout the length of the heater rod. Thus, all values in array T_{sink} will numerically be the same.

The program will now access an interpolation subroutine (subroutine tbl) to compute the saturation temperature, rod power, and the clad temperature at each value in array $time$ (the time values at which results are desired). The value of sink temperature computed, T_{sink} , will be written to the output file at this time as well.

Preparation of an array, q , that will contain volumetric heat generation rates at each value of array $time$ is performed next. Each interpolated value of rod power (at a given value of time) is multiplied by the axial power factor, fax , and the radial power factor (if applicable), fp , and is divided by the total rod length. Then, each resulting value of q is converted to a volumetric heat generation rate by means of appropriate conversion factors and rod dimensions.

It should be noted that the values for fax , fp , and fka have been calculated for each thermocouple location in the RBHT rod bundle and are hardwired into the DATARH source code. Although placeholders still exist in the required input file they are not used during calculations and it is recommended that the values of these variables be set to zero in the input file.

The program investigates the curvature of the future three data points next. The subroutine that performs the inverse conduction calculation is called after this computation. Once the inverse conduction calculation is completed for all time values desired, values of heat flux and heat transfer coefficient at the rod surface are computed. These values along with the computed rod surface temperature at each time value are then written to the output file. The program will then continue onto the next case (if input data are present), or will terminate if the end of input data has been reached.

3.1.4 RBHT Rod Geometry and Materials

Figure 2.4 shows the cross section of the RBHT bundle. The bundle has forty-five heater rods and four unheated corner rods. The corner rods are used to support the bundle and provide exits for the grid thermocouple leads. The support rods are made from Inconel 600 tubing having a diameter of 9.525 mm (0.375 in), a wall thickness of 2.108 mm (0.083 in) and a form length of 3.96 m (156 in). Figure 2.5 shows the cross section of an electrically heated rod. The heater rods are single ended and consist of a Monel 500 electrical resistance element filled and surrounded by hot pressed Boron Nitride (BN) insulation and enclosed in an Inconel 600 cladding as shown in the figure. The heater rods are 3.66 m (12 ft) in heated length with a skewed axial power profile, as shown in Figure 2.6, with the peak power located at 2.74 m (9 ft) elevation. The bundle has a uniform radial power distribution. The maximum to average power ratio (P_{max}/P_{avg}) is 1.5, and the minimum to average power ratio (P_{min}/P_{avg}) is 0.5 at both ends of the heated length.

Table 3.1 shows the description of the geometry for the RBHT heater rod geometry and dimensions.

Table 3.1 Geometry and Dimensions of RBHT Heater Rod

Material	r (mm, in)	Thickness of each region dr (mm, in)
Boron Nitride	0,0	1.71, 0.07
Monel K-500	1.71, 0.07	1.14, 0.045
Boron Nitride	2.86, 0.113	1.18, 0.047
Inconel 600	4.04, 0.159	0.71, 0.028
Rod Radius	4.75, 0.187	

3.1.5 Input File Required for Executing the Current Version of the Program

The program reads input data via an input file names datarhin.dat. This file must exist at the time the executable is run.

The input file, datarhin.dat should contain sets of input data arranged in lines, one line being required per reflood experiment analyzed. Each line must have values for the following input variables in the specified format, separated by one or more spaces:

IFAC:	Integer.	Test facility identifier, 4 for RBHT facility.
ITEST:	Integer.	Identifier for experimental run.
ICHAN:	Integer.	Identifier for thermocouple channel.
IMETRIC:	Integer.	Units of input data, 0 for British, 1 for SI.
NSCAN:	Integer.	Number of input data points.
DT:	Real.	Desired time interval between successive values of heat flux and heat transfer coefficient calculated [s].
TFLOOD:	Real.	Time of reflood start [s].
TSTOP:	Real.	Time of reflood stop [s].
TITLE:	Character, A15.	Identifier for each experimental run.
RLOC:	Character, A15.	Rod location/elevation.
FAX:	Real.	Axial power factor (hardwired in source code but value of 0.0 must be present in input file).
FP:	Real.	Fraction of zone power to this rod (hardwired in source code but value of 0.0 must be present in input file).
FKA:	Real.	Volumetric fraction of Monel 500 (hardwired in source code but value of 0.0 must be present in input file).
PRES:	Real.	System pressure [psia].

NSCAN sets of time, bundle power, and clad temperature follow. One set of values must appear on each successive line and each value must be separated by at least one space. A description of the data required follows:

TIME:	Real.	Array of experimental time values [s].
POWER:	Real.	Bundle Power at corresponding TIME value [kW].
TEMP:	Real.	Experimental temperature at corresponding TIME value for ICHAN [degrees F or K] (depending on IMETRIC value).

The sample input and output files from DATARH are given at the end of this section.

Sample input file: datarhin.dat

```
IFAC ITEST ICHAN IMETRIC NSCAN DT TFLOOD TSTOP
4 937 56 0 6025 0.50 301.30 1362.00
TITLE RLOC FAX FP FKA PRES
RBHT_TEST_937 RodB2-38.4 0.0 0.0 0.0 20.0
TIME POWER TEMP
0.25 -0.0005 674.2396
0.50 -0.0005 674.1904
0.75 -0.0005 674.1823
1.00 -0.0005 674.1577
1.25 -0.0005 674.1331
1.50 -0.0005 674.0920
1.75 -0.0005 674.0593
2.00 -0.0005 674.0183
...
300.00 142.3709 921.2880
300.25 143.8328 922.3034
300.50 143.3725 923.3672
300.75 143.2022 924.5842
301.00 142.5886 925.6238
301.25 143.2425 926.7762
301.50 143.3150 927.7829
301.75 142.7787 928.9585
302.00 142.9874 929.9327
302.25 151.4578 930.9714
302.50 151.2813 931.9538
302.75 143.6488 933.1535
303.00 154.7328 934.2566
...
1516.00 0.0000 218.2863
1516.25 0.0000 218.3030
1516.50 0.0000 218.2947
1516.75 0.0000 218.2697
1517.00 0.0000 218.2947
1517.25 0.0000 218.2614
1517.50 0.0000 218.2531
1517.75 0.0000 218.2614
1506.50 0.0000 218.3530
```

Sample Output File

***** Program DATARH - Universal Rev. 01
 ***** Revision Date: 01-14-2010
 ***** RBHT Test 937
 ***** CHANNEL = 56
 ***** Rod ID = RodB2-38.4

Initial Run Conditions :

Number of data points : 6025
 Axial Power Factor : 0.84700
 Fraction of Zone Power to rod : 0.02222
 Volumetric fraction of wire : 0.85212
 System pressure : 20.00000 psi
 System pressure : 0.13790 MPa
 Start of reload : 301.30 sec
 End time : 1362.00 sec
 Output interval : 0.50 sec
 Saturation Temperature is : 227.92000 deg. F
 : 381.99444 K

Temperature at reflood : 926.96 deg F
 Temperature at reflood : 770.36 K
 Turn around time : 22.45 sec
 Turn around temperature : 999.46 deg F
 Turn around temperature : 810.64 K
 Quench time : 156.45 sec
 Quench temperature : 656.08 deg F
 Quench temperature : 619.87 K

***** Summary of Results *****

TIME	TEMP	TSURF	QSURF	HTC	TIME	TSURF	DT	QSURF	HTC
sec	deg F	deg F	Btu/hr-ft2	Btu/hr-ft2-F	sec	K	K	W/m2	W/m2-K
0.45	928.96	928.03	1.64E+03	2.34E+00	0.45	770.96	388.95	5.16E+03	1.33E+01
0.95	930.97	930.07	2.10E+03	2.99E+00	0.95	772.09	390.09	6.62E+03	1.70E+01
1.45	933.15	932.28	1.73E+03	2.45E+00	1.45	773.32	391.31	5.44E+03	1.39E+01
1.95	935.33	934.4	1.76E+03	2.50E+00	1.95	774.49	392.49	5.57E+03	1.42E+01
2.45	937.36	936.5	1.78E+03	2.51E+00	2.45	775.66	393.66	5.61E+03	1.43E+01
2.95	939.5	938.52	2.00E+03	2.81E+00	2.95	776.78	394.78	6.30E+03	1.60E+01
3.45	941.54	940.54	2.00E+03	2.81E+00	3.45	777.9	395.9	6.31E+03	1.59E+01
3.95	943.48	942.54	2.03E+03	2.84E+00	3.95	779.01	397.01	6.41E+03	1.61E+01
4.45	945.42	944.55	2.01E+03	2.80E+00	4.45	780.13	398.13	6.33E+03	1.59E+01
4.95	947.46	946.46	2.42E+03	3.36E+00	4.95	781.19	399.19	7.62E+03	1.91E+01
5.45	949.46	948.51	2.09E+03	2.90E+00	5.45	782.33	400.33	6.59E+03	1.65E+01
5.95	951.46	950.46	2.18E+03	3.02E+00	5.95	783.41	401.41	6.89E+03	1.72E+01
6.45	953.37	952.45	2.11E+03	2.91E+00	6.45	784.52	402.51	6.66E+03	1.65E+01
6.95	955.28	954.39	2.47E+03	3.40E+00	6.95	785.6	403.6	7.78E+03	1.93E+01
7.45	957.37	956.5	2.03E+03	2.79E+00	7.45	786.77	404.76	6.40E+03	1.58E+01

3.1.6 Calculation of the Power Factor at Each Thermocouple Location

Stern Laboratories, Inc. measured the resistance of each heater rod filament beginning from the bottom of the heated length to the end of the heated length. The measurements were made over increments of one tenth of the length of the rod and the cumulative resistances were reported. Table 3.2 shows a sample table of data from Stern.

Table 3.2 Heater Number 1

Length (in)	Resistance (Ohm)
0	0.000
14.28	0.018
28.55	0.040
42.83	0.066
57.1	0.096
71.38	0.129
85.65	0.166
99.93	0.211
114.20	0.258
128.48	0.291
142.75	0.315

WINDOWS (EAST)

Rod A1 Support Rod	Rod B1 GR-7 PSP-15	Rod C1 GR-0 PSP-45	Rod D1 GR-7 PSP-16	Rod E1 GR-0 PSP-48	Rod F1 GR-0 PSP-42	Rod G1 Support Rod
Rod A2 GR-0 PSP-40	Rod B2 GR-1 PSP-36	Rod C2 GR-2 PSP-32	Rod D2 GR-6 PSP-12	Rod E2 GR-8 PSP-6	Rod F2 GR-1 PSP-37	Rod G2 GR-0 PSP-47
Rod A3 GR-0 PSP-49	Rod B3 GR-8 PSP-27	Rod C3 GR-5 PSP-4	Rod D3 GR-3 PSP-21	Rod E3 GR-4 PSP-7	Rod F3 GR-8 PSP-28	Rod G3 GR-0 PSP-43
Rod A4 GR-7 PSP-17	Rod B4 GR-3 PSP-22	Rod C4 GR-3 PSP-23	Rod D4 GR-3 PSP-25	Rod E4 GR-3 PSP-24	Rod F4 GR-5 PSP-2	Rod G4 GR-0 PSP-44
Rod A5 GR-0 PSP-41	Rod B5 GR-2 PSP-33	Rod C5 GR-4 PSP-8	Rod D5 GR-8 PSP-29	Rod E5 GR-4 PSP-9	Rod F5 GR-2 PSP-34	Rod G5 GR-0 PSP-50
Rod A6 GR-7 PSP-18	Rod B6 GR-1 PSP-38	Rod C6 GR-2 PSP-35	Rod D6 GR-6 PSP-13	Rod E6 GR-8 PSP-30	Rod F6 GR-1 PSP-39	Rod G6 GR-0 PSP-3
Rod A7 Support Rod	Rod B7 GR-0 PSP-1	Rod C7 GR-6 PSP-11	Rod D7 GR-7 PSP-19	Rod E7 GR-0 PSP-46	Rod F7 GR-7 PSP-20	Rod G7 Support Rod

WINDOWS (WEST)

Figure 3.1 RBHT Test Facility, Heater Rod Locations (Looking Down from Top).

Figure 3.1 shows the schematic of the RBHT Test Facility heater rod layout. The 7x7 bundle consists of 8 groups of rods as indicated by GR - # (group number), these are instrumented rods while GR-0 rods are un-instrumented. The PSP - # is the serial number of the rods as given by Stern.

Axial Power Ratio Vs. Length for Rod F4

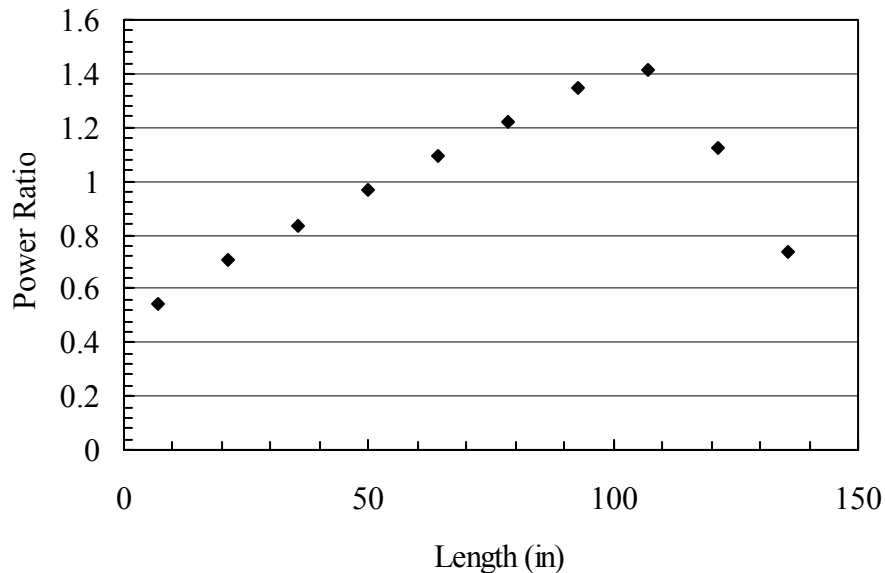


Figure 3.2 Axial Power Ratio for Rod F4.

The heater rod is composed of a series of resistances along the length. The power shape is obtained by appropriately changing the pitch of the heater element.

Using the data, the resistance for every incremental length (one tenth of the total length) is calculated by subtracting the value of resistance over the total length (0 to that axial location) from the previous value (0 to the previous axial location). This would give the resistance of the filament portion for that region (one-tenth of the total length). The incremental length over which the measurements are made is also calculated.

The axial power factor is defined as the ratio of the incremental resistance for that incremental length over the incremental length to the total resistance of the rod over the total heated length. Using this definition, the axial power factor over each incremental length is calculated.

This is plotted as a function of length to get the power shape for each rod. Since the measurements provided by Stern was over every tenth of the heated length, these points were plotted at an average axial position (for example, for the length between 14.28 and 28.55 in, the incremental resistance and hence the power factor over this span was plotted at a location of 21.415 in). Such a plot is shown in Figure 3.2, for Rod F4 (Stern heater number 2)

Measurements from Stern were such that they bypassed the peak power location, meaning the measurement was taken at 99.93 and 114.20 in elevations. The peak power location was 108 in. In order to calculate the power factor at the peak power location and for any arbitrary location along the length of the heater rod, a straight line is fit for the power factor calculated using the data points between 0 and 108 in. The equation for the power factor is a function of length along the heater rod. Using this equation, the peak power factor is calculated for each rod (i.e., the value of power factor is calculated at 108 in location). This is then used along with the remaining calculated values of power factors (for length beyond 108 in) and another such plot is made. An equation relating the power ratio and the heated length is obtained for the region beyond 108 in. Thus, for each heater rod, two plots are made, one for the length of the heater rod below the peak power location and the other beyond the peak power location to the end of the heated length. Using the equations for the power ratio as a function of axial position, the power factor at any location along the heater rod is obtained.

This procedure is followed for each rod with thermocouples and the power factor for every thermocouple location is obtained. Table 3.3 shows a typical calculation for one rod. (The resistances are values before swaging.)

Table 3.3 Sample Power Factor Calculation for One Heater Rod

Stern Lab Heater Number 2: RBHT ROD F4								
Length	Increment	Averaged	Heater # 2	Difference	Power	Channel #	Instrument	Power
(in)	(in)	(in)	Resistance	Ohm	Ratio	THERMOCOUPLE INFORMATION		
							Location	ratio
0	14.28	7.14	0	0.017	0.55	98	85.6	1.29
14.28	14.27	21.415	0.017	0.022	0.71	99	88.4	1.31
28.55	14.28	35.69	0.039	0.026	0.84	100	92.4	1.35
42.83	14.27	49.965	0.065	0.03	0.96	101	94.3	1.37
57.1	14.28	64.24	0.095	0.034	1.09	102	97.2	1.39
71.38	14.27	78.515	0.129	0.038	1.22		108	1.49
85.65	14.28	92.79	0.167	0.042	1.35	103	108.8	1.47
99.93	14.27	107.065	0.209	0.044	1.42	104	111	1.41
		108			1.49			
114.2	14.28	121.34	0.253	0.035	1.13			
128.48	14.27	135.615	0.288	0.023	0.74			
142.75			0.311					

Figure 3.3 and Figure 3.4 show plots of the power ratio as a function of length along the heater rod. Figure 3.3 is the plot from the beginning of the heated length to the peak power location (108 in), while Figure 3.4 is the plot from the peak power location (108 in) to the end of heated length.

The values of the axial power factor for all the thermocouples used in the RBHT Test Facility is shown in Table 3.4. The values of the axial power factors range from 0 to 1.5, which is the value at peak power location of 108 in. For example: RodB1_47.9 refers to the thermocouple at

47.9 in elevation for rod B1. These values are directly used in DATARH for the local rod heat flux and heat transfer coefficient calculations.

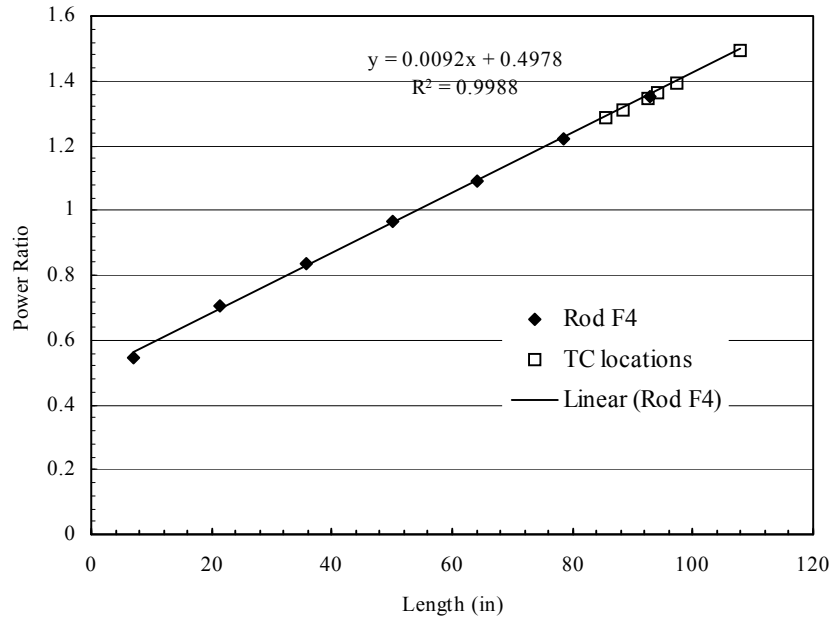


Figure 3.3 Power Factor as a Function of Length (Beginning of Heated Length to Peak Clad Temperature Location).

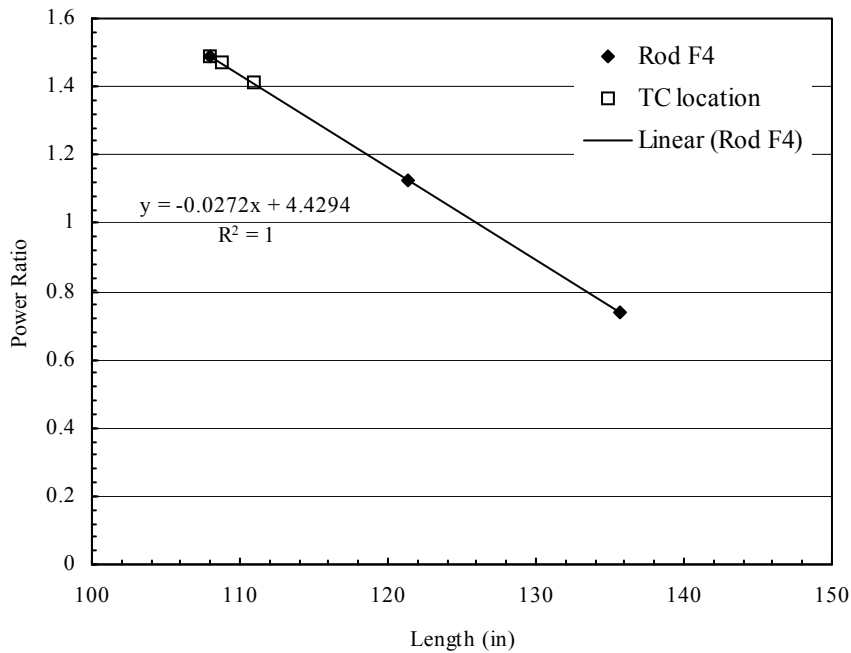


Figure 3.4 Power Factor as a Function of Length (From Peak Clad Temperature Location to the End of Heated Length).

Table 3.4 Axial Power Factors for the RBHT Heater Rods

Rod ID Elevation (inches)	Power Factor	Rod ID Elevation (inches)	Power Factor	Rod ID Elevation (inches)	Power Factor
RodB1_47.9	0.936	RodE2_66	1.111	RodF3_54	0.993
RodB1_63.6	1.082	RodE2_69.8	1.147	RodF3_57	1.022
RodB1_68.6	1.128	RodE2_72.9	1.176	RodF3_60	1.05
RodB1_79.7	1.231	RodE2_74.9	1.195	RodF3_66.1	1.108
RodB1_97.1	1.393	RodF2_4.1	0.519	RodF3_69.9	1.145
RodB1_114.8	1.314	RodF2_11.2	0.586	RodF3_73	1.174
RodB1_126.7	0.99	RodF2_16.2	0.634	RodF3_75	1.193
RodB1_139.4	0.644	RodF2_23.3	0.701	RodA4_48	0.94
RodD1_47.9	0.941	RodF2_29.2	0.757	RodA4_63.8	1.084
RodD1_63.8	1.093	RodF2_33.3	0.796	RodA4_68.8	1.13
RodD1_68.8	1.141	RodF2_35.3	0.815	RodA4_79.9	1.231
RodD1_79.9	1.248	RodF2_38.3	0.843	RodA4_97.1	1.387
RodD1_97.3	1.415	RodB3_50.2	0.956	RodA4_115	1.291
RodD1_115	1.317	RodB3_54.1	0.992	RodA4_126.8	0.977
RodD1_126.6	0.99	RodB3_56.9	1.018	RodA4_139.4	0.642
RodD1_139.4	0.629	RodB3_60.1	1.048	RodB4_88.4	1.303
RodB2_4.1	0.521	RodB3_66.1	1.104	RodB4_91.3	1.329
RodB2_11.2	0.589	RodB3_69.9	1.139	RodB4_93.3	1.347
RodB2_16.2	0.636	RodB3_73	1.168	RodB4_95.1	1.363
RodB2_23.3	0.704	RodB3_75	1.187	RodB4_100	1.407
RodB2_29.3	0.761	RodC3_79.8	1.228	RodB4_106	1.461
RodB2_33.3	0.799	RodC3_85.6	1.281	RodB4_109.9	1.414
RodB2_35.3	0.818	RodC3_88.5	1.308	RodB4_142.3	0.549
RodB2_38.4	0.847	RodC3_92.4	1.344	RodC4_88.4	1.328
RodC2_41	0.87	RodC3_94.4	1.362	RodC4_91.1	1.354
RodC2_53.1	0.983	RodC3_97.2	1.388	RodC4_93.4	1.376
RodC2_55	1	RodC3_108.8	1.463	RodC4_95.3	1.394
RodC2_57.8	1.026	RodD3_88.3	1.313	RodC4_100.1	1.439
RodC2_63.9	1.083	RodD3_91.3	1.341	RodC4_106.1	1.496
RodC2_73.8	1.175	RodD3_93.1	1.358	RodC4_110	1.448
RodC2_75.8	1.194	RodD3_95.3	1.378	RodC4_142.2	0.553
RodC2_76.8	1.203	RodD3_100.1	1.423	RodD4_88.3	1.323
RodD2_103.2	1.455	RodD3_106.1	1.479	RodD4_91.3	1.351
RodD2_106	1.481	RodD3_110	1.46	RodD4_93.2	1.369
RodD2_112.6	1.358	RodD3_142.1	0.51	RodD4_95.2	1.388
RodD2_114.9	1.295	RodE3_63.4	1.079	RodD4_100.1	1.434
RodD2_117.4	1.227	RodE3_113.6	1.331	RodD4_106.1	1.491
RodD2_120.8	1.134	RodE3_115.5	1.281	RodD4_110	1.44
RodD2_124.8	1.024	RodE3_118.5	1.203	RodD4_142.1	0.534
RodD2_128.6	0.92	RodE3_122.7	1.094	RodE4_88.4	1.303
RodE2_50.1	0.962	RodE3_126.5	0.995	RodE4_91.2	1.329
RodE2_54	0.998	RodE3_131.7	0.86	RodE4_93.2	1.347
RodE2_56.9	1.025	RodE3_135.6	0.759	RodE4_95.3	1.365
RodE2_59.9	1.054	RodF3_50.1	0.956	RodE4_100.9	1.416

Table 3.4 Axial Power Factors for the RBHT Heater Rods (Continued)

Rod ID Elevation (inches)	Power Factor	Rod ID Elevation (inches)	Power Factor	Rod ID Elevation (inches)	Power Factor
RodE4_106.1	1.463	RodF5_57.8	1.022	RodE6_75	1.184
RodE4_110	1.428	RodF5_64	1.08	RodF6_4.1	0.528
RodE4_142.3	0.54	RodF5_73.8	1.171	RodF6_11.2	0.593
RodF4_85.6	1.285	RodF5_75.8	1.19	RodF6_16.3	0.639
RodF4_88.4	1.311	RodF5_76.8	1.199	RodF6_23.3	0.703
RodF4_92.4	1.348	RodA6_47.7	0.942	RodF6_29.3	0.757
RodF4_94.3	1.365	RodA6_63.6	1.085	RodF6_33.3	0.794
RodF4_97.2	1.392	RodA6_68.5	1.129	RodF6_35.3	0.812
RodF4_108.8	1.47	RodA6_79.8	1.231	RodF6_38.3	0.839
RodF4_111	1.41	RodA6_97.4	1.389	RodC7_112.6	1.323
RodB5_41	0.872	RodA6_115.1	1.29	RodC7_116.6	1.224
RodB5_52.9	0.982	RodA6_126.6	0.986	RodC7_124.4	1.03
RodB5_55	1.002	RodA6_139.9	0.633	RodC7_128.4	0.931
RodB5_57.8	1.028	RodB6_4.1	0.526	RodD7_47.9	0.948
RodB5_64	1.085	RodB6_11.2	0.592	RodD7_63.6	1.091
RodB5_73.9	1.177	RodB6_16.2	0.638	RodD7_68.8	1.138
RodB5_75.9	1.196	RodB6_23.3	0.703	RodD7_79.8	1.238
RodB5_76.9	1.205	RodB6_29.3	0.758	RodD7_97.1	1.396
RodC5_63.7	1.059	RodB6_33.3	0.795	RodD7_114.9	1.293
RodC5_113.6	1.298	RodB6_35.3	0.813	RodD7_126.7	0.958
RodC5_115.7	1.246	RodB6_38.4	0.842	RodD7_139.4	0.598
RodC5_122.7	1.073	RodC6_40.9	0.866	RodF7_47.9	0.946
RodC5_126.7	0.974	RodC6_52.8	0.981	RodF7_63.8	1.101
RodC5_131.6	0.853	RodC6_54.8	1.001	RodF7_68.9	1.15
RodC5_135.7	0.752	RodC6_57.8	1.03	RodF7_79.9	1.257
RodD5_50	0.959	RodC6_63.8	1.088	RodF7_97.2	1.425
RodD5_54.1	0.996	RodC6_73.7	1.184	RodF7_114.9	1.333
RodD5_56.9	1.022	RodC6_75.8	1.204	RodF7_126.8	0.953
RodD5_60	1.051	RodC6_76.8	1.214	RodF7_139.4	0.551
RodD5_66.1	1.107	RodD6_103.1	1.457		
RodD5_69.9	1.142	RodD6_106	1.484		
RodD5_72.9	1.169	RodD6_112.9	1.354		
RodD5_74.9	1.188	RodD6_114.9	1.298		
RodE5_63.6	1.085	RodD6_116.8	1.246		
RodE5_113.6	1.339	RodD6_120.9	1.132		
RodE5_115.4	1.292	RodD6_124.8	1.024		
RodE5_118.7	1.208	RodD6_128.7	0.916		
RodE5_122.6	1.108	RodE6_50.2	0.956		
RodE5_126.6	1.006	RodE6_54.1	0.992		
RodE5_131.6	0.878	RodE6_57	1.018		
RodE5_135.6	0.775	RodE6_60.2	1.048		
RodF5_41	0.866	RodE6_66.1	1.102		
RodF5_53.1	0.978	RodE6_70	1.138		
RodF5_55	0.996	RodE6_73.1	1.166		

3.2 Quench Front Determination

A simple program was developed and added to the DATARH source code to determine the quench front progress for the RBHT reflood experiments. As a result of the program, the location of the quench front as a function of time is obtained.

The quench front program uses the outside rod temperatures predicted by DATARH, locations of these temperatures, and the test time as input. The reflood start time is the starting time for the program. The program runs as part of DATARH and outputs results in the same output file as seen in the sample output file presented above.

A simple criterion is used to determine the quench front location from the heated rod temperature data. One sample of plot for change in rod temperature with time is presented in Figure 3.5 and quench time is indicated on the figure.

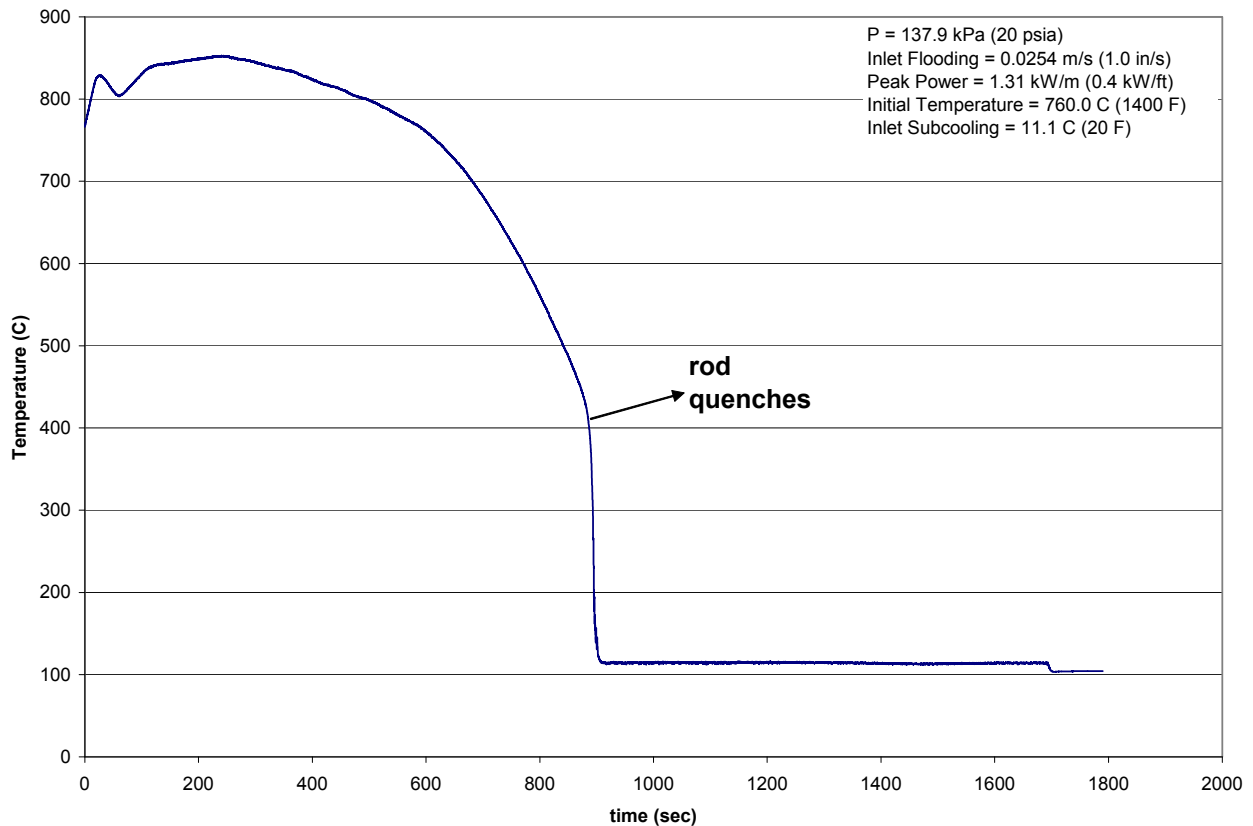


Figure 3.5 Clad Temperature at 2.24 m, Experiment 1096.

The first attempt to determine the quench front time was to use a simple numerical approach to get the first derivative for the above data. The time at which the first derivative reaches its maximum value was assumed as the quench time since the rate of change of the heater rod temperature would be the greatest.

Equation (3-28) gives the relationship used to evaluate the first derivative from the heater rod data:

$$\frac{dT}{dt} = \frac{T_{i+1} - 2T_i + T_{i-1}}{\Delta t} \quad (3-28)$$

where in the program, Δt is the variable DT defined in the input file datarhin.dat and T_{i+1} , T_i , T_{i-1} are predicted heater rod outside surface temperatures from DATARH predictions.

Figure 3.6 presents the change in the first derivative of temperature with respect to reflow time on two different scales. The figure shows that the first derivative reaches its maximum value approximately 10 s after rod quenches. In order to obtain a more accurate value of the quench time, an additional requirement was added to the program. This requirement determines the quench time when the first derivative of temperature versus time curve is greater than 11.1 degrees K/s (20.0 degrees F/s). The value of 11.1 degrees K/s (20 degrees F/s) was determined by examining most of the rod temperature data for all tests and several elevations, although this value is set to 28 degrees K/s (50 degrees F/s) in FLECHT-SEASET analysis (Ref. 1), since the data recording frequency in RBHT tests is smaller (10 samples/s, in FLECHT-SEASET it was 2 samples/s or less), 11.1 degrees K/s (20.0 degrees F/s) is a suitable criterion for these tests.

For the case illustrated in Figure 3.6, the quench time was determined to be 892 s, and the quench temperature for this case is 618 degrees K (653 degrees F).

Figure 3.7 and Figure 3.8 present samples of calculations performed to analyze quench front progress.

As a result of the program, the rod surface temperature at the quenched elevation is also obtained. Figure 3.9 and Figure 3.10 present the data for quenched temperature versus elevation for experiments 1096 and 1383, respectively. As the figures show, the quench temperature data follows a distribution. The mean quench temperatures and standard deviation for these mean temperatures are also presented in the figures. The mean quench temperature for the reference (40 psia) experiment was found to be 694 degrees K (789 degrees F) and for the reference (20 psia) experiment the mean quench temperature was found to be 667 degrees K (741 degrees F).

The quench front program developed for rods was also used to determine the quench front progress for the bundle housing to prepare an input for the energy balance programs to calculate housing heat release. Figure 3.11 and Figure 3.12 present the housing quench front locations versus time for experiments 1096 and 1383, respectively.

The quench front locations for the housing and the rods are shown in Figure 3.13 and Figure 3.14 for the reference experiments. Since the housing is an unpowered structure, it quenches slightly earlier than the heated rods. The figures show that housing and rods quench almost at the same time up to 2 m (6.5 ft) elevation and the peak clad temperature turnaround occurs during this period. This indicates that the housing quench does not affect the turnaround time for the heater rods. At the higher elevations, the difference between quench time of the heater rods and housing does increase.

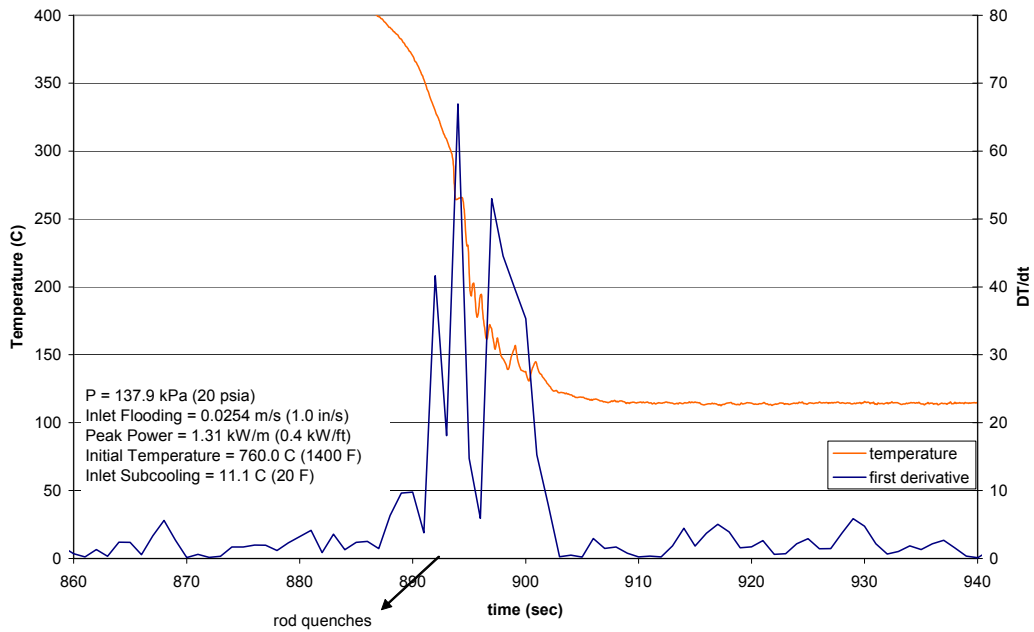
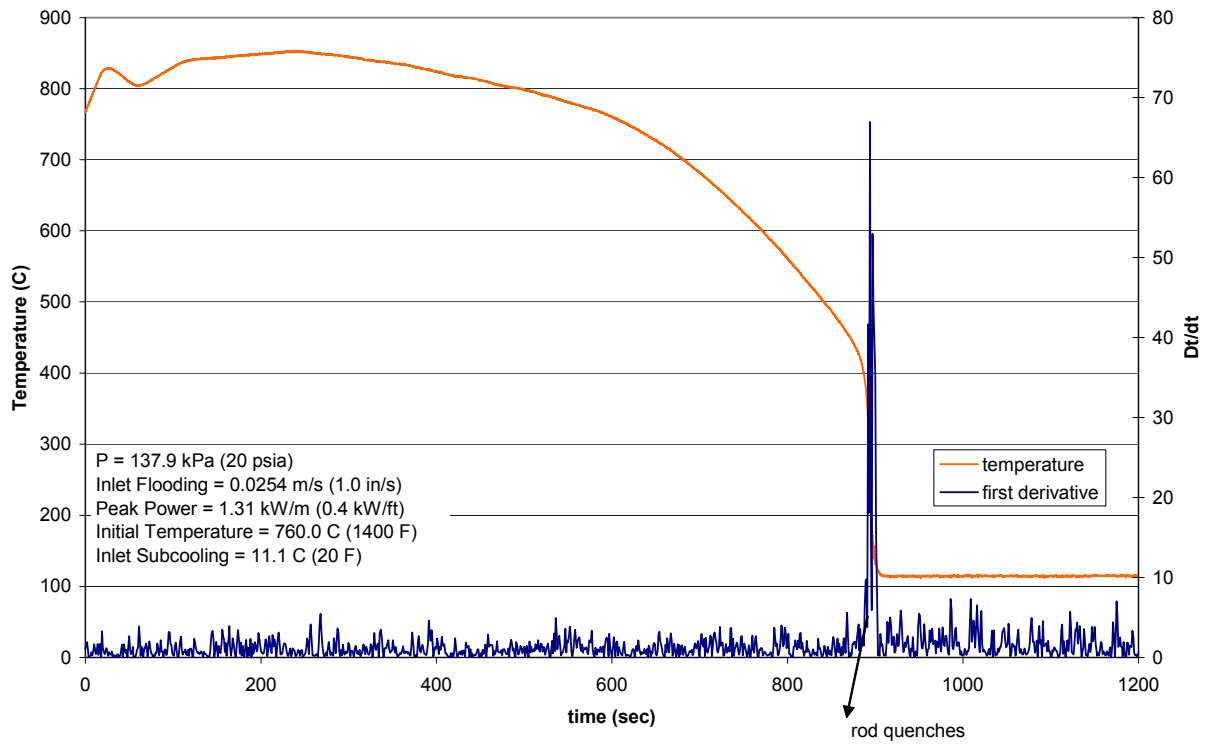


Figure 3.6 Temperature and First Derivative of Temperature at 2.24 m, Experiment 1096.

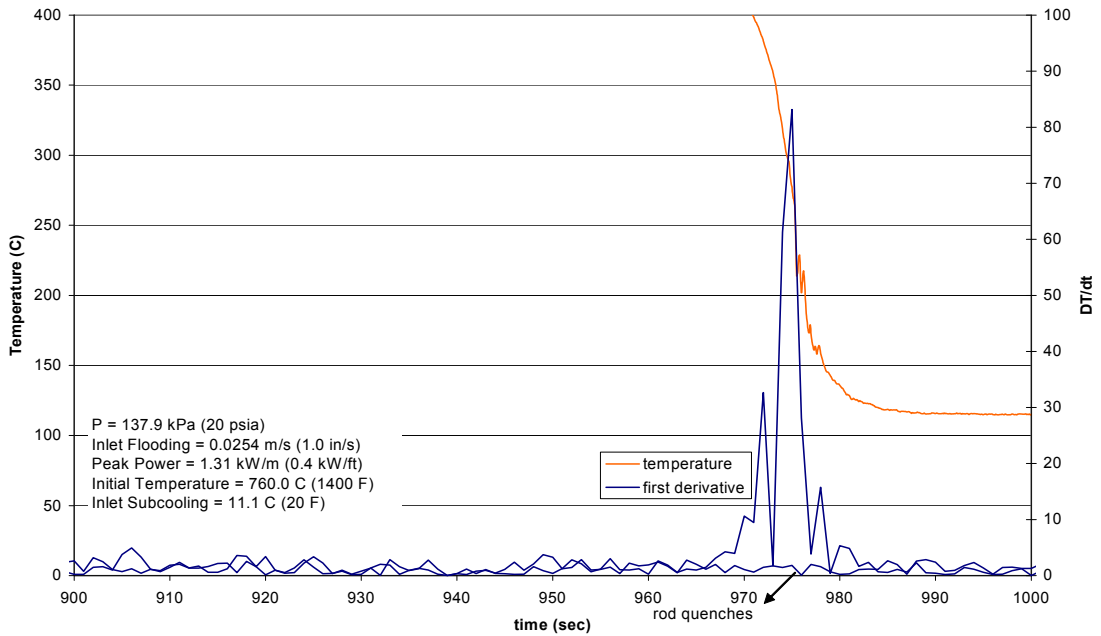
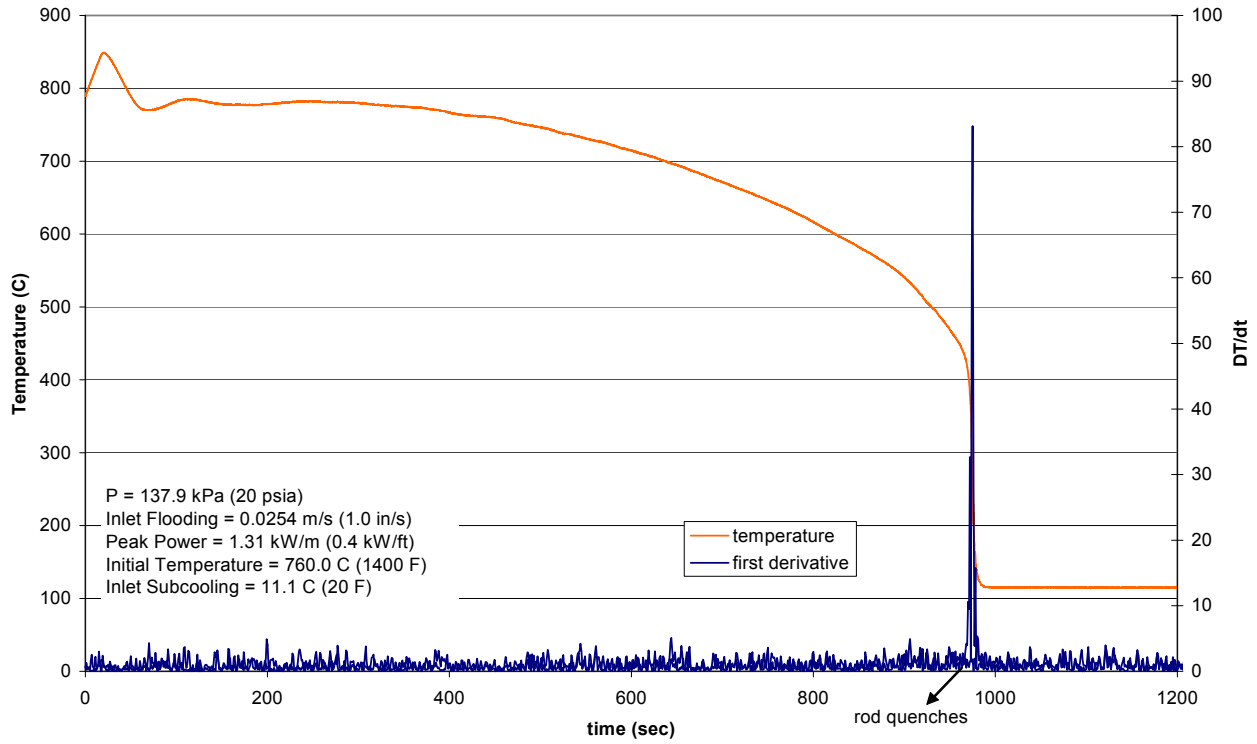


Figure 3.7 Temperature and First Derivative of Temperature Curve at 2.42 m, Experiment 1096.

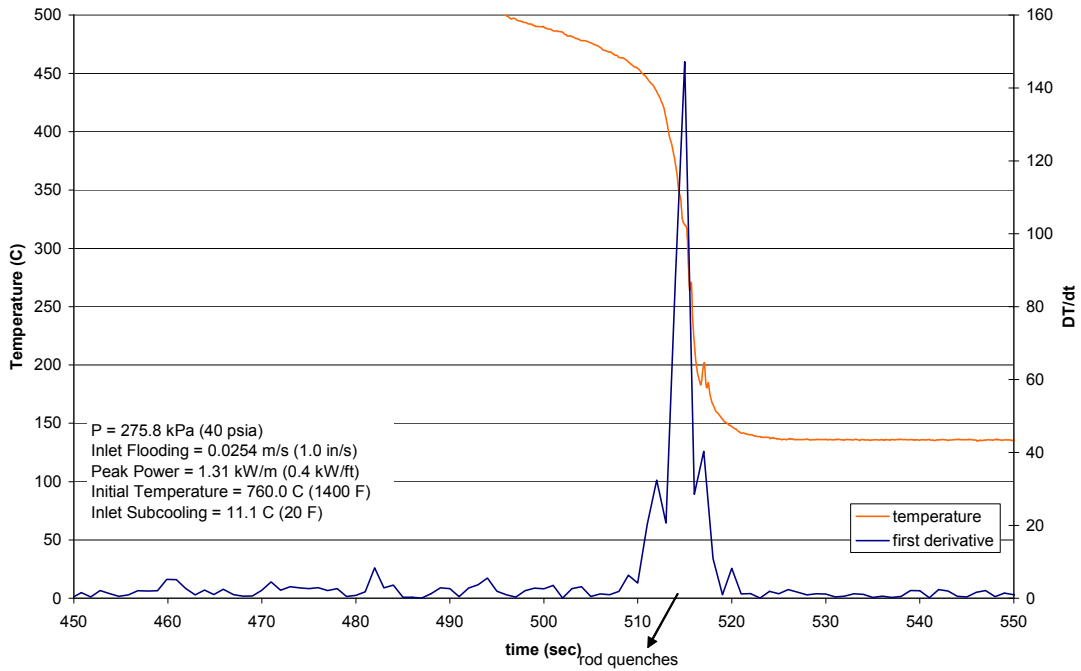
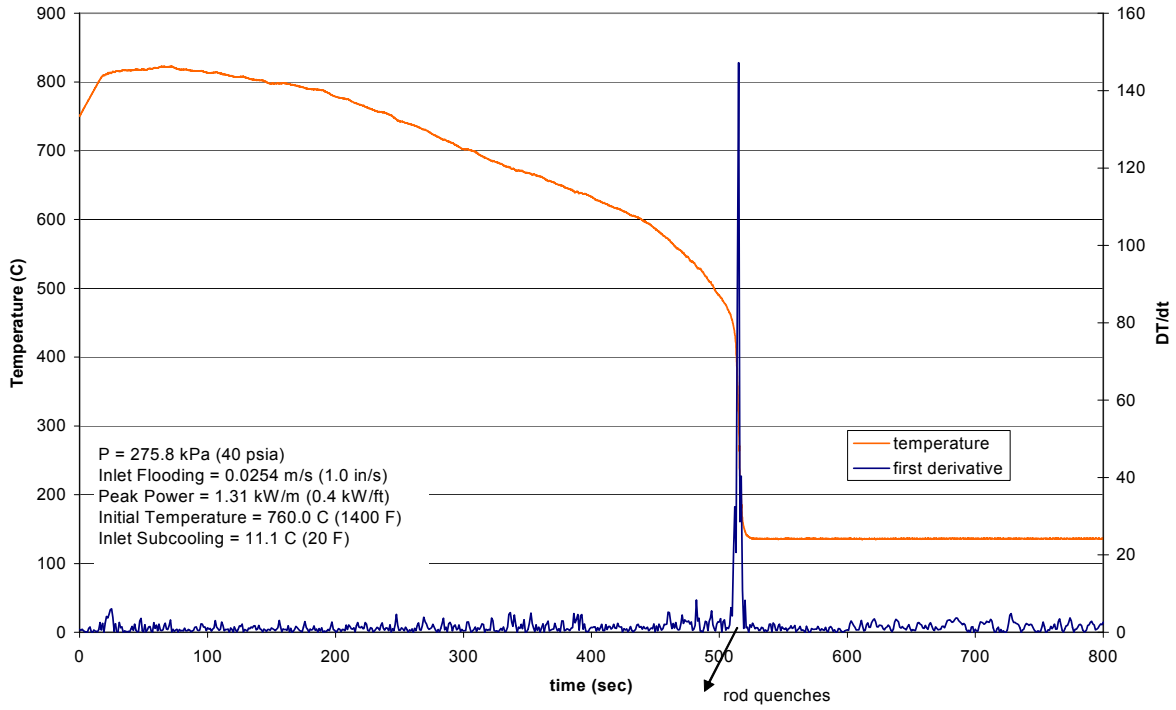


Figure 3.8 Temperature and First Derivative of Temperature Curve at 2.42 m, Experiment 1383.

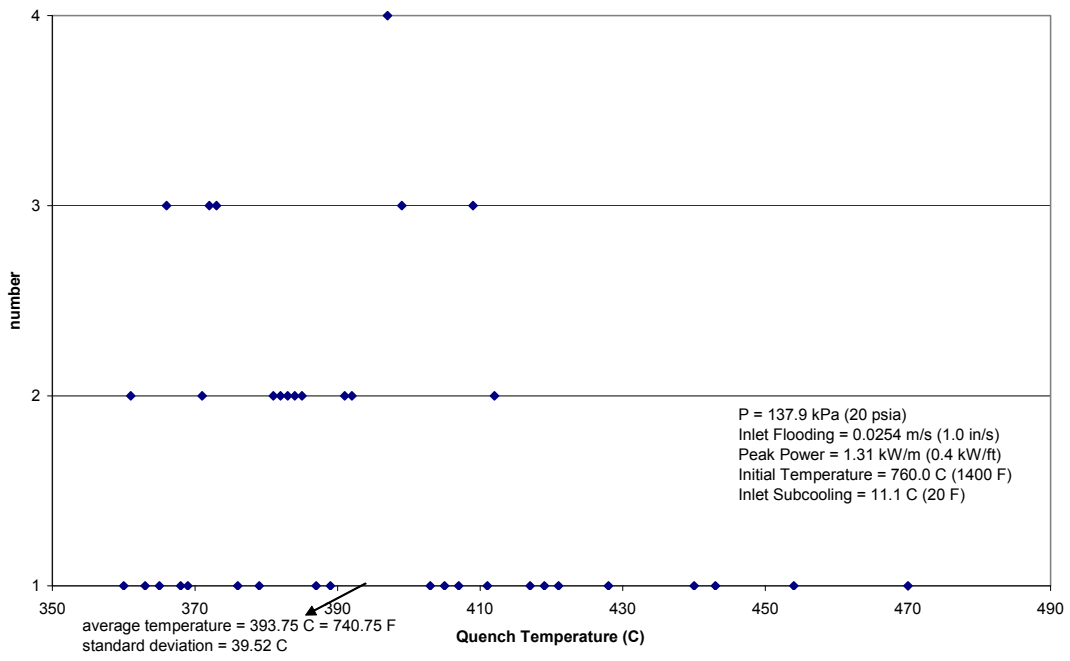


Figure 3.9 Quench Temperature at Different Quench Locations, Experiment 1096.

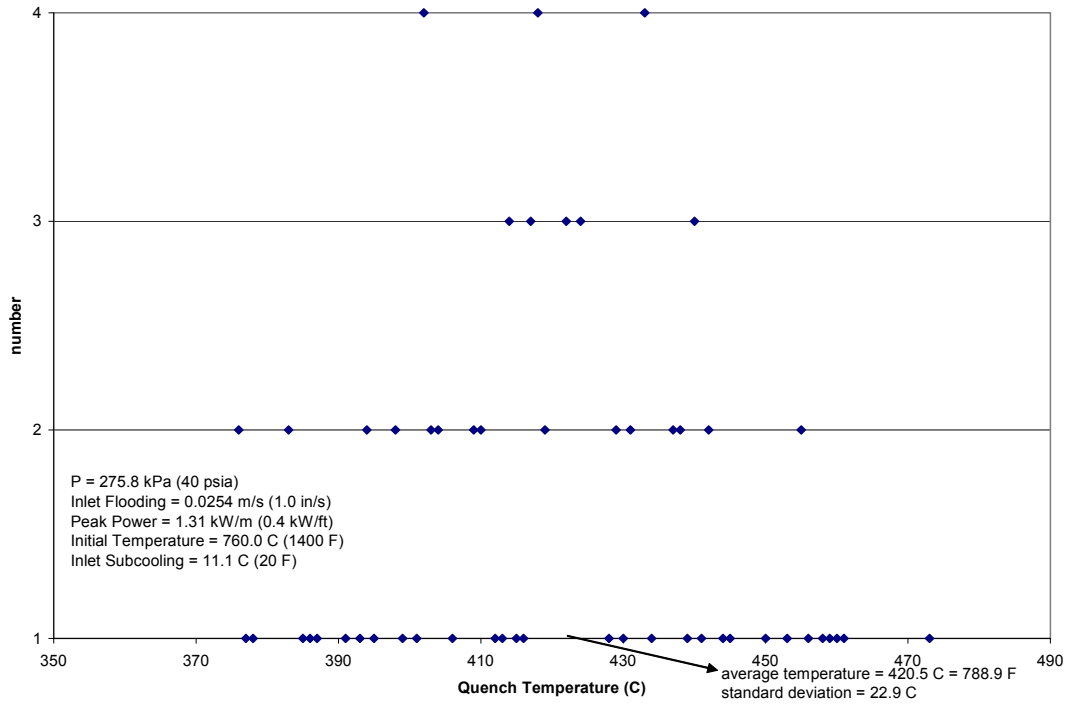


Figure 3.10 Quench Temperature at Different Quench Locations, Experiment 1383.

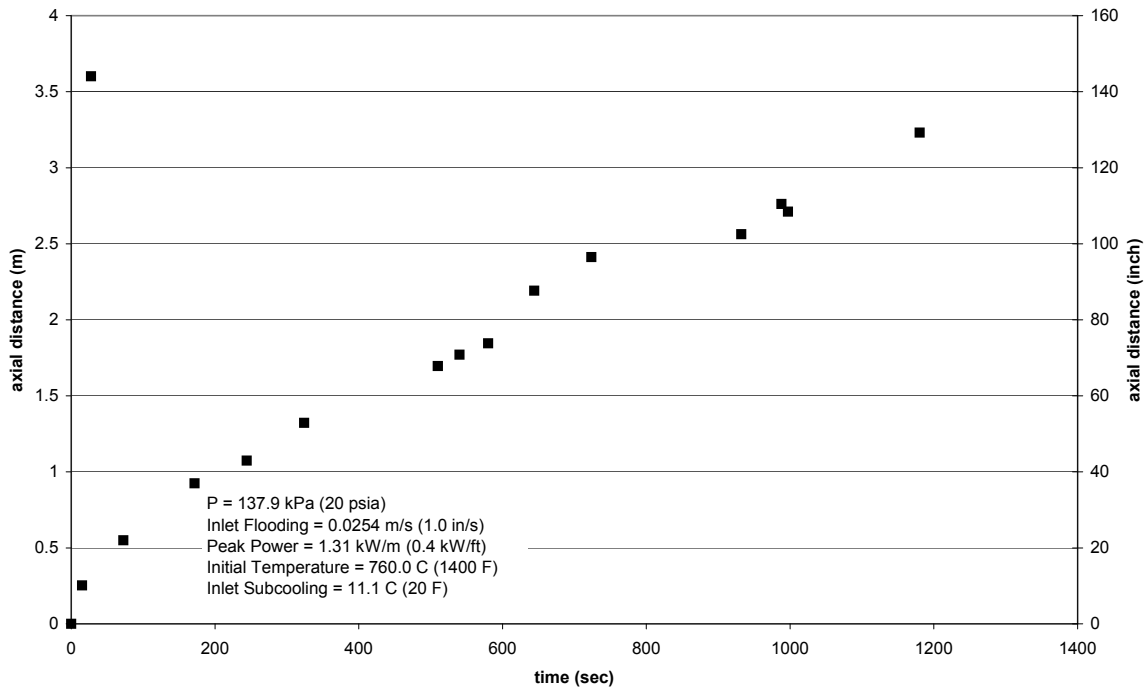


Figure 3.11 Housing Quench Front, Experiment 1096.

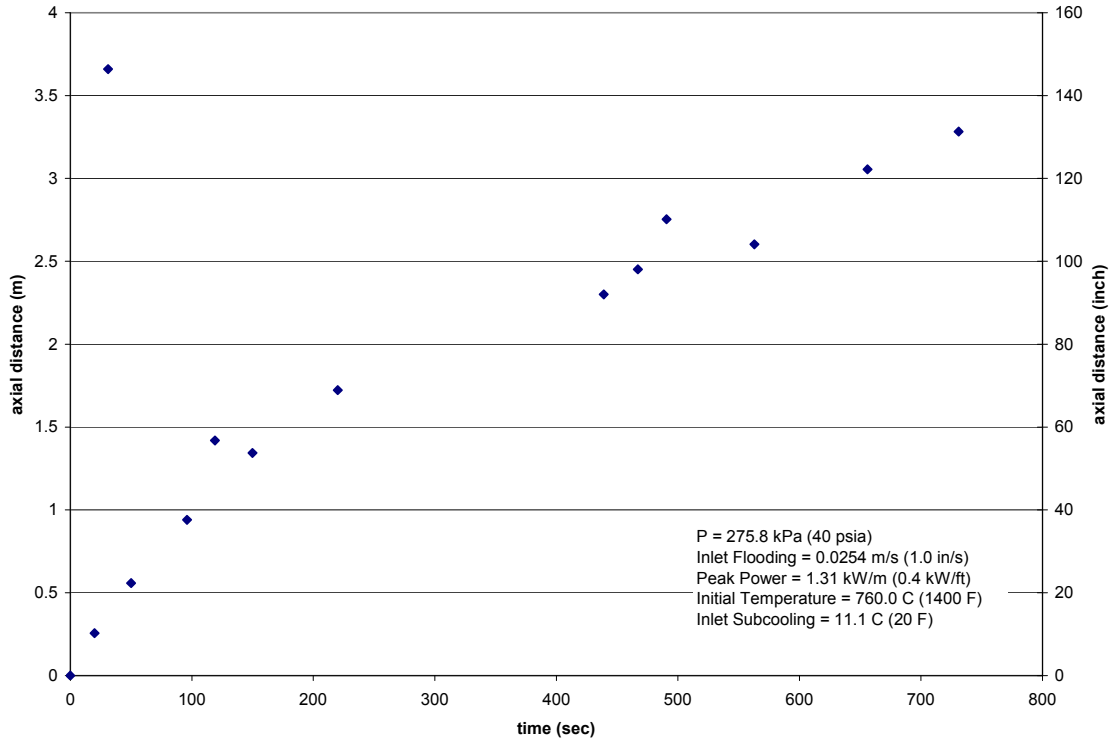


Figure 3.12 Housing Quench Front, Experiment 1383.

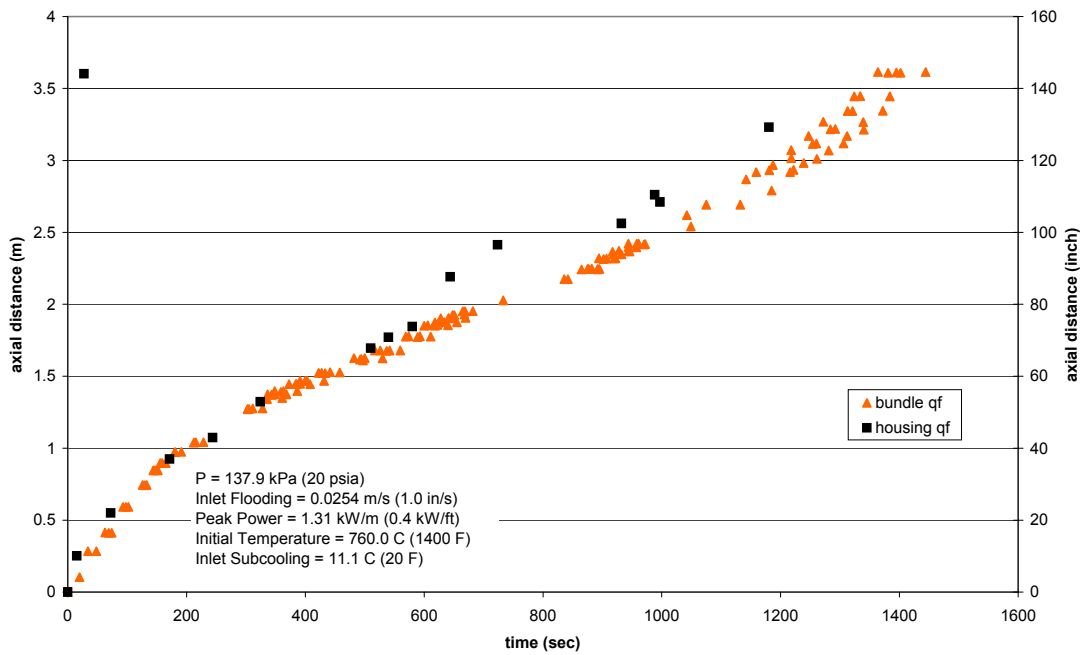


Figure 3.13 Rod and Housing Quench Front, Experiment 1096.

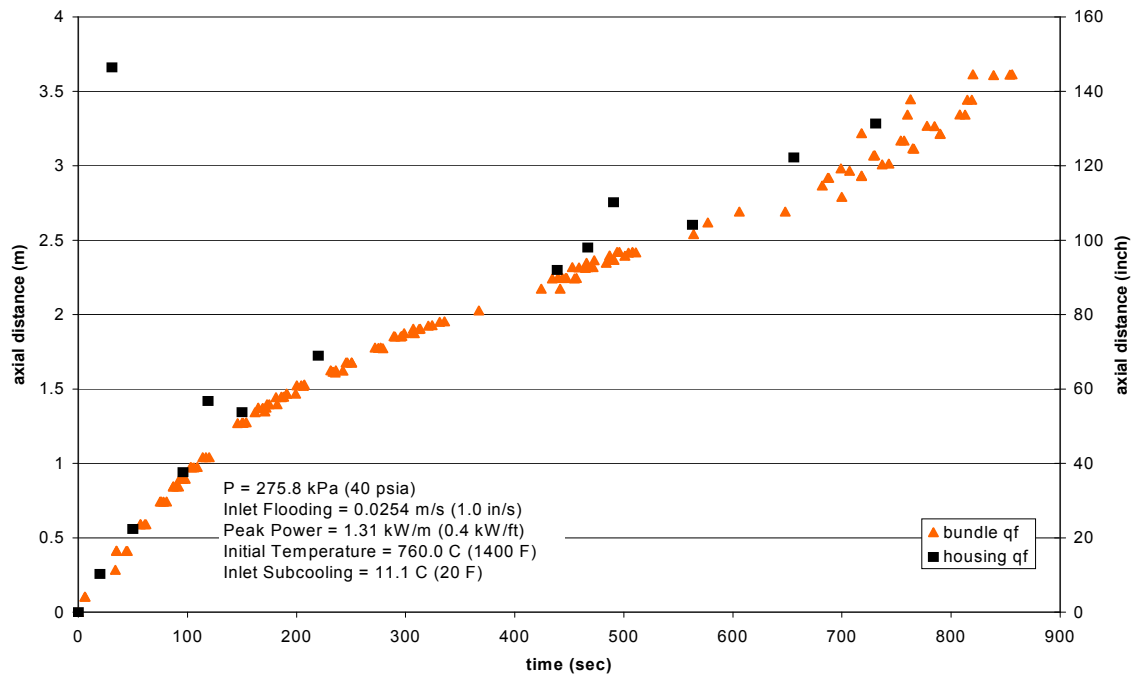


Figure 3.14 Rod and Housing Quench Front, Experiment 1383.

3.3 RBHT Mass Balance

3.3.1 Introduction

As part of the validation of the experiments performed at the RBHT test facility, it was necessary to perform a mass balance using the experimental data. A Fortran program was written to read the output data files and perform the mass balance calculations. The program incorporates steam tables used for calculating density and is input-deck driven, which allows for flexibility in changing key parameters such as the facility dimensions. Finally, the program outputs the finished mass balance information for easy plotting and analysis.

3.3.2 Methodology

In order to calculate the mass balance for the rod bundle test loop it is necessary to determine the locations where mass is stored and where mass flow rate measurements should be taken. For the rod bundle test loop, the elements needed to make up the mass balance are summarized as follows:

$$\left\{ \begin{array}{l} \text{Mass Storage} \\ \text{in the Bundle} \end{array} \right\} + \left\{ \begin{array}{l} \text{Drain \& Carryover} \\ \text{Tanks Mass Storage} \end{array} \right\} + \left\{ \begin{array}{l} \text{Upper Plenum} \\ \text{Mass Storage} \end{array} \right\} + \left\{ \begin{array}{l} \text{Steam Outlet} \\ \text{Mass Flow} \end{array} \right\} = \left\{ \begin{array}{l} \text{Inlet Mass} \\ \text{Flow} \end{array} \right\}$$

The mass storage in the bundle is calculated using the overall pressure drop in the bundle. The calculation can be done one or two ways. First, it can be done by simply considering the overall

pressure drop in the bundle and calculating the mass storage directly from this value using the cross-sectional area of the bundle. This approach calculates the mass storage, where there is no pressure drop correction due to acceleration or friction and may tend to be an over-estimate of the mass storage. The second method is more involved and includes a frictional pressure drop correction of the overall pressure drop. The frictional pressure drop component is made up of friction from both the rods and grids. Acceleration pressure drop is ignored.

It was found for the calculations when the frictional pressure drop was considered; it caused the mass storage in the bundle to be much lower than expected. This is probably due to models for grid and rod friction that were used and the calculation method. However, when only the overall pressure drop was used, the agreement between the expected and predicted bundle mass storage was improved. Although the frictional pressure calculation is still included in the mass balance code for completeness, for all results presented in this report the friction calculation was turned off.

The mass storage in each of the tanks (small and large carryover tanks and drain tank) was calculated from the liquid elevation, taken from a differential pressure cell, and the cross-sectional area of the tank. The differential pressure cells were calibrated at standard conditions and reported in inches of H₂O. The liquid head is taken directly from this reading and the mass storage is calculated as the product of the liquid head, the density at STP, and the cross sectional area of the tank.

The upper plenum mass storage calculation is done very differently from the rest. The reason for this is that there are no direct indicators of the liquid level in the upper plenum. Consequently, an estimate of the liquid level must be made. To achieve this, the upper plenum is assumed to begin filling when the large carryover tank has already filled. Also, the liquid flow rate into the plenum is assumed to be constant and equal to the flow rate into the large carryover tank for the few seconds before it is filled. For the mass balanced performed, the estimate fits the expected values quite well.

When the upper plenum fills liquid overflows into the steam separator drain tank, as indicated by an increase in the rate at which the tank is filling. This additional flow into the drain tank is assumed to be at the same rate at which the large carryover tank and upper plenum are filled.

Eventually, liquid carryover from the steam separator drain tank begins to fill the pressure oscillating tank. This tank does not have a level indicator, however, the liquid is drained from the tank and weighed when the test concludes. In performing the transient mass balance, it is assumed that the rate of liquid collection is the same as the rate at which the steam separator drain tank is filled. In some of the shorter reflood tests, no water was collected in the pressure oscillating tank.

The steam flow from the facility was calculated simply from the measured steam flow and the density at the exit. A thermocouple and a pressure transducer near the exit of the exhaust allowed the density to be calculated. Using the density and volumetric flow rate from the exhaust line, the mass flow rate could be calculated. In experiments where the exhaust flow meter was over-ranged, for example 1143, a calculation was performed using a relationship of pressure drop to flow rate developed from other experimental data. The pressure drop data was then used to calculate an exhaust flow rate.

Finally, each of the mass accumulations calculated so far must sum together to equal the mass flowed into the bundle at the inlet. For some experiments the inlet mass flow was calculated using the level and density of the water in the supply tank. (This method was used rather than the direct measurement of flow rate because of an error found in the inlet flow meter reading. Although the problem with the flow meter did not emerge until later in the test series, each test was re-calculated using the supply tank measurement). The change in the mass storage of the supply tank is equal to the mass injected into the bundle. The mass storage in the supply tank is calculated the same as the mass accumulation in the carryover and drain tanks. The liquid level is reported as inches of H₂O and the cross-sectional area and standard density are known. The only slight difference between this calculation and the calculation of the mass accumulation in the other tanks is that this tank has a cross-sectional area that varies with elevation. A table of cross-section area was used in the program to determine the tank cross-sectional area depending on the liquid elevation.

The mass balance must be concluded when either the drain or large carryover tank is filled. After this point, an accurate estimation of mass accumulation cannot be performed. The mass imbalance is calculated as the difference in the total inlet mass and the sum of all of the other contributions at then end of the experiment or when the drain or large carryover tank is filled. The percent of mass imbalance is calculated as this difference divided by the total inlet mass. In general, the mass imbalance was greater for higher flooding rate tests.

3.3.3 Summary of Mass Imbalances

Figure 3.15 gives a summary of the mass imbalance for each of the RBHT experiments. In general, the calculation of the mass balance agrees within five percent of the injected mass for most of the experiments. The exceptions are two experiments with more than 15 percent imbalance, and three experiments with a mass imbalance of more than 10 percent. The two experiments with the greatest imbalance were both high flooding rate cases (6 in/s). One possible explanation for this imbalance occurring for high flooding rates is that some liquid was able to pass through the steam separator and out of the facility with the steam flow or it was collected in the pressure damping tank and was not measured. The exit flow rate from the facility is calculated bases on the properties of steam, so this extra liquid flow would be unaccounted for. In addition, the short duration of these runs may cause additional error due to transient effects that would not be as pronounced in longer duration runs, such as liquid storage in facility piping and equipment. Individual mass balance calculations for each experiment are given in the next section and the details of the mass balance program.

Percent Mass Imbalance vs. Experiment Number

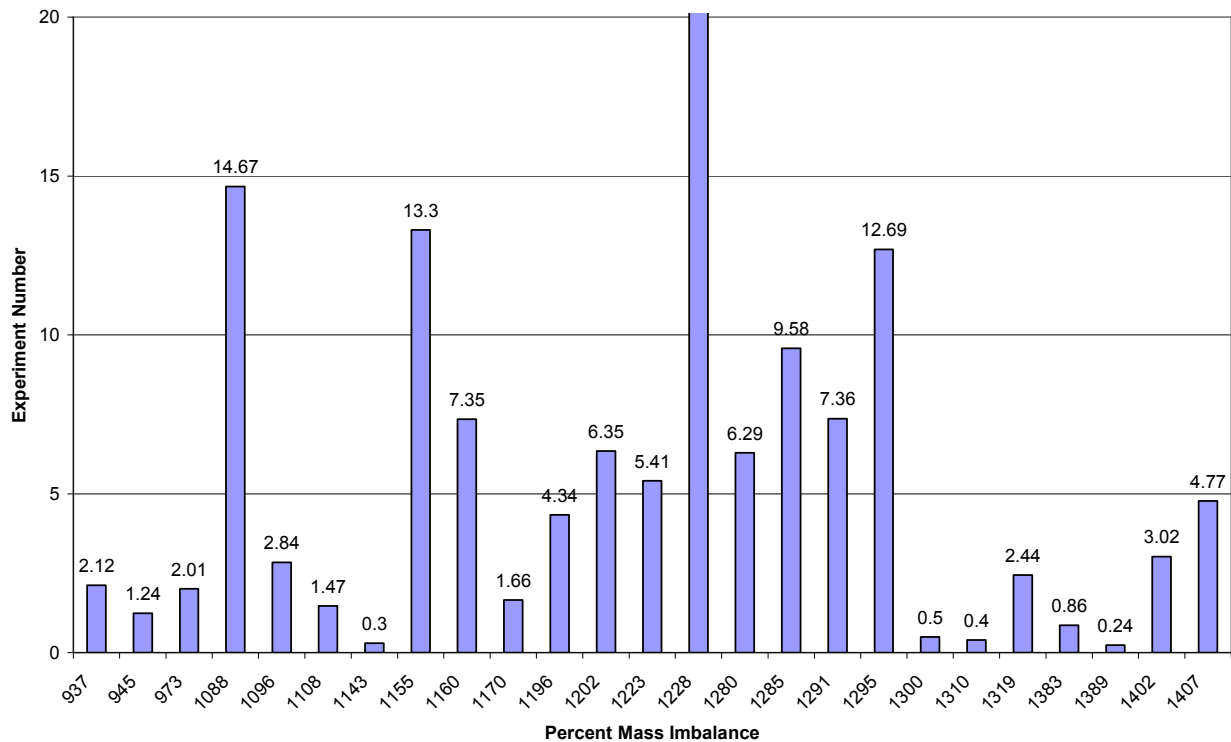


Figure 3.15 Summary of Mass Imbalances.

3.3.4 Transient Mass Balance

3.3.4.1 Bundle Inlet Mass

The bundle inlet mass flow is calculated from the level in the supply tank. Table 3.5 lists the parameters required for calculating the mass flow rate from the level in the supply tank. The supply tank cross-sectional area is taken from the facility design description report and is calculated as a function of elevation. A look-up and interpolation table is include in the code and follows the cross-sectional area profile in Figure 3.16.

Table 3.5 Supply Tank Parameters

Description	Location	Base Units	Fortran Variable
Supply Tank Level	Supply Tank (0-119 in)	in H ₂ O	suplvl
Supply Tank Area	Supply Tank	in ²	suparea
Supply Tank Pressure	Supply Tank	psig	suppr
Supply Tank Liquid Temp.	Supply Tank (bottom)	degrees F	suptmp
Supply Tank Liquid Dens.	Supply Tank (bottom)	lbm/ft ³	rhotk
Supply Line Pressure	Supply Line (after valve)	psig	suppr
Supply Line Liquid Temp.	Supply Line (after valve)	degrees F	suptmp
Supply Line Liquid Dens.	Supply Tank (after valve)	lbm/ft ³	rho

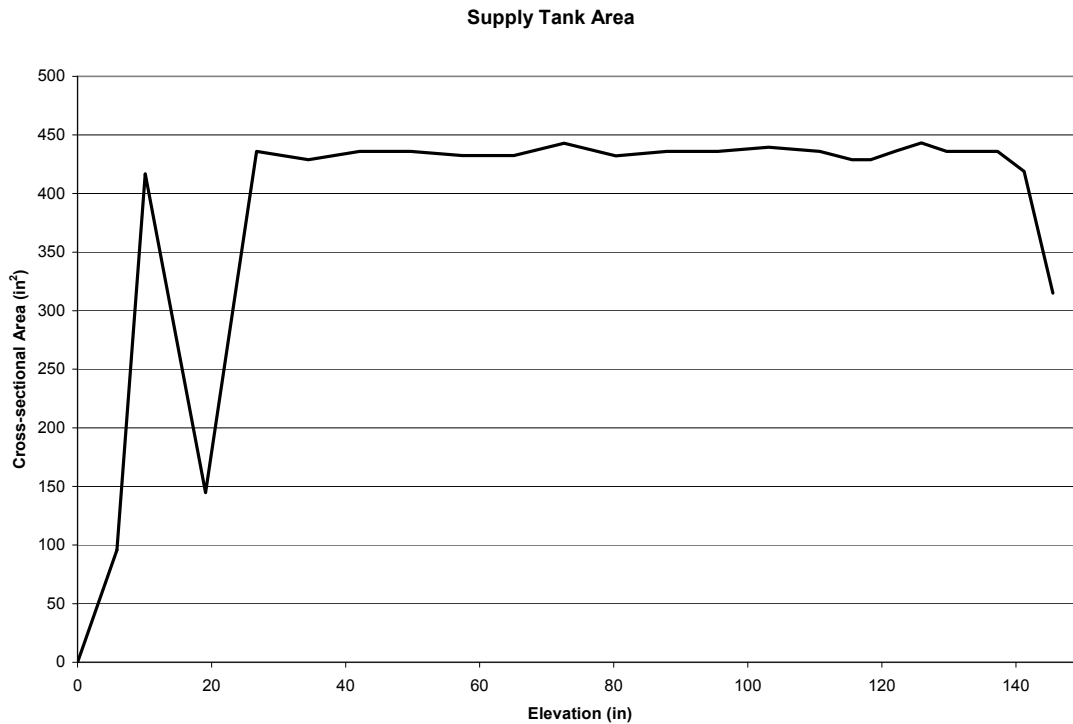


Figure 3.16 Supply Tank Cross-Sectional Area.

The temperature and pressure parameters were taken directly from the data acquisition output data and are used to calculate the density at the corresponding location using an algorithm based on “Properties of Water and Steam in SI-Units,” 2nd Revised and Updated Printing, Springer 1979, and written in 1998 by Bernhard Spang of *The Mining Company*.

In order to determine the flow rate from the supply tank, it is first necessary to determine the correct change in level. The level transducer for the supply tank measures the level as if it were water at STP. This is a *key point*. If the water in the supply tank is not at standard conditions, a correction must be made to calculate the correct change in level. This is done by correcting the level by the ratio of densities at STP and tank conditions respectively.

$$\Delta L_{\text{corrected}} = \Delta L_{\text{measured}} \cdot \frac{\rho_{STP}}{\rho_{\text{tank}}} \tag{3-29}$$

Next, multiplying this corrected level change by the cross sectional area of the tank at that elevation will give the volumetric displacement.

$$\Delta V = \Delta L_{\text{corrected}} \cdot A_{\text{tank}}(x) \tag{3-30}$$

Since the volume is coming from the conditions in the tank, the mass displaced should be calculated from the density at that location.

$$\tilde{m} = \Delta V \cdot \rho_{\text{tank}} \quad (3-31)$$

Now, simplifying the expression for the mass, we see that the tank density is no longer considered.

$$\tilde{m} = \Delta L_{\text{measured}} \cdot \rho_{\text{STP}} \cdot A_{\text{tank}}(x) \quad (3-32)$$

This mass represents the additional mass supplied over the length of time that ΔL is determined. The level is reported as in H₂O, and the change in level gives the mass decrease in the tank over time. The decrease in supply tank mass is the mass supplied to the bundle. The mass flowed into the bundle between two times is:

$$m_{\text{inlet}} = (\Delta P_{t-\Delta t} - \Delta P_t) \cdot \rho_{\text{STP}} \cdot A(z)_{\text{sup.tk.}} \quad (3-33)$$

where $A(z)_{\text{sup.tk.}}$ is the area of the supply tank, which is a function of the water level.

3.3.4.2 Steam Exhaust

The exhaust steam flow is reported in the output file as ft³/min.

The mass flowing from the exhaust (lbm) is given as:

$$m_{\text{exh}} = \rho_{\text{exh}} \dot{V}_{\text{exh}} \Delta T \quad (3-34)$$

where the density is calculated from the temperature and pressure at the exhaust.

3.3.4.3 Large and Small Carryover Tanks and Drain Tank

The mass storage (lbm) in the tanks is calculated by the liquid head in the tank and the cross-sectional area of the tank. The liquid head is reported as inH₂O and the density of reference is the density at STP. Therefore, the mass of liquid in the tank is simply calculated as:

$$m_{\text{tank}} = \Delta P_{\text{tank}} \rho_{\text{STP}} A_{\text{tank}} \quad (3-35)$$

This mass will be cumulative at each time. This calculation is done for the small and large carryover tanks and the drain tank.

3.3.5 Mass Storage in the Bundle

To calculate the mass storage in the bundle the elevation pressure drop must be isolated from the overall pressure drop. The acceleration pressure drop will be ignored, so the frictional

pressure drop across each grid and for the rods must be calculated. In order to do this, the quench front information must be entered to the code in the form of an input deck with as few or as many points as is necessary to describe the quench front behavior. The code then uses those points to generate a polynomial of the desired order to describe the quench front elevation over time. Using this polynomial, the code determines at each time step whether the quench front has reached any given grid location. If the quench front has not reached the grid, the pressure drop is calculated for that grid.

First, the velocity must be found so that the Reynolds number can be calculated. This is done using the exit volumetric flow rate.

$$V = \dot{V}_{exit} \frac{\rho_{exit}}{\rho_{vap} A_{grid}} \quad (3-36)$$

where

$$A_{grid} = 0.877 A_{bundle}$$

The Reynolds number can now be calculated.

$$Re = \frac{\rho_{vap} V D_h}{\mu_{vap}} \quad (3-37)$$

The k value for the grid is taken as a polynomial function of Reynolds number.

$$k_{grid} = -6.965 \times 10^{-14} Re^3 + 5.222 \times 10^{-9} Re^2 - 1.456 \times 10^{-4} Re + 3.249 \quad (3-38)$$

The frictional pressure drop over the grid can now be calculated by

$$\Delta P_{grid} = \frac{k_{grid} \rho_{vap} V^2}{2 g_c} \quad (3-39)$$

The pressure is taken at the location closest to the grid and the temperature is taken as the largest of the three grid thermocouples in the flow.

The frictional pressure drop over the rods is calculated by a correlation by Wantland (Ref. 2) which gives the rod friction factor as

$$f = \frac{0.44}{Re^{0.39}} \quad (3-40)$$

Then, the rod frictional pressure drop is

$$\Delta P_{rods} = f \frac{L}{D_h} \frac{\rho_{vap} V^2}{2g_c} \quad (3-41)$$

Where L is the length of the rods above the quench front.

The elevation pressure drop is calculated by subtracting the frictional pressure drops from the overall pressure drop.

$$\Delta P_{elev} = \Delta P_{tot} - \sum \Delta P_{grid} - \Delta P_{rods} \quad (3-42)$$

Finally, the mass storage in the bundle is calculated by

$$m_{bundle} = A_{bundle} \Delta P_{elev} \frac{g_c}{g} \quad (3-43)$$

A sample of mass balance calculation is presented in Figure 3.17. For the valid experiments, the results of the mass balance calculations are presented in Quick Look Reports.

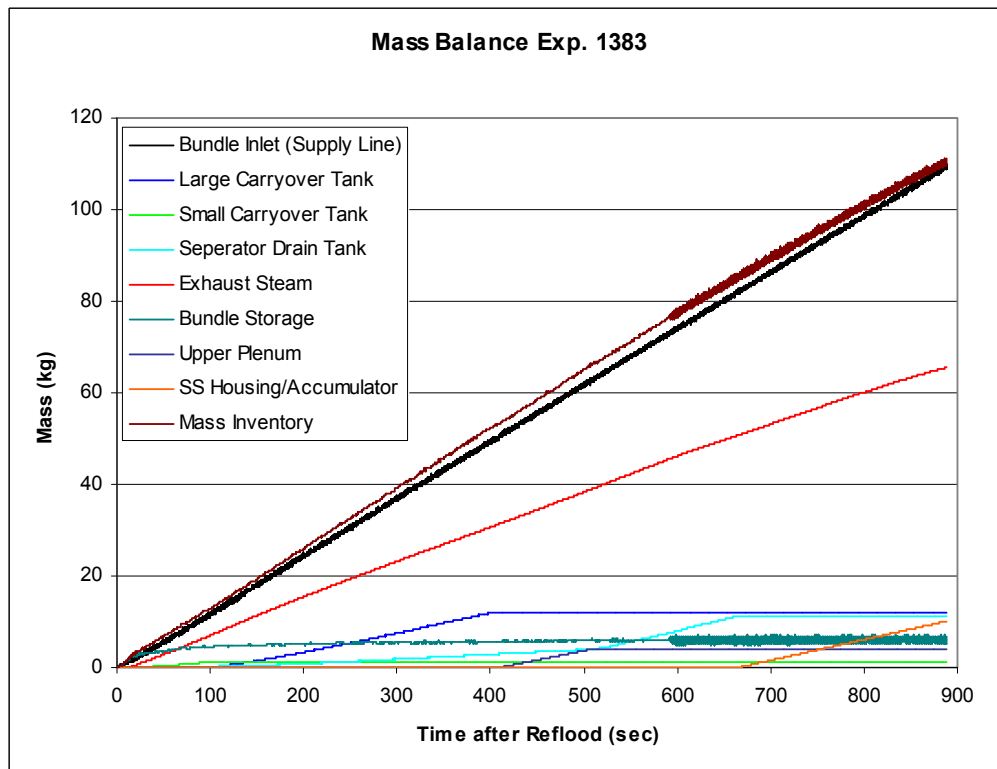


Figure 3.17 Mass Balance Plot for Experiment 1383.

3.4 Droplet Measurements

3.4.1 Droplet Measurement Instrumentation

The method of analyzing the droplet distributions in the rod bundle involves the use of a system known as VisiSizer, shown in Figure 3.18 and Figure 3.19, which is capable of real-time analysis of droplet size and velocity distributions. The system consists of a high-resolution digital camera, infrared laser, data analysis software, and associated computer and control equipment.

The camera, a Kodak Megaplug™ digital camera, has a resolution of over 1.0 megapixels. The laser system incorporates an infrared beam of wavelength 805 nm and is capable of pulsing at frequencies up to 1000 Hz. The laser can also pulse twice during a single camera frame to produce a double image used in determining velocity information. The beam of the laser is scattered with an opaque sheet of plastic to produce uniform background lighting for imaging. The system captures high-resolution images of the injection streams and analyzes the images at a rate of about 7 frames per second, identifying droplets as dark images in front of the laser-illuminated scattering sheet. The diameter of each droplet is determined automatically by referencing the number of dark pixels in the droplet image to the pixel area of a calibration circle.

A variety of user-defined parameters control the counting of the droplets, including focus rejection and sphericity criteria. Those data that do not meet the user set criteria are rejected. Focus rejection is determined by considering the sharpness of the droplet image by quantifying the intensity gradient at the outer edge of the droplet. In addition, the droplet analysis duration can be controlled by elapsed time, number of frames, or number of droplets counted. The software also calculates real-time statistics such as the mean and Sauter-mean diameters as well as displays the diameter distribution and, if applicable, the velocity distribution. Velocity is determined by double-pulsing the laser to capture the motion of a droplet. Analysis of the velocity is done automatically using criteria such as direction of motion, velocity range, and size matching.

The test setup for this analysis involves positioning the camera such that the view is through the quartz windows on the sides of the facility housing. The laser is placed opposite to the housing such that it provides a backlighting through the rod bundle. The size of the area imaged is large enough for only two subchannels to be analyzed for each position of the camera. A general schematic of the camera setup is shown in Figure 3.18.

It can also be seen in Figure 3.18 that the size of the probe volume will not be bounded by the edges of the rods at the focal plane. The width of the focal plane will be smaller than the gap size due to the parallax of viewing through the depth of the rod bundle. Figure 3.19 is an example of the image produced when viewing through the bundle, where the black images are the heater rods and the light image is the gap between the rods. The center of the image is the row of rods directly in front of the camera and the white regions are the row of gaps on either side of the rod. The width of the probe volume will be a function of the distance of the camera from the rod bundle. It is also important to note that fuzzy borders produced by out-of-focus rods in the image decrease the width of the probe volume even more. The variation of the gap size in the image is due to the difficulty in aligning the camera to a high degree of precision. For

the experiments presented here, the width of the focal plane is approximately 2.16 mm (0.085 in), which is about 70 percent of the overall gap width.

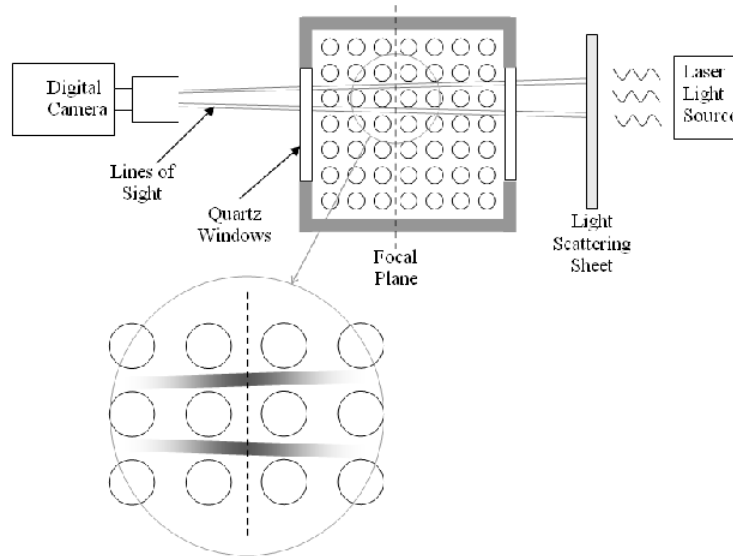


Figure 3.18 General Schematic of the Imaging System.

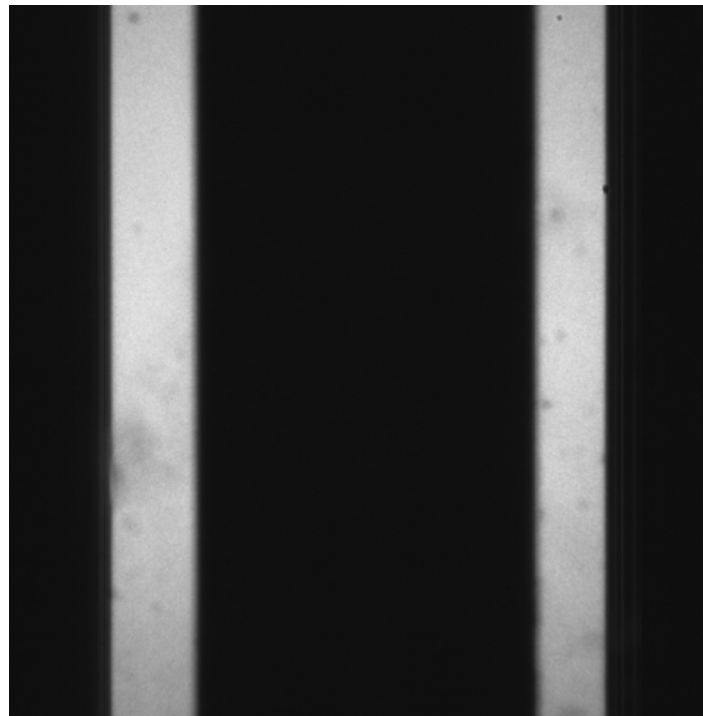


Figure 3.19 Typical VisiSizer Image Through the Rod Bundle (No Droplets Present).

The depth of the probe volume is also dependent on the distance of the camera from the bundle, but more directly on the focus rejection setting. The focus rejection setting is used to

reject droplets that appear out-of-focus due to their distance from the focal plane. In the experiments presented here this depth is approximately 5 mm.

The imaging system is calibrated using a small calibration reticule. The system is trained and focused on the reticule which is attached to a quartz window on the housing. Using the known size of the calibration circles on the reticule, the distance can be determined between the camera and the quartz window using a calibration curve that was developed. The camera can then be focused on the center of the desired subchannel in the bundle by adjusting the focus setting to the desired new distance from the camera.

A very detailed set of characterization and calibration bench tests separate from the rod bundle experiments were performed on the VisiSizer system. These bench tests helped determine the effects of the various rejection parameters on the droplet data acquisition as well as define the functional range and effectiveness of the system.

3.4.2 Droplet Size Measurements

For each test in the matrix a series of droplet measurements were taken at a single elevation. Runs were divided into ten-second periods in which droplet sizes were measured. For each of the ten-second period statistics were performed and the results were plotted as a function of both time and the quench front elevation.

It should be noted that the droplet diameters measured in these experiments are lower than those found in the FLECHT-SEASET series of tests. A number of causes may have contributed to a smaller droplet diameter for the RBHT tests.

The bias of the measuring technique to smaller droplets can be caused by the difference in behavior of large droplets compared to small droplets. First, the image of a large droplet is more likely to be overlapping with the image of a heater rod. The VisiSizer system is not able to determine the size of a droplet that is touching a rod because the entire droplet is not visible and it cannot distinguish the droplet image from that of the rod. In addition, images of larger droplets are more likely to be overlapping with images of other droplets. If the two droplet images are overlapping and offset, then both droplets in the overlapped area will be seen as a single droplet and will be rejected due to the sphericity criteria. Finally, larger droplets may also tend to be less spherical than small droplets. This causes the large droplets to be more likely to be rejected by the sphericity criteria even if it is in-focus and not overlapping any other droplet images.

3.4.3 Droplet Size and Elevation

The size of the droplets present in the rod bundle is dependent on the elevation for two reasons. First, droplets will tend to evaporate as they travel upward in the bundle with the superheated steam flow. Also, the droplets may impact on spacer grids and shatter into smaller droplets. These effects can be seen on the diameter distributions of the droplets measured with the VisiSizer system.

In the preliminary shakedown reflood testing, the VisiSizer system was used to determine the effect of spacer grids on the diameters of droplets. The elevations within the bundle were approximately 2.74 m (108 in) and 2.90 m (114 in), with a grid located at about 2.79 m (110 in).

The bundle was pressurized to 1.38 bar (25 psia) and the reflooding rate was set to 25.4 mm/s (1 in/s). The injected water was 339 degrees K (150 degrees F) subcooled.

The diameter distributions obtained from the two locations can be seen in Figure 3.20. It can be seen that the droplet distribution changes shape from upstream to downstream of the grid, and that the mean size decreases. As had been done in the FLECHT-SEASET series of tests, the data from Figure 3.20 was fitted to a log-normal distribution as shown in Figure 3.21. The figure shows the log-normal fit for the distributions upstream and downstream of the grid in the same manner as Figure 3.20. The log normal distribution curves show more dramatically the effect of spacer grid on droplet breakup.

The arithmetic mean diameters for the droplets upstream and downstream of the spacer grid are 0.64 and 0.45 mm (0.025 and 0.018 in) respectively, which represents a 29 percent decrease in the mean size of the droplets.

A series of separate effects tests were performed on an individual grid strap with individual droplets impinging on a thin strip of metal simulating a grid strap. There have also been laser-doppler experiments by Lee et al (Ref. 7) and similar experiments by Clare (Ref. 8) to examine droplet breakup caused by spacer grids. Figure 3.22 shows a plot of drop breakup data for different drop size to grid strap thickness ratios as a function of drop impact Weber number. Figure 3.22 also shows the curve fit correlated to the data as a function of the drop diameter to strap thickness.

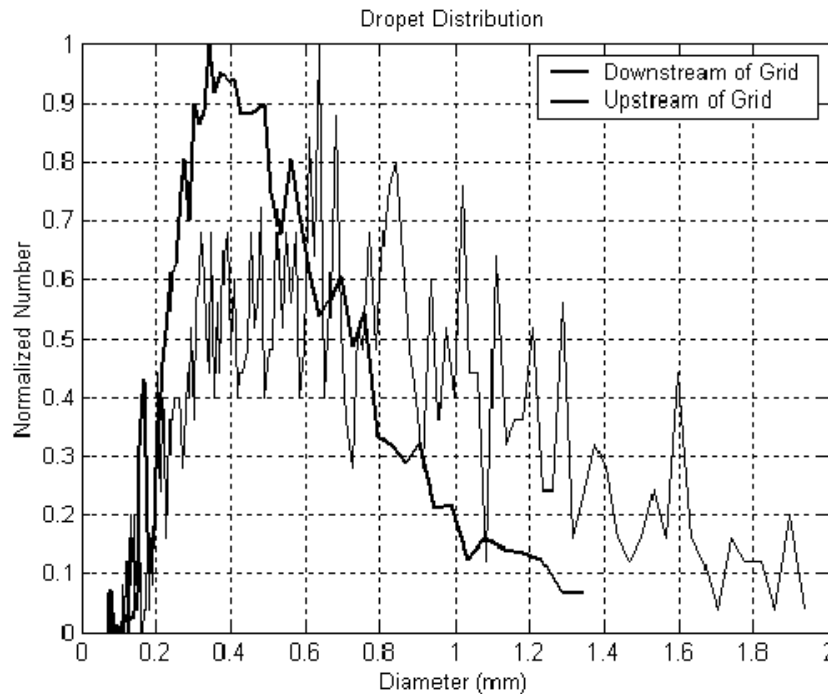


Figure 3.20 Normalized Droplet Distributions Upstream and Downstream of the Spacer Grid.

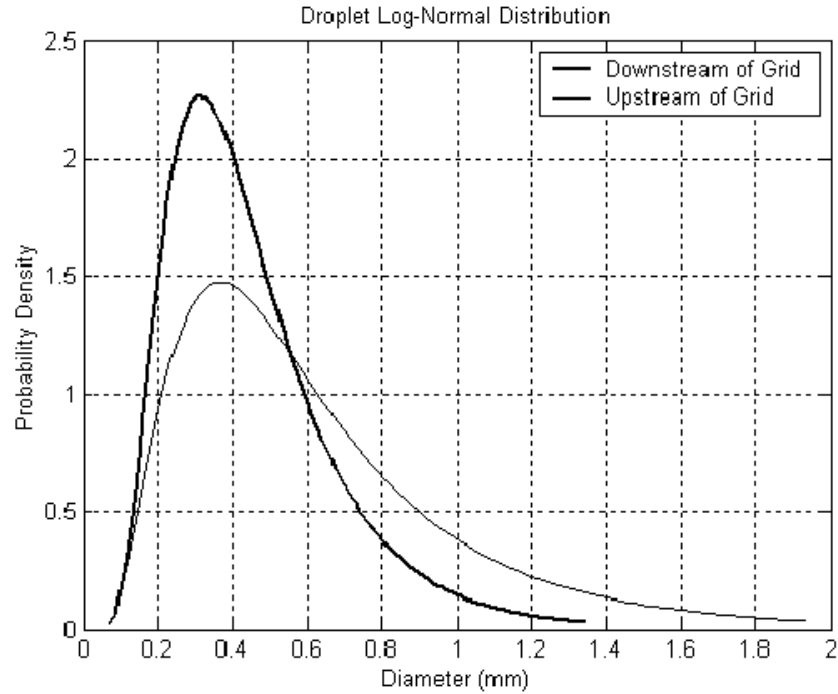


Figure 3.21 Probability Distribution Log-Normal Curve Fits Upstream and Downstream of the Spacer Grid.

For the RBHT experiments, the unshattered droplet diameter to grid strap thickness ratio (d_o/W) is 2.1. COBRA-TF computer code calculations were performed for this experiment, and the prediction for the velocity of the droplets upstream of the spacer grid is 1.78 m/s (5.85 ft/s). The corresponding droplet Weber number (using properties at saturation) is 55.24. Using the correlation form given in Figure 3.22 for droplet breakup, the resulting droplet diameter ratio (d_{en}/d_o) should be about 0.74. For this RBHT experiment, the ratio is 0.71, using the peak values from the distributions shown in Figure 3.21.

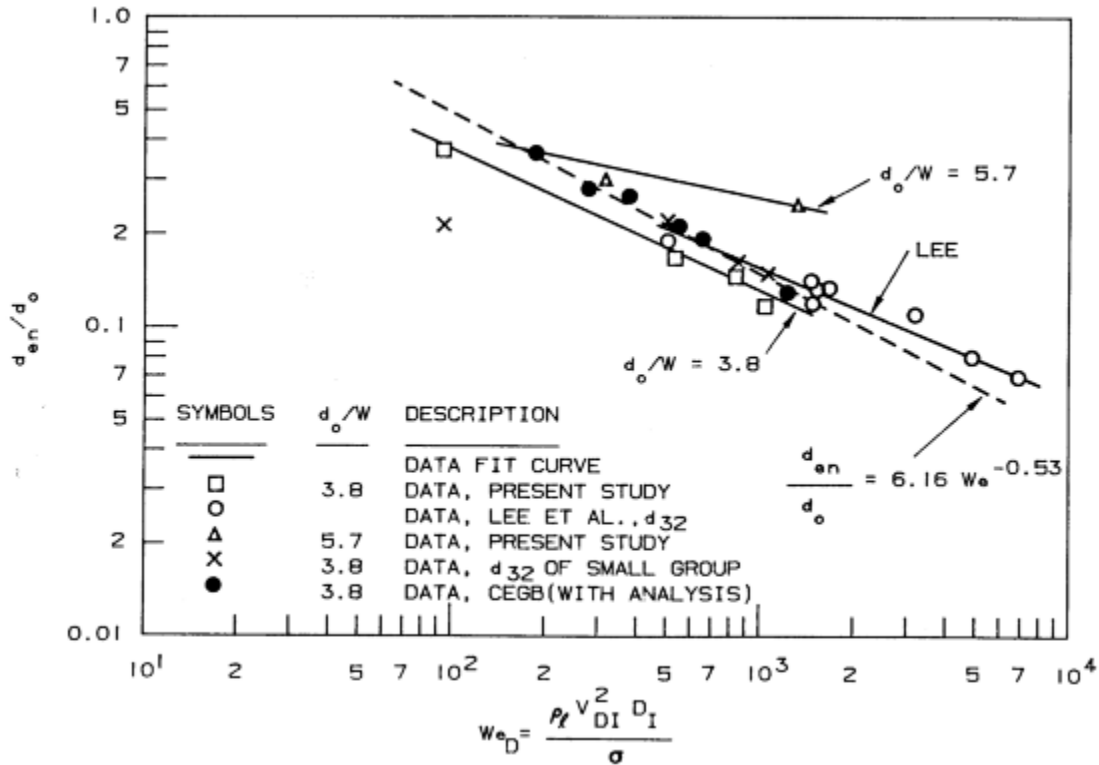


Figure 3.22 Drop Breakup Data as a Function of Droplet Impact Weber Number.

The change in droplet diameter due to evaporation was another factor considered in the FLECHT-SEASET tests. For droplet evaporation over a 76 mm (3 in) length, the droplet diameter was calculated to reduce by less than one percent. Therefore, it can be assumed that the overall change in droplet diameter due to evaporation would be less than two percent, which would not account for much of the 29 percent reduction in diameter over the grid span, as seen in Figure 3.21.

Additional evidence of droplet breakup can be seen in the results from the test matrix. A few examples of measurements of mean droplet diameter at different elevations are shown in Figure 3.23 through Figure 3.25. In these figures, one can clearly see that for tests with identical conditions, the droplet diameter decreases with elevation. Figure 3.23 should show the effect of a single grid on the droplet diameter. Figure 3.24, likewise shows the effect of a single grid, but over a greater length within the bundle. Figure 3.25 represents the effects of two spacer grids on the droplet diameter.

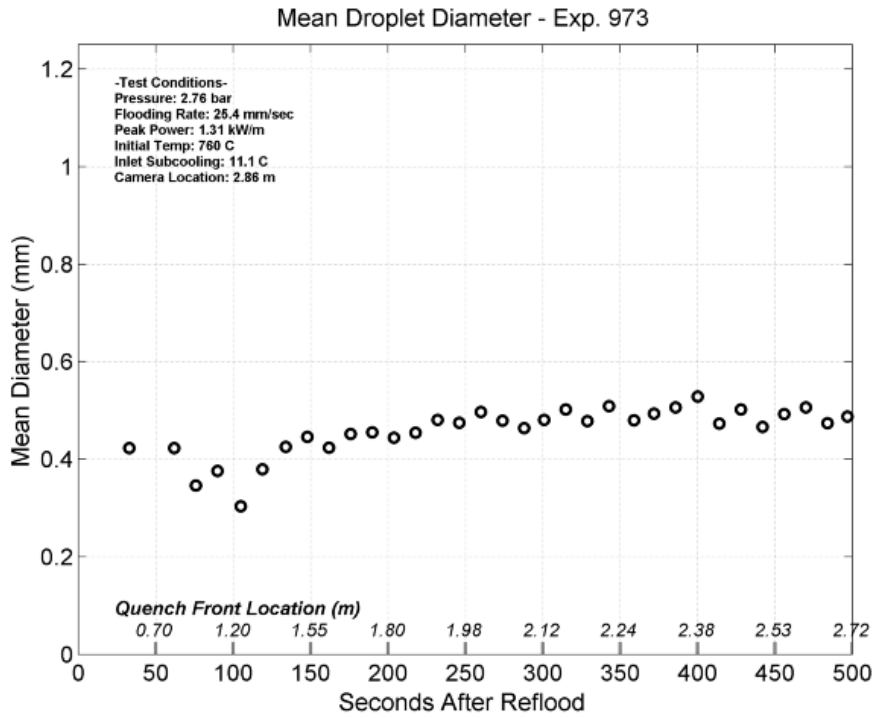
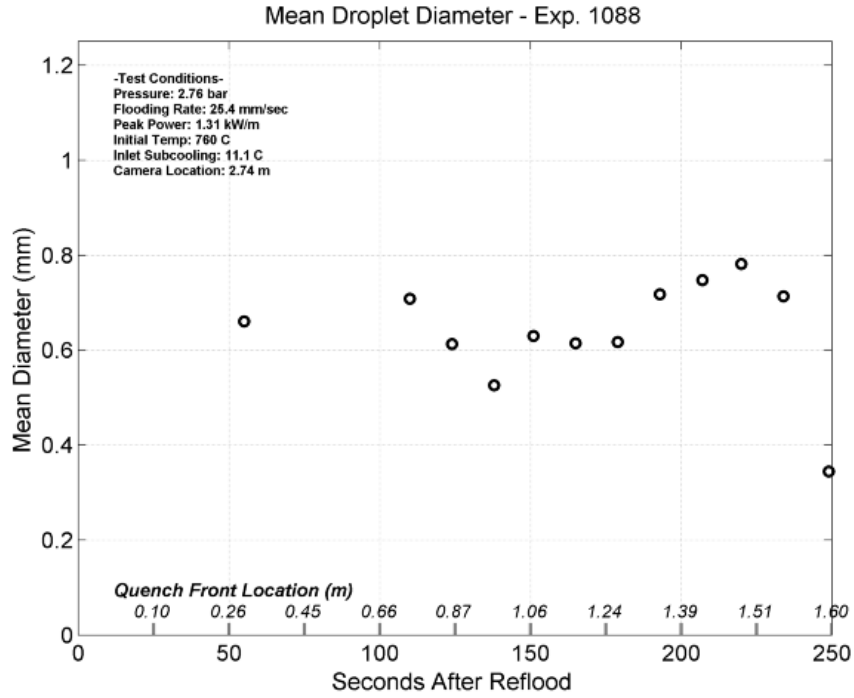


Figure 3.23 Comparison of Droplet Diameter from Experiment 1088 (2.74 m) and Experiment 973 (2.86 m).

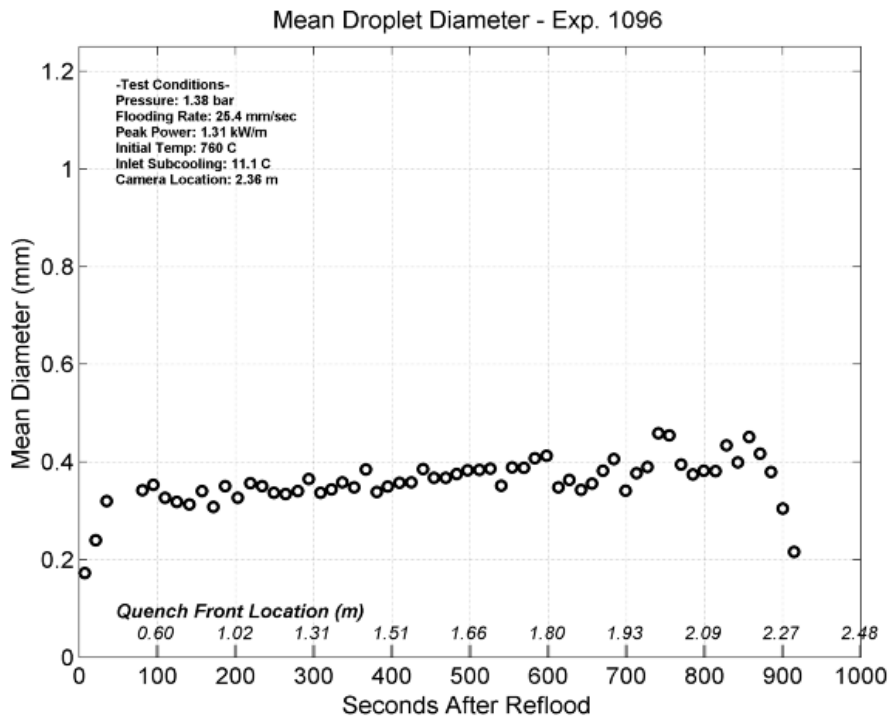
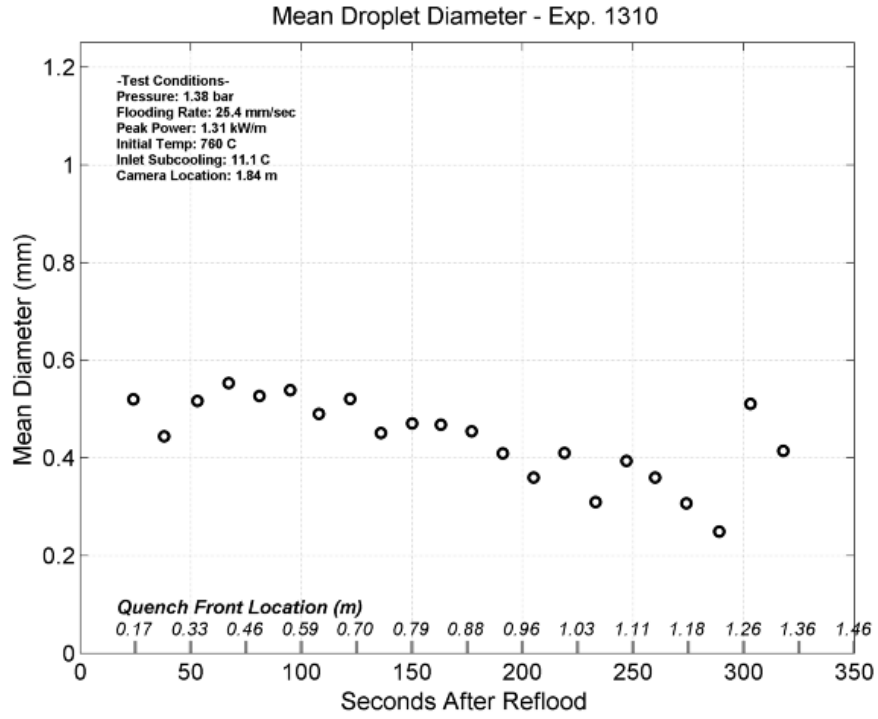


Figure 3.24 Comparison of Droplet Diameter from Experiment 1310 (1.84 m) and Experiment 1096 (2.36 m).

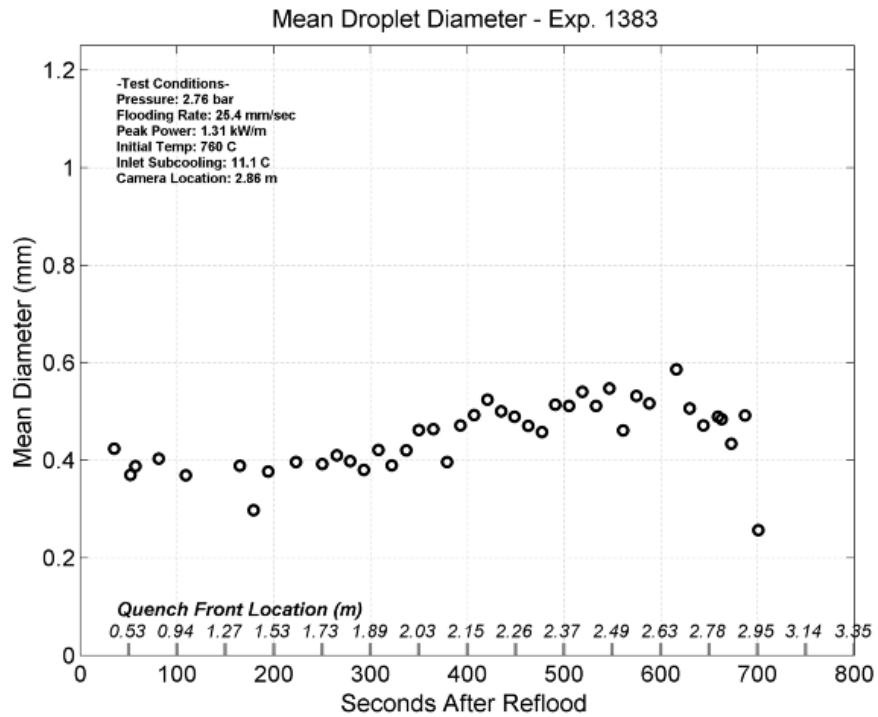
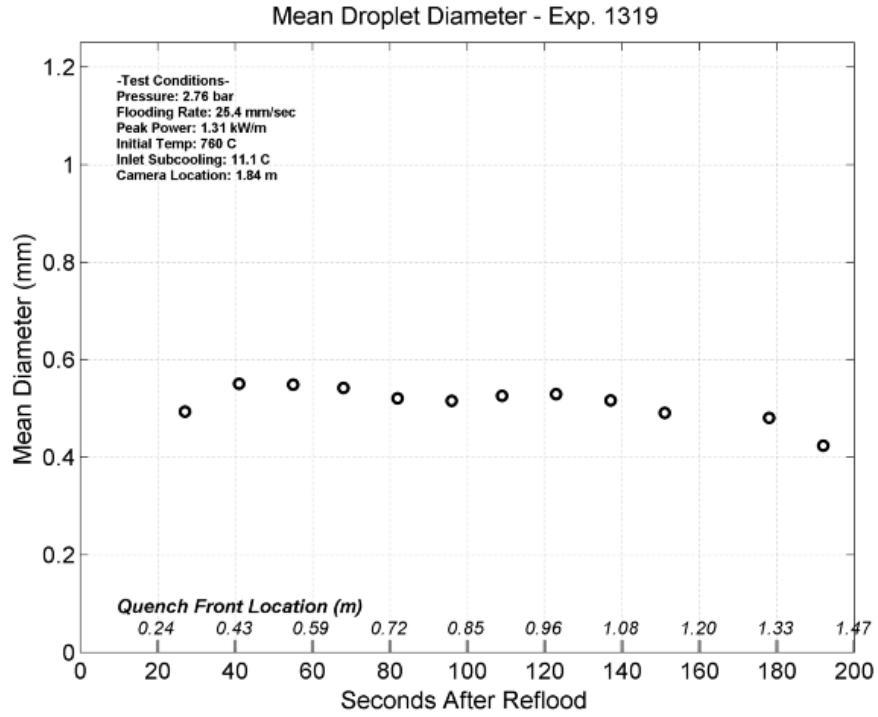


Figure 3.25 Comparison of Droplet Diameter from Experiment 1319 (1.84 m) and Experiment 1383 (2.86 m).

3.4.4 Droplet Velocity

Although the VisiSizer system is capable of obtaining velocity information, its ability to do so in the bundle geometry is severely limited. The system uses a double-pulse technique to capture a double exposure of the droplet images. The system then compares the location of similar droplets to determine the velocity. However, when using the double-pulse mode, contrast in the image is much less compared to the single-pulse mode. This makes the droplet recognition much harder since the droplets will not be much darker than the background. In addition, velocity mode tends to reject more droplets because the diameter rejection criteria are compounded by velocity rejection criteria. As a result, the velocity mode captures fewer droplets than diameter-only mode.

However, despite these limitations, some preliminary droplet velocity information was collected with the VisiSizer system during one of the early shakedown reflood tests. Figure 3.26 shows a plot representing the diameter and velocity distribution for an experiment where the camera was located at 2.74 m (108 in) and shows the resulting velocity and size distribution downstream of the grid.

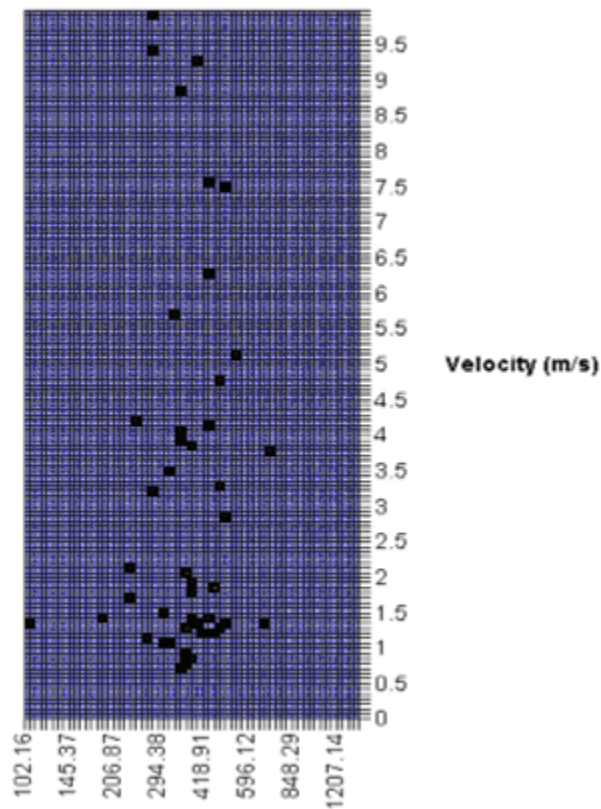


Figure 3.26 Size and Velocity Distribution Downstream of the Spacer Grid.

Figure 3.26 shows that there is very little correlation between droplet size and velocity for droplets immediately downstream of a spacer grid. This lack of correlation between drop velocity and size has also been observed in the FLECHT-SEASET experiments.

3.4.5 Calculation of Interfacial Area from Droplet Distribution Data

In order to estimate the droplet interfacial area in the dispersed flow region of the bundle, the digital droplet imaging data is used along with calculations of total liquid flow. In this section, the procedure for determining droplet interfacial area will be outlined.

The dispersed flow film boiling region is extremely complex since the dispersed droplets act as heat sinks and alter the vapor superheat temperature such that the film boiling is a two-step process. That is, heat is transferred to the continuous vapor phase from the heated walls, and then heat is transferred to the entrained water droplets by interfacial heat and mass transfer. As a result, the vapor temperature is a dependent parameter that is a function of both the wall heat transfer and the interfacial heat transfer. Therefore, the droplet interfacial area is a parameter of great importance when investigating these heat transfer processes.

The droplet data from the digital imaging system can be collected to give a time-line of droplet diameter information for a given location within the rod bundle. In addition, the Sauter mean diameter (SMD) can also be determined using the conventional formulation.

$$d_{32} = \frac{\sum (f_i d_i^3)}{\sum (f_i d_i^2)} \quad (3-44)$$

where

d_{32} SMD
 f_i fraction of droplet group i ,
 d_i diameter of droplet group i

The SMD represents the diameter of a particle whose ratio of volume to surface area is the same as the complete sample. The SMD is calculated over many time intervals in order to observe the trend in droplet size. For example, Figure 3.27 shows the SMD evolution for Experiment 1383.

The near flow of droplets is determined from the mass and energy balance program.

The total interfacial area of the droplets can be estimated from the total droplet volume using the calculated mass flow and density and the droplet SMD.

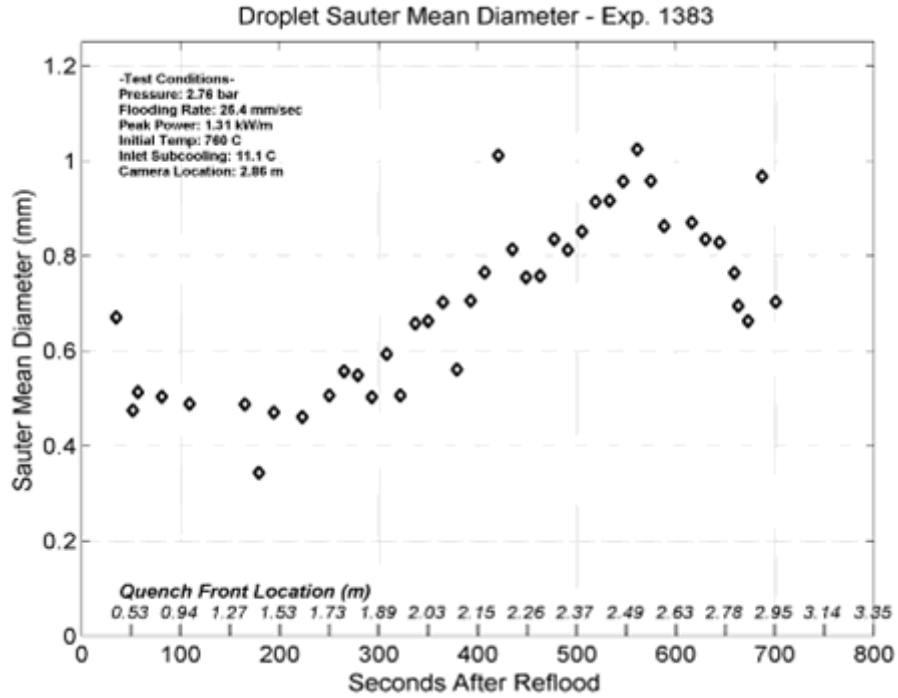


Figure 3.27 Sauter Mean Diameter Time History for Experiment 1383.

The volume of n droplets:

$$V = \frac{1}{6} \pi n \sum (f_i d_i^3) \quad (3-45)$$

where

f_i = fraction of droplet group i

d_i = diameter of droplet group i

Surface area of n droplets:

$$A = \pi n \sum (f_i d_i^2) \quad (3-46)$$

So, solving of area in terms of volume:

$$A = 6V \frac{\sum (f_i d_i^2)}{\sum (f_i d_i^3)} = \frac{6 \cdot V}{d_{32}} \quad (3-47)$$

which represents the simple formula for converting the total measured droplet volume into surface area using the SMD measurement.

Finally, this equation must be converted to a rate equation, since the reported parameter is rate of liquid mass. In addition, the mass rate is converted to a volume rate by the liquid density at saturation. The resulting rate of interfacial area because:

$$\dot{A} = 6 \cdot \frac{\dot{m}_{liq}}{\rho_{sat} \cdot d_{32}} \quad (3-48)$$

The mass rate for Experiment 1383 is shown in Figure 3.28. Using this formula at several times over the reflood transient, a curve representing the evolution of droplet interfacial area can be obtained, as shown in Figure 3.29.

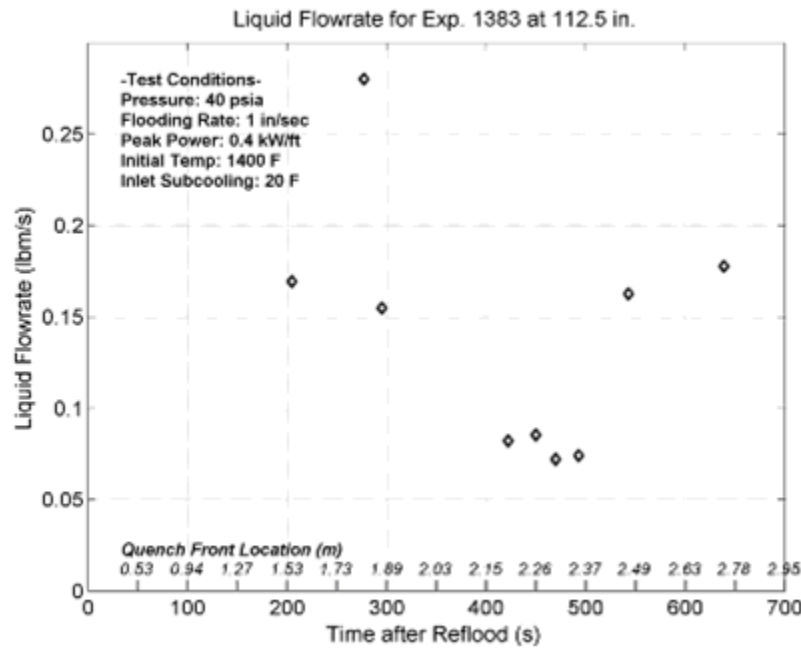


Figure 3.28 Liquid Flow rate for Experiment 1383.

3.4.6 Droplet Measurement Data for Individual Experiments

The droplet data and individual number of droplet counts are given in the Appendix A for each experiment in which data was obtained. The test run number, camera location, and test conditions are given on each plot. The data is taken as a function of time and the moving quench front location is also indicated on each plot. Drop mass diameter and Sauter mean diameters are also plotted.

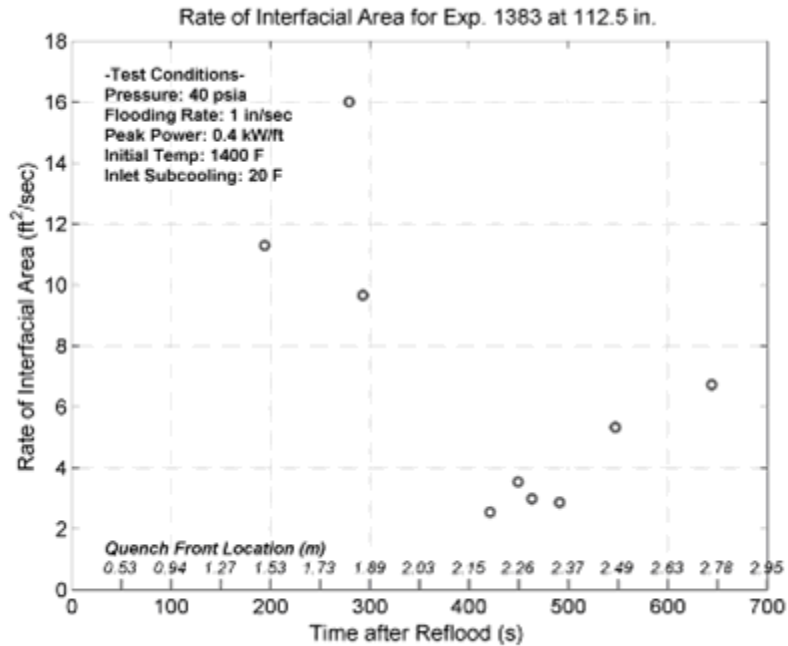


Figure 3.29 Rate of Interfacial Area for Experiment 1383.

3.5 References

1. Lee, N., Wong, S., Yeh, H.C., and Hochreiter, L.E., "PWR FLECHT-SEASET Unblocked Bundle, Forced and Gravity Reflood Task Data Evaluation and Analysis Report," WCAP-9891, February 1982.
2. Oxford Lasers. "HSI1000 Fast Illumination System," Operation Manual, Issue 2, Rev. 1 (1997), Oxford Lasers, Ltd.
3. Todd, Donald R., "Characterization of the VisiSizer Particle/Drop Sizing System," MS Thesis, Pennsylvania State University, 1999.
4. Lee, N., et. al., "PWR FLECHT SEASET Unblocked Bundle, Forced and Gravity Reflood Task Data Evaluation and Analysis Report," NUREG/CR-2256, Feb. 1982.
5. C.Y. Paik, L.E. Hochreiter, J.M. Kelly, R.J. Kohrt "Analysis of FLECHT-SEASET 163-Rod Blocked Bundle Data Using COBRA-TF", NUREG/CR-4166, 1985.
6. Yao, S. C., et al., "Dynamics of Droplets Impacting in Thin Heated Strips," submitted to National Heat Transfer Conference, Denver, 1985.
7. Lee, Richard S. L., et. al, "A Study of Droplet Hydrodynamics Across a Grid Spacer," NUREG/CR-4034, 1983.

8. Clare, A. J. and Fairbairn, S. A., "Droplet Dynamics and Heat Transfer in Dispersed Two-Phase Flow," CONF-8410331, 1985.
9. Rehme, K. "Pressure Drop Correlations for Fuel Element Spacers," Nuclear Technology, Vol. 17, January 1973.
10. Wantland, J. L., "Compact Tubular Heat Exchangers," TID 7529, Reactor Heat Transfer Conference (Pt. 1), Book 2, 1957.

4. CONCLUSIONS

A series of forced reflood heat transfer experiments has been completed in the RBHT Test Facility. The reflood heat transfer experiments which were performed provided additional and new data which has not been obtained in other rod bundle reflood tests. The new data included:

1. Detailed non-equilibrium vapor superheat temperature measurements along the axial length of the bundle, and immediately downstream of the spacer grids.
2. Spacer grid temperature surface measurements within the rod bundle at the different axial positions.
3. Detailed entrained droplet size measurements as observed between the heater rods both upstream and downstream of the spacer grids.
4. Detailed heater rod temperature measurements along the axial length of the rod bundle specifically downstream of the spacer grids.
5. Detailed pressure drop along the bundle to determine the spacer grid losses and void fraction distribution along the bundle length.
6. Liquid carryover measurements of the entrained liquid flow out of the bundle measured using both a small carryover tank and a large carryover tank such that detecting entrained water was faster.
7. Both liquid and steam flows from the bundle exit were measured such that a system mass balance could be performed on each test.

The RBHT reflood heat transfer experiments were specifically designed for use in Best-Estimate computer code validation efforts, not as tests to determine licensing limits. As such, these tests were designed with more complete instrumentation such that local heat transfer phenomena could be identified and quantified more accurately. The experiments were also designed for easier computer code modeling with a linear axial power distribution, no radial power gradient, and constant power rather than decay power. Using the constant power results in quasi-steady reflood tests of much longer duration such that it is easier to model and study the dispersed flow film boiling phenomena which is the heat transfer regime of interest.

The spacer grids used in these experiments are similar in design to prototypical PWR production mixing vanes grids found on most PWR fuel assembly designs. The heat transfer phenomena associated with the spacers observed in the RBHT Test Facility is expected to be similar to that of a commercial PWR. The spacer grids have a first order effect on the local heat transfer downstream of the spacer grid. The grids can re-wet, shatter entrained droplets, and enhance the convective heat transfer downstream. All these effects enhance the dispersed flow film boiling downstream of the grids resulting in lower measured heater rod temperatures downstream of the grids. This was clearly observable in the RBHT reflood heat transfer experiments.

The heater rod instrumentation has also been designed such that detailed axial quench front information can be obtained for comparisons to Best-Estimate computer codes. The quasi-steady nature of the experiments along with the extended reflood times due to the constant power which was used, provide a significant challenge to today's computer code predictions. The longer transients will provide an opportunity for errors in the calculations to accumulate and cause a deviation from the experimental data. The code developer will have a much clearer indication of which models are causing this deviation, since the tests are quasi-steady, such that they can more easily correct the problem. The RBHT reflood heat transfer experiments have provided new and needed data which can be used for Best-Estimate computer code development and validation.

APPENDIX A. TEST RESULTS

This appendix contains the tables and plots for the selected data of 25 valid reflood heat transfer tests performed at the RBHT Test Facility.

For each test run, the following tables and plots are presented:

- List of the run conditions
- Listing of the measurements for the selected thermocouples
- Upper plenum pressure
- Inlet liquid flow rate, outlet vapor flow rate
- Inlet flow temperature
- Bundle Voltage and Current
- Rod surface temperatures – calculated as described in Chapter 3, Section 1 at five selected locations, corresponding to steam probe locations and at the top section of the bundle
- Steam temperatures - data from 5 steam probes at the upper section of the bundle
- Grid temperatures for the top 3 spacer grids
- Heat transfer coefficients - calculated as described in Chapter 3, Section 1
- Heater rod quench data - calculations performed for this is described in Chapter 3, Section 2
- Droplet Measurements - described in Chapter 3, Section 4

In temperature, heat transfer coefficient, and quench front plots, time zero represents when the reflood starts.

RBHT - REFLOOD TESTS

SUMMARY SHEET

RUN NO: **937**

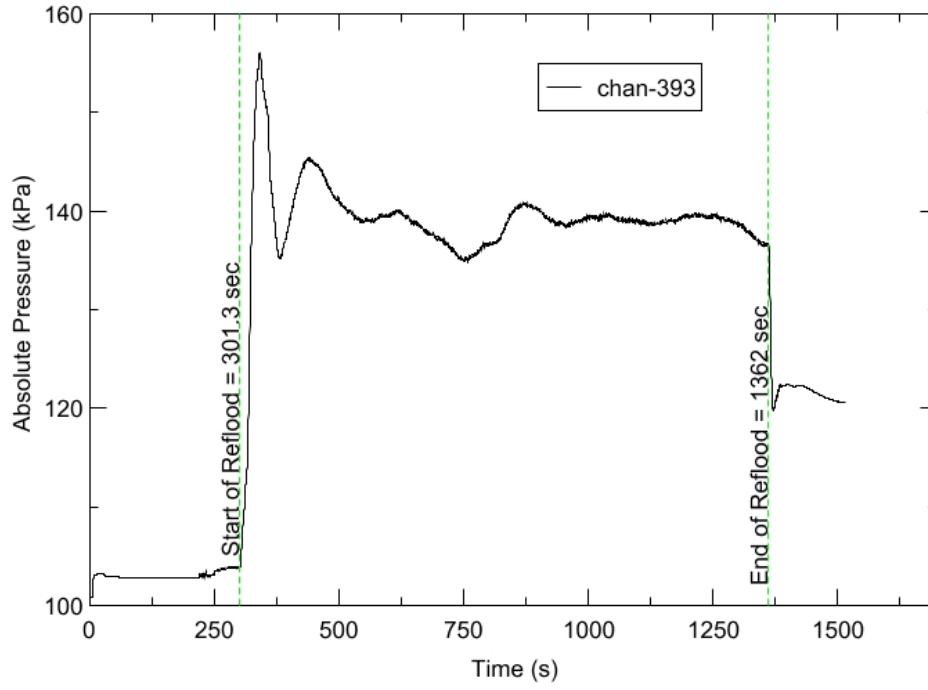
RUN CONDITIONS

Upper Plenum Pressure:	138 kPa (20 psia)
Initial Peak Clad Temperature:	1033 degrees K (1400 degrees F)
Rod Peak Power:	1.31 kW/m (0.4 kW/ft)
Flooding Rate:	0.0254 m/s (1 in/s)
Inlet Subcooling:	11 degrees K (20 degrees F)
Start of Reflood:	301.3 s
End of Reflood:	1362 s
Test Date:	5/13/2002
Comments:	No droplet data

Rod_Elevation	Channel Number	Temperature at Reflood (K)	Temperature at Reflood (°F)	Tumaround Time (sec.)	Tumaround Temperature (K)	Tumaround Temperature (°F)	Quench Time (sec.)	Quench Temperature (K)	Quench Temperature (°F)
B6_0.592m	148	691.42	784.86	15.95	719.63	835.65	90.45	537.15	507.19
B6_0.744m	149	712.94	823.61	17.45	743.74	879.05	119.45	555.1	539.49
B6_0.846m	150	745.7	882.58	19.45	781.38	946.79	136.95	571.83	569.6
B6_0.897m	151	755.42	900.07	18.95	793.09	967.88	147.45	572.53	570.87
C6_1.04m	137	801.34	982.73	24.95	846.15	1063.38	173.45	632.94	679.61
D5_1.27m	217	846.11	1063.3	24.95	891.1	1144.3	241.45	587.23	597.32
C6_1.34m	138	837.55	1047.9	26.95	890.22	1142.71	262.95	629.08	672.65
D5_1.37m	218	870.19	1106.65	30.95	927.33	1209.51	267.45	633.46	680.55
C6_1.39m	139	845.35	1061.94	30.95	901.52	1163.05	280.45	621.51	659.02
D5_1.45m	219	882.72	1129.21	31.95	942.27	1236.4	292.95	650.26	710.79
C6_1.47m	140	861.02	1090.15	33.95	918.6	1193.8	307.95	654.78	718.92
D5_1.52m	220	894.33	1150.11	37.45	957.87	1264.48	321.45	694.44	790.31
C6_1.62m	141	878	1120.71	99.95	971.96	1289.84	373.45	662.21	732.3
D5_1.68m	221	906.65	1172.28	99.95	1010.64	1359.47	388.45	684.78	772.92
D5_1.78m	222	896.63	1154.24	25.95	959.63	1267.65	430.45	629.49	673.4
D5_1.85m	223	923.24	1202.14	27.95	984.83	1313.01	451.95	682.74	769.25
C6_1.87m	142	903.57	1166.75	31.45	988.34	1283.33	473.95	680.62	765.43
D5_1.90m	224	931.23	1216.53	31.45	998.06	1336.82	472.45	708.15	814.98
C6_1.95m	144	917.29	1191.43	88.95	986.59	1316.18	507.95	656.98	722.87
C3_2.17m	178	966.31	1279.67	123.95	1075.68	1476.53	595.45	745.2	881.67
D4_2.24m	241	985.83	1314.8	122.95	1094.04	1509.58	652.45	594.39	610.21
D4_2.32m	242	991.53	1325.06	22.95	1052.94	1435.6	673.95	613	643.7
C3_2.35m	180	988.25	1319.17	22.95	1051.57	1433.14	649.45	669.43	745.29
D4_2.37m	243	1000.19	1340.66	23.95	1066.69	1460.36	689.95	623.79	663.14
C3_2.40m	181	990.08	1322.46	24.95	1057.6	1444	663.45	671.28	748.62
D4_2.54m	245	1022.57	1380.94	25.45	1096.41	1513.86	759.45	658.63	725.85
D6_2.62m	129	1015.62	1368.44	98.95	1097.11	1515.11	755.45	679.41	763.25
D6_2.69m	130	1009.67	1357.72	110.45	1110.45	1539.13	786.45	685.9	774.93
C3_2.76m	183	1009.1	1356.69	114.45	1100.57	1521.33	810.45	694.44	790.3
D6_2.87m	131	973.73	1293.03	20.95	1038.54	1409.68	846.45	666.09	739.27
D6_2.92m	132	954.9	1259.14	24.45	1025.81	1386.77	860.45	693.4	788.43
D6_2.97m	133	934.22	1221.9	25.95	1004.29	1348.04	876.95	708.26	815.18
D6_3.07m	134	904.49	1168.39	26.95	973.86	1293.26	897.95	689.48	781.37
E3_3.12m	197	899.34	1159.13	27.95	969.45	1285.32	954.95	647.89	706.52
D6_3.17m	135	868.24	1103.14	27.95	935.34	1223.92	919.95	689.15	780.78
D6_3.27m	136	824.13	1023.75	111.45	902.35	1164.54	940.45	671.4	748.83
D4_3.61m	248	642.5	696.81	113.45	723.07	841.83	1032.95	544.69	520.76

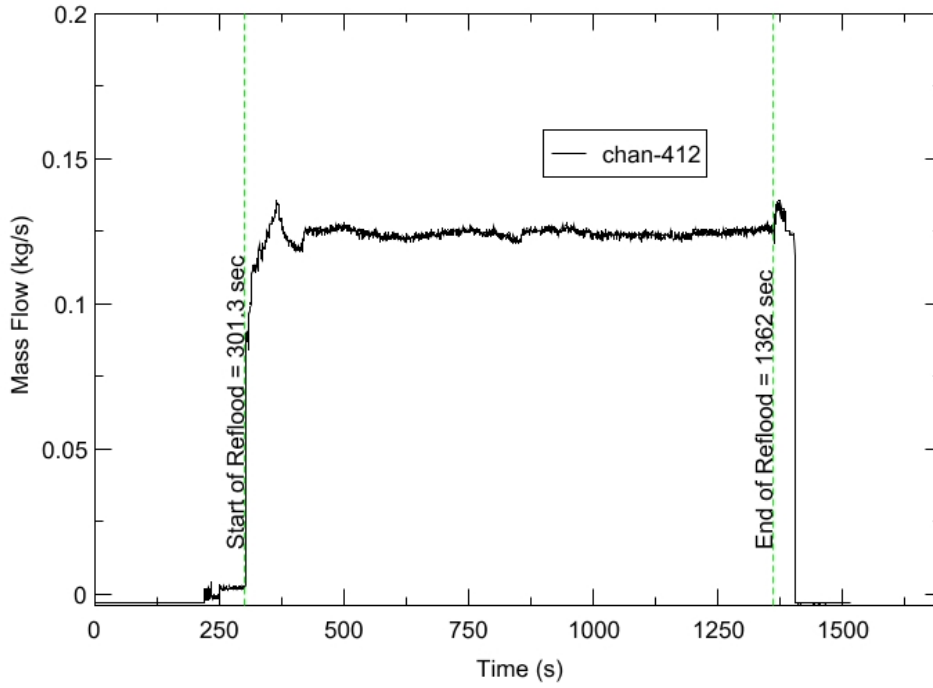
RBHT - TEST FACILITY

Upper Plenum Pressure vs. Time, Exp 937



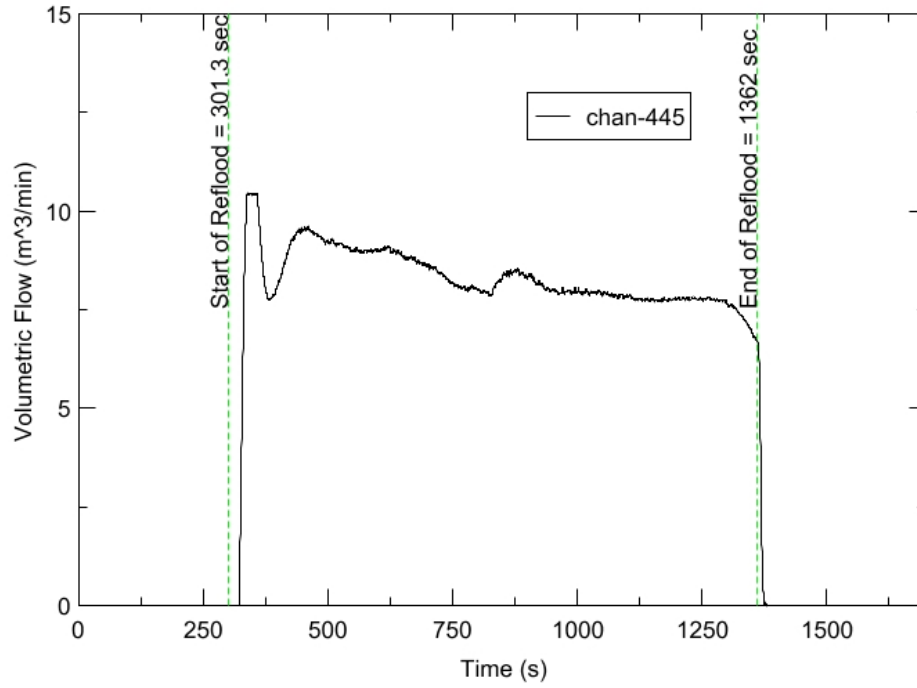
RBHT - TEST FACILITY

Inlet Flow vs. Time, Exp 937



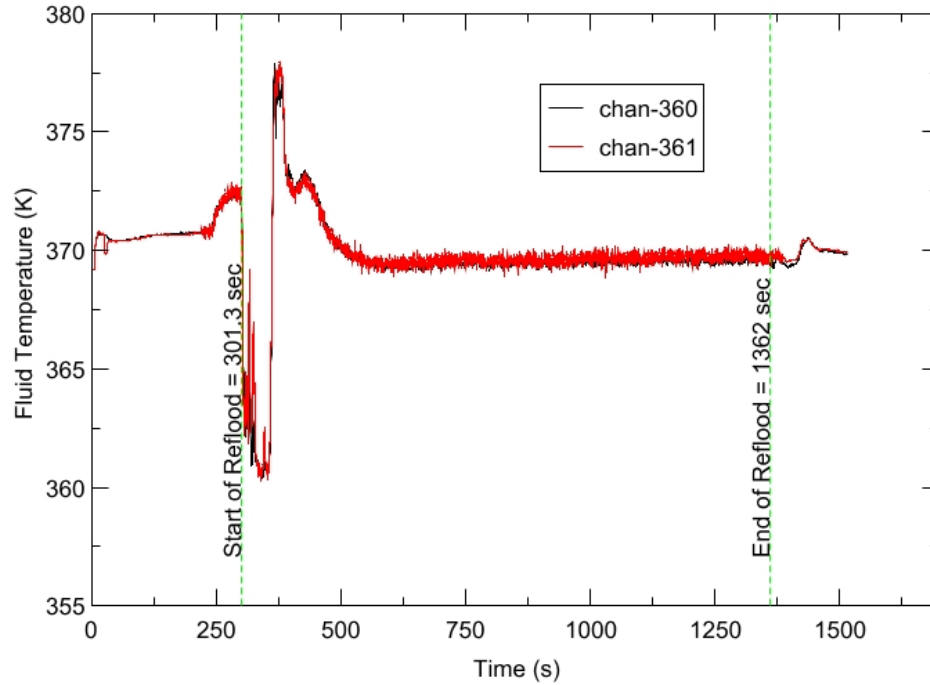
RBHT - TEST FACILITY

Steam Exhaust Flow vs. Time, Exp 937



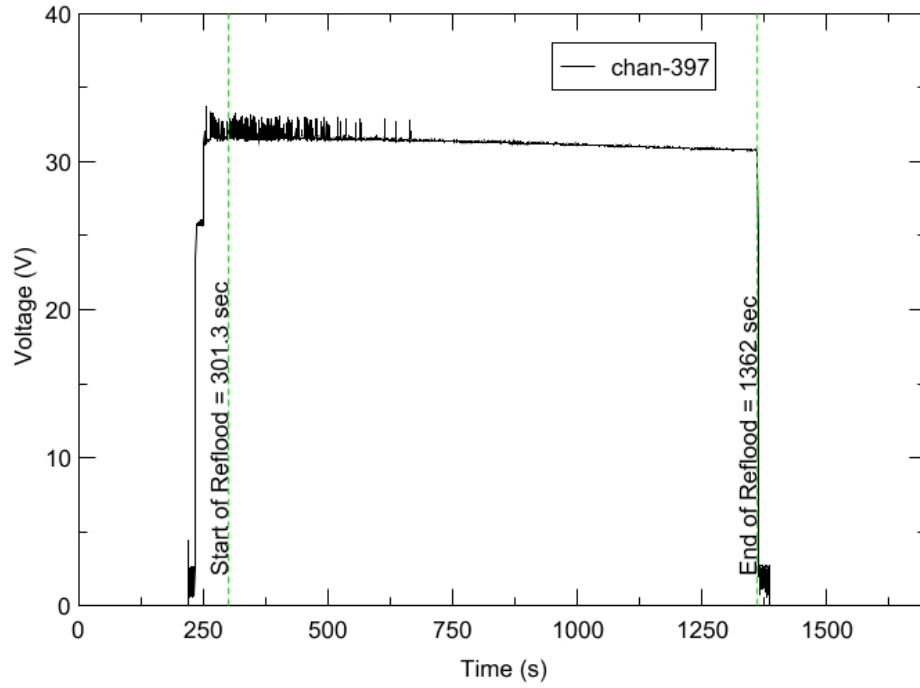
RBHT - TEST FACILITY

Inlet Flow Temperature vs. Time, Exp 937



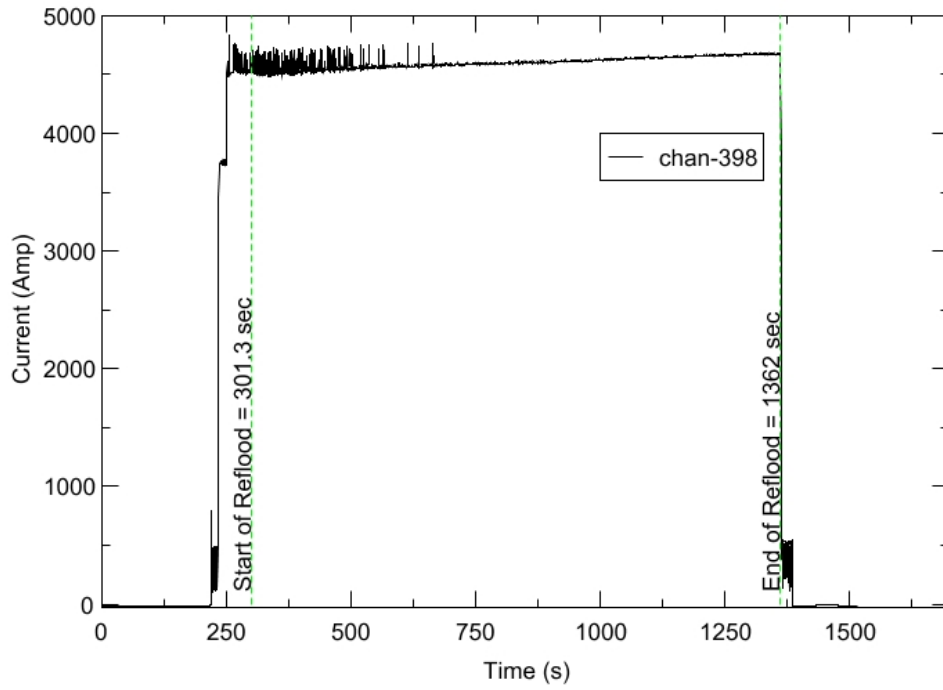
RBHT - TEST FACILITY

Test Section Voltage vs. Time, Exp 937

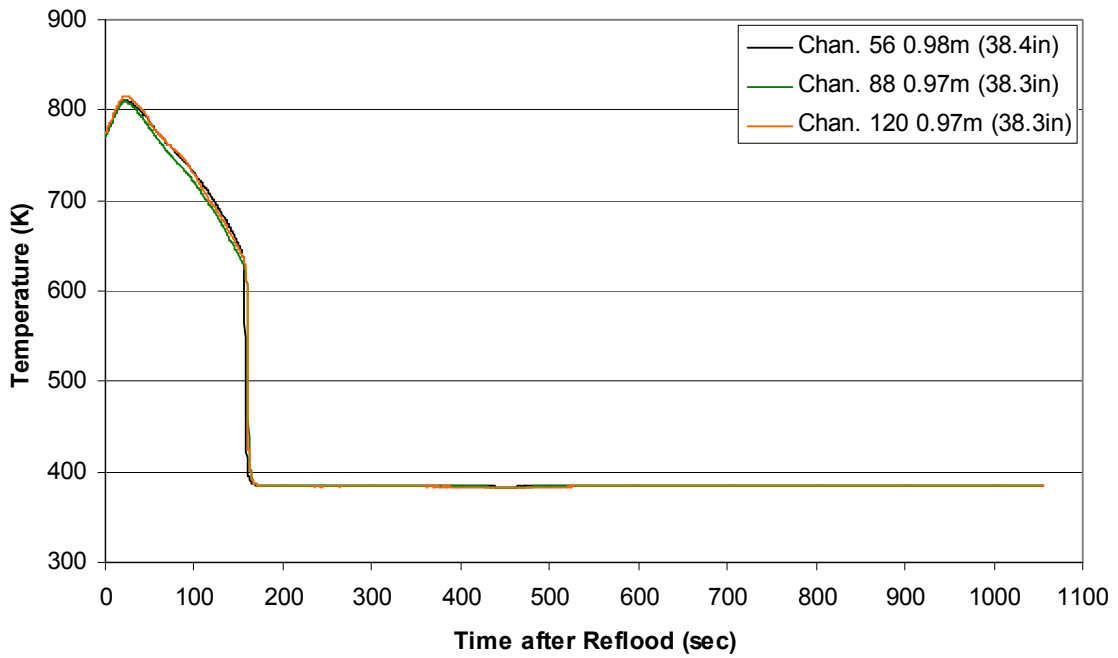


RBHT - TEST FACILITY

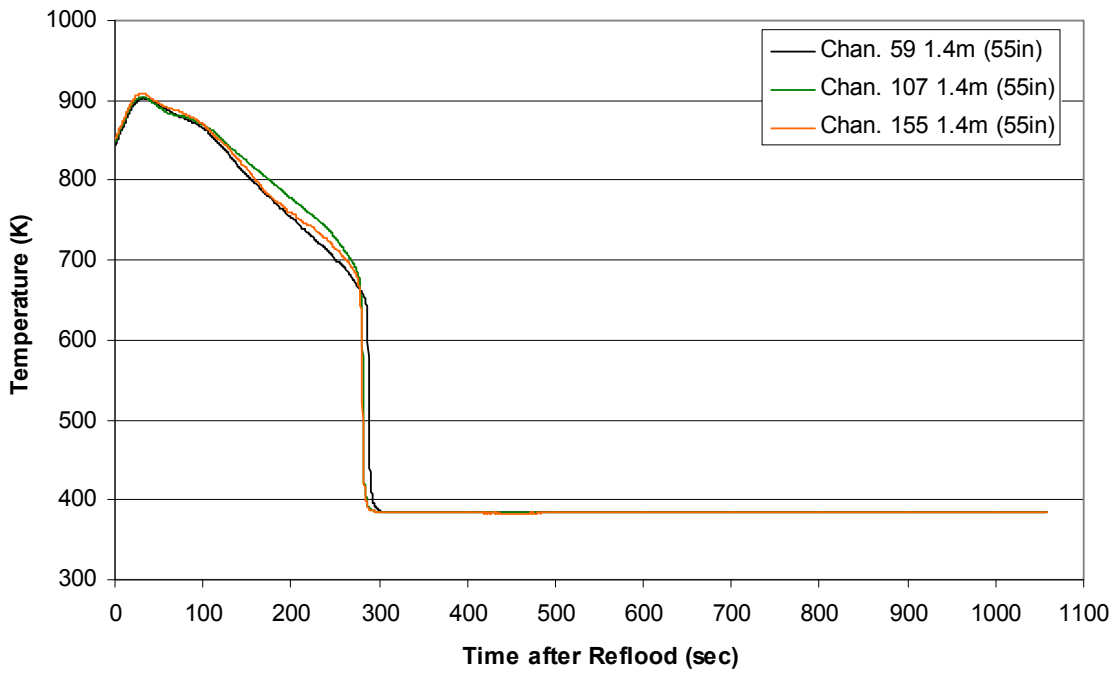
Test Section Current vs. Time, Exp 937



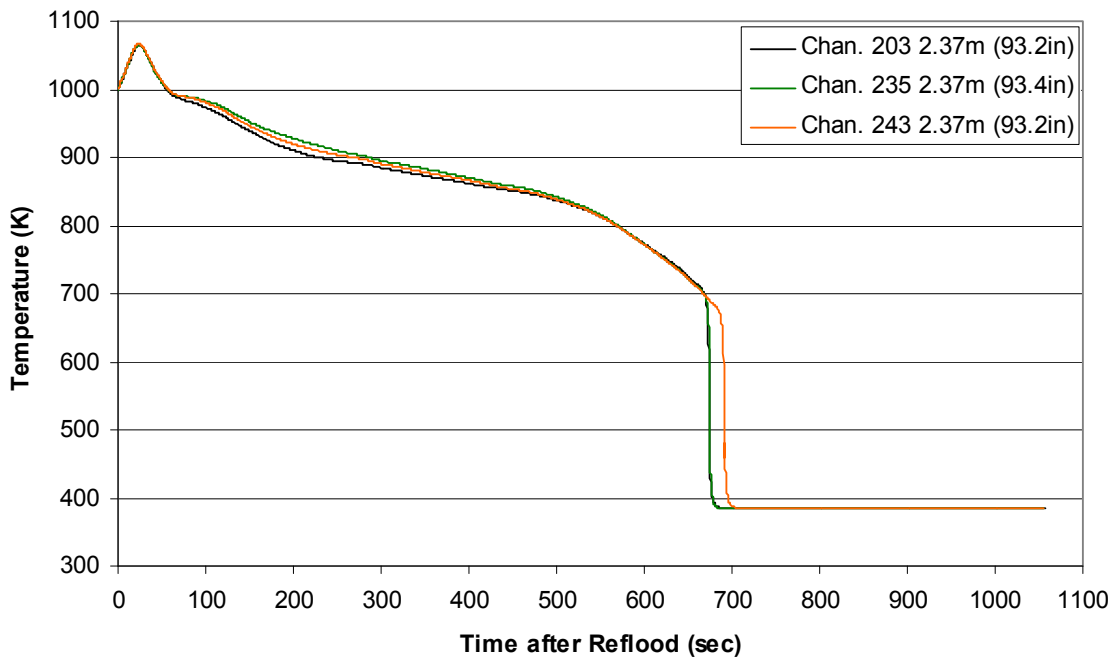
**Heater Rod Temperature during Reflood
RBHT Exp. 937**



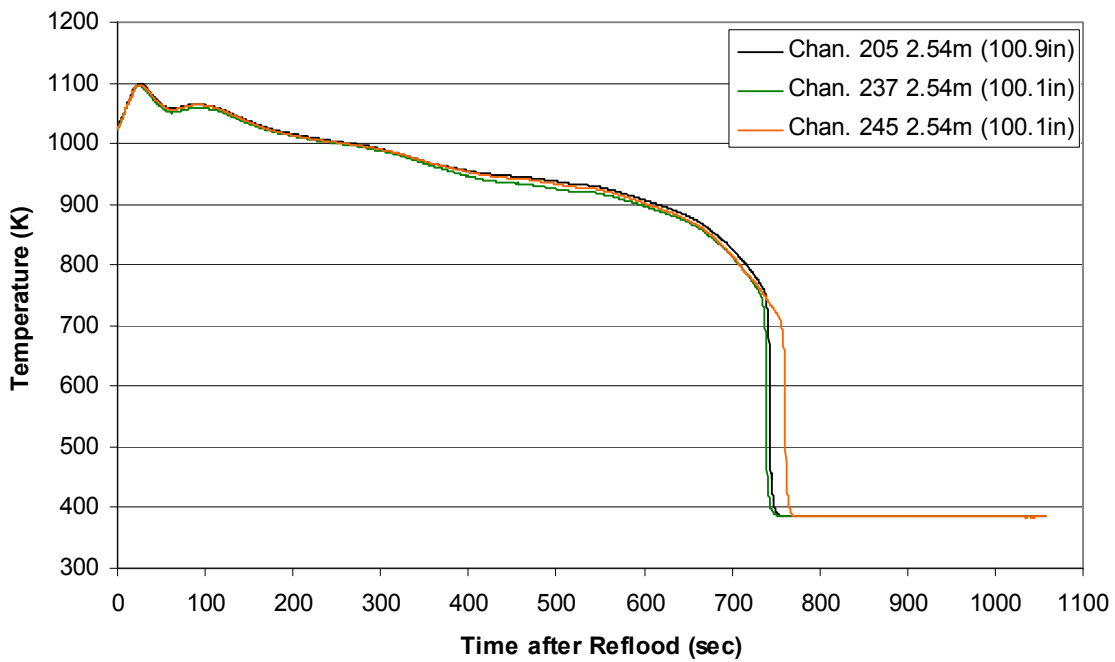
**Heater Rod Temperature during Reflood
RBHT Exp. 937**



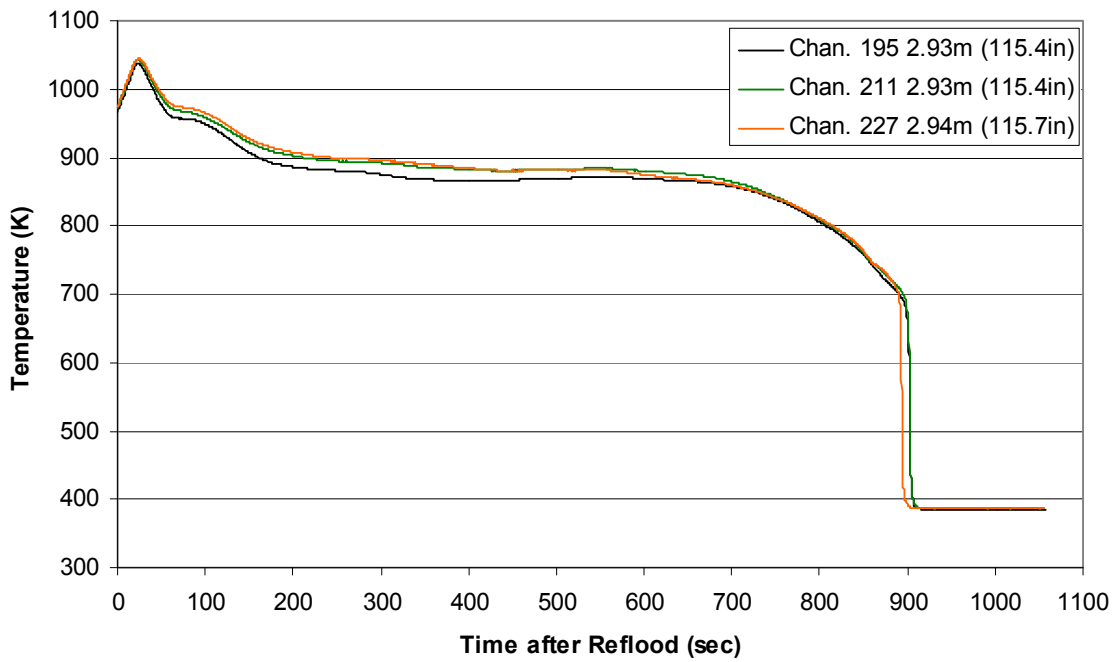
**Heater Rod Temperature during Reflood
RBHT Exp. 937**



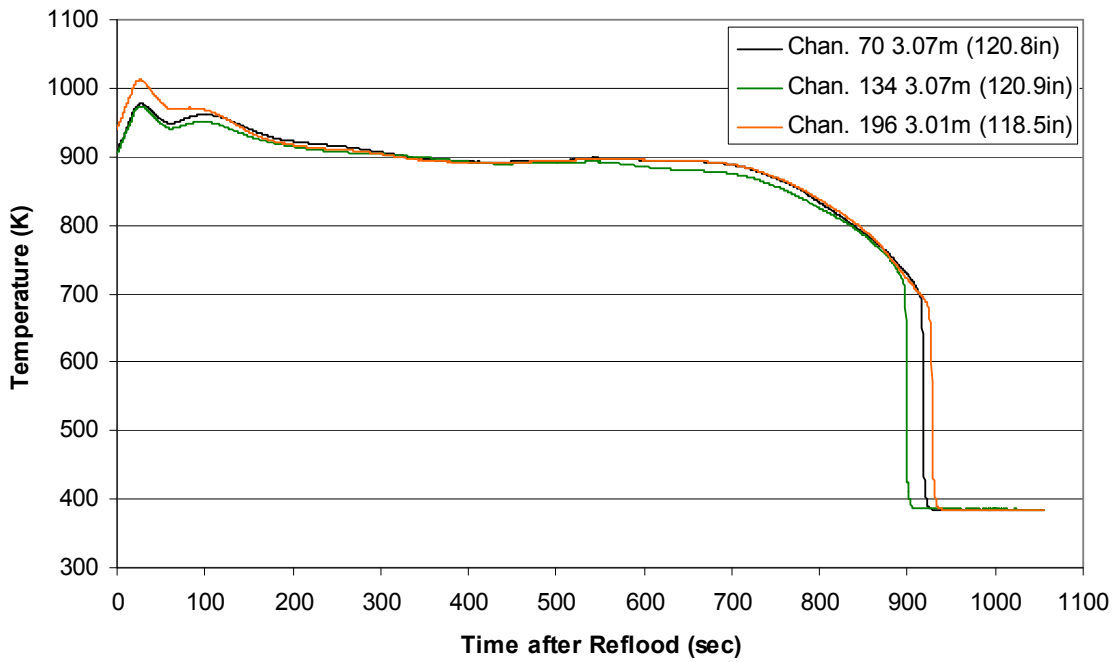
**Heater Rod Temperature during Reflood
RBHT Exp. 937**



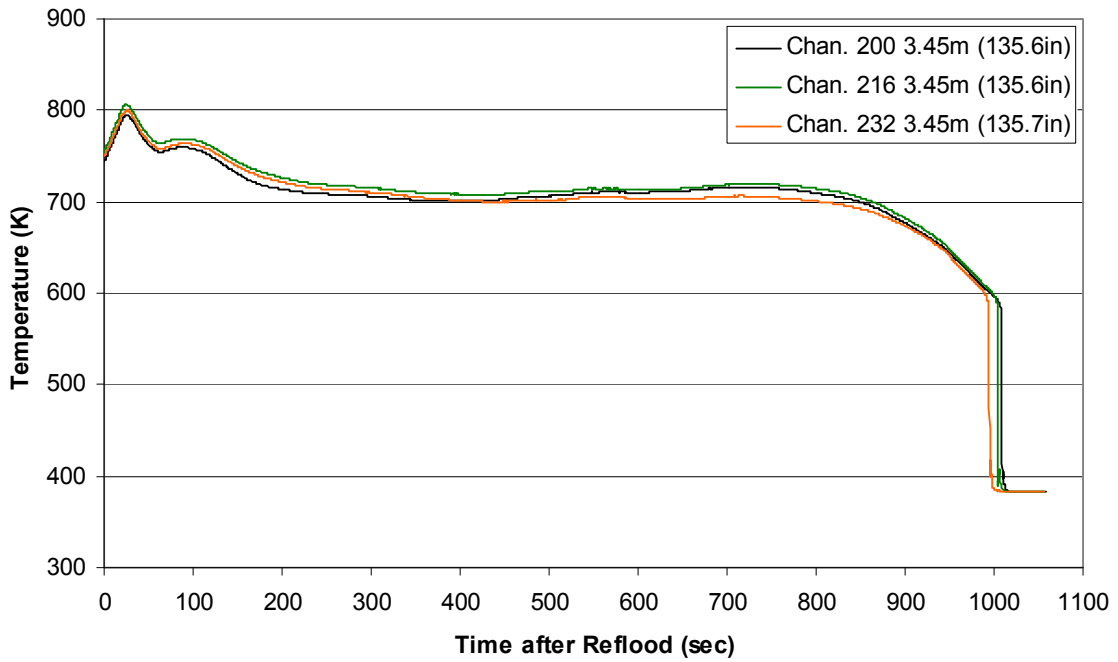
**Heater Rod Temperature during Reflood
RBHT Exp. 937**



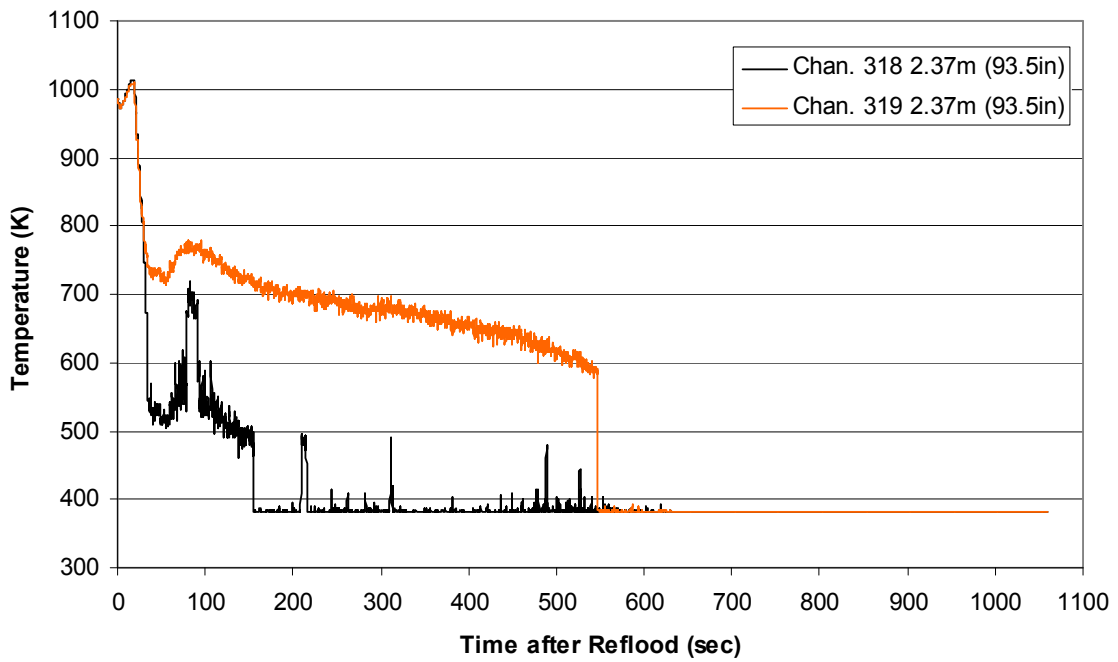
**Heater Rod Temperature during Reflood
RBHT Exp. 937**



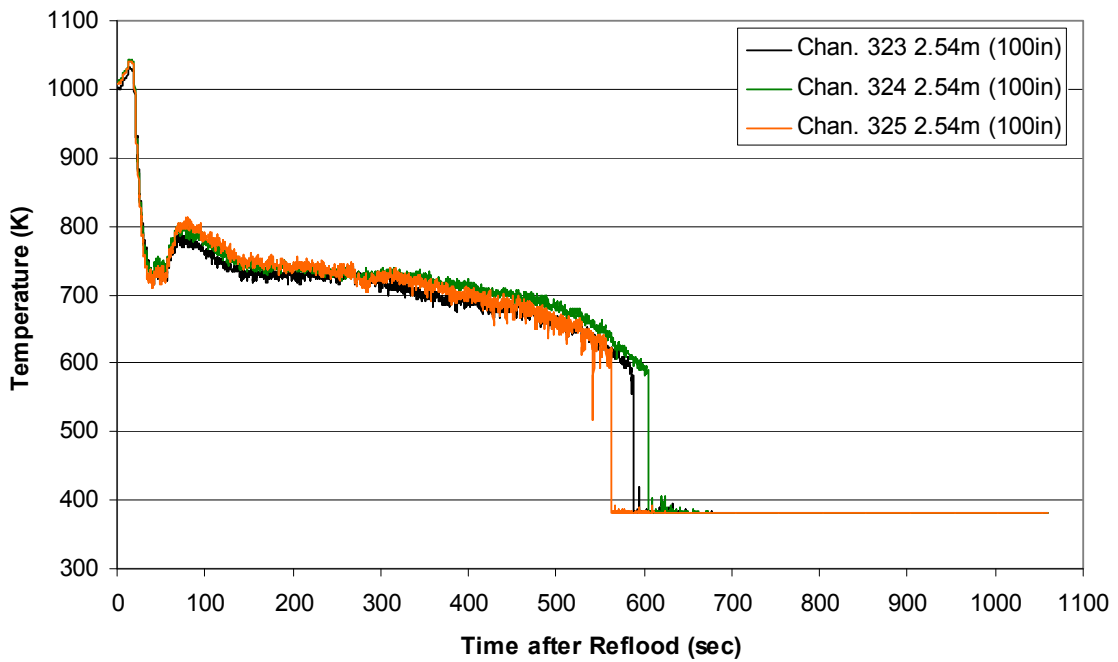
Heater Rod Temperature during Reflood RBHT Exp. 937



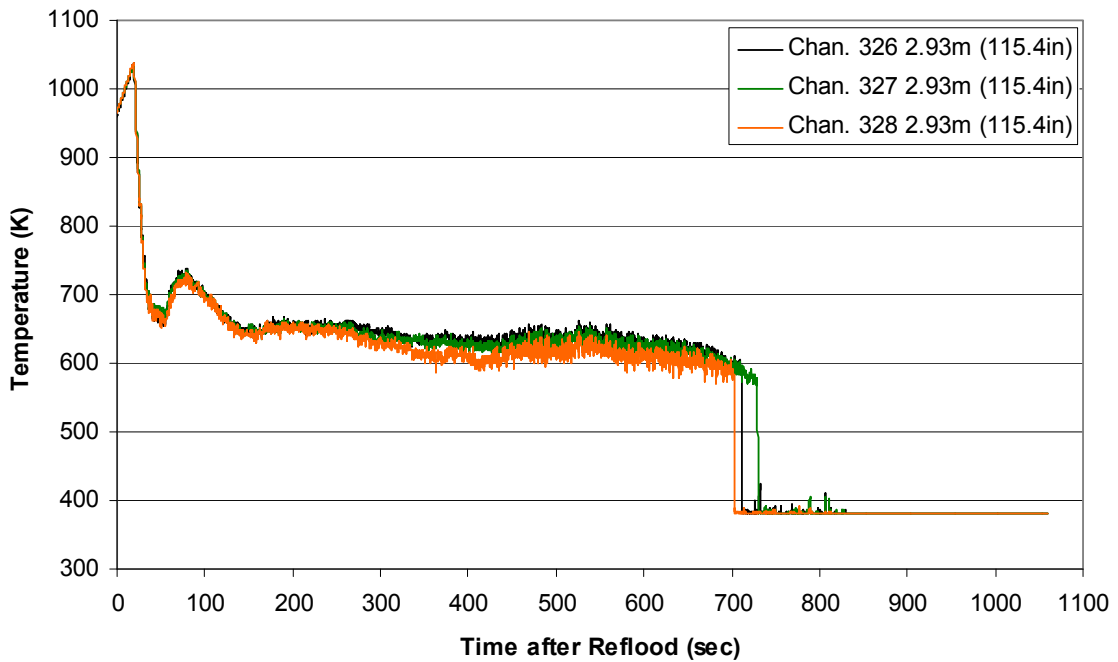
Steam Probe Temperature during Reflood RBHT Exp. 937



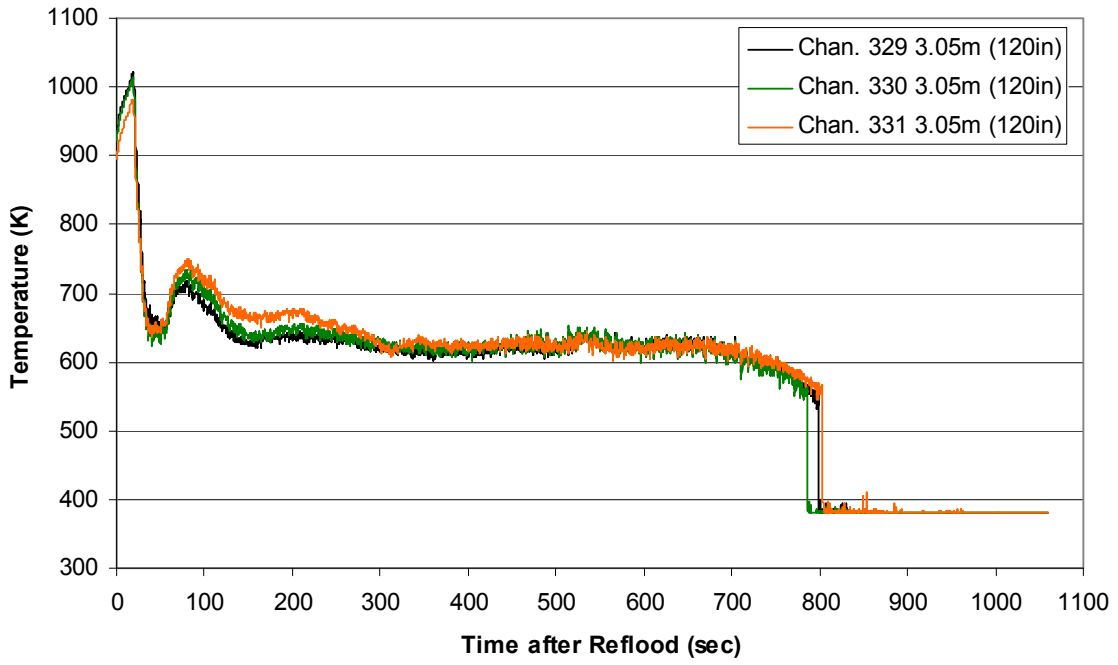
Steam Probe Temperature during Reflood
RBHT Exp. 937



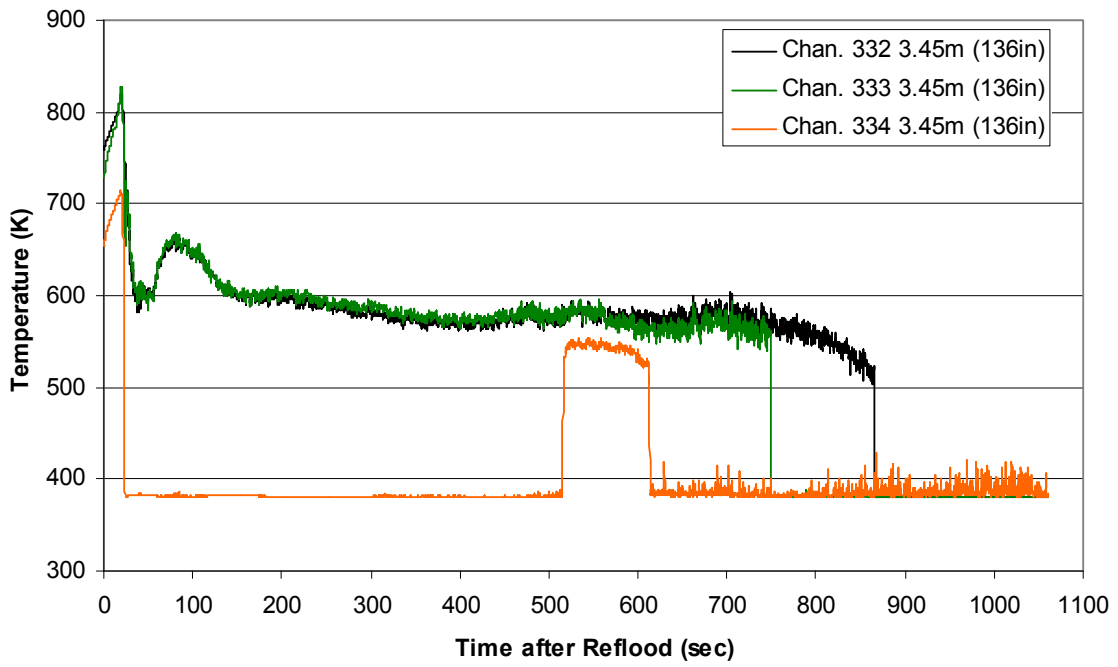
Steam Probe Temperature during Reflood
RBHT Exp. 937



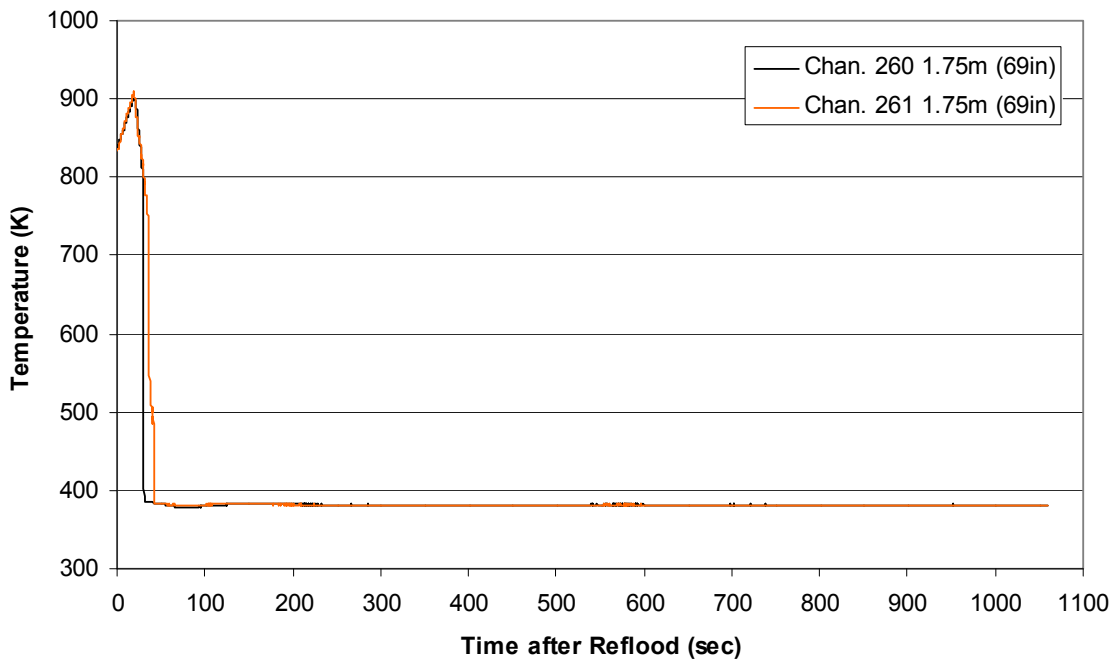
Steam Probe Temperature during Reflood RBHT Exp. 937



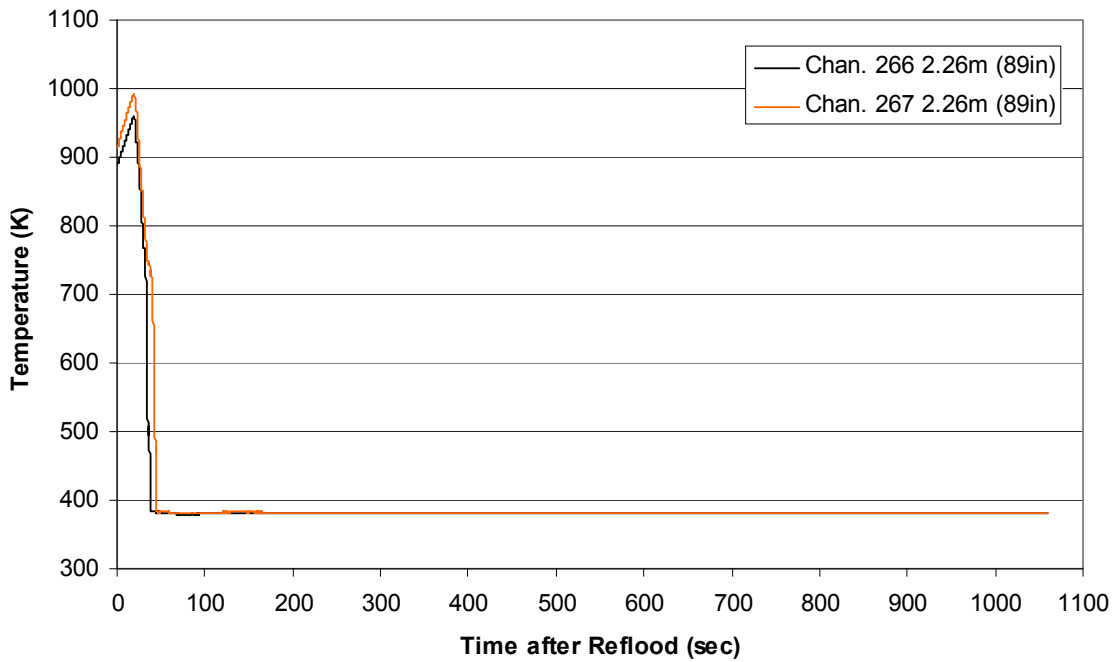
Steam Probe Temperature during Reflood RBHT Exp. 937



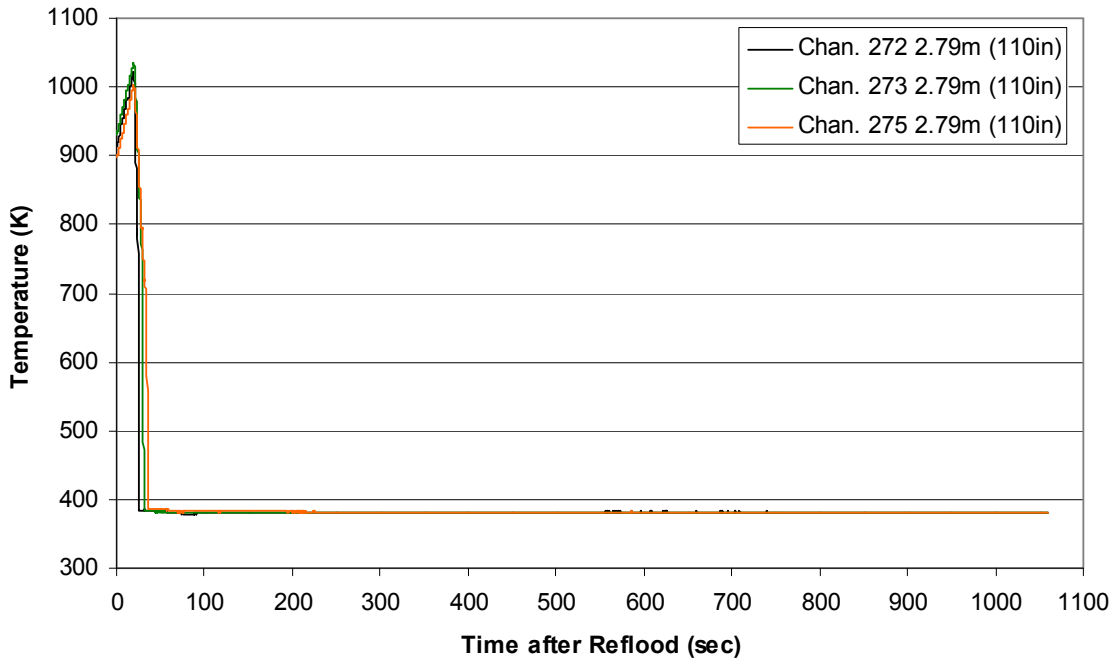
Spacer Grid Temperature during Reflood RBHT Exp. 937



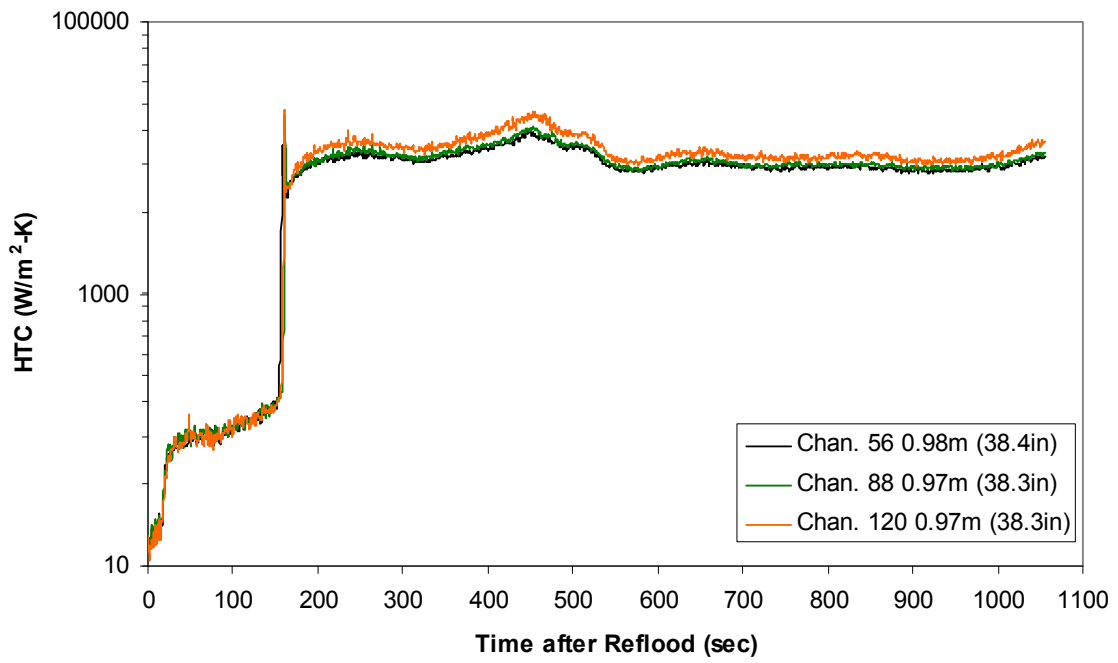
Spacer Grid Temperature during Reflood RBHT Exp. 937



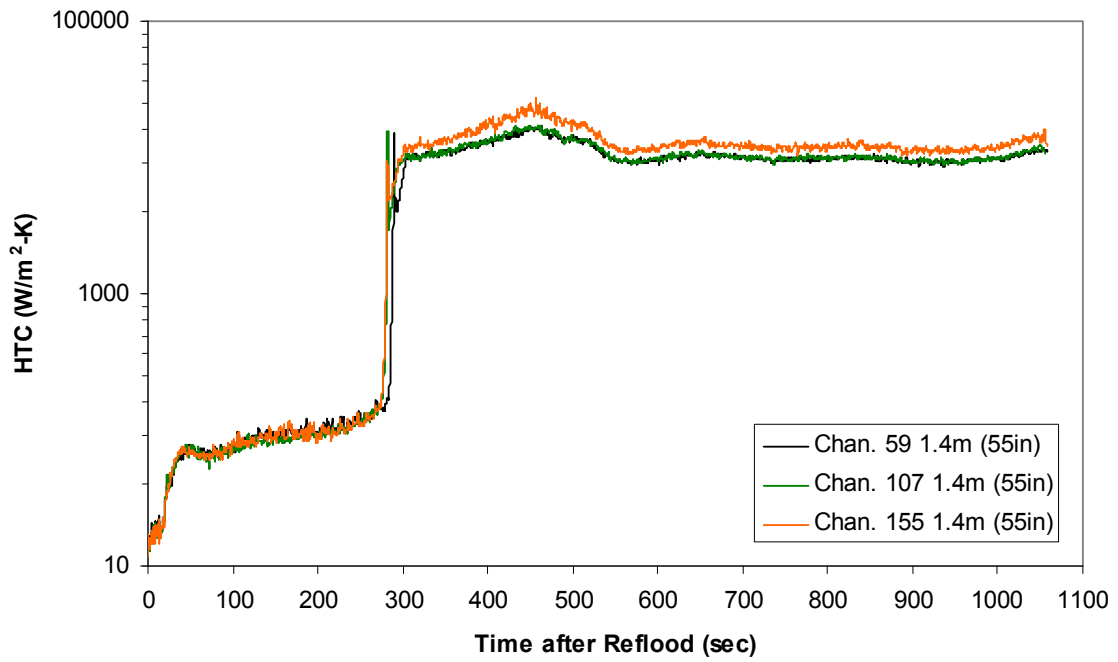
Spacer Grid Temperature during Reflood RBHT Exp. 937



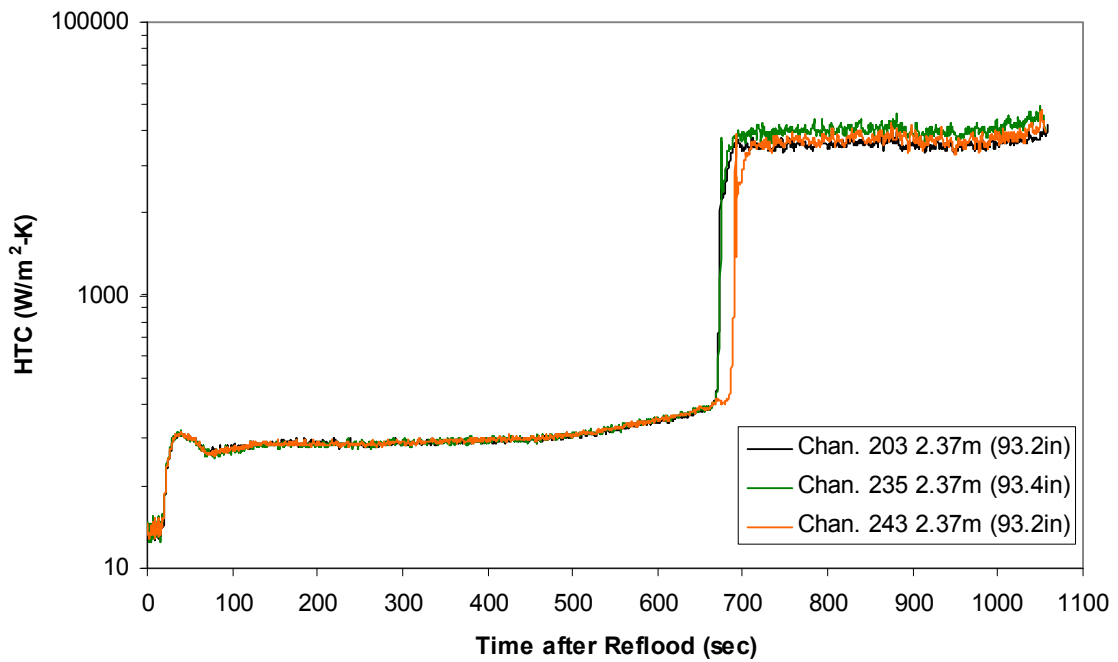
Heat Transfer Coefficient during Reflood RBHT Exp. 937



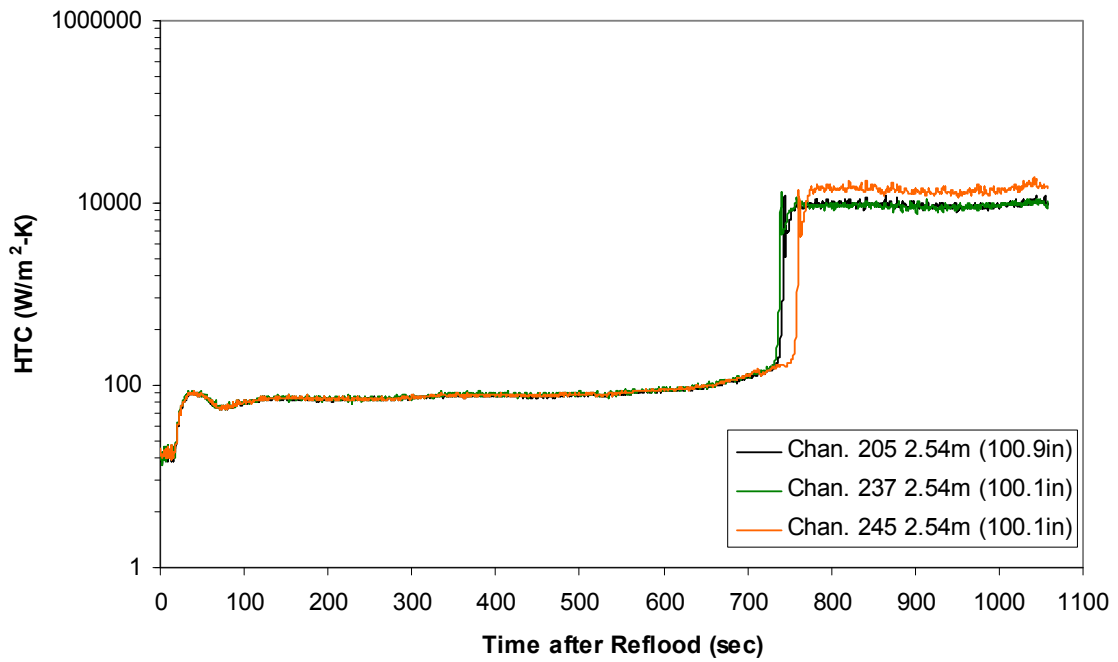
Heat Transfer Coefficient during Reflood
RBHT Exp. 937



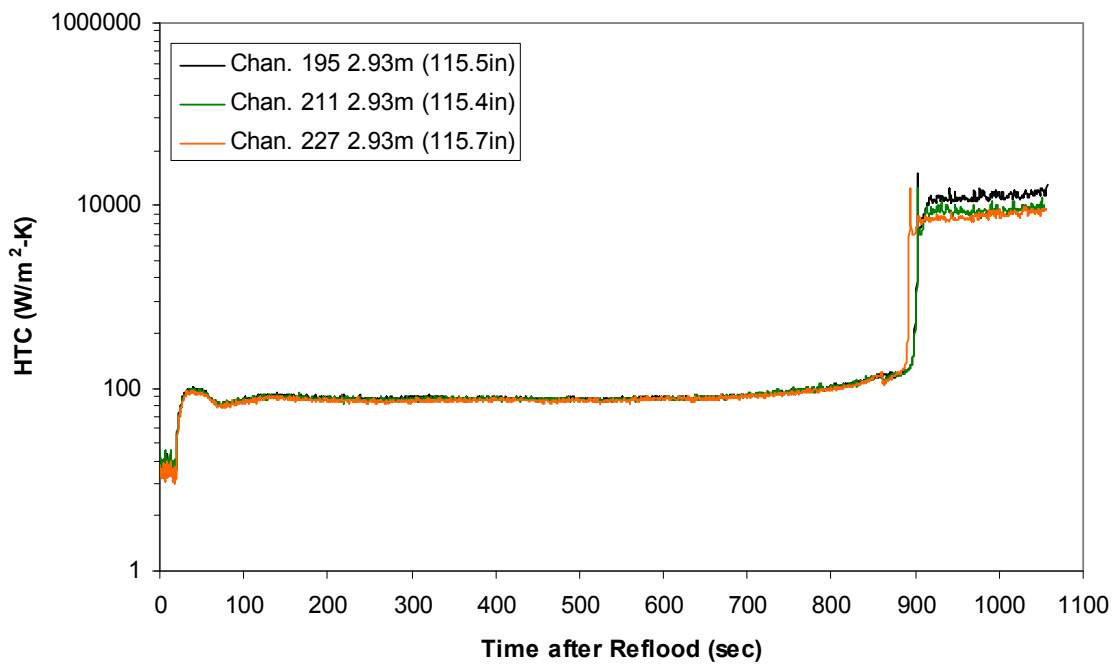
Heat Transfer Coefficient during Reflood
RBHT Exp. 937



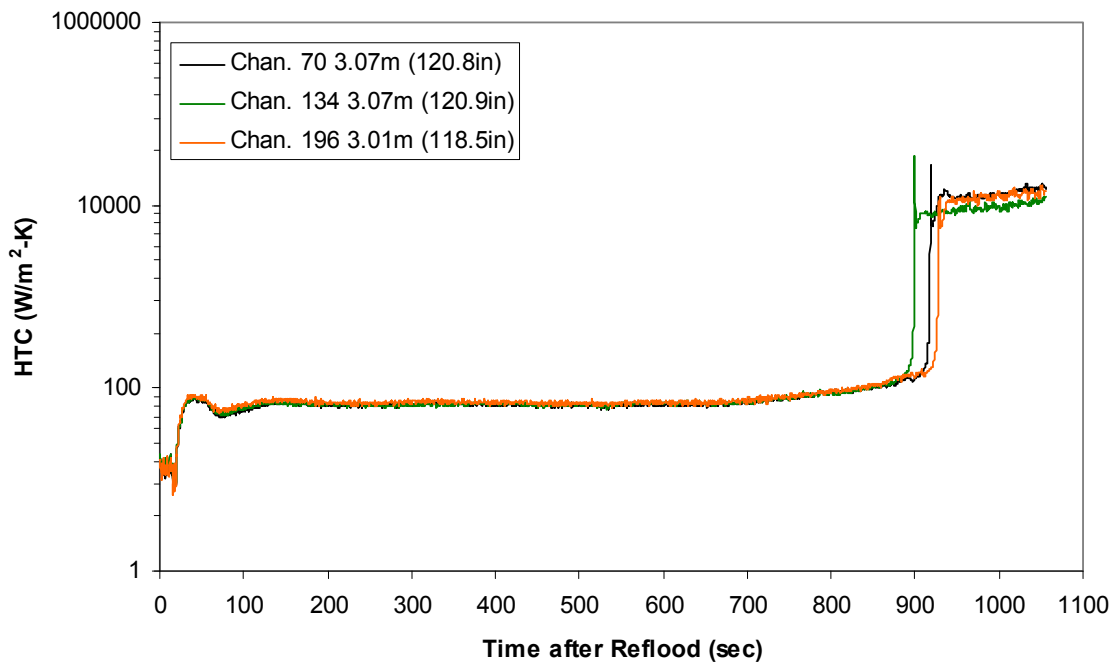
Heat Transfer Coefficient during Reflood RBHT Exp. 937



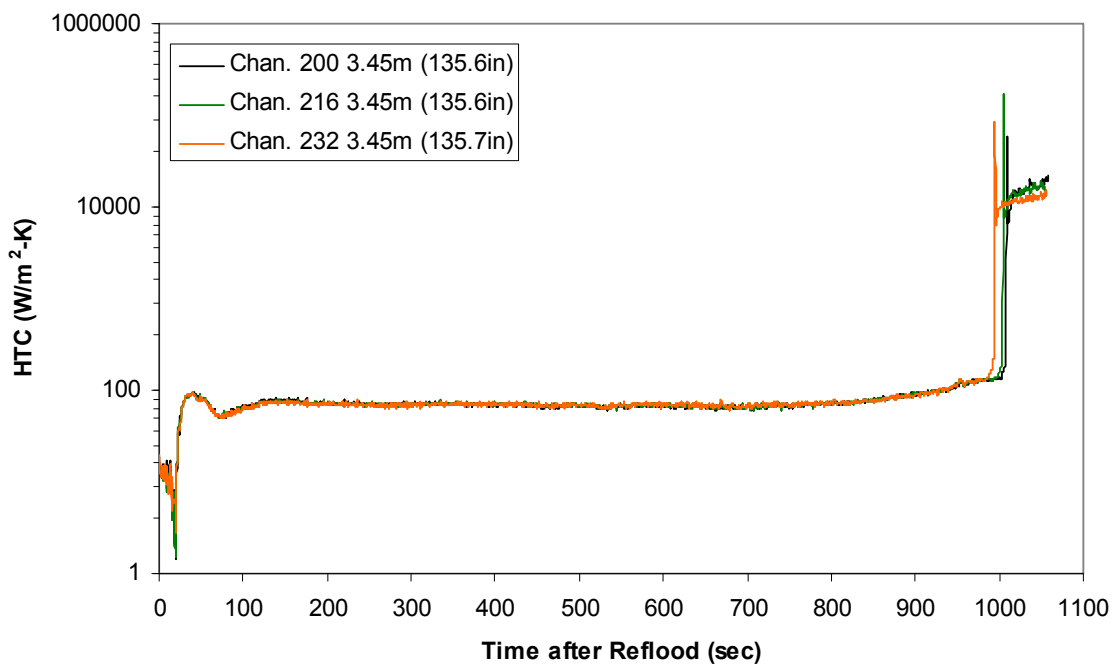
Heat Transfer Coefficient during Reflood RBHT Exp. 937



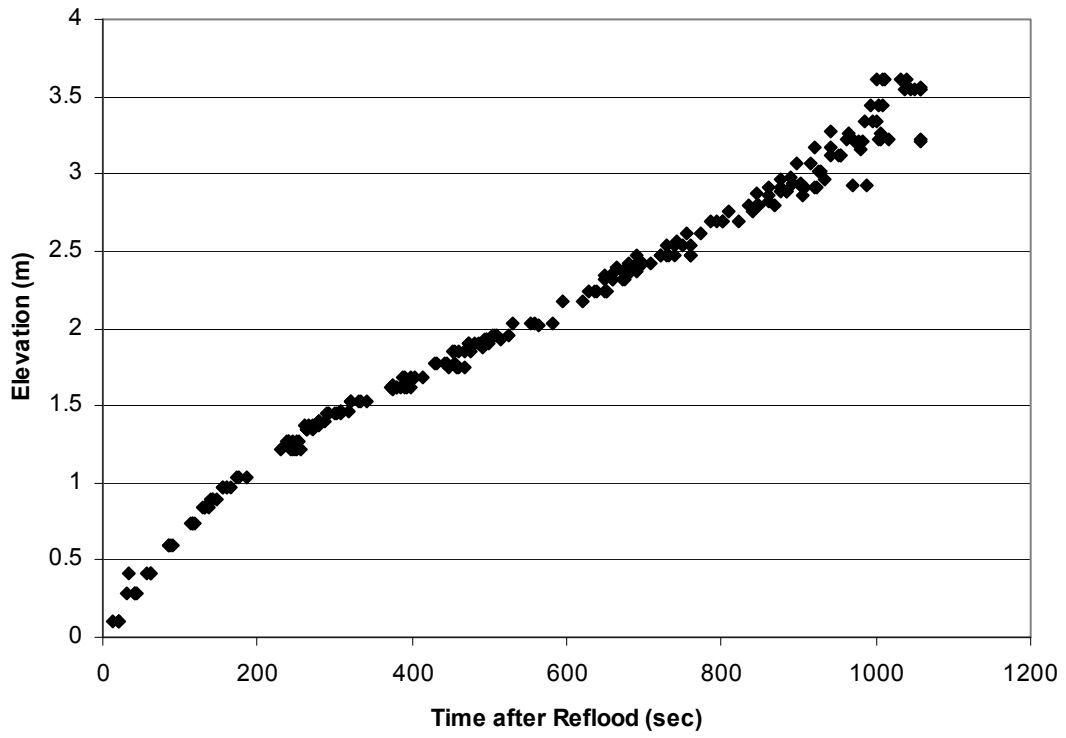
Heat Transfer Coefficient during Reflood RBHT Exp. 937



Heat Transfer Coefficient during Reflood RBHT Exp. 937



Quench Data, RBHT Exp. 937



RBHT - REFLOOD TESTS

SUMMARY SHEET

RUN NO: **945**

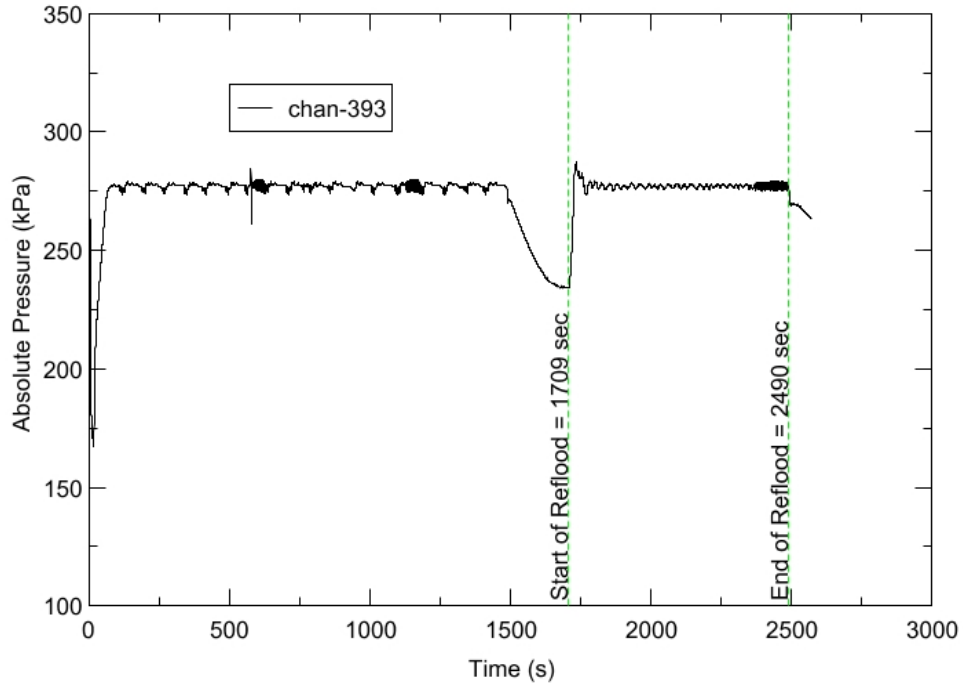
RUN CONDITIONS

Upper Plenum Pressure:	276 kPa (40 psia)
Initial Peak Clad Temperature:	1033 degrees K (1400 degrees F)
Rod Peak Power:	1.31 kW/m (0.4 kW/ft)
Flooding Rate:	0.0254 m/s (1 in/s)
Inlet Subcooling:	11 degrees K (20 degrees F)
Start of Reflood:	1709 s
End of Reflood:	2490 s
Test Date:	5/13/2002
Comments:	No droplet data

Rod_Elevation	Channel Number	Temperature at Reflood (K)	Temperature at Reflood (°F)	Turnaround Time (sec.)	Turnaround Temperature (K)	Turnaround Temperature (°F)	Quench Time (sec.)	Quench Temperature (K)	Quench Temperature (°F)
B6 0.592m	148	717.94	832.6	15.25	743.62	878.83	66.75	563.72	555
B6 0.744m	149	724.52	844.45	18.25	756.61	902.21	85.75	566.12	559.33
B6 0.846m	150	756.96	902.84	18.25	791.1	964.3	95.75	574.34	574.12
B6 0.897m	151	767.92	922.57	19.25	804.37	988.17	100.75	592.69	607.16
C6 1.04m	137	812.76	1003.29	20.75	863.11	1075.9	113.75	631.68	677.33
D5 1.27m	217	853.48	1076.57	19.75	894.62	1150.62	148.25	588.89	600.31
C6 1.34m	138	851	1072.12	24.75	897.54	1155.88	153.75	632.47	678.76
D5 1.37m	218	879.26	1122.98	25.75	928.45	1211.53	160.25	634.23	681.92
C6 1.39m	139	860.84	1089.83	25.75	909.84	1178.02	161.25	659.71	727.79
D5 1.45m	219	894.5	1150.41	25.75	946.32	1243.68	172.25	665.88	738.9
C6 1.47m	140	878.49	1121.6	25.75	928.96	1212.44	174.25	679.15	762.78
D5 1.52m	220	910.81	1179.77	26.25	963.5	1274.61	186.25	683.93	771.38
C6 1.62m	141	899.84	1160.03	34.75	957.76	1264.28	205.25	695.82	792.79
D5 1.68m	221	927.29	1209.44	67.25	989.8	1321.95	218.25	709.37	817.19
D5 1.78m	222	909.82	1177.99	23.25	965.46	1278.14	239.75	631.4	676.83
D5 1.85m	223	940.35	1232.94	23.25	993.81	1329.17	251.25	676.5	758.02
C6 1.87m	142	925.47	1206.16	24.75	981.61	1307.21	256.75	694.67	790.72
D5 1.90m	224	948.94	1248.4	25.25	1006.54	1352.08	216.75	793.41	968.44
C6 1.95m	144	940.79	1233.74	34.75	998.2	1337.07	275.25	692.53	786.86
C3 2.17m	178	987.06	1317.01	71.75	1057.9	1444.54	326.25	756.46	901.95
D4 2.24m	241	1003.69	1346.95	87.25	1077.15	1479.19	358.75	706.25	811.57
D4 2.32m	242	1007.72	1354.21	20.75	1066.39	1459.82	374.25	630.48	675.17
C3 2.35m	180	1008.88	1356.3	20.75	1068.59	1463.77	364.25	683.81	771.17
D4 2.37m	243	1019.46	1375.33	21.25	1081.82	1487.59	383.25	675.98	757.07
C3 2.40m	181	1011.91	1361.75	21.75	1075.54	1476.28	375.25	716.85	830.64
D4 2.54m	245	1029.93	1394.19	23.75	1100.84	1521.82	435.25	703.36	806.36
D6 2.62m	129	1017.76	1372.28	75.25	1096.41	1513.85	442.25	743.28	878.22
D6 2.69m	130	1002.43	1344.68	89.25	1104.67	1528.73	465.25	769.99	926.3
C3 2.76m	183	1003	1345.72	92.25	1105.82	1530.79	489.75	711.31	820.67
D6 2.87m	131	934.32	1222.09	21.75	1002.32	1344.49	511.75	661.14	730.37
D6 2.92m	132	919.75	1195.86	25.25	992.7	1327.18	519.75	699.19	798.86
D6 2.97m	133	899.74	1159.84	26.25	971.57	1289.14	532.75	696.29	793.63
D6 3.07m	134	863.4	1094.43	91.75	954.32	1258.09	550.25	698.93	798.39
E3 3.12m	197	853.26	1076.18	221.75	963.04	1273.78	581.25	659.56	727.51
D6 3.17m	135	808.15	994.98	222.25	946.21	1243.48	571.25	701.32	802.69
D6 3.27m	136	735.59	864.38	249.25	933.72	1221	591.25	685.63	774.45
D4 3.61m	248	562.82	553.39	249.25	750.91	891.94	649.75	567.41	561.65

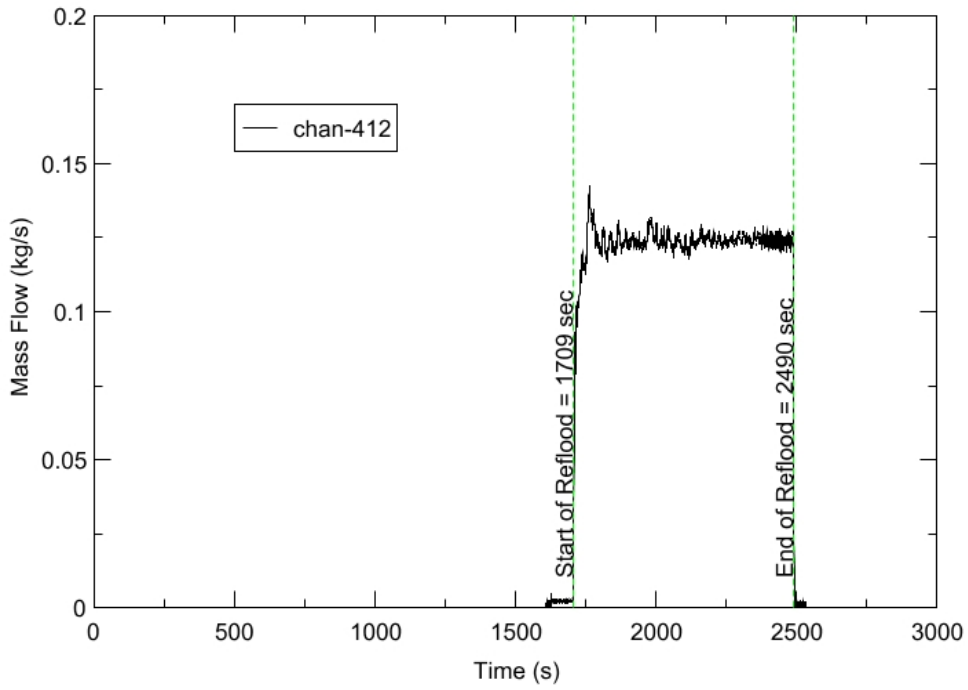
RBHT - TEST FACILITY

Upper Plenum Pressure vs. Time, Exp 945



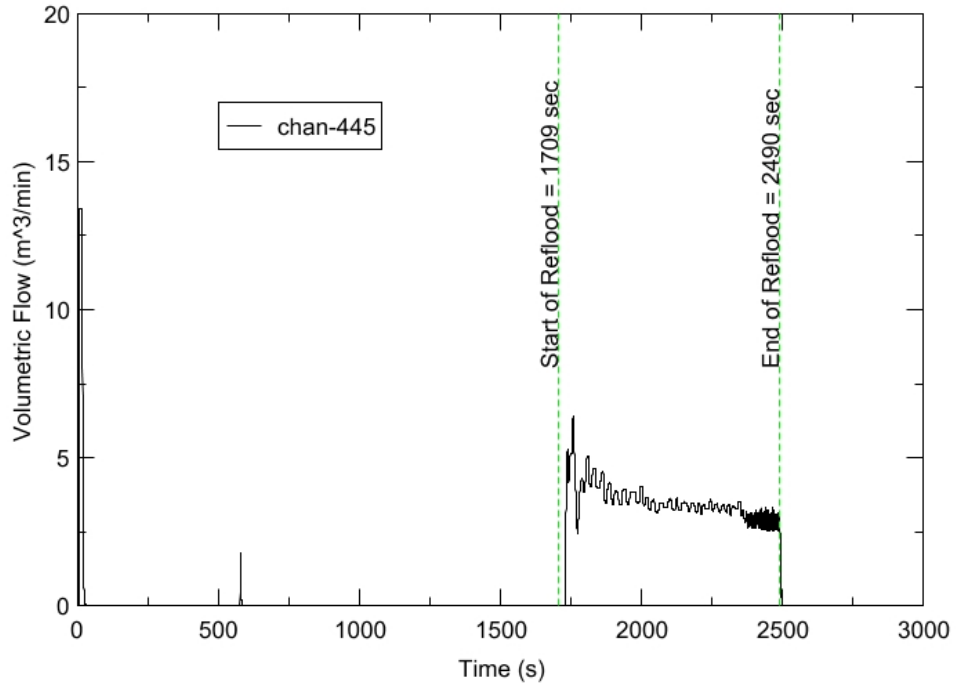
RBHT - TEST FACILITY

Inlet Flow vs. Time, Exp 945



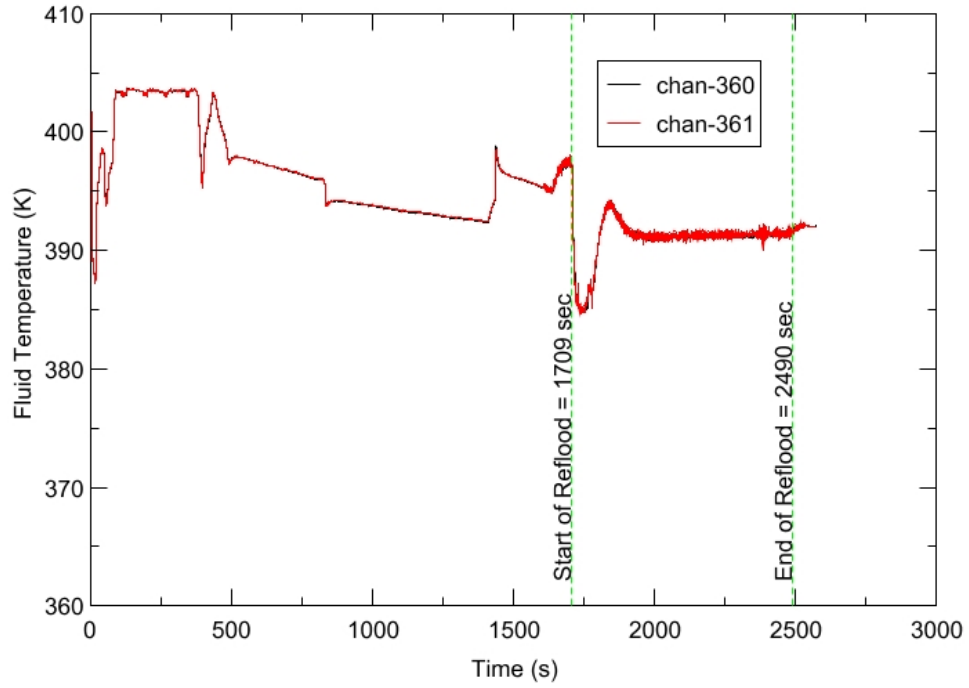
RBHT - TEST FACILITY

Steam Exhaust Flow vs. Time, Exp 945



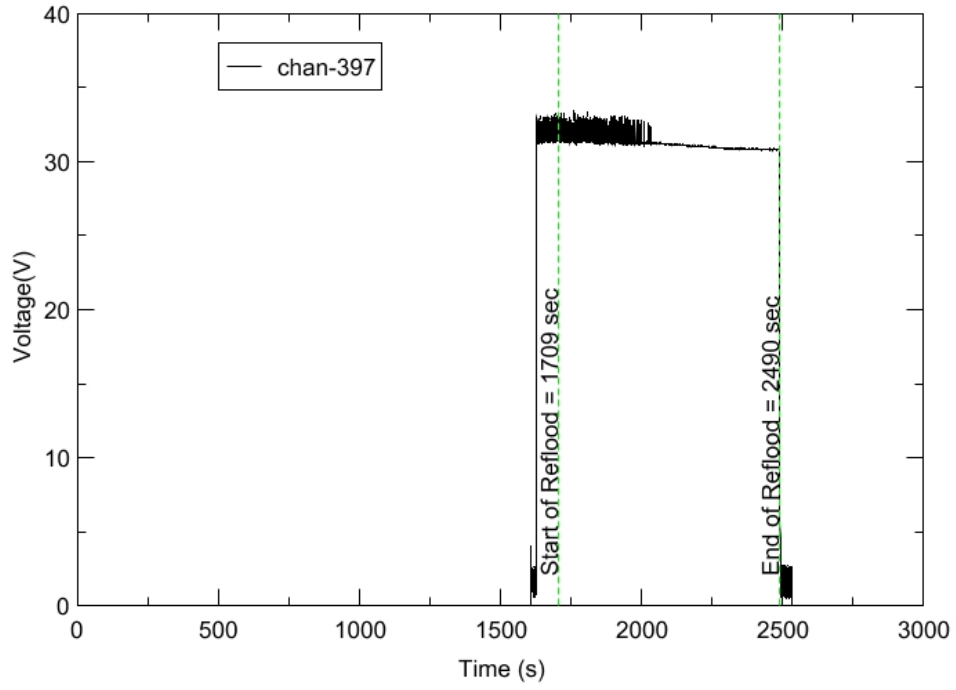
RBHT - TEST FACILITY

Inlet Flow Temperature vs. Time, Exp 945



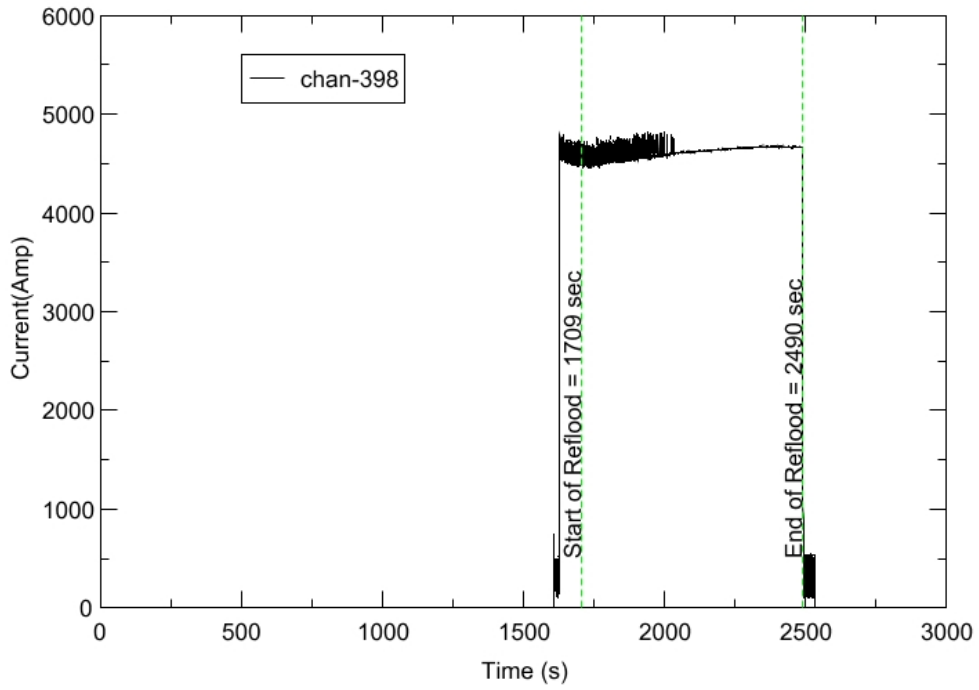
RBHT - TEST FACILITY

Test Section Voltage vs. Time, Exp 945

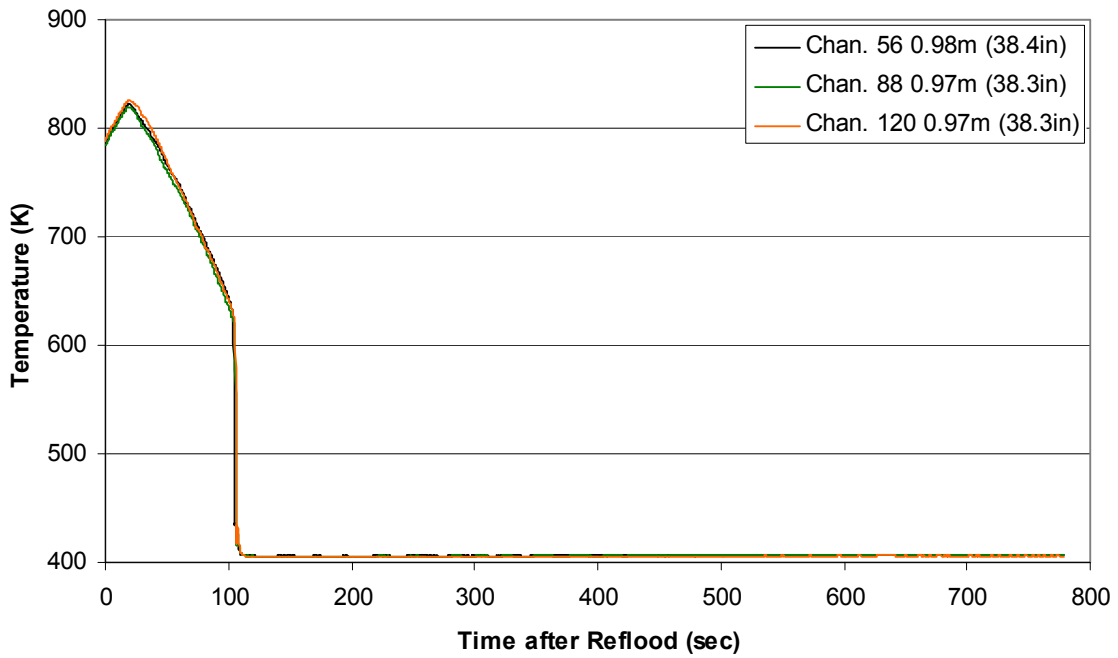


RBHT - TEST FACILITY

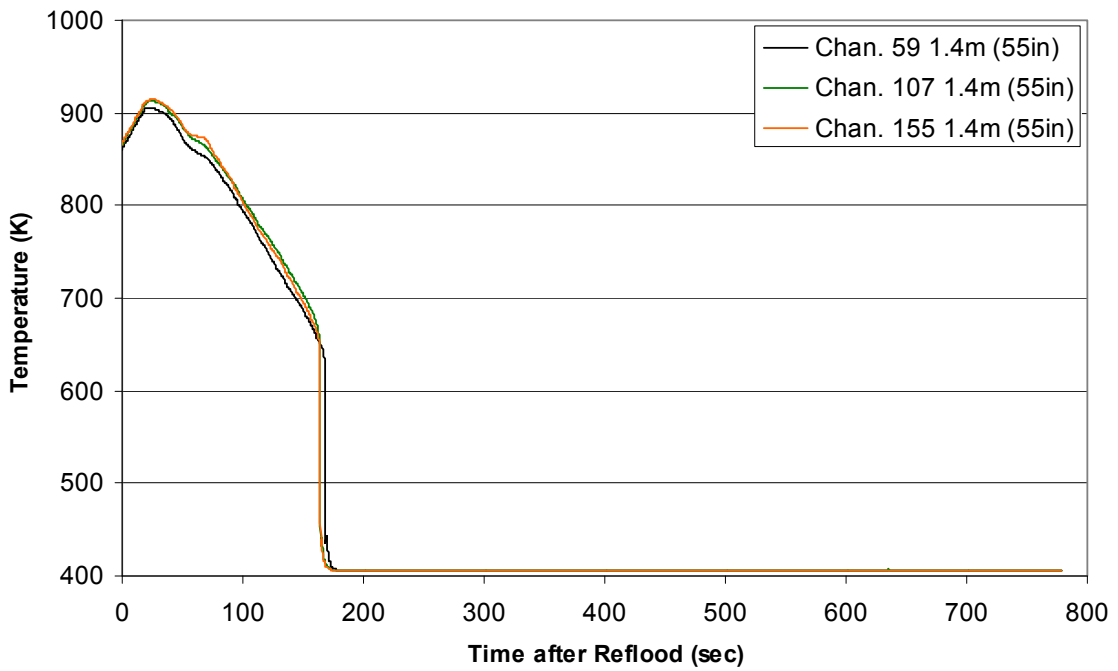
Test Section Current vs. Time, Exp 945



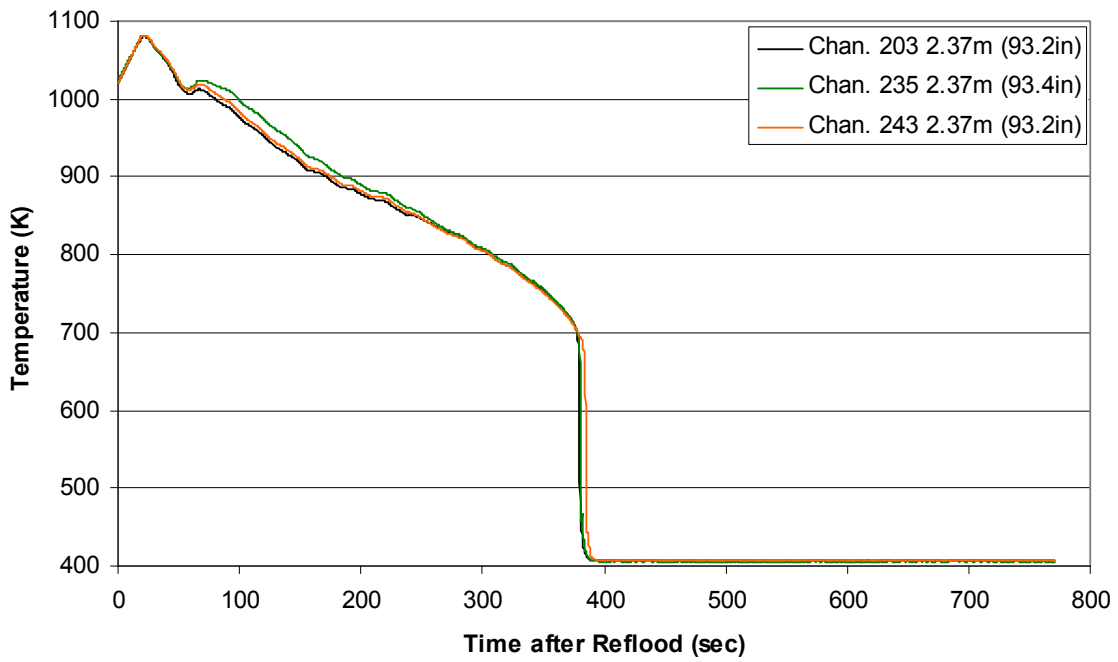
**Heater Rod Temperature during Reflood
RBHT Exp. 945**



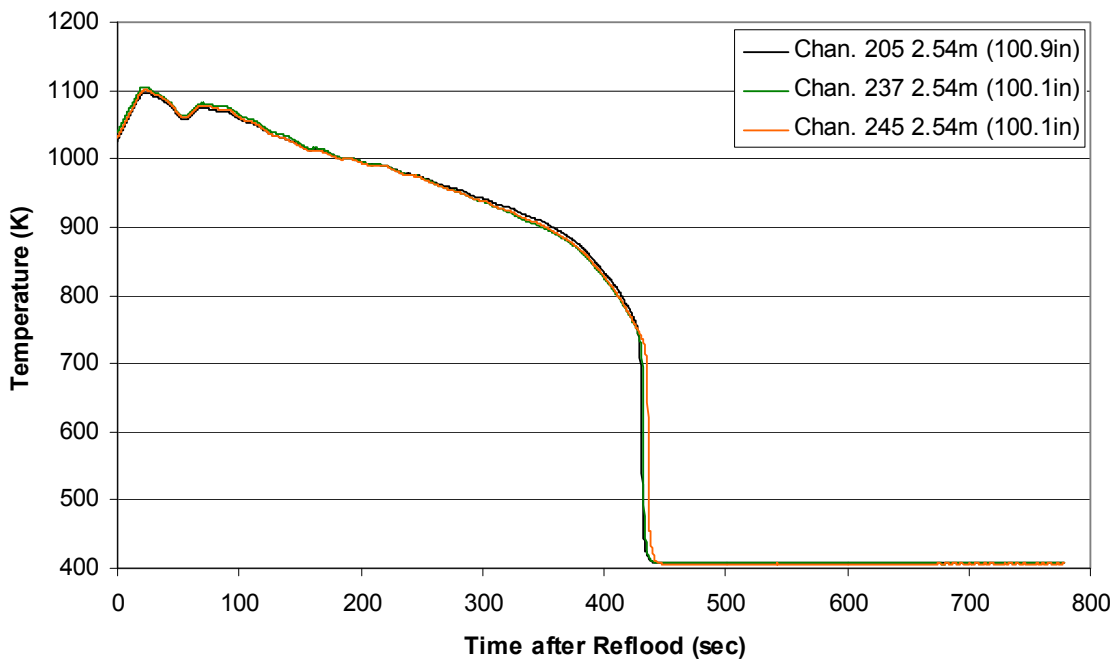
**Heater Rod Temperature during Reflood
RBHT Exp. 945**



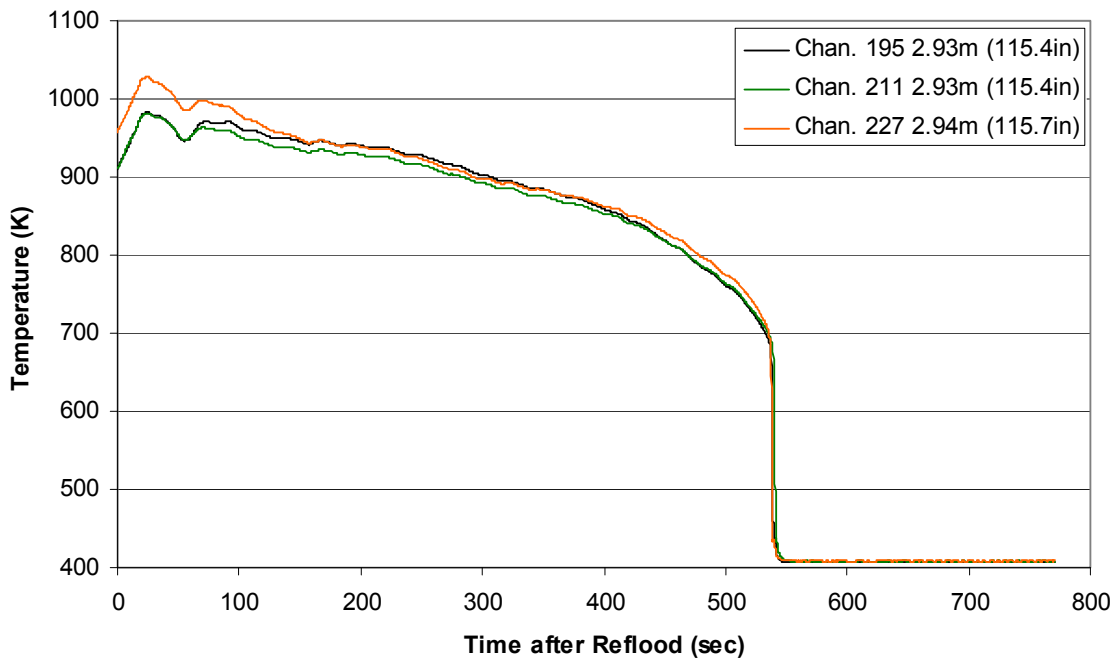
**Heater Rod Temperature during Reflood
RBHT Exp. 945**



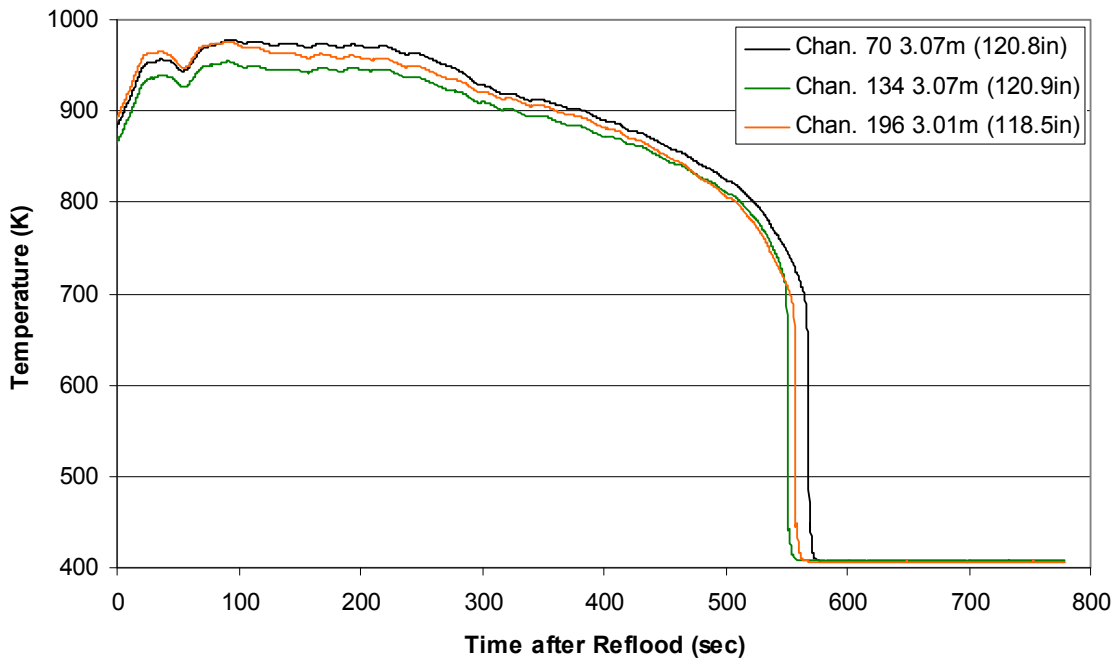
**Heater Rod Temperature during Reflood
RBHT Exp. 945**



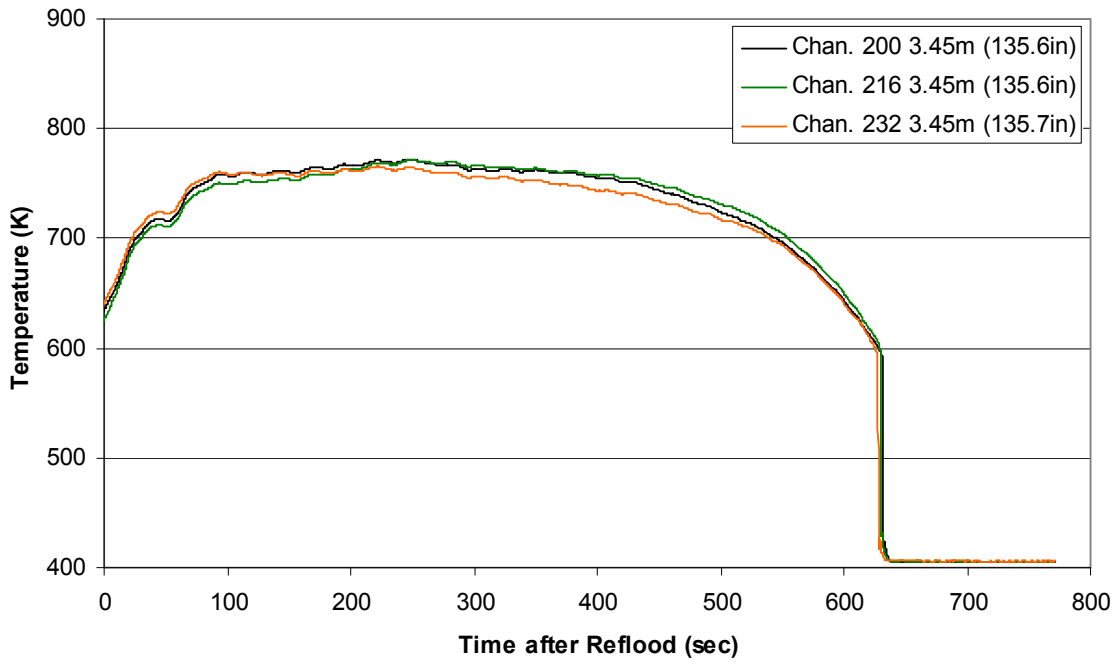
**Heater Rod Temperature during Reflood
RBHT Exp. 945**



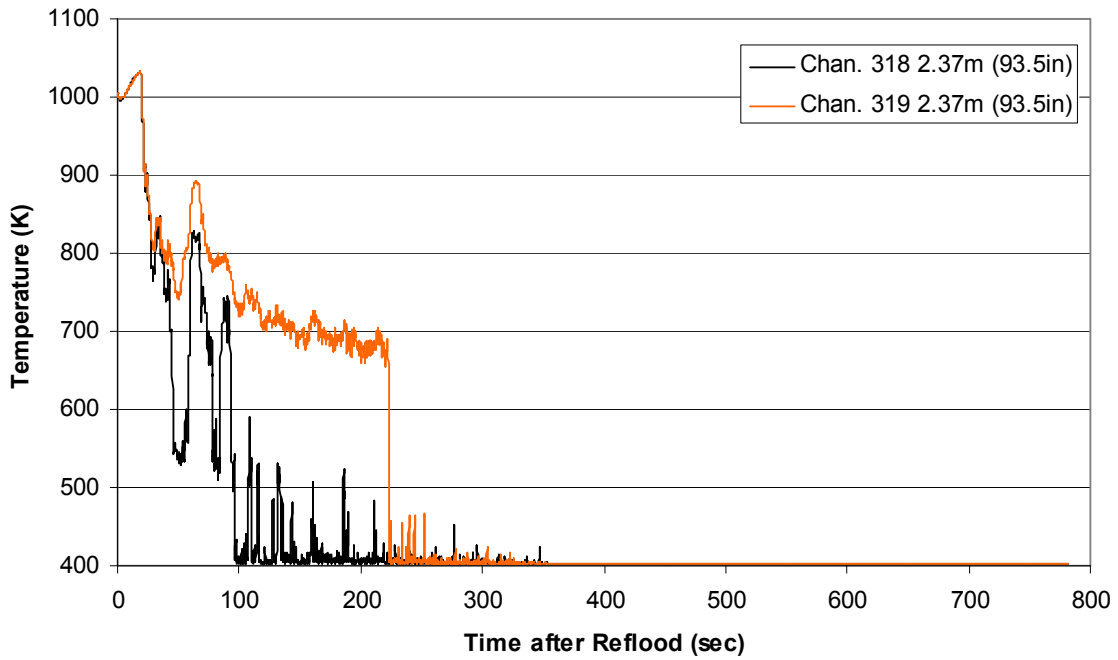
**Heater Rod Temperature during Reflood
RBHT Exp. 945**



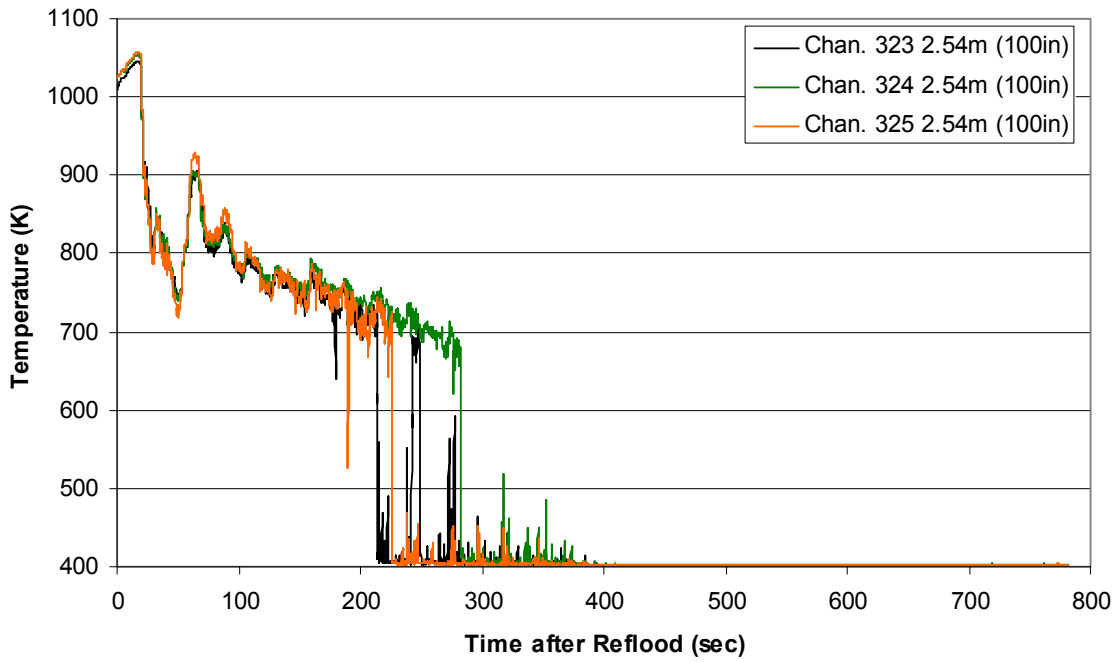
Heater Rod Temperature during Reflood RBHT Exp. 945



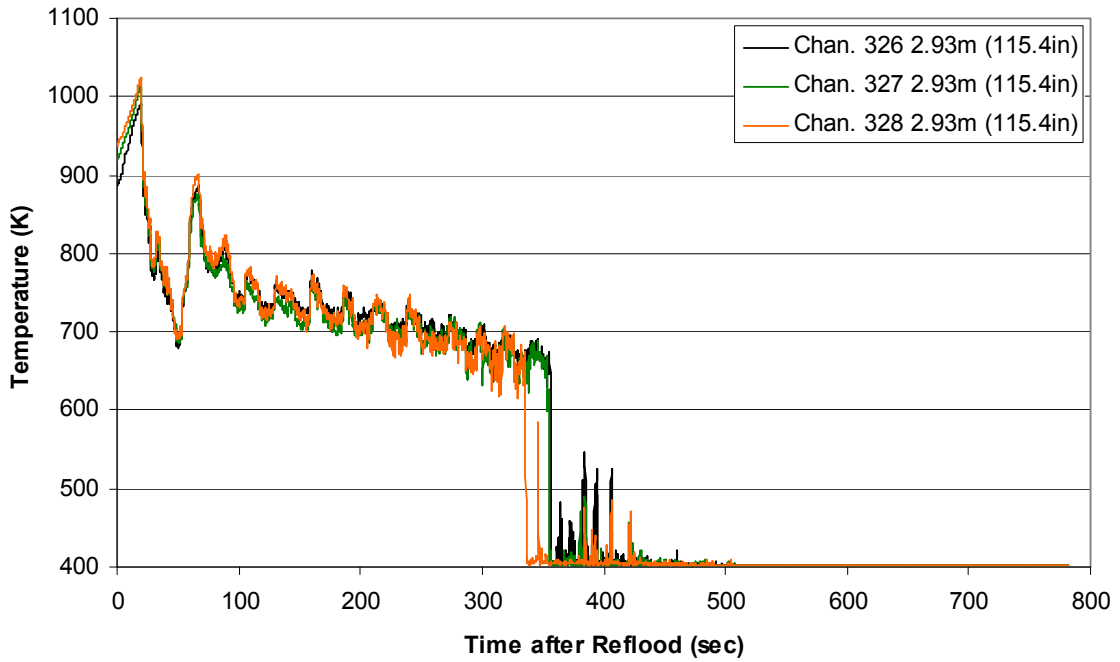
Steam Probe Temperature during Reflood RBHT Exp. 945



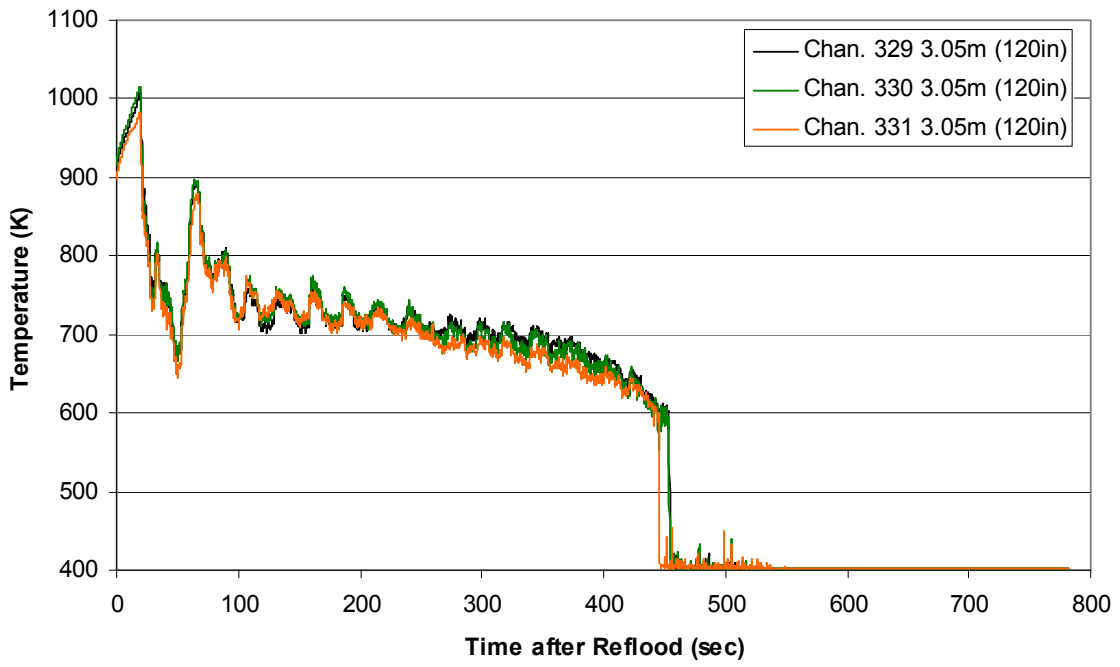
**Steam Probe Temperature during Reflood
RBHT Exp. 945**



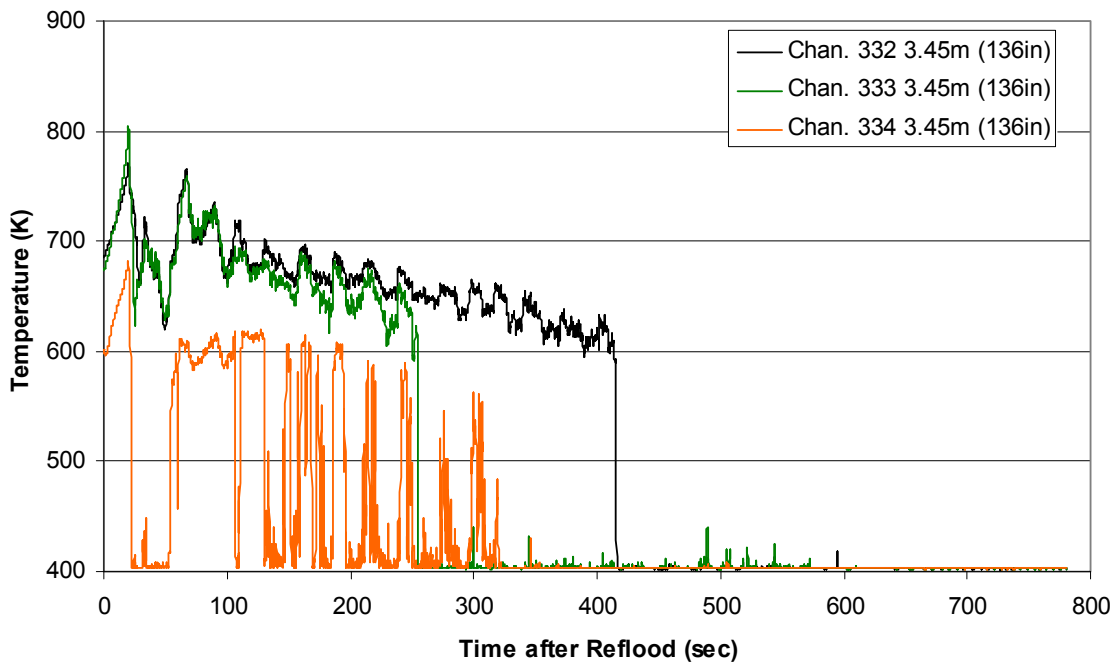
**Steam Probe Temperature during Reflood
RBHT Exp. 945**



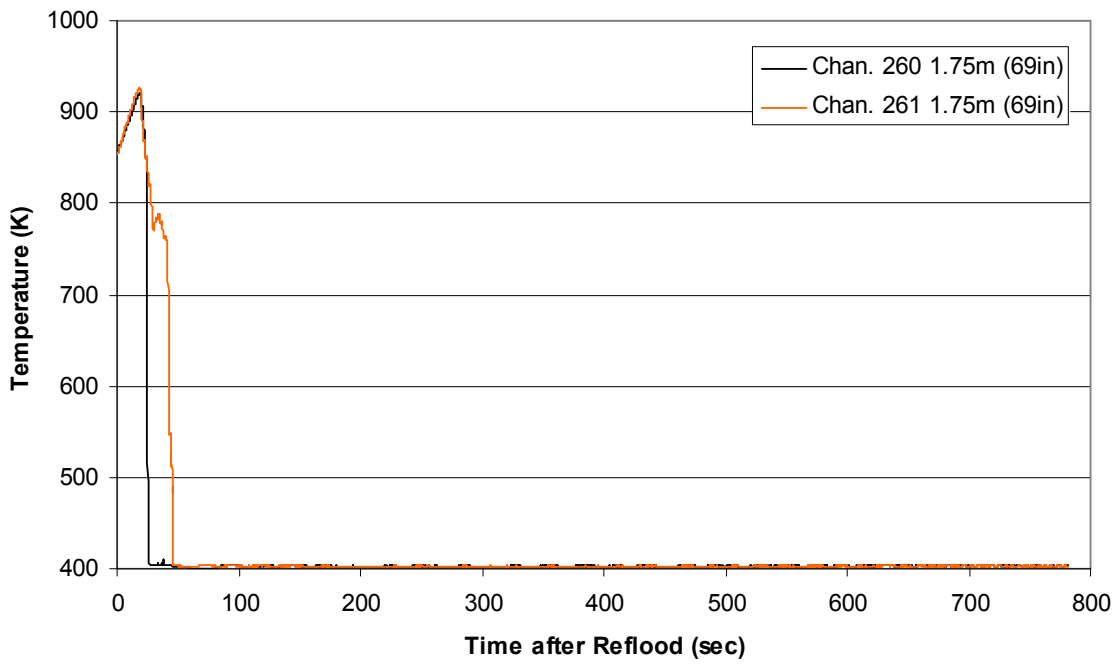
Steam Probe Temperature during Reflood
RBHT Exp. 945



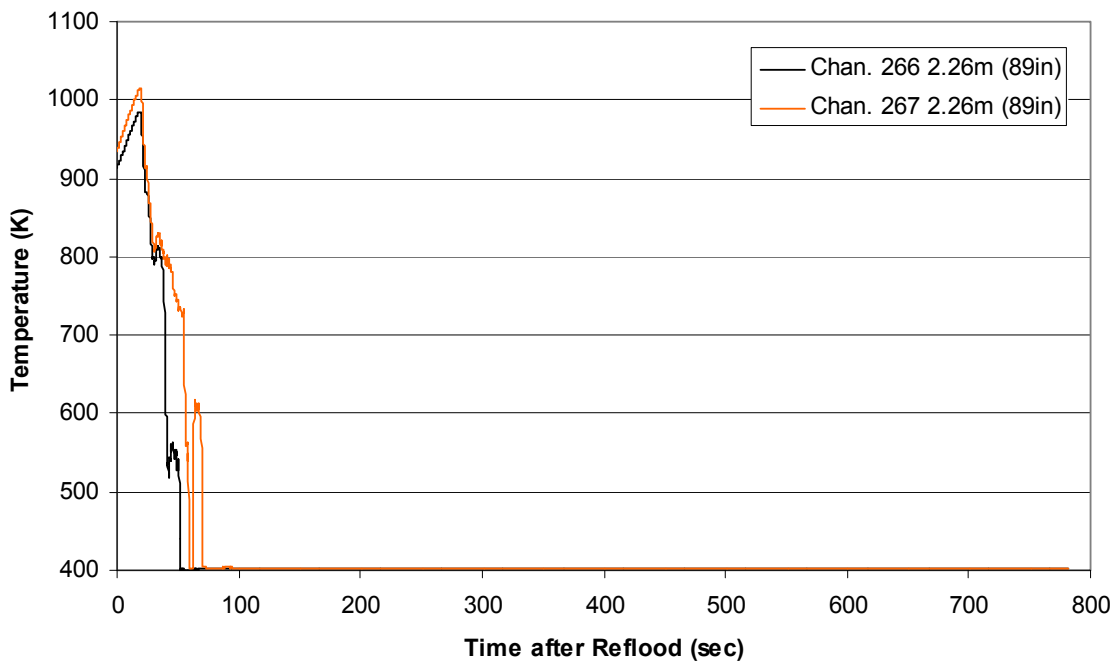
Steam Probe Temperature during Reflood
RBHT Exp. 945



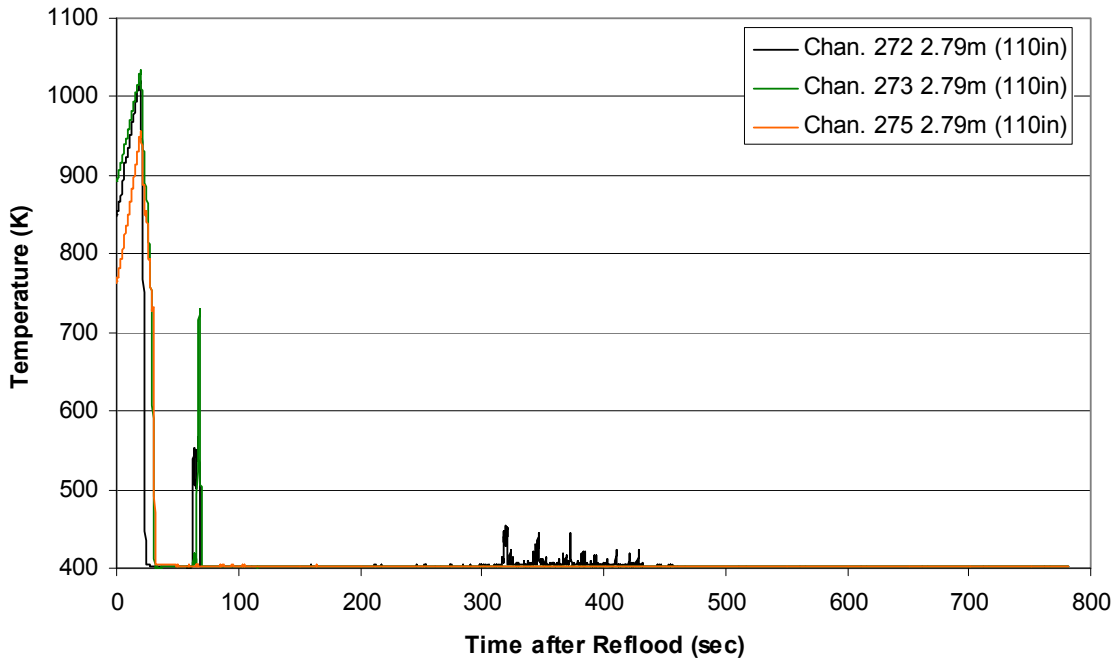
Spacer Grid Temperature during Reflood RBHT Exp. 945



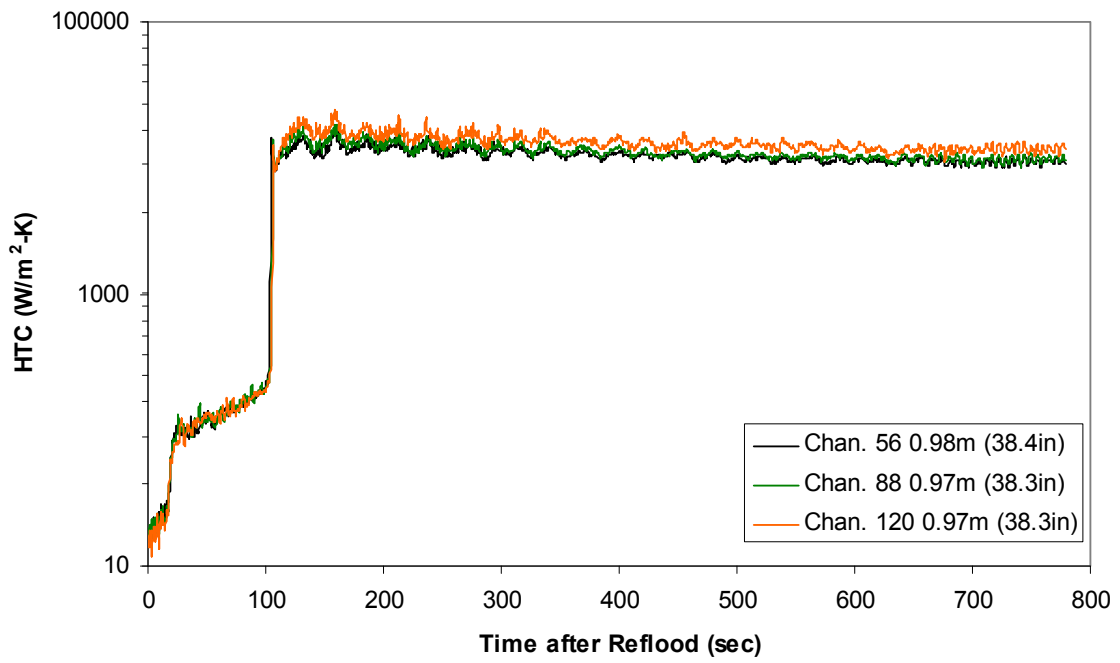
Spacer Grid Temperature during Reflood RBHT Exp. 945



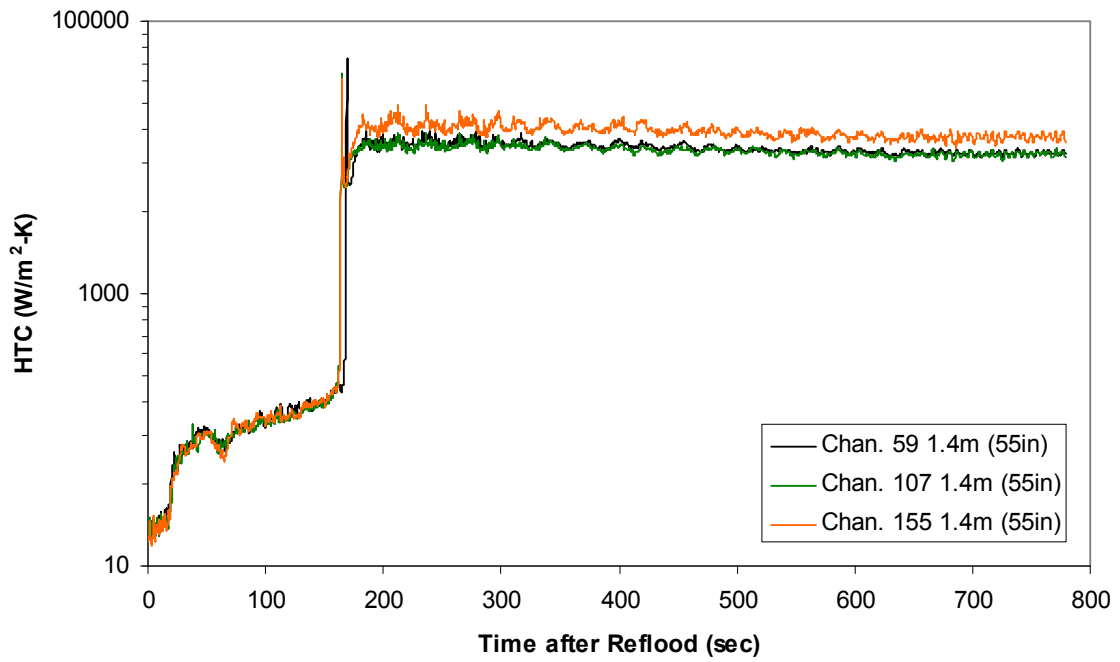
Spacer Grid Temperature during Reflood RBHT Exp. 945



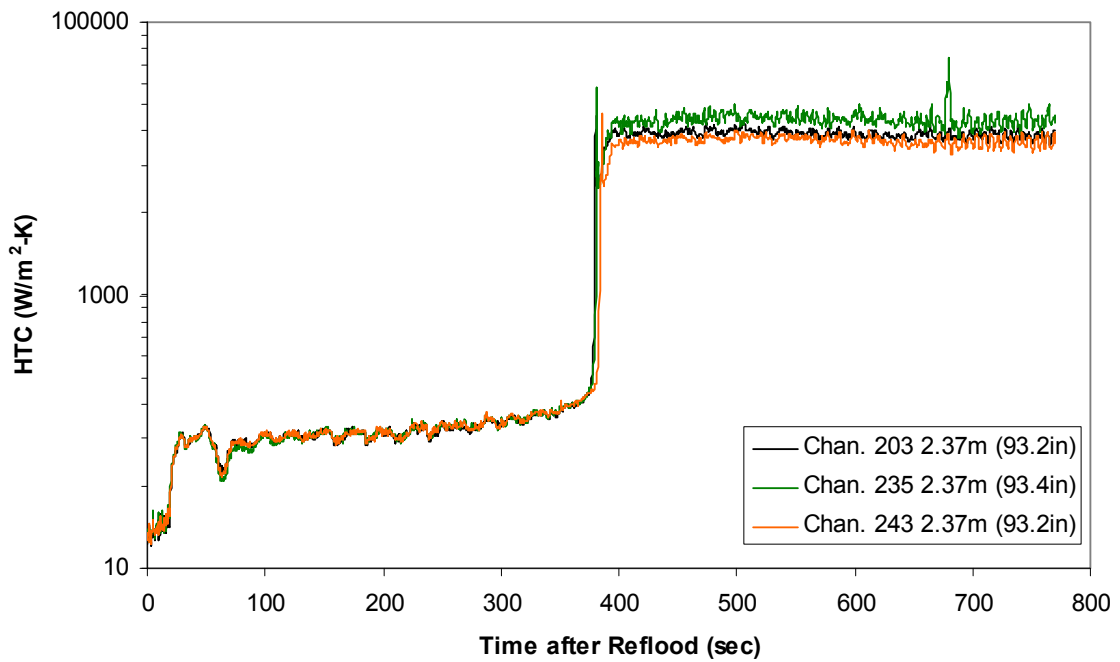
Heat Transfer Coefficient during Reflood RBHT Exp. 945



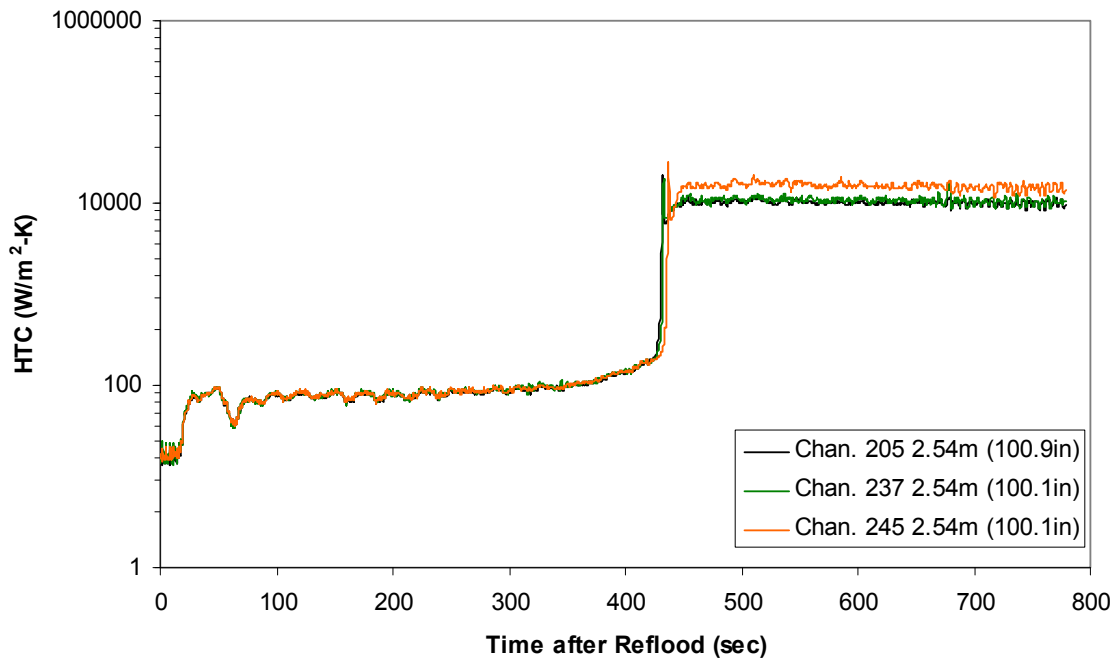
Heat Transfer Coefficient during Reflood
RBHT Exp. 945



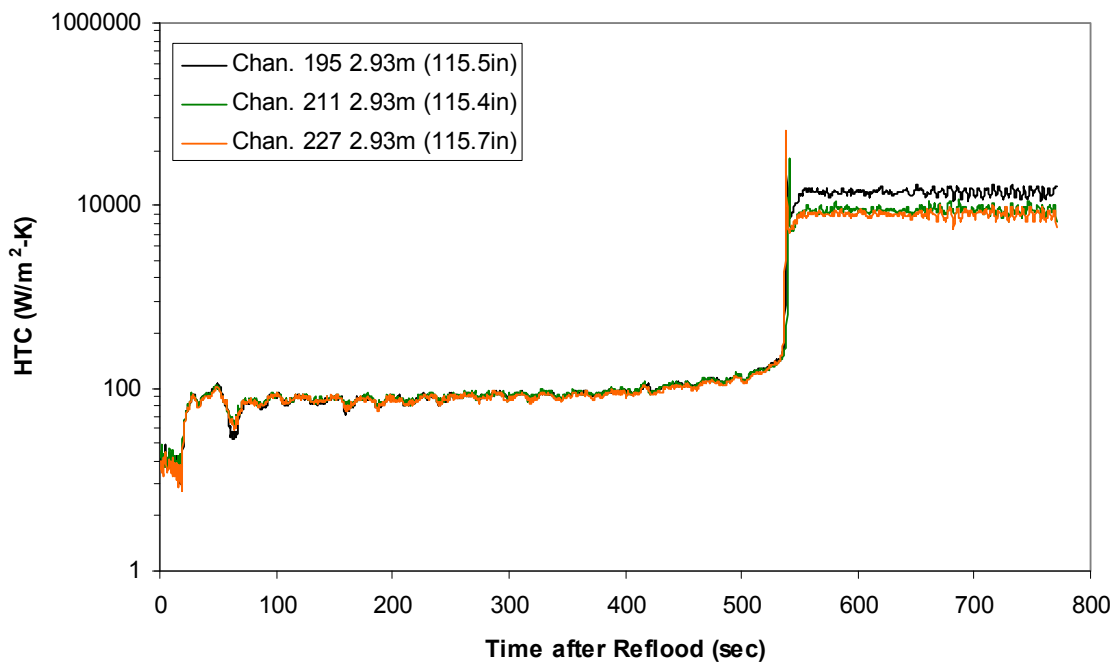
Heat Transfer Coefficient during Reflood
RBHT Exp. 945



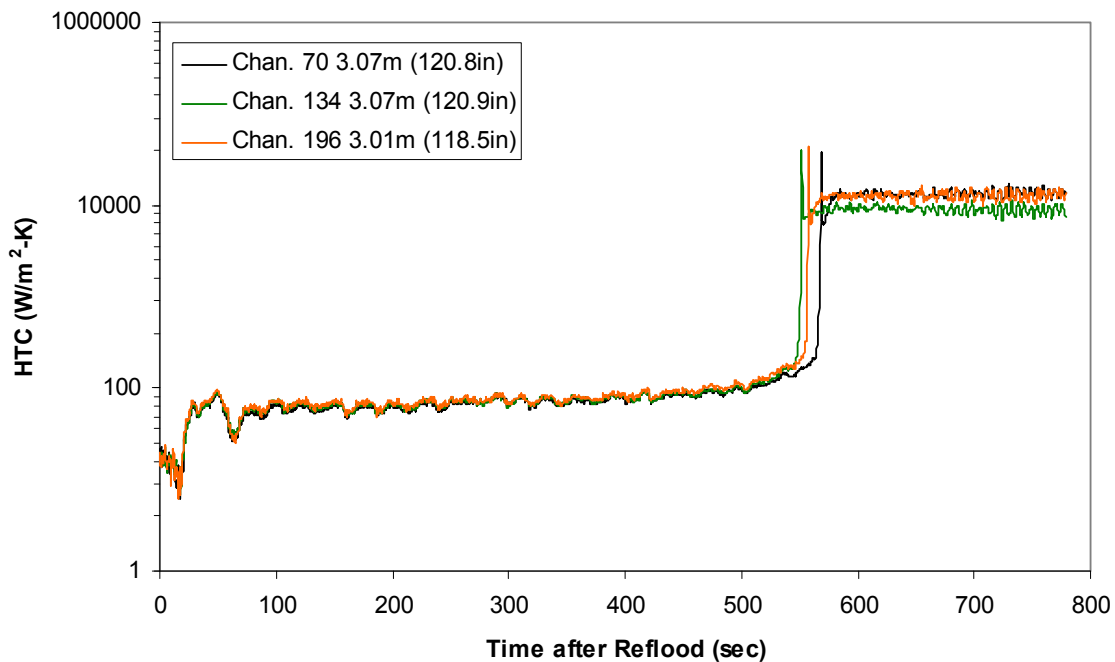
Heat Transfer Coefficient during Reflood RBHT Exp. 945



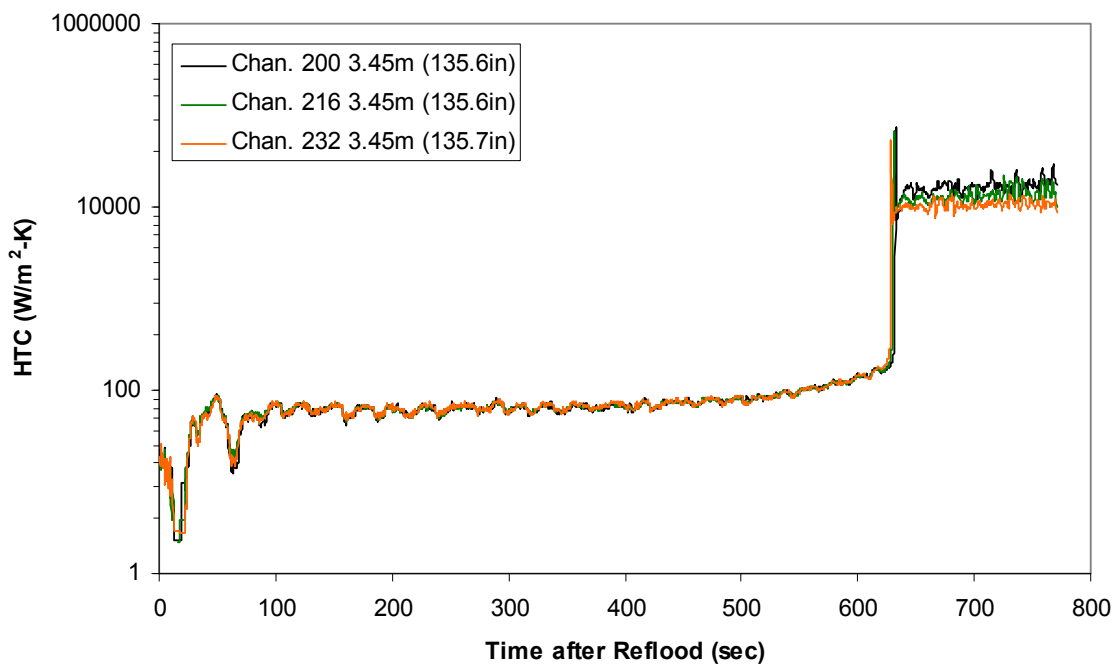
Heat Transfer Coefficient during Reflood RBHT Exp. 945



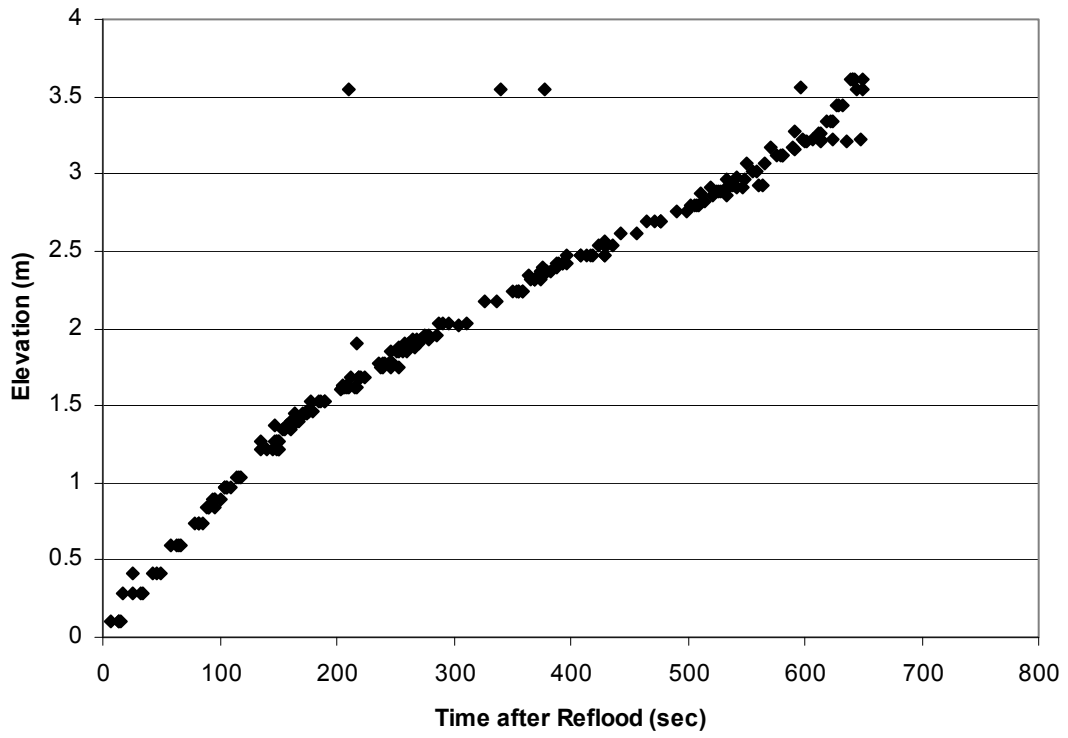
Heat Transfer Coefficient during Reflood RBHT Exp. 945



Heat Transfer Coefficient during Reflood RBHT Exp. 945



Quench Data, RBHT Exp. 945



RBHT - REFLOOD TESTS

SUMMARY SHEET

RUN NO: **973**

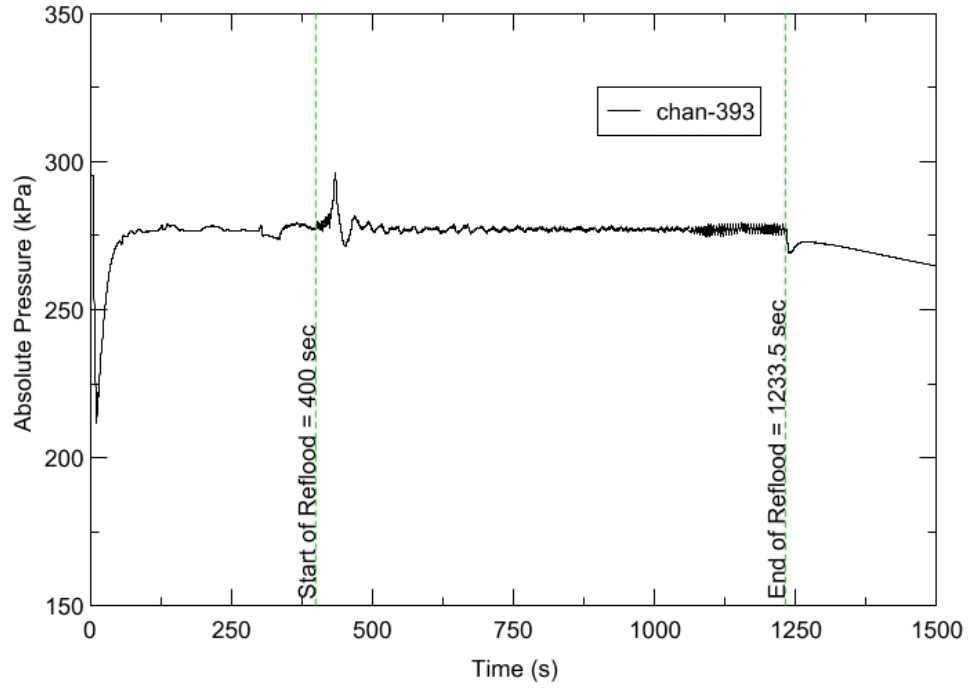
RUN CONDITIONS

Upper Plenum Pressure:	276 kPa (40 psia)
Initial Peak Clad Temperature:	1033 degrees K (1400 degrees F)
Rod Peak Power:	1.31 kW/m (0.4 kW/ft)
Flooding Rate:	0.0254 m/s (1 in/s)
Inlet Subcooling:	11 degrees K (20 degrees F)
Start of Reflood:	400 s
End of Reflood:	1233.5 s
Test Date:	5/16/2002
Comments:	Steam probes positioned in subchannel gaps.

Rod_Elevation	Channel Number	Temperature at Reflood (K)	Temperature at Reflood (°F)	Turnaround Time (sec.)	Turnaround Temperature (K)	Turnaround Temperature (°F)	Quench Time (sec.)	Quench Temperature (K)	Quench Temperature (°F)
B6 0.592m	148	561.51	551.03	17.25	596.77	614.5	45.25	521.81	479.57
B6 0.744m	149	552.35	534.54	19.25	592.89	607.51	58.25	526.16	487.39
B6 0.846m	150	577.92	580.57	21.75	624.89	665.11	64.75	538.58	509.75
B6 0.897m	151	583.16	590.01	22.75	633.96	681.44	68.75	541.49	514.99
C6 1.04m	137	598.93	618.38	25.75	659	726.51	72.75	587.23	597.33
D5 1.27m	217	722.18	840.23	25.25	770.03	926.37	98.75	586.51	596.03
C6 1.34m	138	785.88	954.89	26.75	835.3	1043.85	109.25	631.24	676.54
D5 1.37m	218	828.39	1031.41	26.75	876.39	1117.81	112.25	653.03	715.76
C6 1.39m	139	820.57	1017.34	26.25	870.65	1107.48	115.75	659	726.52
D5 1.45m	219	868.17	1103.01	28.25	920.46	1197.15	127.75	663.61	734.82
C6 1.47m	140	853.12	1075.93	28.25	907.37	1173.57	130.25	682.8	769.35
D5 1.52m	220	891.07	1144.24	28.25	949.26	1248.98	144.75	684.8	772.95
C6 1.62m	141	878.98	1122.48	29.75	943.81	1239.17	166.25	689.69	781.76
D5 1.68m	221	905.62	1170.43	64.75	978.98	1302.48	180.75	714.8	826.94
D5 1.78m	222	886.68	1136.33	29.75	961.69	1271.36	205.25	636.5	686.01
D5 1.85m	223	915.61	1188.42	30.25	989.89	1322.11	216.75	683.87	771.28
C6 1.87m	142	897.71	1156.19	31.25	973.68	1292.93	222.75	681.67	767.32
D5 1.90m	224	928.05	1210.8	31.25	1005.69	1350.56	228.75	697.5	795.82
C6 1.95m	144	912.44	1182.71	30.75	990.06	1322.41	244.75	691.17	784.42
C3 2.17m	178	952.19	1254.25	66.25	1064.58	1456.55	311.75	711	820.11
D4 2.24m	241	961.5	1271.01	66.75	1079.04	1482.58	344.75	692.6	787
D4 2.32m	242	965.08	1277.46	29.75	1051.13	1432.34	361.75	638.64	689.87
C3 2.35m	180	964.61	1276.61	29.75	1050.74	1431.65	354.25	687.53	777.86
D4 2.37m	243	981.16	1306.39	30.25	1069.51	1465.43	373.25	669.87	746.09
C3 2.40m	181	975.87	1296.88	30.25	1063.83	1455.21	366.75	710.44	819.11
D4 2.54m	245	1019.26	1374.99	65.75	1118.93	1554.39	431.25	673.53	752.66
D6 2.62m	129	1013.77	1365.1	64.75	1121.26	1558.58	442.25	745.34	881.93
D6 2.69m	130	1011.89	1361.72	88.75	1130.96	1576.05	469.25	745.47	882.16
C3 2.76m	183	1006.37	1351.78	87.75	1138.1	1588.88	494.75	741.98	875.87
D4 2.79m	247	988.29	1319.24	29.25	1094.73	1510.83	517.75	657.63	724.05
D6 2.87m	131	972.87	1291.48	29.25	1064.15	1455.78	519.25	660.72	729.6
D6 2.92m	132	962.73	1273.23	30.75	1056.95	1442.82	529.75	691.88	785.7
D6 2.97m	133	948.33	1247.3	30.75	1039.27	1411	545.75	696.62	794.23
D6 3.07m	134	925.23	1205.72	66.75	1021.78	1379.52	567.25	686.83	776.6
E3 3.12m	197	917.56	1191.92	66.75	1024.32	1384.09	589.25	665.73	738.62
D6 3.17m	135	895.9	1152.93	89.25	998.36	1337.36	587.25	678.44	761.5
D6 3.27m	136	853.43	1076.49	89.25	968.26	1283.19	605.25	673.84	753.23
D4 3.61m	248	729.46	853.34	68.75	799.42	979.27	663.25	576.04	577.19

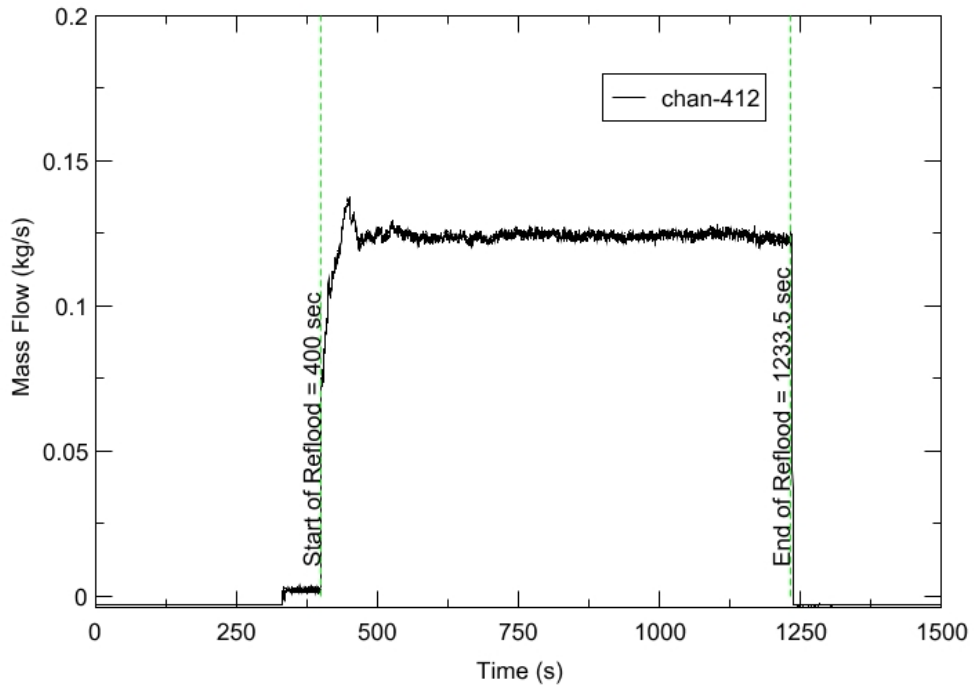
RBHT - TEST FACILITY

Upper Plenum Pressure vs. Time, Exp 973



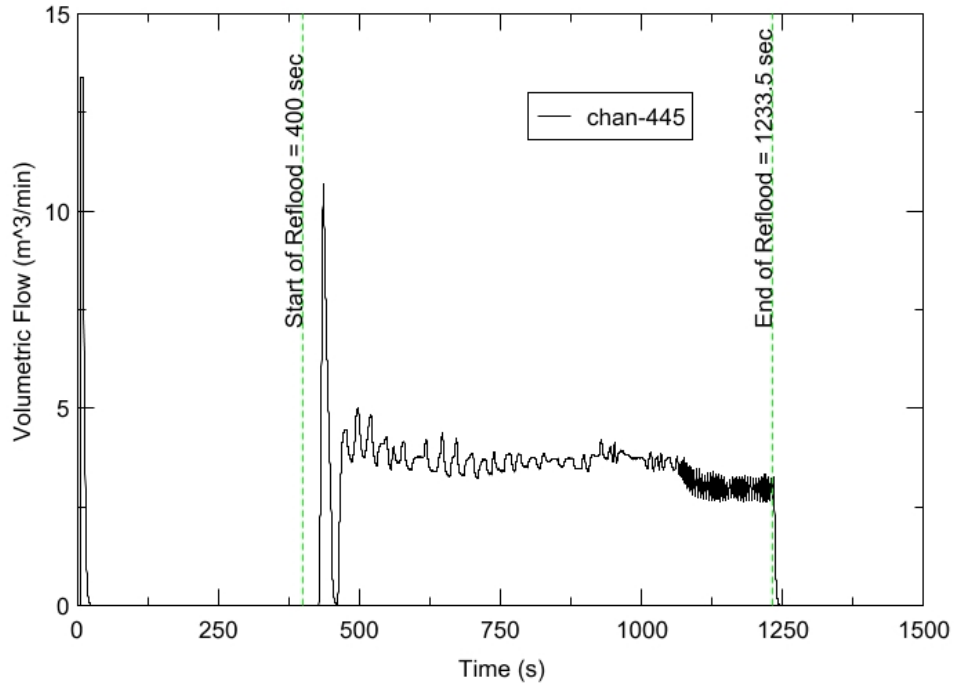
RBHT - TEST FACILITY

Inlet Flow vs. Time, Exp 973



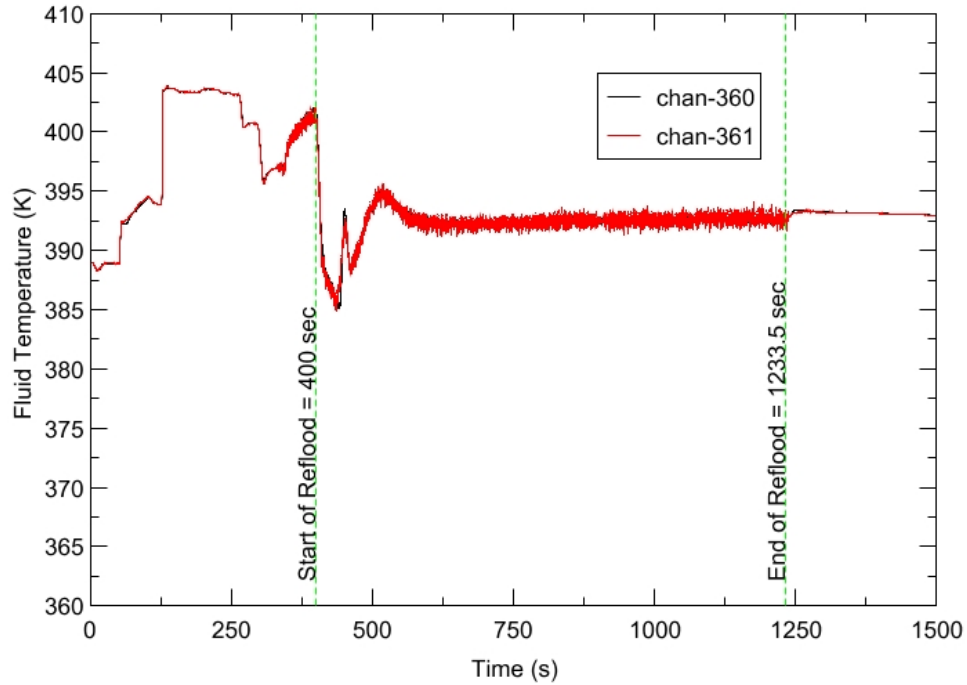
RBHT - TEST FACILITY

Steam Exhaust Flow vs. Time, Exp 973



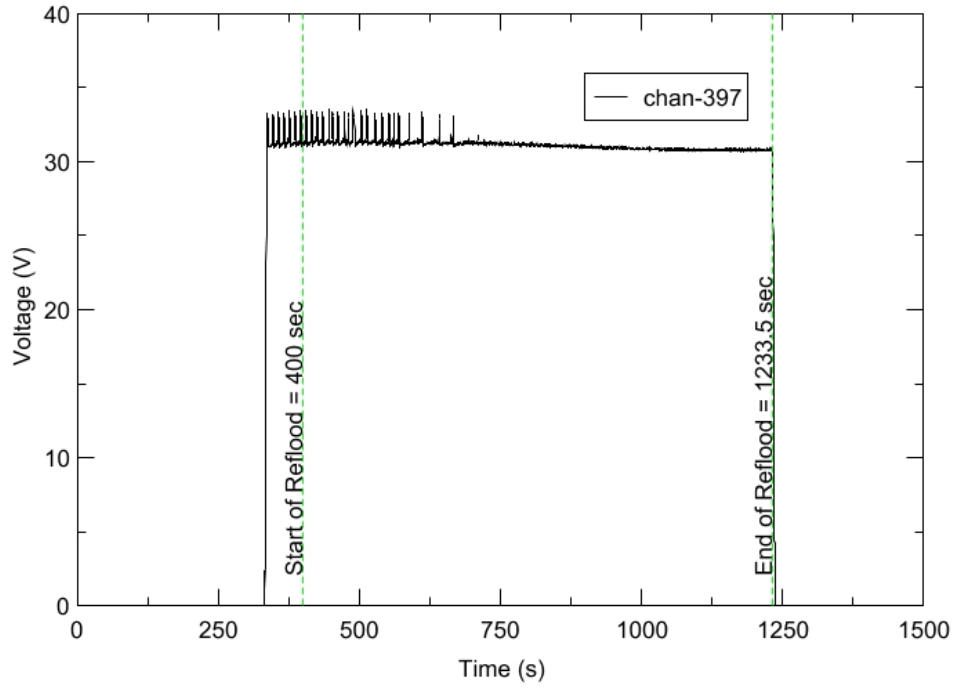
RBHT - TEST FACILITY

Inlet Flow Temperature vs. Time, Exp 973



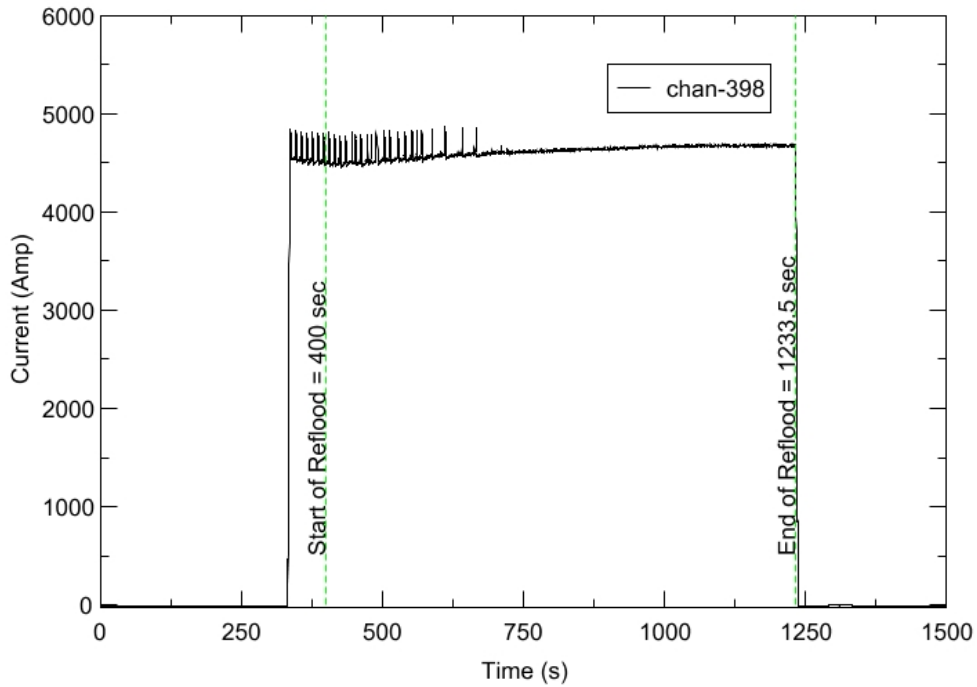
RBHT - TEST FACILITY

Test Section Voltage vs. Time, Exp 973

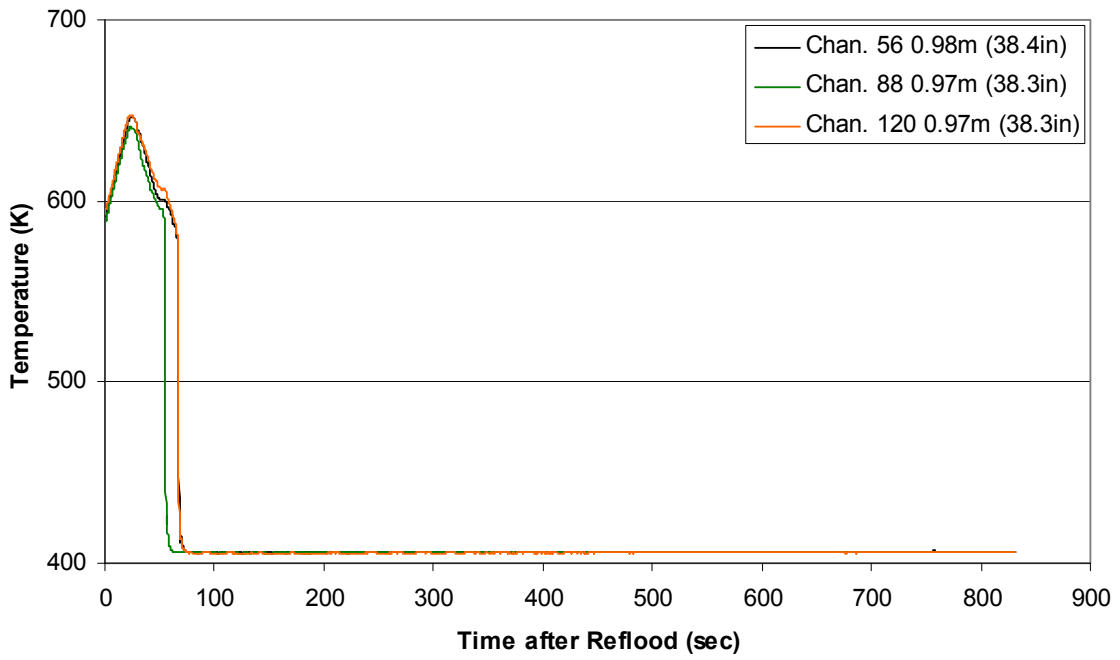


RBHT - TEST FACILITY

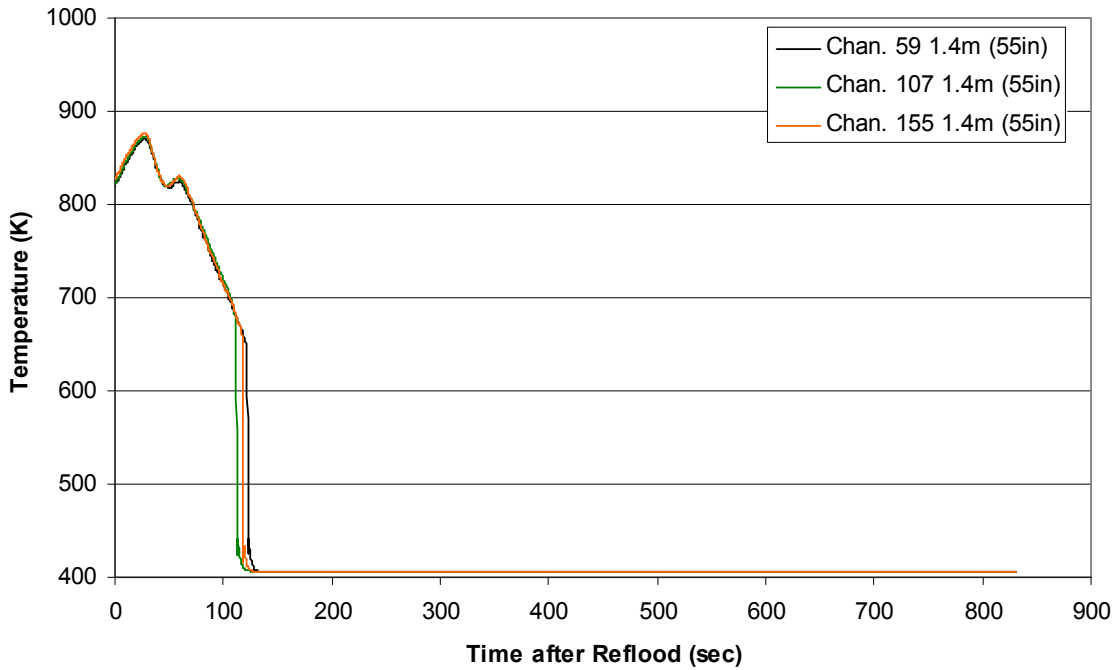
Test Section Current vs. Time, Exp 973



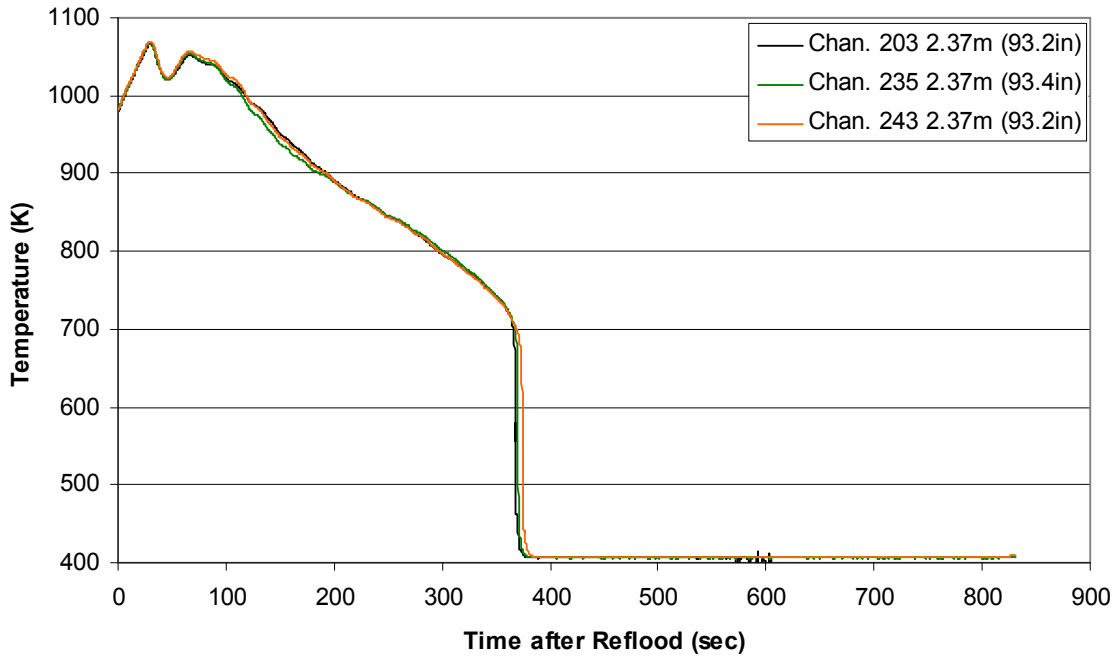
Heater Rod Temperature during Reflood
RBHT Exp. 973



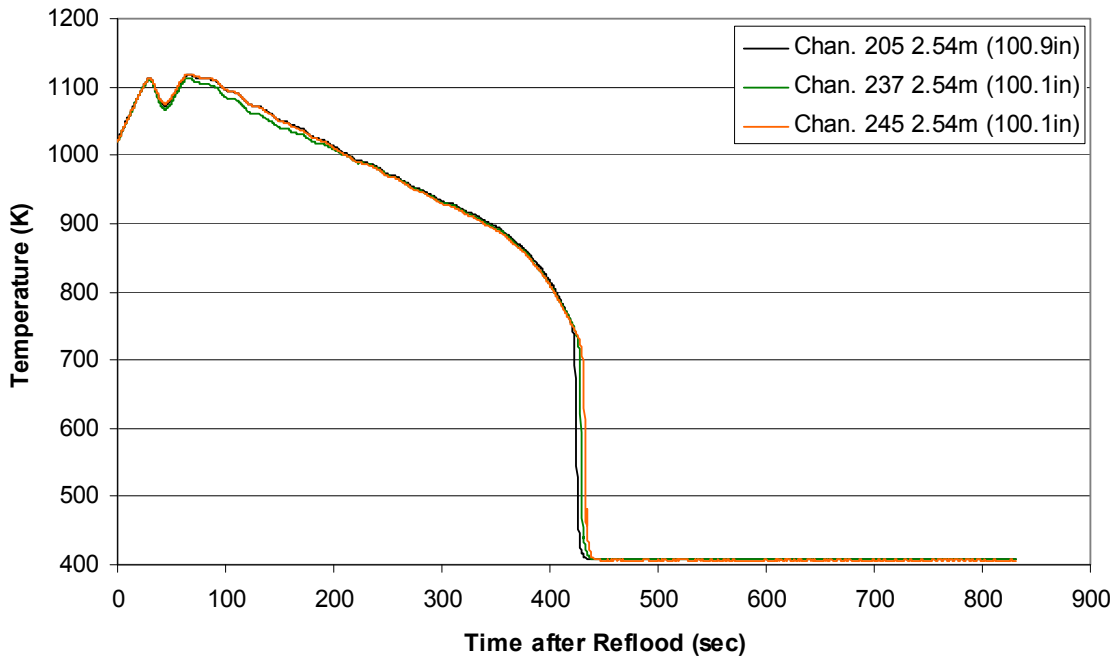
Heater Rod Temperature during Reflood
RBHT Exp. 973



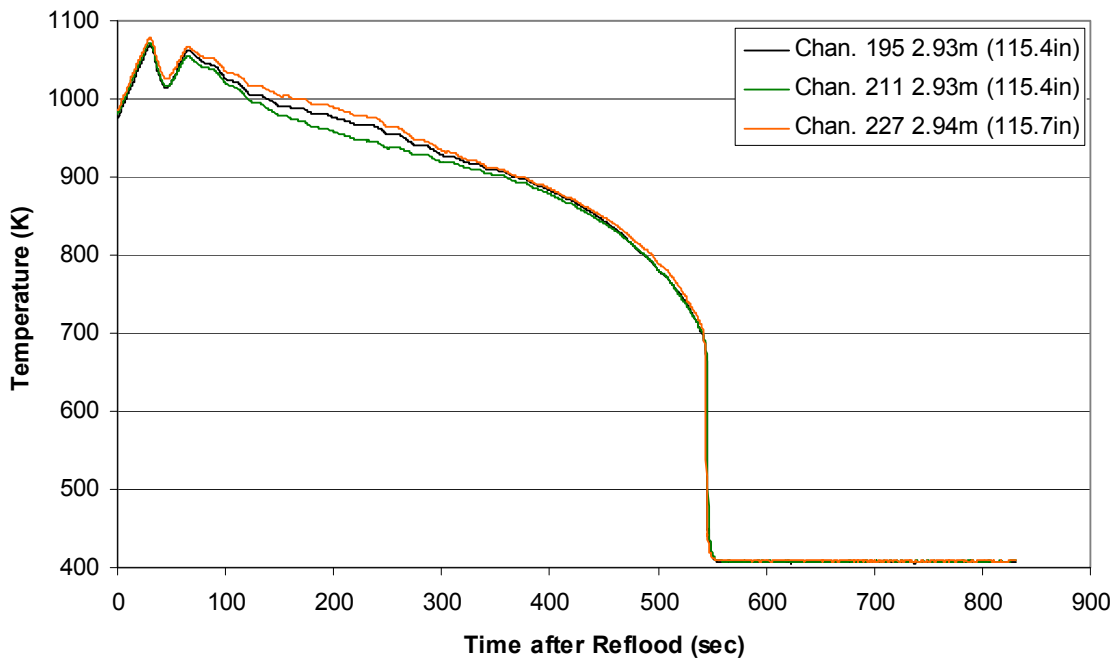
**Heater Rod Temperature during Reflood
RBHT Exp. 973**



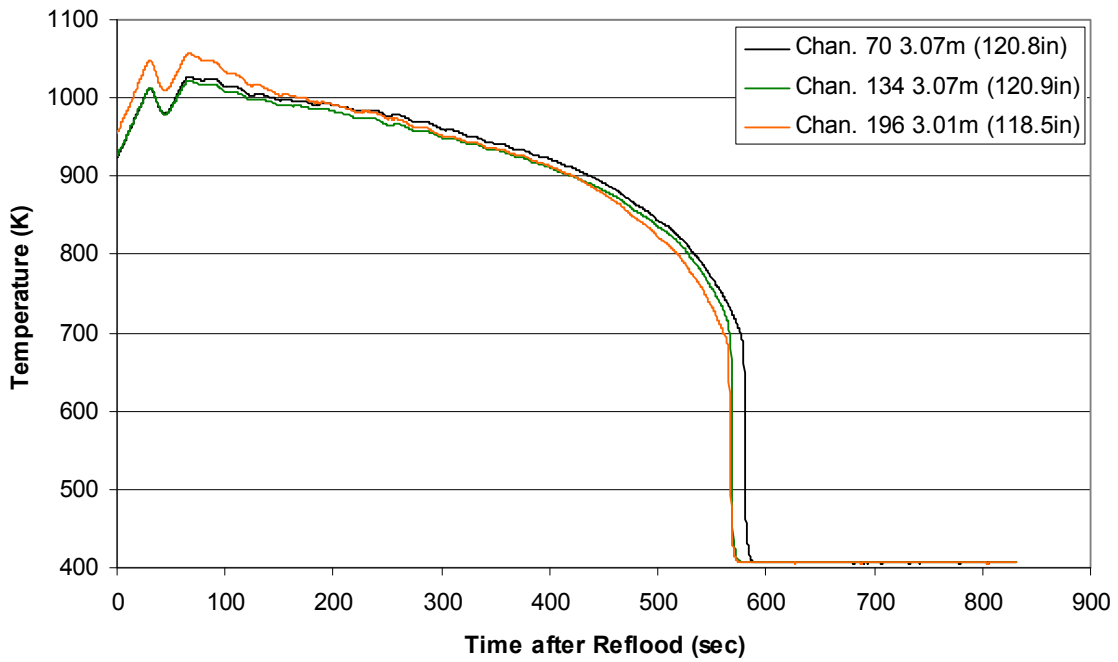
**Heater Rod Temperature during Reflood
RBHT Exp. 973**



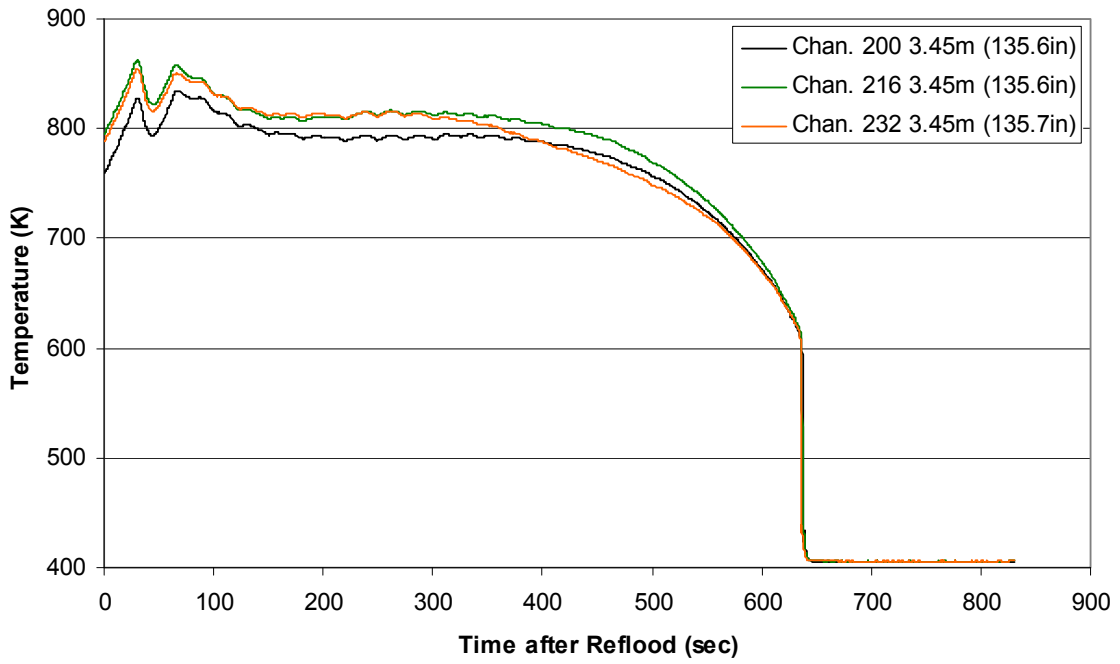
**Heater Rod Temperature during Reflood
RBHT Exp. 973**



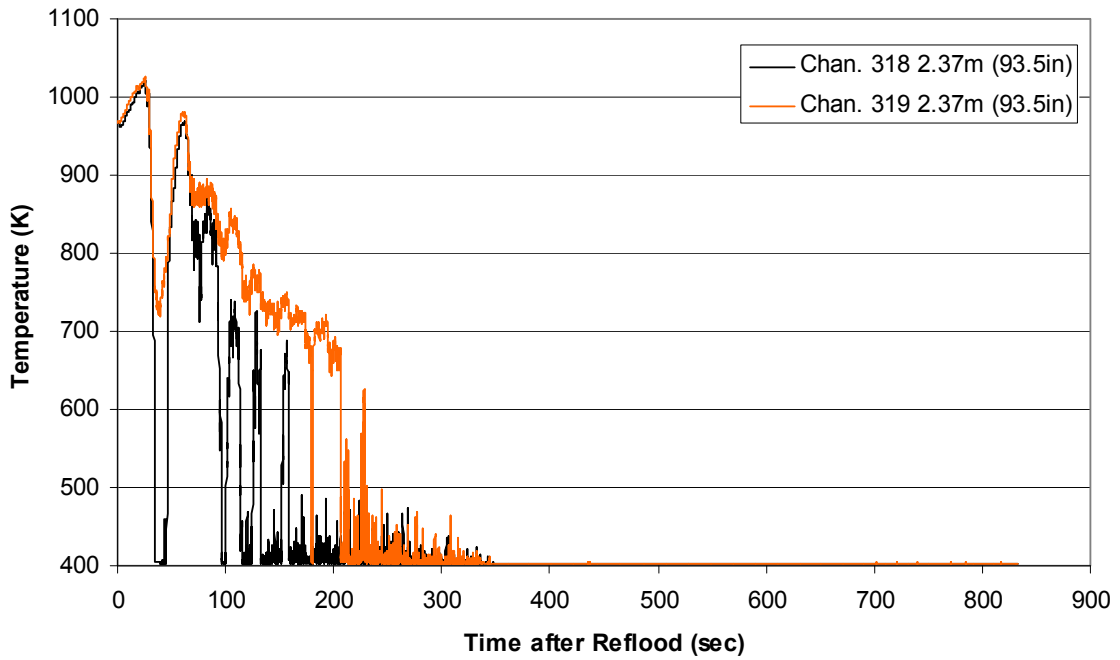
**Heater Rod Temperature during Reflood
RBHT Exp. 973**



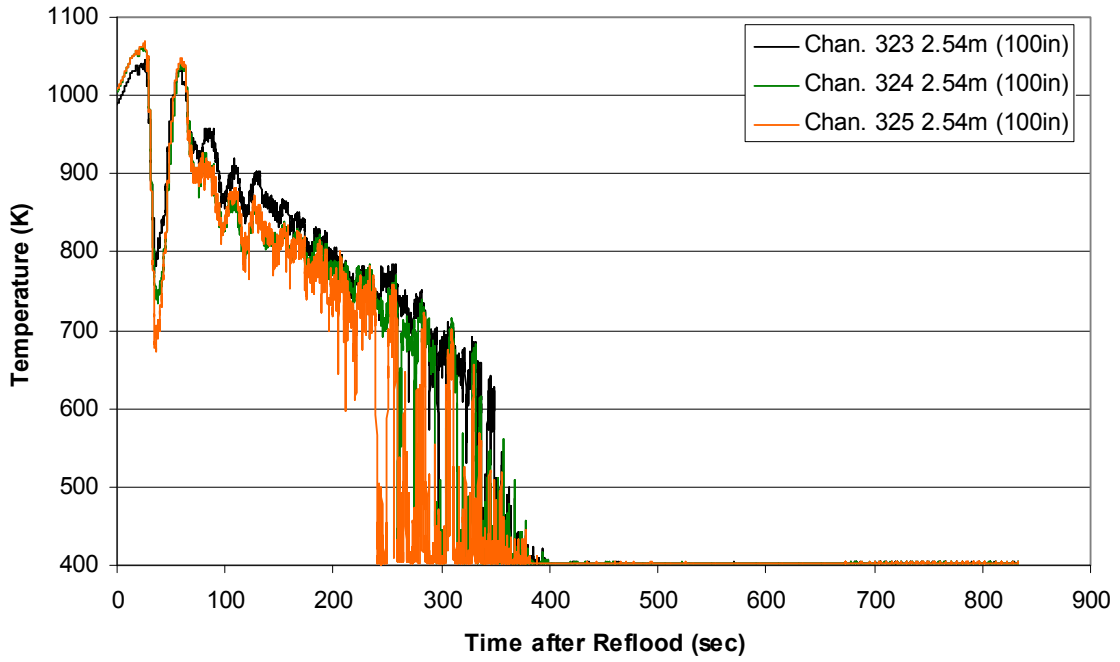
Heater Rod Temperature during Reflood RBHT Exp. 973



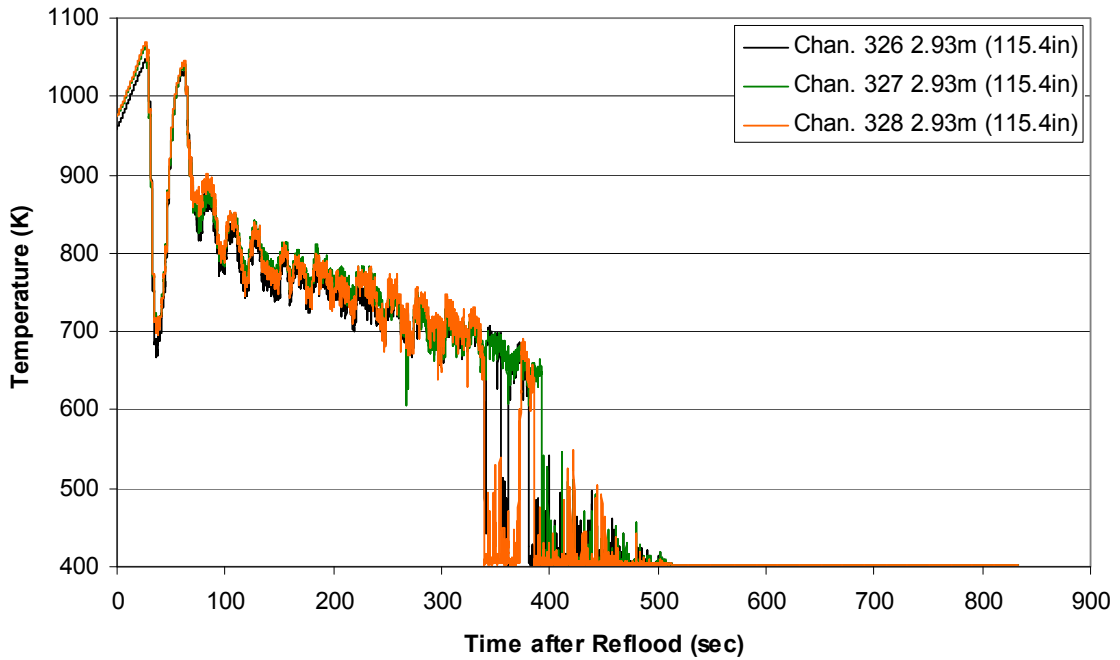
Steam Probe Temperature during Reflood RBHT Exp. 973



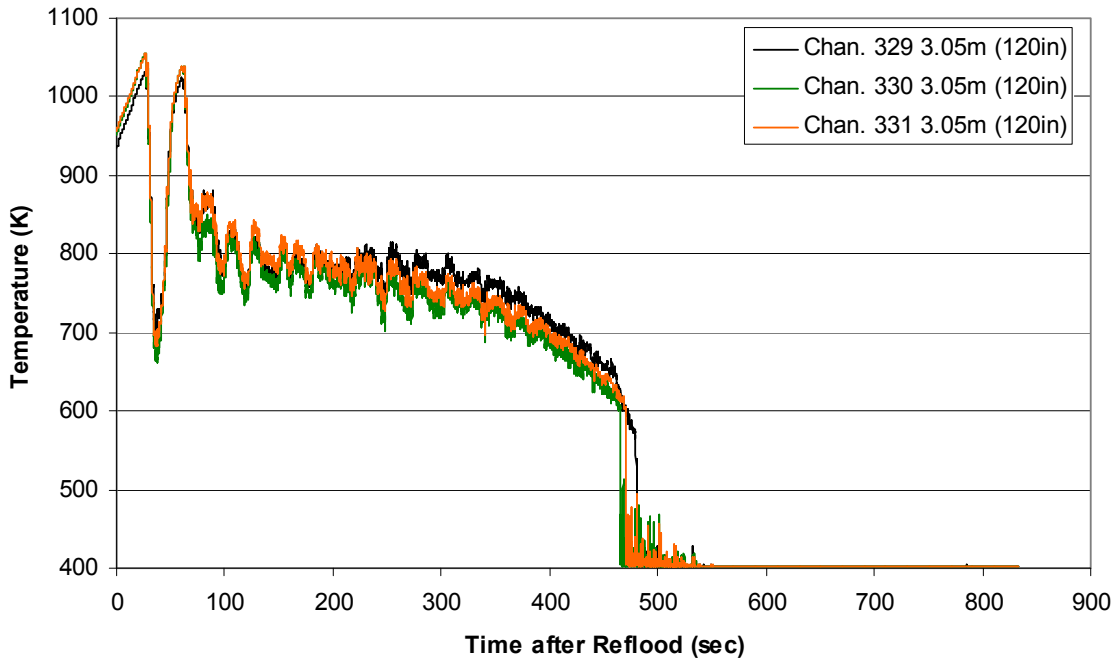
Steam Probe Temperature during Reflood
RBHT Exp. 973



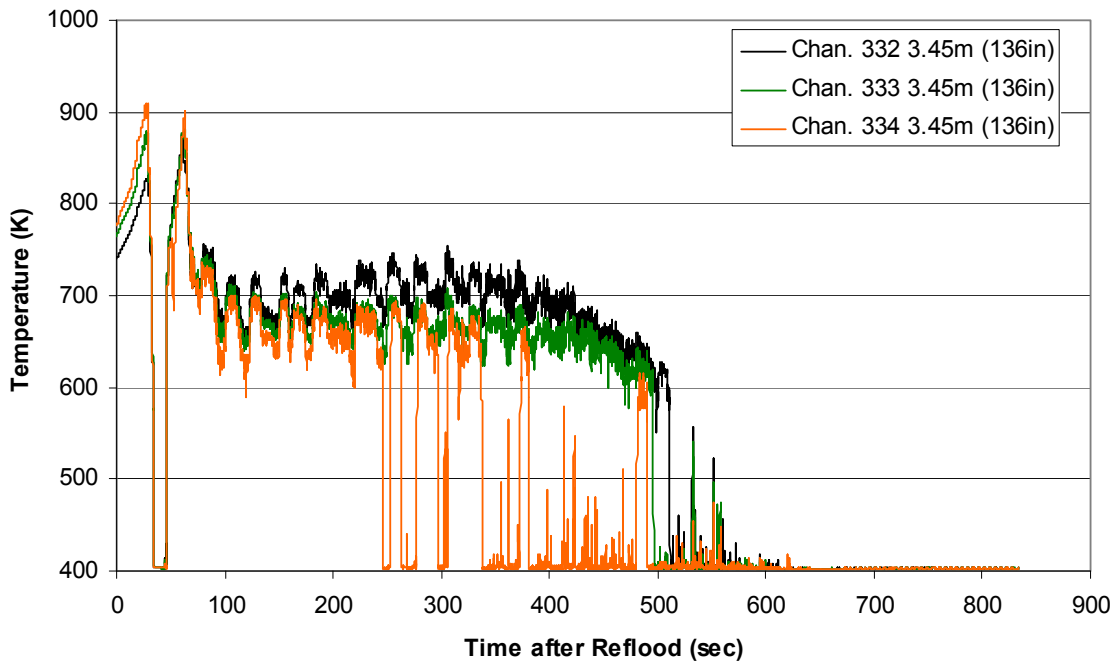
Steam Probe Temperature during Reflood
RBHT Exp. 973



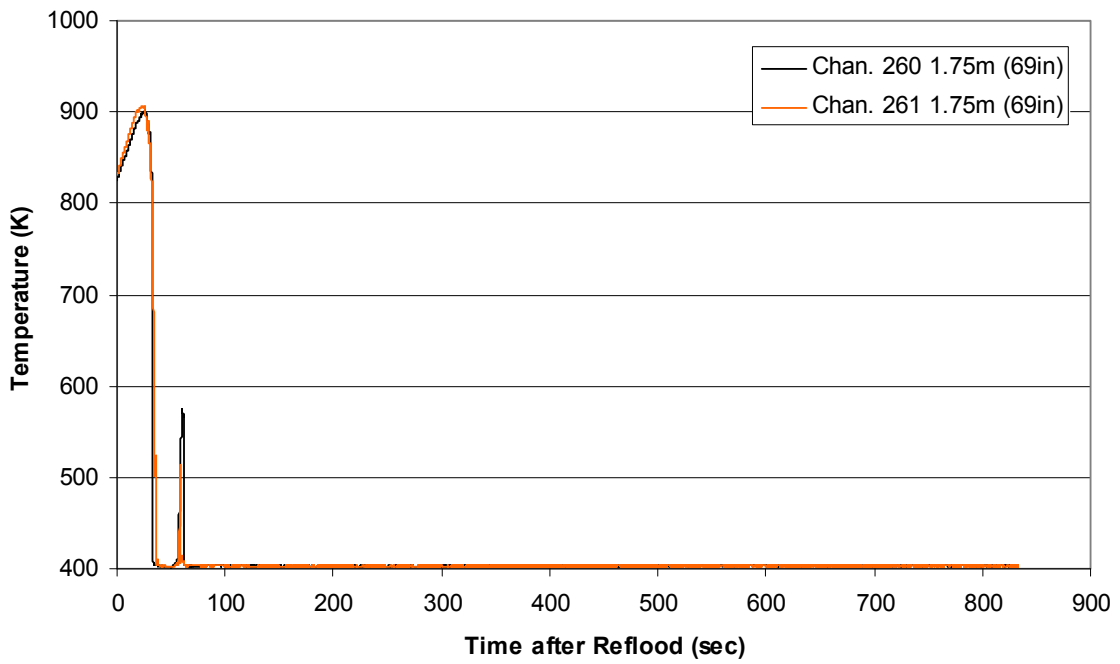
**Steam Probe Temperature during Reflood
RBHT Exp. 973**



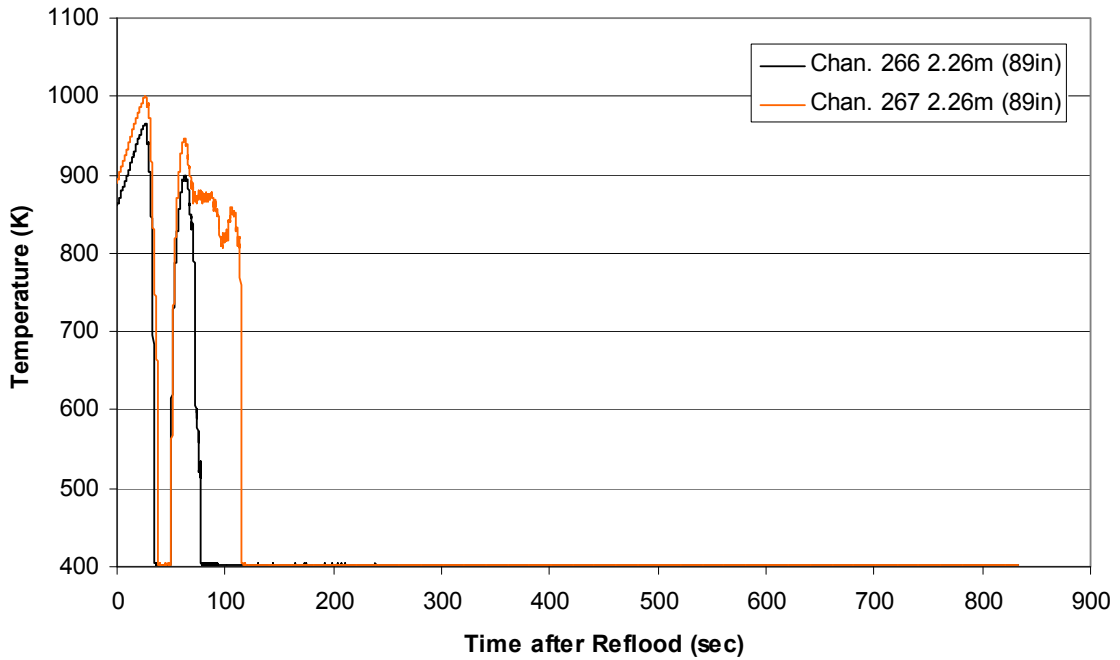
**Steam Probe Temperature during Reflood
RBHT Exp. 973**



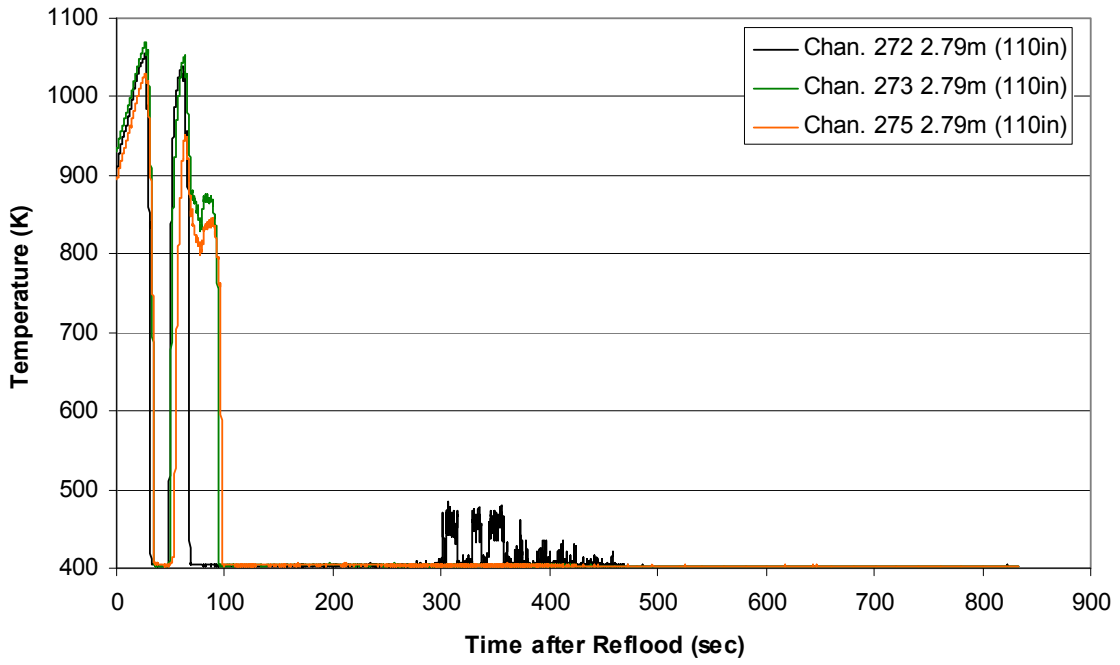
Spacer Grid Temperature during Reflood RBHT Exp. 973



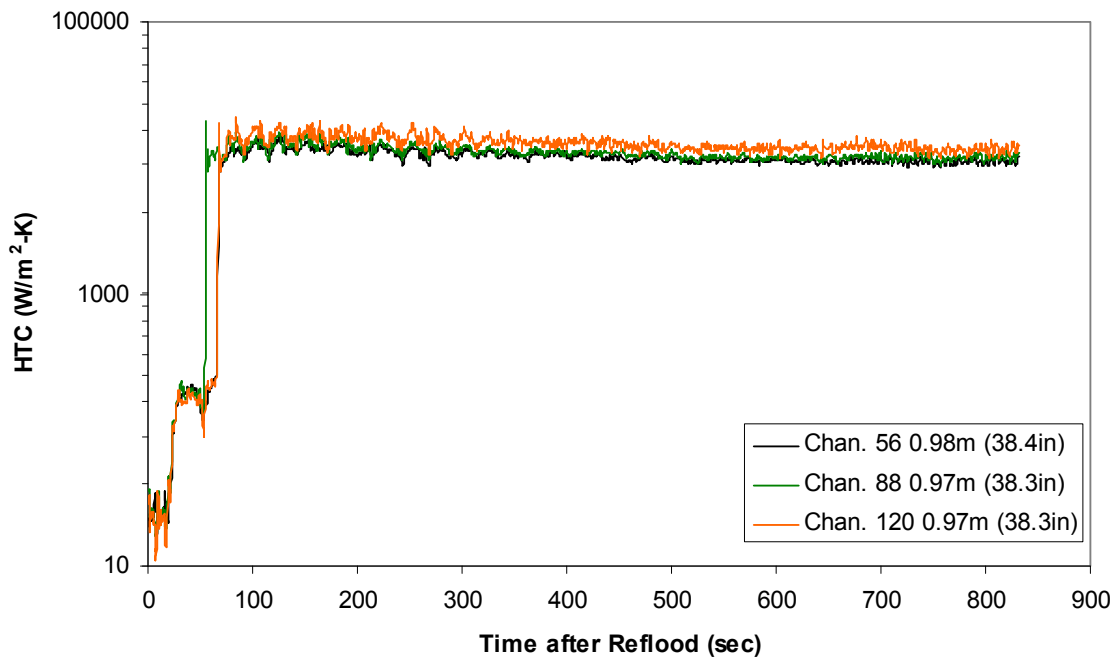
Spacer Grid Temperature during Reflood RBHT Exp. 973



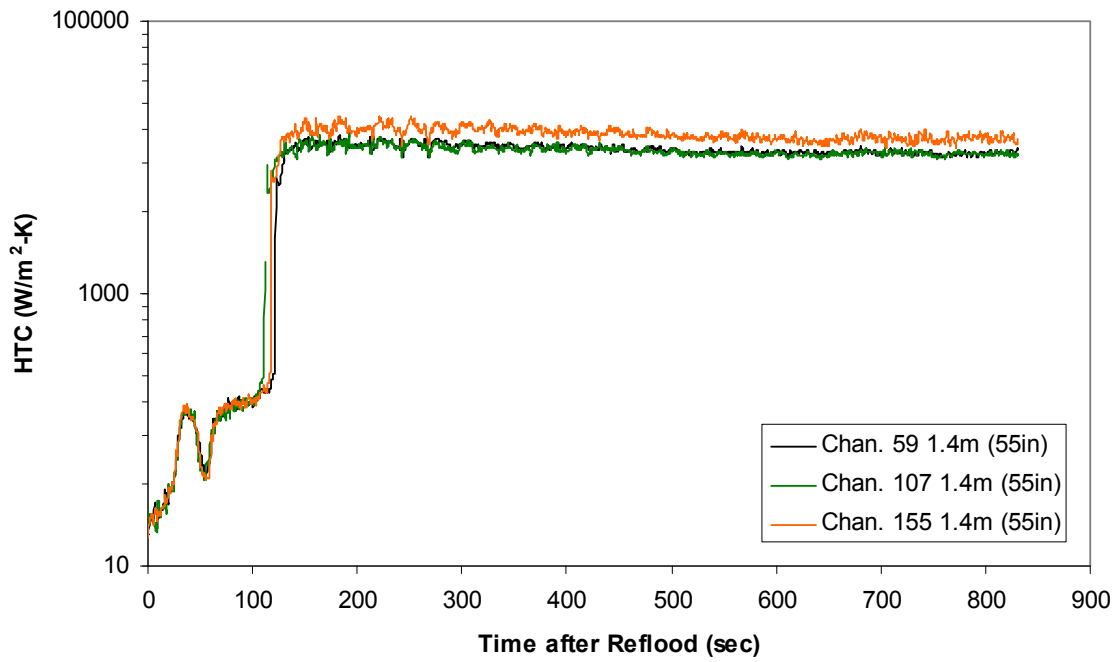
Spacer Grid Temperature during Reflood RBHT Exp. 973



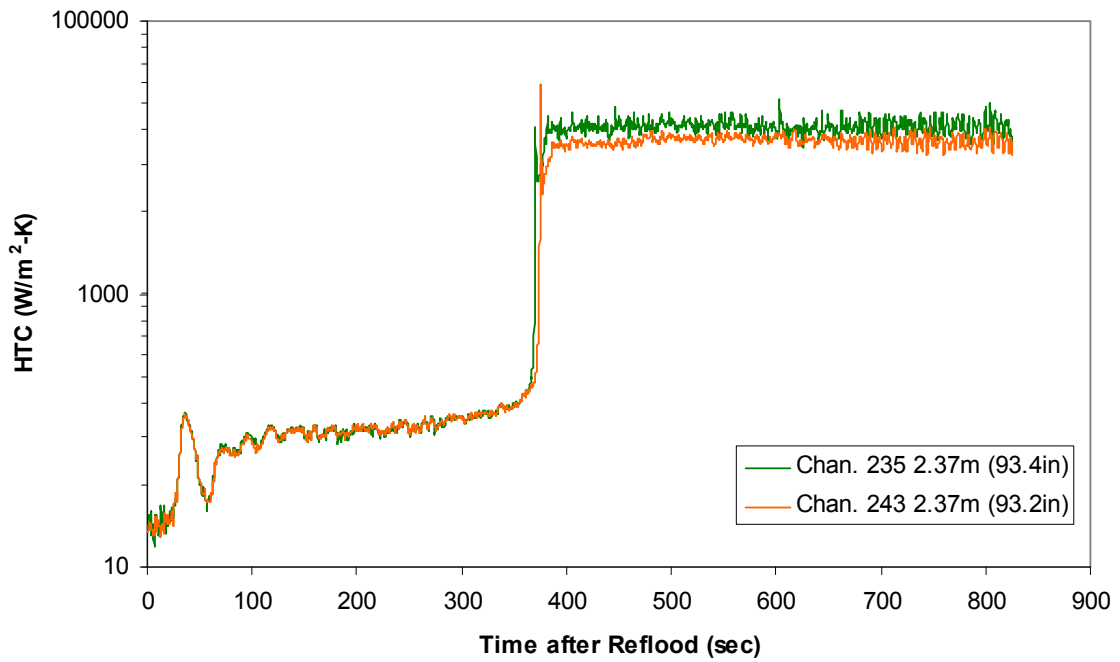
Heat Transfer Coefficient during Reflood RBHT Exp. 973



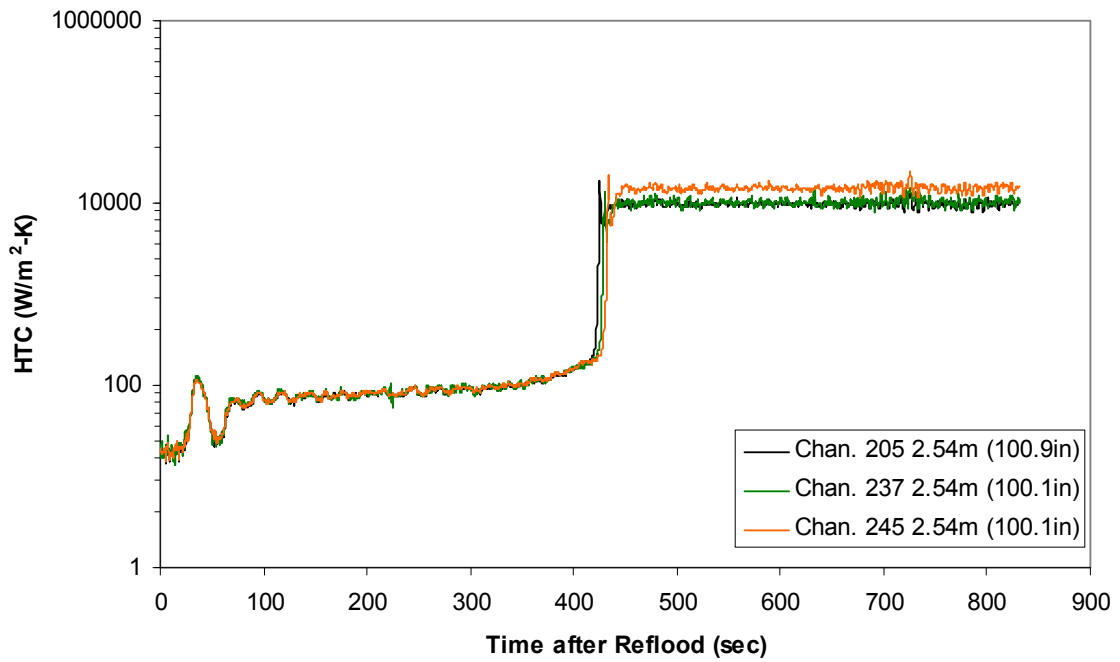
Heat Transfer Coefficient during Reflood RBHT Exp. 973



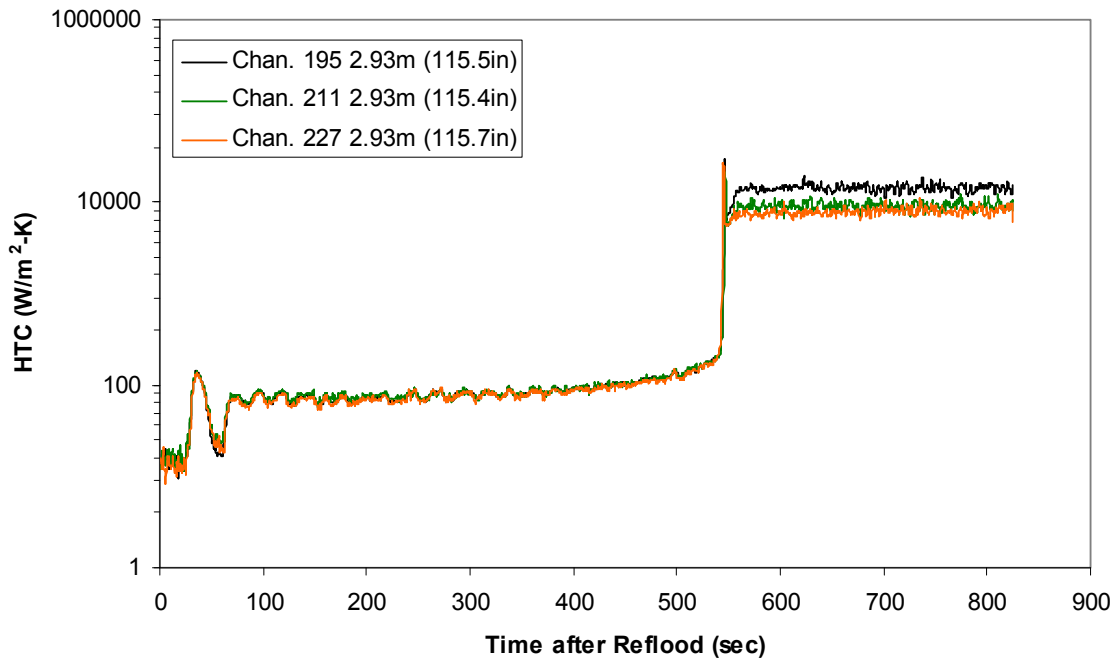
Heat Transfer Coefficient during Reflood RBHT Exp. 973



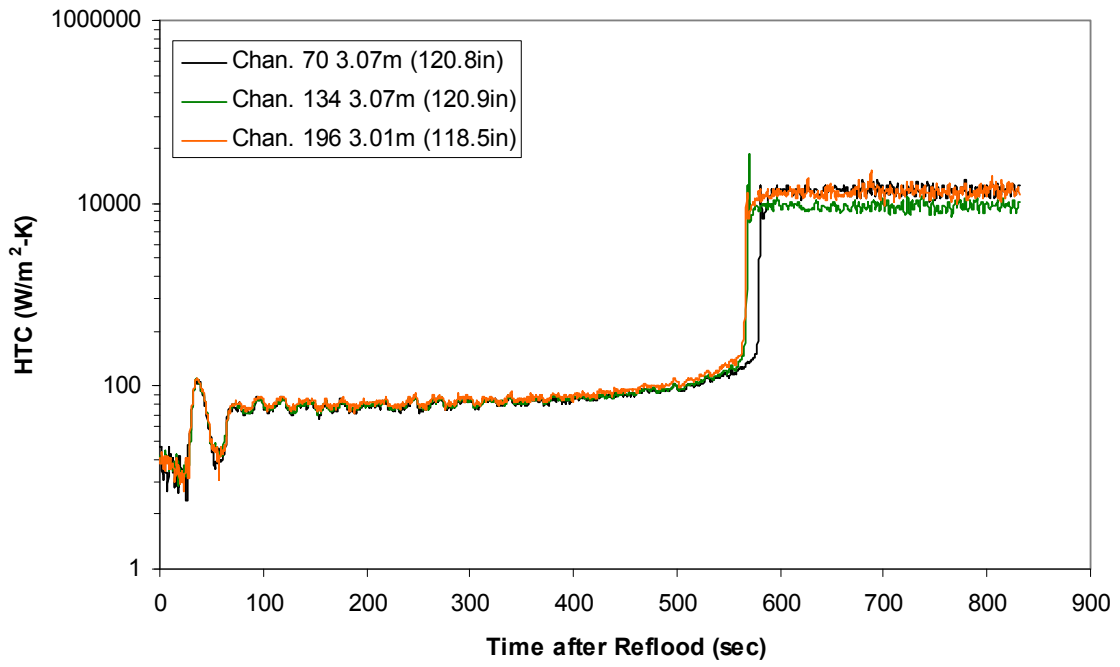
Heat Transfer Coefficient during Reflood RBHT Exp. 973



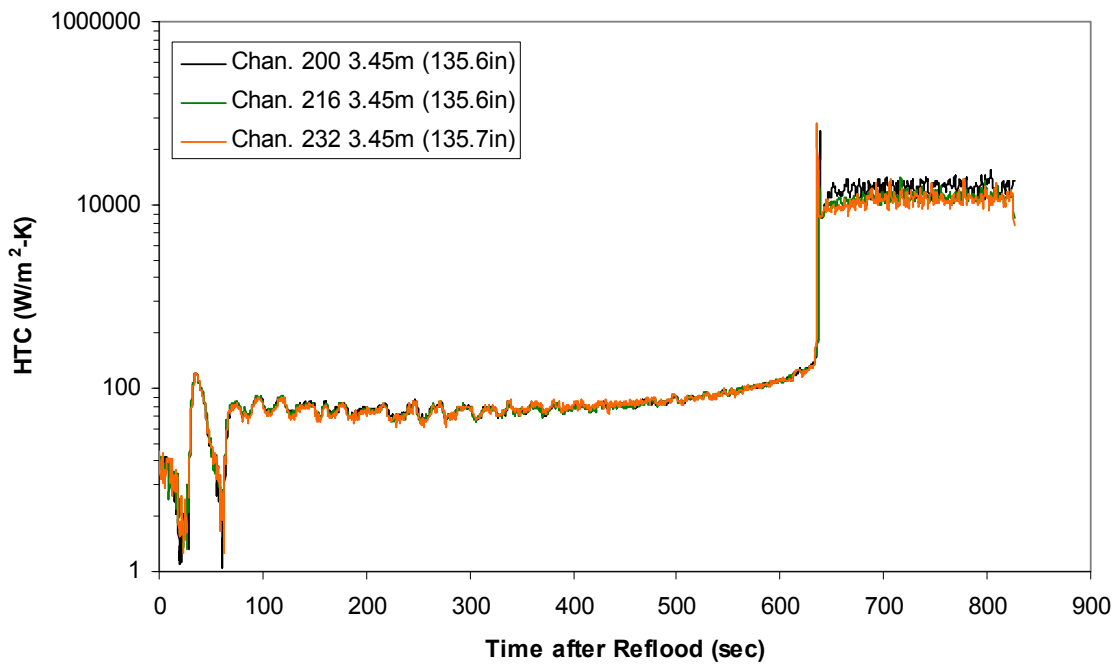
Heat Transfer Coefficient during Reflood RBHT Exp. 973



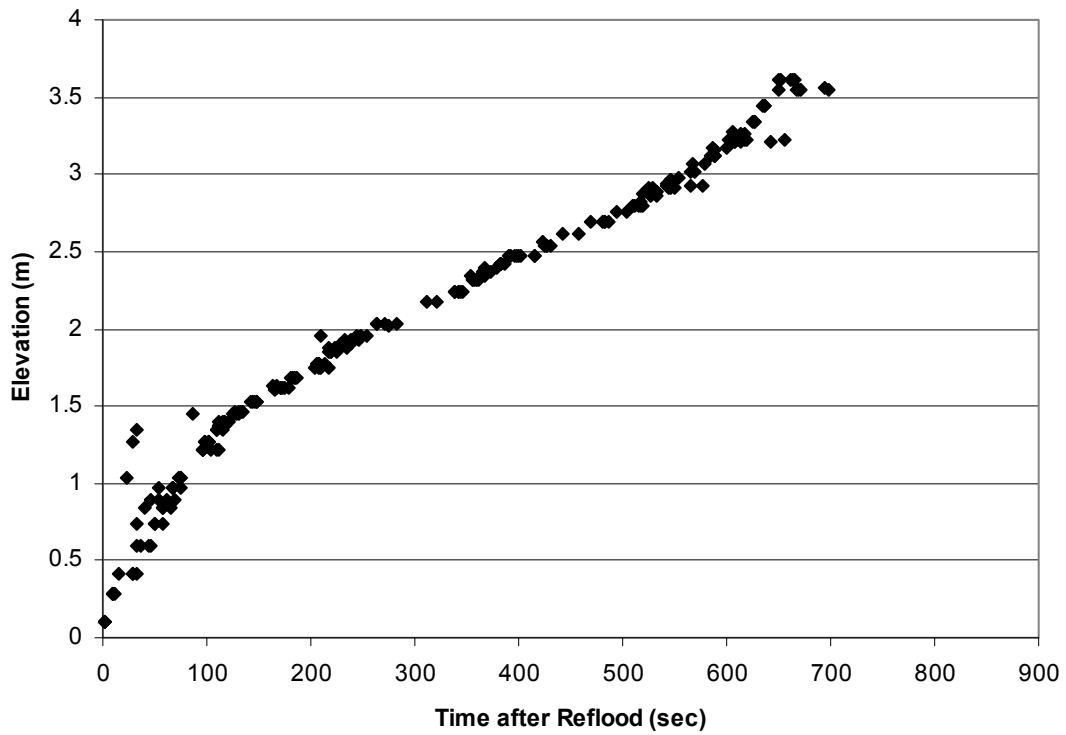
Heat Transfer Coefficient during Reflood RBHT Exp. 973



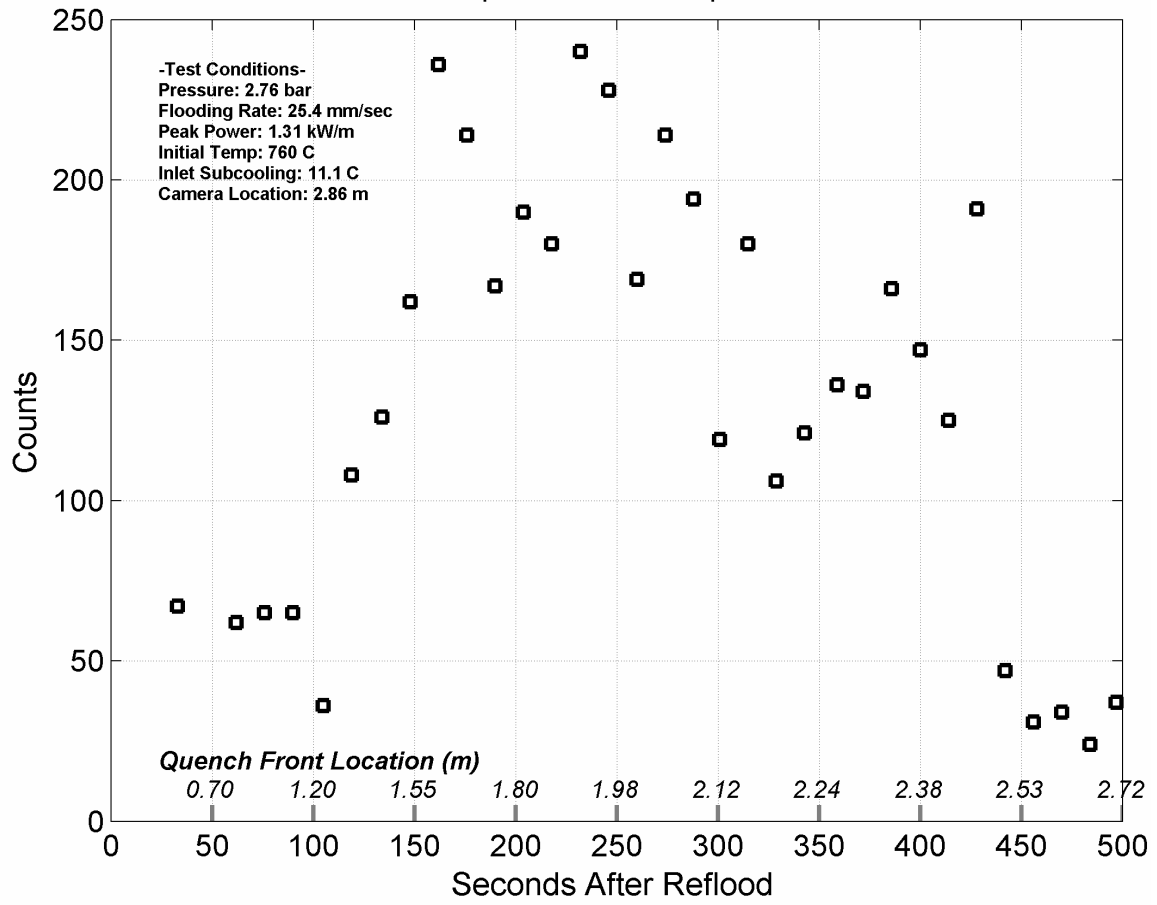
Heat Transfer Coefficient during Reflood RBHT Exp. 973



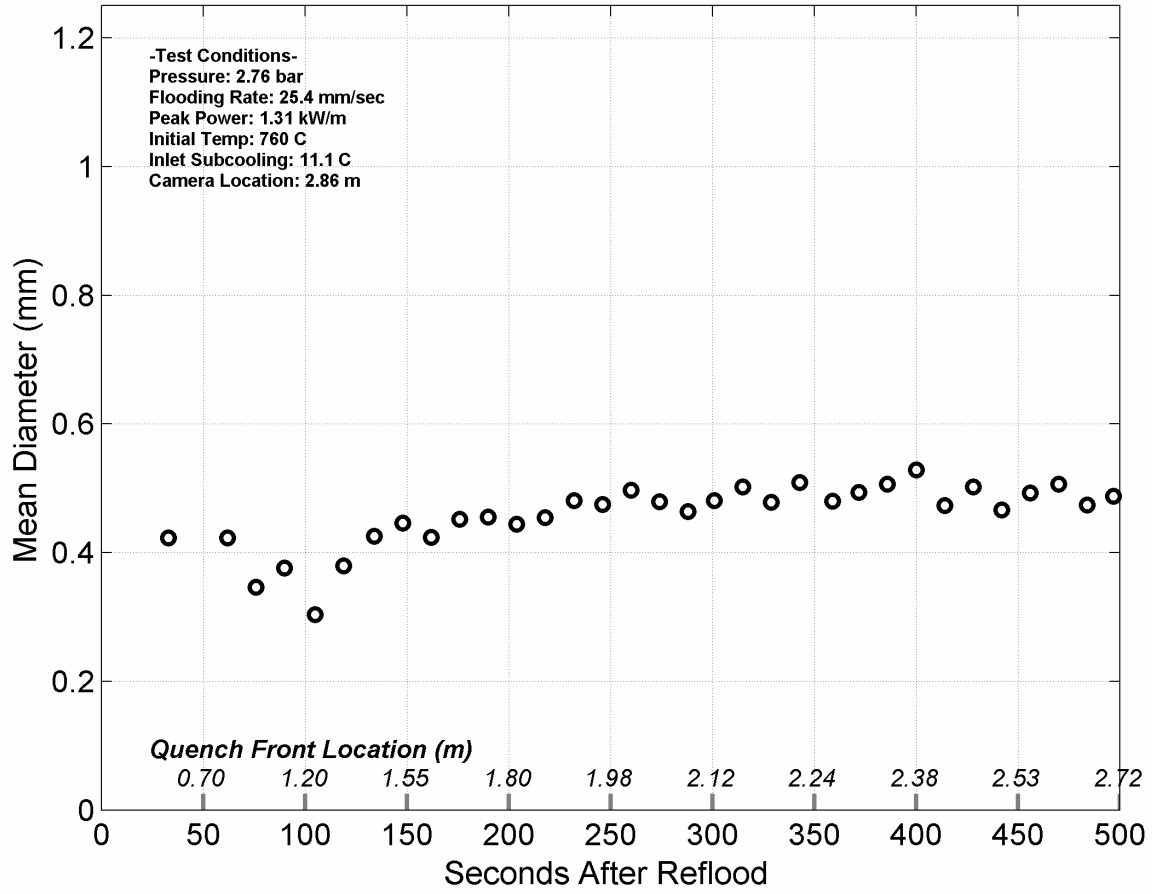
Quench Data, RBHT Exp. 973



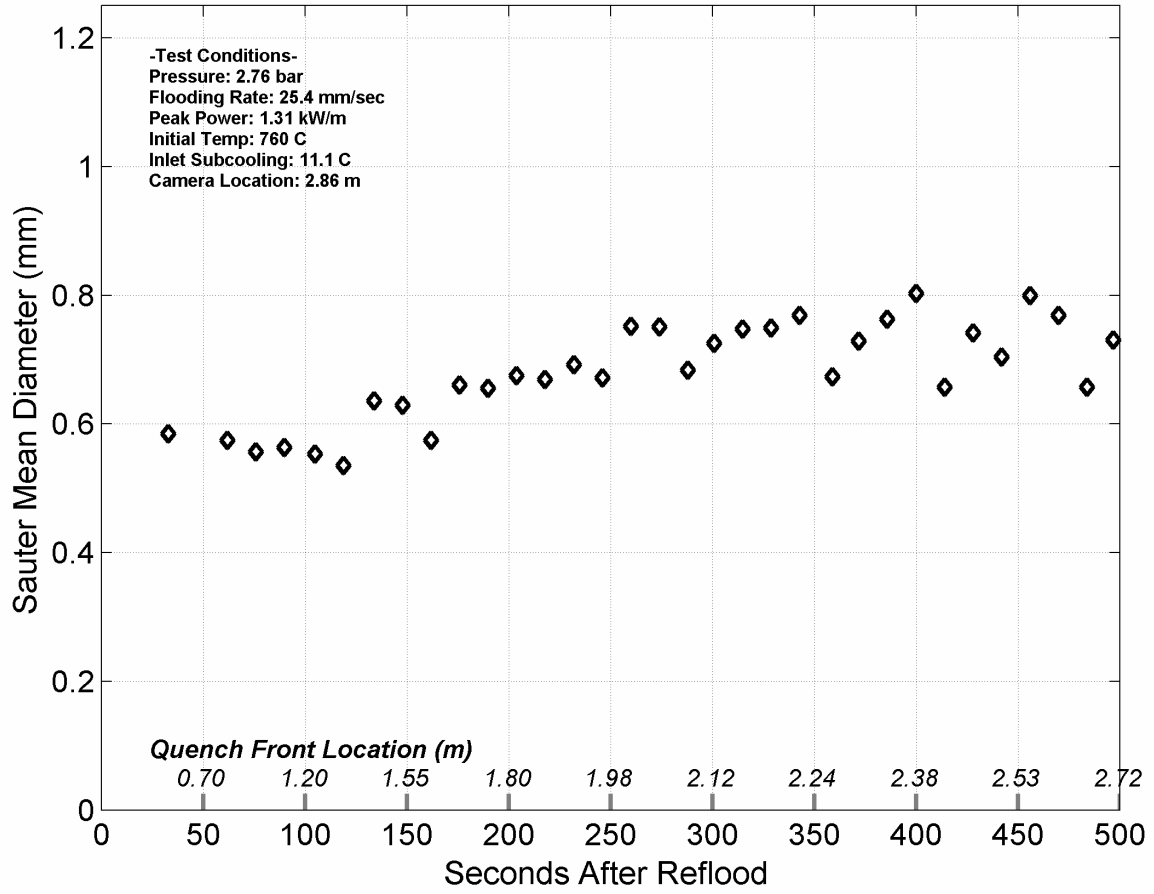
Droplet Counts - Exp. 973



Mean Droplet Diameter - Exp. 973



Droplet Sauter Mean Diameter - Exp. 973



RBHT - REFLOOD TESTS

SUMMARY SHEET

RUN NO: **1088**

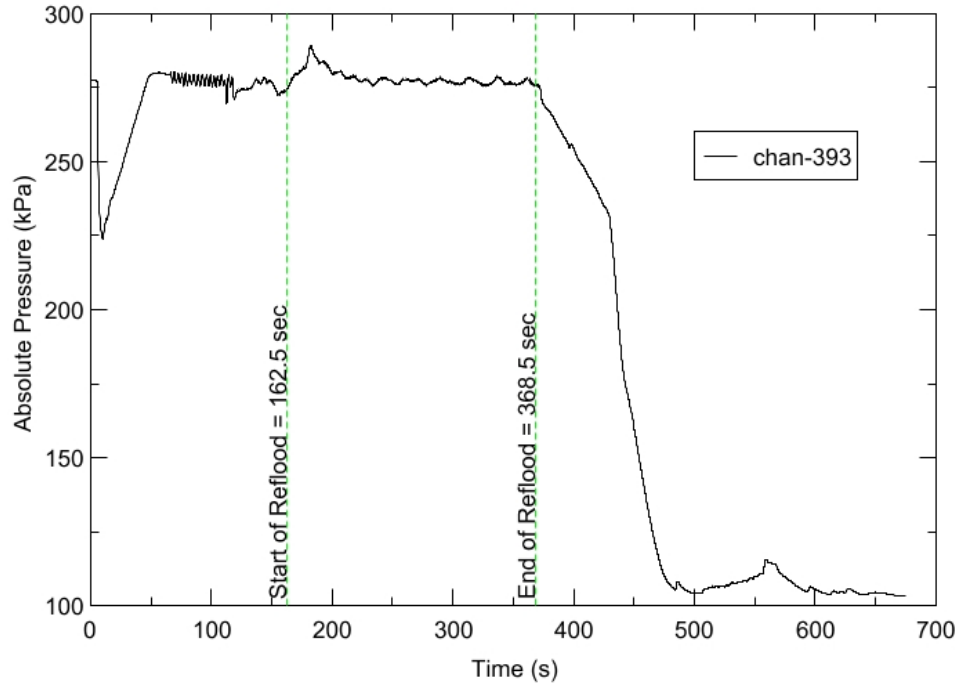
RUN CONDITIONS

Upper Plenum Pressure:	276 kPa (40 psia)
Initial Peak Clad Temperature:	1033 degree K (1400 degree F)
Rod Peak Power:	1.31 kW/m (0.4 kW/ft)
Flooding Rate:	0.0254 m/s (1 in/s)
Inlet Subcooling:	11 degree K (20 degree F)
Start of Reflood:	162.5 s
End of Reflood:	368.5 s
Test Date:	5/31/2002
Comments:	Test terminated early but valid to end time. Quench front at 1.52 m (60 in) at test termination.

Rod_Elevation	Channel Number	Temperature at Reflood (K)	Temperature at Reflood (F)	Turnaround Time (sec.)	Turnaround Temperature (K)	Turnaround Temperature (F)	Quench Time (sec.)	Quench Temperature (K)	Quench Temperature (F)
B6 0.592m	148	751.13	892.34	13.75	772.87	931.47	63.75	555.39	540.01
B6 0.744m	149	768.61	923.82	15.25	794.34	970.12	80.75	577.85	580.44
B6 0.846m	150	807.29	993.44	15.75	834.38	1042.19	90.25	586.21	595.49
B6 0.897m	151	822.52	1020.85	15.75	850.37	1070.98	95.25	604.54	628.48
C6 1.04m	137	881.53	1127.06	16.75	913.41	1184.46	109.25	651.29	712.63
D5 1.27m	217	937.52	1227.85	17.25	970.18	1286.63	149.75	596.42	613.86
C6 1.34m	138	926.35	1207.74	18.75	963.45	1274.53	154.75	642.96	697.64
D5 1.37m	218	966.17	1279.42	20.75	1004.36	1348.16	162.75	647.25	705.35
C6 1.39m	139	938.93	1230.39	19.25	976.51	1298.04	162.75	669.83	746.01
D5 1.45m	219	983.86	1311.25	21.25	1023.68	1382.93	175.75	671.6	749.18
C6 1.47m	140	958.34	1265.32	19.25	996.35	1333.74	177.75	682.17	768.23
D5 1.52m	220	1000.53	1341.27	21.25	1042.25	1416.36	191.75	691.03	784.17

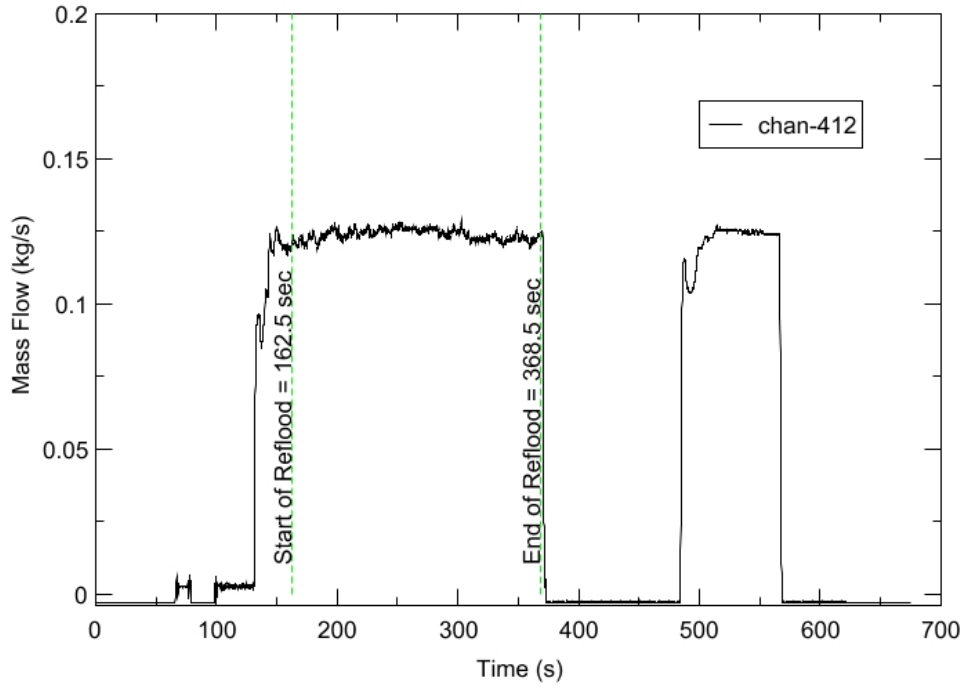
RBHT - TEST FACILITY

Upper Plenum Pressure vs. Time, Exp 1088



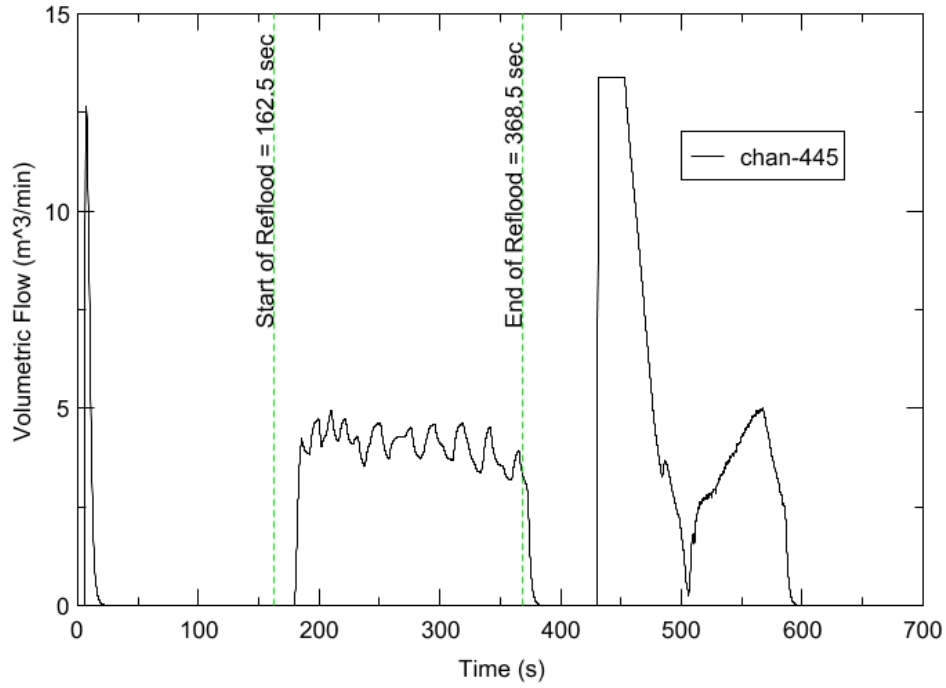
RBHT - TEST FACILITY

Inlet Flow vs. Time, Exp 1088



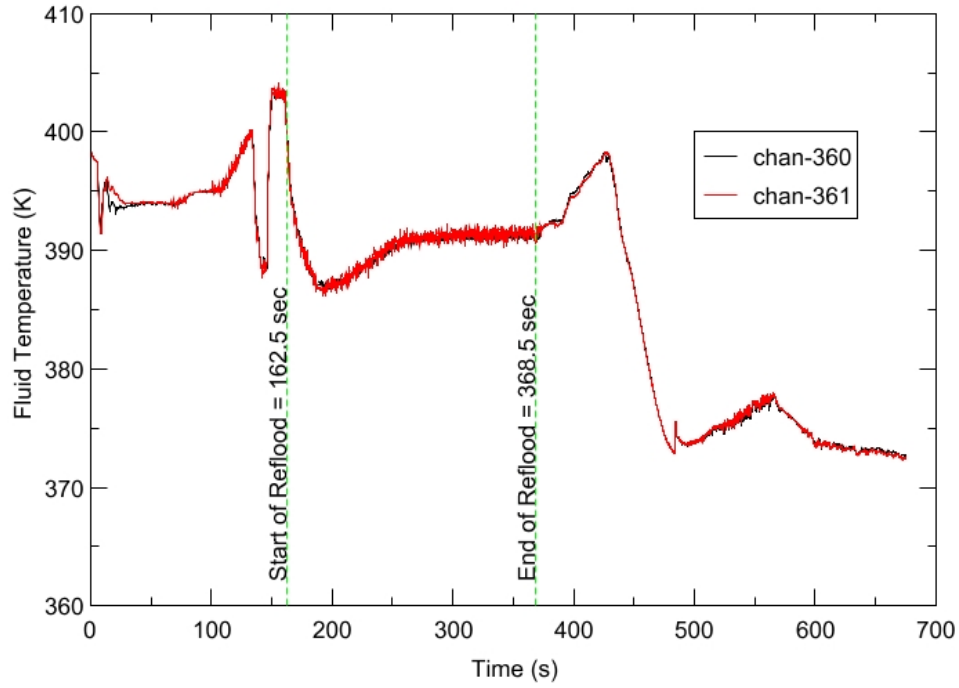
RBHT - TEST FACILITY

Steam Exhaust Flow vs. Time, Exp 1088



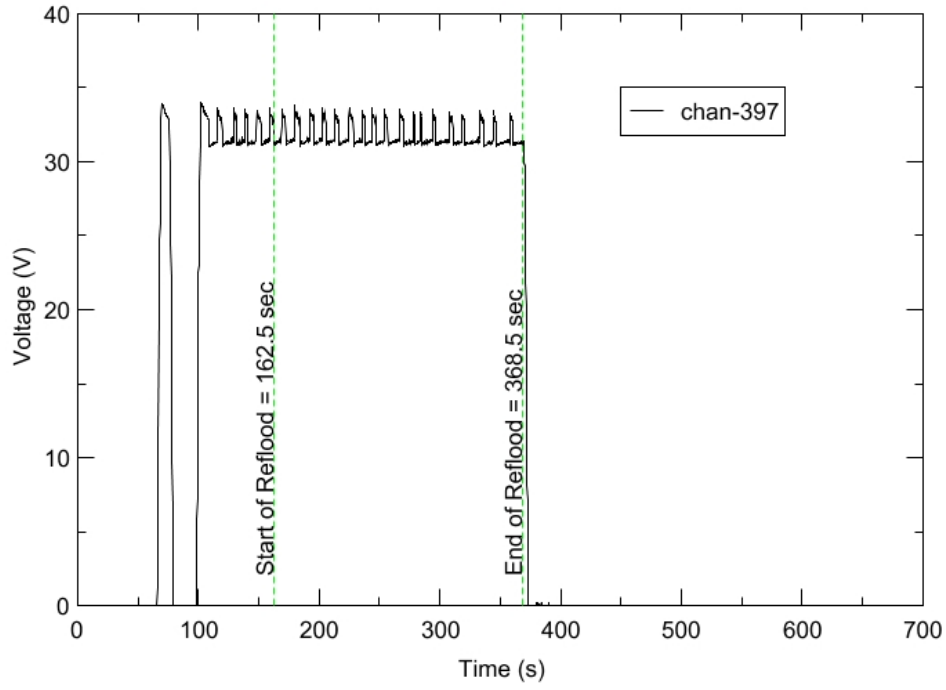
RBHT - TEST FACILITY

Inlet Flow Temperature vs. Time, Exp 1088



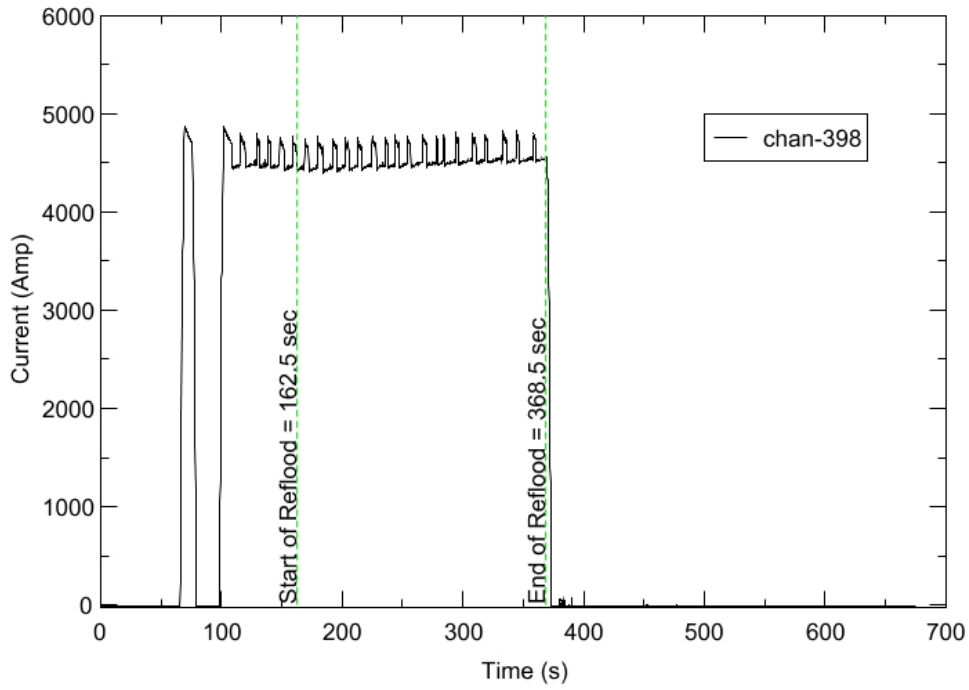
RBHT - TEST FACILITY

Test Section Voltage vs. Time, Exp 1088

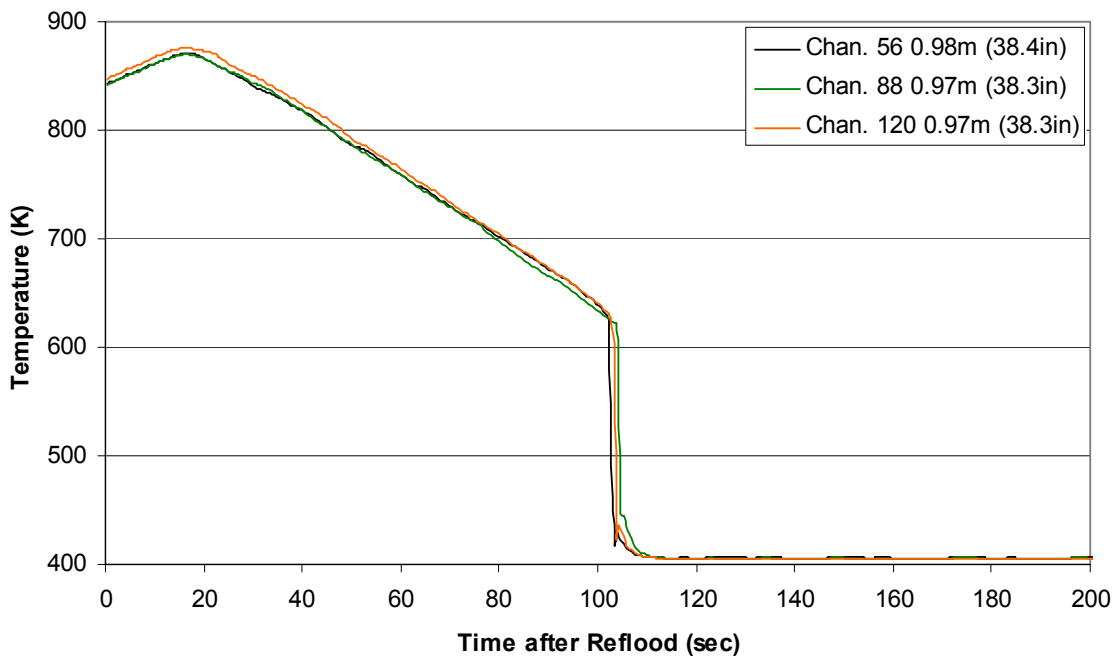


RBHT - TEST FACILITY

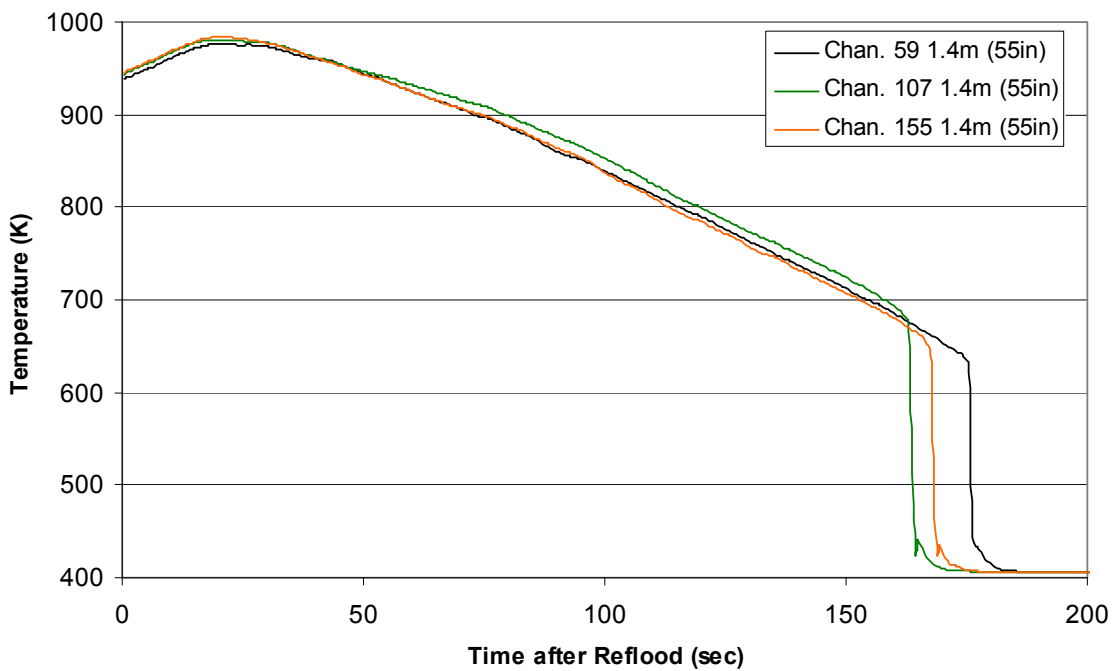
Test Section Current vs. Time, Exp 1088



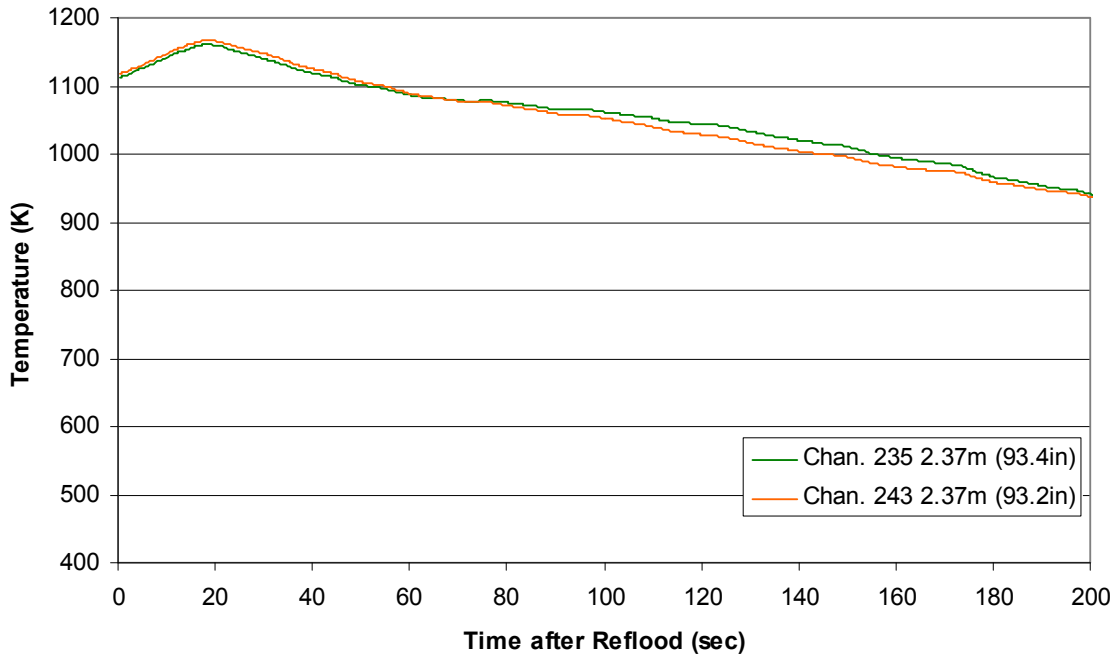
Heater Rod Temperature during Reflood RBHT Exp. 1088



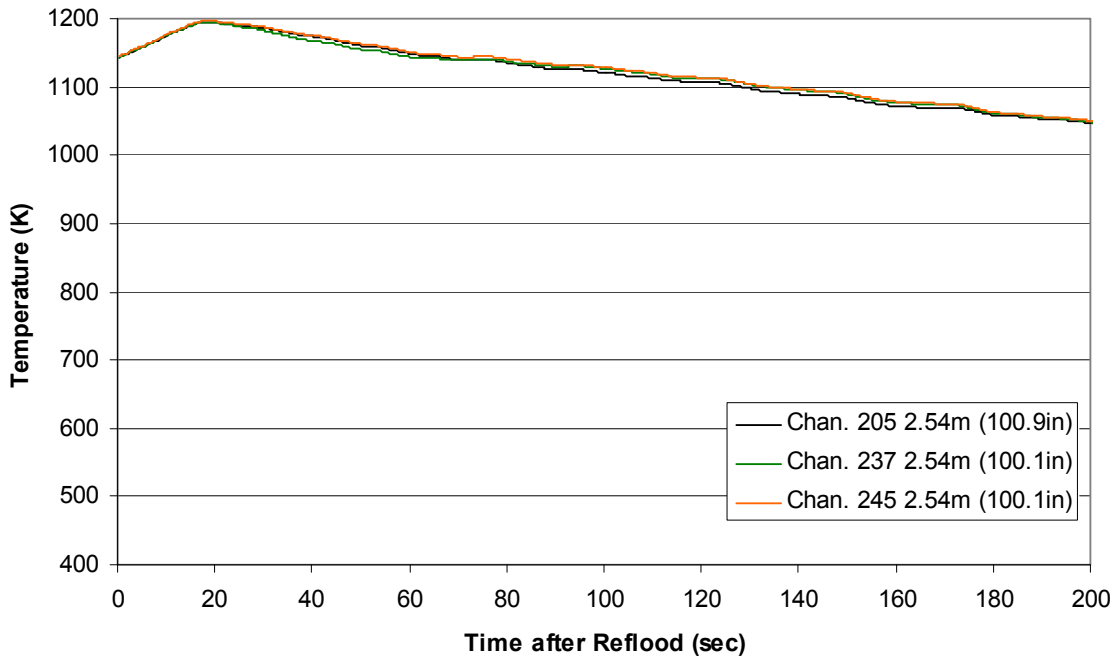
Heater Rod Temperature during Reflood RBHT Exp. 1088



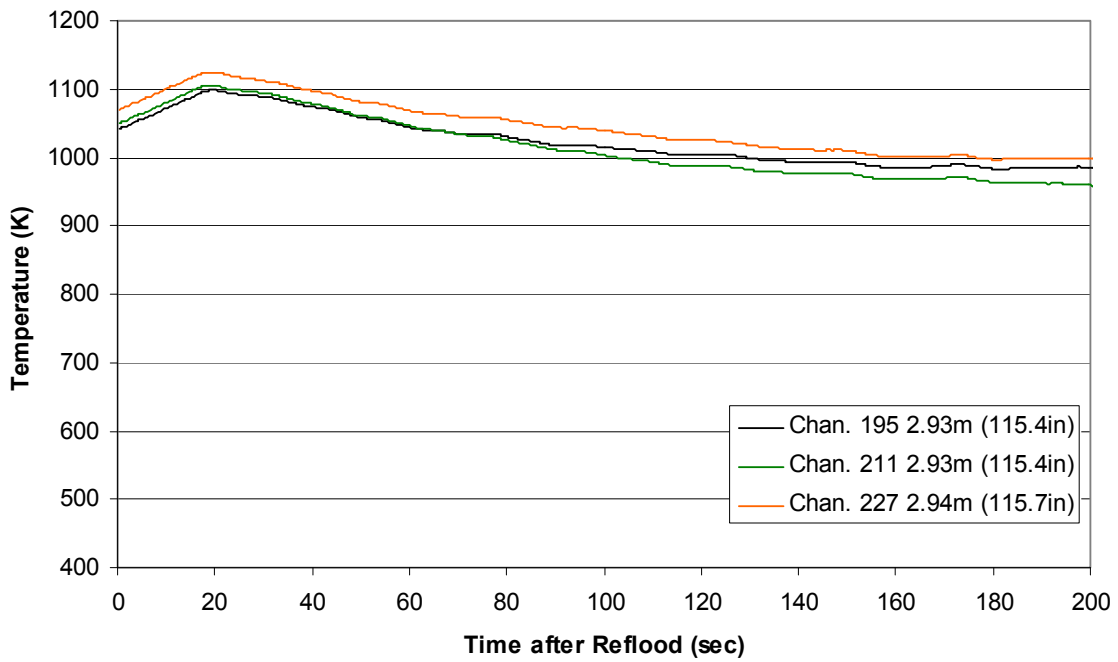
**Heater Rod Temperature during Reflood
RBHT Exp. 1088**



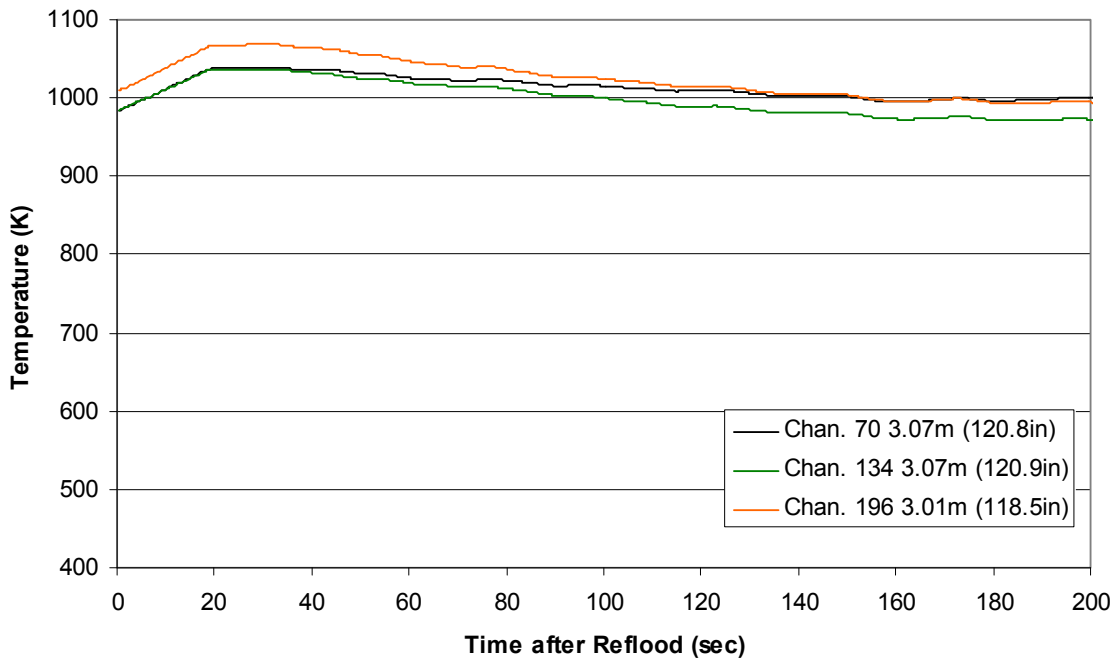
**Heater Rod Temperature during Reflood
RBHT Exp. 1088**



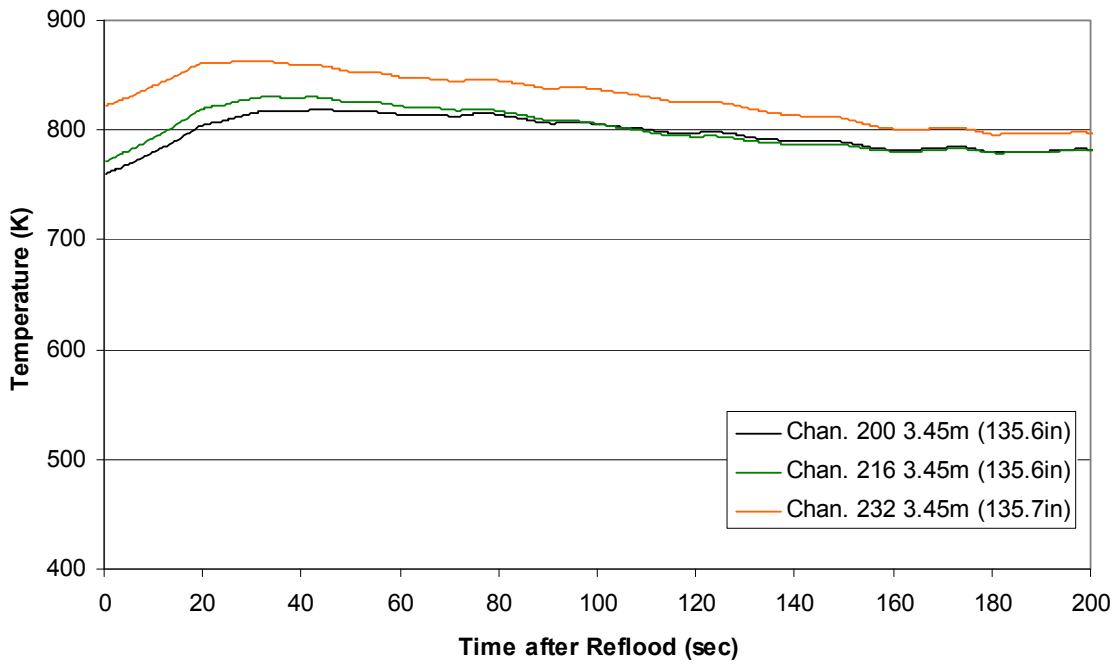
Heater Rod Temperature during Reflood
RBHT Exp. 1088



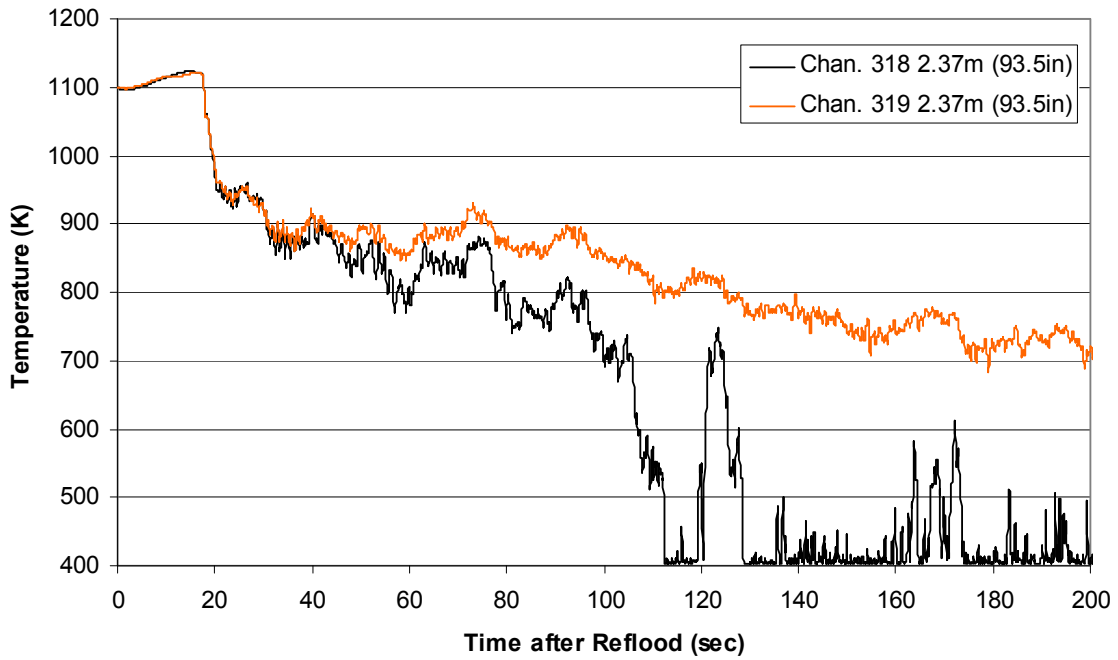
Heater Rod Temperature during Reflood
RBHT Exp. 1088



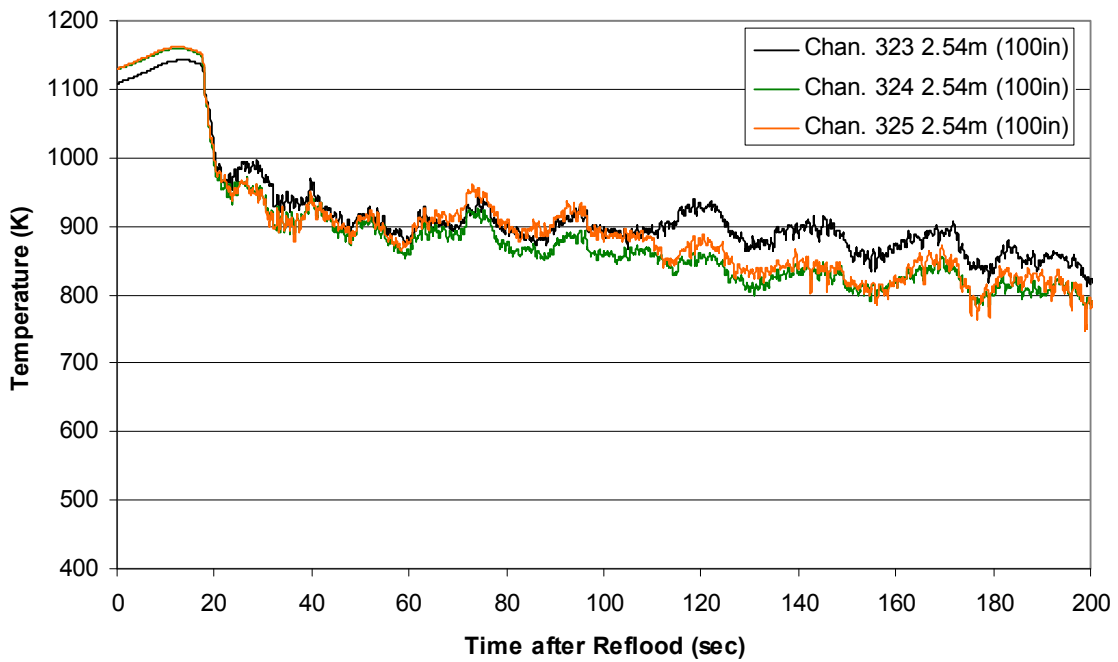
Heater Rod Temperature during Reflood RBHT Exp. 1088



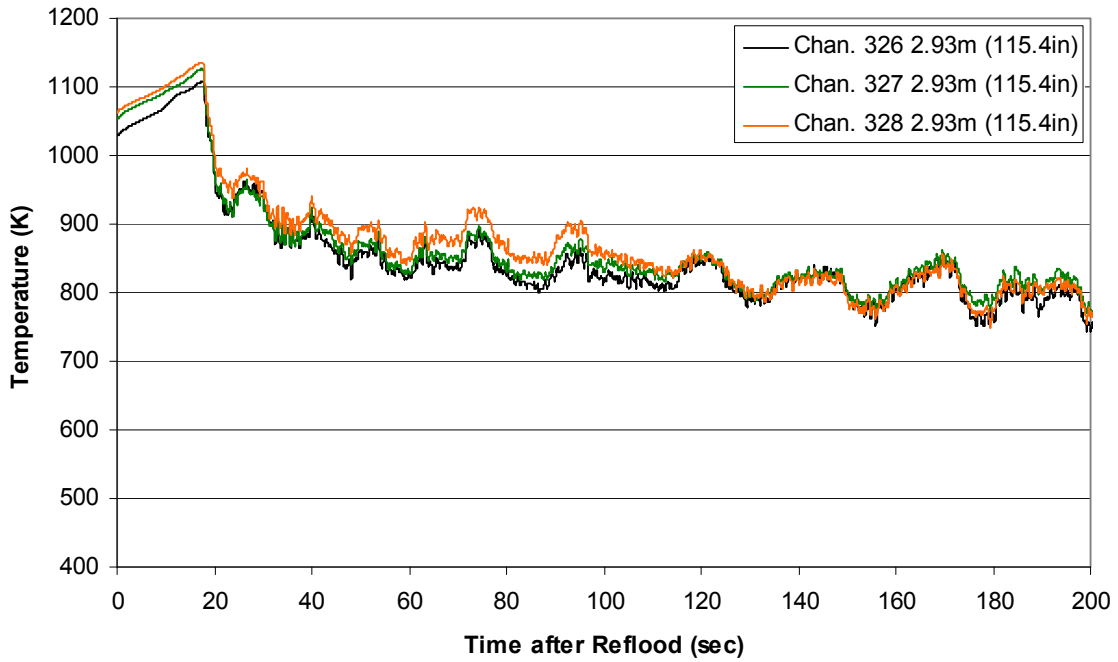
Steam Probe Temperature during Reflood RBHT Exp. 1088



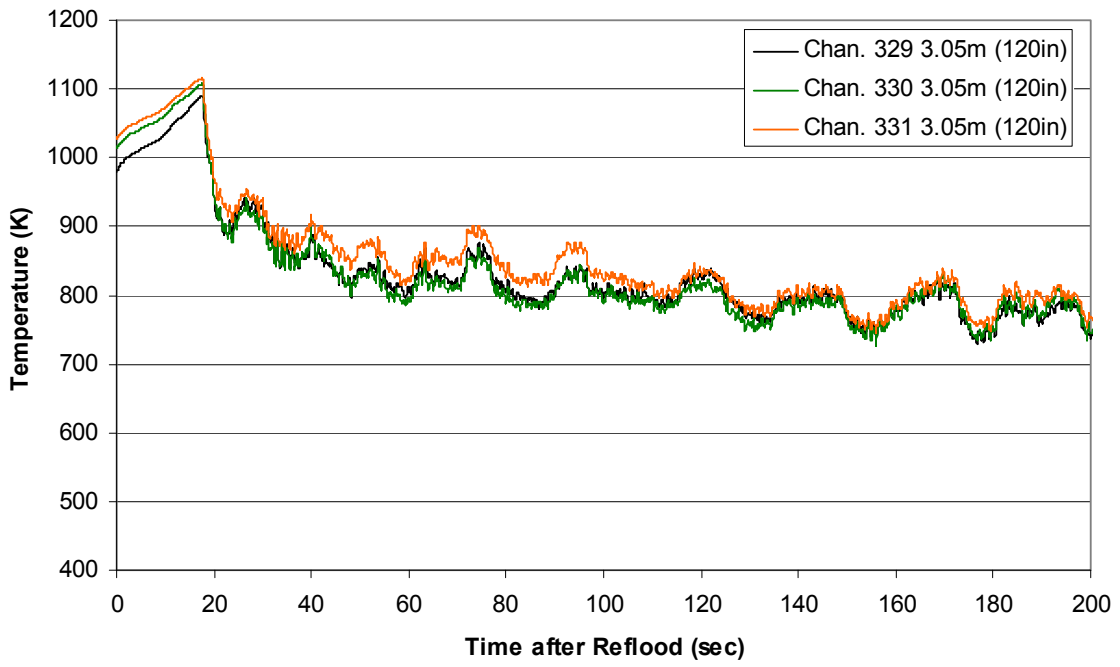
Steam Probe Temperature during Reflood
RBHT Exp. 1088



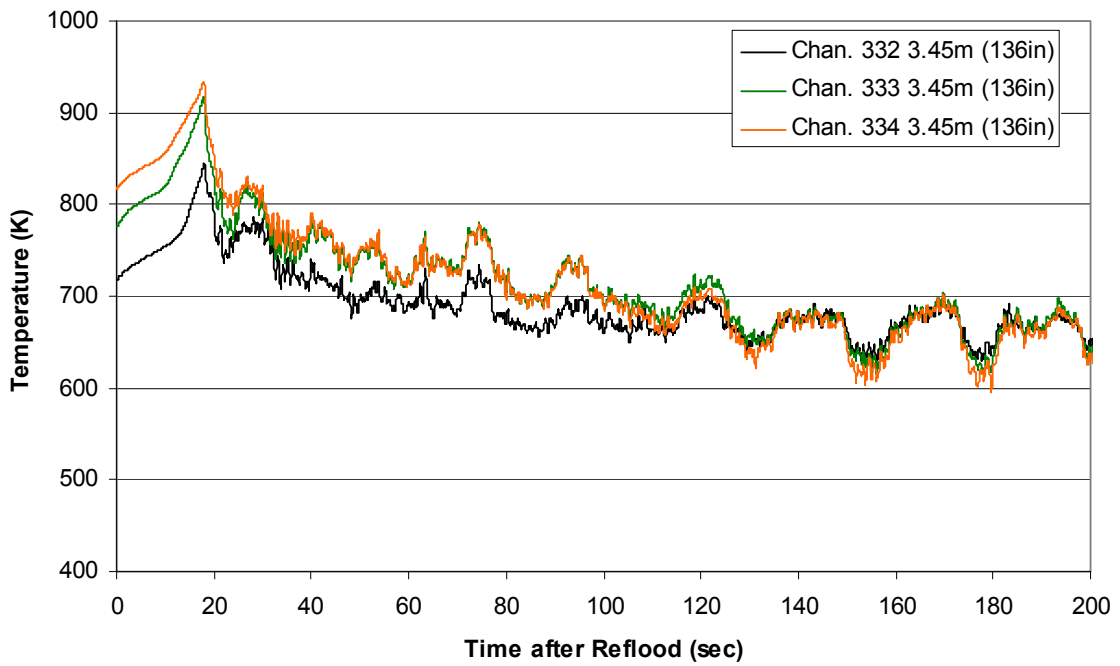
Steam Probe Temperature during Reflood
RBHT Exp. 1088



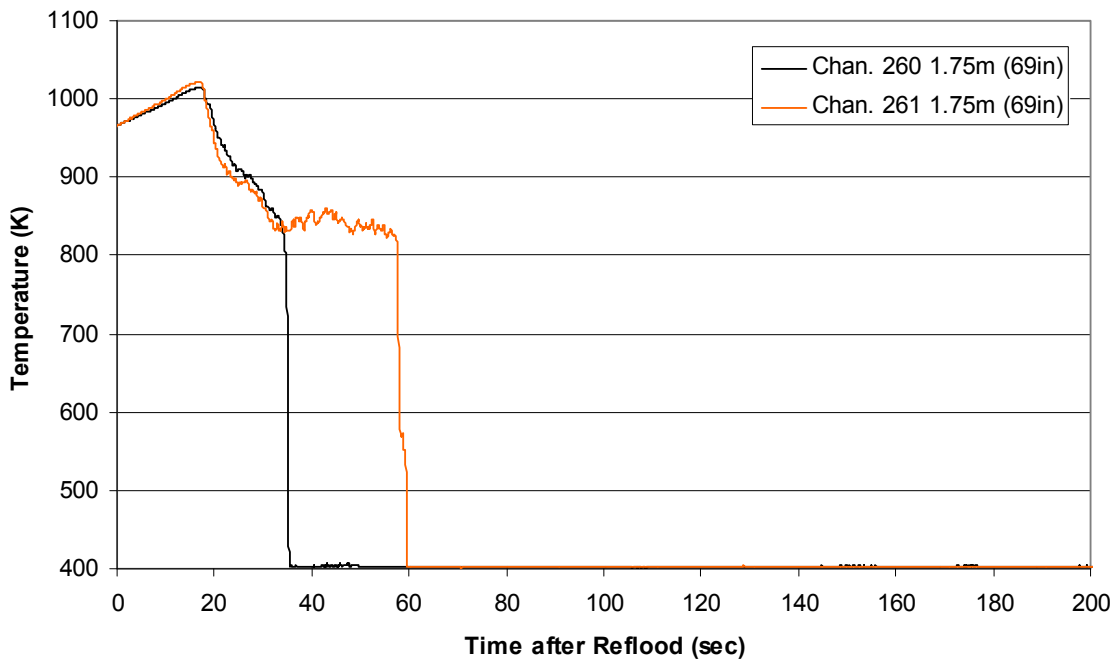
Steam Probe Temperature during Reflood
RBHT Exp. 1088



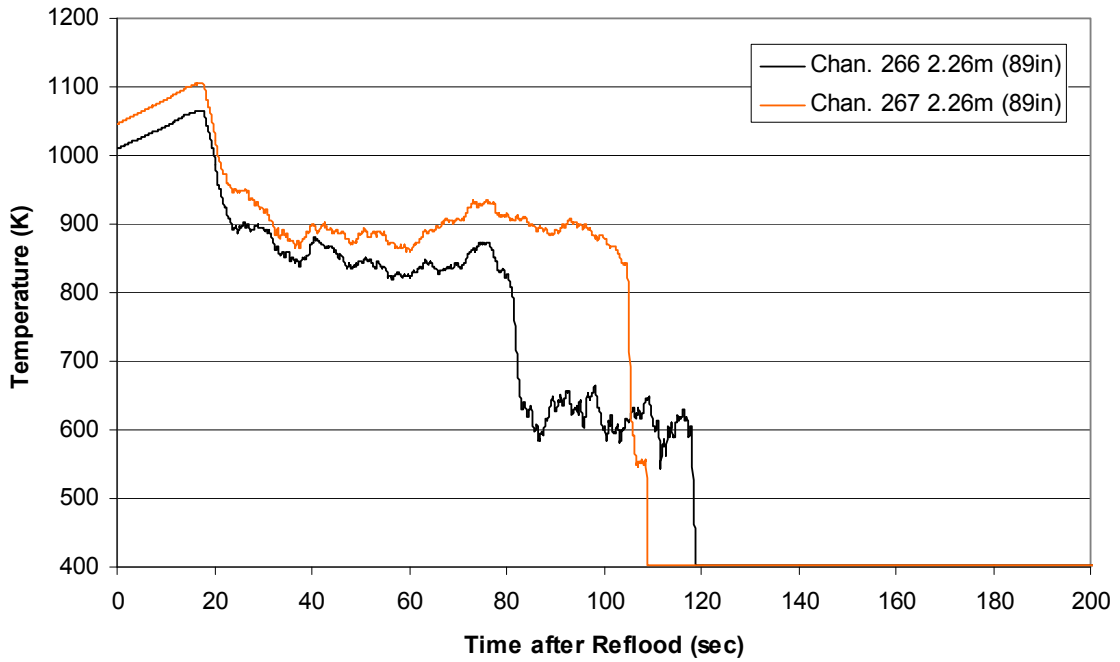
Steam Probe Temperature during Reflood
RBHT Exp. 1088



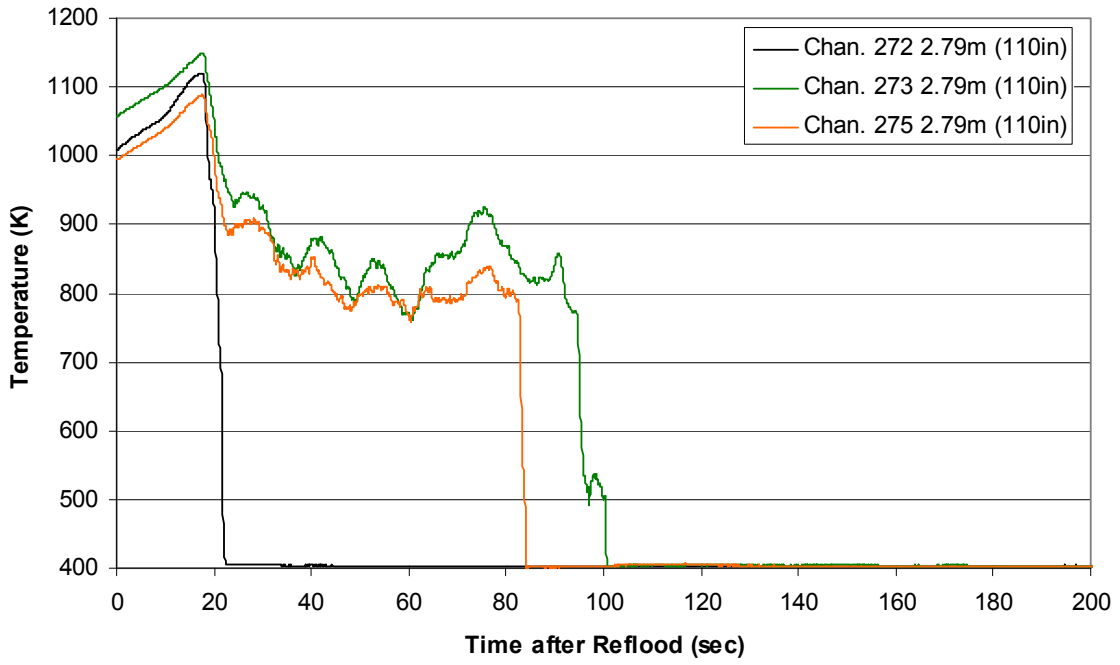
Spacer Grid Temperature during Reflood
RBHT Exp. 1088



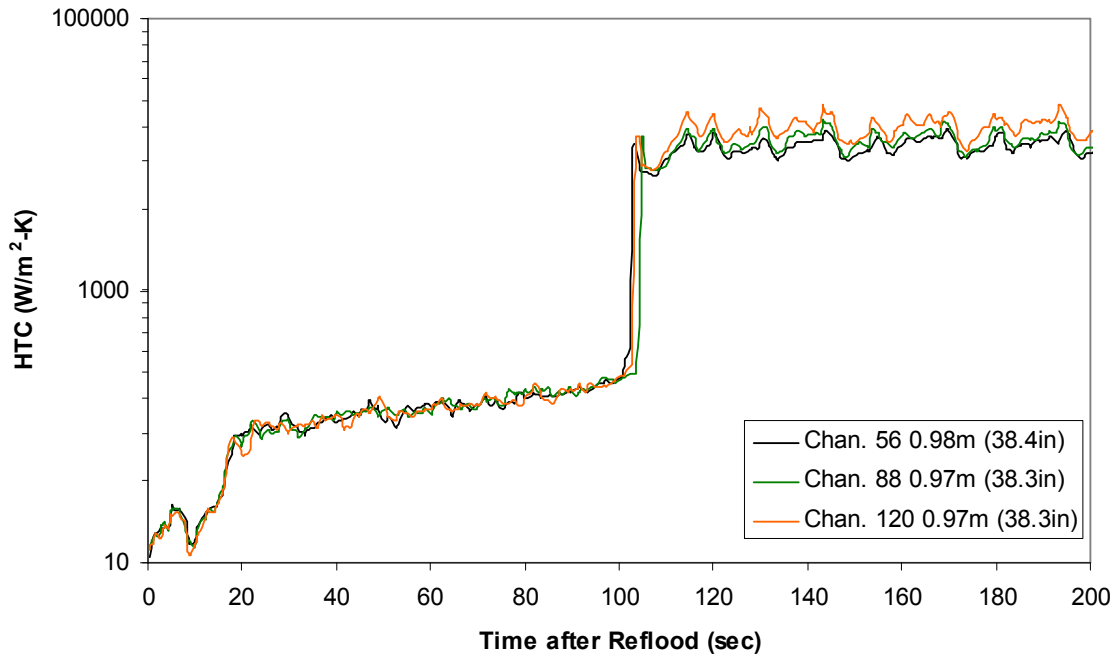
Spacer Grid Temperature during Reflood
RBHT Exp. 1088



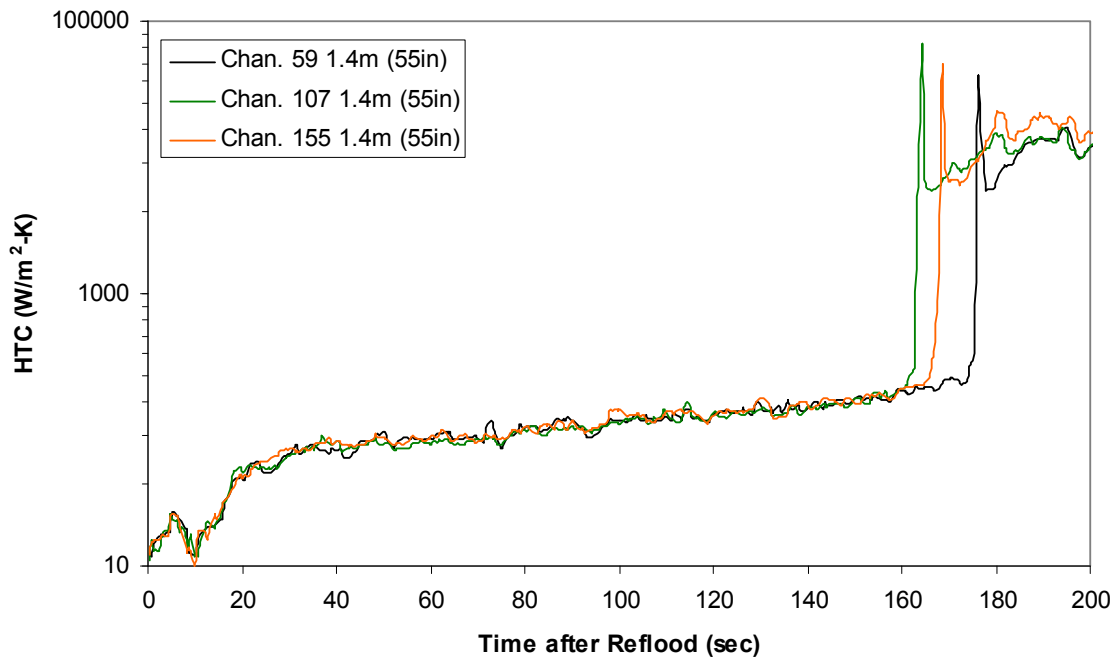
Spacer Grid Temperature during Reflood
RBHT Exp. 1088



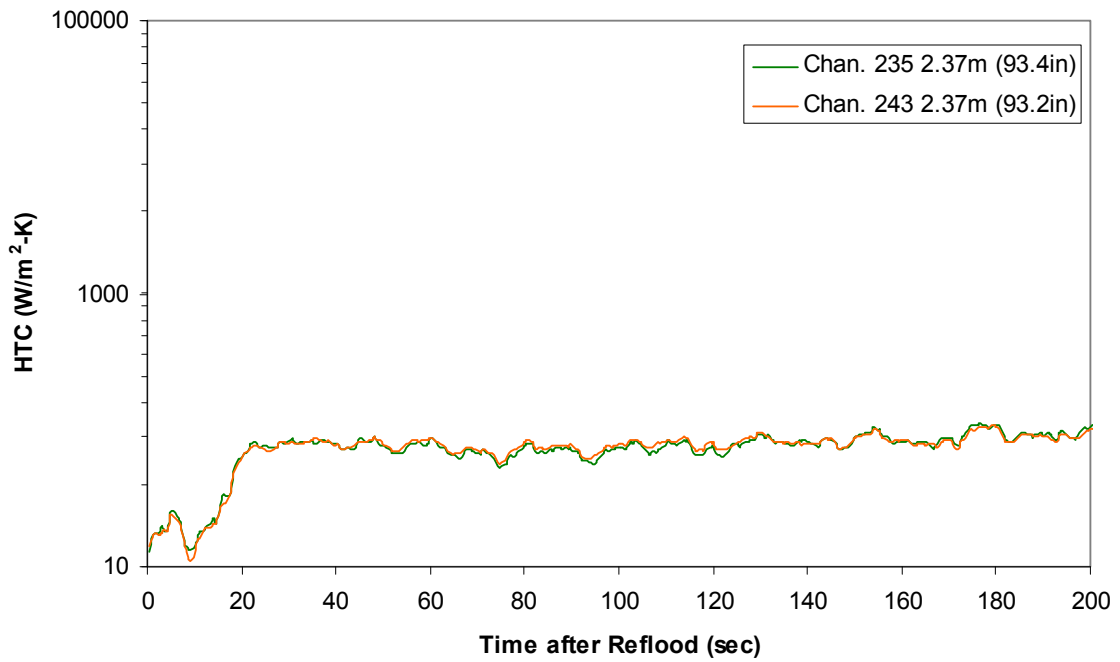
Heat Transfer Coefficient during Reflood
RBHT Exp. 1088



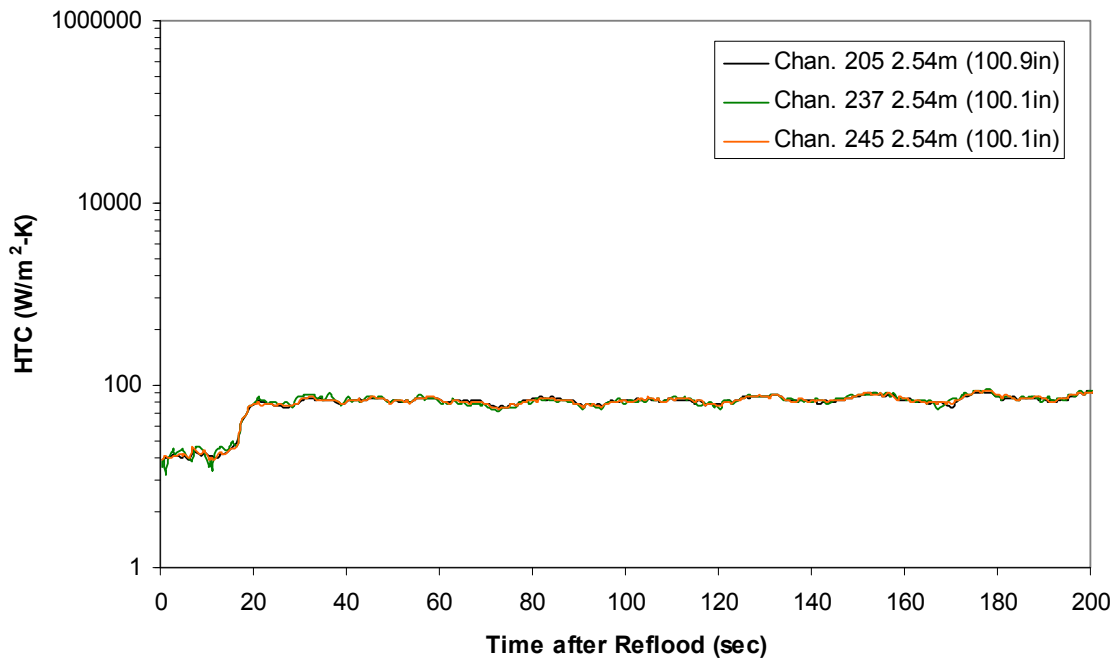
Heat Transfer Coefficient during Reflood RBHT Exp. 1088



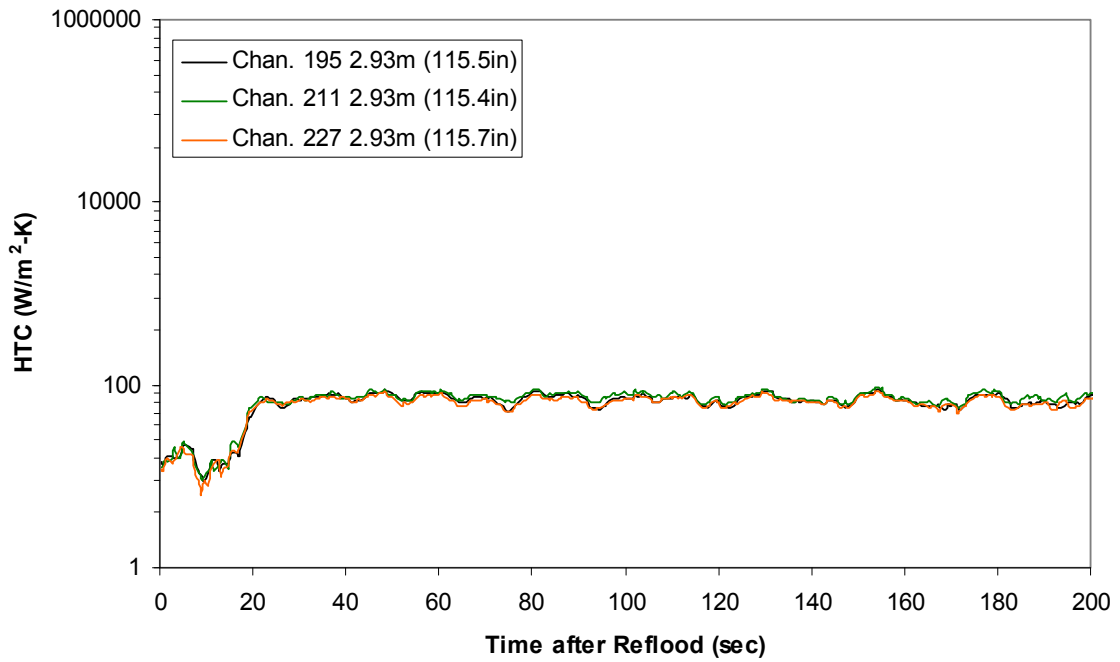
Heat Transfer Coefficient during Reflood RBHT Exp. 1088



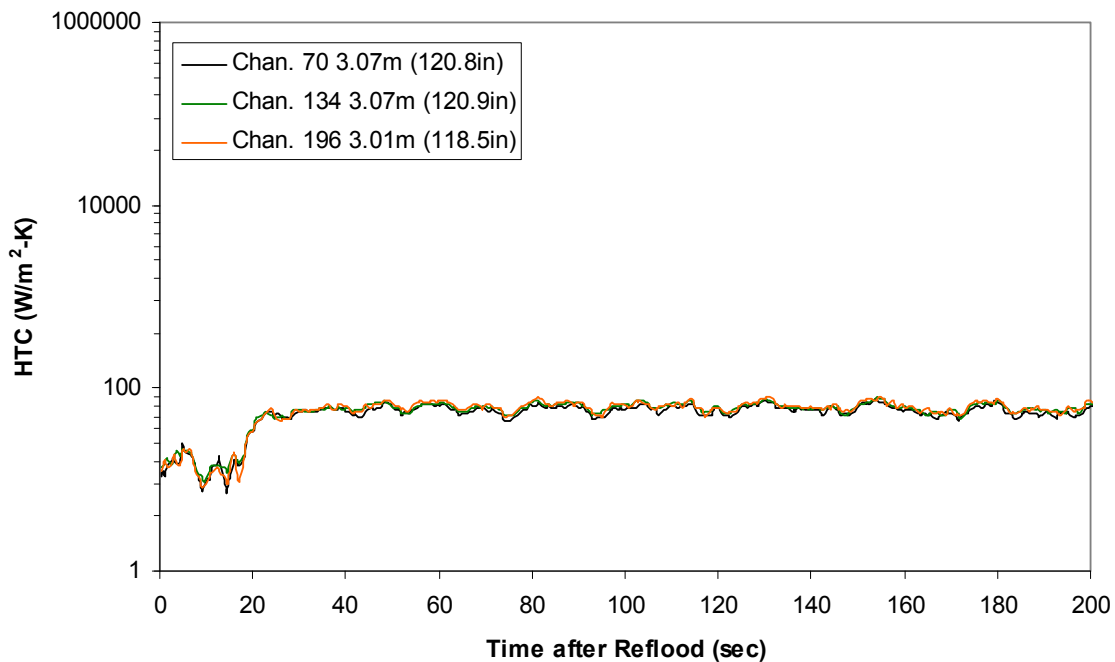
Heat Transfer Coefficient during Reflood RBHT Exp. 1088



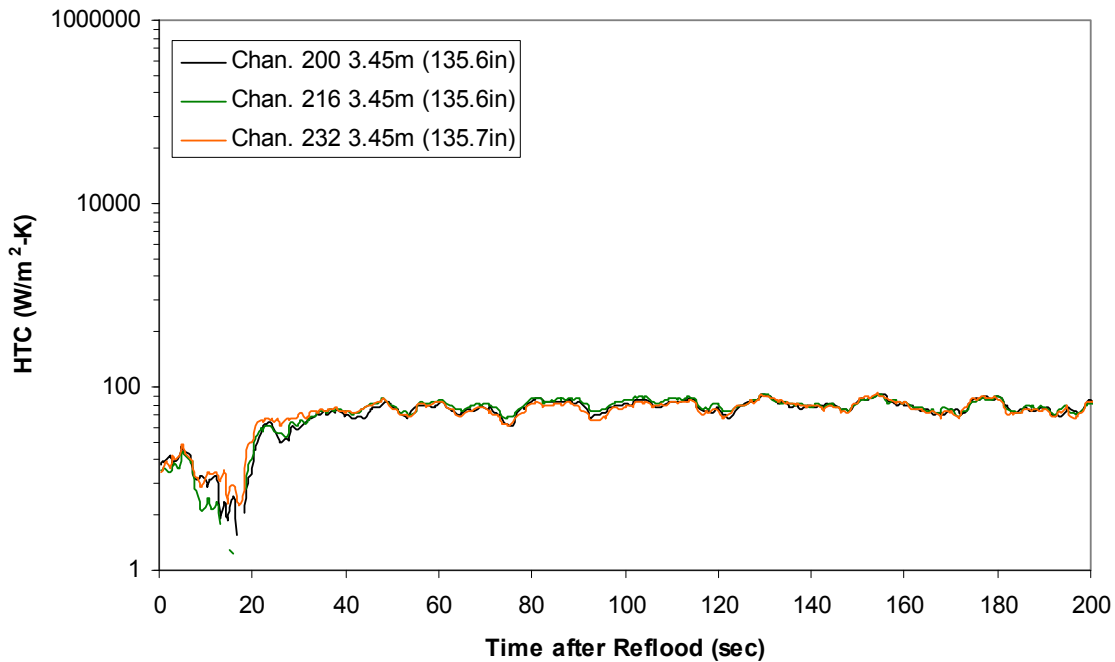
Heat Transfer Coefficient during Reflood RBHT Exp. 1088



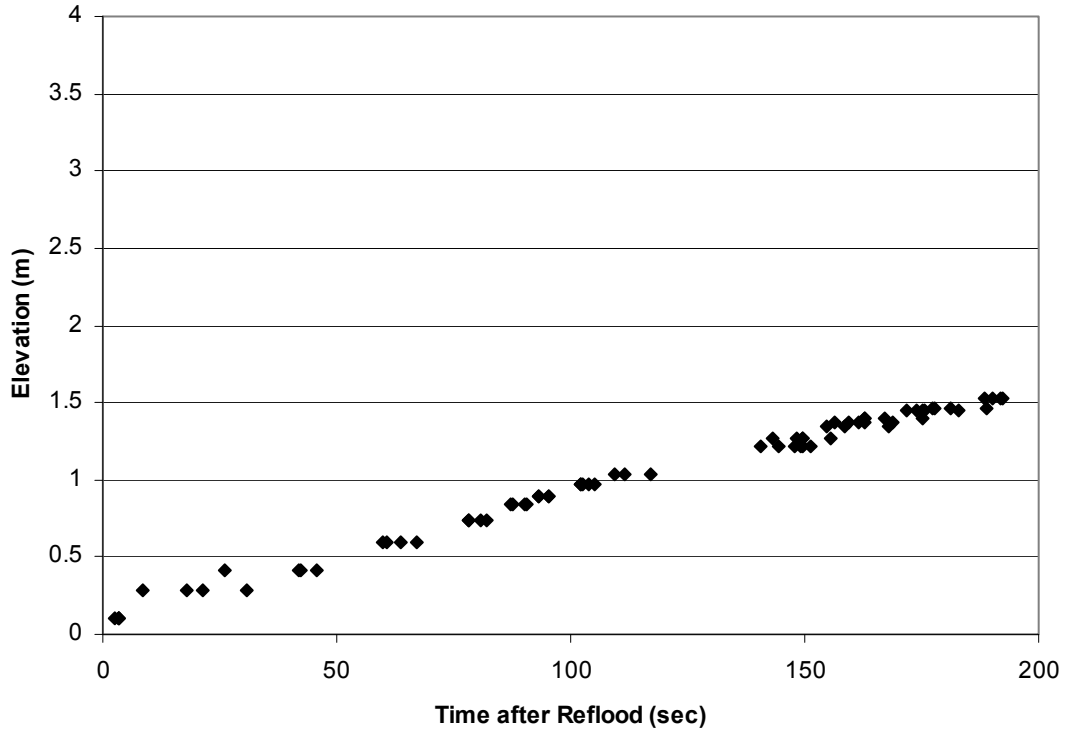
Heat Transfer Coefficient during Reflood RBHT Exp. 1088



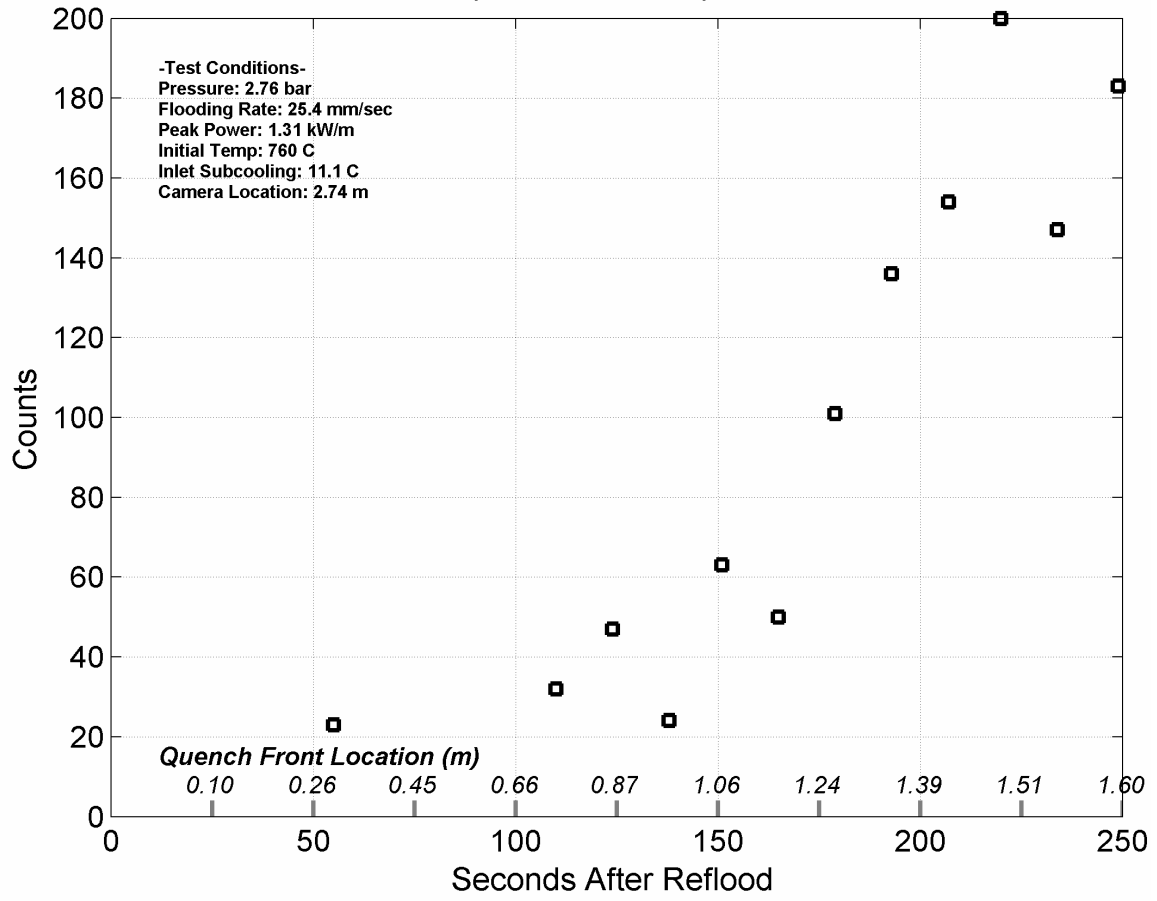
Heat Transfer Coefficient during Reflood RBHT Exp. 1088



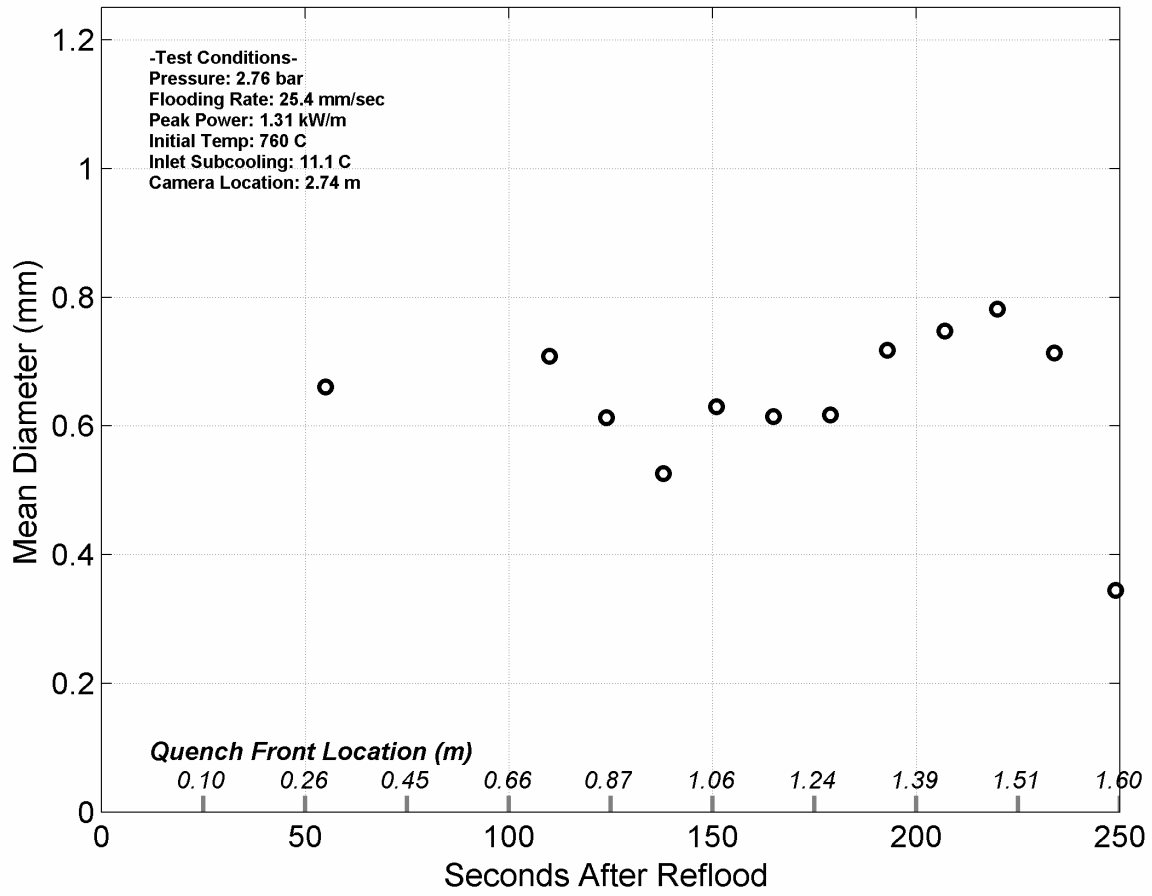
Quench Data, RBHT Exp. 1088



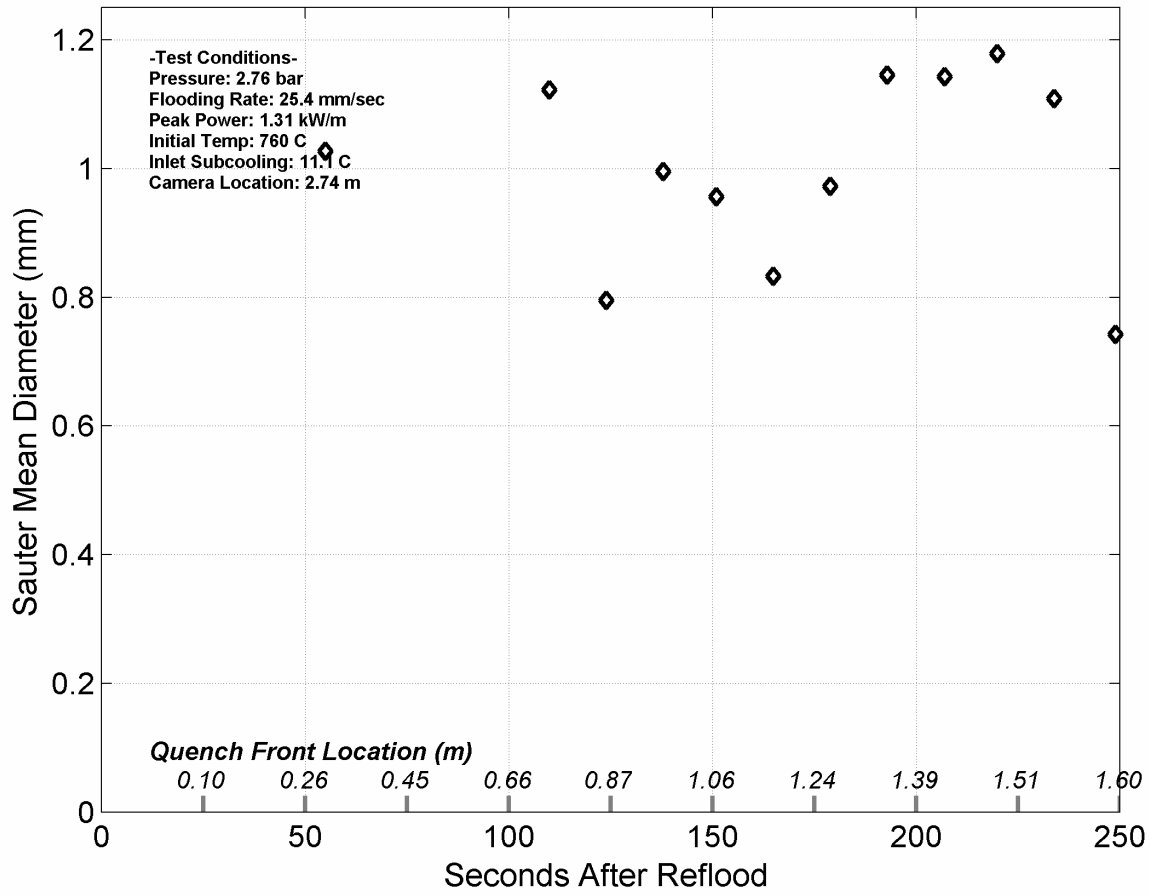
Droplet Counts - Exp. 1088



Mean Droplet Diameter - Exp. 1088



Droplet Sauter Mean Diameter - Exp. 1088



RBHT - REFLOOD TESTS

SUMMARY SHEET

RUN NO: **1096**

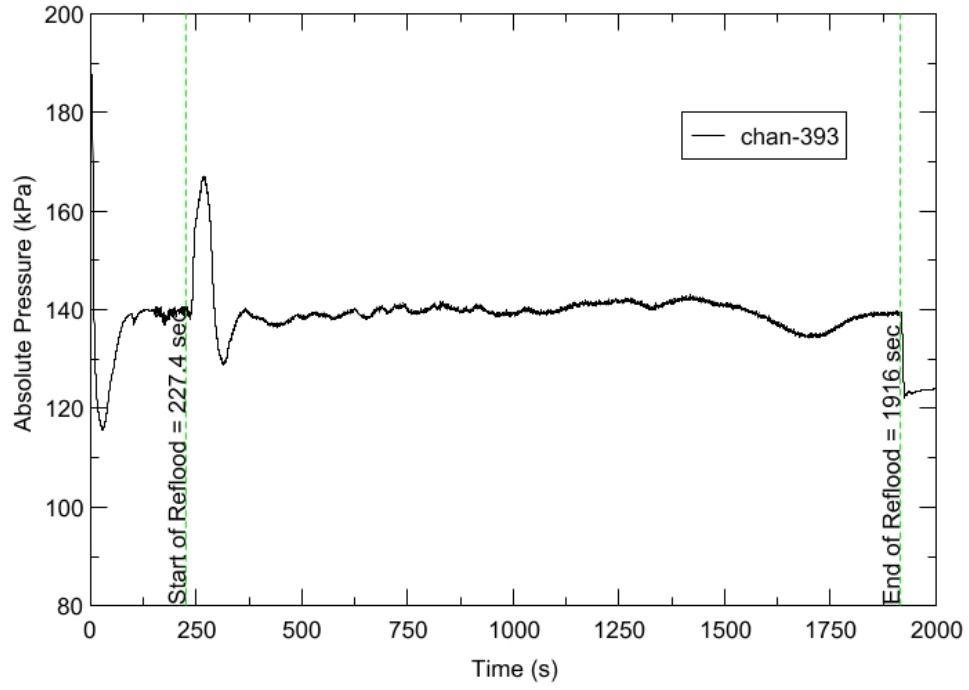
RUN CONDITIONS

Upper Plenum Pressure:	138 kPa (20 psia)
Initial Peak Clad Temperature:	1033 degrees K (1400 degrees F)
Rod Peak Power:	1.31 kW/m (0.4 kW/ft)
Flooding Rate:	0.0254 m/s (1 in/s)
Inlet Subcooling:	11 degrees K (20 degrees F)
Start of Reflood:	227.4 s
End of Reflood:	1916 s
Test Date:	6/4/2002
Comments:	

Rod_Elevation	Channel Number	Temperature at Reflood (K)	Temperature at Reflood (°F)	Turnaround Time (sec.)	Turnaround Temperature (K)	Turnaround Temperature (°F)	Quench Time (sec.)	Quench Temperature (K)	Quench Temperature (°F)
B6 0.592m	148	753.98	897.48	11.85	774.04	933.59	96.85	550.57	531.34
B6 0.744m	149	761.08	910.26	13.35	783.89	951.31	131.85	548.92	528.37
B6 0.846m	150	792.83	967.41	13.35	818.01	1012.74	150.85	583.43	590.48
B6 0.897m	151	802.81	985.36	13.35	829.26	1032.98	163.85	600.16	620.6
C6 1.04m	137	853.61	1076.81	18.35	883.6	1130.78	211.35	578.31	581.27
D5 1.27m	217	903.05	1165.8	15.35	931.83	1217.61	305.85	590.21	602.7
D6 1.34m	138	888.23	1139.12	19.85	924.1	1203.69	332.35	597.62	616.03
D5 1.37m	218	926.98	1208.87	25.35	963.94	1275.41	339.35	630.32	674.88
C6 1.39m	139	896.74	1154.44	23.85	934.59	1222.57	356.35	634.4	682.23
D5 1.45m	219	941.78	1235.51	25.85	980.27	1304.8	372.35	663.47	734.55
C6 1.47m	140	914.14	1185.76	24.35	952.65	1255.09	396.85	646.82	704.59
D5 1.52m	220	956.17	1261.43	23.35	996.56	1334.13	421.35	587.98	598.68
C6 1.62m	141	938.88	1230.3	114.85	1006.36	1351.76	490.85	594.34	610.13
D5 1.68m	221	975.73	1296.63	156.85	1058.74	1446.05	513.85	628.68	671.93
D5 1.78m	222	968.97	1284.45	17.85	1007.7	1354.18	566.35	628.19	671.06
D5 1.85m	223	996.93	1334.79	17.85	1036.66	1406.31	597.85	657.85	724.43
C6 1.87m	142	975.55	1296.31	20.35	1018.15	1372.98	621.35	639.12	690.74
D5 1.90m	224	1003.67	1346.92	19.85	1046.25	1423.56	626.35	667.91	742.55
C6 1.95m	144	983.33	1310.31	114.85	1035.66	1404.5	666.35	602.63	625.04
C3 2.17m	178	1028.76	1392.08	232.35	1131.48	1576.98	834.35	578.64	581.87
D4 2.24m	241	1049.97	1430.26	239.85	1124.04	1563.59	890.35	567.23	561.32
D4 2.32m	242	1060.85	1449.84	15.35	1101.68	1523.34	919.35	630.29	674.84
C3 2.35m	180	1054.48	1438.38	15.85	1097.66	1516.09	917.85	607.06	633.02
D4 2.37m	243	1068.99	1464.49	15.85	1113.81	1545.16	944.85	548.82	528.19
C3 2.40m	181	1056.19	1441.45	16.35	1101.72	1523.41	942.85	572.43	570.69
D4 2.54m	245	1091.52	1505.04	16.85	1139.01	1590.53	1040.85	629.2	672.88
D6 2.62m	129	1081.44	1486.9	253.85	1137.44	1587.71	1036.85	682.94	769.61
D6 2.69m	130	1081.35	1486.74	278.85	1161.24	1630.55	1069.35	716.01	829.13
C3 2.76m	183	1079.99	1484.3	559.35	1164.38	1636.2	1151.35	614.69	646.76
D4 2.79m	247	1066.75	1460.47	14.85	1116.21	1549.48	1167.85	627.2	669.26
D6 2.87m	131	1047.05	1425.01	14.85	1090.37	1502.98	1135.85	662.2	732.28
D6 2.92m	132	1026.14	1387.36	16.35	1074.53	1474.47	1157.85	602.44	624.71
D6 2.97m	133	998.64	1337.87	16.85	1045.51	1422.23	1184.85	606.02	631.14
D6 3.07m	134	962.48	1272.78	17.85	1008.3	1355.26	1215.85	650.79	711.74
E3 3.12m	197	955.16	1259.6	17.35	999.96	1340.24	1303.85	613.15	643.98
D6 3.17m	135	923.17	1202.02	787.35	988.4	1319.43	1244.85	662.89	733.52
D6 3.27m	136	879.18	1122.84	788.85	968.77	1284.1	1270.35	636.34	685.73
D4 3.61m	248	628.32	671.29	1115.35	740.17	872.62	1400.35	549.81	529.98

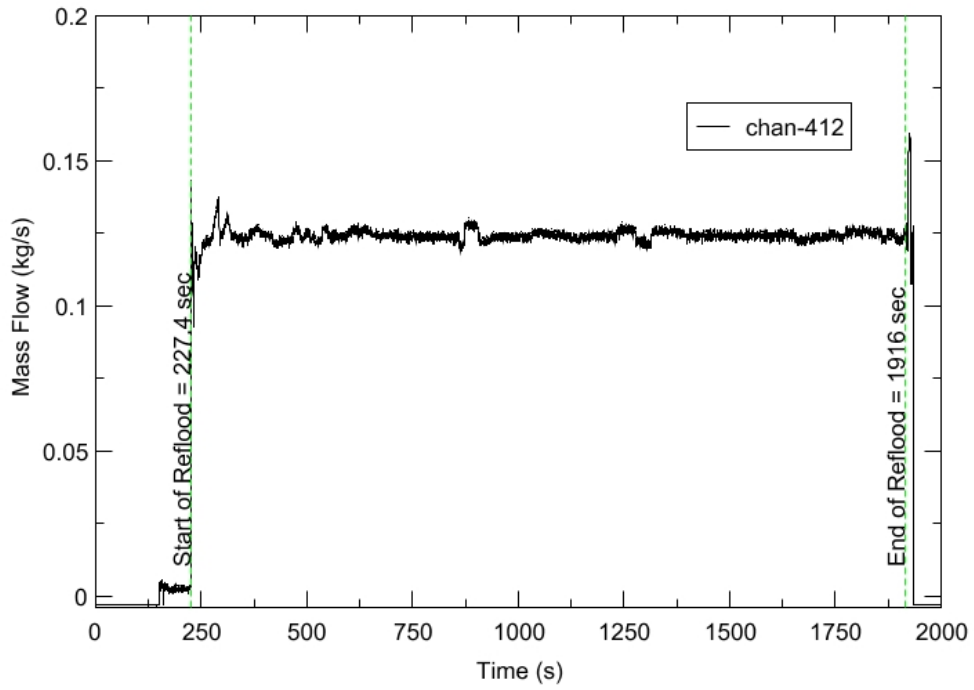
RBHT - TEST FACILITY

Upper Plenum Pressure vs. Time, Exp 1096



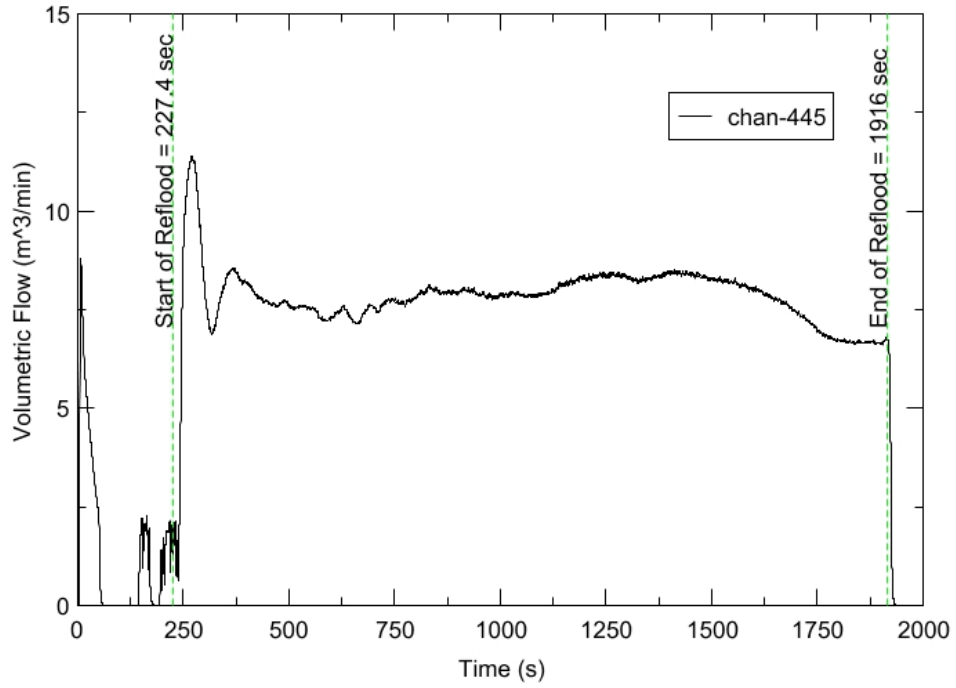
RBHT - TEST FACILITY

Inlet Flow vs. Time, Exp 1096



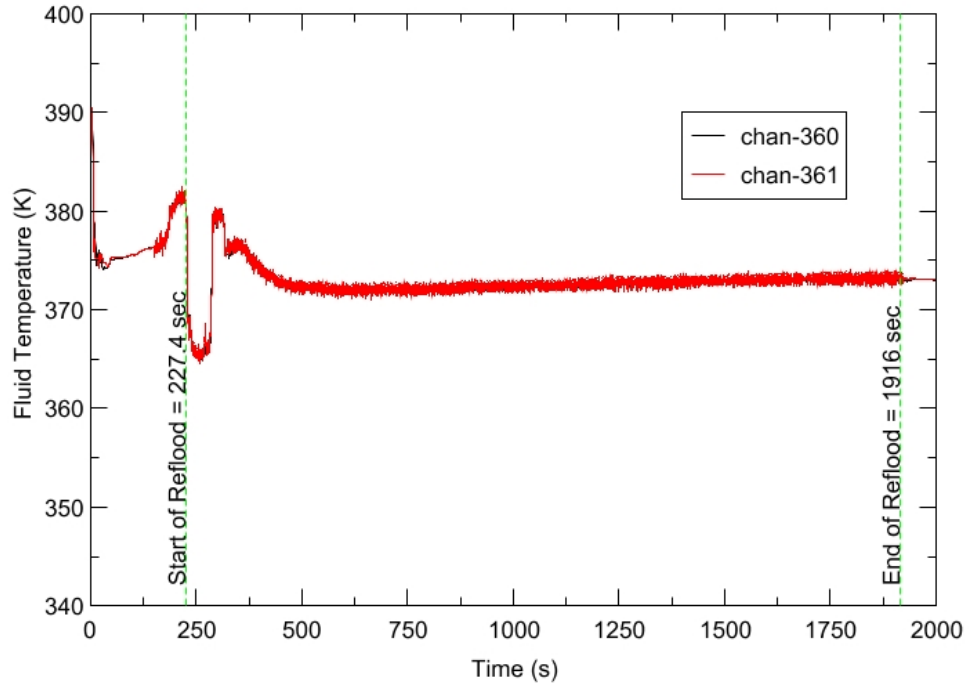
RBHT - TEST FACILITY

Steam Exhaust Flow vs. Time, Exp 1096



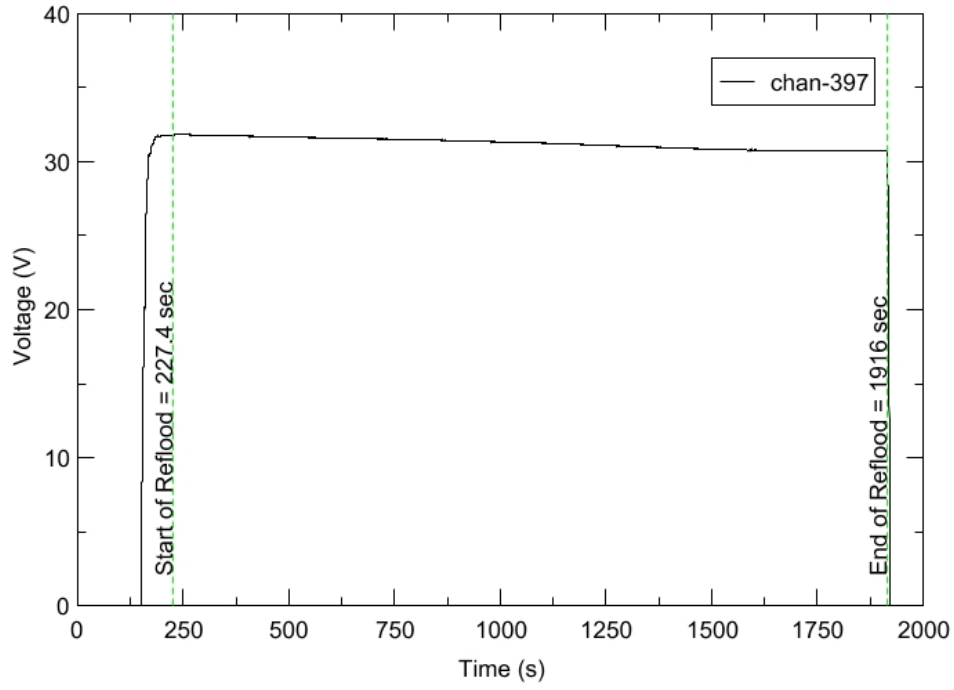
RBHT - TEST FACILITY

Inlet Flow Temperature vs. Time, Exp 1096



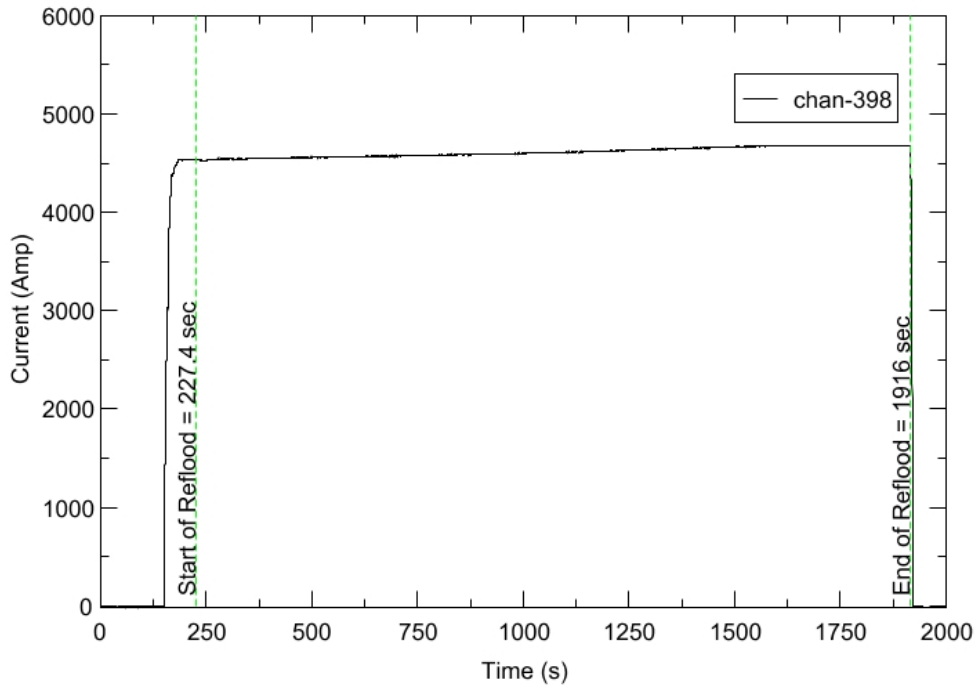
RBHT - TEST FACILITY

Test Section Voltage vs. Time, Exp 1096

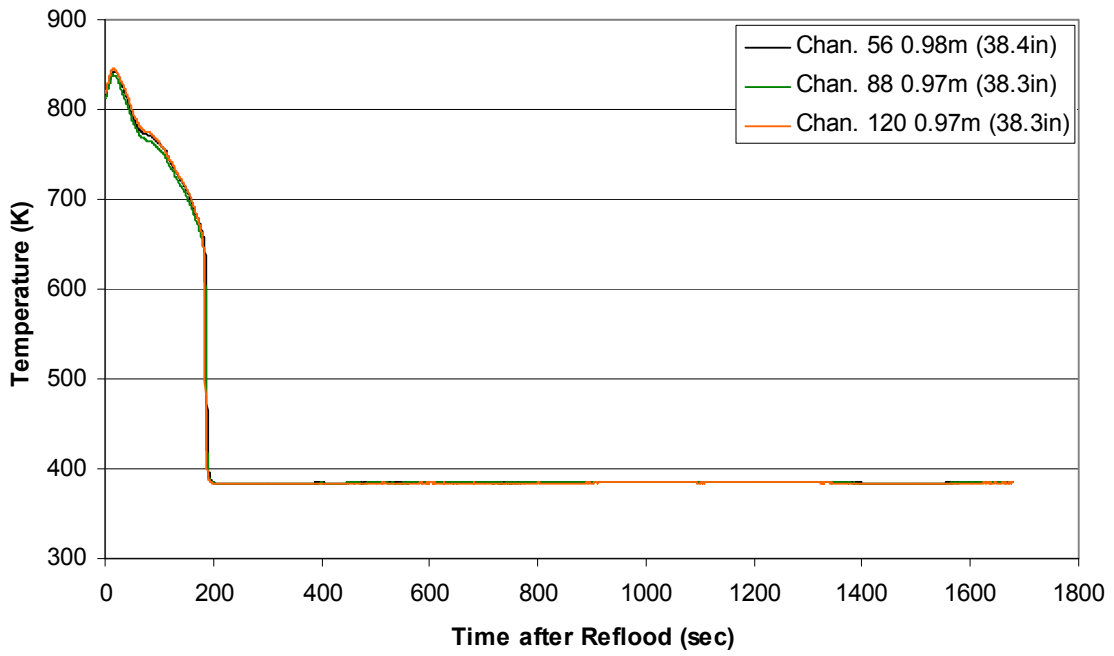


RBHT - TEST FACILITY

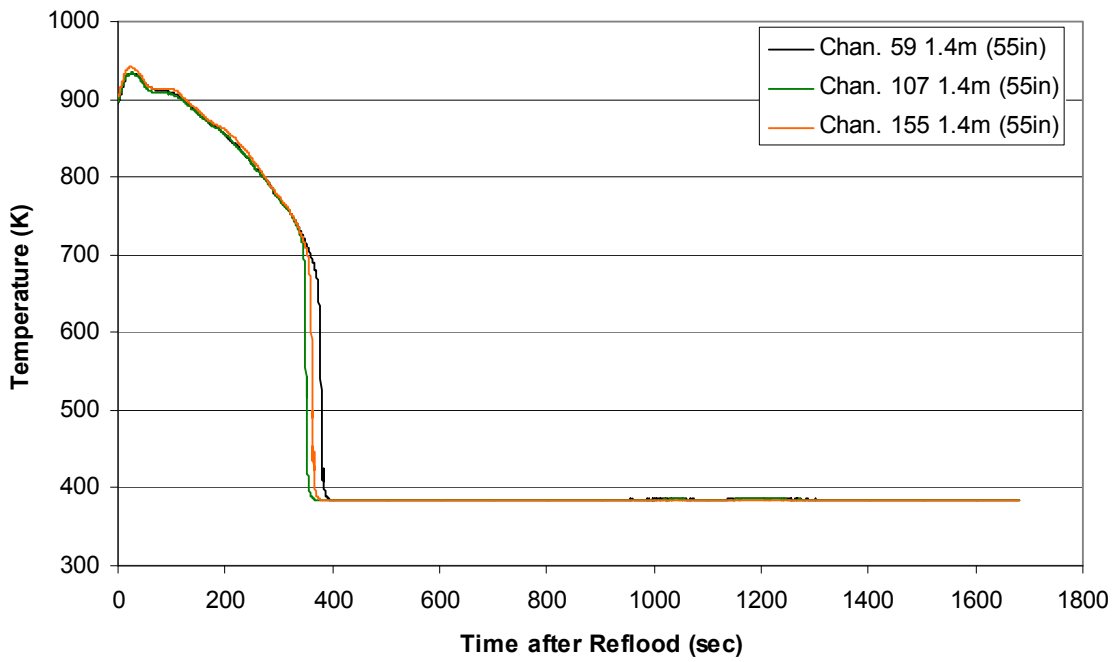
Test Section Current vs. Time, Exp 1096



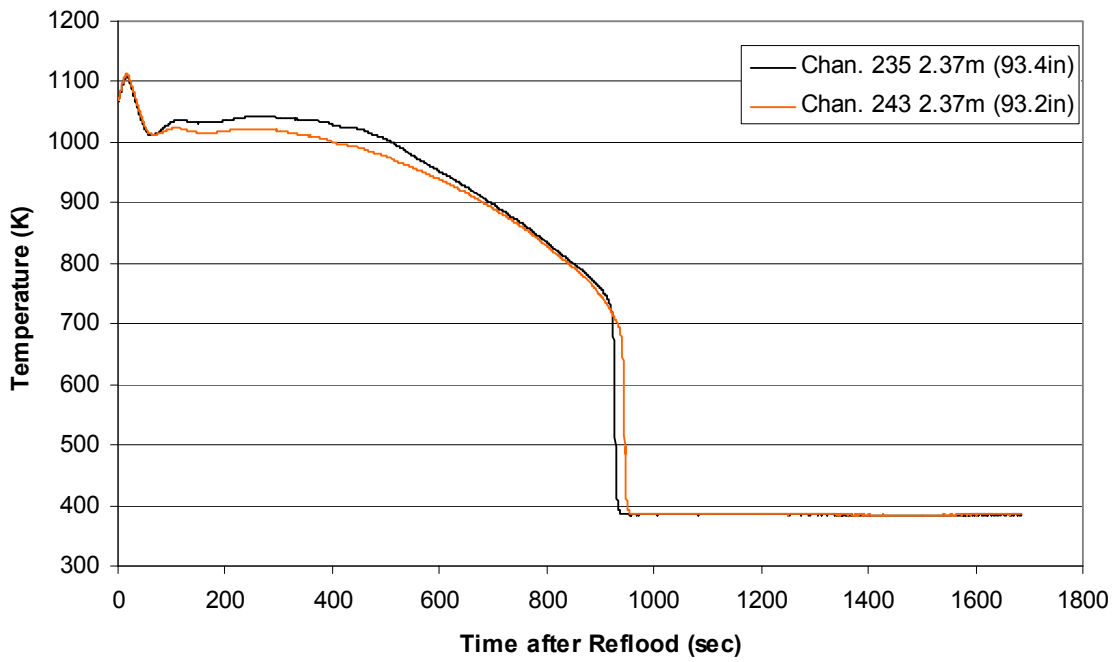
Heater Rod Temperature during Reflood
RBHT Exp. 1096



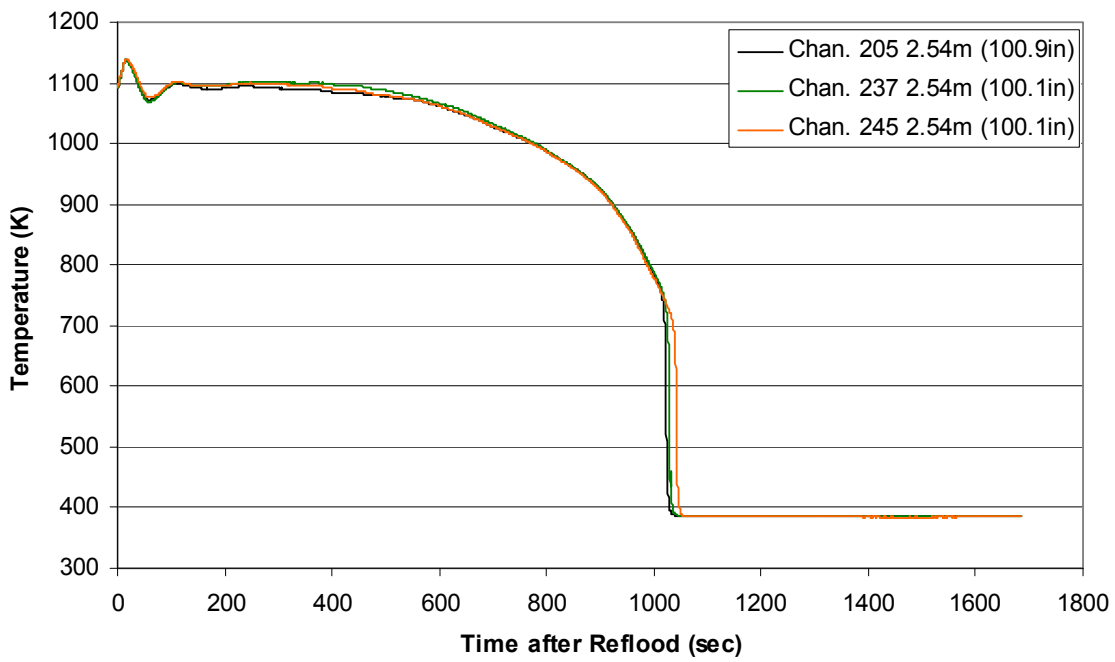
Heater Rod Temperature during Reflood
RBHT Exp. 1096



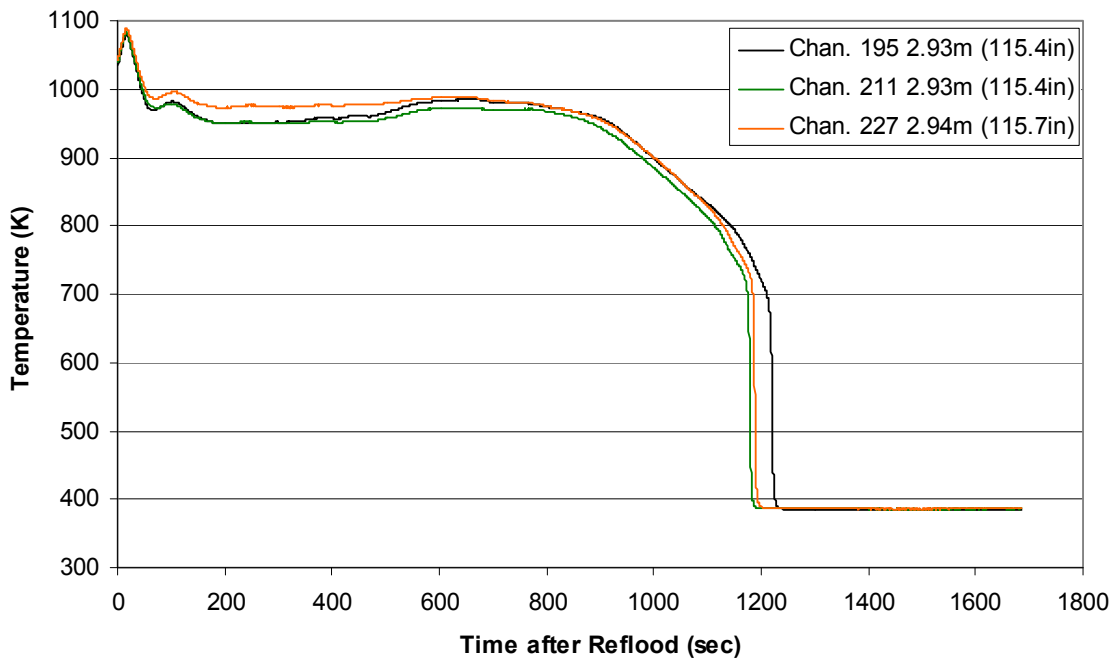
**Heater Rod Temperature during Reflood
RBHT Exp. 1096**



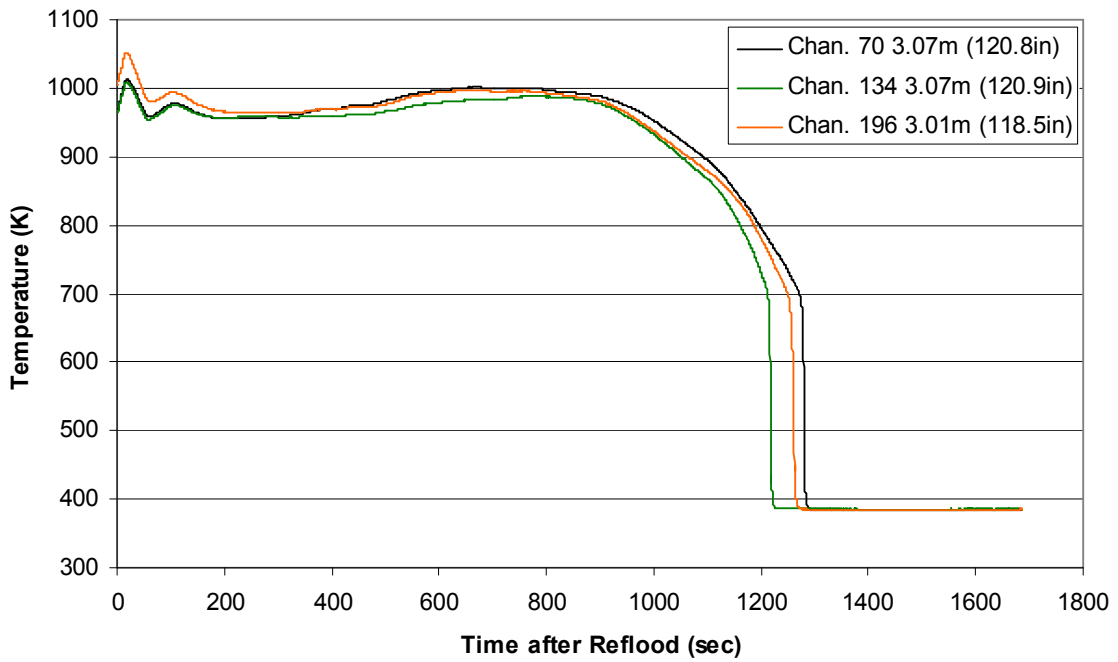
**Heater Rod Temperature during Reflood
RBHT Exp. 1096**



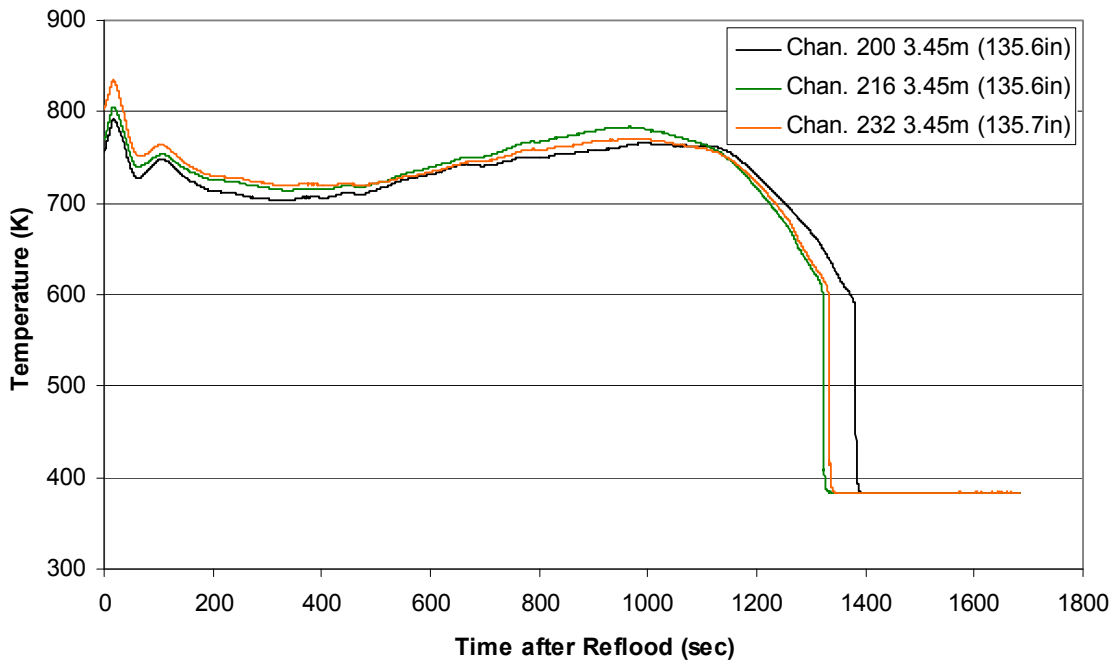
**Heater Rod Temperature during Reflood
RBHT Exp. 1096**



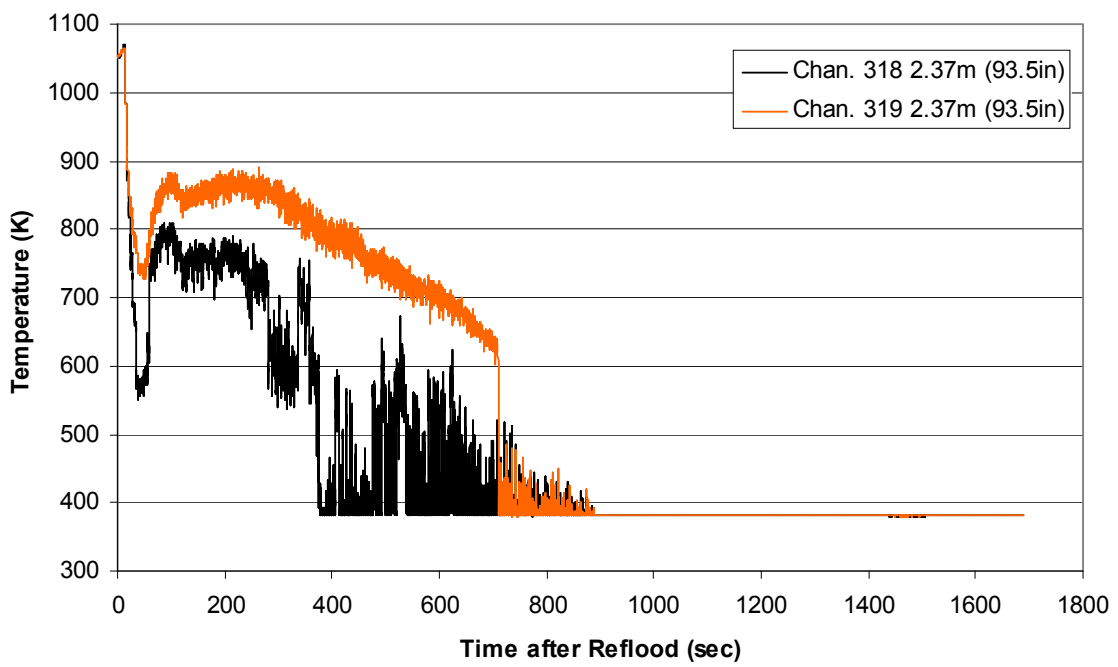
**Heater Rod Temperature during Reflood
RBHT Exp. 1096**



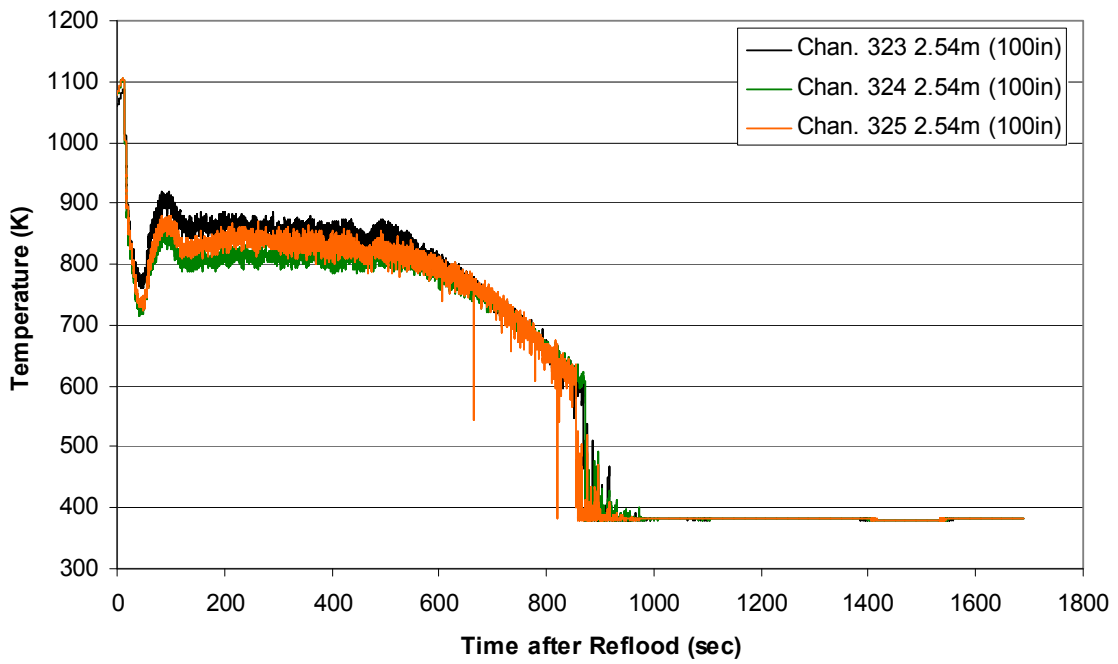
Heater Rod Temperature during Reflood
RBHT Exp. 1096



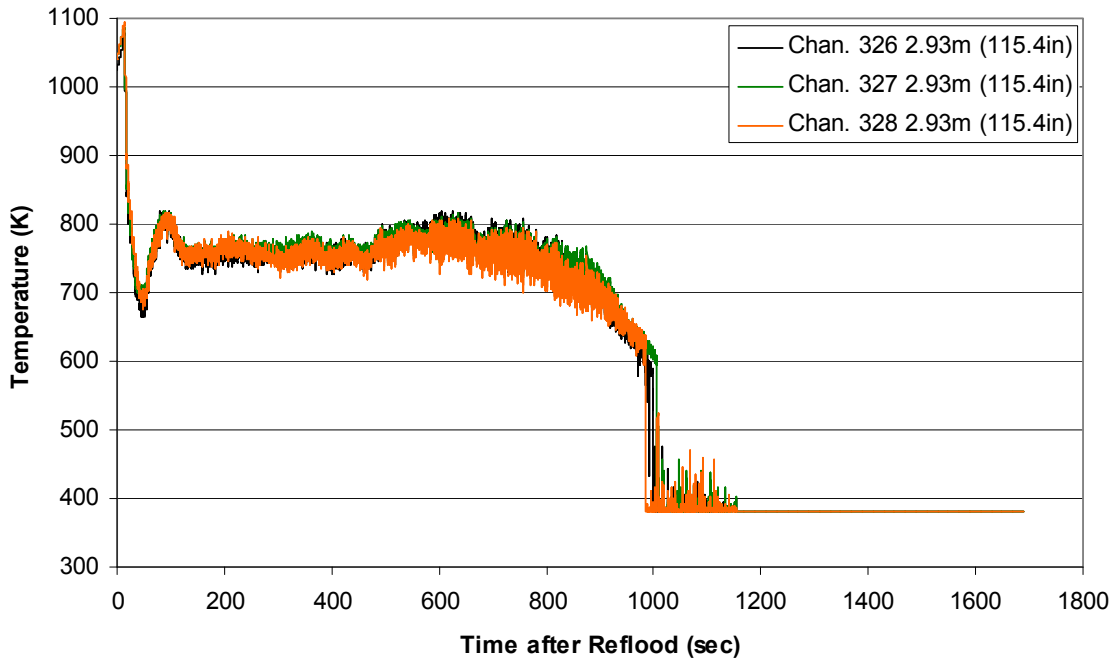
Steam Probe Temperature during Reflood
RBHT Exp. 1096



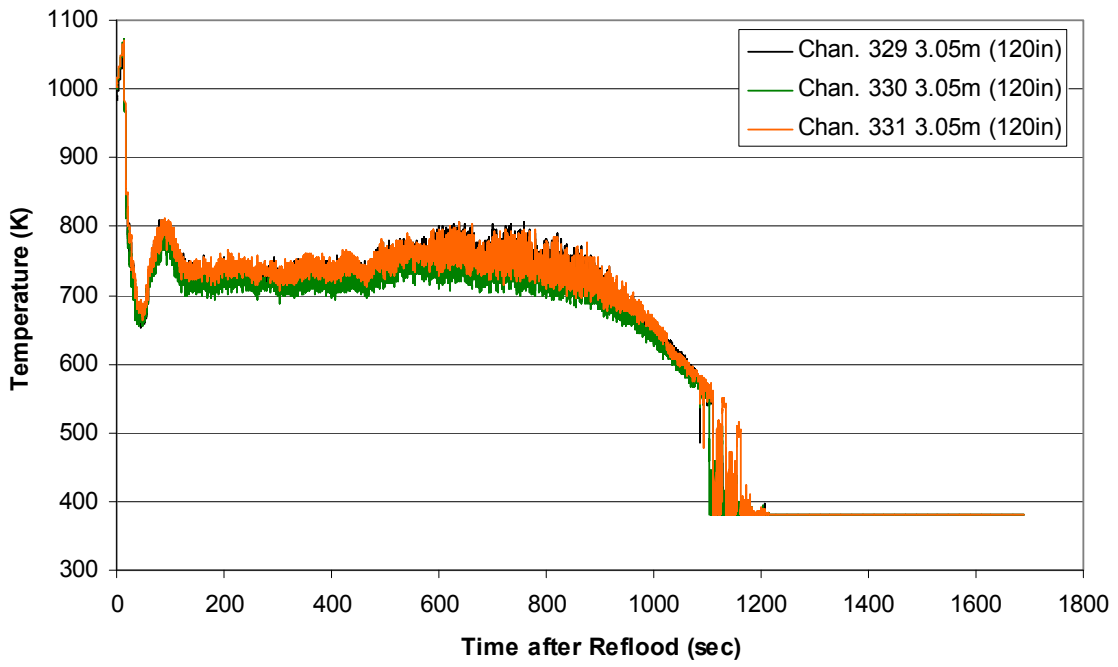
Steam Probe Temperature during Reflood
RBHT Exp. 1096



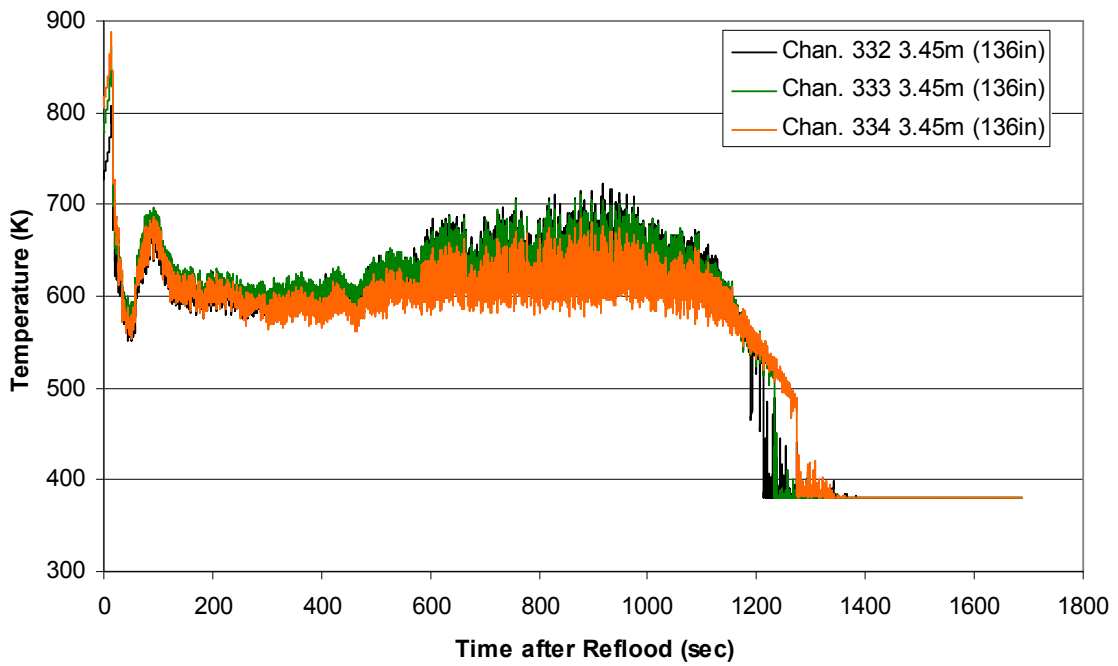
Steam Probe Temperature during Reflood
RBHT Exp. 1096



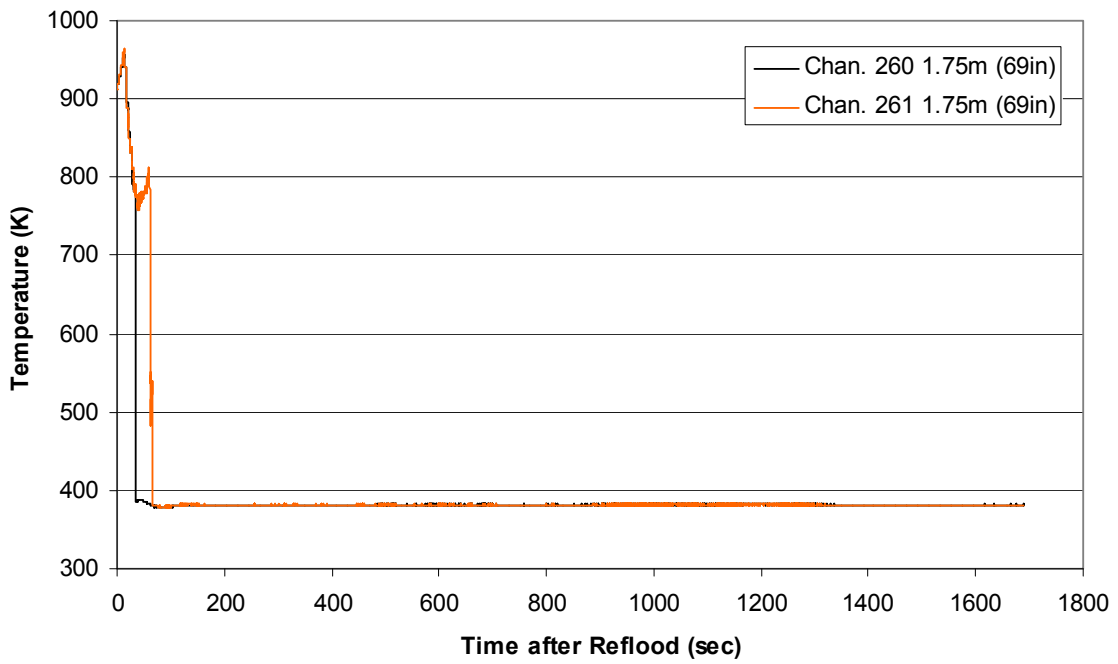
Steam Probe Temperature during Reflood
RBHT Exp. 1096



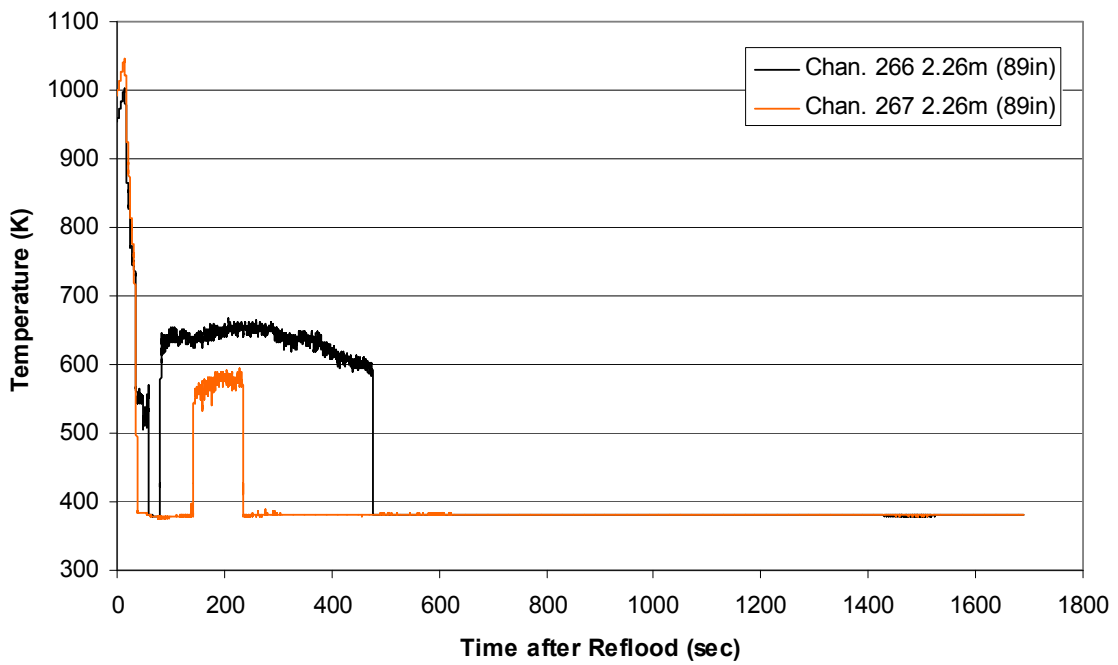
Steam Probe Temperature during Reflood
RBHT Exp. 1096



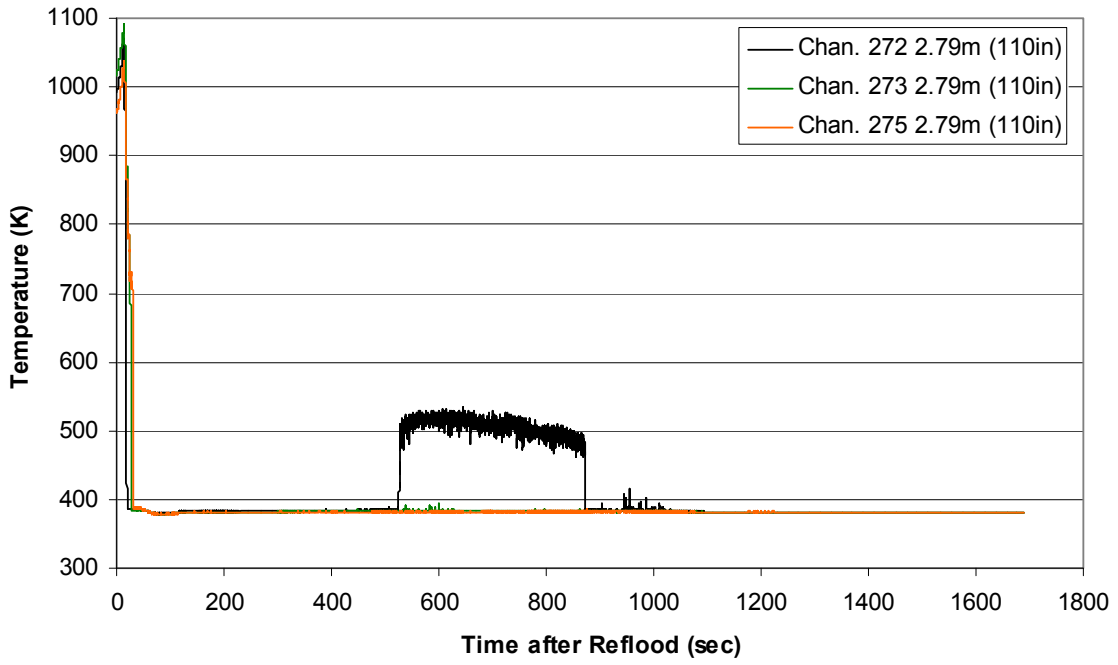
Spacer Grid Temperature during Reflood
RBHT Exp. 1096



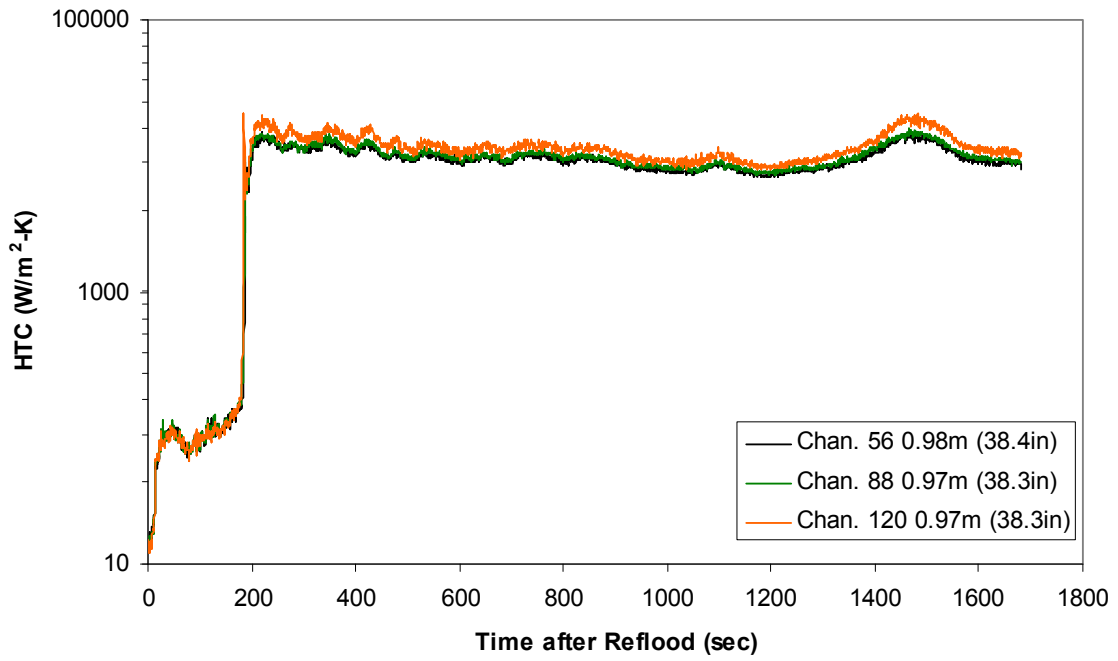
Spacer Grid Temperature during Reflood
RBHT Exp. 1096



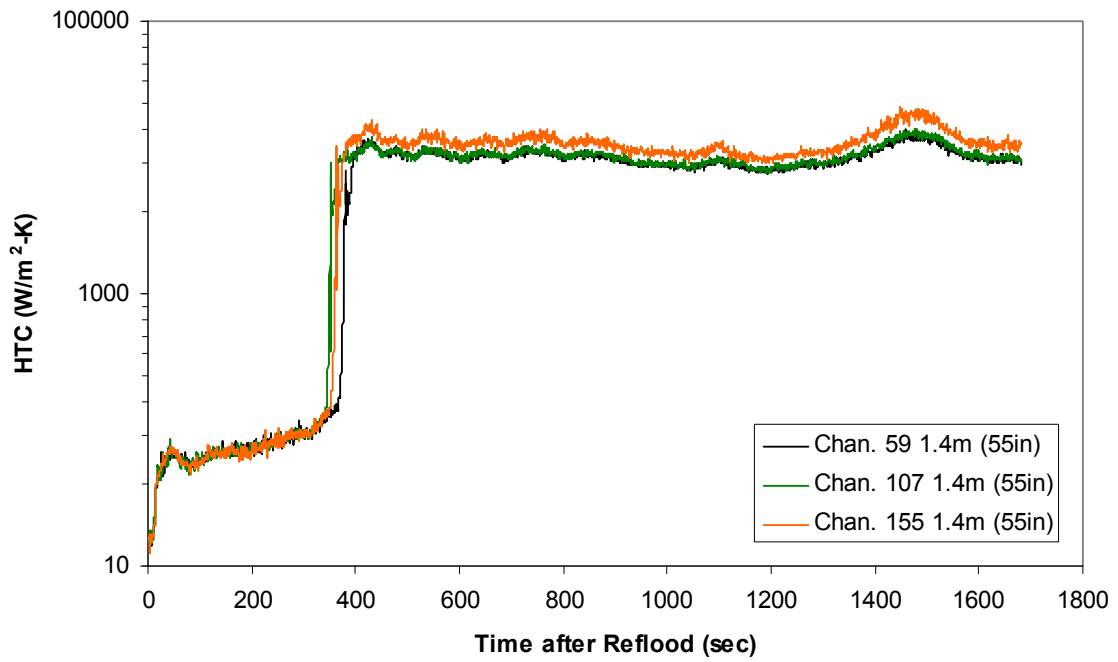
Spacer Grid Temperature during Reflood RBHT Exp. 1096



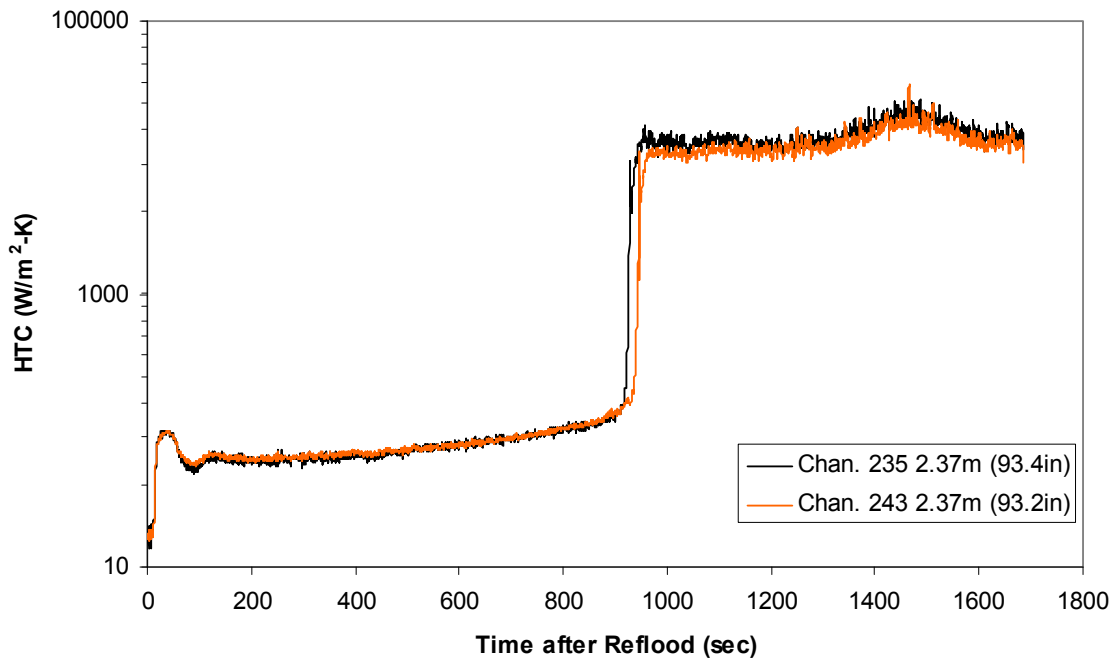
Heat Transfer Coefficient during Reflood RBHT Exp. 1096



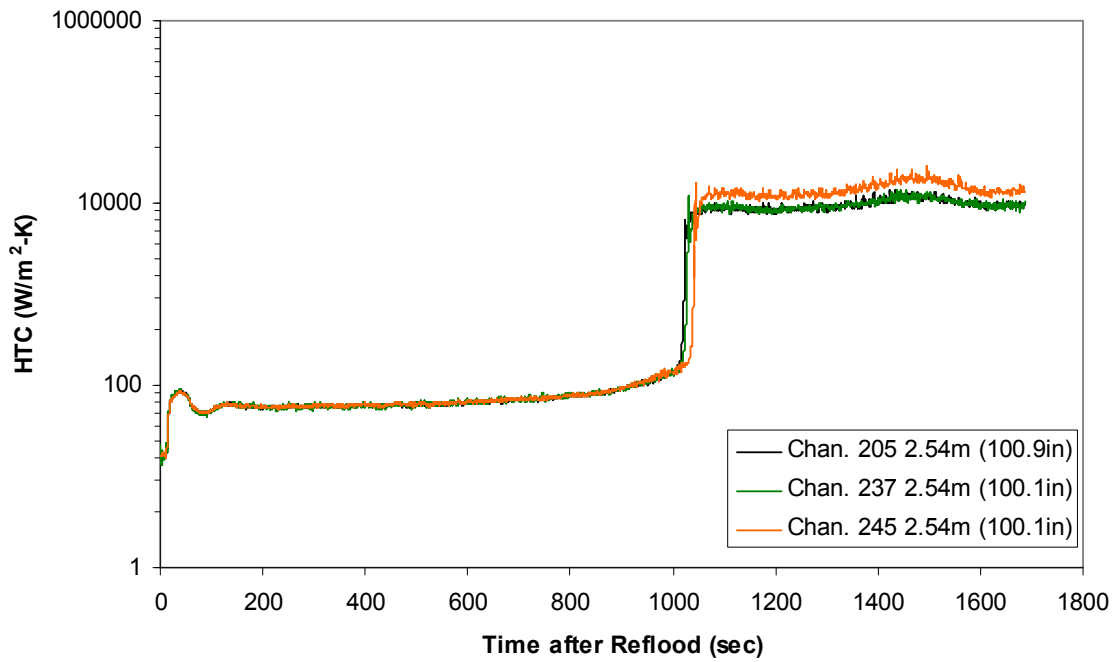
Heat Transfer Coefficient during Reflood
RBHT Exp. 1096



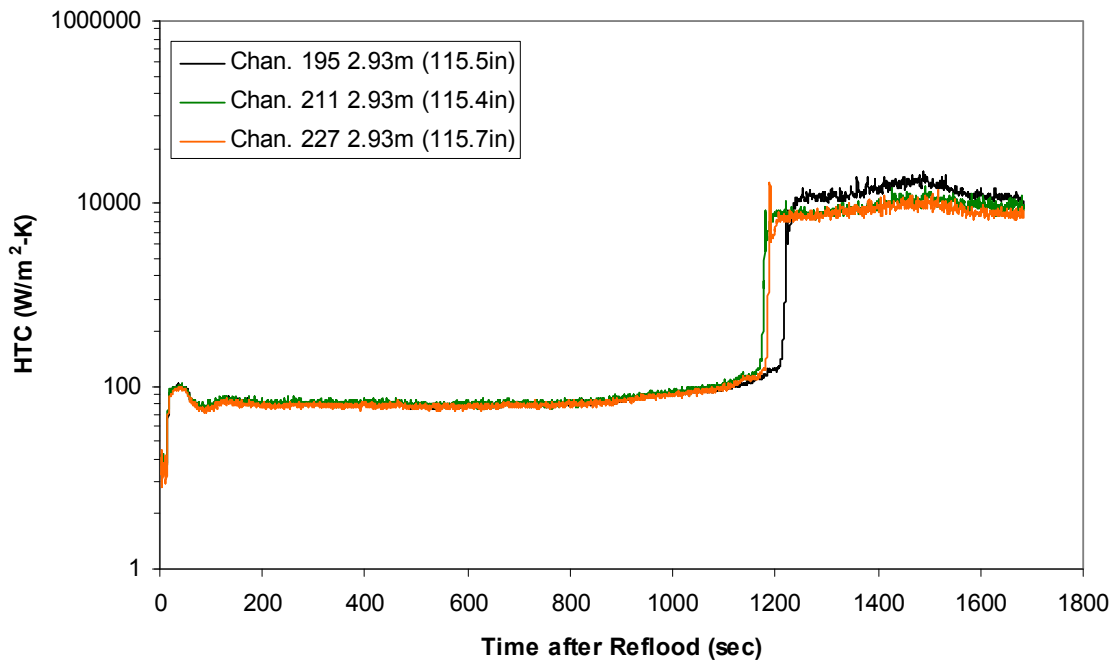
Heat Transfer Coefficient during Reflood
RBHT Exp. 1096



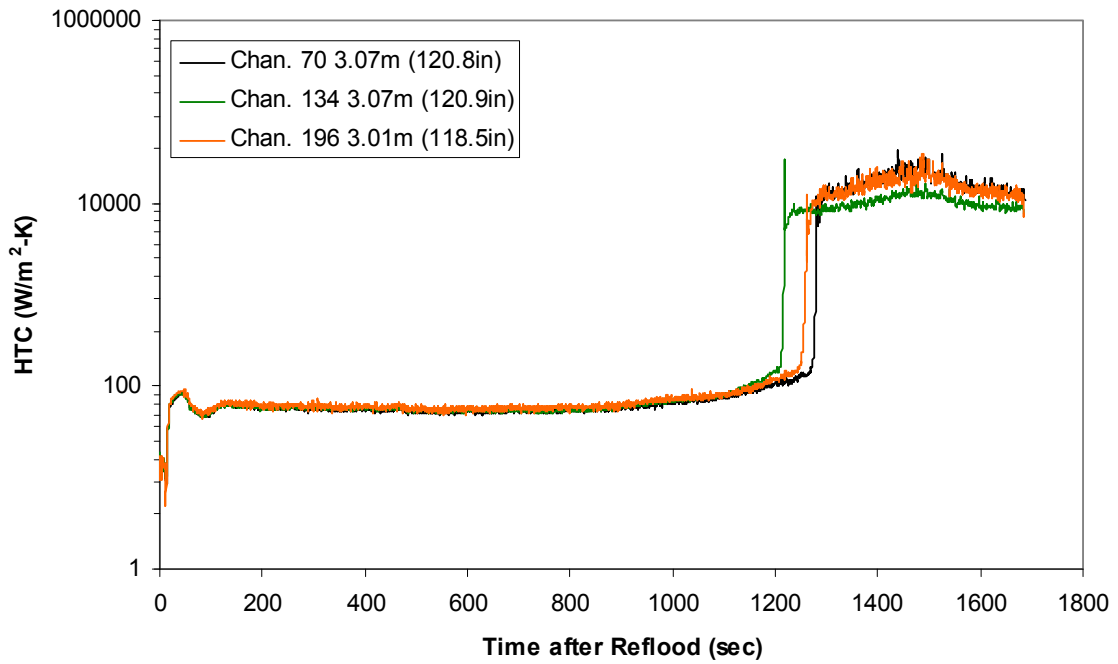
Heat Transfer Coefficient during Reflood RBHT Exp. 1096



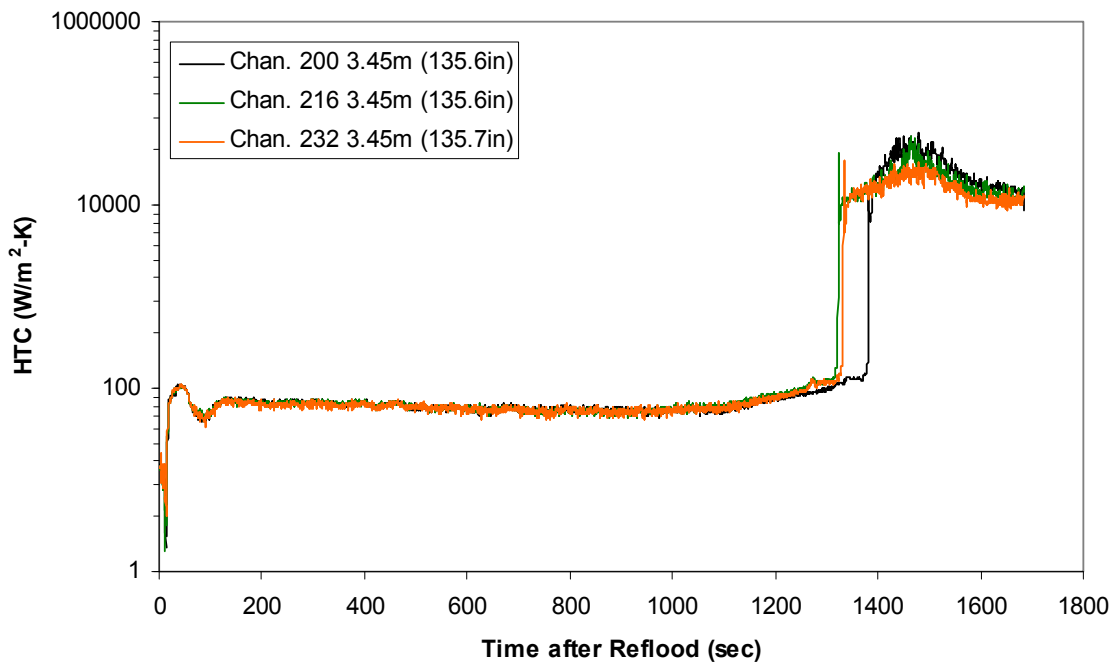
Heat Transfer Coefficient during Reflood RBHT Exp. 1096



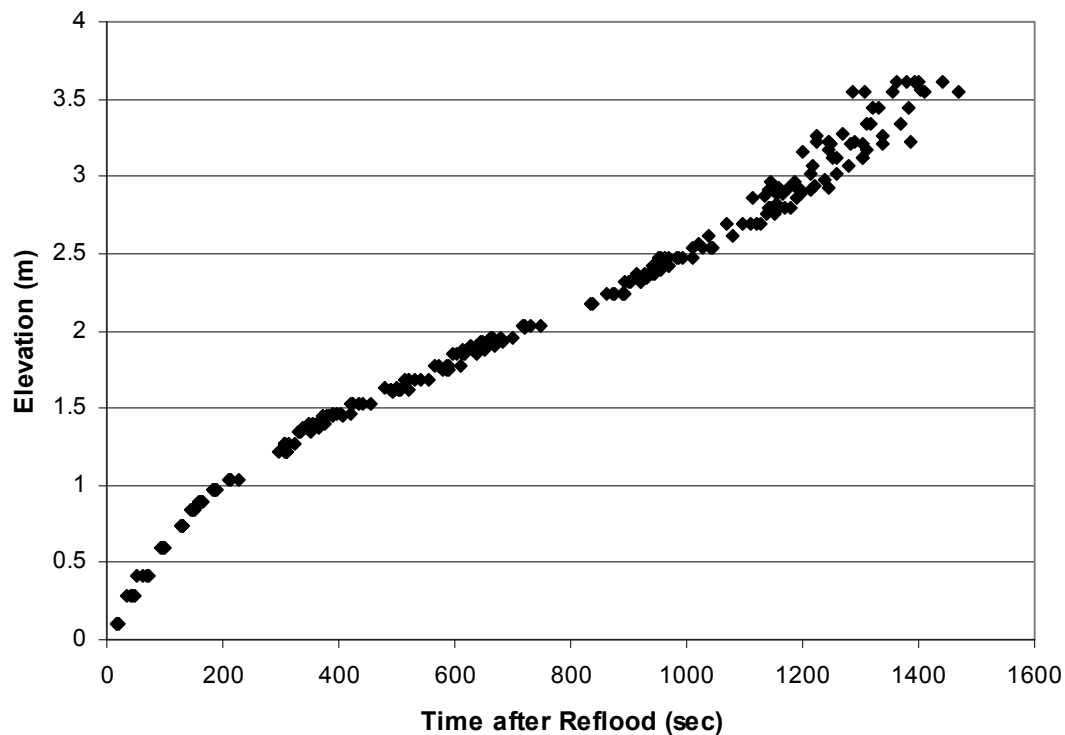
Heat Transfer Coefficient during Reflood RBHT Exp. 1096



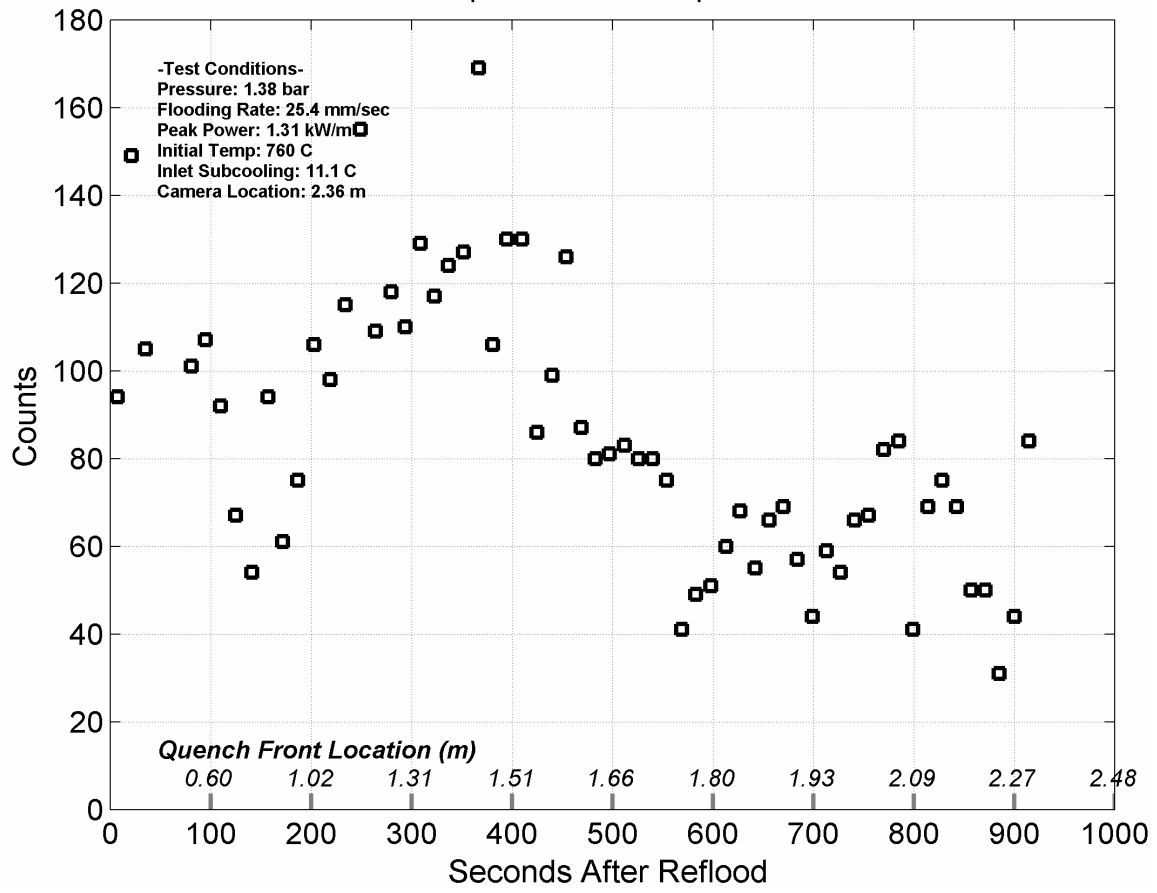
Heat Transfer Coefficient during Reflood RBHT Exp. 1096



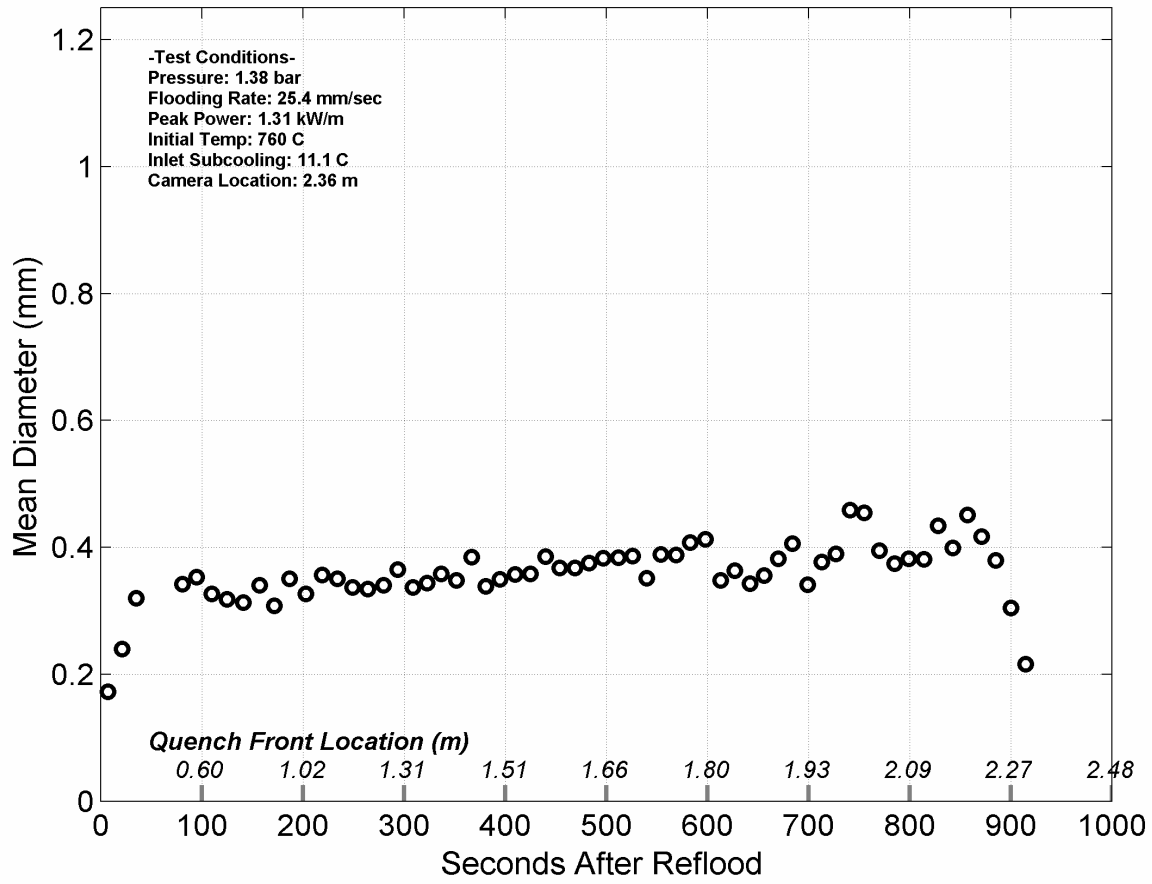
Quench Data, RBHT Exp. 1096



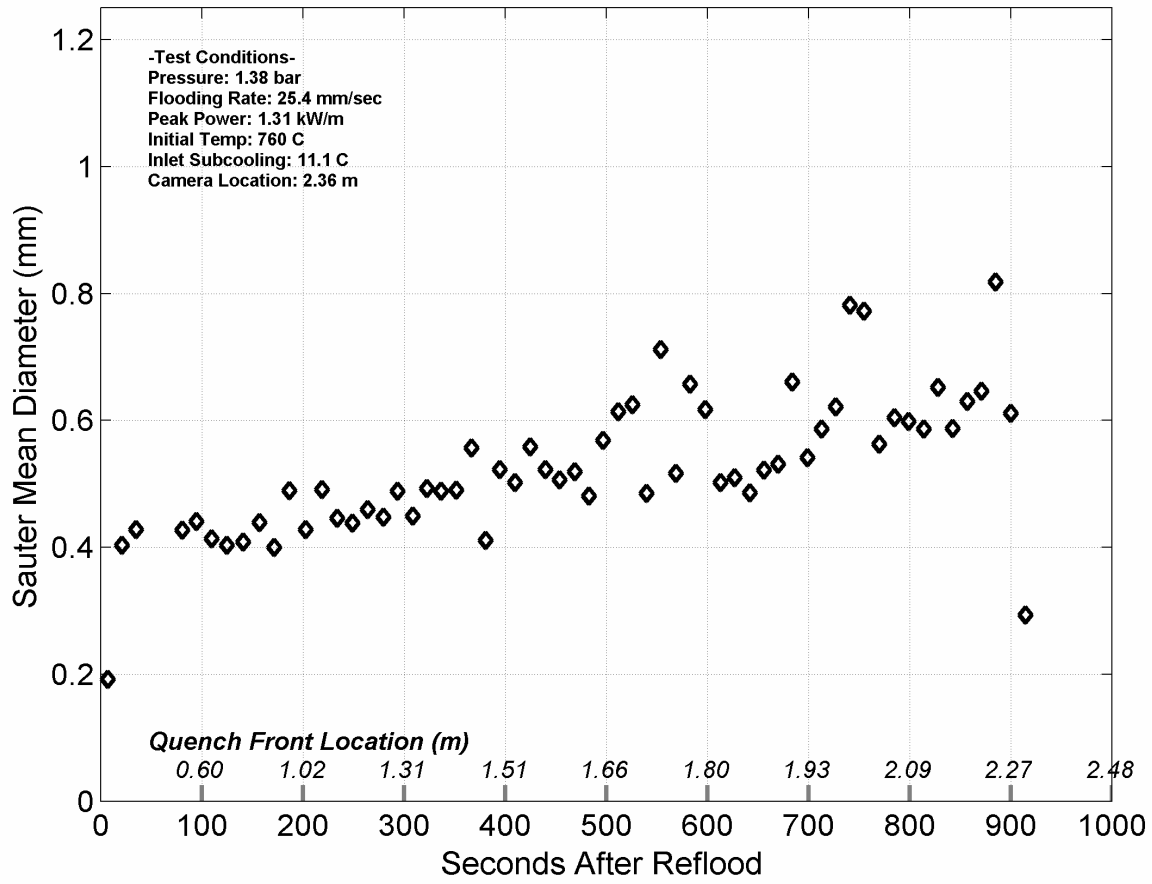
Droplet Counts - Exp. 1096



Mean Droplet Diameter - Exp. 1096



Droplet Sauter Mean Diameter - Exp. 1096



RBHT - REFLOOD TESTS

SUMMARY SHEET

RUN NO: **1108**

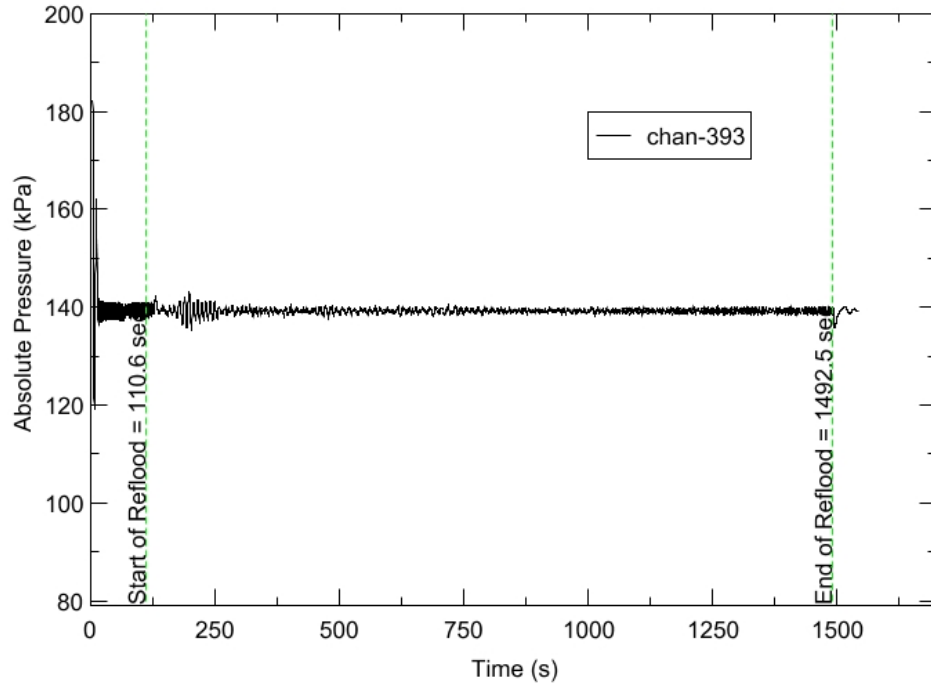
RUN CONDITIONS

Upper Plenum Pressure:	138 kPa (20 psia)
Initial Peak Clad Temperature:	1033 degrees K (1400 degrees F)
Rod Peak Power:	1.31 kW/m (0.4 kW/ft)
Flooding Rate:	0.0254 m/s (1 in/s)
Inlet Subcooling:	83 degrees K (150 degrees F)
Start of Reflood:	110.6 s
End of Reflood:	1492.5 s
Test Date:	6/6/2002
Comments:	Heater rod surfaces below 1m (40 in) quench to a temperature below saturation due to the high inlet subcooling. Therefore DATARH calculated heat transfer coefficients are not presented below this elevation after rod quench.

Rod_Elevation	Channel Number	Temperature at Reflood (K)	Temperature at Reflood (°F)	Turnaround Time (sec.)	Turnaround Temperature (K)	Turnaround Temperature (°F)	Quench Time (sec.)	Quench Temperature (K)	Quench Temperature (°F)
B6 0.592m	148	671.94	749.81	13.65	693.9	789.33	62.15	540.91	513.95
B6 0.744m	149	727.95	850.63	14.15	753.24	896.14	85.15	564.9	557.14
B6 0.846m	150	767.19	921.26	14.65	796.23	973.52	99.65	554.74	538.85
B6 0.897m	151	780.63	945.45	15.15	811.14	1000.37	107.15	570.61	567.41
C6 1.04m	137	835.11	1043.52	18.65	871.06	1108.22	130.65	593.02	607.75
D5 1.27m	217	891.98	1145.87	18.65	926.77	1208.51	179.65	578.99	582.49
C6 1.34m	138	871.59	1109.18	25.15	914.35	1186.15	189.15	583.27	590.2
D5 1.37m	218	910.36	1178.96	32.15	956.44	1261.9	195.15	597.42	615.66
C6 1.39m	139	878.72	1122.02	36.15	924.66	1204.7	198.15	608.41	635.44
D5 1.45m	219	923	1201.71	39.15	973.09	1291.87	207.65	613.82	645.19
C6 1.47m	140	892.45	1146.73	47.15	945.57	1242.34	214.15	613.7	644.97
D5 1.52m	220	934.42	1222.27	64.65	993.63	1328.85	225.15	641.34	694.73
C6 1.62m	141	910.6	1179.4	84.15	996	1333.12	252.15	650.24	710.74
D5 1.68m	221	949.28	1249.01	84.65	1042.15	1416.18	268.15	668.3	743.25
D5 1.78m	222	949.45	1249.32	21.15	995.73	1332.63	304.15	607.13	633.15
D5 1.85m	223	967.12	1281.13	76.65	1031.59	1397.18	321.65	648.92	708.38
C6 1.87m	142	940.75	1233.66	68.15	1016.32	1369.68	331.65	599.88	620.1
D5 1.90m	224	971.2	1288.47	84.65	1055.29	1439.83	336.65	677.53	759.87
C6 1.95m	144	943.5	1238.61	85.15	1039.94	1412.2	361.15	660.88	729.89
C3 2.17m	178	974.69	1294.76	193.65	1133.26	1580.17	479.65	644.55	700.51
D4 2.24m	241	996.67	1334.31	193.65	1151.47	1612.96	548.15	588.41	599.44
D4 2.32m	242	1005	1349.31	237.65	1091.04	1504.19	581.15	657.26	723.39
C3 2.35m	180	992.68	1327.14	242.65	1084.37	1492.17	571.15	679.11	762.72
D4 2.37m	243	1010.34	1358.92	237.15	1102.69	1525.16	607.15	610.5	639.21
C3 2.40m	181	995.53	1332.26	243.15	1095.46	1512.13	607.65	665.28	737.82
D4 2.54m	245	1041.68	1415.33	250.15	1179.95	1664.22	736.65	602.38	624.59
D6 2.62m	129	1023.82	1383.18	280.15	1191.99	1685.89	779.65	642.4	696.64
D6 2.69m	130	1026.91	1388.75	302.15	1221.09	1738.27	828.15	606.71	632.38
C3 2.76m	183	1033.75	1401.06	360.15	1247.6	1785.99	859.15	677.13	759.14
D4 2.79m	247	1025.14	1385.56	393.65	1170.46	1647.15	898.15	636.34	685.73
D6 2.87m	131	997.01	1334.93	18.15	1053.29	1436.24	919.65	674.61	754.6
D6 2.92m	132	978.16	1300.99	432.65	1059.65	1447.68	945.65	649.69	709.76
D6 2.97m	133	953.97	1257.46	470.65	1067.94	1462.61	974.65	660.17	728.61
D6 3.07m	134	922.38	1200.6	516.15	1073.28	1472.22	1015.15	523.32	482.29
E3 3.12m	197	918.23	1193.13	516.15	1097.16	1515.19	1047.65	586.33	595.71
D6 3.17m	135	887.54	1137.88	556.15	1077.2	1479.28	1051.65	656.53	722.07
D6 3.27m	136	847.77	1066.3	594.65	1065.37	1457.98	1091.65	538.8	510.16
D4 3.61m	248	614.3	646.06	697.65	807.28	993.42	1201.15	564.7	556.76

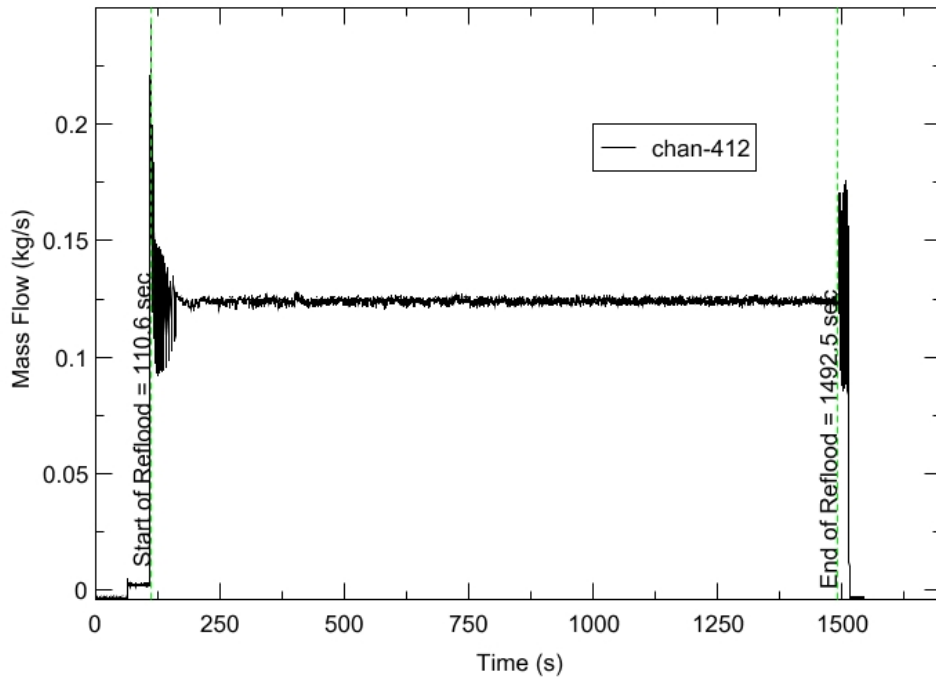
RBHT - TEST FACILITY

Upper Plenum Pressure vs. Time, Exp 1108



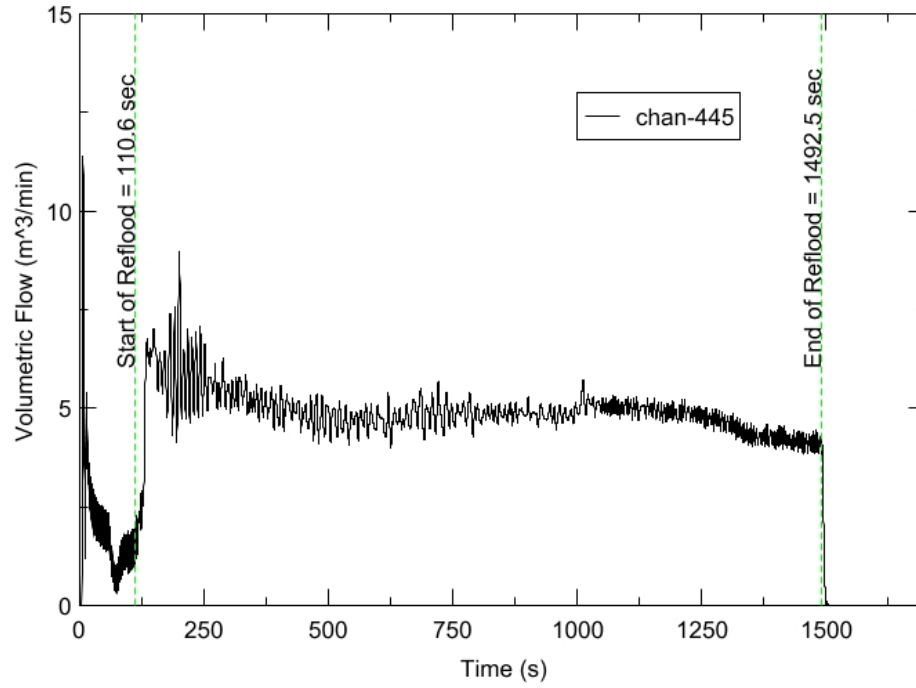
RBHT - TEST FACILITY

Inlet Flow vs. Time, Exp 1108



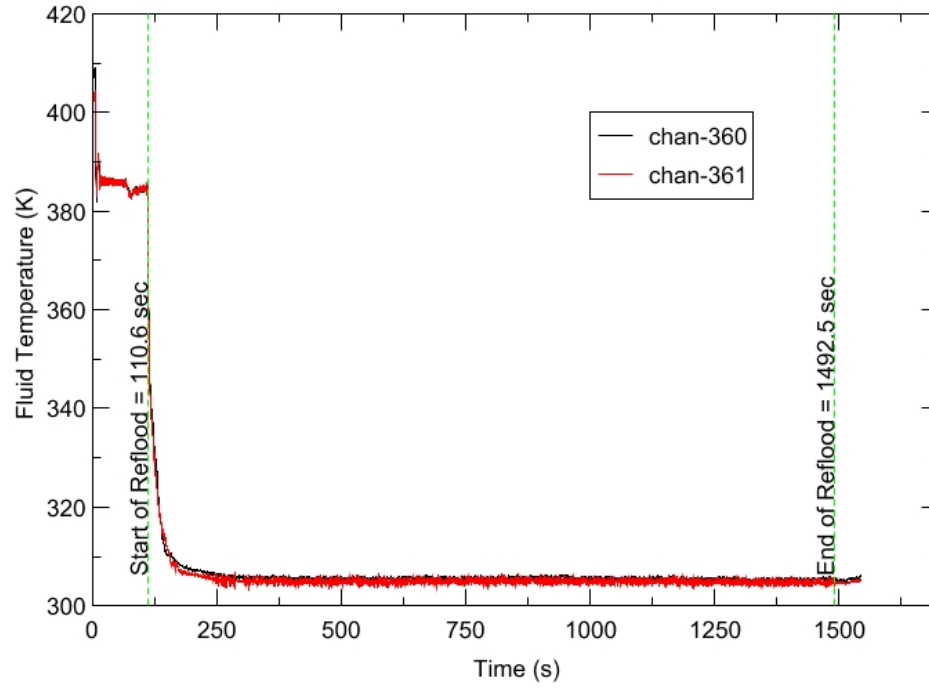
RBHT - TEST FACILITY

Steam Exhaust Flow vs. Time, Exp 1108



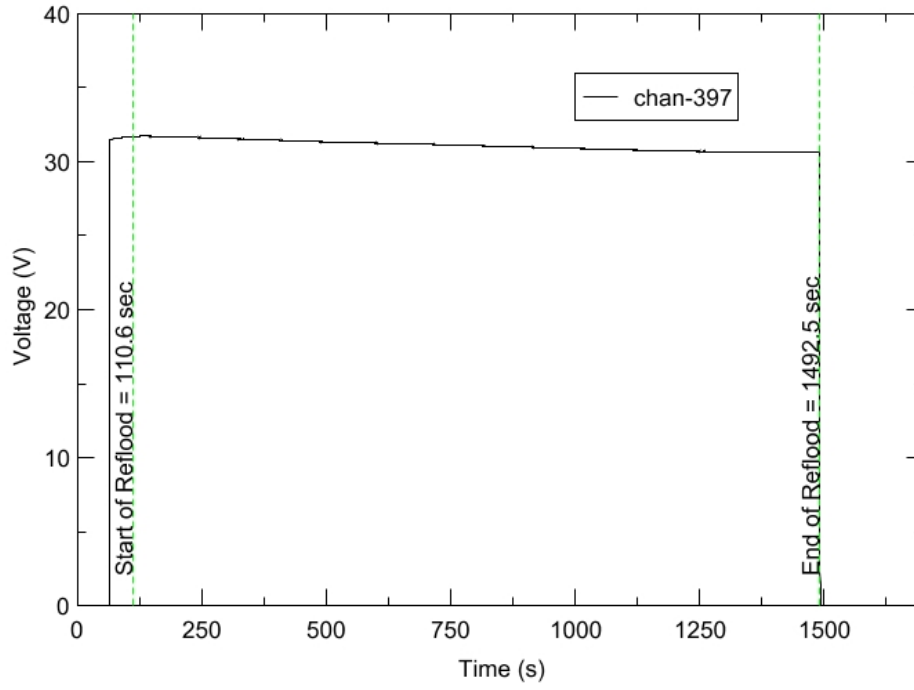
RBHT - TEST FACILITY

Inlet Flow Temperature vs. Time, Exp 1108



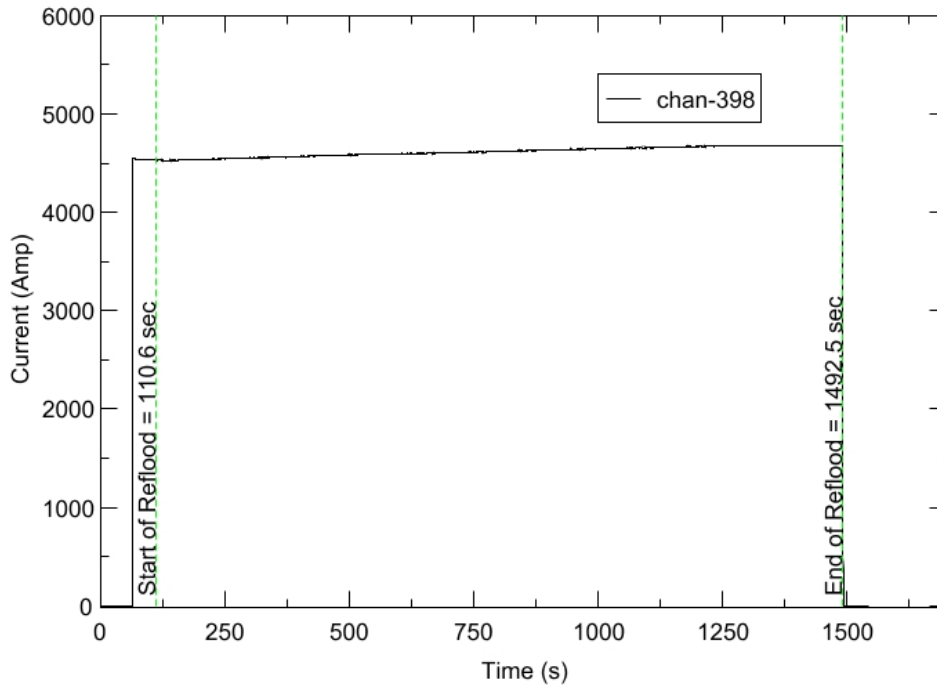
RBHT - TEST FACILITY

Test Section Voltage vs. Time, Exp 1108

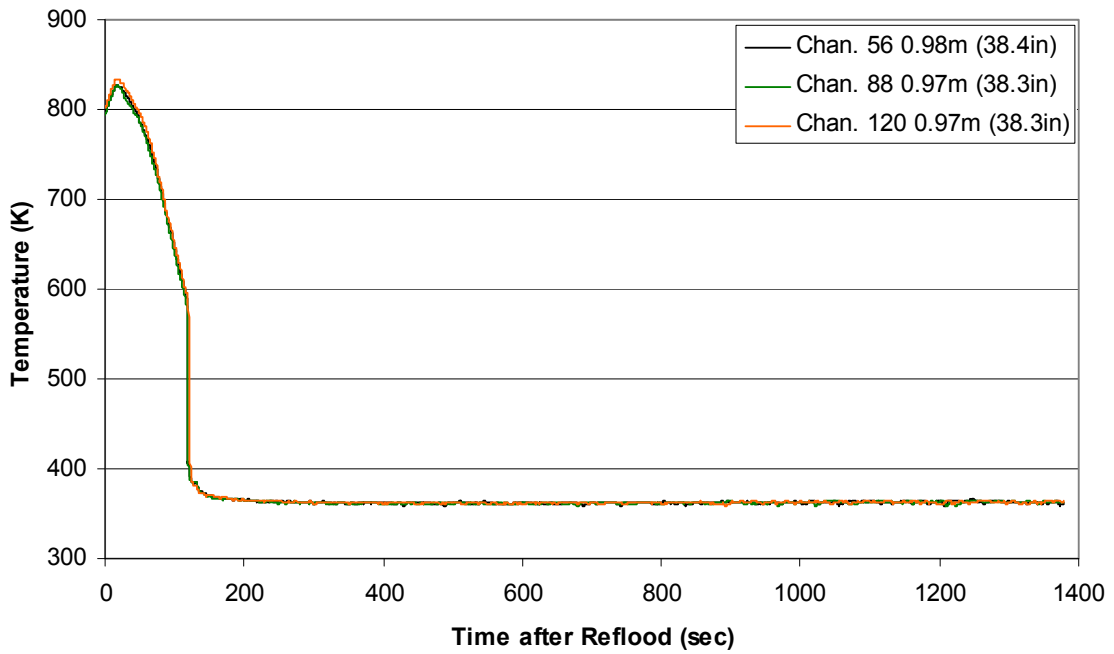


RBHT - TEST FACILITY

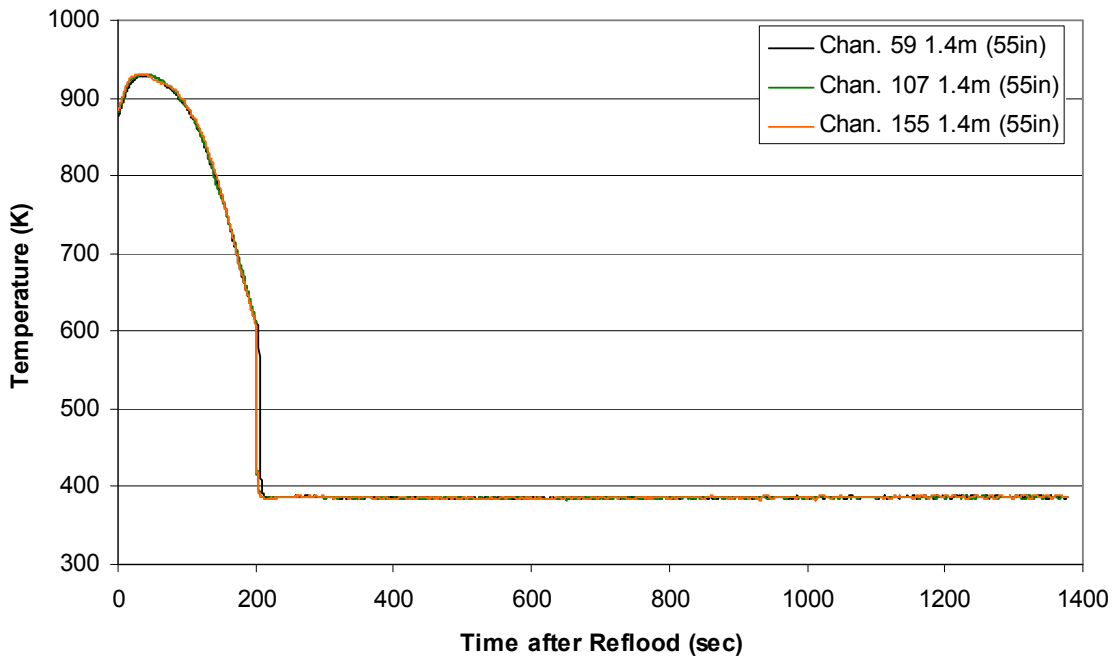
Test Section Current vs. Time, Exp 1108



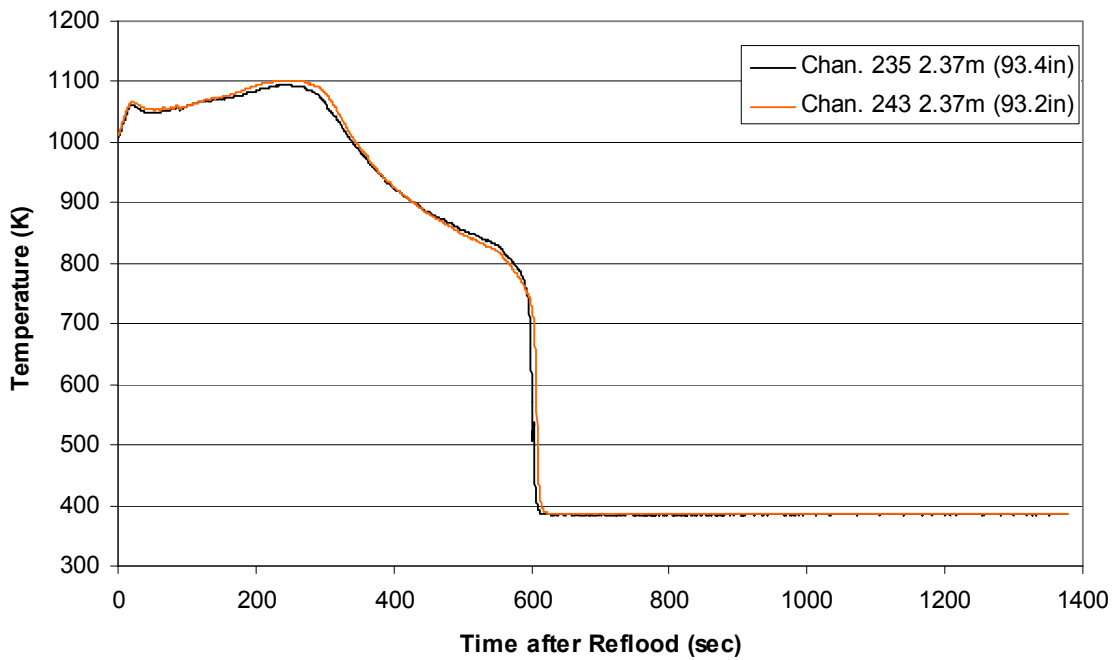
**Heater Rod Temperature during Reflood
RBHT Exp. 1108**



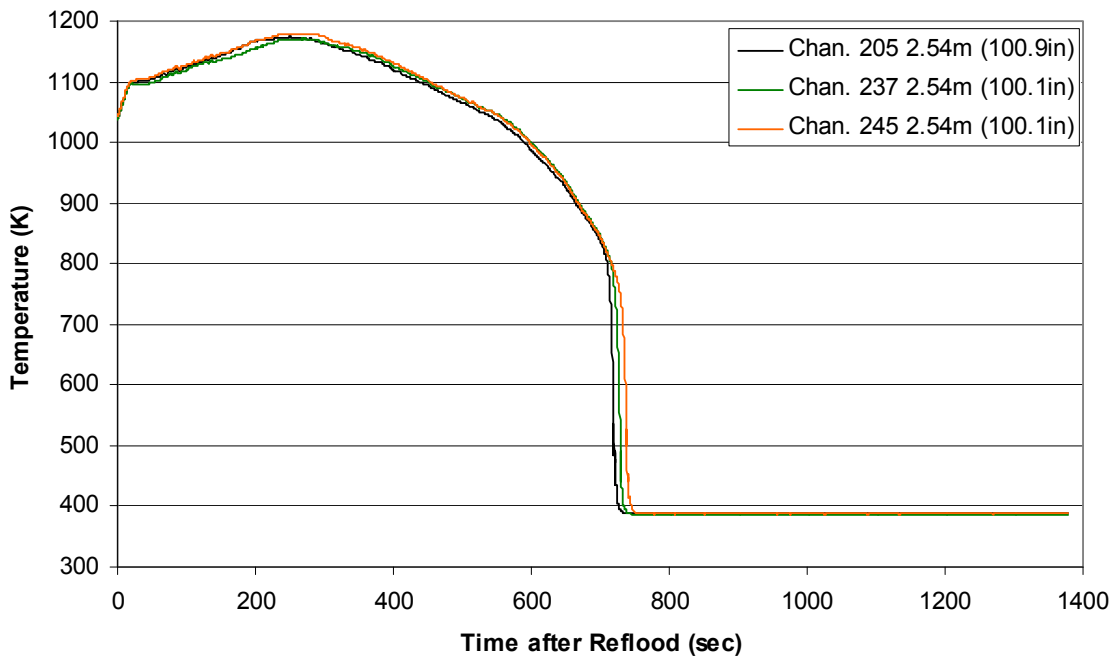
**Heater Rod Temperature during Reflood
RBHT Exp. 1108**



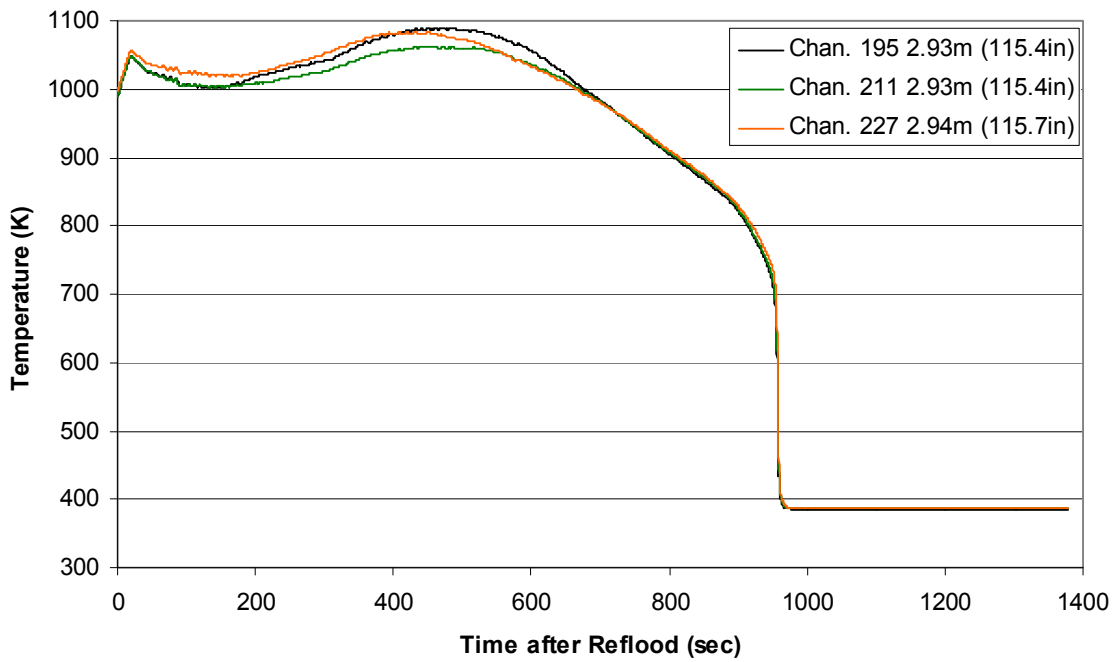
Heater Rod Temperature during Reflood
RBHT Exp. 1108



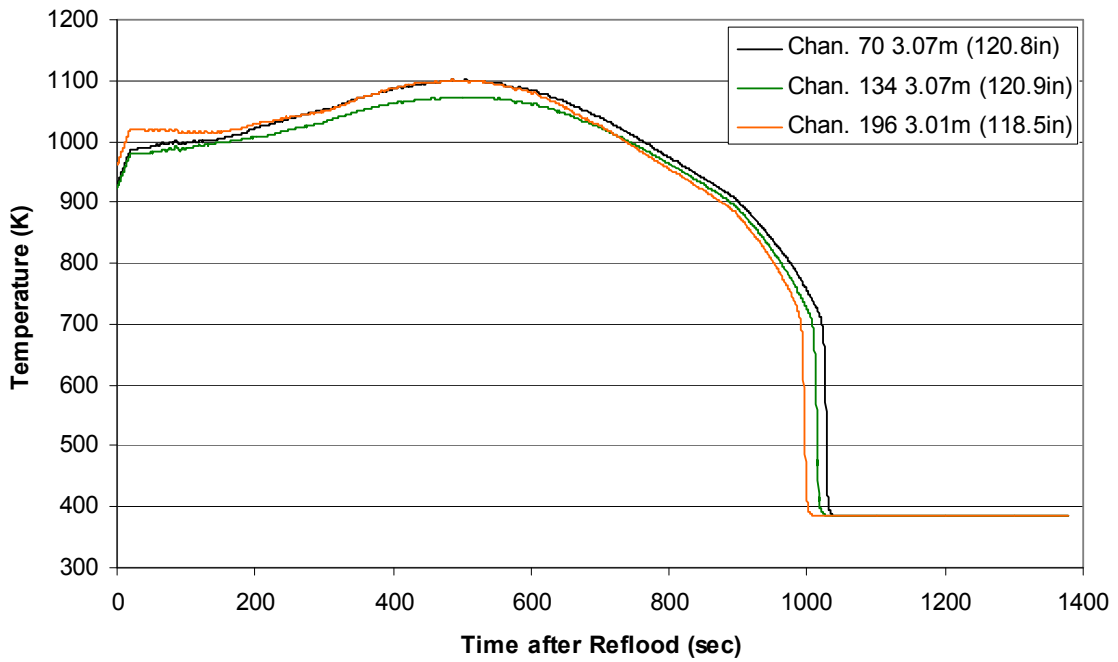
Heater Rod Temperature during Reflood
RBHT Exp. 1108



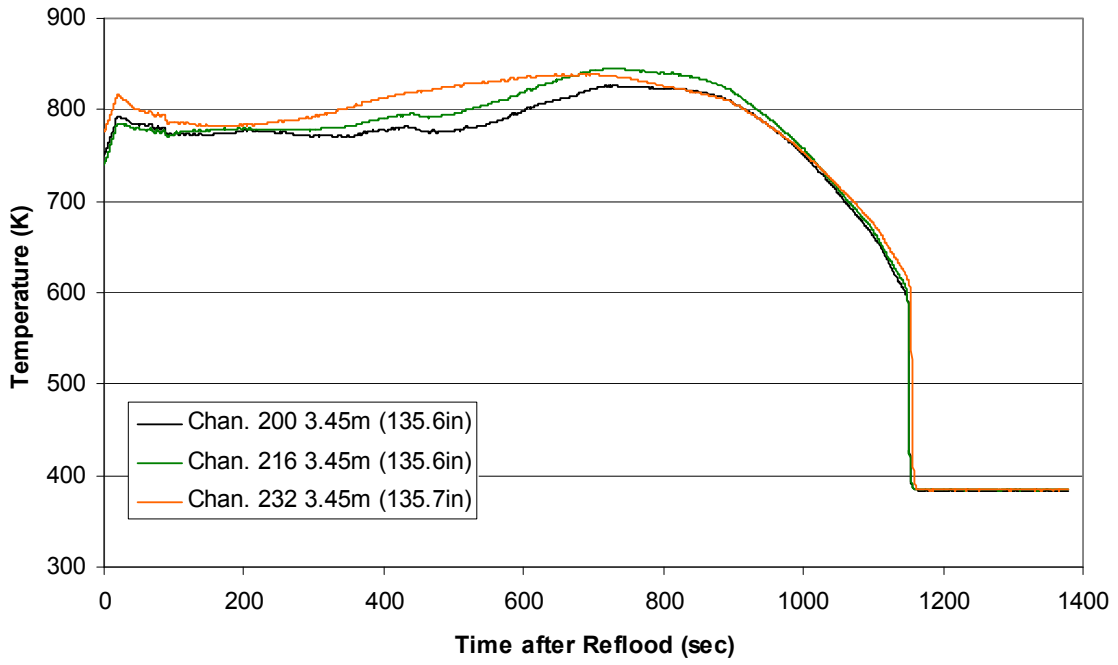
Heater Rod Temperature during Reflood
RBHT Exp. 1108



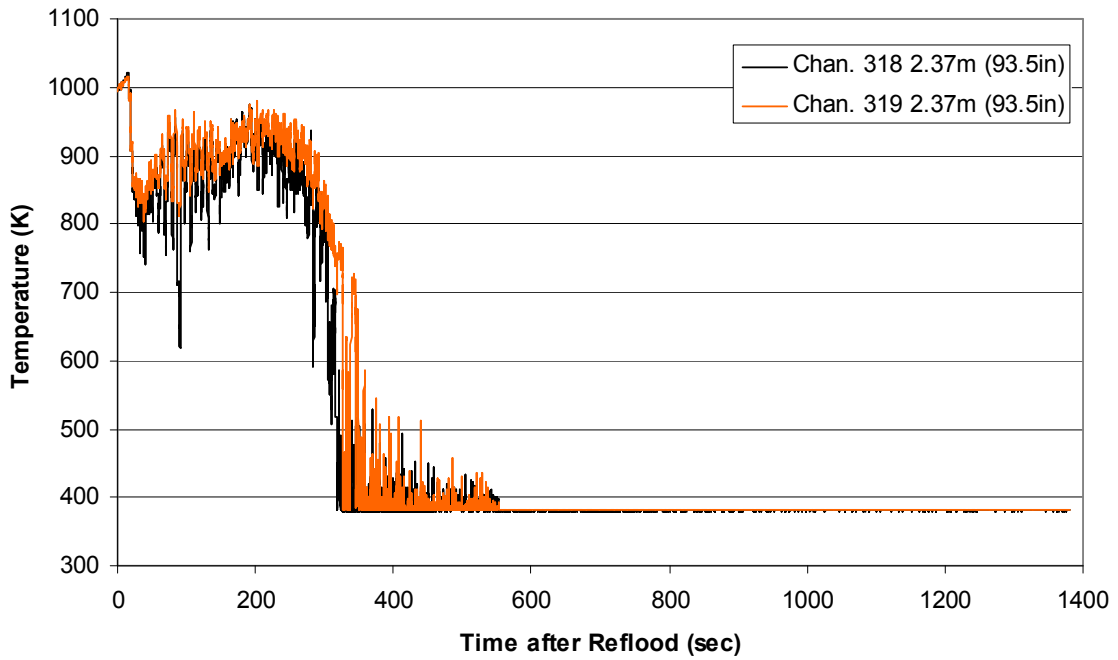
Heater Rod Temperature during Reflood
RBHT Exp. 1108



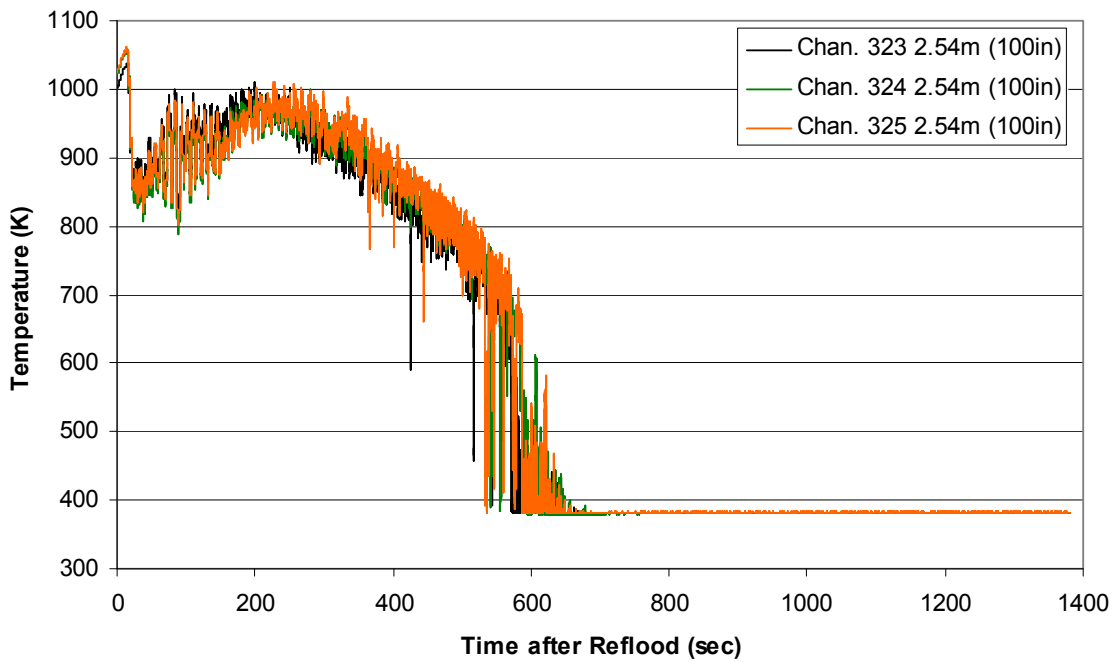
Heater Rod Temperature during Reflood RBHT Exp. 1108



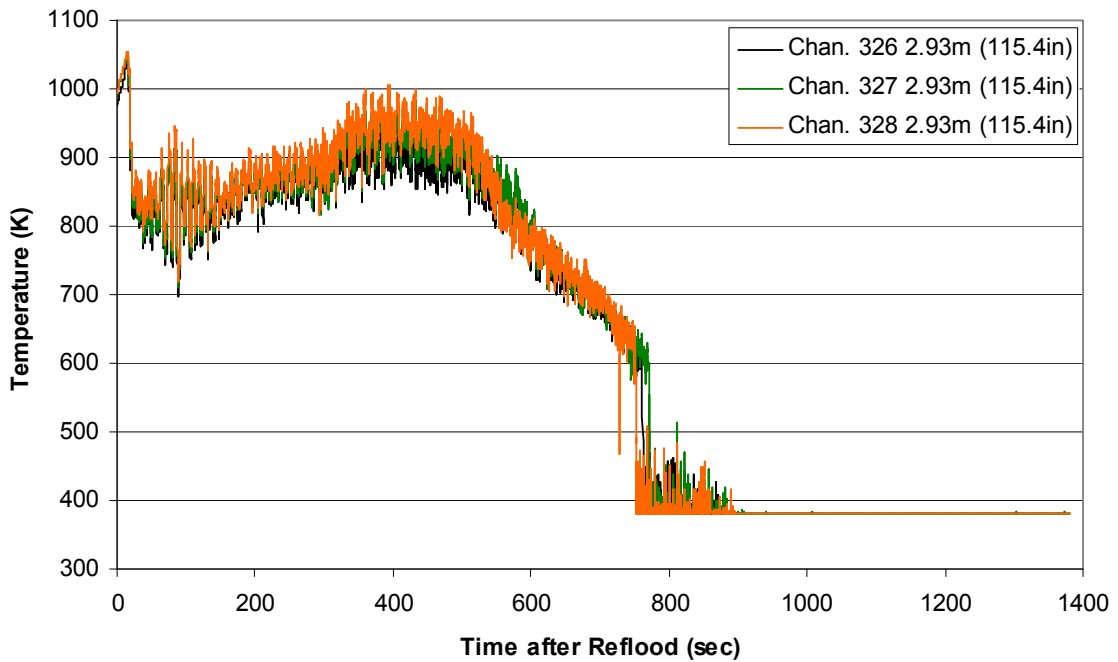
Steam Probe Temperature during Reflood RBHT Exp. 1108



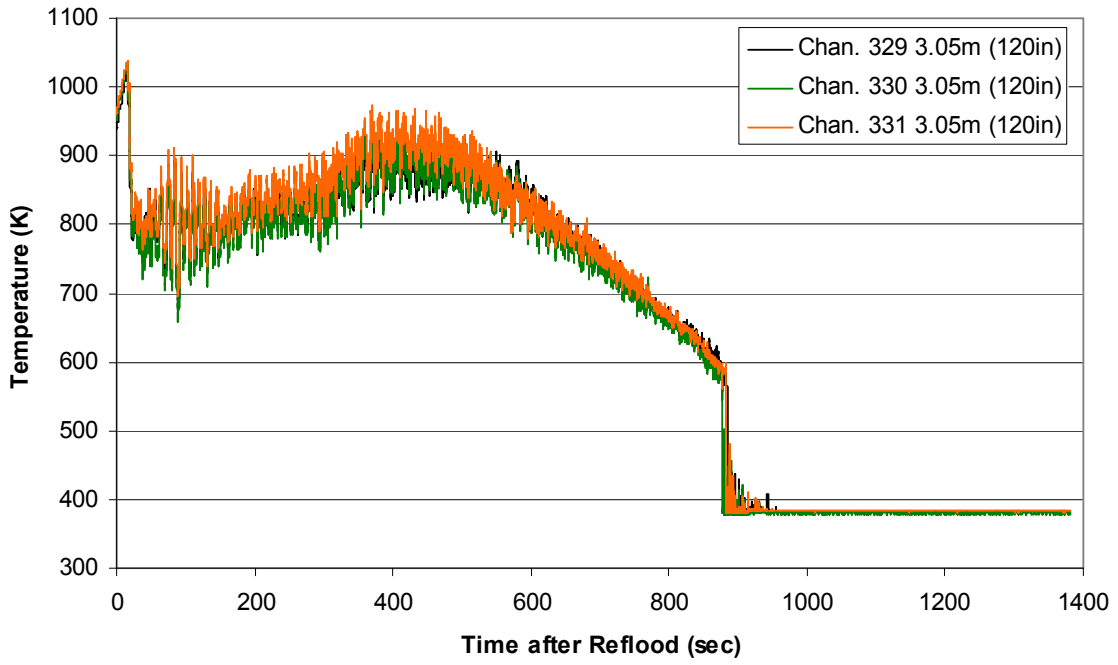
Steam Probe Temperature during Reflood
RBHT Exp. 1108



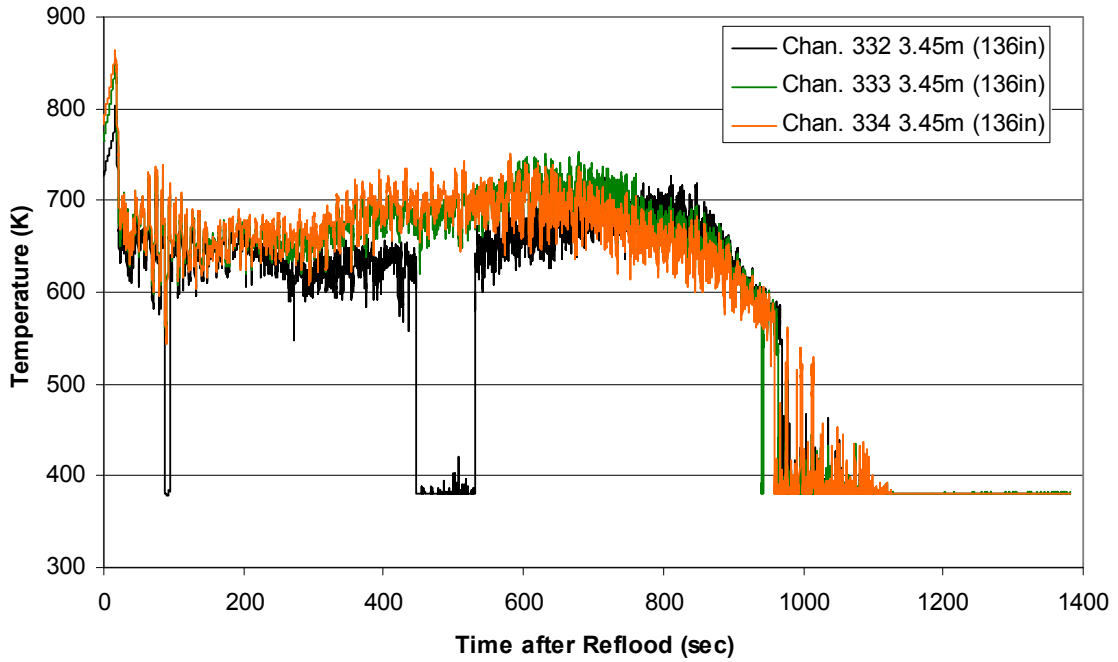
Steam Probe Temperature during Reflood
RBHT Exp. 1108



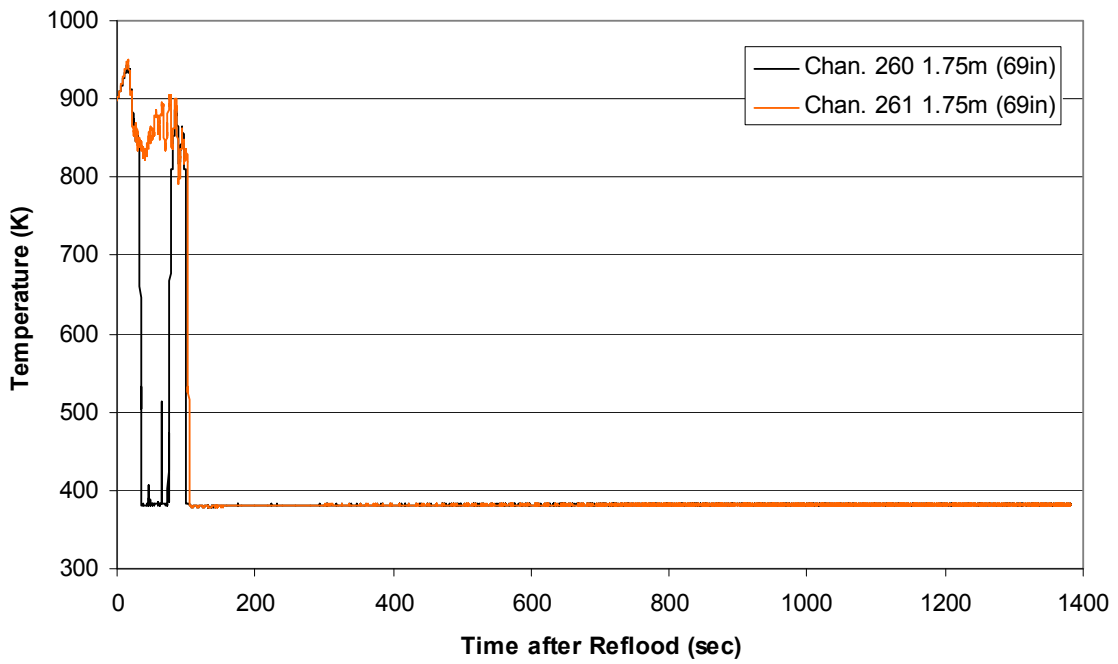
Steam Probe Temperature during Reflood
RBHT Exp. 1108



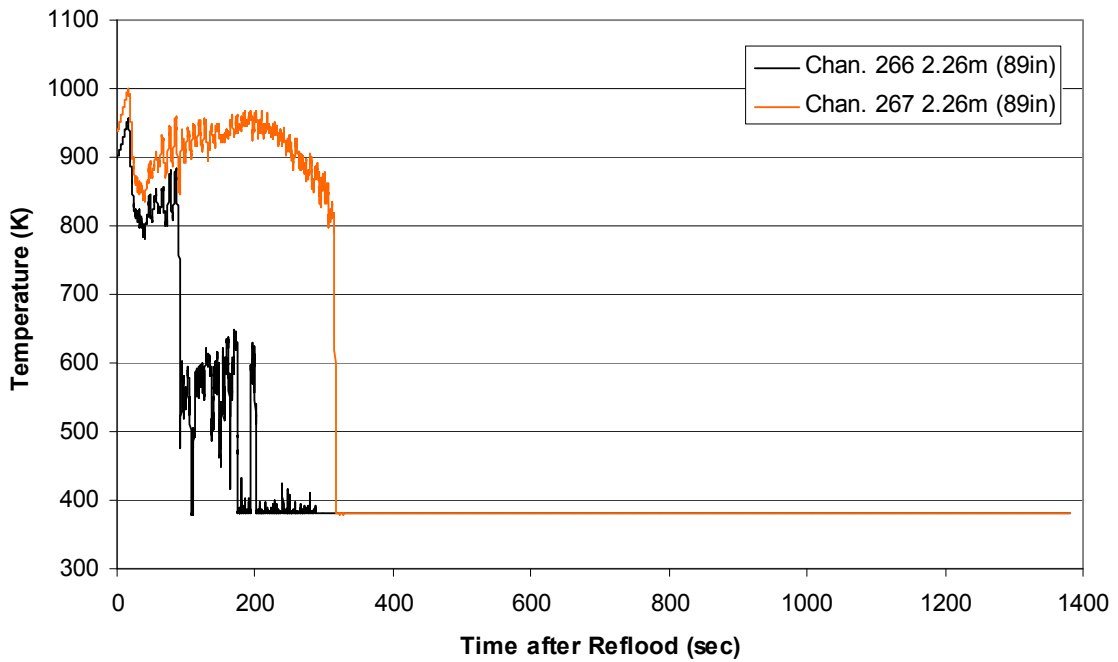
Steam Probe Temperature during Reflood
RBHT Exp. 1108



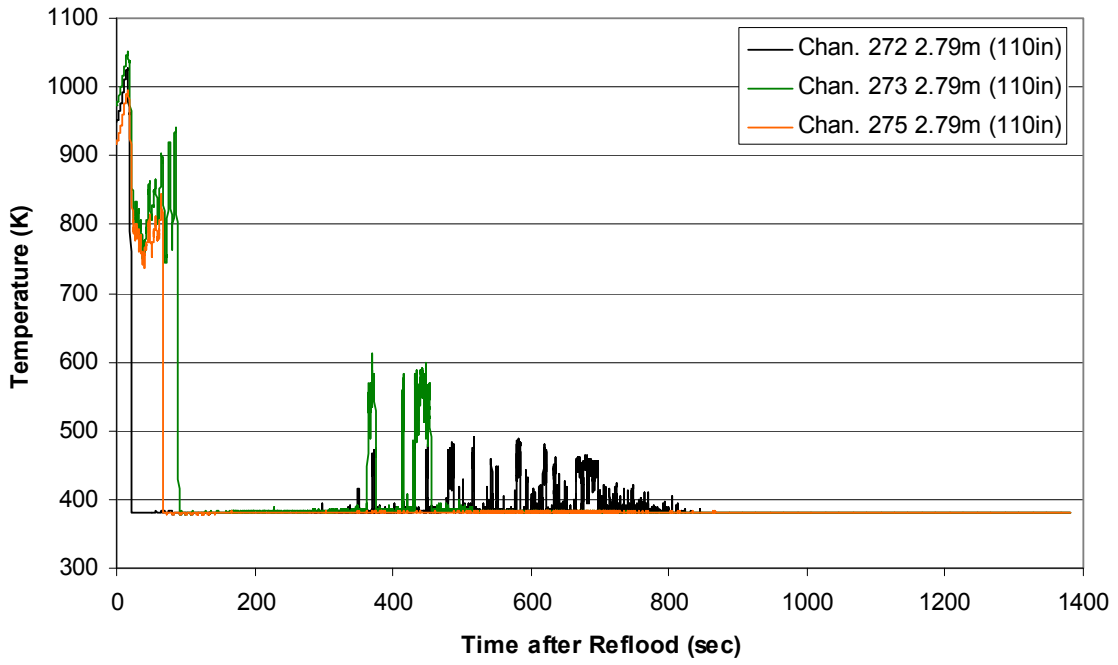
Spacer Grid Temperature during Reflood
RBHT Exp. 1108



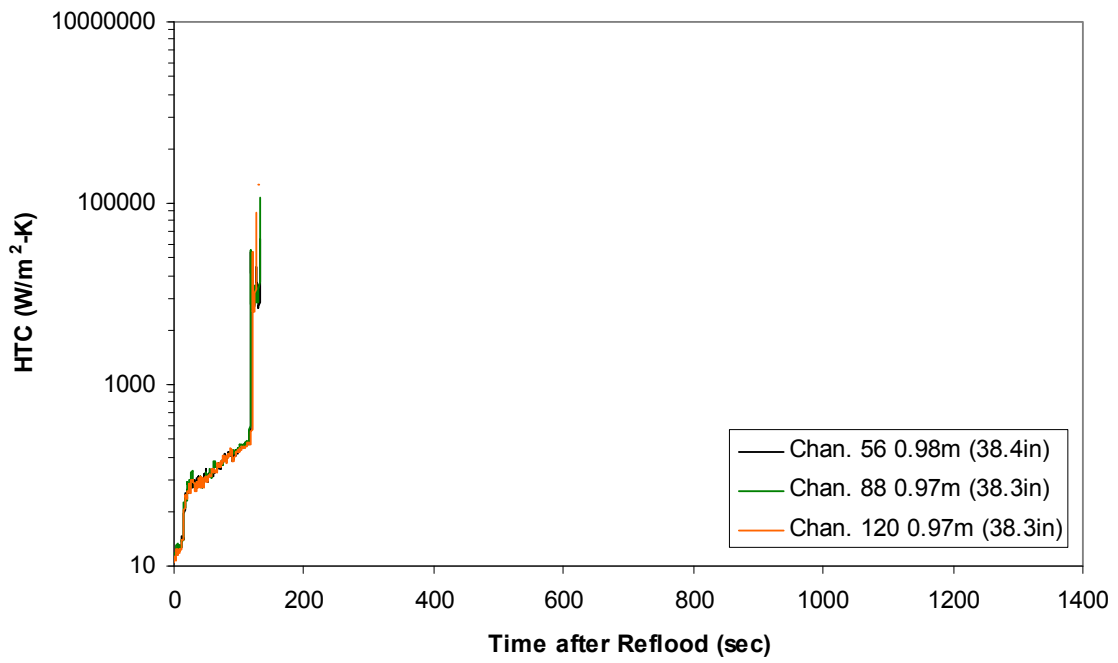
Spacer Grid Temperature during Reflood
RBHT Exp. 1108



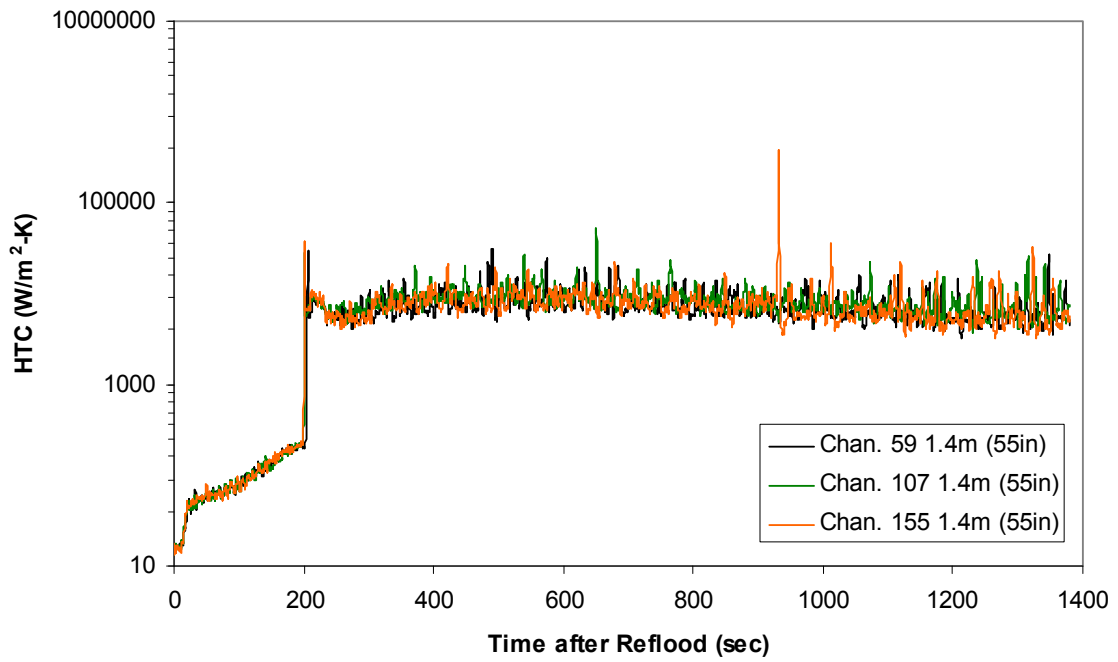
Spacer Grid Temperature during Reflood RBHT Exp. 1108



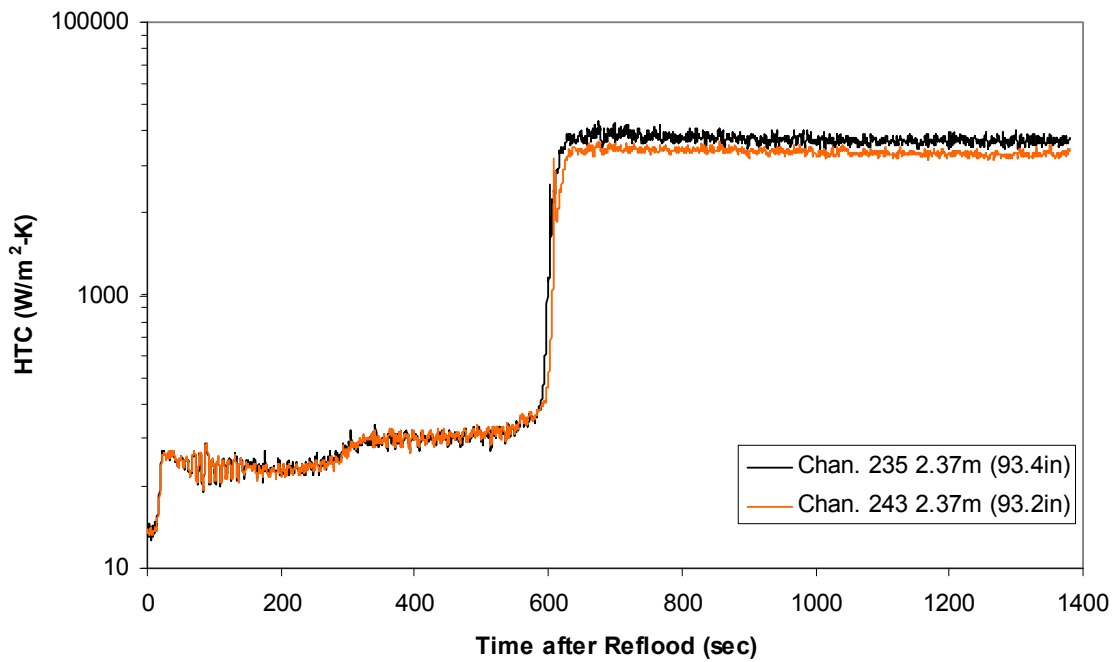
Heat Transfer Coefficient during Reflood RBHT Exp. 1108



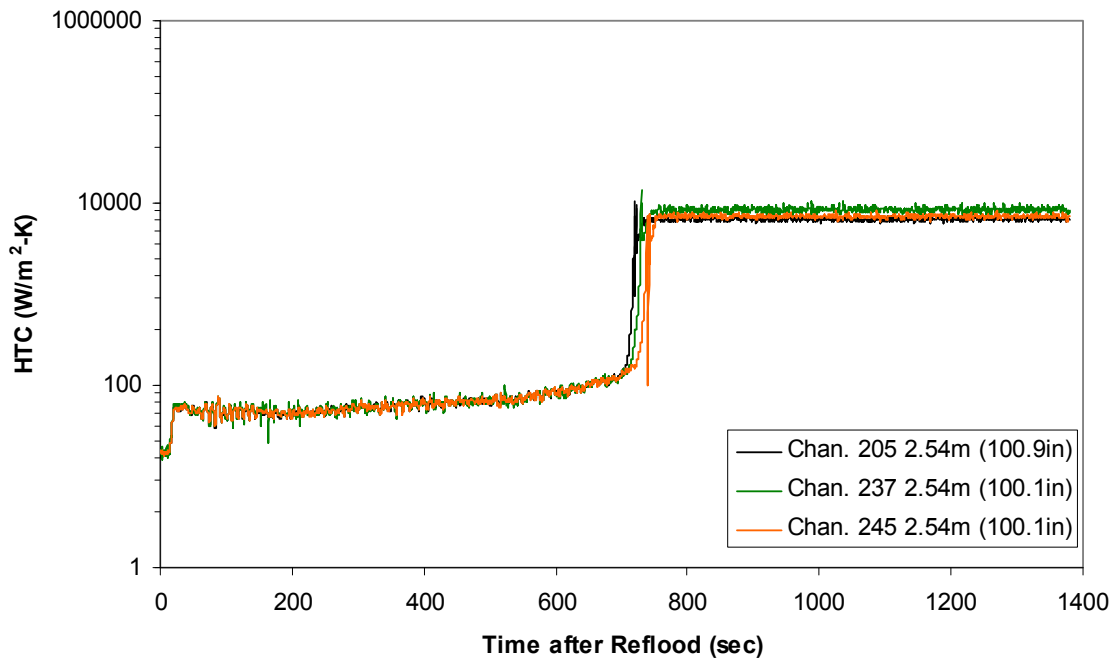
Heat Transfer Coefficient during Reflood RBHT Exp. 1108



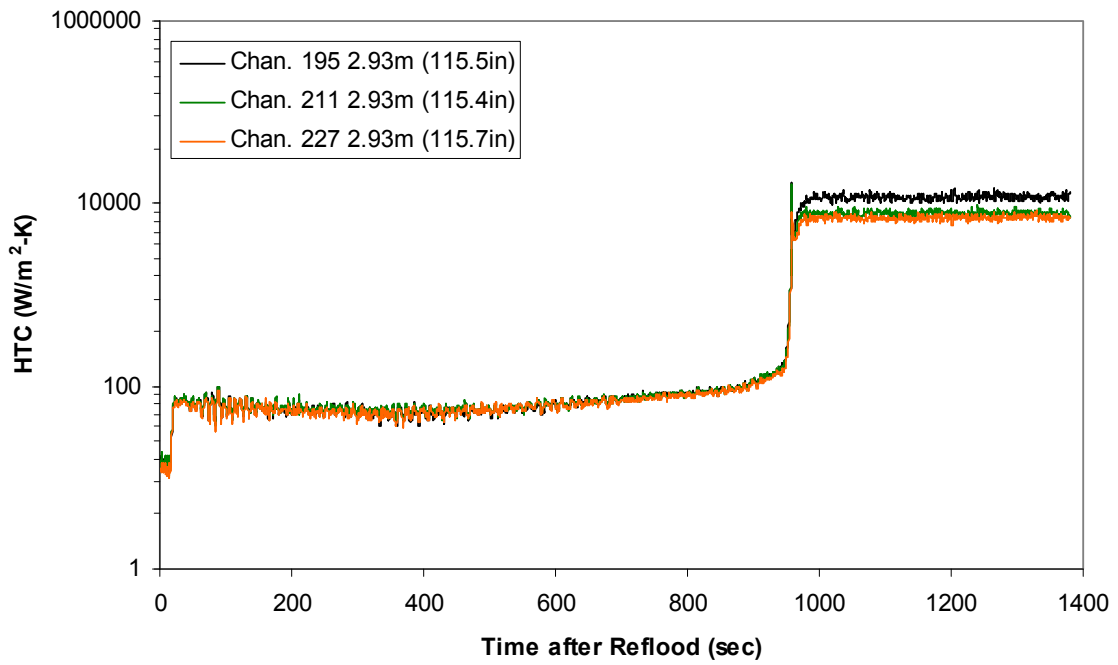
Heat Transfer Coefficient during Reflood RBHT Exp. 1108



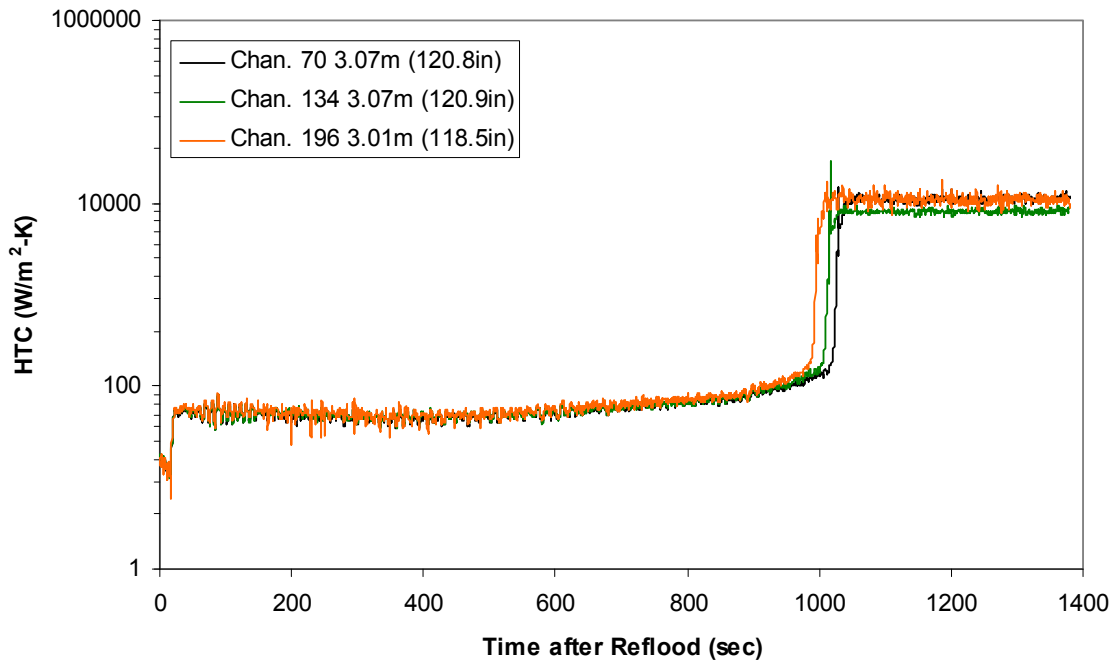
Heat Transfer Coefficient during Reflood RBHT Exp. 1108



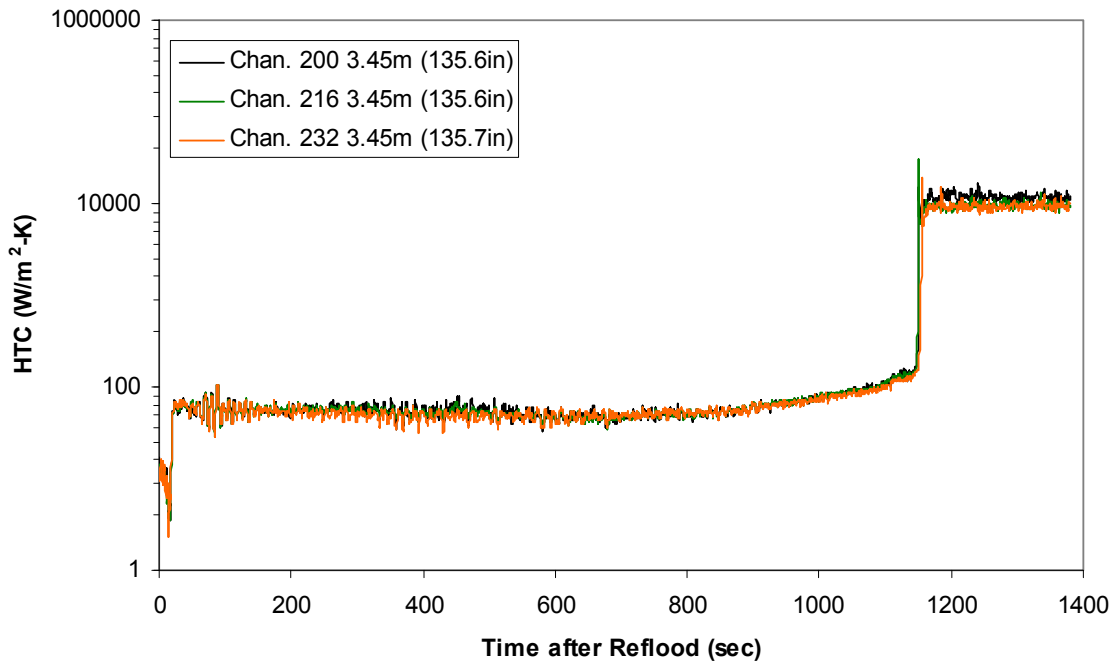
Heat Transfer Coefficient during Reflood RBHT Exp. 1108



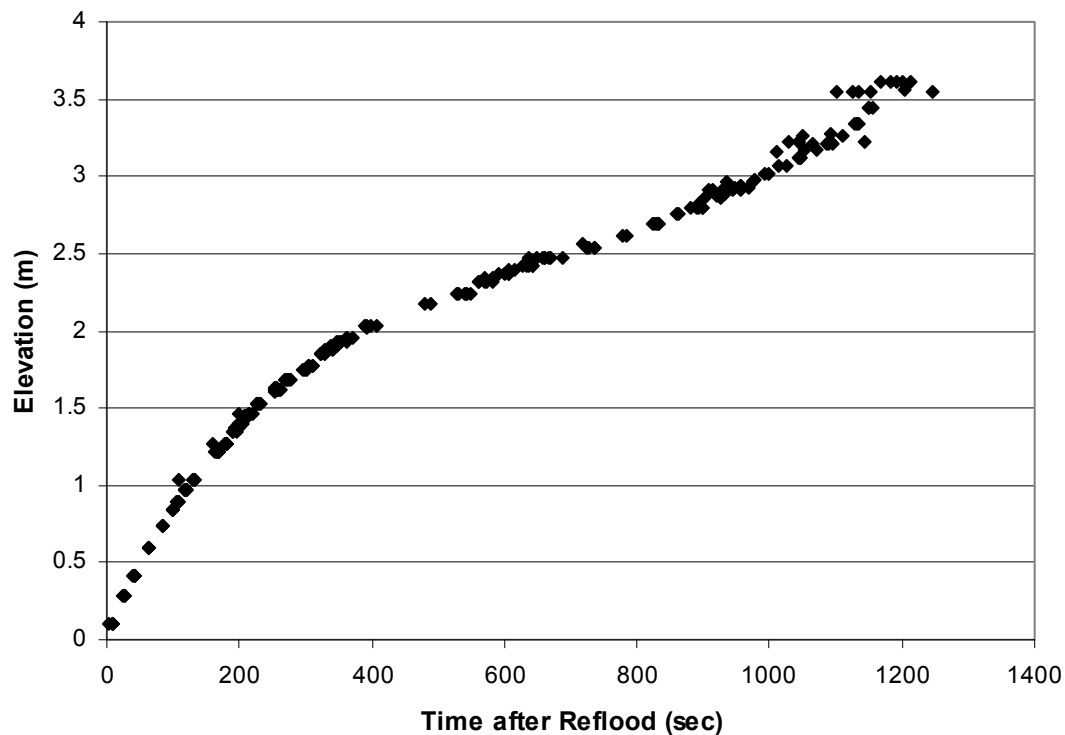
Heat Transfer Coefficient during Reflood RBHT Exp. 1108



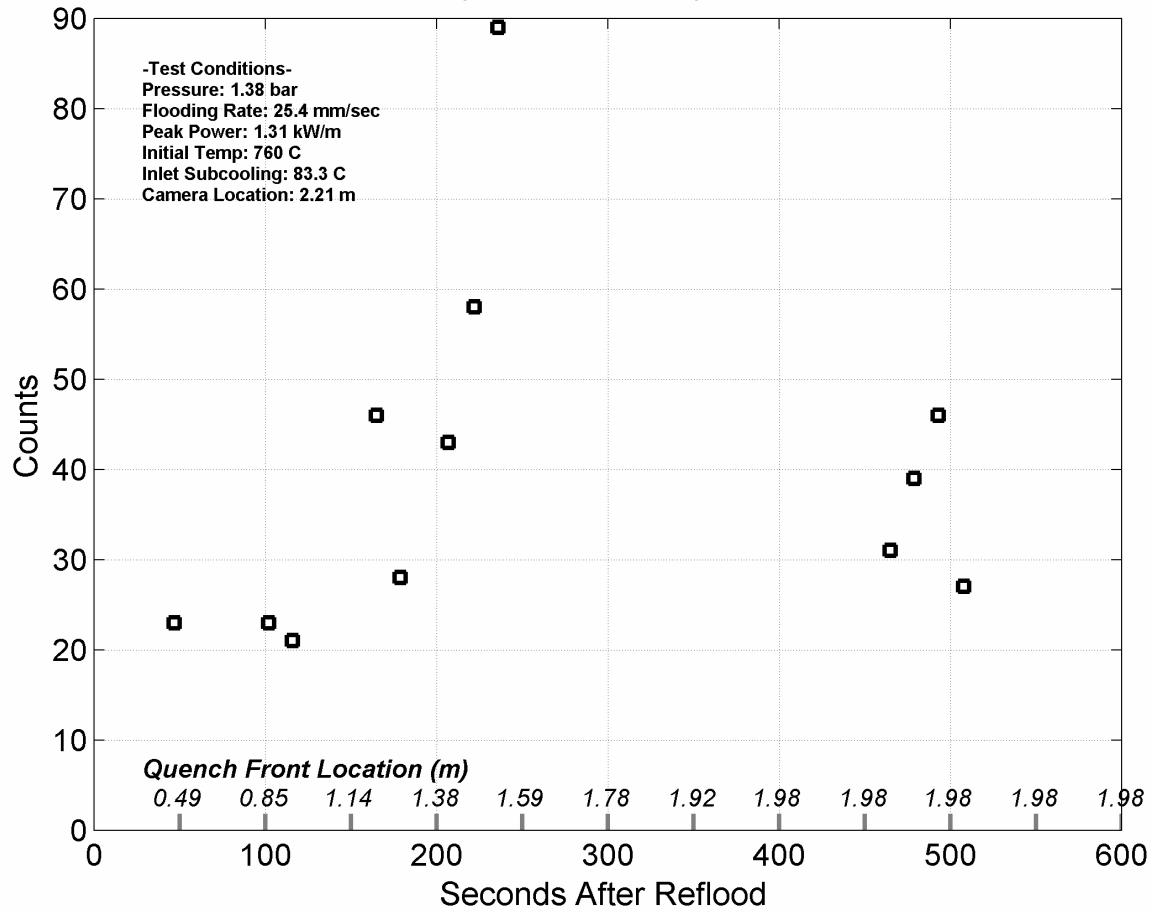
Heat Transfer Coefficient during Reflood RBHT Exp. 1108



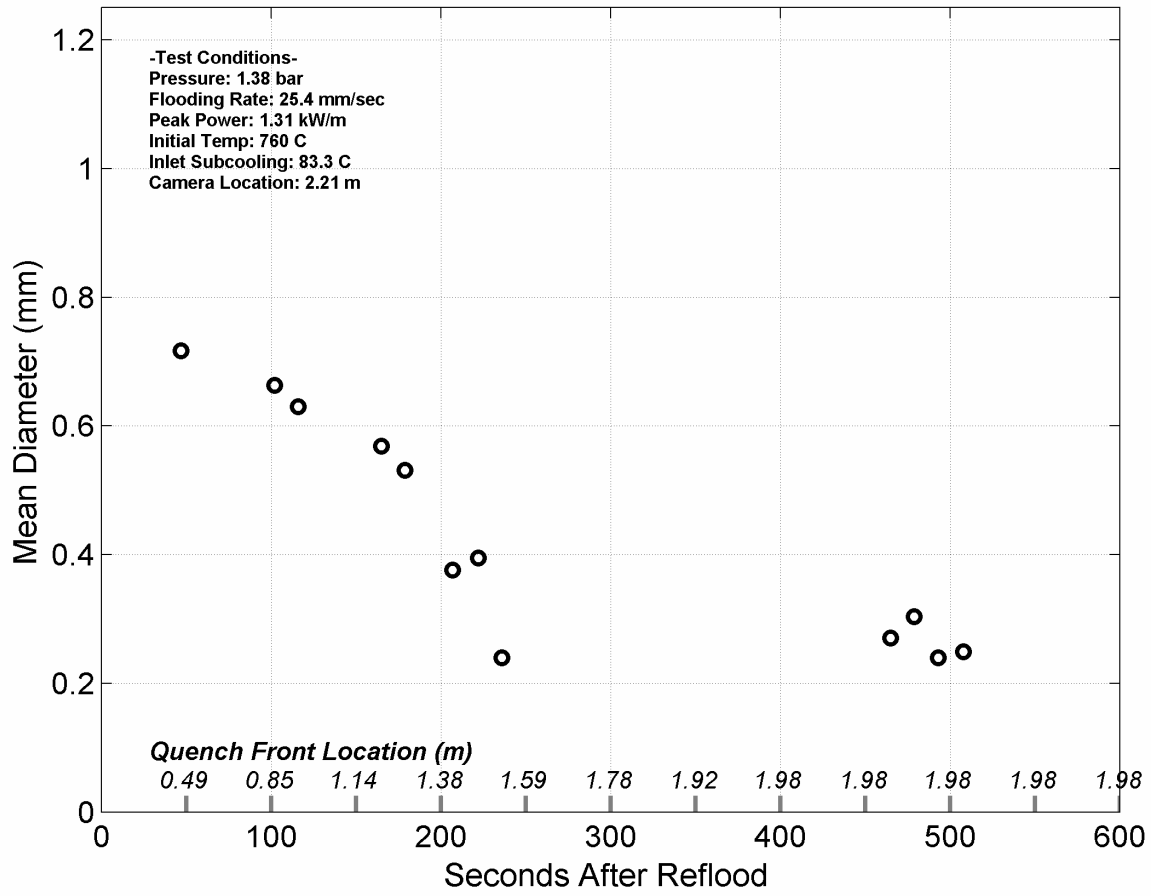
Quench Data, RBHT Exp. 1108



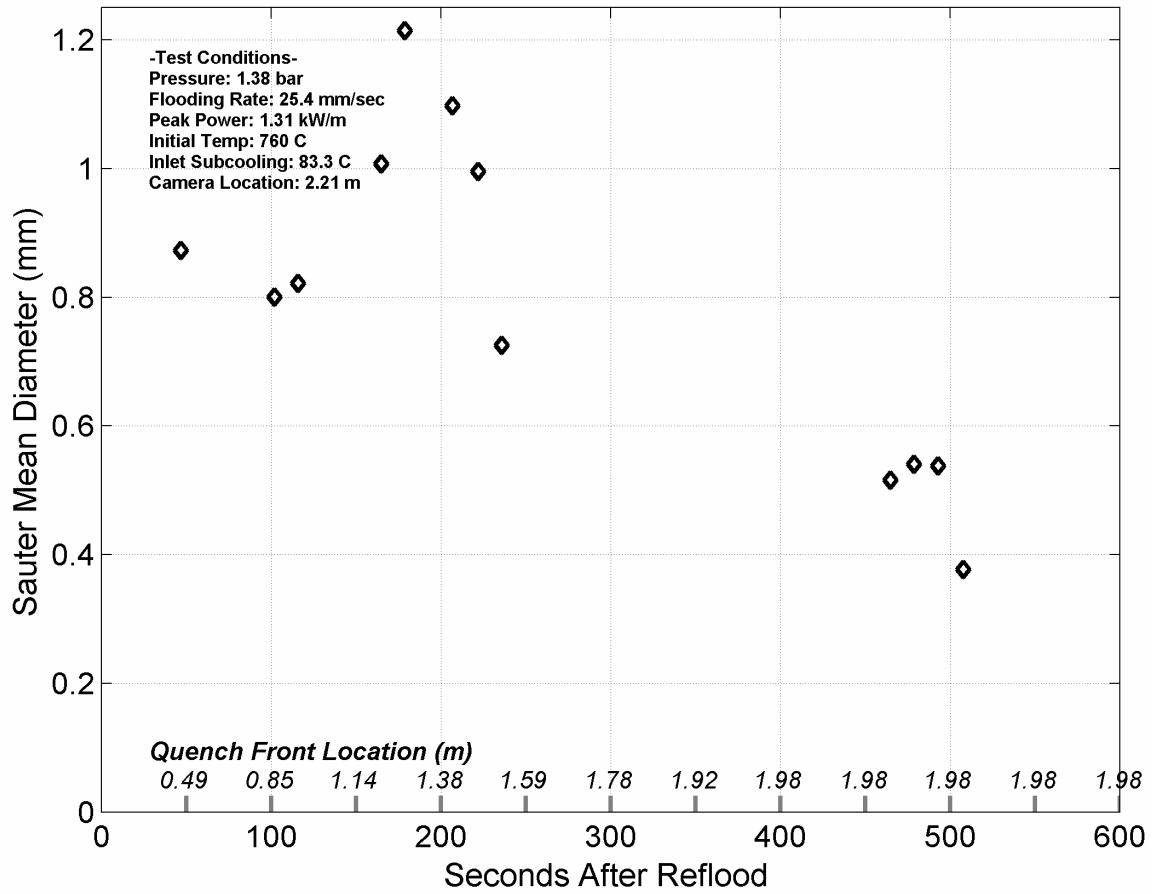
Droplet Counts - Exp. 1108



Mean Droplet Diameter - Exp. 1108



Droplet Sauter Mean Diameter - Exp. 1108



RBHT - REFLOOD TESTS

SUMMARY SHEET

RUN NO: **1143**

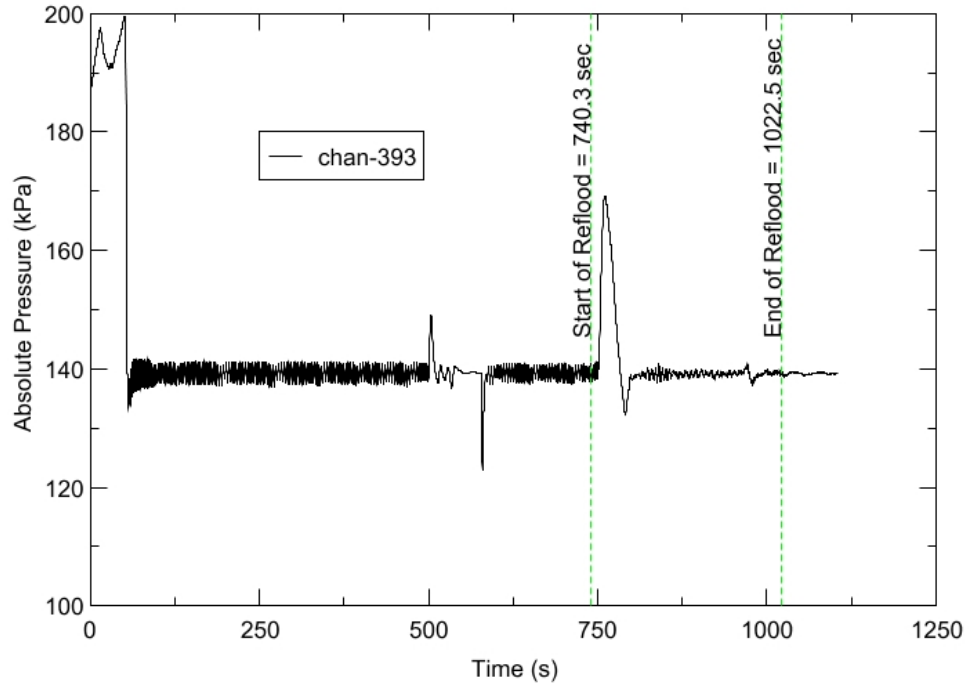
RUN CONDITIONS

Upper Plenum Pressure:	138 kPa (20 psia)
Initial Peak Clad Temperature:	1144 degrees K (1600 degrees F)
Rod Peak Power:	2.3 kW/m (0.7 kW/ft)
Flooding Rate:	0.1524 m/s (6 in/s)
Inlet Subcooling:	83 degrees K (150 degrees F)
Start of Reflood:	740.3 s
End of Reflood:	1022.5 s
Test Date:	6/12/2002
Comments:	Heater rod surfaces below 2.4 m (94 in) quench to a temperature below saturation due to the high inlet subcooling. Therefore DATARH calculated heat transfer coefficients are not presented below this elevation after rod quench.

Rod_Elevation	Channel Number	Temperature at Reflood (K)	Temperature at Reflood (°F)	Turnaround Time (sec.)	Turnaround Temperature (K)	Turnaround Temperature (°F)	Quench Time (sec.)	Quench Temperature (K)	Quench Temperature (°F)
B2_0.592m	52	799.73	979.82	10.95	832.22	1038.31	25.45	712.51	822.83
B2_0.744m	53	820.34	1016.92	12.45	857.19	1083.26	30.95	731.69	857.36
B6_0.846m	150	857.57	1083.95	12.45	896.44	1153.9	34.95	730.24	854.74
B6_0.897m	151	867.31	1101.46	13.45	908.74	1176.04	35.45	753.48	896.57
C6_1.04m	137	918.32	1193.28	13.95	964.95	1277.22	42.45	761.75	911.47
D5_1.27m	217	984.05	1311.59	12.95	1028.55	1391.71	52.95	729.5	853.41
C6_1.34m	138	971.69	1289.35	13.95	1024.8	1384.95	56.45	709.92	818.17
D5_1.37m	218	1004.43	1348.29	13.95	1057.46	1443.74	58.45	762.57	912.94
C6_1.39m	139	975.97	1297.06	13.95	1030.64	1395.47	59.95	744.58	880.56
D5_1.45m	219	1015.62	1368.43	13.95	1070.59	1467.37	62.45	753.64	896.86
C6_1.47m	140	989.19	1320.85	14.45	1044.76	1420.88	63.95	740.6	873.39
D5_1.52m	220	1026.91	1388.75	14.45	1083.9	1491.34	67.45	752.16	894.19
C6_1.62m	141	1010.26	1358.79	14.95	1070.36	1466.97	72.45	761.29	910.63
D5_1.68m	221	1046.07	1423.24	14.45	1106.74	1532.45	75.95	773.42	932.46
D5_1.78m	222	1031.35	1396.74	12.95	1085.48	1494.17	82.45	697.27	795.4
D5_1.85m	223	1064.15	1455.78	12.95	1123.29	1562.24	86.45	692.35	786.55
C6_1.87m	142	1044.95	1421.23	13.45	1106.65	1532.28	86.95	734.69	862.76
D5_1.90m	224	1068.32	1463.28	13.45	1130.4	1575.03	87.95	696.34	793.73
C6_1.95m	144	1047.84	1426.43	13.45	1111.1	1540.29	92.45	694.79	790.94
C3_2.17m	178	1079.69	1483.76	13.95	1148.87	1608.28	111.95	701.87	803.69
D4_2.24m	241	1087.85	1498.44	13.95	1157.35	1623.55	116.95	690.72	783.6
D4_2.32m	242	1107.94	1534.61	12.45	1170.43	1647.09	121.45	664.57	736.53
C3_2.35m	180	1103.05	1525.8	12.95	1169.43	1645.28	123.95	671.55	749.1
D4_2.37m	243	1114.69	1546.75	12.45	1181.75	1667.46	125.45	673.81	753.16
C3_2.40m	181	1104.03	1527.57	12.95	1172.51	1650.83	128.45	684.85	773.05
D4_2.54m	245	1146.16	1603.41	12.45	1214.37	1726.17	141.45	692.98	787.68
D6_2.62m	129	1144.39	1600.22	12.45	1213.76	1725.08	149.95	701.59	803.18
D6_2.69m	130	1146.37	1603.78	12.45	1218.42	1733.46	159.95	697.69	796.15
C3_2.76m	183	1145.26	1601.78	12.95	1216.2	1729.48	171.45	674.24	753.95
D4_2.79m	247	1103.13	1525.95	11.95	1172.92	1651.58	175.45	666.03	739.16
D6_2.87m	131	1093.63	1508.85	11.45	1156.26	1621.59	184.45	628.59	671.78
D6_2.92m	132	1063.9	1455.34	12.95	1133.35	1580.34	192.95	619.47	655.36
D6_2.97m	133	1029.37	1393.17	12.95	1094.94	1511.21	201.95	614.83	647
D6_3.07m	134	985.81	1314.78	12.95	1046.9	1424.73	214.95	609.23	636.93
E3_3.12m	197	971.84	1289.62	13.45	1030.67	1395.52	223.45	588.84	600.22
D6_3.17m	135	942.25	1236.35	12.95	999.11	1338.71	229.95	597.58	615.95
D6_3.27m	136	892.36	1146.56	13.45	945.82	1242.79	217.95	606.41	631.85
D4_3.61m	248	650.11	710.51	14.45	700.83	801.81	39.95	498.91	438.34

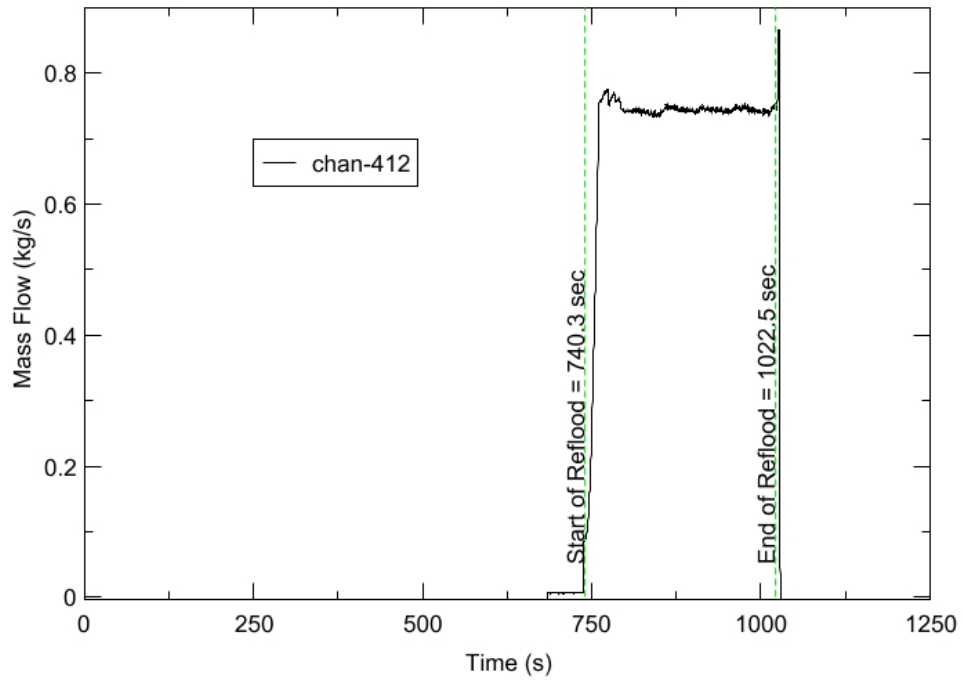
RBHT - TEST FACILITY

Upper Plenum Pressure vs. Time, Exp 1143



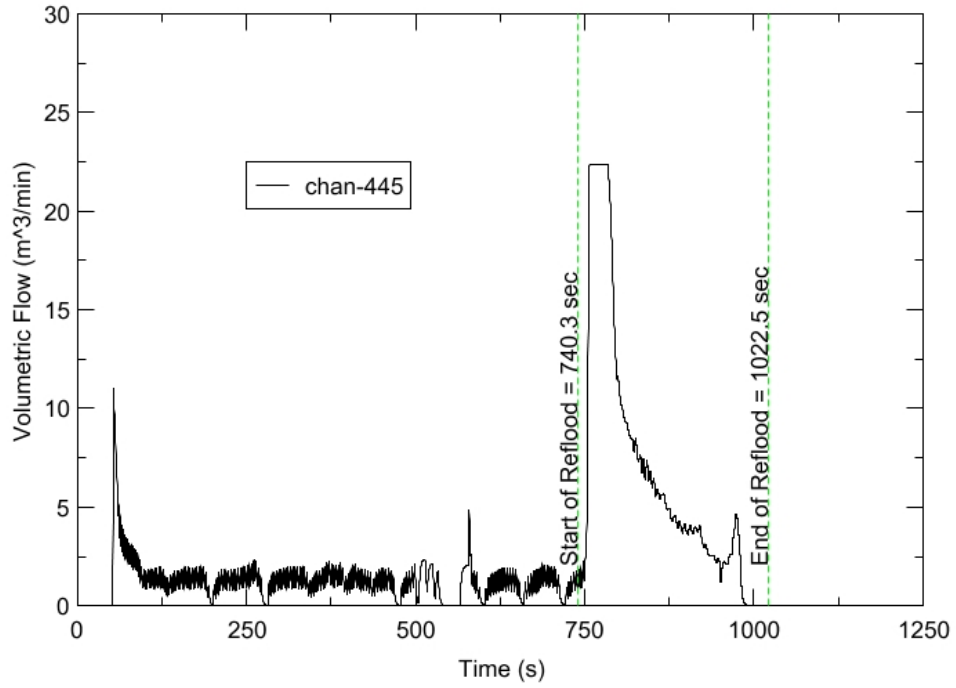
RBHT - TEST FACILITY

Inlet Flow vs. Time, Exp 1143



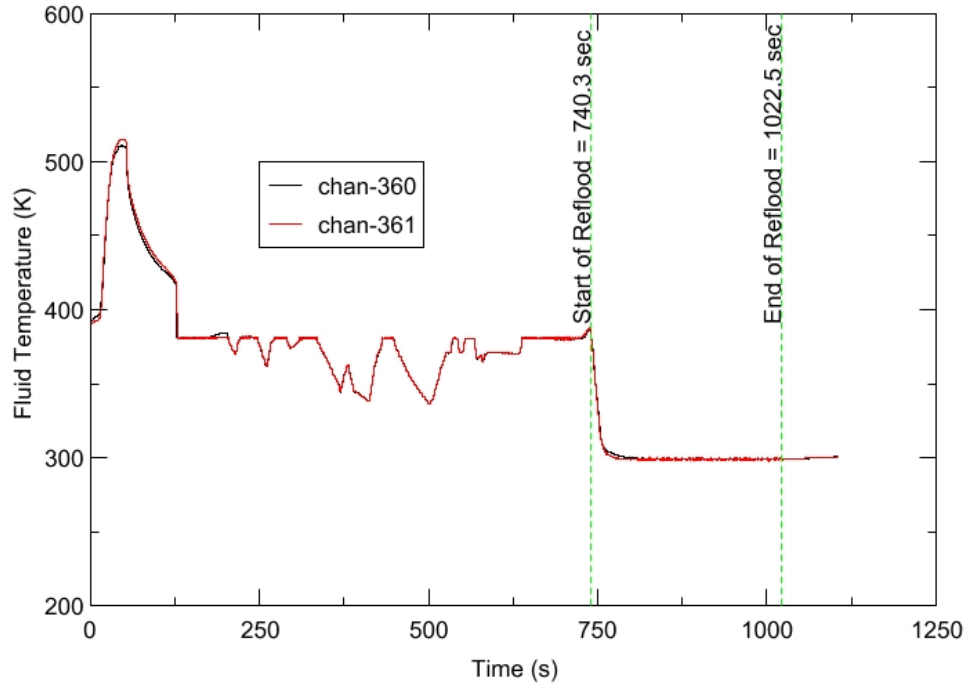
RBHT - TEST FACILITY

Steam Exhaust Flow vs. Time, Exp 1143



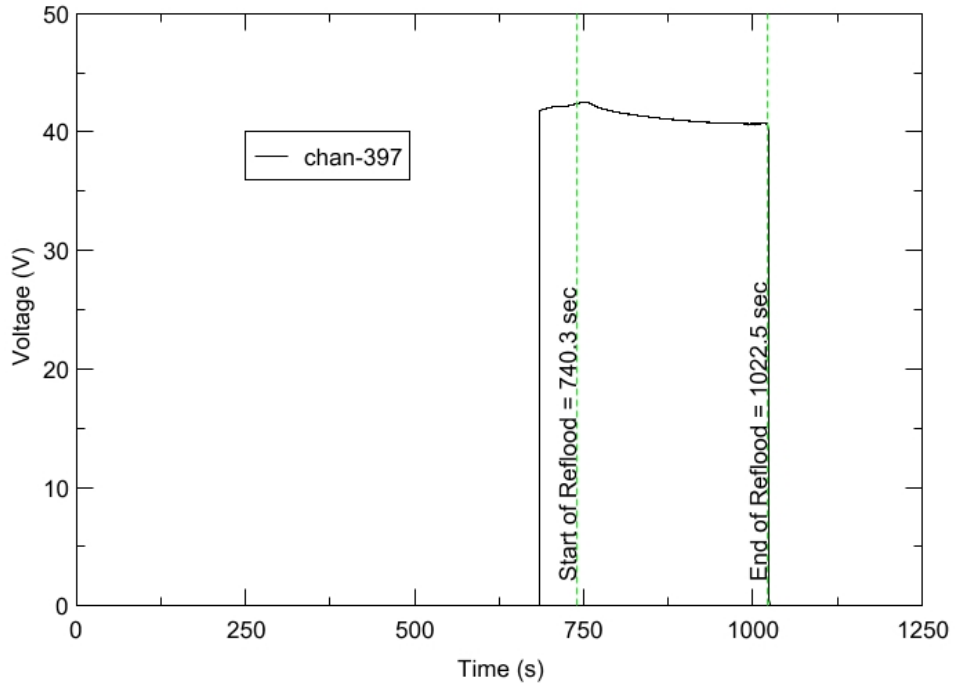
RBHT - TEST FACILITY

Inlet Flow Temperature vs. Time, Exp 1143



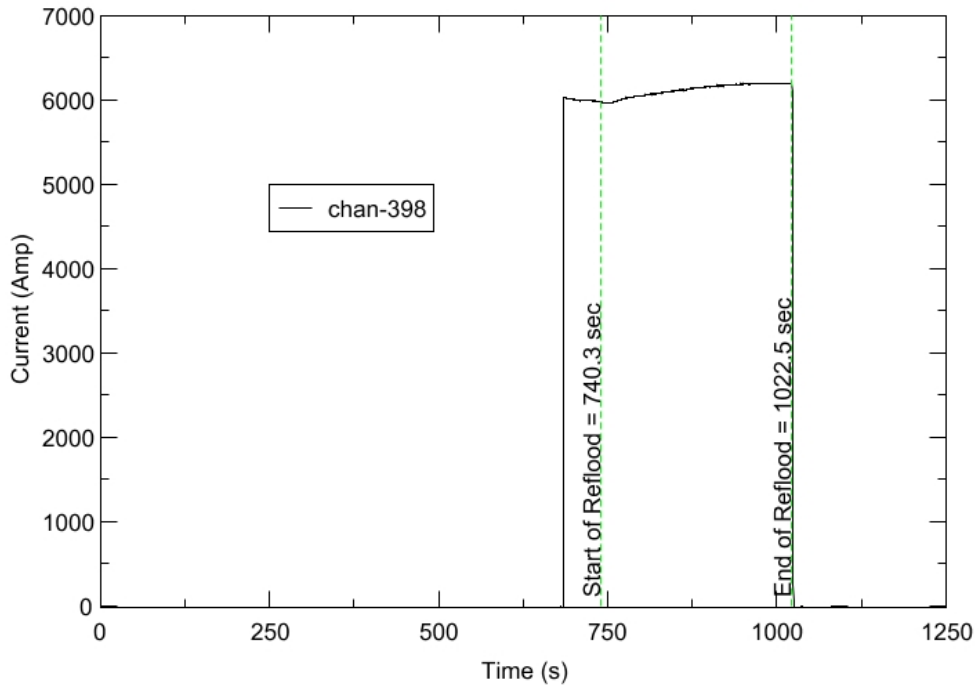
RBHT - TEST FACILITY

Test Section Voltage vs. Time, Exp 1143

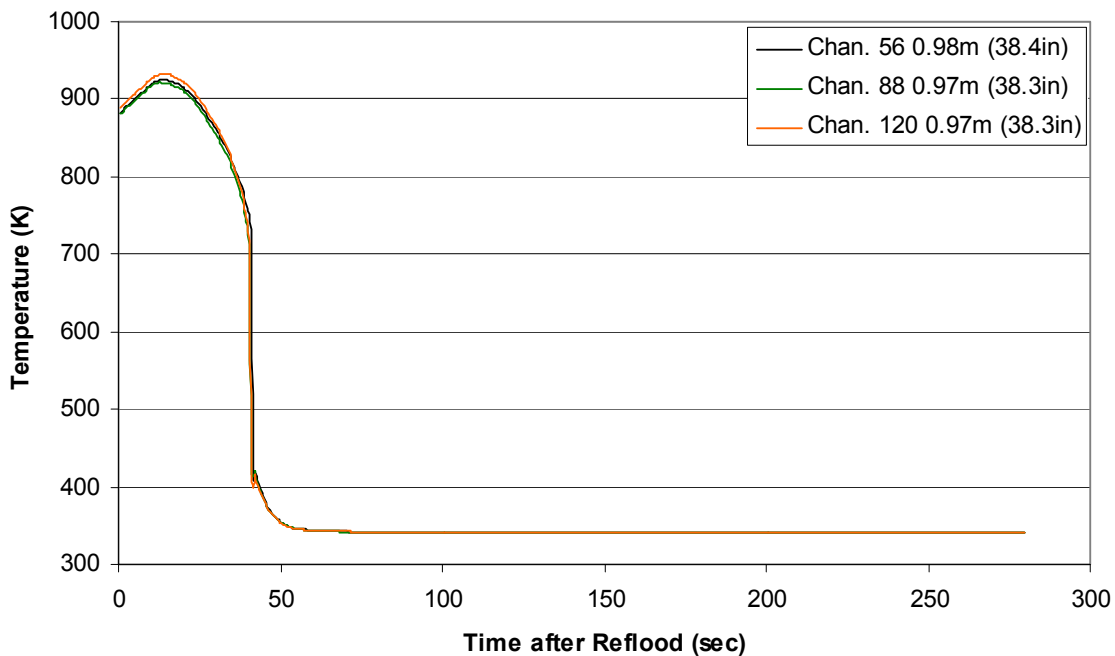


RBHT - TEST FACILITY

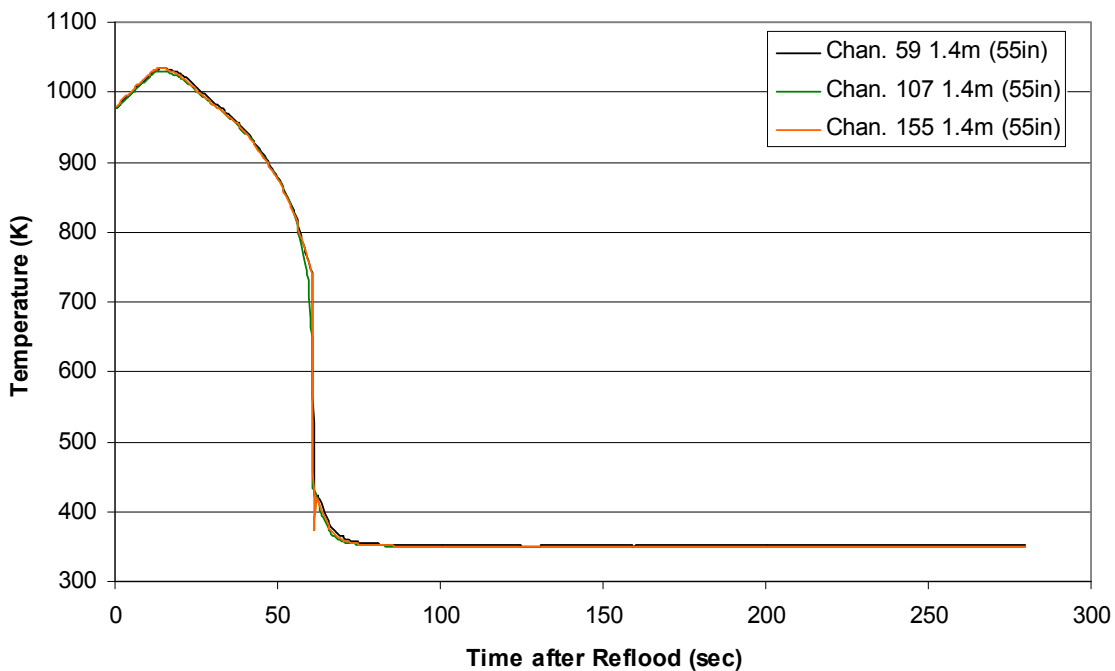
Test Section Current vs. Time, Exp 1143



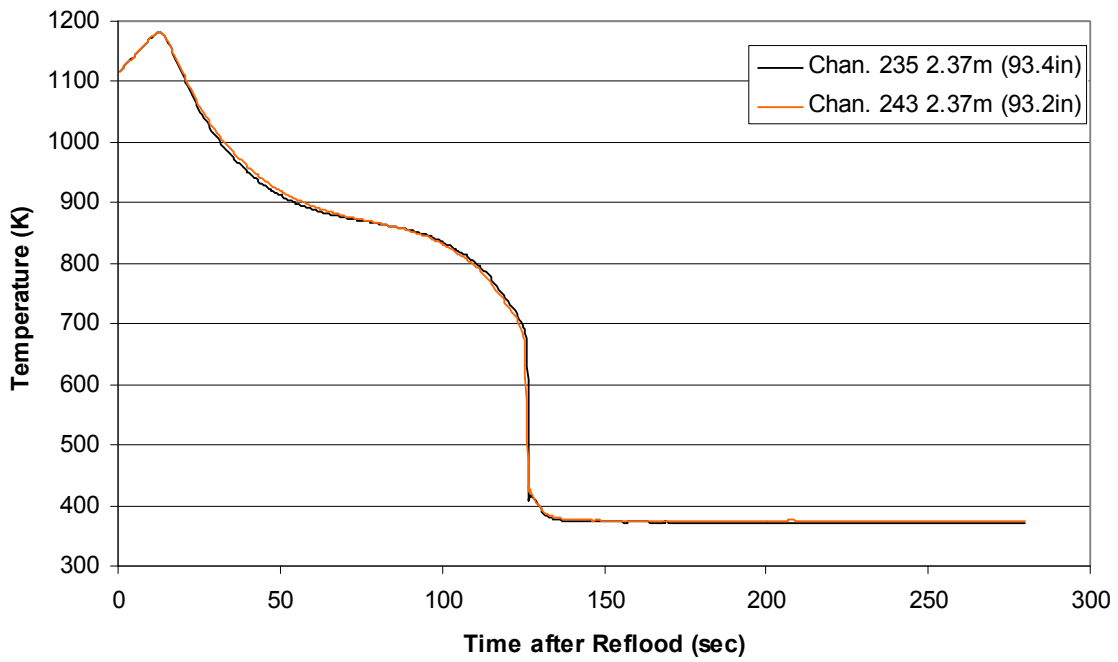
**Heater Rod Temperature during Reflood
RBHT Exp. 1143**



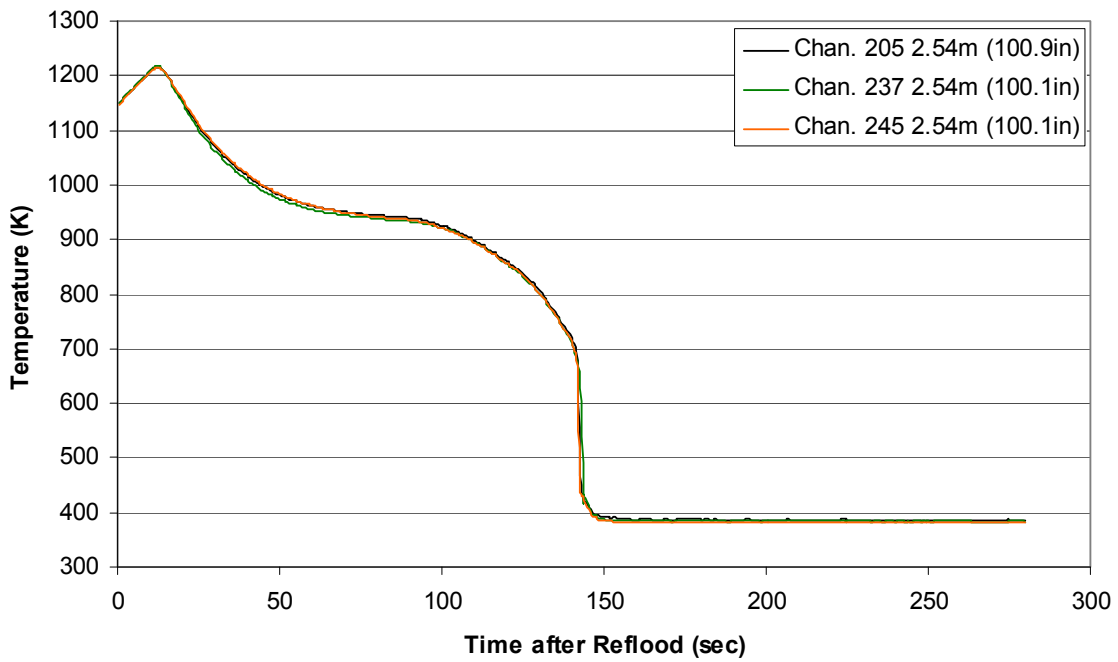
**Heater Rod Temperature during Reflood
RBHT Exp. 1143**



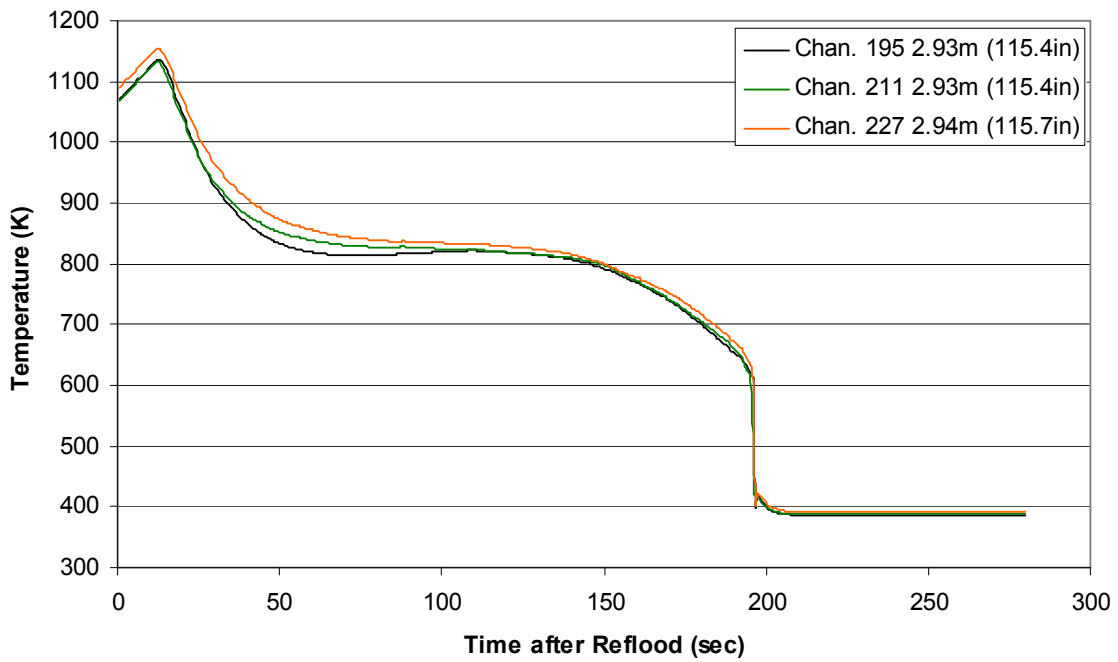
Heater Rod Temperature during Reflood
RBHT Exp. 1143



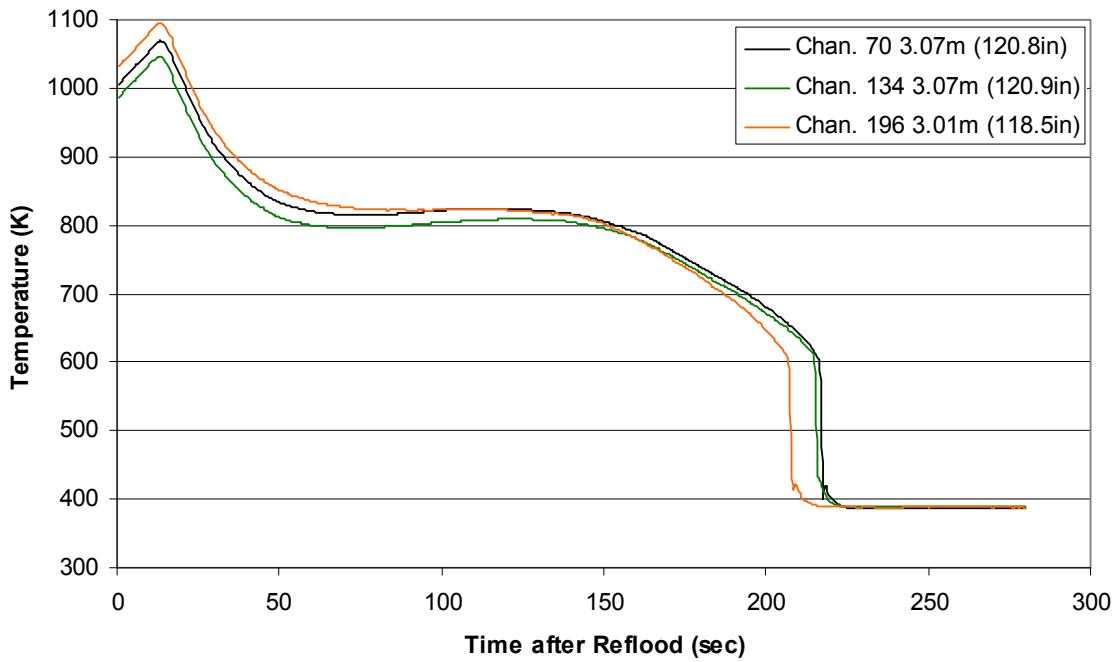
Heater Rod Temperature during Reflood
RBHT Exp. 1143



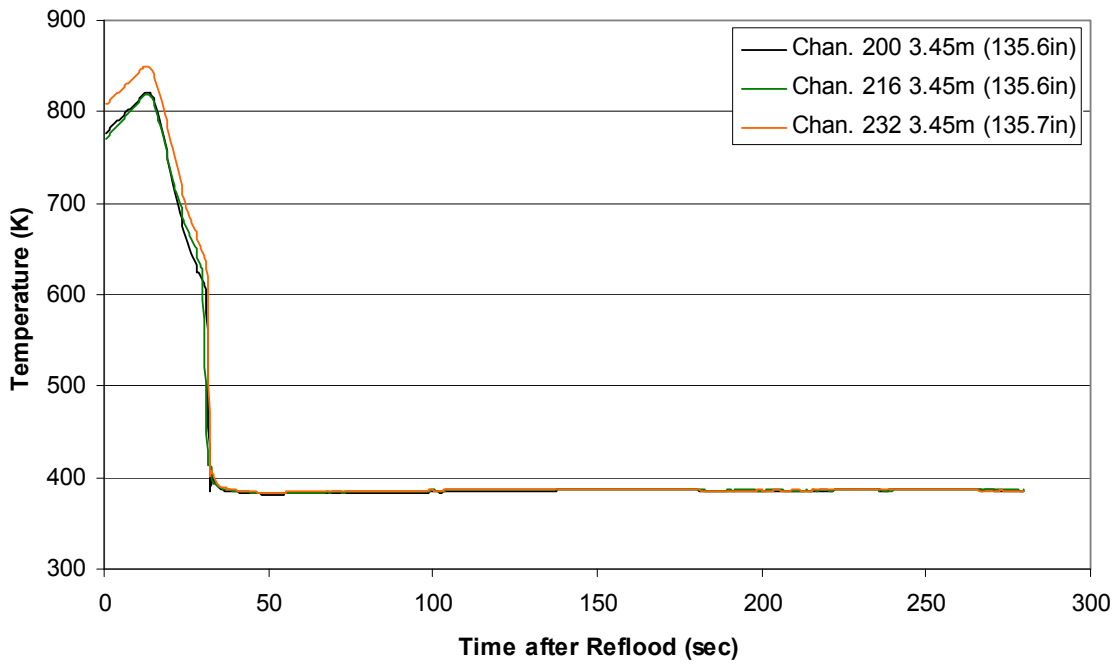
Heater Rod Temperature during Reflood RBHT Exp. 1143



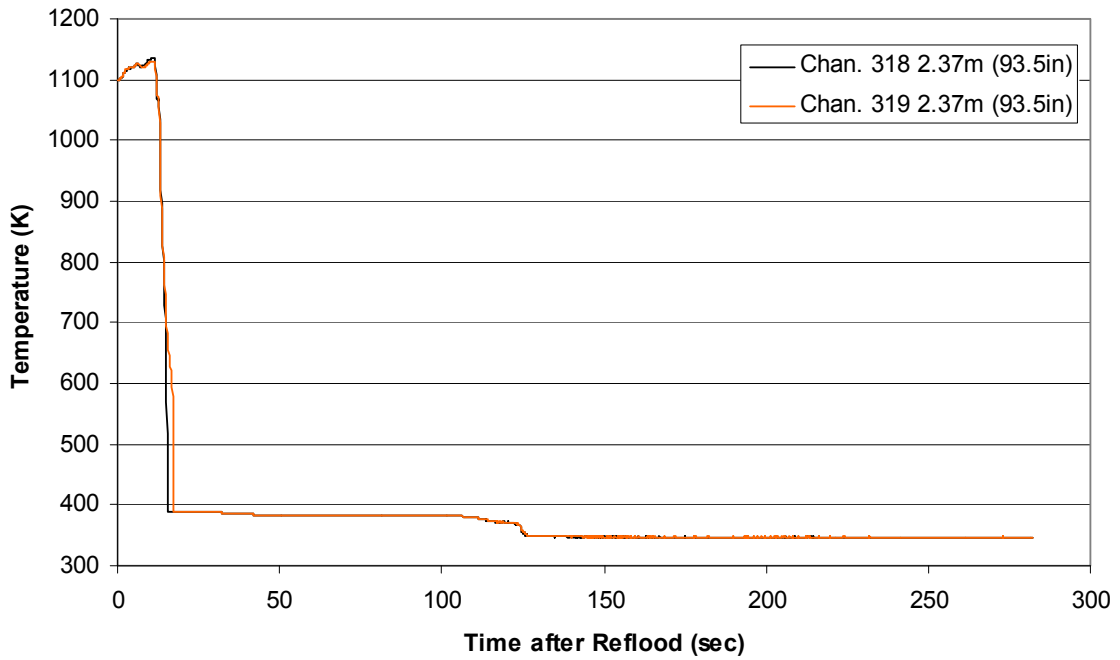
Heater Rod Temperature during Reflood RBHT Exp. 1143



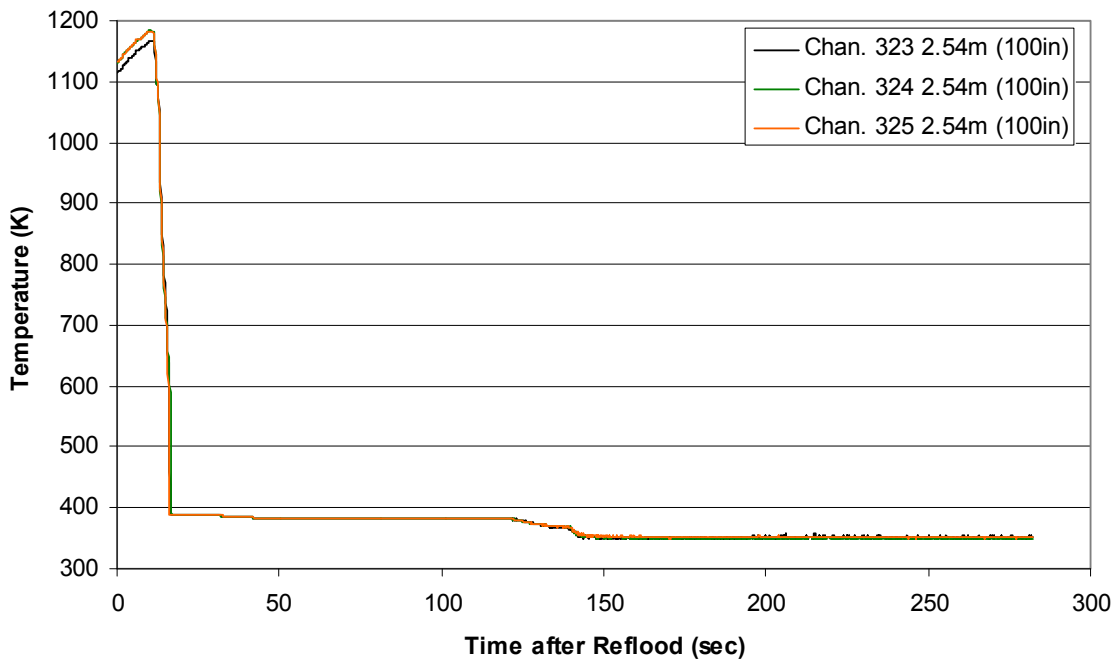
Heater Rod Temperature during Reflood RBHT Exp. 1143



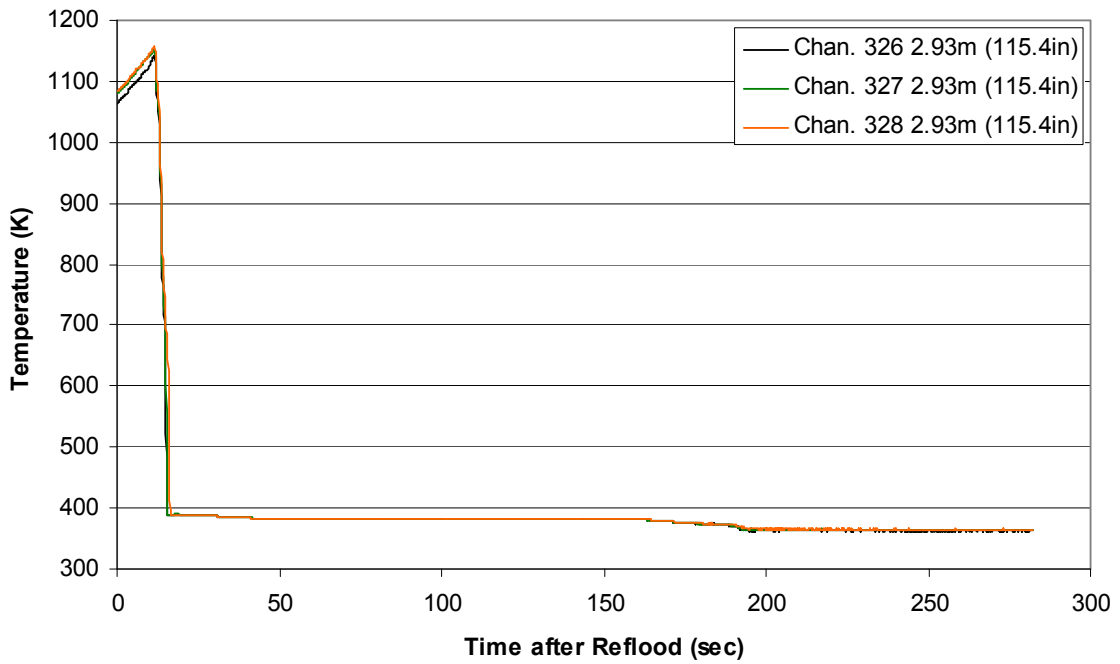
Steam Probe Temperature during Reflood RBHT Exp. 1143



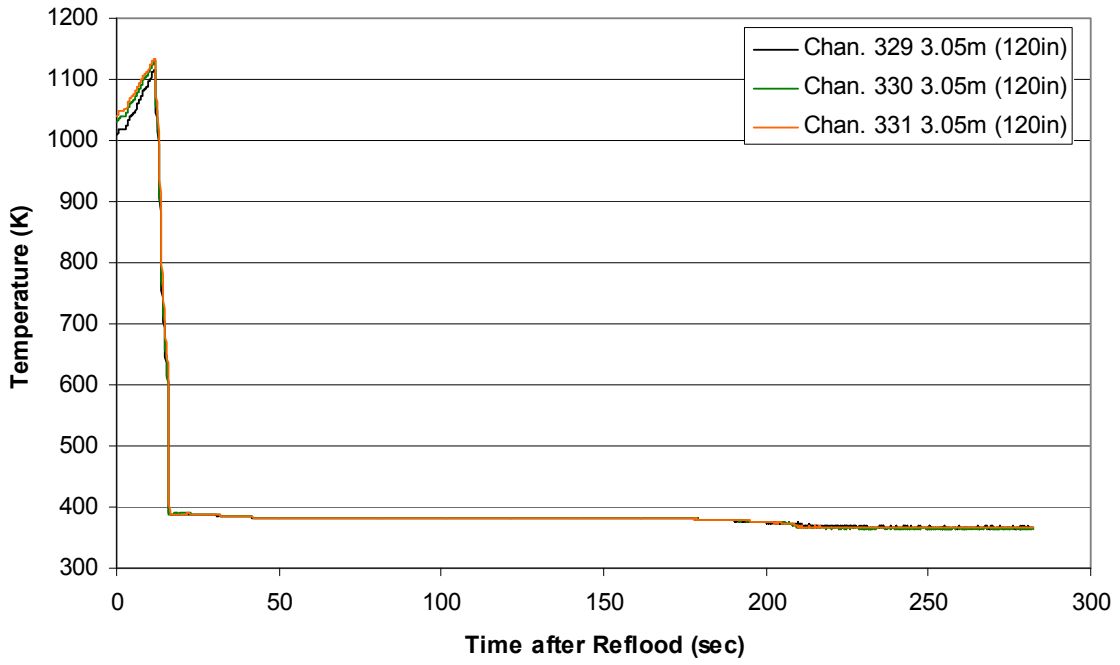
Steam Probe Temperature during Reflood RBHT Exp. 1143



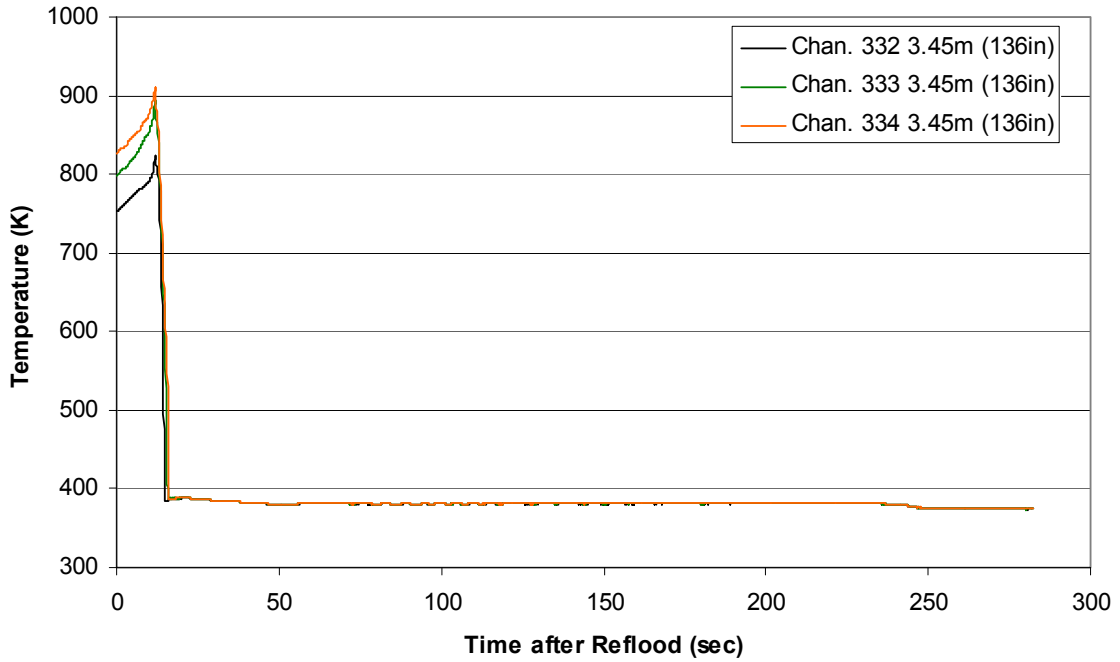
Steam Probe Temperature during Reflood RBHT Exp. 1143



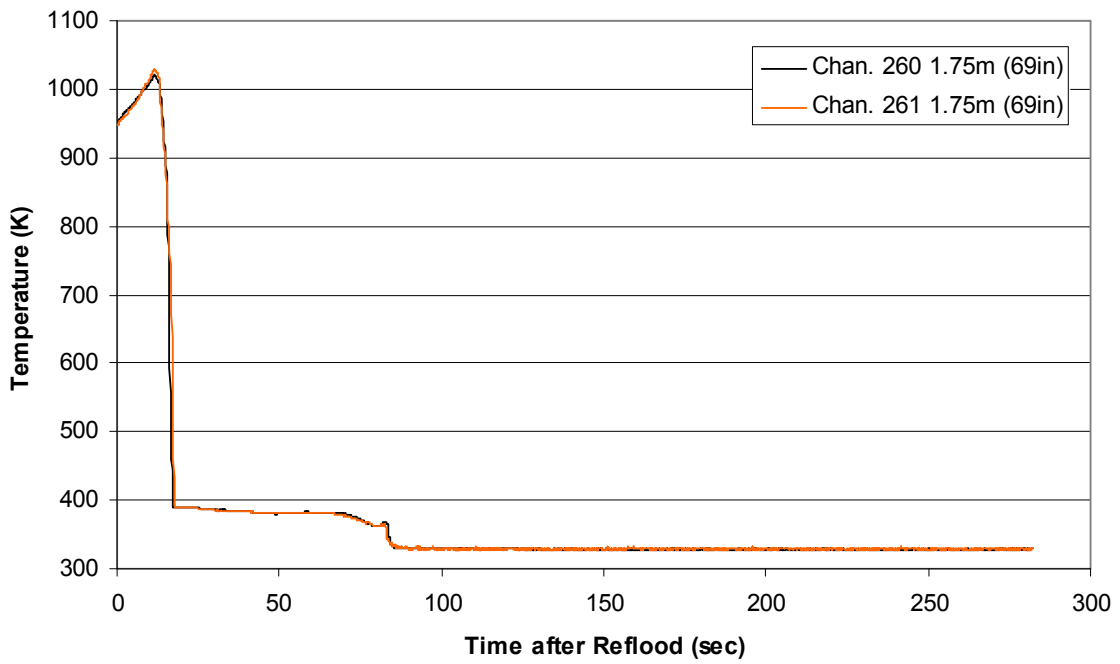
Steam Probe Temperature during Reflood
RBHT Exp. 1143



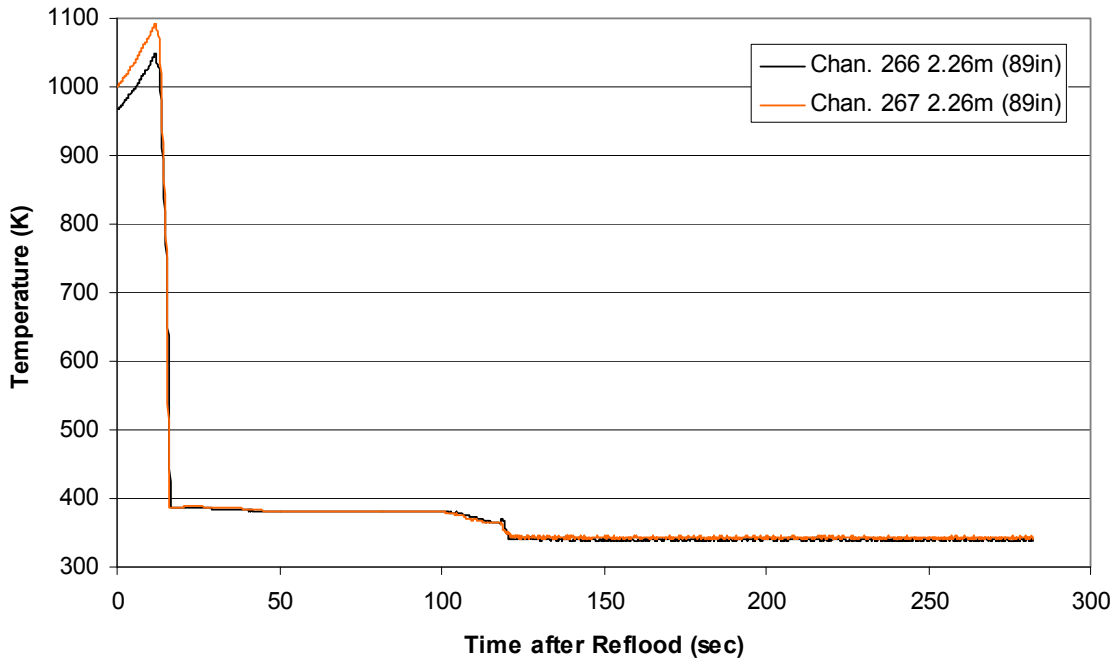
Steam Probe Temperature during Reflood
RBHT Exp. 1143



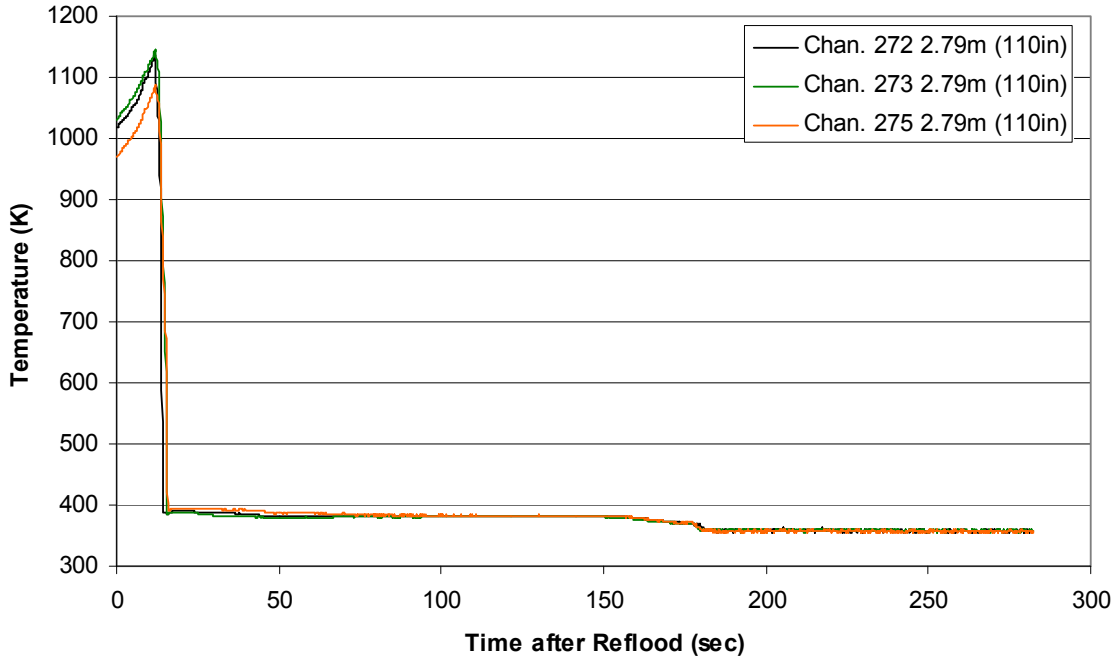
Spacer Grid Temperature during Reflood RBHT Exp. 1143



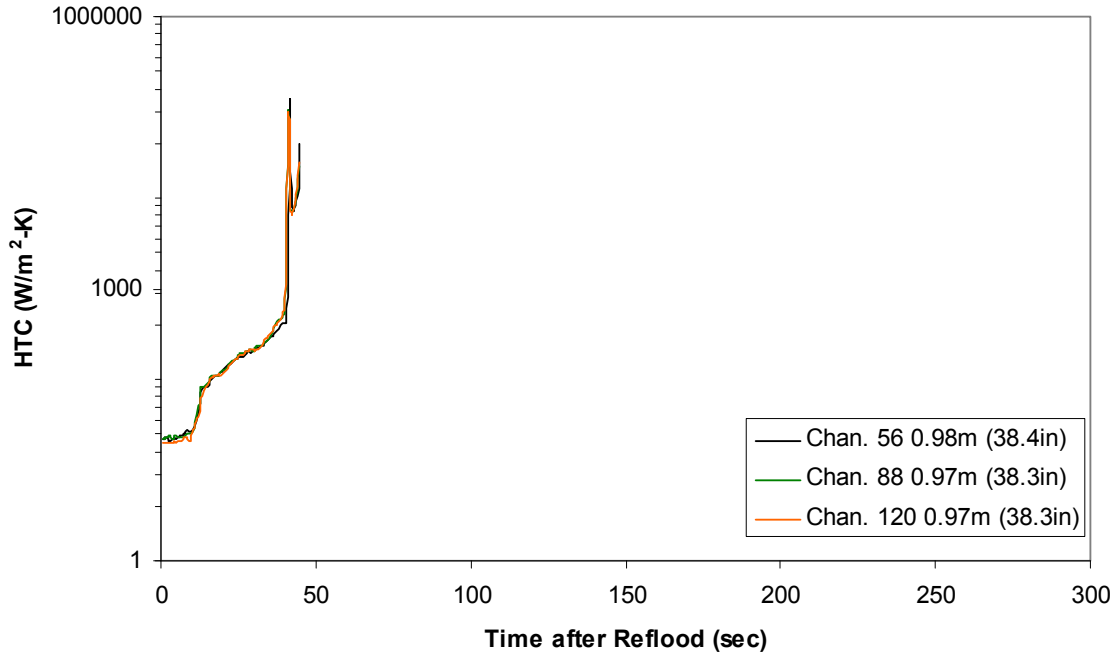
Spacer Grid Temperature during Reflood RBHT Exp. 1143



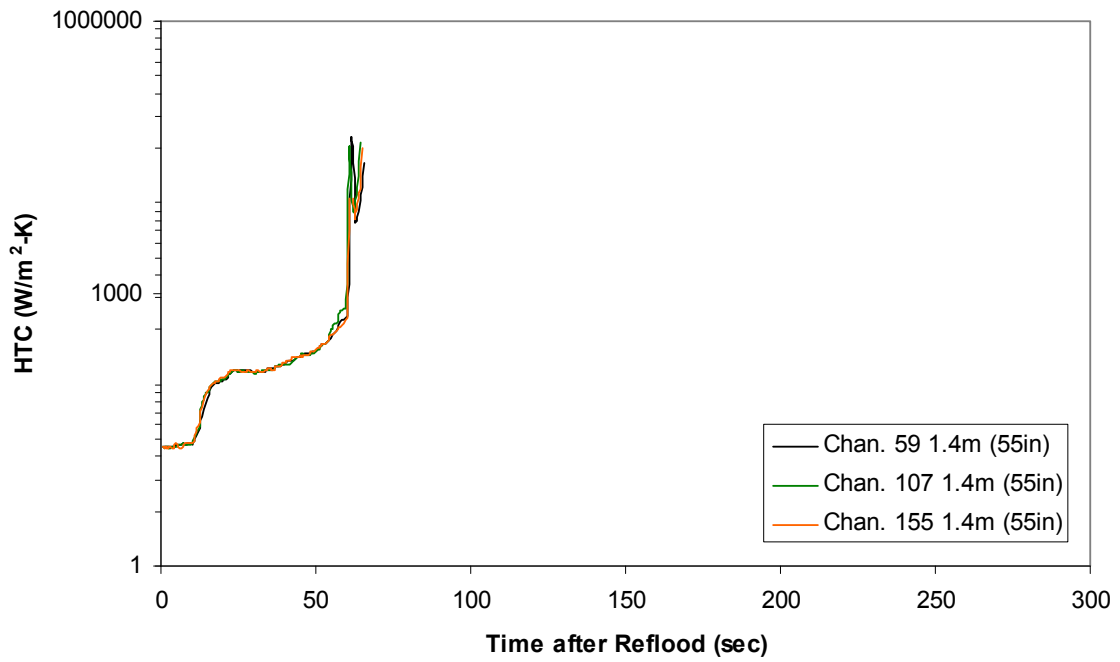
Spacer Grid Temperature during Reflood RBHT Exp. 1143



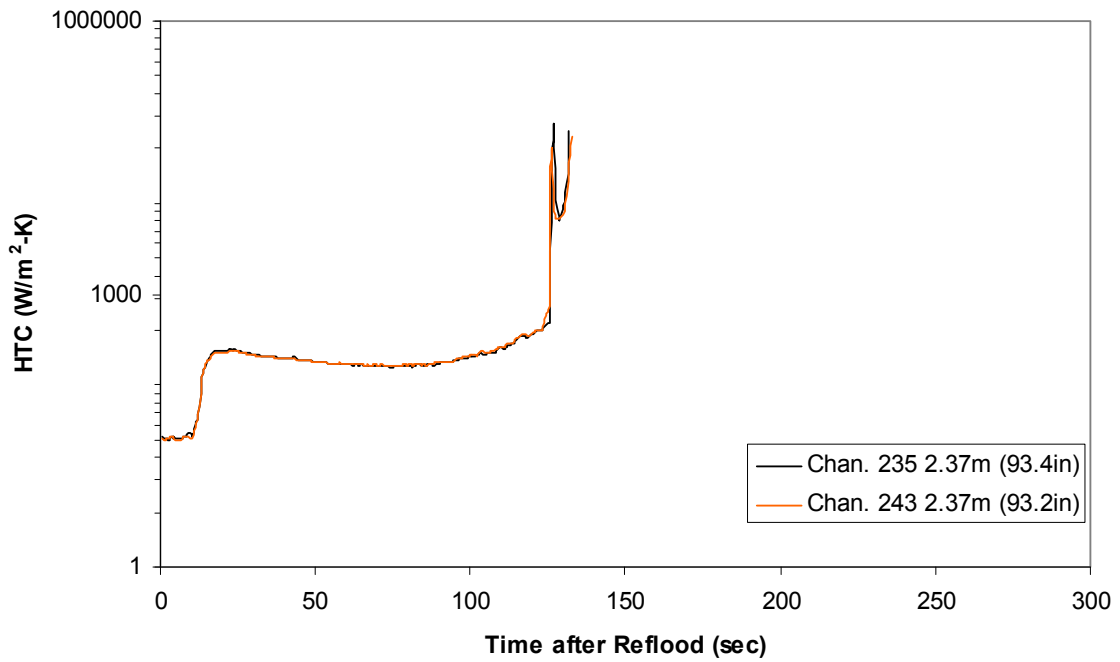
Heat Transfer Coefficient during Reflood RBHT Exp. 1143



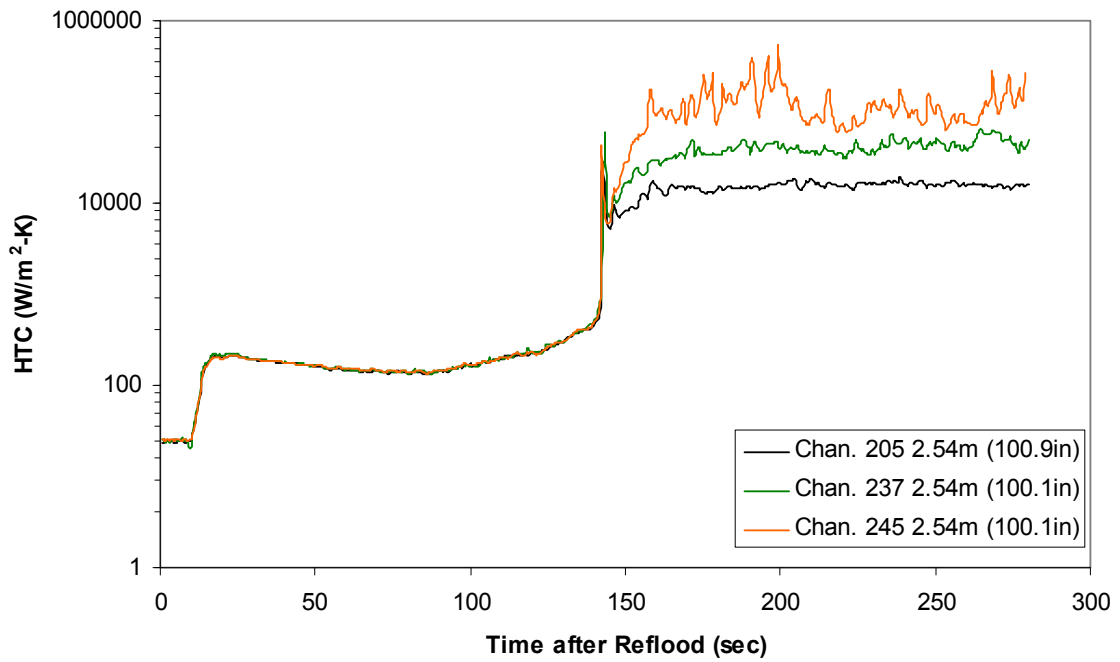
Heat Transfer Coefficient during Reflood
RBHT Exp. 1143



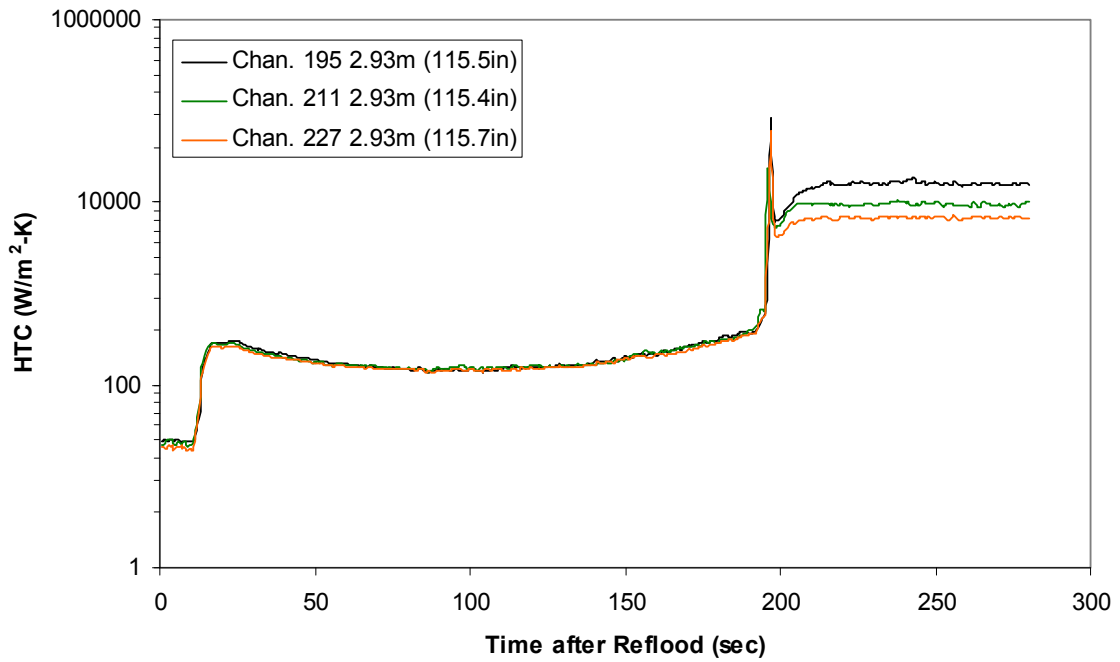
Heat Transfer Coefficient during Reflood
RBHT Exp. 1143



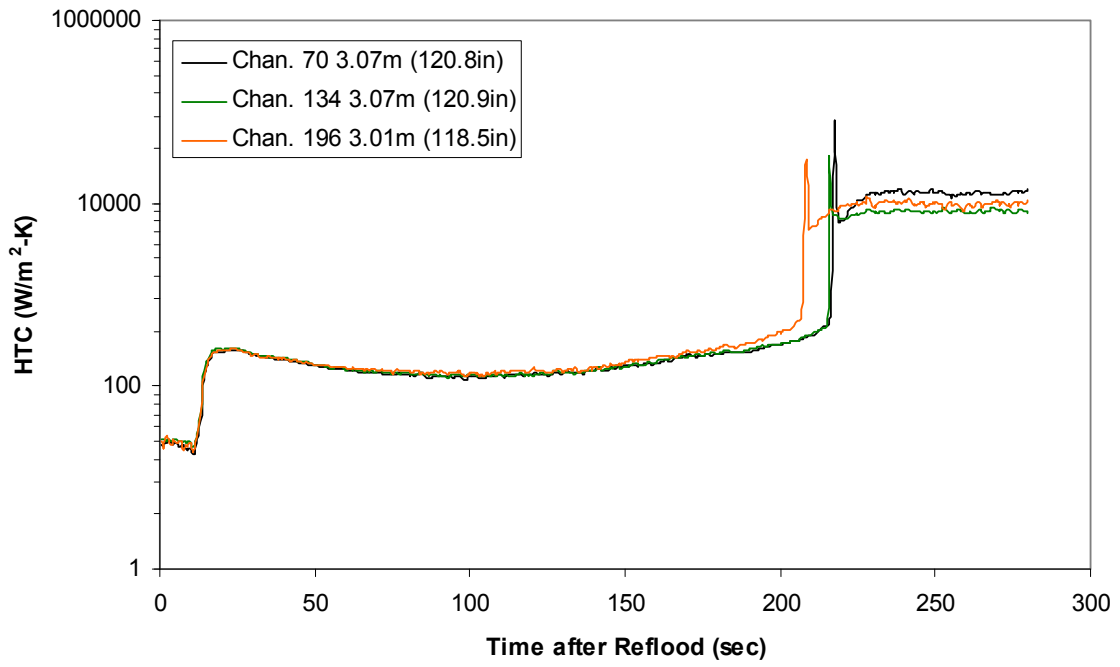
Heat Transfer Coefficient during Reflood RBHT Exp. 1143



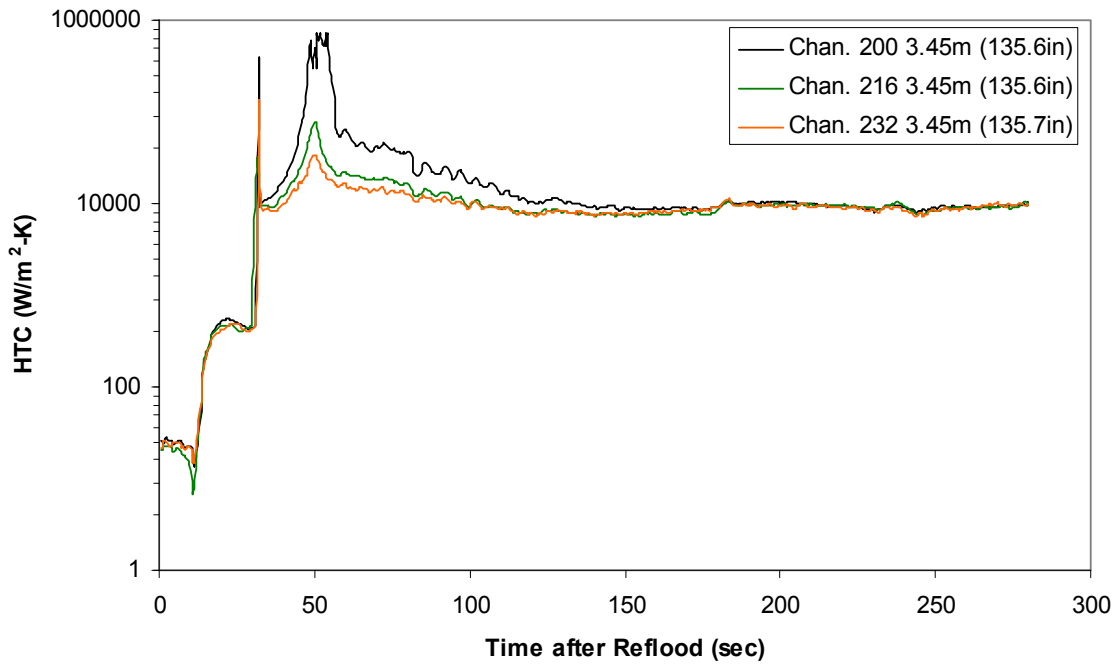
Heat Transfer Coefficient during Reflood RBHT Exp. 1143



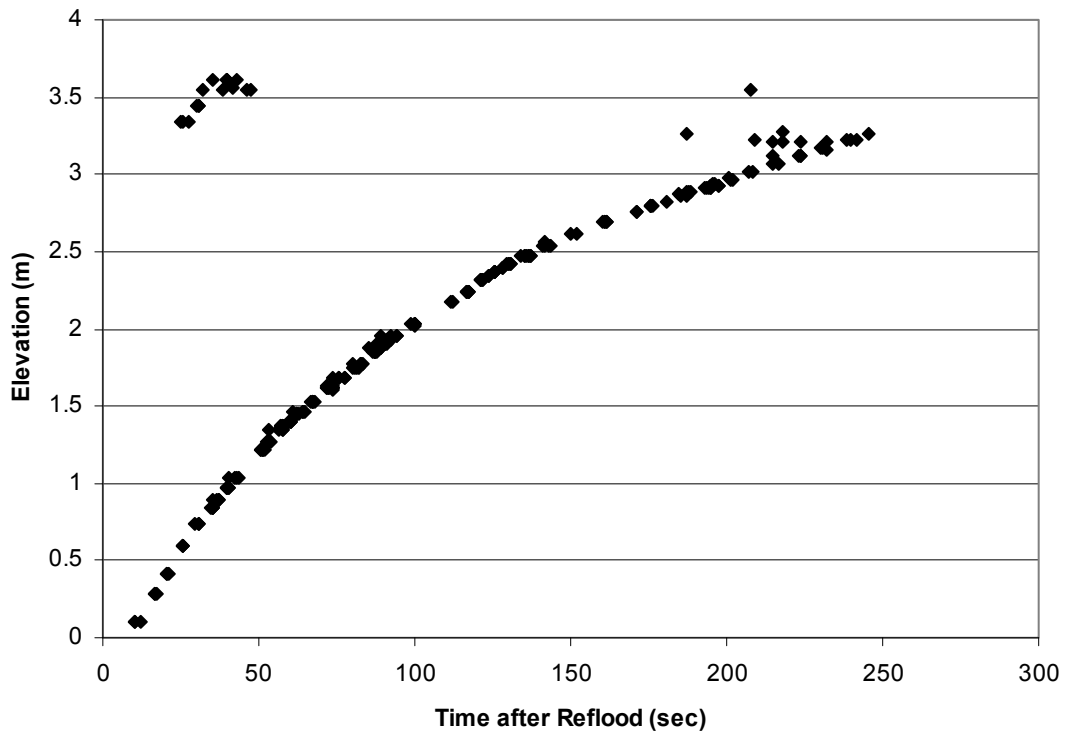
Heat Transfer Coefficient during Reflood RBHT Exp. 1143



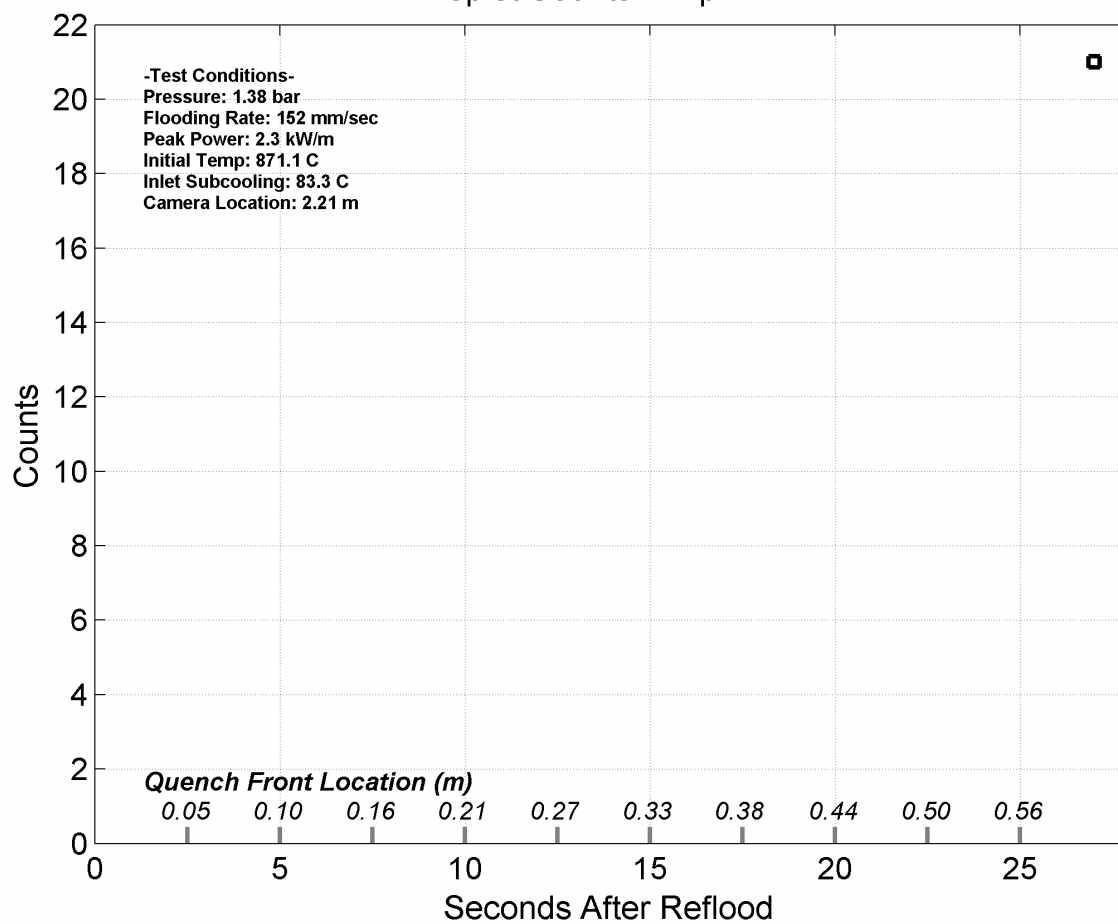
Heat Transfer Coefficient during Reflood RBHT Exp. 1143



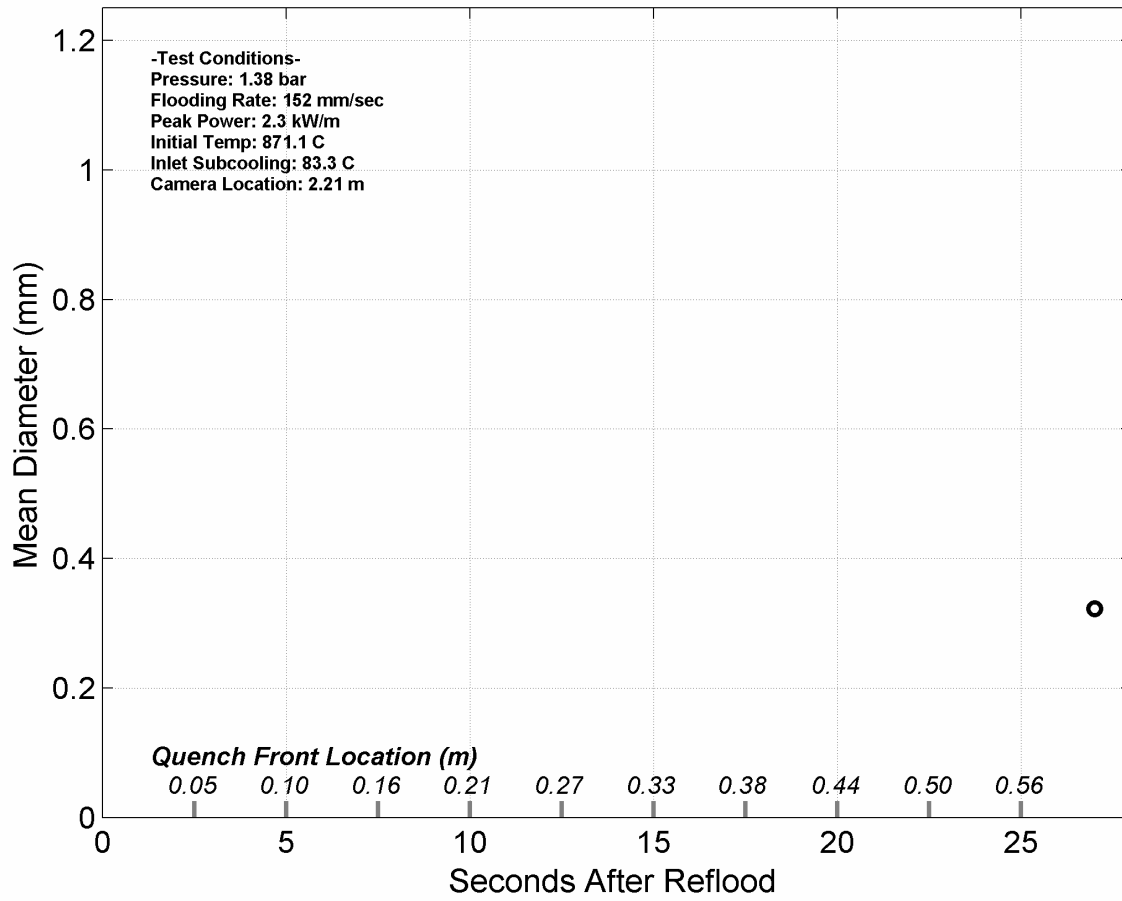
Quench Data, RBHT Exp. 1143



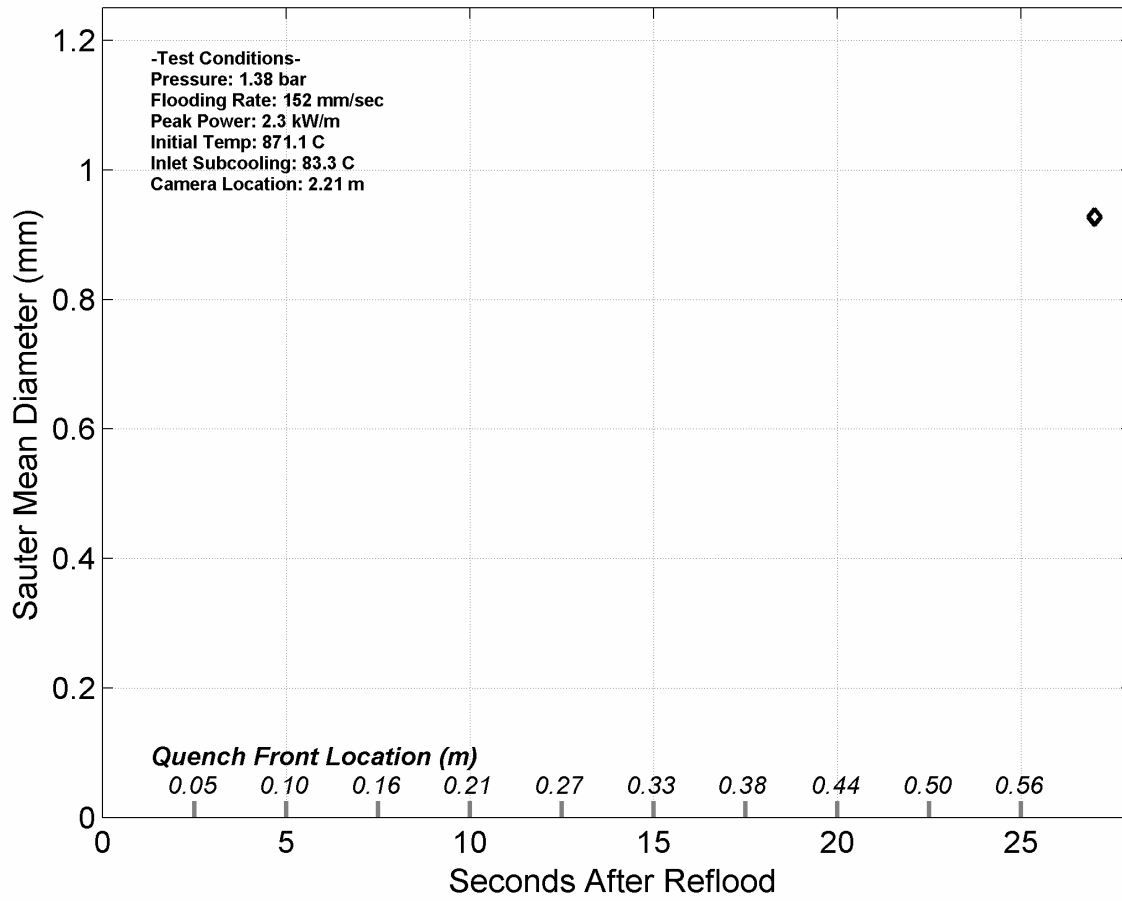
Droplet Counts - Exp. 1143



Mean Droplet Diameter - Exp. 1143



Droplet Sauter Mean Diameter - Exp. 1143



RBHT - REFLOOD TESTS

SUMMARY SHEET

RUN NO: **1155**

RUN CONDITIONS

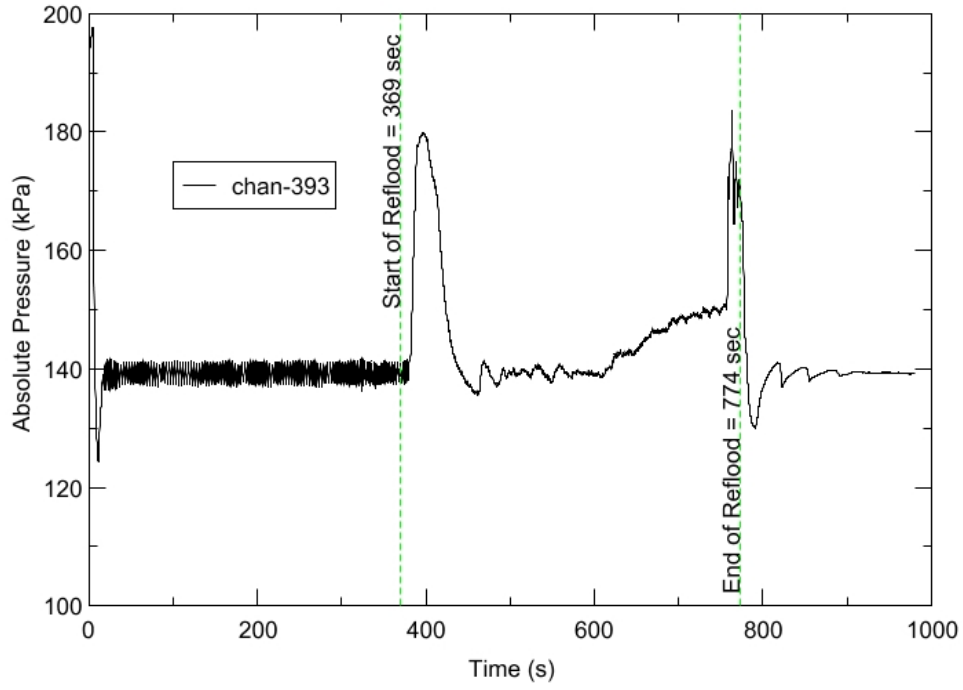
Upper Plenum Pressure:	138 kPa (20 psia)
Initial Peak Clad Temperature:	1144 degrees K (1600 degrees F)
Rod Peak Power:	2.3 kW/m (0.7 kW/ft)
Flooding Rate:	0.1524 m/s (6 in/s)
Inlet Subcooling:	11 degrees K (20 degrees F)
Start of Reflood:	369 s
End of Reflood:	774 s
Test Date:	6/14/2002
Comments:	Test terminated early, valid up to end of reflood time. Quench front at 2.35 m (93 in) at test termination.

No Droplet Data

Rod_Elevation	Channel Number	Temperature at Reflood (K)	Temperature at Reflood (°F)	Turnaround Time (sec.)	Turnaround Temperature (K)	Turnaround Temperature (°F)	Quench Time (sec.)	Quench Temperature (K)	Quench Temperature (°F)
B6 0.592m	148	806.43	991.89	12.25	843.36	1058.35	64.75	579.62	583.63
B6 0.744m	149	813.78	1005.12	14.25	854.99	1079.29	88.75	606.24	631.54
B6 0.846m	150	845.93	1062.98	14.75	890.89	1143.92	105.75	588.51	599.62
B6 0.897m	151	856.54	1082.08	15.25	902.93	1165.59	114.75	596.24	613.54
C6 1.04m	137	909.31	1177.06	15.25	961.27	1270.6	137.75	635.6	684.4
D5 1.27m	217	971.45	1288.93	13.75	1022.39	1380.62	182.75	633.45	680.52
C6 1.34m	138	956.58	1262.15	15.25	1014.03	1365.57	198.25	642.86	697.45
D5 1.37m	218	991.85	1325.65	14.75	1049.09	1428.67	200.25	665.21	737.7
C6 1.39m	139	961.87	1271.69	15.25	1020.87	1377.87	208.25	656.02	721.15
D5 1.45m	219	1003.75	1347.06	15.25	1062.92	1453.57	213.25	679.57	763.54
C6 1.47m	140	974.8	1294.94	15.75	1035.1	1403.49	222.75	681.33	766.71
D5 1.52m	220	1015.5	1368.2	15.75	1076.8	1478.54	228.75	699.87	800.07
C6 1.62m	141	995.04	1331.39	15.75	1059.86	1448.07	256.75	711.62	821.22
D5 1.68m	221	1034.01	1401.53	15.75	1099.44	1519.3	263.75	743.77	879.1
D5 1.78m	222	1021.54	1379.09	13.75	1080.21	1484.68	286.75	671.16	748.4
D5 1.85m	223	1050.77	1431.7	13.75	1114.03	1545.56	299.75	700.09	800.48
C6 1.87m	142	1027.47	1389.77	14.25	1093.23	1508.13	313.75	708.58	815.76
D5 1.90m	224	1056.79	1442.54	14.25	1122.99	1561.7	309.75	723.29	842.24
C6 1.95m	144	1033.55	1400.7	14.25	1101.13	1522.35	331.25	713.83	825.21
C3 2.17m	178	1069.76	1465.89	14.75	1143.53	1598.66	364.75	746.55	884.09
D4 2.24m	241	1076.16	1477.41	13.75	1145.27	1601.8	389.25	700.77	801.7
C3 2.35m	180	1086.68	1496.34	13.75	1158.25	1625.17	394.75	714.36	826.15
D4 3.61m	248	667.78	742.31	15.25	726.89	848.72	41.25	503.84	447.23

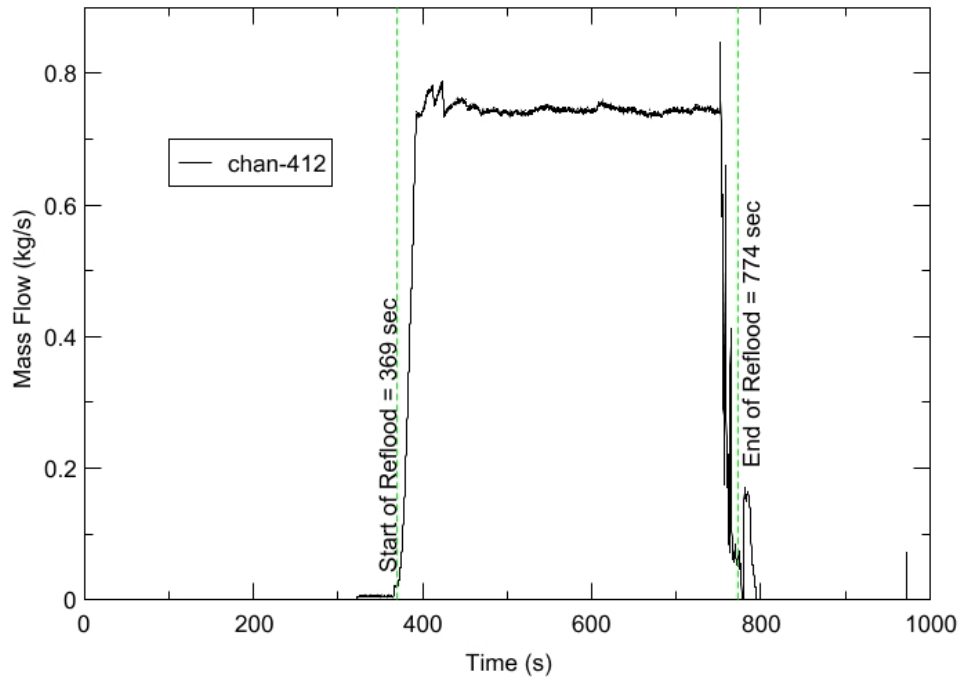
RBHT - TEST FACILITY

Upper Plenum Pressure vs. Time, Exp 1155



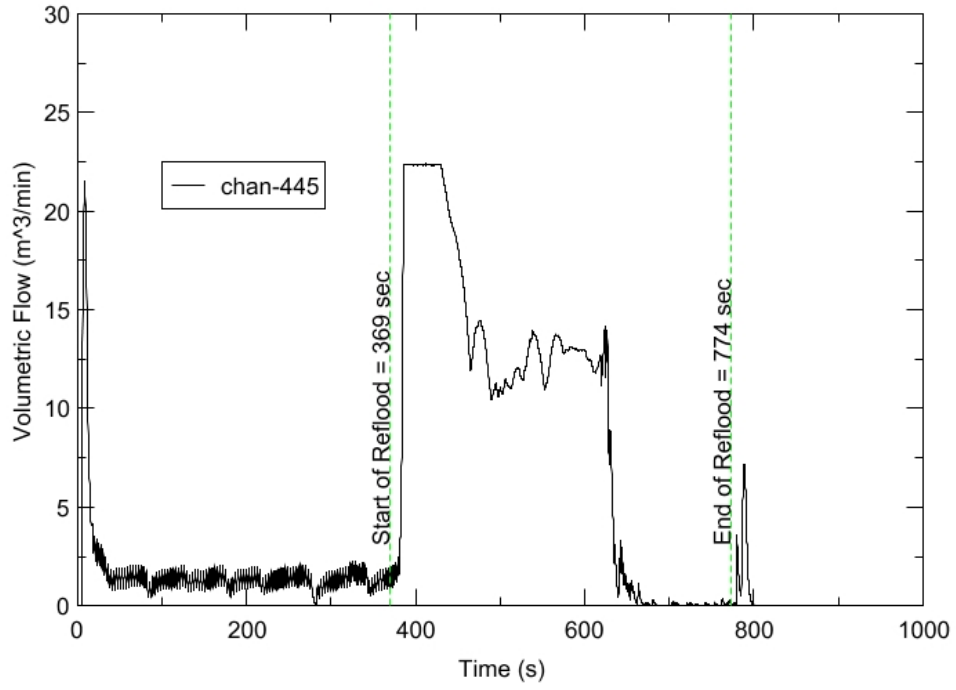
RBHT - TEST FACILITY

Inlet Flow vs. Time, Exp 1155



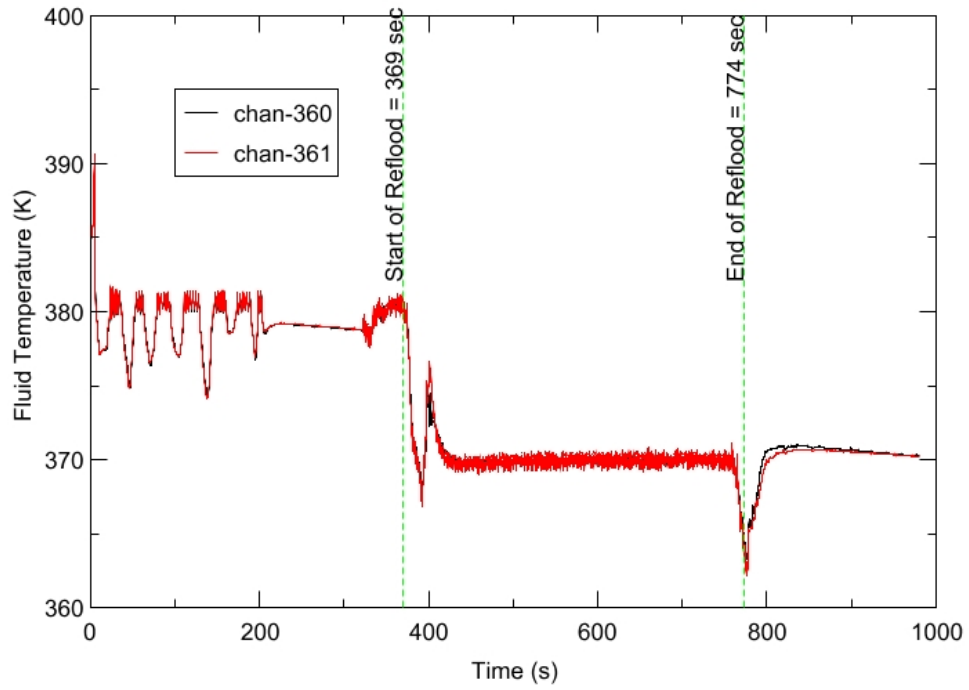
RBHT - TEST FACILITY

Steam Exhaust Flow vs. Time, Exp 1155



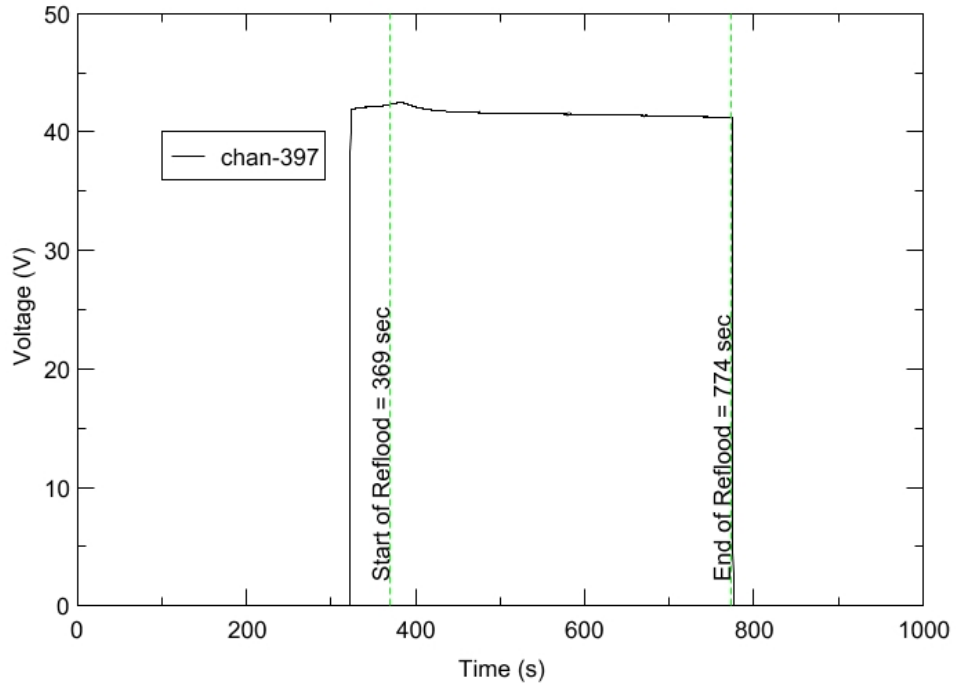
RBHT - TEST FACILITY

Inlet Flow Temperature vs. Time, Exp 1155



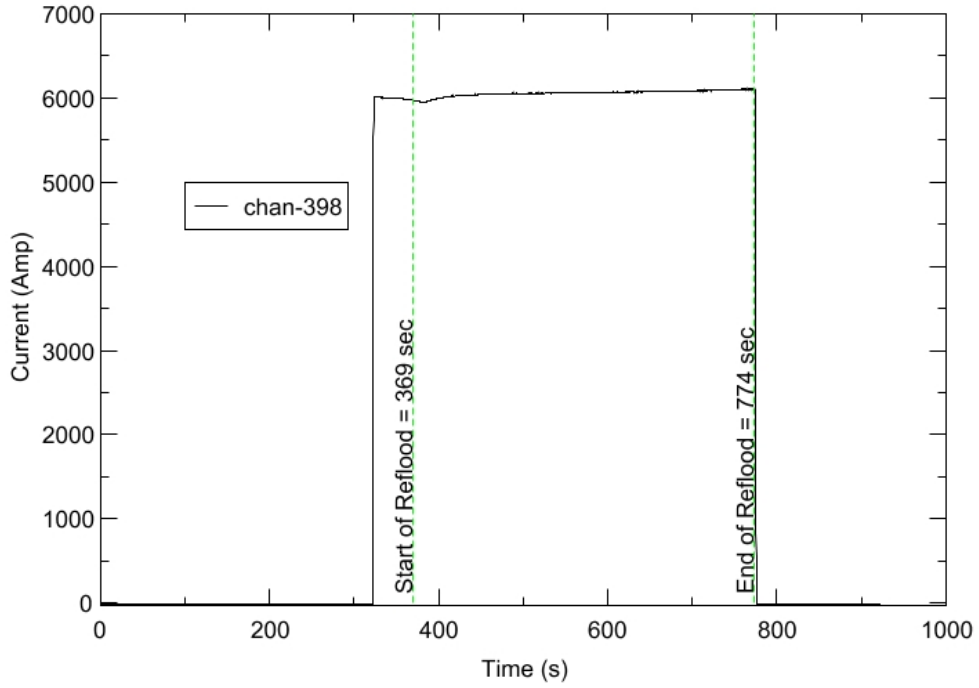
RBHT - TEST FACILITY

Test Section Voltage vs. Time, Exp 1155

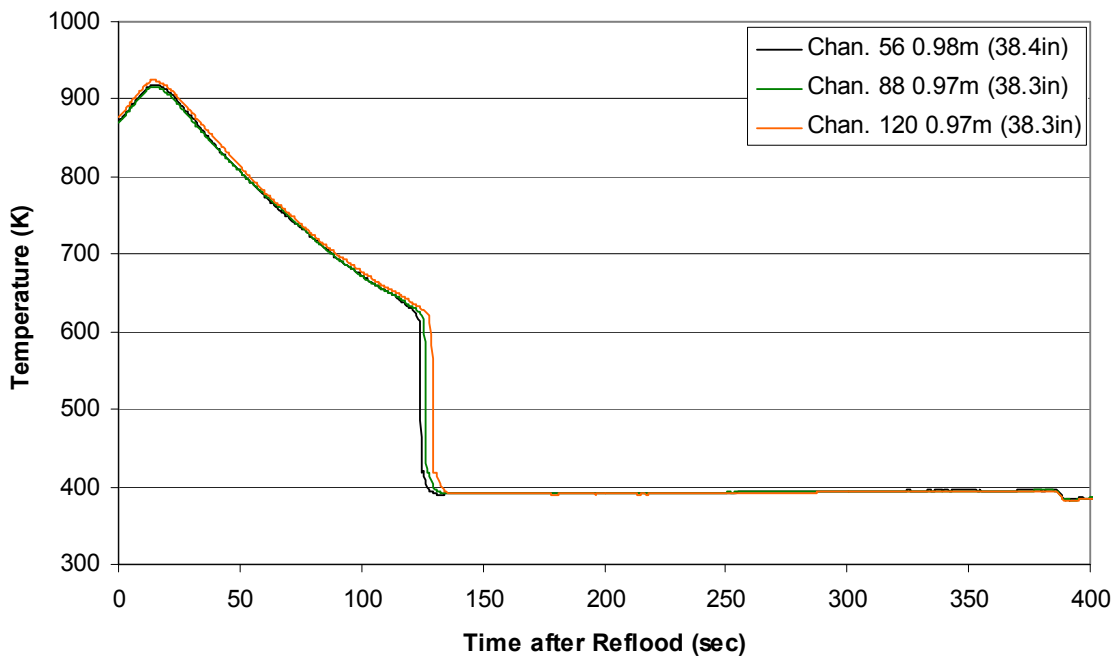


RBHT - TEST FACILITY

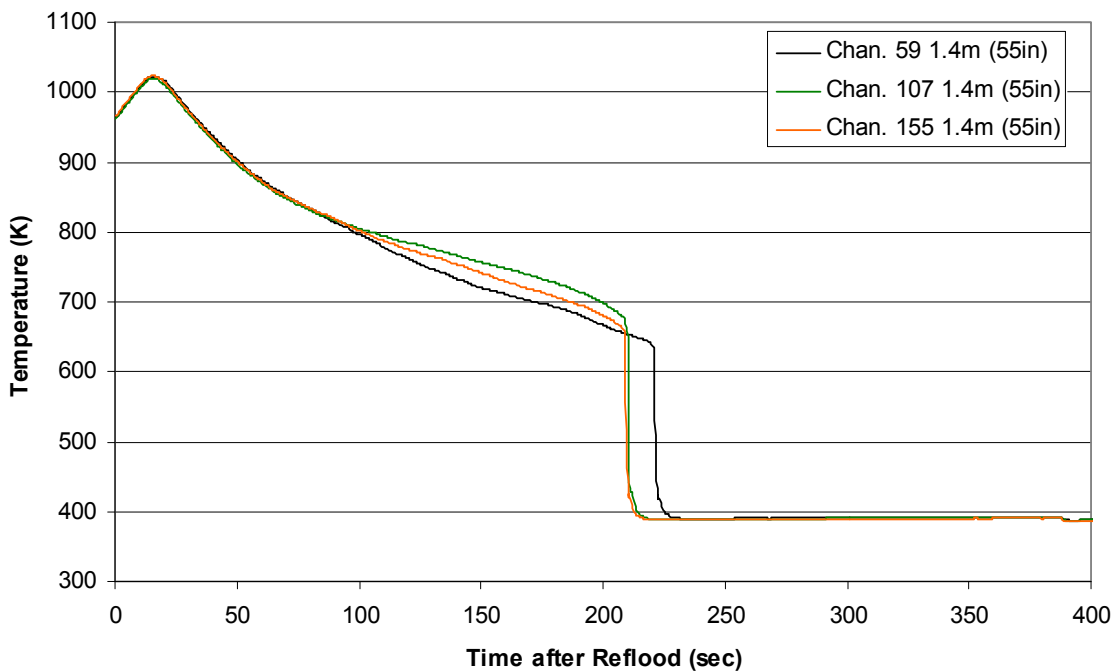
Test Section Current vs. Time, Exp 1155



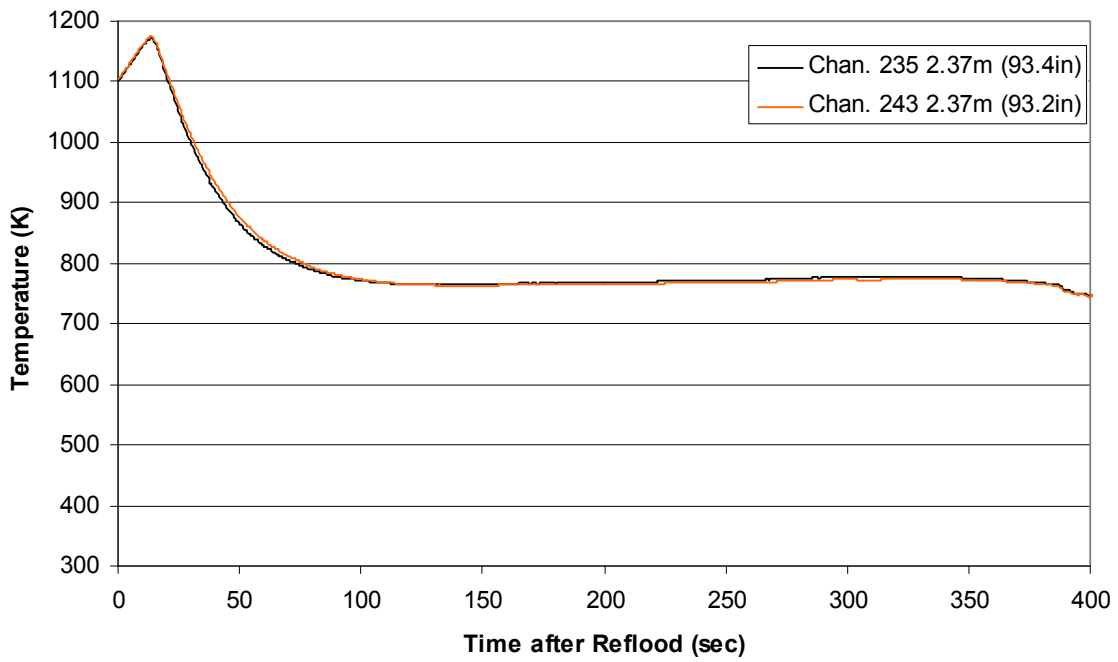
Heater Rod Temperature during Reflood
RBHT Exp. 1155



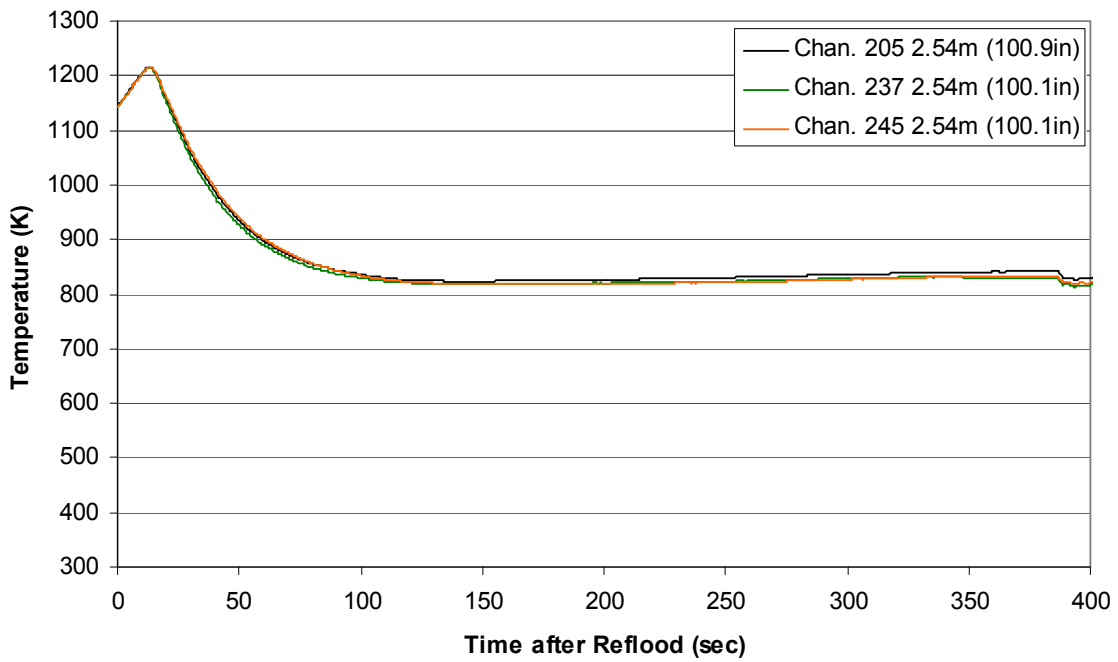
Heater Rod Temperature during Reflood
RBHT Exp. 1155



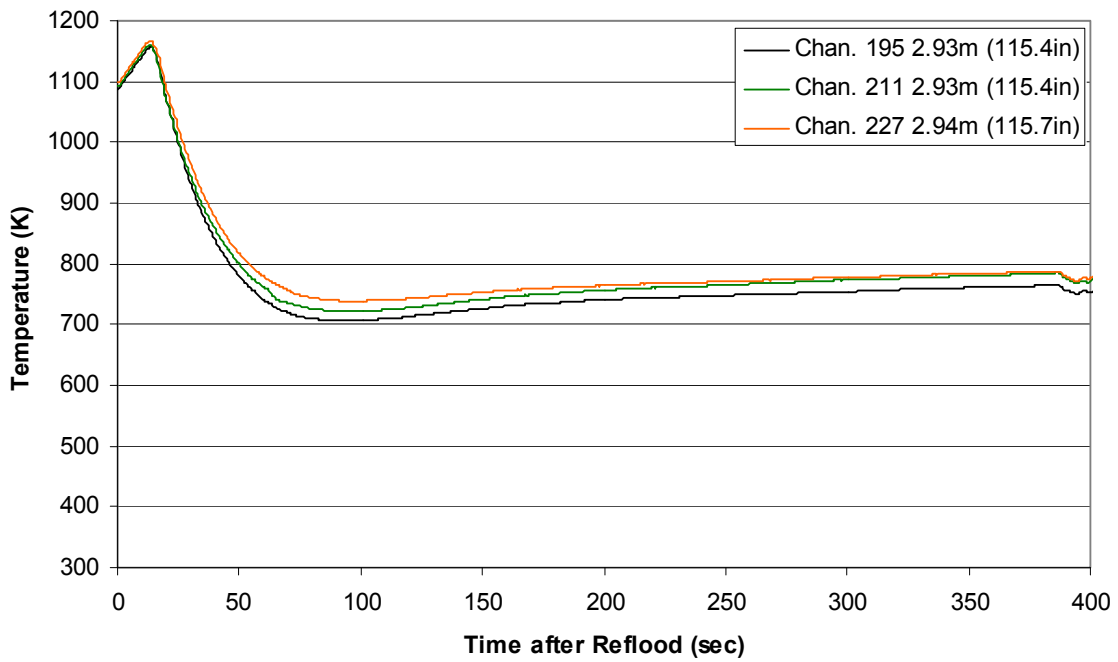
**Heater Rod Temperature during Reflood
RBHT Exp. 1155**



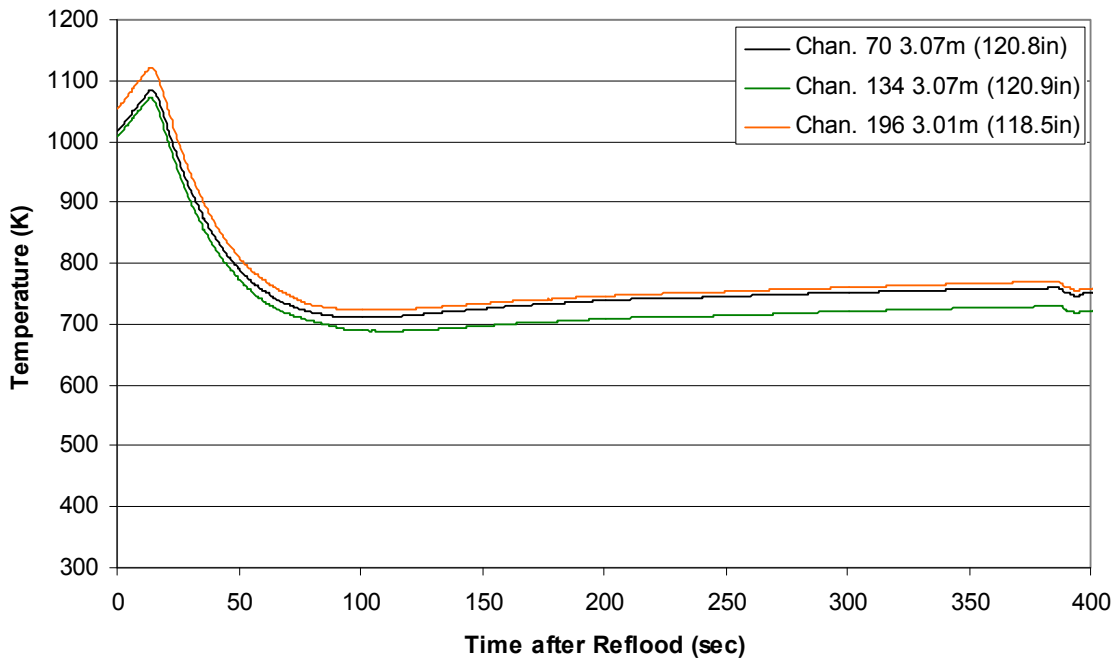
**Heater Rod Temperature during Reflood
RBHT Exp. 1155**



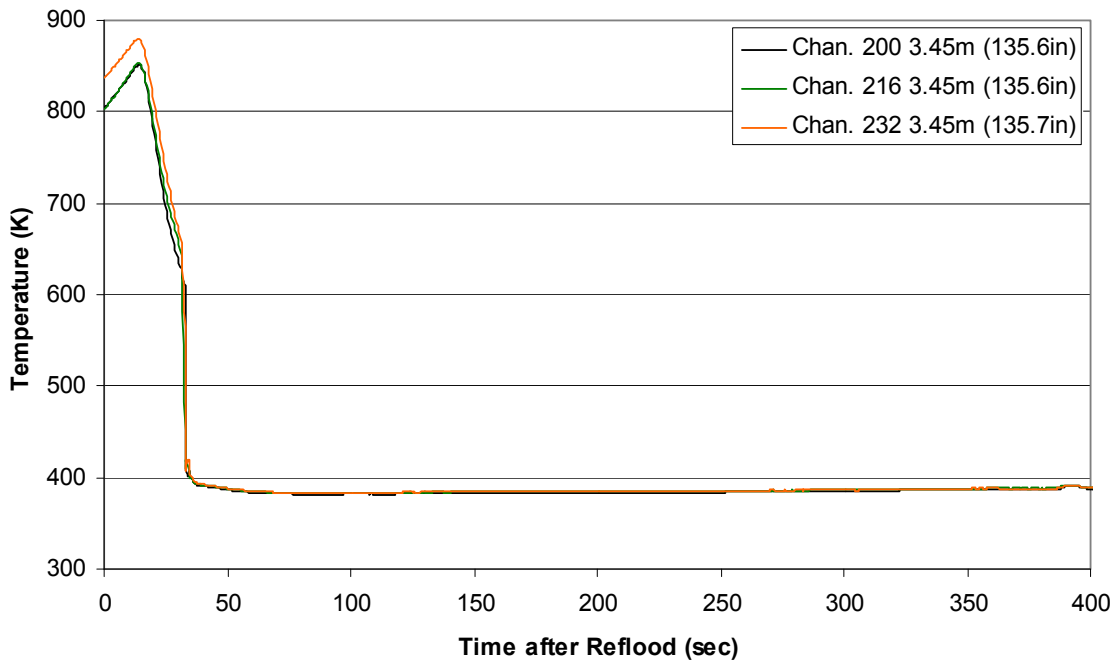
**Heater Rod Temperature during Reflood
RBHT Exp. 1155**



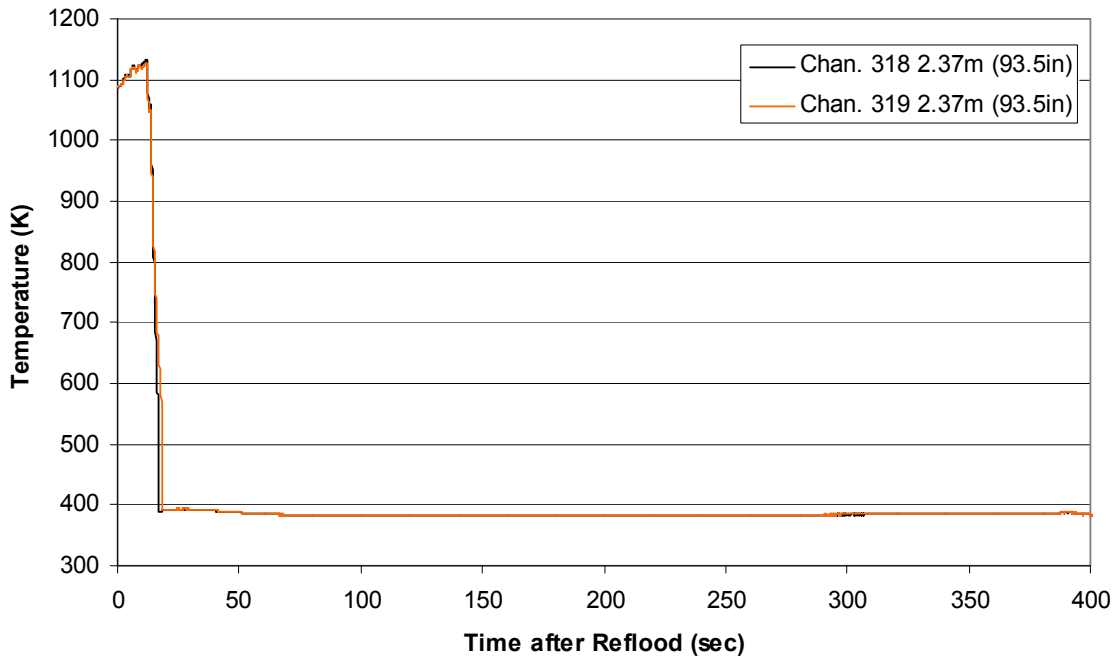
**Heater Rod Temperature during Reflood
RBHT Exp. 1155**



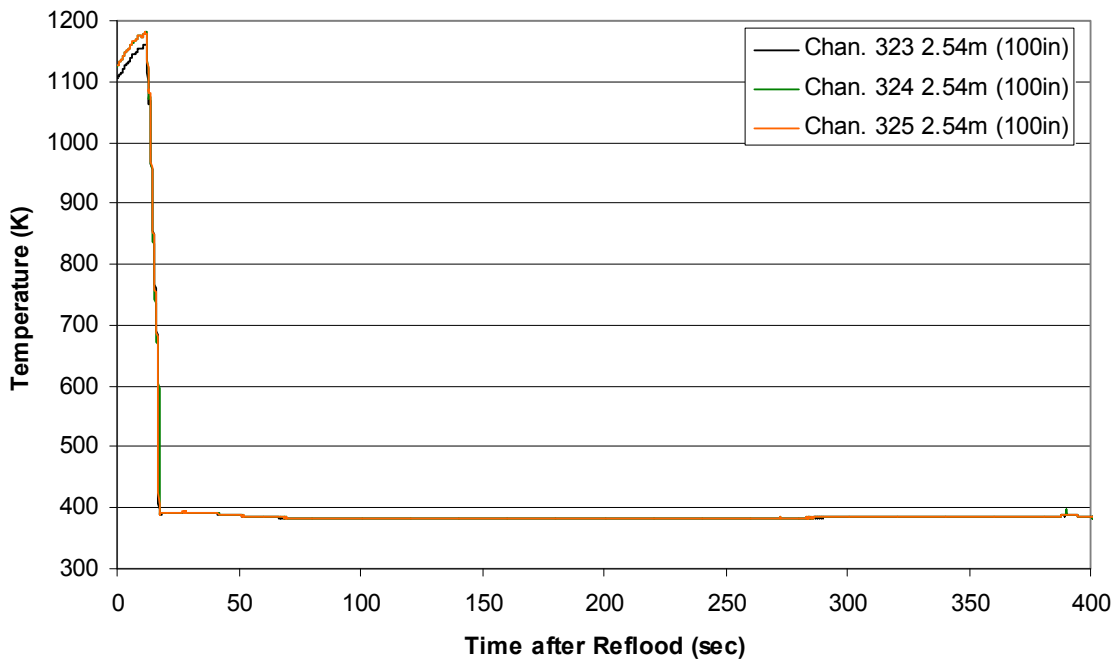
Heater Rod Temperature during Reflood RBHT Exp. 1155



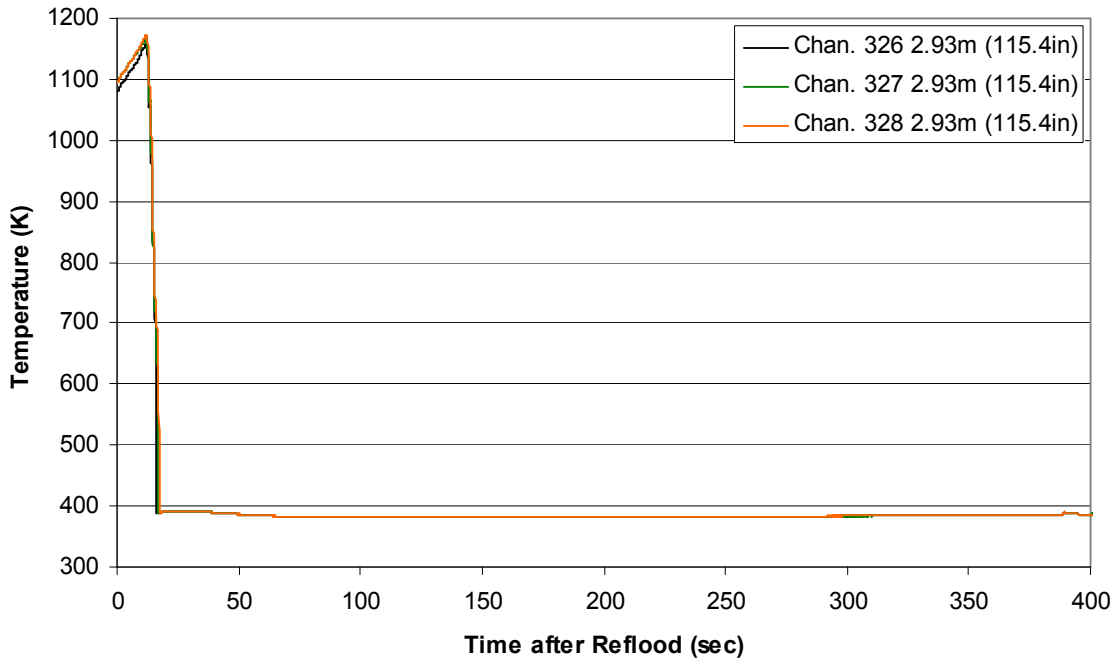
Steam Probe Temperature during Reflood RBHT Exp. 1155



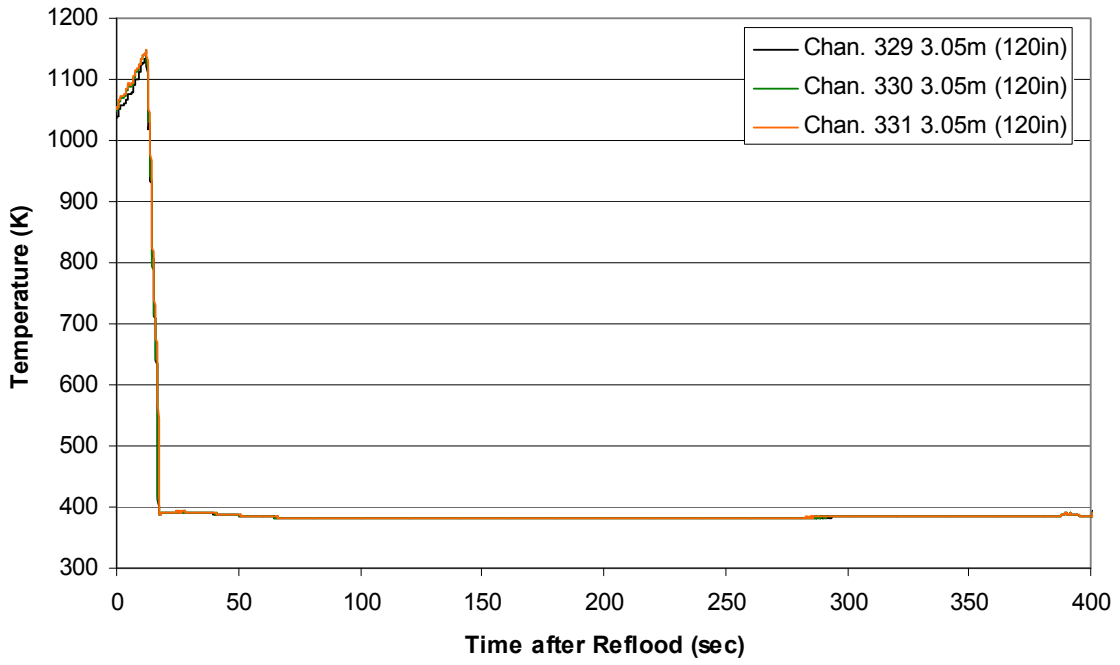
Steam Probe Temperature during Reflood RBHT Exp. 1155



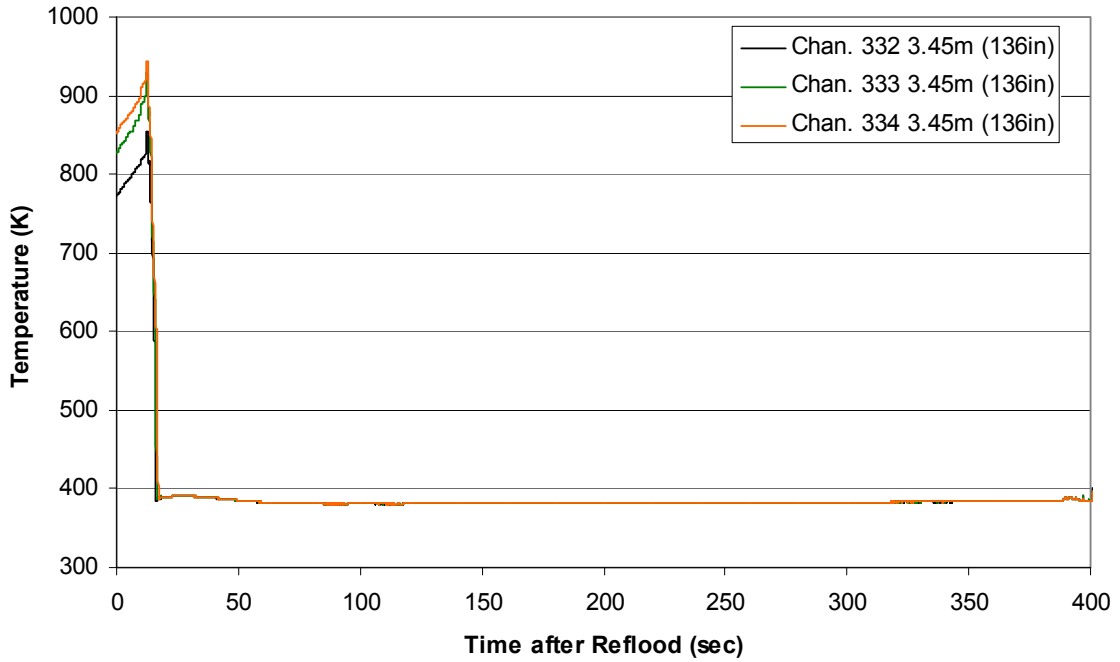
Steam Probe Temperature during Reflood RBHT Exp. 1155



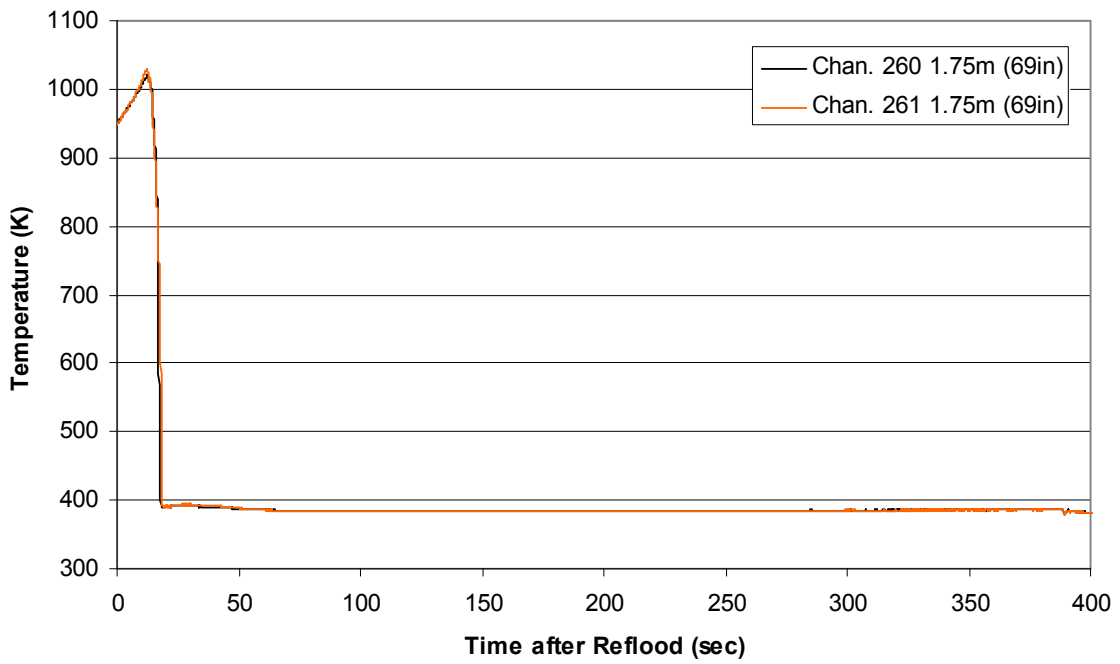
Steam Probe Temperature during Reflood RBHT Exp. 1155



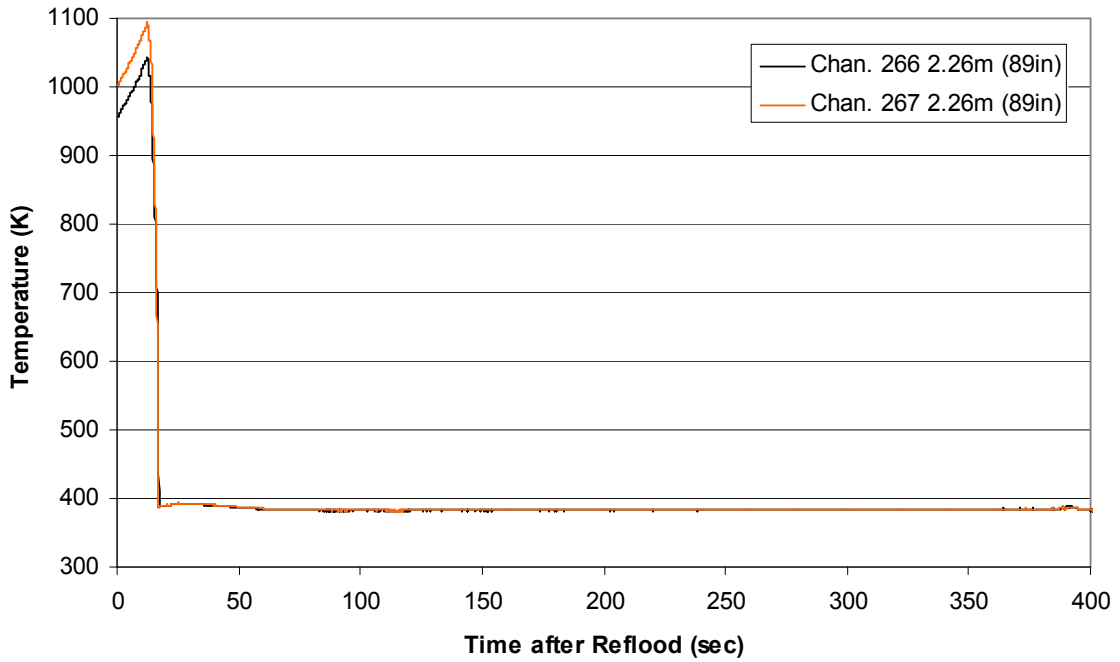
Steam Probe Temperature during Reflood RBHT Exp. 1155



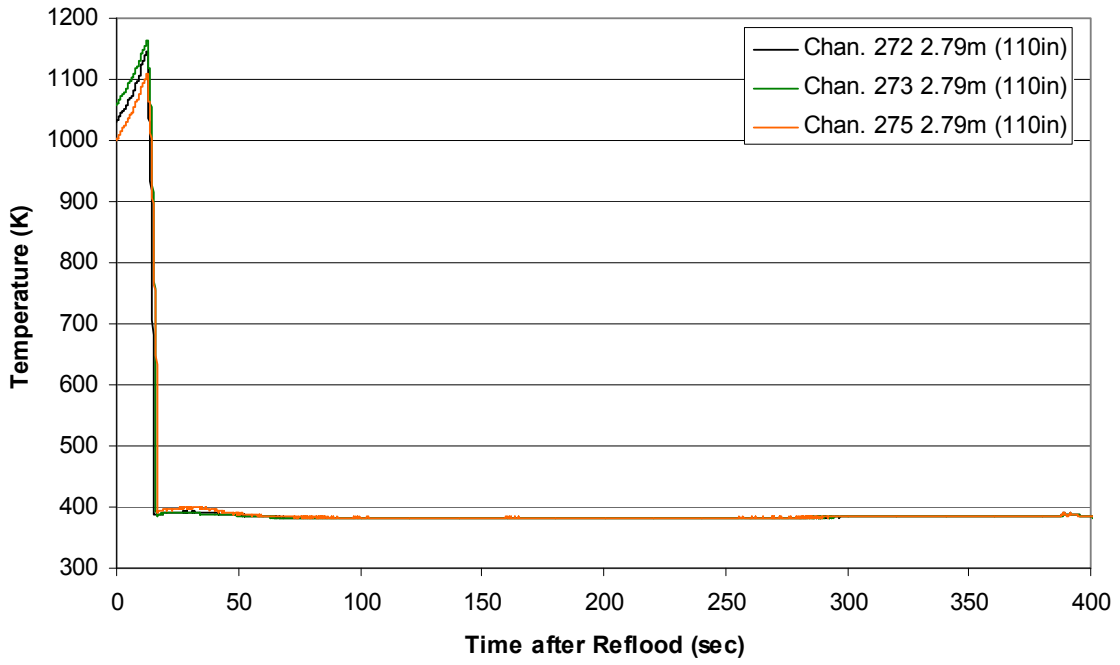
Spacer Grid Temperature during Reflood
RBHT Exp. 1155



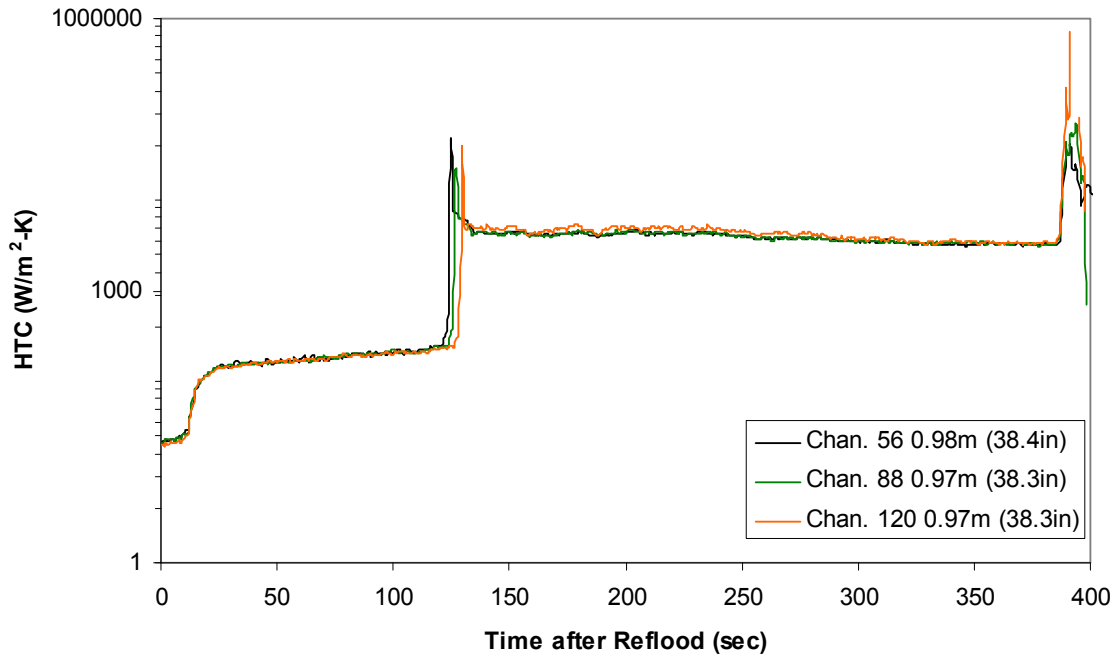
Spacer Grid Temperature during Reflood
RBHT Exp. 1155



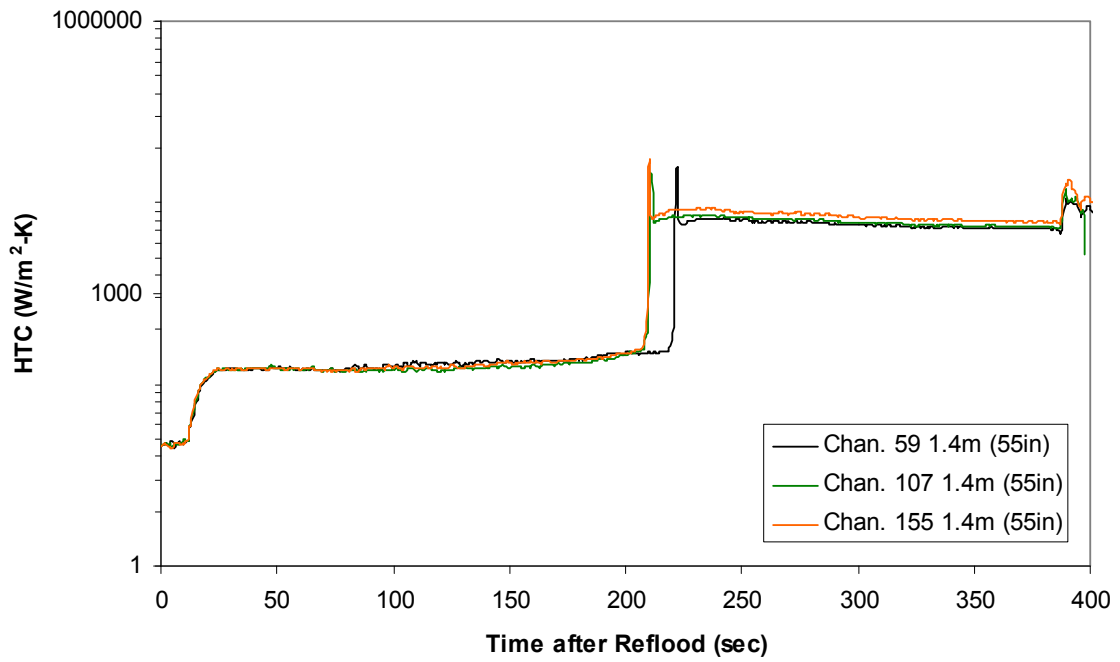
Spacer Grid Temperature during Reflood RBHT Exp. 1155



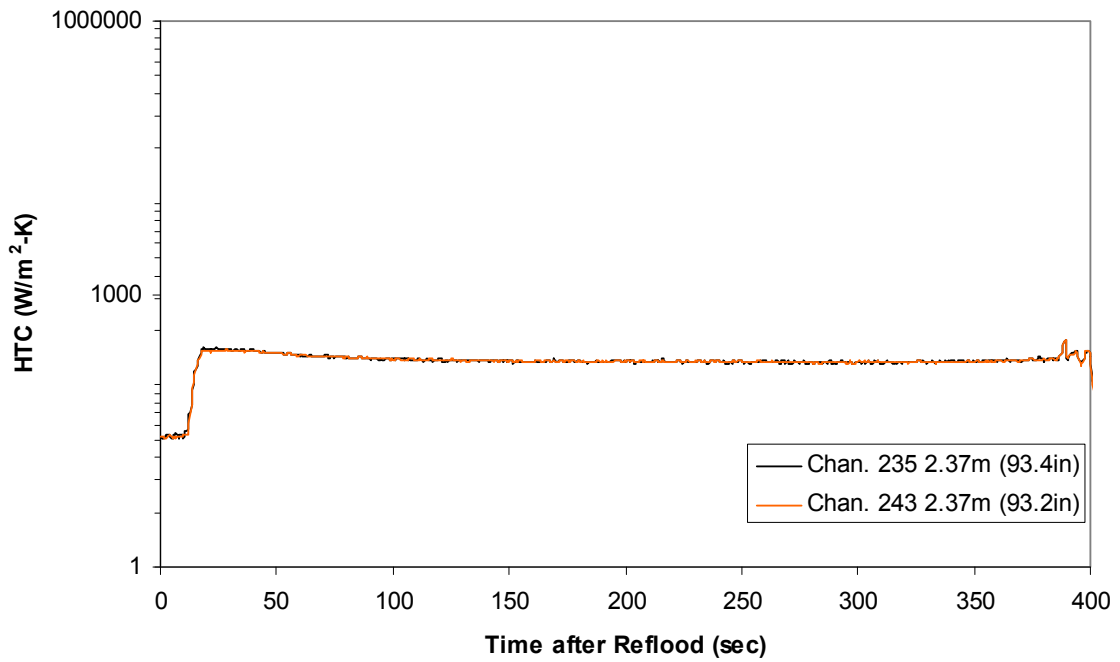
Heat Transfer Coefficient during Reflood RBHT Exp. 1155



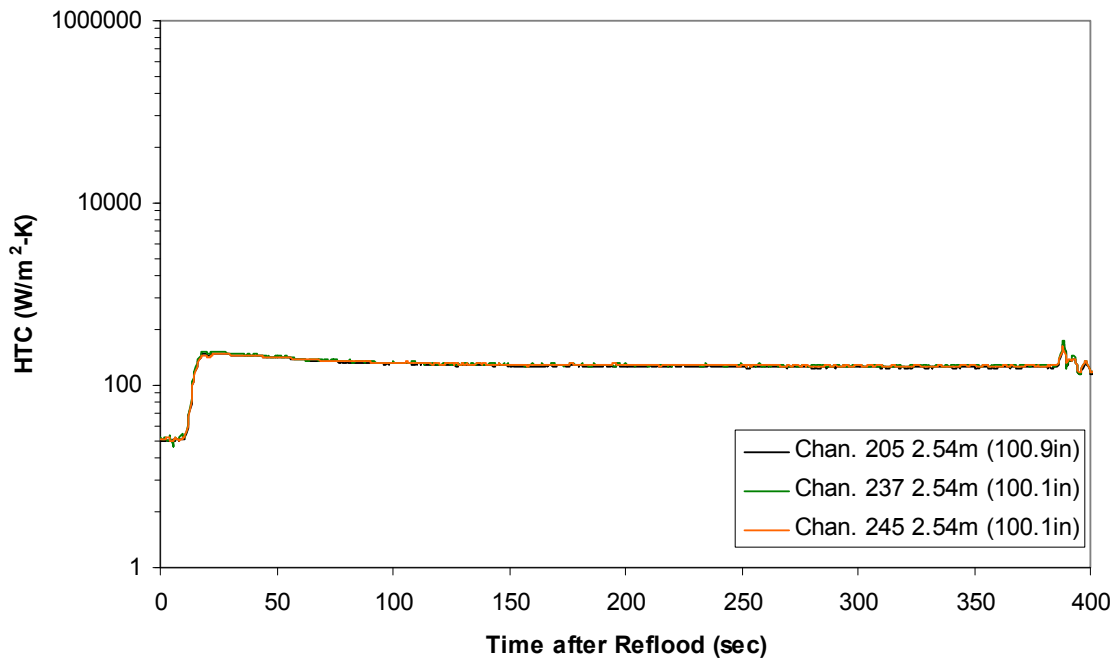
Heat Transfer Coefficient during Reflood
RBHT Exp. 1155



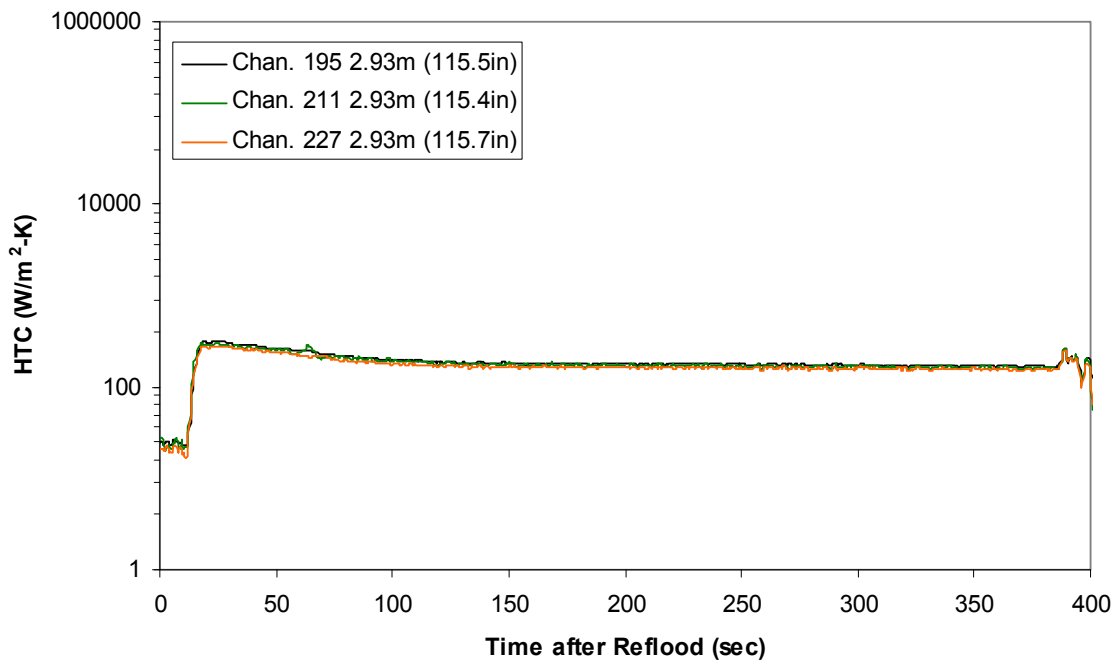
Heat Transfer Coefficient during Reflood
RBHT Exp. 1155



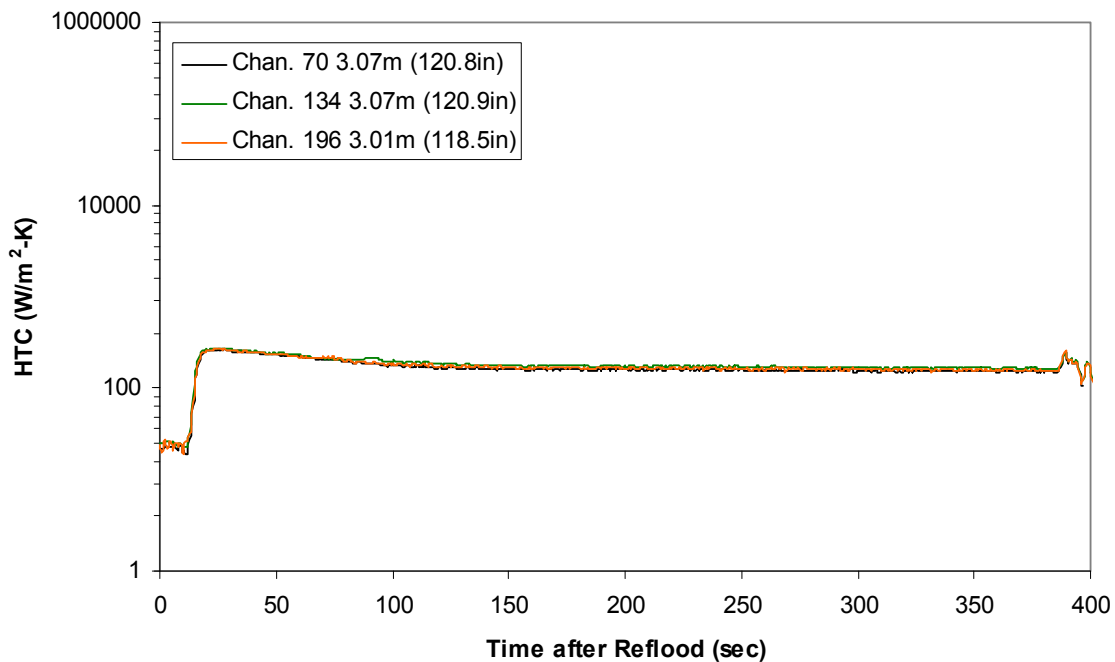
Heat Transfer Coefficient during Reflood RBHT Exp. 1155



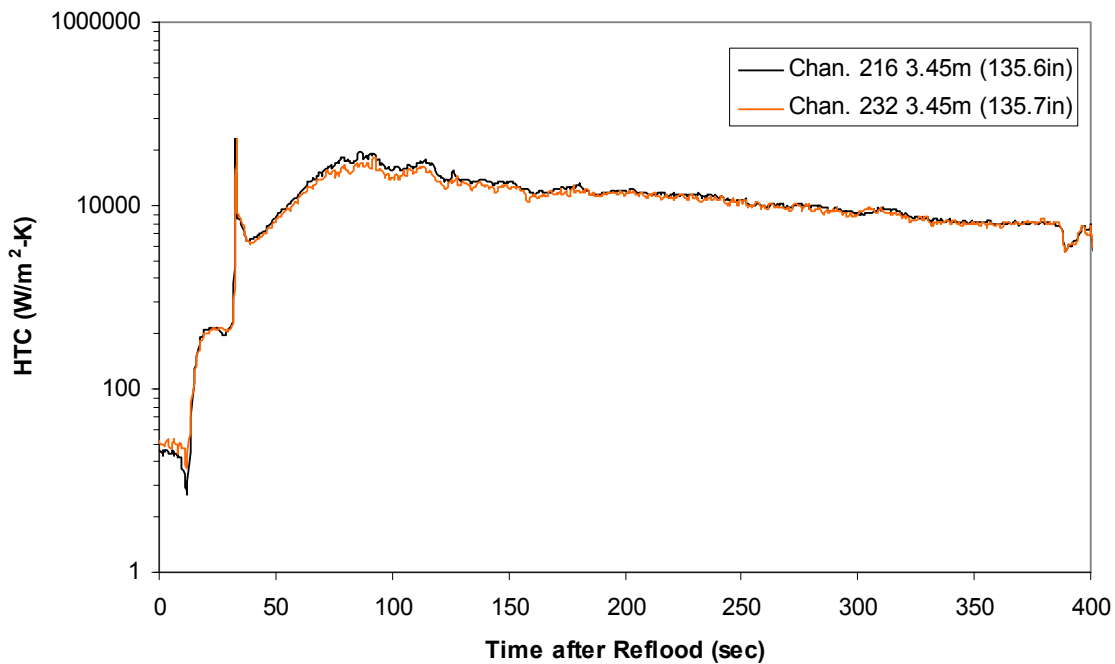
Heat Transfer Coefficient during Reflood RBHT Exp. 1155



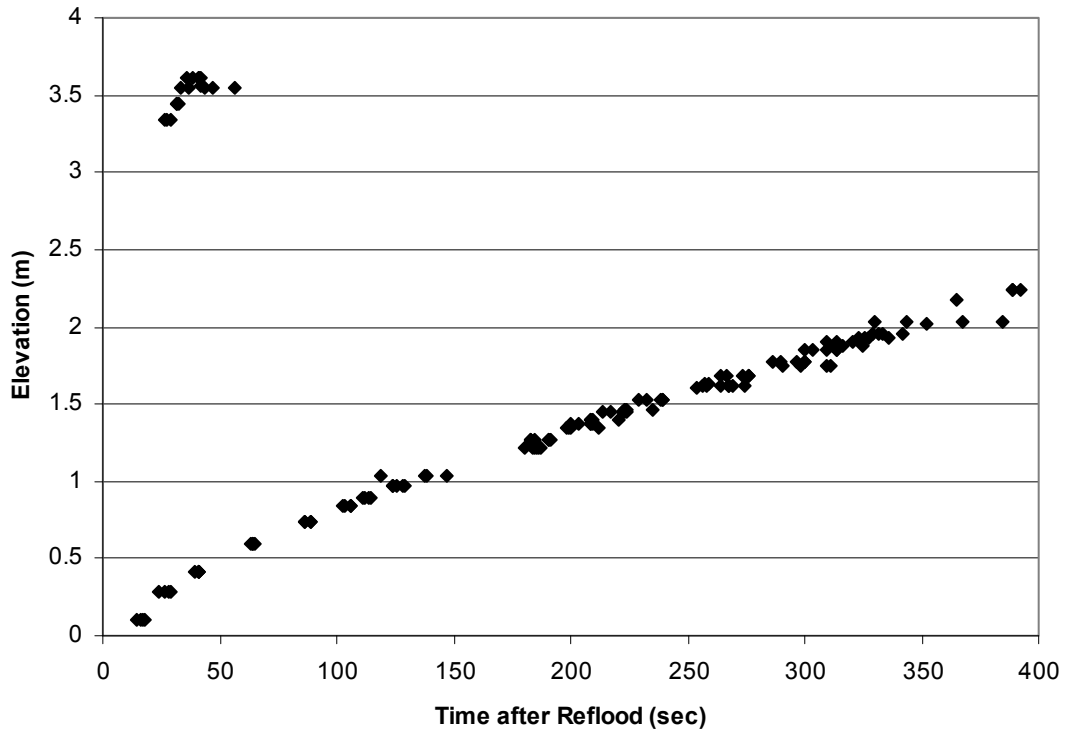
Heat Transfer Coefficient during Reflood RBHT Exp. 1155



Heat Transfer Coefficient during Reflood RBHT Exp. 1155



Quench Data, RBHT Exp. 1155



RBHT - REFLOOD TESTS

SUMMARY SHEET

RUN NO: **1160**

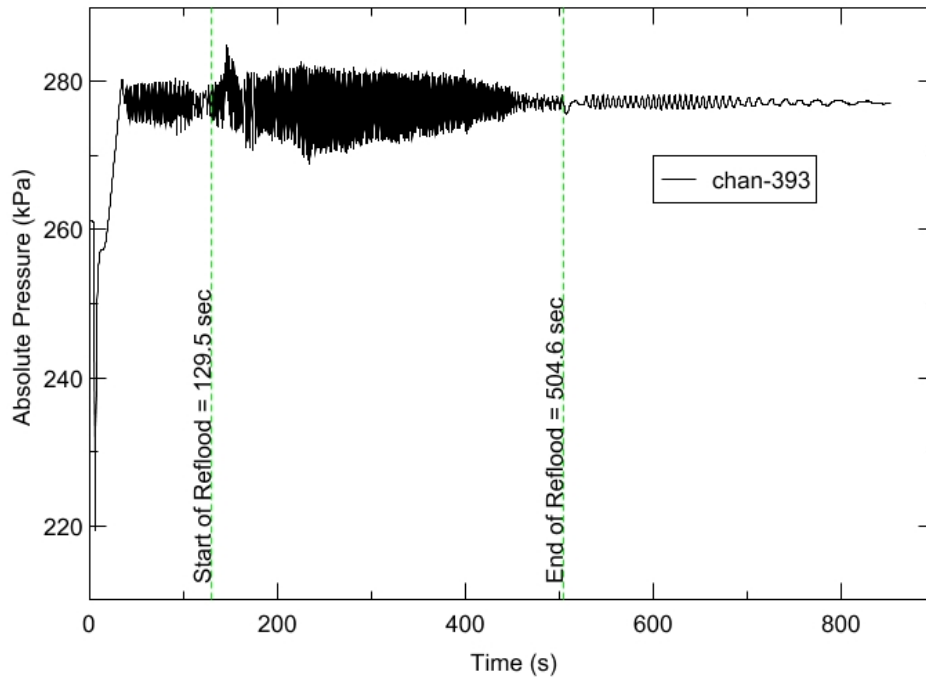
RUN CONDITIONS

Upper Plenum Pressure:	276 kPa (40 psia)
Initial Peak Clad Temperature:	1144 degrees K (1600 degrees F)
Rod Peak Power:	2.3 kW/m (0.7 kW/ft)
Flooding Rate:	0.127 m/s (5 in/s)
Inlet Subcooling:	83 degrees K (150 degrees F)
Start of Reflood:	129.5 s
End of Reflood:	504.6 s
Test Date:	6/17/2002
Comments:	Heater rod surfaces below 2.4 m (94 in) quench to a temperature below saturation due to the high inlet subcooling. Therefore DATARH calculated heat transfer coefficients are not presented below this elevation after rod quench.

Rod_Elevation	Channel Number	Temperature at Reflood (K)	Temperature at Reflood (°F)	Turnaround Time (sec.)	Turnaround Temperature (K)	Turnaround Temperature (°F)	Quench Time (sec.)	Quench Temperature (K)	Quench Temperature (°F)
B6 0.592m	148	818.33	1013.31	14.25	860.05	1088.4	34.25	713.04	823.78
B6 0.744m	149	818.69	1013.96	14.25	862.97	1093.65	41.25	697.24	795.35
B6 0.846m	150	852.36	1074.56	15.75	901.64	1163.26	45.25	699.56	799.52
B6 0.897m	151	863.86	1095.26	15.75	914.66	1186.7	47.25	691.87	785.68
C6 1.04m	137	917.12	1191.12	17.25	973.98	1293.48	54.25	724.27	844
D5 1.27m	217	976.23	1297.53	15.75	1033.59	1400.77	64.75	708.29	815.24
C6 1.34m	138	962.16	1272.19	17.25	1026.62	1388.23	67.75	716.06	829.21
D5 1.37m	218	997.21	1335.3	17.25	1061.4	1450.83	71.75	701.91	803.76
C6 1.39m	139	969.31	1285.06	18.75	1034.59	1402.57	72.75	706.48	811.98
D5 1.45m	219	1010.47	1359.15	17.25	1076.87	1478.67	75.75	702.68	805.14
C6 1.47m	140	982.43	1308.68	18.75	1049.05	1428.6	77.25	696.78	794.52
D5 1.52m	220	1022.67	1381.12	18.75	1091.98	1505.87	80.75	718.86	834.26
C6 1.62m	141	1001.92	1343.77	20.75	1074.55	1474.51	84.75	752.91	895.55
D5 1.68m	221	1042.03	1415.96	21.75	1116.85	1550.64	89.75	738	868.71
D5 1.78m	222	1030.49	1395.19	15.75	1096.85	1514.65	97.25	682.93	769.58
D5 1.85m	223	1055.81	1440.76	15.75	1128.03	1570.77	100.75	684.31	772.06
C6 1.87m	142	1031.79	1397.53	17.25	1106.62	1532.23	103.75	661.6	731.2
D5 1.90m	224	1062.37	1452.58	17.25	1137.41	1587.66	97.75	738.65	869.88
C6 1.95m	144	1039.09	1410.68	17.25	1115.78	1548.71	108.25	665.51	738.24
C3 2.17m	178	1076.12	1477.32	17.75	1159.88	1628.1	129.75	661.72	731.41
D4 2.24m	241	1076.67	1478.32	15.75	1154.72	1618.81	135.75	661.09	730.28
D4 2.32m	242	1099.71	1519.79	16.25	1177.92	1660.56	142.25	651.13	712.35
C3 2.35m	180	1089.4	1501.23	15.75	1171.83	1649.6	145.25	658.16	725
D4 2.37m	243	1105.78	1530.72	15.75	1187.37	1677.58	147.75	645.12	701.53
C3 2.40m	181	1092.23	1506.32	15.75	1175.89	1656.92	150.75	666.73	740.43
D4 2.54m	245	1144.09	1599.67	15.25	1227.11	1749.11	168.75	677.19	759.26
D6 2.62m	129	1136.52	1586.06	15.25	1222.11	1740.11	179.25	690.26	782.78
D6 2.69m	130	1138.76	1590.08	15.25	1227.05	1748.99	190.75	703.45	806.51
C3 2.76m	183	1139.89	1592.12	16.75	1227.82	1750.38	202.75	706.46	811.95
D6 2.87m	131	1088.3	1499.26	14.25	1168.88	1644.29	219.75	669.33	745.11
D6 2.92m	132	1063.23	1454.12	16.25	1147.15	1605.18	226.75	667.81	742.37
D6 2.97m	133	1034.41	1402.26	16.25	1113.4	1544.44	233.75	668.58	743.76
D6 3.07m	134	996.35	1333.74	16.25	1069.86	1466.07	243.25	676.39	757.81
E3 3.12m	197	992.19	1326.25	16.25	1063.15	1453.97	252.25	664.71	736.8
D6 3.17m	135	957.16	1263.19	16.25	1025.58	1386.36	254.75	673.86	753.27
D6 3.27m	136	908.66	1175.9	17.75	974.85	1295.03	266.75	662.26	732.38
D4 3.61m	248	697.64	796.07	20.25	763.02	913.75	235.25	433.79	321.14

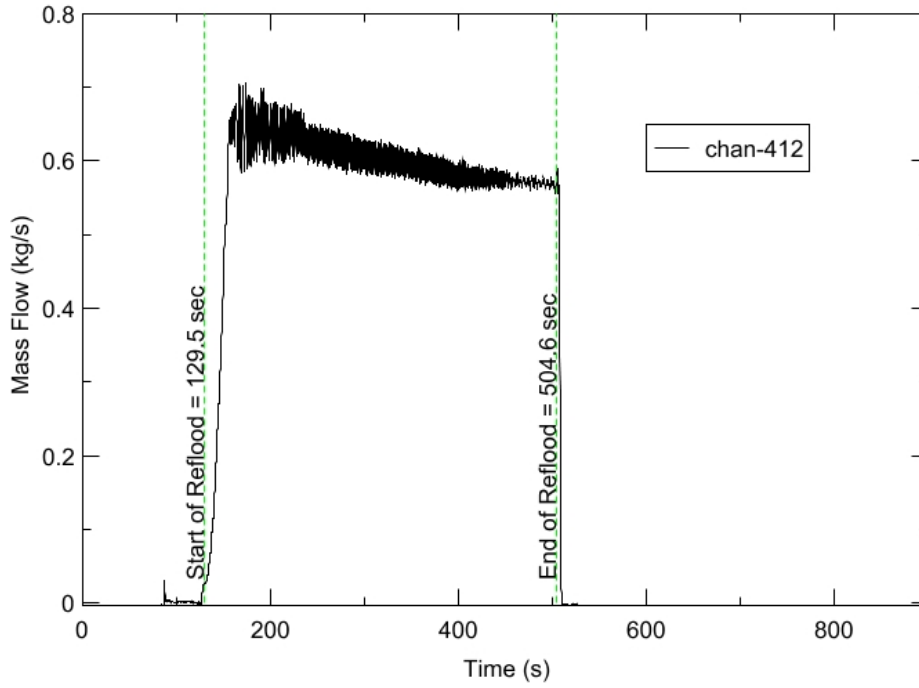
RBHT - TEST FACILITY

Upper Plenum Pressure vs. Time, Exp 1160



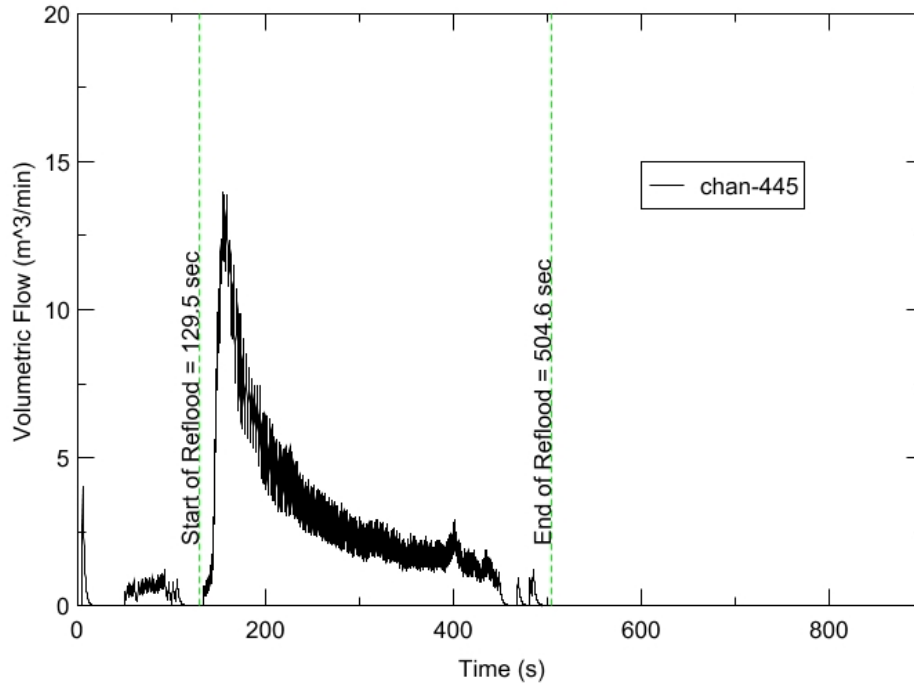
RBHT - TEST FACILITY

Inlet Flow vs. Time, Exp 1160



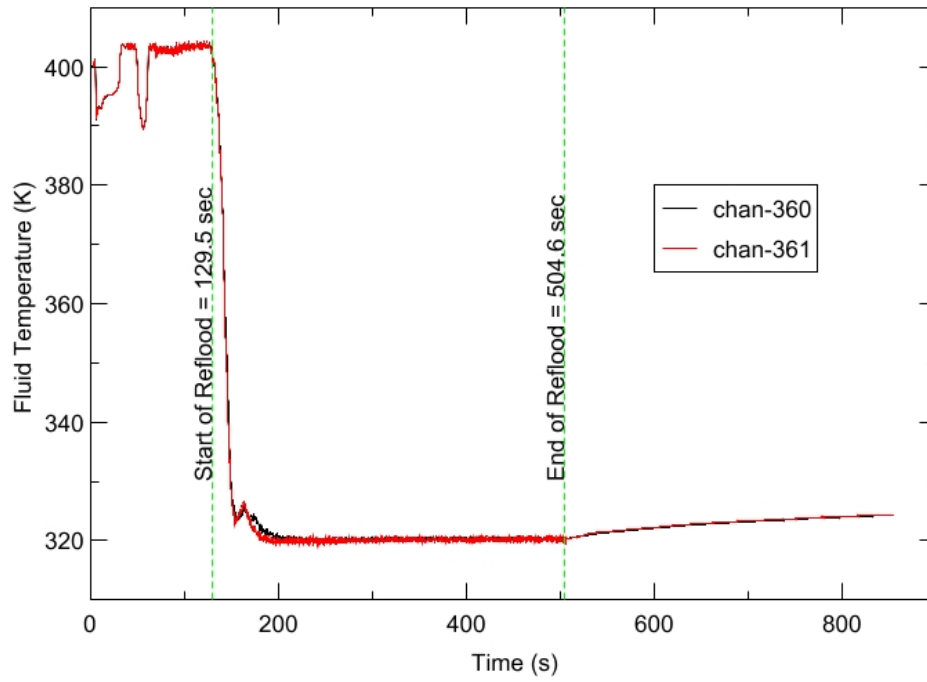
RBHT - TEST FACILITY

Steam Exhaust Flow vs. Time, Exp 1160



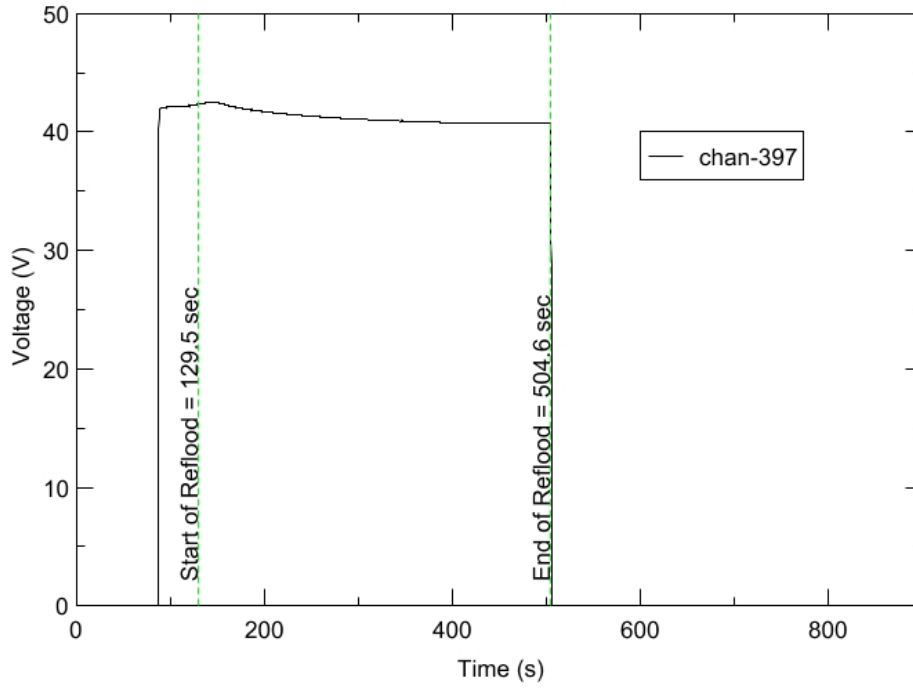
RBHT - TEST FACILITY

Inlet Flow Temperature vs. Time, Exp 1160



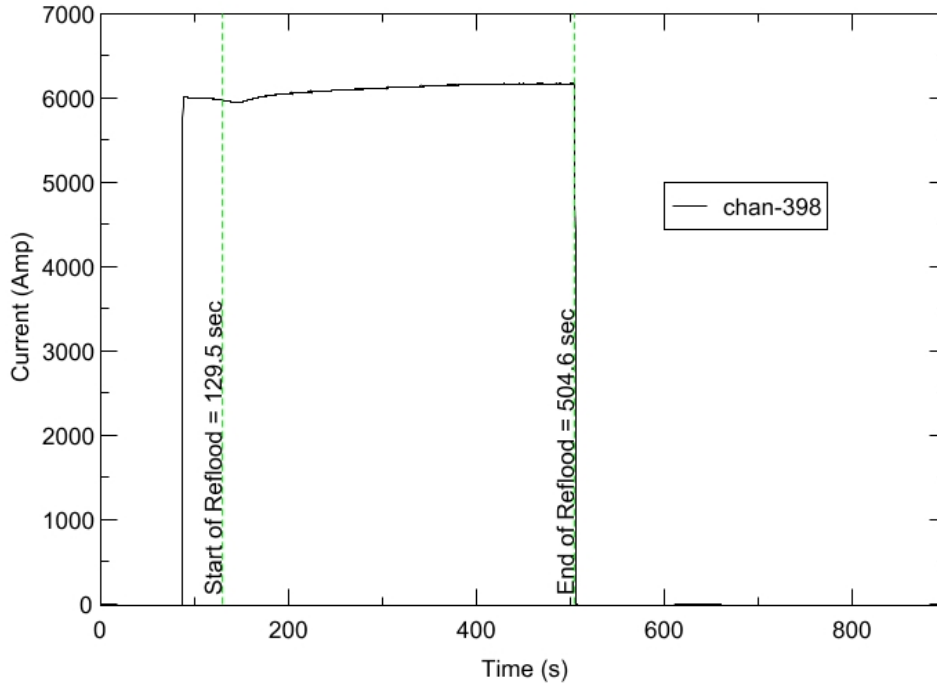
RBHT - TEST FACILITY

Test Section Voltage vs. Time, Exp 1160

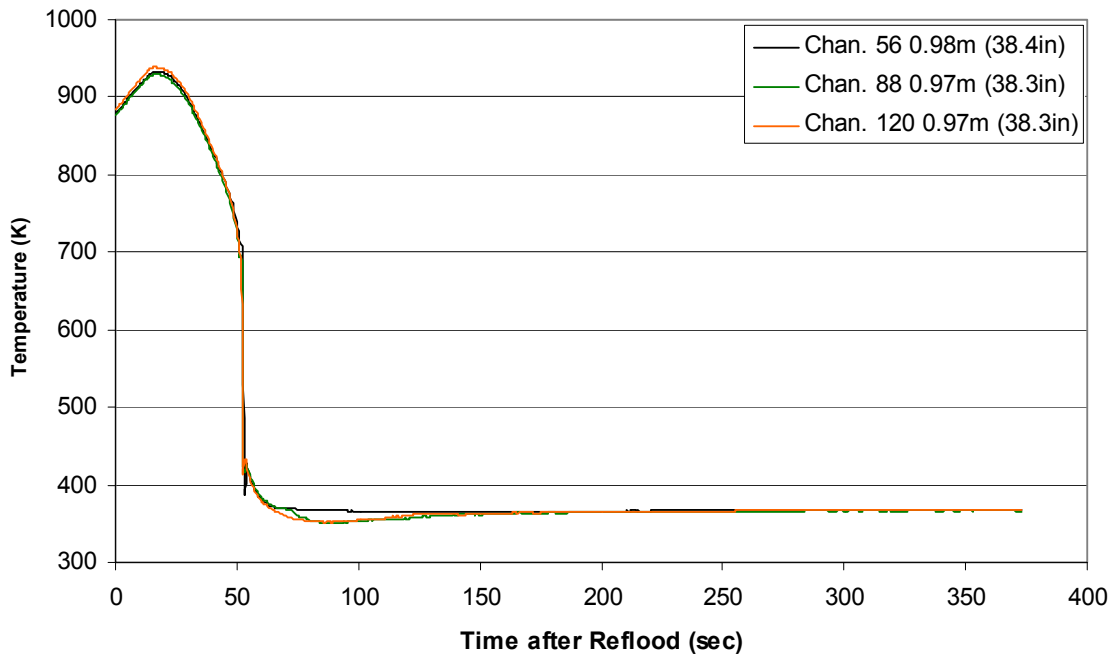


RBHT - TEST FACILITY

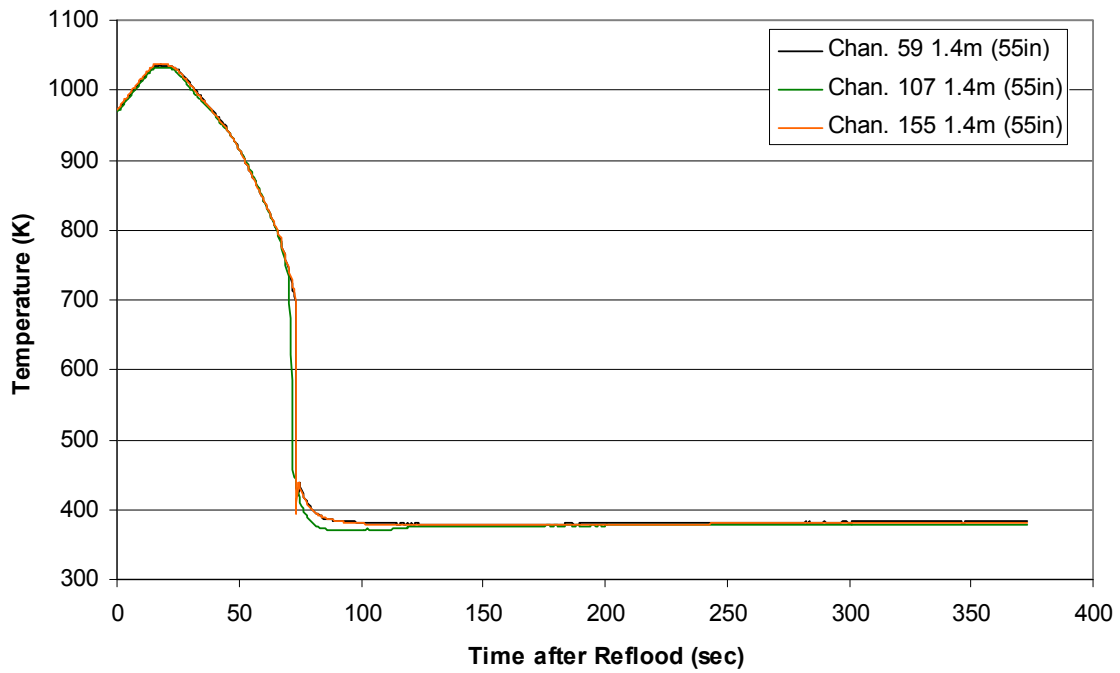
Test Section Current vs. Time, Exp 1160



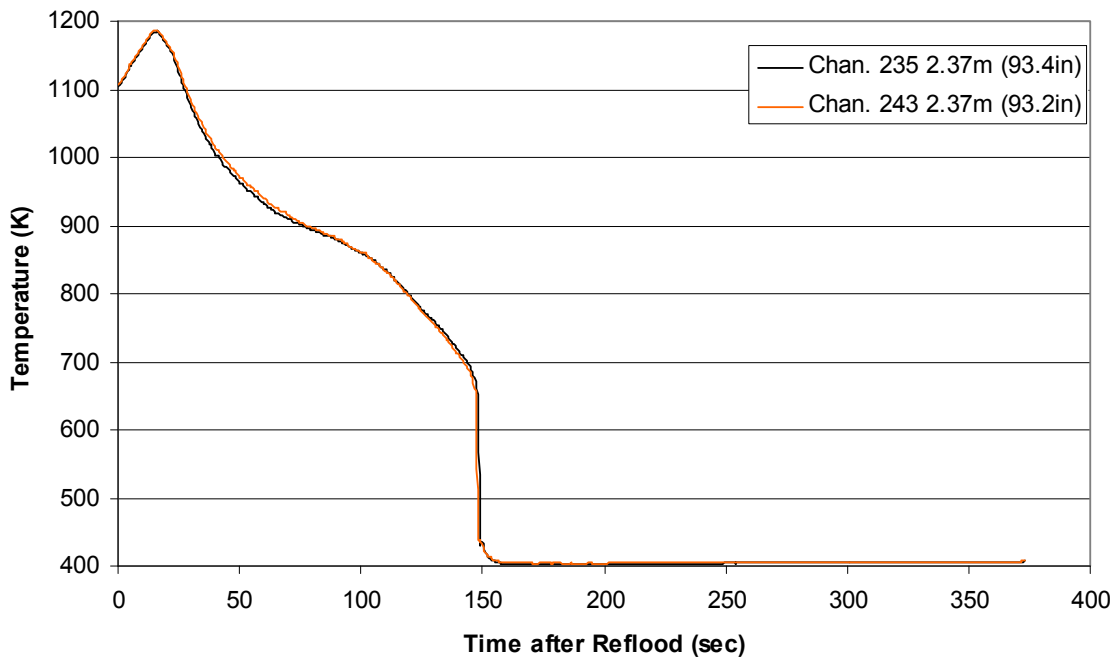
**Heater Rod Temperature during Reflood
RBHT Exp. 1160**



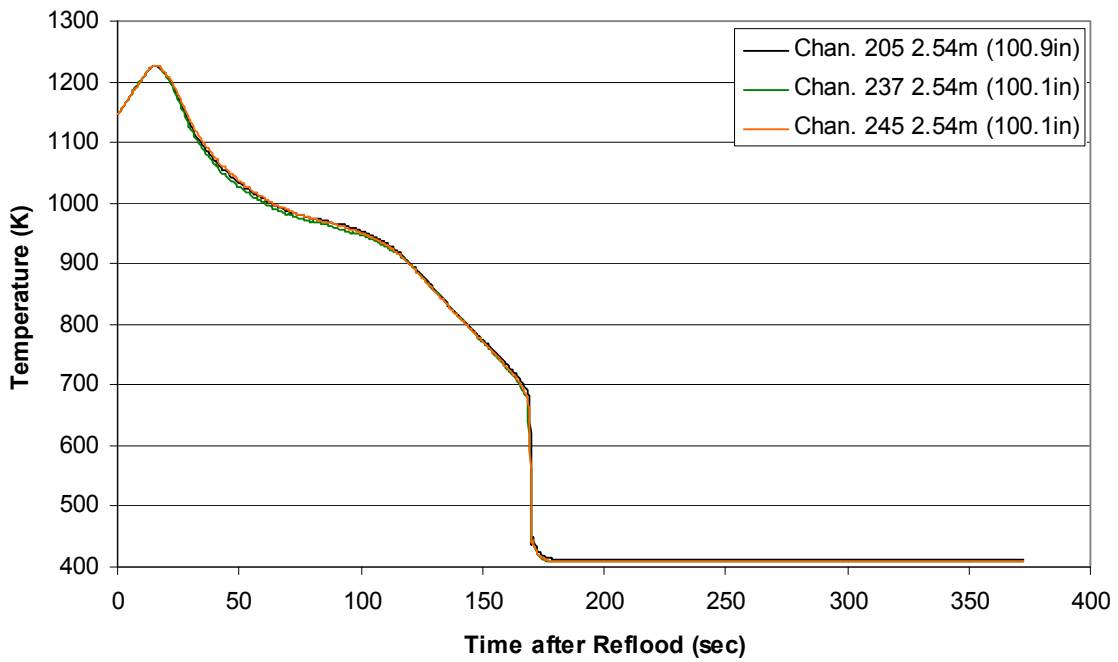
**Heater Rod Temperature during Reflood
RBHT Exp. 1160**



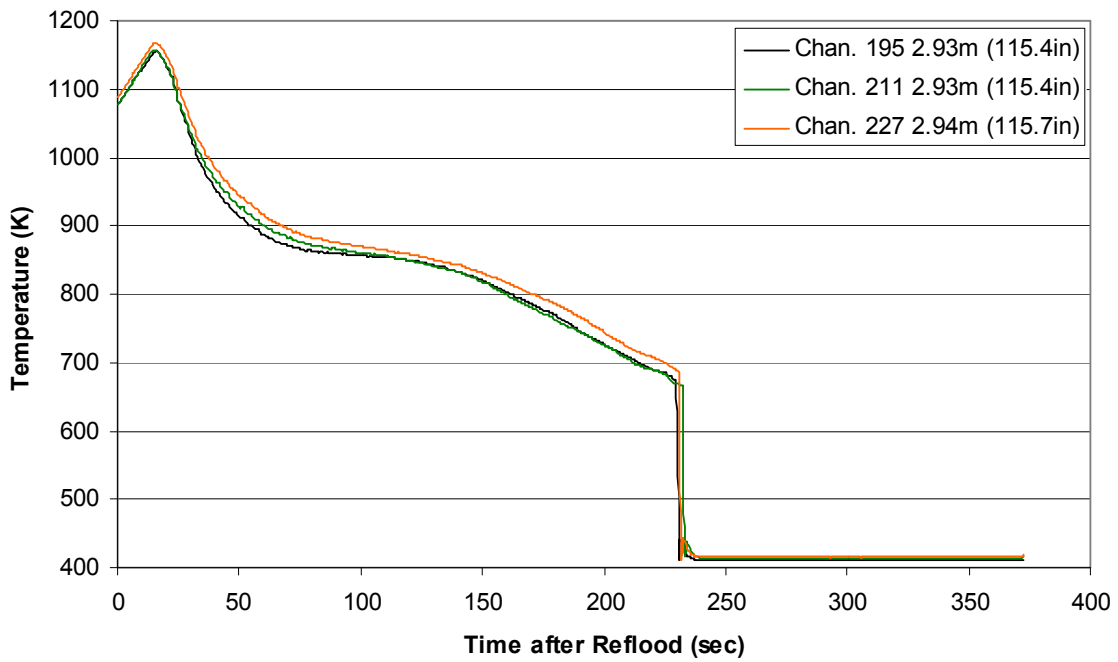
**Heater Rod Temperature during Reflood
RBHT Exp. 1160**



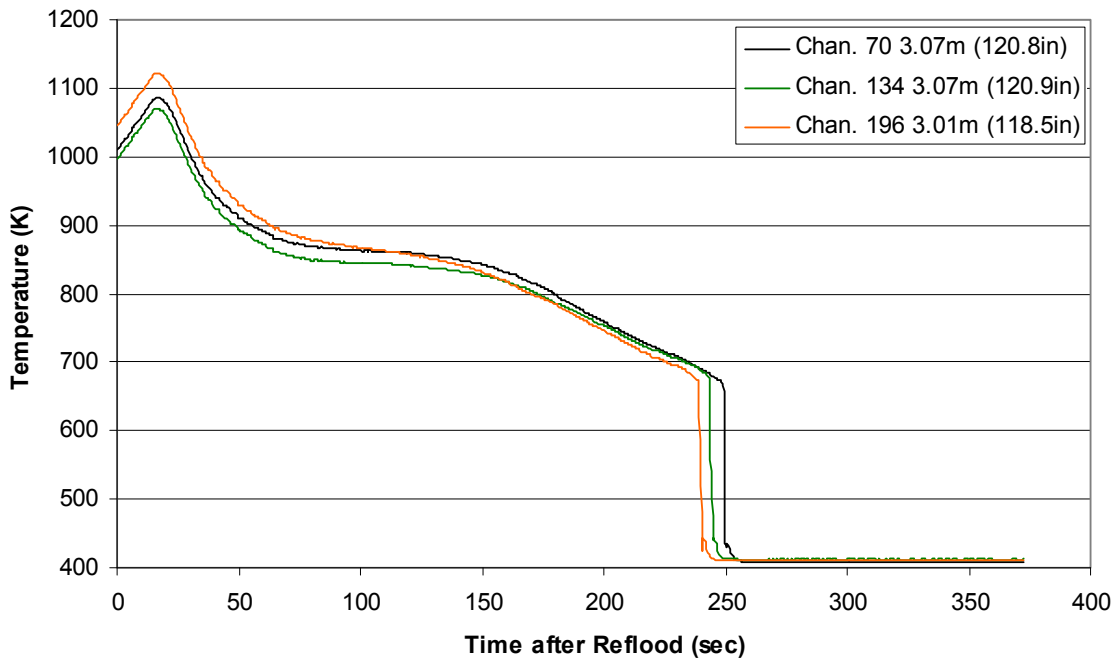
**Heater Rod Temperature during Reflood
RBHT Exp. 1160**



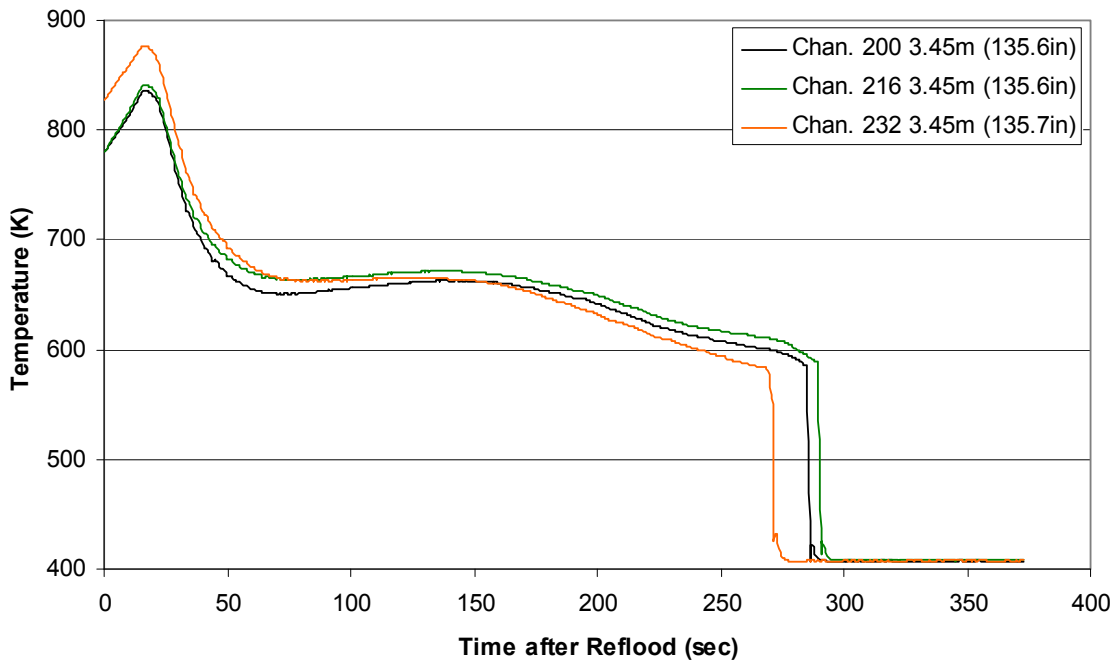
**Heater Rod Temperature during Reflood
RBHT Exp. 1160**



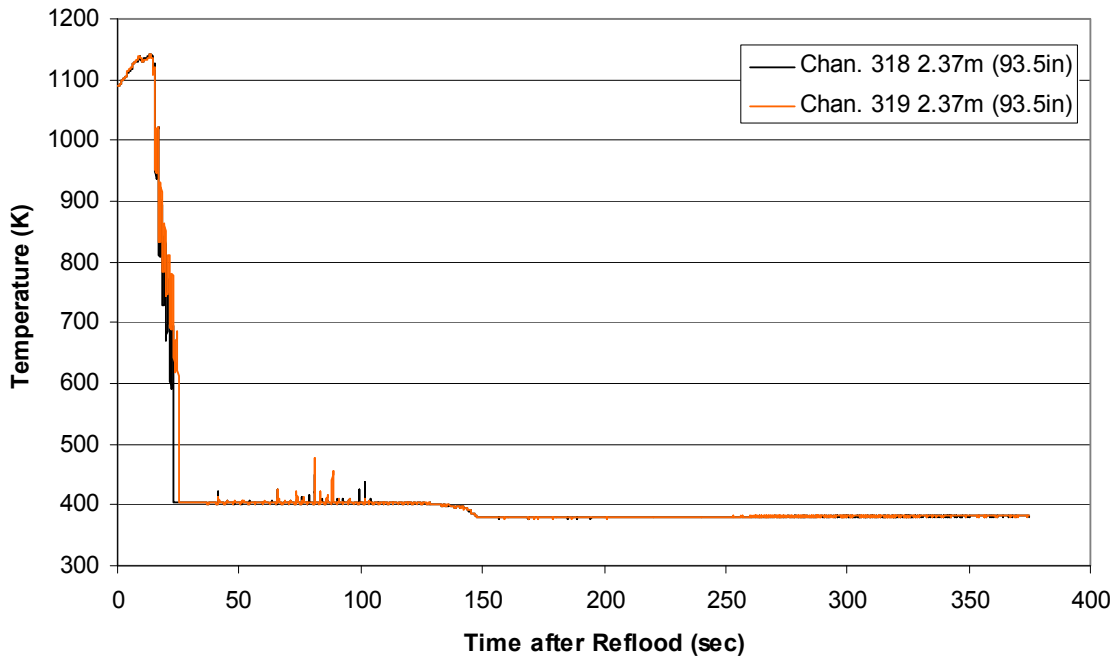
**Heater Rod Temperature during Reflood
RBHT Exp. 1160**



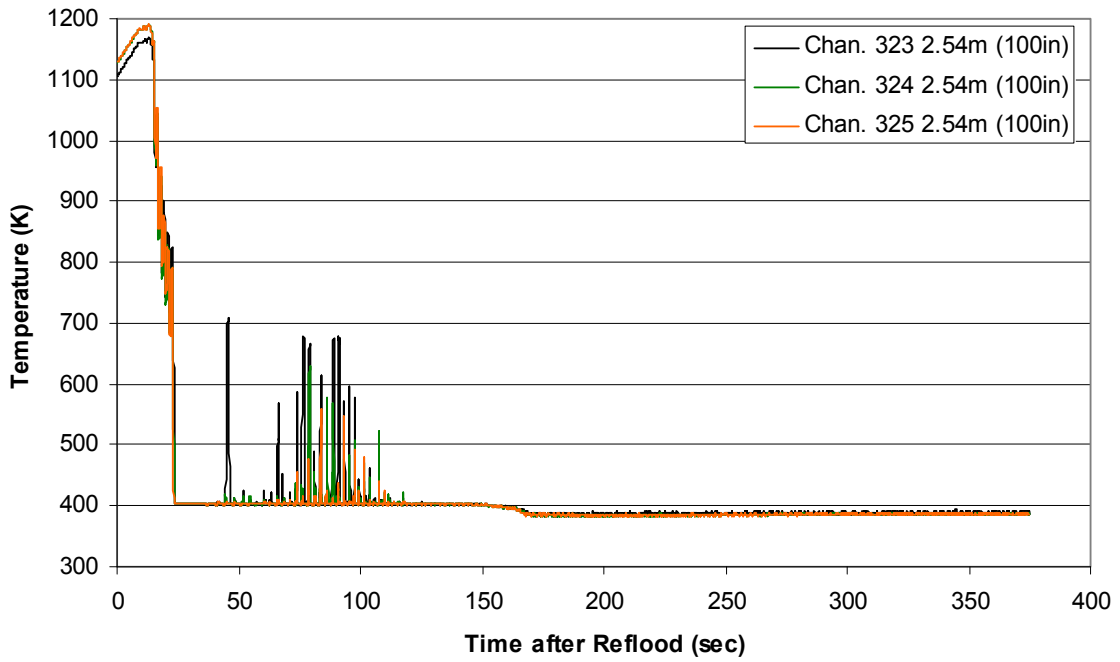
Heater Rod Temperature during Reflood RBHT Exp. 1160



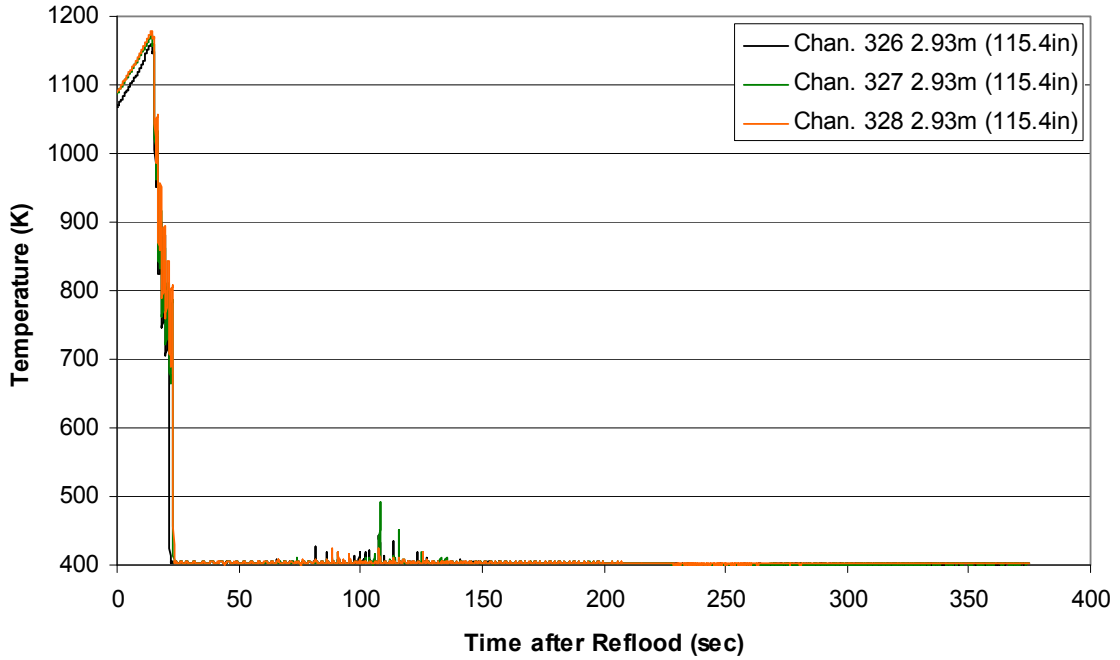
Steam Probe Temperature during Reflood RBHT Exp. 1160



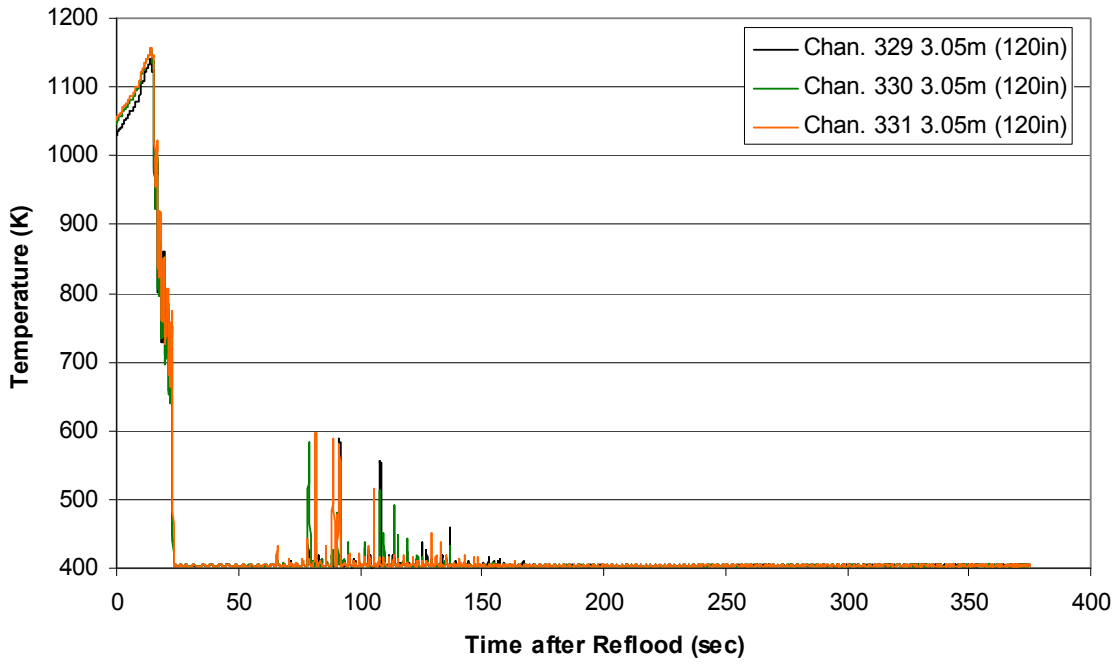
Steam Probe Temperature during Reflood
RBHT Exp. 1160



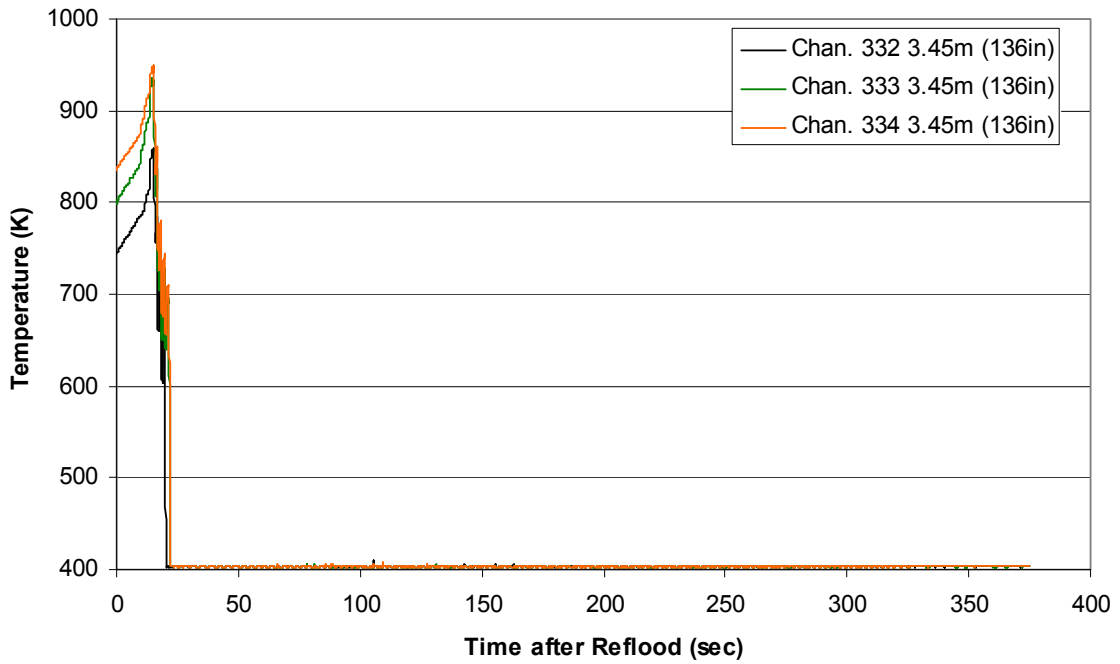
Steam Probe Temperature during Reflood
RBHT Exp. 1160



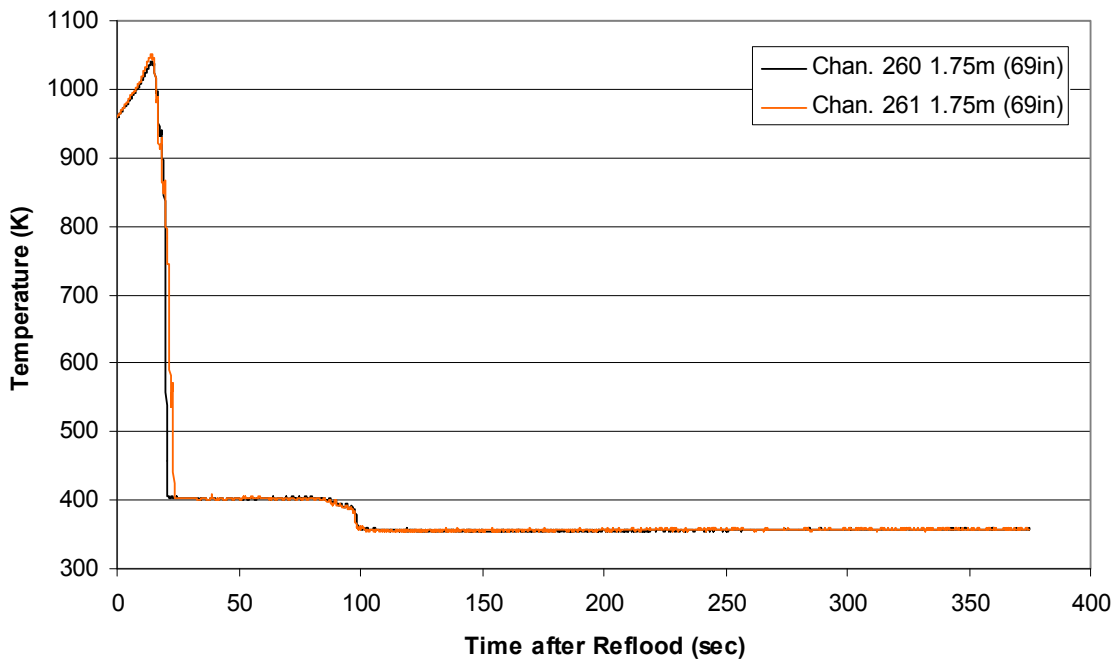
Steam Probe Temperature during Reflood
RBHT Exp. 1160



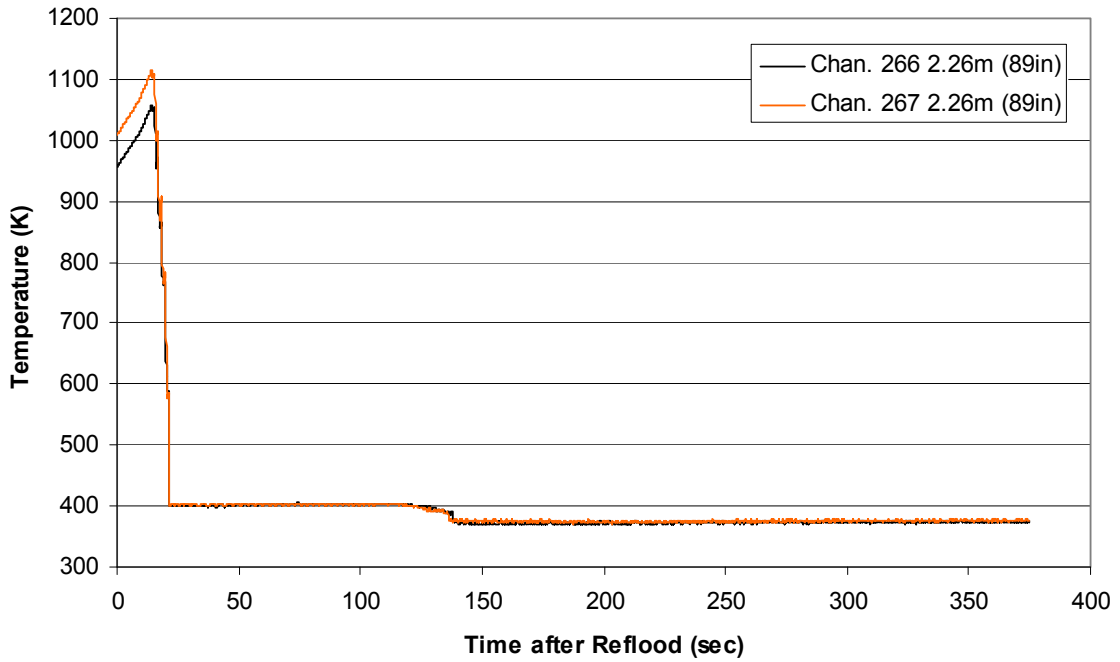
Steam Probe Temperature during Reflood
RBHT Exp. 1160



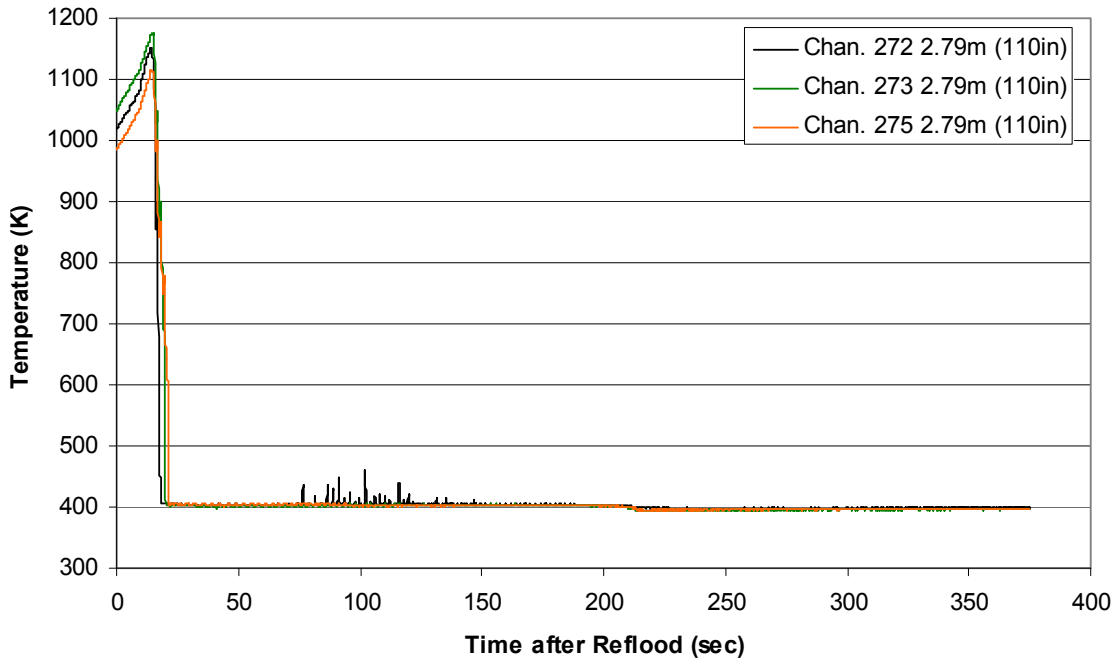
Spacer Grid Temperature during Reflood RBHT Exp. 1160



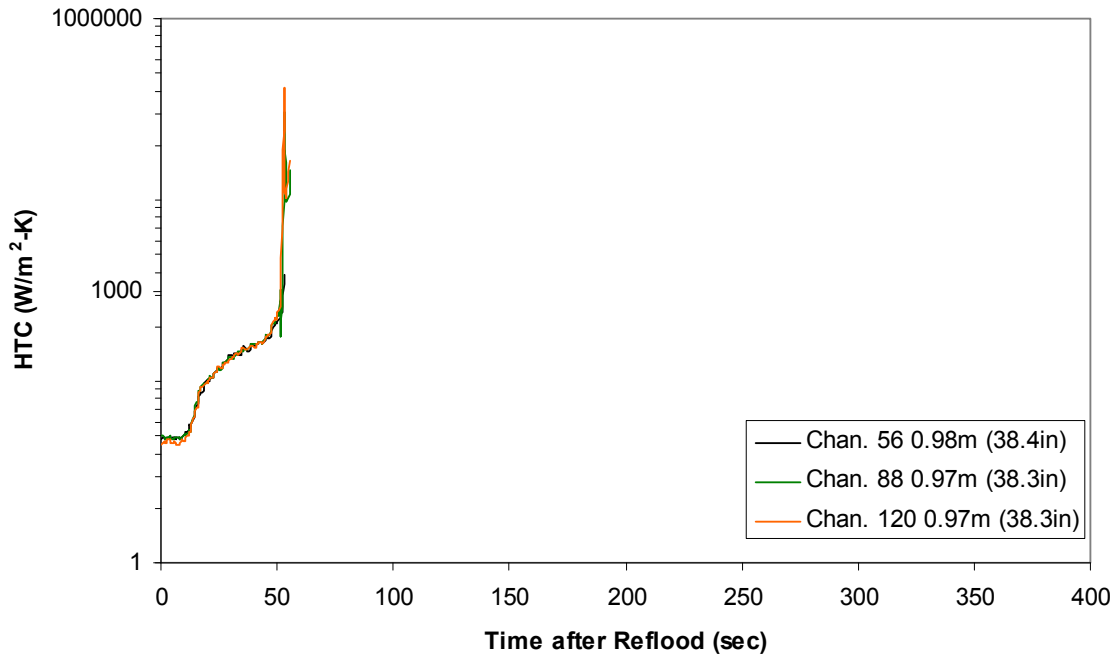
Spacer Grid Temperature during Reflood RBHT Exp. 1160



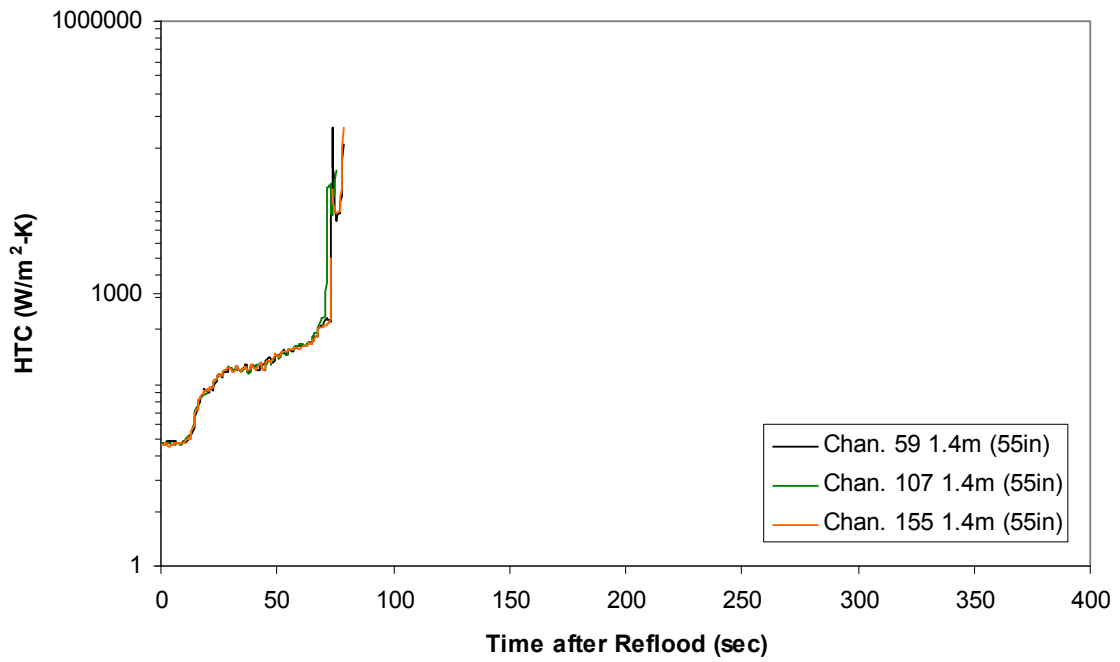
Spacer Grid Temperature during Reflood RBHT Exp. 1160



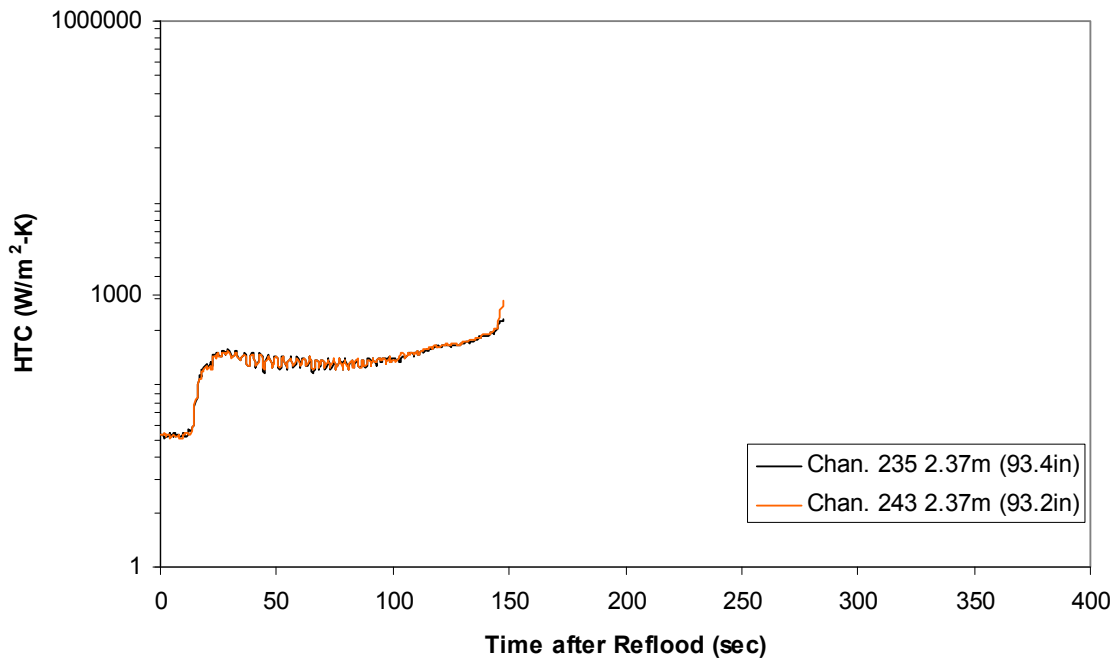
Heat Transfer Coefficient during Reflood RBHT Exp. 1160



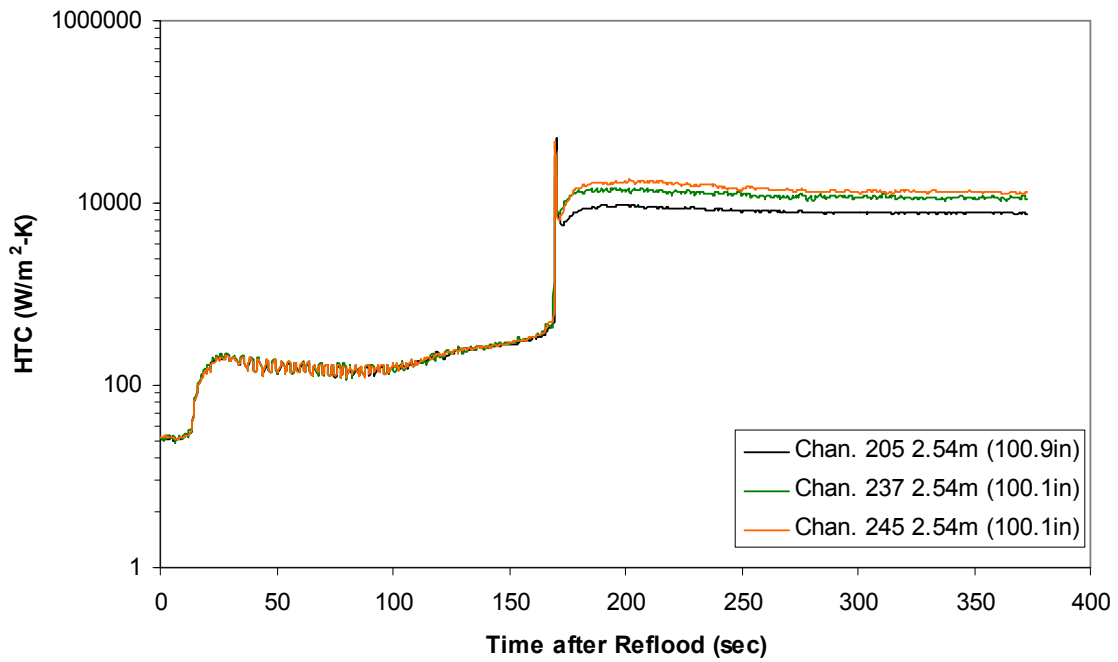
Heat Transfer Coefficient during Reflood
RBHT Exp. 1160



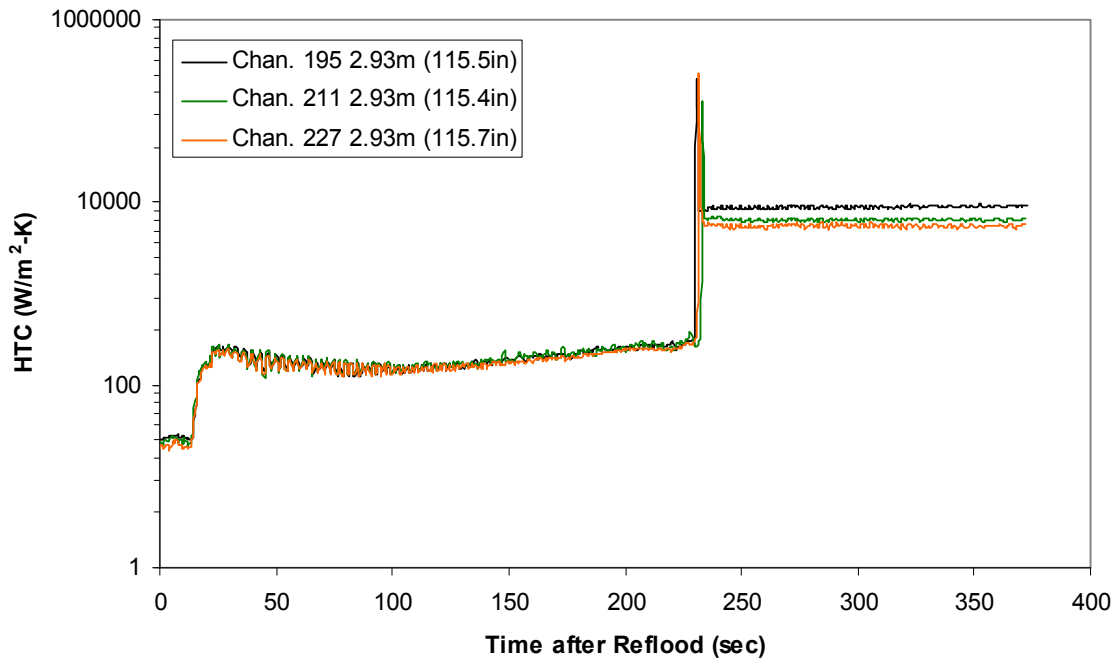
Heat Transfer Coefficient during Reflood
RBHT Exp. 1160



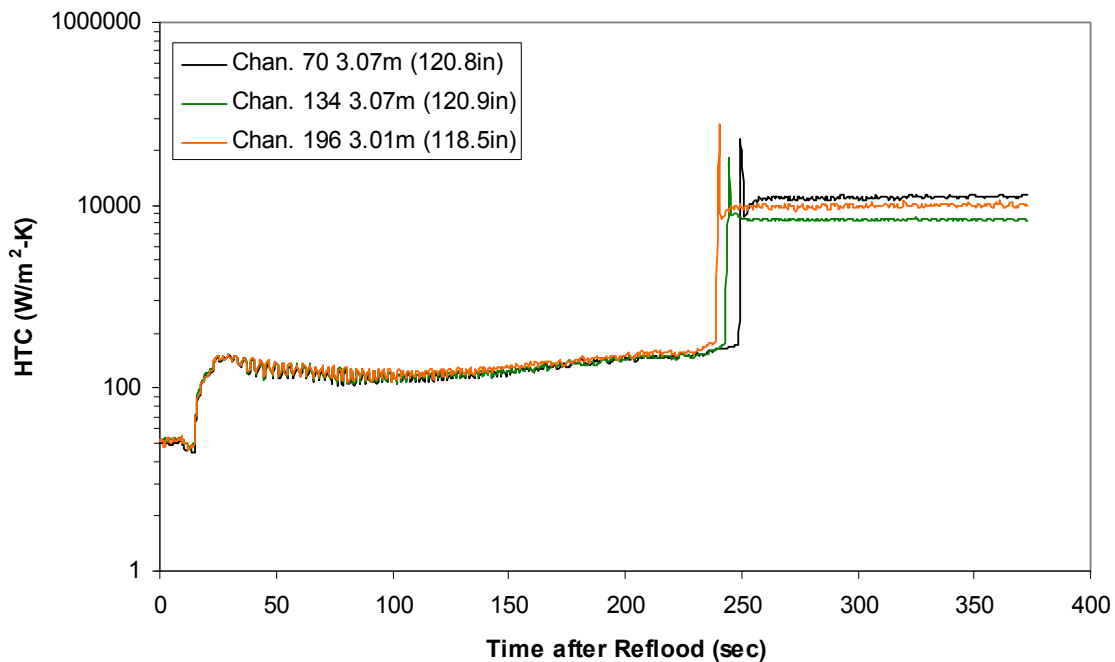
Heat Transfer Coefficient during Reflood RBHT Exp. 1160



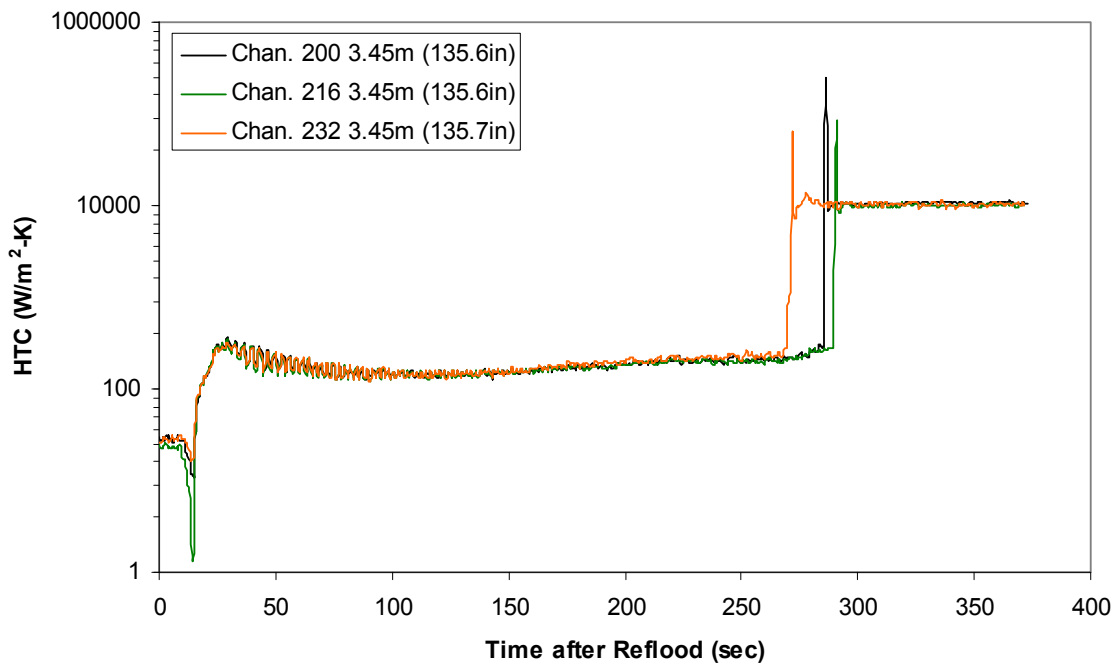
Heat Transfer Coefficient during Reflood RBHT Exp. 1160



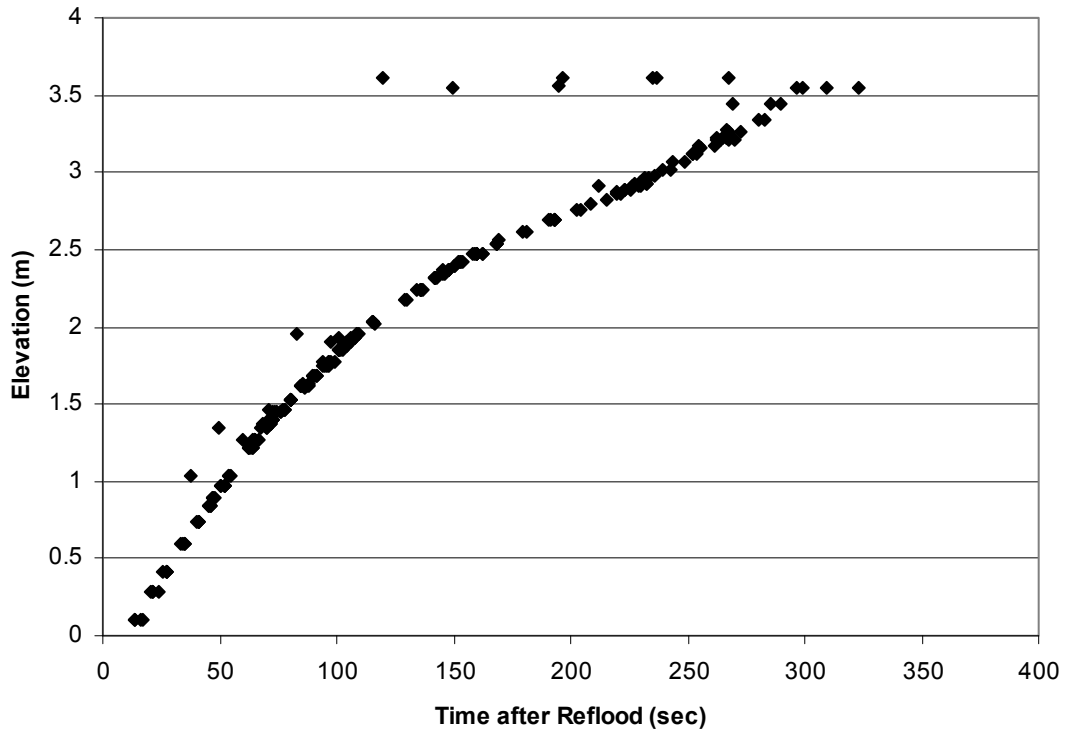
Heat Transfer Coefficient during Reflood RBHT Exp. 1160



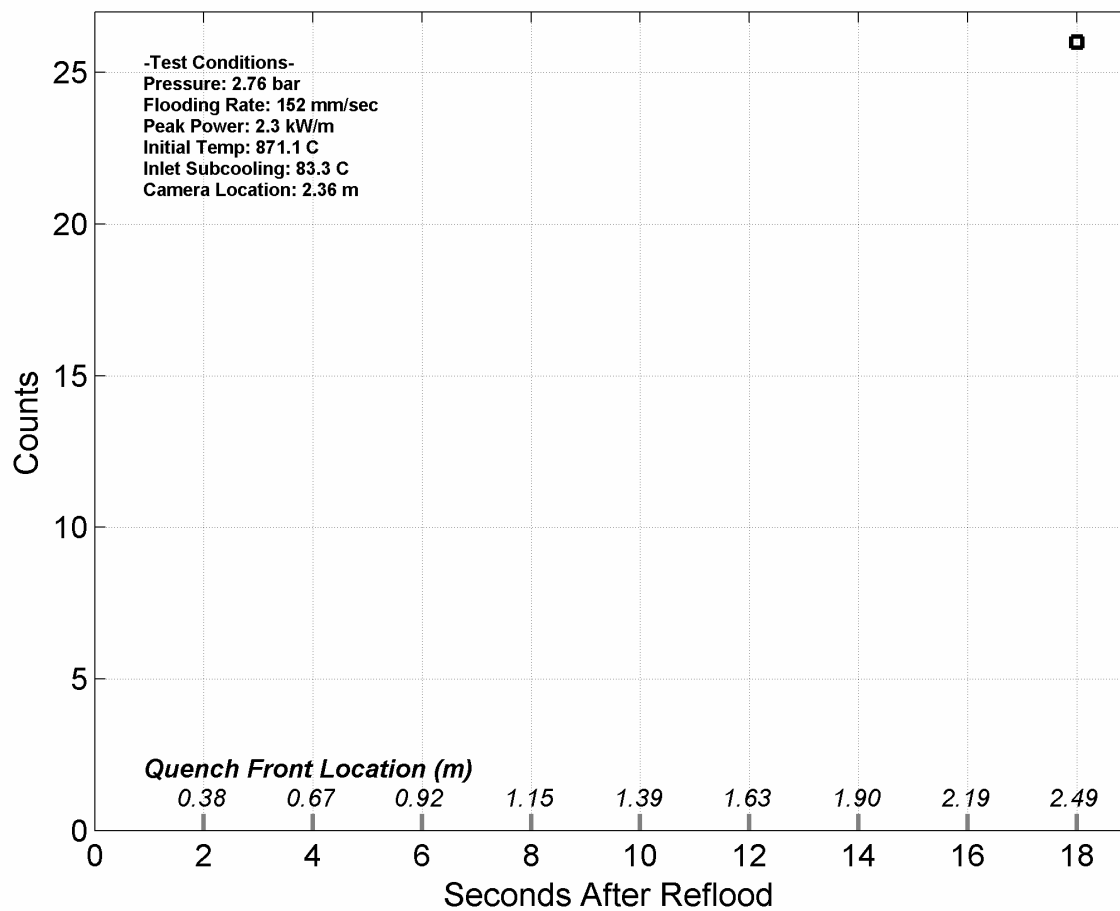
Heat Transfer Coefficient during Reflood RBHT Exp. 1160



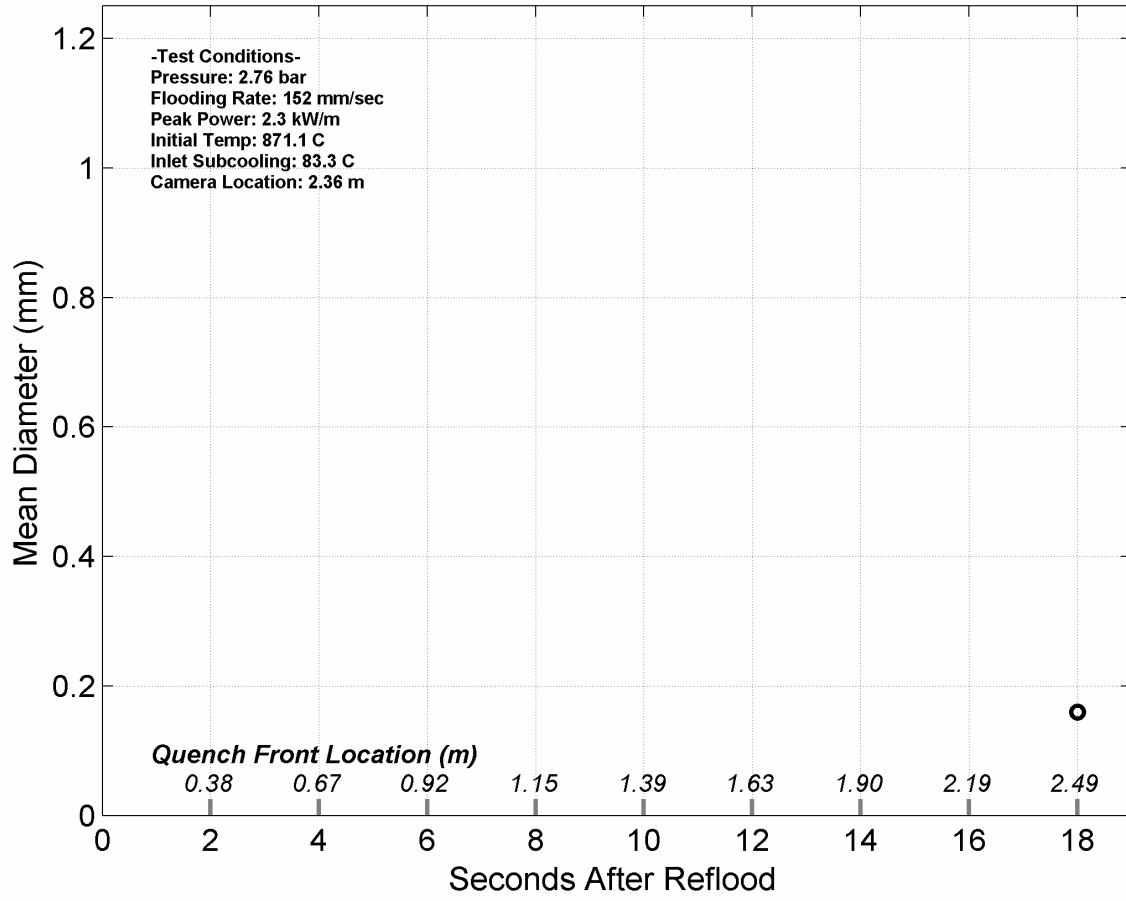
Quench Data, RBHT Exp. 1160



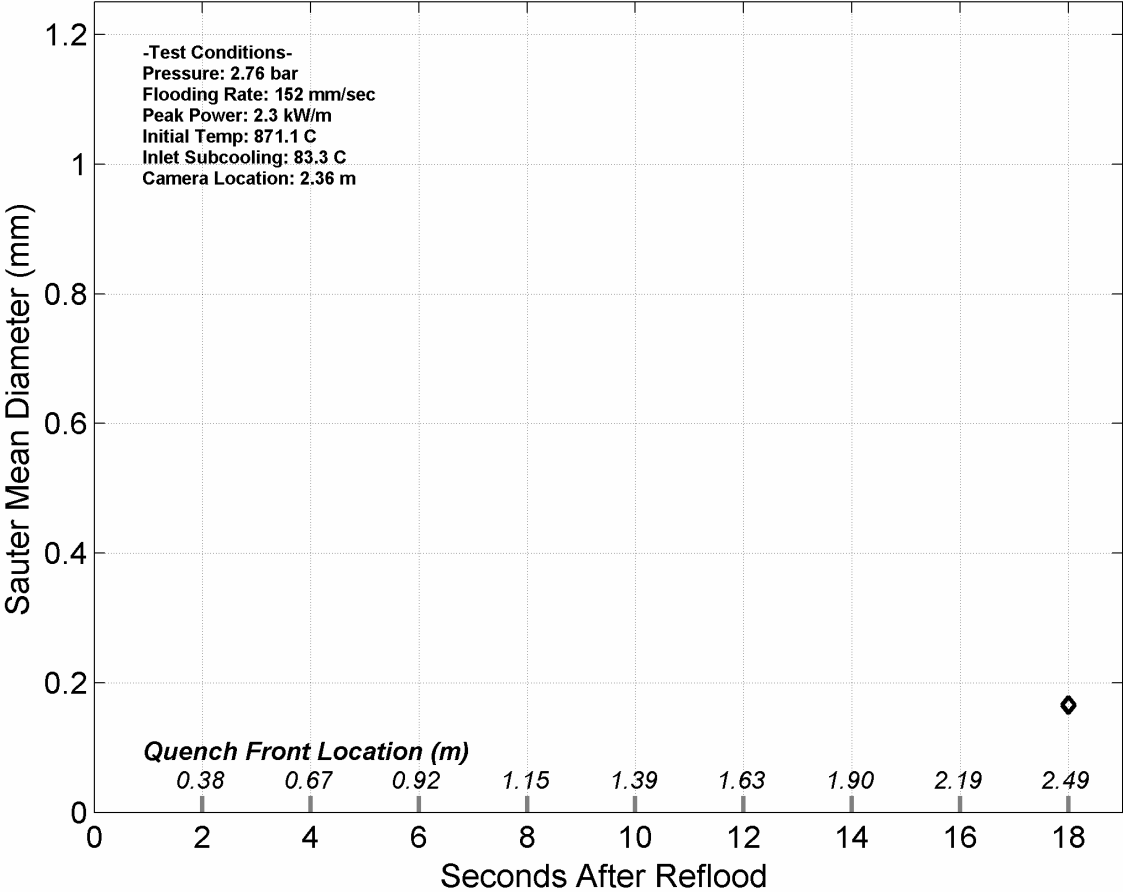
Droplet Counts - Exp. 1160



Mean Droplet Diameter - Exp. 1160



Droplet Sauter Mean Diameter - Exp. 1160



RBHT - REFLOOD TESTS

SUMMARY SHEET

RUN NO: **1170**

RUN CONDITIONS

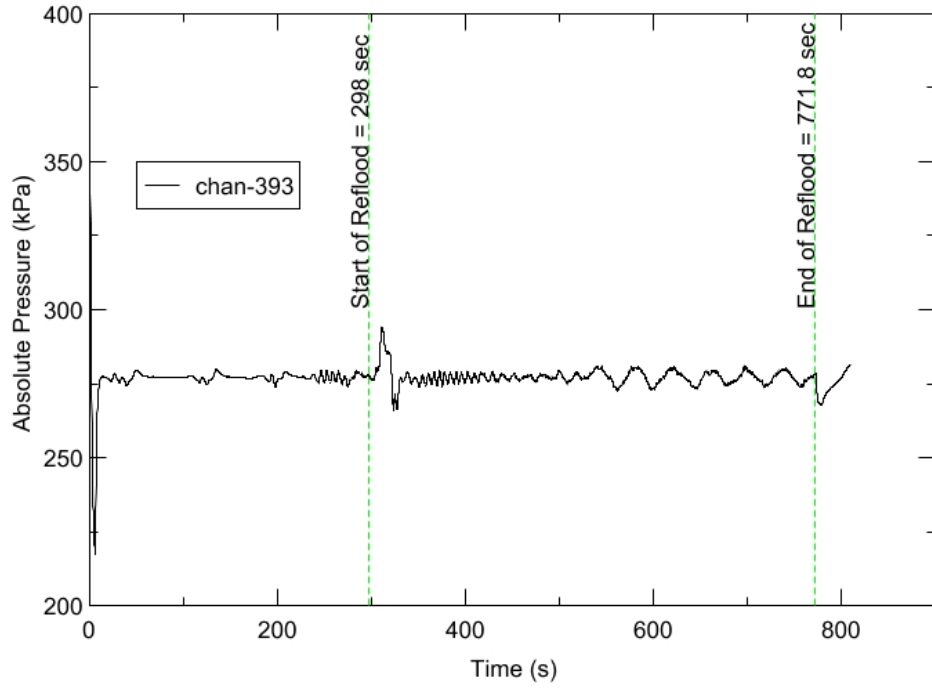
Upper Plenum Pressure:	276 kPa (40 psia)
Initial Peak Clad Temperature:	1144 degrees K (1600 degrees F)
Rod Peak Power:	2.3 kW/m (0.7 kW/ft)
Flooding Rate:	0.1524 m/s (6 in/s)
Inlet Subcooling:	11 degrees K (20 degrees F)
Start of Reflood:	298 s
End of Reflood:	771.8 s
Test Date:	6/19/2002
Comments:	No droplet data

A heater rod surface (chan. 200) at 3.45 m (135.6 in) quenches to a temperature below saturation due to bottom reflood from subcooled liquid accumulation in the upper plenum. Therefore DATARH calculated heat transfer coefficients are not presented for this channel.

Rod_Elevation	Channel Number	Temperature at Reflood (K)	Temperature at Reflood (°F)	Turnaround Time (sec.)	Turnaround Temperature (K)	Turnaround Temperature (°F)	Quench Time (sec.)	Quench Temperature (K)	Quench Temperature (°F)
B6_0.592m	148	825.48	1026.17	8.75	851.96	1073.84	58.75	607.5	633.81
B6_0.744m	149	832.44	1038.7	10.25	864.3	1096.05	75.75	629.52	673.46
B6_0.846m	150	862.56	1092.92	10.25	896.68	1154.34	86.25	606.51	632.02
B6_0.897m	151	874.8	1114.95	10.75	910.37	1178.97	90.75	622.74	661.24
C6_1.04m	137	930.88	1215.89	11.25	970.1	1286.49	101.75	662.74	733.24
D5_1.27m	217	986.05	1315.2	11.75	1027.54	1389.88	126.75	631.07	676.24
C6_1.34m	138	975.74	1296.65	12.25	1021.93	1379.79	133.75	647.78	706.31
D5_1.37m	218	1009.13	1356.74	12.25	1055.06	1439.42	136.25	674.05	753.61
C6_1.39m	139	983.69	1310.95	12.75	1030.39	1395.02	139.25	655.06	719.41
D5_1.45m	219	1023.55	1382.69	12.25	1071.05	1468.21	143.75	674.54	754.49
C6_1.47m	140	998.61	1337.8	12.75	1046.3	1423.65	146.75	663.92	735.37
D5_1.52m	220	1037.25	1407.36	12.75	1086.58	1496.16	152.75	680.19	764.66
C6_1.62m	141	1021.86	1379.66	13.25	1073.26	1472.18	164.75	696.12	793.34
D5_1.68m	221	1058.62	1445.83	13.25	1111.11	1540.31	172.25	722.75	841.26
D5_1.78m	222	1043.92	1419.37	11.25	1093.16	1508	185.75	657.48	723.78
D5_1.85m	223	1069	1464.51	11.75	1120.6	1557.38	192.75	673.85	753.24
C6_1.87m	142	1048.68	1427.94	12.25	1102.81	1525.37	196.25	676.01	757.12
D5_1.90m	224	1076.69	1478.36	11.75	1130.7	1575.58	198.25	685.89	774.91
C6_1.95m	144	1056.63	1442.25	12.25	1111.76	1541.48	205.25	685.26	773.78
C3_2.17m	178	1095.23	1511.72	12.75	1156.39	1621.82	226.25	728.7	851.97
D4_2.24m	241	1096.23	1513.53	11.25	1153.61	1616.8	259.75	655.41	720.05
D4_2.32m	242	1118.36	1553.36	11.25	1175.36	1655.96	267.25	684.27	772
C3_2.35m	180	1109.57	1537.54	11.75	1168.8	1644.15	245.25	714.44	826.31
D4_2.37m	243	1127.21	1569.29	11.25	1186.28	1675.61	274.25	690.42	783.06
C3_2.40m	181	1114.65	1546.68	11.75	1175.2	1655.67	251.75	718.87	834.28
D4_2.54m	245	1170.6	1647.4	11.25	1229.64	1753.66	299.75	708.59	815.77
D6_2.62m	129	1166.43	1639.88	11.25	1226.61	1748.22	296.75	731.23	856.53
D6_2.69m	130	1169.91	1646.15	11.25	1232.15	1758.19	308.25	742.59	876.97
C3_2.76m	183	1172.97	1651.65	11.75	1235.68	1764.54	305.25	751.08	892.26
D4_2.79m	247	1153.08	1615.85	10.75	1212.68	1723.13	339.75	670.6	747.39
D6_2.87m	131	1123.6	1562.78	10.25	1178.73	1662.03	330.75	667.12	741.13
D6_2.92m	132	1102.6	1524.99	11.75	1162.76	1633.28	337.25	689.66	781.7
D6_2.97m	133	1076.53	1478.07	11.75	1133.08	1579.85	344.25	681.21	766.49
D6_3.07m	134	1043.11	1417.91	11.75	1095.76	1512.69	352.75	666.47	739.96
E3_3.12m	197	1032.57	1398.94	11.75	1083.91	1491.34	361.75	663.92	735.37
D6_3.17m	135	1005.87	1350.88	11.75	1054.87	1439.09	361.75	651.84	713.62
D6_3.27m	136	961.46	1270.94	12.25	1009.25	1356.96	369.75	621.38	658.79
D4_3.61m	248	755.58	900.36	13.25	804.23	987.92	52.25	574.18	573.84

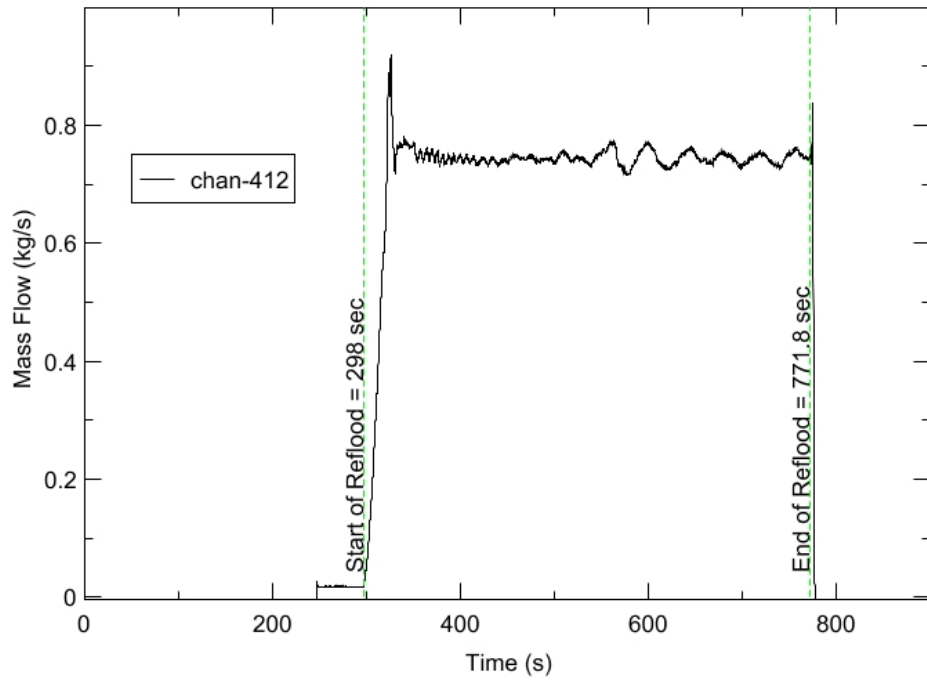
RBHT - TEST FACILITY

Upper Plenum Pressure vs. Time, Exp 1170



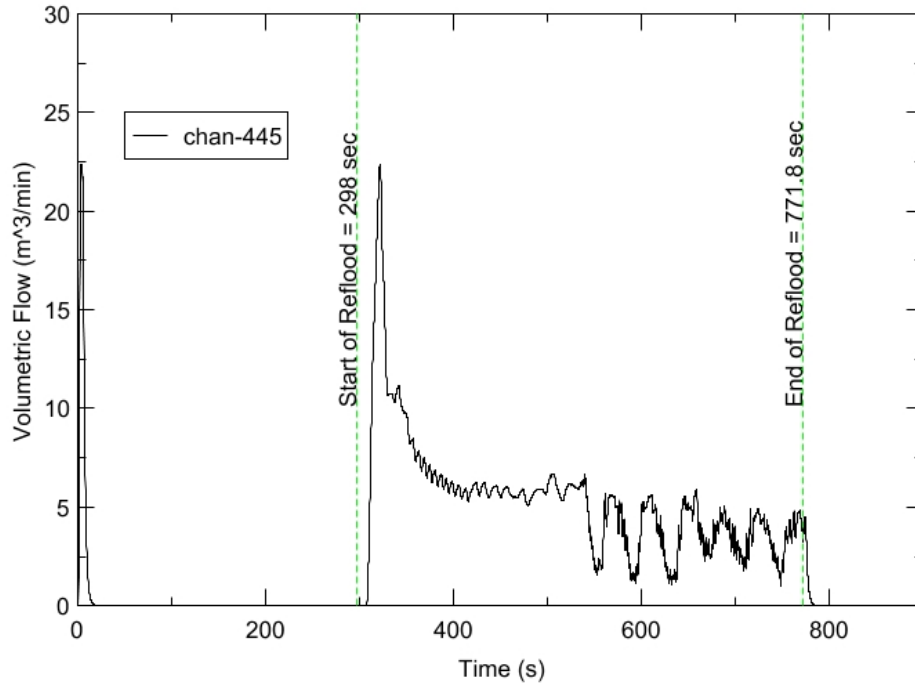
RBHT - TEST FACILITY

Inlet Flow vs. Time, Exp 1170



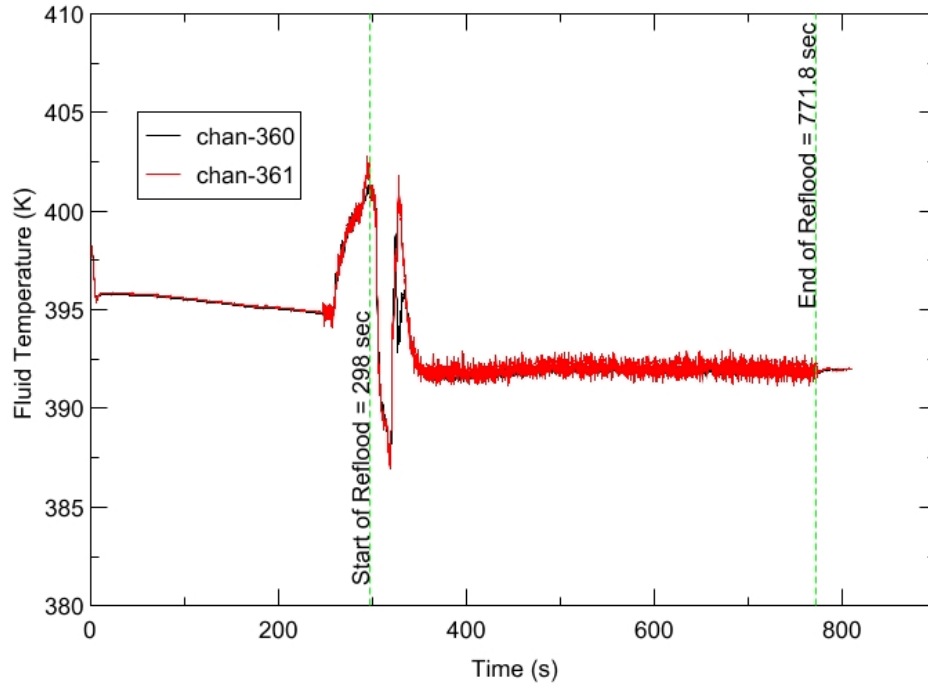
RBHT - TEST FACILITY

Steam Exhaust Flow vs. Time, Exp 1170



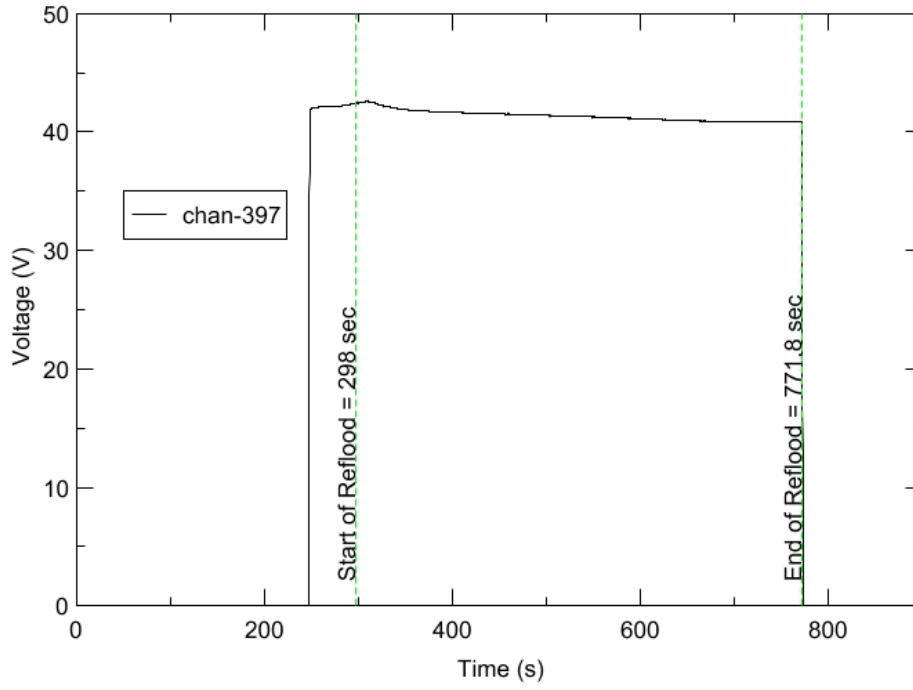
RBHT - TEST FACILITY

Inlet Flow Temperature vs. Time, Exp 1170



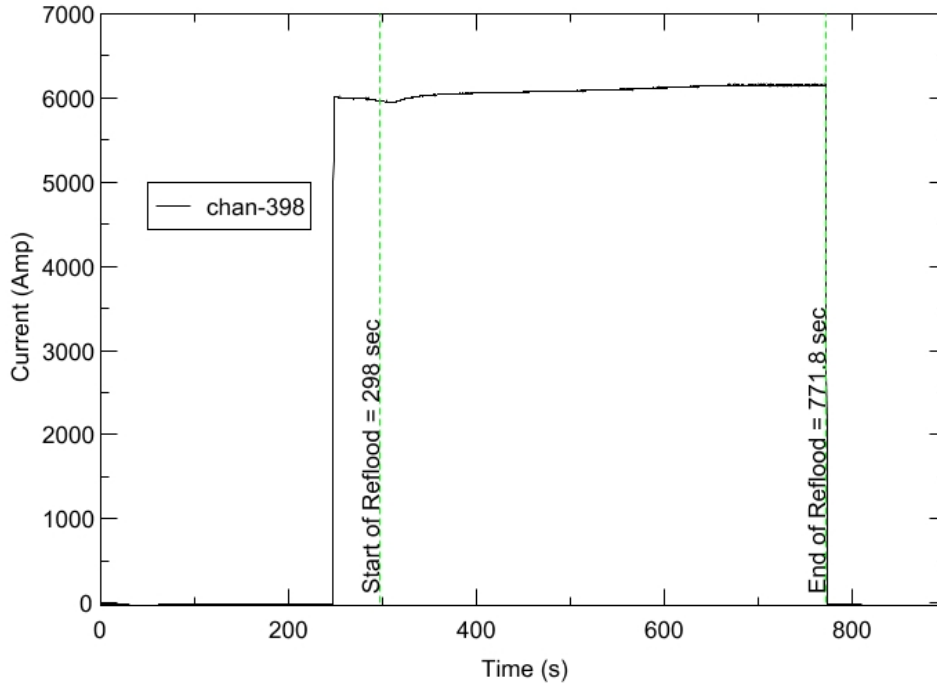
RBHT - TEST FACILITY

Test Section Voltage vs. Time, Exp 1170

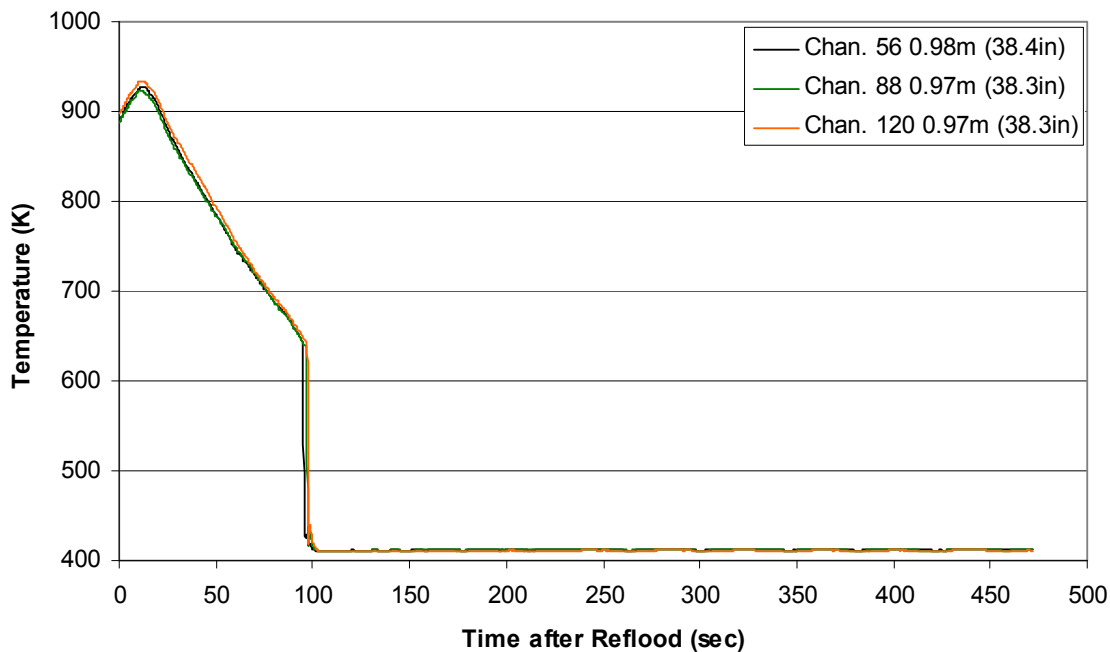


RBHT - TEST FACILITY

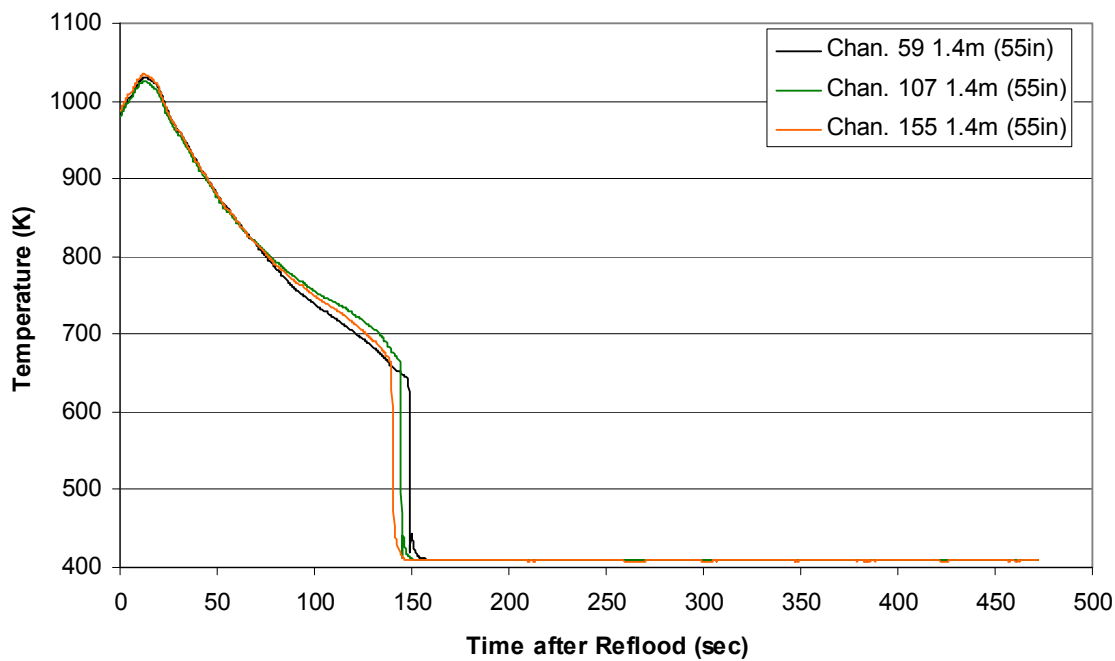
Test Section Current vs. Time, Exp 1170



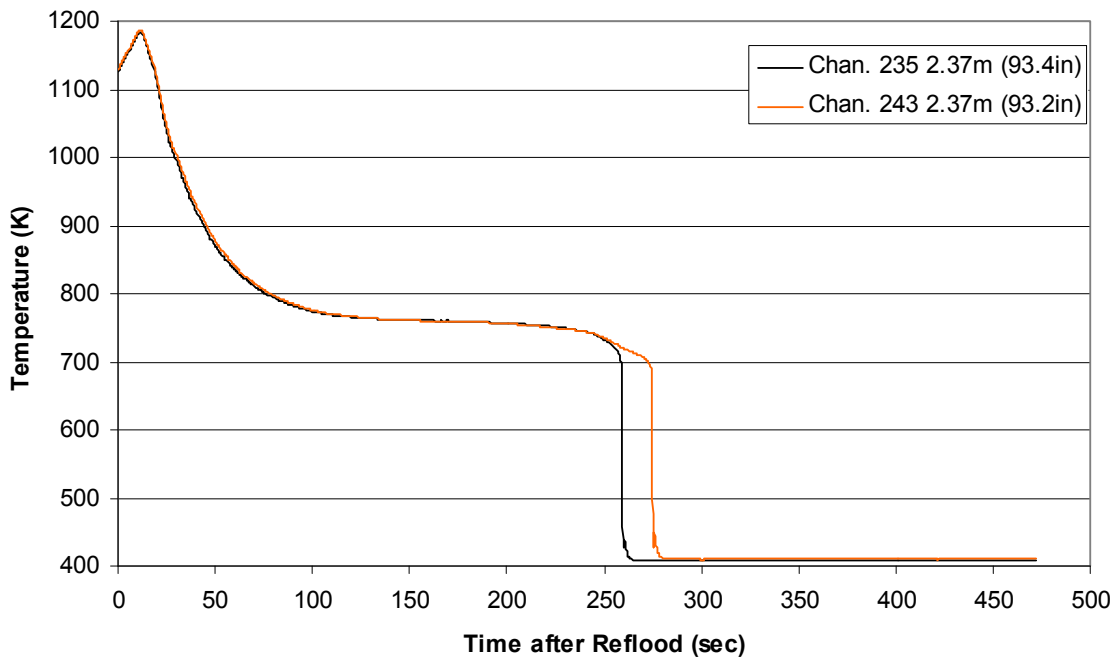
Heater Rod Temperature during Reflood RBHT Exp. 1170



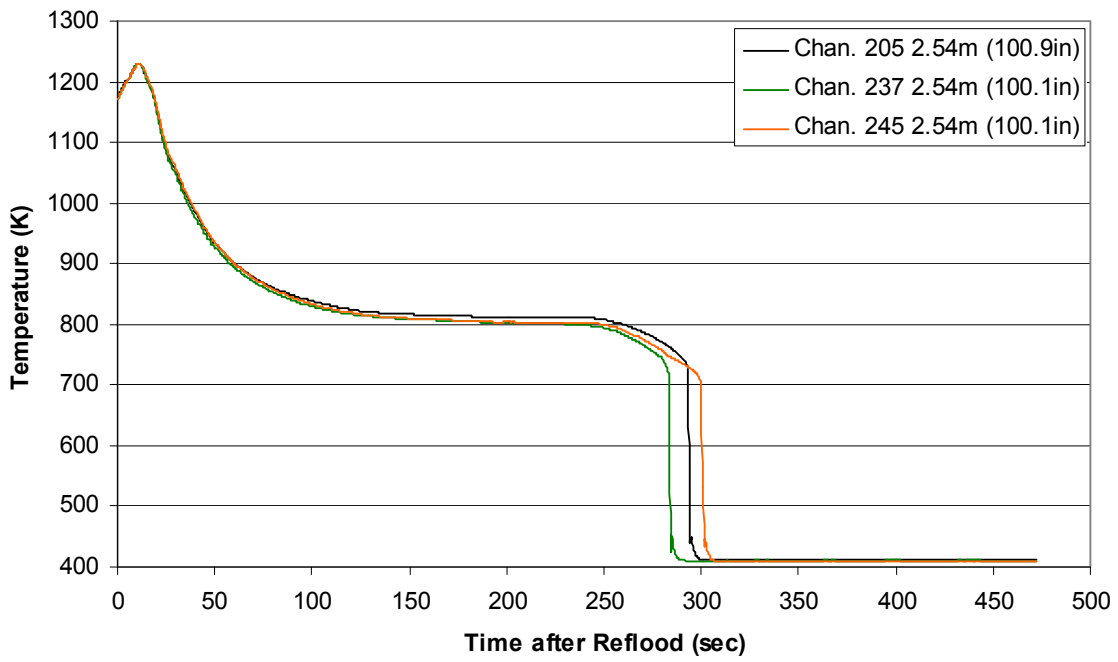
Heater Rod Temperature during Reflood RBHT Exp. 1170



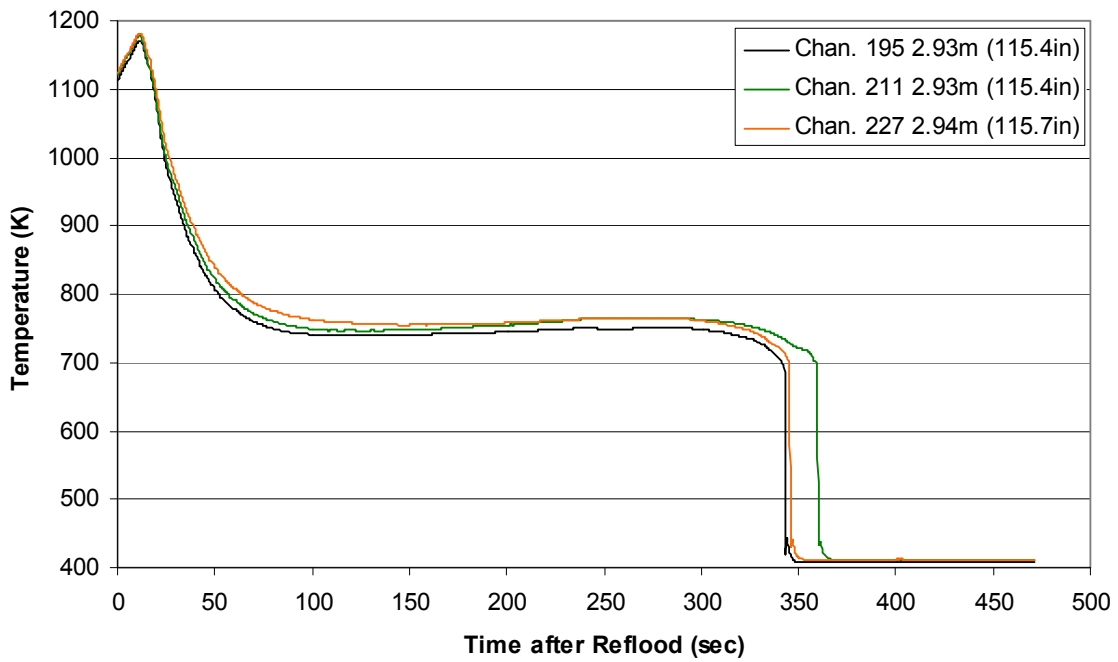
Heater Rod Temperature during Reflood
RBHT Exp. 1170



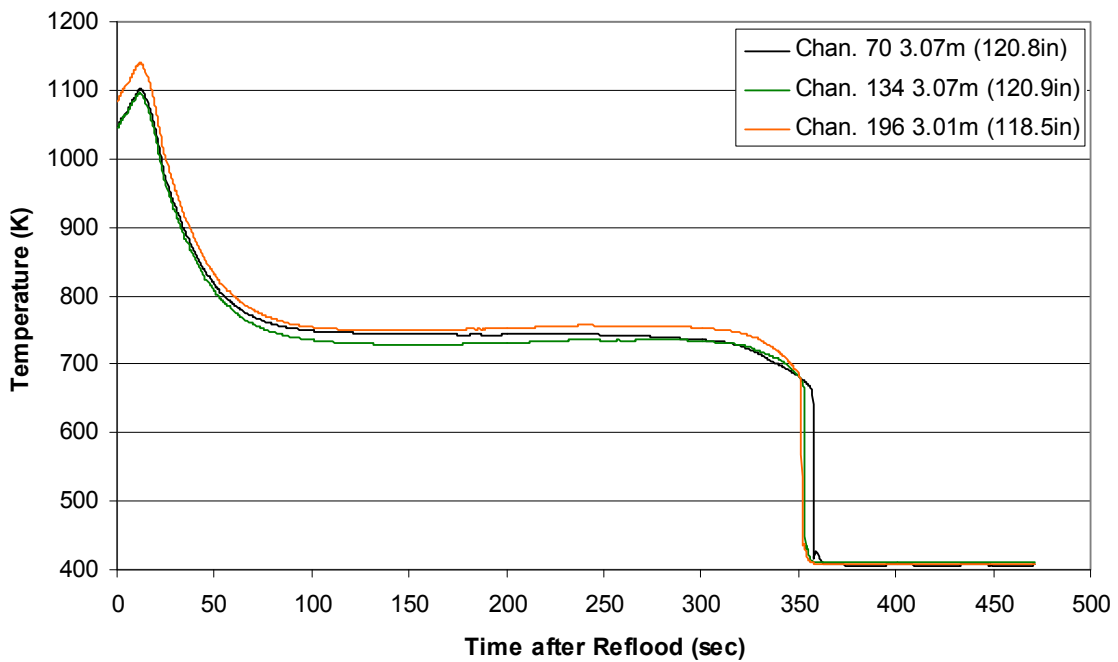
Heater Rod Temperature during Reflood
RBHT Exp. 1170



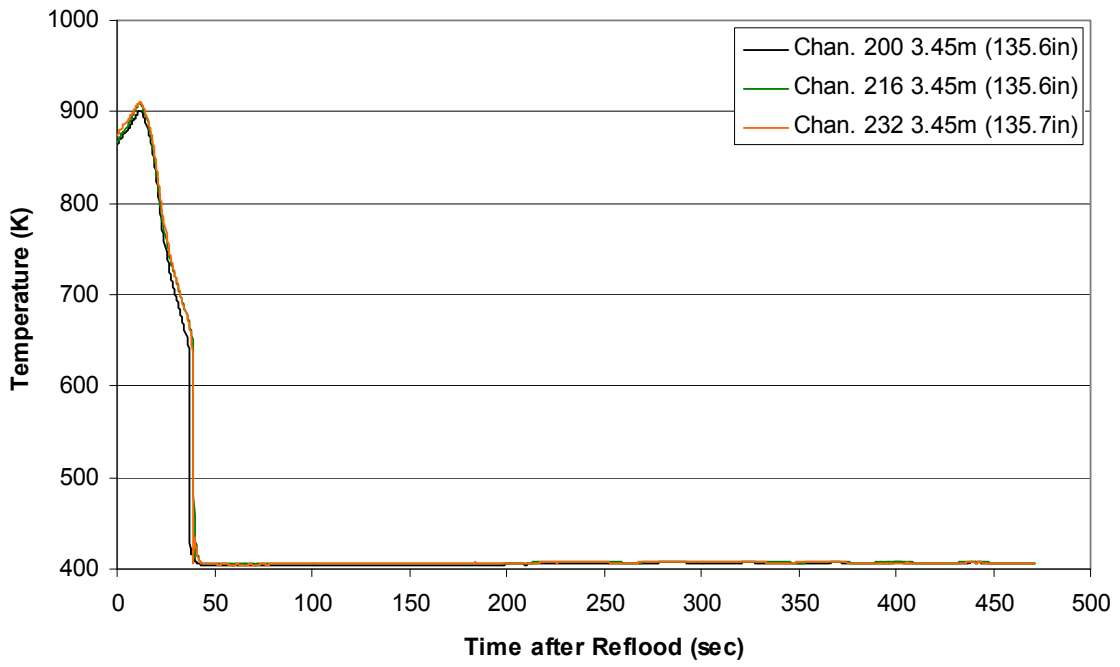
Heater Rod Temperature during Reflood
RBHT Exp. 1170



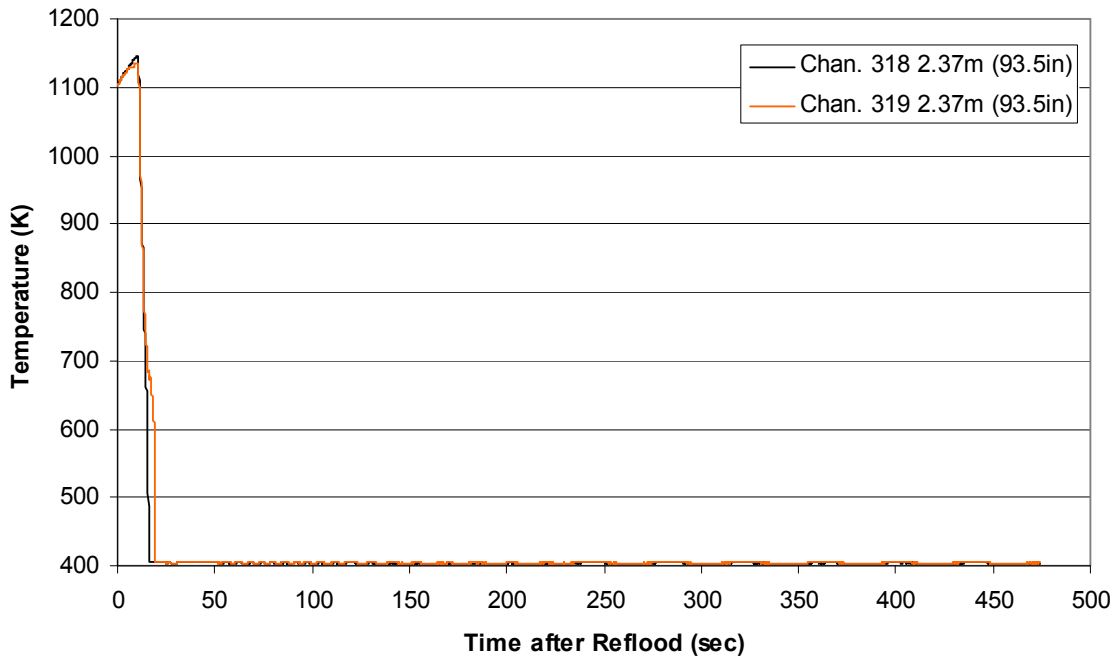
Heater Rod Temperature during Reflood
RBHT Exp. 1170



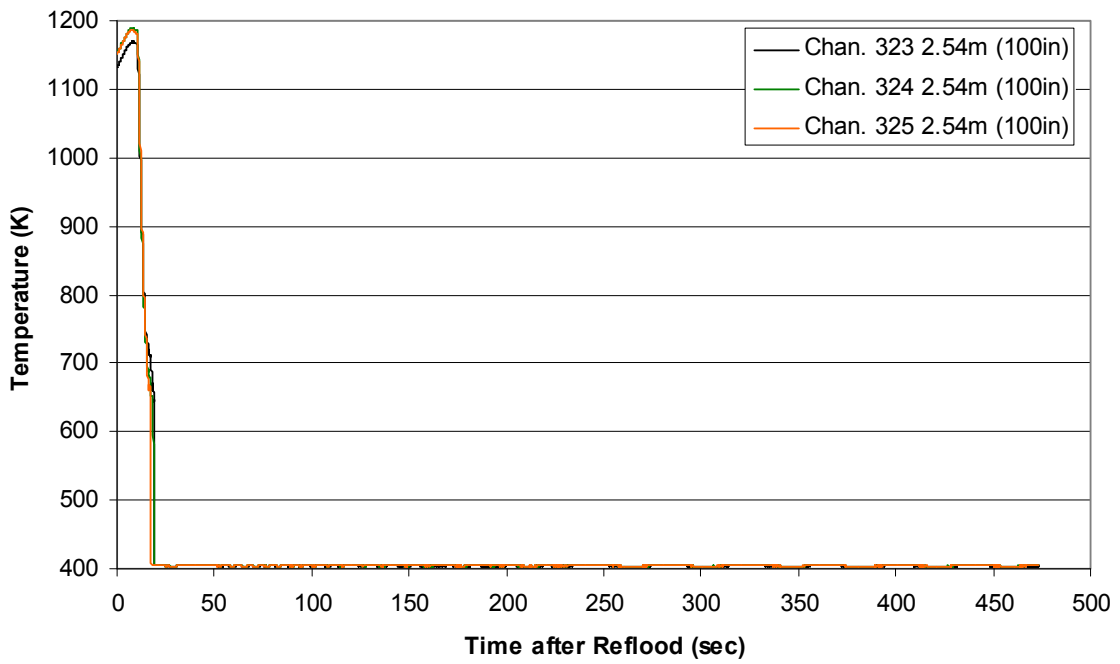
Heater Rod Temperature during Reflood RBHT Exp. 1170



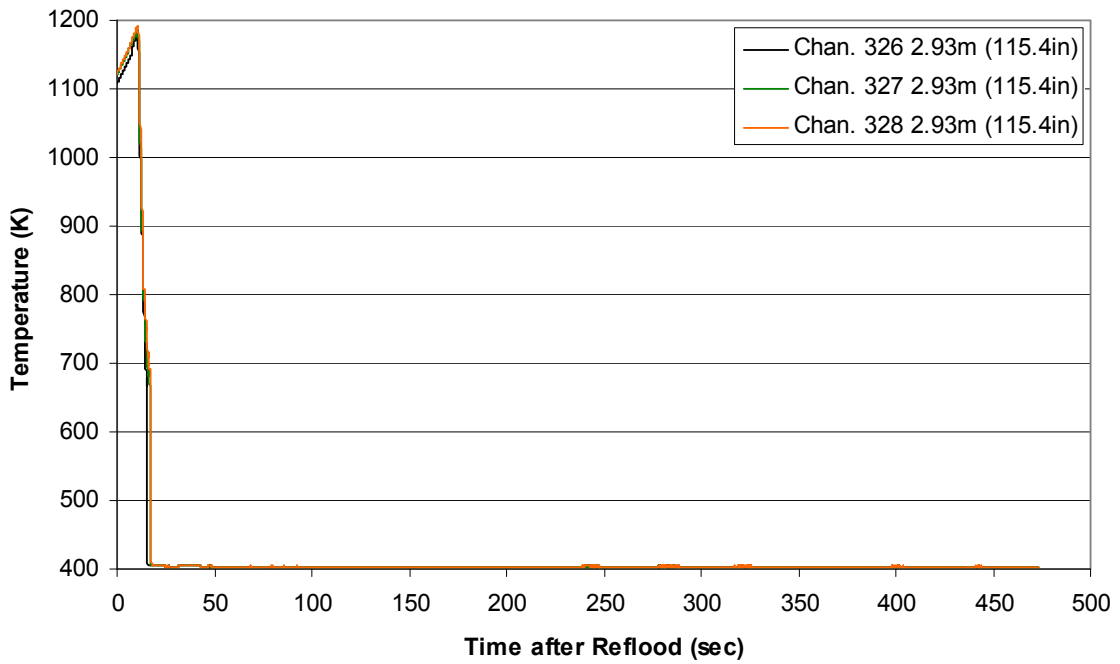
Steam Probe Temperature during Reflood RBHT Exp. 1170



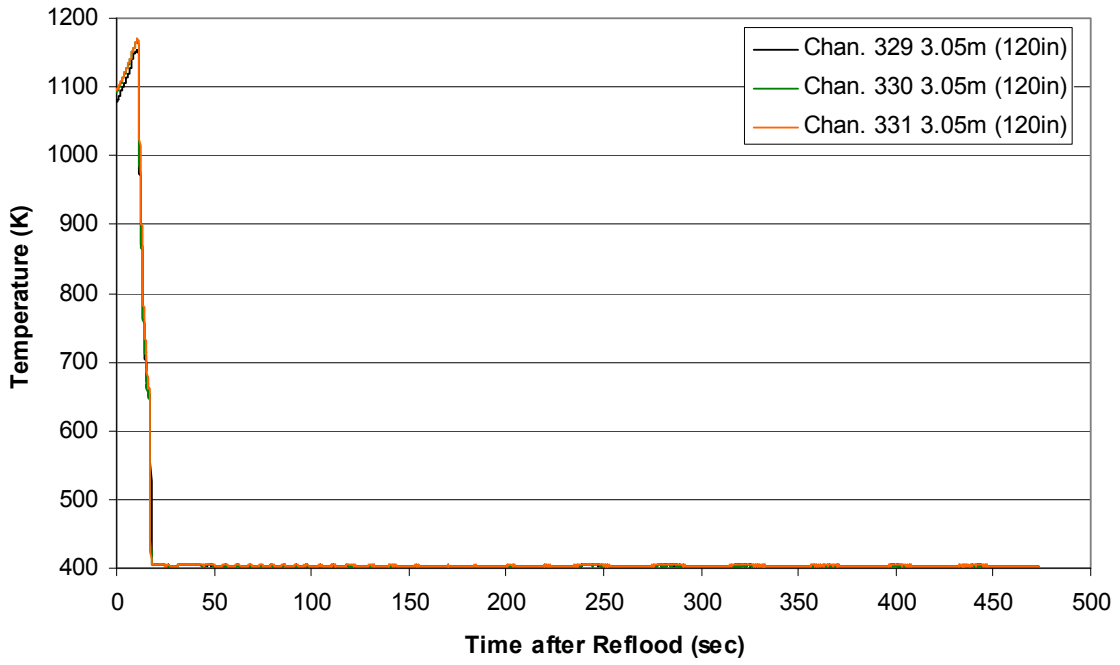
Steam Probe Temperature during Reflood RBHT Exp. 1170



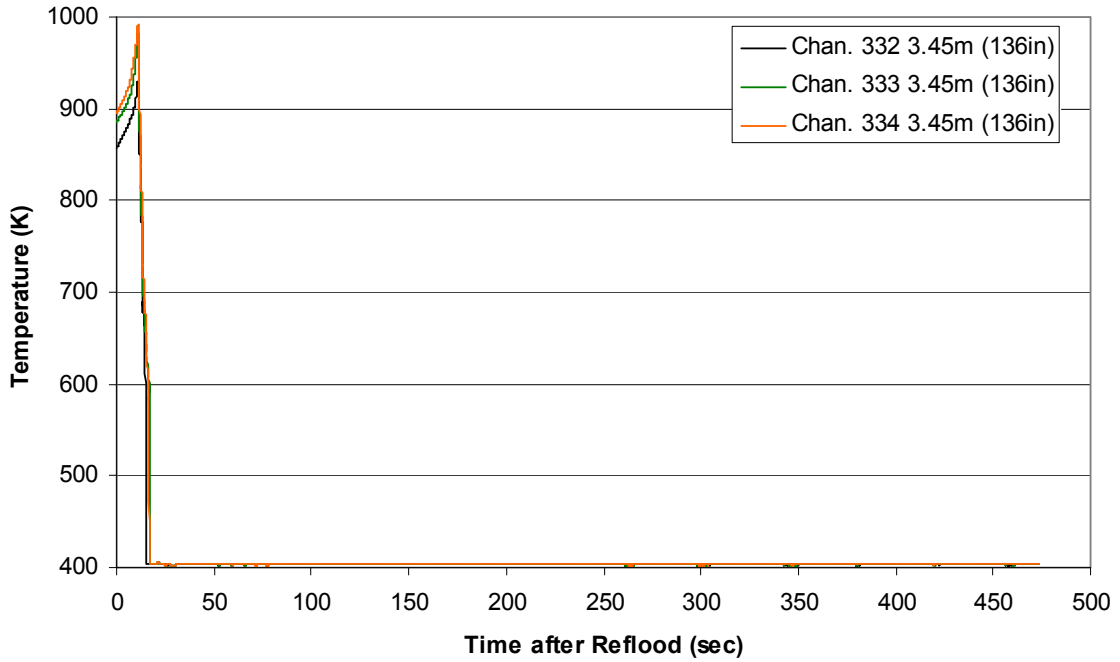
Steam Probe Temperature during Reflood RBHT Exp. 1170



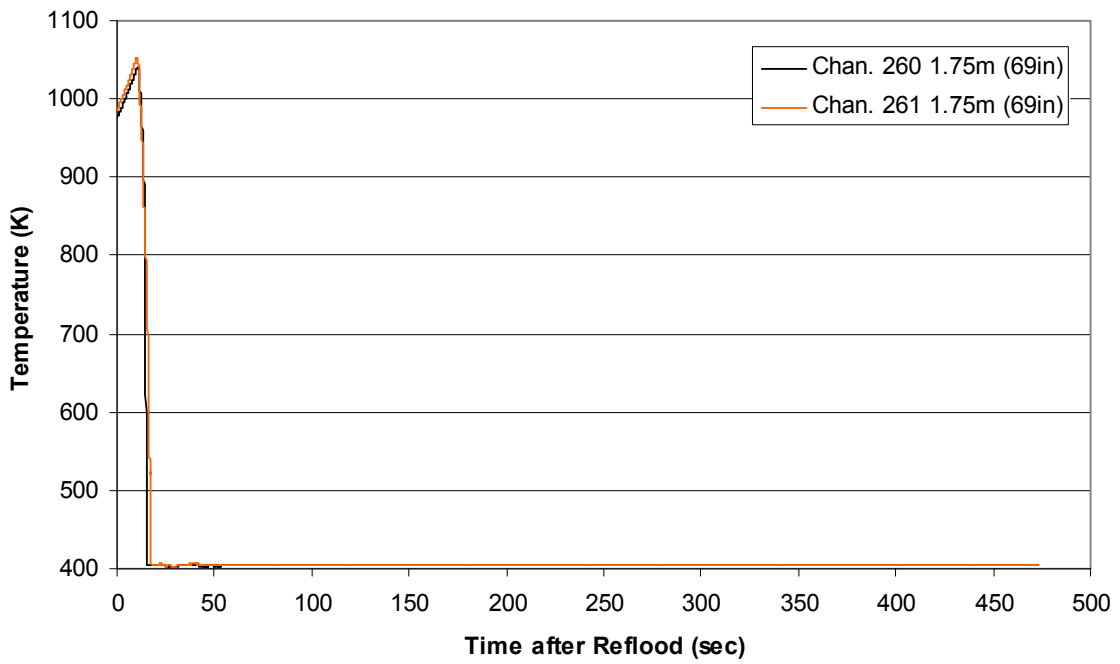
Steam Probe Temperature during Reflood RBHT Exp. 1170



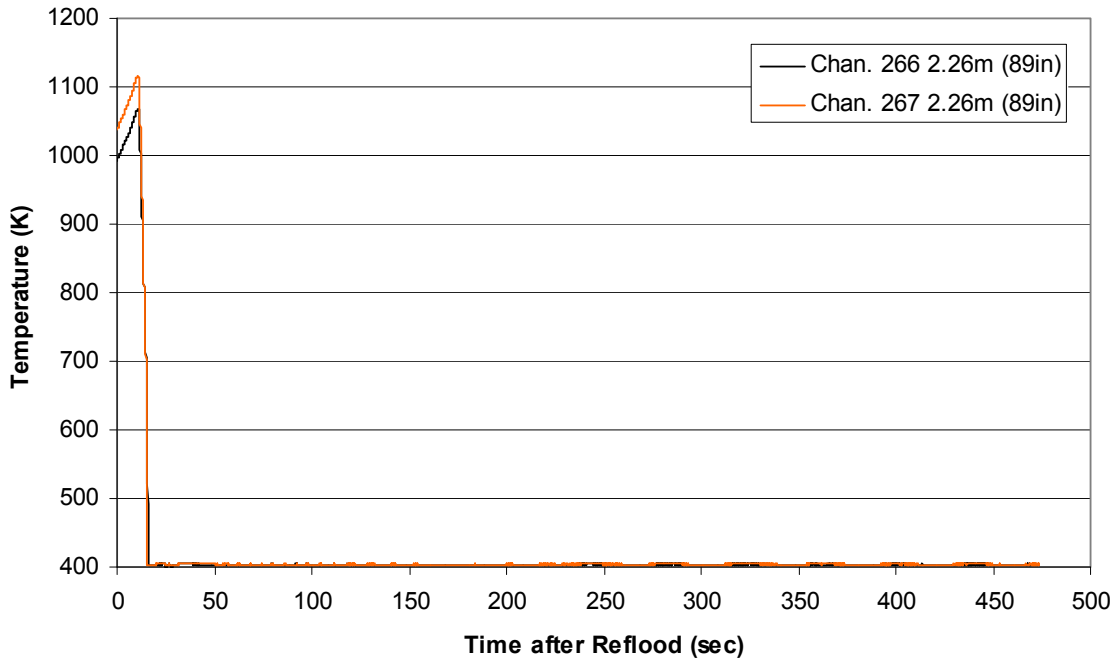
Steam Probe Temperature during Reflood RBHT Exp. 1170



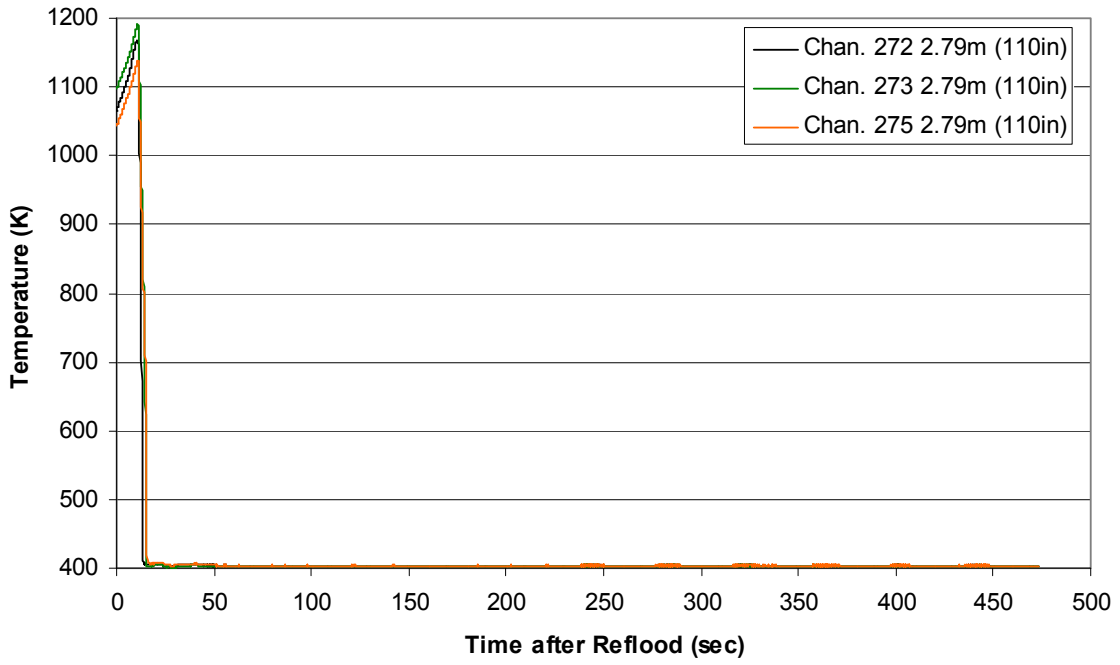
Spacer Grid Temperature during Reflood
RBHT Exp. 1170



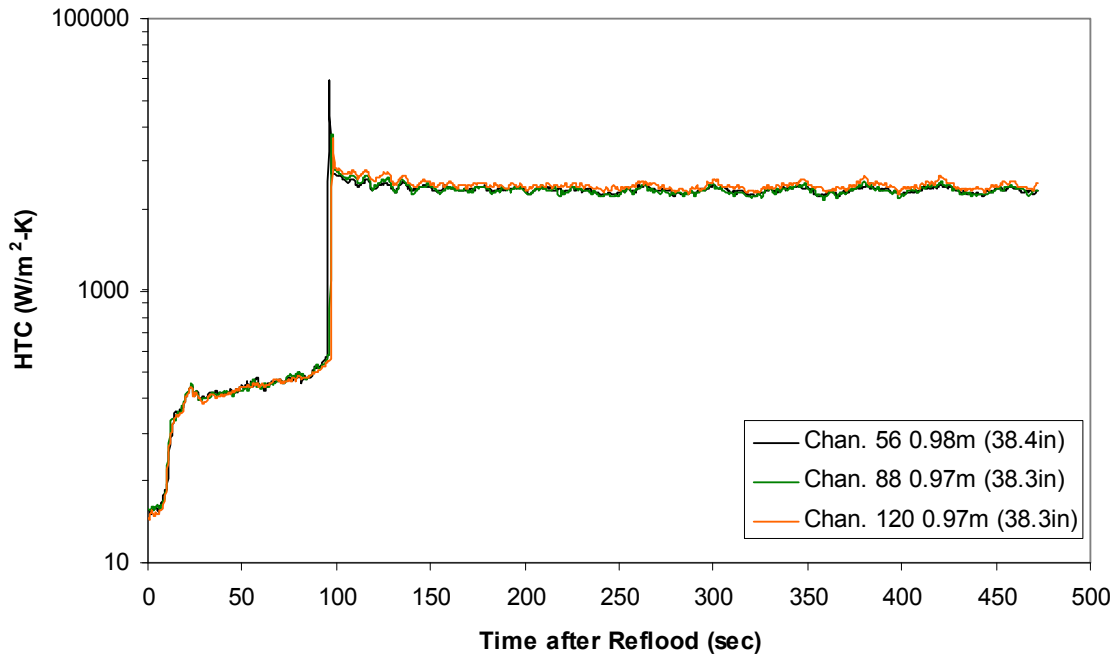
Spacer Grid Temperature during Reflood
RBHT Exp. 1170



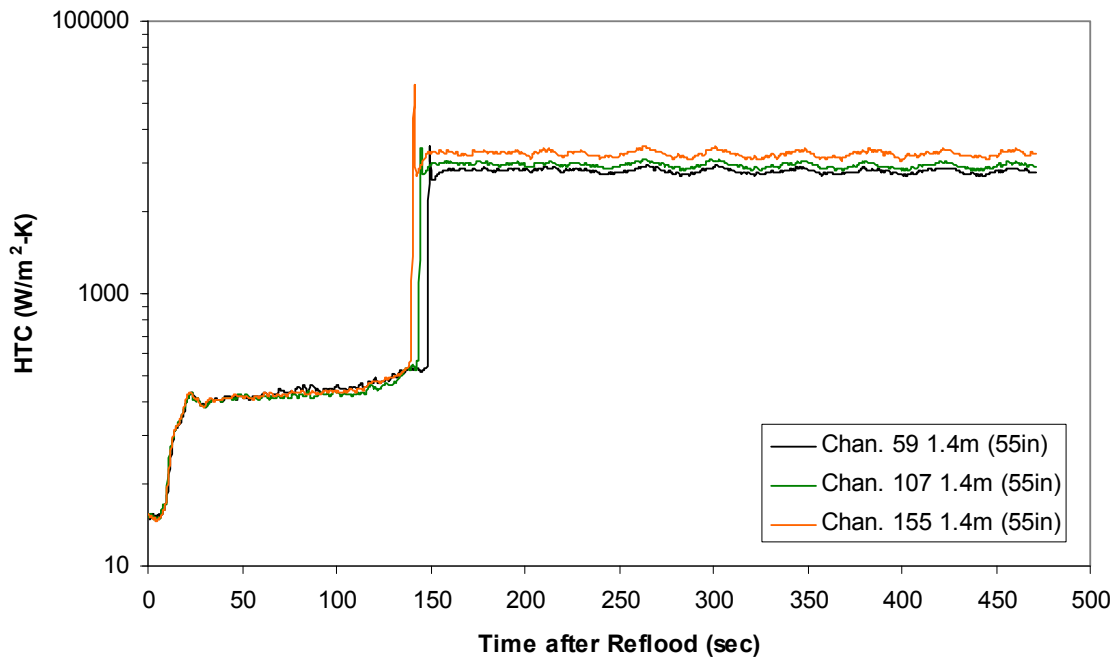
Spacer Grid Temperature during Reflood RBHT Exp. 1170



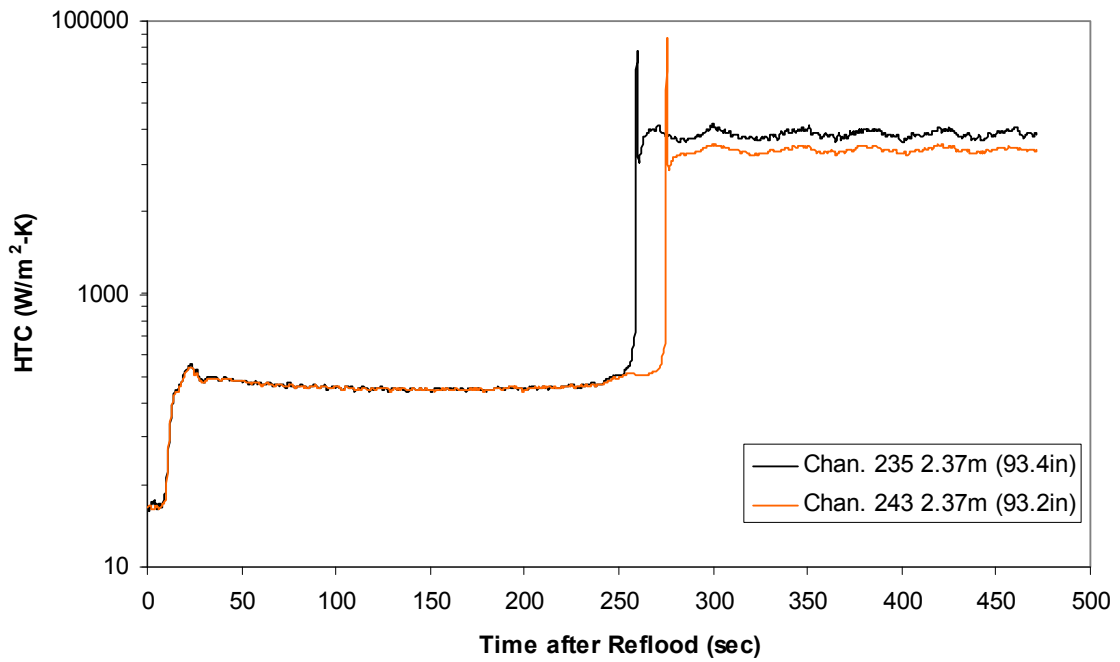
Heat Transfer Coefficient during Reflood RBHT Exp. 1170



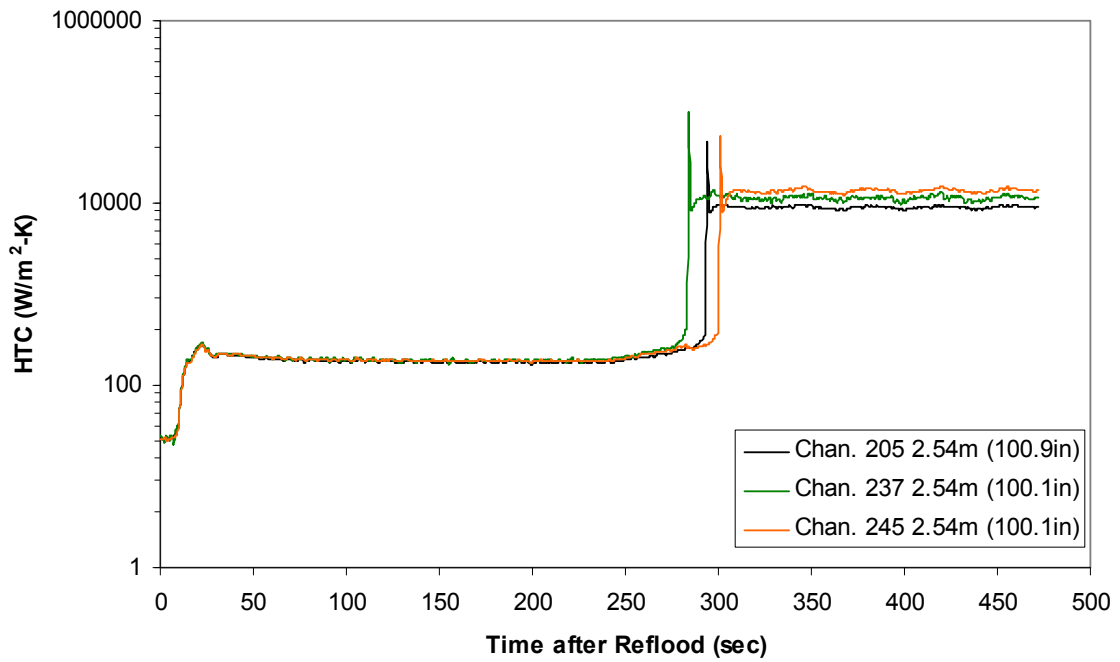
Heat Transfer Coefficient during Reflood
RBHT Exp. 1170



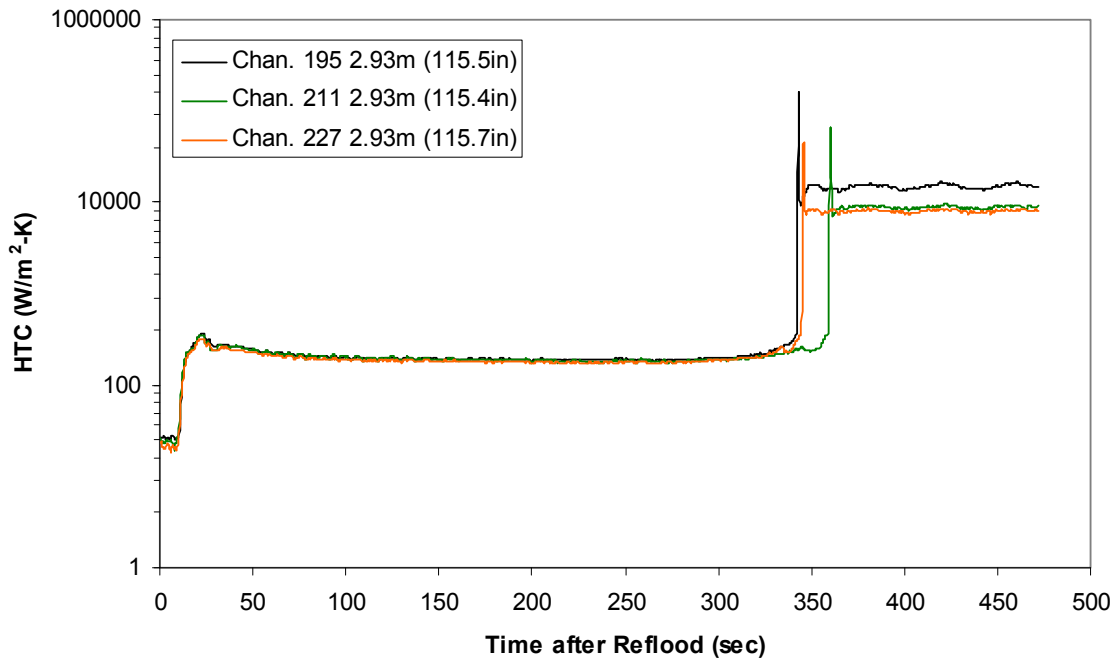
Heat Transfer Coefficient during Reflood
RBHT Exp. 1170



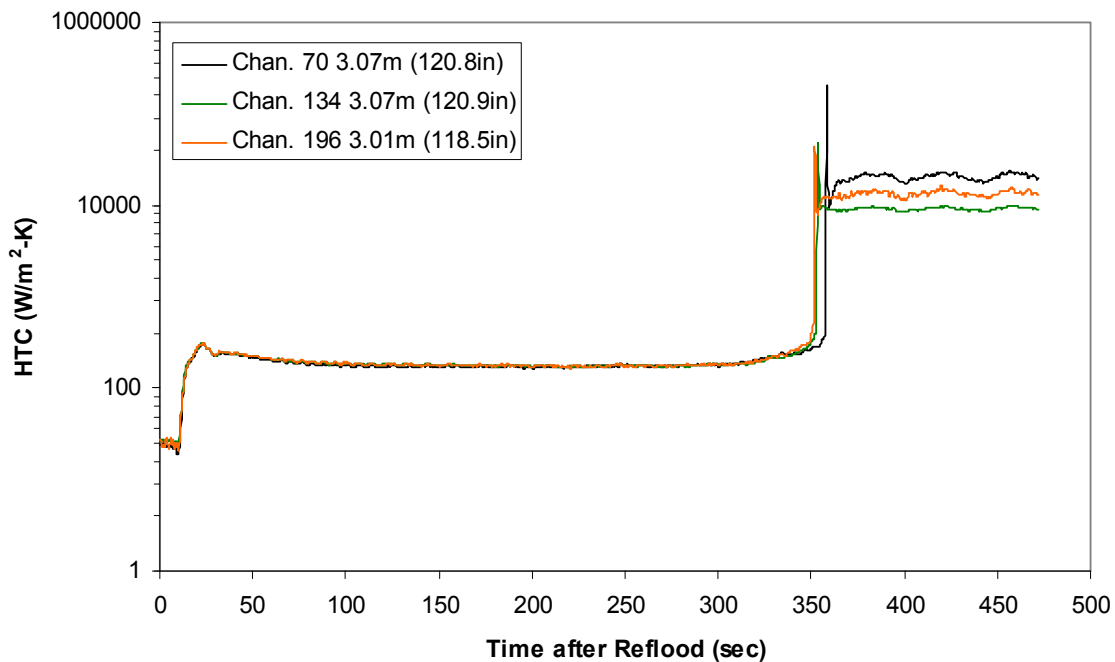
Heat Transfer Coefficient during Reflood RBHT Exp. 1170



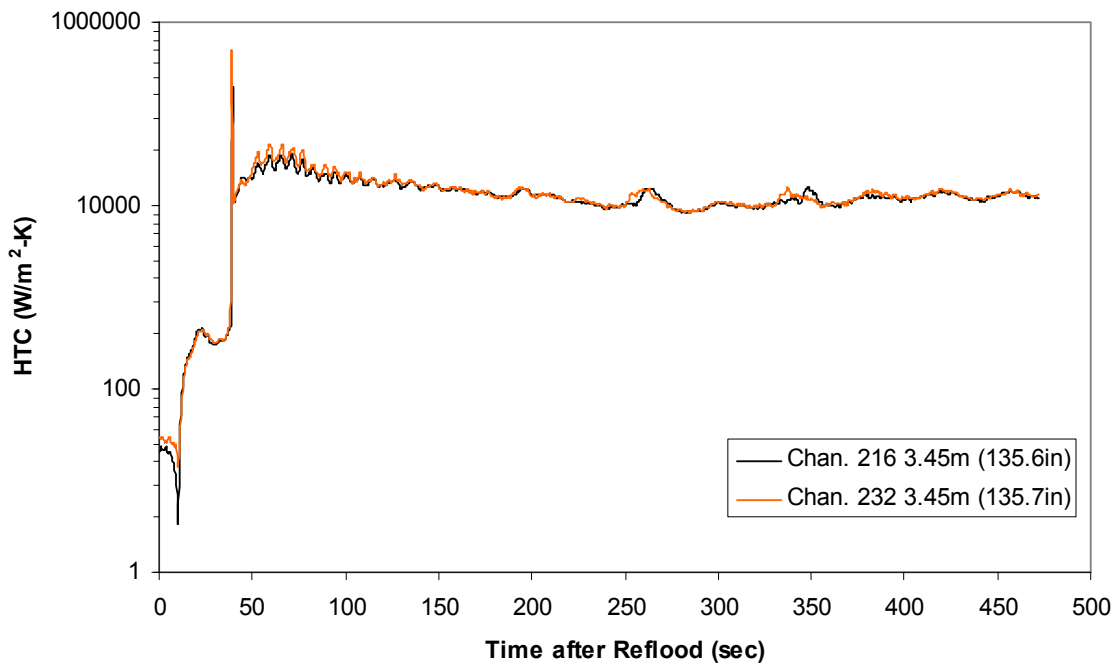
Heat Transfer Coefficient during Reflood RBHT Exp. 1170



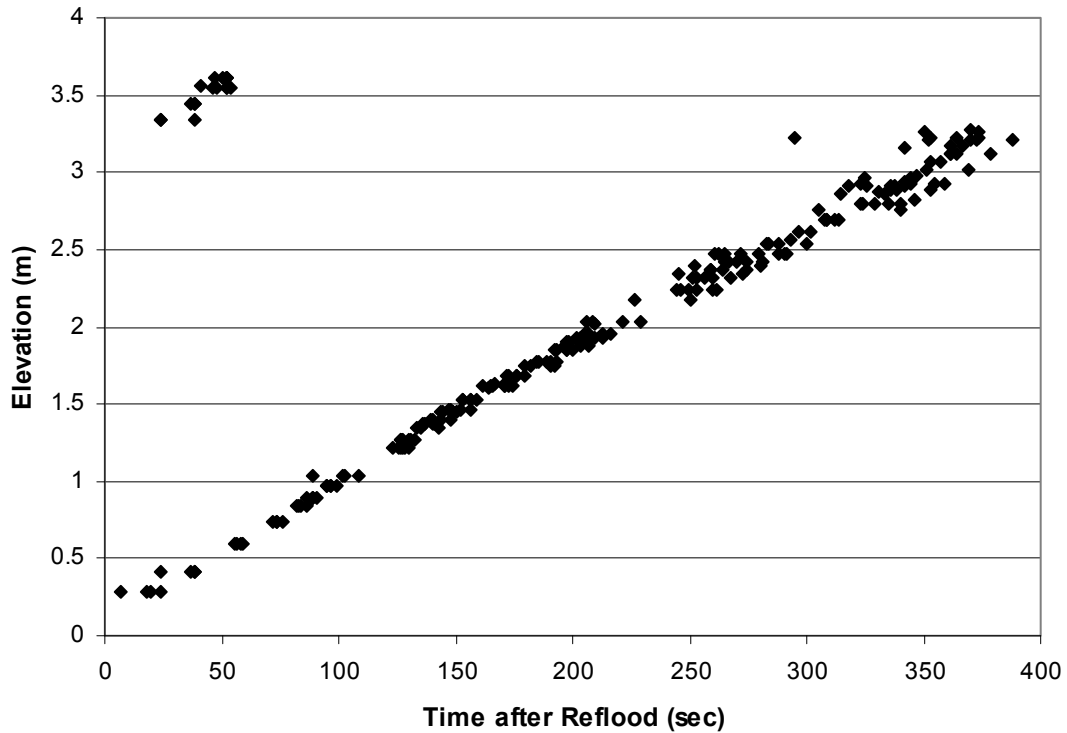
Heat Transfer Coefficient during Reflood RBHT Exp. 1170



Heat Transfer Coefficient during Reflood RBHT Exp. 1170



Quench Data, RBHT Exp. 1170



RBHT - REFLOOD TESTS

SUMMARY SHEET

RUN NO: **1196**

RUN CONDITIONS

Upper Plenum Pressure: 276 kPa (40 psia)
Initial Peak Clad Temperature: 1144 degrees K (1600 degrees F)
Rod Peak Power: 2.3 kW/m (0.7 kW/ft)
Flooding Rate: 0.1524 m/s (6 in/s)
Inlet Subcooling: 53 degrees K (96 degrees F)
Start of Reflood: 226.6 s
End of Reflood: 718.7 s
Test Date: 6/25/2002

Comments:

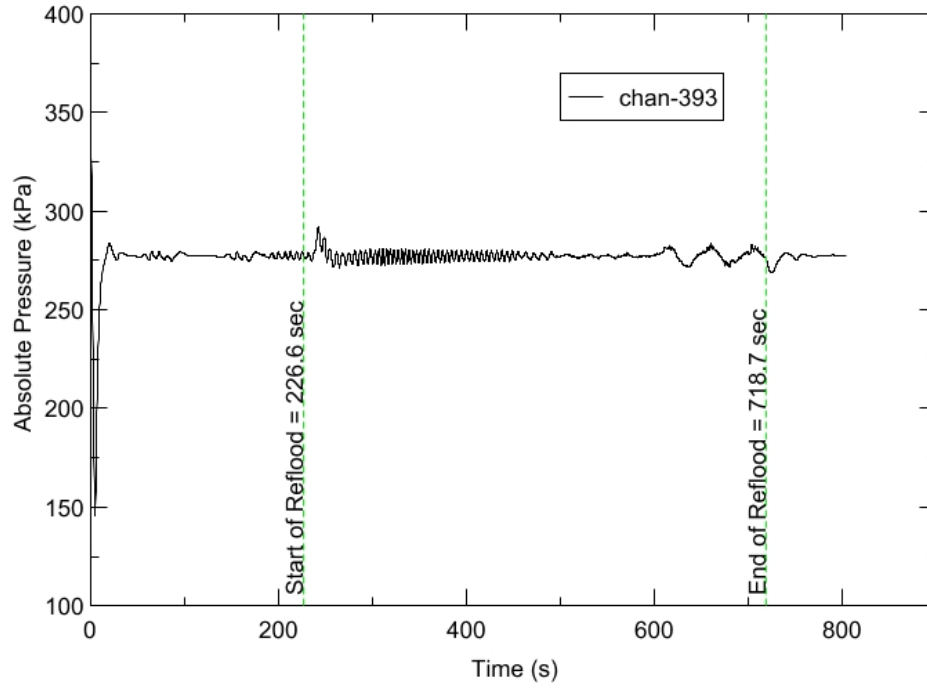
No Droplet Data

Heater rod surfaces below 2.29 m (90 in) quench to a temperature below saturation due to the high inlet subcooling. Therefore DATARH calculated heat transfer coefficients are not presented below this elevation after rod quench.

Rod_Elevation	Channel Number	Temperature at Reflood (K)	Temperature at Reflood (°F)	Turnaround Time (sec.)	Turnaround Temperature (K)	Turnaround Temperature (°F)	Quench Time (sec.)	Quench Temperature (K)	Quench Temperature (°F)
B6 0.592m	148	802.7	985.18	11.65	838.84	1050.23	34.15	692.59	786.97
B6 0.744m	149	808.8	996.14	12.65	847.97	1066.65	43.65	659.63	727.65
B6 0.846m	150	839.93	1052.19	13.15	883.72	1131.01	49.15	660.93	729.98
B6 0.897m	151	852.7	1075.17	13.65	897.79	1156.33	54.15	632.91	679.55
C6 1.04m	137	904.99	1169.29	15.15	956.01	1261.14	62.15	651.18	712.44
D5 1.27m	217	961.9	1271.73	15.15	1015.43	1368.08	74.65	655.66	720.5
C6 1.34m	138	949.48	1249.38	15.65	1008.81	1356.17	78.15	650.31	710.88
D5 1.37m	218	982.09	1308.08	15.65	1041.34	1414.72	84.15	639.46	691.35
C6 1.39m	139	955.8	1260.75	15.65	1015.83	1368.81	84.65	652.83	715.4
D5 1.45m	219	994.2	1329.86	15.65	1055.8	1440.76	89.15	647.73	706.23
C6 1.47m	140	968.12	1282.94	16.15	1029.71	1393.79	91.65	622.85	661.45
D5 1.52m	220	1005	1349.3	20.15	1069.4	1465.23	95.65	649.24	708.94
C6 1.62m	141	985.53	1314.27	20.65	1054.68	1438.74	104.65	634.9	683.13
D5 1.68m	221	1022.31	1380.47	20.65	1093.83	1509.2	110.15	634.61	682.62
D5 1.78m	222	1006.68	1352.34	14.15	1068.8	1464.14	119.15	644.88	701.1
D5 1.85m	223	1033.51	1400.62	14.65	1099.74	1519.84	125.65	621.87	659.68
C6 1.87m	142	1011.64	1361.27	15.65	1081.19	1486.45	127.15	632.68	679.14
D5 1.90m	224	1040.09	1412.47	15.15	1109.44	1537.3	130.15	630.37	674.98
C6 1.95m	144	1018.03	1372.76	15.65	1089.86	1502.06	134.65	638.69	689.96
C3 2.17m	178	1055.97	1441.05	15.65	1133.79	1581.13	161.65	665.1	737.48
D4 2.24m	241	1057.34	1443.52	14.65	1129.03	1572.57	174.15	681.81	767.57
D4 2.32m	242	1084.53	1492.47	14.15	1159.05	1626.6	183.15	647.44	705.7
C3 2.35m	180	1077.6	1479.99	14.65	1154.82	1618.99	183.15	661.74	731.45
D4 2.37m	243	1092.42	1506.66	14.65	1168.83	1644.21	189.65	662.83	733.41
C3 2.40m	181	1082.33	1488.5	14.65	1160.97	1630.06	189.15	672.67	751.12
D4 2.54m	245	1129.26	1572.98	14.15	1207	1712.92	216.15	692.16	786.2
D6 2.62m	129	1117.66	1552.1	14.15	1197.17	1695.21	222.15	723.24	842.14
D6 2.69m	130	1116.47	1549.96	14.65	1199.3	1699.04	236.15	731.82	857.6
C3 2.76m	183	1121.59	1559.18	14.65	1203.87	1707.27	246.65	738.76	870.07
D4 2.79m	247	1096.1	1513.29	13.65	1175.92	1656.97	263.15	704.92	809.16
D6 2.87m	131	1062.44	1452.7	13.15	1136.57	1586.15	267.15	670.71	747.59
D6 2.92m	132	1038.62	1409.82	14.65	1118.88	1554.29	273.65	679.36	763.17
D6 2.97m	133	1010.43	1359.08	15.15	1086.97	1496.85	281.15	689.27	780.99
D6 3.07m	134	974.02	1293.54	15.15	1045.73	1422.62	291.65	681.59	767.17
E3 3.12m	197	977.46	1299.73	14.65	1048.54	1427.68	304.15	676.53	758.06
D6 3.17m	135	936.96	1226.84	15.15	1004.18	1347.84	303.15	691.75	785.47
D6 3.27m	136	889.22	1140.91	16.15	954.5	1258.41	315.65	685.4	774.04
D4 3.61m	248	668.72	744	17.15	738.05	868.8	489.65	407.72	274.2

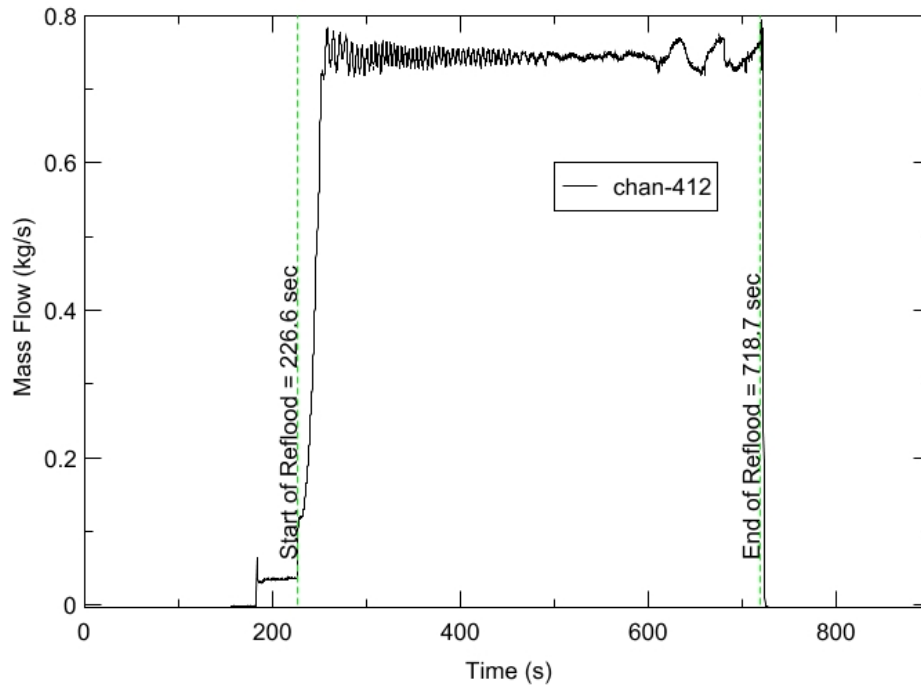
RBHT - TEST FACILITY

Upper Plenum Pressure vs. Time, Exp 1196



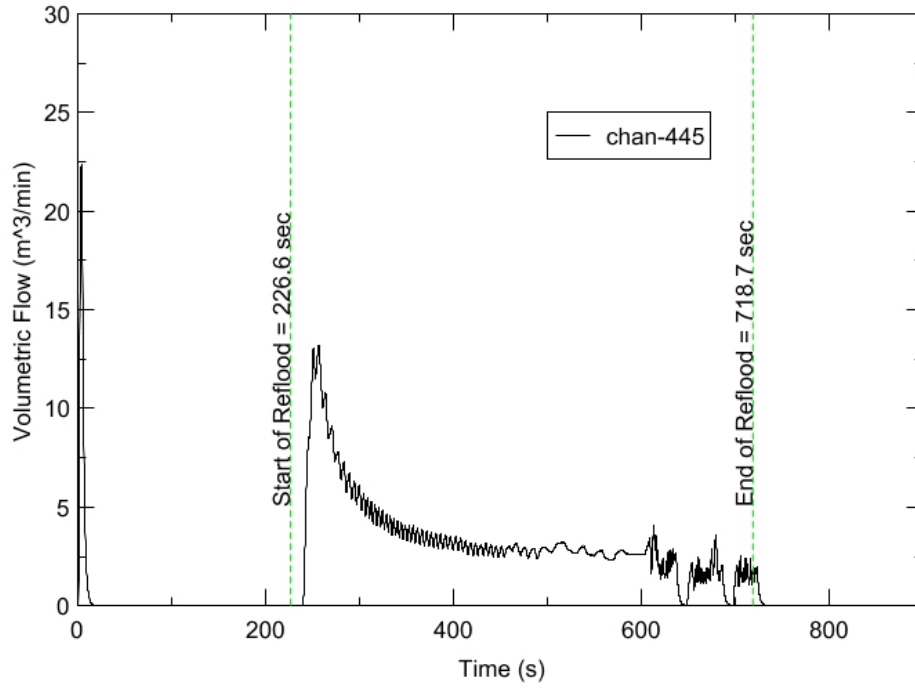
RBHT - TEST FACILITY

Inlet Flow vs. Time, Exp 1196



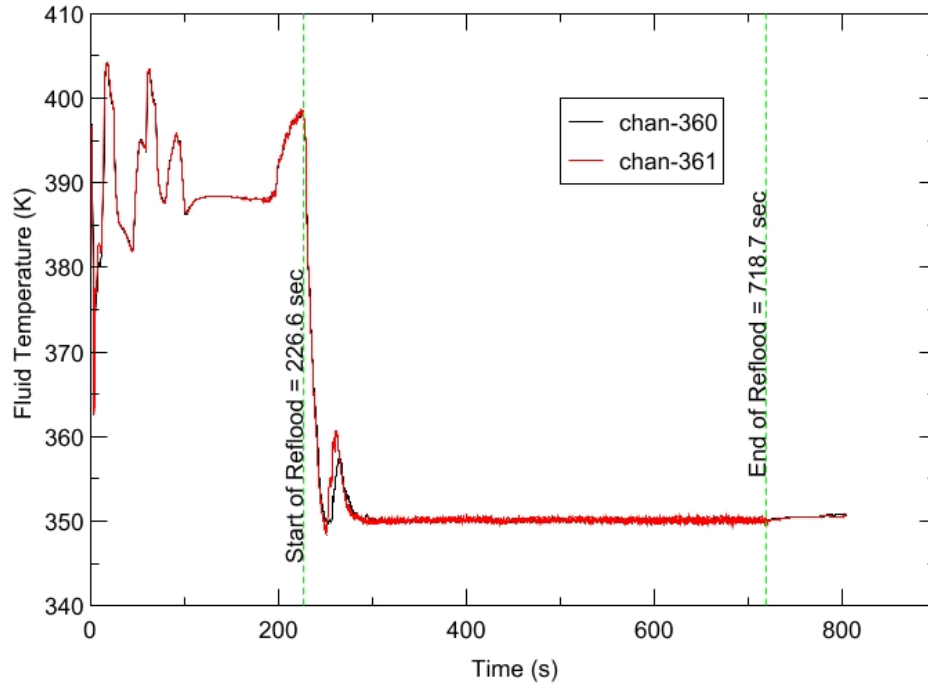
RBHT - TEST FACILITY

Steam Exhaust Flow vs. Time, Exp 1196



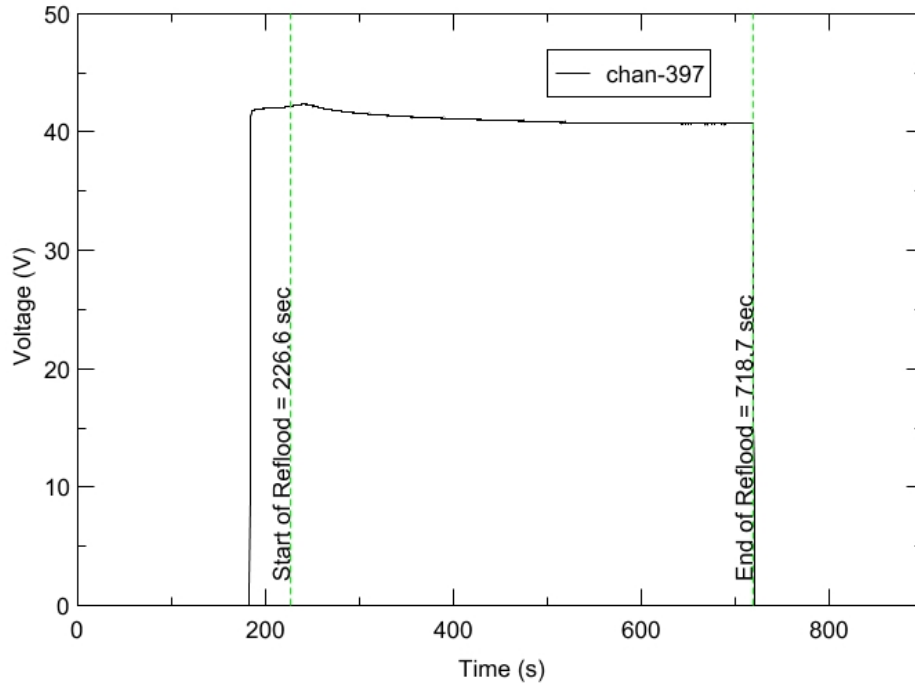
RBHT - TEST FACILITY

Inlet Flow Temperature vs. Time, Exp 1196



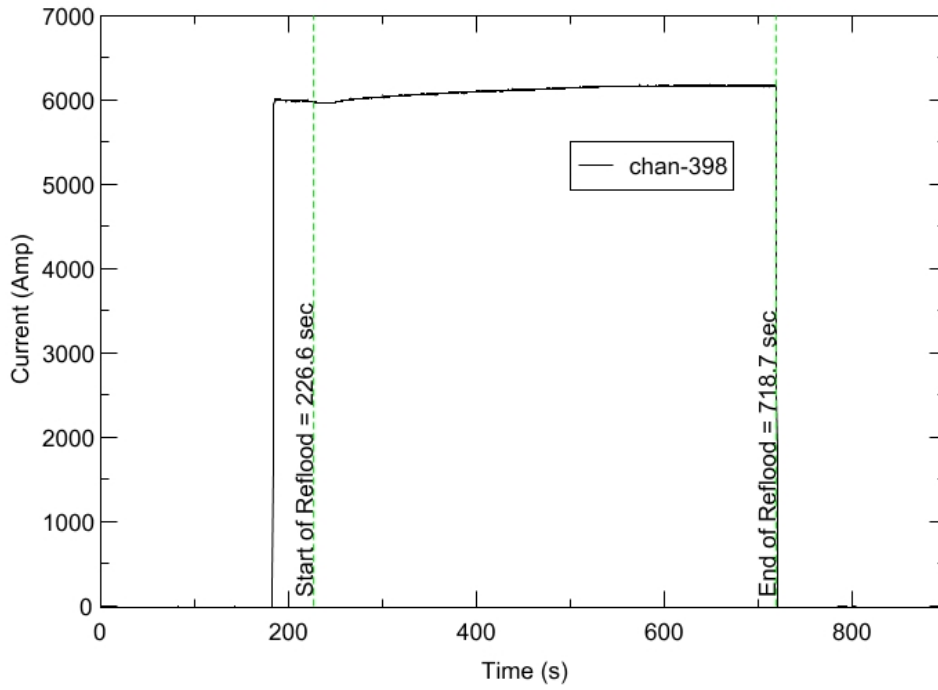
RBHT - TEST FACILITY

Test Section Voltage vs. Time, Exp 1196

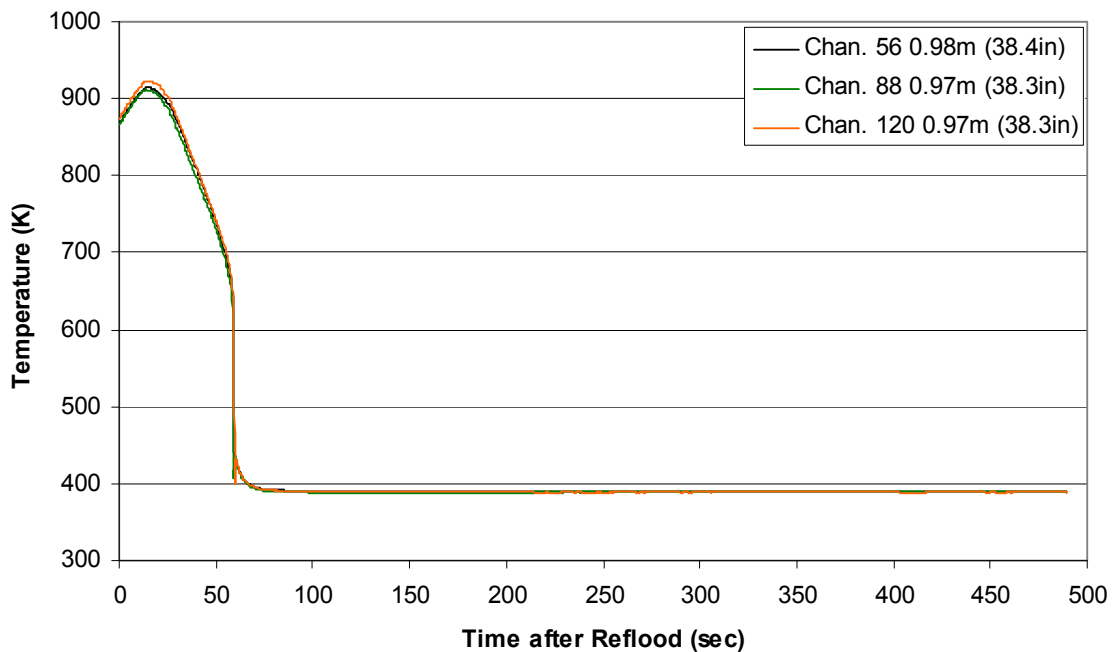


RBHT - TEST FACILITY

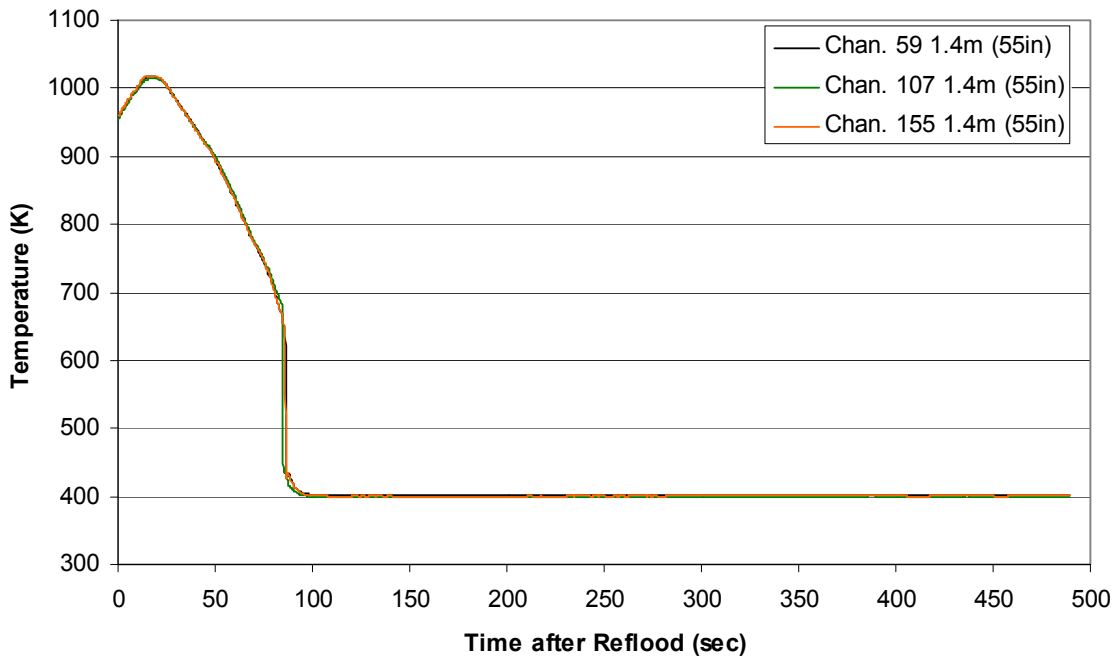
Test Section Current vs. Time, Exp 1196



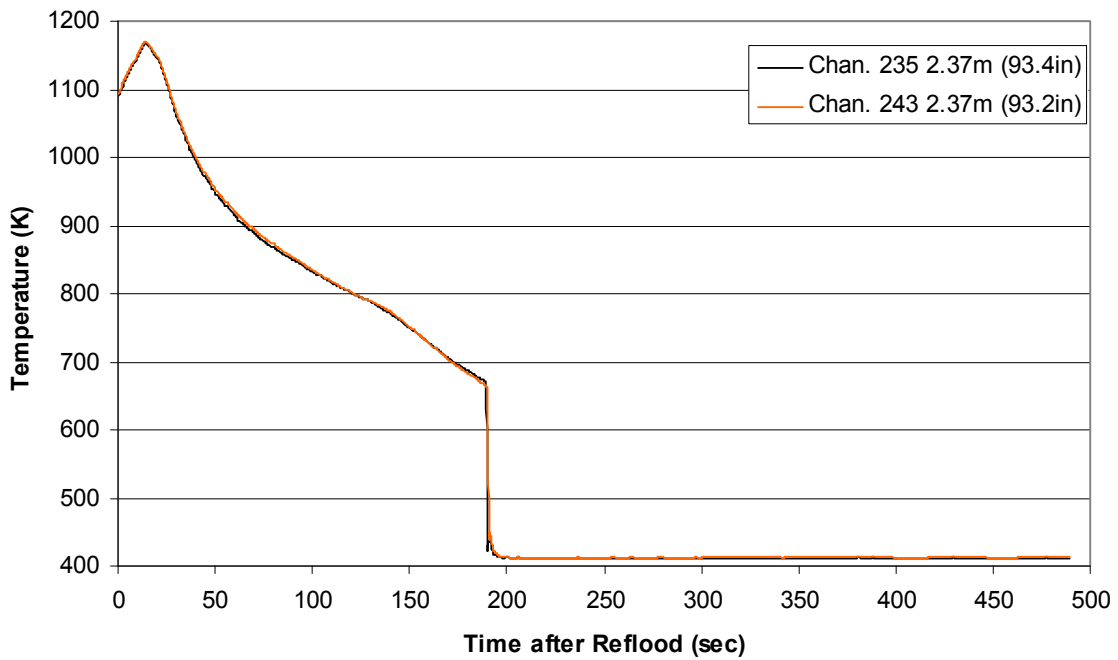
Heater Rod Temperature during Reflood
RBHT Exp. 1196



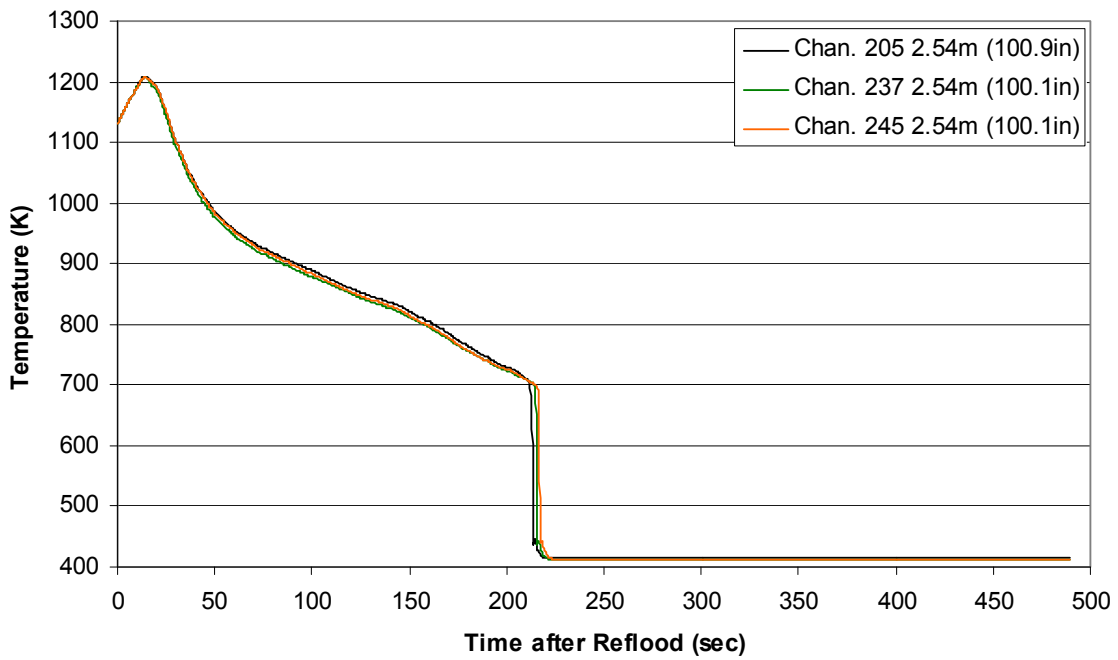
Heater Rod Temperature during Reflood
RBHT Exp. 1196



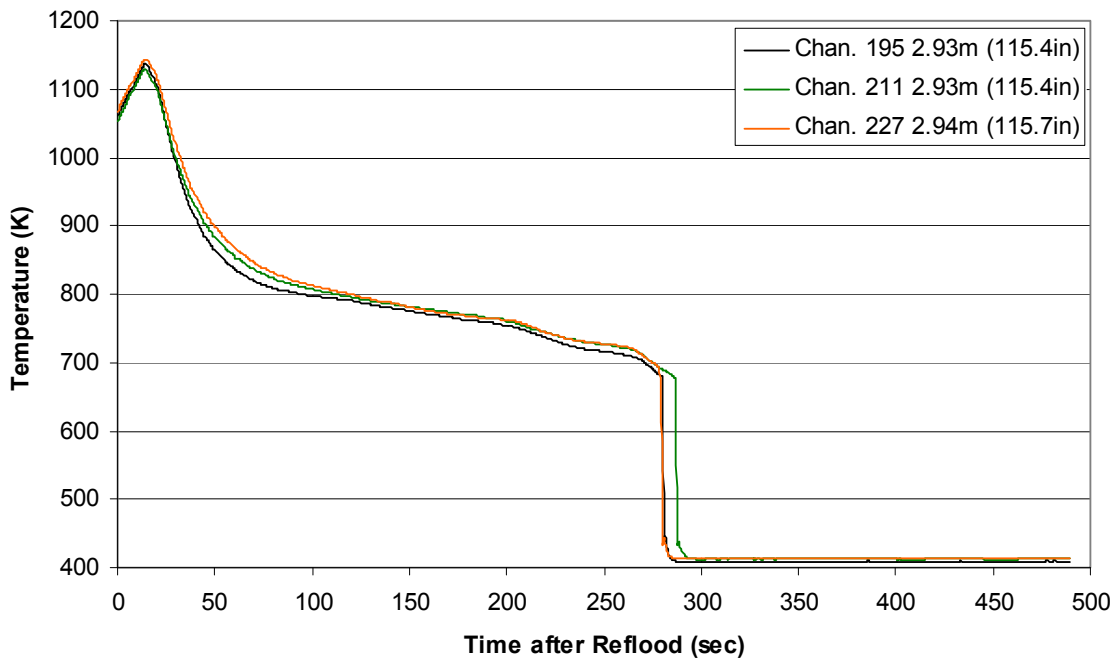
**Heater Rod Temperature during Reflood
RBHT Exp. 1196**



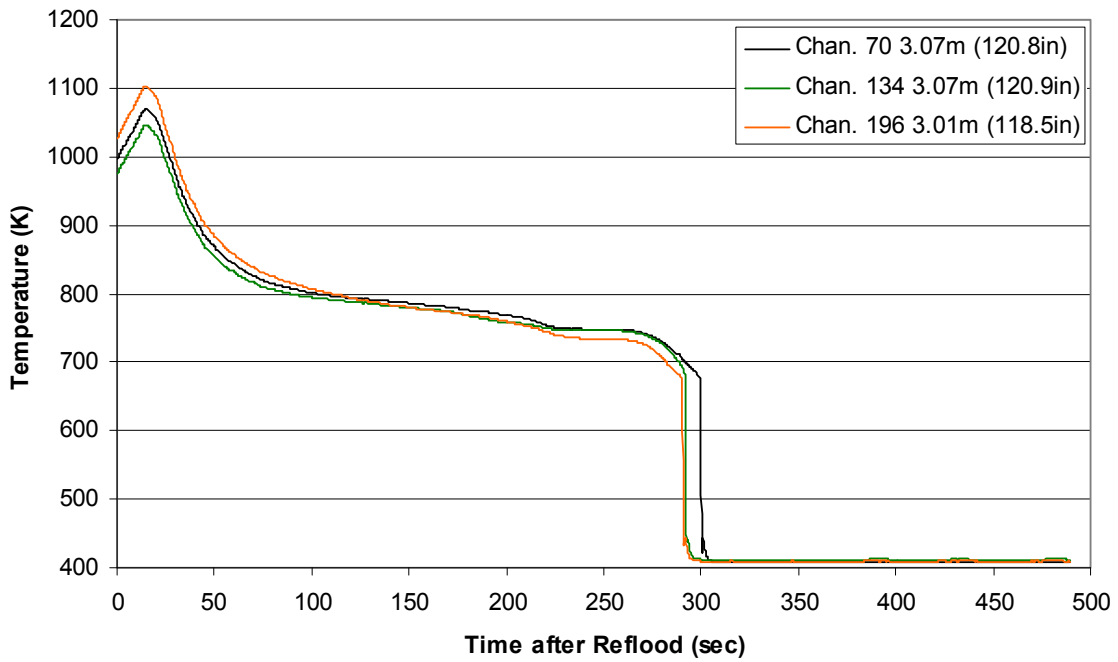
**Heater Rod Temperature during Reflood
RBHT Exp. 1196**



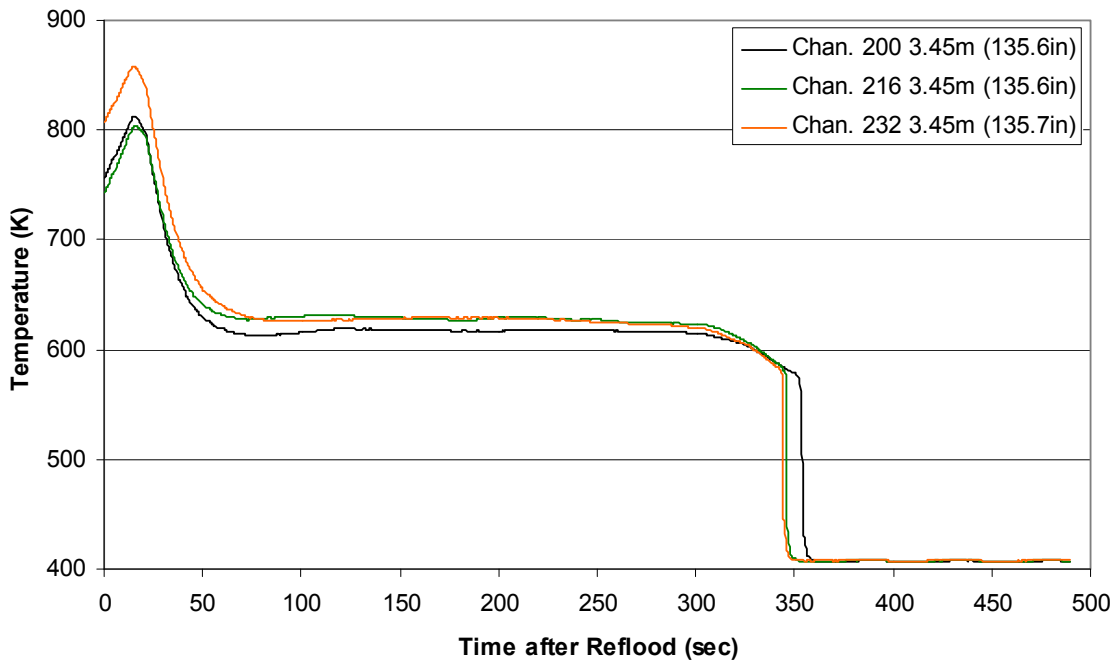
**Heater Rod Temperature during Reflood
RBHT Exp. 1196**



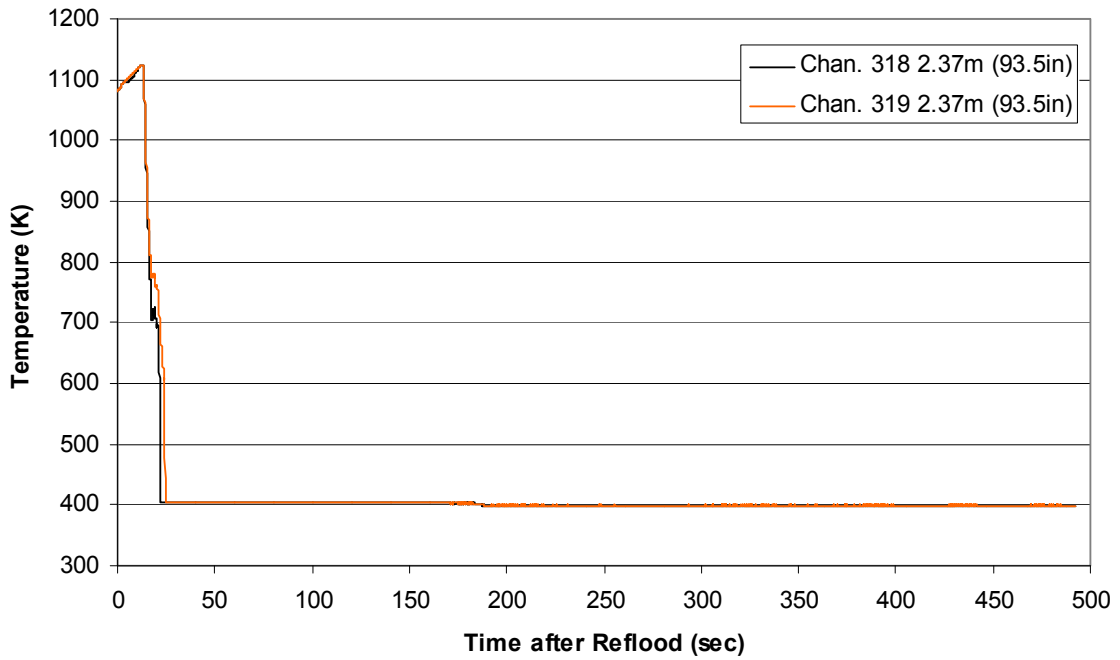
**Heater Rod Temperature during Reflood
RBHT Exp. 1196**



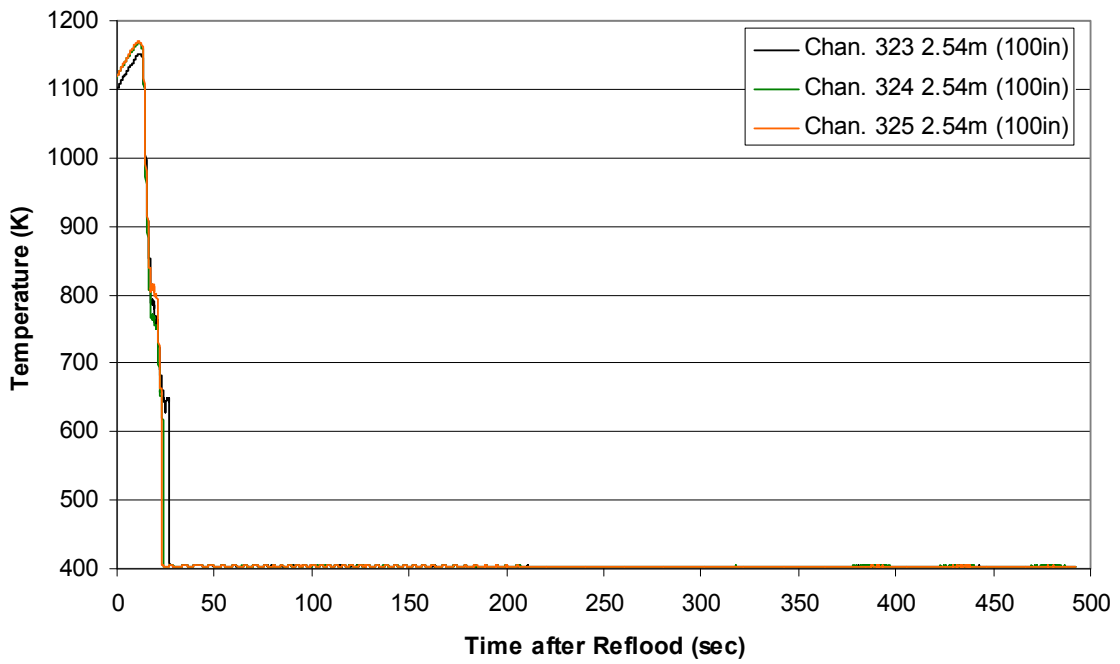
Heater Rod Temperature during Reflood RBHT Exp. 1196



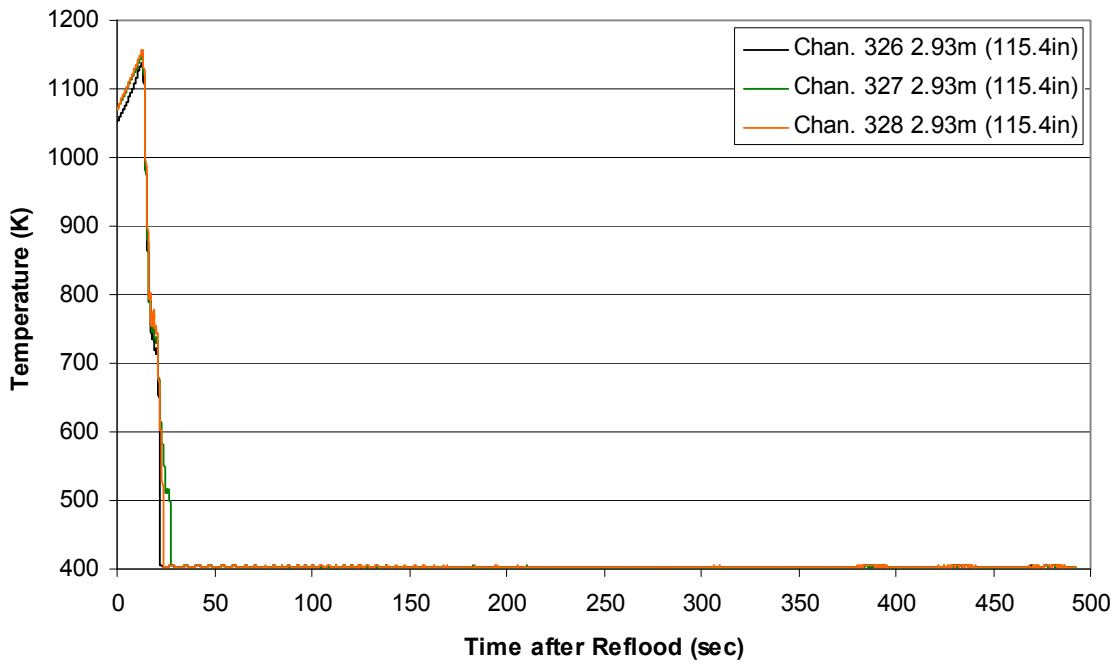
Steam Probe Temperature during Reflood RBHT Exp. 1196



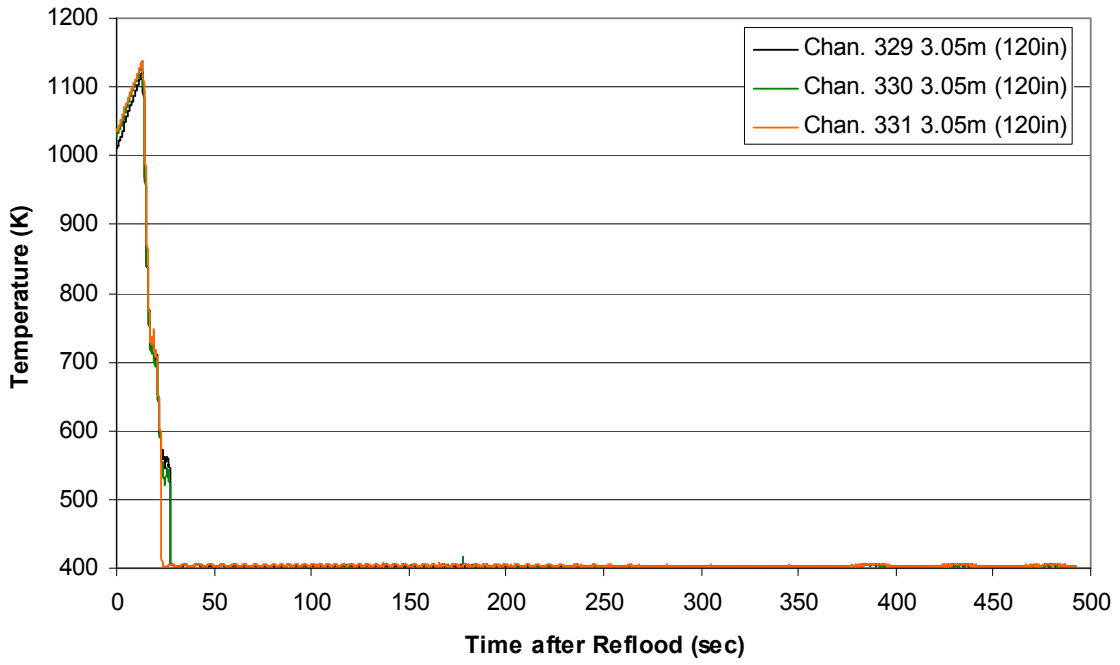
Steam Probe Temperature during Reflood RBHT Exp. 1196



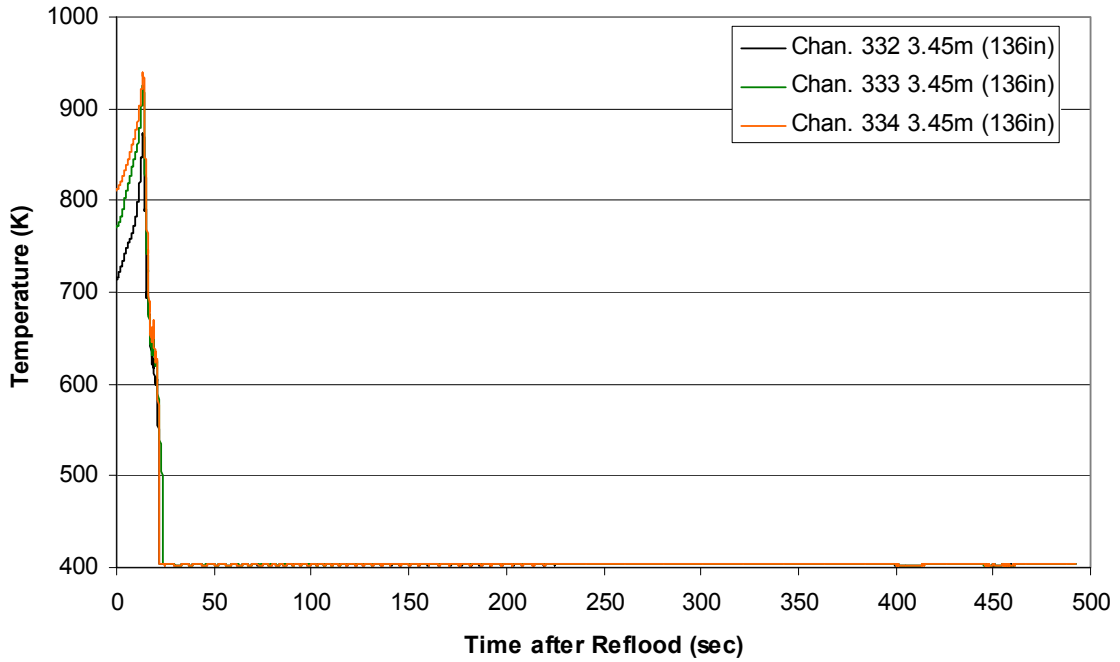
Steam Probe Temperature during Reflood RBHT Exp. 1196



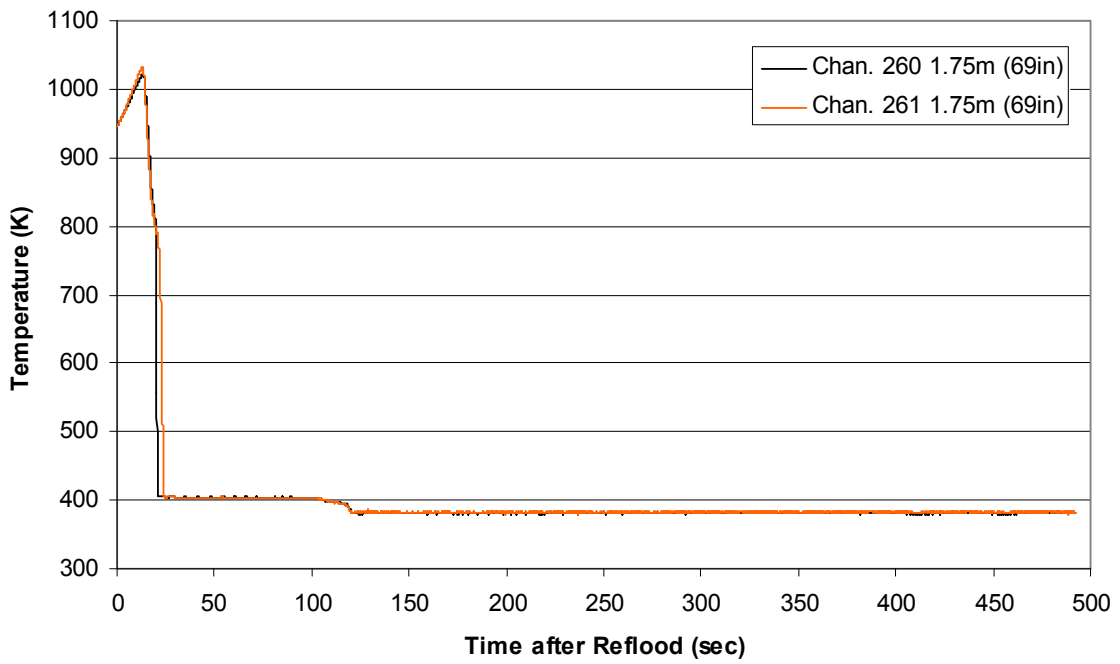
Steam Probe Temperature during Reflood
RBHT Exp. 1196



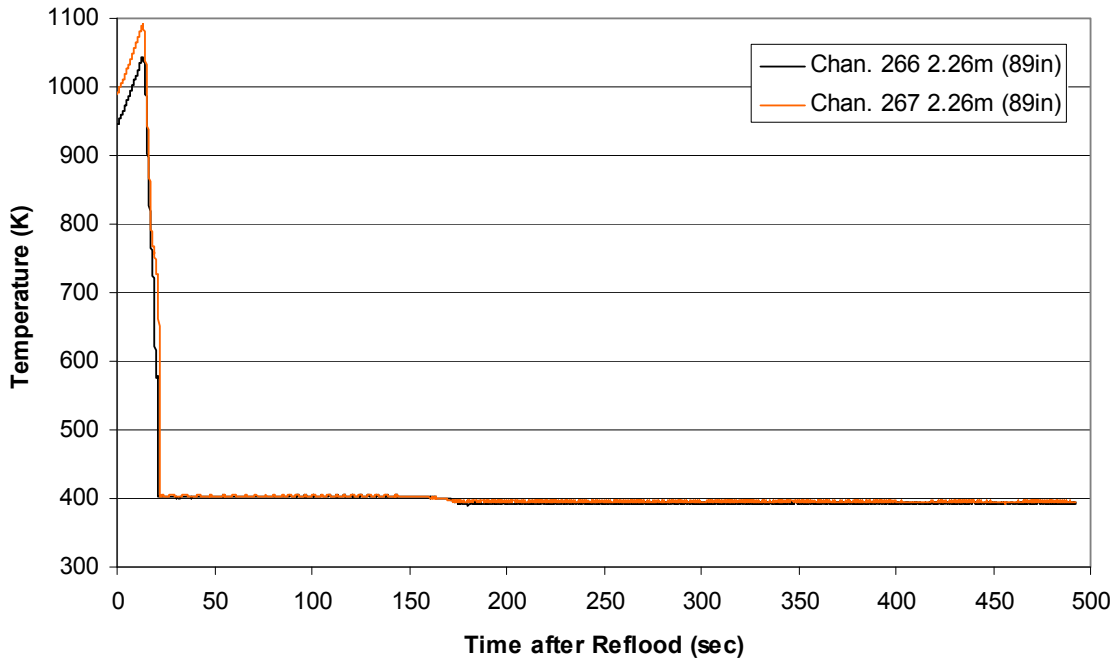
Steam Probe Temperature during Reflood
RBHT Exp. 1196



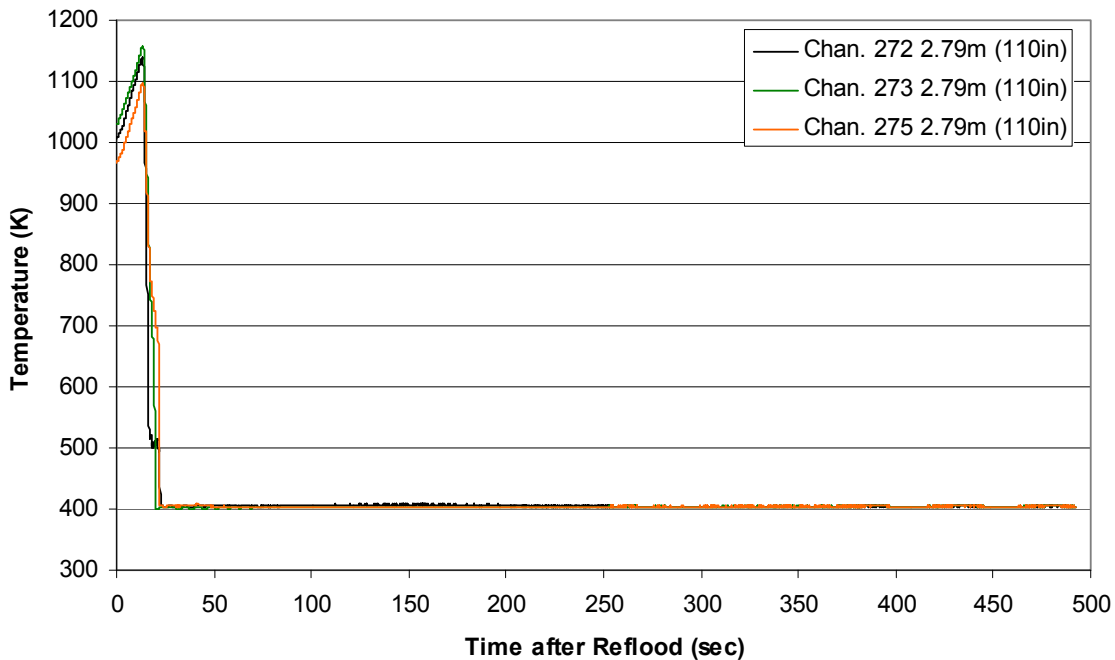
Spacer Grid Temperature during Reflood RBHT Exp. 1196



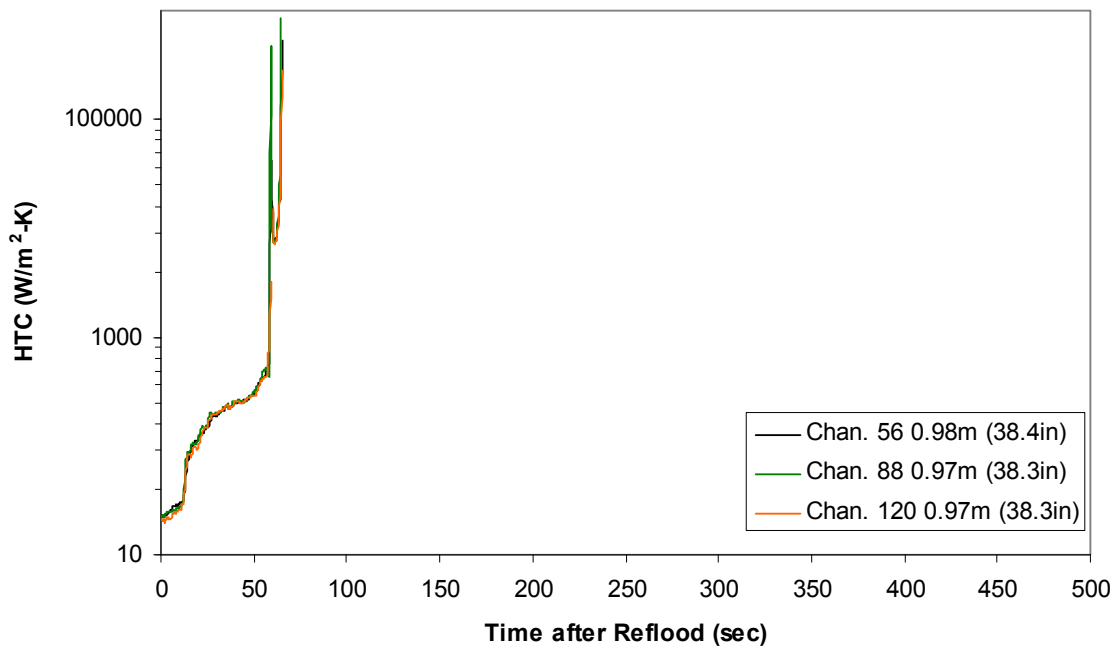
Spacer Grid Temperature during Reflood RBHT Exp. 1196



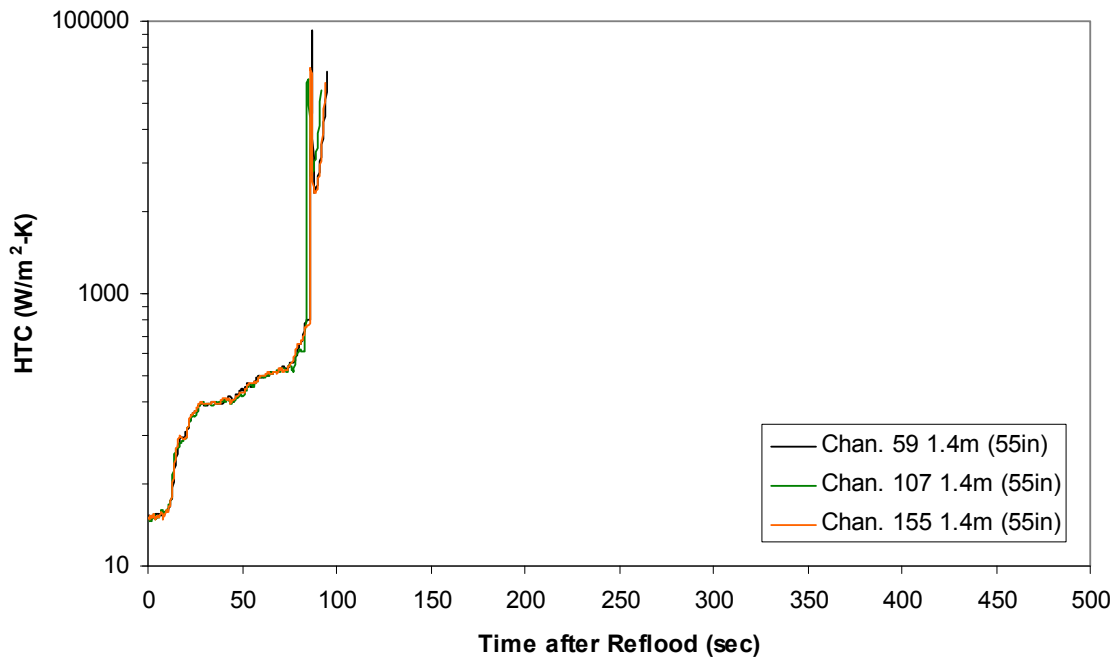
Spacer Grid Temperature during Reflood RBHT Exp. 1196



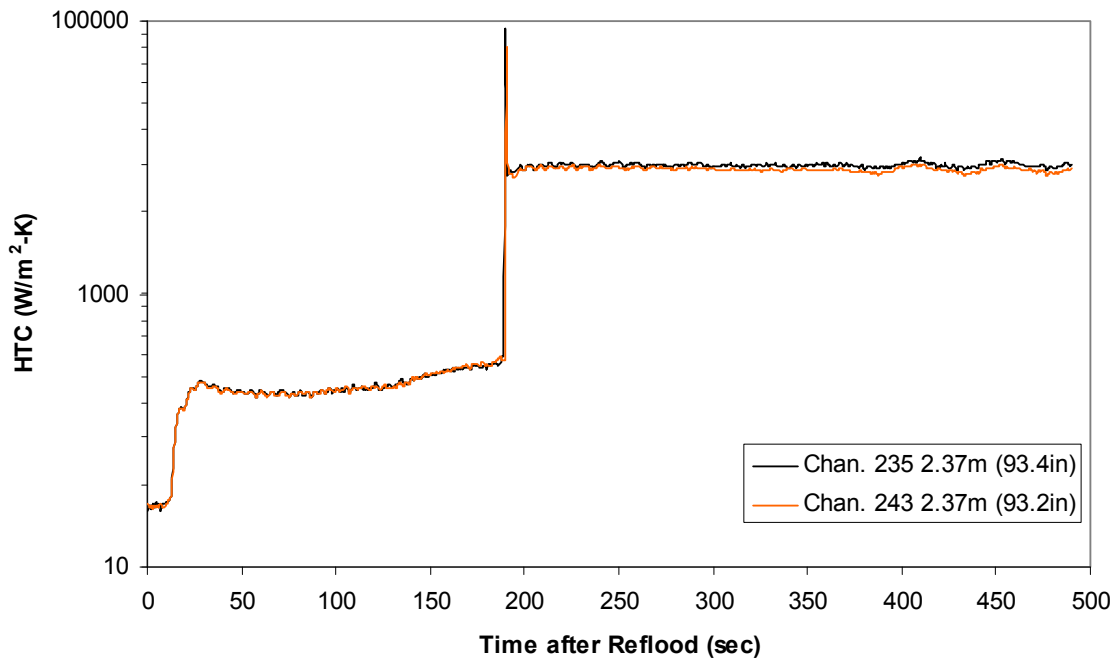
Heat Transfer Coefficient during Reflood RBHT Exp. 1196



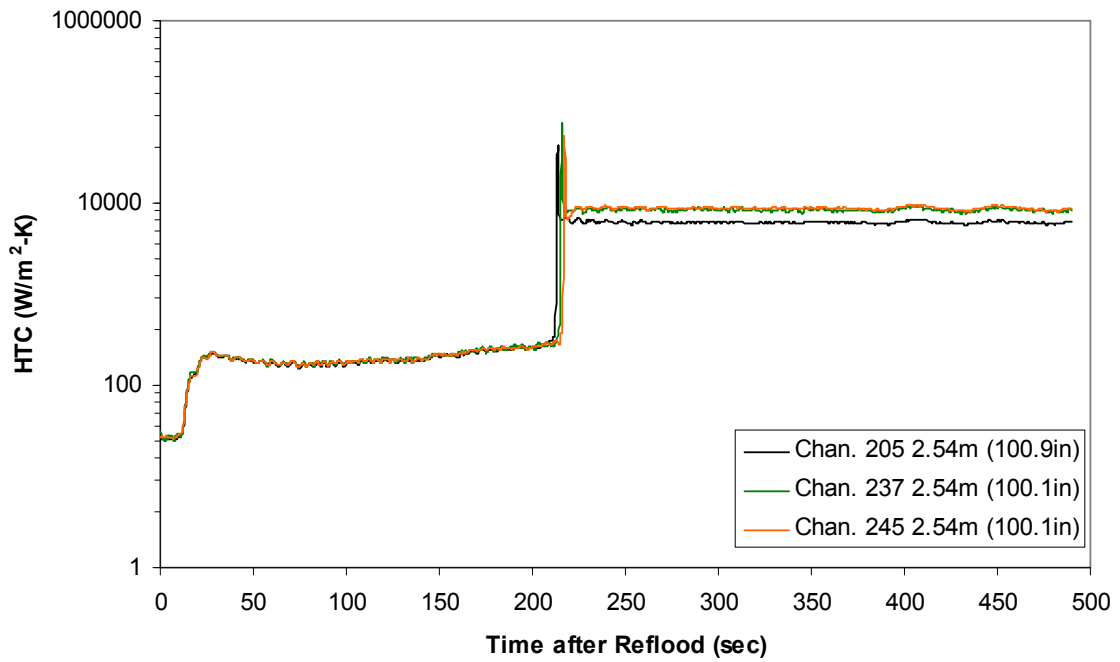
Heat Transfer Coefficient during Reflood RBHT Exp. 1196



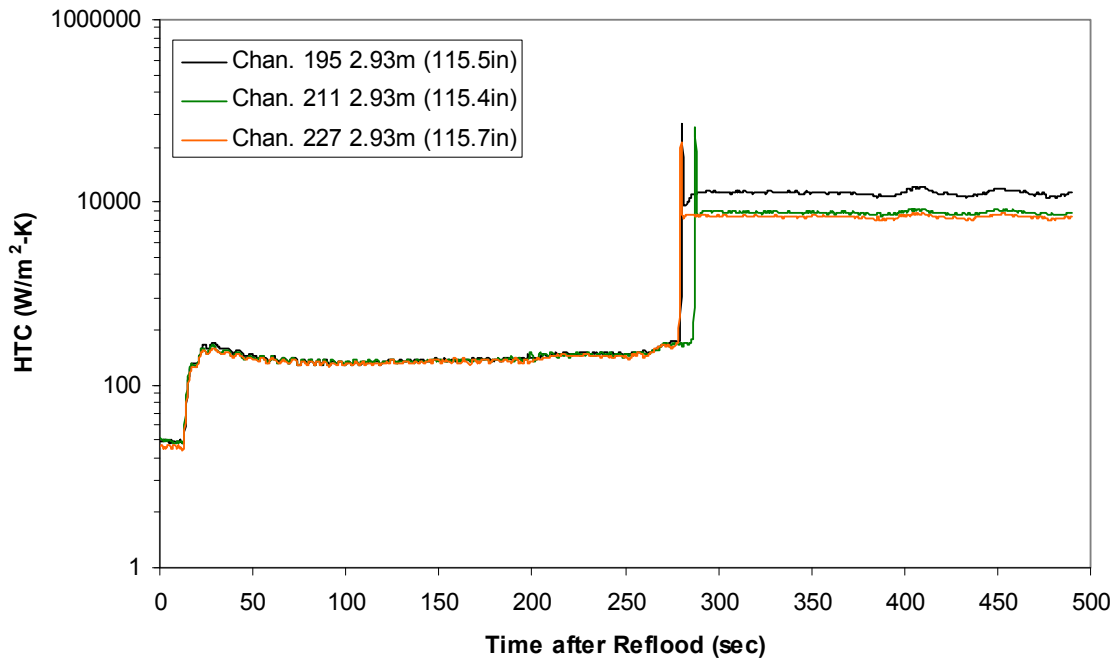
Heat Transfer Coefficient during Reflood RBHT Exp. 1196



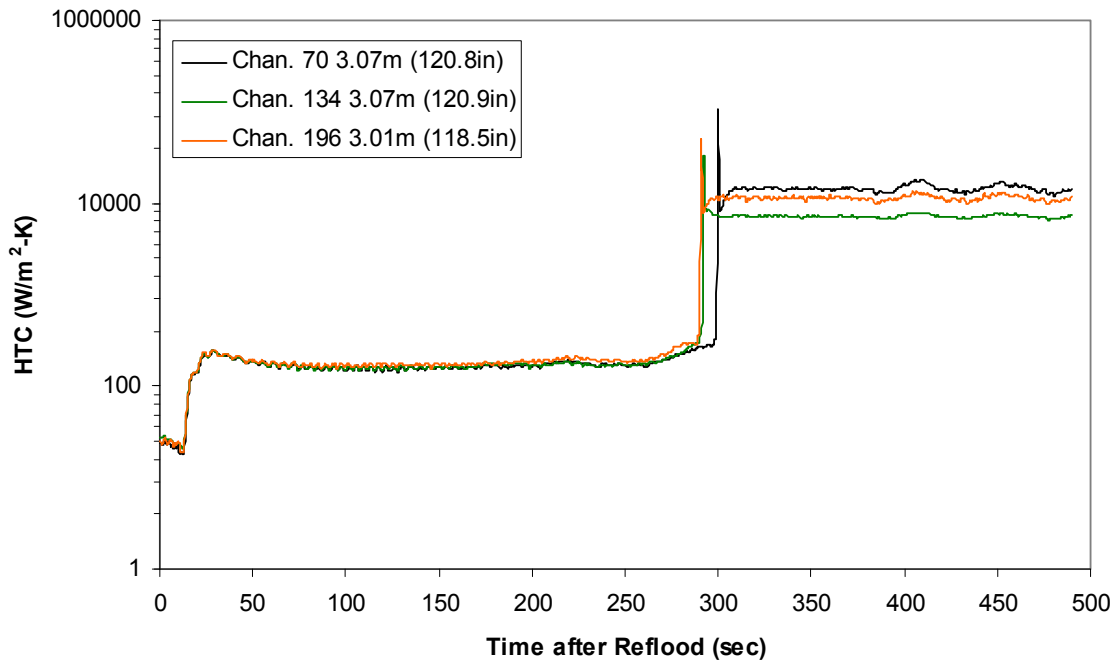
Heat Transfer Coefficient during Reflood RBHT Exp. 1196



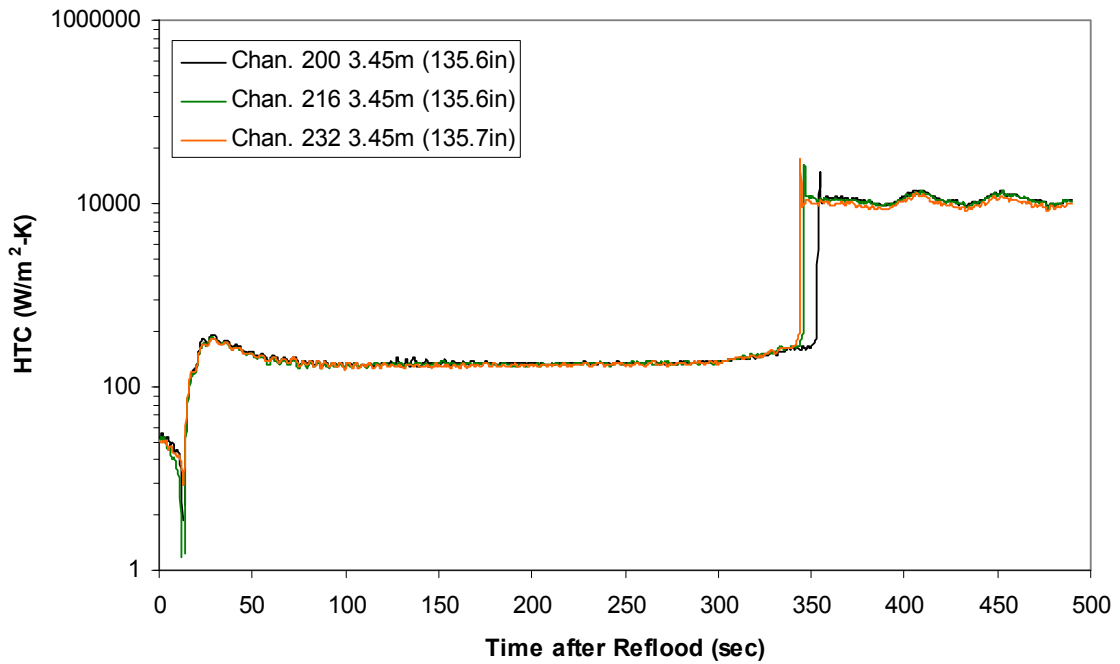
Heat Transfer Coefficient during Reflood RBHT Exp. 1196



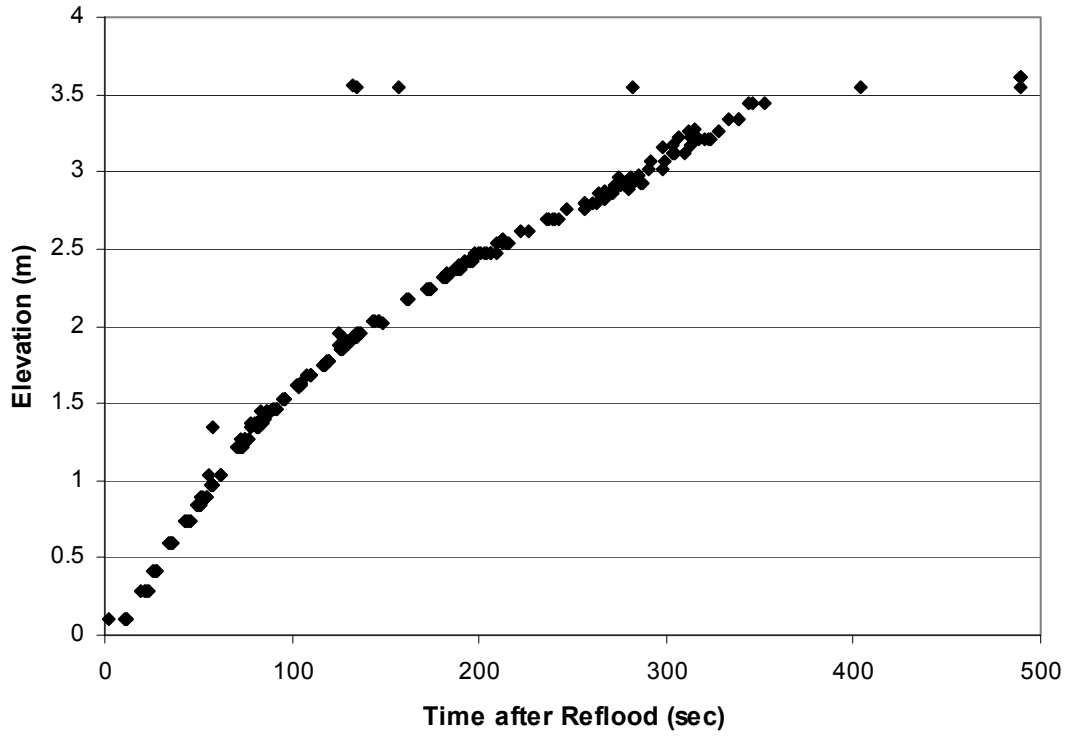
Heat Transfer Coefficient during Reflood RBHT Exp. 1196



Heat Transfer Coefficient during Reflood RBHT Exp. 1196



Quench Data, RBHT Exp. 1196



RBHT - REFLOOD TESTS

SUMMARY SHEET

RUN NO: **1202**

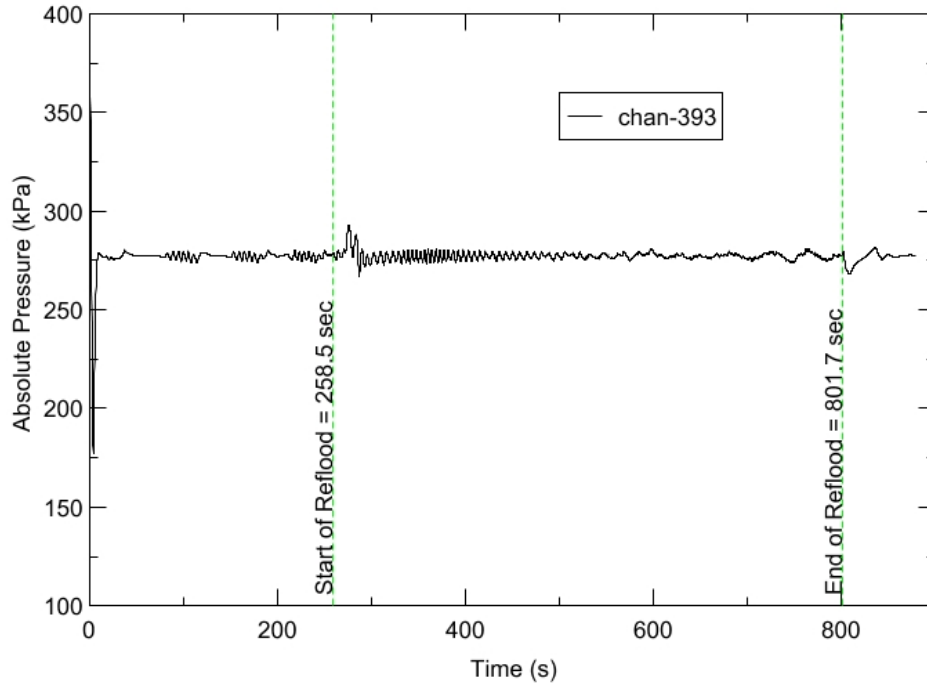
RUN CONDITIONS

Upper Plenum Pressure:	276 kPa (40 psia)
Initial Peak Clad Temperature:	1144 degrees K (1600 degrees F)
Rod Peak Power:	2.3 kW/m (0.7 kW/ft)
Flooding Rate:	0.1524 m/s (6 in/s)
Inlet Subcooling:	23 degrees K (42 degrees F)
Start of Reflood:	258.5 s
End of Reflood:	801.7 s
Test Date:	6/26/2002
Comments:	No droplet data

Rod_Elevation	Channel Number	Temperature at Reflood (K)	Temperature at Reflood (°F)	Turnaround Time (sec.)	Turnaround Temperature (K)	Turnaround Temperature (°F)	Quench Time (sec.)	Quench Temperature (K)	Quench Temperature (°F)
B6 0.592m	148	785.2	953.67	12.75	826.38	1027.8	53.75	601.82	623.59
B6 0.744m	149	793.17	968.02	13.75	838.07	1048.83	67.75	594.16	609.8
B6 0.846m	150	832.62	1039.03	15.25	881.9	1127.73	76.75	604.66	628.71
B6 0.897m	151	846.74	1064.44	15.25	897.77	1156.29	81.25	609.06	636.62
C6 1.04m	137	899.19	1158.85	15.75	954.66	1258.71	92.75	639.32	691.09
D5 1.27m	217	953.82	1257.19	15.25	1013.81	1365.18	115.75	626.45	667.91
C6 1.34m	138	943.26	1238.19	16.25	1006.86	1352.66	122.25	640.6	693.39
D5 1.37m	218	975.26	1295.78	16.25	1039.42	1411.27	125.25	659.19	726.85
C6 1.39m	139	949.78	1249.92	16.25	1014.06	1365.62	127.25	653.78	717.12
D5 1.45m	219	987.26	1317.39	16.25	1053.52	1436.65	132.75	661.59	731.17
C6 1.47m	140	962.65	1273.09	16.25	1027.99	1390.69	135.25	658.22	725.1
D5 1.52m	220	998.37	1337.38	16.25	1066.31	1459.67	141.25	669.88	746.1
C6 1.62m	141	981.42	1306.87	16.75	1052.3	1434.46	153.25	683.3	770.25
D5 1.68m	221	1017.85	1372.43	17.25	1090.43	1503.08	160.75	706.07	811.25
D5 1.78m	222	1000.69	1341.56	15.25	1069.11	1464.71	174.75	674.22	753.9
D5 1.85m	223	1029.2	1392.88	15.75	1101.96	1523.84	182.25	666.46	739.93
C6 1.87m	142	1008.66	1355.9	16.25	1083.89	1491.31	185.25	675.83	756.8
D5 1.90m	224	1037.05	1407	15.75	1112.8	1543.35	187.75	689.2	780.87
C6 1.95m	144	1016.74	1370.45	16.25	1093.92	1509.36	194.75	692.61	787.01
C3 2.17m	178	1060.58	1449.35	16.75	1143.98	1599.48	228.25	736.63	866.24
D4 2.24m	241	1062.08	1452.05	15.75	1138.89	1590.31	257.75	676.06	757.22
D4 2.32m	242	1092.44	1506.7	15.25	1173.75	1653.06	269.25	697.53	795.87
C3 2.35m	180	1085.18	1493.63	15.75	1169.22	1644.91	253.25	727.72	850.21
D4 2.37m	243	1100.75	1521.65	15.25	1184.09	1671.68	277.75	707.88	814.49
C3 2.40m	181	1089.25	1500.96	15.75	1174.93	1655.18	261.25	734.78	862.91
D4 2.54m	245	1130.93	1575.98	15.25	1216.07	1729.23	310.25	710.26	818.78
D6 2.62m	129	1119.25	1554.97	15.25	1207.24	1713.34	306.25	738.45	869.52
D6 2.69m	130	1116.66	1550.3	15.25	1206.92	1712.76	319.75	749.49	889.4
C3 2.76m	183	1119.31	1555.06	15.75	1208.58	1715.76	324.25	761.46	910.94
D4 2.79m	247	1093.75	1509.06	14.75	1179.97	1664.26	357.75	686.13	775.35
D6 2.87m	131	1059.62	1447.62	14.75	1140.88	1593.89	346.25	681.91	767.74
D6 2.92m	132	1037.1	1407.1	15.75	1123.33	1562.3	353.25	702.94	805.6
D6 2.97m	133	1011.16	1360.39	15.75	1092.56	1506.92	360.75	682.03	767.96
D6 3.07m	134	977.86	1300.47	16.25	1053.28	1436.22	369.75	667.06	741.03
E3 3.12m	197	987.23	1317.32	16.25	1061.33	1450.71	390.75	663.43	734.49
D6 3.17m	135	943.69	1238.95	16.25	1013.75	1365.07	378.75	658.9	726.33
D6 3.27m	136	897.32	1155.48	16.25	965.05	1277.4	387.25	626.8	668.56
D4 3.61m	248	682.83	769.4	17.25	752.89	895.52	62.25	559.36	547.16

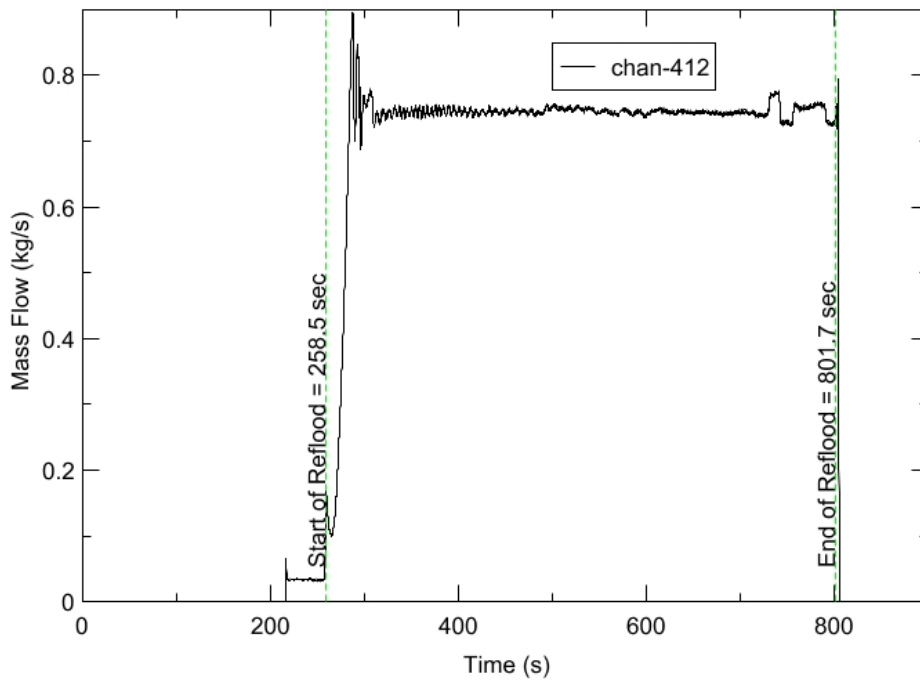
RBHT - TEST FACILITY

Upper Plenum Pressure vs. Time, Exp 1202



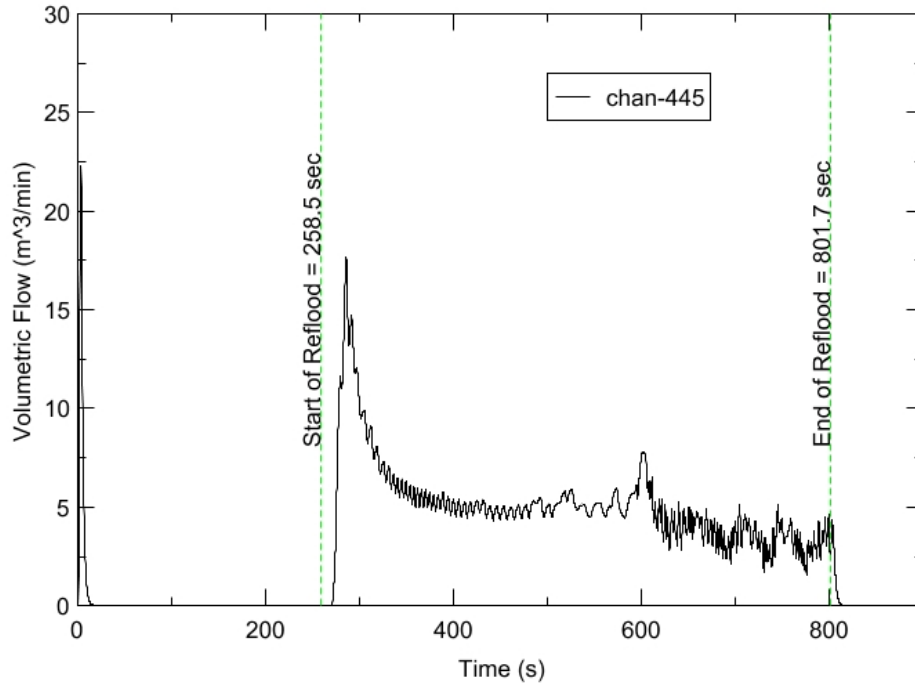
RBHT - TEST FACILITY

Inlet Flow vs. Time, Exp 1202



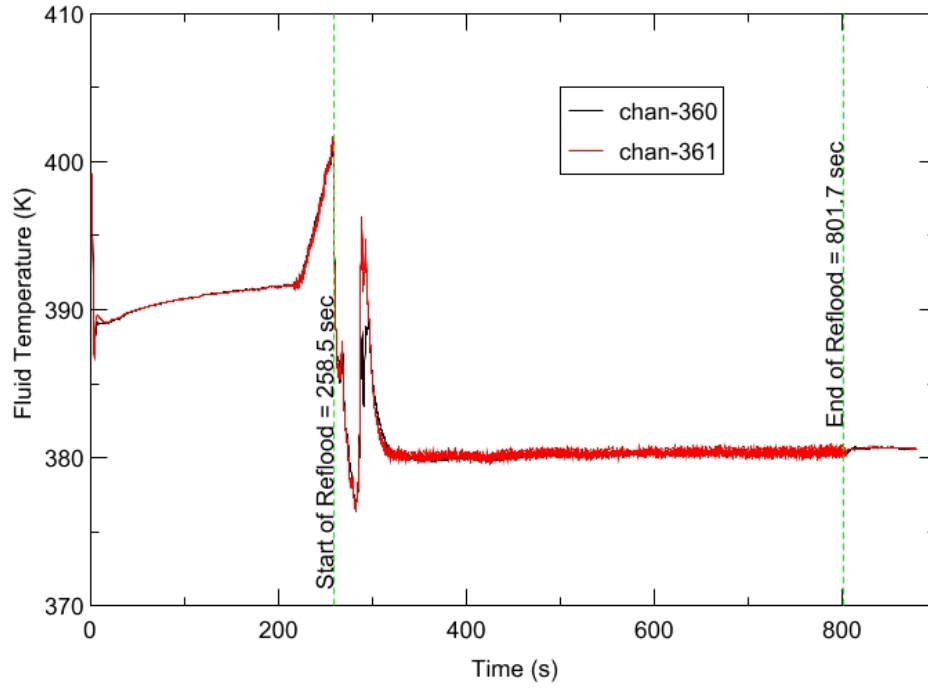
RBHT - TEST FACILITY

Steam Exhaust Flow vs. Time, Exp 1202



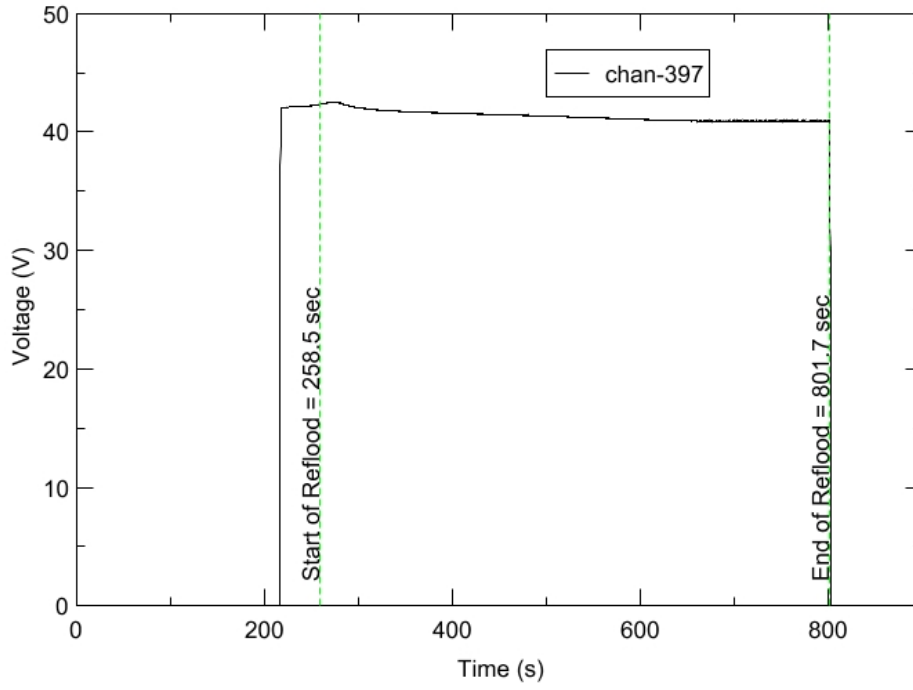
RBHT - TEST FACILITY

Inlet Flow Temperature vs. Time, Exp 1202



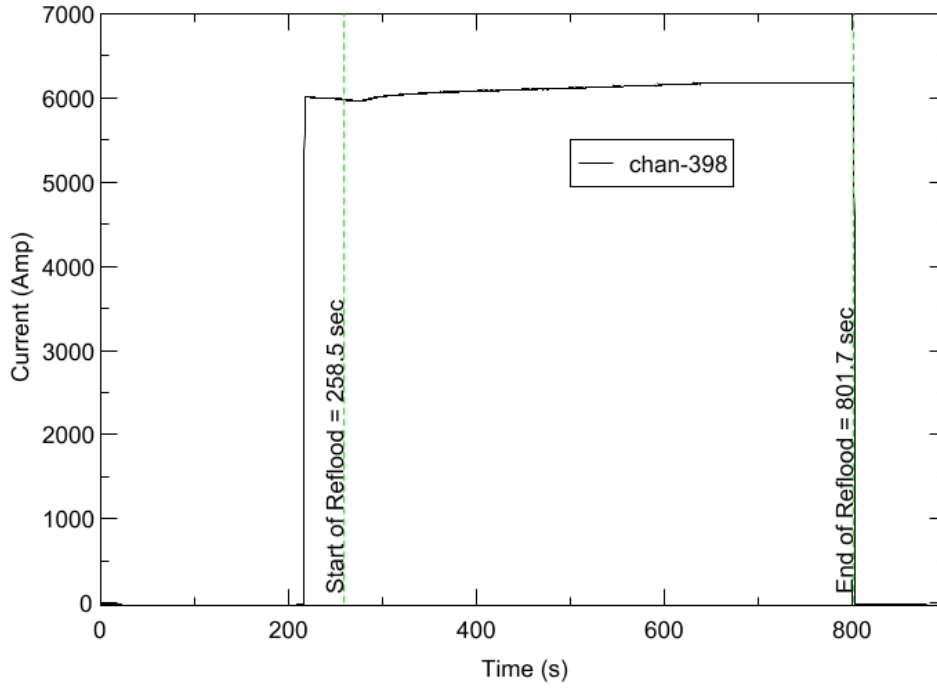
RBHT - TEST FACILITY

Test Section Voltage vs. Time, Exp 1202

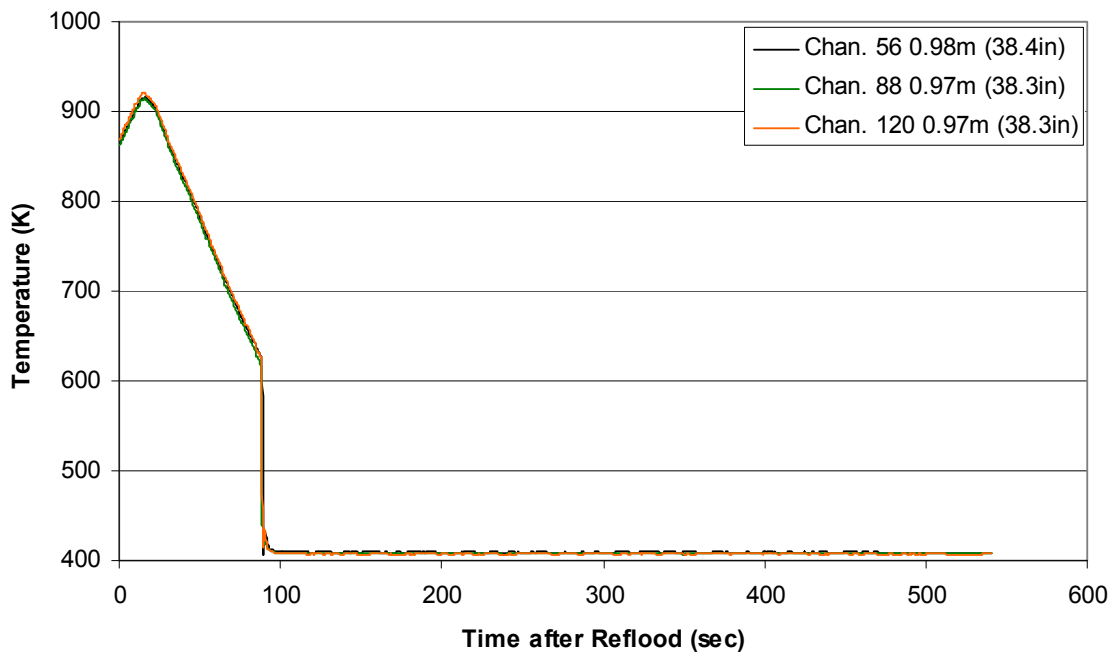


RBHT - TEST FACILITY

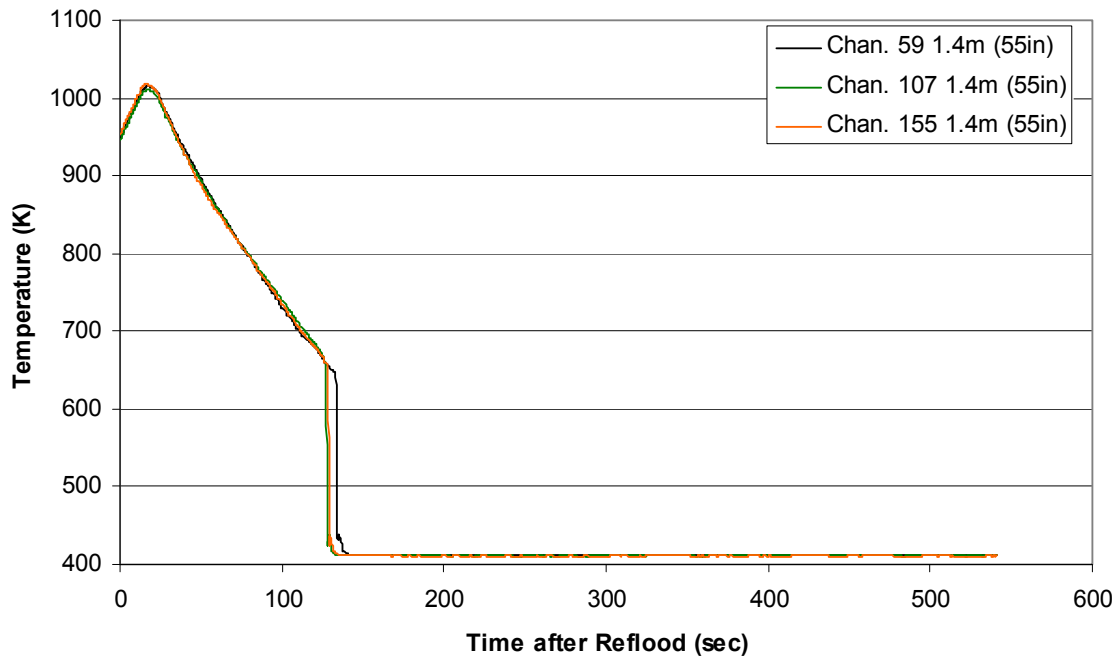
Test Section Current vs. Time, Exp 1202



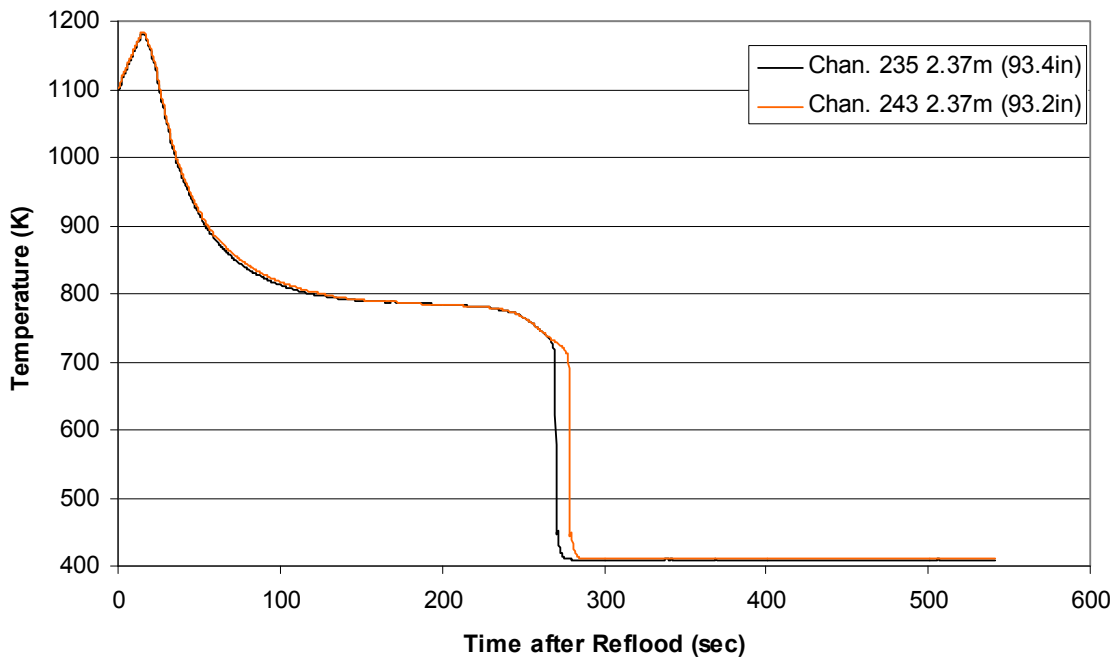
Heater Rod Temperature during Reflood
RBHT Exp. 1202



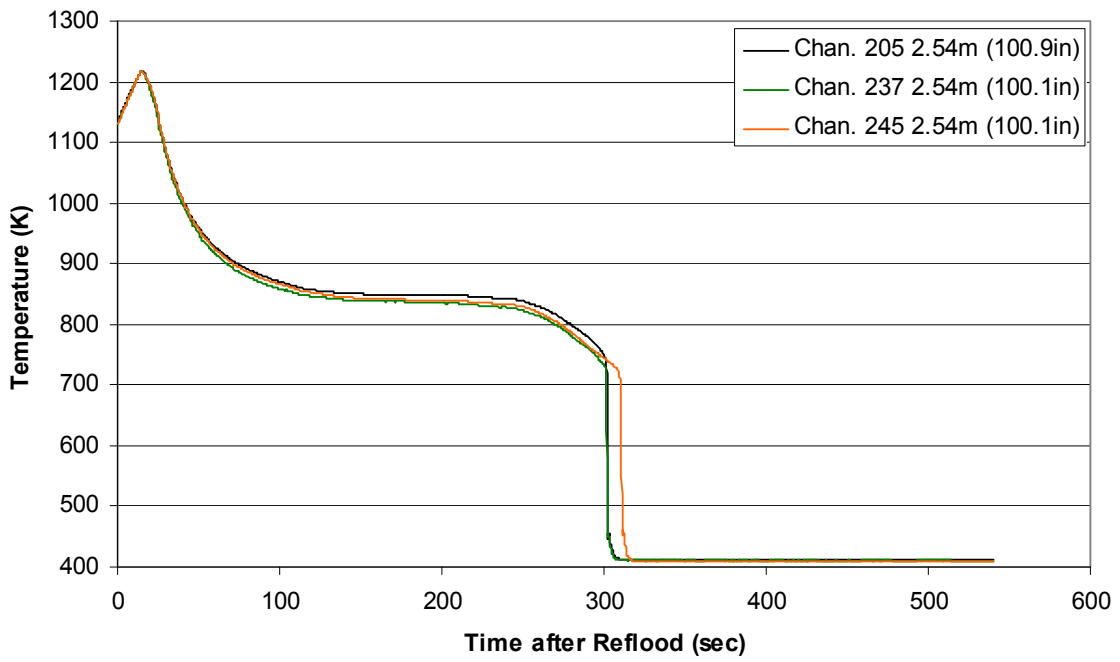
Heater Rod Temperature during Reflood
RBHT Exp. 1202



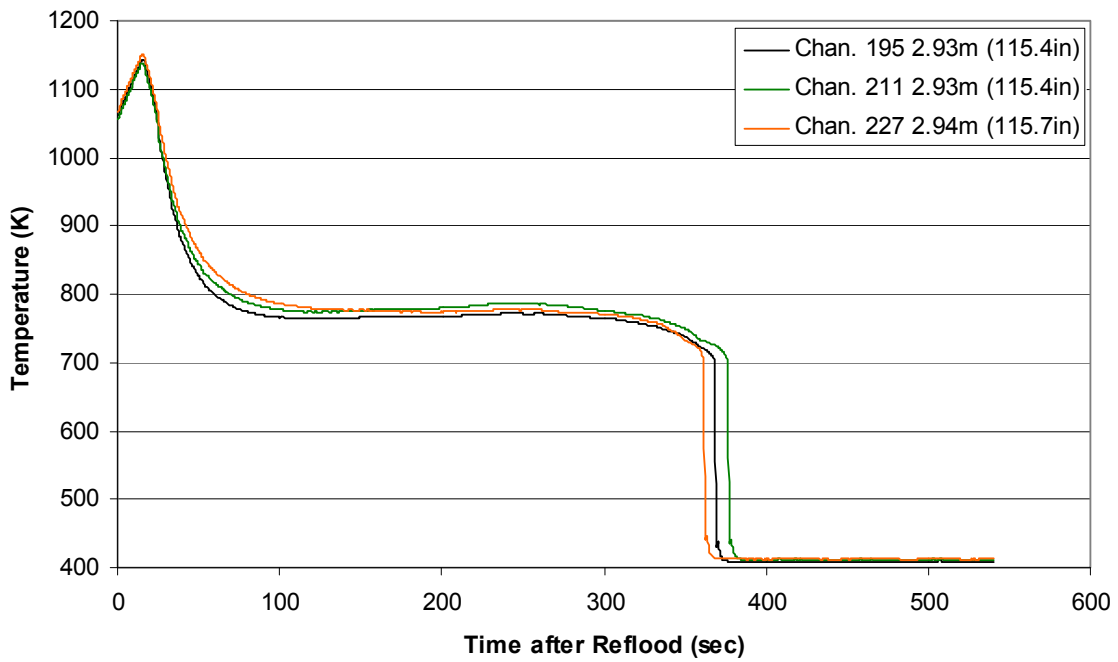
Heater Rod Temperature during Reflood
RBHT Exp. 1202



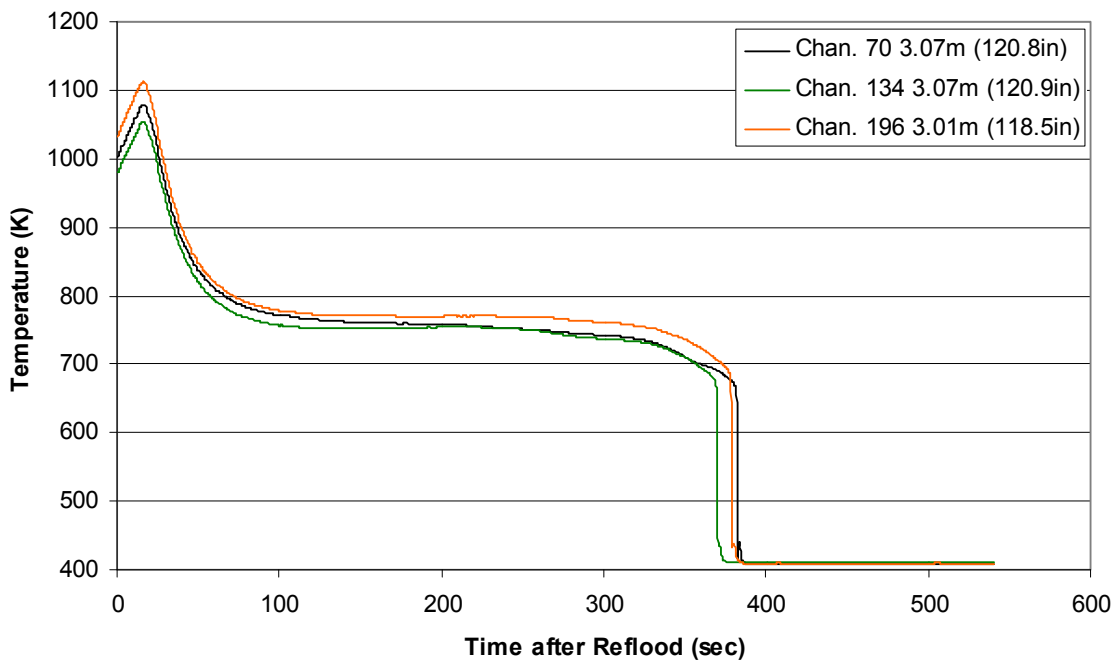
Heater Rod Temperature during Reflood
RBHT Exp. 1202



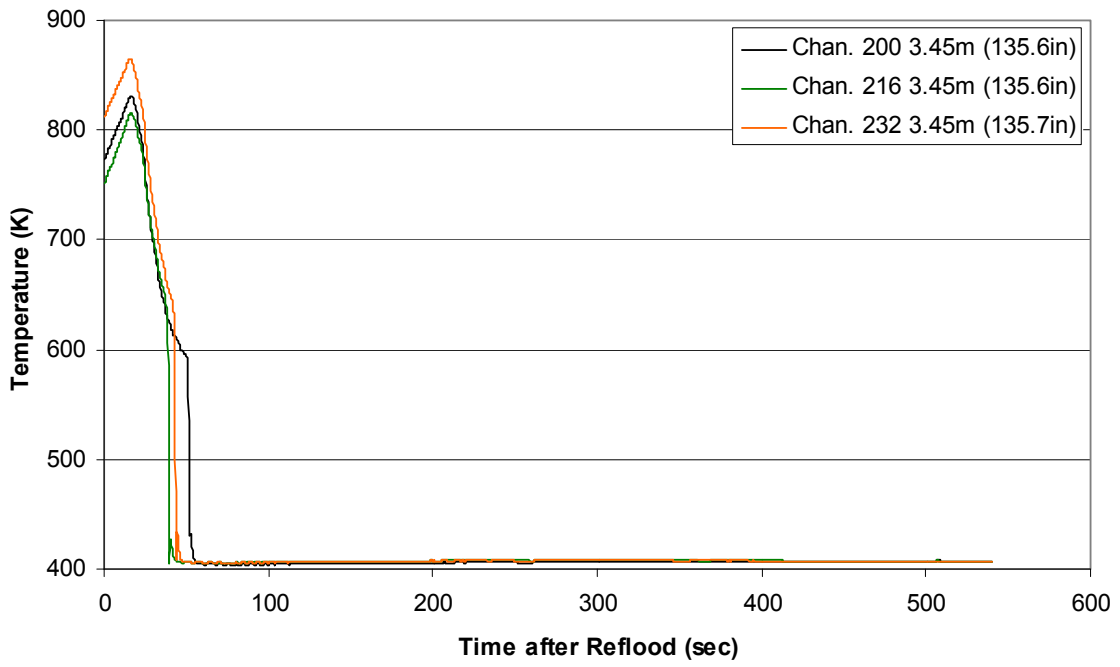
**Heater Rod Temperature during Reflood
RBHT Exp. 1202**



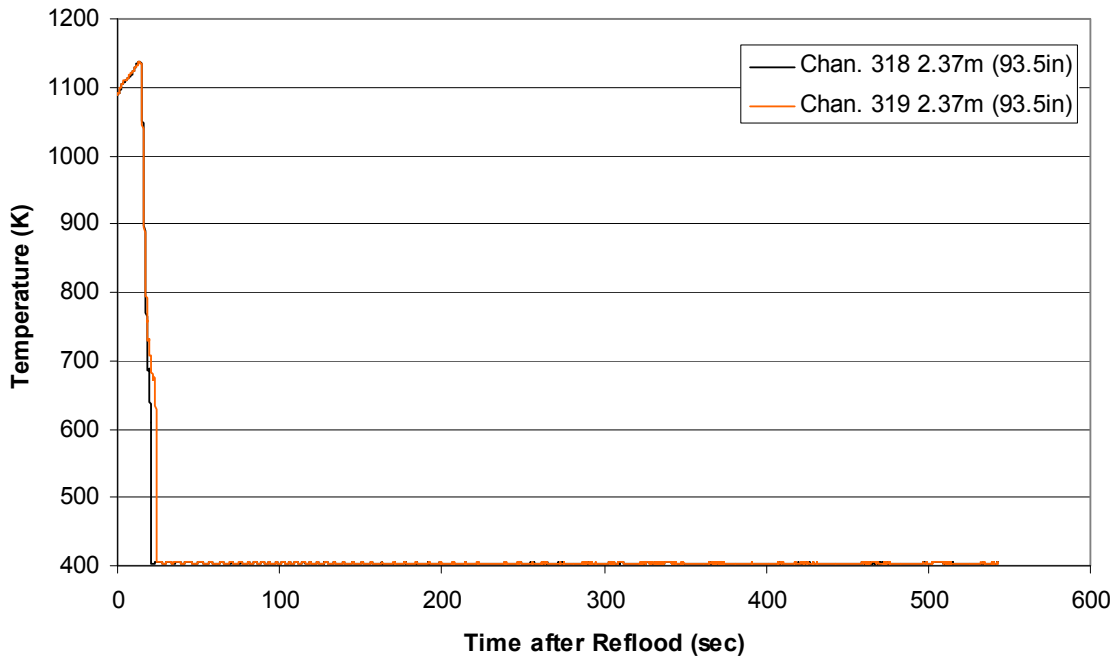
**Heater Rod Temperature during Reflood
RBHT Exp. 1202**



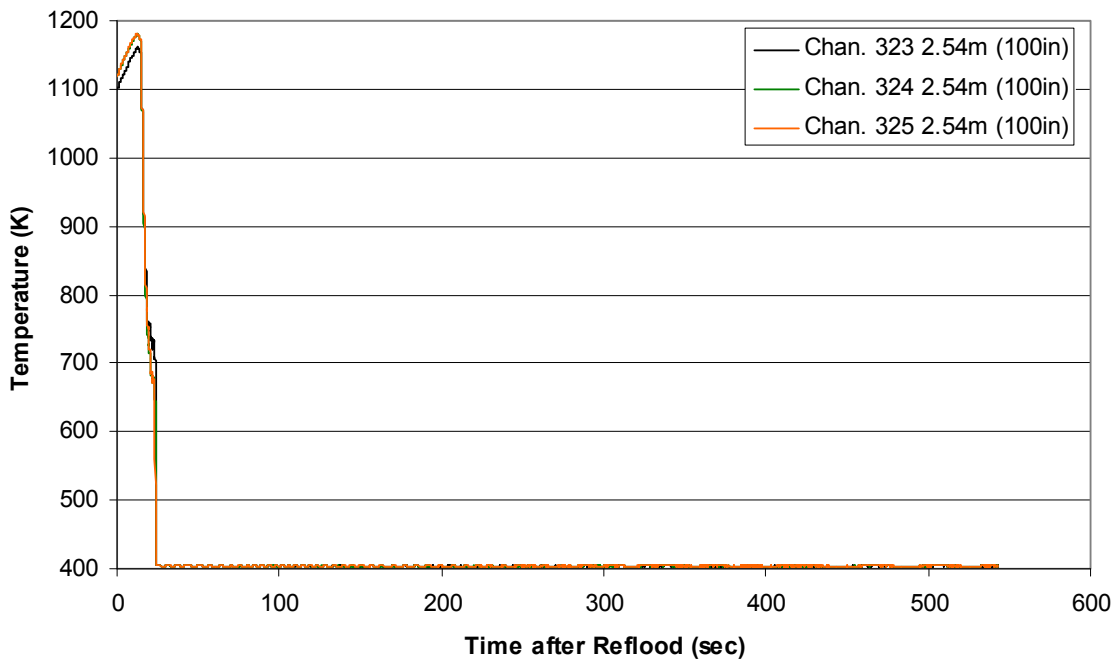
Heater Rod Temperature during Reflood RBHT Exp. 1202



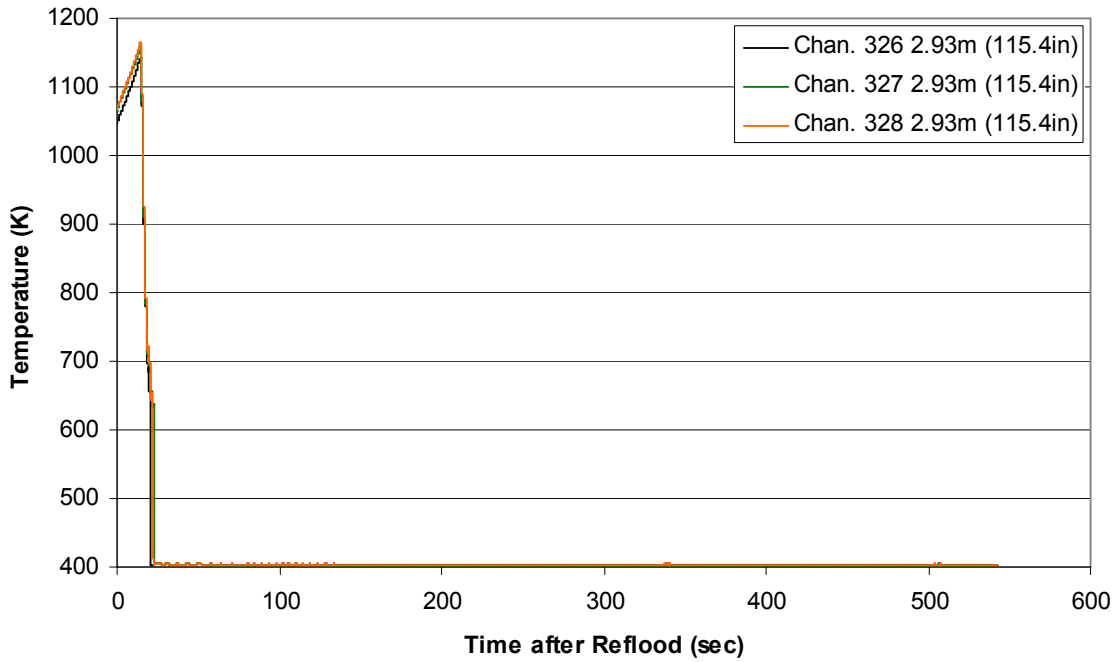
Steam Probe Temperature during Reflood RBHT Exp. 1202



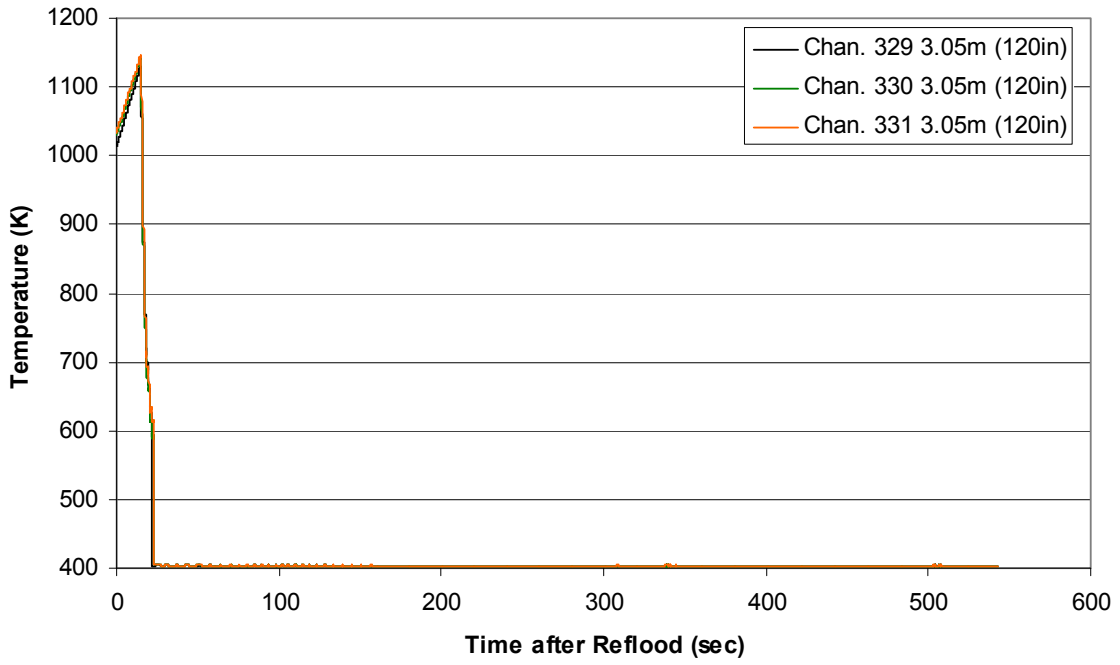
Steam Probe Temperature during Reflood RBHT Exp. 1202



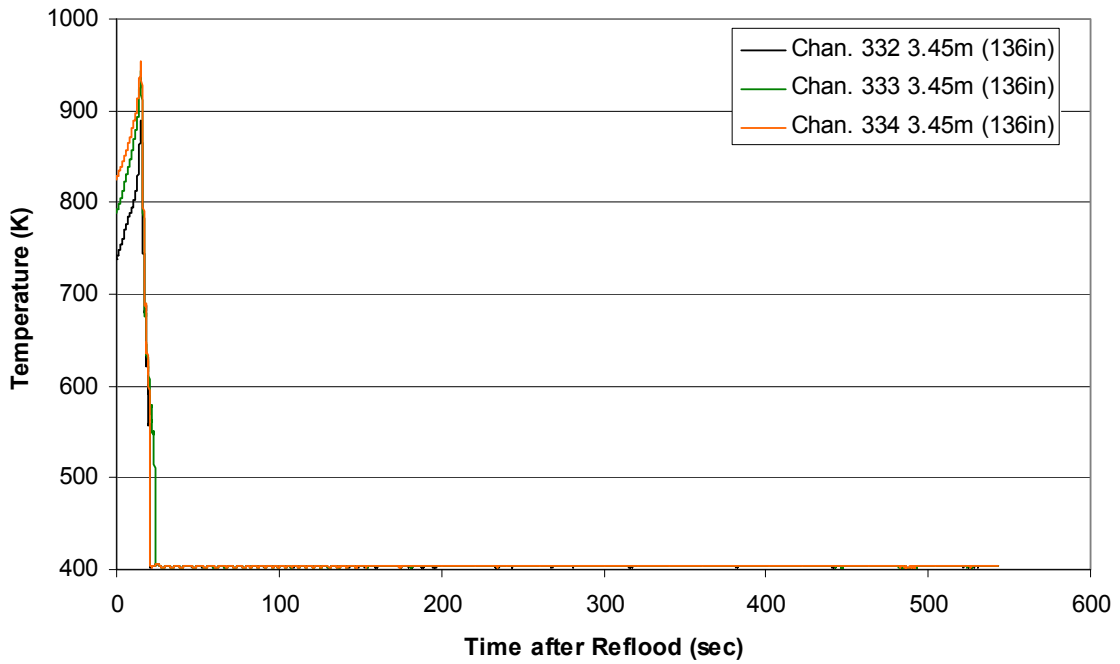
Steam Probe Temperature during Reflood RBHT Exp. 1202



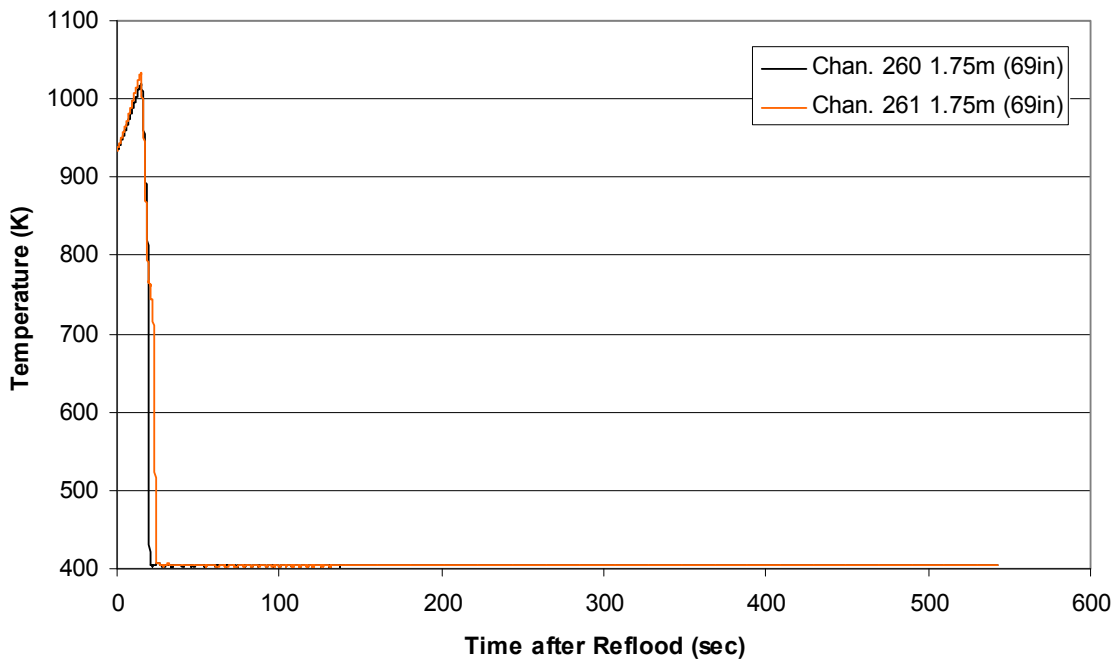
Steam Probe Temperature during Reflood
RBHT Exp. 1202



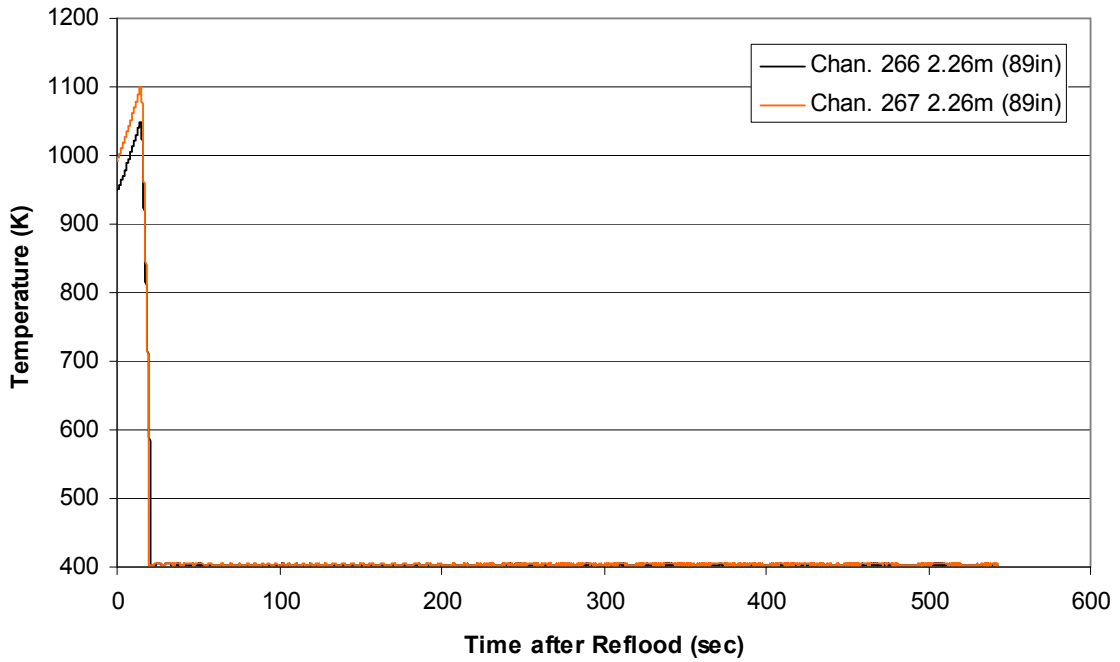
Steam Probe Temperature during Reflood
RBHT Exp. 1202



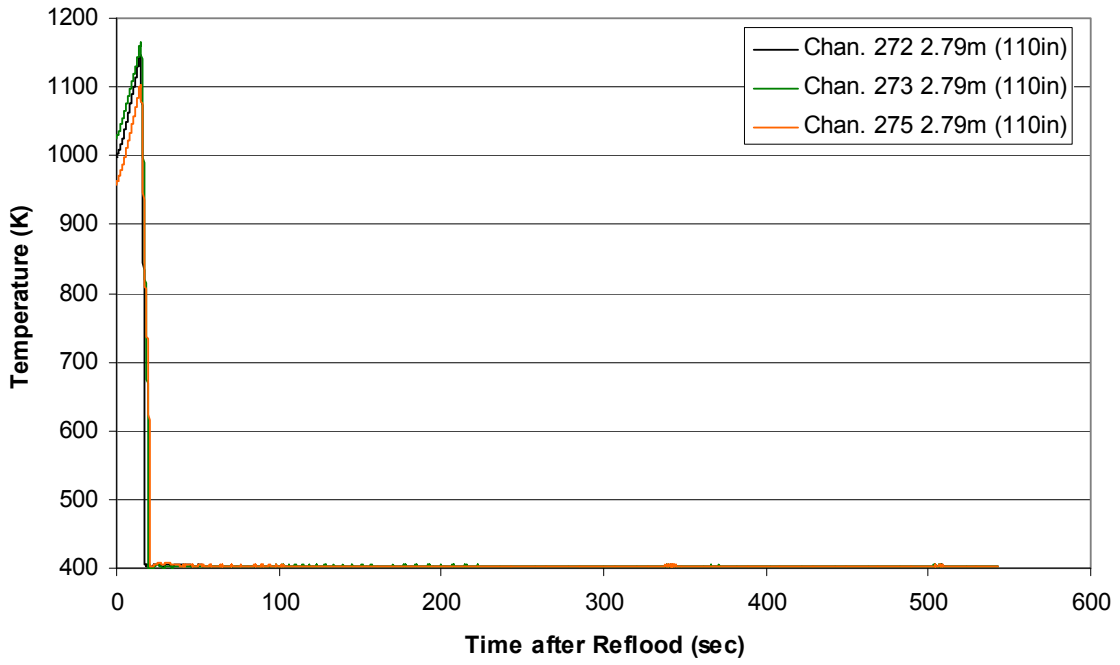
Spacer Grid Temperature during Reflood RBHT Exp. 1202



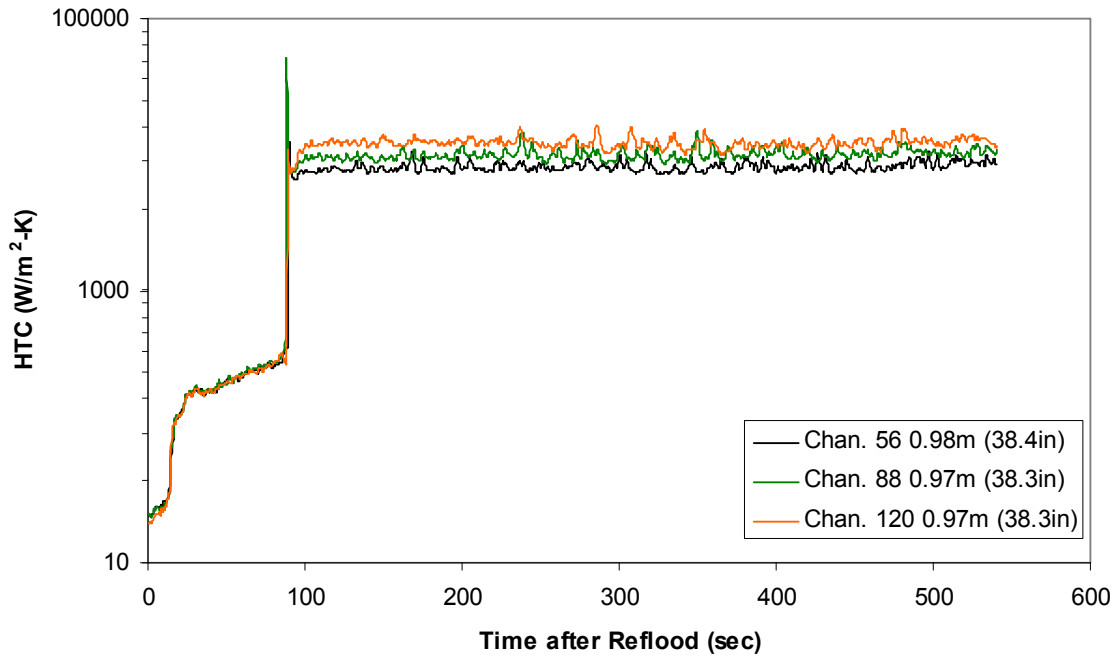
Spacer Grid Temperature during Reflood RBHT Exp. 1202



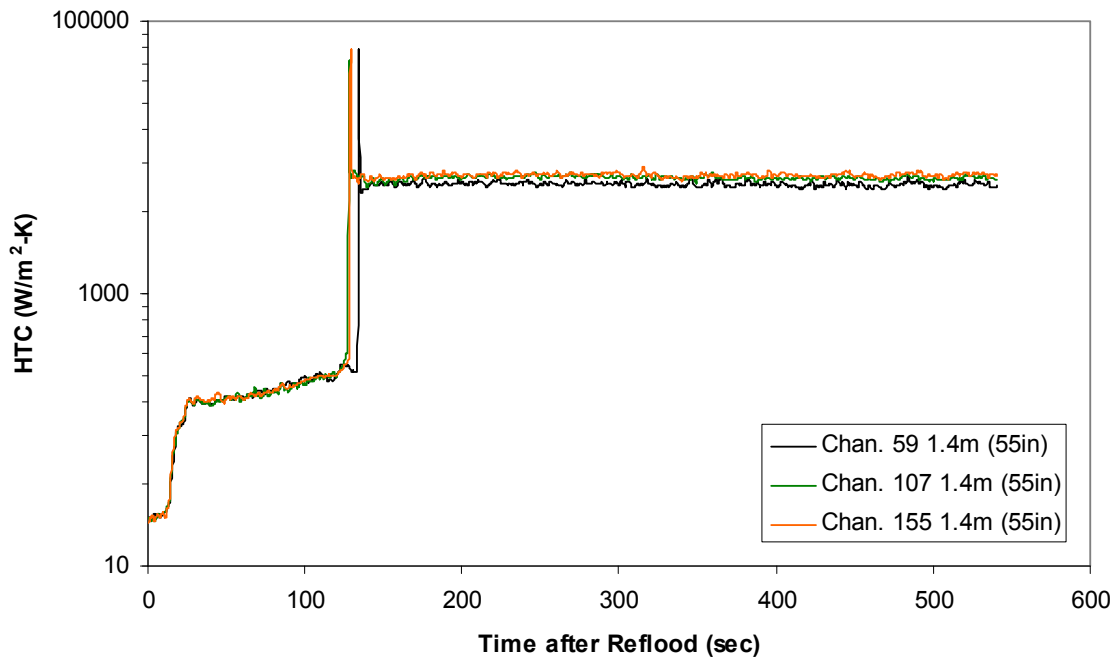
Spacer Grid Temperature during Reflood RBHT Exp. 1202



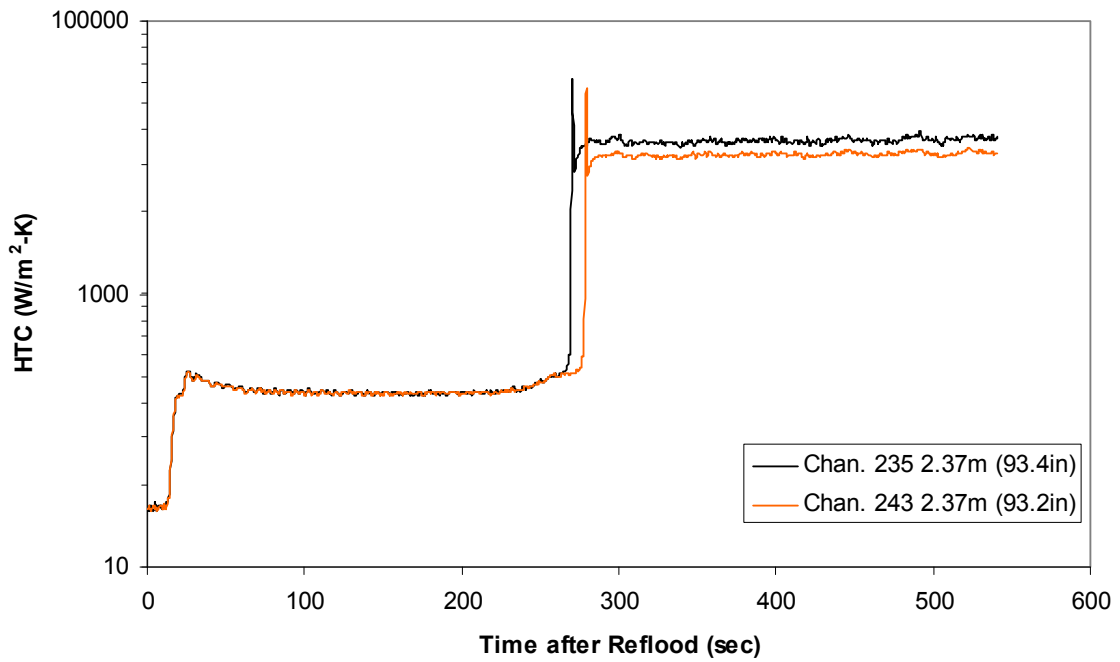
Heat Transfer Coefficient during Reflood RBHT Exp. 1202



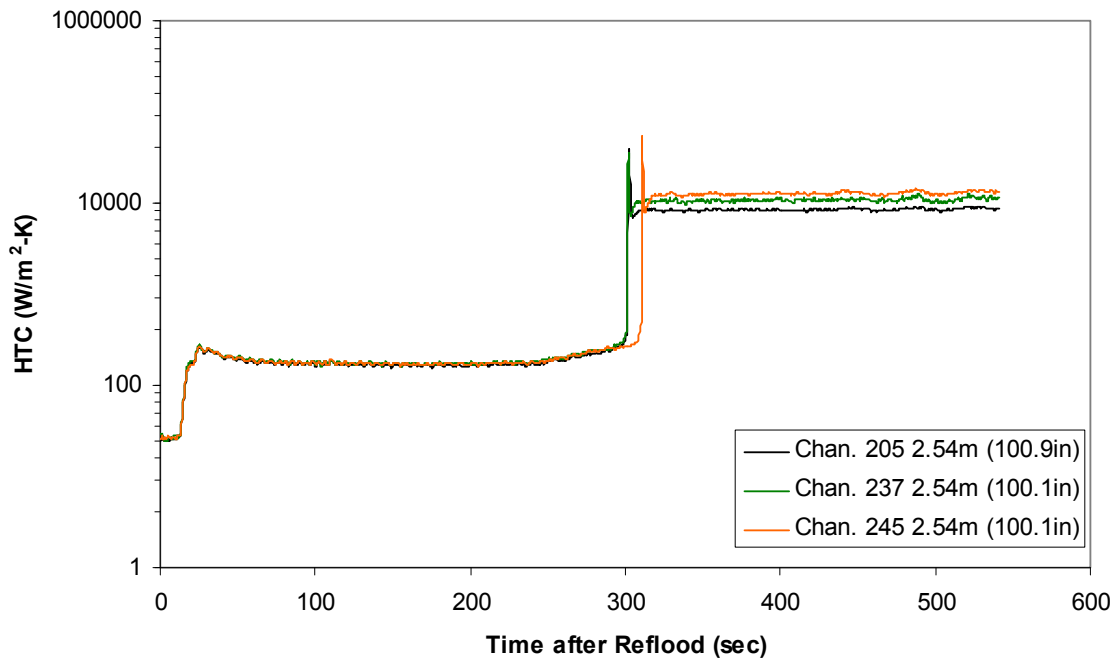
Heat Transfer Coefficient during Reflood
RBHT Exp. 1202



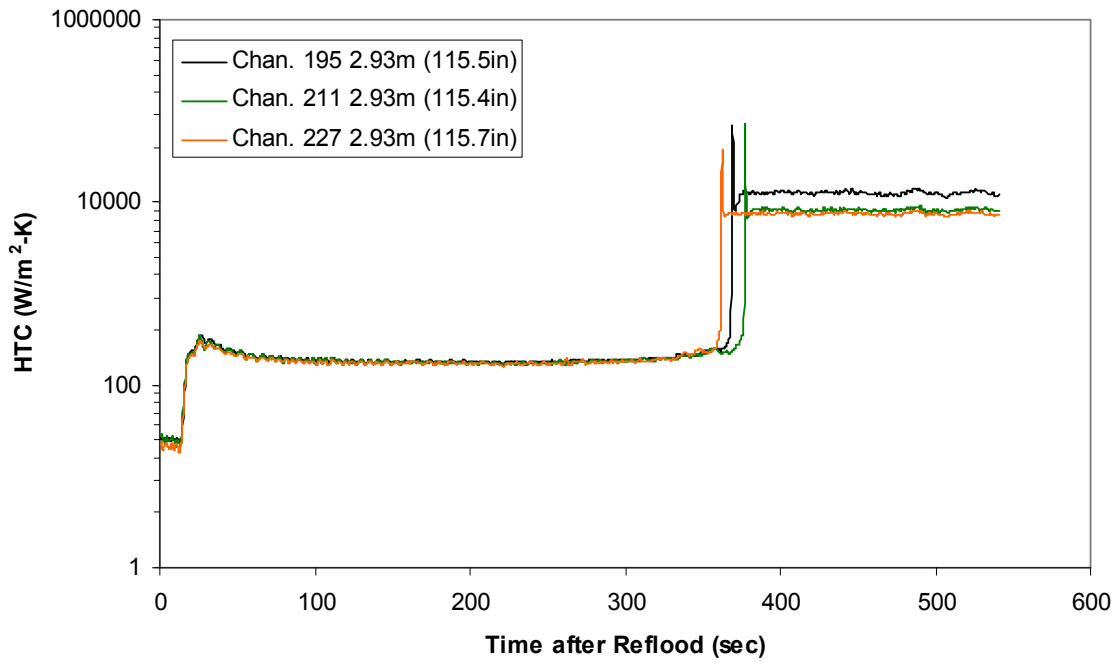
Heat Transfer Coefficient during Reflood
RBHT Exp. 1202



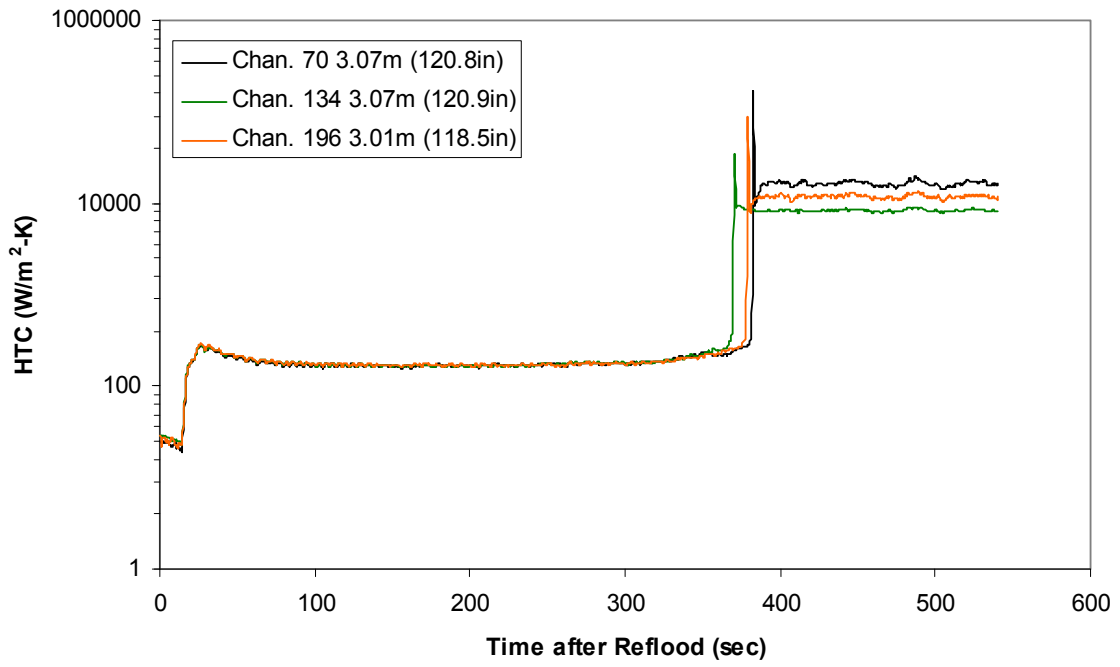
Heat Transfer Coefficient during Reflood RBHT Exp. 1202



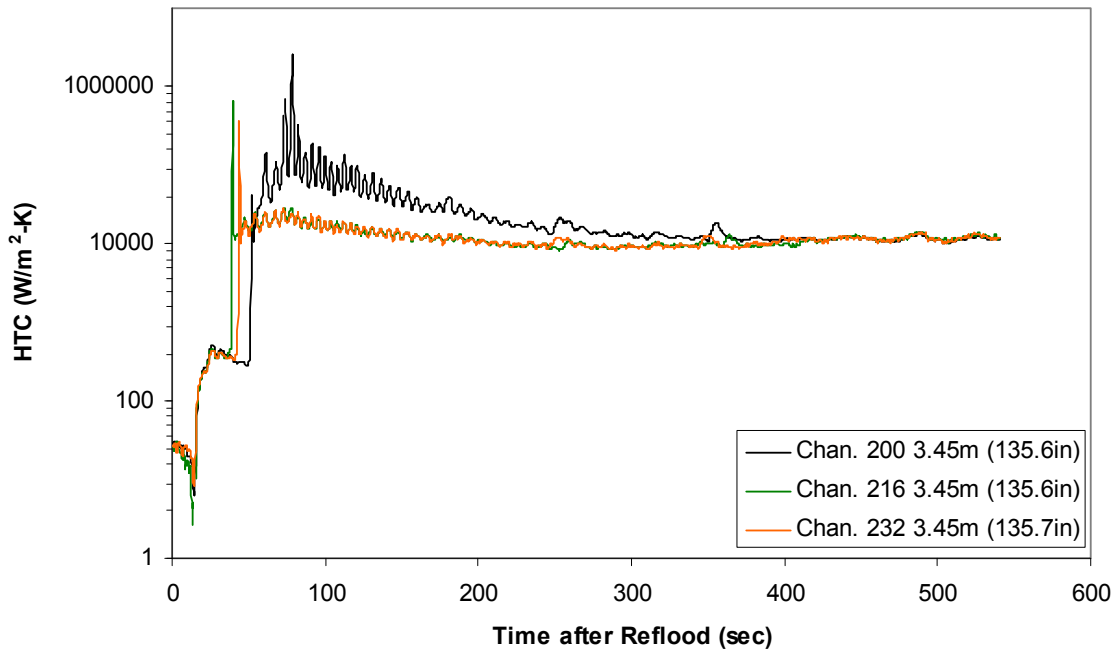
Heat Transfer Coefficient during Reflood RBHT Exp. 1202



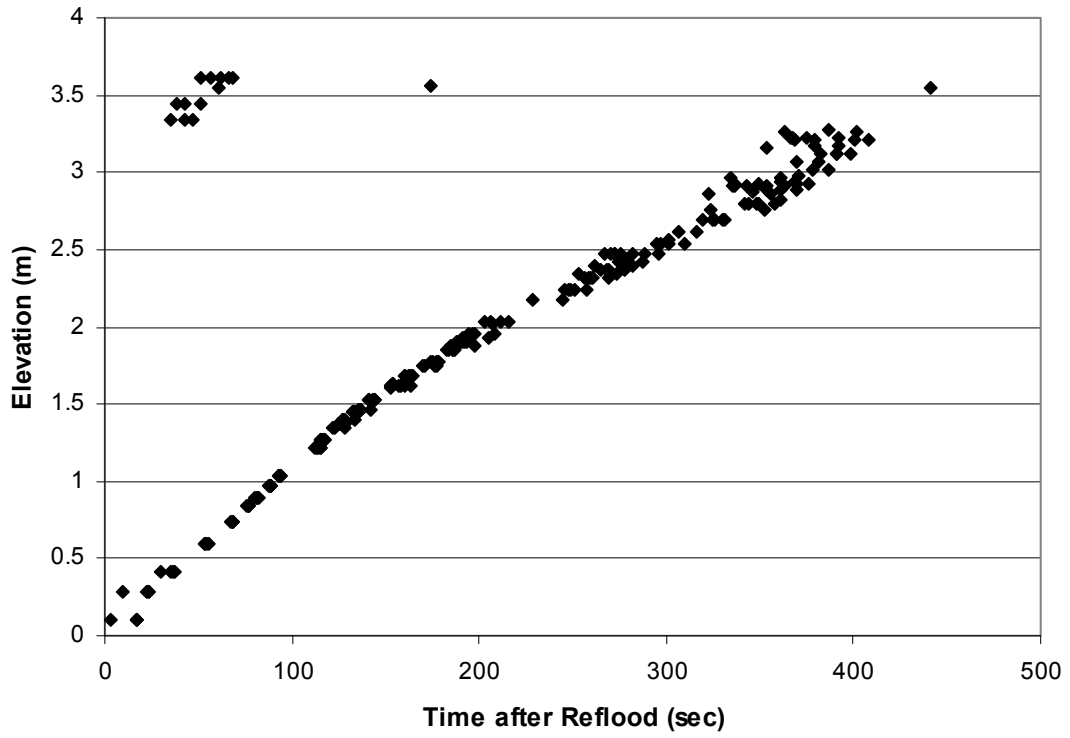
Heat Transfer Coefficient during Reflood RBHT Exp. 1202



Heat Transfer Coefficient during Reflood RBHT Exp. 1202



Quench Data, RBHT Exp. 1202



RBHT - REFLOOD TESTS

SUMMARY SHEET

RUN NO: **1223**

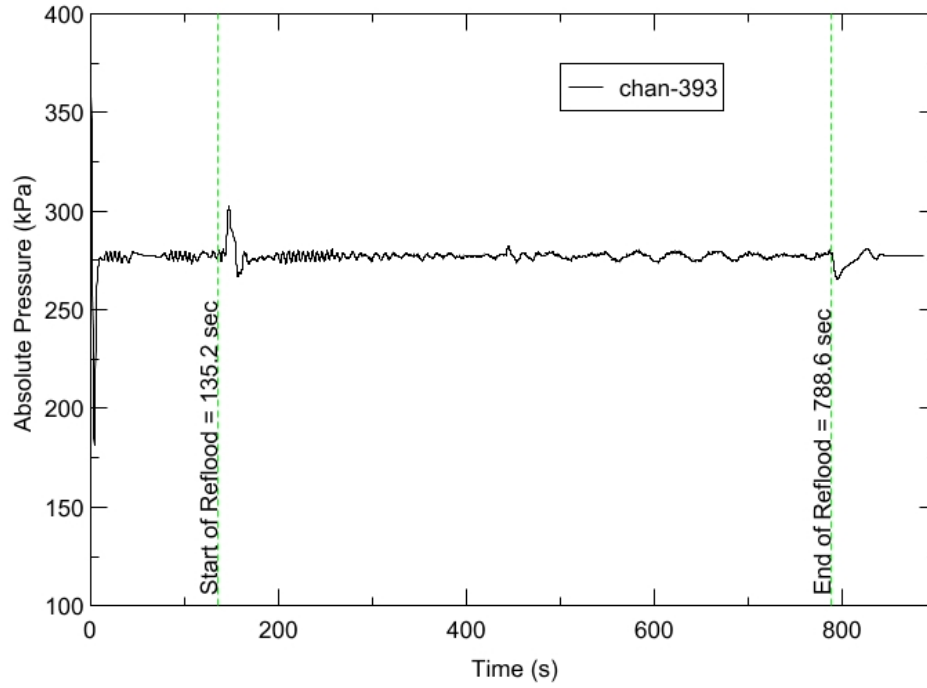
RUN CONDITIONS

Upper Plenum Pressure:	276 kPa (40 psia)
Initial Peak Clad Temperature:	1144 degrees K (1600 degrees F)
Rod Peak Power:	2.3 kW/m (0.7 kW/ft)
Flooding Rate:	0.1524 m/s (6 in/s)
Inlet Subcooling:	11 degrees K (20 degrees F)
Start of Reflood:	135.2 s
End of Reflood:	788.6 s
Test Date:	6/28/2002
Comments:	No droplet data

Rod_Elevation	Channel Number	Temperature at Reflood (K)	Temperature at Reflood (°F)	Turnaround Time (sec.)	Turnaround Temperature (K)	Turnaround Temperature (°F)	Quench Time (sec.)	Quench Temperature (K)	Quench Temperature (°F)
B6 0.592m	148	815.75	1008.67	8.05	841.44	1054.9	57.05	604.52	628.45
B6 0.744m	149	814.49	1006.4	9.05	842.14	1056.17	73.55	595.32	611.89
B6 0.846m	150	863.85	1095.25	9.05	893.99	1149.5	82.55	624.38	664.2
B6 0.897m	151	876.88	1118.69	9.05	908.08	1174.86	88.05	632.66	679.1
C6 1.04m	137	929.28	1213.01	10.05	965.39	1278.01	101.55	663.86	735.27
D5 1.27m	217	986.93	1316.79	9.55	1024.03	1383.57	127.55	635.06	683.43
C6 1.34m	138	978.65	1301.87	10.55	1019.77	1375.9	132.05	654.93	719.18
D5 1.37m	218	1010.85	1359.84	10.05	1051.34	1432.73	138.55	668.55	743.71
C6 1.39m	139	984.71	1312.8	10.55	1026.4	1387.84	137.55	669.03	744.57
D5 1.45m	219	1023.55	1382.7	10.05	1065.5	1458.21	146.55	672.62	751.02
C6 1.47m	140	997.01	1334.93	10.55	1039.86	1412.07	146.05	663.72	735
D5 1.52m	220	1035.14	1403.56	10.55	1078.69	1481.96	155.55	675.9	756.93
C6 1.62m	141	1017.25	1371.36	11.05	1063.39	1454.41	164.05	696.84	794.62
D5 1.68m	221	1056.13	1441.35	11.05	1102.5	1524.81	175.05	715.94	829.01
D5 1.78m	222	1025.41	1386.04	10.05	1069.11	1464.71	188.55	658.7	725.97
D5 1.85m	223	1065.98	1459.08	10.05	1111.09	1540.28	195.55	673.38	752.4
C6 1.87m	142	1046.34	1423.73	10.55	1094.18	1509.84	195.55	679.34	763.13
D5 1.90m	224	1077.53	1479.87	10.05	1125.11	1565.51	201.55	683.68	770.93
C6 1.95m	144	1057.99	1444.69	10.55	1106.75	1532.46	204.55	692.25	786.36
C3 2.17m	178	1111.34	1540.73	10.55	1164.78	1636.91	229.55	732.41	858.66
D4 2.24m	241	1102.01	1523.94	10.05	1151.56	1613.13	260.55	658.89	726.32
D4 2.32m	242	1143.71	1598.99	9.55	1194.86	1691.07	270.05	691.88	785.69
C3 2.35m	180	1139.61	1591.61	10.05	1193.57	1688.73	250.05	721	838.11
D4 2.37m	243	1153.21	1616.1	9.55	1205.81	1710.76	277.55	706.4	811.83
C3 2.40m	181	1143.16	1598	10.05	1198.42	1697.47	257.05	728.15	850.98
D4 2.54m	245	1182.24	1668.34	9.55	1234.08	1761.65	306.55	705.27	809.8
D6 2.62m	129	1172.6	1650.99	9.55	1226.25	1747.56	302.05	740.86	873.86
D6 2.69m	130	1174.06	1653.61	9.55	1228.88	1752.3	314.55	746.06	883.21
C3 2.76m	183	1173.74	1653.05	9.55	1228.42	1751.46	313.55	752.44	894.7
D6 2.92m	132	1084.66	1492.71	10.05	1138.96	1590.44	344.55	701.9	803.74
D6 2.97m	133	1052.16	1434.21	10.55	1103.96	1527.45	352.05	686.13	775.34
D6 3.07m	134	1011.27	1360.61	10.55	1058.82	1446.19	360.55	672.82	751.4
E3 3.12m	197	1018.93	1374.39	10.05	1065.54	1458.28	372.05	670.16	746.59
D6 3.17m	135	975.12	1295.53	10.55	1018.73	1374.03	369.55	658.76	726.07
D6 3.27m	136	923.94	1203.4	10.55	966.94	1280.81	378.05	620.05	656.4
D4 3.61m	248	708.78	816.12	10.55	761.21	910.49	40.05	569	564.52

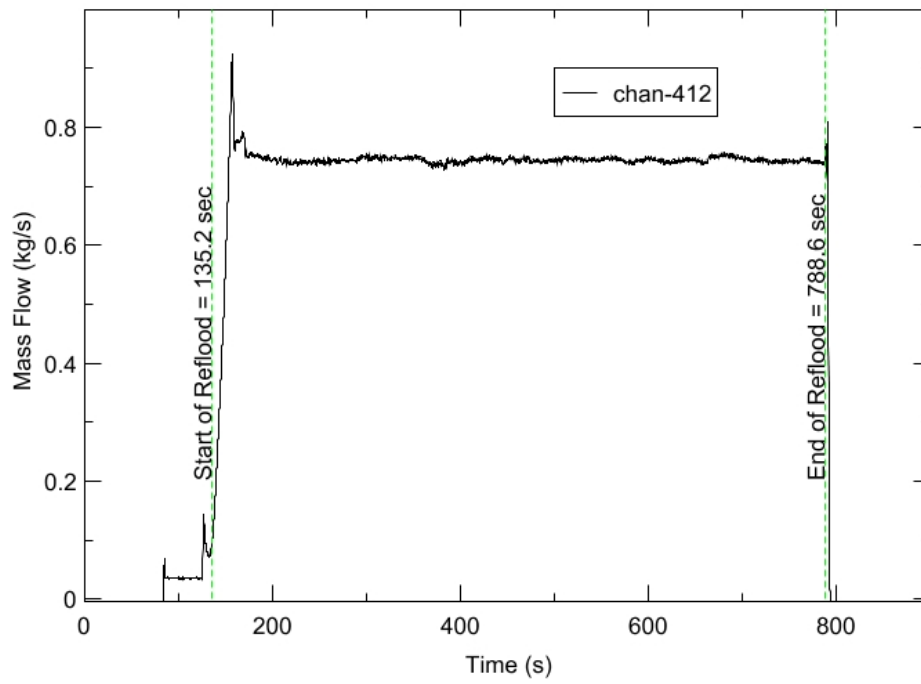
RBHT - TEST FACILITY

Upper Plenum Pressure vs. Time, Exp 1223



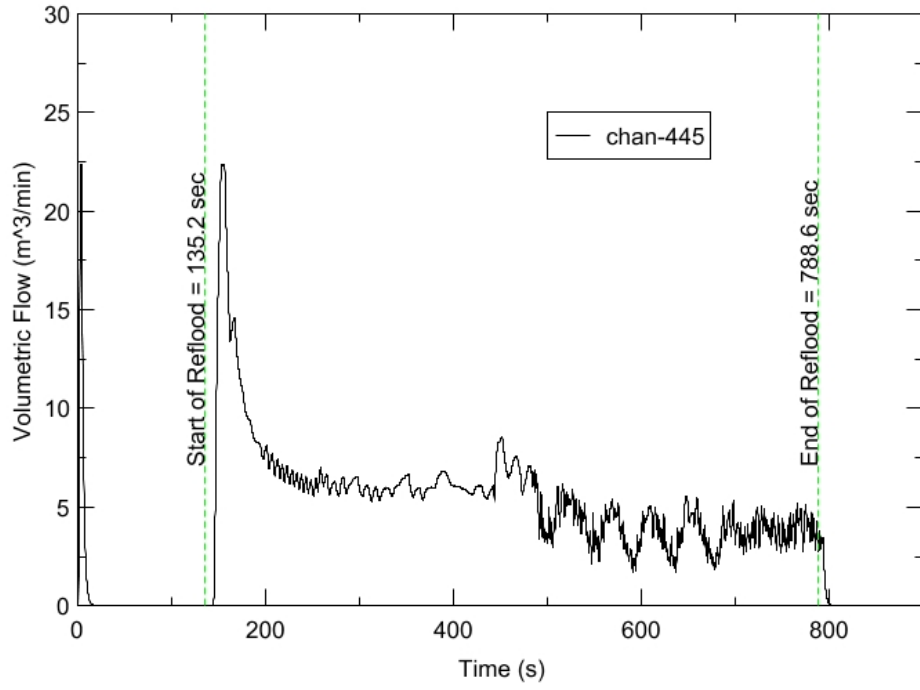
RBHT - TEST FACILITY

Inlet Flow vs. Time, Exp 1223



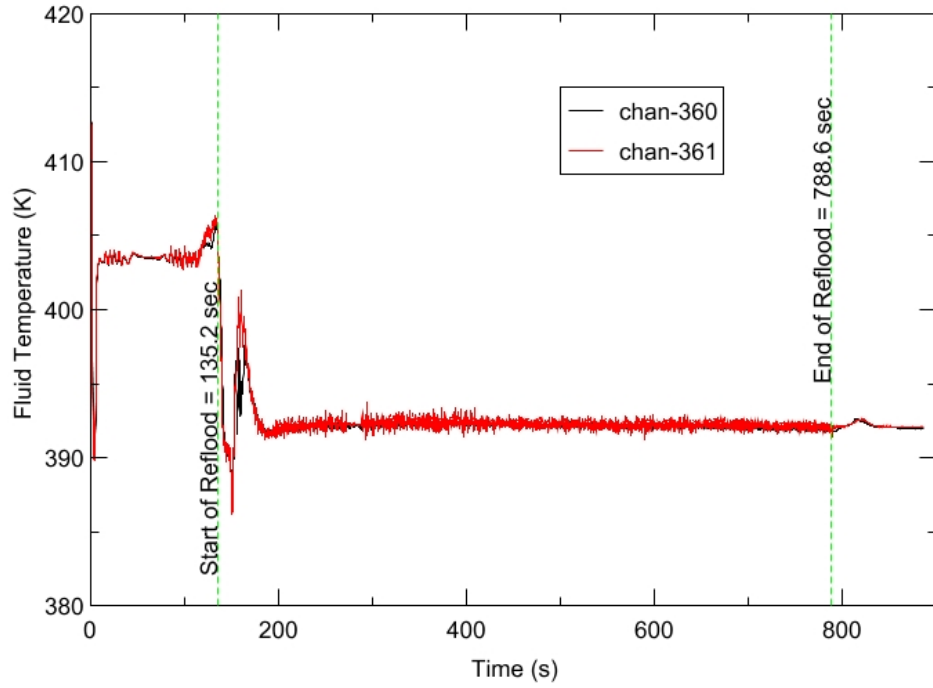
RBHT - TEST FACILITY

Steam Exhaust Flow vs. Time, Exp 1223



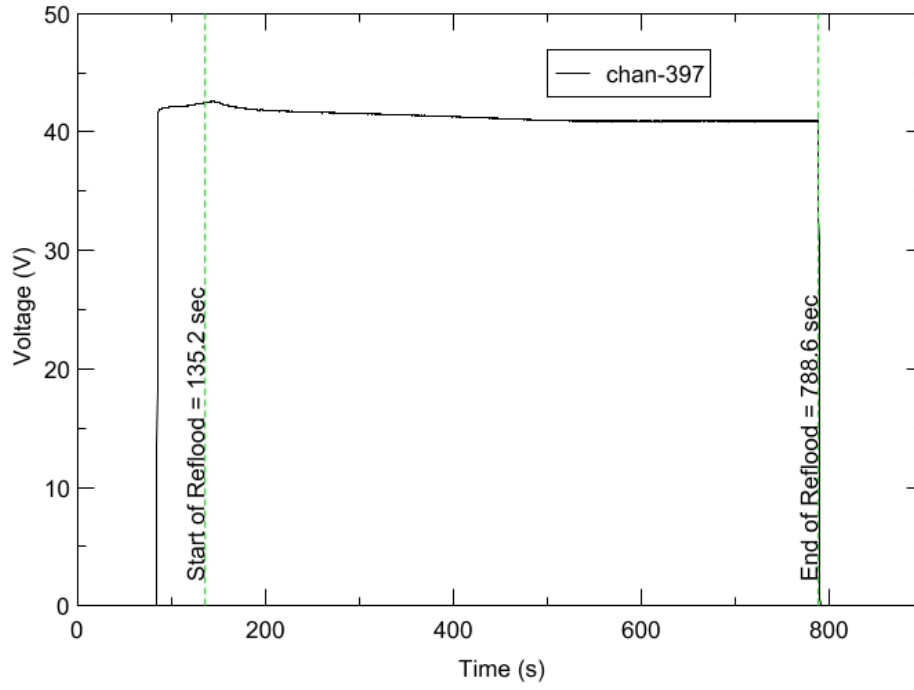
RBHT - TEST FACILITY

Inlet Flow Temperature vs. Time, Exp 1223



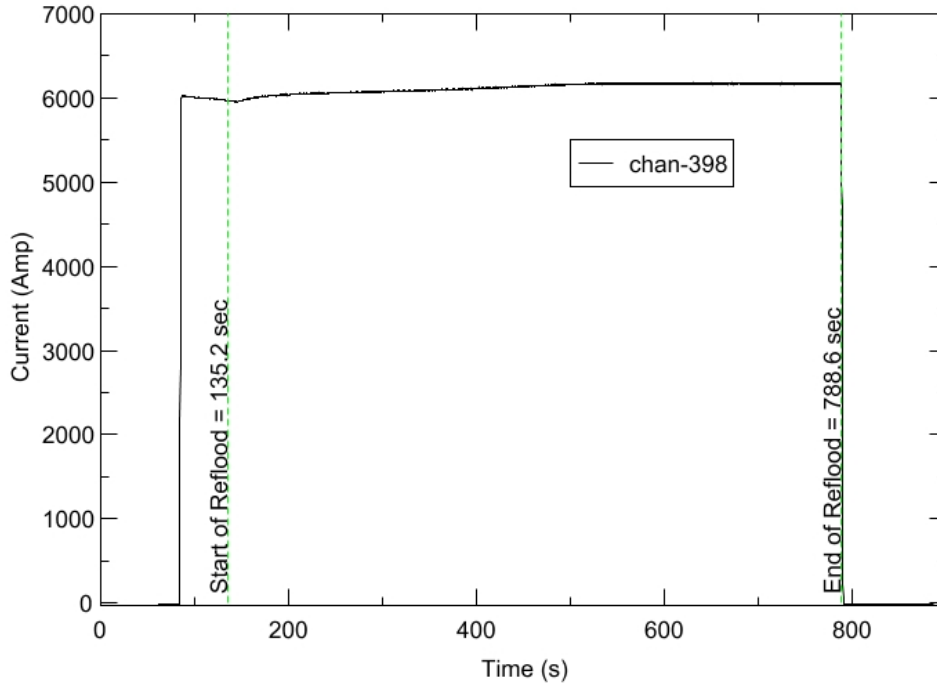
RBHT - TEST FACILITY

Test Section Voltage vs. Time, Exp 1223

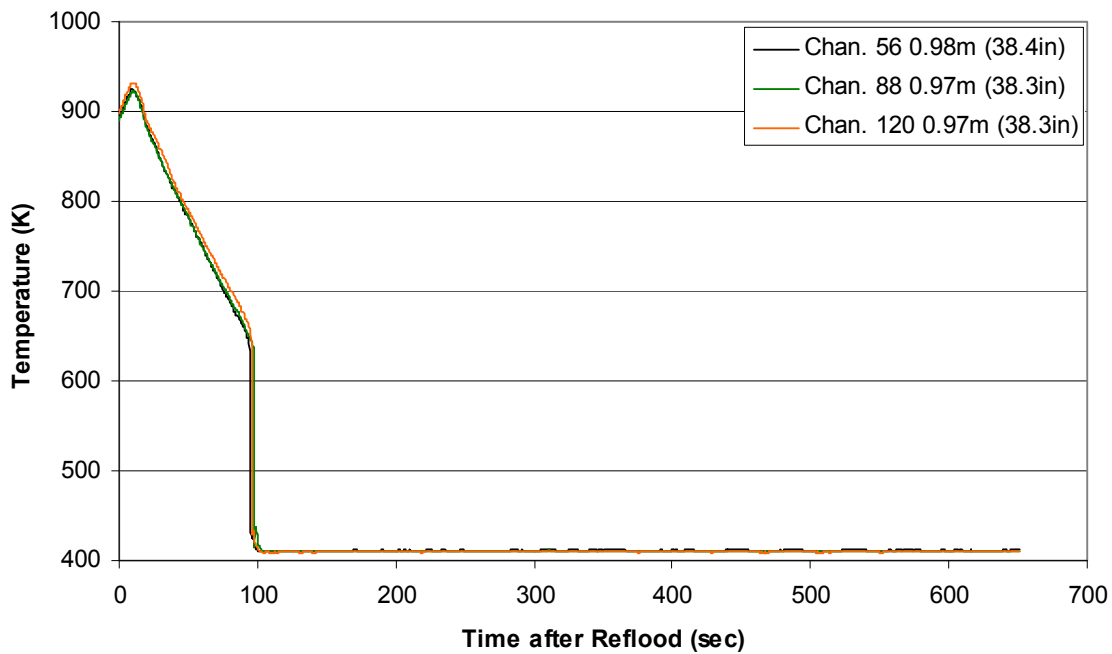


RBHT - TEST FACILITY

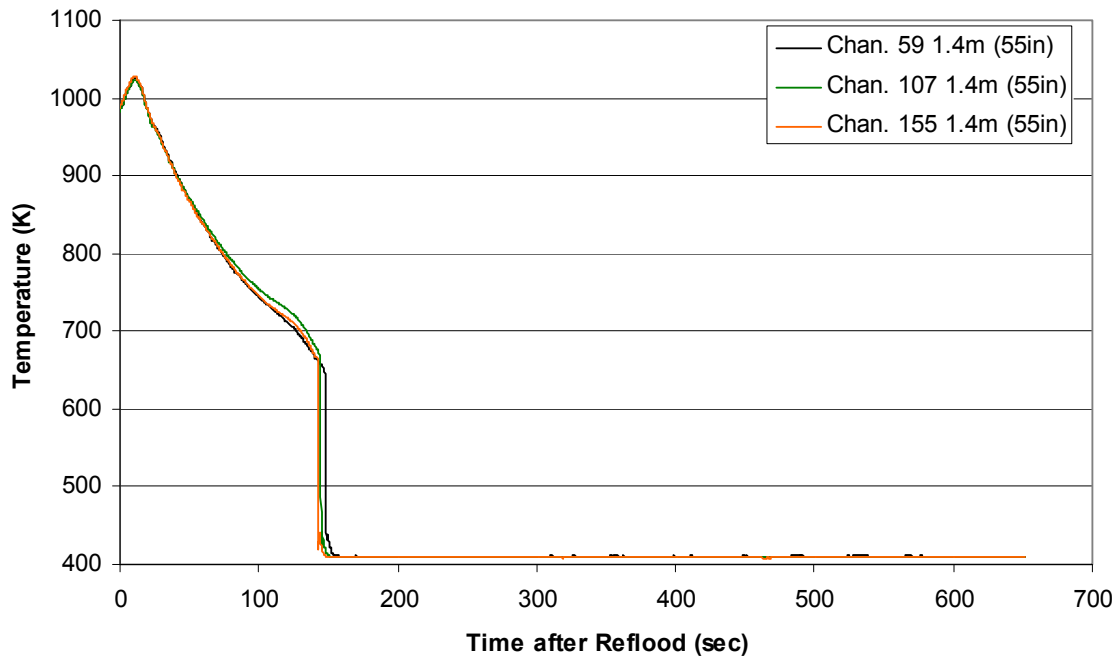
Test Section Current vs. Time, Exp 1223



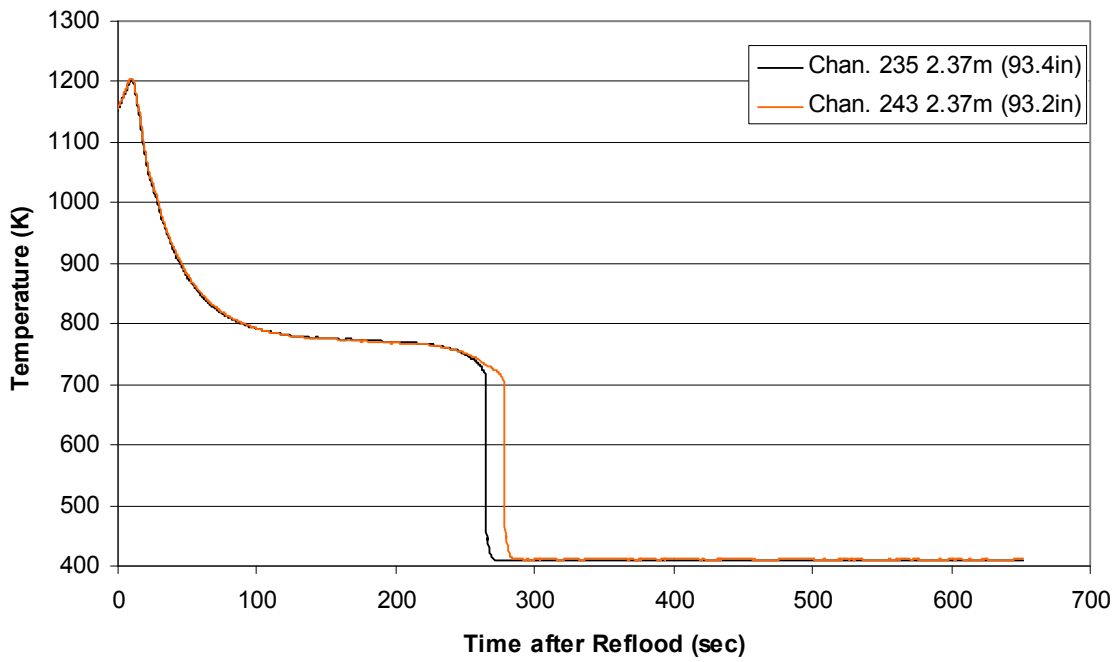
Heater Rod Temperature during Reflood RBHT Exp. 1223



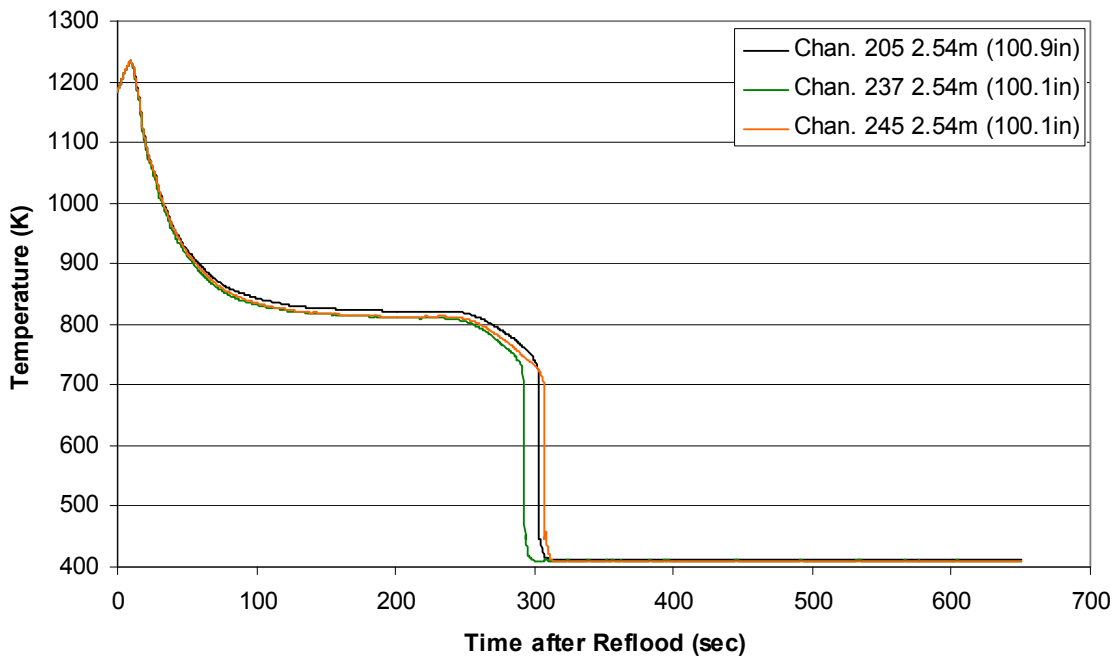
Heater Rod Temperature during Reflood RBHT Exp. 1223



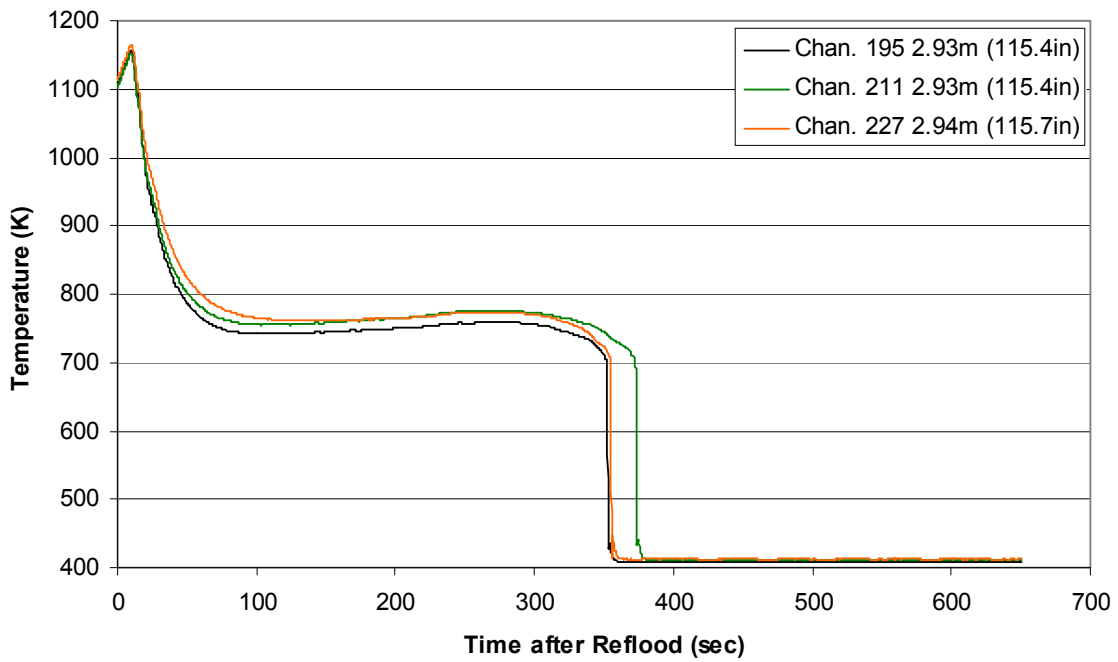
**Heater Rod Temperature during Reflood
RBHT Exp. 1223**



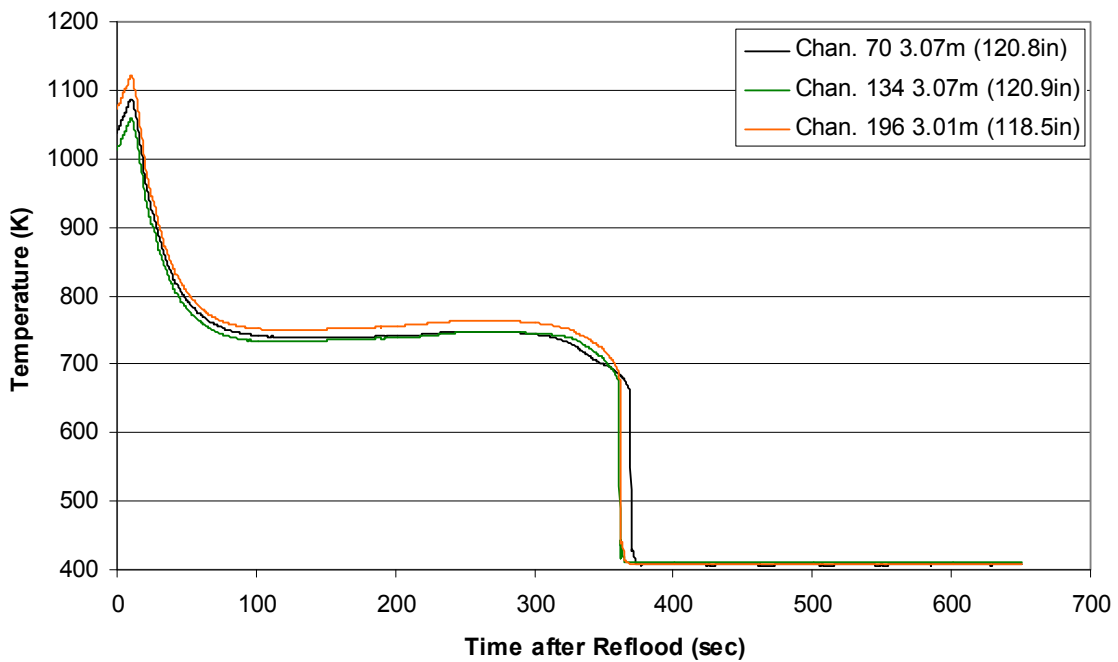
**Heater Rod Temperature during Reflood
RBHT Exp. 1223**



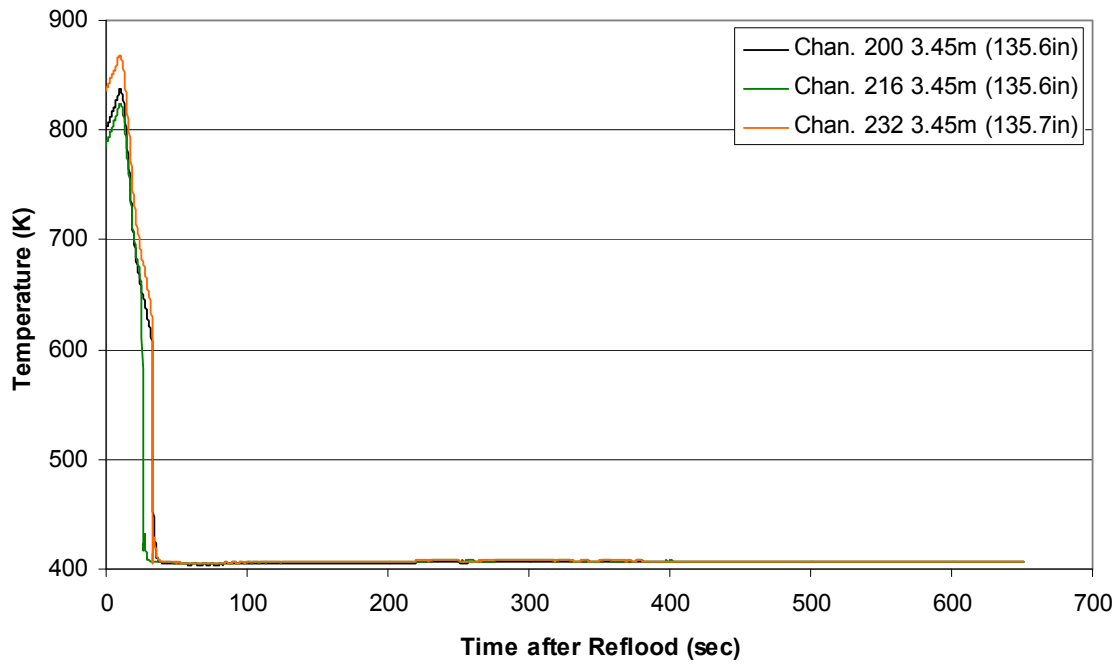
Heater Rod Temperature during Reflood
RBHT Exp. 1223



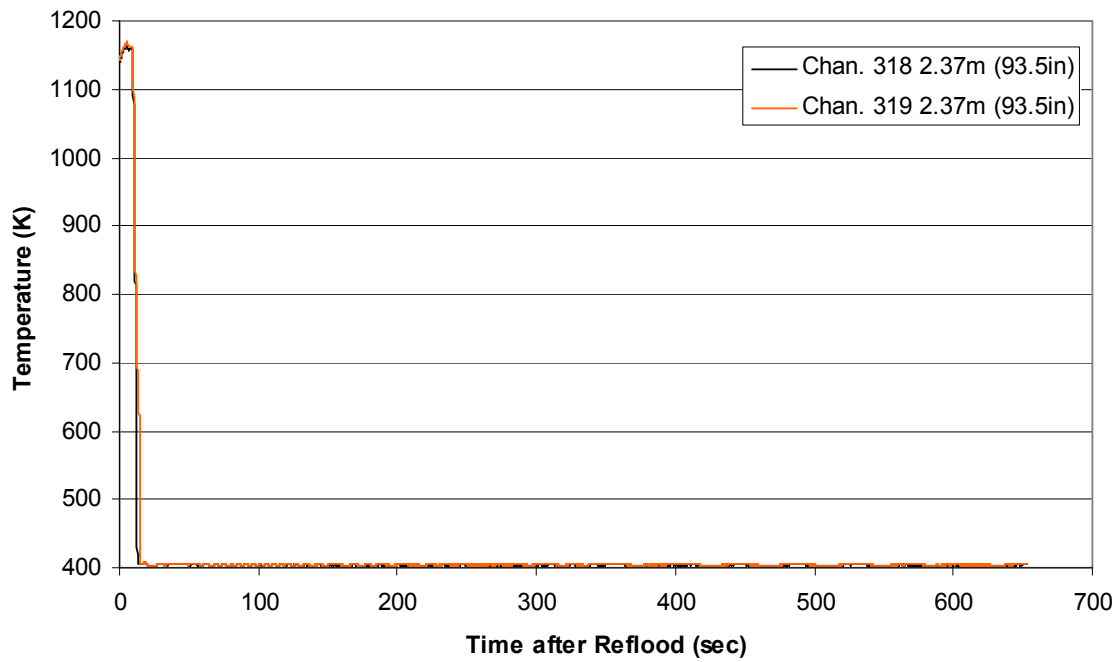
Heater Rod Temperature during Reflood
RBHT Exp. 1223



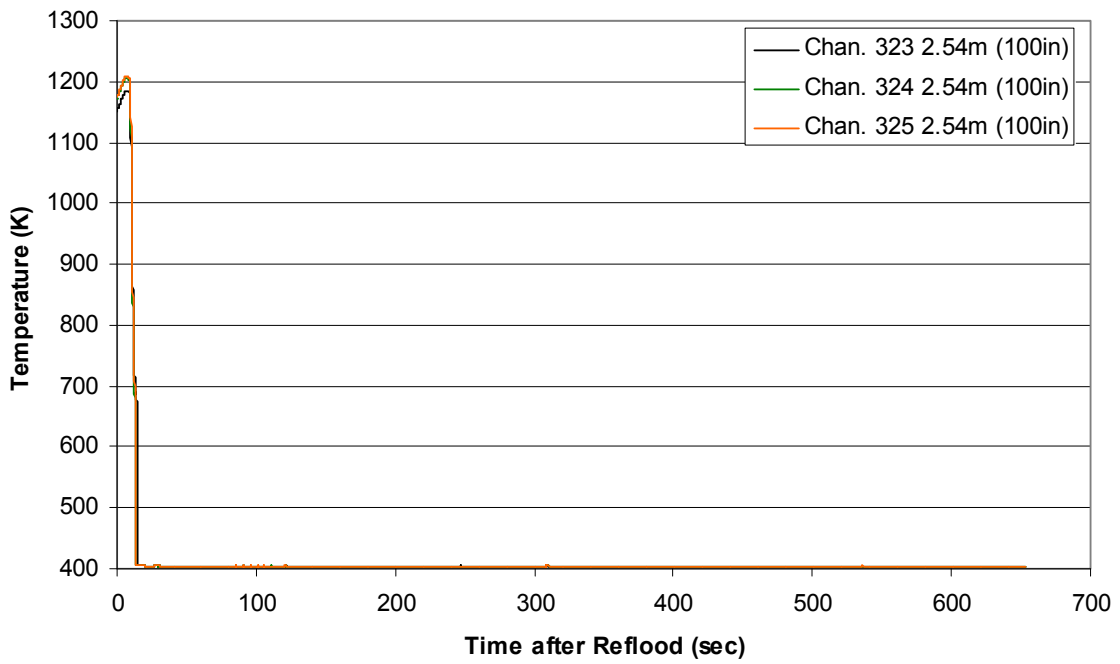
Heater Rod Temperature during Reflood RBHT Exp. 1223



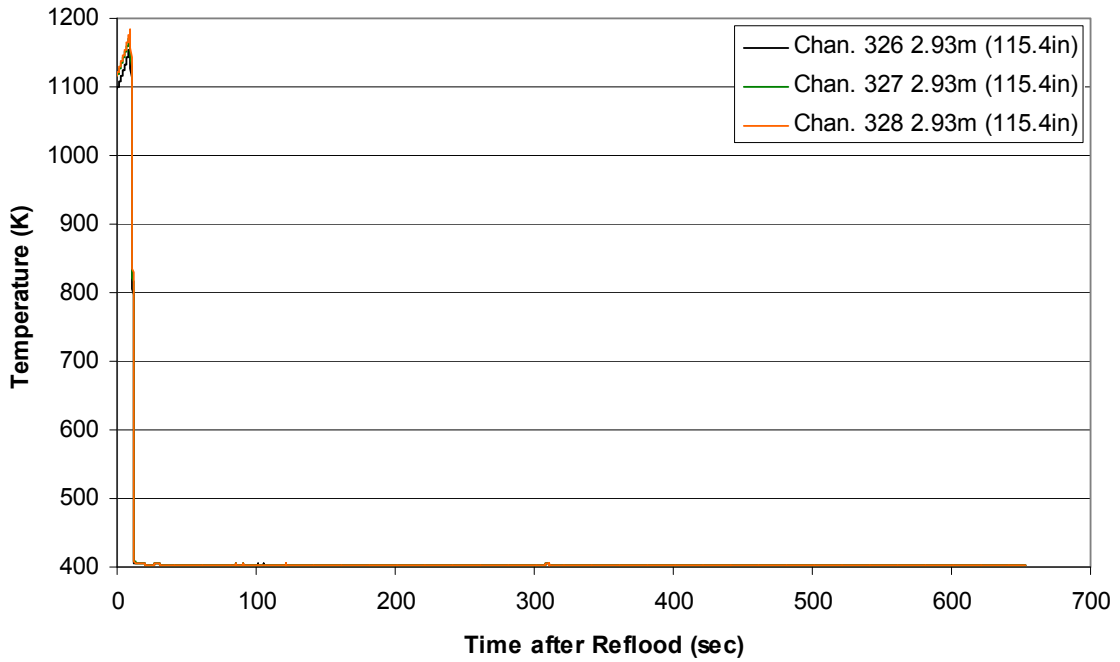
Steam Probe Temperature during Reflood RBHT Exp. 1223



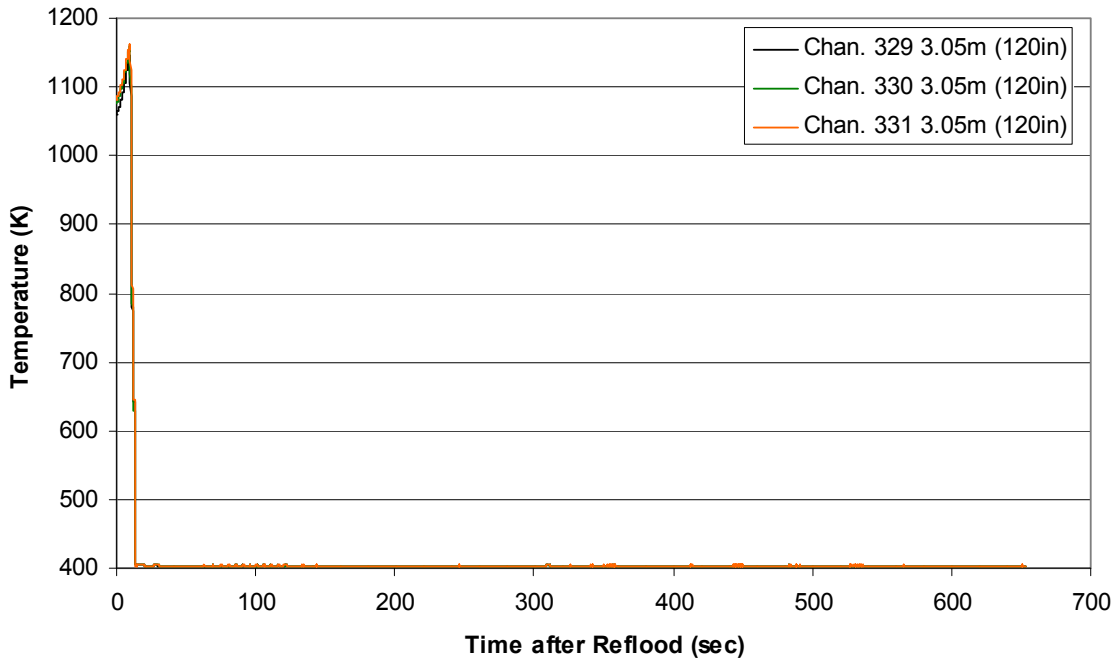
Steam Probe Temperature during Reflood RBHT Exp. 1223



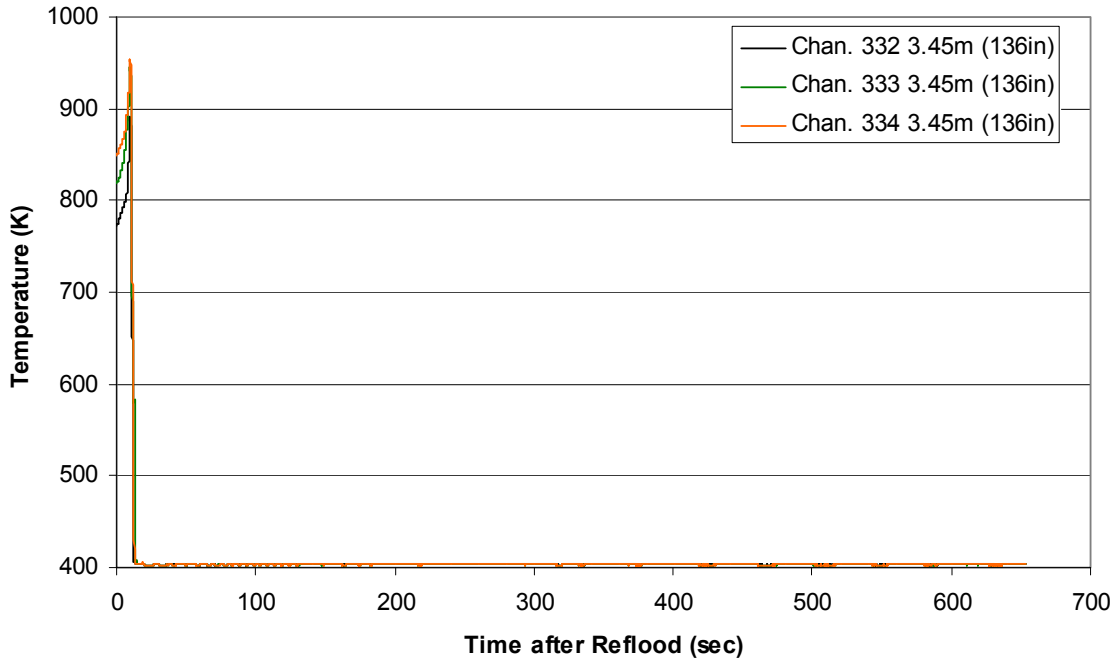
Steam Probe Temperature during Reflood RBHT Exp. 1223



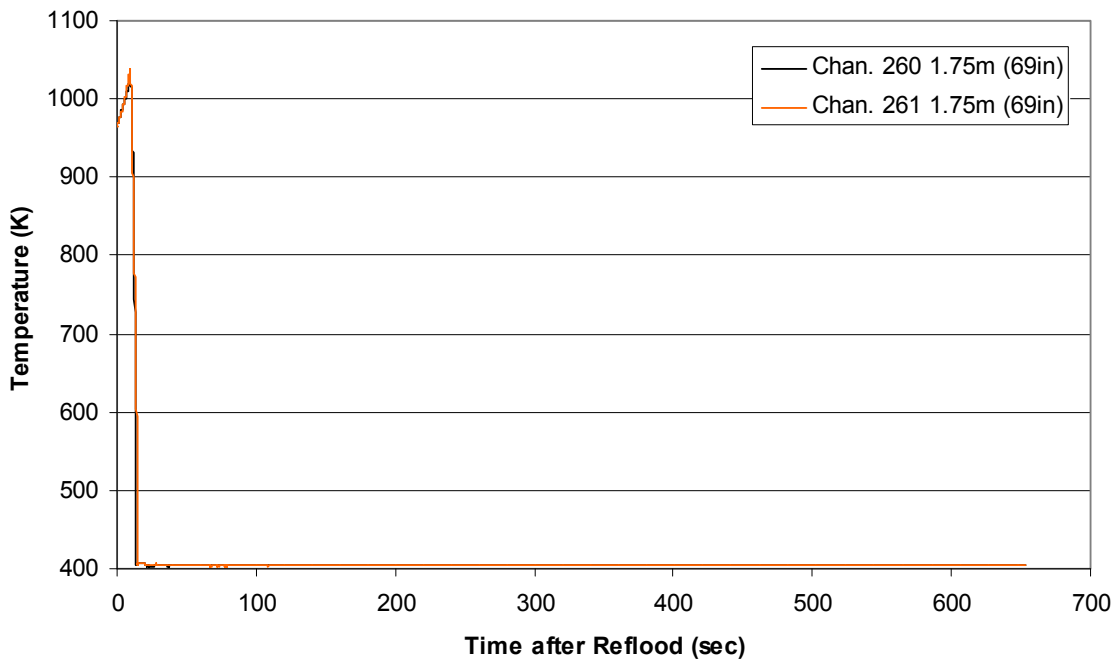
Steam Probe Temperature during Reflood RBHT Exp. 1223



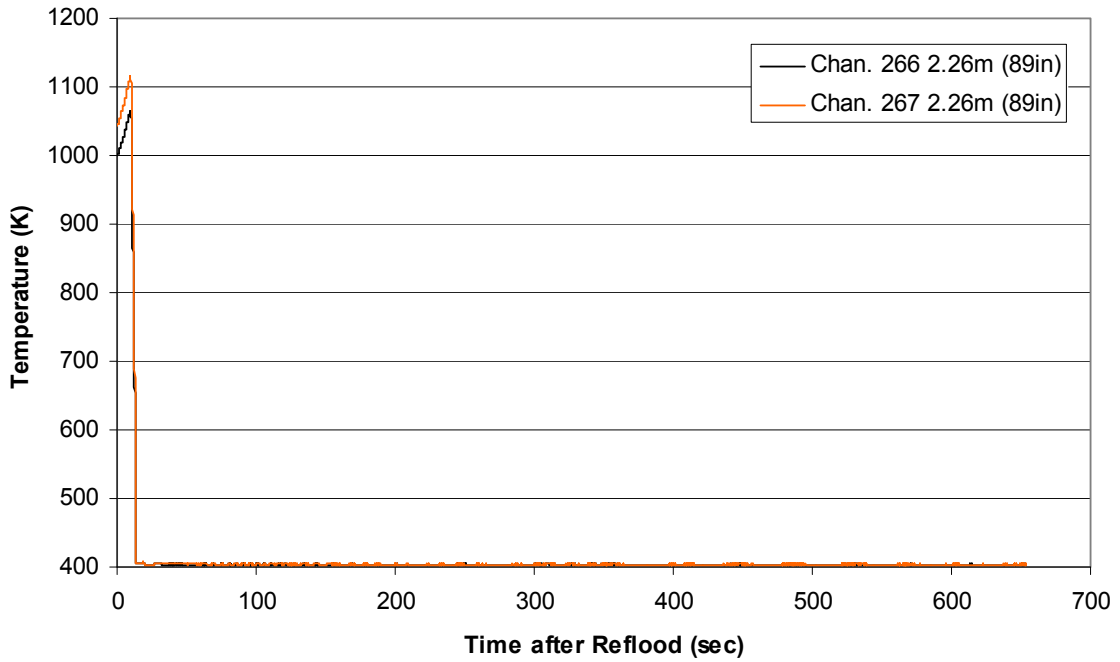
Steam Probe Temperature during Reflood RBHT Exp. 1223



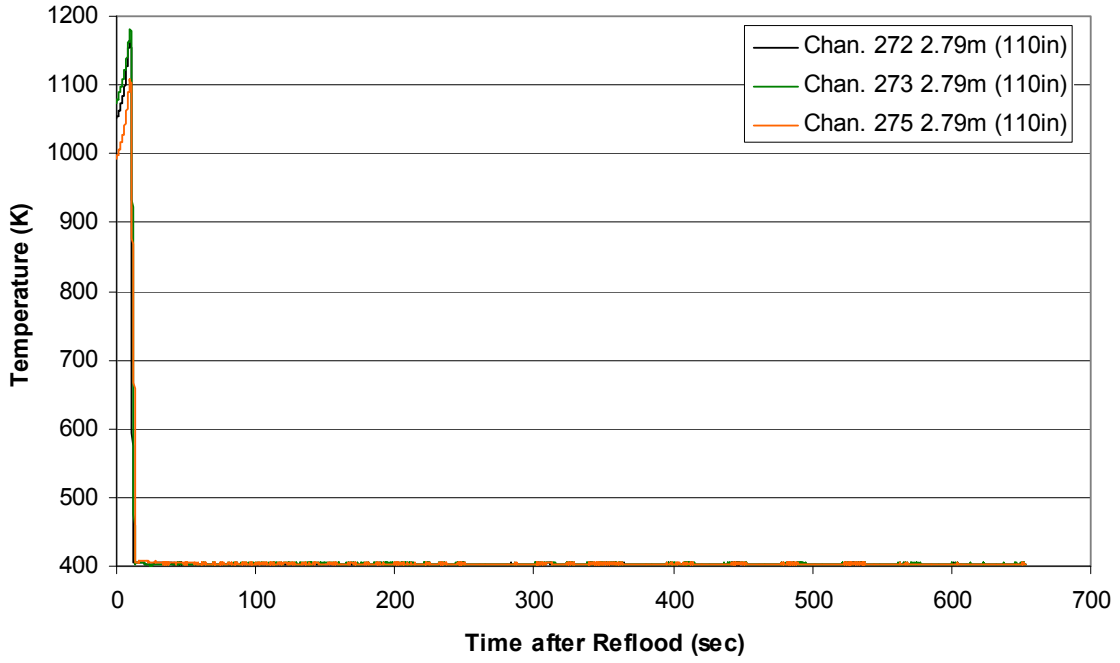
Spacer Grid Temperature during Reflood
RBHT Exp. 1223



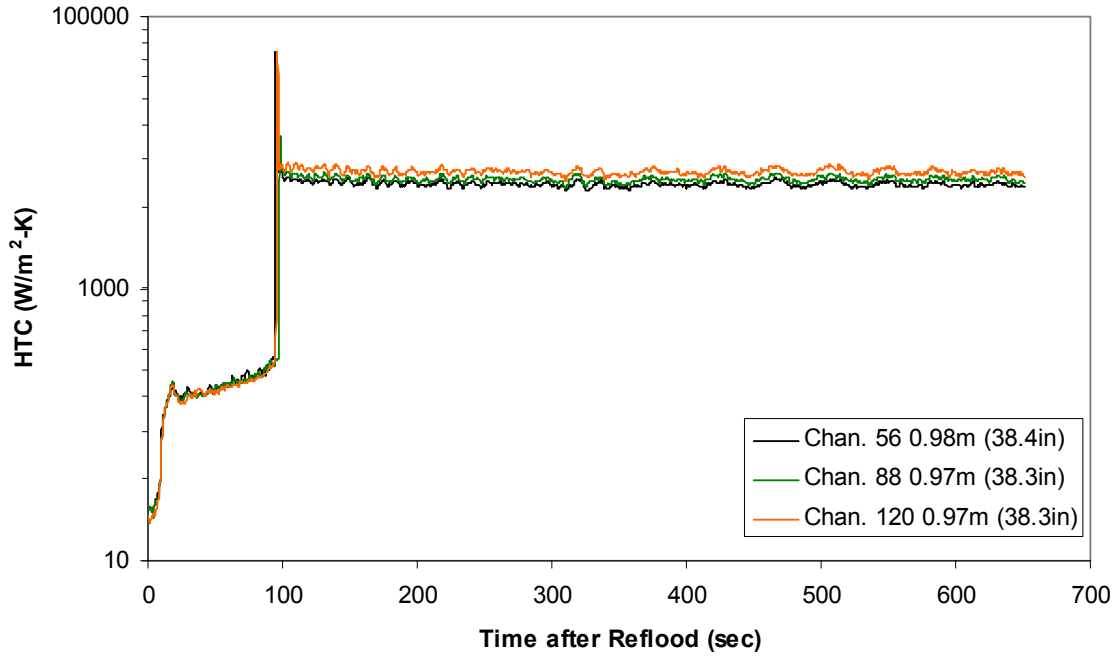
Spacer Grid Temperature during Reflood
RBHT Exp. 1223



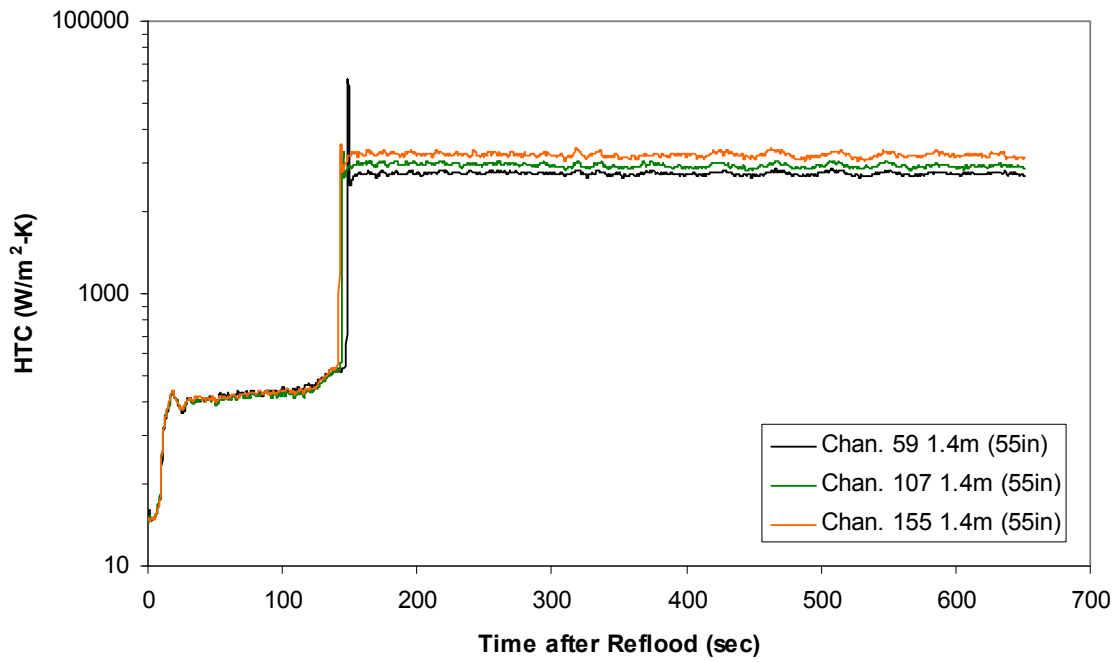
Spacer Grid Temperature during Reflood RBHT Exp. 1223



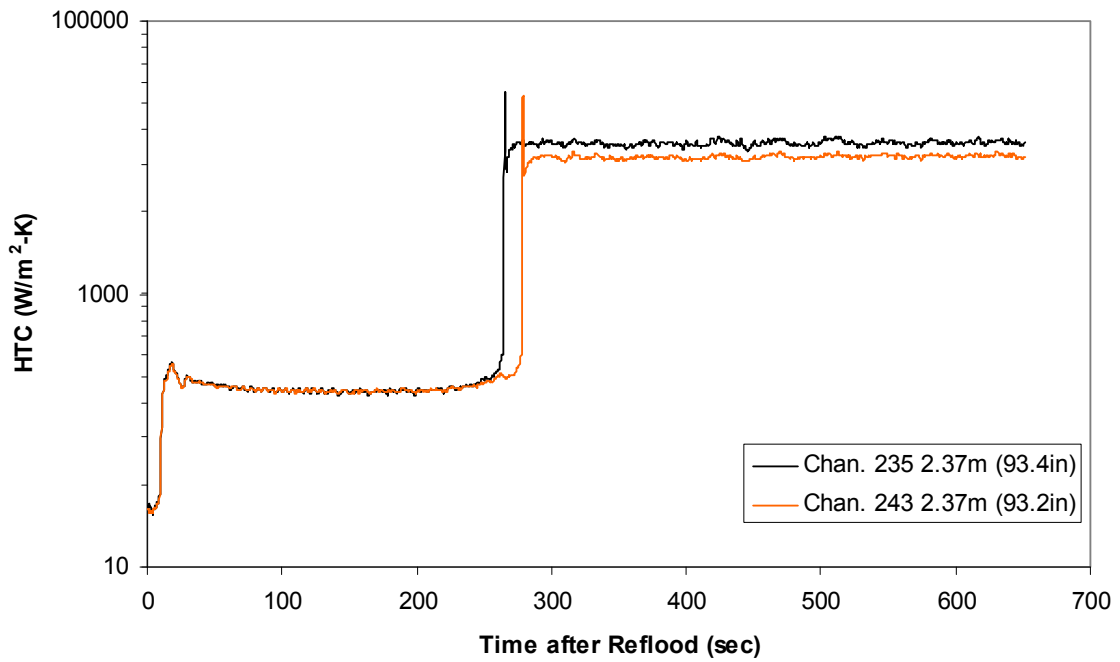
Heat Transfer Coefficient during Reflood RBHT Exp. 1223



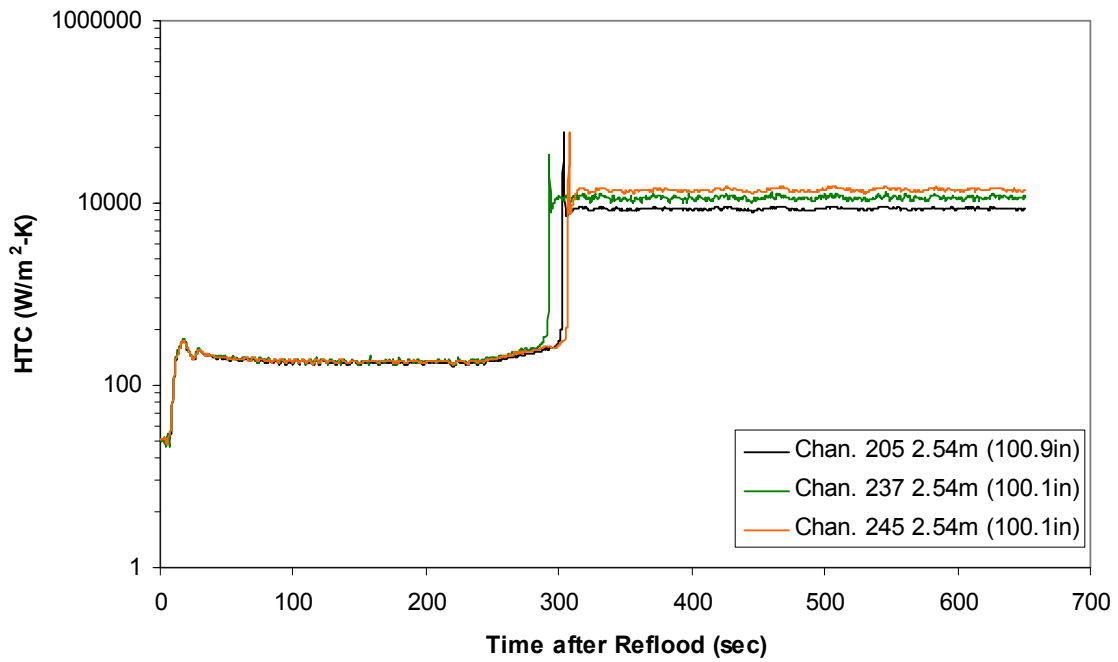
Heat Transfer Coefficient during Reflood RBHT Exp. 1223



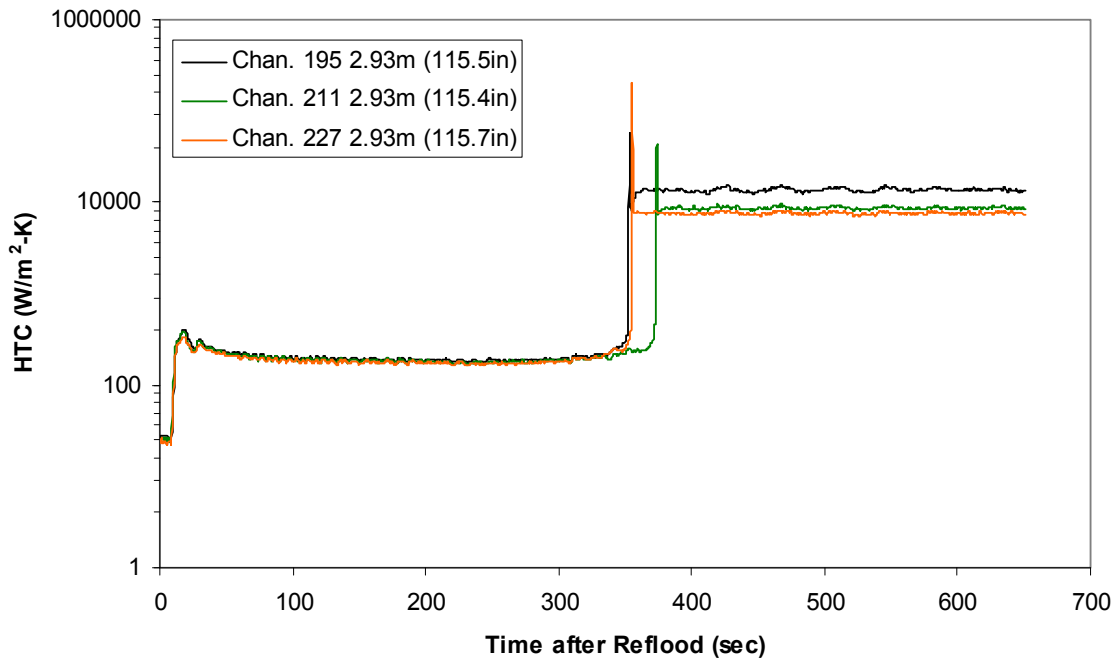
Heat Transfer Coefficient during Reflood RBHT Exp. 1223



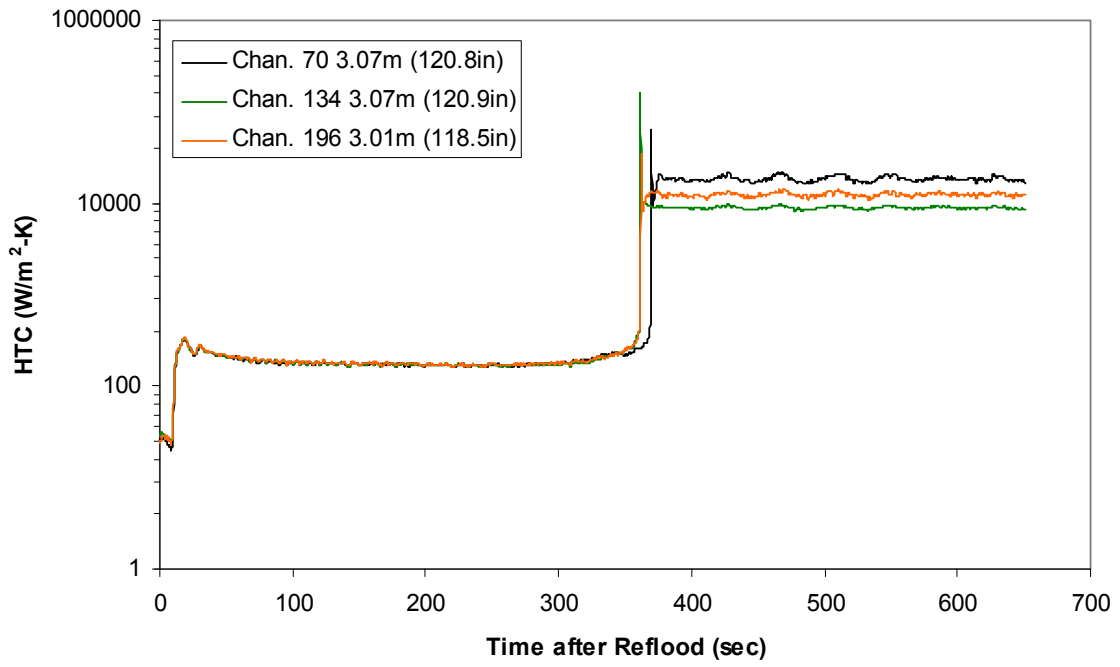
Heat Transfer Coefficient during Reflood RBHT Exp. 1223



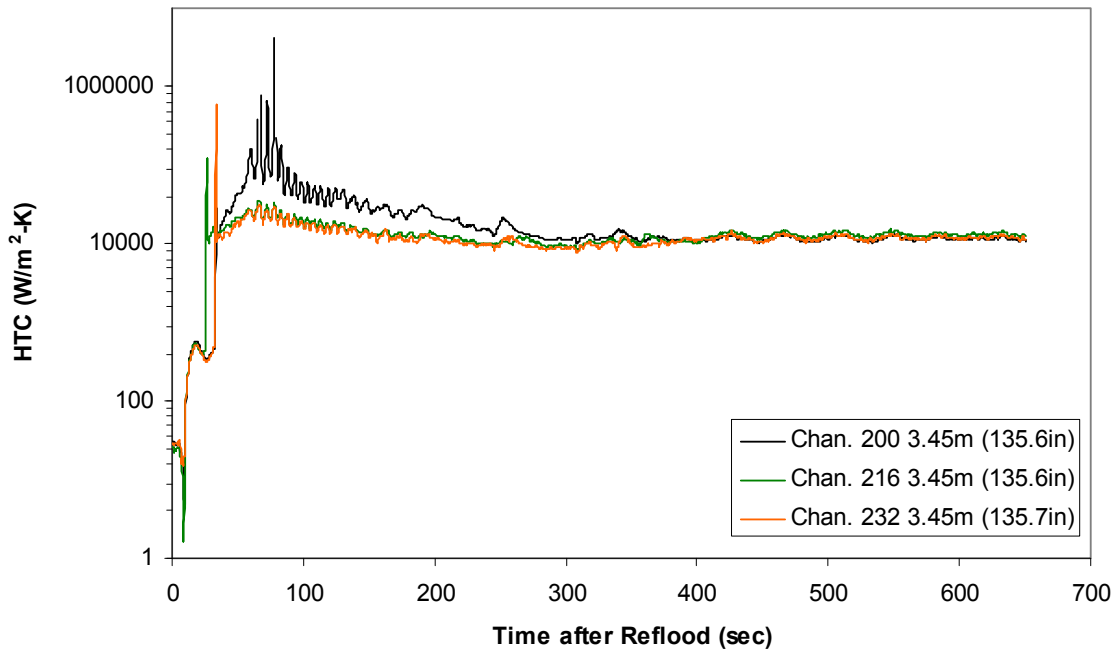
Heat Transfer Coefficient during Reflood RBHT Exp. 1223



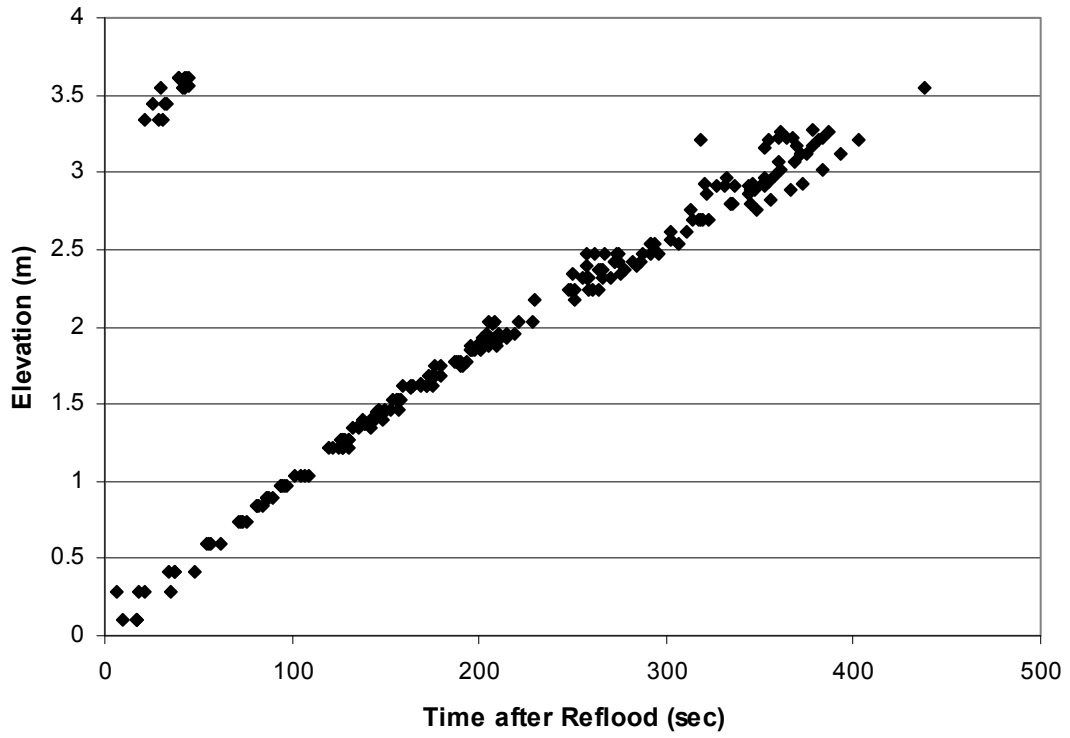
Heat Transfer Coefficient during Reflood RBHT Exp. 1223



Heat Transfer Coefficient during Reflood RBHT Exp. 1223



Quench Data, RBHT Exp. 1223



RBHT - REFLOOD TESTS

SUMMARY SHEET

RUN NO: **1228**

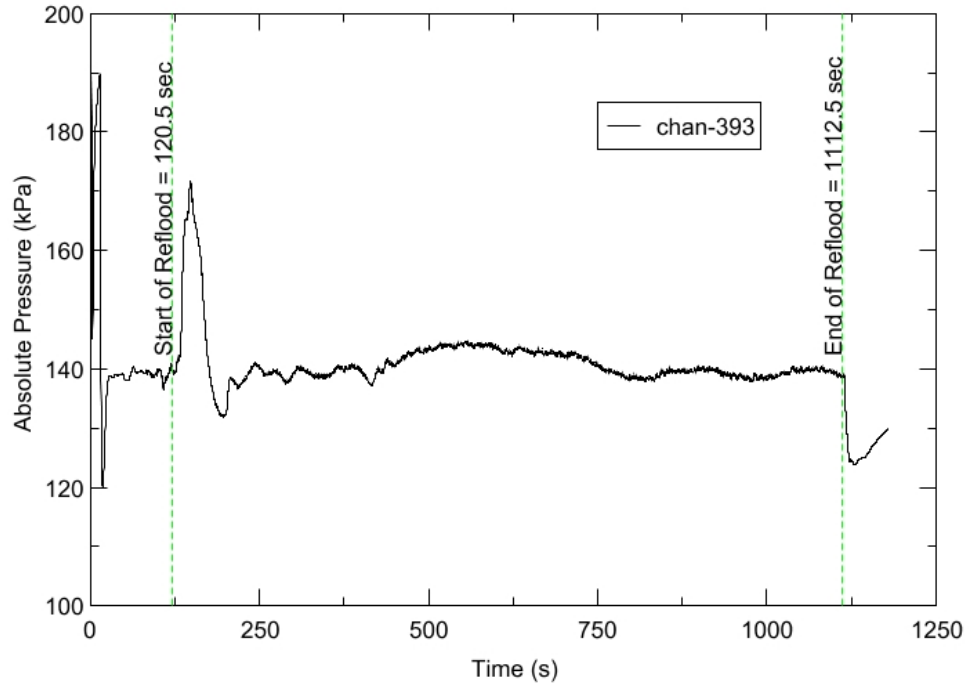
RUN CONDITIONS

Upper Plenum Pressure:	138 kPa (20 psia)
Initial Peak Clad Temperature:	1144 degrees K (1600 degrees F)
Rod Peak Power:	2.3 kW/m (0.7 kW/ft)
Flooding Rate:	0.1524 m/s (6 in/s)
Inlet Subcooling:	23 degrees K (42 degrees F)
Start of Reflood:	120.5 s
End of Reflood:	1112.5 s
Test Date:	7/1/2002
Comments:	No droplet data

Rod_Elevation	Channel Number	Temperature at Reflood (K)	Temperature at Reflood (F)	Tumaround Time (sec.)	Tumaround Temperature (K)	Tumaround Temperature (F)	Quench Time (sec.)	Quench Temperature (K)	Quench Temperature (F)
B6 0.592m	148	761.37	910.79	12.25	800.53	981.26	52.25	590.12	602.53
B6 0.744m	149	776.89	938.72	14.75	820.55	1017.3	68.25	569.43	565.29
B6 0.846m	150	803.11	985.91	15.75	851.66	1073.3	81.25	580.75	585.66
B6 0.897m	151	812.78	1003.31	15.75	861.96	1091.83	88.25	581.18	586.43
C6 1.04m	137	859.65	1087.68	18.75	915.55	1188.29	106.75	606.47	631.95
C6 1.34m	138	912.79	1183.33	17.25	975.55	1296.3	154.75	625.78	666.72
C6 1.39m	139	917.65	1192.09	18.75	981.61	1307.2	163.75	636.32	685.68
C6 1.47m	140	929.36	1213.17	18.25	995.12	1331.53	178.25	649.39	709.21
C6 1.62m	141	949.36	1249.16	19.25	1021.57	1379.15	212.25	683.07	769.84
C6 1.87m	142	986.16	1315.41	16.25	1058.02	1444.75	273.25	695.27	791.8
C6 1.95m	144	995.36	1331.95	16.75	1069.61	1465.61	291.75	716.68	830.34
D6 2.62m	129	1117.36	1551.56	14.75	1199.02	1698.54	480.25	762.28	912.42
D6 2.69m	130	1117.63	1552.05	15.25	1201.77	1703.5	500.75	774.97	935.25
D6 2.87m	131	1064.17	1455.81	13.25	1136.96	1586.85	540.25	699.19	798.85
D6 2.92m	132	1037.96	1408.63	14.75	1116.51	1550.04	551.25	728.65	851.89
D6 2.97m	133	1005.08	1349.46	15.25	1080.49	1485.19	563.75	718.04	832.79
D6 3.07m	134	960.71	1269.6	15.25	1031.78	1397.52	578.75	702.73	805.23
D6 3.17m	135	917.39	1191.62	15.25	983.51	1310.62	594.75	686.51	776.02
D6 3.27m	136	866.18	1099.44	15.75	930.27	1214.8	608.75	630.77	675.69
D5 1.27m	217	923.51	1202.64	16.25	981.83	1307.6	143.75	614.81	646.97
D5 1.37m	218	941.91	1235.75	17.75	1005.95	1351.03	160.25	640.83	693.8
D5 1.45m	219	953.44	1256.5	17.75	1019.46	1375.34	173.25	643.04	697.79
D5 1.52m	220	964.76	1276.88	17.75	1033.35	1400.34	188.75	661.88	731.7
D5 1.68m	221	984.96	1313.24	19.25	1059.27	1447.01	224.25	706.29	811.63
D5 1.78m	222	974.11	1293.71	14.75	1038.28	1409.22	249.75	690.18	782.63
D5 1.85m	223	1005.49	1350.2	15.25	1073.94	1473.41	265.25	684.55	772.5
D5 1.90m	224	1014.7	1366.78	15.75	1086.33	1495.71	276.25	703.72	807.01
D4 2.24m	241	1062.56	1452.92	14.75	1132.05	1578.01	400.25	683.94	771.41
D4 2.32m	242	1095.9	1512.93	14.75	1170.79	1647.73	419.25	727.9	850.53
D4 2.37m	243	1104.91	1529.15	14.75	1182	1667.91	434.75	719.65	835.69
D4 2.54m	245	1129.86	1574.07	14.75	1208.63	1715.85	489.25	733.89	861.32
D4 2.79m	247	1096.23	1513.52	13.25	1172.44	1650.71	564.75	694.15	789.78
D4 3.61m	248	611.47	640.95	16.75	682.33	768.51	39.75	514.89	467.12
C3 2.17m	178	1052.4	1434.63	16.75	1132	1577.92	351.75	751.25	892.56
E3 3.12m	197	961.01	1270.12	15.25	1030.23	1394.73	614.25	684.22	771.92
C3 2.35m	180	1090.85	1503.84	14.75	1168.46	1643.54	394.75	753.38	896.39
C3 2.40m	181	1094.62	1510.63	15.25	1173.7	1652.97	408.75	762.24	912.34
C3 2.76m	183	1122.24	1560.35	15.25	1206	1711.11	510.75	775.34	935.92

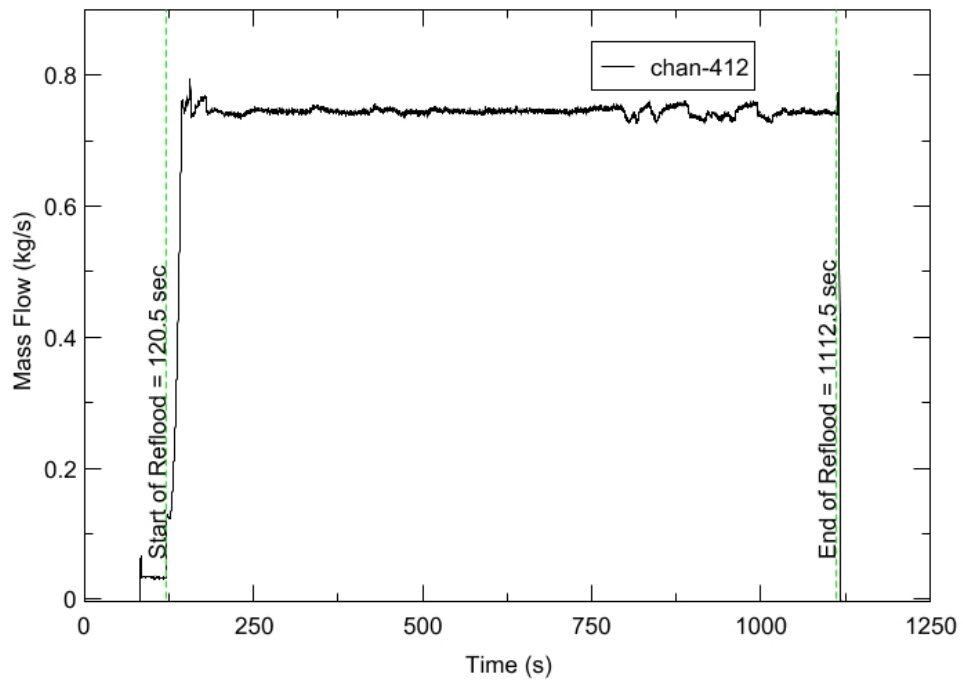
RBHT - TEST FACILITY

Upper Plenum Pressure vs. Time, Exp 1228



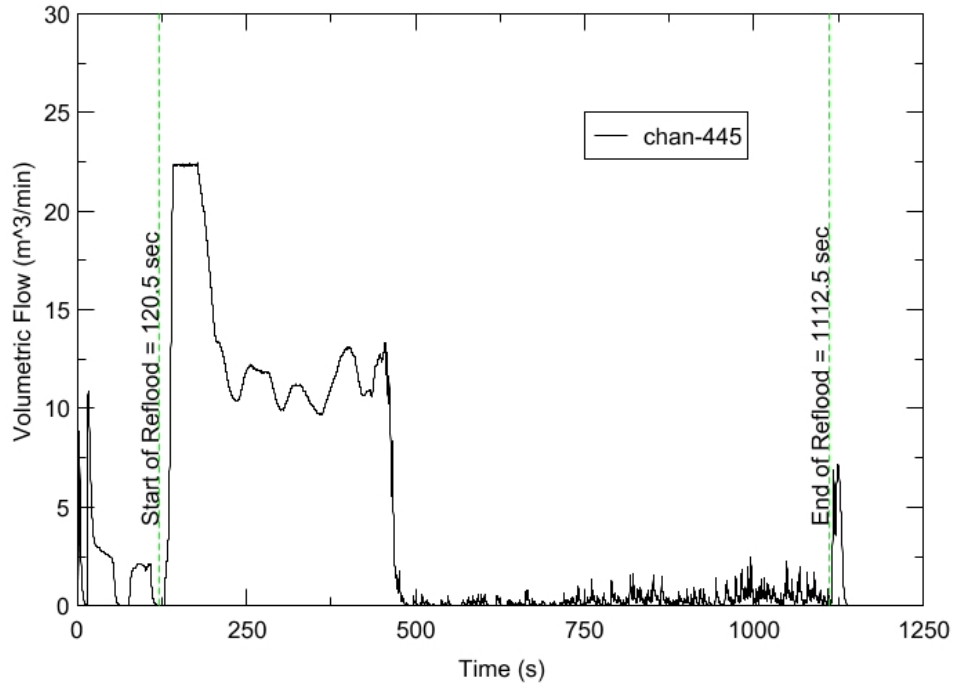
RBHT - TEST FACILITY

Inlet Flow vs. Time, Exp 1228



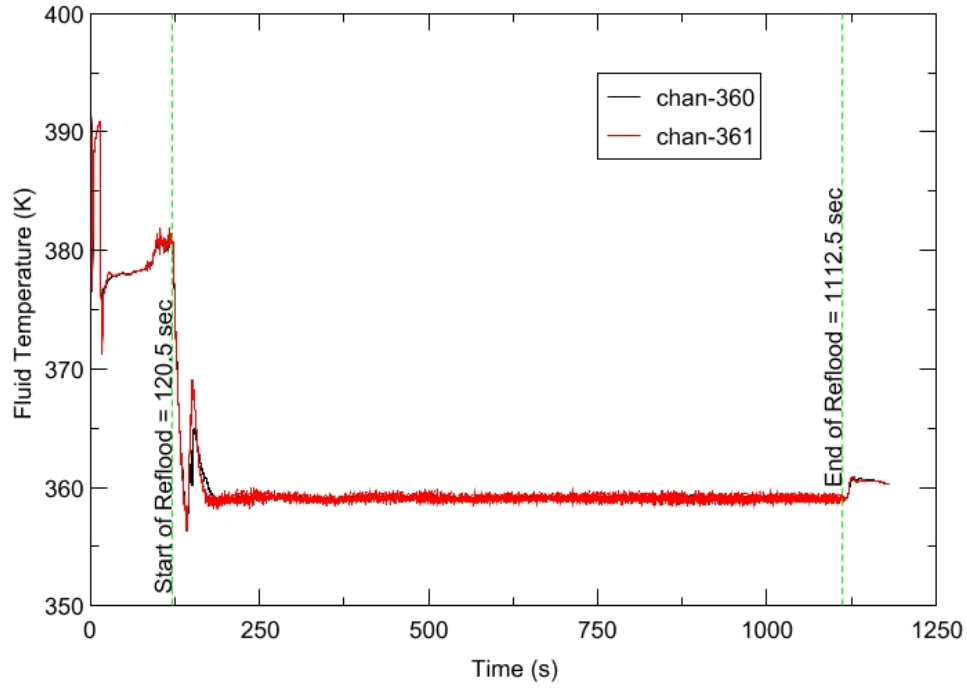
RBHT - TEST FACILITY

Steam Exhaust Flow vs. Time, Exp 1228



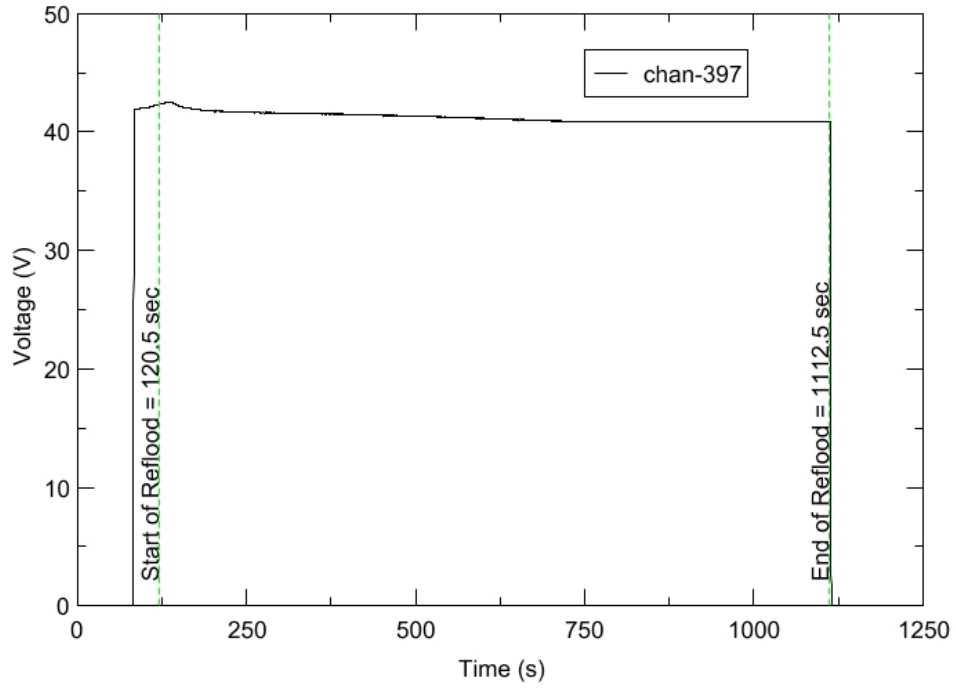
RBHT - TEST FACILITY

Inlet Flow Temperature vs. Time, Exp 1228



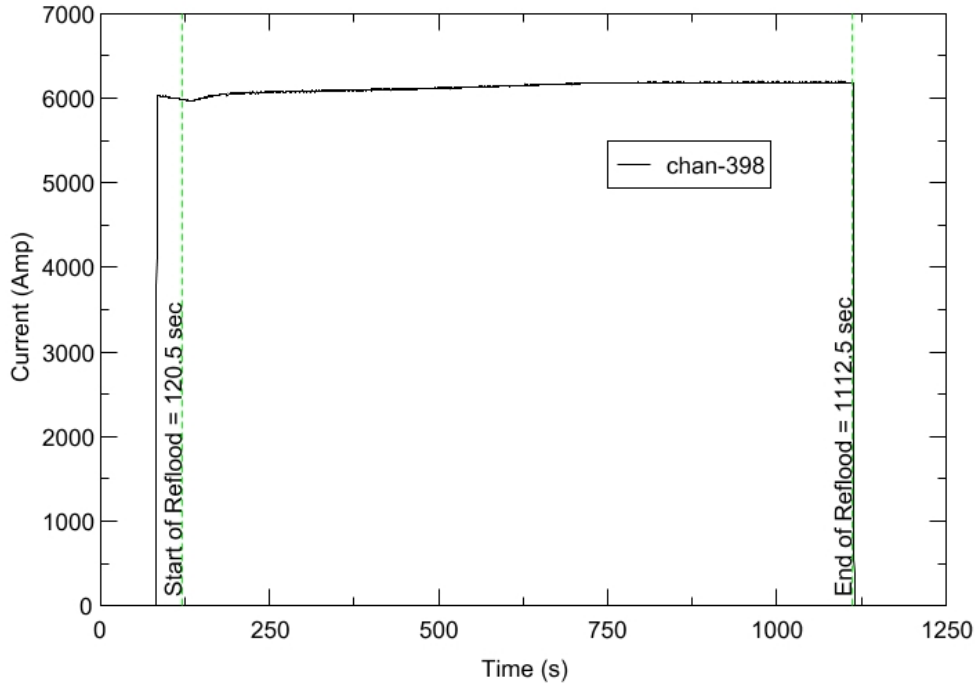
RBHT - TEST FACILITY

Test Section Voltage vs. Time, Exp 1228

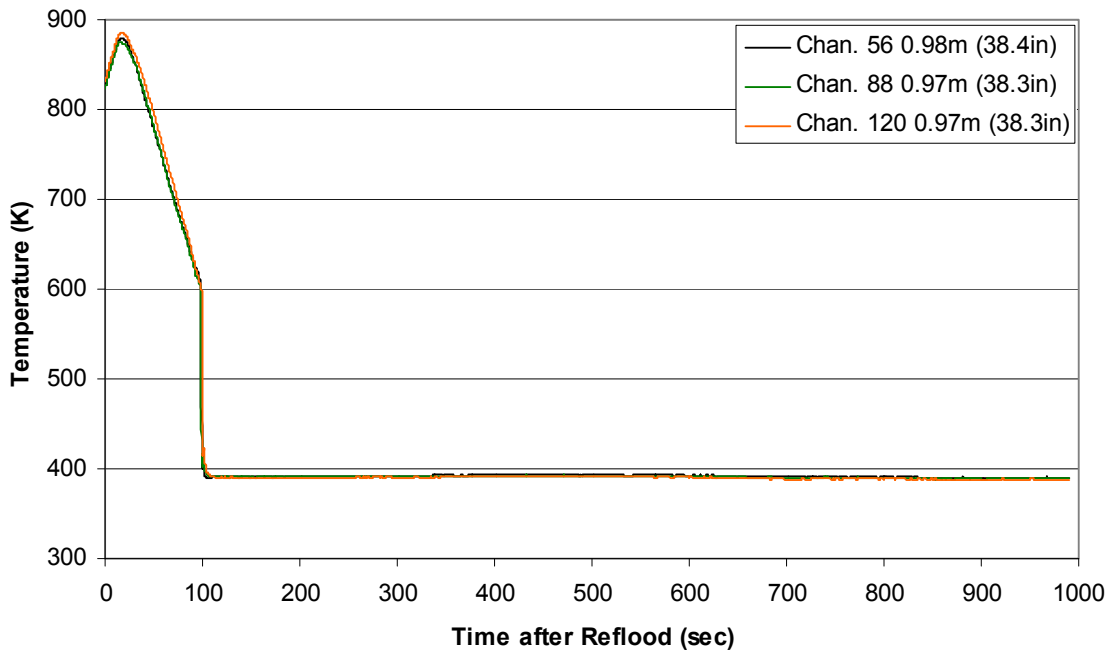


RBHT - TEST FACILITY

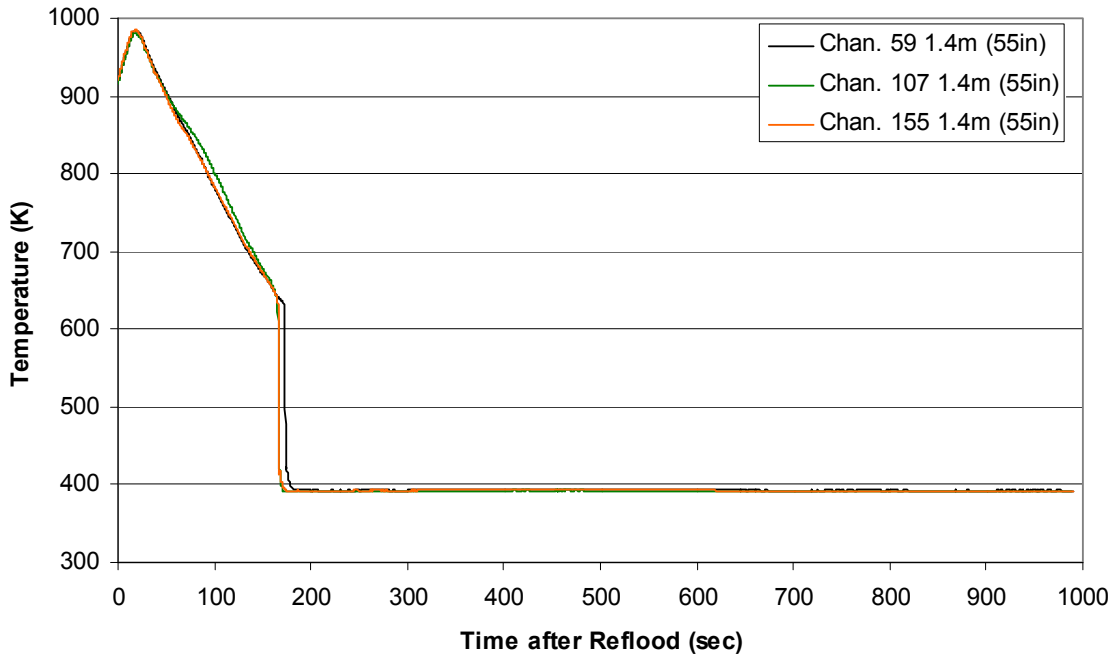
Test Section Current vs. Time, Exp 1228



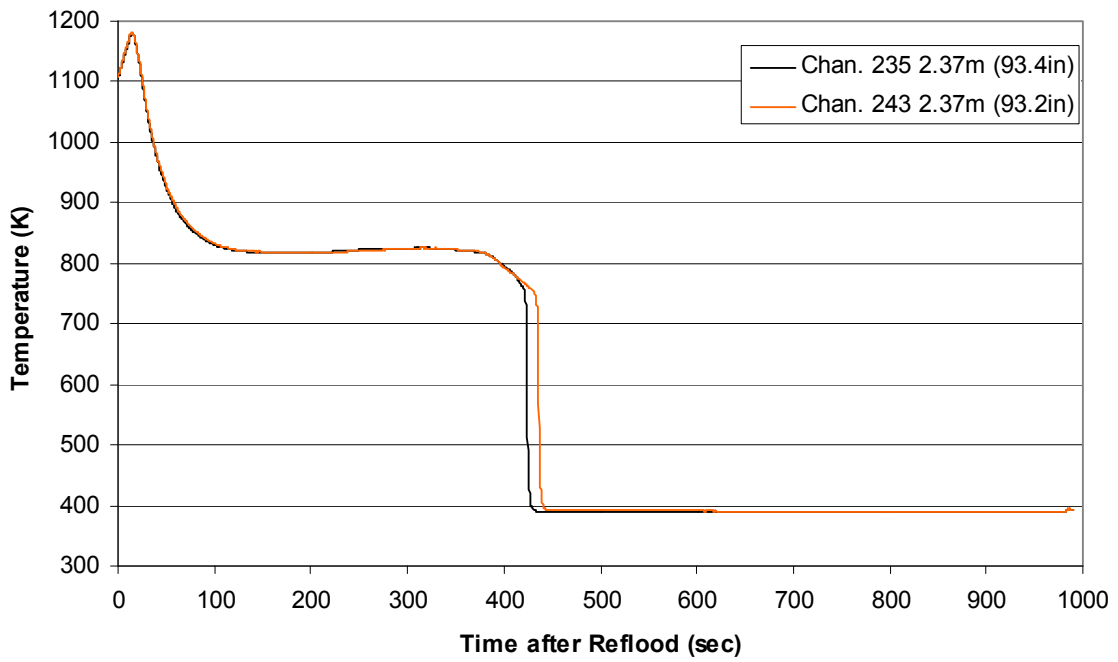
Heater Rod Temperature during Reflood
RBHT Exp. 1228



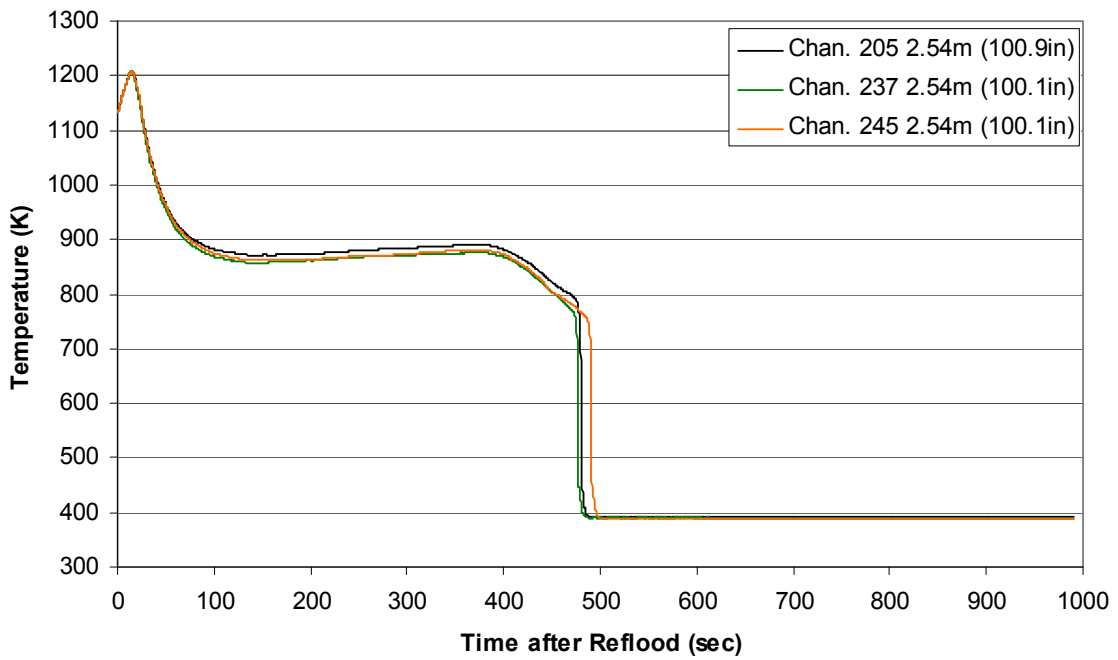
Heater Rod Temperature during Reflood
RBHT Exp. 1228



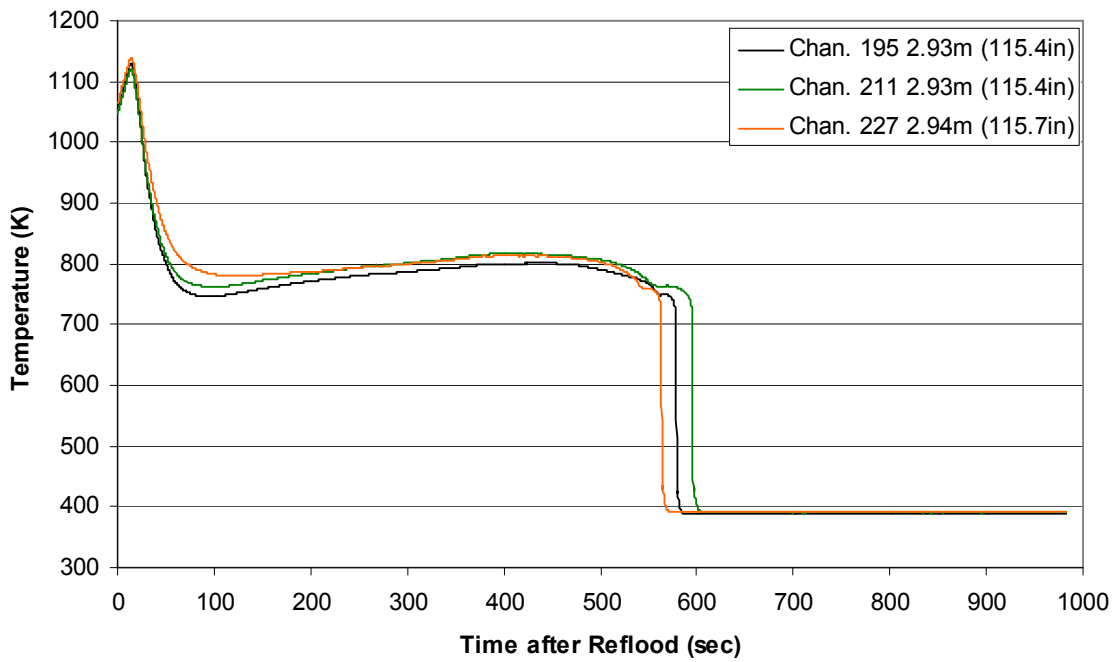
Heater Rod Temperature during Reflood
RBHT Exp. 1228



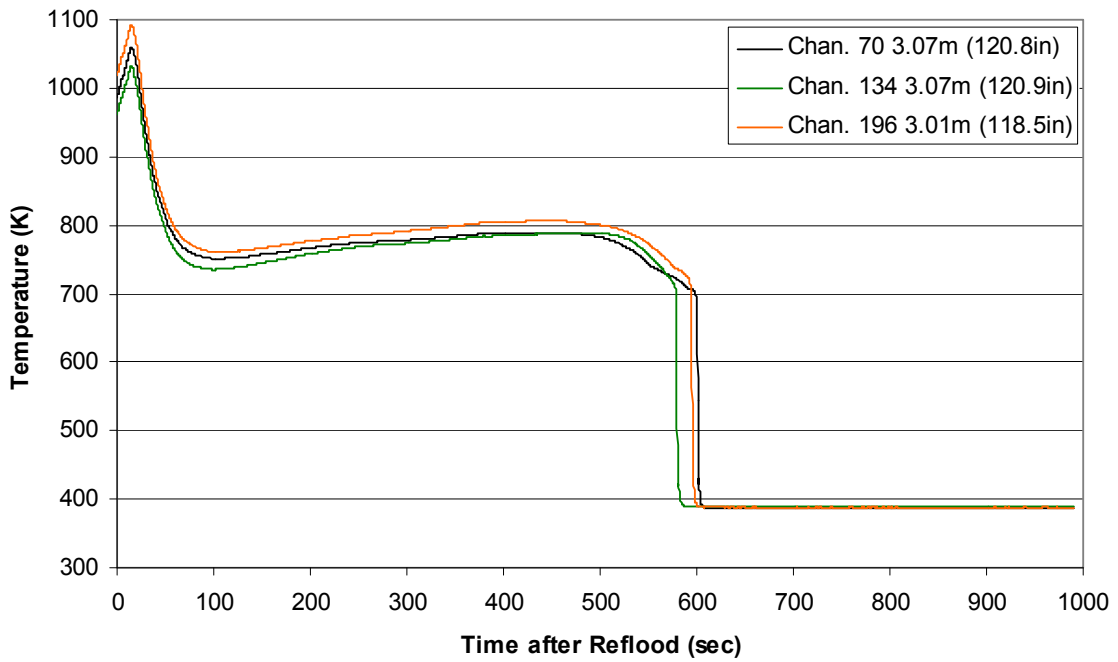
Heater Rod Temperature during Reflood
RBHT Exp. 1228



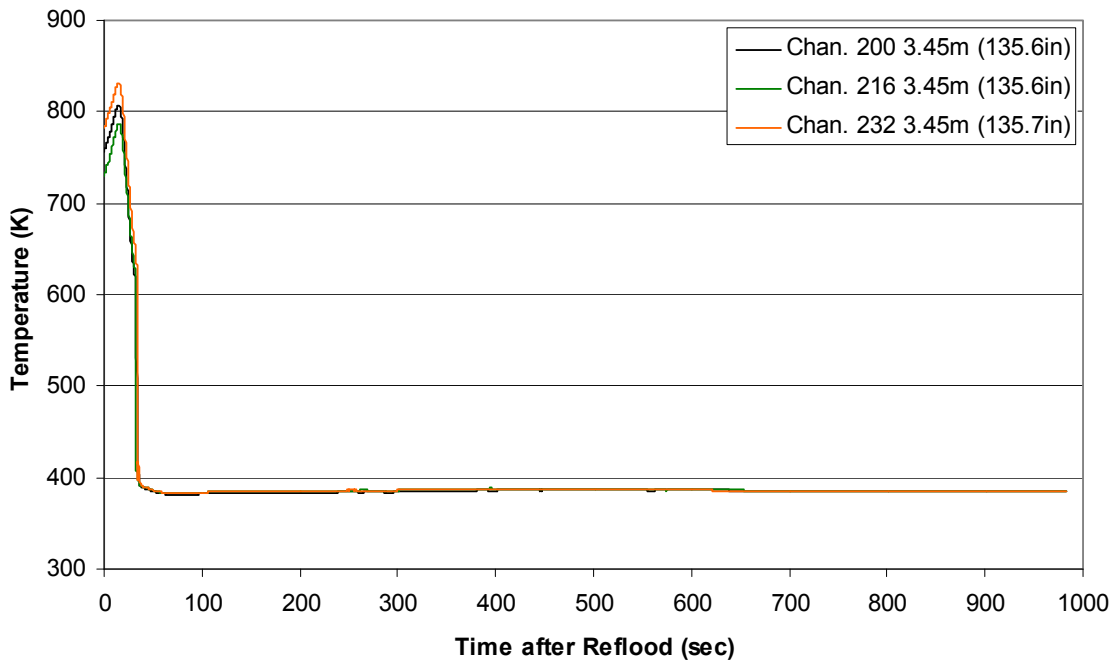
**Heater Rod Temperature during Reflood
RBHT Exp. 1228**



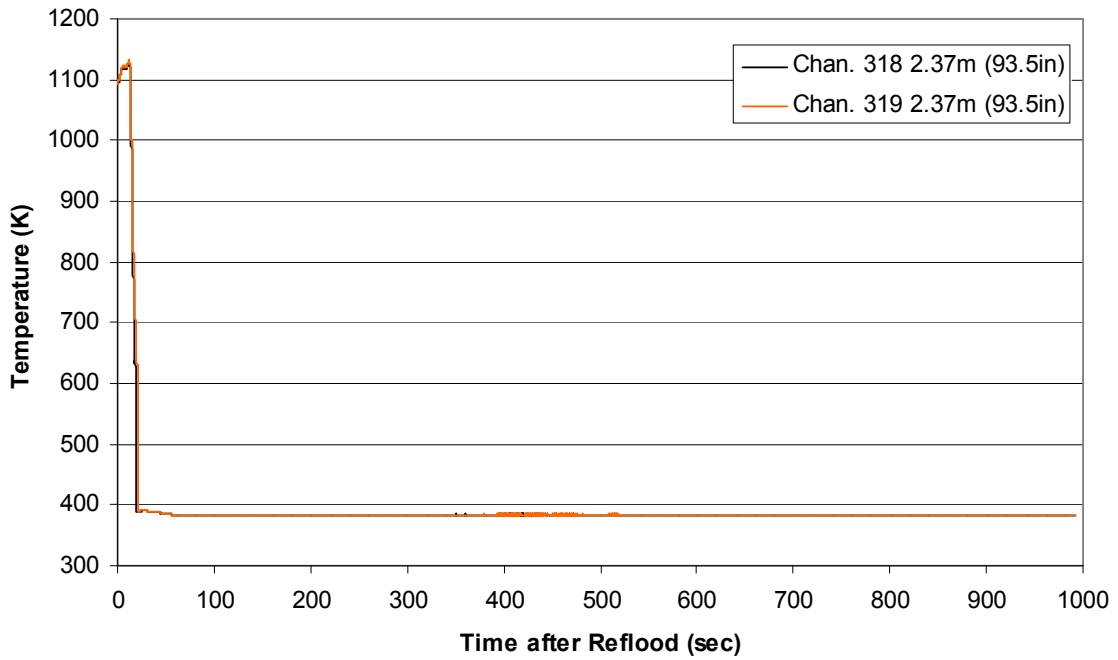
**Heater Rod Temperature during Reflood
RBHT Exp. 1228**



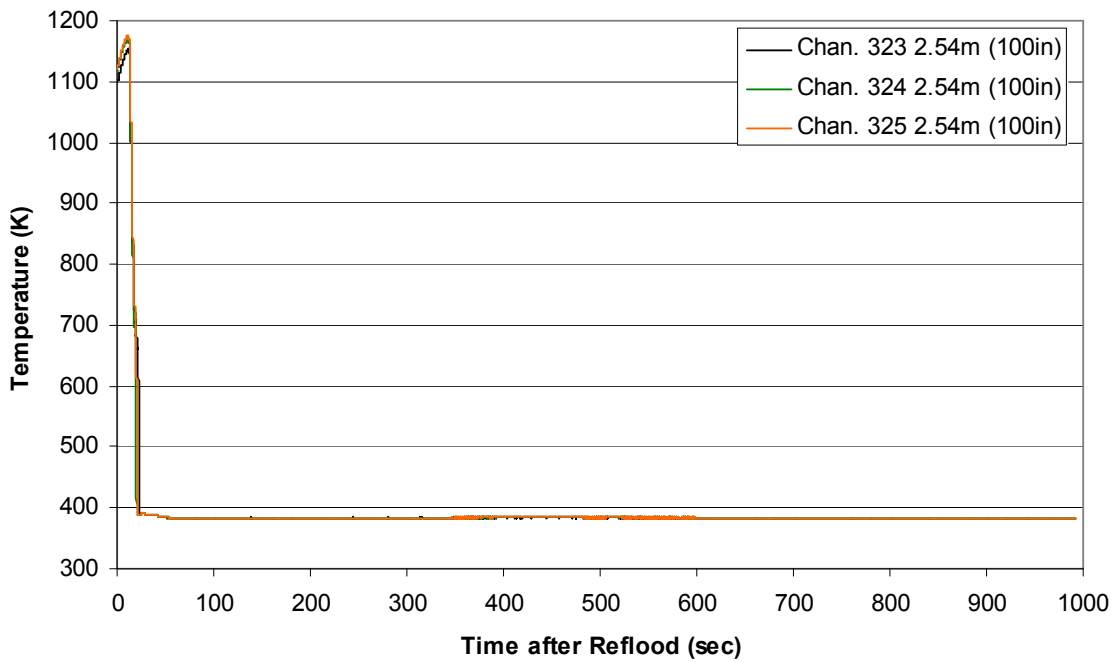
Heater Rod Temperature during Reflood RBHT Exp. 1228



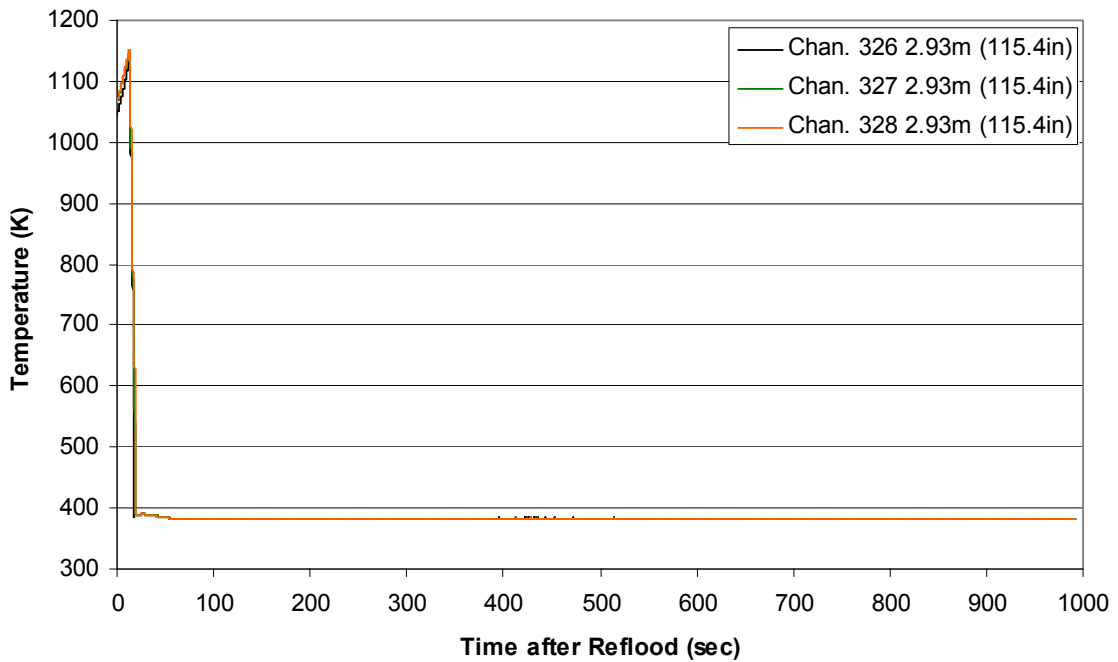
Steam Probe Temperature during Reflood RBHT Exp. 1228



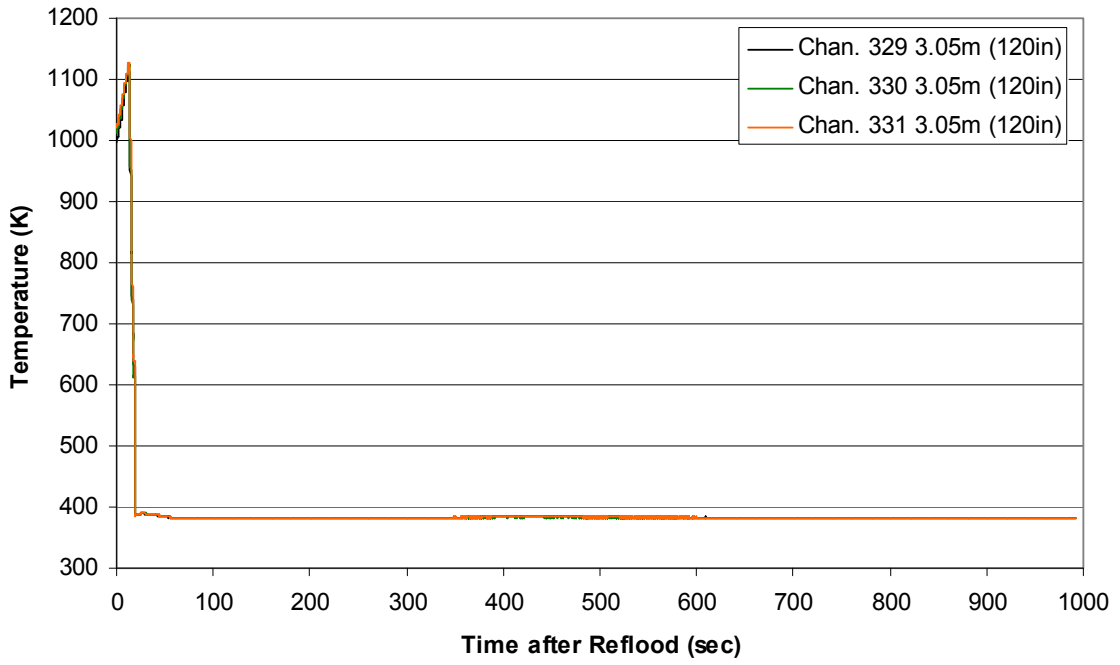
Steam Probe Temperature during Reflood RBHT Exp. 1228



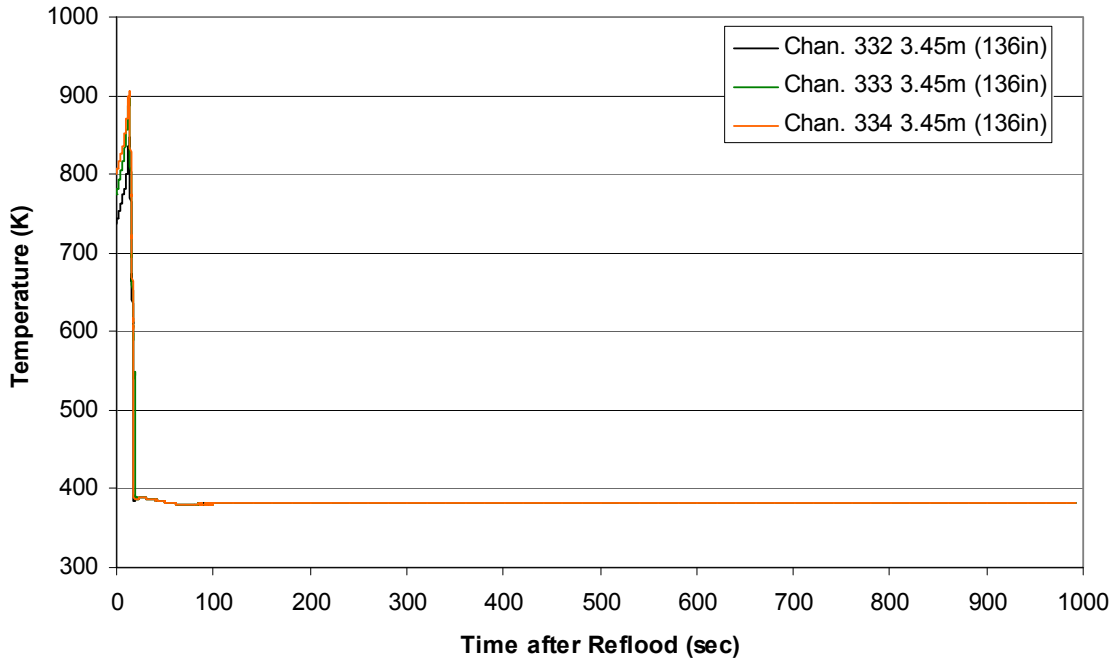
Steam Probe Temperature during Reflood RBHT Exp. 1228



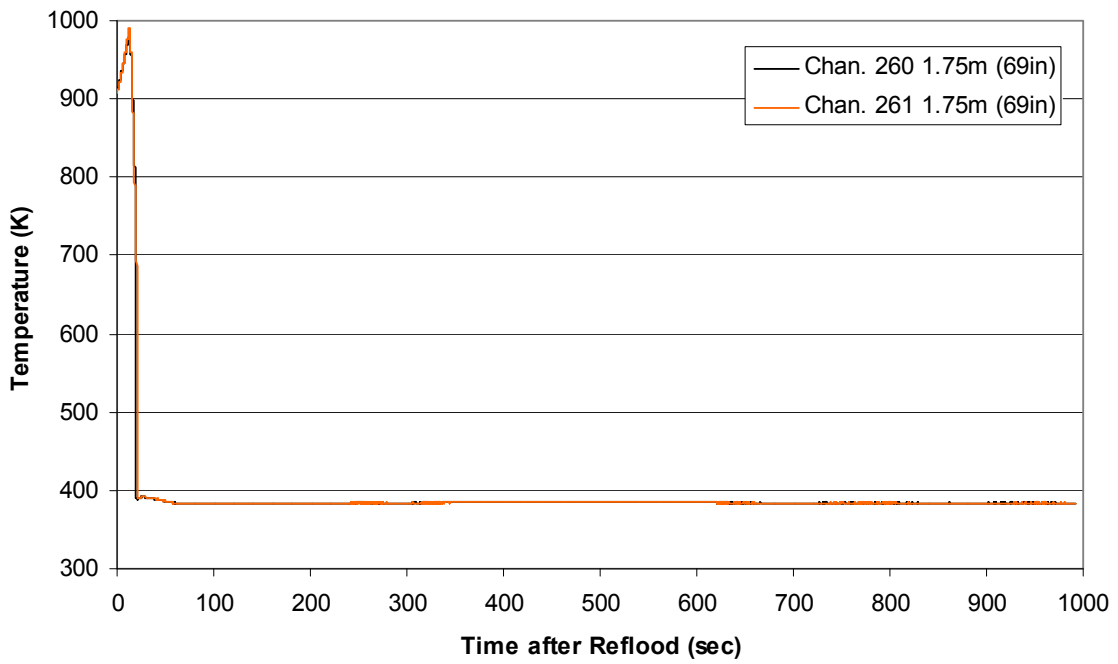
Steam Probe Temperature during Reflood
RBHT Exp. 1228



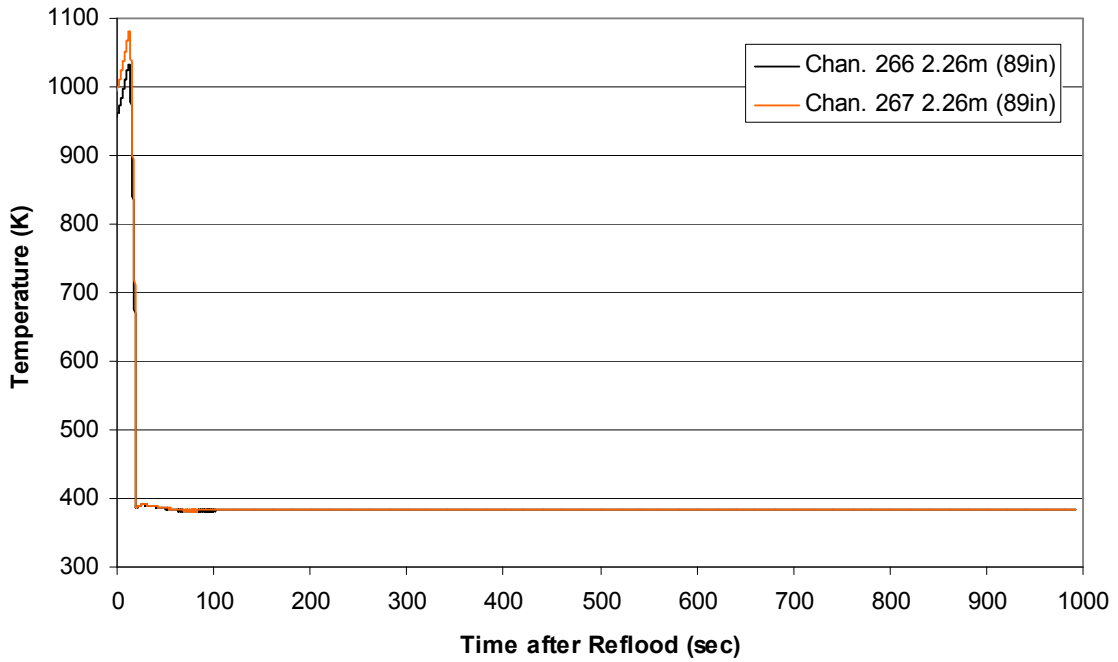
Steam Probe Temperature during Reflood
RBHT Exp. 1228



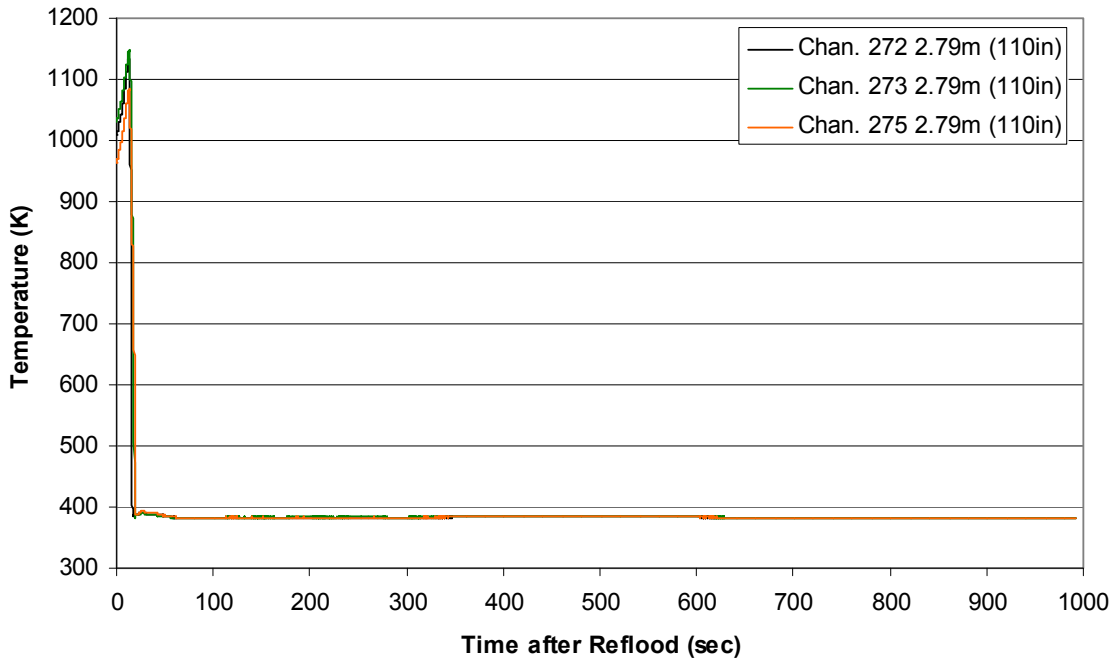
Spacer Grid Temperature during Reflood RBHT Exp. 1228



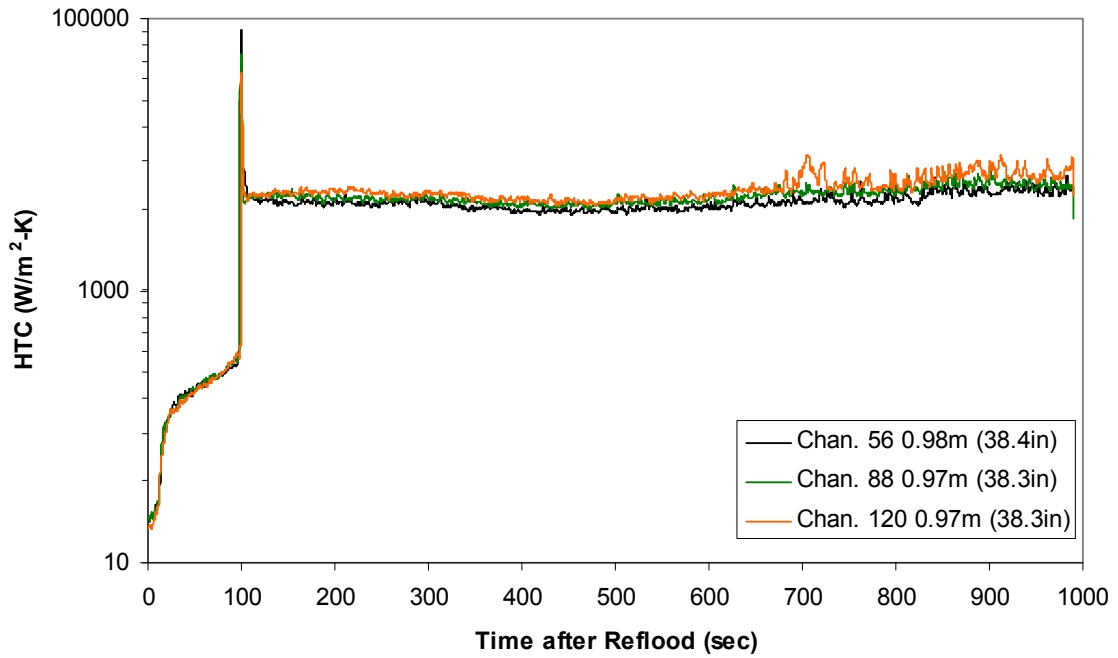
Spacer Grid Temperature during Reflood RBHT Exp. 1228



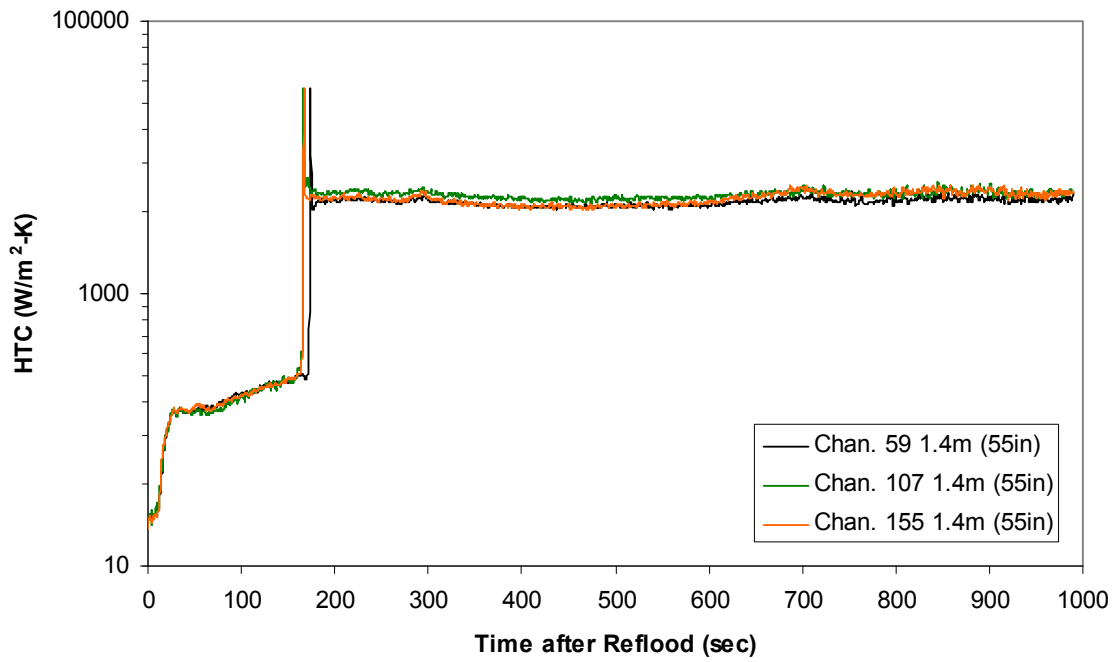
Spacer Grid Temperature during Reflood RBHT Exp. 1228



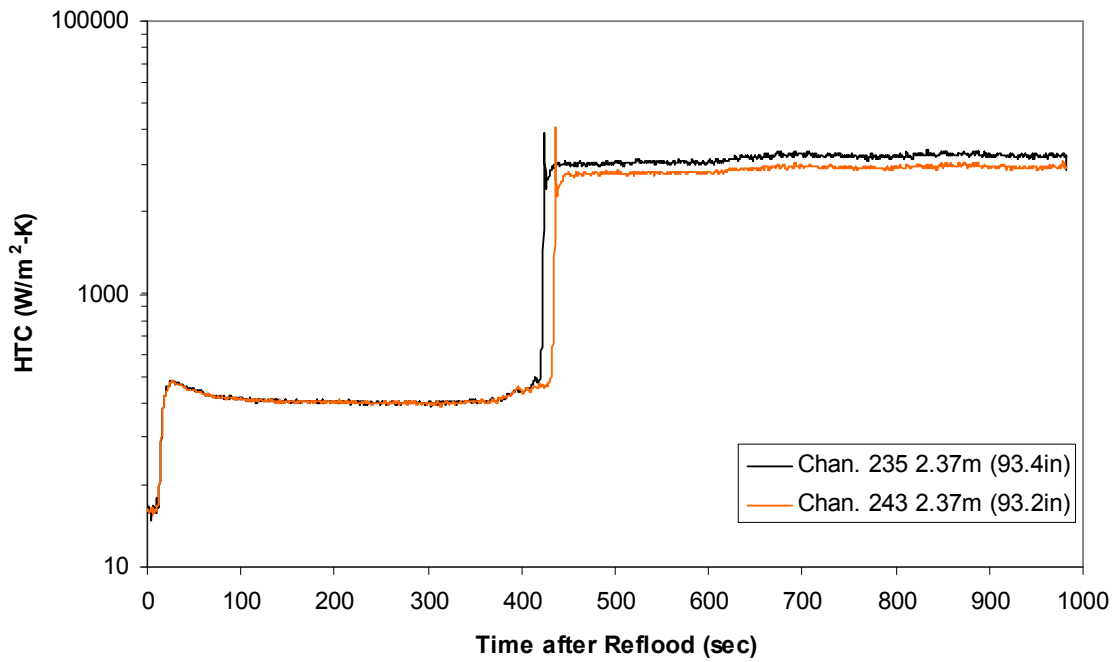
Heat Transfer Coefficient during Reflood RBHT Exp. 1228



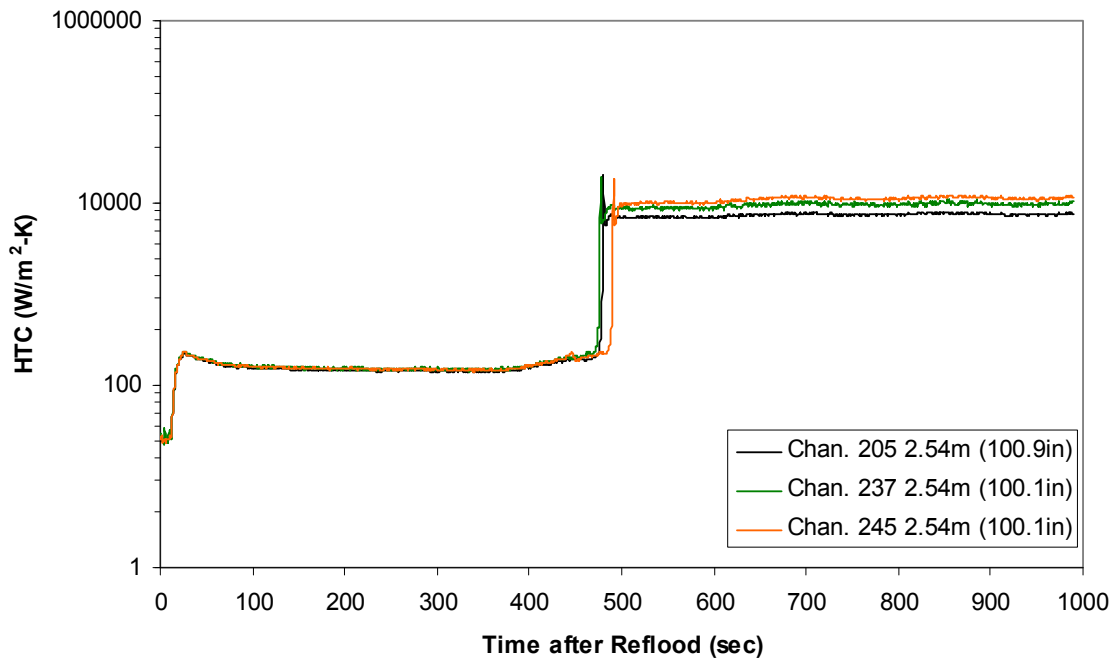
Heat Transfer Coefficient during Reflood
RBHT Exp. 1228



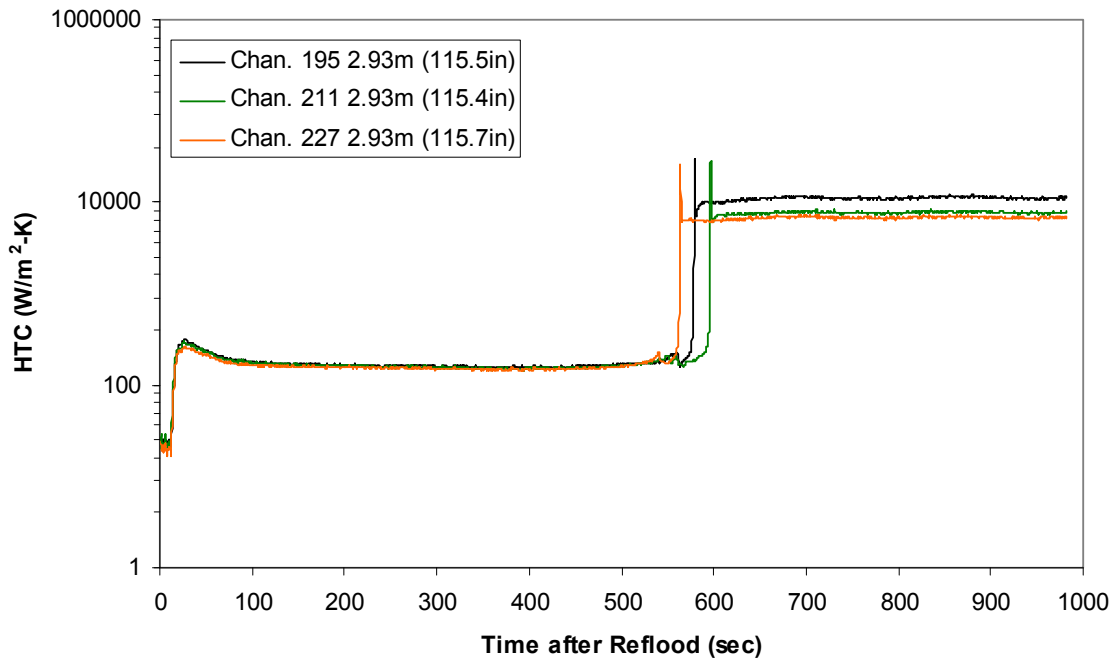
Heat Transfer Coefficient during Reflood
RBHT Exp. 1228



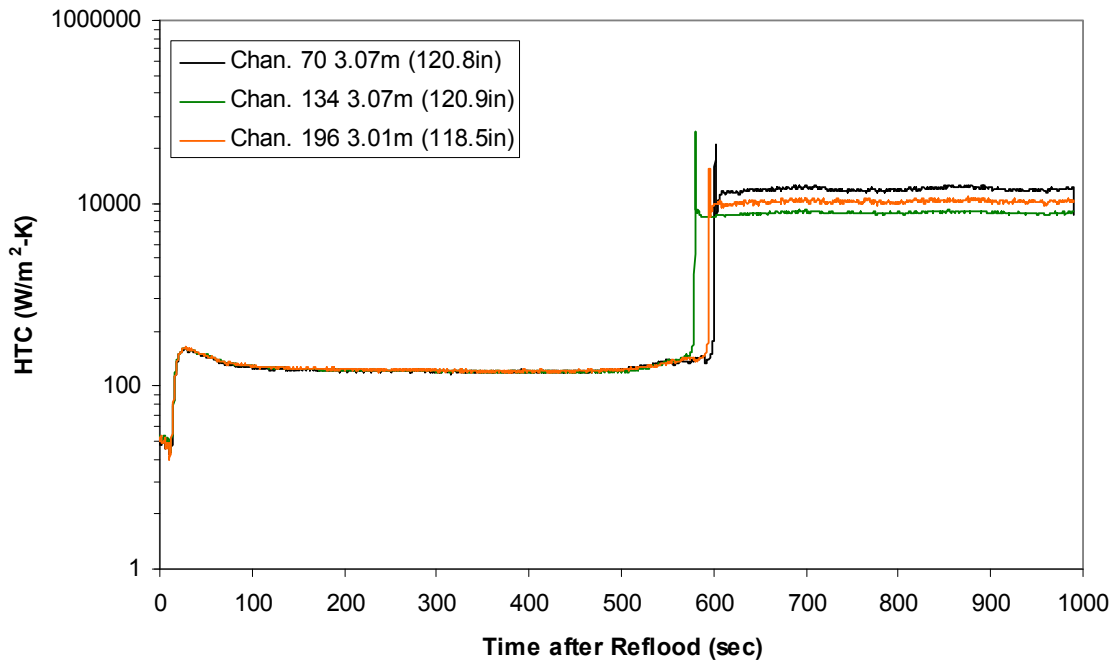
Heat Transfer Coefficient during Reflood RBHT Exp. 1228



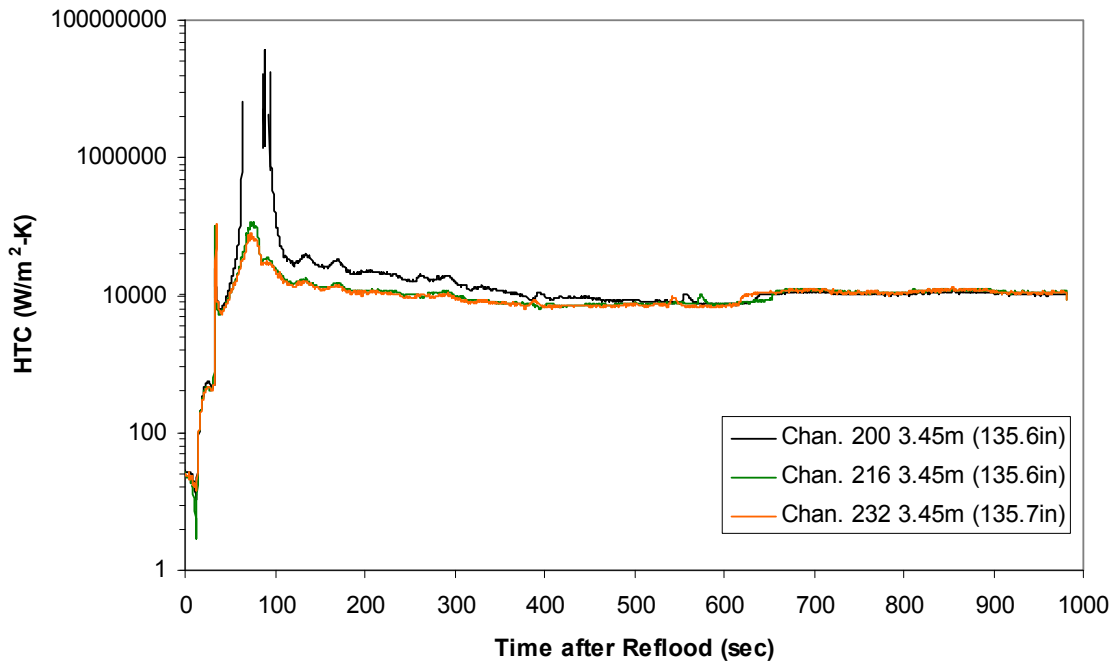
Heat Transfer Coefficient during Reflood RBHT Exp. 1228



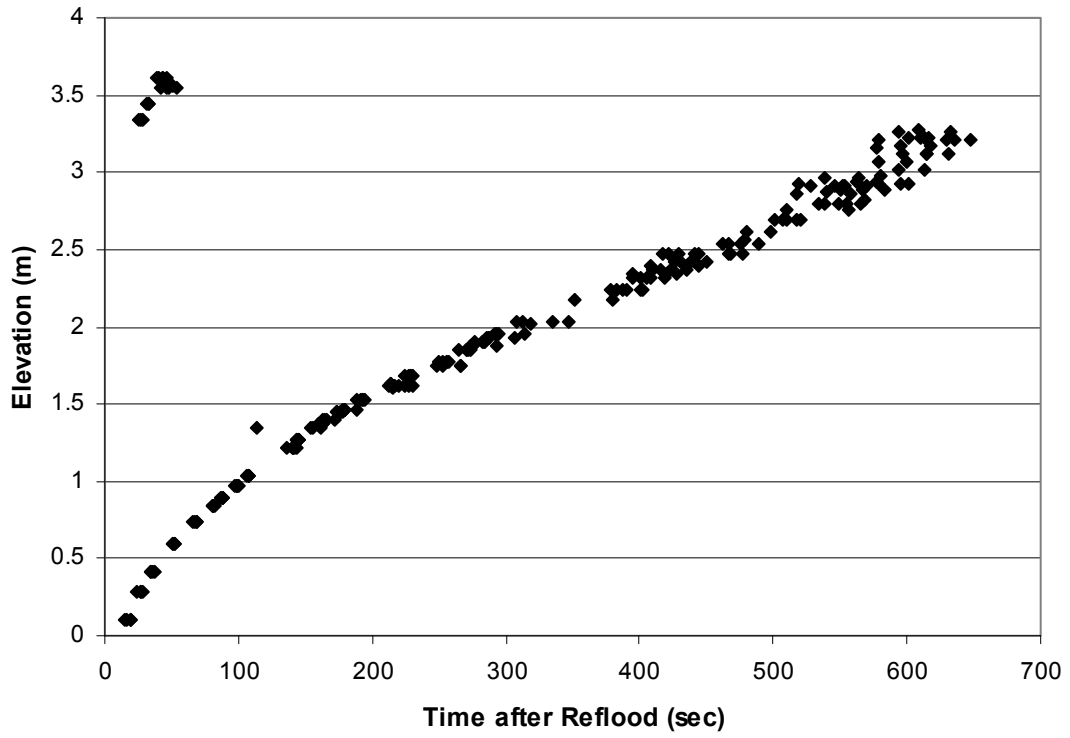
Heat Transfer Coefficient during Reflood RBHT Exp. 1228



Heat Transfer Coefficient during Reflood RBHT Exp. 1228



Quench Data, RBHT Exp. 1228



RBHT - REFLOOD TESTS

SUMMARY SHEET

RUN NO: **1280**

RUN CONDITIONS

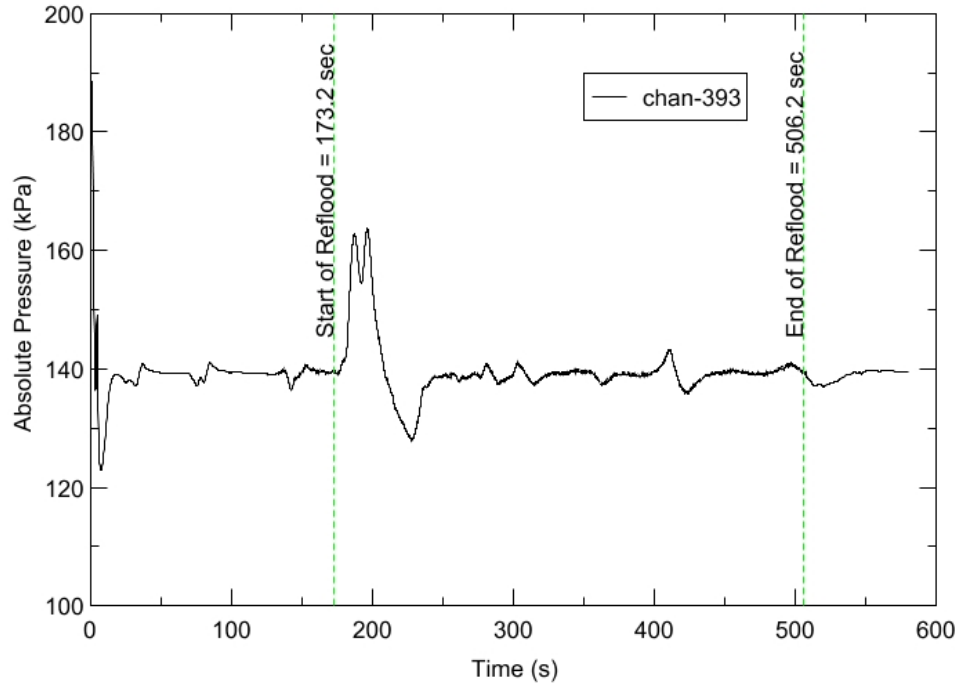
Upper Plenum Pressure:	138 kPa (20 psia)
Initial Peak Clad Temperature:	1144 degrees K (1600 degrees F)
Rod Peak Power:	2.3 kW/m (0.7 kW/ft)
Flooding Rate:	0.1524 m/s (6 in/s)
Inlet Subcooling:	83 degrees K (150 degrees F)
Start of Reflood:	173.2 s
End of Reflood:	506.2 s
Test Date:	7/17/2002
Comments:	No Droplet Data

Heater rod surfaces below 2.54 m (100 in) quench to a temperature below saturation due to the high inlet subcooling. Therefore DATARH calculated heat transfer coefficients are not presented below this elevation after rod quench.

Rod_Elevation	Channel Number	Temperature at Reflood (K)	Temperature at Reflood (F)	Turnaround Time (sec.)	Turnaround Temperature (K)	Turnaround Temperature (F)	Quench Time (sec.)	Quench Temperature (K)	Quench Temperature (F)
B6_0.592m	148	775.59	936.37	8.55	802.21	984.3	25.55	694.65	790.69
B6_0.744m	149	802.94	985.6	9.55	832.6	1038.99	30.55	705.74	810.64
B6_0.846m	150	824.46	1024.35	11.05	858.84	1086.22	34.55	707.4	813.64
B6_0.897m	151	833.22	1040.11	11.55	869.42	1105.27	35.55	723.97	843.45
C6_1.04m	137	880.16	1124.6	16.55	921.35	1198.74	42.05	733.83	861.2
D5_1.27m	217	951.56	1253.12	14.05	993	1327.71	51.55	759.24	906.94
C6_1.34m	138	935.21	1223.68	15.05	982.39	1308.62	54.55	744.99	881.3
D5_1.37m	218	968.15	1282.98	16.05	1015.24	1367.74	58.55	738.21	869.09
C6_1.39m	139	938.85	1230.24	16.55	987.31	1317.47	59.05	736.16	865.39
D5_1.45m	219	978.45	1301.51	16.55	1027.38	1389.59	62.05	746.83	884.61
C6_1.47m	140	949.82	1249.99	16.05	999.85	1340.05	63.05	735.87	864.88
D5_1.52m	220	988.33	1319.31	16.55	1040.04	1412.39	66.55	742.83	877.41
C6_1.62m	141	967.35	1281.55	18.05	1024.83	1385	71.55	763.62	914.82
D5_1.68m	221	1005.85	1350.84	17.55	1064.34	1456.13	76.05	746.29	883.63
D5_1.78m	222	993.19	1328.05	11.05	1037.95	1408.62	82.05	702.35	804.54
D5_1.85m	223	1023.02	1381.75	11.05	1071.24	1468.54	86.05	695.53	792.27
C6_1.87m	142	1000.1	1340.5	12.05	1052.33	1434.5	88.05	702.29	804.44
D5_1.90m	224	1029.41	1393.24	12.05	1081.03	1486.16	89.05	698.22	797.1
C6_1.95m	144	1006.44	1351.91	12.55	1061	1450.11	93.05	704.41	808.25
C3_2.17m	178	1043.61	1418.82	10.55	1094.95	1511.22	111.55	683.94	771.4
D4_2.24m	241	1088.62	1499.82	10.05	1137.84	1588.42	116.05	662.76	733.28
D4_2.32m	242	1097.62	1516.03	10.55	1151.69	1613.35	122.55	696.25	793.56
C3_2.35m	180	1089.89	1502.11	11.05	1147.39	1605.61	126.05	684.96	773.24
D4_2.37m	243	1104.1	1527.69	10.55	1159.62	1627.64	127.05	713.15	823.98
C3_2.40m	181	1091.96	1505.84	11.05	1149.79	1609.93	131.55	684.65	772.69
D4_2.54m	245	1126.86	1568.66	10.55	1182.64	1669.07	148.05	689.84	782.03
D6_2.62m	129	1115.25	1547.76	10.55	1173.44	1652.5	158.05	690.49	783.19
D6_2.69m	130	1116.39	1549.81	11.05	1175.5	1656.21	169.05	699.51	799.43
C3_2.76m	183	1116.78	1550.52	11.05	1176.49	1657.99	182.05	684.8	772.95
D4_2.79m	247	1091.36	1504.76	9.05	1142.44	1596.7	187.05	657.69	724.16
D6_2.87m	131	1066.87	1460.68	9.05	1117.04	1550.98	199.55	628.44	671.5
D6_2.92m	132	1039.4	1411.22	10.55	1095.67	1512.52	209.05	633.49	680.59
D6_2.97m	133	1008.24	1355.14	11.05	1062.59	1452.98	220.05	626.21	667.5
D6_3.07m	134	967.25	1281.37	11.05	1018.38	1373.39	235.05	623.27	662.2
E3_3.12m	197	965.95	1279.02	10.55	1015.91	1368.95	245.55	607.1	633.1
D6_3.17m	135	926.7	1208.36	11.05	974.56	1294.52	252.55	620.13	656.55
D6_3.27m	136	880.35	1124.94	11.55	926.19	1207.46	215.05	562.71	553.19
D4_3.61m	248	623.01	661.73	12.55	678.09	760.87	42.05	476.4	397.83

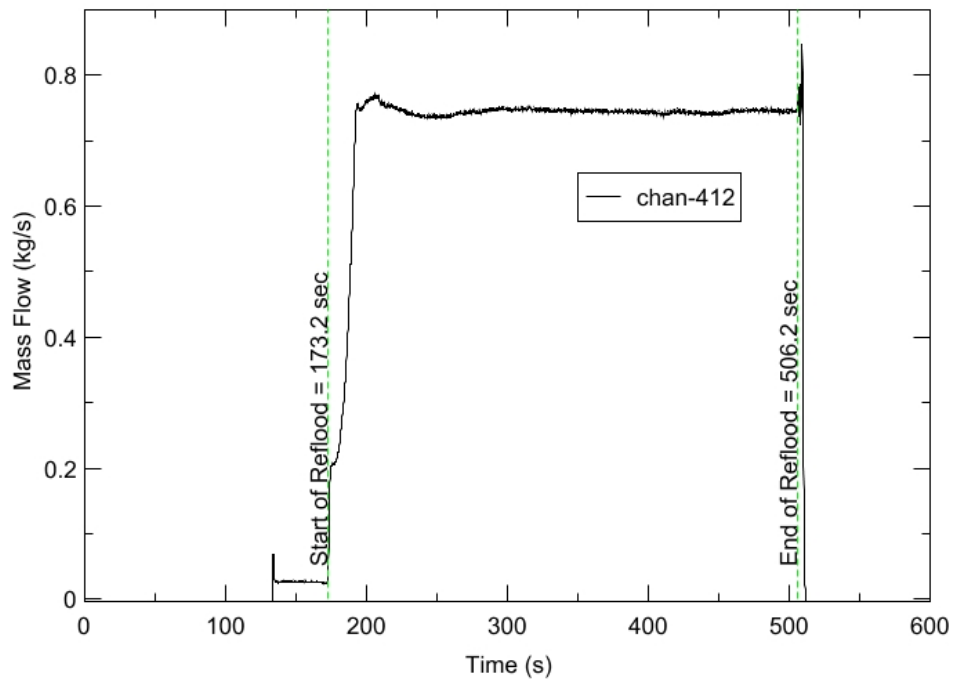
RBHT - TEST FACILITY

Upper Plenum Pressure vs. Time, Exp 1280



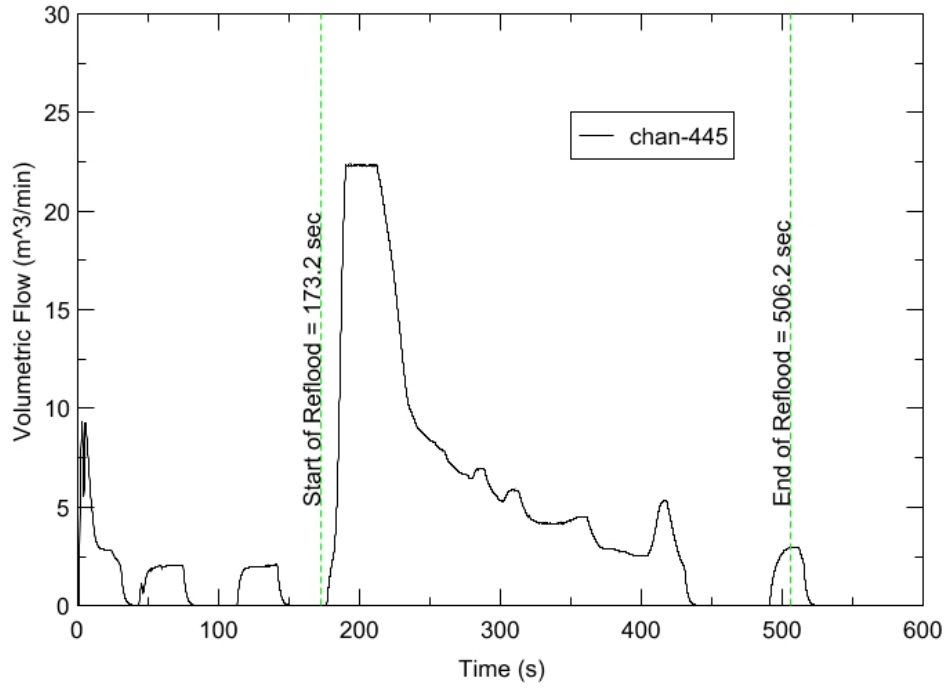
RBHT - TEST FACILITY

Inlet Flow vs. Time, Exp 1280



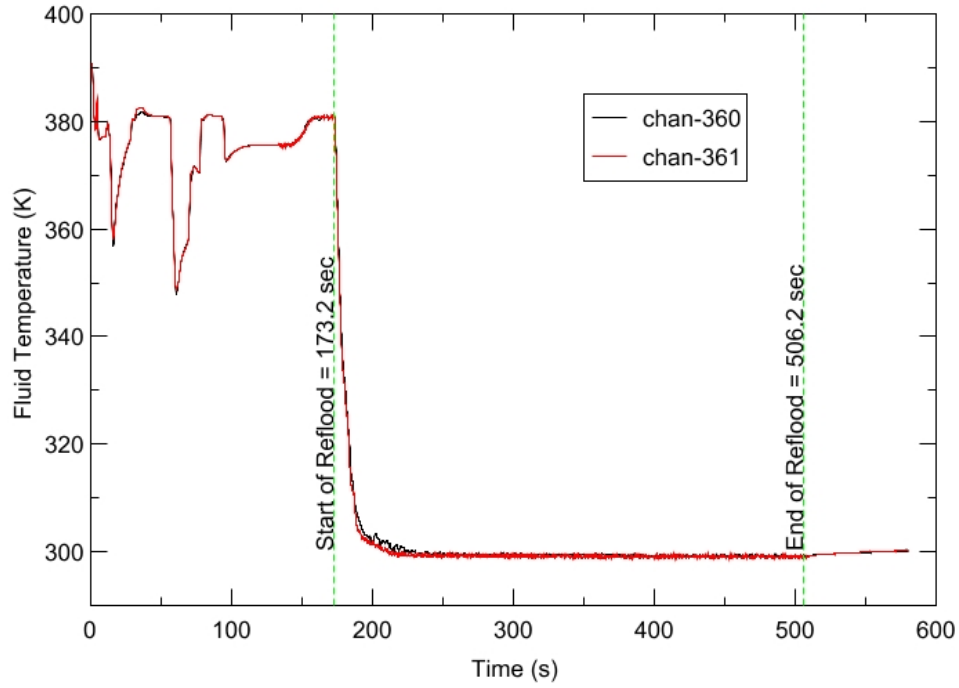
RBHT - TEST FACILITY

Steam Exhaust Flow vs. Time, Exp 1280



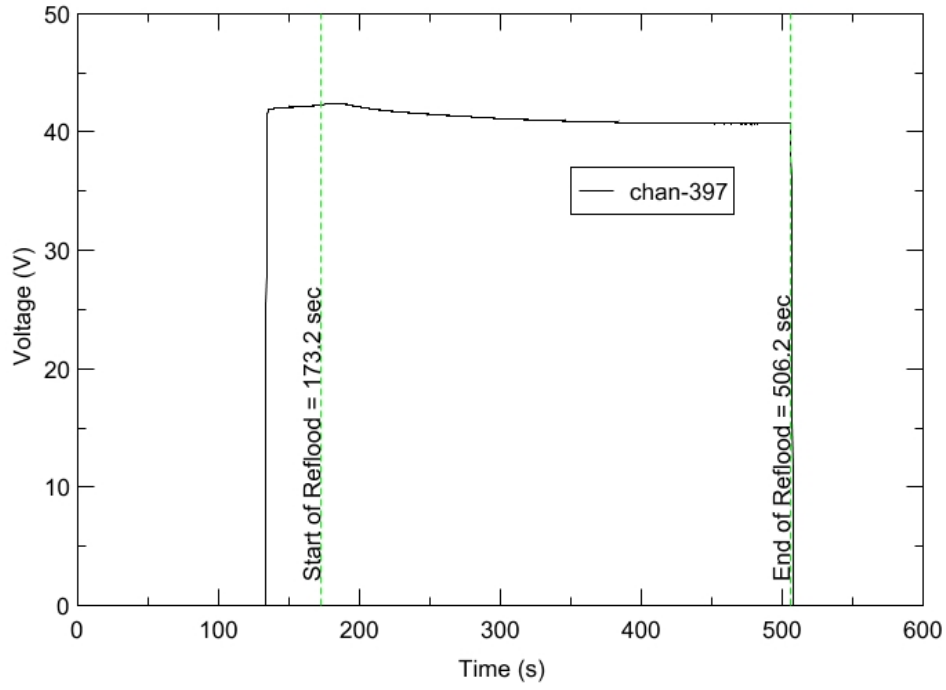
RBHT - TEST FACILITY

Inlet Flow Temperature vs. Time, Exp 1280



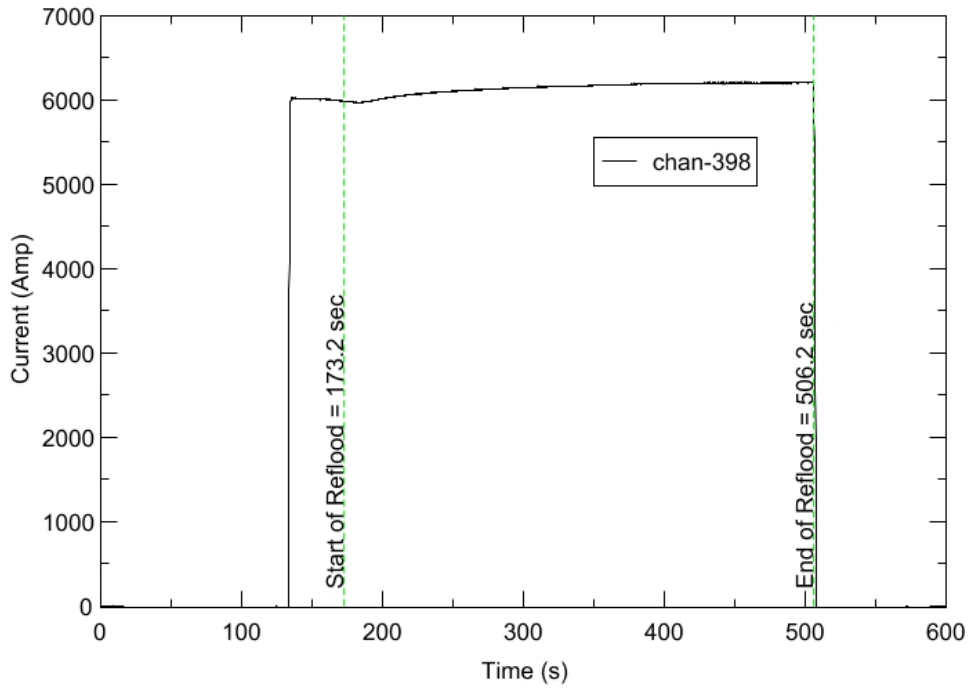
RBHT - TEST FACILITY

Test Section Voltage vs. Time, Exp 1280

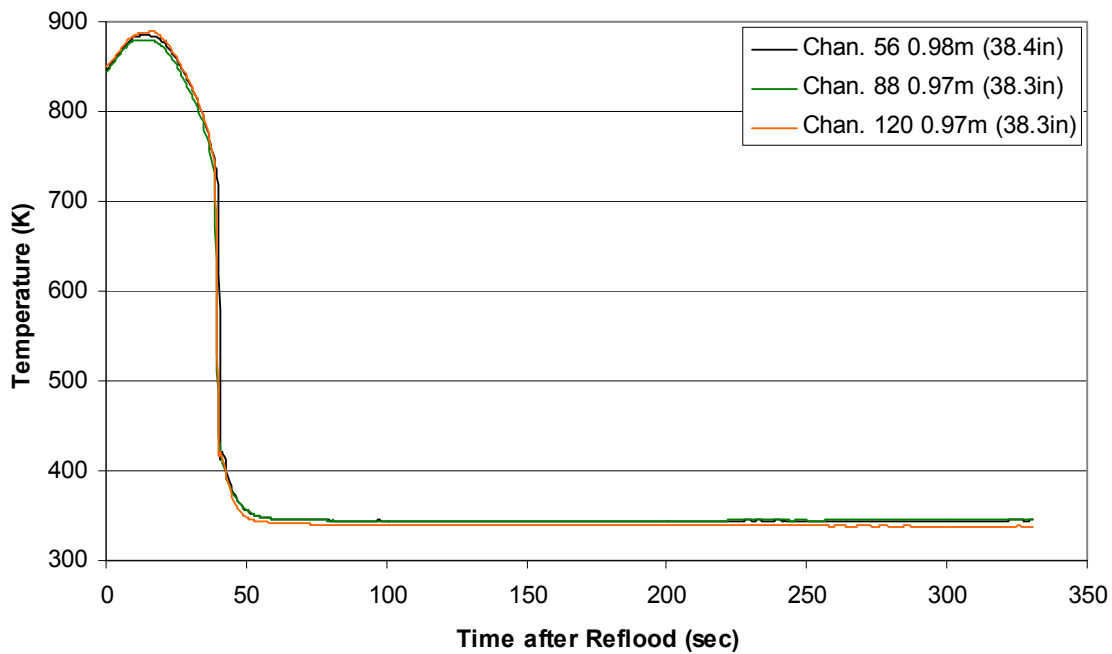


RBHT - TEST FACILITY

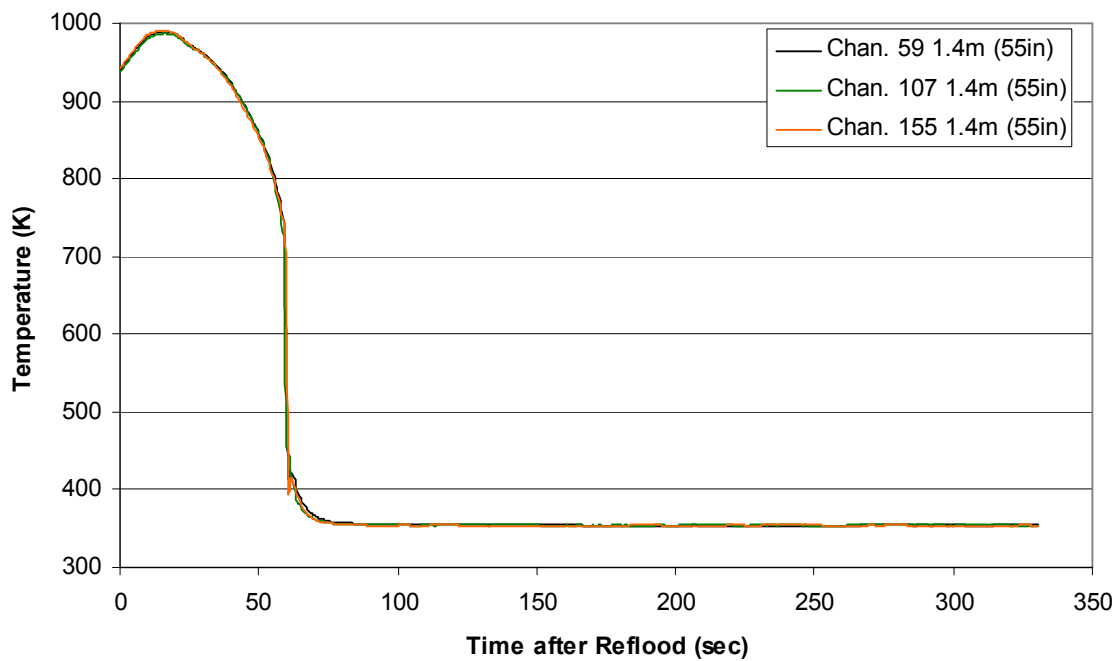
Test Section Current vs. Time, Exp 1280



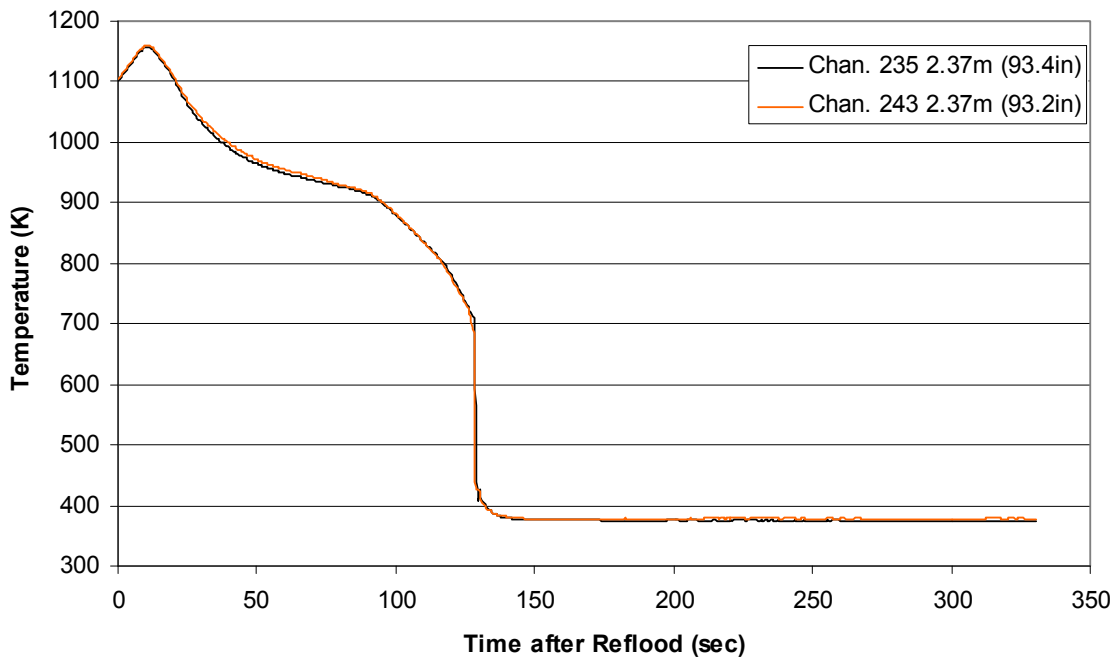
**Heater Rod Temperature during Reflood
RBHT Exp. 1280**



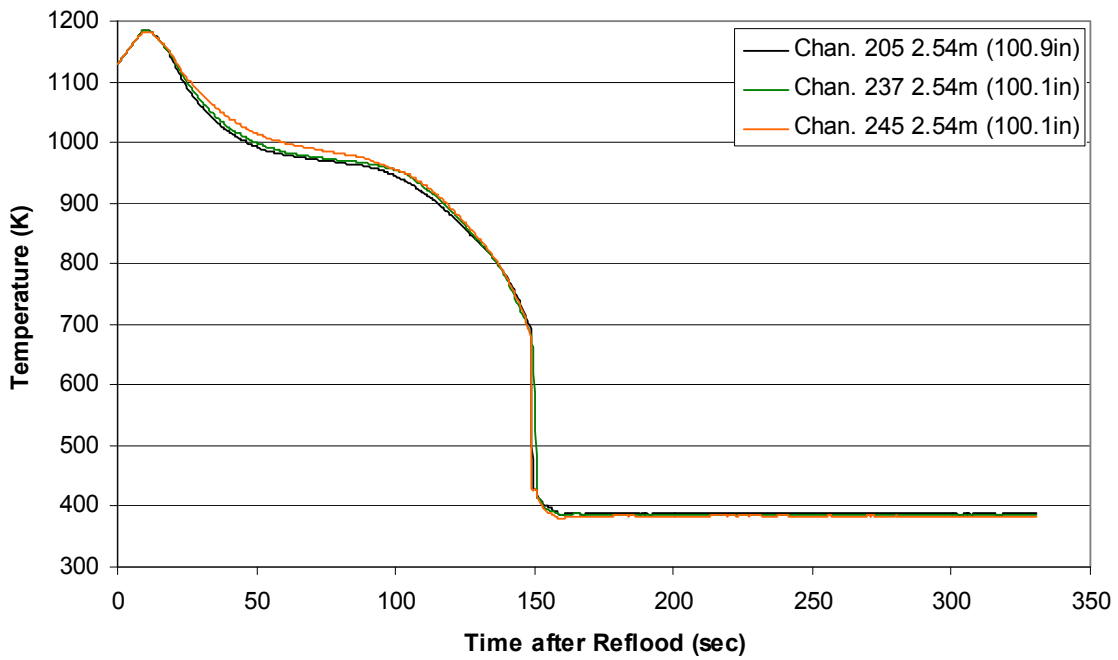
**Heater Rod Temperature during Reflood
RBHT Exp. 1280**



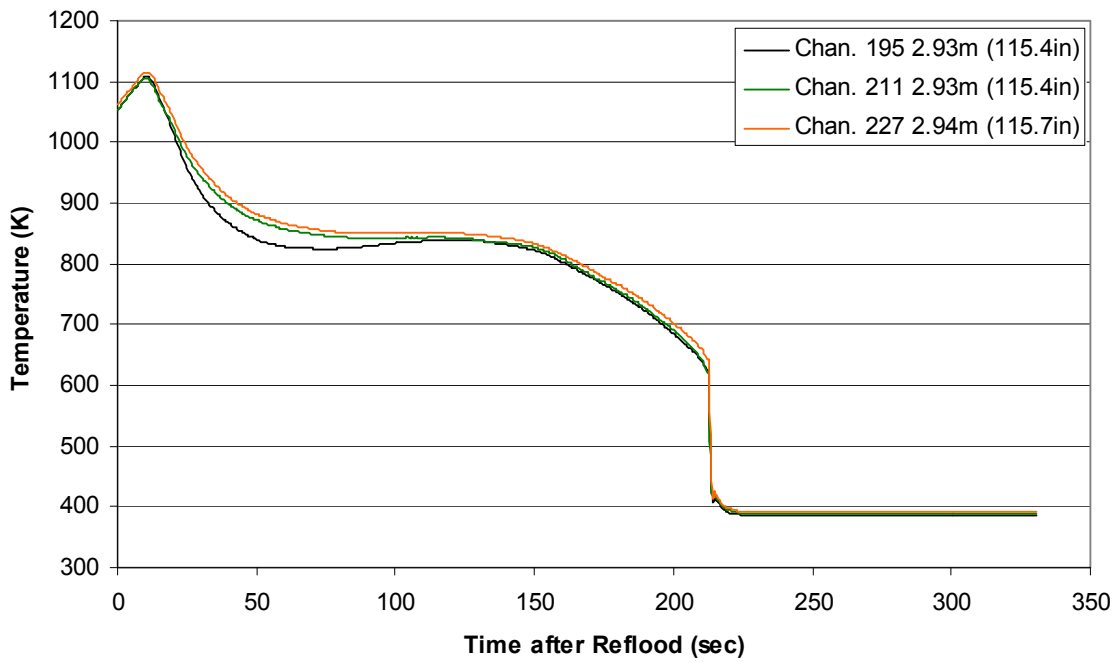
**Heater Rod Temperature during Reflood
RBHT Exp. 1280**



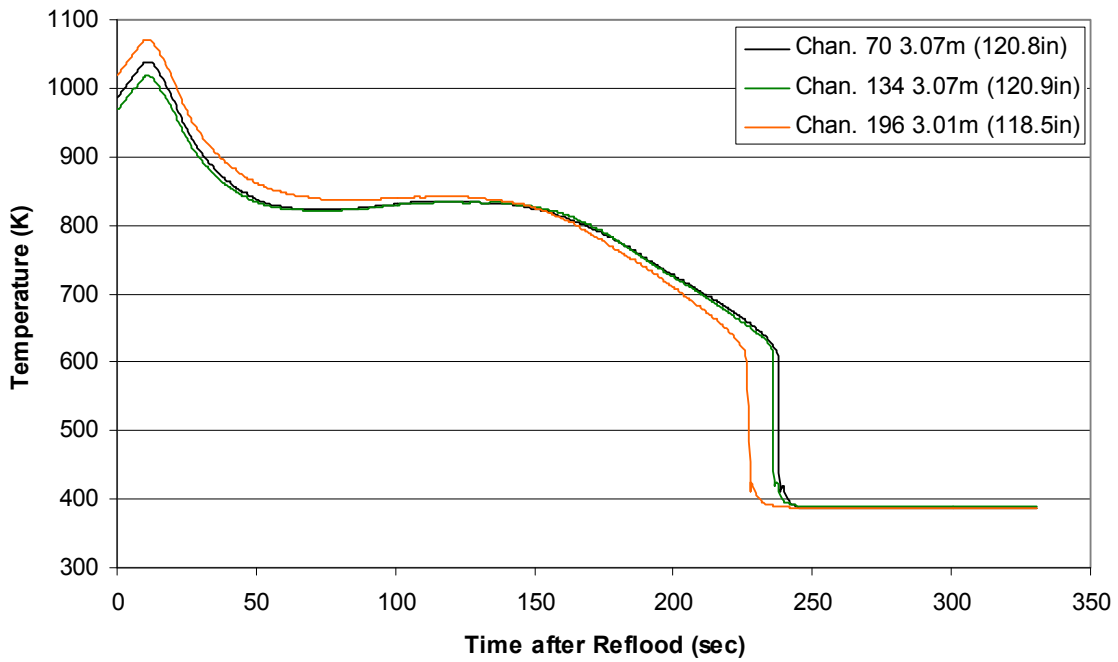
**Heater Rod Temperature during Reflood
RBHT Exp. 1280**



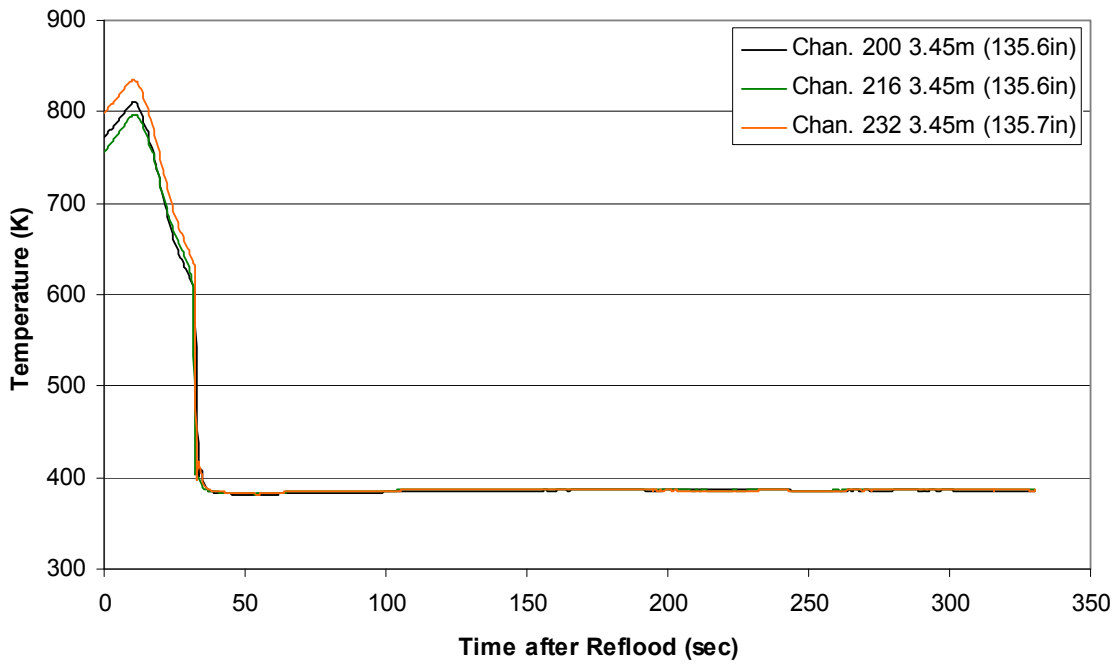
**Heater Rod Temperature during Reflood
RBHT Exp. 1280**



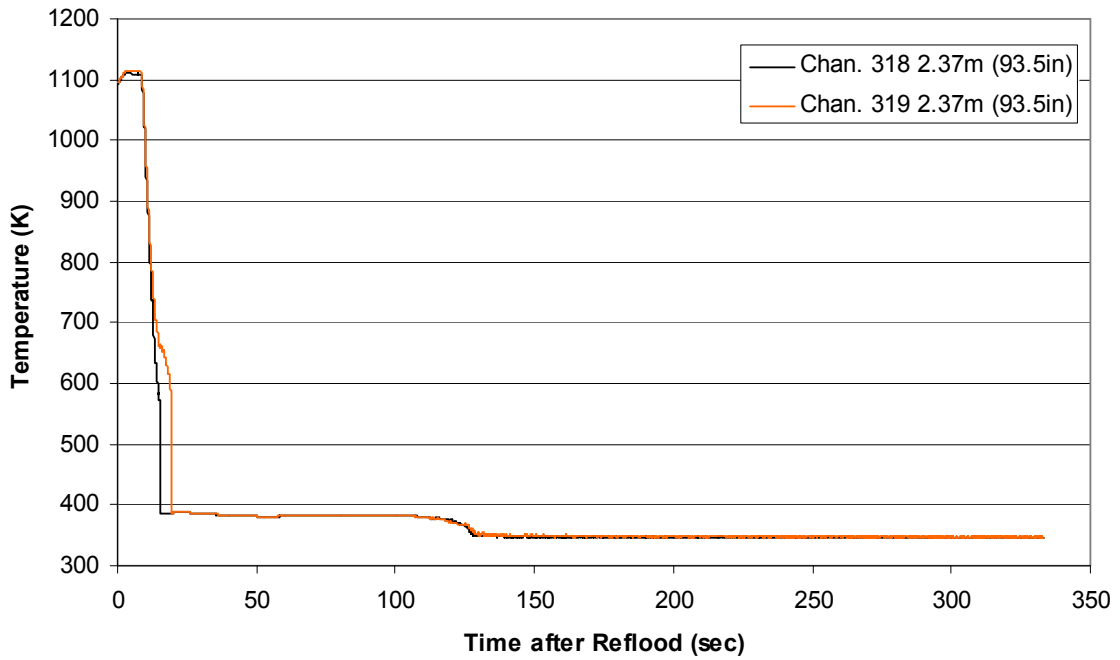
**Heater Rod Temperature during Reflood
RBHT Exp. 1280**



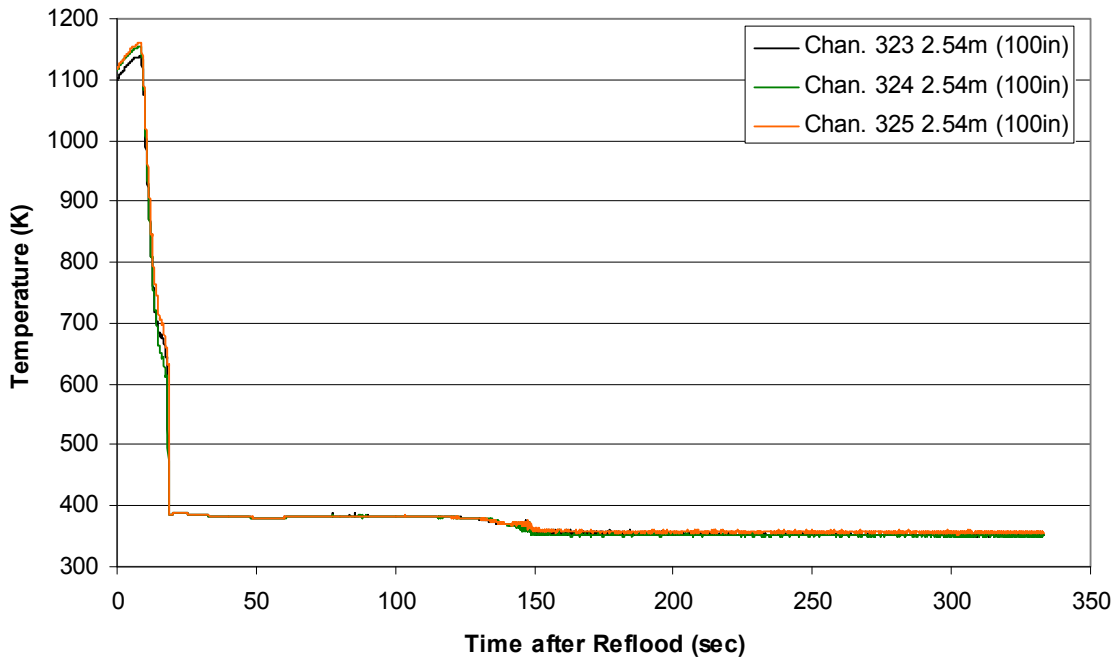
Heater Rod Temperature during Reflood RBHT Exp. 1280



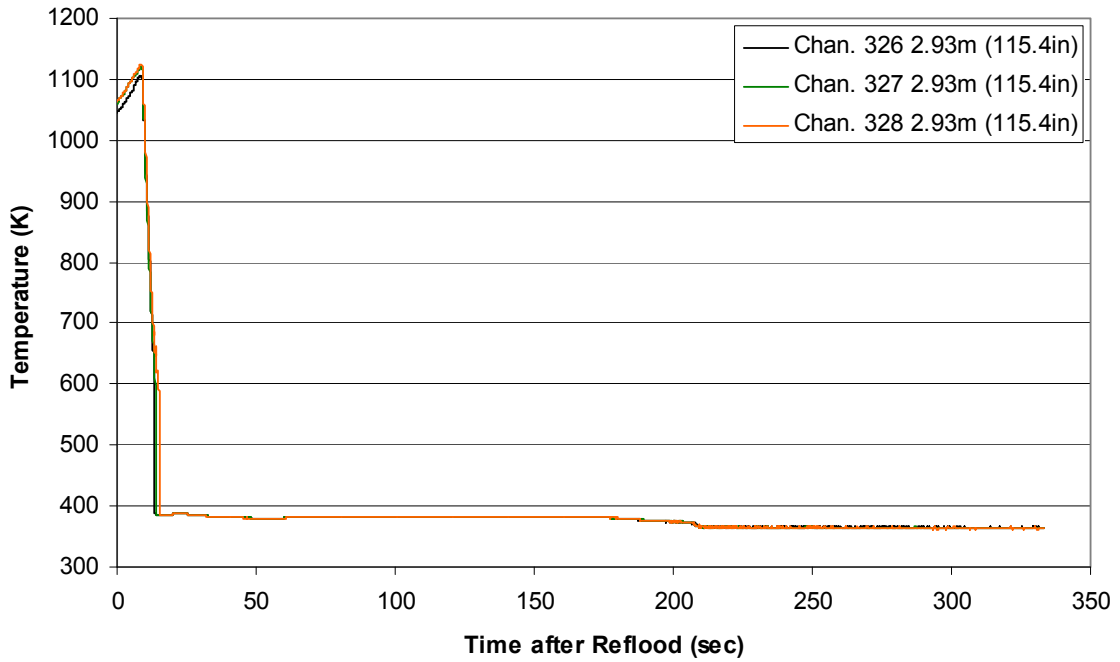
Steam Probe Temperature during Reflood RBHT Exp. 1280



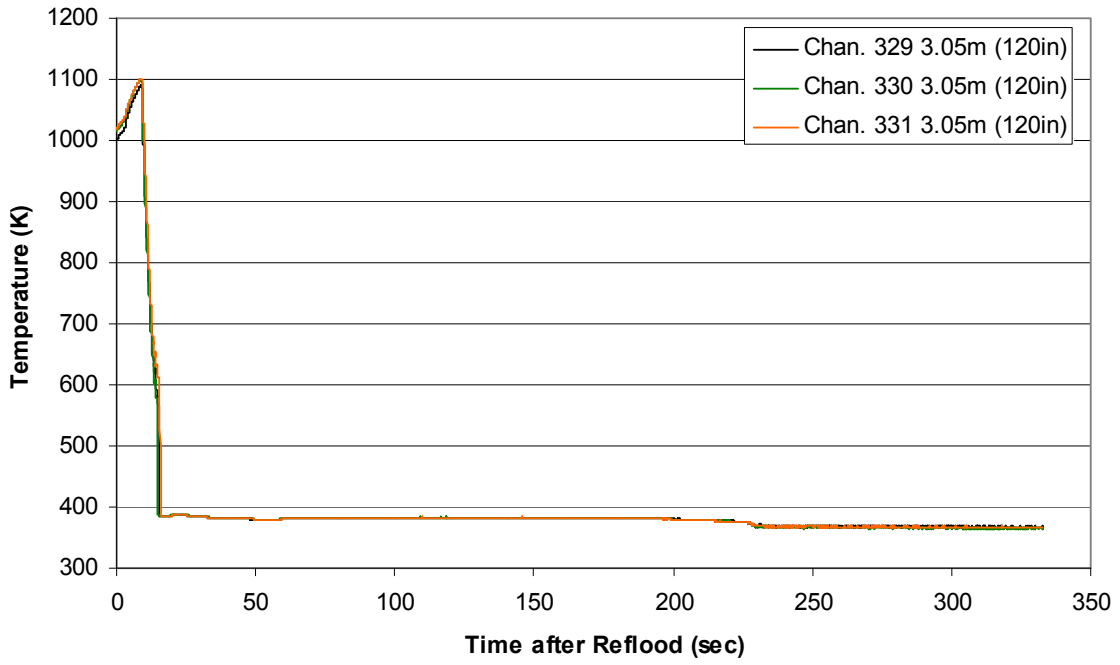
Steam Probe Temperature during Reflood RBHT Exp. 1280



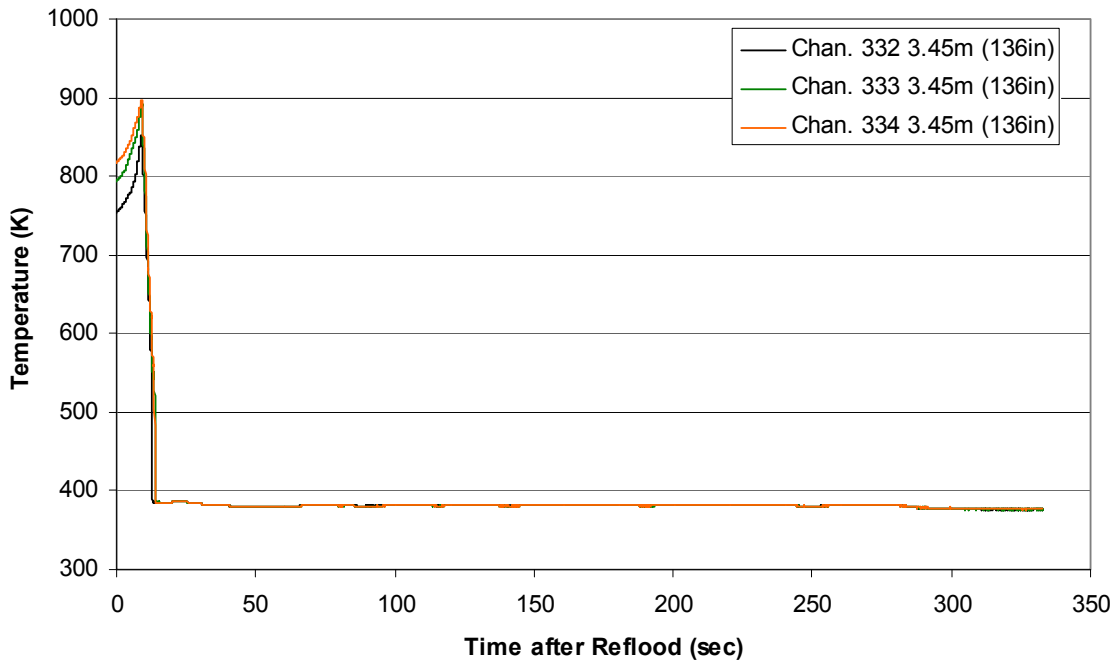
Steam Probe Temperature during Reflood RBHT Exp. 1280



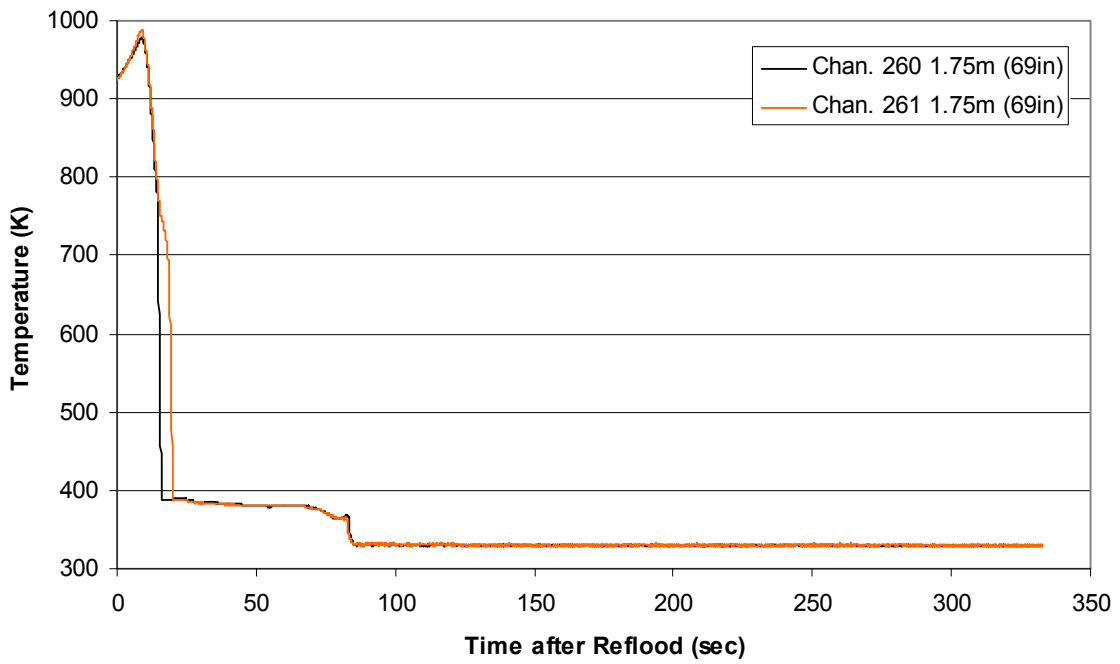
Steam Probe Temperature during Reflood RBHT Exp. 1280



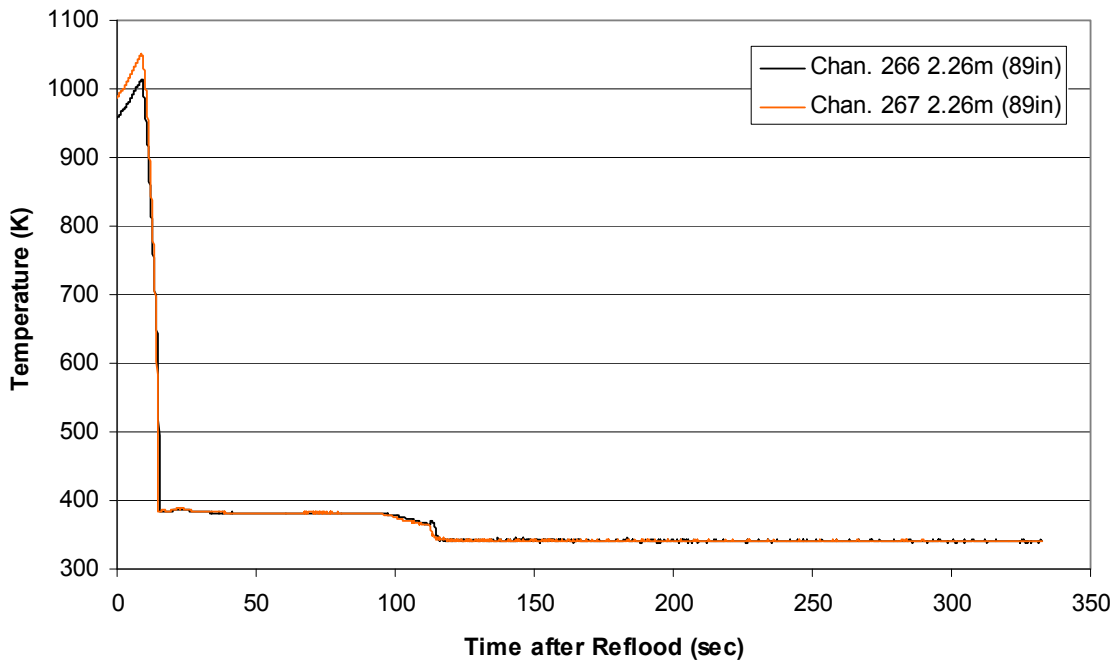
Steam Probe Temperature during Reflood RBHT Exp. 1280



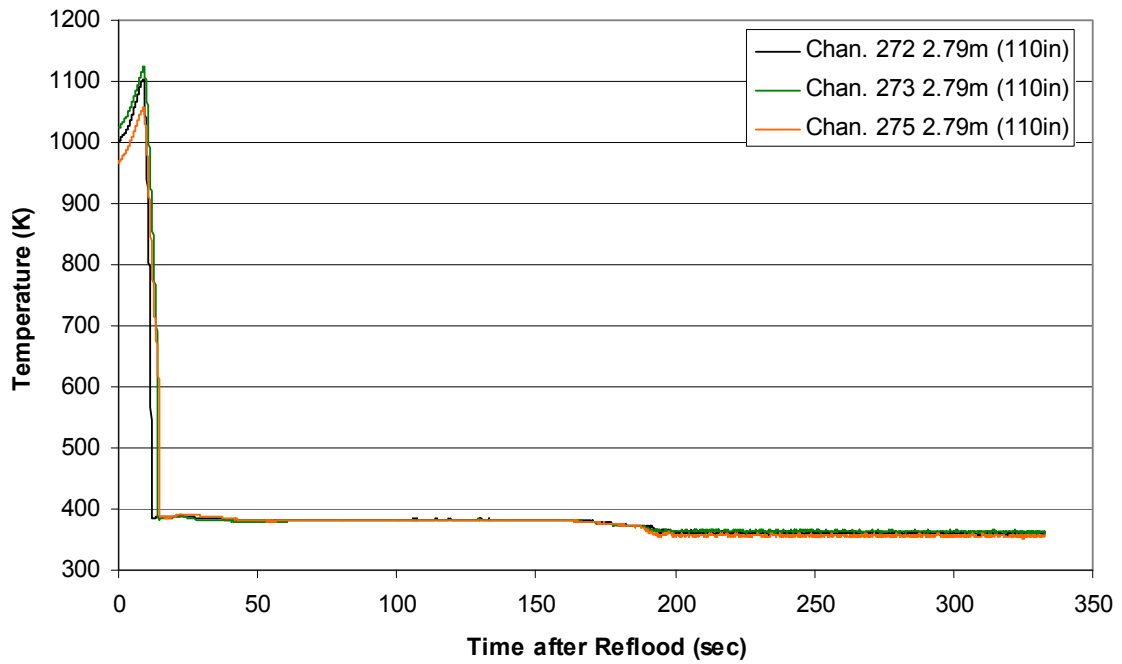
Spacer Grid Temperature during Reflood
RBHT Exp. 1280



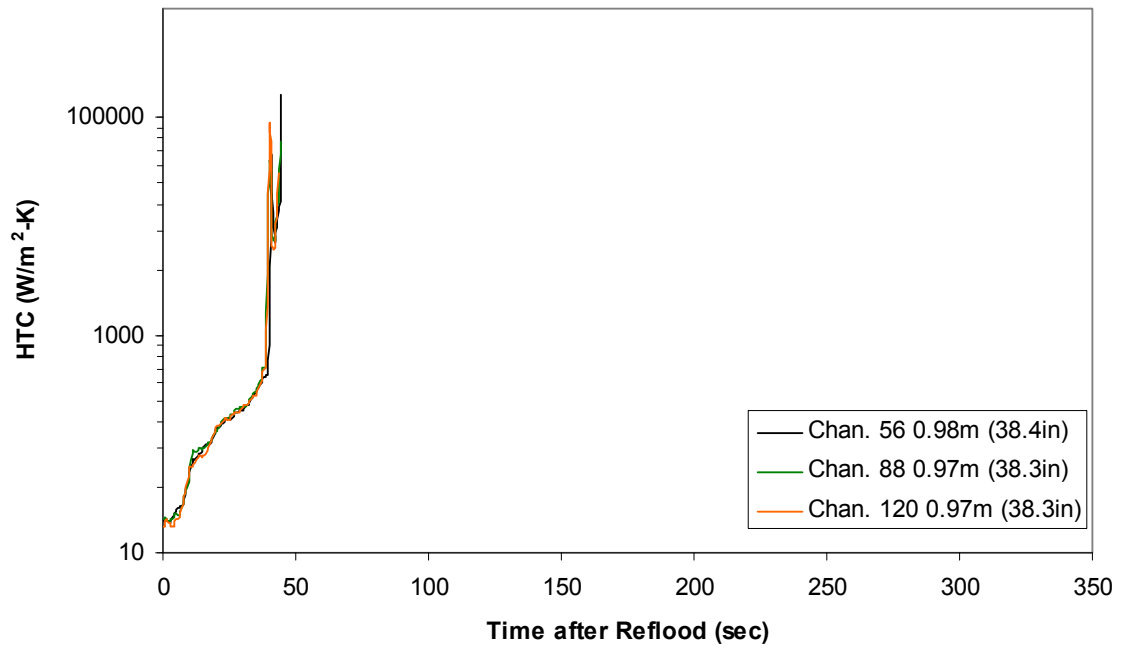
Spacer Grid Temperature during Reflood
RBHT Exp. 1280



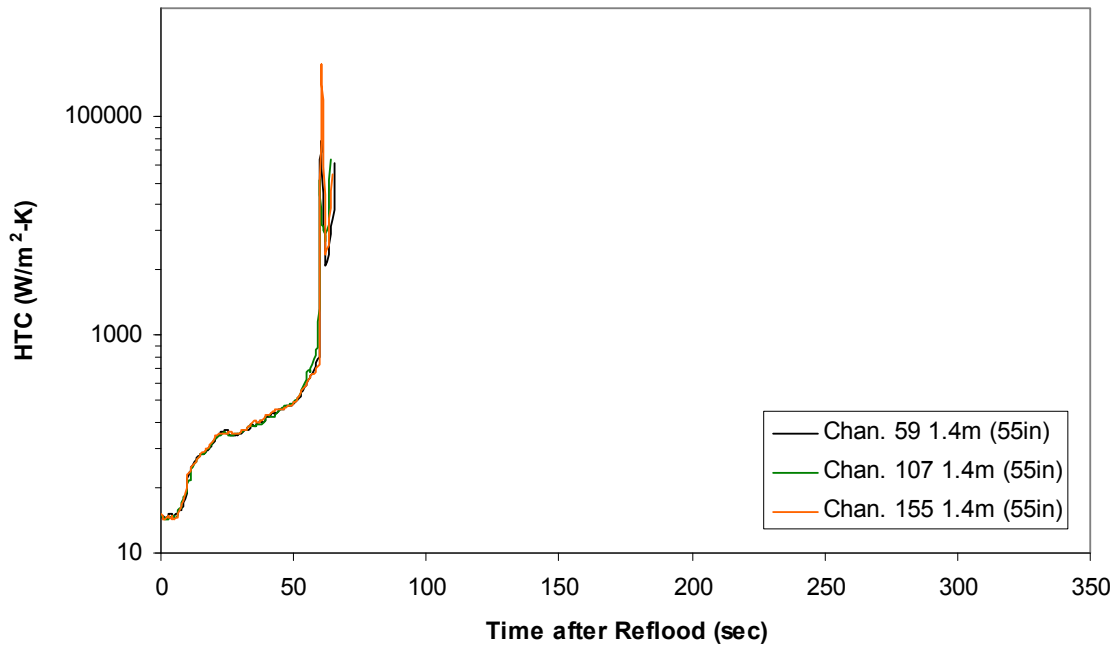
Spacer Grid Temperature during Reflood RBHT Exp. 1280



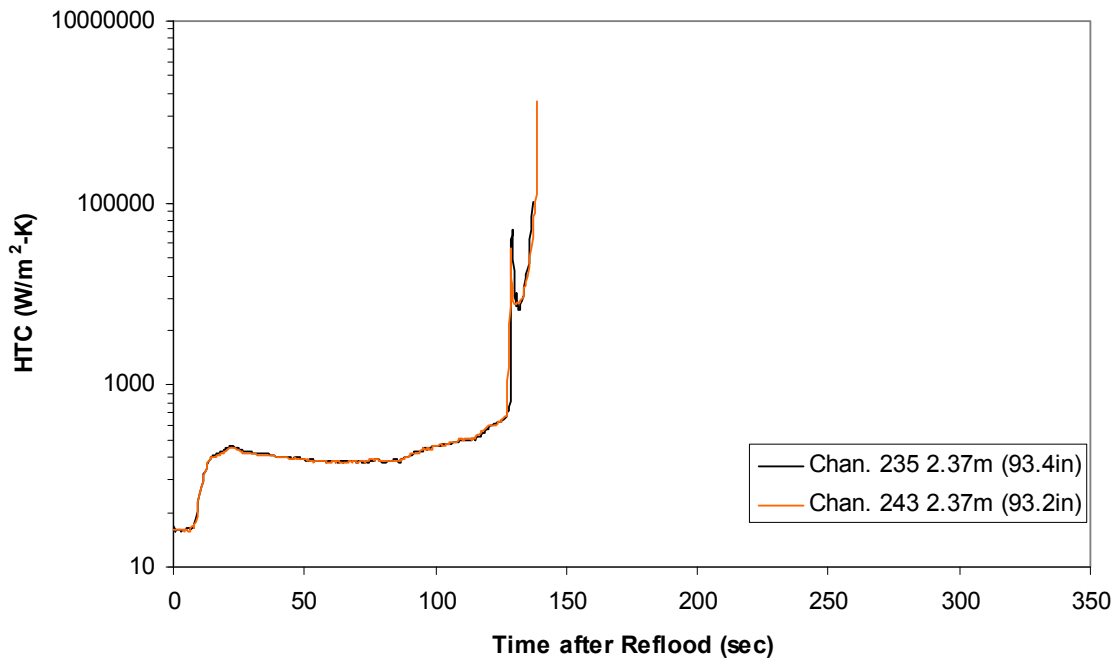
Heat Transfer Coefficient during Reflood RBHT Exp. 1280



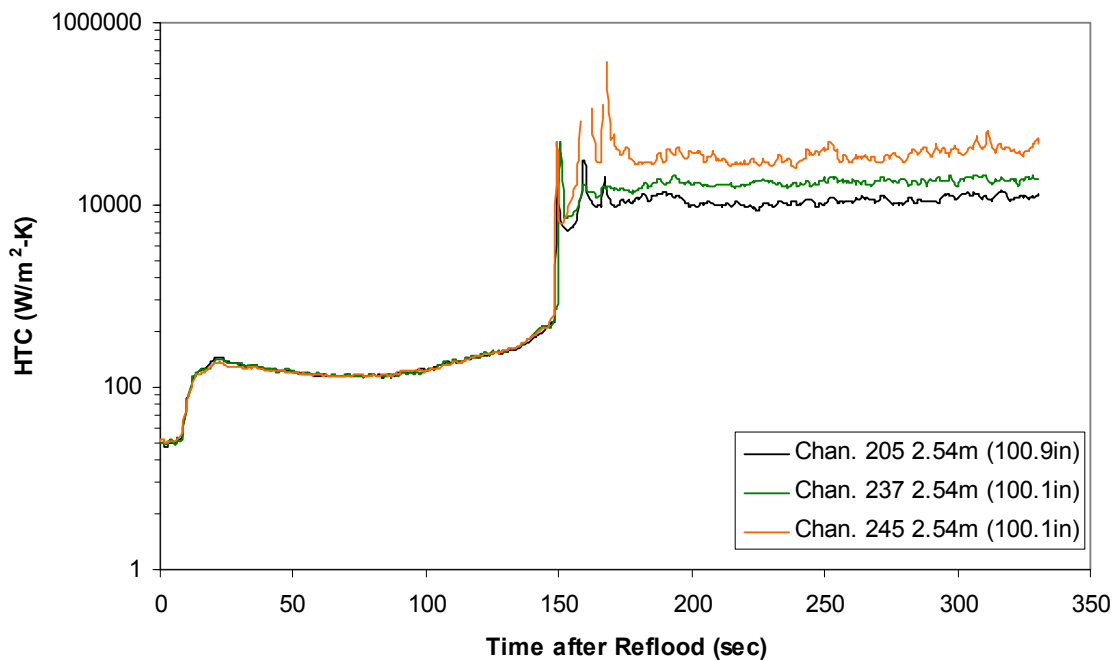
Heat Transfer Coefficient during Reflood RBHT Exp. 1280



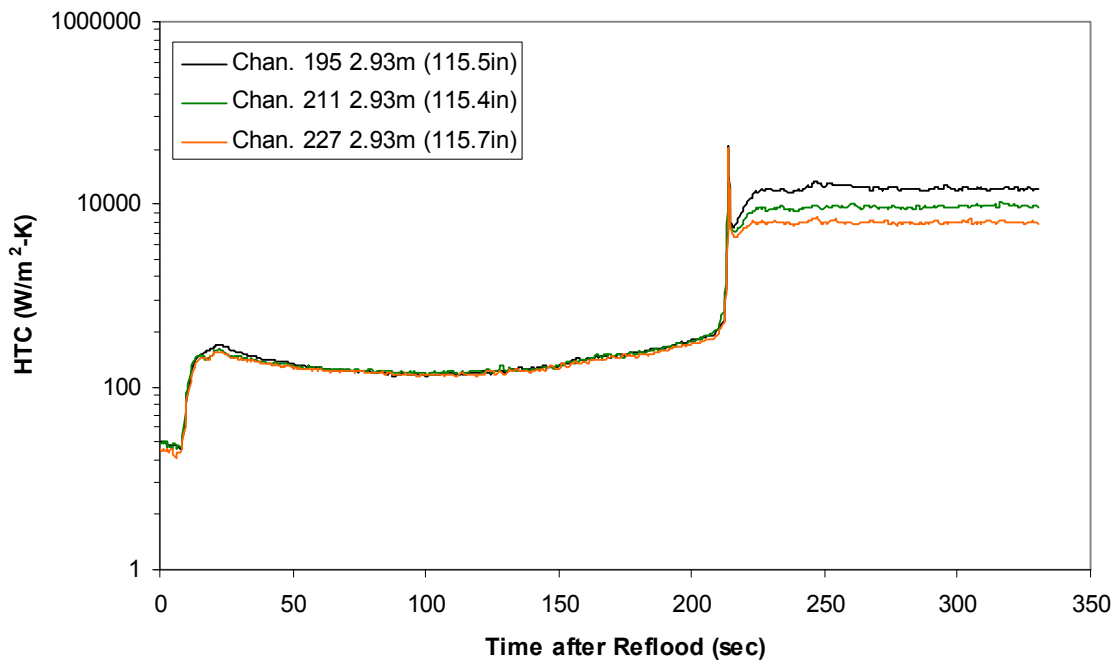
Heat Transfer Coefficient during Reflood RBHT Exp. 1280



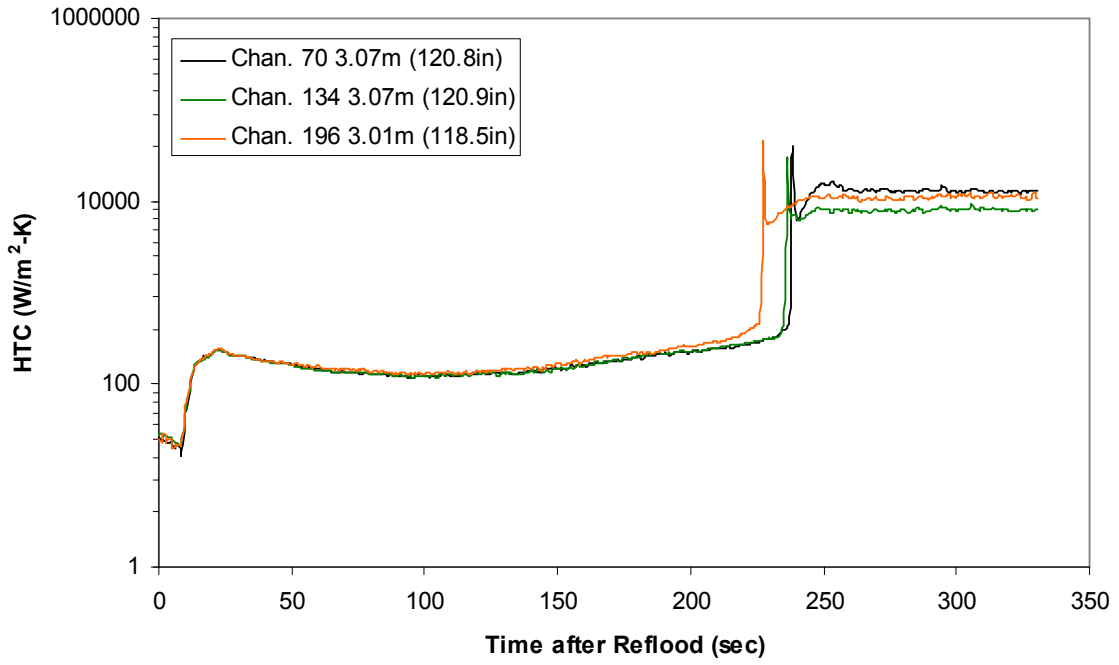
Heat Transfer Coefficient during Reflood RBHT Exp. 1280



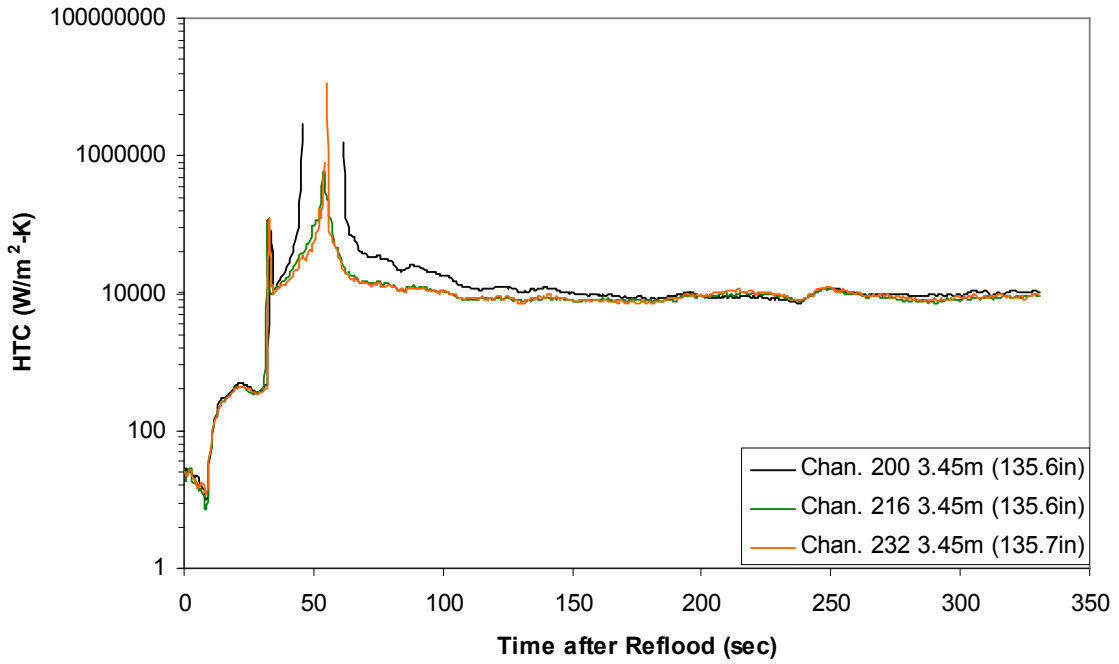
Heat Transfer Coefficient during Reflood RBHT Exp. 1280



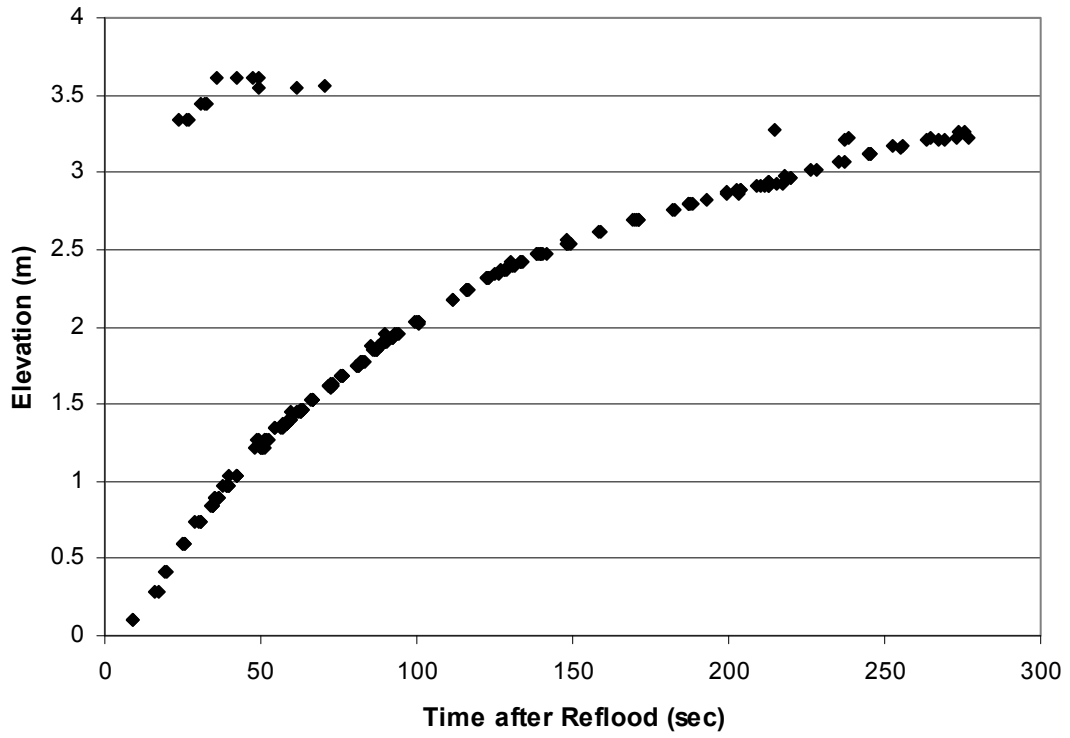
Heat Transfer Coefficient during Reflood RBHT Exp. 1280



Heat Transfer Coefficient during Reflood RBHT Exp. 1280



Quench Data, RBHT Exp. 1280



RBHT - REFLOOD TESTS

SUMMARY SHEET

RUN NO: **1285**

RUN CONDITIONS

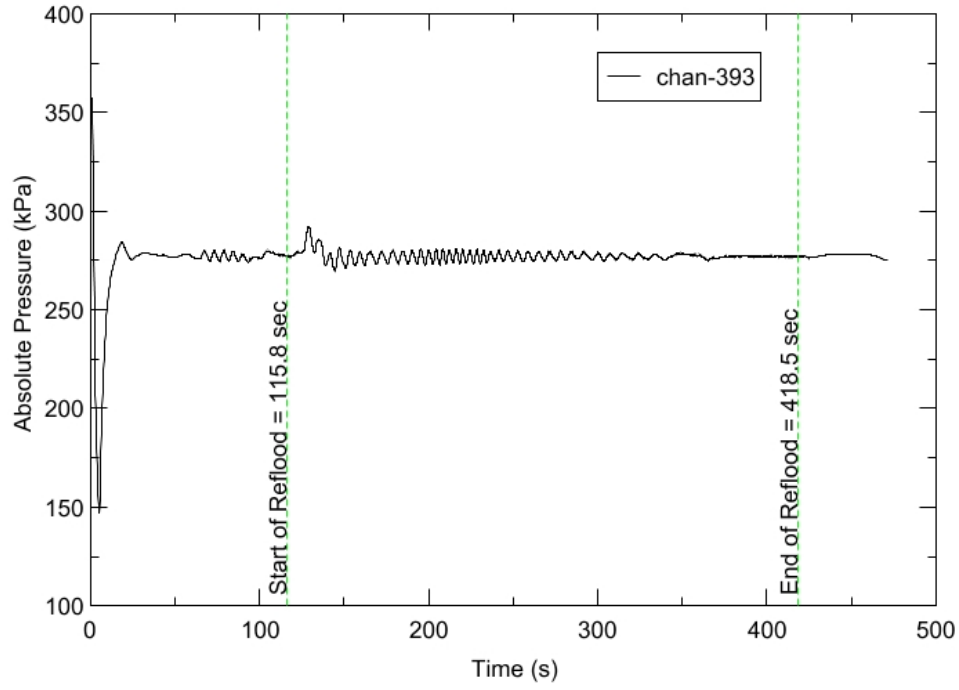
Upper Plenum Pressure:	276 kPa (40 psia)
Initial Peak Clad Temperature:	1144 degrees K (1600 degrees F)
Rod Peak Power:	2.3 kW/m (0.7 kW/ft)
Flooding Rate:	0.1524 m/s (6 in/s)
Inlet Subcooling:	83 degrees K (150 degrees F)
Start of Reflood:	115.8 s
End of Reflood:	418.5 s
Test Date:	7/18/2002
Comments:	No droplet data

Heater rod surfaces below 2.54 m (100 in) quench to a temperature below saturation due to the high inlet subcooling. Therefore DATARH calculated heat transfer coefficients are not presented below this elevation after rod quench.

Rod_Elevation	Channel Number	Temperature at Reflood (K)	Temperature at Reflood (°F)	Turnaround Time (sec.)	Turnaround Temperature (K)	Turnaround Temperature (°F)	Quench Time (sec.)	Quench Temperature (K)	Quench Temperature (°F)
B6 0.592m	148	777.82	940.38	9.45	805.82	990.8	25.95	675.33	755.91
B6 0.744m	149	805.63	990.44	10.45	838	1048.71	30.95	686.68	776.34
B6 0.846m	150	836.51	1046.02	10.95	871.23	1108.52	33.95	705.93	810.99
B6 0.897m	151	848.04	1066.78	10.95	883.6	1130.79	35.95	701.38	802.79
C6 1.04m	137	897.55	1155.9	11.45	936.7	1226.37	41.95	703.33	806.31
D5 1.27m	217	955.95	1261.02	12.45	1000.19	1340.65	50.95	732.96	859.64
C6 1.34m	138	941.71	1235.4	11.95	987.66	1318.09	53.45	722.83	841.4
D5 1.37m	218	975.46	1296.14	12.45	1022.11	1380.11	56.95	711.68	821.34
C6 1.39m	139	947	1244.91	12.95	992.4	1326.64	57.45	715.61	828.41
D5 1.45m	219	986.67	1316.31	12.95	1034.99	1403.29	58.45	741.62	875.23
C6 1.47m	140	958.59	1265.77	11.95	1006.99	1352.89	60.95	695.89	792.92
D5 1.52m	220	997.15	1335.19	13.95	1046.99	1424.9	63.45	726.71	848.38
C6 1.62m	141	976.4	1297.83	16.95	1029.64	1393.66	67.45	745.49	882.2
D5 1.68m	221	1015.78	1368.72	16.95	1071.85	1469.64	69.95	761.61	911.22
D5 1.78m	222	999.97	1340.26	11.95	1050.55	1431.31	76.45	709.52	817.45
D5 1.85m	223	1027.87	1390.48	11.95	1080.33	1484.91	79.95	686.82	776.58
C6 1.87m	142	1004.53	1348.47	12.45	1059.96	1448.24	81.45	694.05	789.6
D5 1.90m	224	1036.01	1405.12	11.95	1090.93	1503.98	80.95	699.39	799.21
C6 1.95m	144	1014.25	1365.97	12.45	1071.42	1468.87	85.45	697.64	796.07
C3 2.17m	178	1043.89	1419.32	11.45	1100.79	1521.74	101.45	678.35	761.35
D4 2.24m	241	1088.94	1500.41	11.45	1143.63	1598.85	105.95	649.58	709.56
D4 2.32m	242	1098.18	1517.04	11.45	1157.73	1624.22	111.45	672.08	750.06
C3 2.35m	180	1088.56	1499.72	11.95	1151.25	1612.56	113.95	675.35	755.94
D4 2.37m	243	1105.56	1530.32	11.95	1166.57	1640.14	115.45	676.65	758.28
C3 2.40m	181	1091.48	1504.98	11.95	1154.94	1619.2	118.95	663.52	734.64
D4 2.54m	245	1131.28	1576.61	11.45	1192.05	1686	131.45	678.83	762.21
D6 2.62m	129	1121.02	1558.15	11.45	1183.81	1671.16	137.95	688.59	779.77
D6 2.69m	130	1121.34	1558.72	11.45	1185.52	1674.25	147.95	675.32	755.88
C3 2.76m	183	1120.45	1557.13	11.95	1184.63	1672.64	156.95	679.92	764.17
D4 2.79m	247	1095.3	1511.86	10.45	1155.74	1620.64	160.45	688.77	780.1
D6 2.87m	131	1063.49	1454.6	10.45	1121.96	1559.83	167.95	634.13	681.75
D6 2.92m	132	1037.93	1408.58	11.95	1102.15	1524.18	173.95	642.68	697.13
D6 2.97m	133	1009.1	1356.69	11.95	1070.17	1466.62	179.95	631.76	677.47
D6 3.07m	134	972.34	1290.53	12.45	1029.17	1392.82	187.45	633.29	680.23
E3 3.12m	197	978.47	1301.55	11.95	1034.49	1402.4	193.45	615.77	648.7
D6 3.17m	135	937.94	1228.6	12.45	990.68	1323.54	195.95	628.87	672.28
D6 3.27m	136	893.11	1147.91	12.45	944.36	1240.16	204.45	622.53	660.87
D4 3.61m	248	681.06	766.21	12.95	736.52	866.05	165.45	482.08	408.06

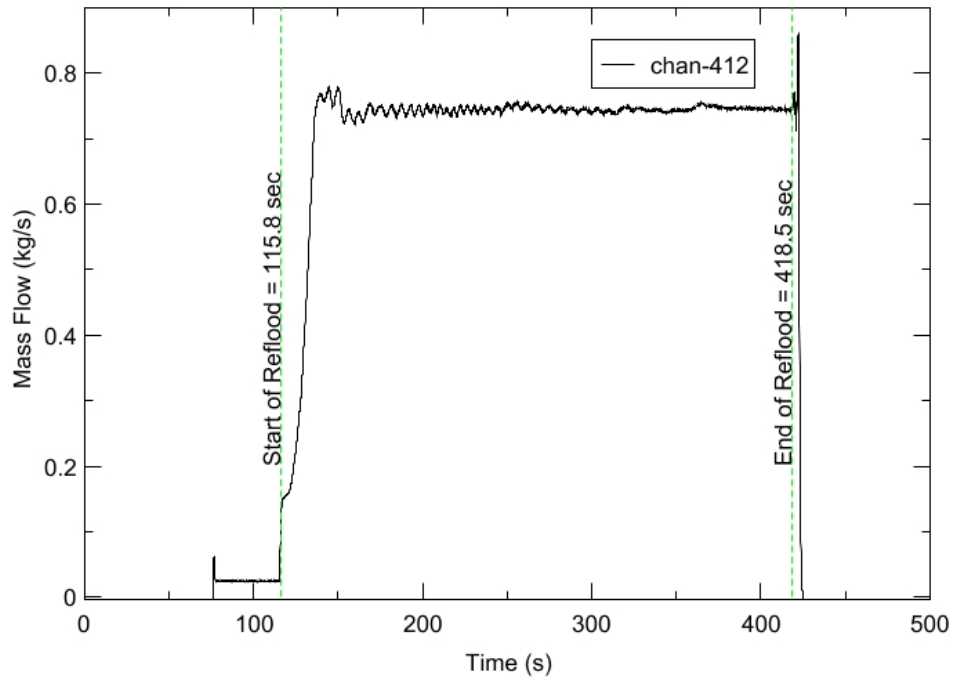
RBHT - TEST FACILITY

Upper Plenum Pressure vs. Time, Exp 1285



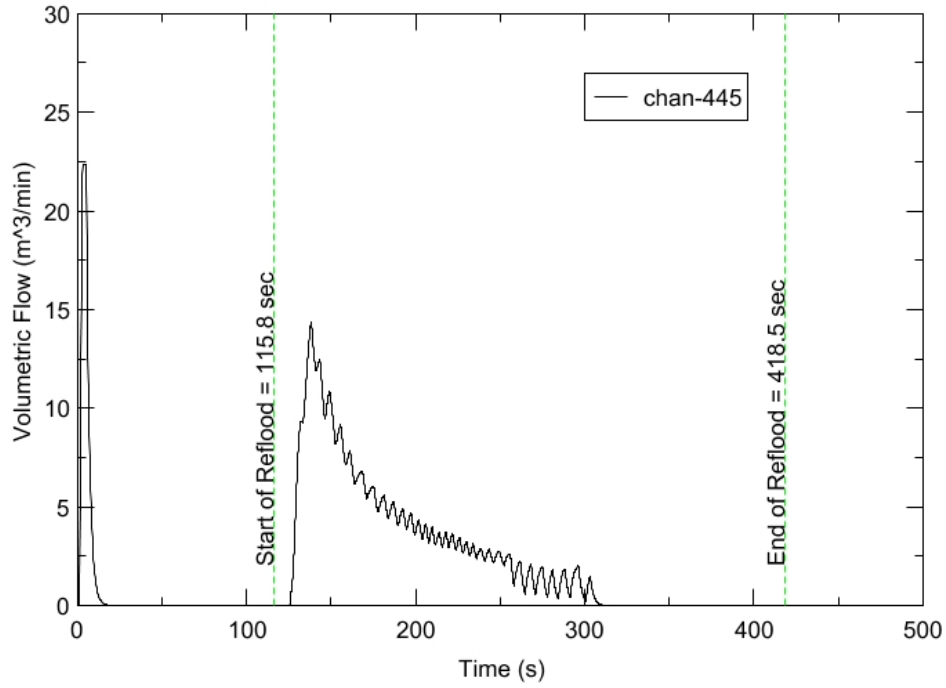
RBHT - TEST FACILITY

Inlet Flow vs. Time, Exp 1285



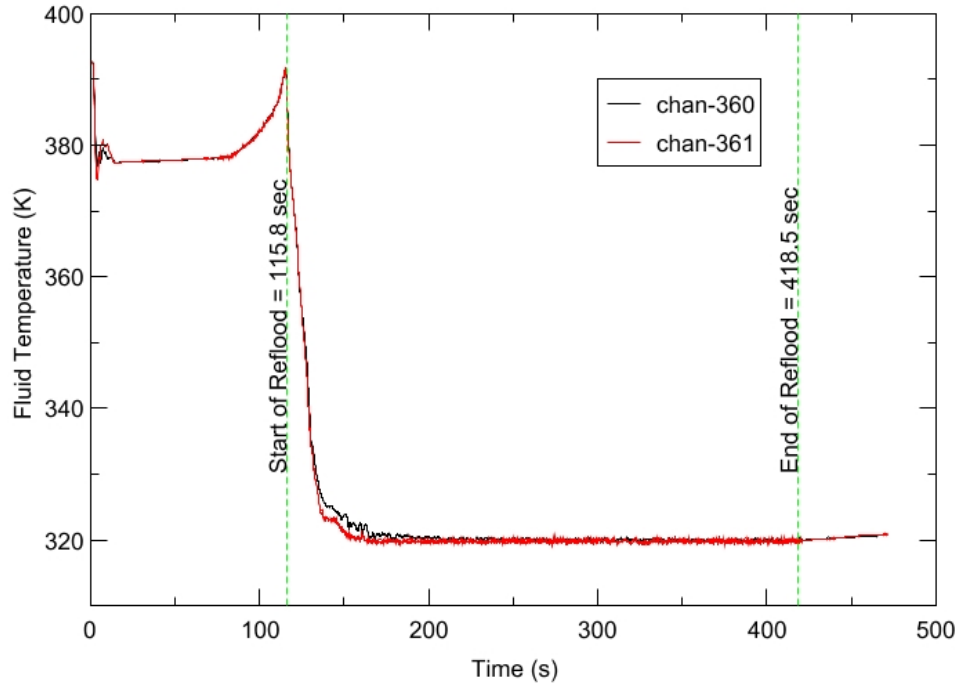
RBHT - TEST FACILITY

Steam Exhaust Flow vs. Time, Exp 1285



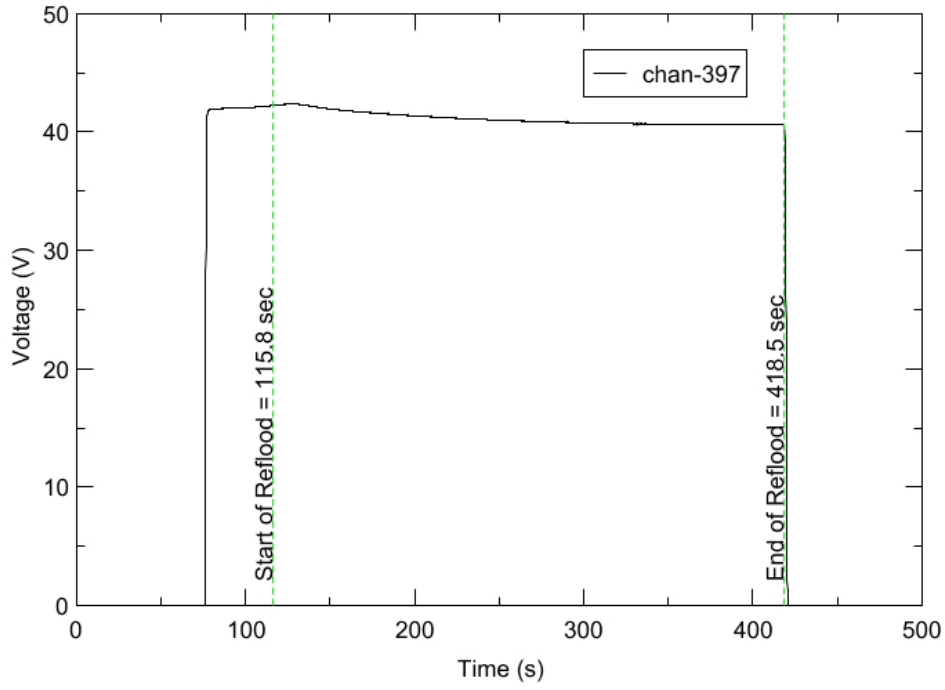
RBHT - TEST FACILITY

Inlet Flow Temperature vs. Time, Exp 1285



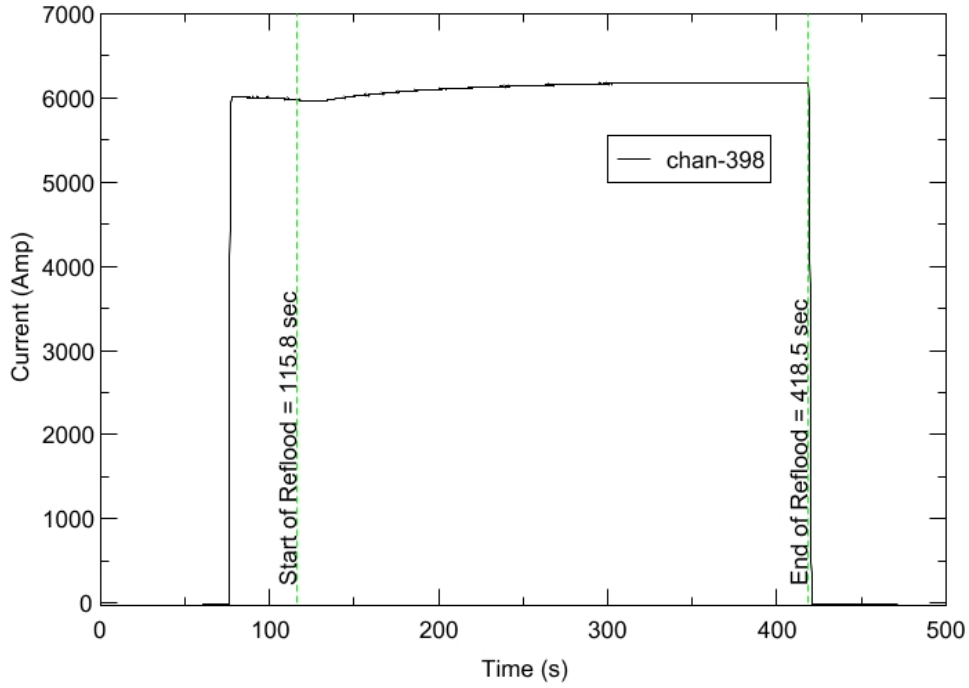
RBHT - TEST FACILITY

Test Section Voltage vs. Time, Exp 1285

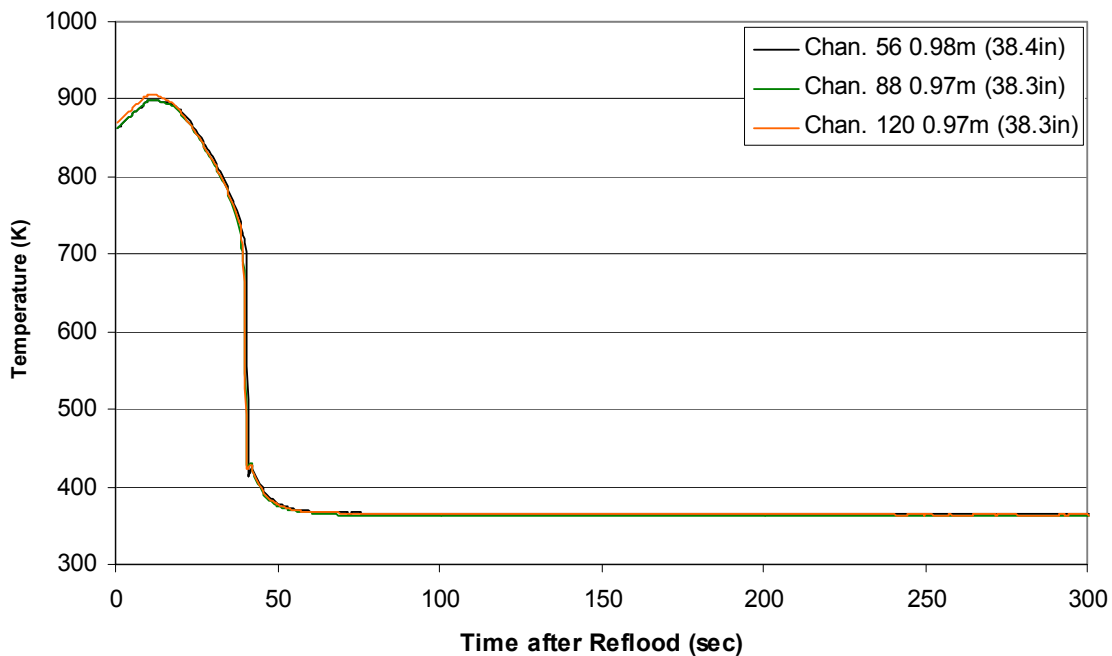


RBHT - TEST FACILITY

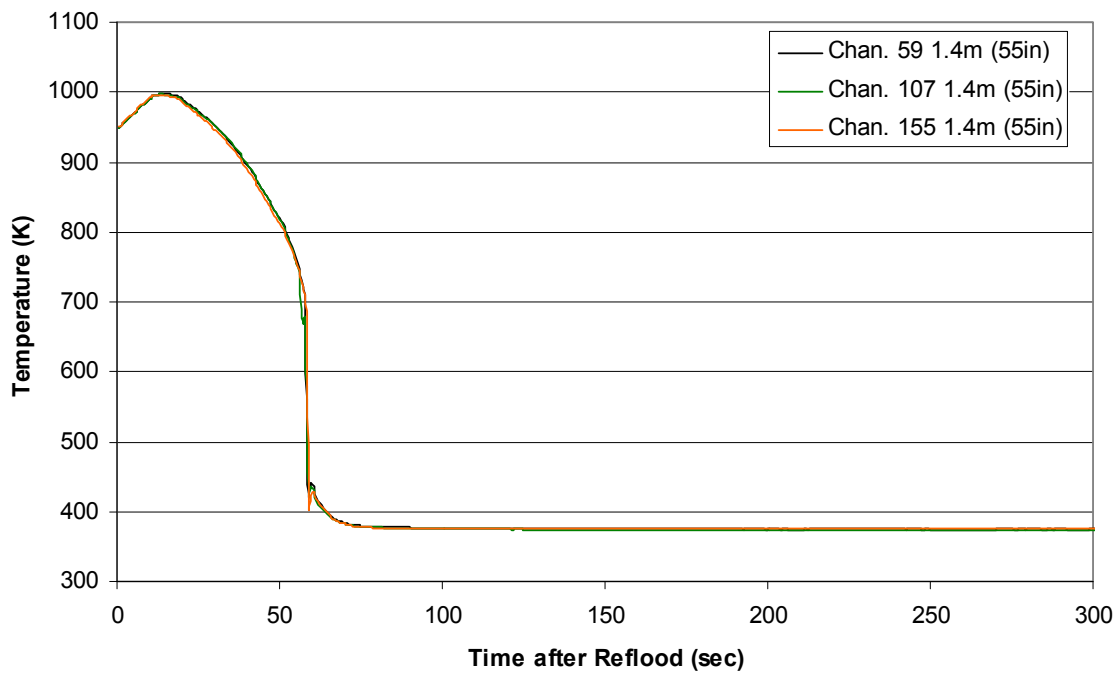
Test Section Current vs. Time, Exp 1285



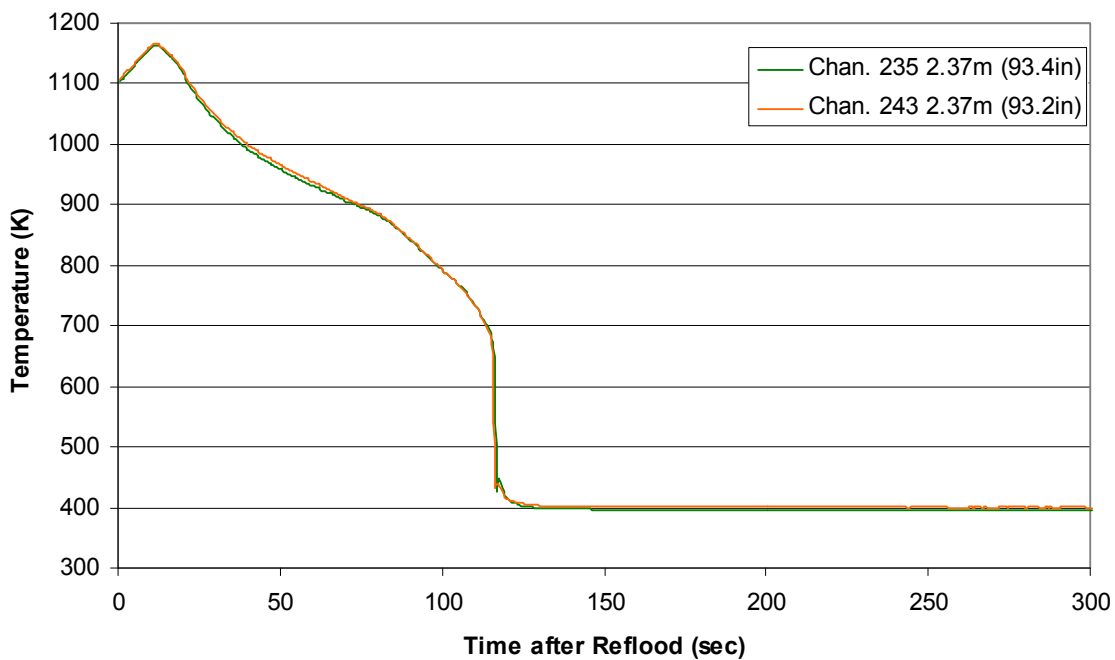
Heater Rod Temperature during Reflood RBHT Exp. 1285



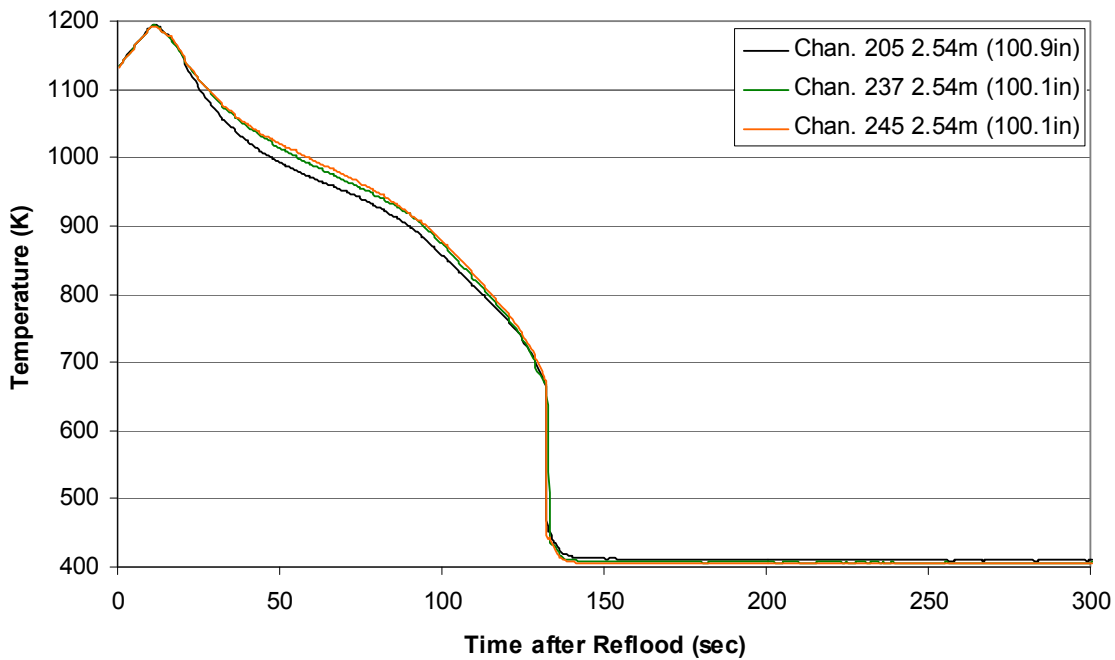
Heater Rod Temperature during Reflood RBHT Exp. 1285



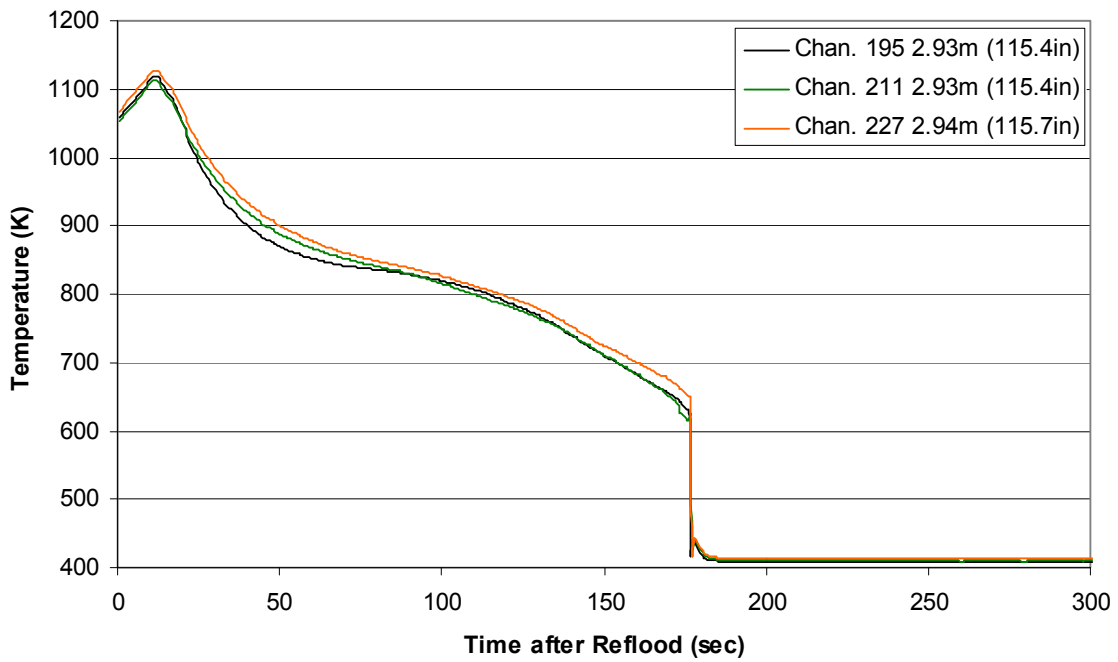
**Heater Rod Temperature during Reflood
RBHT Exp. 1285**



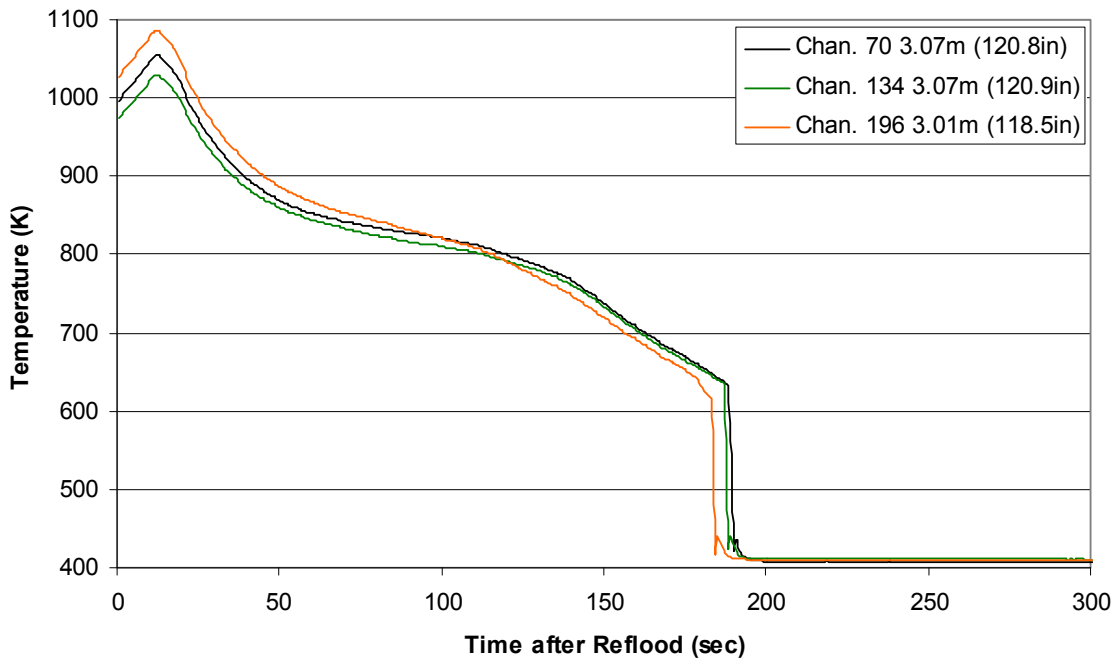
**Heater Rod Temperature during Reflood
RBHT Exp. 1285**



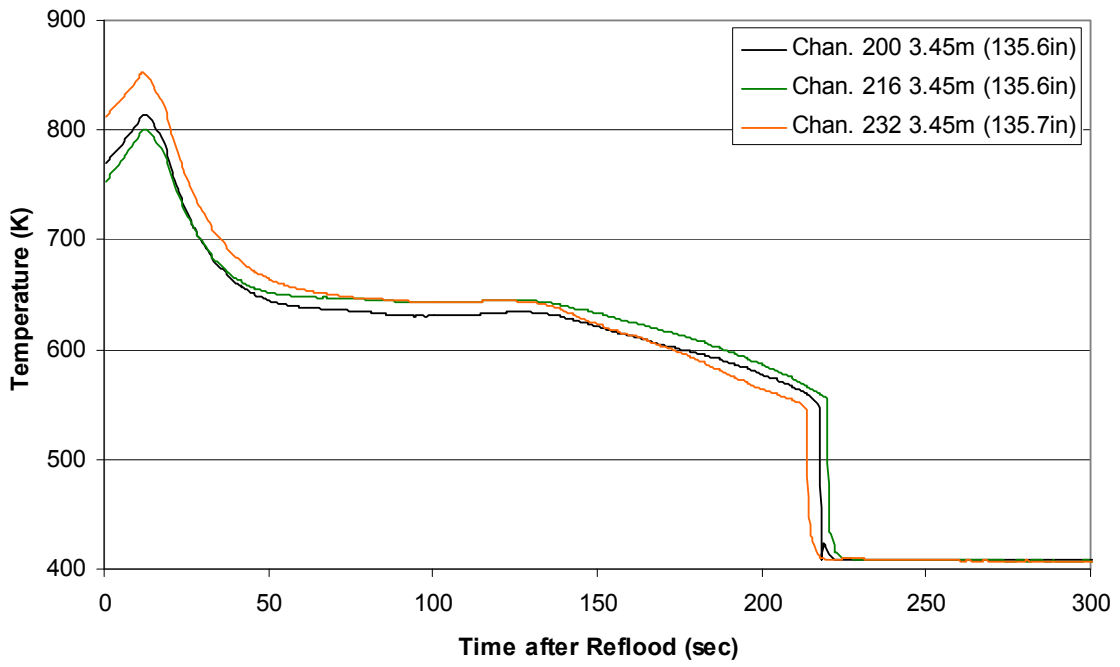
Heater Rod Temperature during Reflood RBHT Exp. 1285



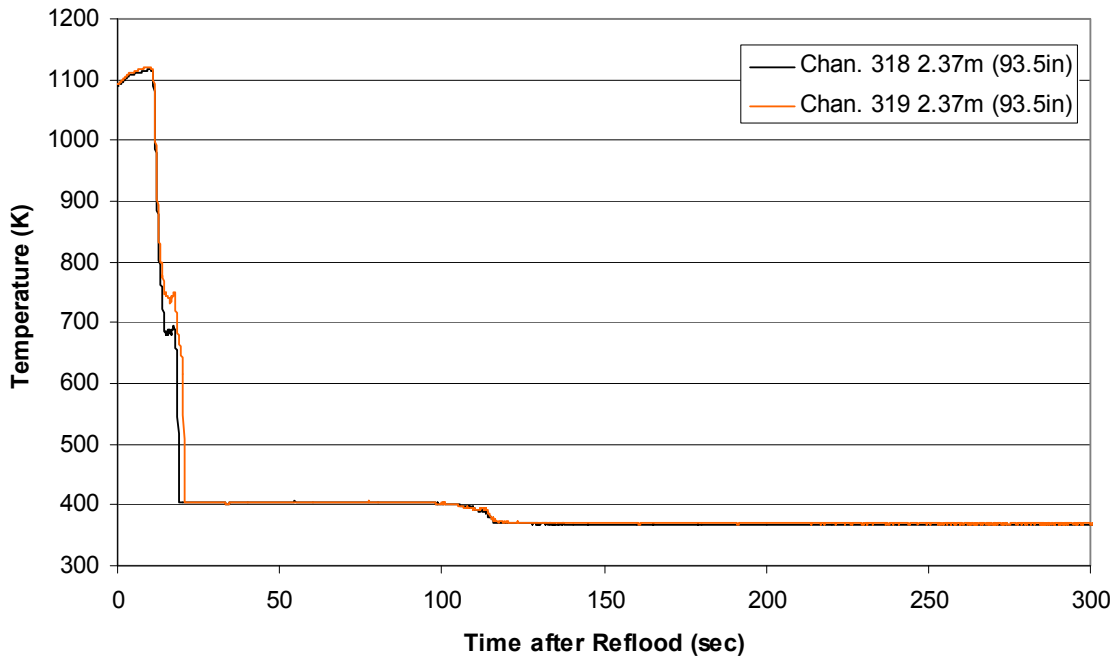
Heater Rod Temperature during Reflood RBHT Exp. 1285



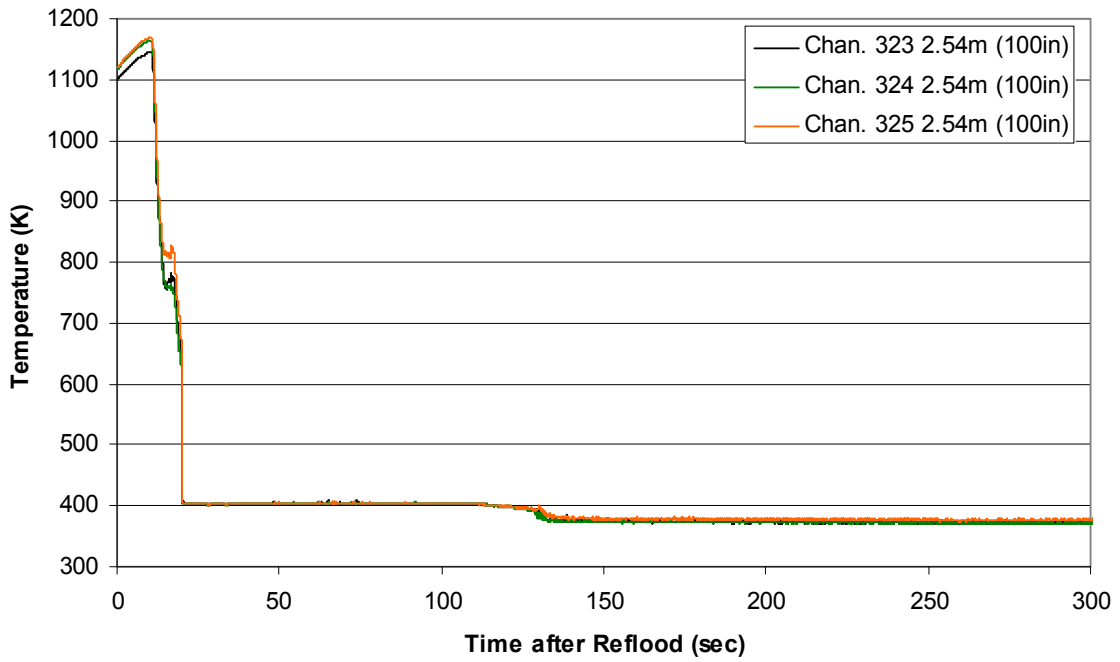
Heater Rod Temperature during Reflood RBHT Exp. 1285



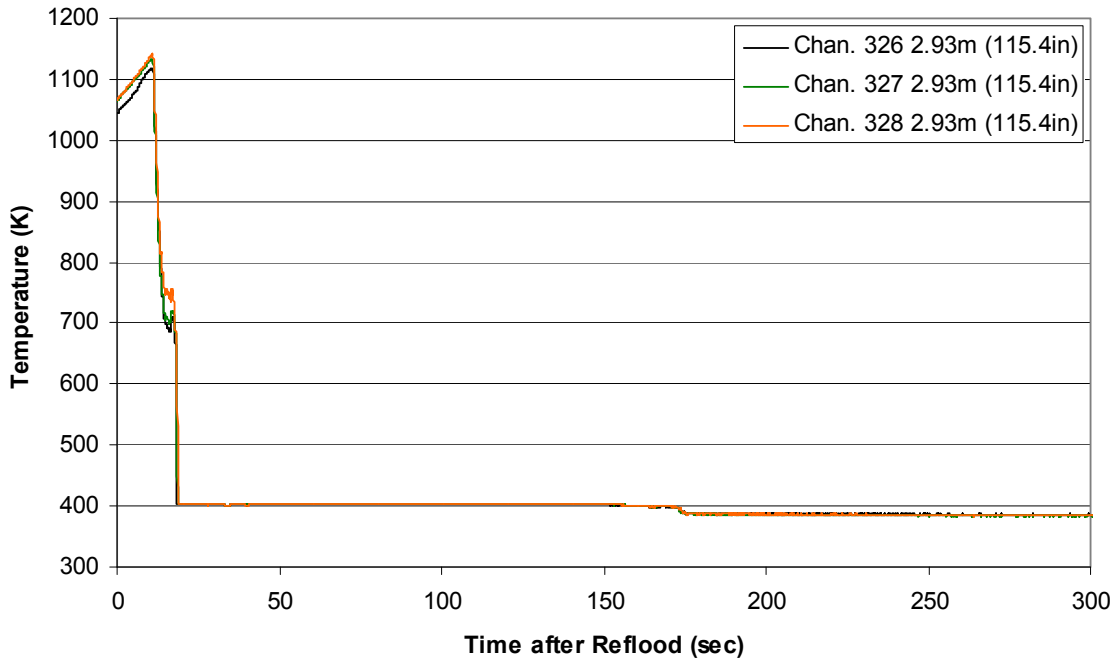
Steam Probe Temperature during Reflood RBHT Exp. 1285



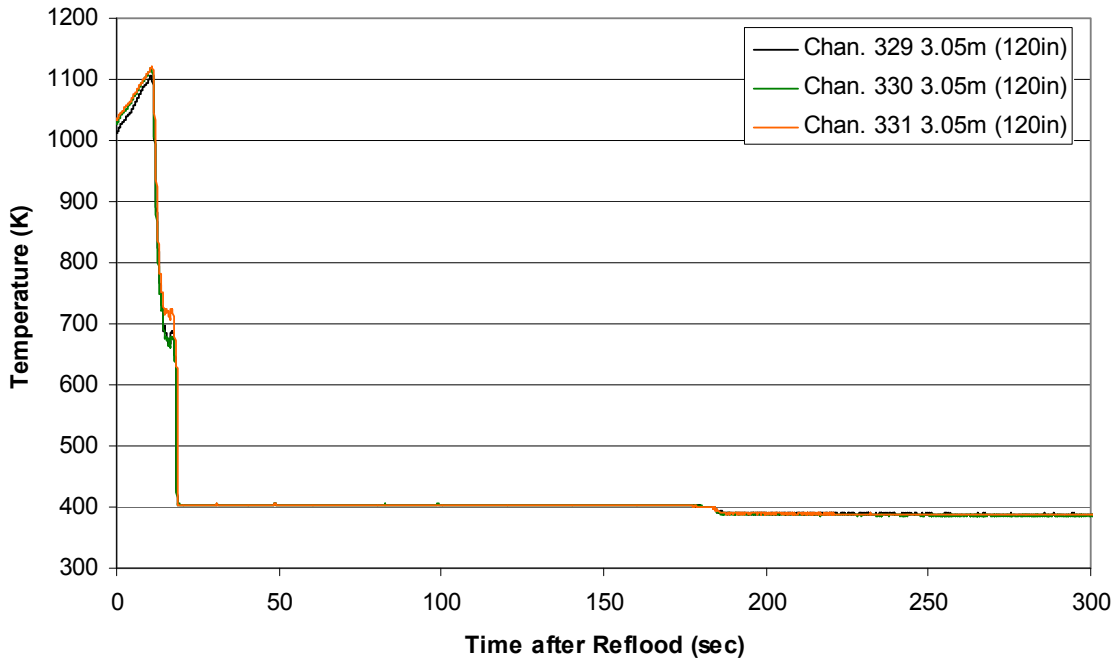
Steam Probe Temperature during Reflood RBHT Exp. 1285



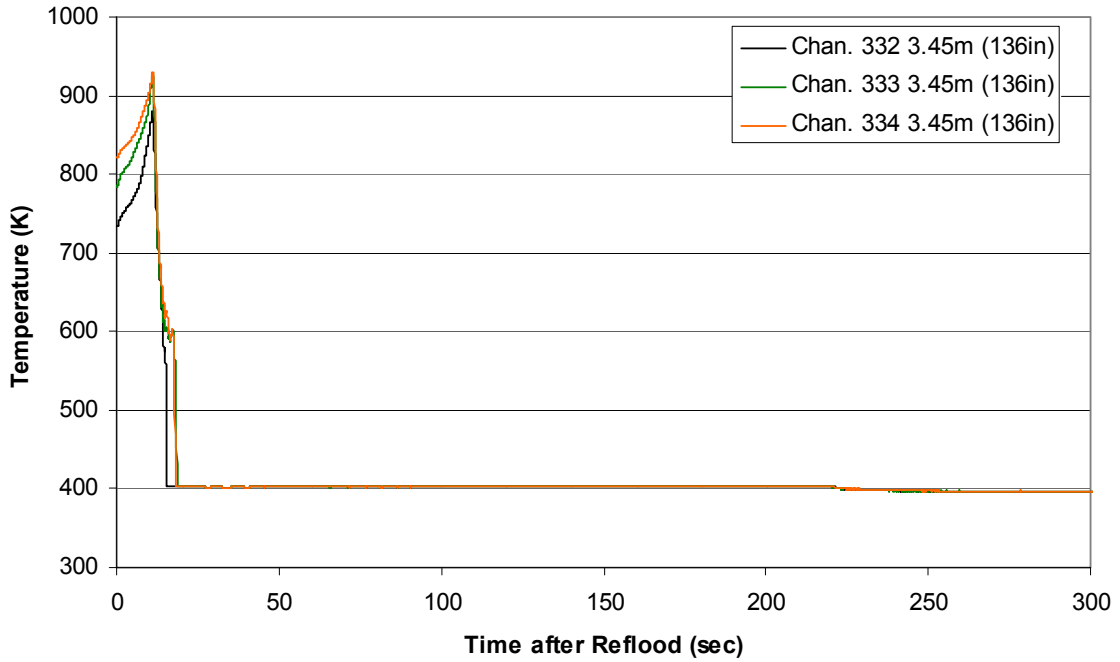
Steam Probe Temperature during Reflood RBHT Exp. 1285



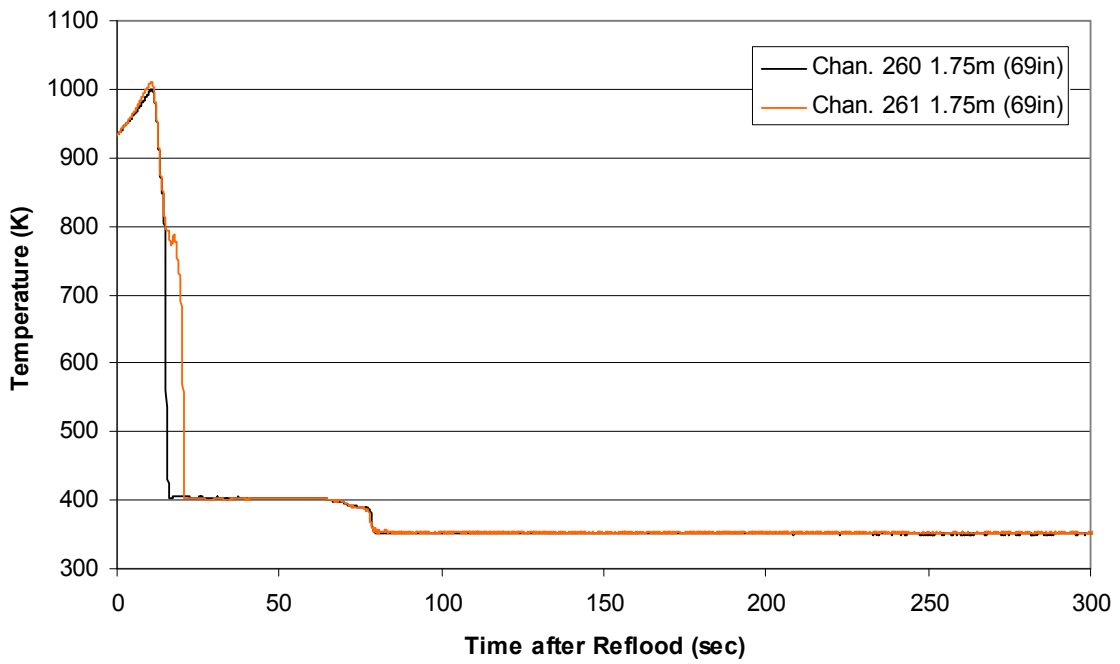
Steam Probe Temperature during Reflood
RBHT Exp. 1285



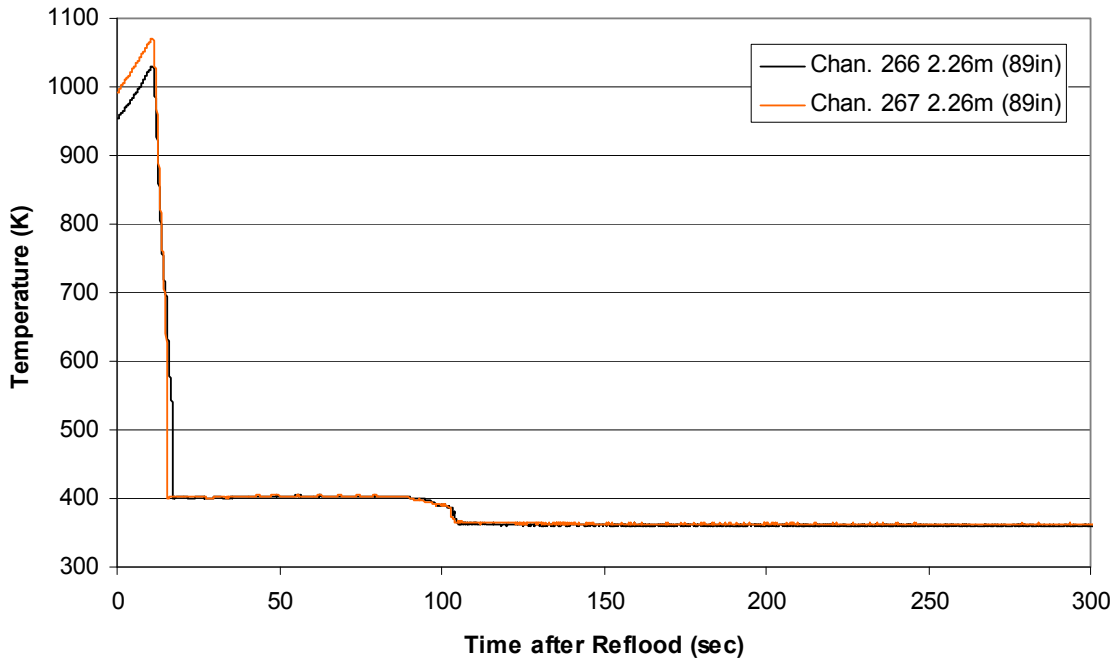
Steam Probe Temperature during Reflood
RBHT Exp. 1285



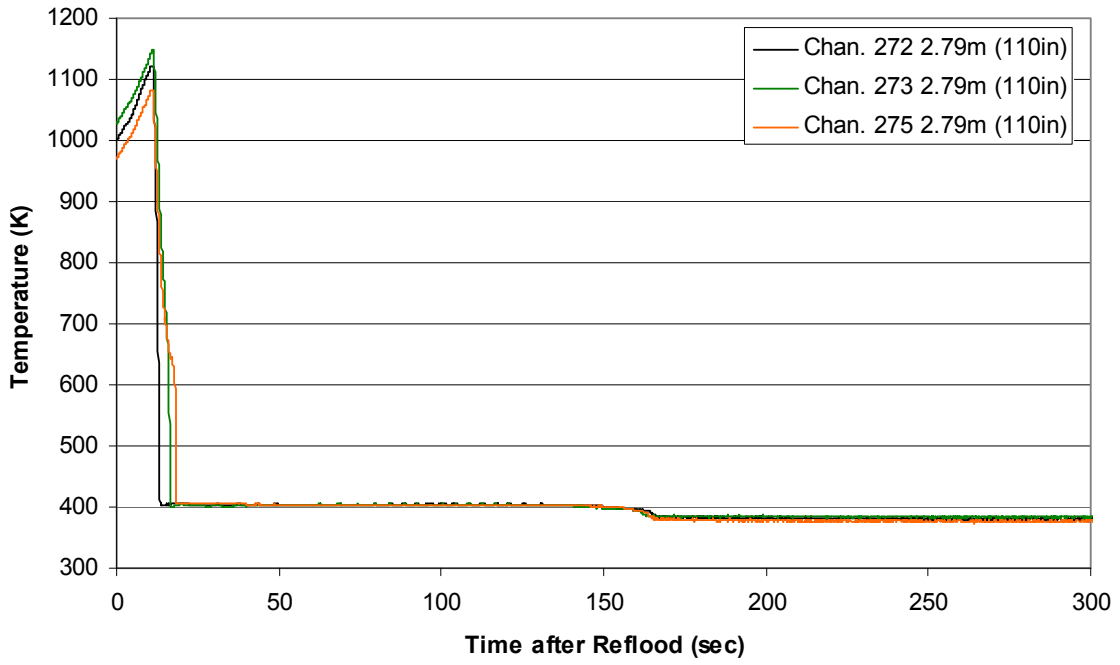
Spacer Grid Temperature during Reflood RBHT Exp. 1285



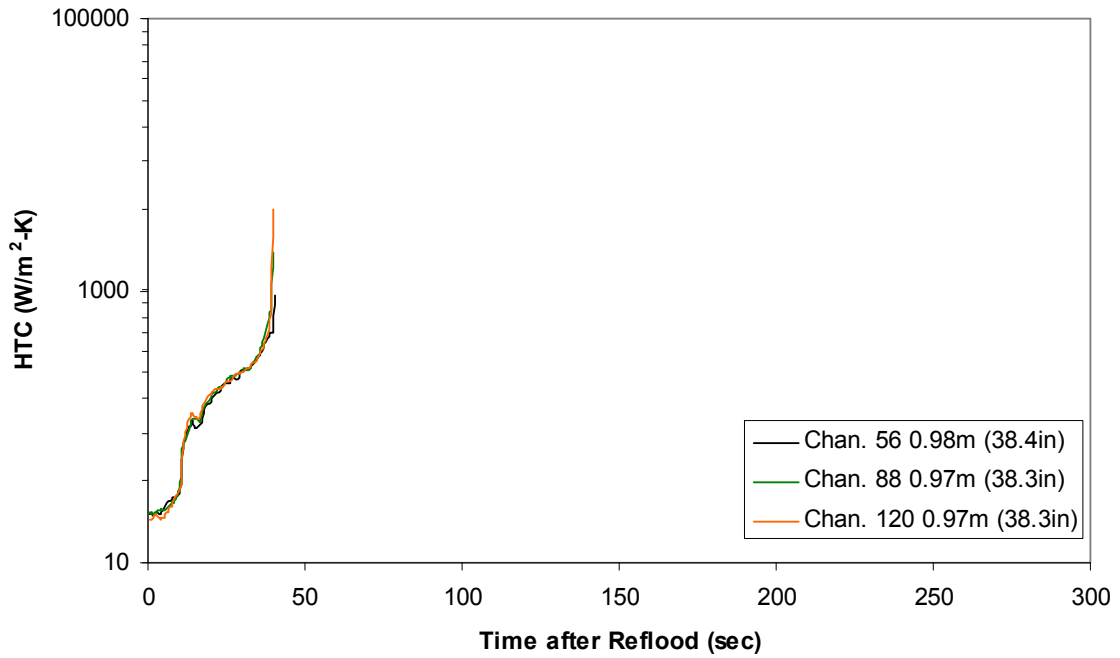
Spacer Grid Temperature during Reflood RBHT Exp. 1285



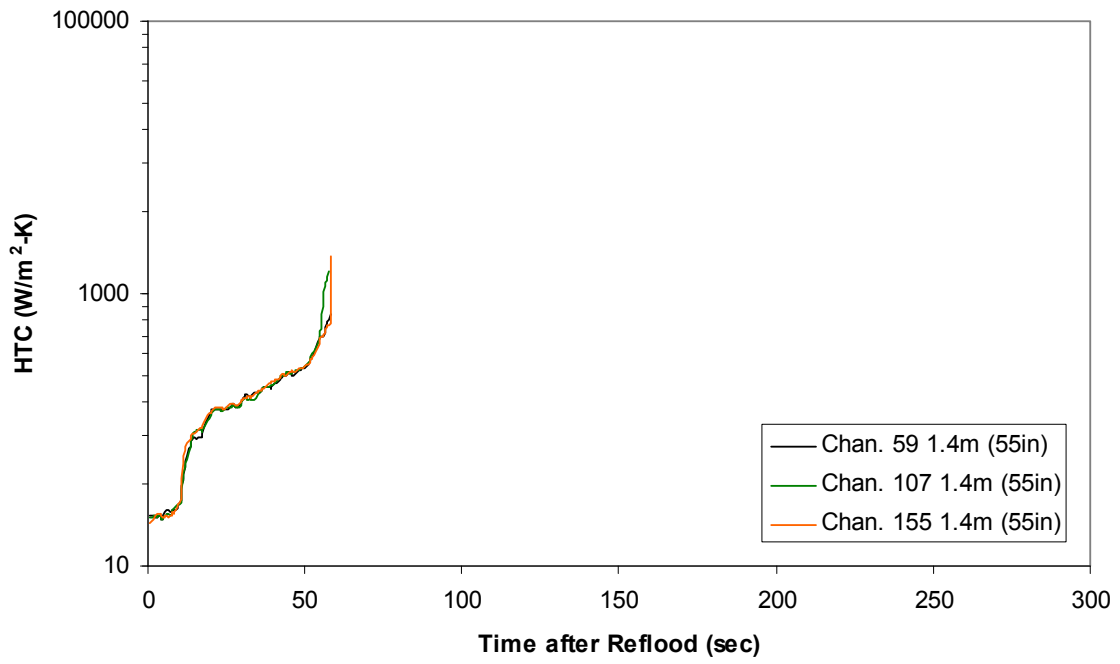
Spacer Grid Temperature during Reflood RBHT Exp. 1285



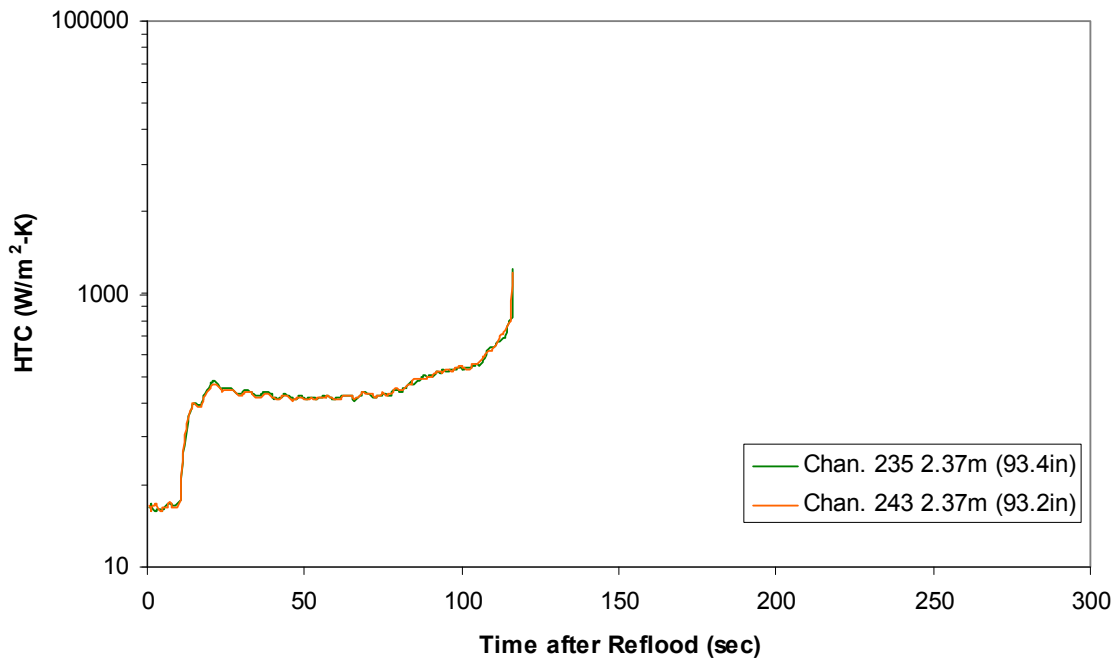
Heat Transfer Coefficient during Reflood RBHT Exp. 1285



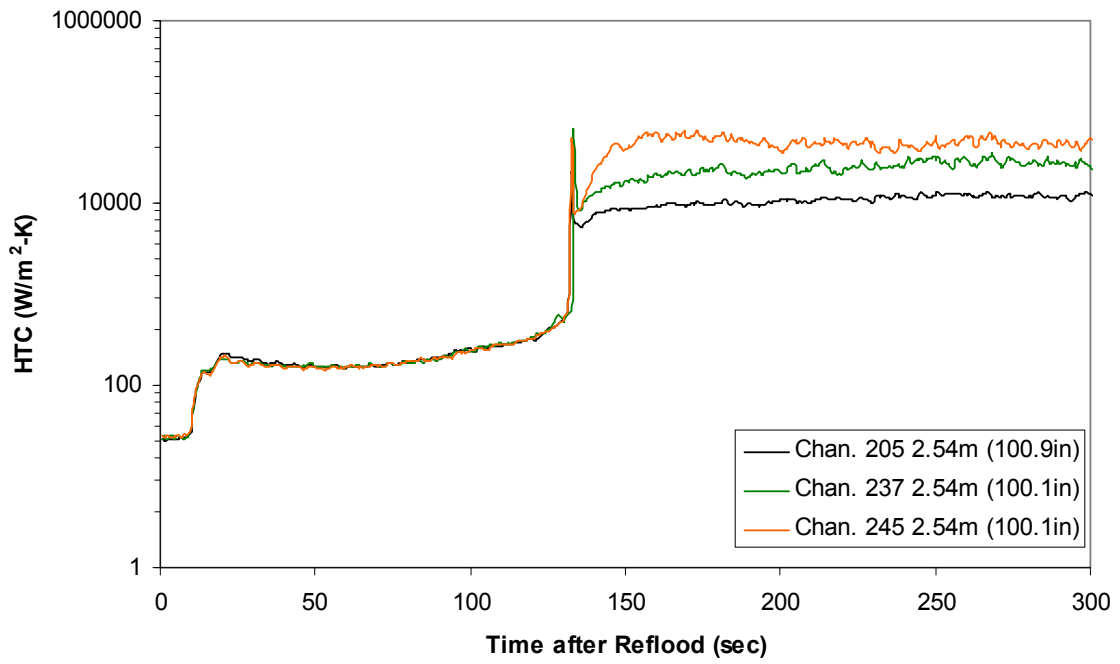
Heat Transfer Coefficient during Reflood RBHT Exp. 1285



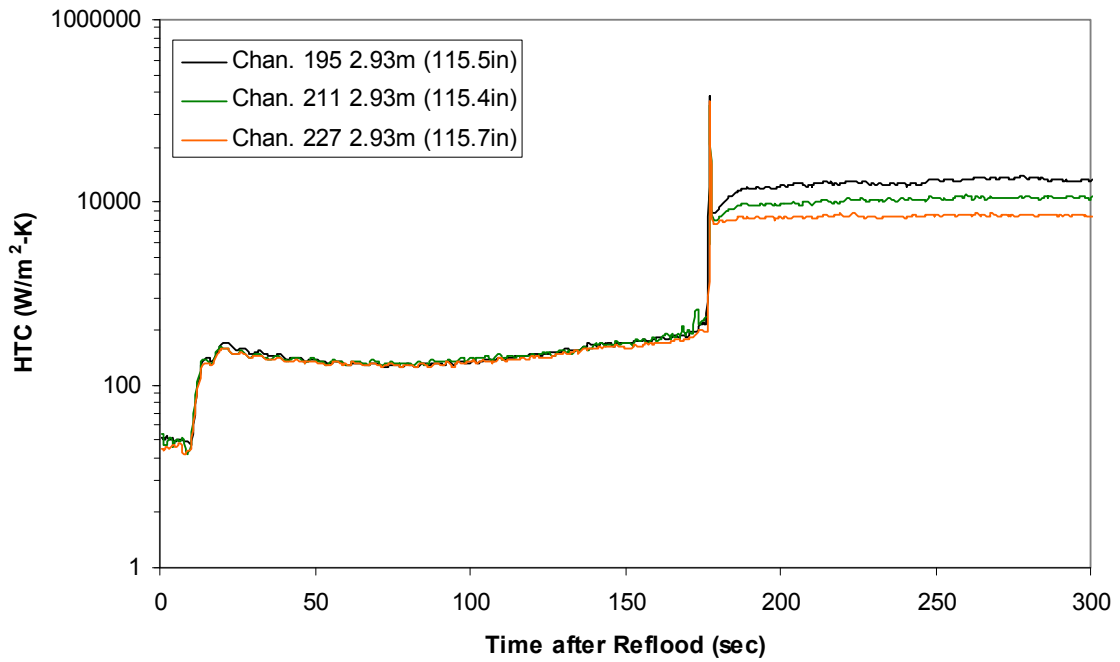
Heat Transfer Coefficient during Reflood RBHT Exp. 1285



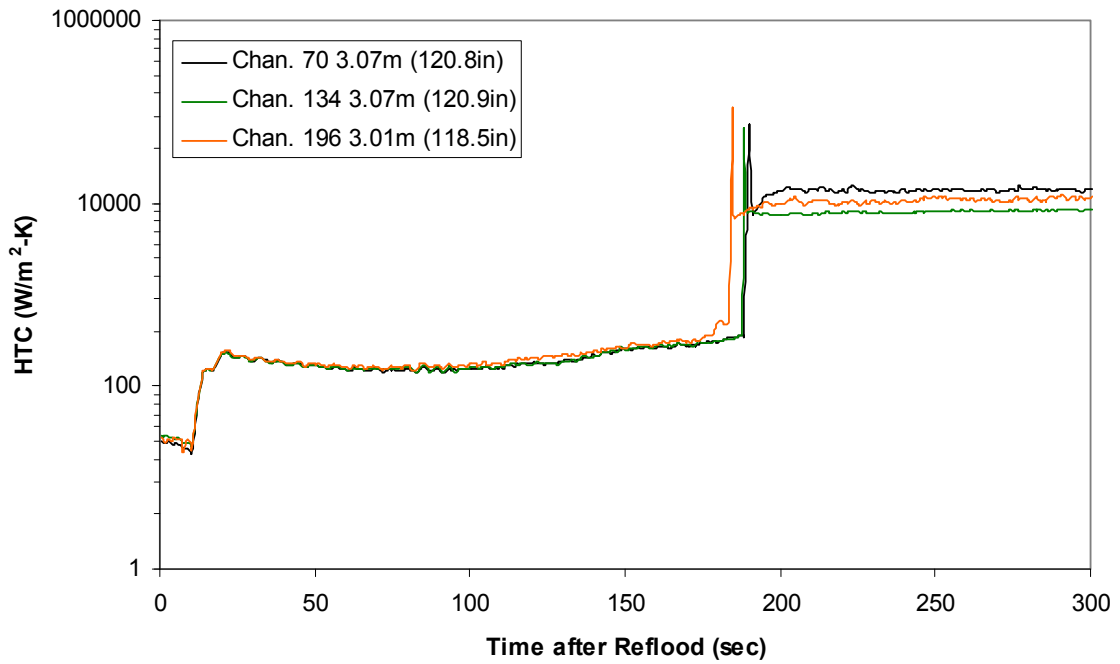
Heat Transfer Coefficient during Reflood RBHT Exp. 1285



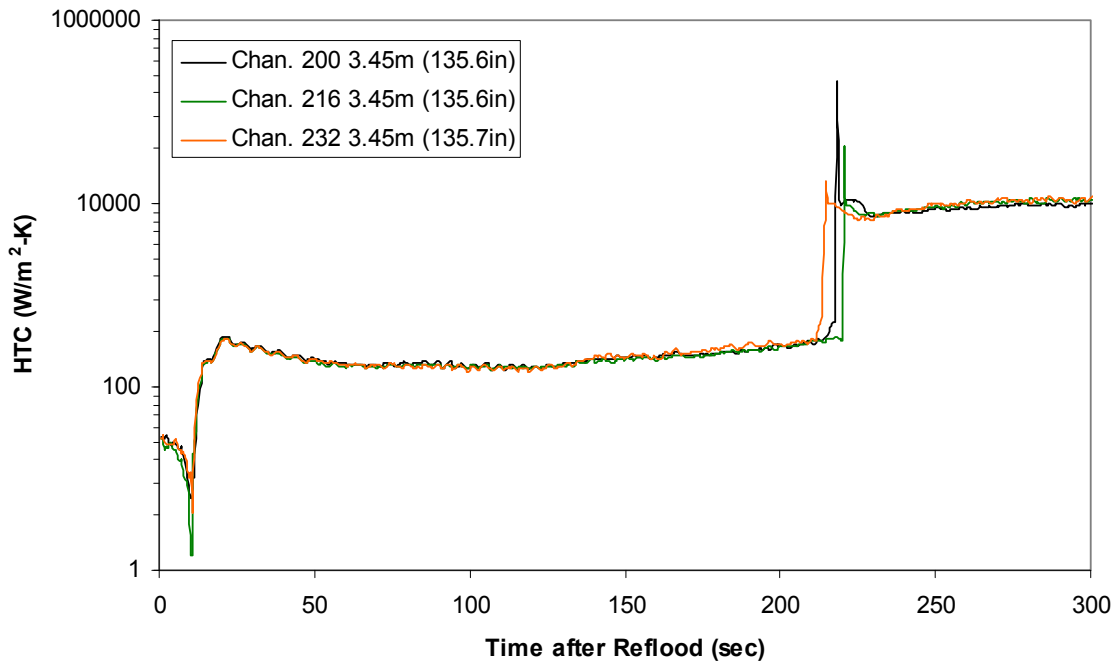
Heat Transfer Coefficient during Reflood RBHT Exp. 1285



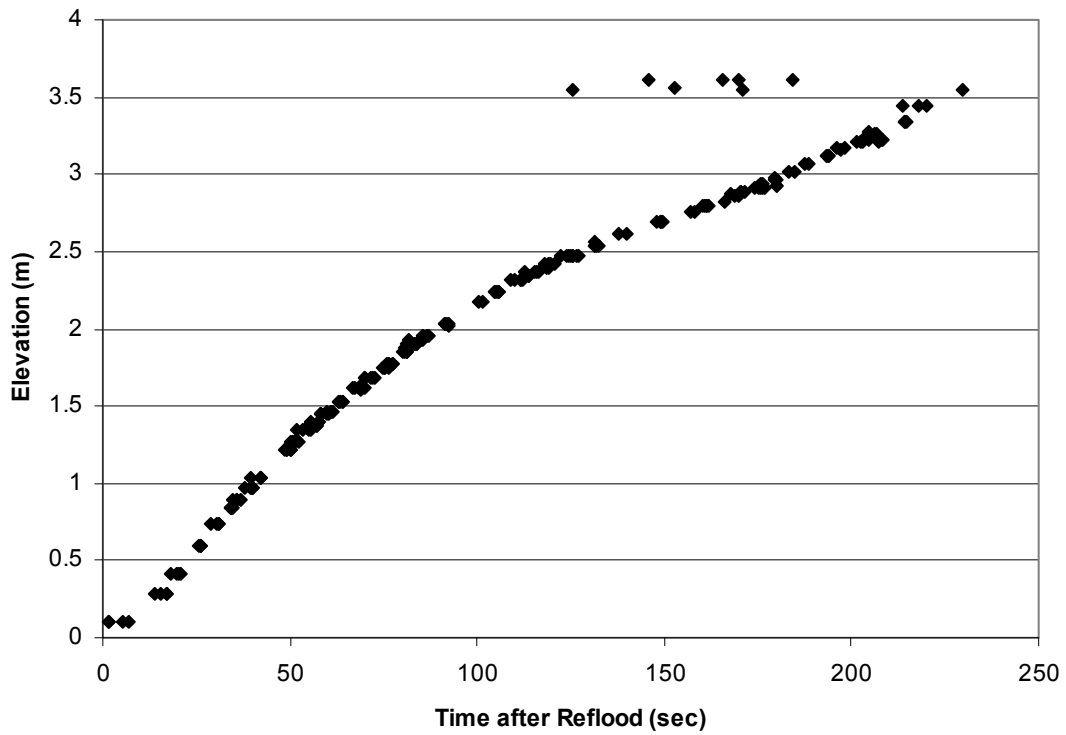
Heat Transfer Coefficient during Reflood RBHT Exp. 1285



Heat Transfer Coefficient during Reflood RBHT Exp. 1285



Quench Data, RBHT Exp. 1285



RBHT - REFLOOD TESTS

SUMMARY SHEET

RUN NO: **1291**

RUN CONDITIONS

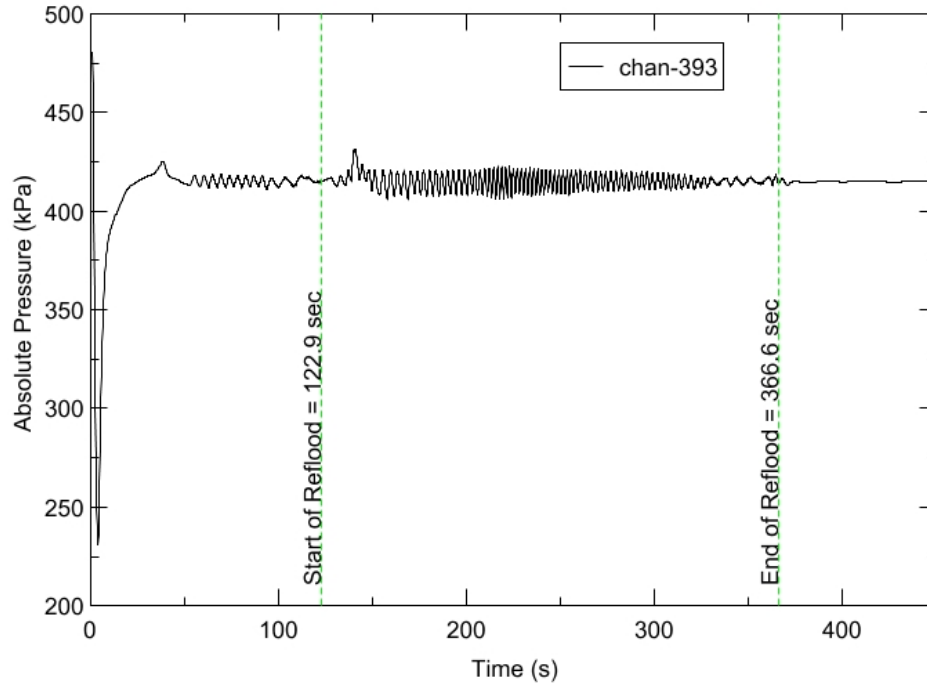
Upper Plenum Pressure:	414 kPa (60 psia)
Initial Peak Clad Temperature:	1144 degrees K (1600 degrees F)
Rod Peak Power:	2.3 kW/m (0.7 kW/ft)
Flooding Rate:	0.1524 m/s (6 in/s)
Inlet Subcooling:	83 degrees K (150 degrees F)
Start of Reflood:	122.9 s
End of Reflood:	366.6 s
Test Date:	7/19/2002
Comments:	No droplet data

Heater rod surfaces below 2.54 m (100 in) quench to a temperature below saturation due to the high inlet subcooling. Therefore DATARH calculated heat transfer coefficients are not presented below this elevation after rod quench.

Rod_Elevation	Channel Number	Temperature at Reflood (K)	Temperature at Reflood (°F)	Turnaround Time (sec.)	Turnaround Temperature (K)	Turnaround Temperature (°F)	Quench Time (sec.)	Quench Temperature (K)	Quench Temperature (°F)
B6_0.592m	148	785.7	954.57	15.35	836.5	1046.01	37.85	678.91	762.35
B6_0.744m	149	823.47	1022.57	16.35	875.58	1116.36	43.35	674.31	754.07
B6_0.846m	150	851.55	1073.11	16.35	906.96	1172.83	47.35	688.13	778.94
B6_0.897m	151	861.61	1091.22	16.35	918.48	1193.57	49.85	675.67	756.51
C6_1.04m	137	901.29	1162.64	16.85	963.08	1273.86	55.35	680.38	764.99
D5_1.27m	217	966.44	1279.91	16.35	1032.63	1399.05	63.85	688.34	779.32
C6_1.34m	138	960.15	1268.58	16.85	1029.15	1392.77	64.35	716.67	830.32
D5_1.37m	218	987.96	1318.64	16.85	1057.88	1444.49	69.35	681.26	766.58
C6_1.39m	139	964.86	1277.05	16.85	1034.54	1402.49	69.35	694.19	789.85
D5_1.45m	219	999.31	1339.07	16.85	1071.17	1468.42	72.35	678.56	761.72
C6_1.47m	140	974.98	1295.28	16.85	1046.24	1423.55	72.35	681.62	767.22
D5_1.52m	220	1008.8	1356.14	17.35	1082.52	1488.84	75.35	688.46	779.54
C6_1.62m	141	990.25	1322.77	17.35	1066.17	1459.41	79.35	696.17	793.42
D5_1.68m	221	1022.5	1380.81	17.35	1101.08	1522.25	82.85	685.51	774.23
D5_1.78m	222	992.07	1326.04	16.85	1067.01	1460.92	87.85	667.22	741.3
D5_1.85m	223	1041.77	1415.49	16.35	1119.47	1555.36	91.35	636.41	685.84
C6_1.87m	142	1025.47	1386.16	16.85	1105.47	1530.16	91.35	663.49	734.59
D5_1.90m	224	1052.66	1435.09	16.85	1133.56	1580.71	89.35	676.34	757.72
C6_1.95m	144	1036.61	1406.22	16.85	1119.18	1554.83	93.85	684.84	773.02
C3_2.17m	178	1047.06	1425.02	16.85	1134.7	1582.77	110.85	648.75	708.06
D4_2.24m	241	1106.66	1532.29	16.35	1190.84	1683.82	113.35	630.47	675.16
D4_2.32m	242	1118.63	1553.84	16.85	1208.25	1715.16	118.85	649.73	709.83
C3_2.35m	180	1112.51	1542.83	16.85	1205.69	1710.56	120.35	650.04	710.39
D4_2.37m	243	1124.22	1563.9	16.85	1215.84	1728.83	121.35	653.23	716.13
C3_2.40m	181	1113.48	1544.57	16.85	1207.51	1713.83	124.35	655.96	721.04
D4_2.54m	245	1142.77	1597.3	16.35	1234.42	1762.27	136.35	652.75	715.26
D6_2.62m	129	1129.04	1572.58	16.35	1224.1	1743.68	141.85	674.54	754.48
D6_2.69m	130	1121.03	1558.16	16.35	1217.67	1732.12	149.35	683.67	770.92
C3_2.76m	183	1109.04	1536.59	16.35	1204.9	1709.14	155.85	683.51	770.63
D6_2.92m	132	1022.77	1381.29	16.85	1113.35	1544.34	169.35	634.79	682.94
D6_2.97m	133	998.9	1338.33	17.35	1084.12	1491.72	173.35	615.64	648.46
D6_3.07m	134	963.19	1274.05	17.35	1041.61	1415.21	177.85	630.13	674.55
E3_3.12m	197	954.41	1258.26	17.35	1034.65	1402.68	182.35	618.33	653.31
D6_3.17m	135	922.01	1199.93	17.35	995.42	1332.07	184.35	629.63	673.64
D6_3.27m	136	852.24	1074.35	17.85	925.98	1207.07	190.35	623.6	662.79
D4_3.61m	248	633.25	680.16	17.85	722.66	841.09	148.85	498.61	437.81

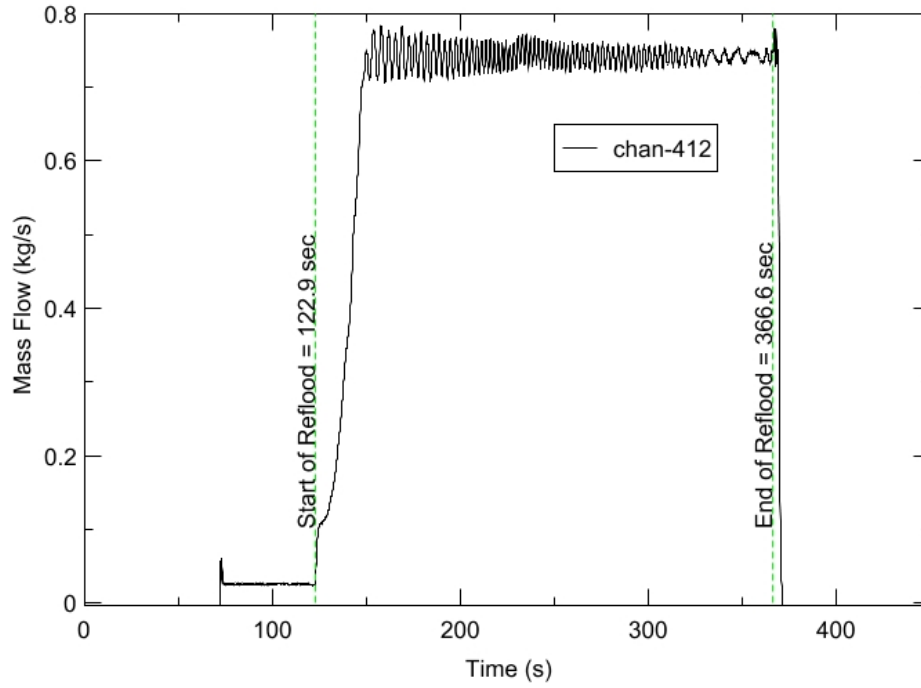
RBHT - TEST FACILITY

Upper Plenum Pressure vs. Time, Exp 1291



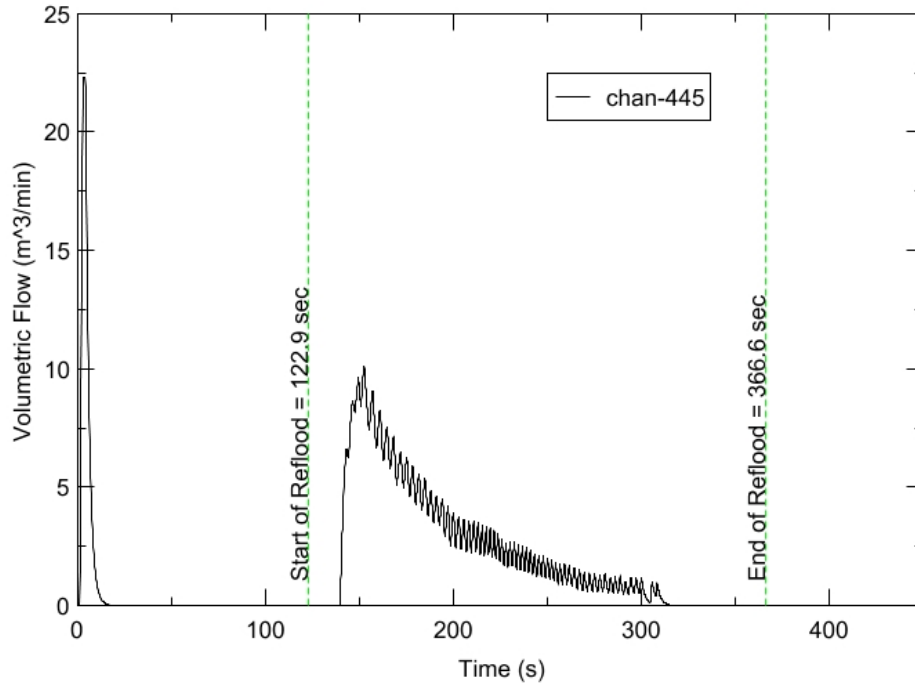
RBHT - TEST FACILITY

Inlet Flow vs. Time, Exp 1291



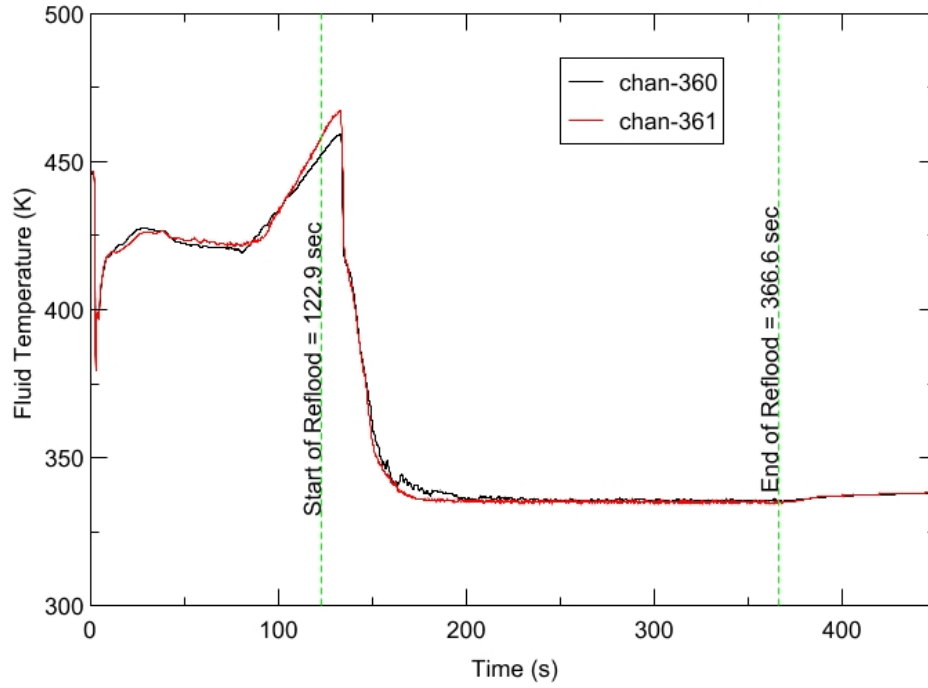
RBHT - TEST FACILITY

Steam Exhaust Flow vs. Time, Exp 1291



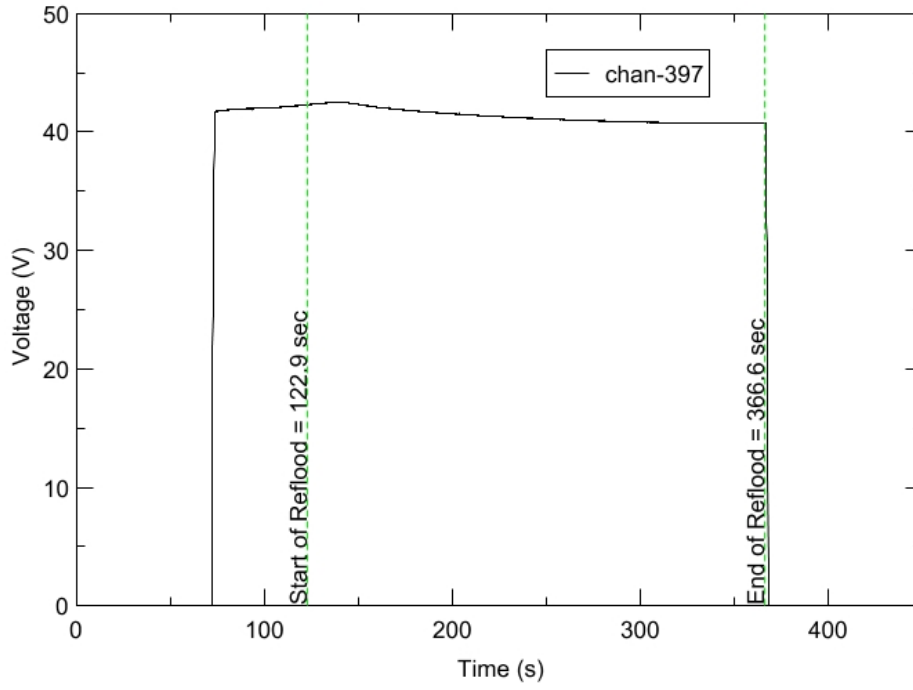
RBHT - TEST FACILITY

Inlet Flow Temperature vs. Time, Exp 1291



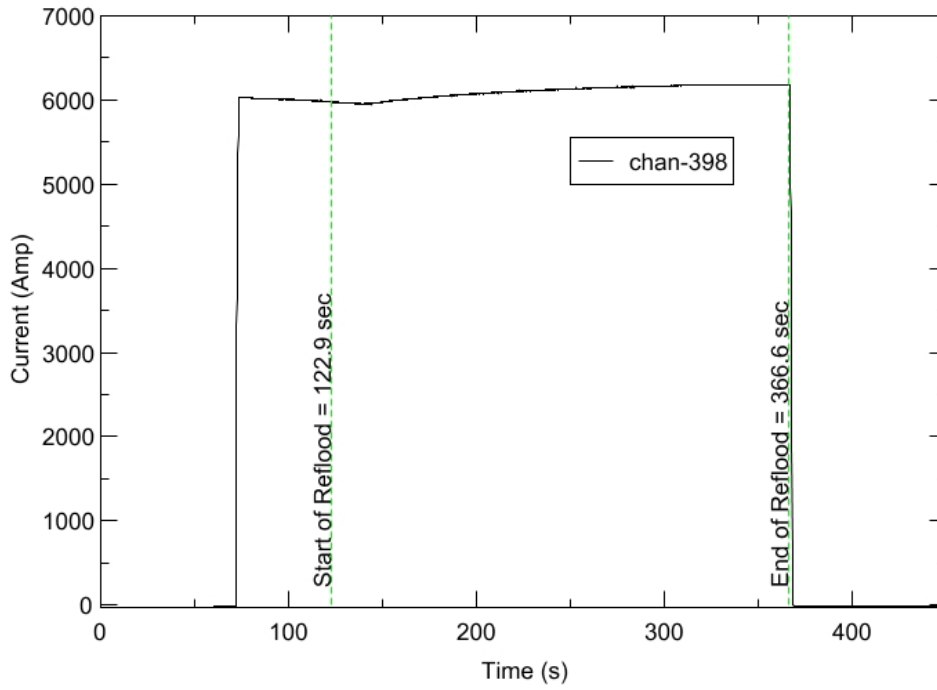
RBHT - TEST FACILITY

Test Section Voltage vs. Time, Exp 1291

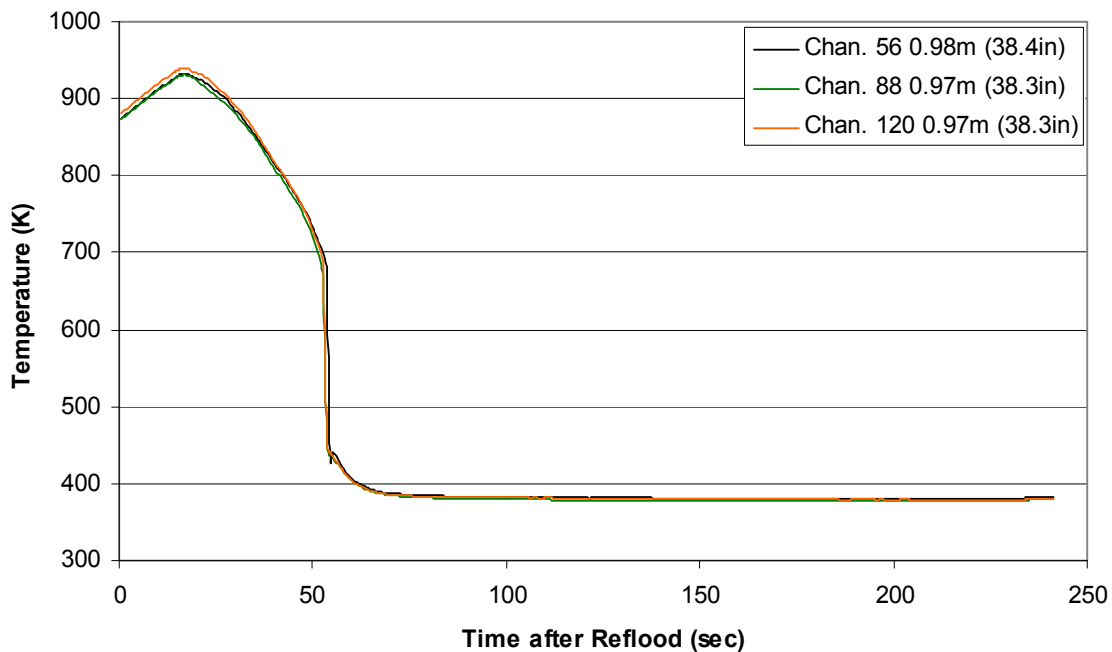


RBHT - TEST FACILITY

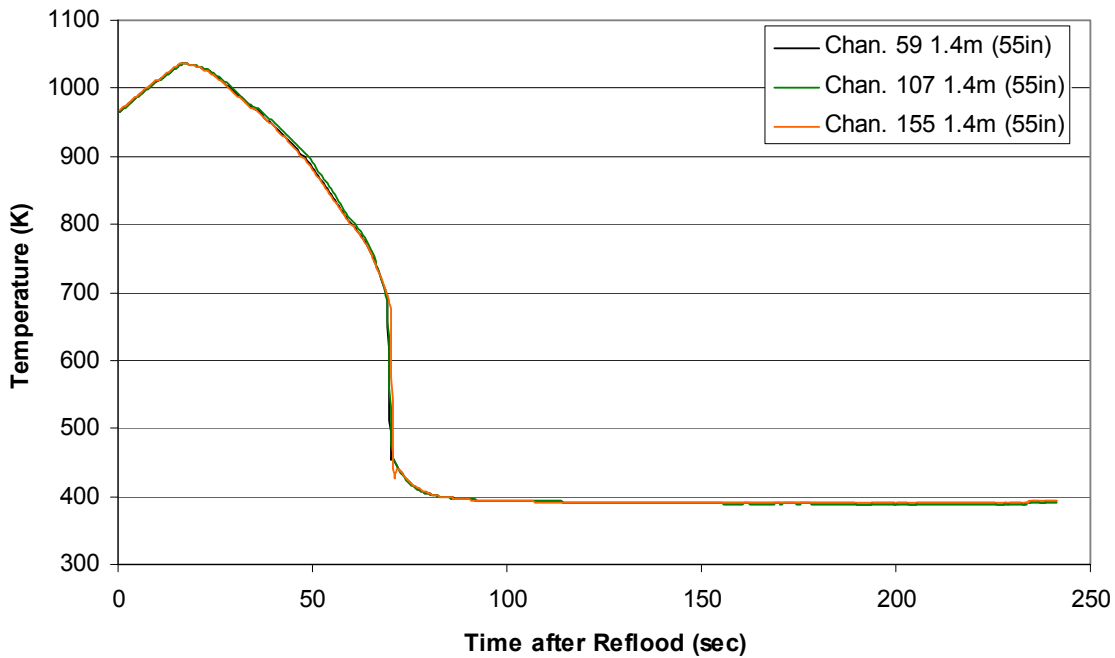
Test Section Current vs. Time, Exp 1291



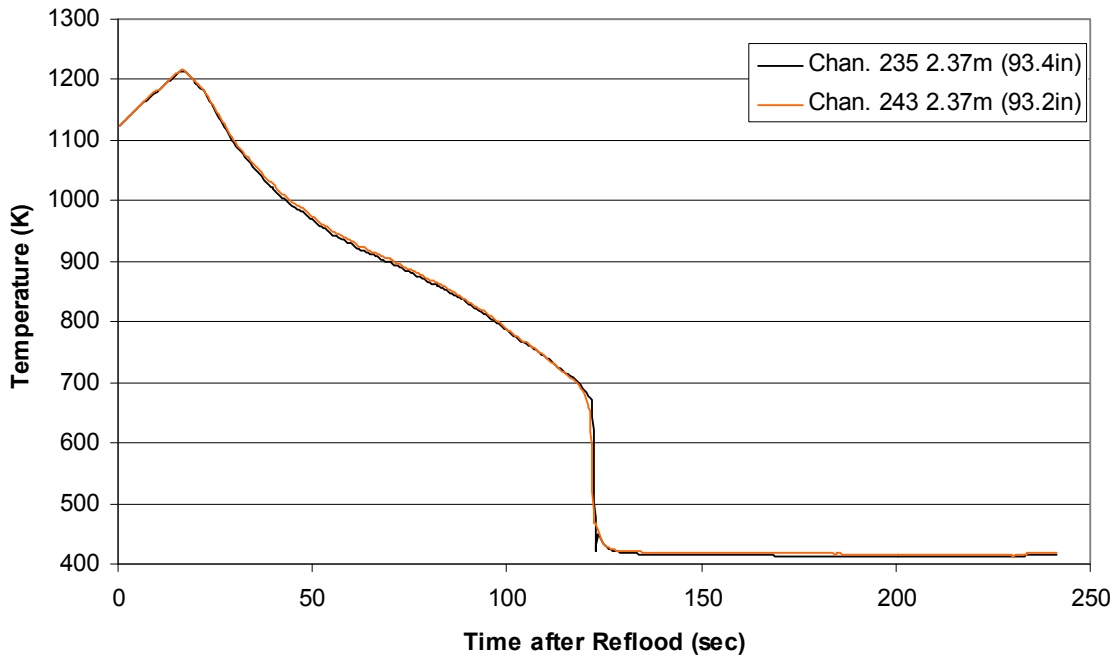
**Heater Rod Temperature during Reflood
RBHT Exp. 1291**



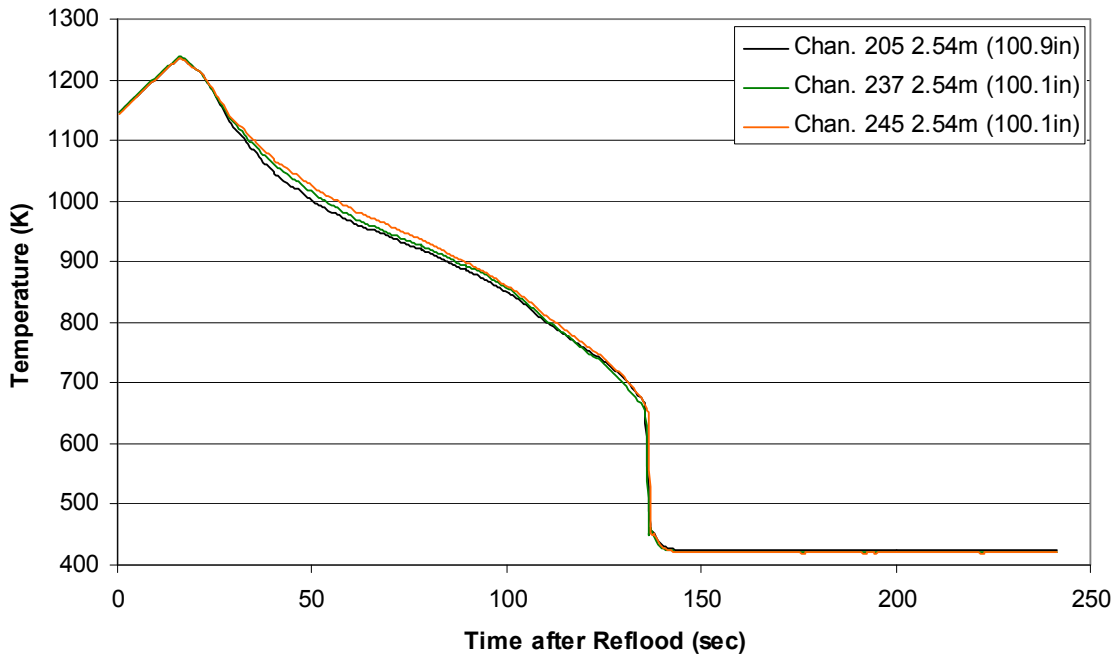
**Heater Rod Temperature during Reflood
RBHT Exp. 1291**



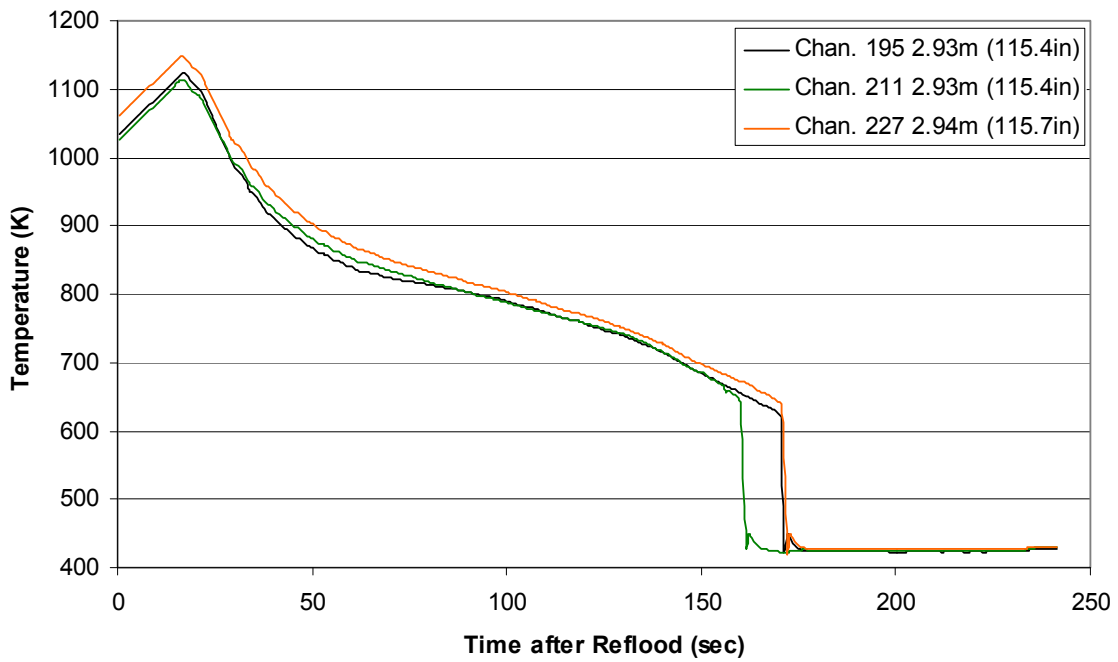
Heater Rod Temperature during Reflood
RBHT Exp. 1291



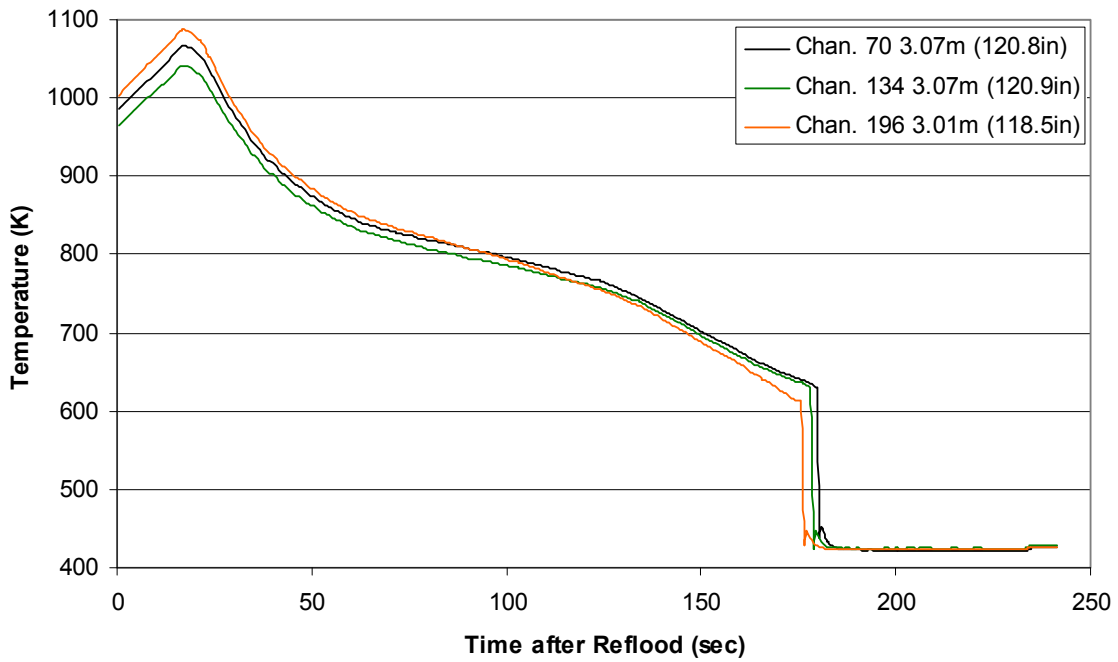
Heater Rod Temperature during Reflood
RBHT Exp. 1291



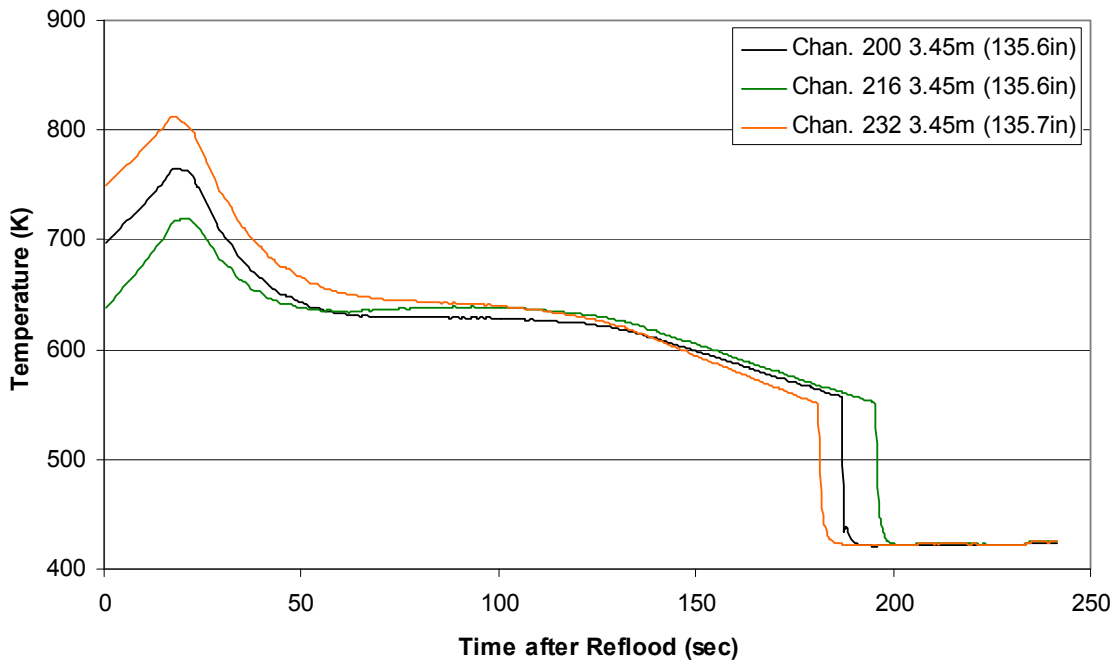
Heater Rod Temperature during Reflood
RBHT Exp. 1291



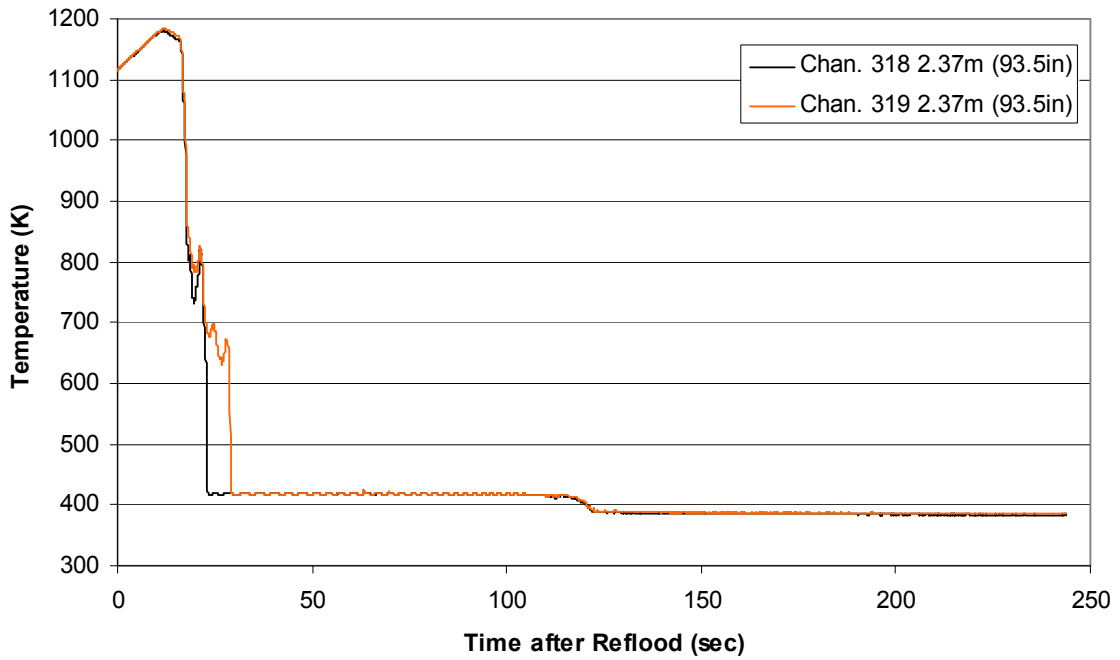
Heater Rod Temperature during Reflood
RBHT Exp. 1291



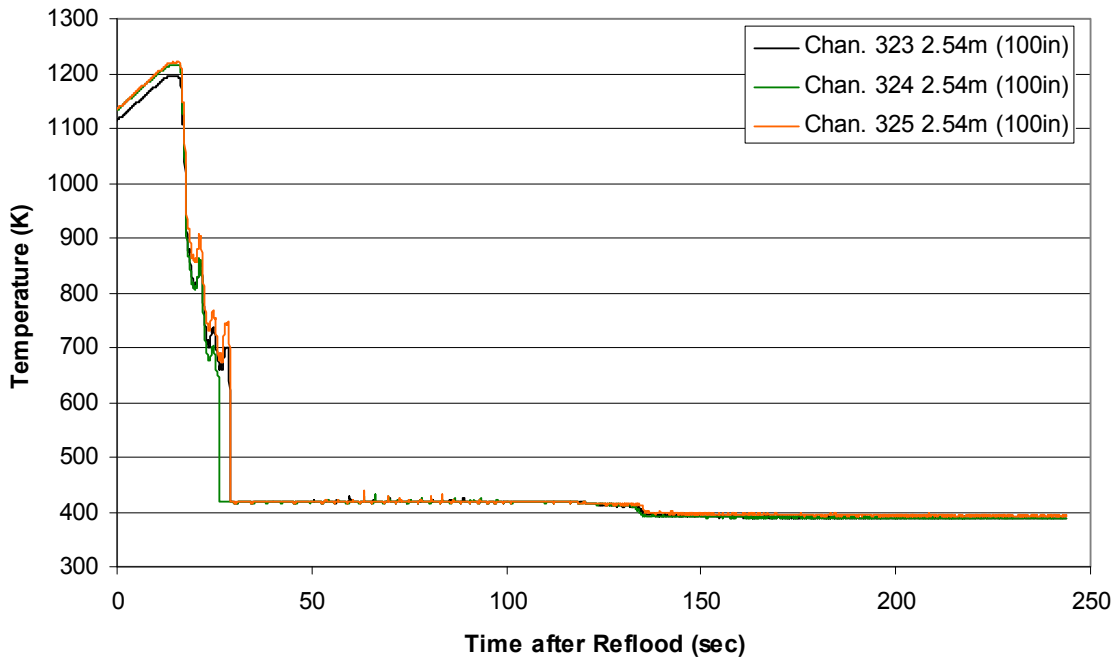
Heater Rod Temperature during Reflood RBHT Exp. 1291



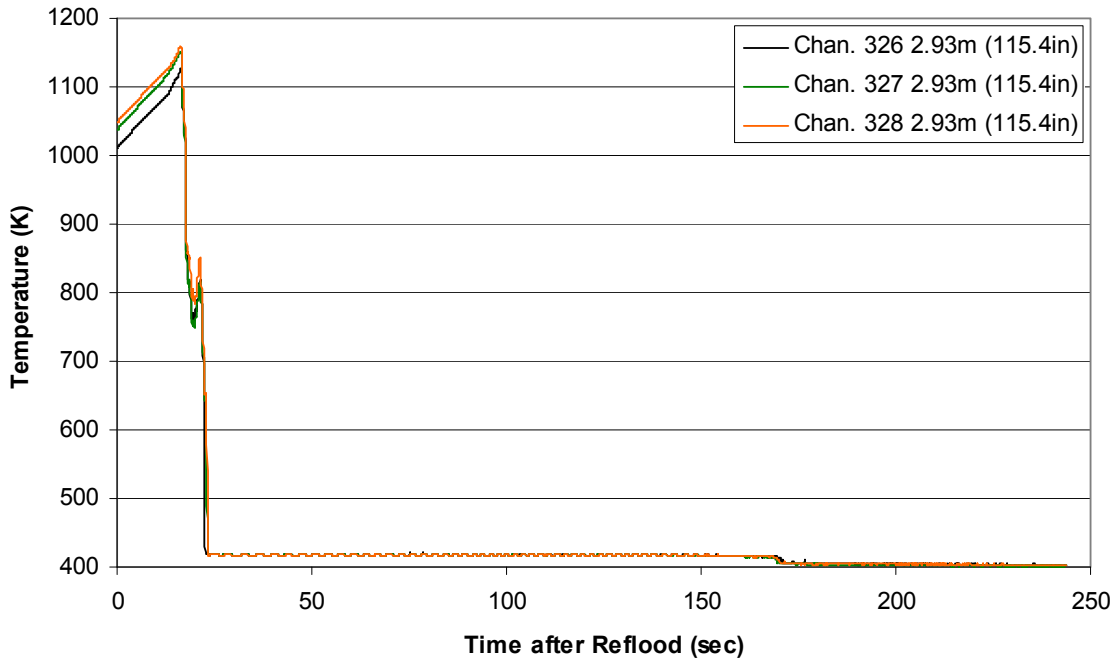
Steam Probe Temperature during Reflood RBHT Exp. 1291



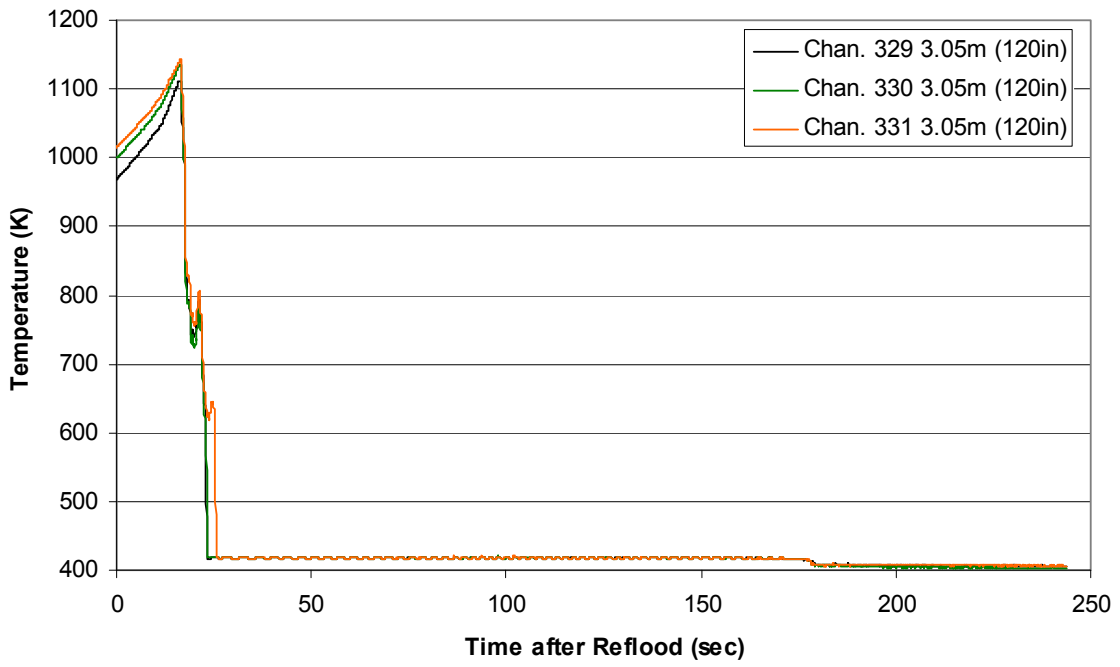
Steam Probe Temperature during Reflood
RBHT Exp. 1291



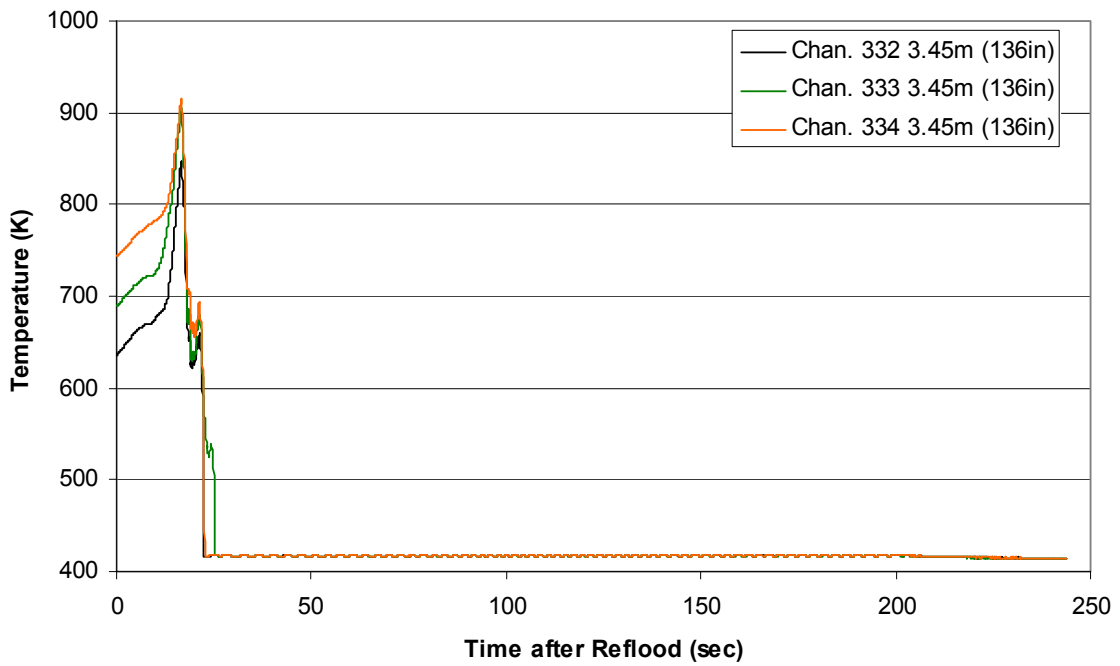
Steam Probe Temperature during Reflood
RBHT Exp. 1291



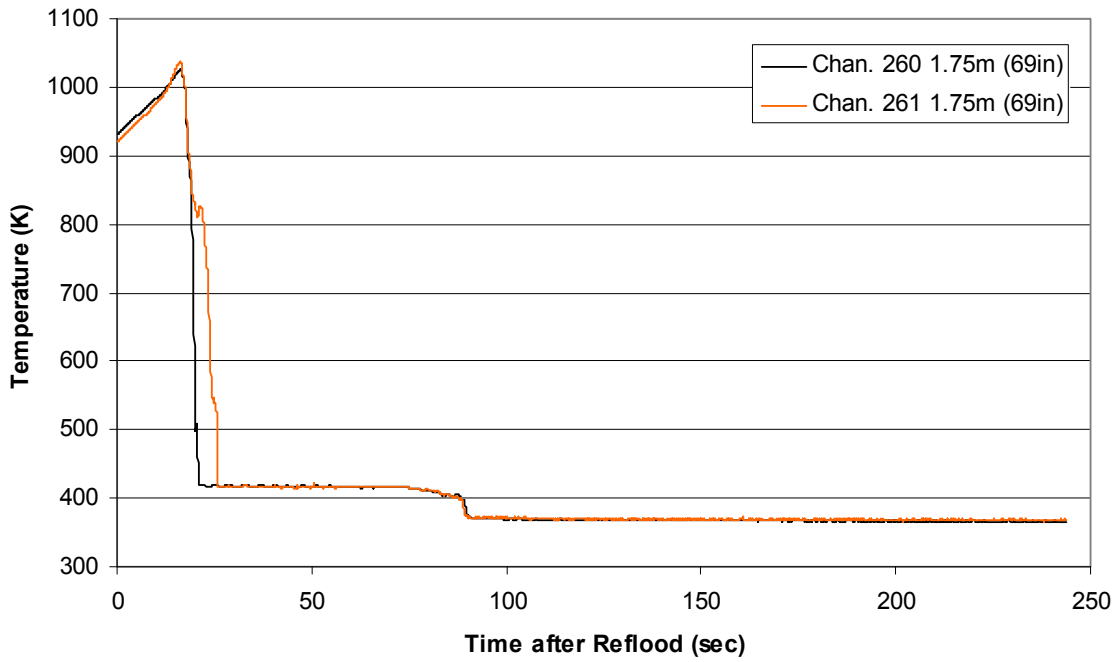
Steam Probe Temperature during Reflood
RBHT Exp. 1291



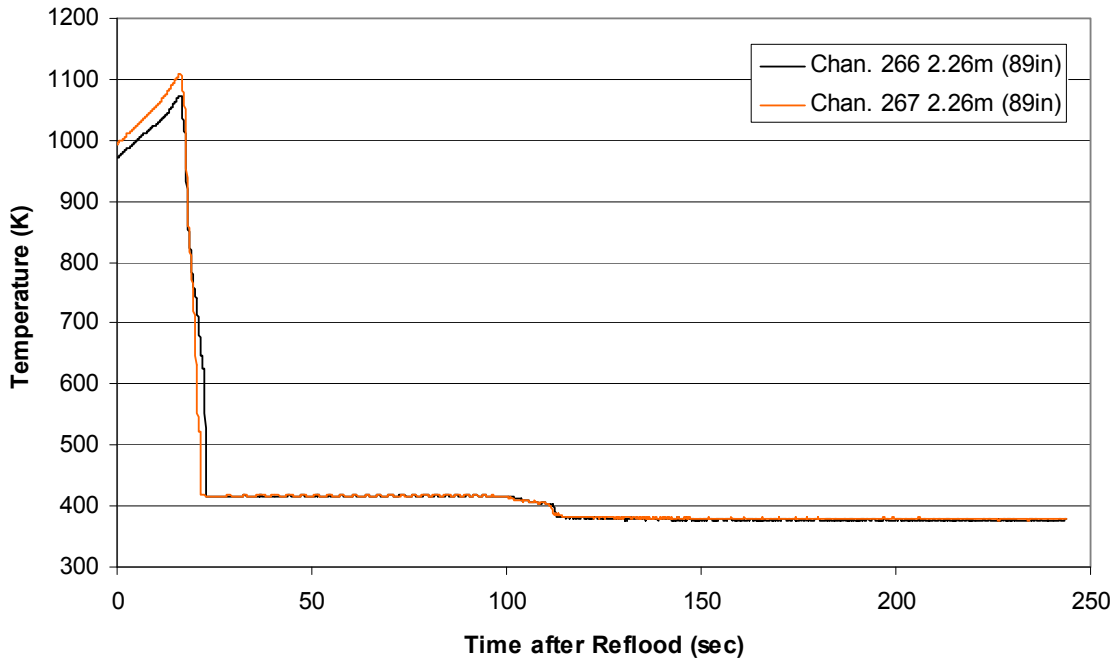
Steam Probe Temperature during Reflood
RBHT Exp. 1291



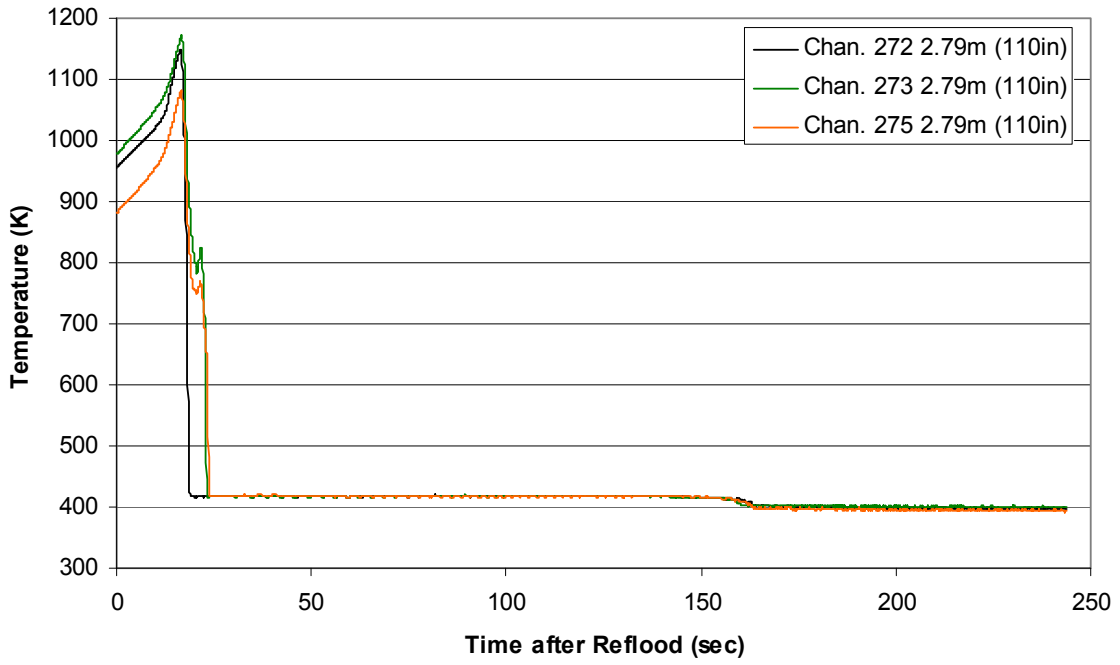
Spacer Grid Temperature during Reflood
RBHT Exp. 1291



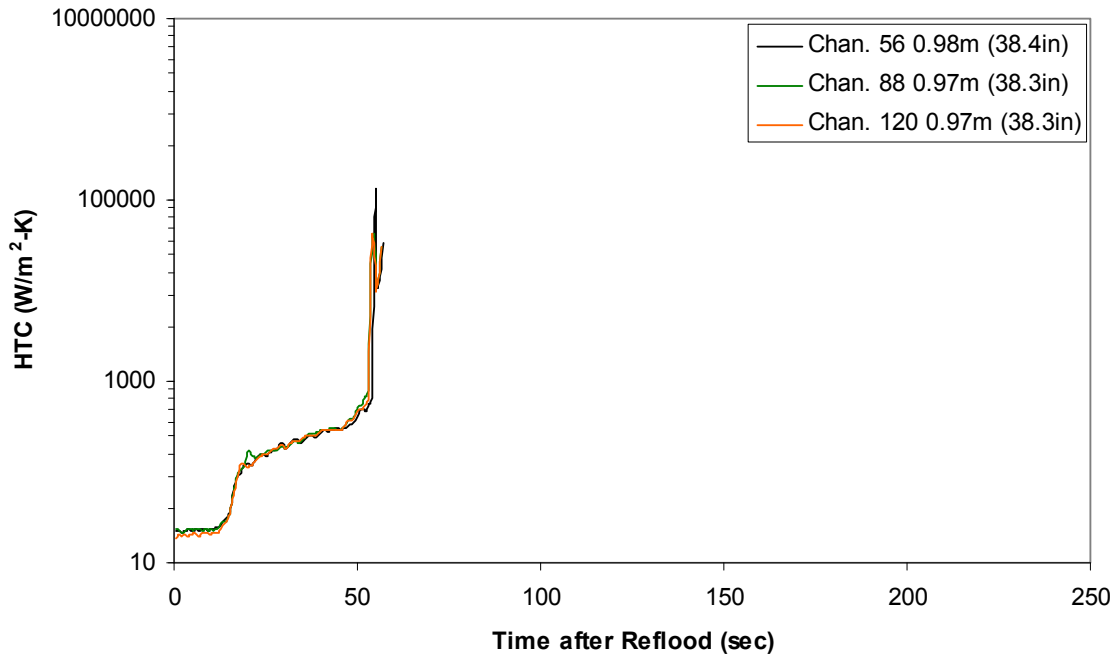
Spacer Grid Temperature during Reflood
RBHT Exp. 1291



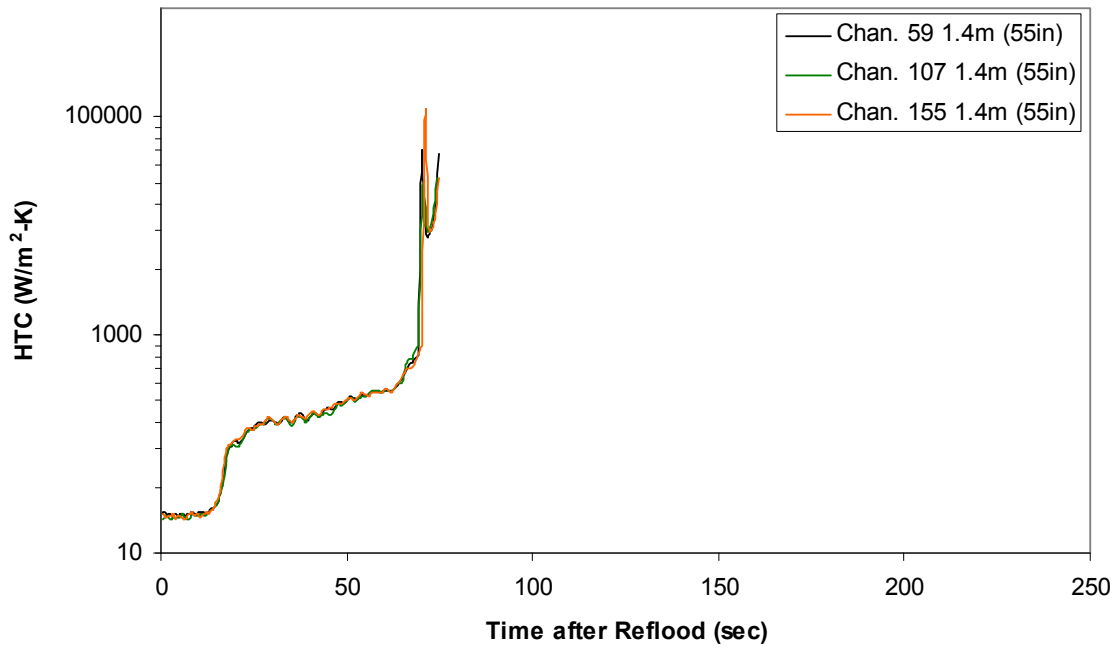
Spacer Grid Temperature during Reflood RBHT Exp. 1291



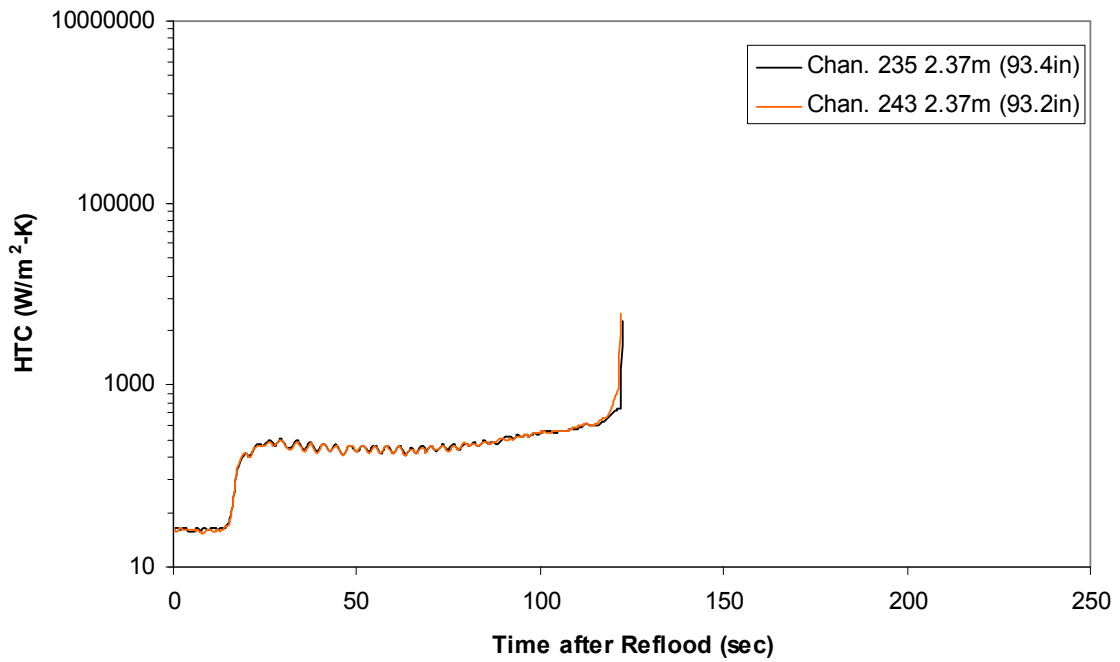
Heat Transfer Coefficient during Reflood RBHT Exp. 1291



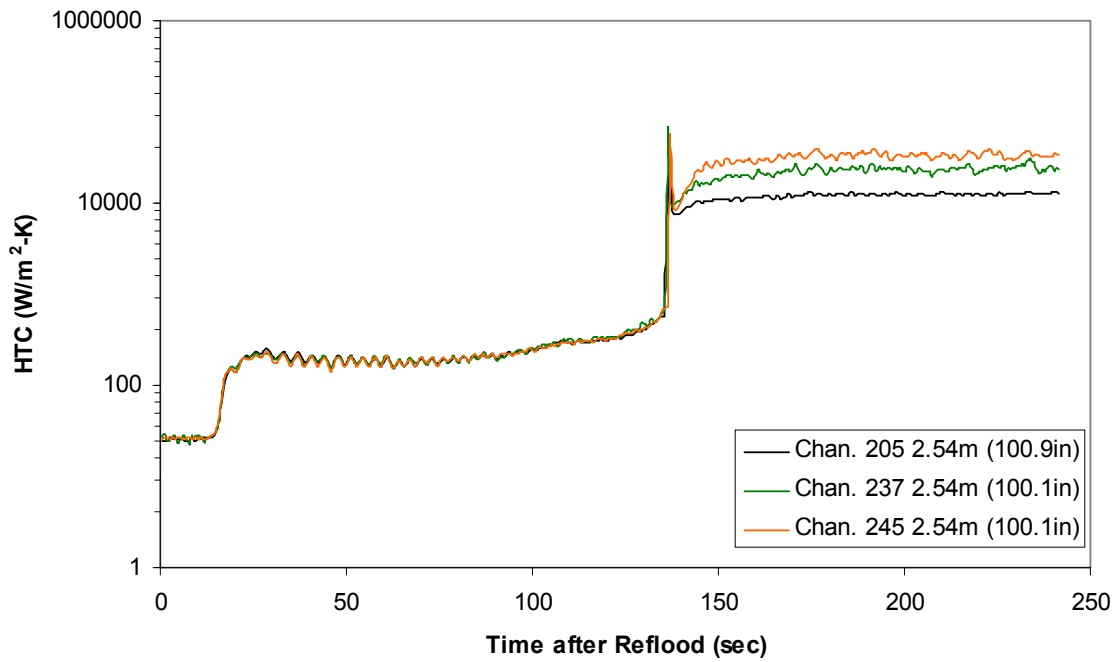
Heat Transfer Coefficient during Reflood RBHT Exp. 1291



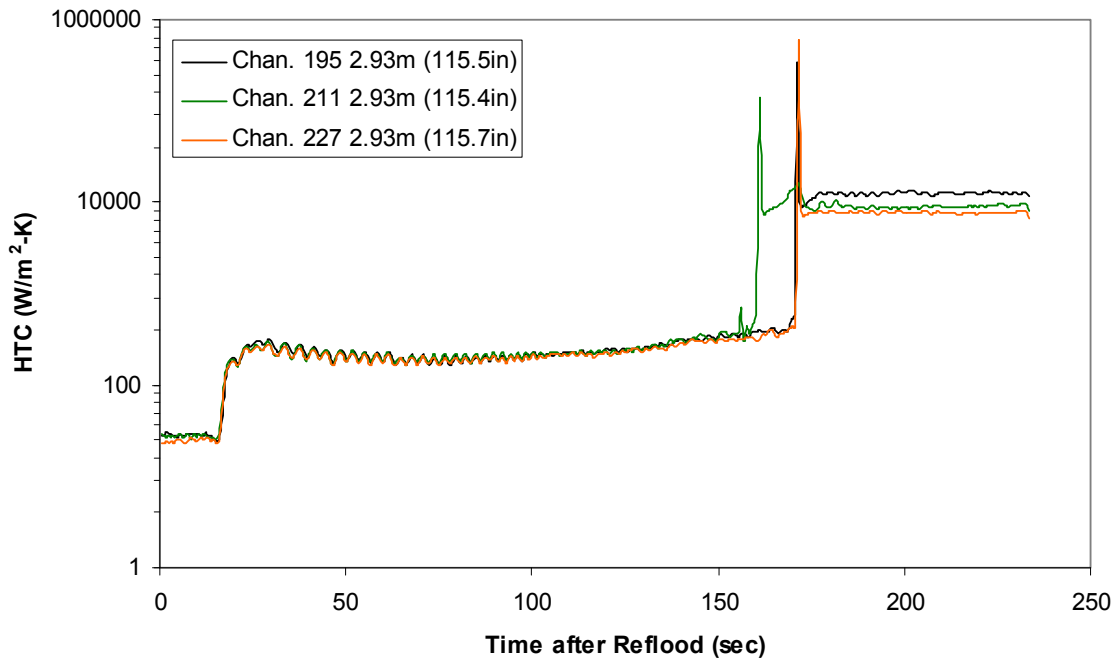
Heat Transfer Coefficient during Reflood RBHT Exp. 1291



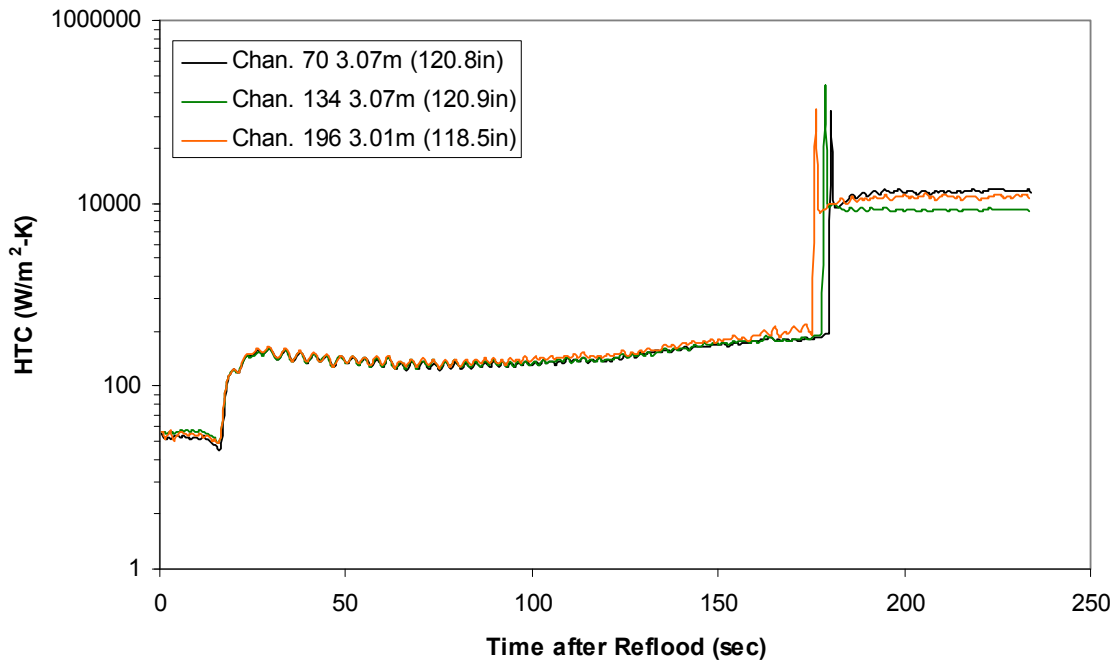
Heat Transfer Coefficient during Reflood RBHT Exp. 1291



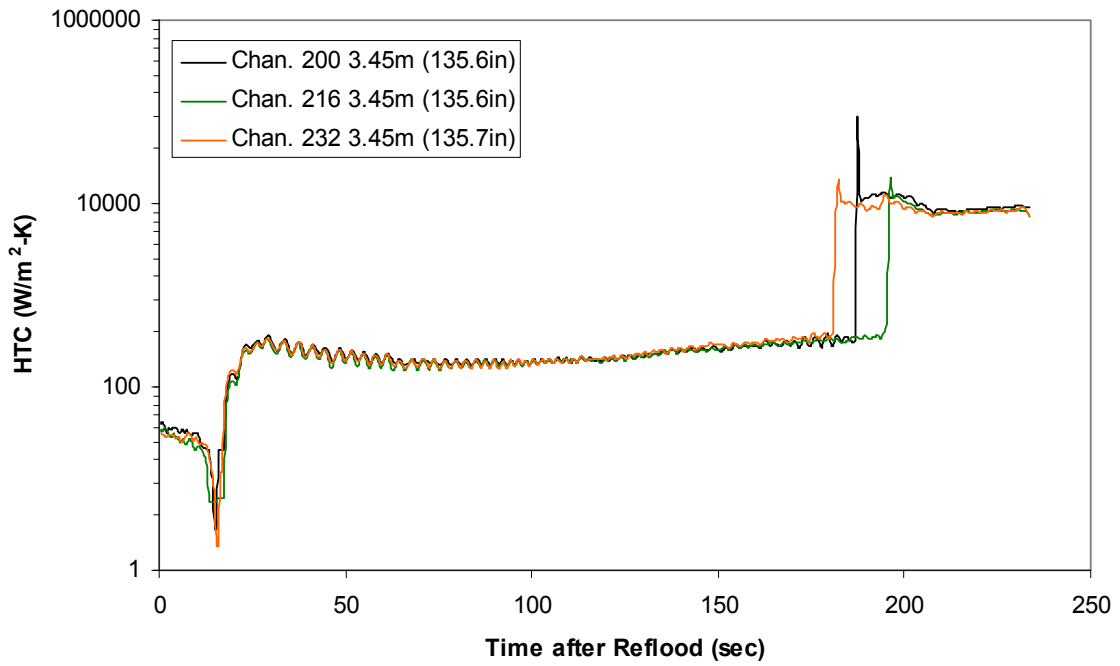
Heat Transfer Coefficient during Reflood RBHT Exp. 1291



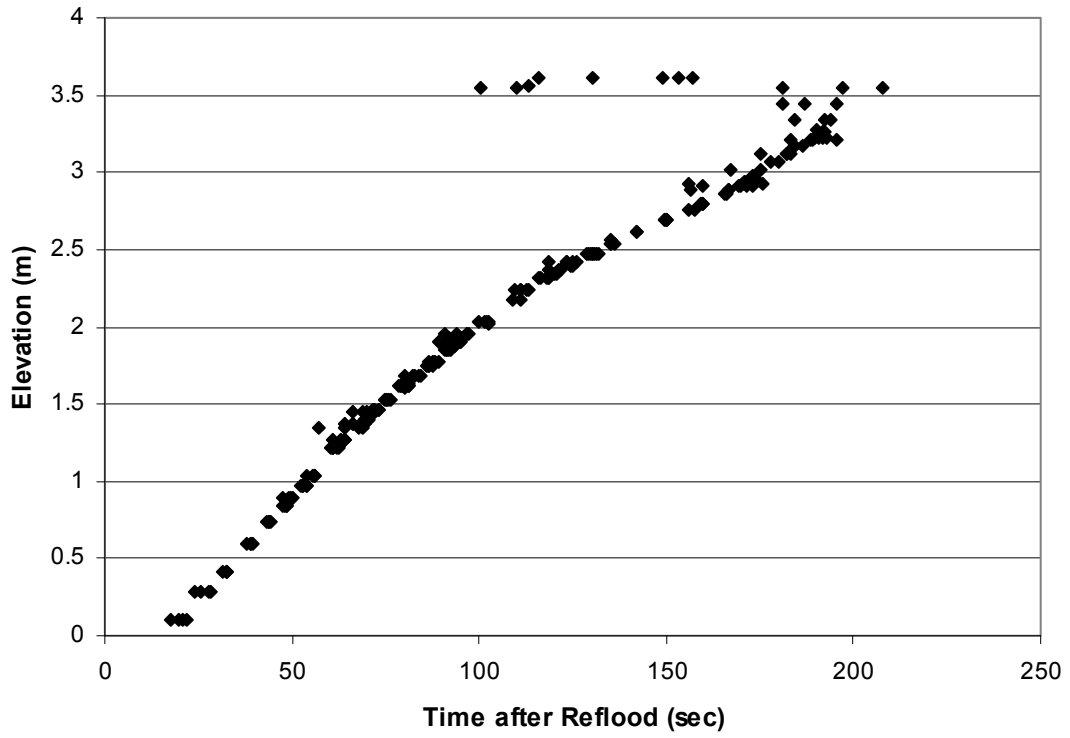
Heat Transfer Coefficient during Reflood RBHT Exp. 1291



Heat Transfer Coefficient during Reflood RBHT Exp. 1291



Quench Data, RBHT Exp. 1291



RBHT - REFLOOD TESTS

SUMMARY SHEET

RUN NO: **1295**

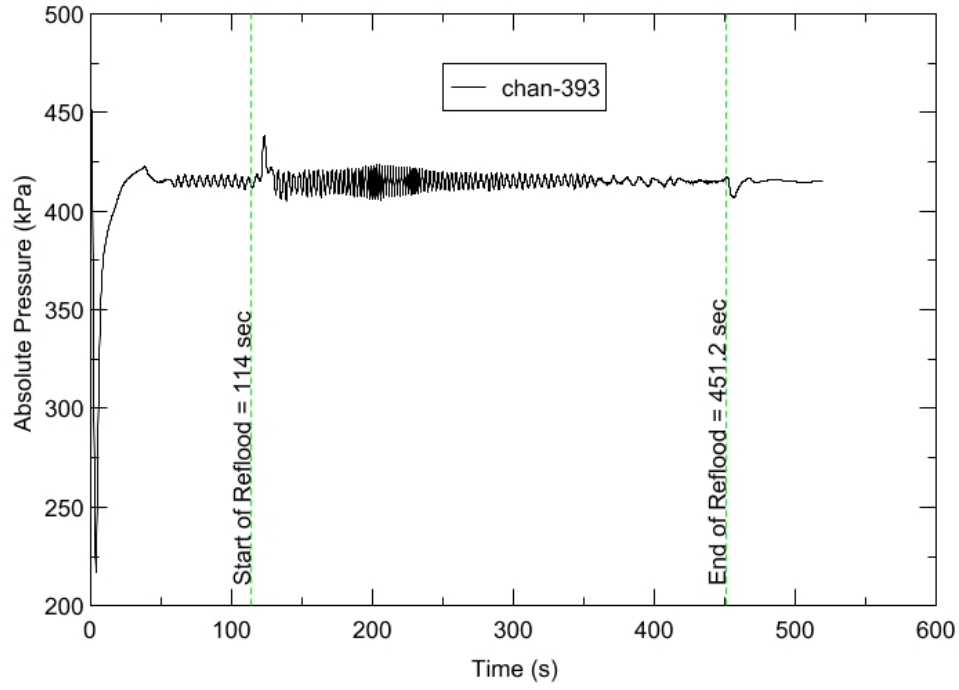
RUN CONDITIONS

Upper Plenum Pressure:	414 kPa (60 psia)
Initial Peak Clad Temperature:	1144 degrees K (1600 degrees F)
Rod Peak Power:	2.3 kW/m (0.7 kW/ft)
Flooding Rate:	0.1524 m/s (6 in/s)
Inlet Subcooling:	23 degrees K (42 degrees F)
Start of Reflood:	114 s
End of Reflood:	451.2 s
Test Date:	7/23/2002
Comments:	No droplet data

Rod_Elevation	Channel Number	Temperature at Reflood (K)	Temperature at Reflood (°F)	Tumaround Time (sec.)	Tumaround Temperature (K)	Tumaround Temperature (°F)	Quench Time (sec.)	Quench Temperature (K)	Quench Temperature (°F)
B6 0.592m	148	809.25	996.96	6.25	829.4	1033.22	41.25	612.56	642.92
B6 0.744m	149	834.26	1041.98	6.75	855.64	1080.47	51.75	598.09	616.88
B6 0.846m	150	863.18	1094.03	7.25	887.04	1136.98	57.75	607.06	633.01
B6 0.897m	151	874.56	1114.52	7.25	899.25	1158.96	60.75	610.94	640.01
C6 1.04m	137	919.91	1196.15	7.75	946.85	1244.64	69.75	642.26	696.38
D5 1.27m	217	970.47	1287.16	7.75	999.2	1338.88	86.25	630.74	675.64
C6 1.34m	138	969.06	1284.62	7.75	1000.04	1340.38	89.75	642.17	696.22
D5 1.37m	218	995.3	1331.86	7.75	1026.46	1387.93	94.25	647.3	705.45
C6 1.39m	139	976.18	1297.43	7.75	1007.58	1353.96	93.75	648.27	707.2
D5 1.45m	219	1010.43	1359.09	7.75	1042.58	1416.96	99.75	654.75	718.87
C6 1.47m	140	991.28	1324.61	7.75	1023.64	1382.86	99.75	651.3	712.66
D5 1.52m	220	1024.48	1384.38	7.75	1057.6	1443.98	106.75	660.28	728.81
C6 1.62m	141	1015.54	1368.28	8.25	1050.41	1431.06	112.75	672.28	750.41
D5 1.68m	221	1048.62	1427.84	8.25	1084.16	1491.8	121.25	676.55	758.1
D5 1.78m	222	993.09	1327.87	7.75	1031.57	1397.14	130.75	662.7	733.17
D5 1.85m	223	1056.44	1441.91	7.75	1091.04	1504.19	136.75	635.33	683.9
C6 1.87m	142	1046.89	1424.72	8.25	1082.67	1489.12	135.75	644.57	700.53
D5 1.90m	224	1072.85	1471.44	7.75	1109.48	1537.37	140.75	649.2	708.87
C6 1.95m	144	1063.96	1455.43	8.25	1101.23	1522.53	141.25	670.66	747.5
C3 2.17m	178	1076.16	1477.39	7.75	1118.57	1553.75	163.25	686.62	776.23
D4 2.24m	241	1137.5	1587.82	7.75	1174.5	1654.42	175.25	648.09	706.88
D4 2.32m	242	1159.62	1627.64	7.75	1200.25	1700.76	182.25	687.17	777.21
C3 2.35m	180	1155.73	1620.63	8.25	1198.51	1697.63	178.75	703.22	806.11
D4 2.37m	243	1167.15	1641.18	7.75	1209.44	1717.3	187.75	700.7	801.57
C3 2.40m	181	1158.51	1625.63	8.25	1202.08	1704.06	184.25	714.66	826.71
D4 2.54m	245	1198.03	1696.77	7.25	1238	1768.71	210.75	711.66	821.3
D6 2.62m	129	1198.33	1697.3	7.25	1238.71	1770	213.75	723.89	843.32
D6 2.69m	130	1199.15	1698.79	7.25	1240.15	1772.57	223.25	732.41	858.64
C3 2.76m	183	1178.26	1661.18	7.75	1220.53	1737.26	230.25	745.05	881.41
D6 2.92m	132	1094.55	1510.5	8.25	1137.55	1587.91	247.75	679.23	762.92
D6 2.97m	133	1064.75	1456.87	8.25	1105.79	1530.74	252.75	666.8	740.55
D6 3.07m	134	1023.74	1383.04	8.25	1061.84	1451.63	258.75	662.99	733.69
E3 3.12m	197	1024.17	1383.82	8.25	1063.18	1454.04	268.25	661.54	731.09
D6 3.17m	135	982.14	1308.16	8.25	1017.97	1372.67	265.75	660.67	729.51
D6 3.27m	136	924.45	1204.32	8.75	960.9	1269.93	272.25	622.49	660.79
D4 3.61m	248	694.59	790.58	8.25	747.45	885.72	334.75	422.11	300.11

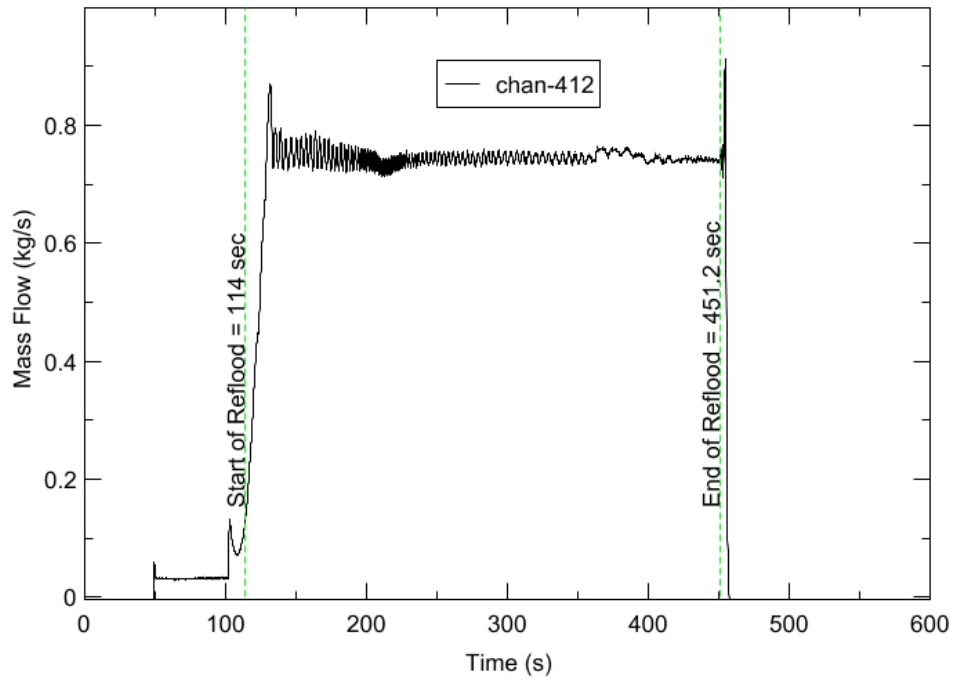
RBHT - TEST FACILITY

Upper Plenum Pressure vs. Time, Exp 1295



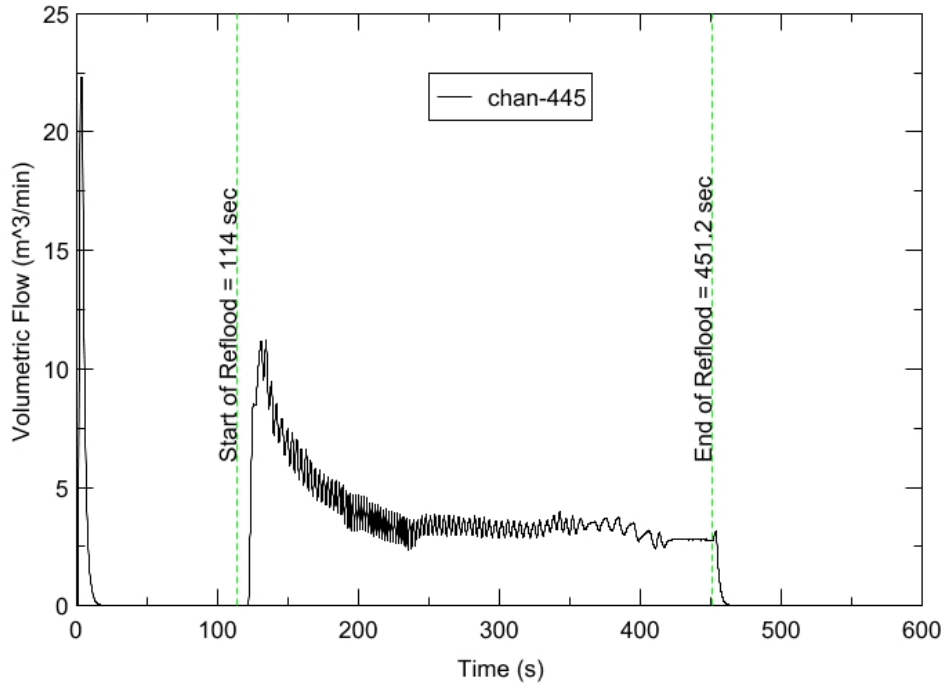
RBHT - TEST FACILITY

Inlet Flow vs. Time, Exp 1295



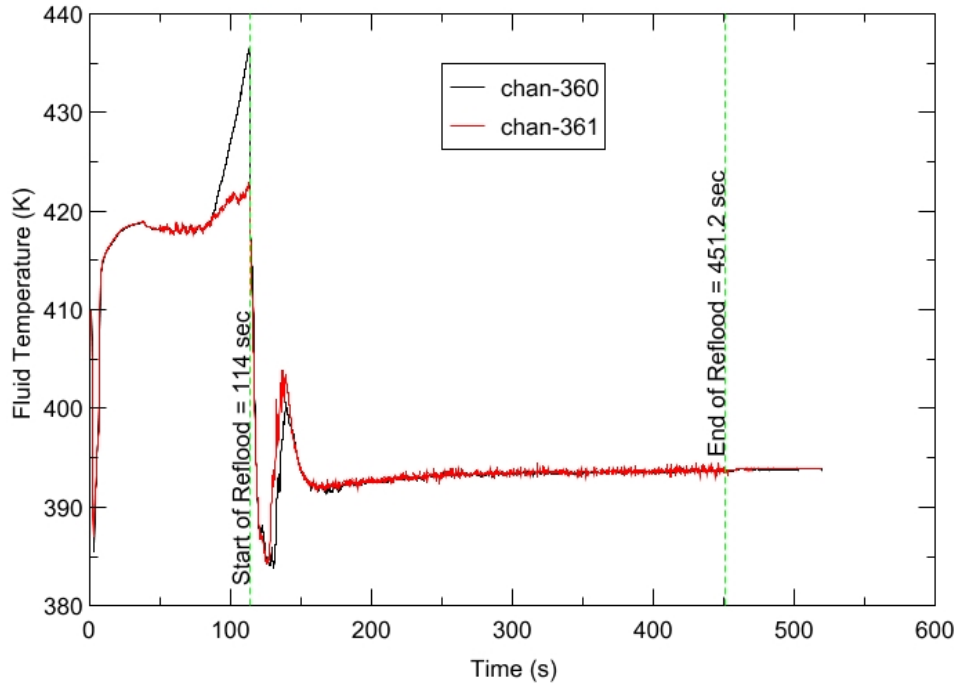
RBHT - TEST FACILITY

Steam Exhaust Flow vs. Time, Exp 1295



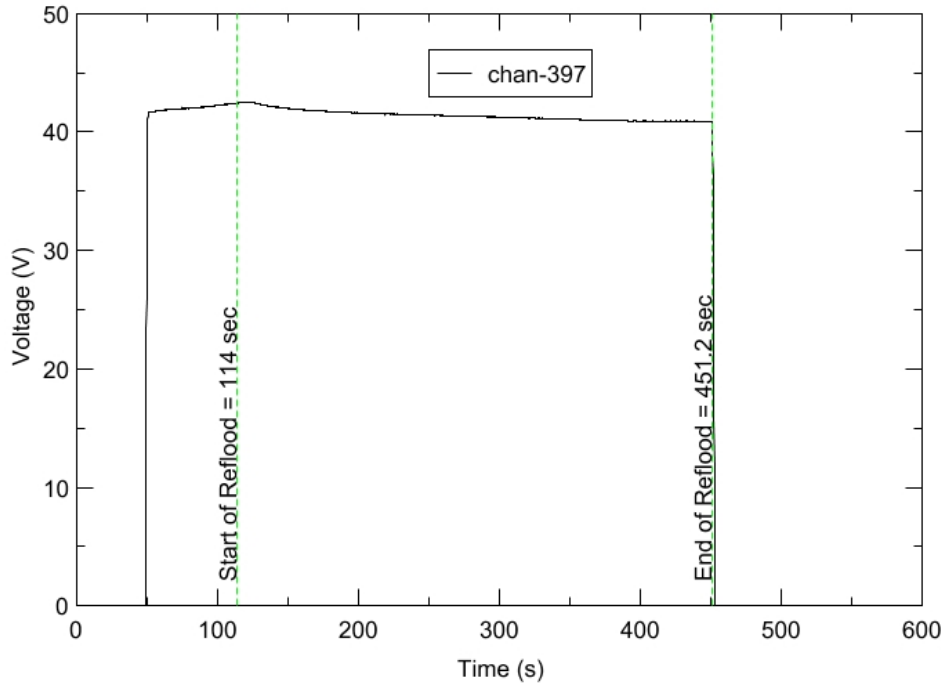
RBHT - TEST FACILITY

Inlet Flow Temperature vs. Time, Exp 1295



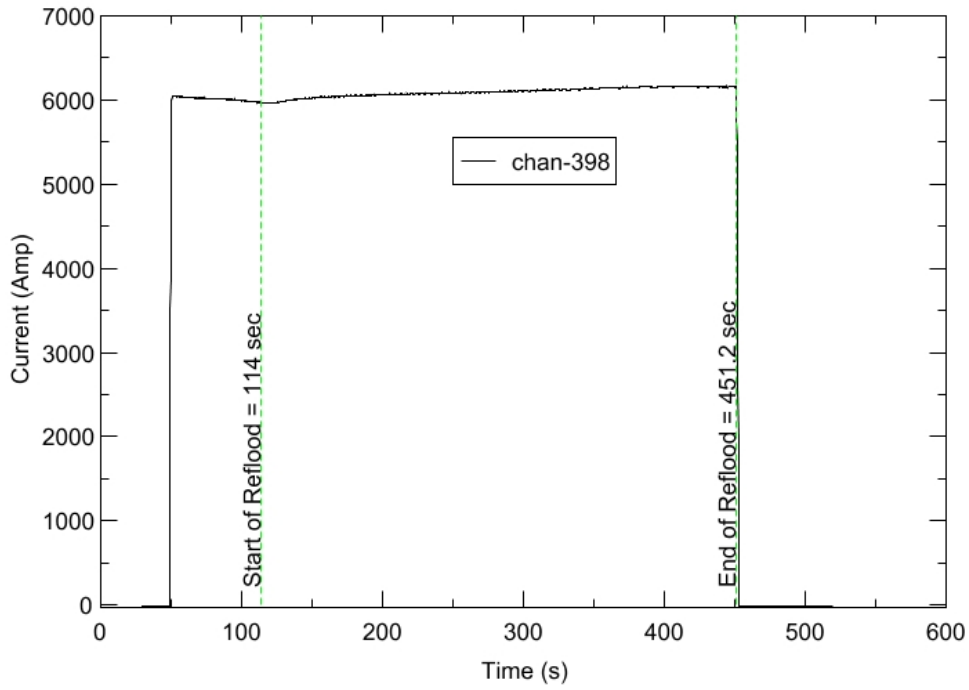
RBHT - TEST FACILITY

Test Section Voltage vs. Time, Exp 1295

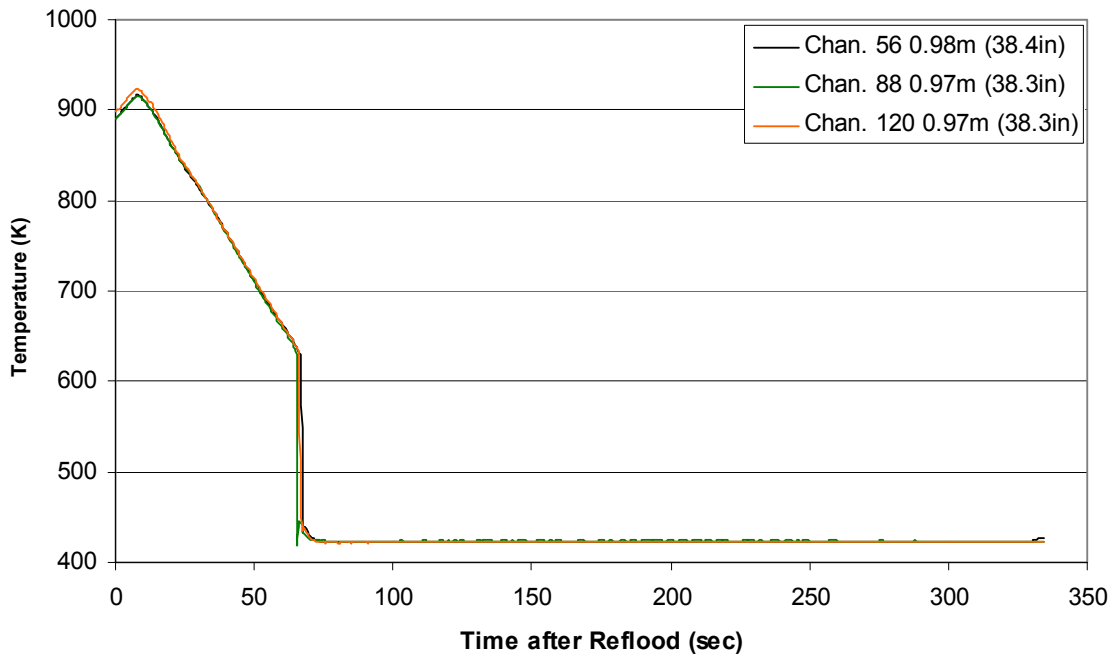


RBHT - TEST FACILITY

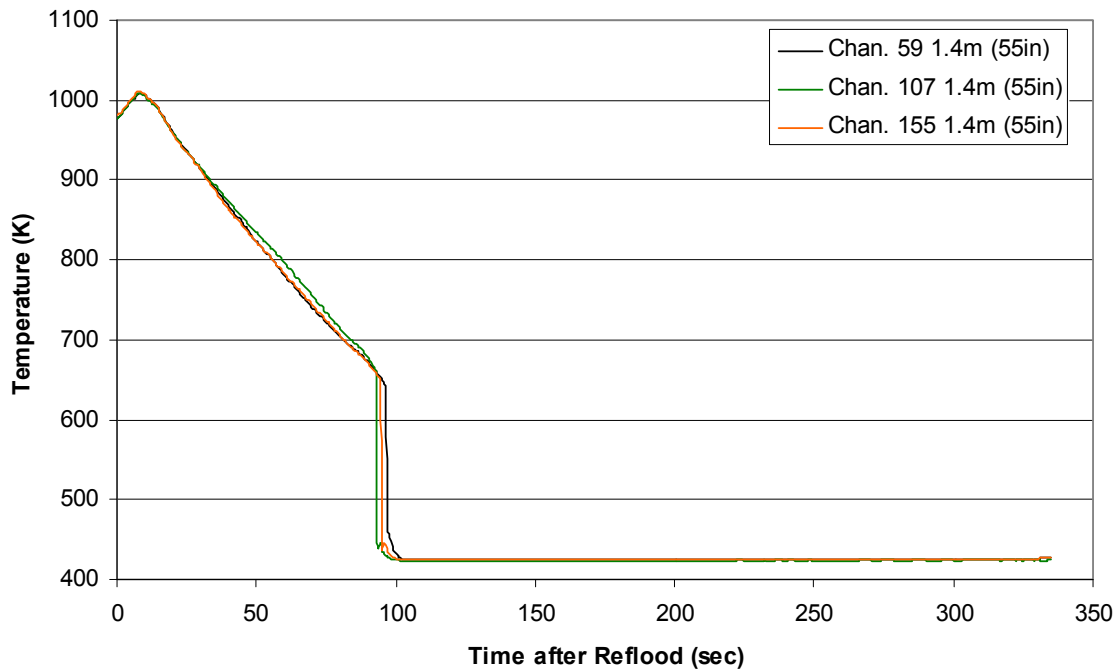
Test Section Current vs. Time, Exp 1295



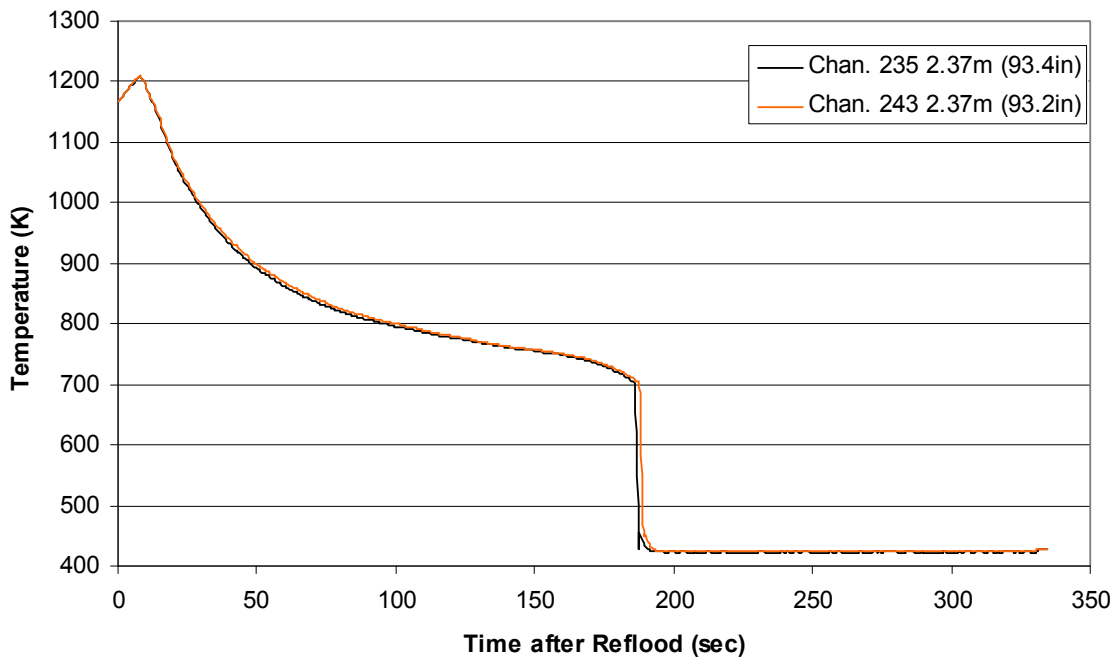
Heater Rod Temperature during Reflood RBHT Exp. 1295



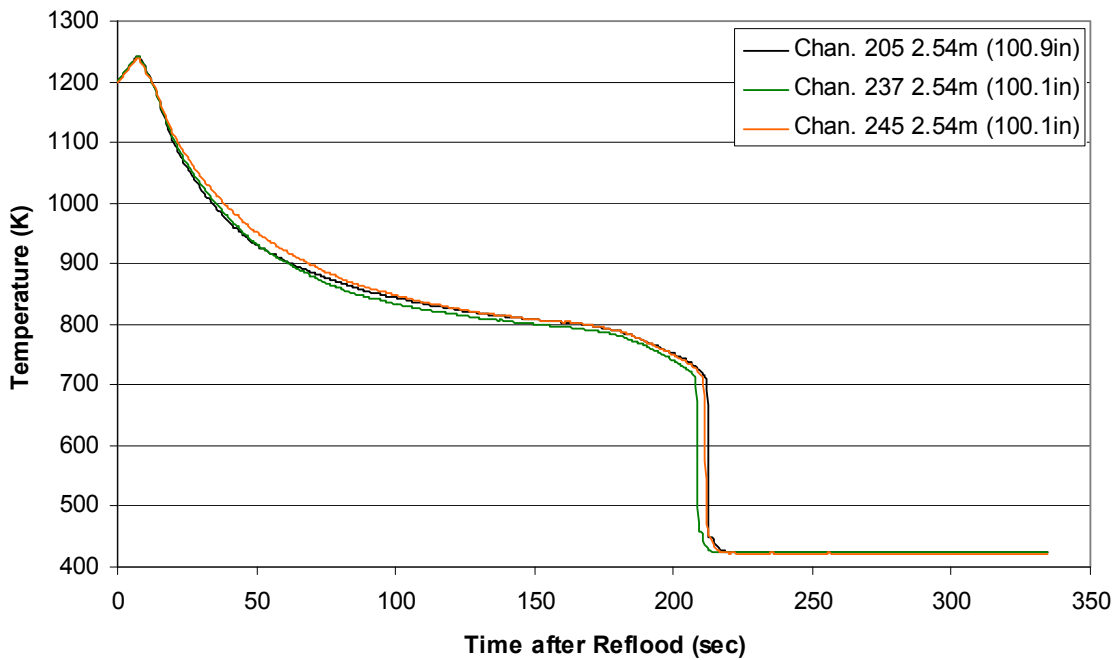
Heater Rod Temperature during Reflood RBHT Exp. 1295



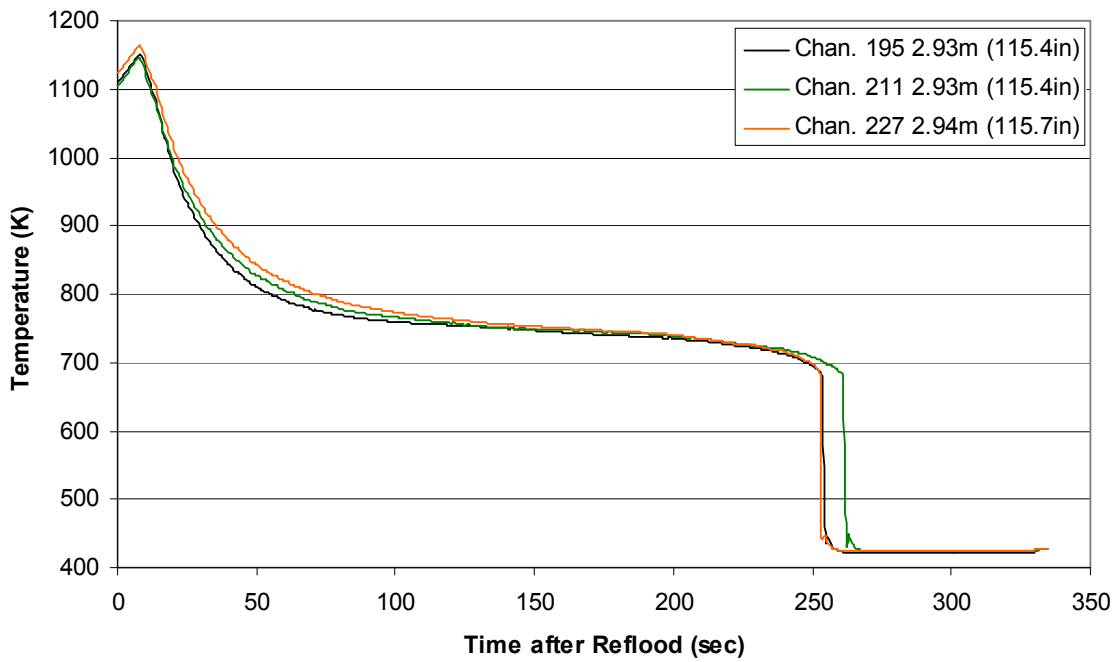
Heater Rod Temperature during Reflood
RBHT Exp. 1295



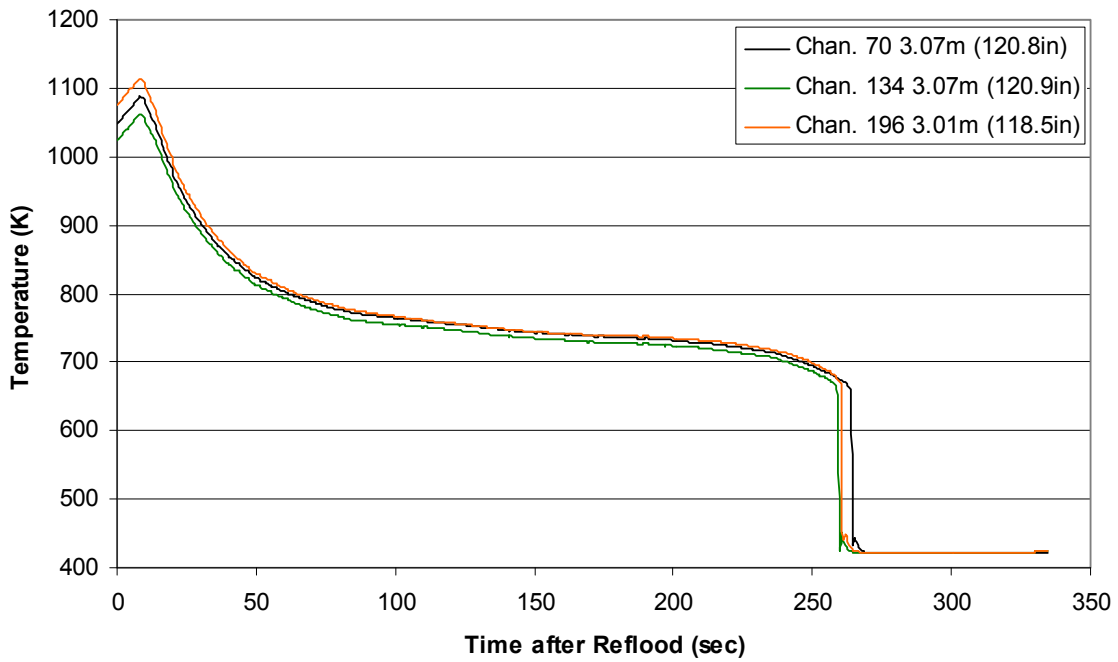
Heater Rod Temperature during Reflood
RBHT Exp. 1295



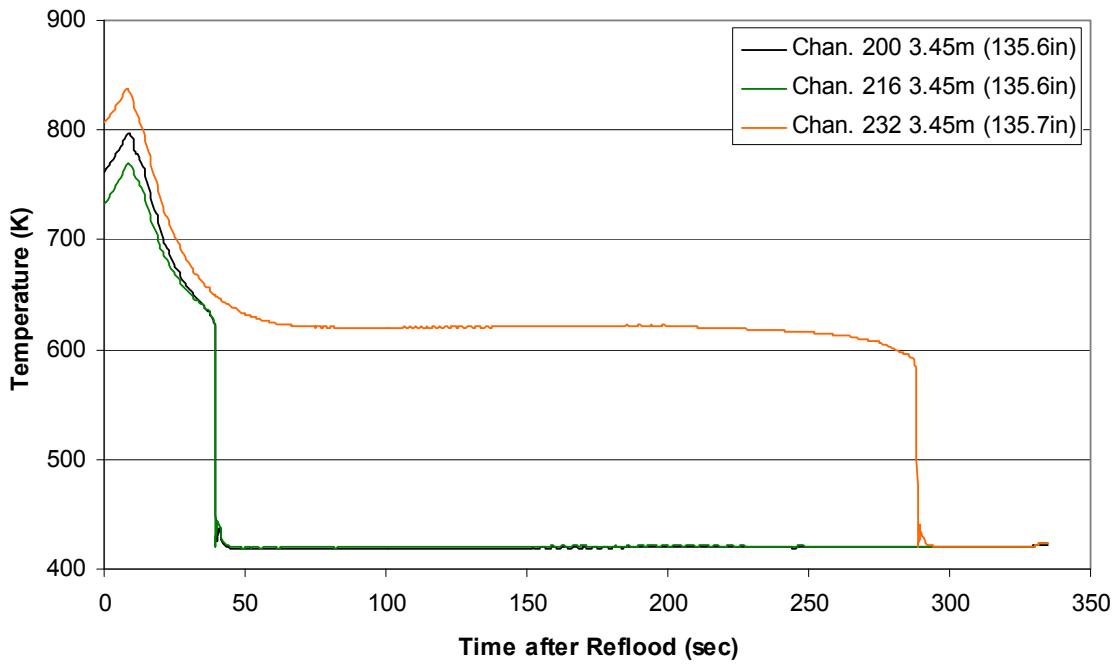
Heater Rod Temperature during Reflood RBHT Exp. 1295



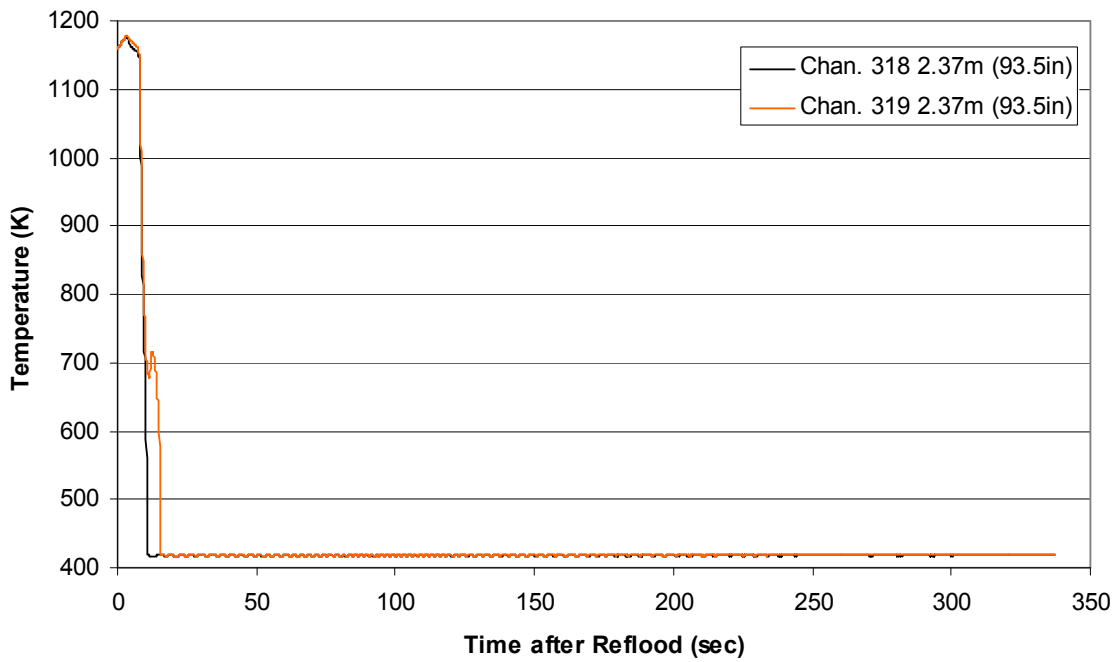
Heater Rod Temperature during Reflood RBHT Exp. 1295



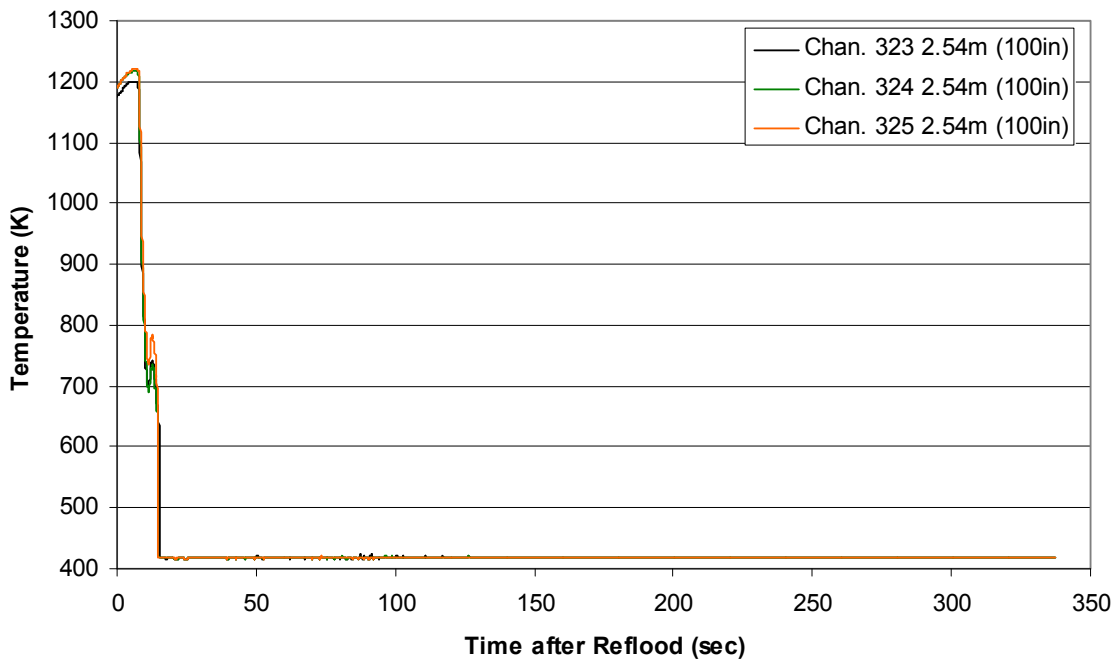
Heater Rod Temperature during Reflood RBHT Exp. 1295



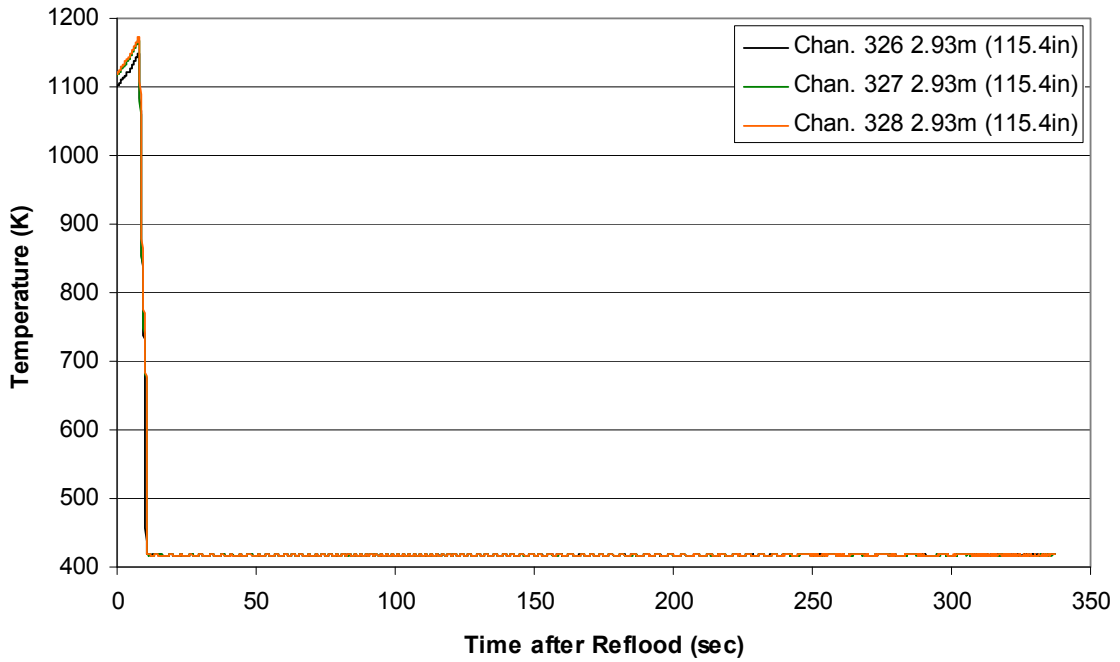
Steam Probe Temperature during Reflood RBHT Exp. 1295



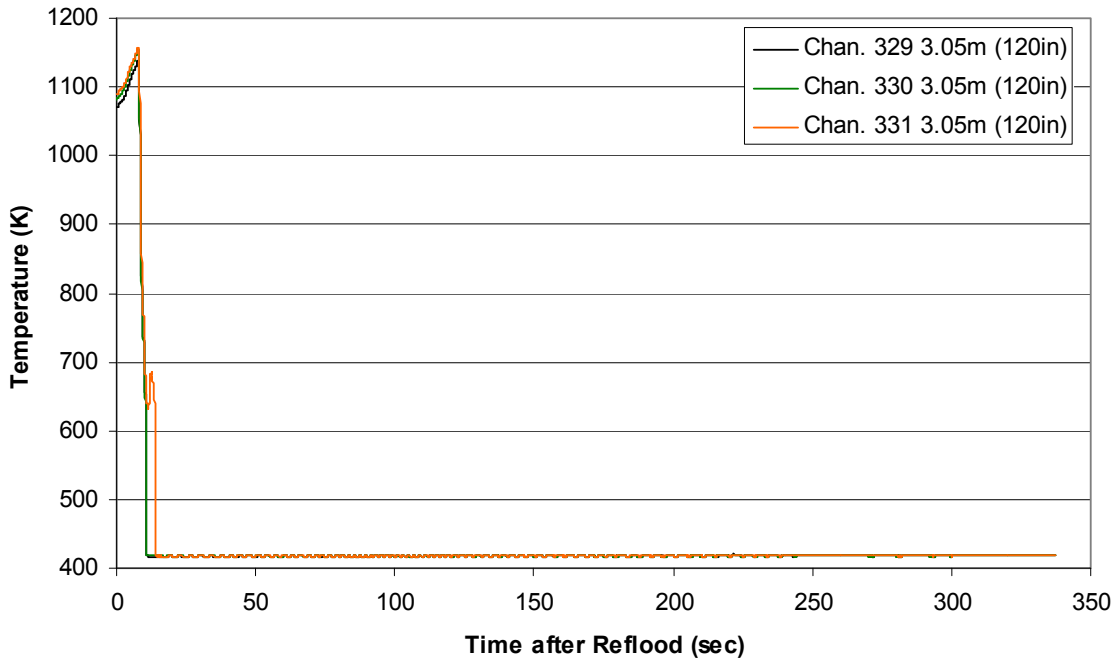
Steam Probe Temperature during Reflood RBHT Exp. 1295



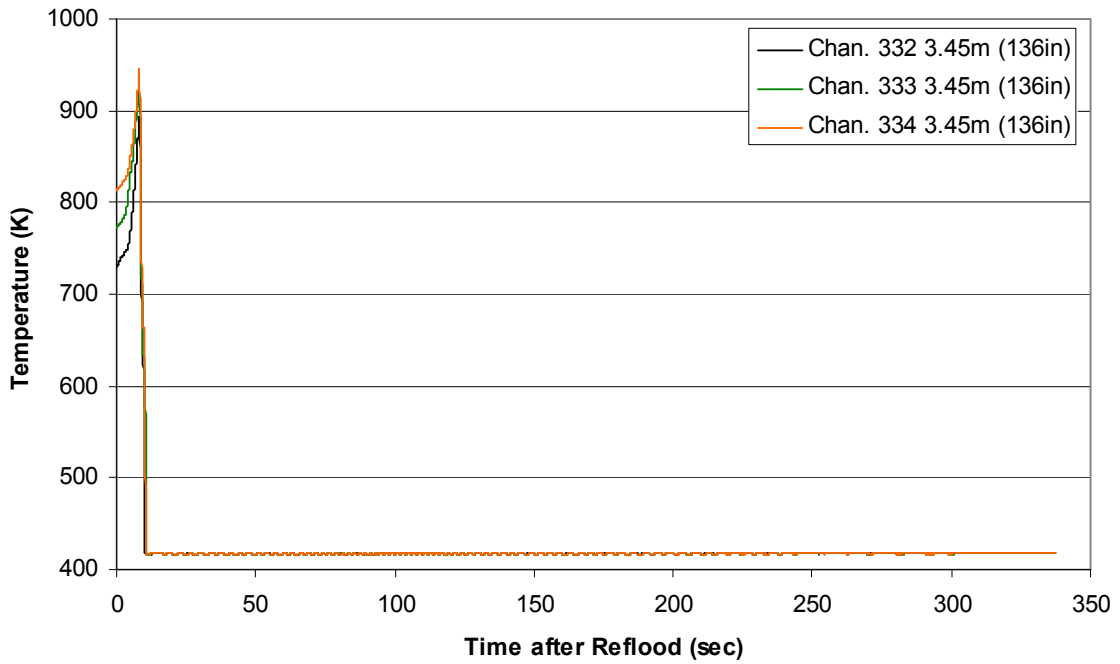
Steam Probe Temperature during Reflood RBHT Exp. 1295



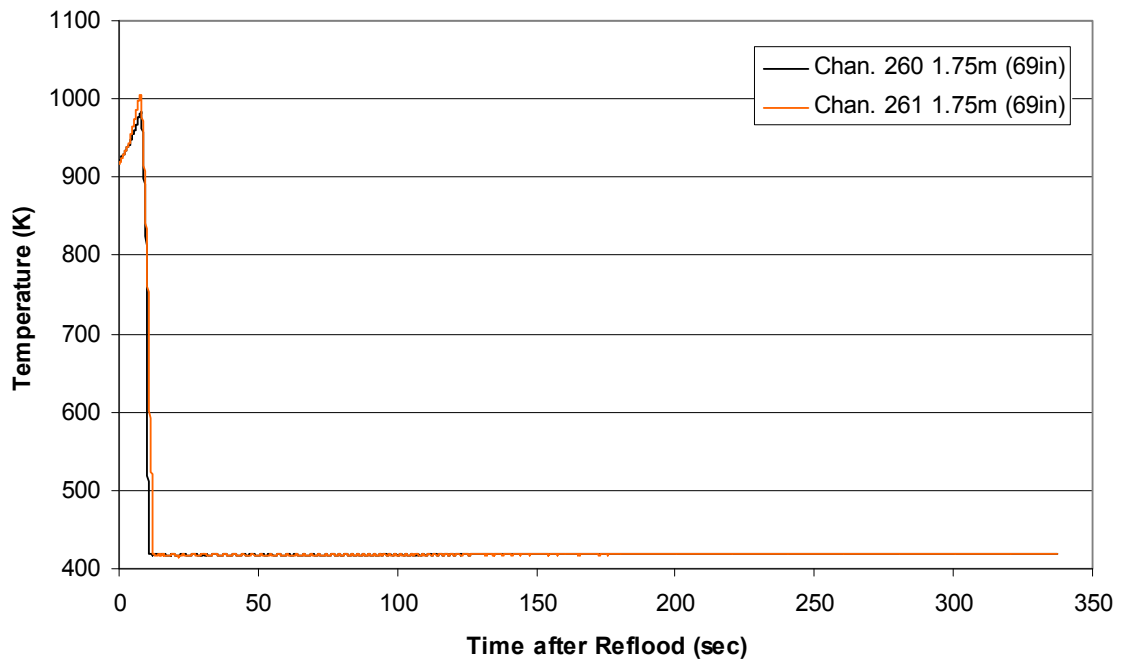
Steam Probe Temperature during Reflood
RBHT Exp. 1295



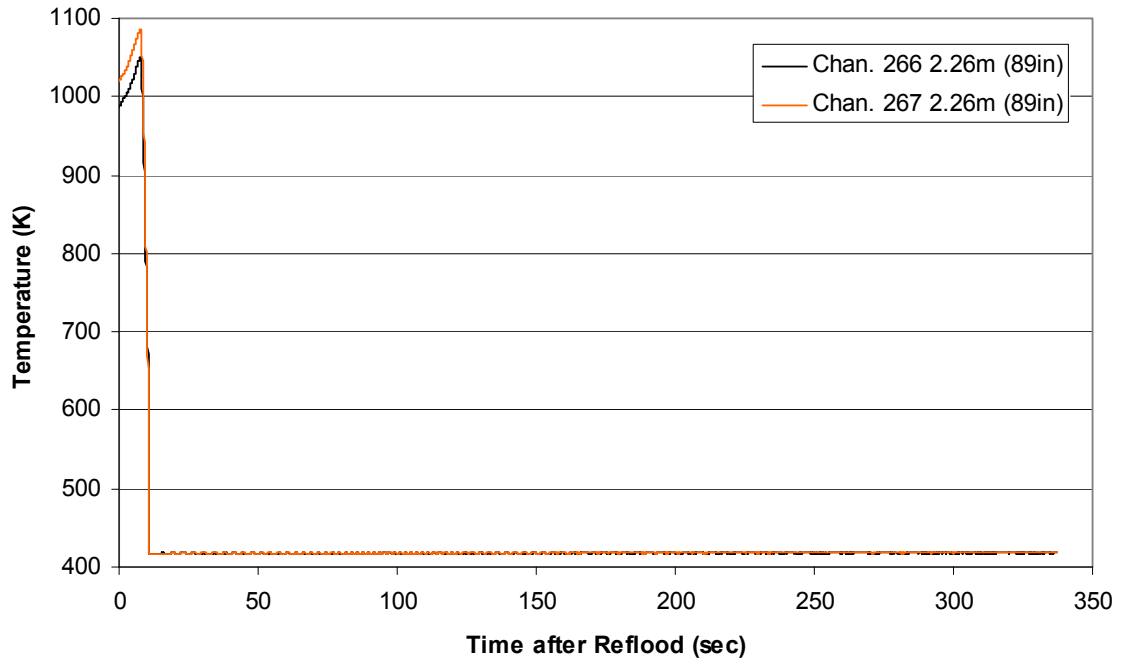
Steam Probe Temperature during Reflood
RBHT Exp. 1295



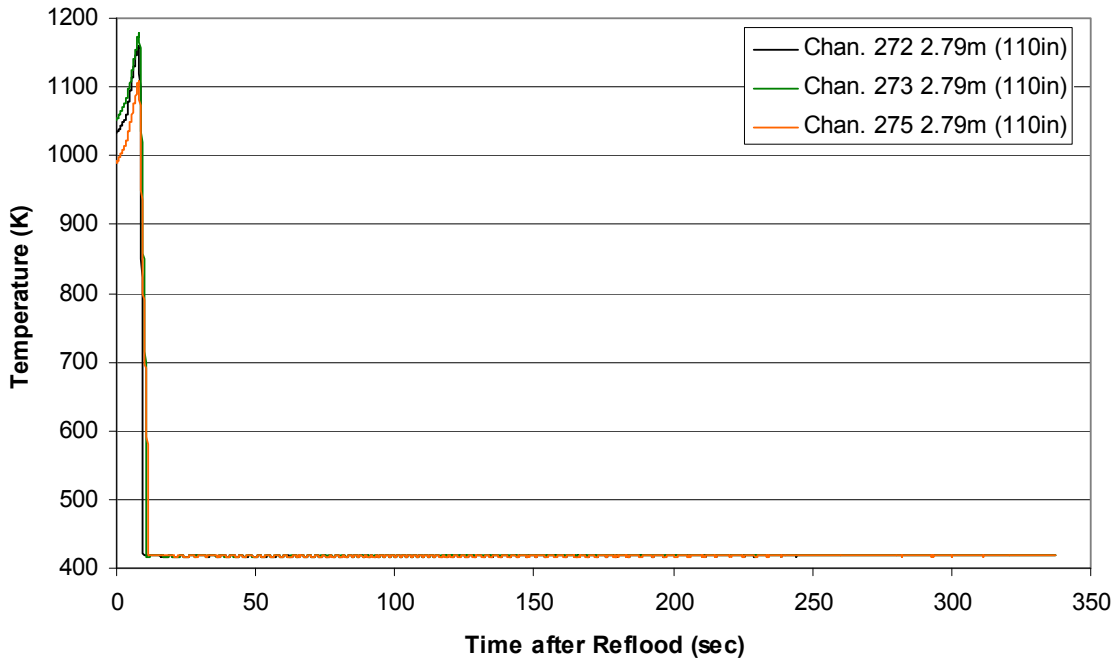
Spacer Grid Temperature during Reflood RBHT Exp. 1295



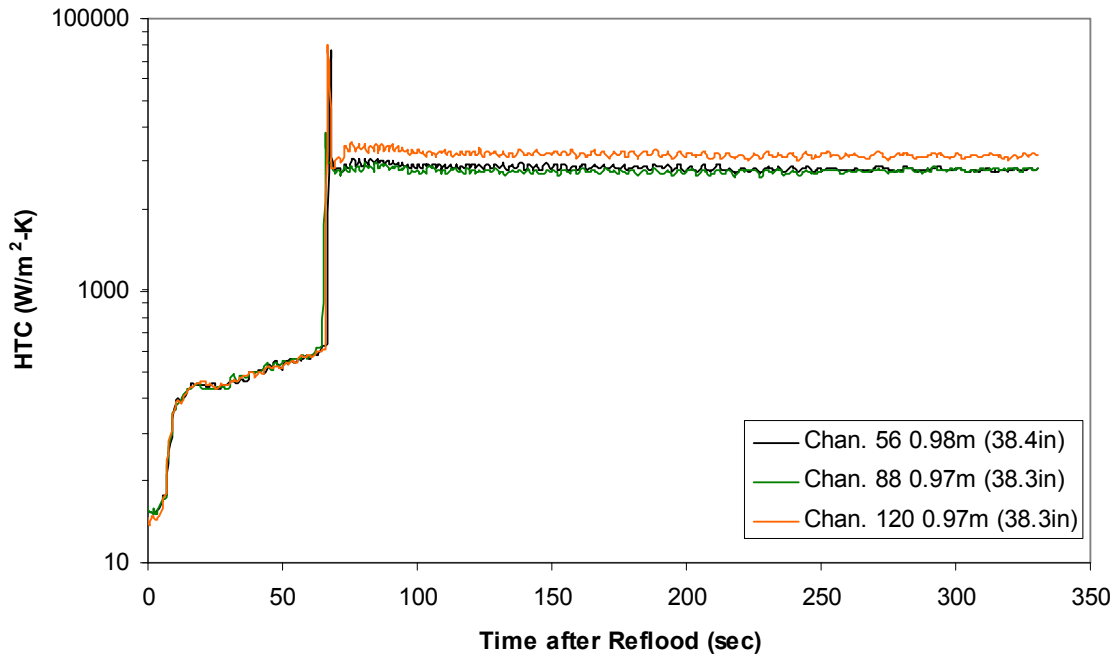
Spacer Grid Temperature during Reflood RBHT Exp. 1295



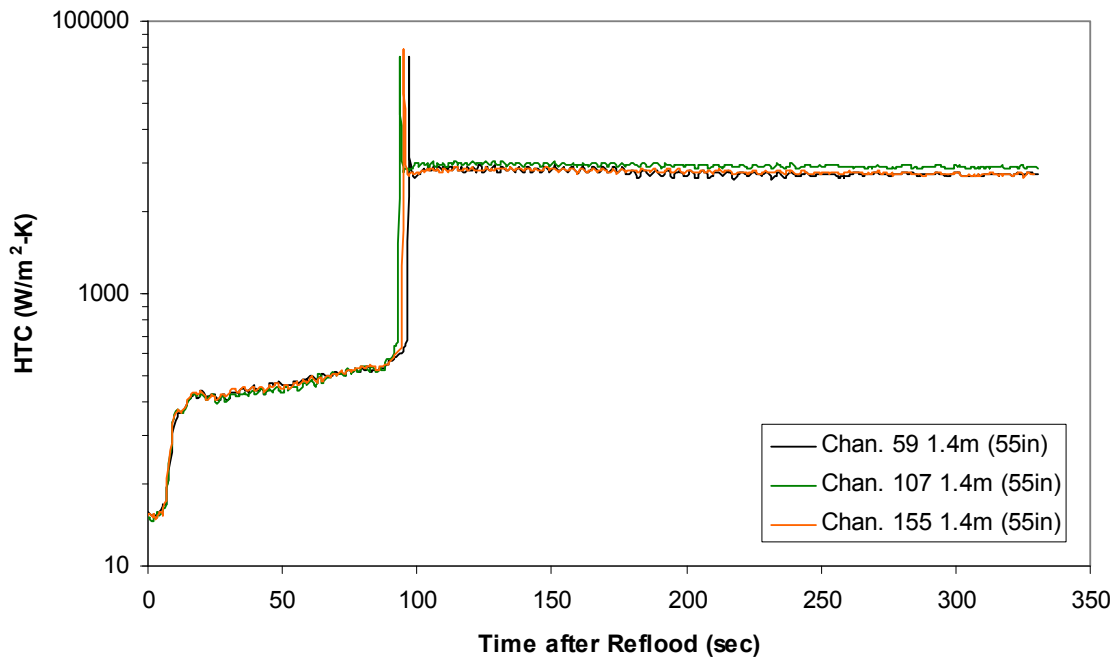
Spacer Grid Temperature during Reflood RBHT Exp. 1295



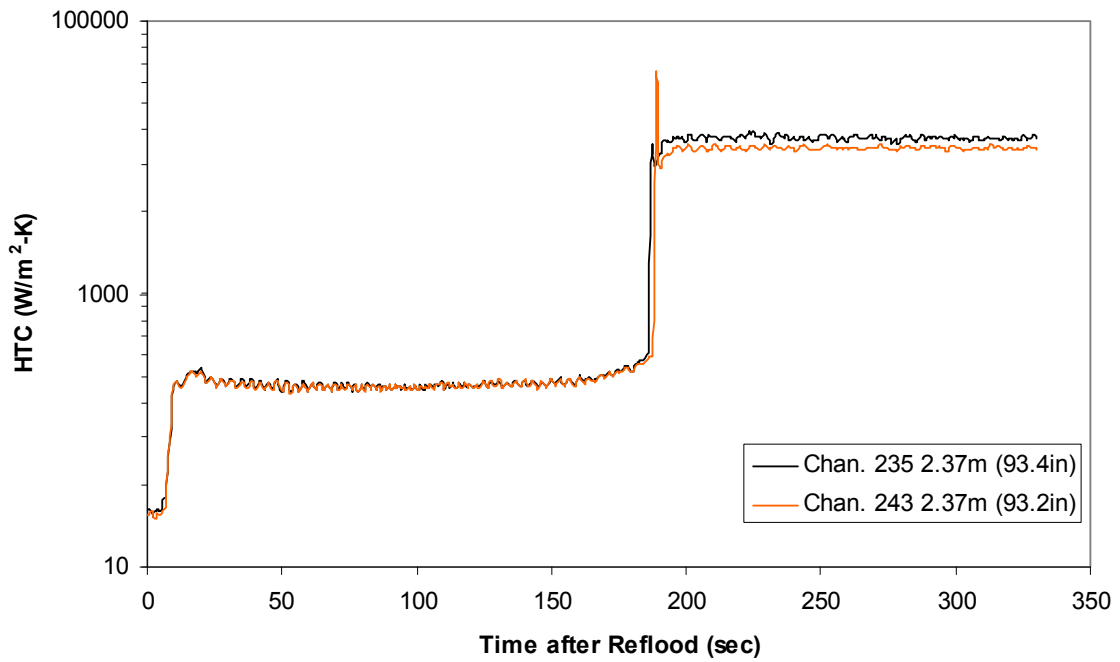
Heat Transfer Coefficient during Reflood RBHT Exp. 1295



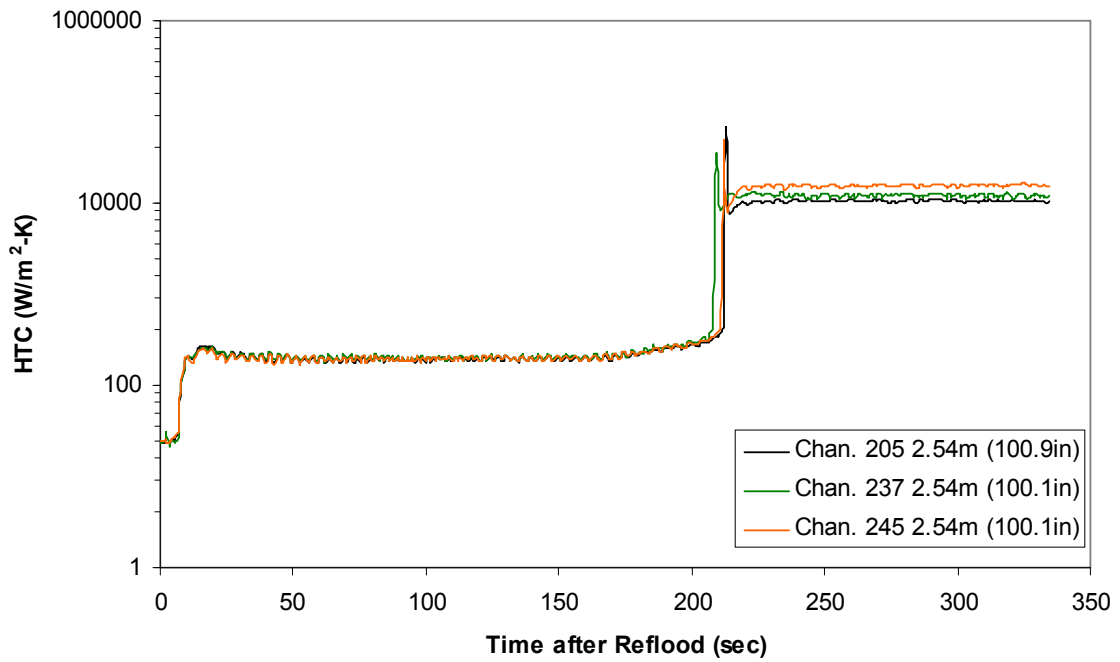
Heat Transfer Coefficient during Reflood
RBHT Exp. 1295



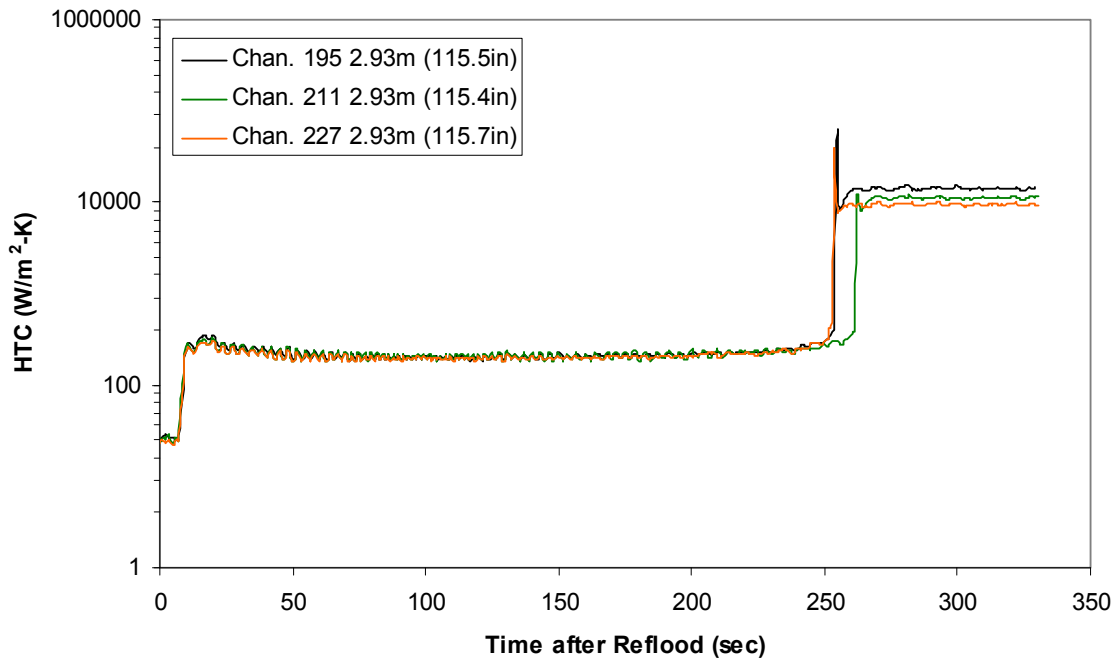
Heat Transfer Coefficient during Reflood
RBHT Exp. 1295



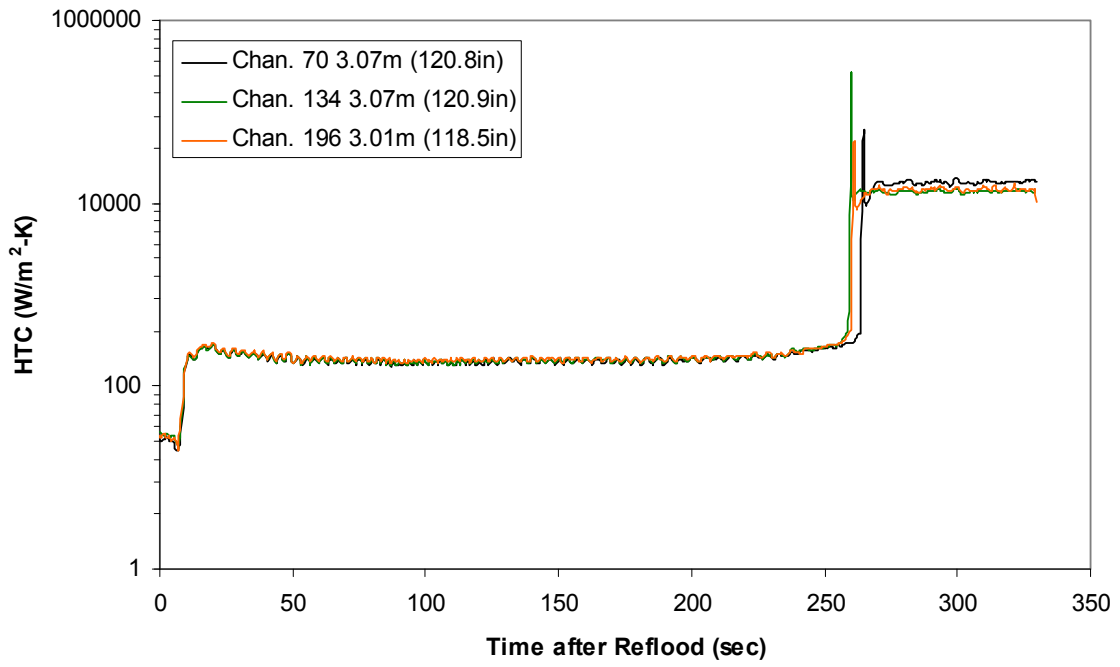
Heat Transfer Coefficient during Reflood RBHT Exp. 1295



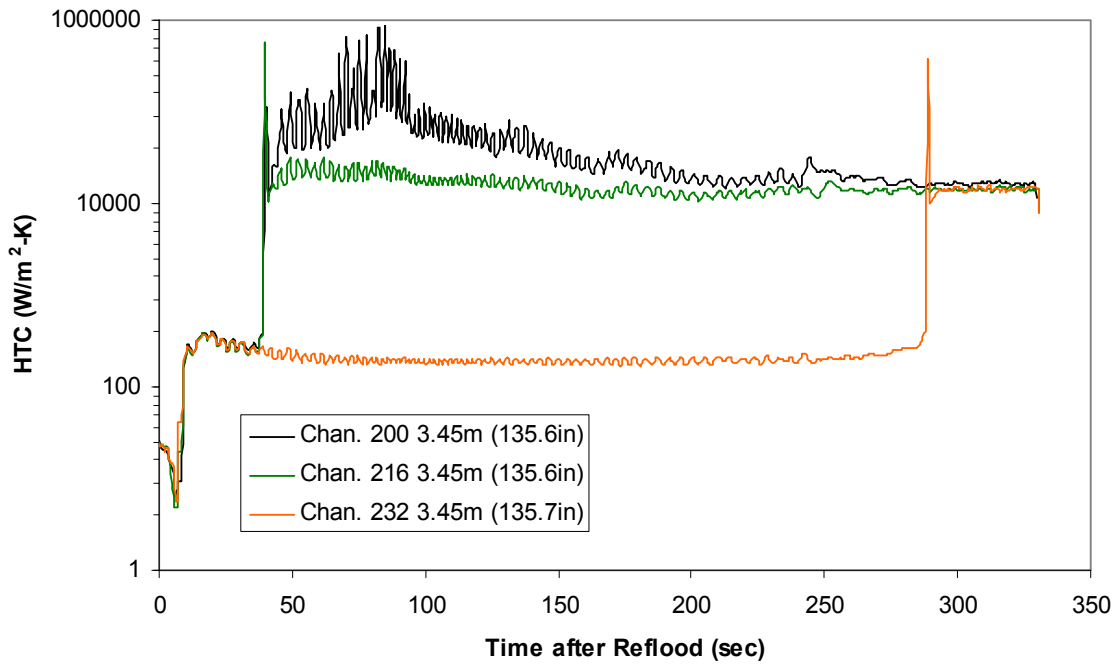
Heat Transfer Coefficient during Reflood RBHT Exp. 1295



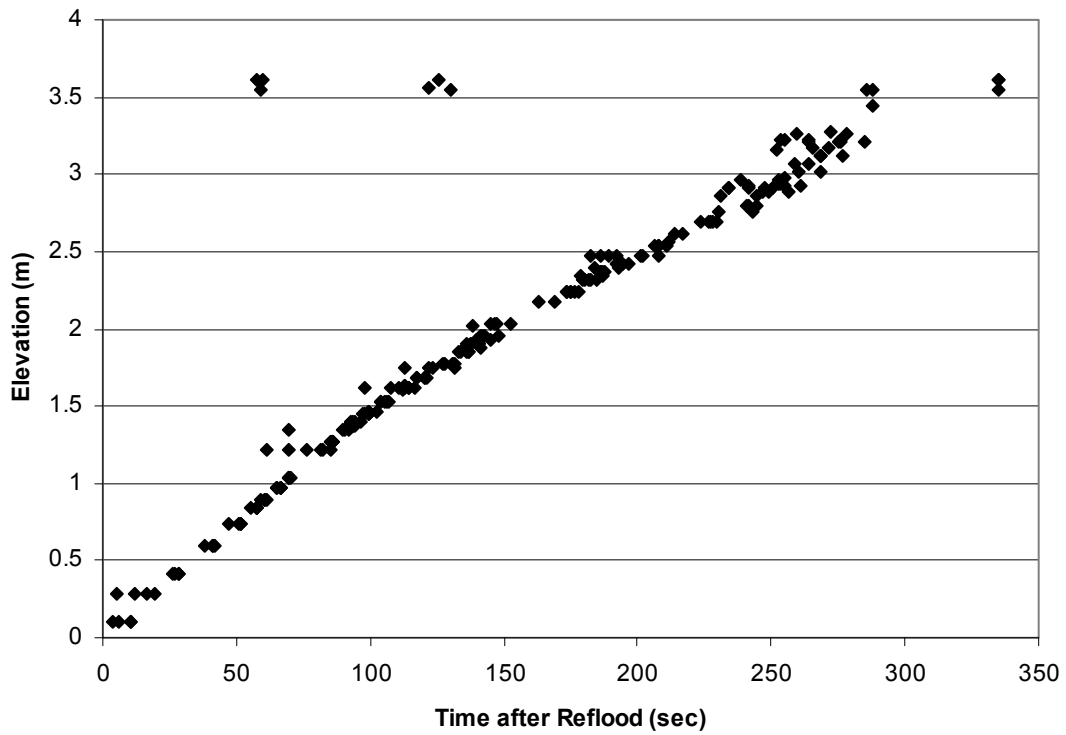
Heat Transfer Coefficient during Reflood RBHT Exp. 1295



Heat Transfer Coefficient during Reflood RBHT Exp. 1295



Quench Data, RBHT Exp. 1295



RBHT - REFLOOD TESTS

SUMMARY SHEET

RUN NO: **1300**

RUN CONDITIONS

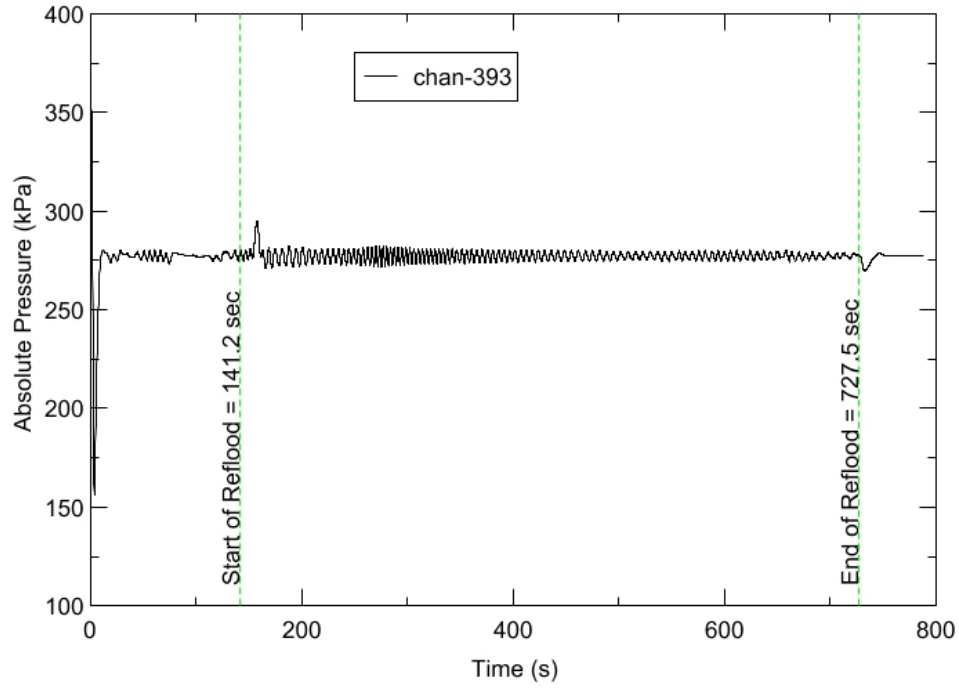
Upper Plenum Pressure:	276 kPa (40 psia)
Initial Peak Clad Temperature:	1144 degrees K (1600 degrees F)
Rod Peak Power:	2.3 kW/m (0.7 kW/ft)
Flooding Rate:	0.0762 m/s (3 in/s)
Inlet Subcooling:	76 degrees K (136 degrees F)
Start of Reflood:	141.2 s
End of Reflood:	727.5 s
Test Date:	7/23/2002
Comments:	No Droplet Data

Heater rod surfaces below 1m (40 in) quench to a temperature below saturation due to the high inlet subcooling. Therefore DATARH calculated heat transfer coefficients are not presented below this elevation after rod quench.

Rod_Elevation	Channel Number	Temperature at Reflood (K)	Temperature at Reflood (F)	Turnaround Time (sec.)	Turnaround Temperature (K)	Turnaround Temperature (F)	Quench Time (sec.)	Quench Temperature (K)	Quench Temperature (F)
B6_0.592m	148	779.38	943.19	13.05	822.85	1021.44	39.55	665.26	737.78
B6_0.744m	149	801.72	983.4	13.55	849.13	1068.75	50.55	653.82	717.18
B6_0.846m	150	830.76	1035.68	13.55	880.7	1125.58	59.55	637.89	688.52
B6_0.897m	151	841.84	1055.63	14.05	893.42	1148.48	63.55	640.86	693.86
C6_1.04m	137	891.56	1145.12	15.05	946.99	1244.89	76.55	655.6	720.4
D5_1.27m	217	951.72	1253.4	15.05	1011.31	1360.68	99.05	667.09	741.08
C6_1.34m	138	940.16	1232.61	15.55	1003.46	1346.54	106.55	658.37	725.38
D5_1.37m	218	972.66	1291.11	15.55	1036.02	1405.15	110.55	678.01	760.74
C6_1.39m	139	945.89	1242.92	16.05	1009.63	1357.64	112.55	667.31	741.47
D5_1.45m	219	985.04	1313.39	15.55	1049.91	1430.15	119.05	681.68	767.33
C6_1.47m	140	958.01	1264.73	15.55	1023.42	1382.47	121.55	676.47	757.95
D5_1.52m	220	996.14	1333.37	15.55	1063.11	1453.92	129.55	682.52	768.85
C6_1.62m	141	975.97	1297.06	27.05	1046.85	1424.65	142.05	686.95	776.82
D5_1.68m	221	1015.74	1368.64	32.05	1088.58	1499.76	151.05	691.19	784.45
D5_1.78m	222	1000.91	1341.94	14.55	1067	1460.91	166.05	712.54	822.88
D5_1.85m	223	1029.02	1392.55	14.55	1099.84	1520.02	177.05	676.86	758.66
C6_1.87m	142	1006.58	1352.15	15.05	1079.46	1483.34	180.05	686.09	775.27
D5_1.90m	224	1037.45	1407.73	15.05	1110.74	1539.64	160.55	758.66	905.89
C6_1.95m	144	1017.76	1372.28	15.05	1092.2	1506.27	191.55	704.02	807.55
C3_2.17m	178	1046.59	1424.18	14.55	1122.02	1559.95	231.05	743.13	877.94
D4_2.24m	241	1096.88	1514.7	14.05	1172.11	1650.11	255.05	697.8	796.36
D4_2.32m	242	1105.58	1530.36	14.55	1185.28	1673.81	270.05	733.12	859.92
C3_2.35m	180	1097.46	1515.74	15.05	1181.17	1666.42	264.05	773.34	932.32
D4_2.37m	243	1112.85	1543.45	14.55	1194.05	1689.61	281.55	740.91	873.94
C3_2.40m	181	1100.04	1520.39	15.05	1184.12	1671.73	275.55	775.81	936.76
D4_2.54m	245	1137.43	1587.69	14.05	1218.87	1734.27	331.05	745.48	882.17
D6_2.62m	129	1126.36	1567.76	14.05	1210.47	1719.16	337.05	784.47	952.36
D6_2.69m	130	1125.98	1567.08	14.05	1211.36	1720.76	359.55	794.27	970
C3_2.76m	183	1124.27	1564	14.55	1208.89	1716.31	377.55	810.77	999.7
D4_2.79m	247	1096.02	1513.15	13.55	1173.45	1652.53	408.05	718.97	834.45
D6_2.87m	131	1067.07	1461.03	13.55	1144.87	1601.07	406.55	734.38	862.19
D6_2.92m	132	1039.57	1411.54	15.05	1121.73	1559.43	418.05	752.87	895.49
D6_2.97m	133	1008.46	1355.54	15.05	1086.09	1495.28	431.55	749.42	889.27
D6_3.07m	134	971.61	1289.21	15.05	1042.84	1417.43	449.55	749.69	889.76
E3_3.12m	197	975.87	1296.88	15.05	1046.37	1423.78	478.05	716.19	829.46
D6_3.17m	135	938.75	1230.06	15.05	1004.53	1348.47	470.05	734.47	862.36
D6_3.27m	136	893.4	1148.44	15.55	957.05	1263	489.05	725.67	846.52
D4_3.61m	248	678.33	761.31	15.55	753.04	895.79	547.05	580.89	585.92

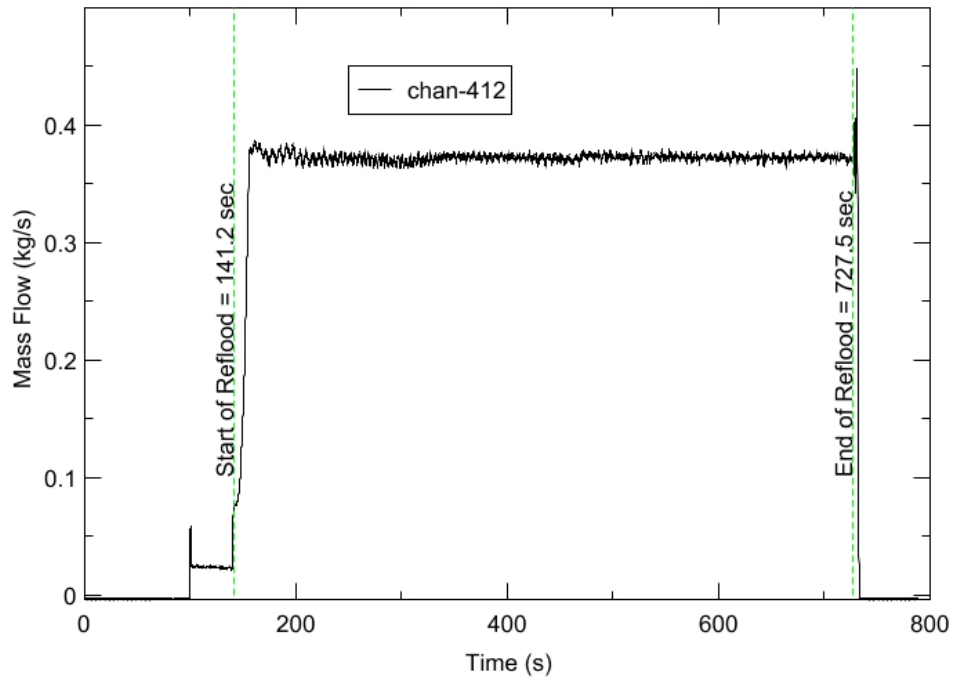
RBHT - TEST FACILITY

Upper Plenum Pressure vs. Time, Exp 1300



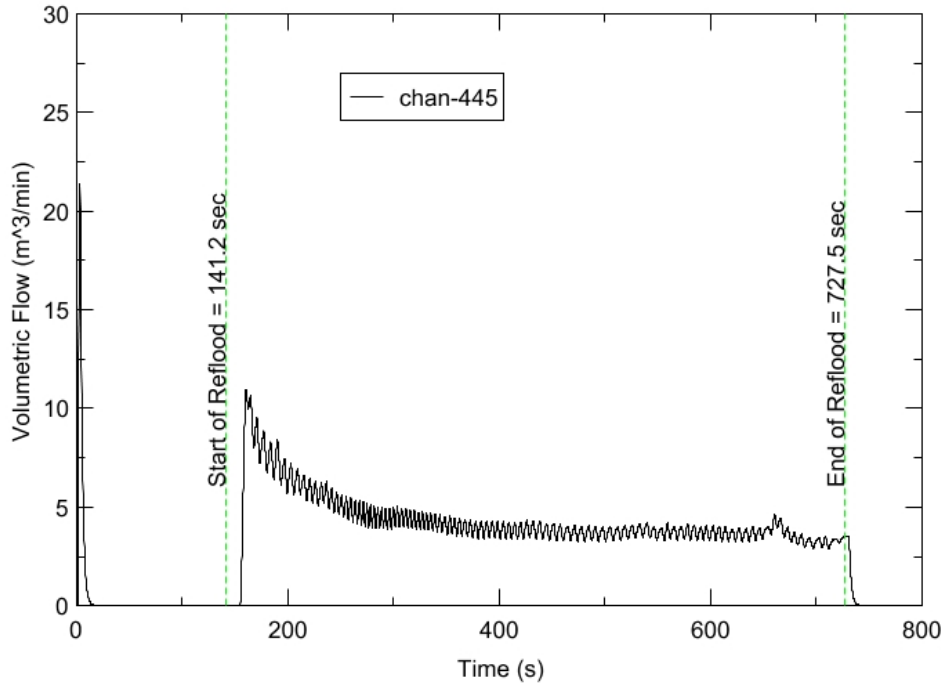
RBHT - TEST FACILITY

Inlet Flow vs. Time, Exp 1300



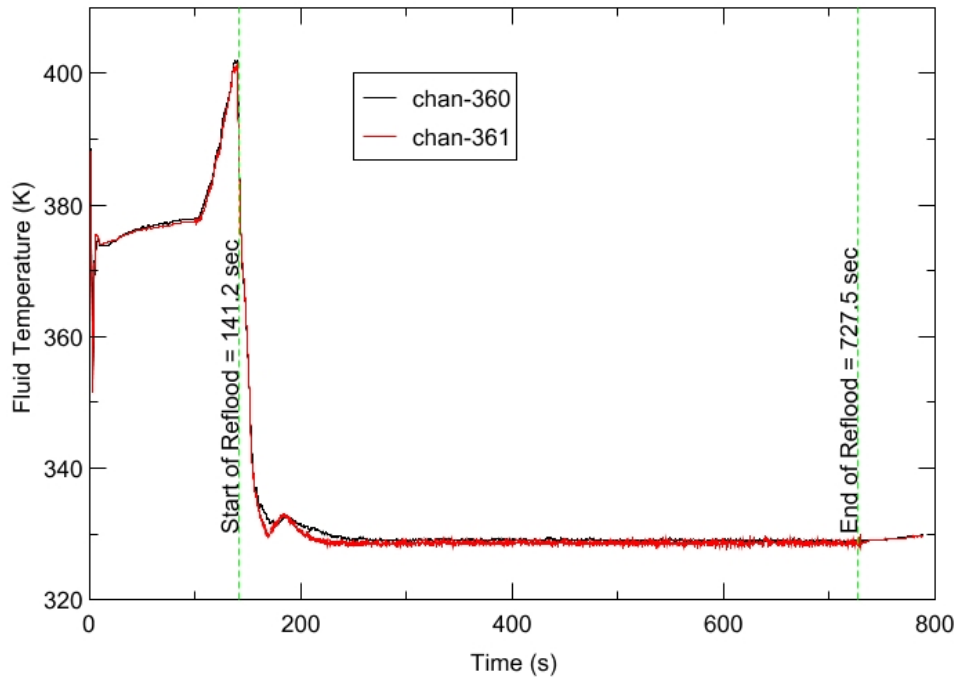
RBHT - TEST FACILITY

Steam Exhaust Flow vs. Time, Exp 1300



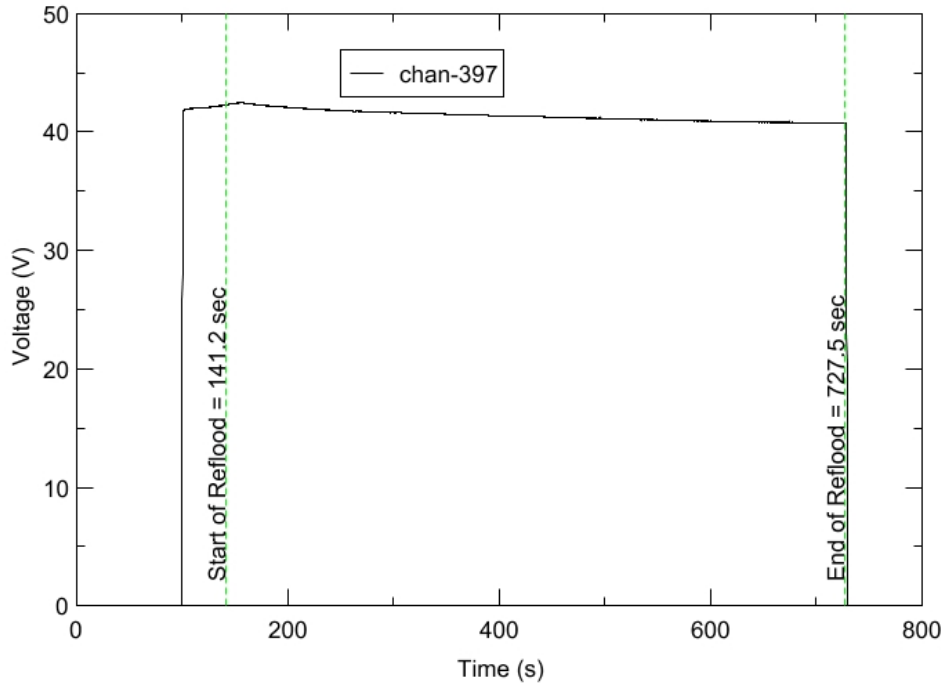
RBHT - TEST FACILITY

Inlet Flow Temperature vs. Time, Exp 1300



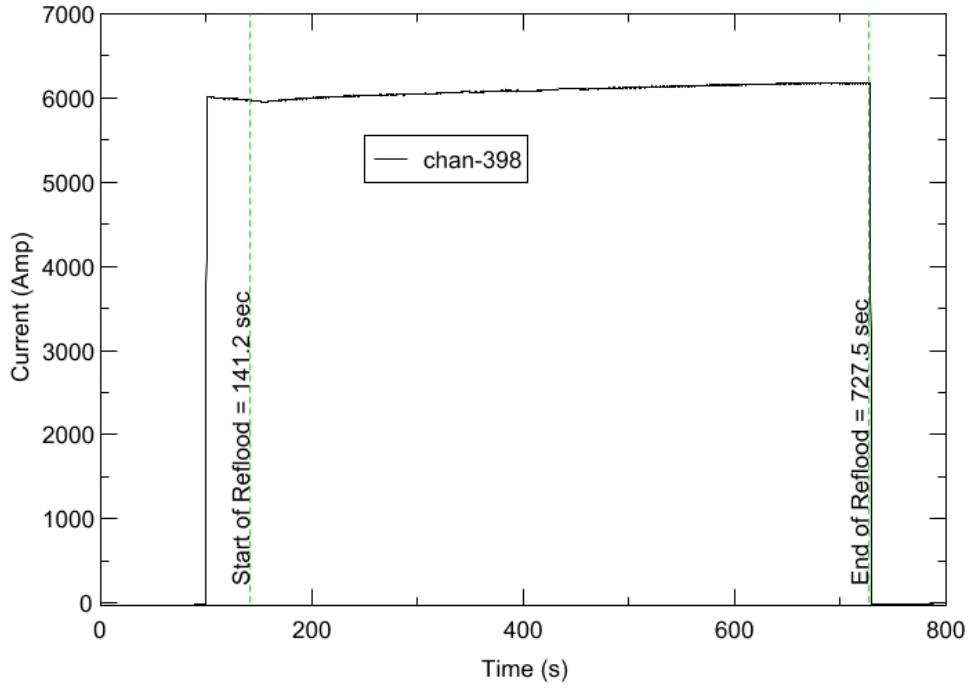
RBHT - TEST FACILITY

Test Section Voltage vs. Time, Exp 1300

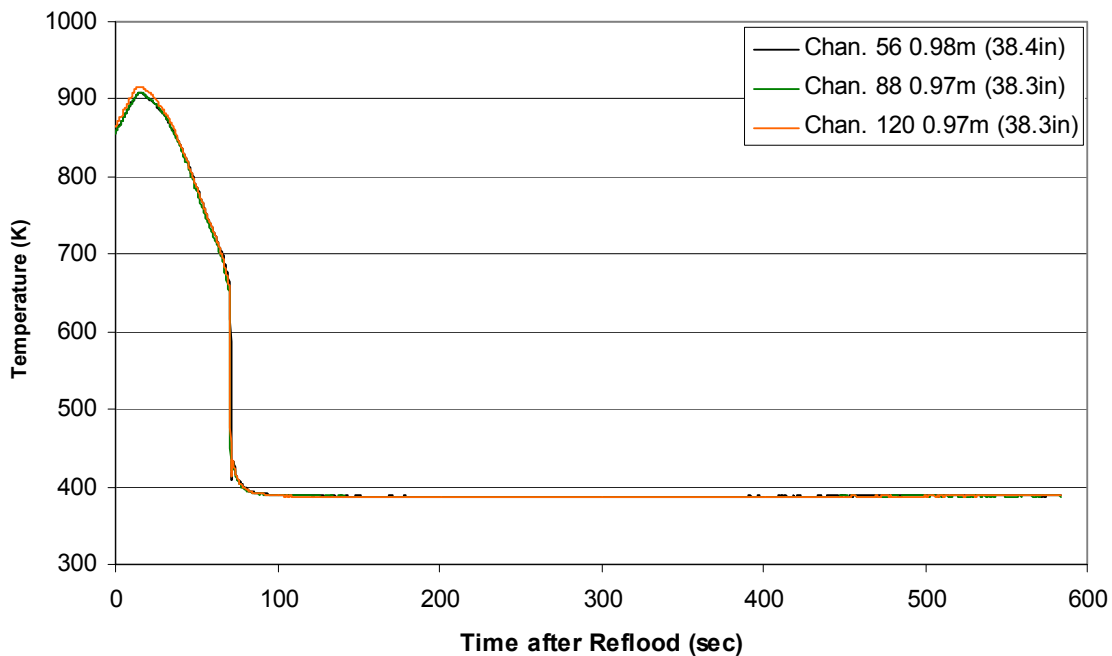


RBHT - TEST FACILITY

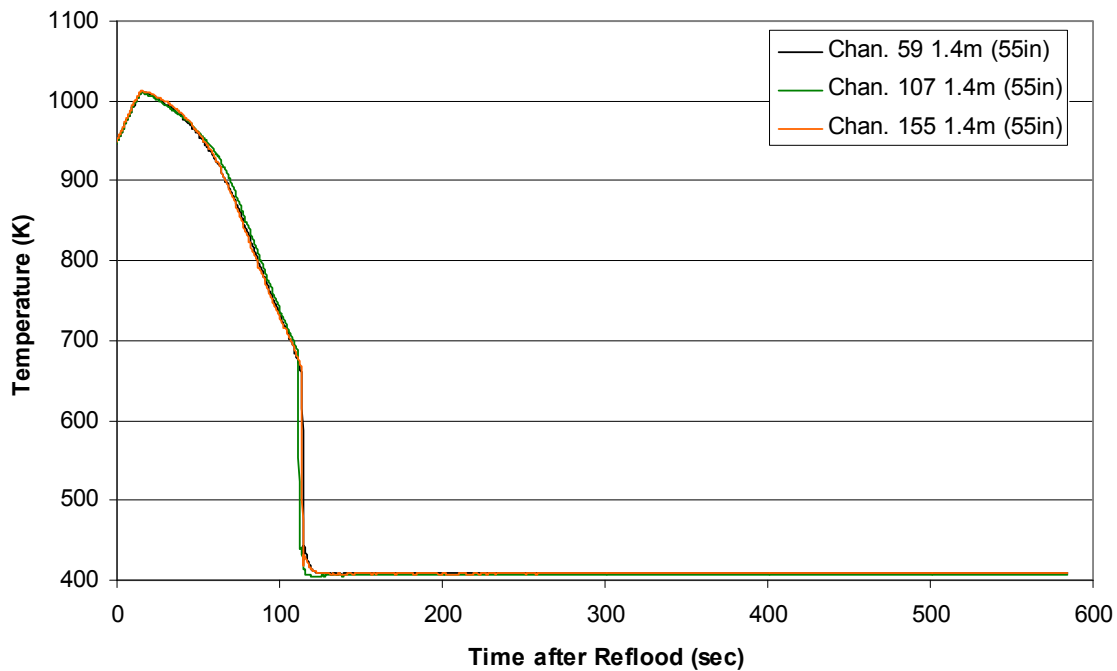
Test Section Current vs. Time, Exp 1300



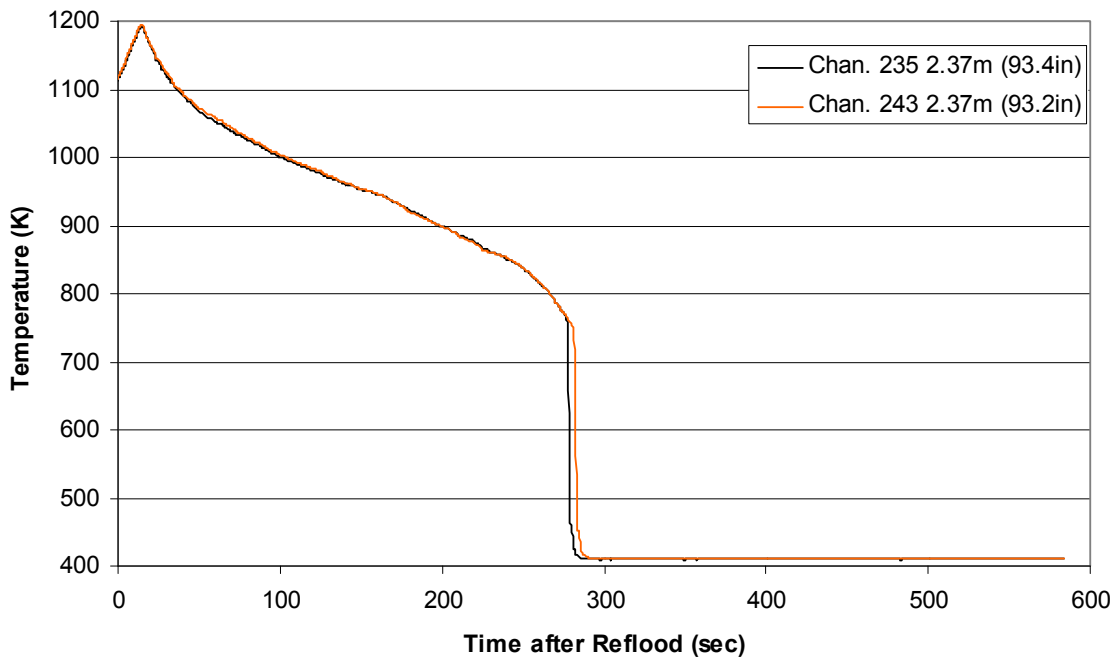
Heater Rod Temperature during Reflood RBHT Exp. 1300



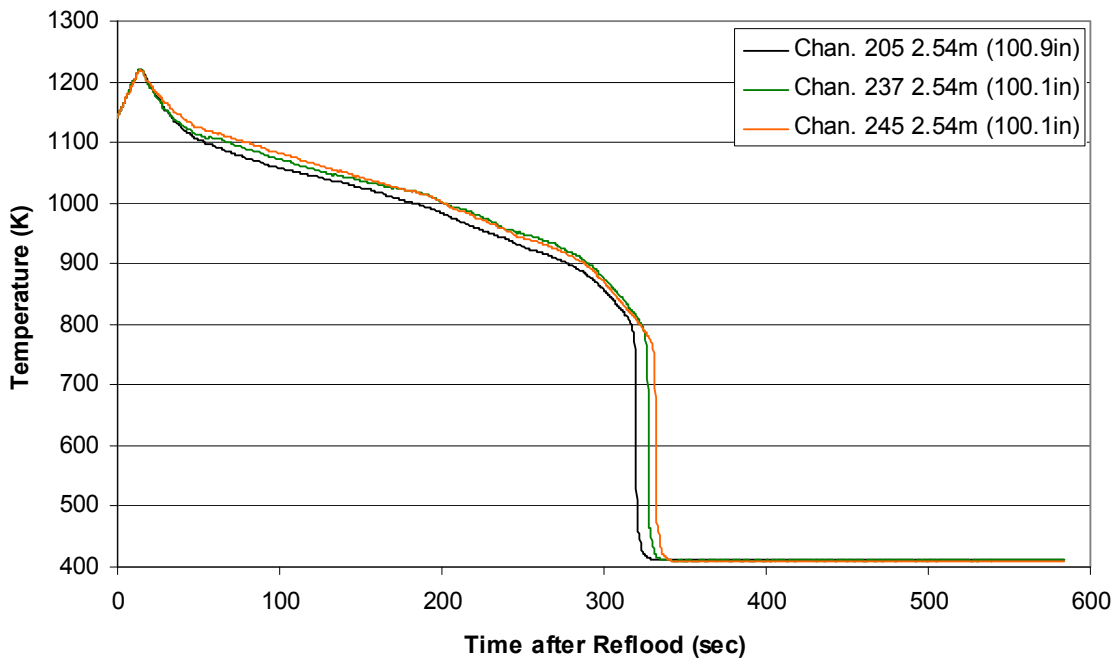
Heater Rod Temperature during Reflood RBHT Exp. 1300



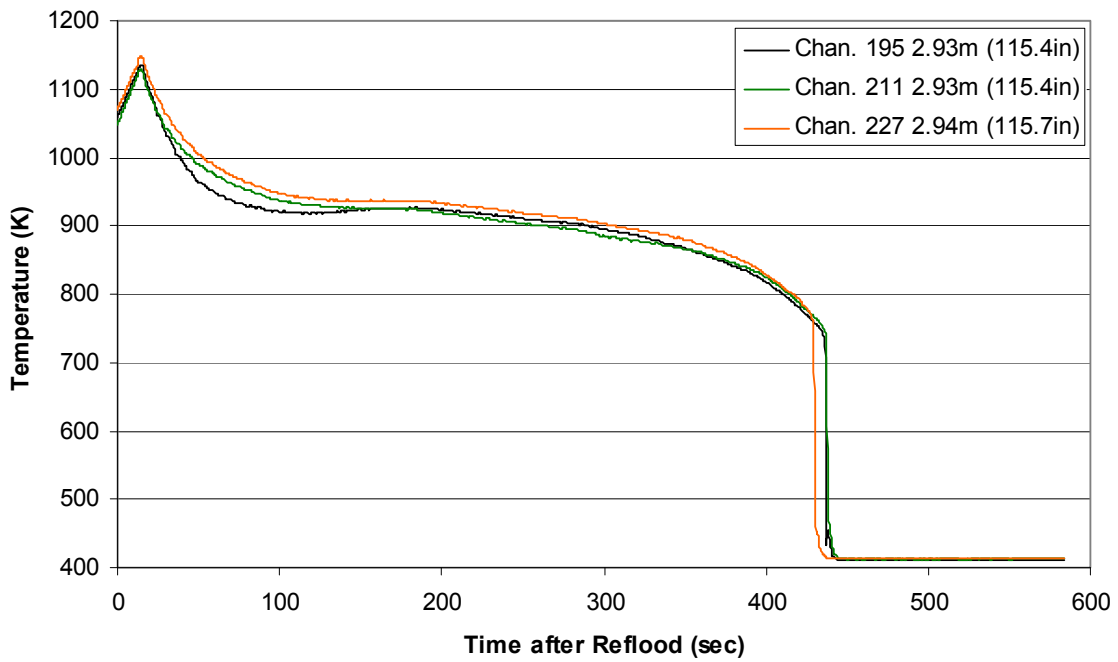
**Heater Rod Temperature during Reflood
RBHT Exp. 1300**



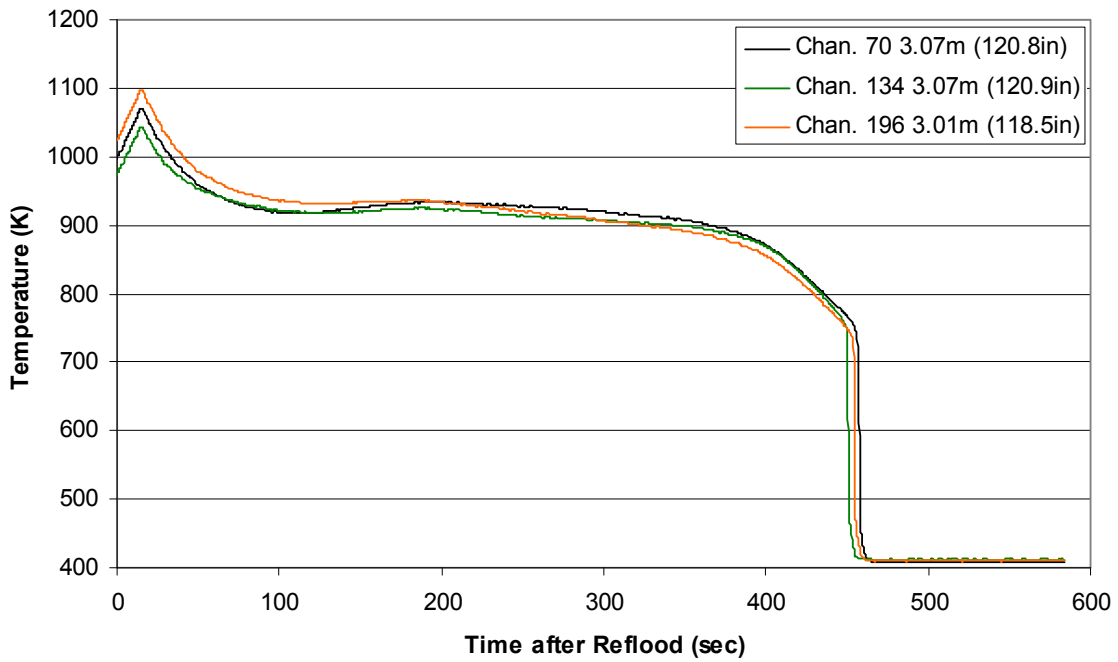
**Heater Rod Temperature during Reflood
RBHT Exp. 1300**



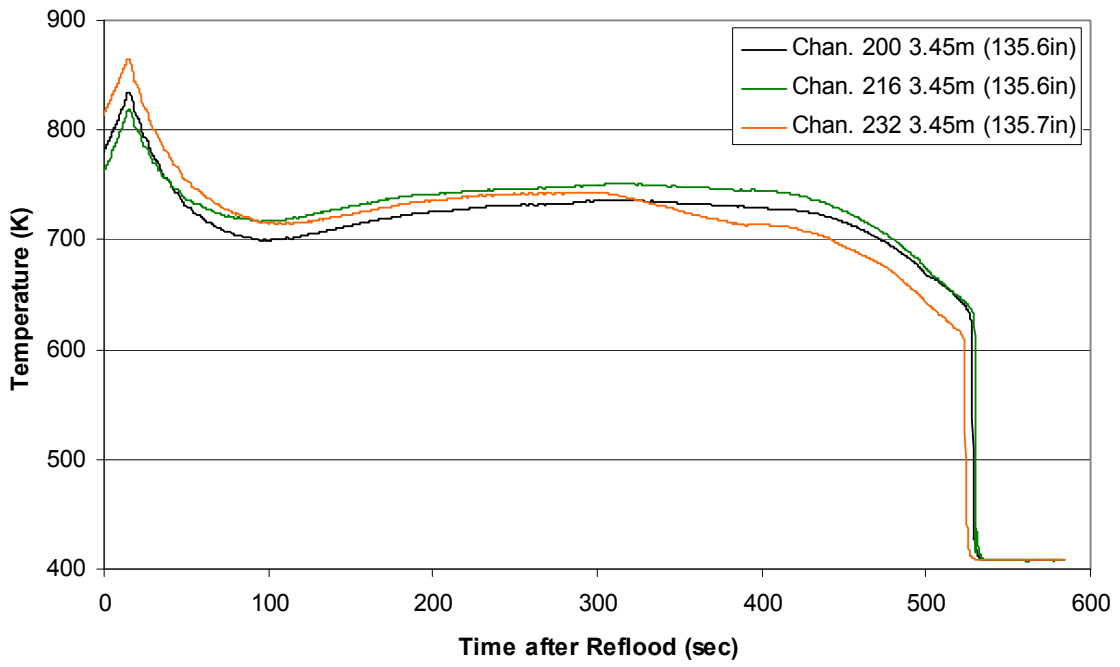
**Heater Rod Temperature during Reflood
RBHT Exp. 1300**



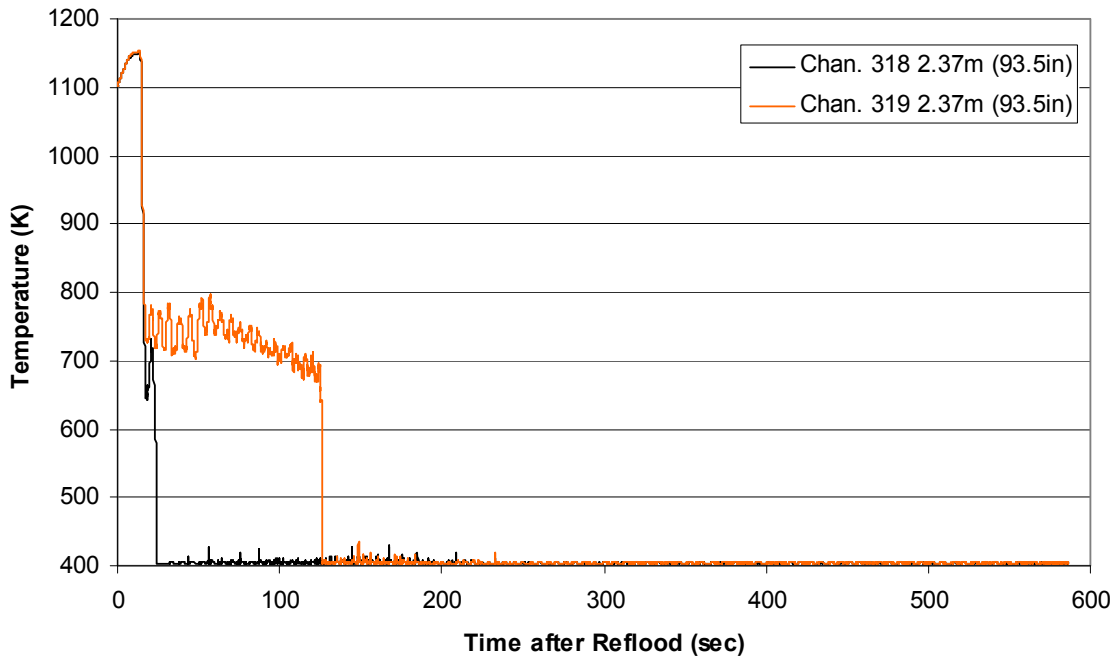
**Heater Rod Temperature during Reflood
RBHT Exp. 1300**



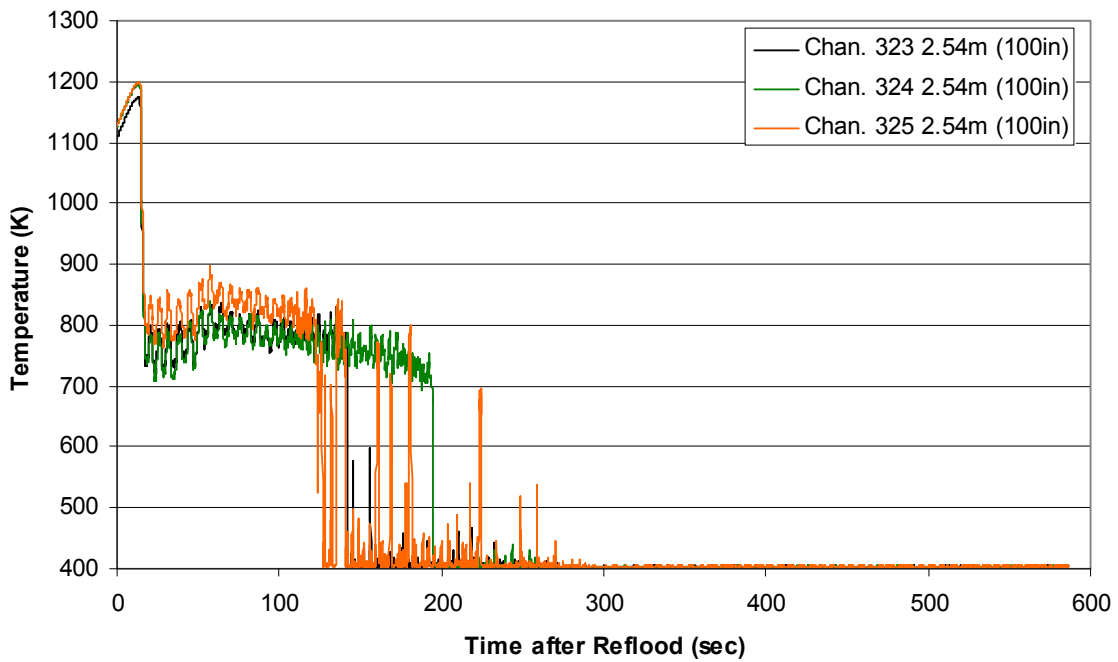
Heater Rod Temperature during Reflood RBHT Exp. 1300



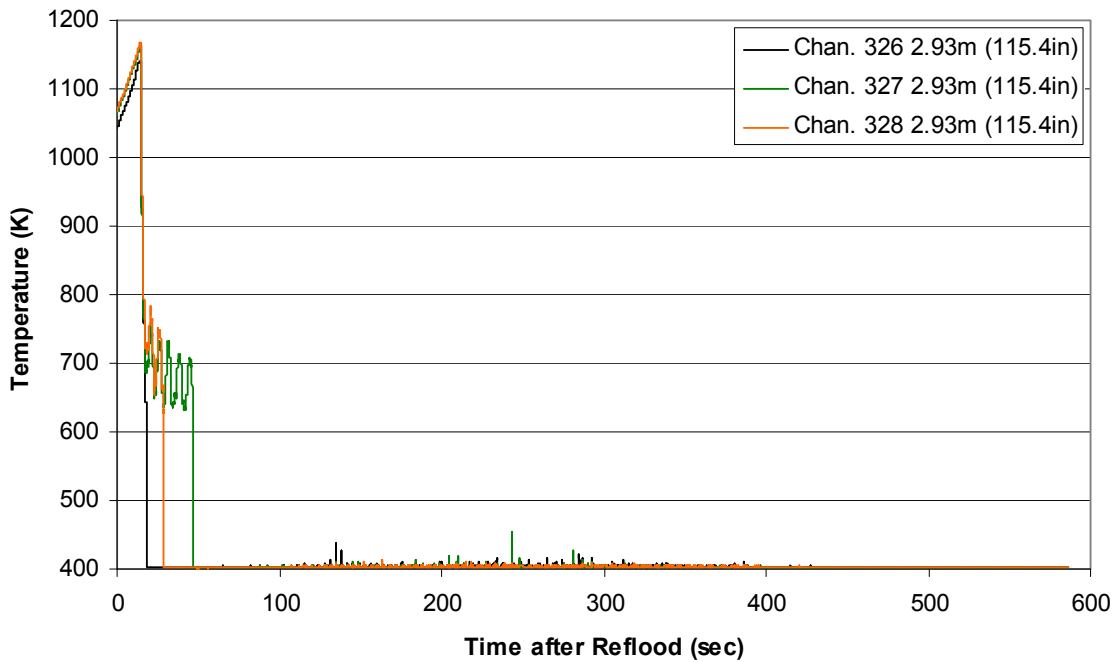
Steam Probe Temperature during Reflood RBHT Exp. 1300



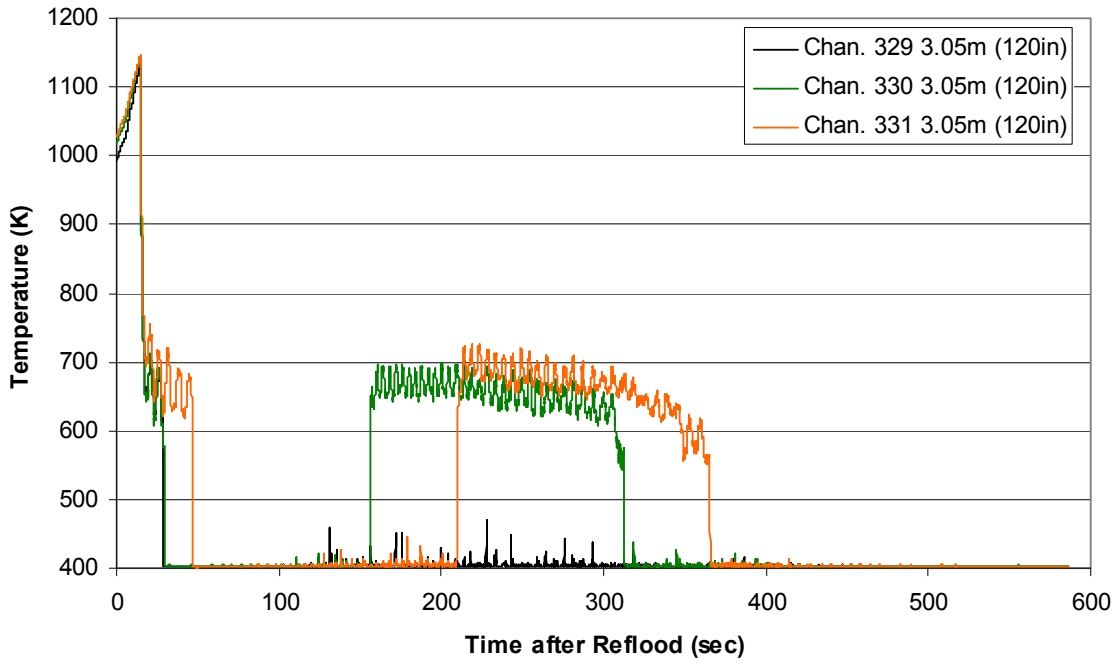
Steam Probe Temperature during Reflood RBHT Exp. 1300



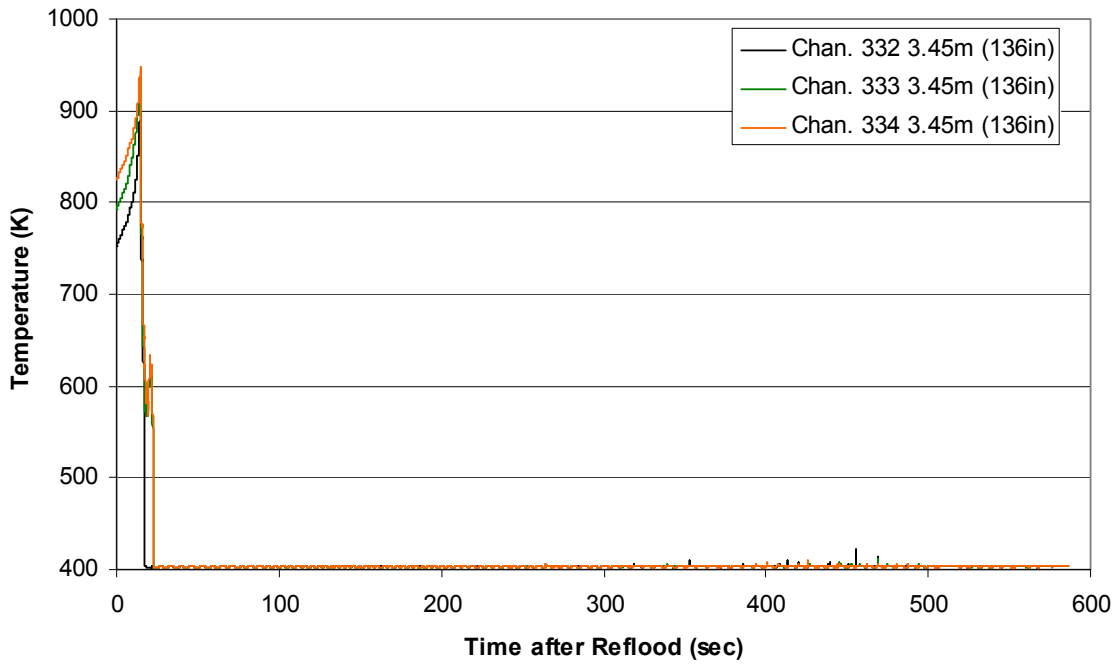
Steam Probe Temperature during Reflood RBHT Exp. 1300



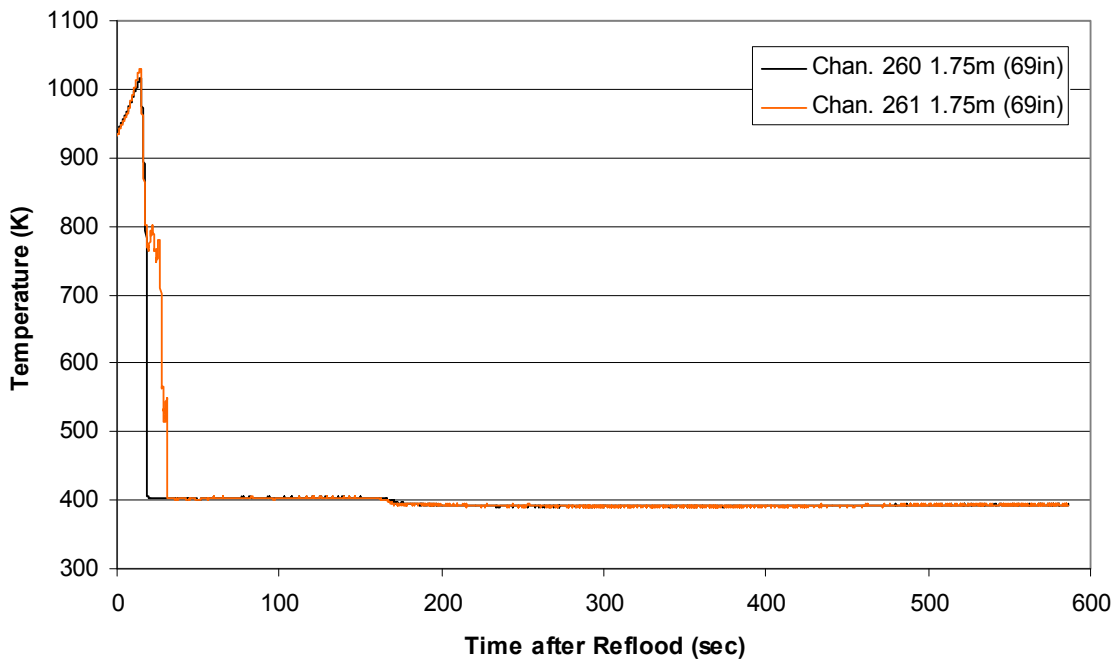
Steam Probe Temperature during Reflood RBHT Exp. 1300



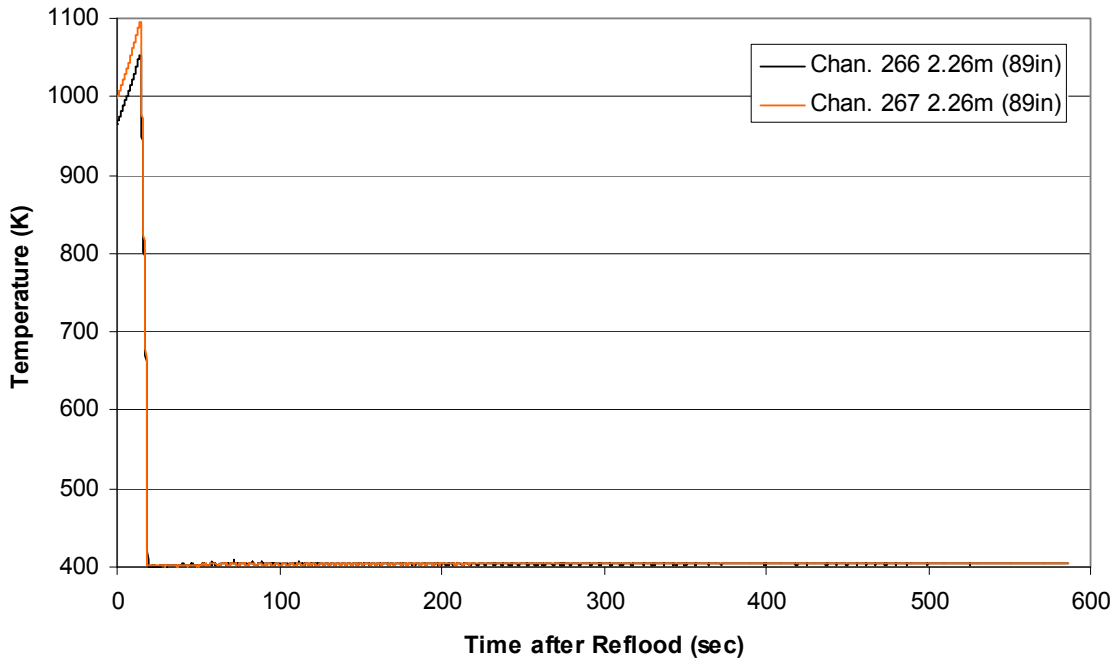
Steam Probe Temperature during Reflood RBHT Exp. 1300



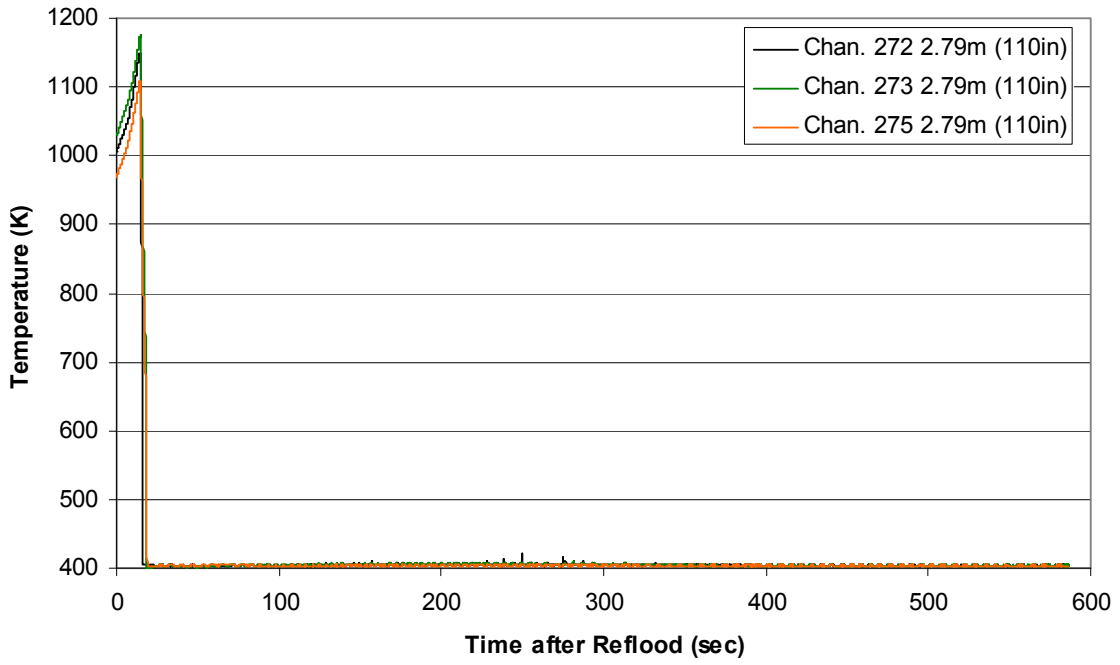
**Spacer Grid Temperature during Reflood
RBHT Exp. 1300**



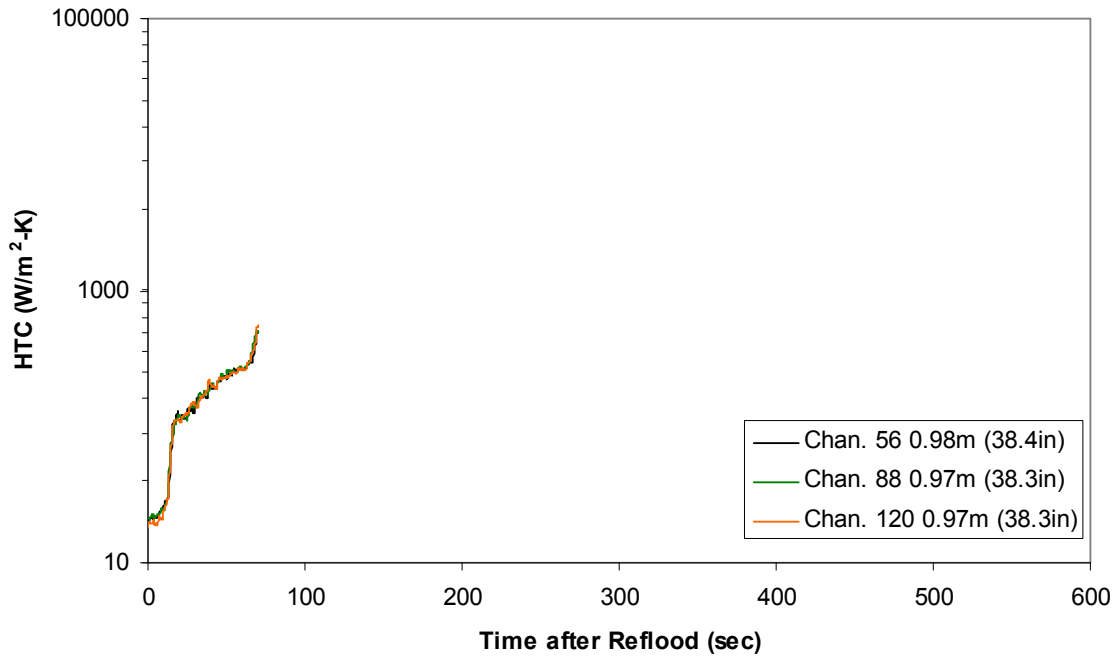
**Spacer Grid Temperature during Reflood
RBHT Exp. 1300**



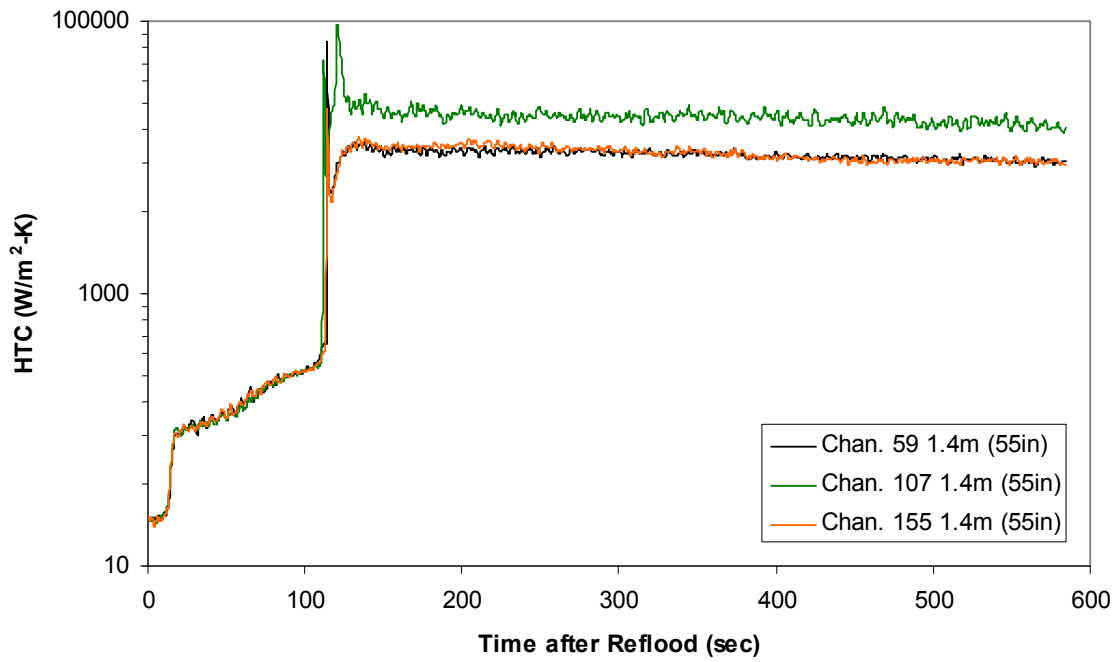
Spacer Grid Temperature during Reflood RBHT Exp. 1300



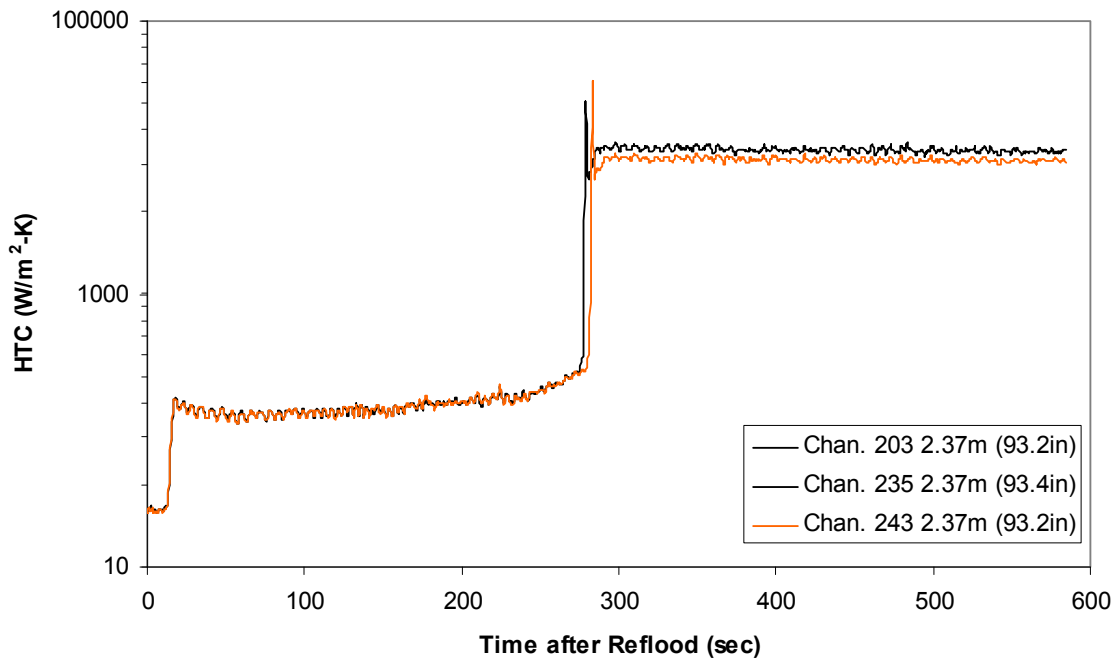
Heat Transfer Coefficient during Reflood RBHT Exp. 1300



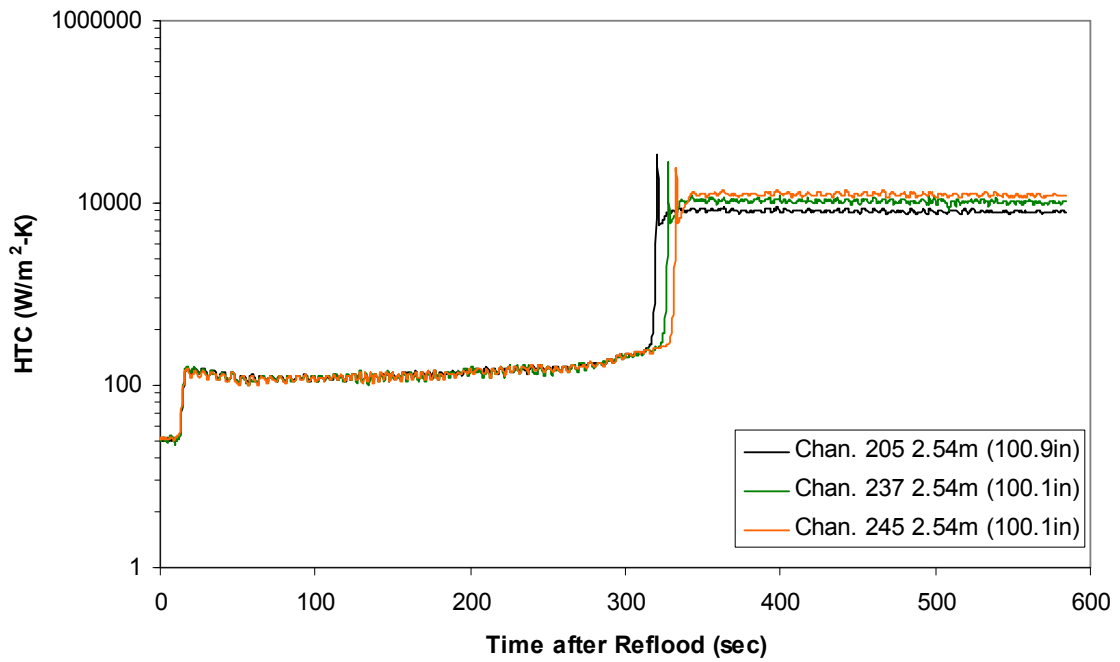
Heat Transfer Coefficient during Reflood
RBHT Exp. 1300



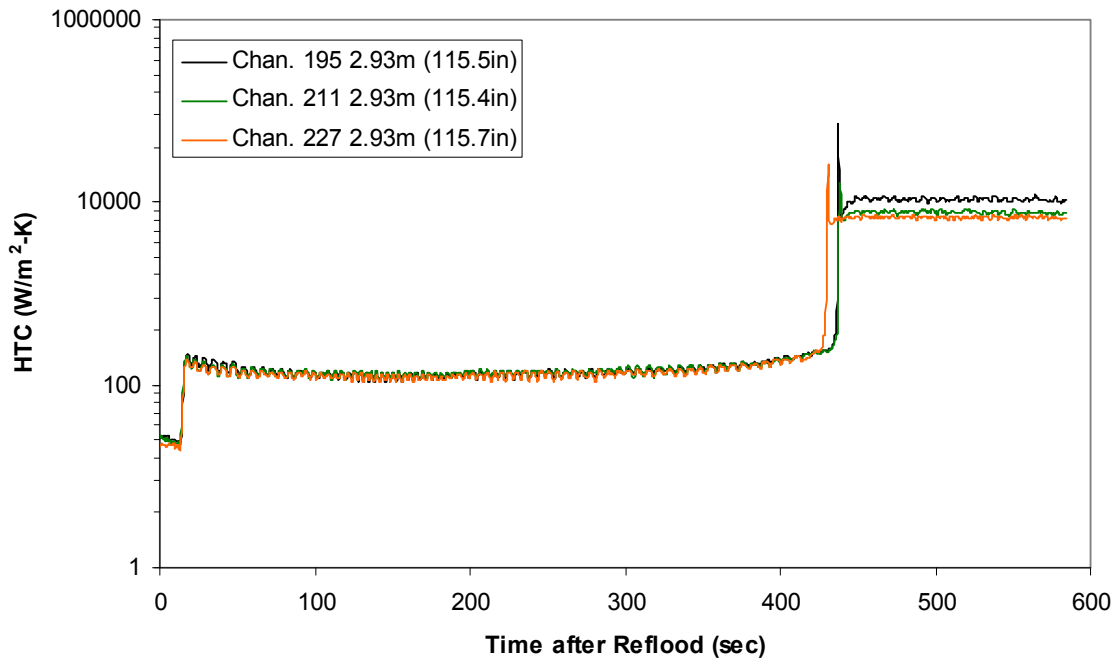
Heat Transfer Coefficient during Reflood
RBHT Exp. 1300



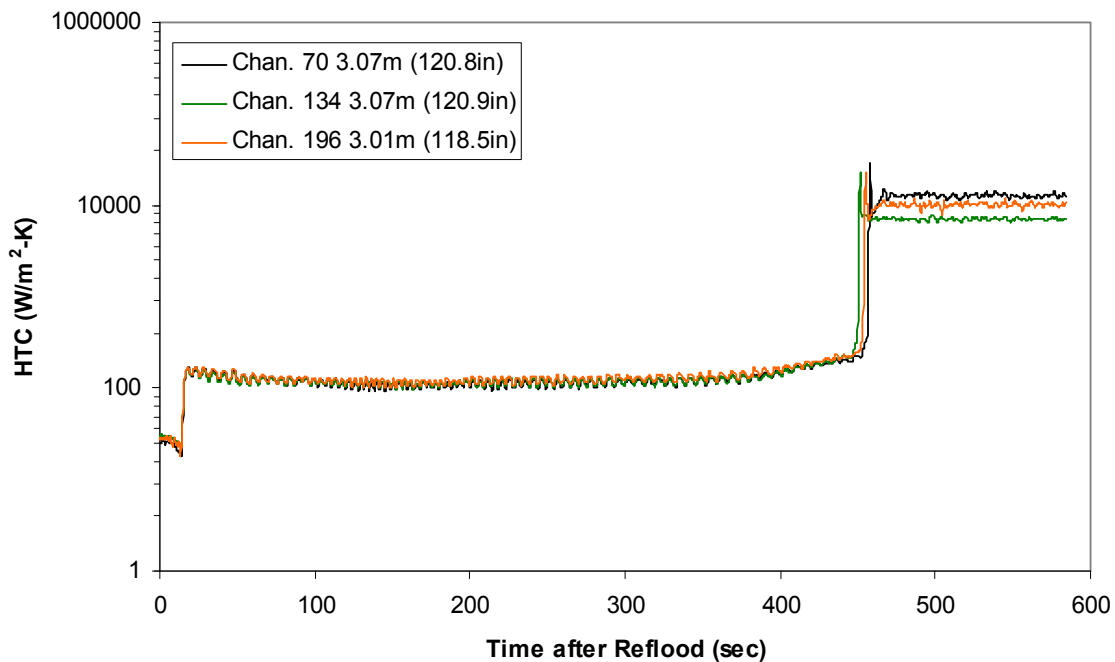
Heat Transfer Coefficient during Reflood RBHT Exp. 1300



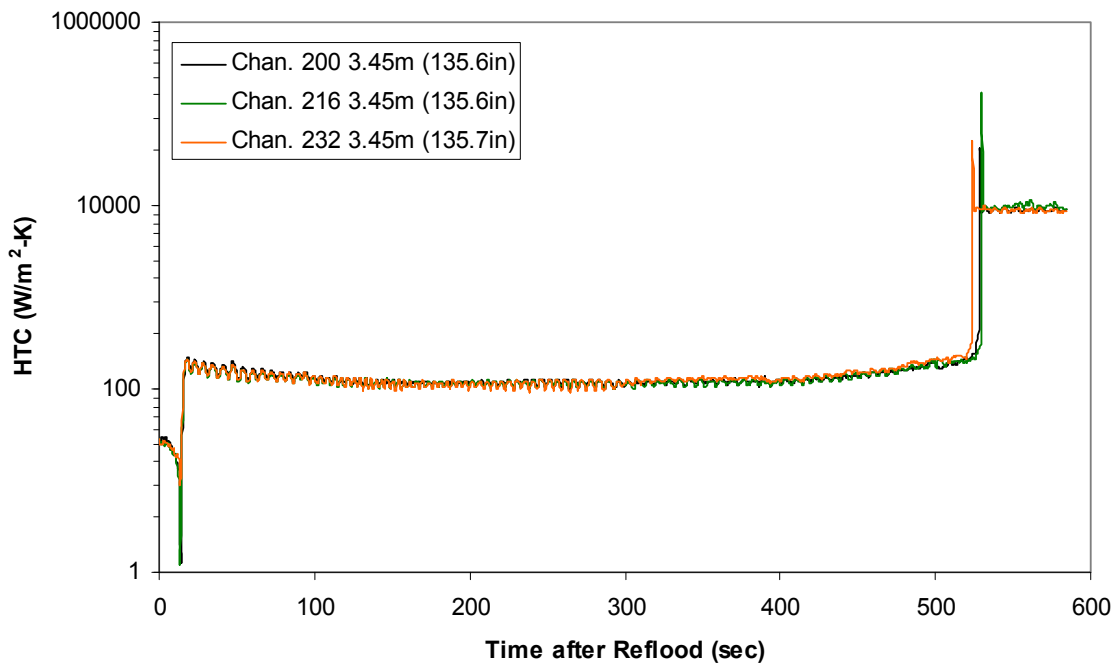
Heat Transfer Coefficient during Reflood RBHT Exp. 1300



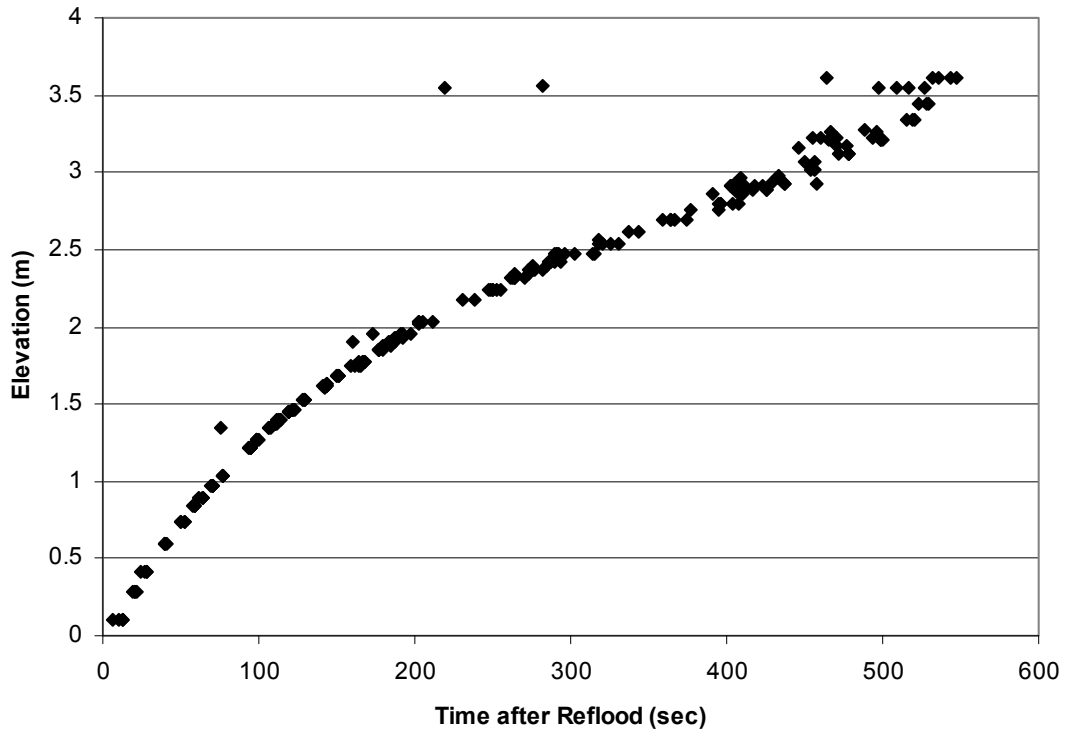
Heat Transfer Coefficient during Reflood RBHT Exp. 1300



Heat Transfer Coefficient during Reflood RBHT Exp. 1300



Quench Data, RBHT Exp. 1300



RBHT - REFLOOD TESTS

SUMMARY SHEET

RUN NO: **1310**

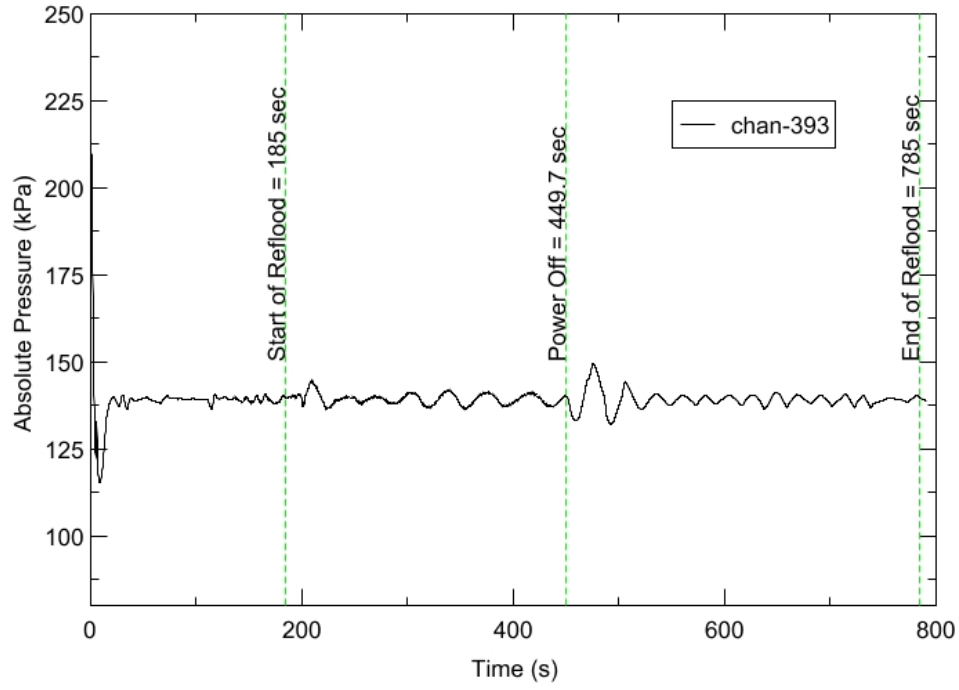
RUN CONDITIONS

Upper Plenum Pressure:	138 kPa (20 psia)
Initial Peak Clad Temperature:	1033 degrees K (1400 degrees F)
Rod Peak Power:	1.31 kW/m (0.4 kW/ft)
Flooding Rate:	0.0254 m/s (1 in/s)
Inlet Subcooling:	11 degrees K (20 degrees F)
Start of Reflood:	185 s
End of Reflood:	785 s
Test Date:	8/1/2002
Comments:	Power turn off at 449.7 seconds. Inlet flow continued until entire bundle quenched. DATARH heat transfer coefficients calculated until power was turned off. Droplet data was collected until approximately 60 seconds after power was turn off.

Rod_Elevation	Channel Number	Temperature at Reflood (K)	Temperature at Reflood (°F)	Turnaround Time (sec.)	Turnaround Temperature (K)	Turnaround Temperature (°F)	Quench Time (sec.)	Quench Temperature (K)	Quench Temperature (°F)
B6 0.592m	148	740.02	872.35	14.25	766.12	919.32	98.75	574.9	575.13
B6 0.744m	149	765.23	917.72	15.25	794.11	969.7	135.25	559.08	546.66
B6 0.846m	150	786.03	955.17	15.75	817.39	1011.61	161.25	587.47	597.75
B6 0.897m	151	794.09	969.67	18.75	826.77	1028.49	179.75	597.05	615.01
C6 1.04m	137	838.52	1049.65	63.25	881.71	1127.38	237.25	564.8	556.96
D5 1.27m	217	896.12	1153.33	47.25	945.76	1242.69	301.75	600.59	621.37
C6 1.34m	138	878.04	1120.78	74.75	940.68	1233.54	317.75	579.98	584.28
D5 1.37m	218	910.69	1179.56	74.75	980.89	1305.91	321.25	602.67	625.11
C6 1.39m	139	882.16	1128.2	118.25	962.42	1272.66	326.25	587.87	598.49
D5 1.45m	219	919.6	1195.6	117.75	1009.5	1357.42	334.25	589.84	602.03
C6 1.47m	140	891.1	1144.29	146.75	993.13	1327.95	339.75	586.15	595.38
D5 1.52m	220	927.5	1209.81	150.75	1046.06	1423.21	348.25	590.66	603.5
C6 1.62m	141	901.29	1162.64	226.75	1063.29	1454.23	367.25	573.74	573.05
D5 1.68m	221	935.25	1223.76	227.75	1121.18	1558.44	376.75	575.65	576.48
D5 1.78m	222	926.16	1207.39	227.75	1073.13	1471.94	393.75	560.96	550.04
D5 1.85m	223	945.82	1242.79	186.75	1092.91	1507.55	398.25	534.73	502.83
C6 1.87m	142	917.57	1191.94	149.25	1060.97	1450.06	396.75	553.27	536.2
D5 1.90m	224	952.69	1255.16	227.75	1124.74	1564.85	402.25	561.6	551.19
C6 1.95m	144	931.53	1217.06	227.75	1102.44	1524.71	406.25	577.99	580.7
C3 2.17m	178	971.53	1289.06	264.75	1148.01	1606.72	446.75	558.5	545.62
D4 2.24m	241	1015.21	1367.7	264.75	1145.8	1602.76	444.75	521.91	479.75
D4 2.32m	242	1023.52	1382.66	264.75	1183.81	1671.16	451.25	566.92	560.77
C3 2.35m	180	1013.96	1365.44	264.75	1186.67	1676.32	456.75	551.37	532.77
D4 2.37m	243	1029.23	1392.93	264.75	1195.43	1692.09	460.25	555.82	540.79
C3 2.40m	181	1016.53	1370.07	264.75	1188.14	1678.97	464.75	555.92	540.97
D4 2.54m	245	1049.99	1430.29	265.25	1265.79	1818.73	488.75	546.25	523.56
D6 2.62m	129	1035.71	1404.59	265.25	1261.81	1811.57	494.25	555.26	539.78
D6 2.69m	130	1036.53	1406.07	265.25	1279.06	1842.62	504.25	561.61	551.22
C3 2.76m	183	1036.61	1406.2	265.25	1288.44	1859.5	515.75	557.88	544.5
D4 2.79m	247	1025.71	1386.59	286.25	1211.09	1720.27	513.25	499	438.51
D6 2.87m	131	998	1336.72	265.25	1083.9	1491.32	510.25	500.9	441.94
D6 2.92m	132	975.72	1296.61	265.25	1095.8	1512.75	513.25	535.31	503.87
D6 2.97m	133	947.16	1245.19	264.75	1094.89	1511.11	520.25	544.13	519.75
D6 3.07m	134	909.85	1178.04	264.75	1091.34	1504.72	527.75	551.57	533.14
E3 3.12m	197	908.67	1175.91	264.75	1099.62	1519.64	538.25	526.54	488.08
D6 3.17m	135	875.08	1115.45	264.75	1080.92	1485.97	538.75	543.65	518.89
D6 3.27m	136	835.23	1043.72	264.75	1057.54	1443.89	549.25	536.33	505.7

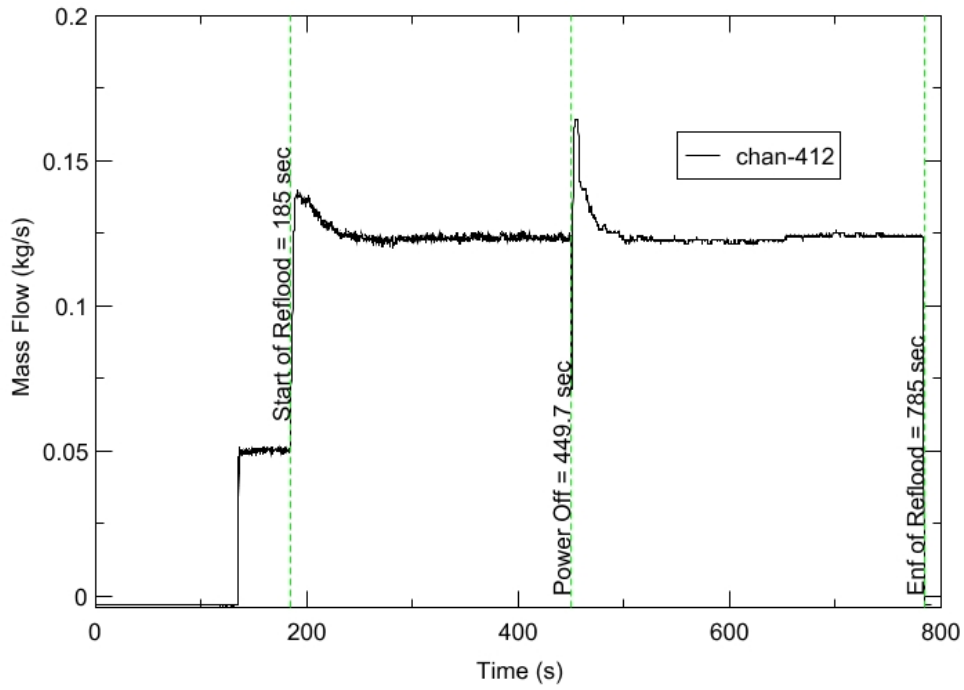
RBHT - TEST FACILITY

Upper Plenum Pressure vs. Time, Exp 1310



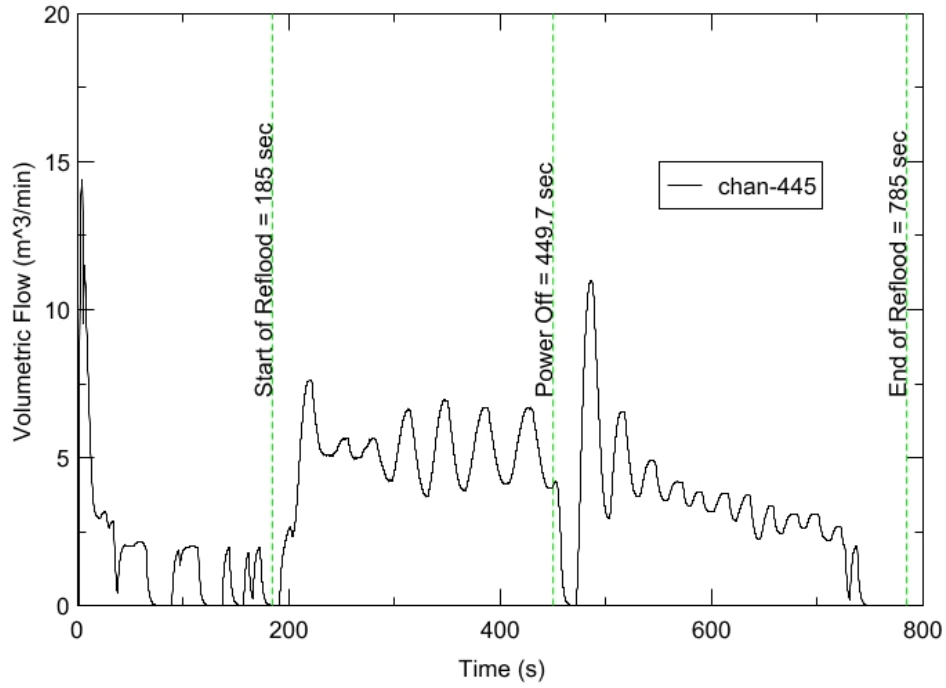
RBHT - TEST FACILITY

Inlet Flow vs. Time, Exp 1310



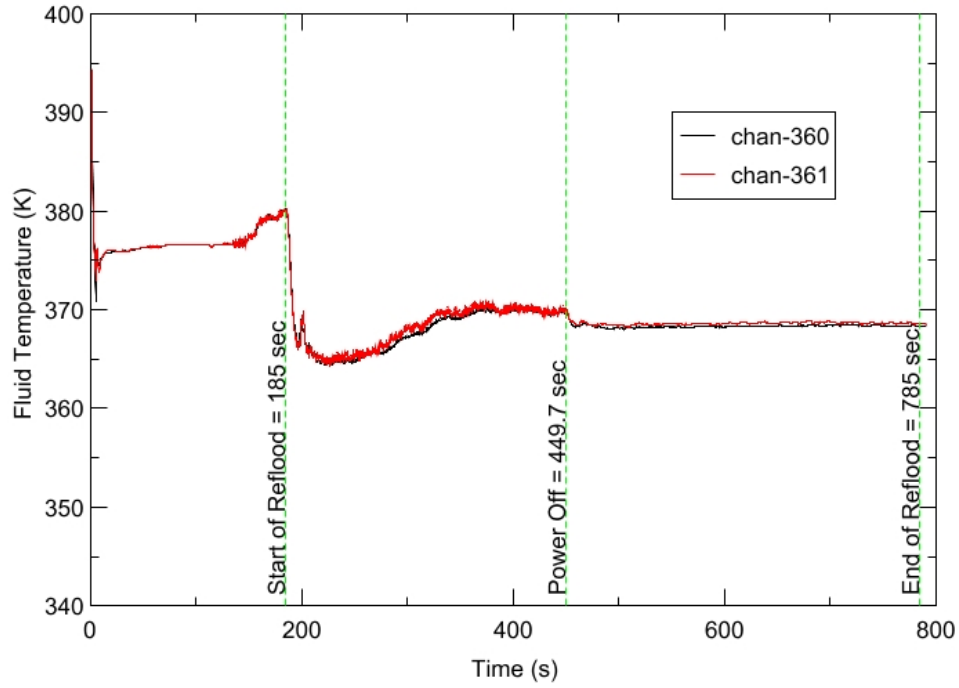
RBHT - TEST FACILITY

Steam Exhaust Flow vs. Time, Exp 1310



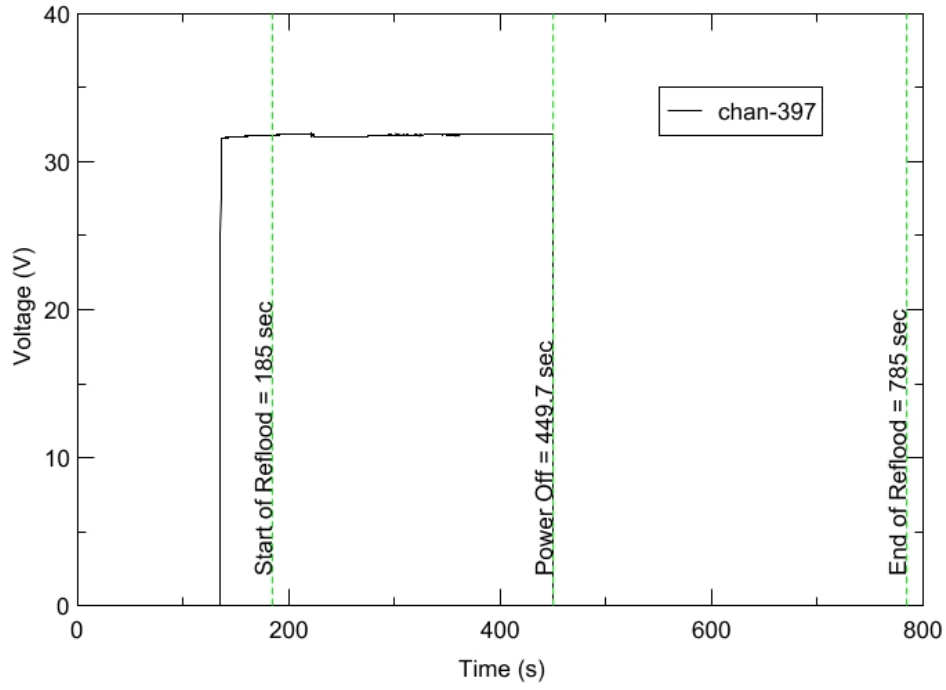
RBHT - TEST FACILITY

Inlet Flow Temperature vs. Time, Exp 1310



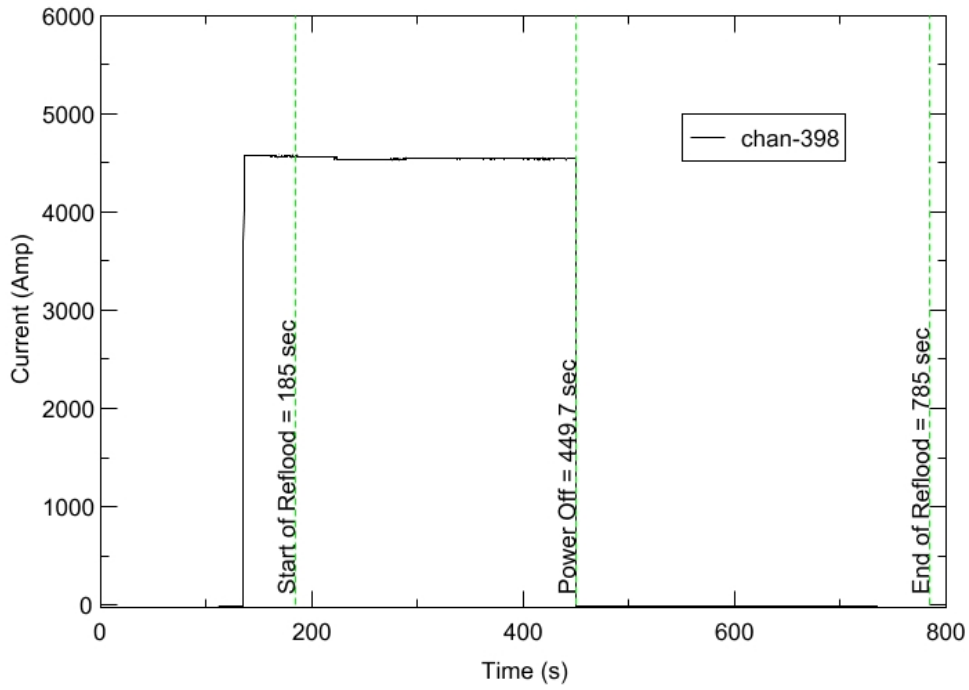
RBHT - TEST FACILITY

Test Section Voltage vs. Time, Exp 1310

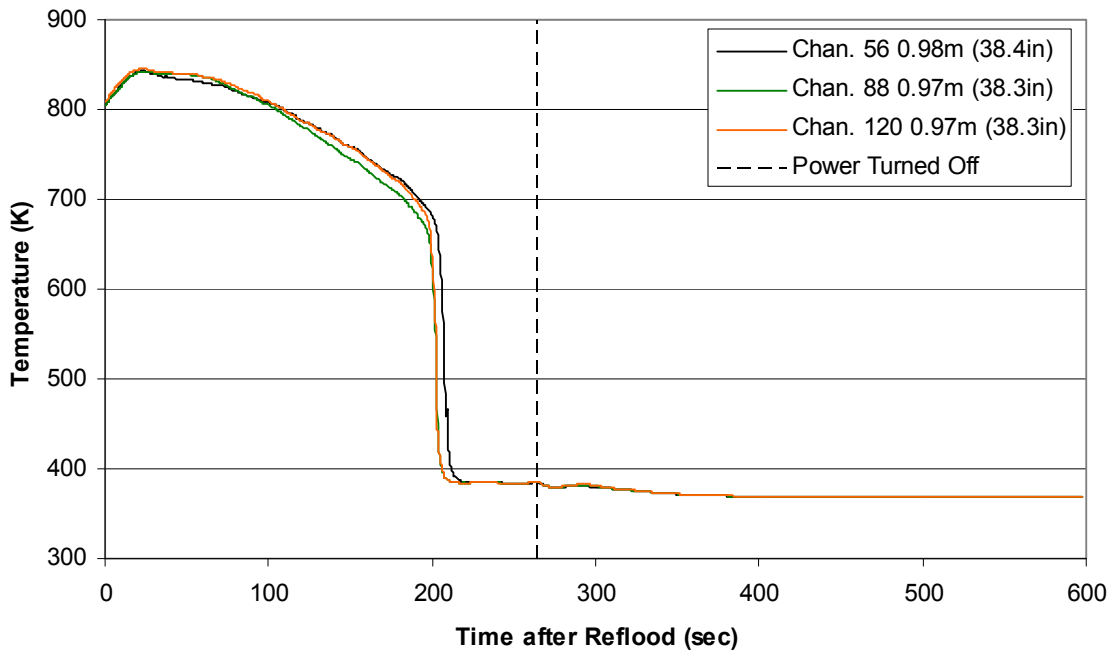


RBHT - TEST FACILITY

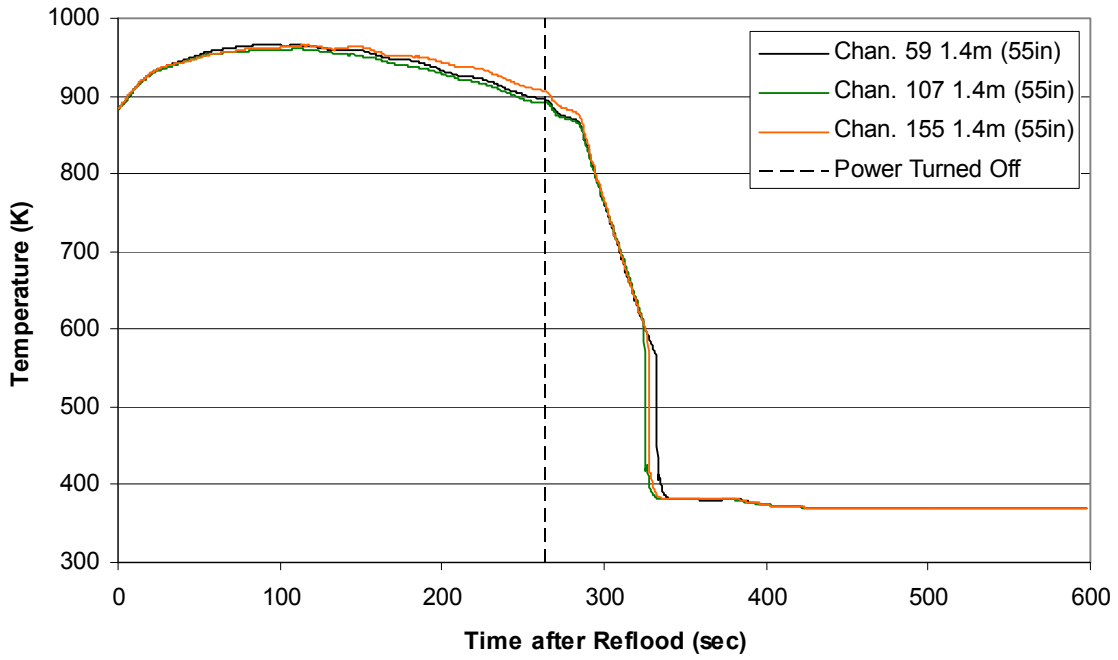
Test Section Current vs. Time, Exp 1310



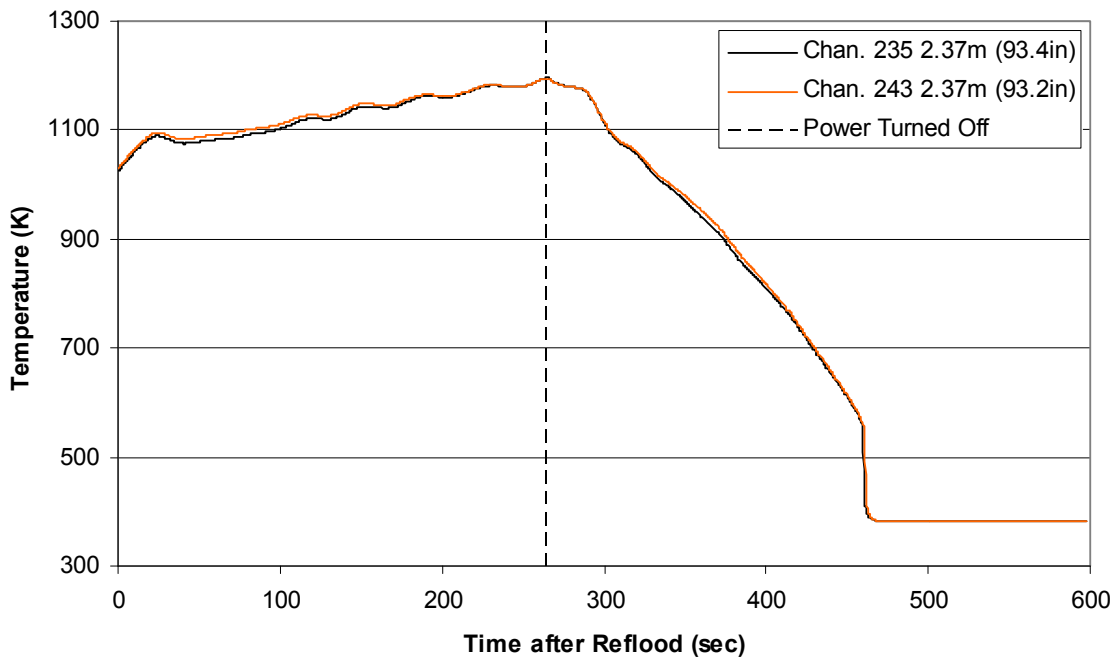
Heater Rod Temperature during Reflood RBHT Exp. 1310



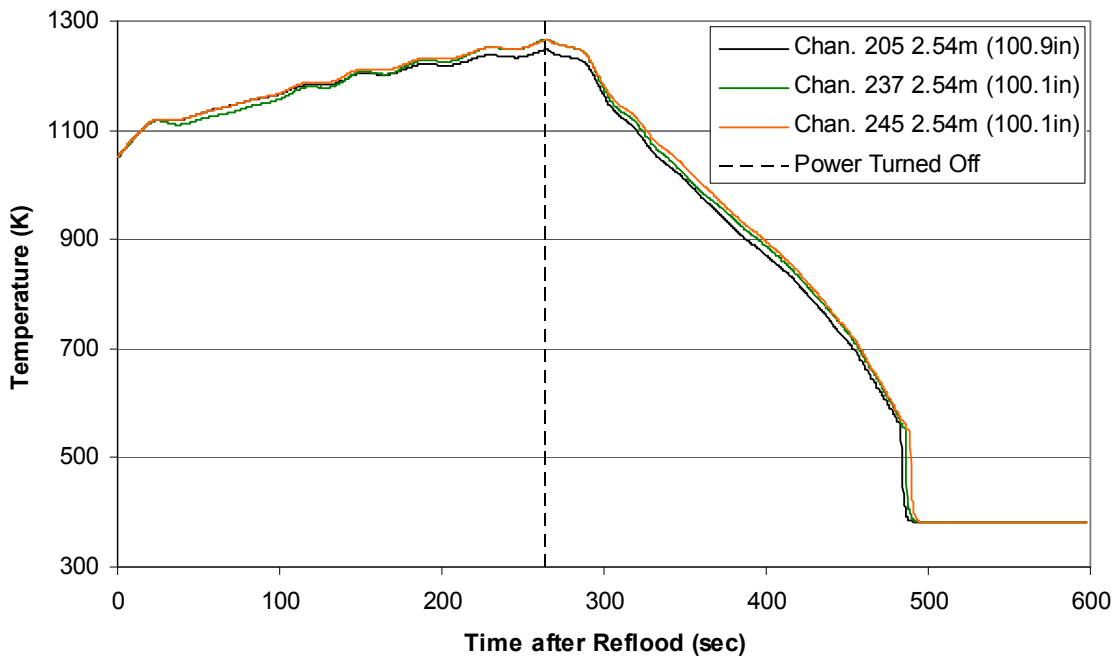
Heater Rod Temperature during Reflood RBHT Exp. 1310



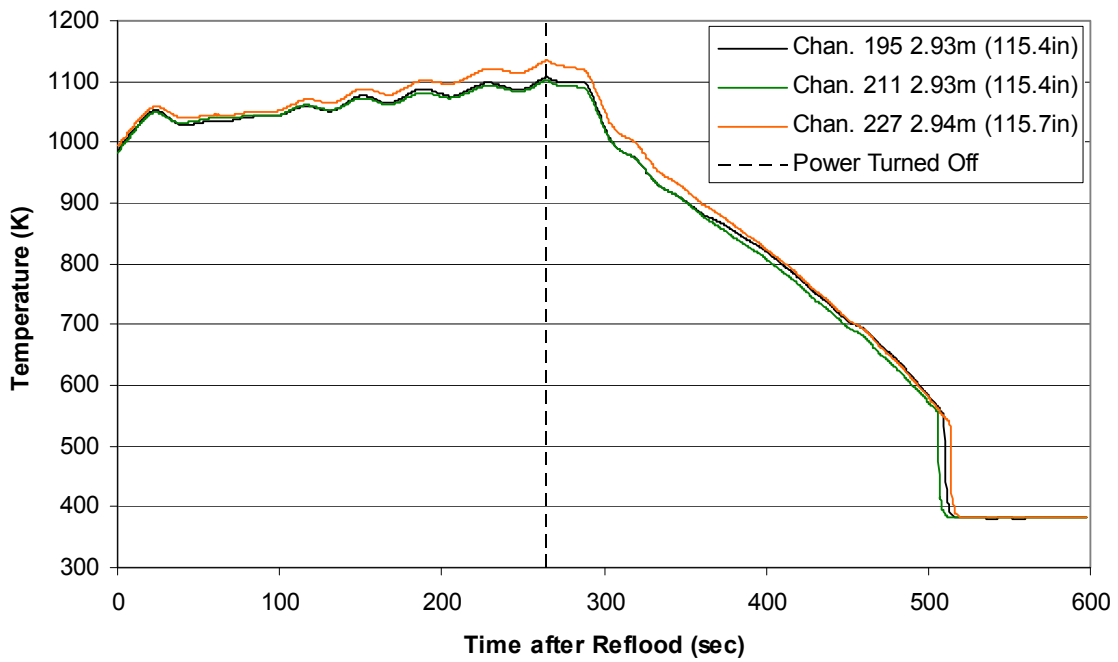
Heater Rod Temperature during Reflood
RBHT Exp. 1310



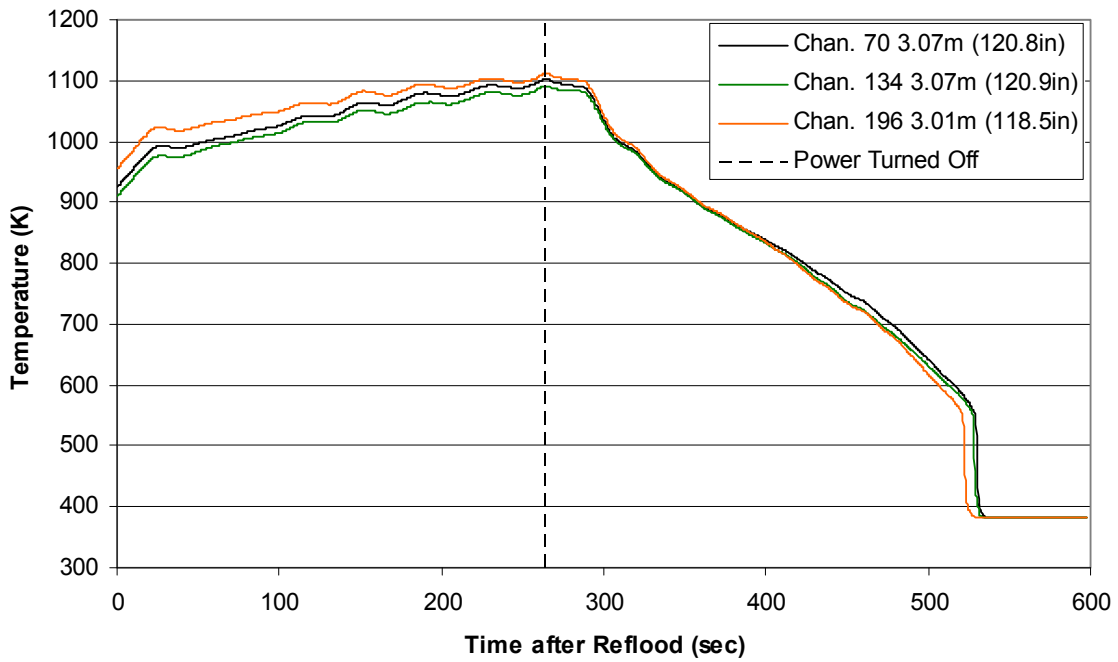
Heater Rod Temperature during Reflood
RBHT Exp. 1310



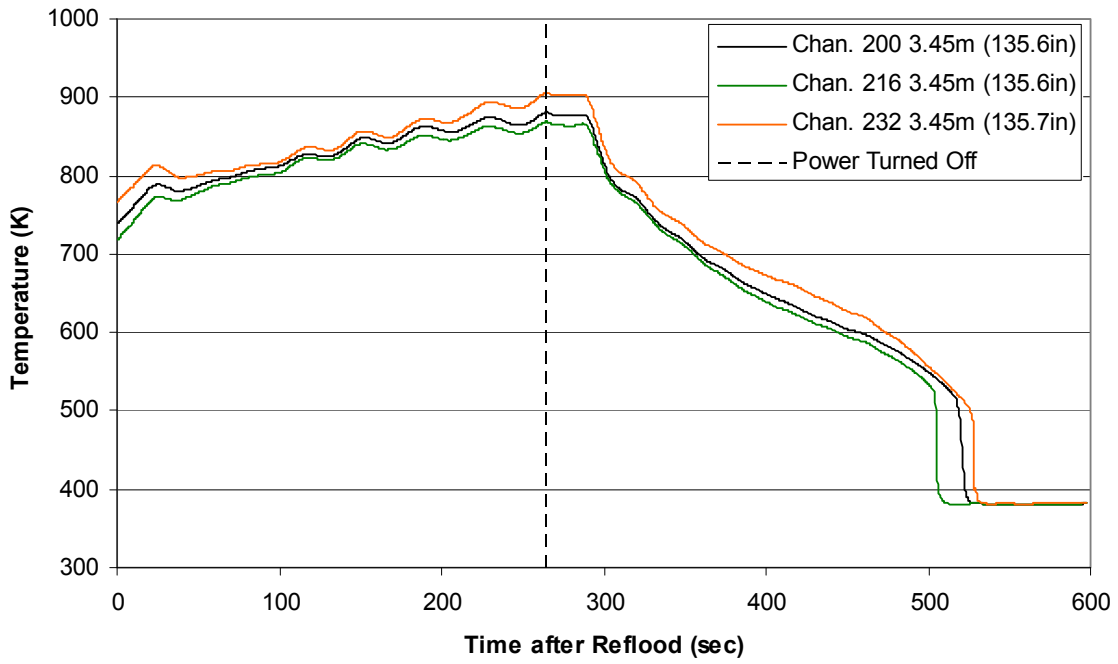
Heater Rod Temperature during Reflood
RBHT Exp. 1310



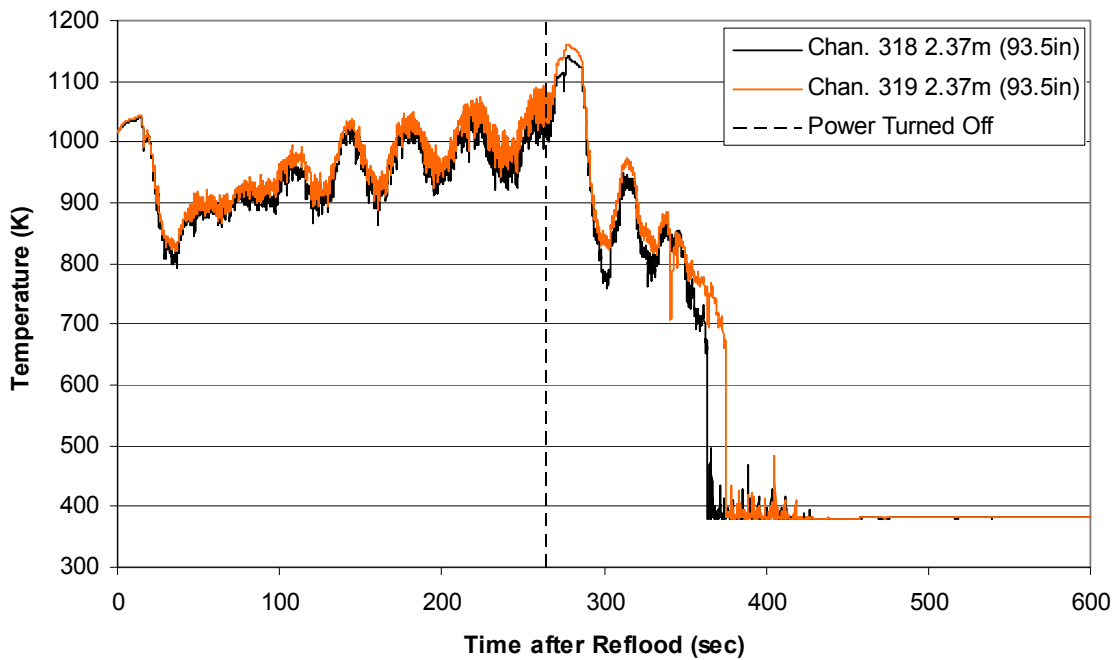
Heater Rod Temperature during Reflood
RBHT Exp. 1310



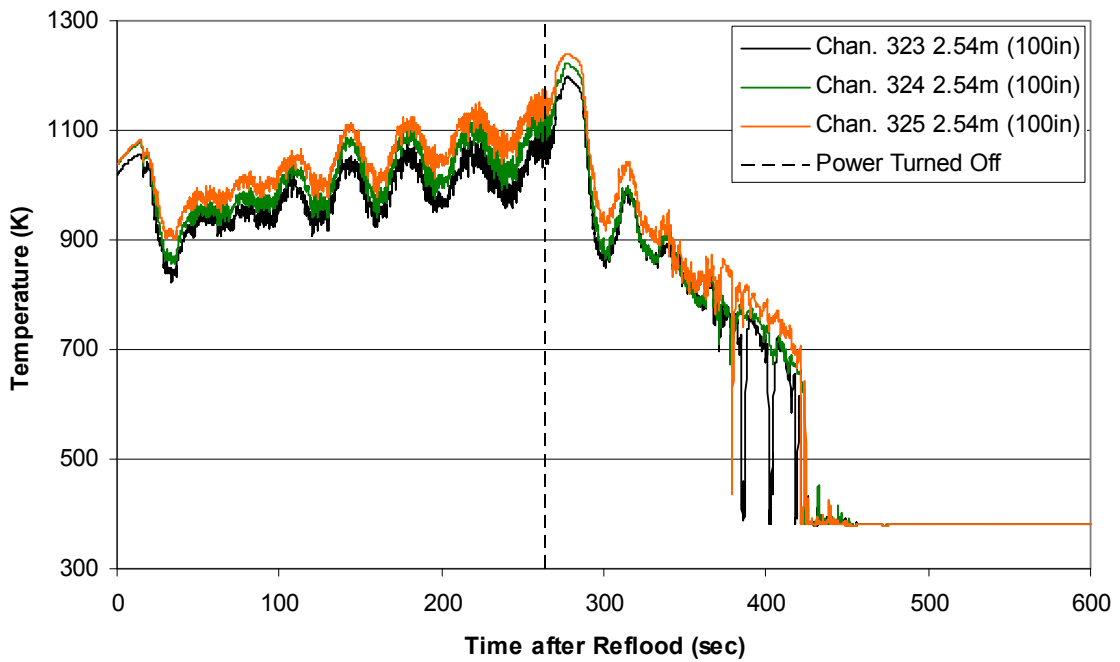
Heater Rod Temperature during Reflood RBHT Exp. 1310



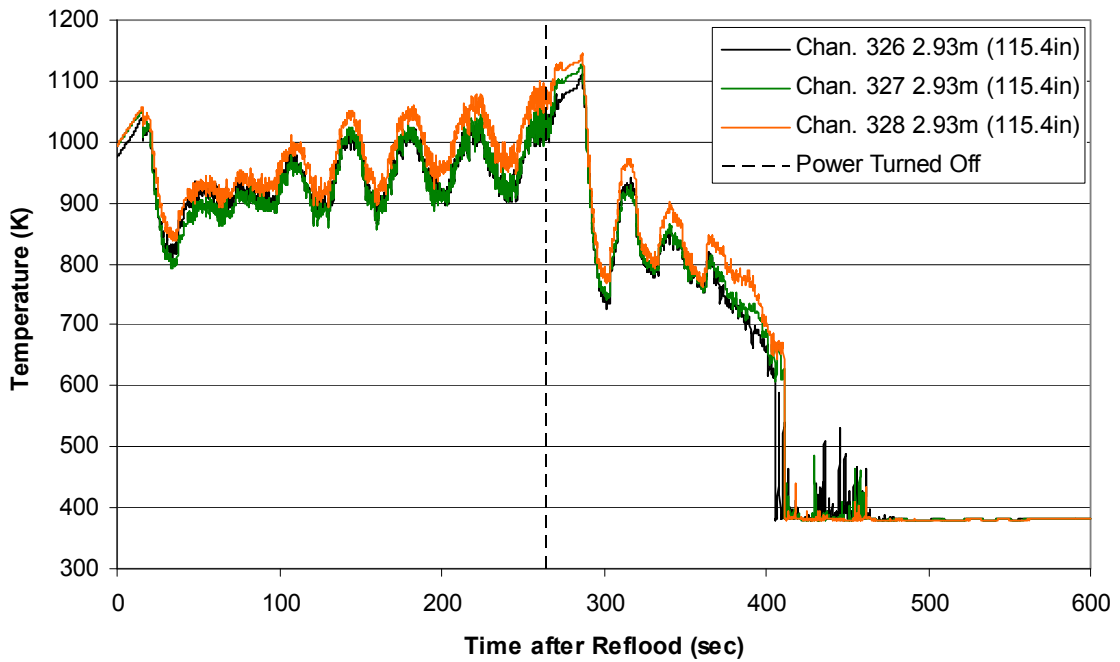
Steam Probe Temperature during Reflood RBHT Exp. 1310



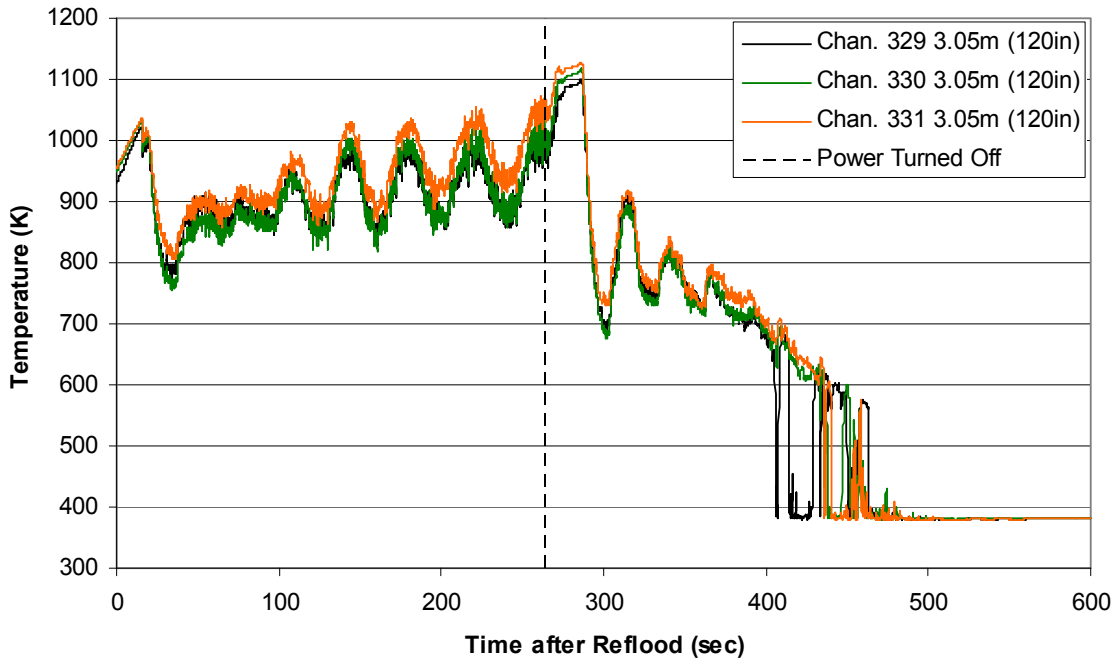
Steam Probe Temperature during Reflood
RBHT Exp. 1310



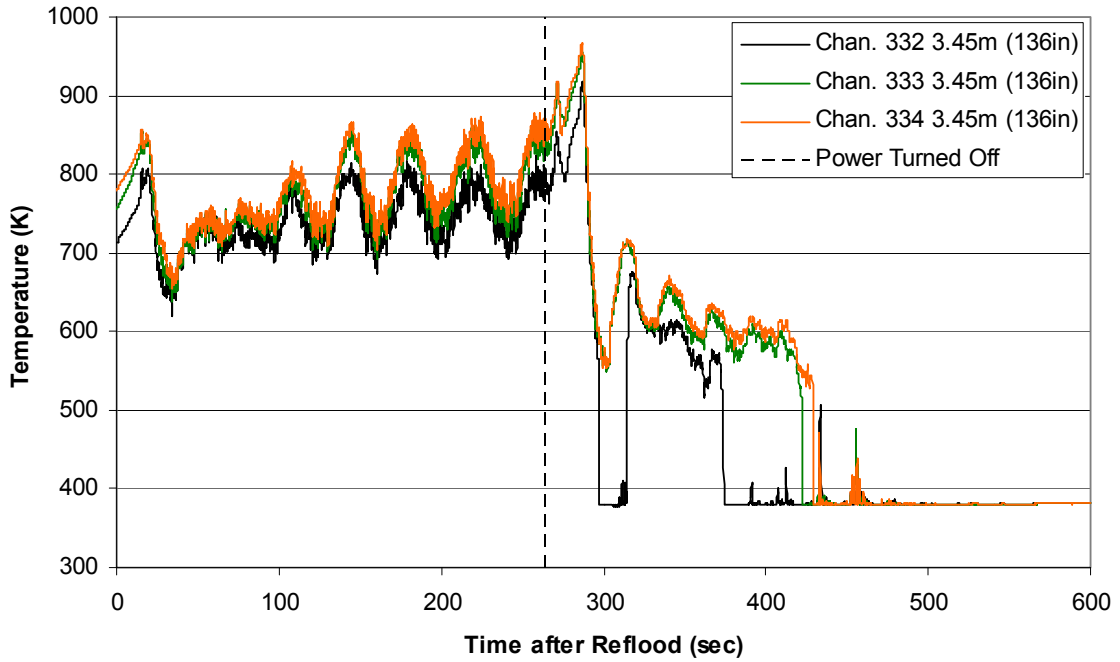
Steam Probe Temperature during Reflood
RBHT Exp. 1310



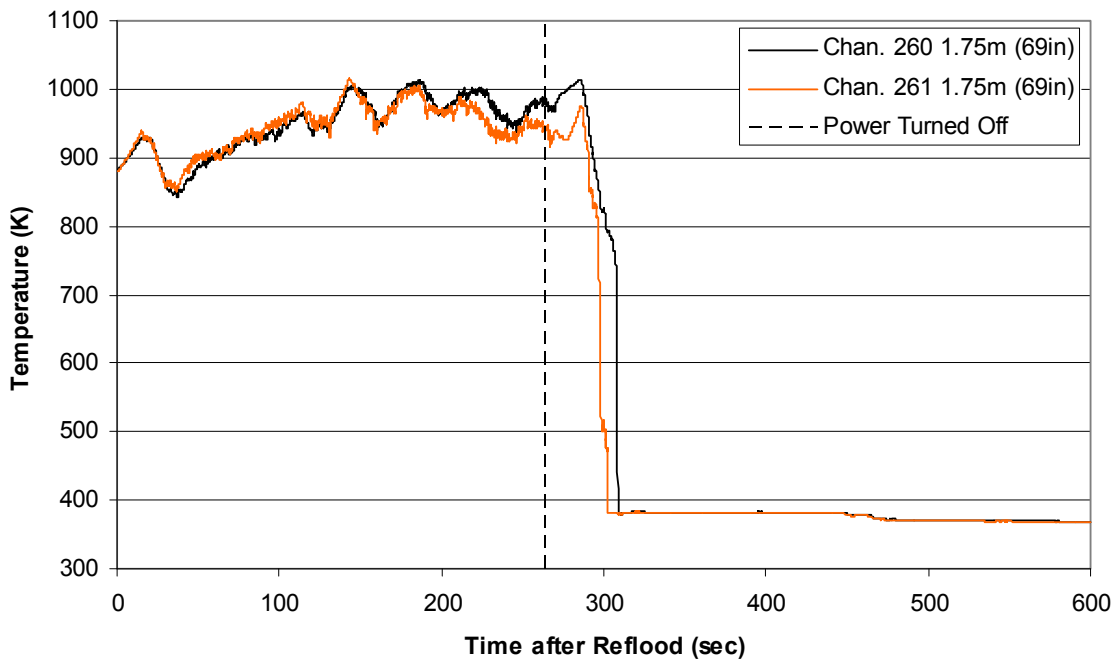
Steam Probe Temperature during Reflood
RBHT Exp. 1310



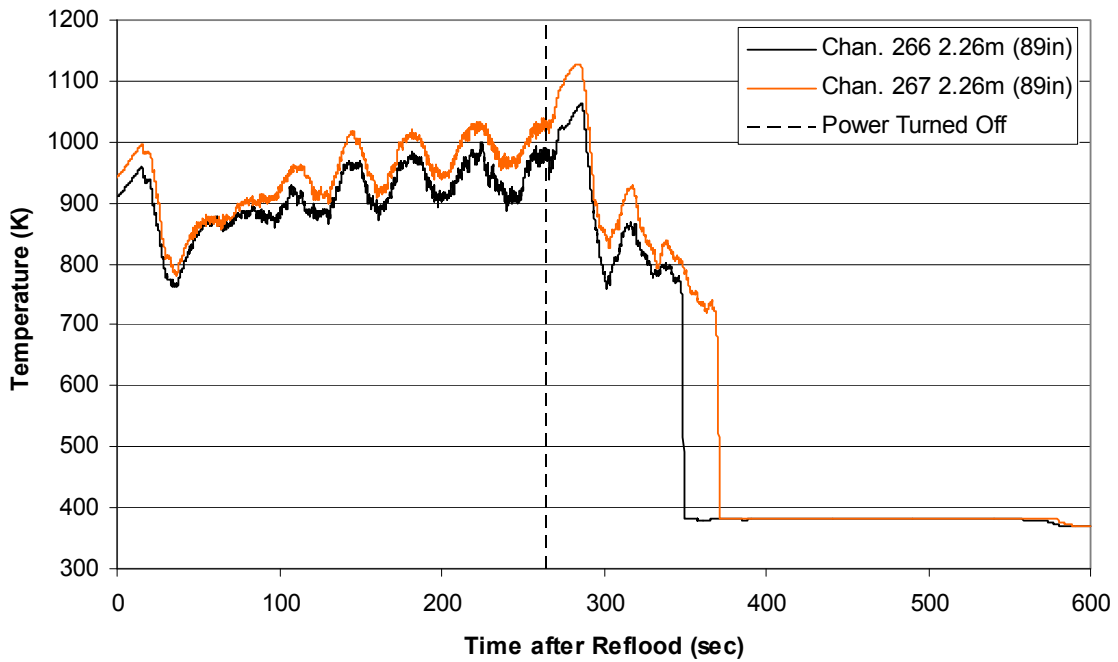
Steam Probe Temperature during Reflood
RBHT Exp. 1310



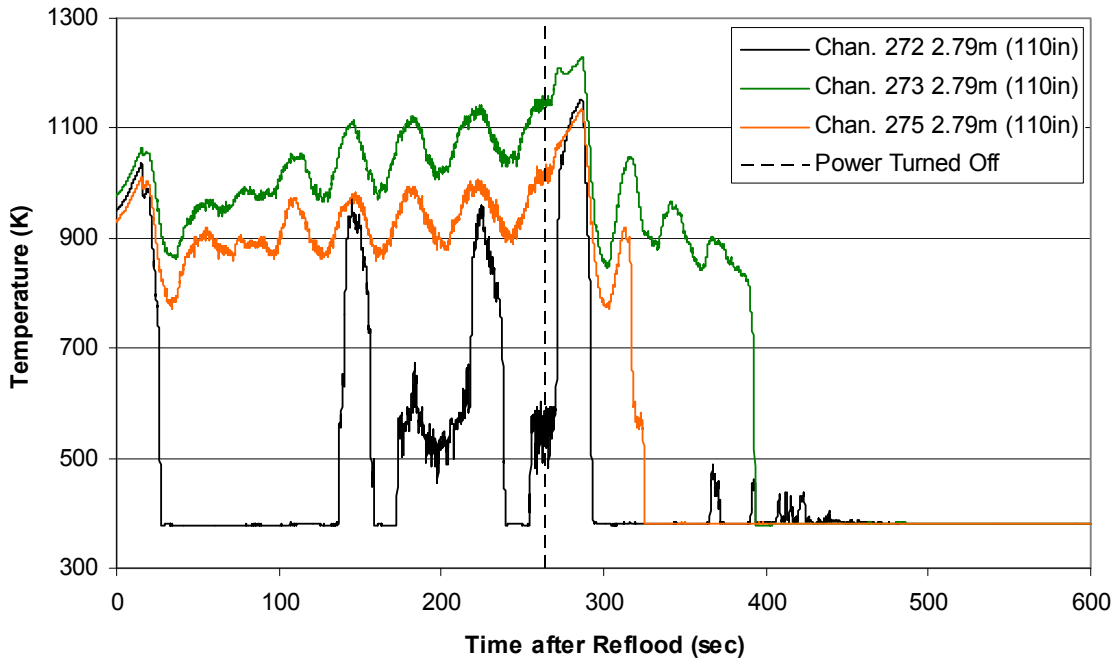
Spacer Grid Temperature during Reflood RBHT Exp. 1310



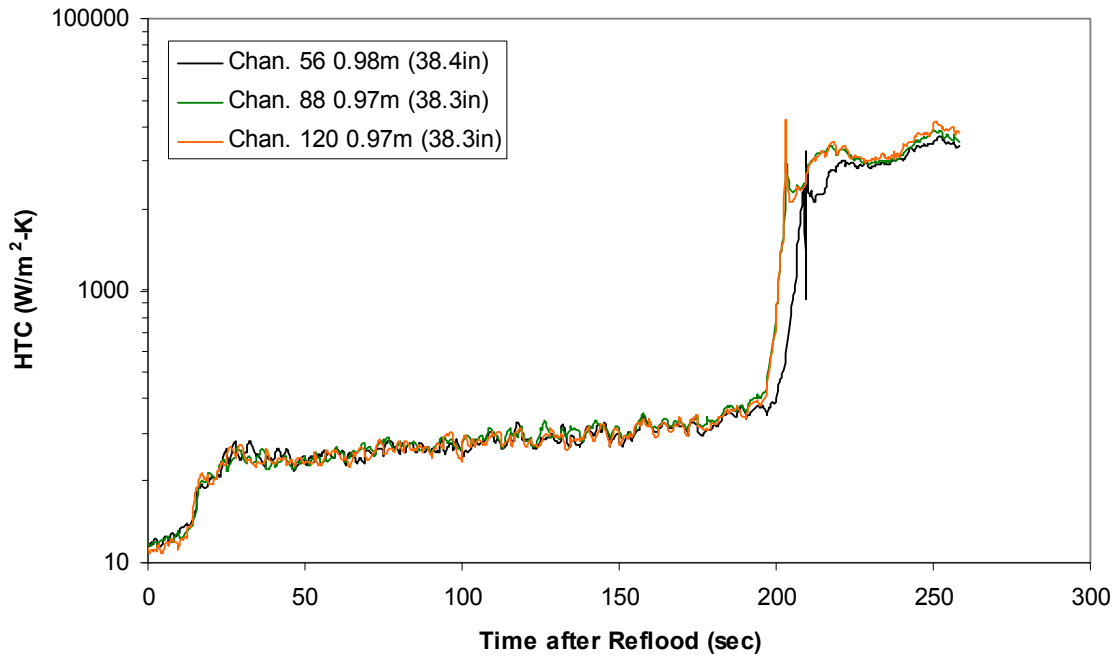
Spacer Grid Temperature during Reflood RBHT Exp. 1310



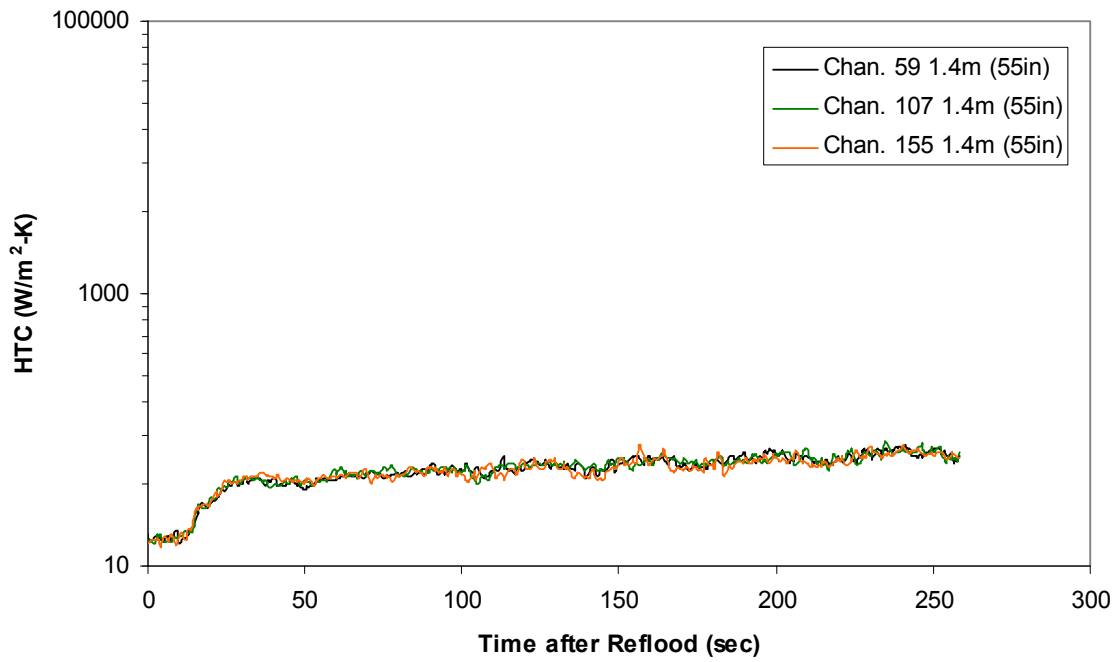
Spacer Grid Temperature during Reflood RBHT Exp. 1310



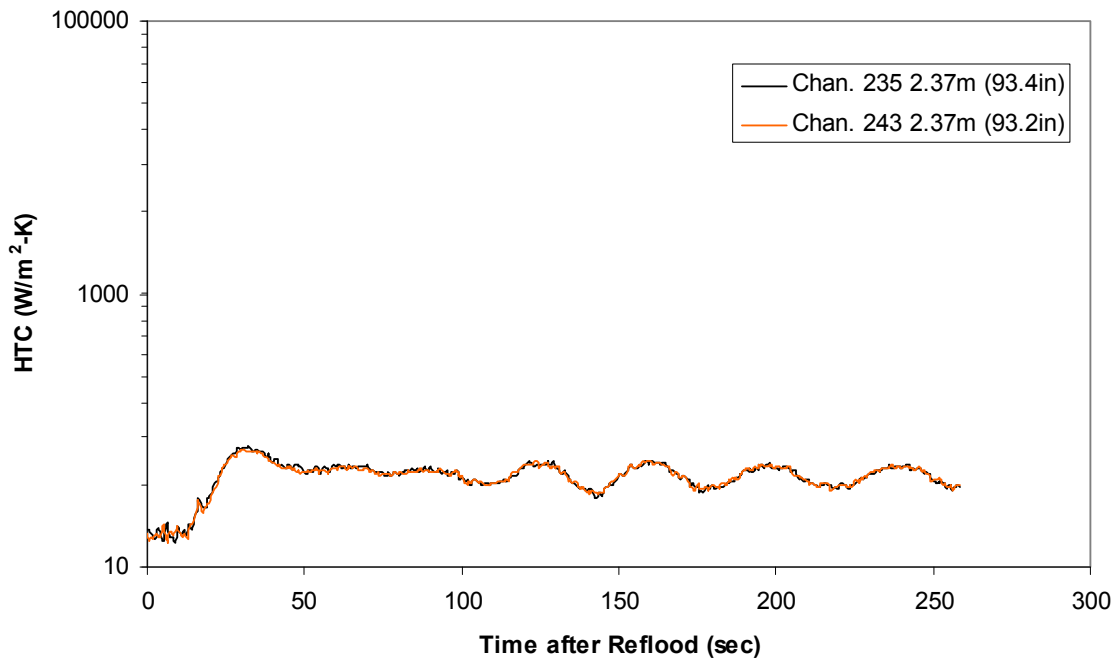
Heat Transfer Coefficient during Reflood RBHT Exp. 1310



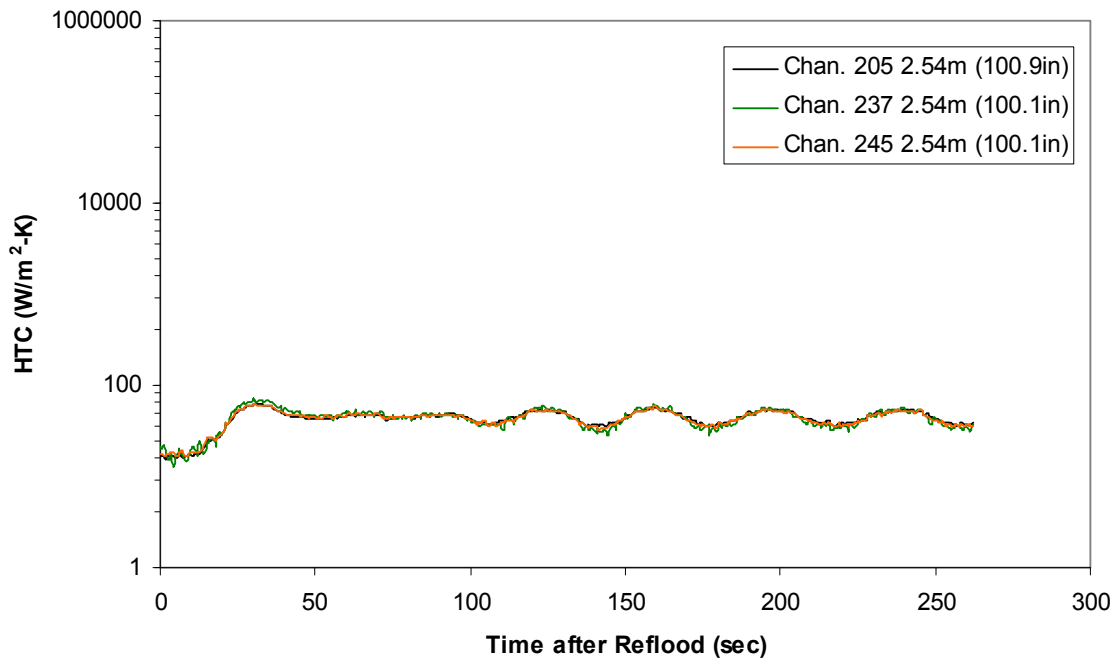
Heat Transfer Coefficient during Reflood RBHT Exp. 1310



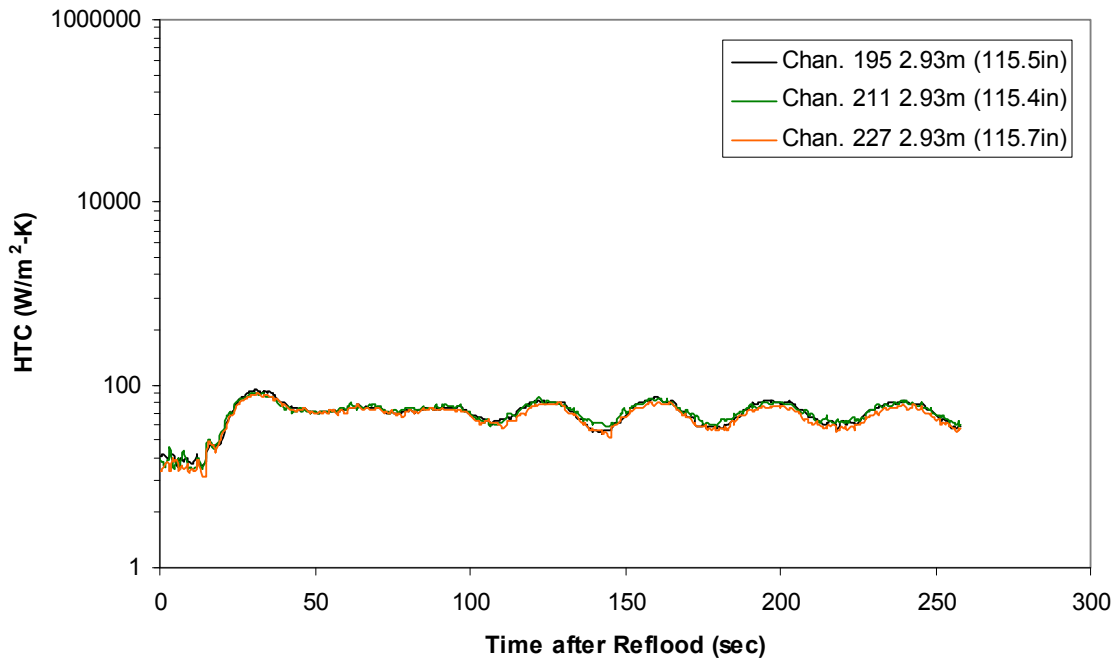
Heat Transfer Coefficient during Reflood RBHT Exp. 1310



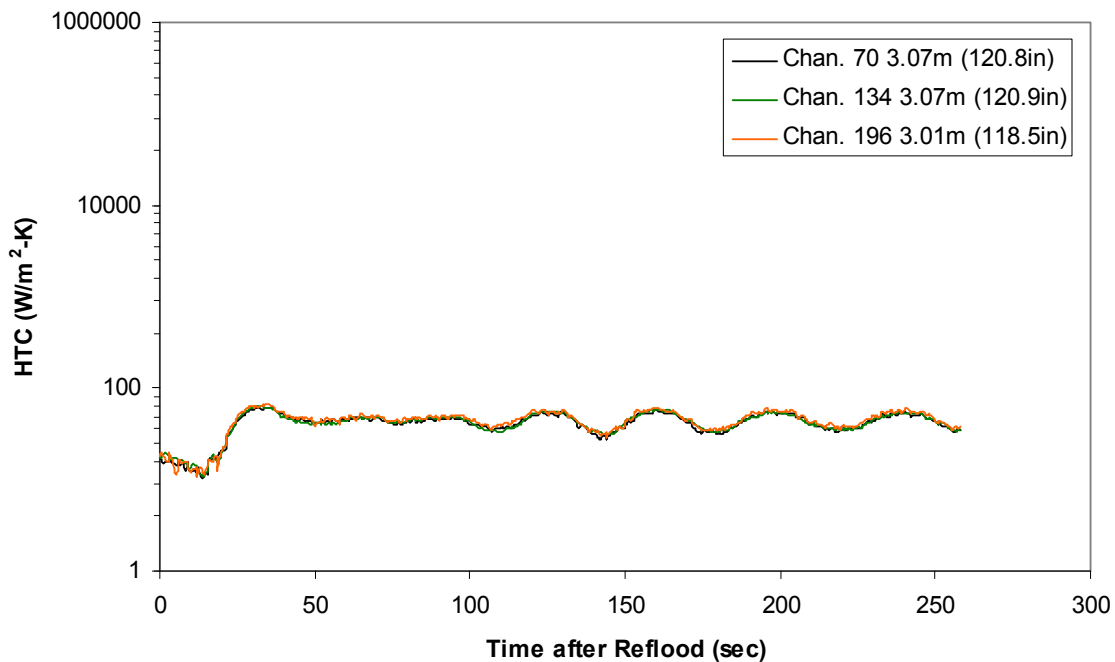
Heat Transfer Coefficient during Reflood RBHT Exp. 1310



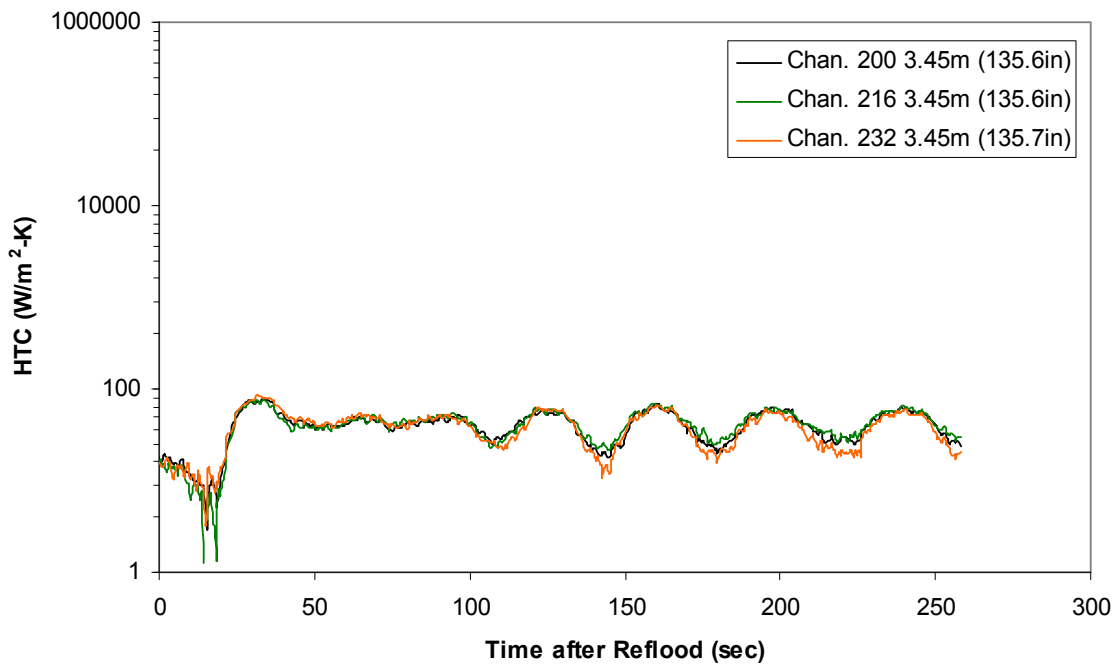
Heat Transfer Coefficient during Reflood RBHT Exp. 1310



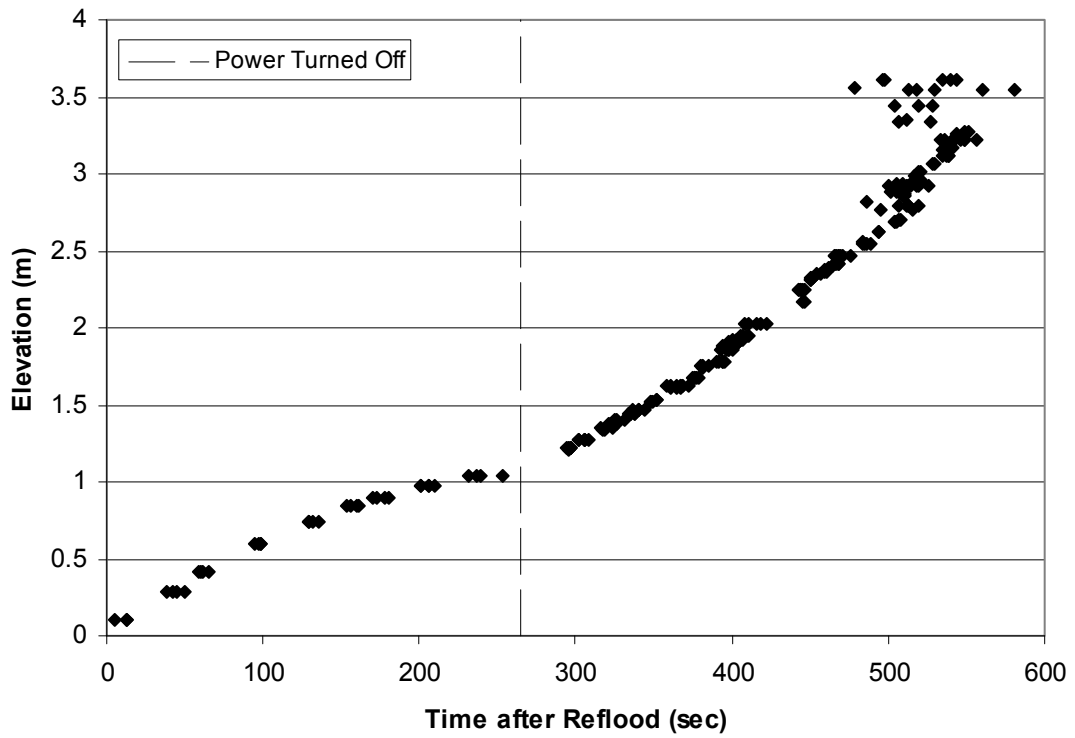
Heat Transfer Coefficient during Reflood RBHT Exp. 1310



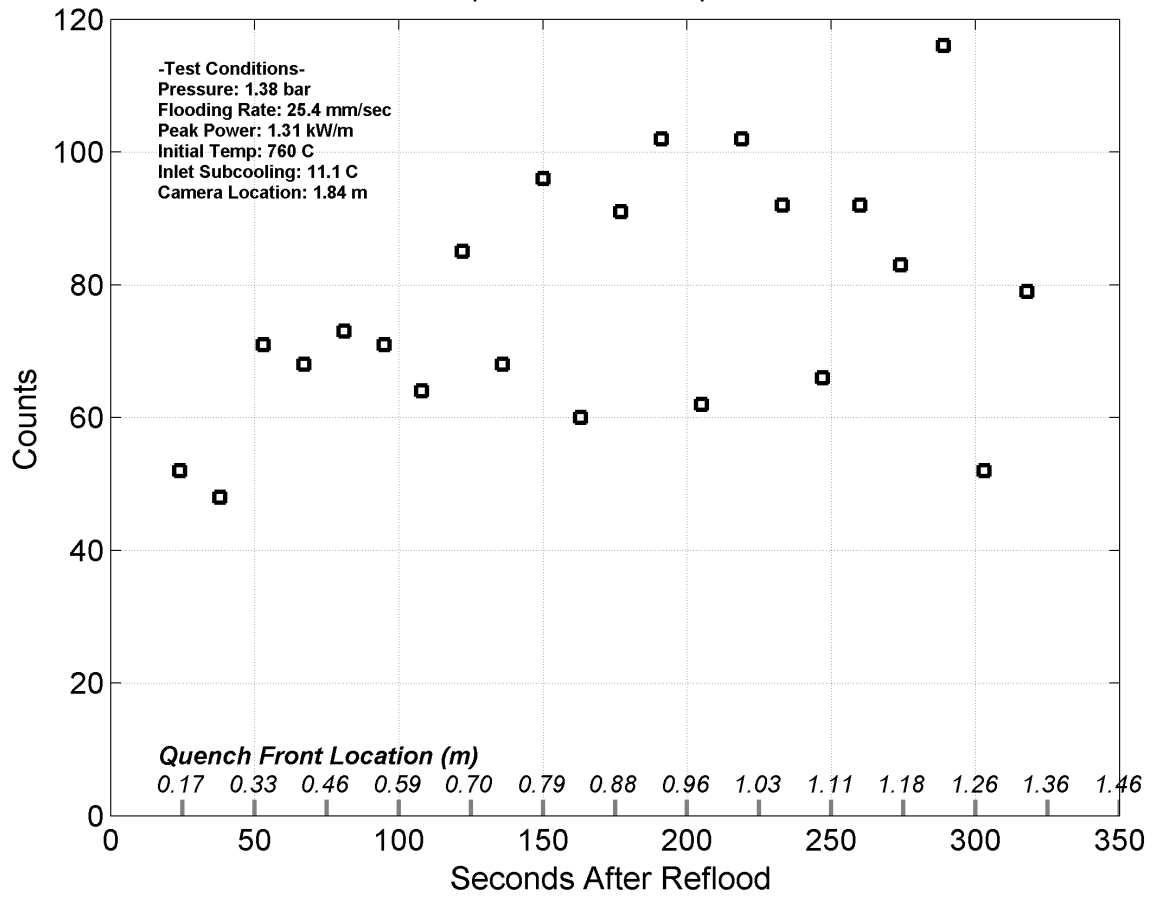
Heat Transfer Coefficient during Reflood RBHT Exp. 1310



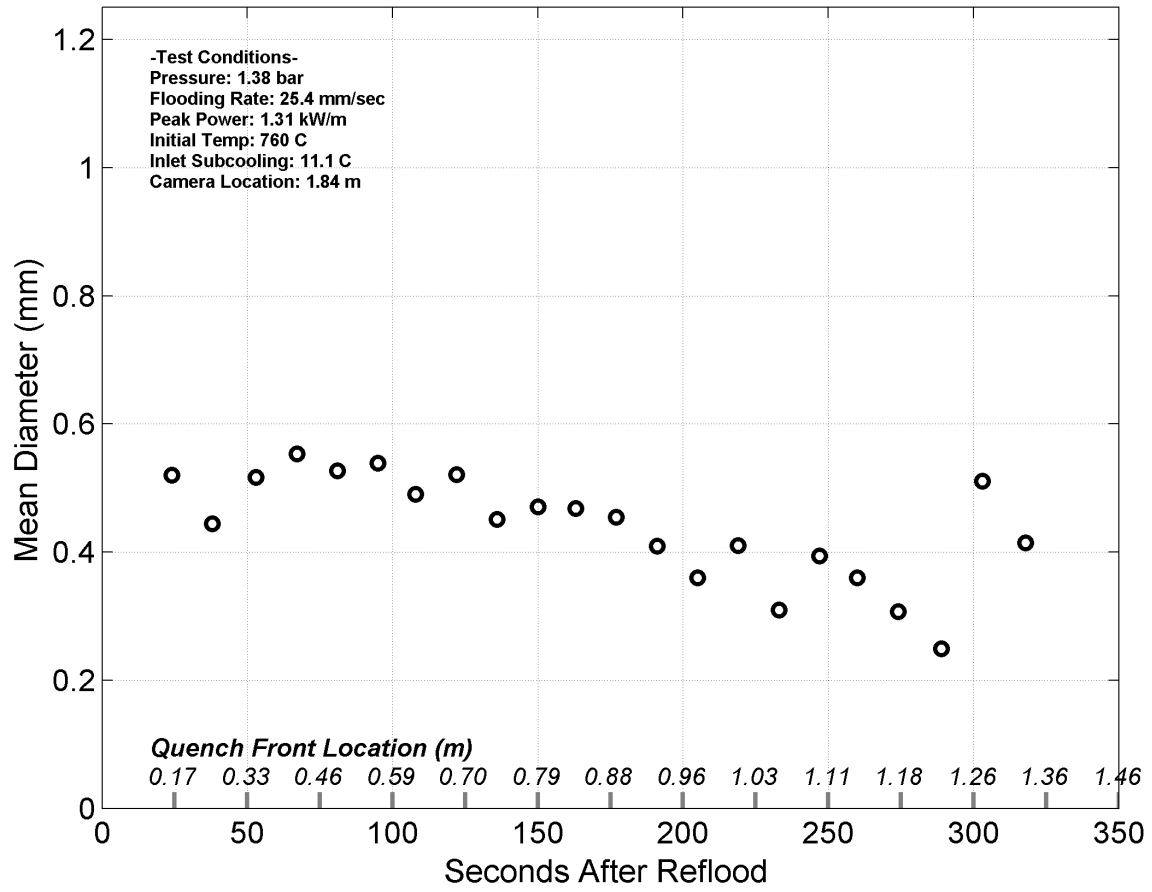
Quench Data, RBHT Exp. 1310



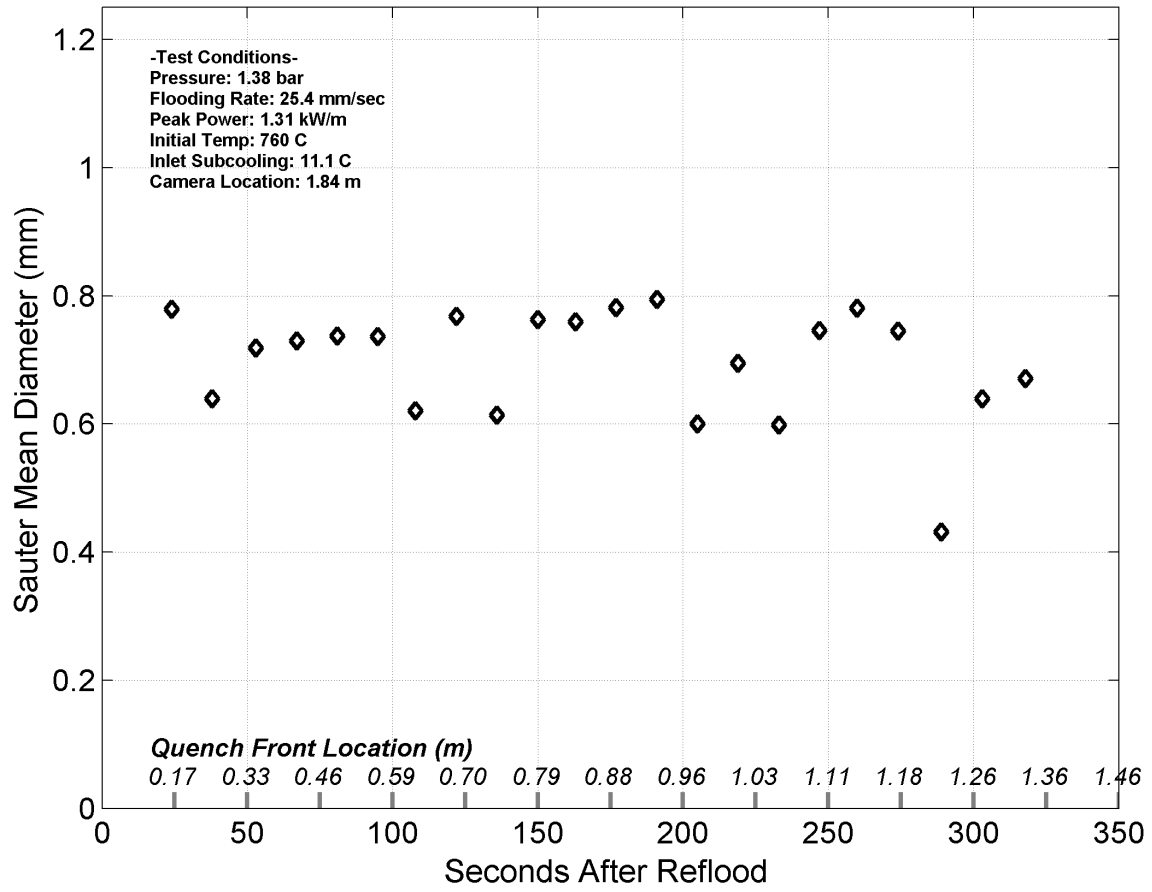
Droplet Counts - Exp. 1310



Mean Droplet Diameter - Exp. 1310



Droplet Sauter Mean Diameter - Exp. 1310



RBHT - REFLOOD TESTS

SUMMARY SHEET

RUN NO: **1319**

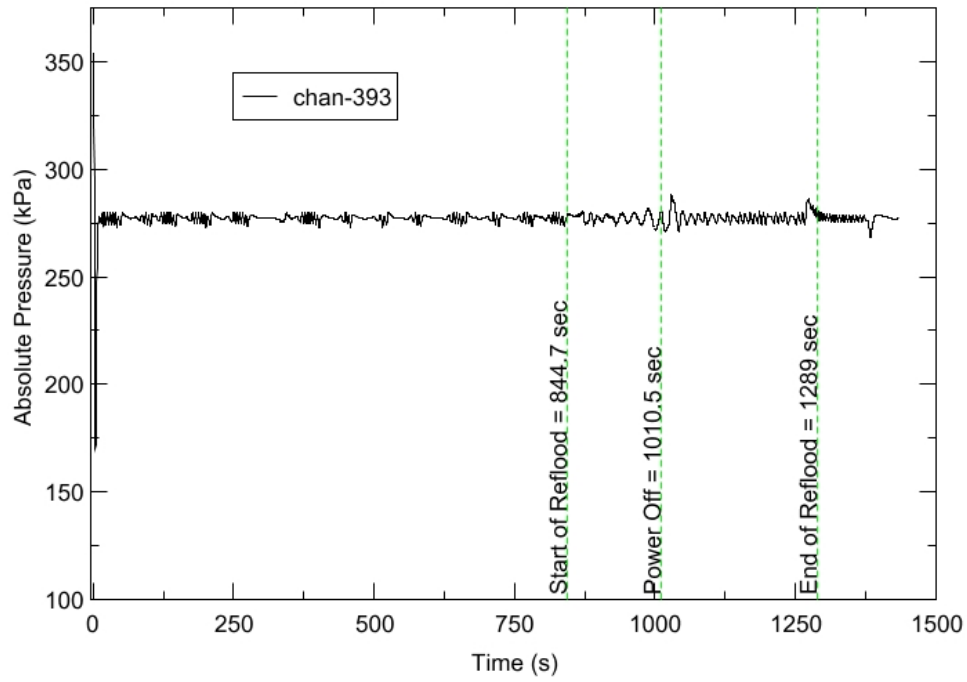
RUN CONDITIONS

Upper Plenum Pressure:	276 kPa (40 psia)
Initial Peak Clad Temperature:	1033 degrees K (1400 degrees F)
Rod Peak Power:	1.31 kW/m (0.4 kW/ft)
Flooding Rate:	0.0254 m/s (1 in/s)
Inlet Subcooling:	11 degrees K (20 degrees F)
Start of Reflood:	844.7 s
End of Reflood:	1289 s
Test Date:	8/5/2002
Comments:	Power turn off at 1010.5 seconds. Inlet flow continued until entire bundle quenched. DATARH heat transfer coefficients calculated until power was turned off. Droplet data was collected until approximately 30 seconds after power was turn off.

Rod_Elevation	Channel Number	Temperature at Reflood (K)	Temperature at Reflood (F)	Turnaround Time (sec.)	Turnaround Temperature (K)	Turnaround Temperature (F)	Quench Time (sec.)	Quench Temperature (K)	Quench Temperature (F)
B6_0.592m	148	707.99	814.7	17.05	737.95	868.62	64.05	595.83	612.81
B6_0.744m	149	732.86	859.46	19.05	767.75	922.26	82.05	573.93	573.39
B6_0.846m	150	759.02	906.55	19.55	797.63	976.05	93.05	606.62	632.23
B6_0.897m	151	768.99	924.49	19.55	809.09	996.67	99.55	616	649.11
C6_1.04m	137	810.79	999.74	21.55	855.75	1080.67	117.55	670.46	747.15
C6_1.34m	138	850.3	1070.86	51.05	909.99	1178.3	186.55	669.57	745.53
C6_1.39m	139	857.35	1083.54	65.55	924.53	1204.46	194.05	666.83	740.6
C6_1.47m	140	868.82	1104.19	71.05	945.88	1242.9	204.55	651.71	713.4
C6_1.62m	141	882.36	1128.56	93.55	995.44	1332.11	223.55	642.22	696.31
C6_1.87m	142	905.52	1170.25	94.05	1015.9	1368.94	246.55	595.34	611.93
C6_1.95m	144	924.97	1205.26	115.55	1051.3	1432.66	253.05	607.14	633.17
D6_2.62m	129	1051.42	1432.86	166.55	1254.2	1797.88	322.55	606.11	631.31
D6_2.69m	130	1050.78	1431.71	166.55	1271.97	1829.86	330.55	614.28	646.01
D6_2.87m	131	987.87	1318.47	167.05	1158.86	1626.27	346.05	543.81	519.17
D6_2.92m	132	967.55	1281.9	168.55	1168.29	1643.24	349.05	583.68	590.94
D6_2.97m	133	943.16	1238	168.55	1163.39	1634.41	354.55	596.07	613.24
D6_3.07m	134	912.69	1183.15	167.05	1154.28	1618.01	362.05	610.52	639.25
D6_3.17m	135	881.32	1126.7	167.55	1137.44	1587.71	372.05	601.84	623.62
D6_3.27m	136	832.83	1039.4	168.05	1115.77	1548.69	381.55	603.03	625.77
D5_1.27m	217	858.15	1084.98	37.05	913.76	1185.08	163.05	592.27	606.4
D5_1.37m	218	878.63	1121.84	51.05	943.64	1238.87	190.05	688.7	779.98
D5_1.45m	219	890.67	1143.51	66.05	964.88	1277.1	200.55	670.37	746.97
D5_1.52m	220	900.32	1160.89	93.05	986.5	1316.01	211.05	655	719.31
D5_1.68m	221	912.85	1183.44	115.05	1039.55	1411.49	230.05	647.56	705.92
D5_1.78m	222	897.16	1155.2	96.05	1002.97	1345.65	241.05	598.66	617.89
D5_1.85m	223	924.27	1203.99	94.55	1033.77	1401.1	245.05	579.47	583.36
D5_1.90m	224	934.93	1223.18	96.05	1061.18	1450.44	248.05	610.06	638.42
D4_2.24m	241	1014.66	1366.69	140.55	1131.24	1576.55	287.55	552.25	534.36
D4_2.32m	242	1026.14	1387.36	166.05	1182.63	1669.04	292.55	593.26	608.18
D4_2.37m	243	1033.27	1400.2	166.55	1203.98	1707.47	297.55	598.5	617.62
D4_2.54m	245	1058.23	1445.12	166.55	1275.33	1835.9	321.05	593.62	608.82
D4_2.79m	247	1015.57	1368.33	184.55	1251.72	1793.4	348.05	573.75	573.06
D4_3.61m	248	616.68	650.33	167.05	986.57	1316.13	399.55	571.87	569.67
C3_2.17m	178	967.27	1281.4	141.05	1108.56	1535.72	279.55	618.01	652.73
E3_3.12m	197	913.71	1185	167.55	1179.92	1664.18	371.05	587.11	597.12
C3_2.35m	180	1021.24	1378.54	166.55	1182.79	1669.33	292.05	616.35	649.75
C3_2.40m	181	1025	1385.31	166.55	1191.19	1684.45	297.55	628.46	671.55
C3_2.76m	183	1045.52	1422.26	166.55	1296.29	1873.64	340.55	625.55	666.31

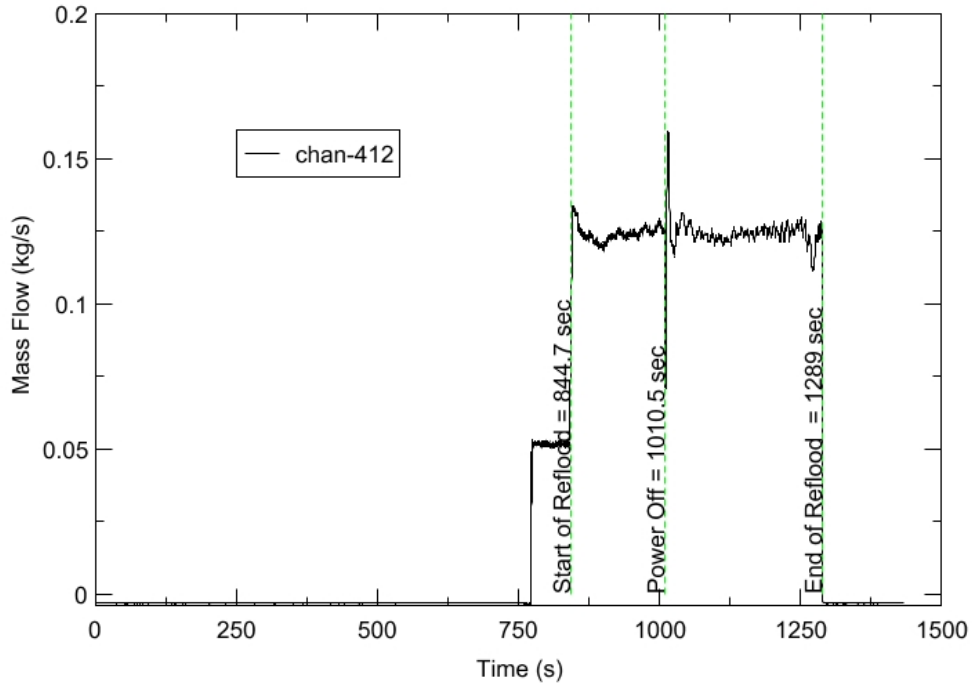
RBHT - TEST FACILITY

Upper Plenum Pressure vs. Time, Exp 1319



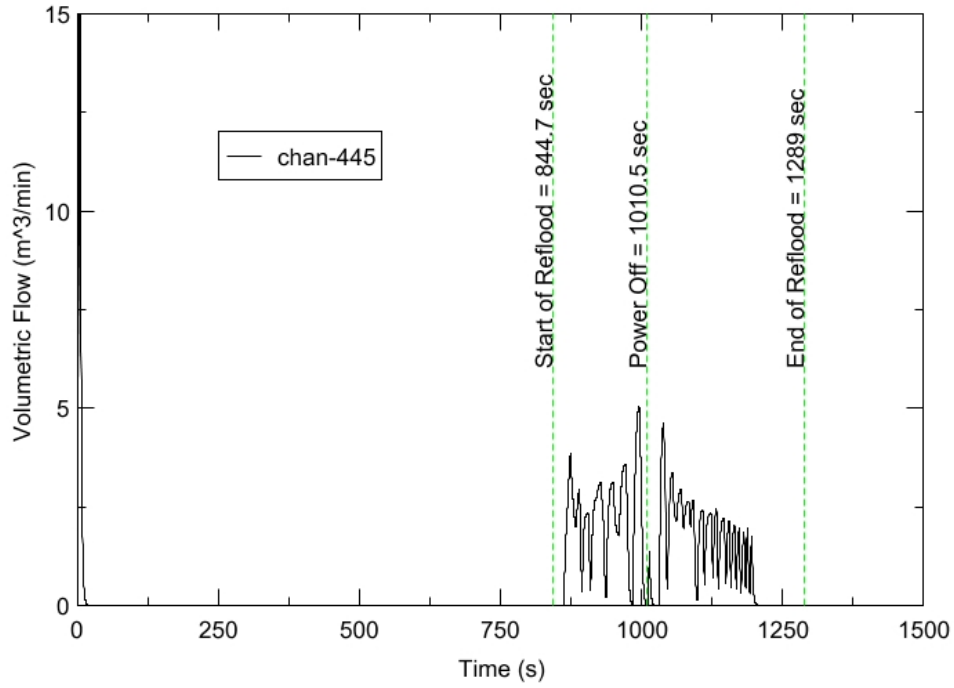
RBHT - TEST FACILITY

Inlet Flow vs. Time, Exp 1319



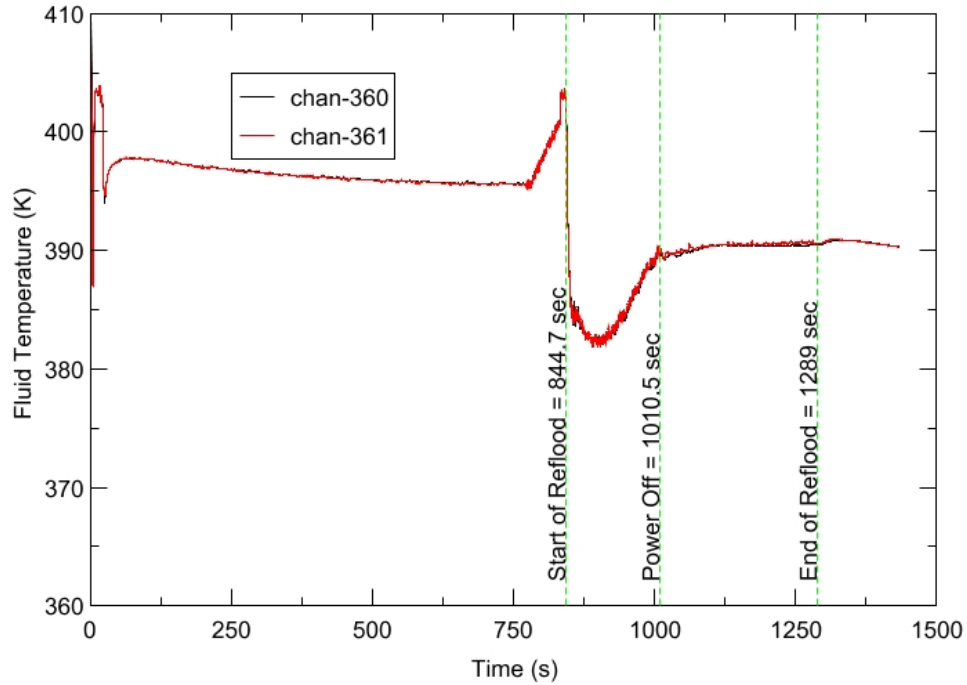
RBHT - TEST FACILITY

Steam Exhaust Flow vs. Time, Exp 1319



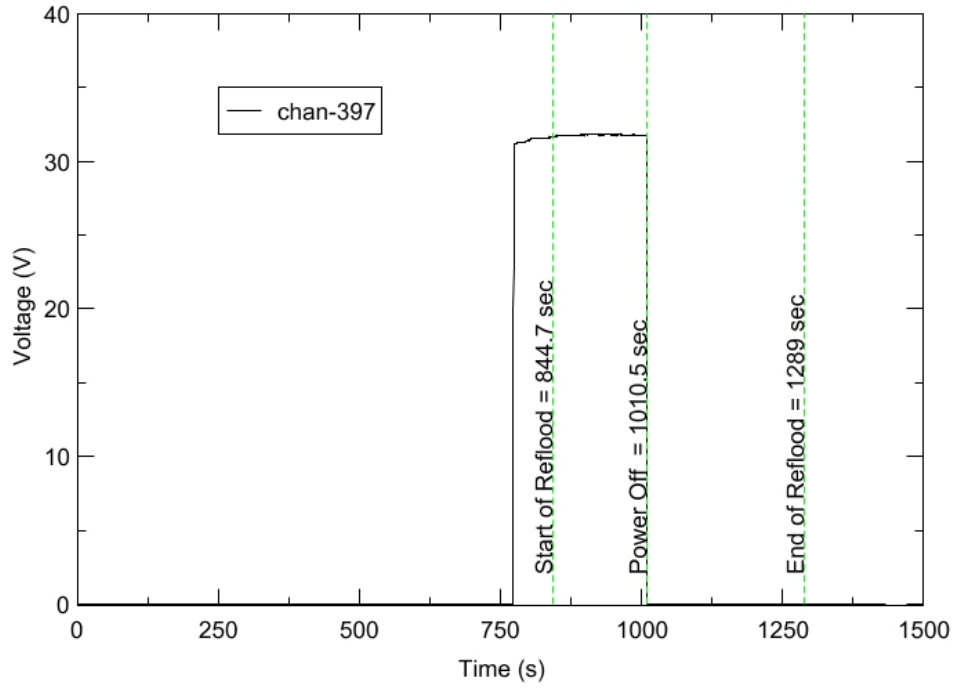
RBHT - TEST FACILITY

Inlet Flow Temperature vs. Time, Exp 1319



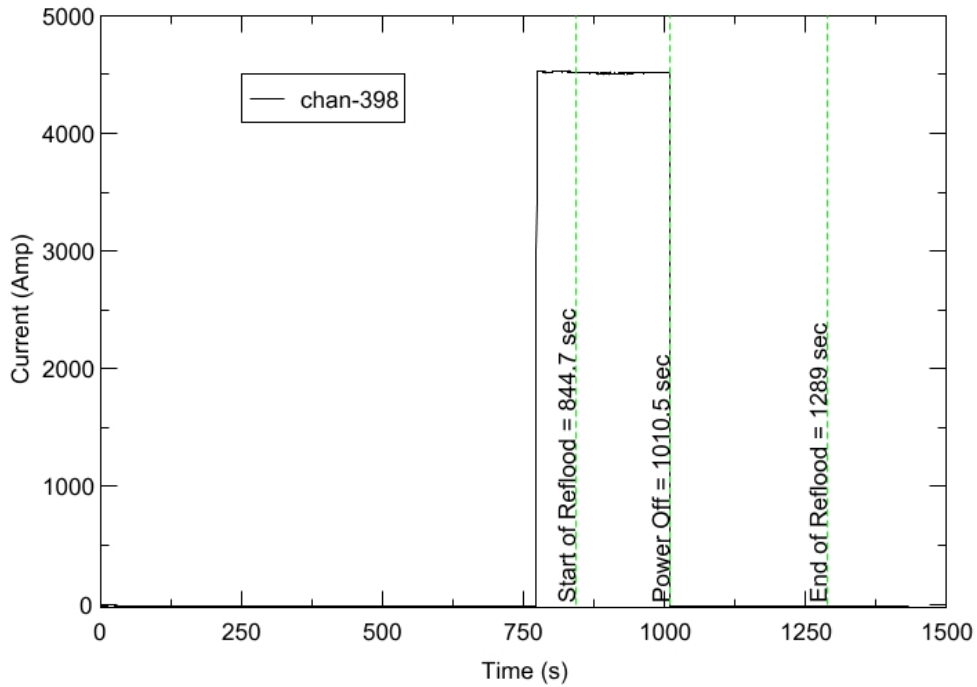
RBHT - TEST FACILITY

Test Section Voltage vs. Time, Exp 1319

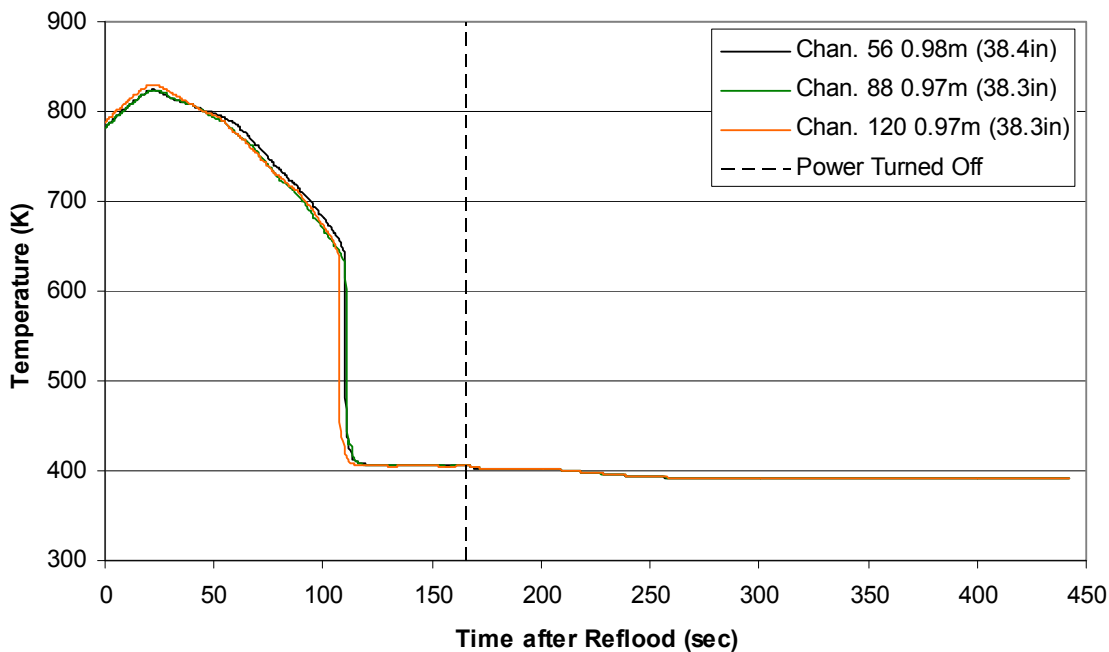


RBHT - TEST FACILITY

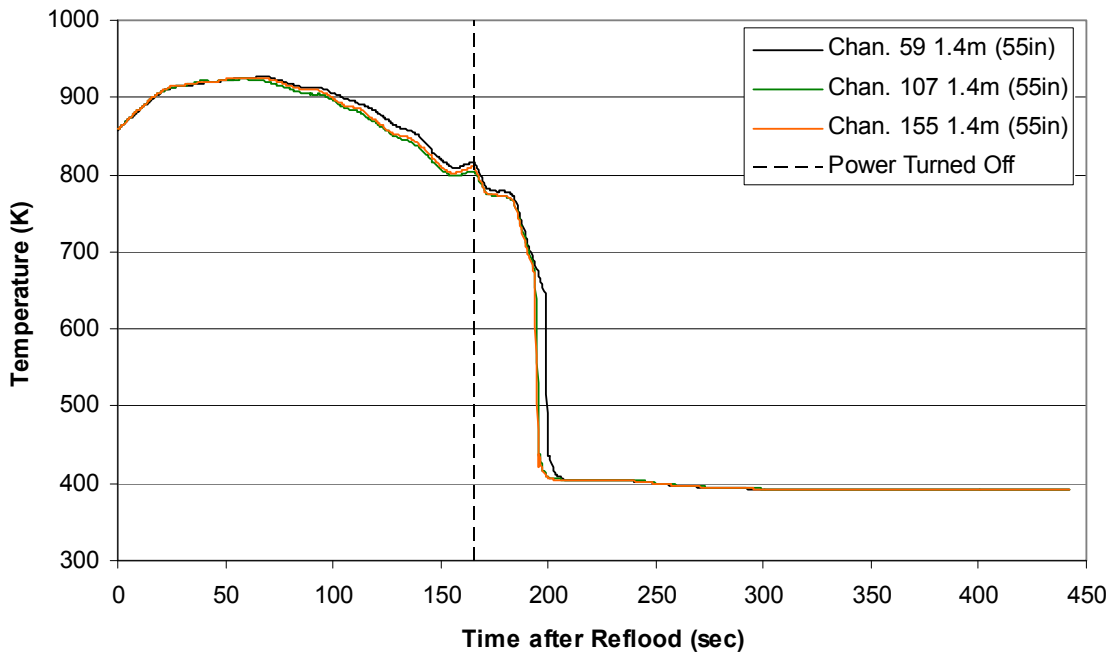
Test Section Current vs. Time, Exp 1319



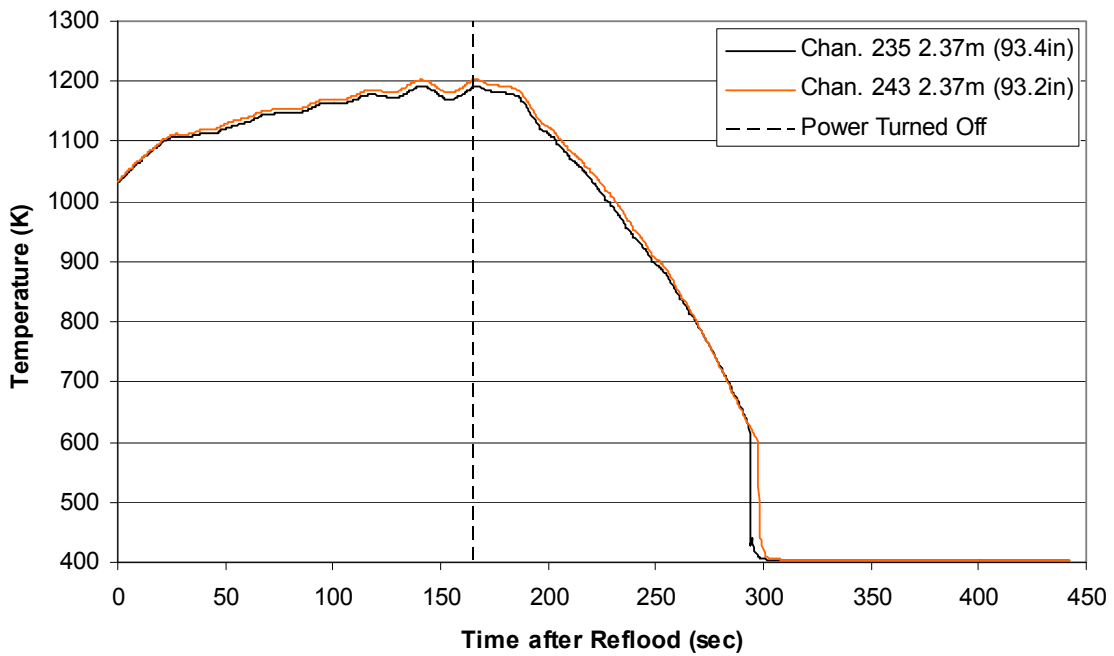
Heater Rod Temperature during Reflood
RBHT Exp. 1319



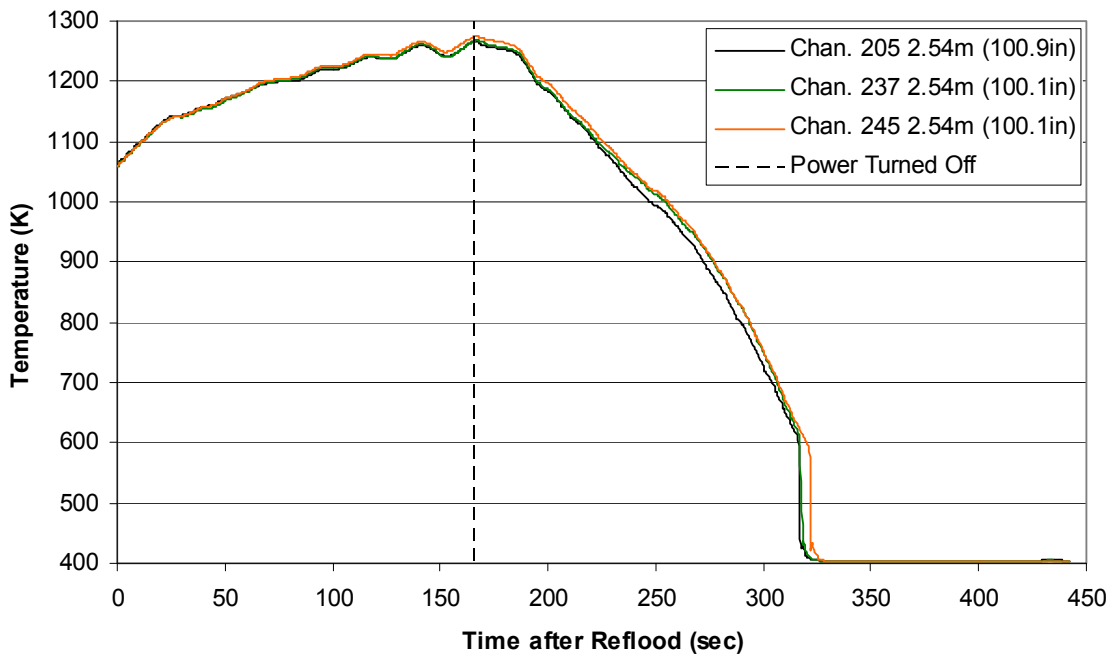
Heater Rod Temperature during Reflood
RBHT Exp. 1319



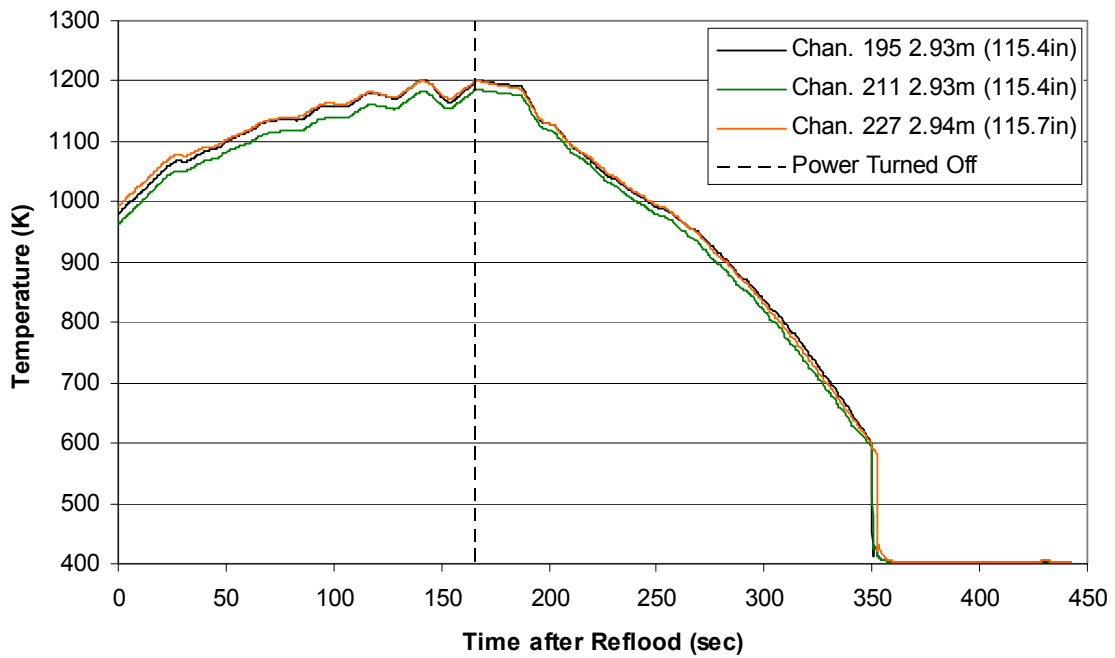
Heater Rod Temperature during Reflood
RBHT Exp. 1319



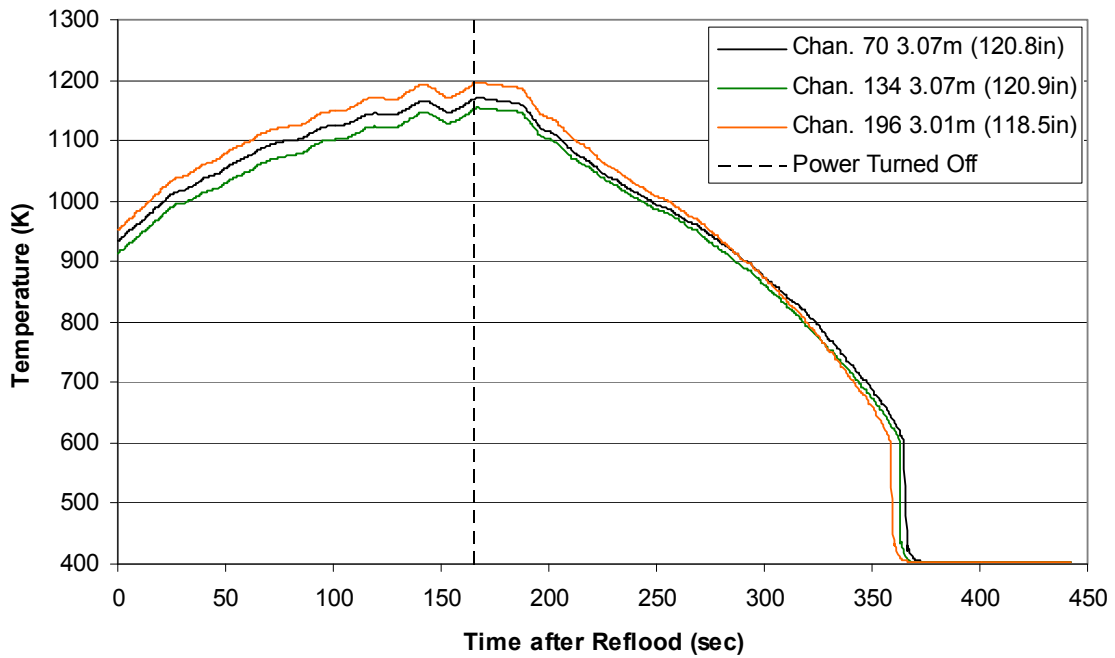
Heater Rod Temperature during Reflood
RBHT Exp. 1319



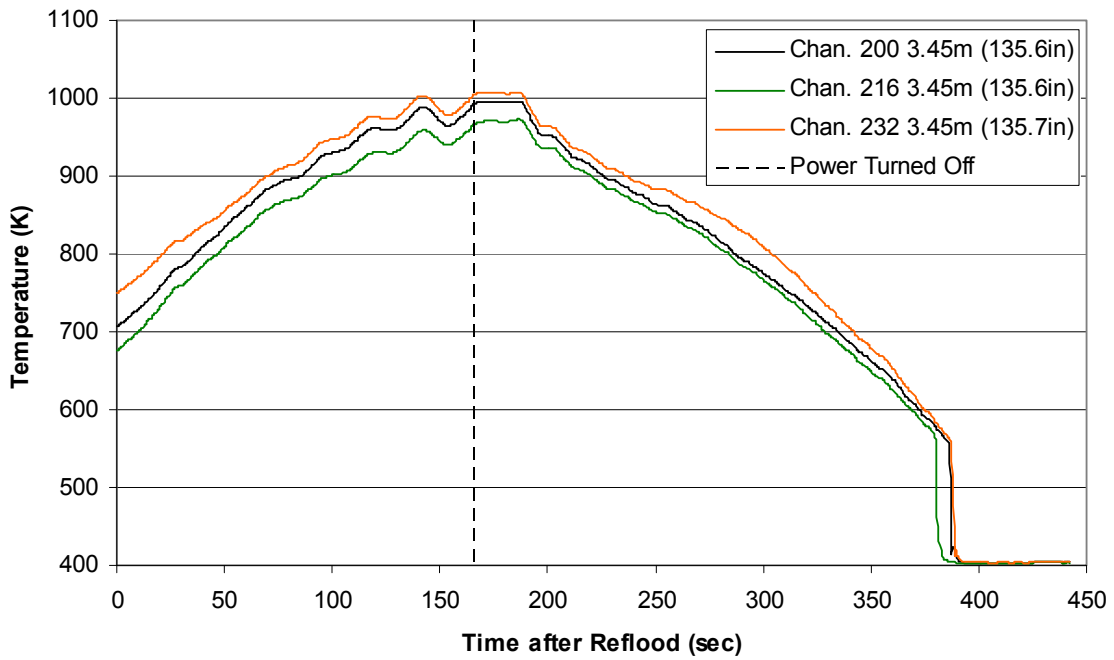
Heater Rod Temperature during Reflood
RBHT Exp. 1319



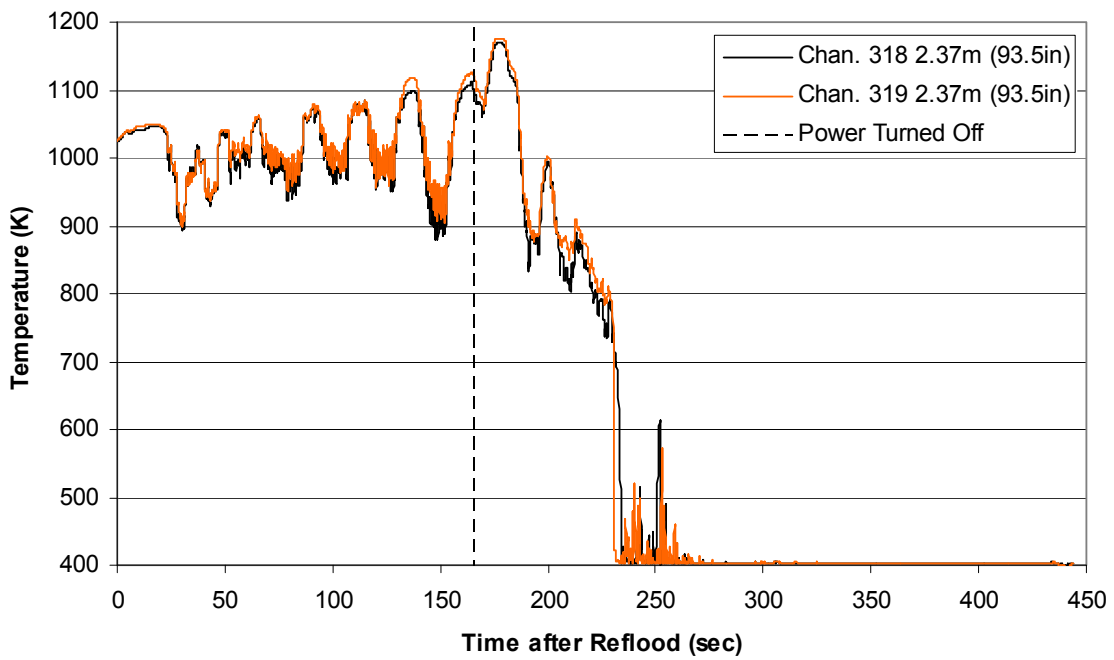
Heater Rod Temperature during Reflood
RBHT Exp. 1319



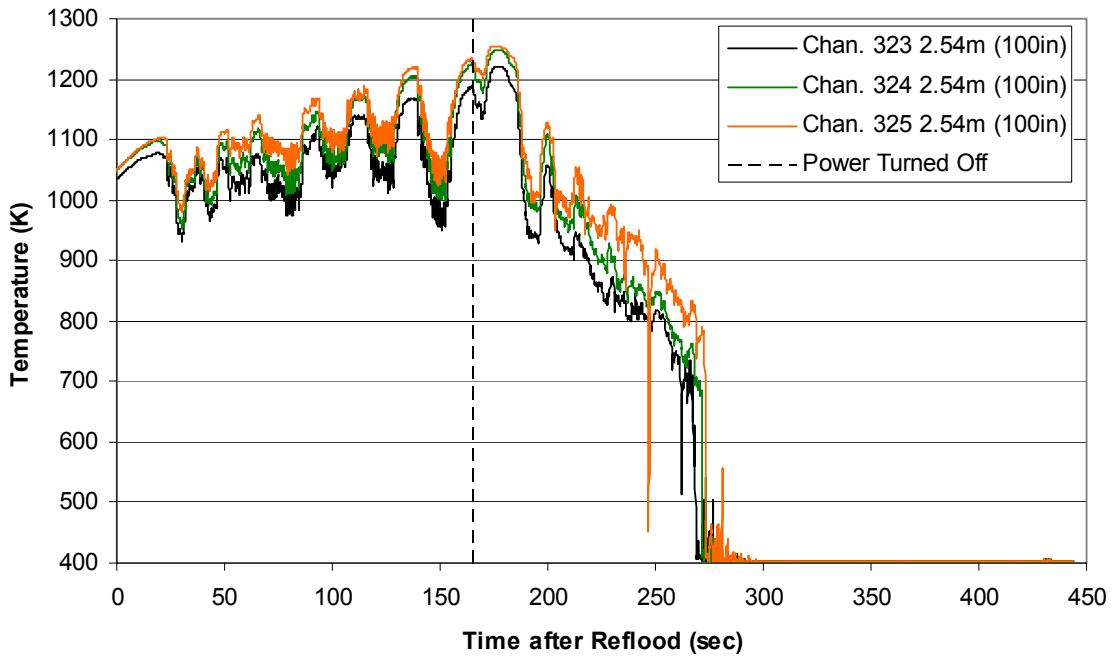
Heater Rod Temperature during Reflood
RBHT Exp. 1319



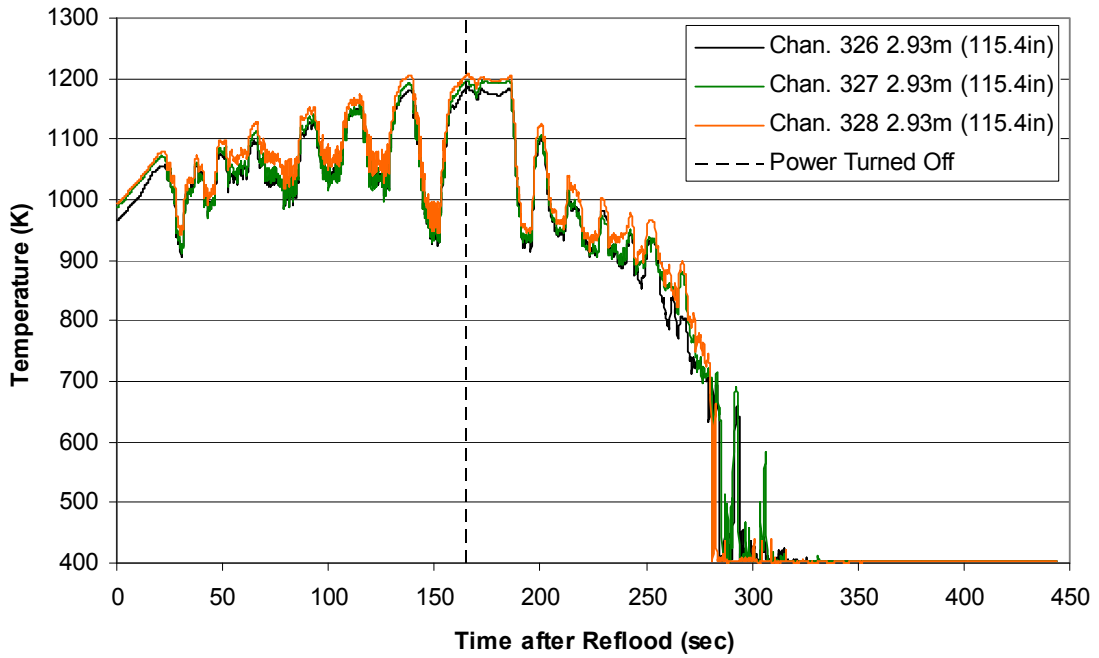
Heater Rod Temperature during Reflood
RBHT Exp. 1319



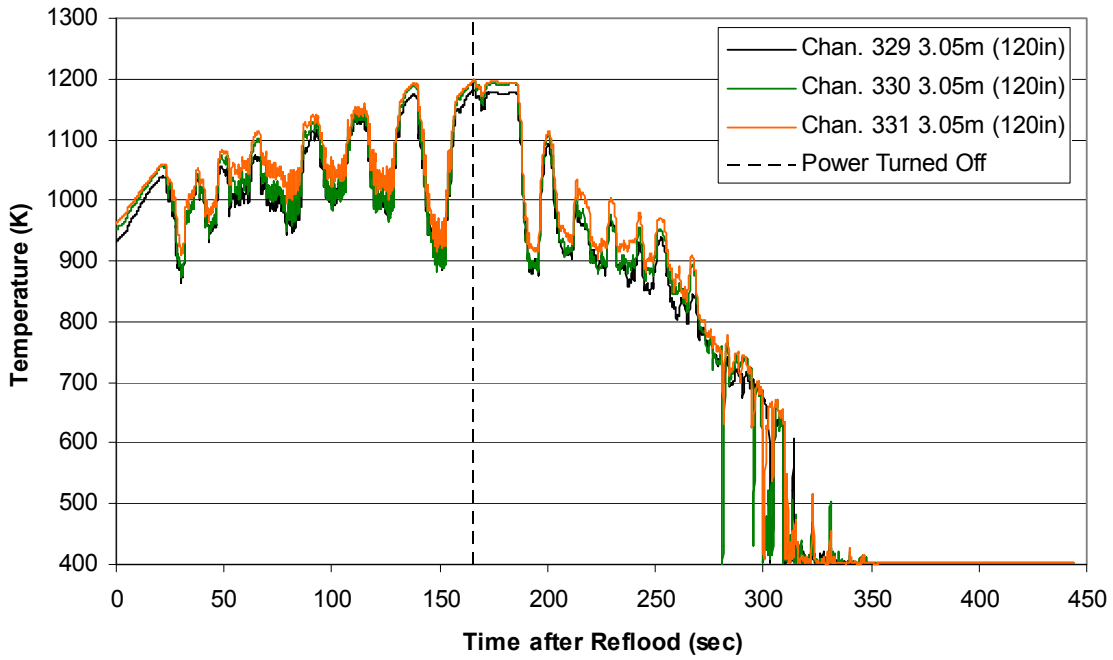
Heater Rod Temperature during Reflood RBHT Exp. 1319



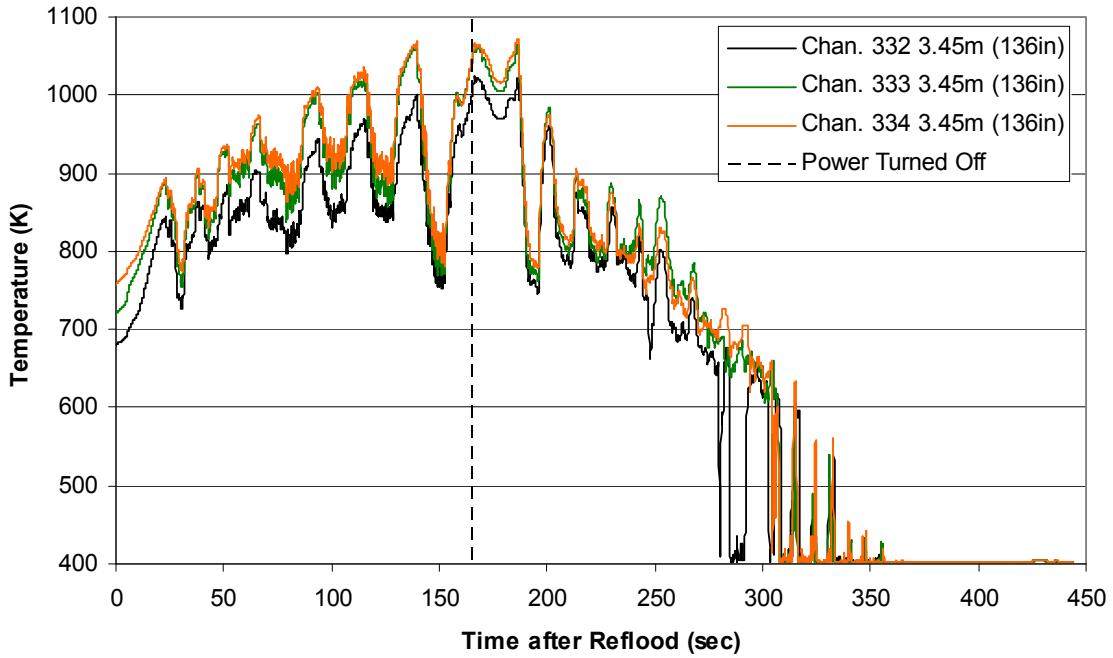
Heater Rod Temperature during Reflood RBHT Exp. 1319



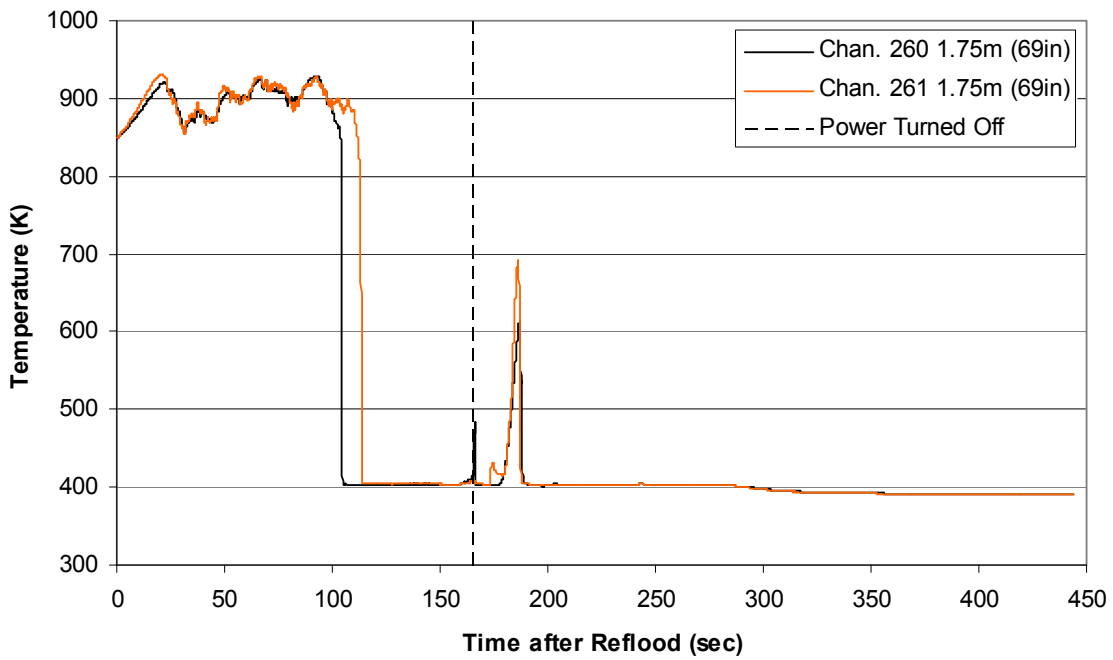
Heater Rod Temperature during Reflood
RBHT Exp. 1319



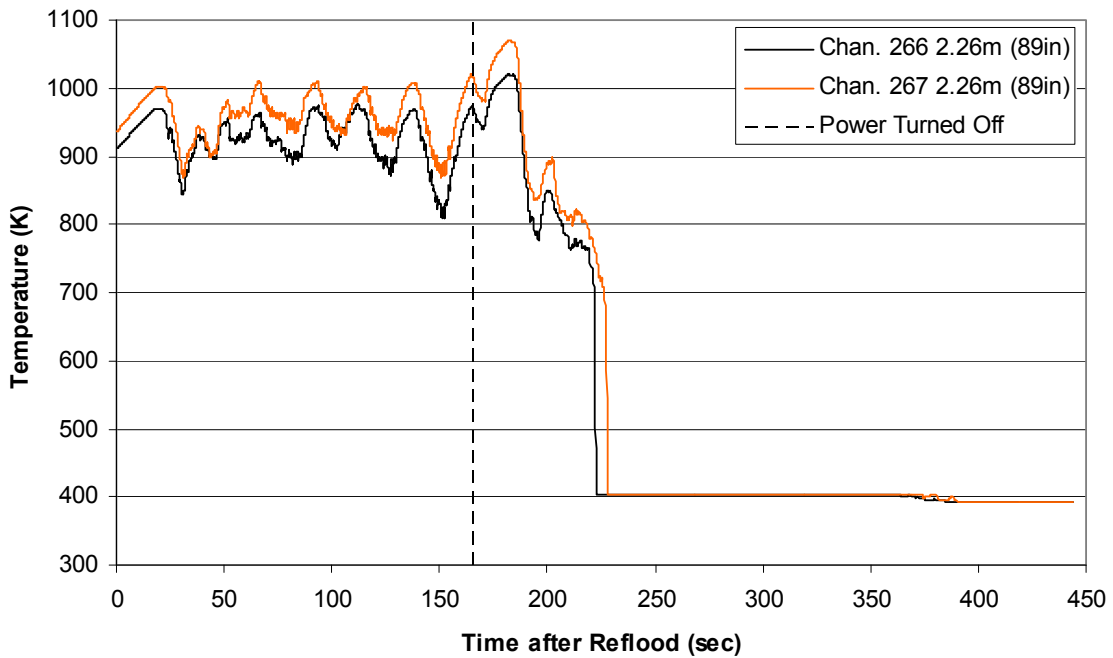
Heater Rod Temperature during Reflood
RBHT Exp. 1319



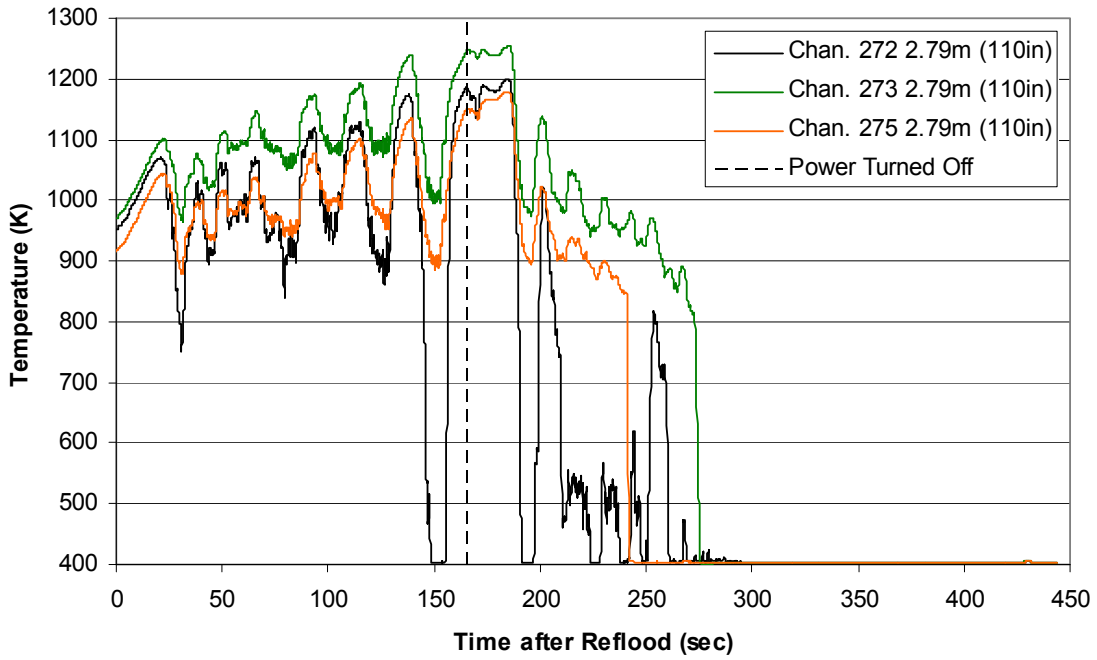
**Heater Rod Temperature during Reflood
RBHT Exp. 1319**



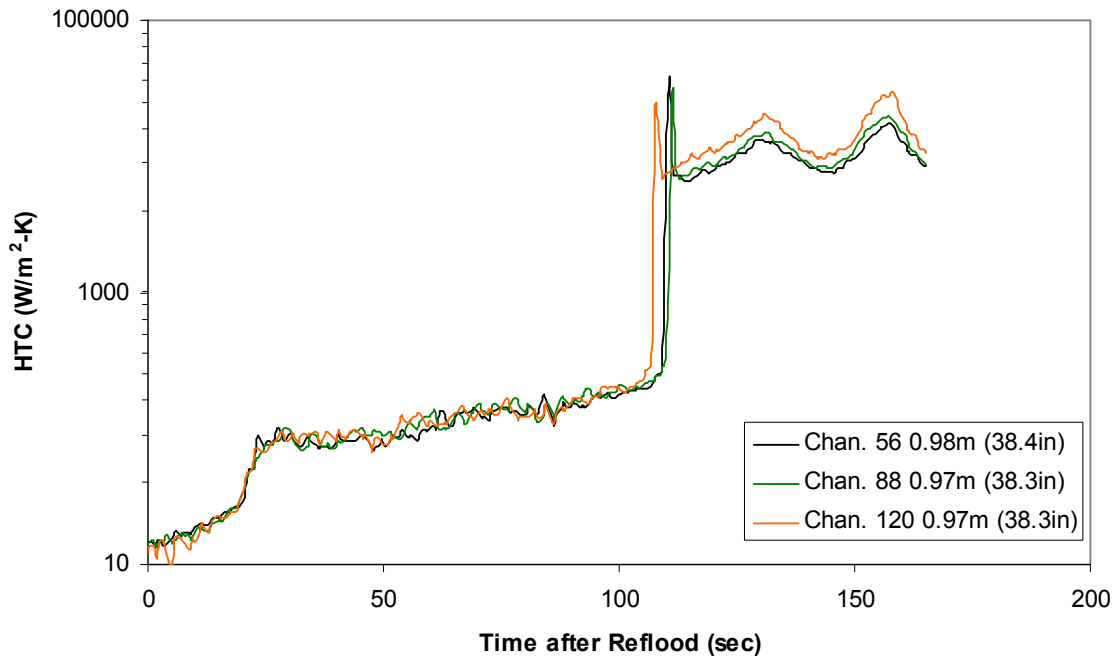
**Heater Rod Temperature during Reflood
RBHT Exp. 1319**



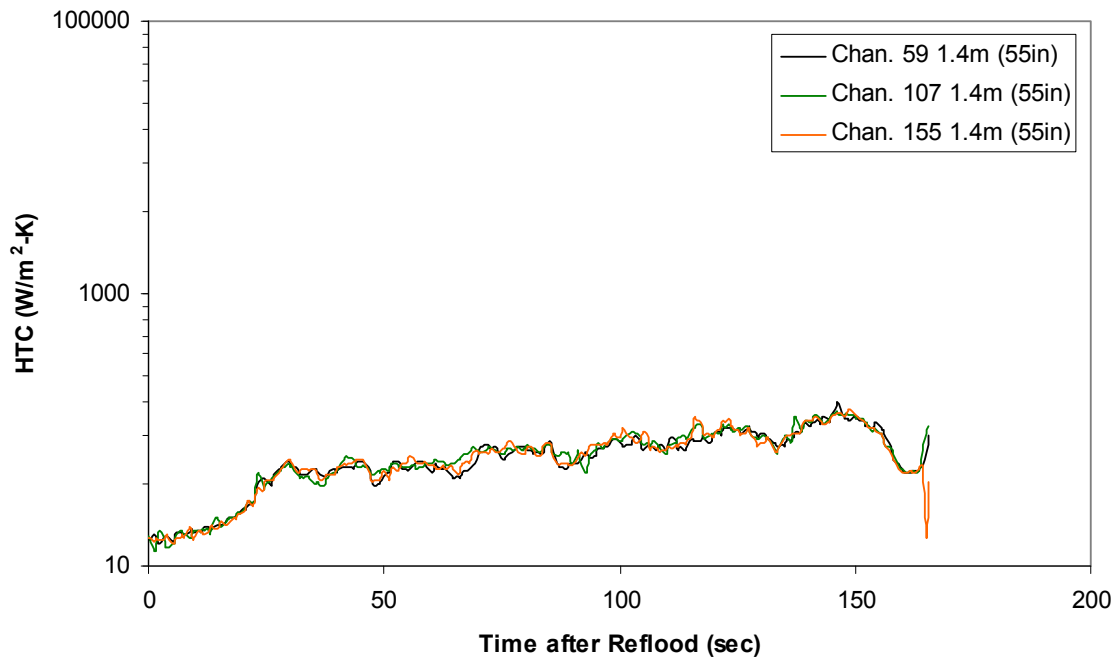
Heater Rod Temperature during Reflood
RBHT Exp. 1319



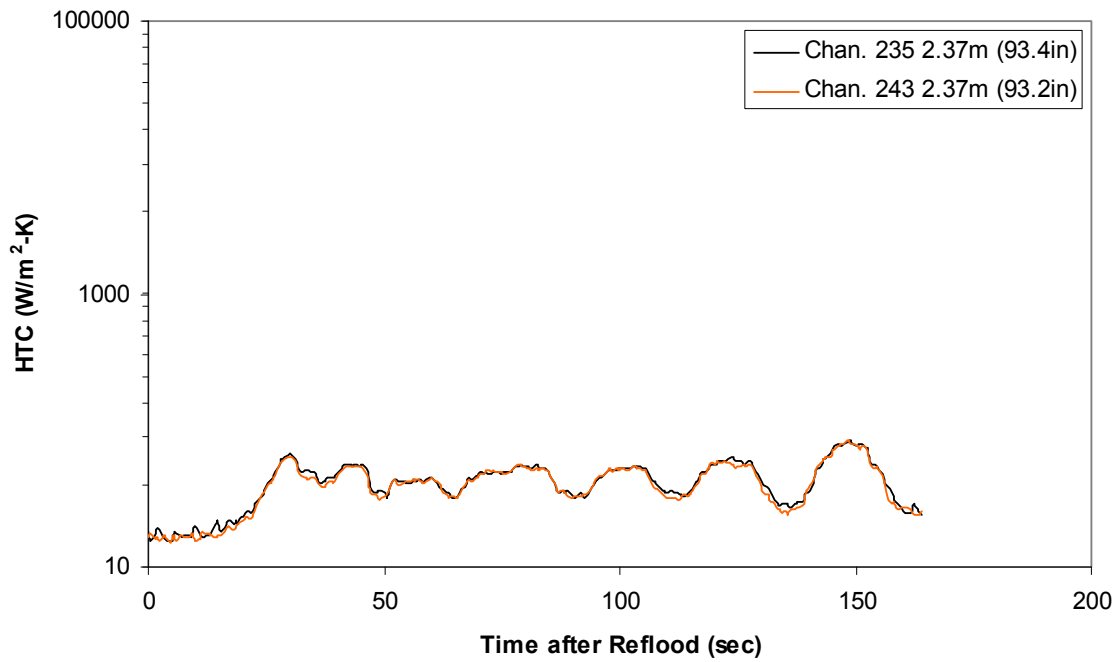
Heat Transfer Coefficient during Reflood
RBHT Exp. 1319



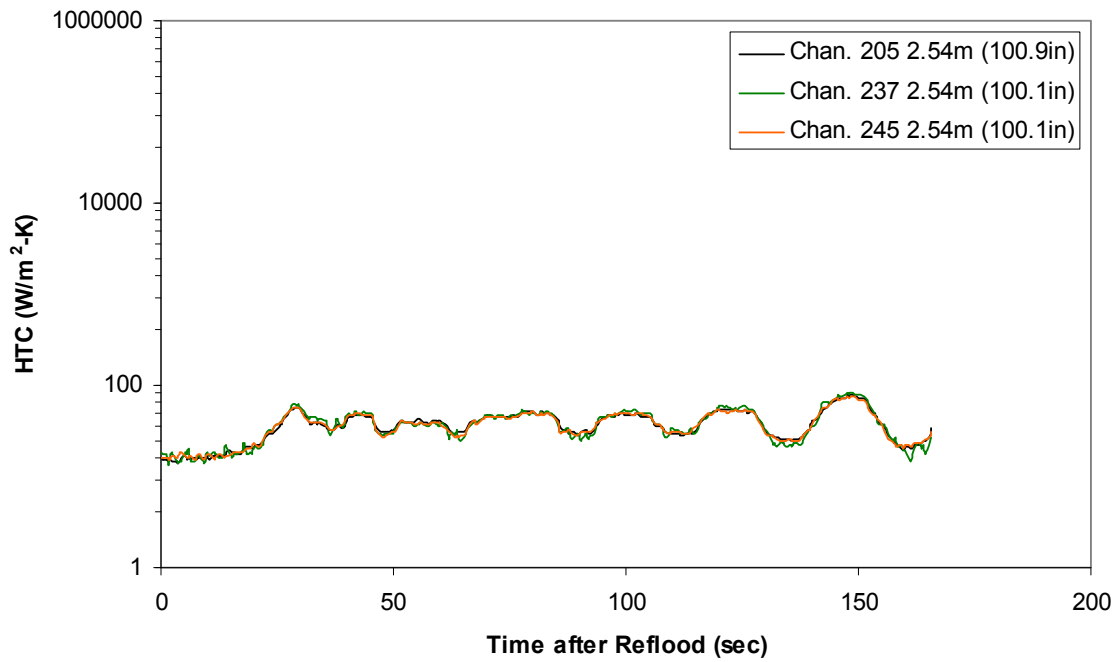
Heat Transfer Coefficient during Reflood RBHT Exp. 1319



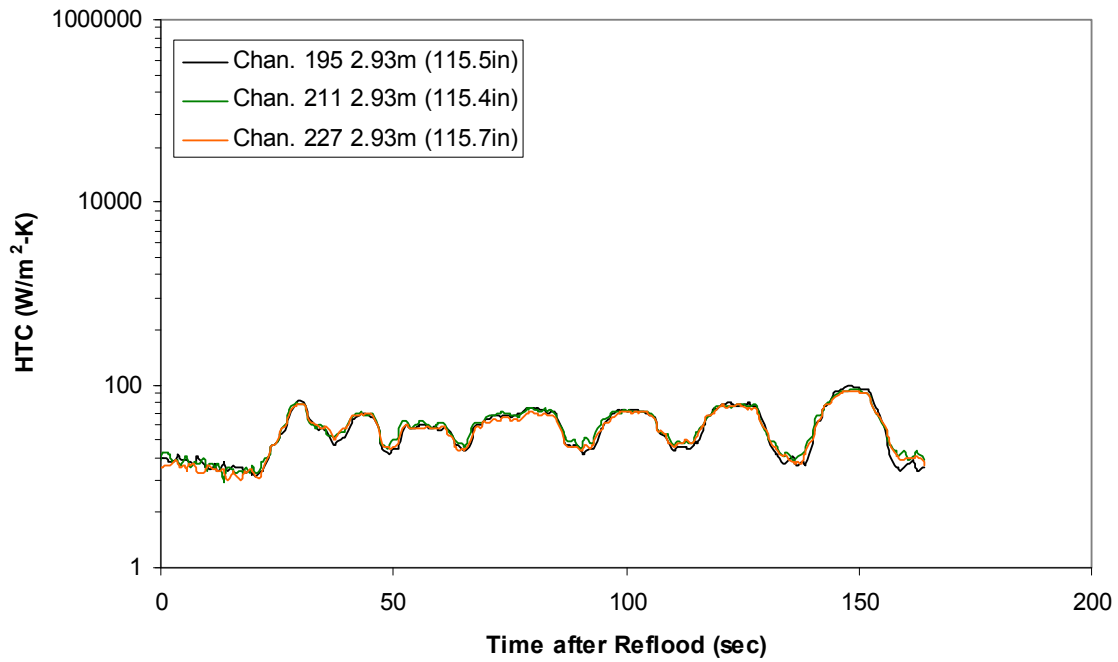
Heat Transfer Coefficient during Reflood RBHT Exp. 1319



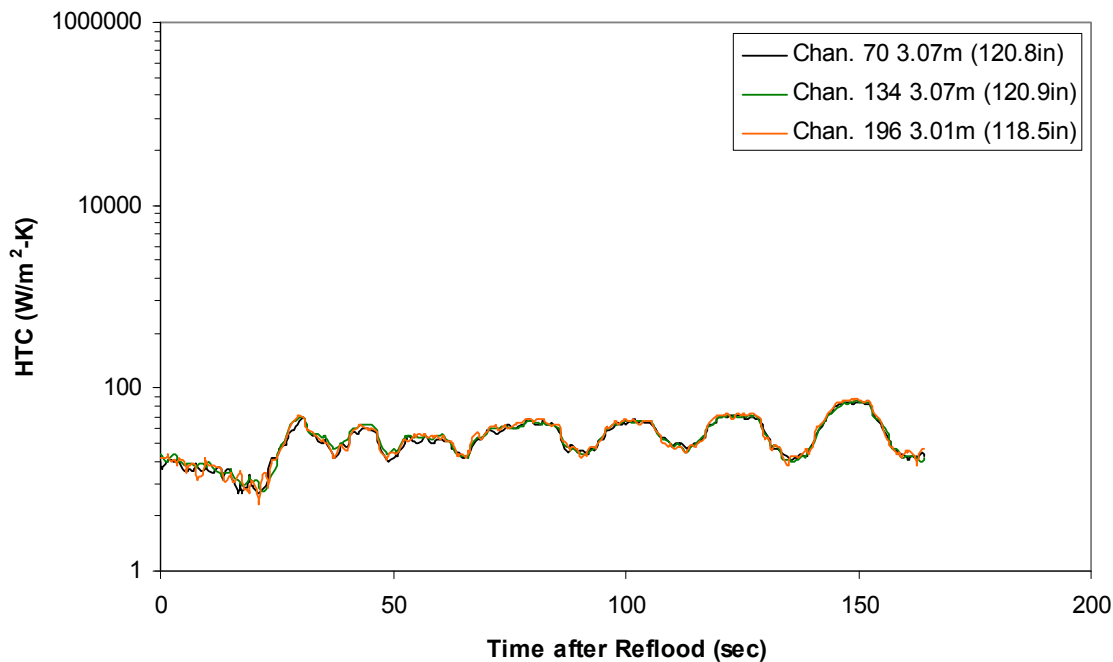
Heat Transfer Coefficient during Reflood RBHT Exp. 1319



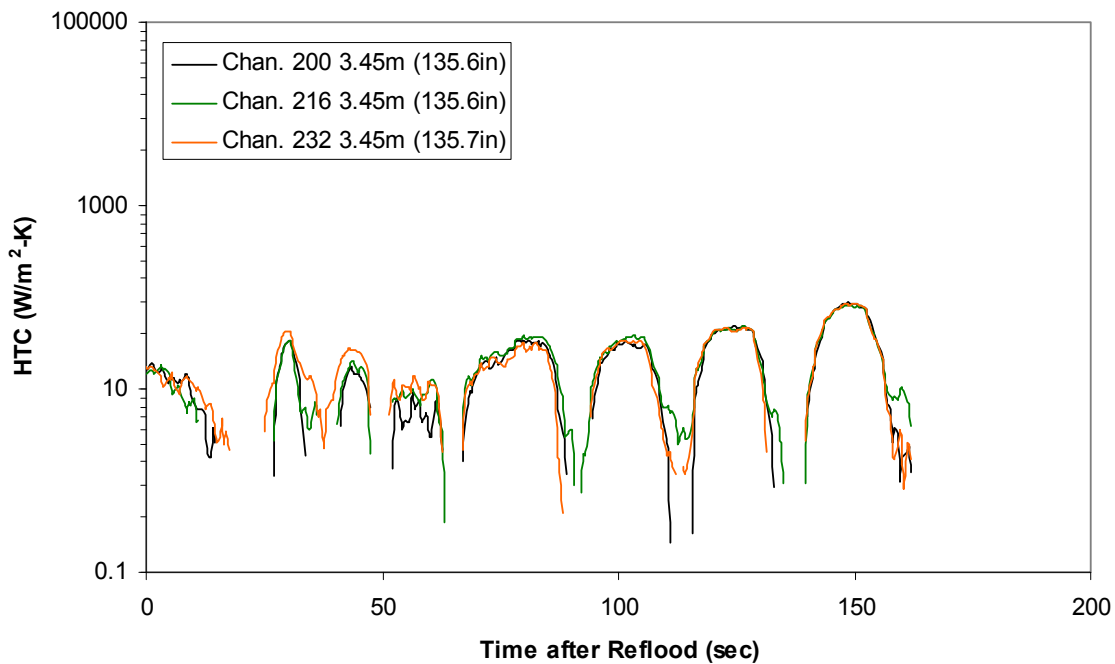
Heat Transfer Coefficient during Reflood RBHT Exp. 1319



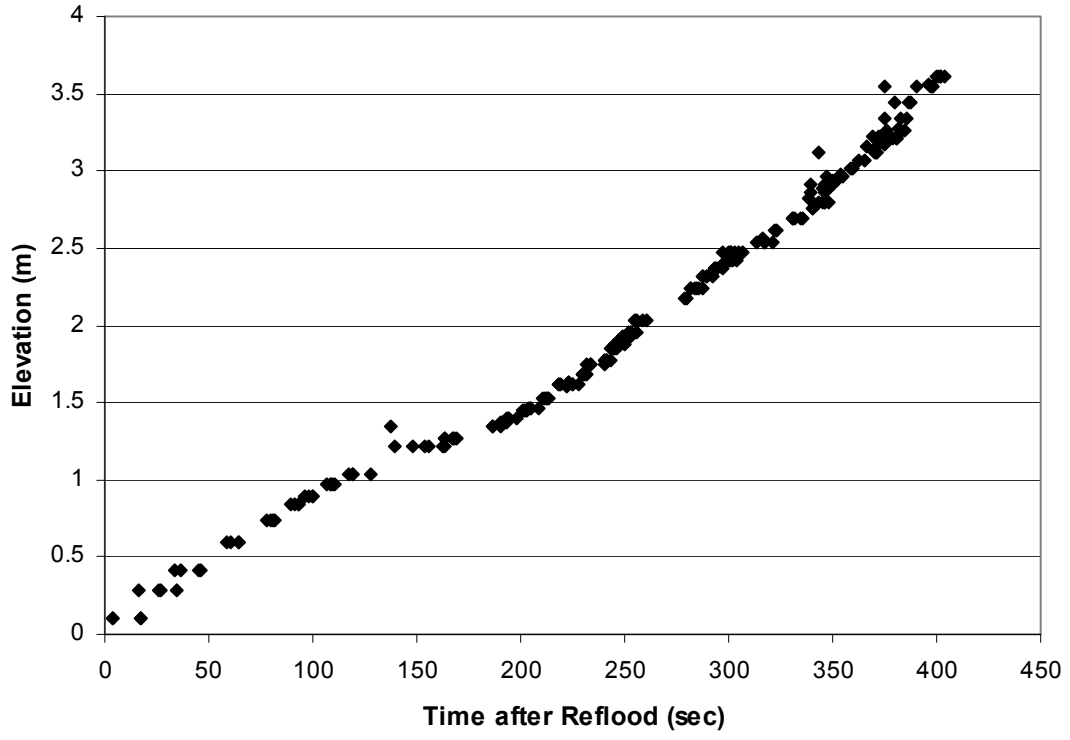
Heat Transfer Coefficient during Reflood RBHT Exp. 1319



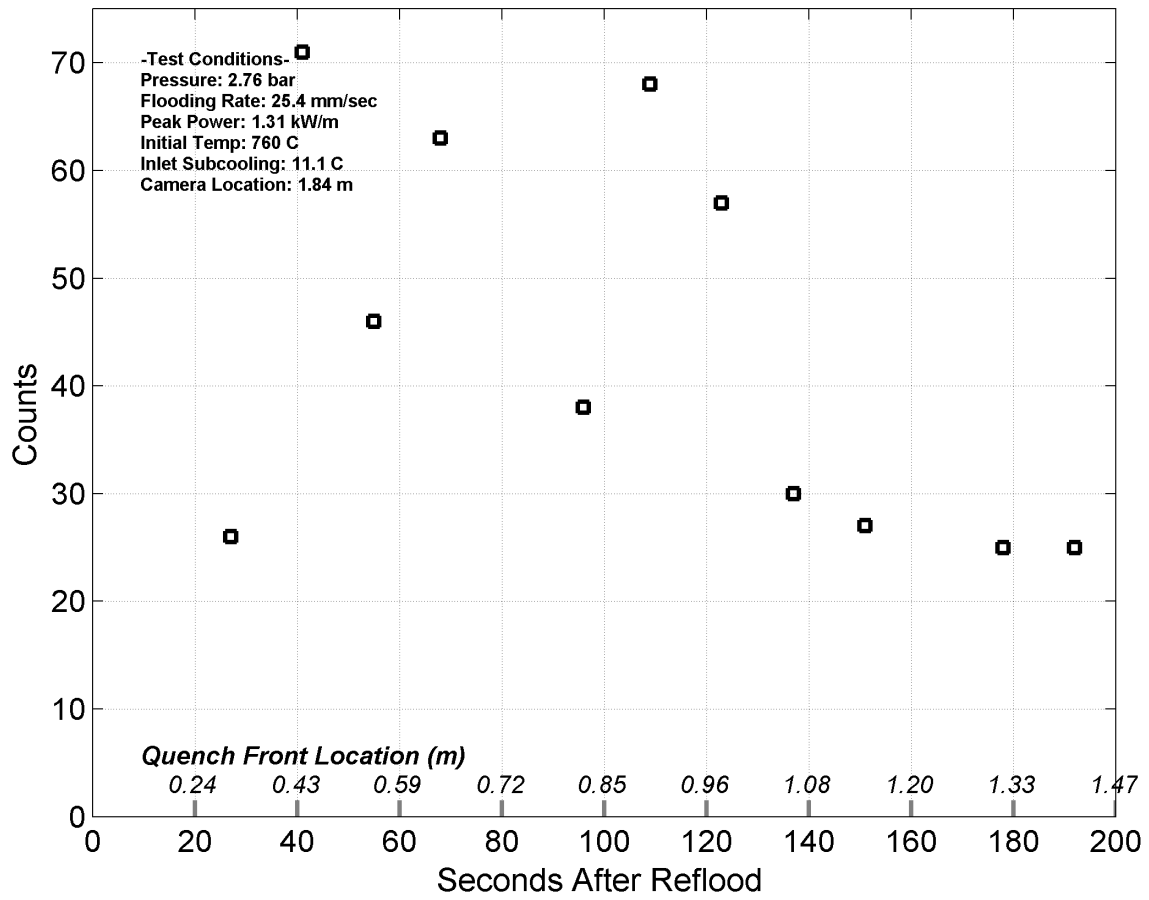
Heat Transfer Coefficient during Reflood RBHT Exp. 1319



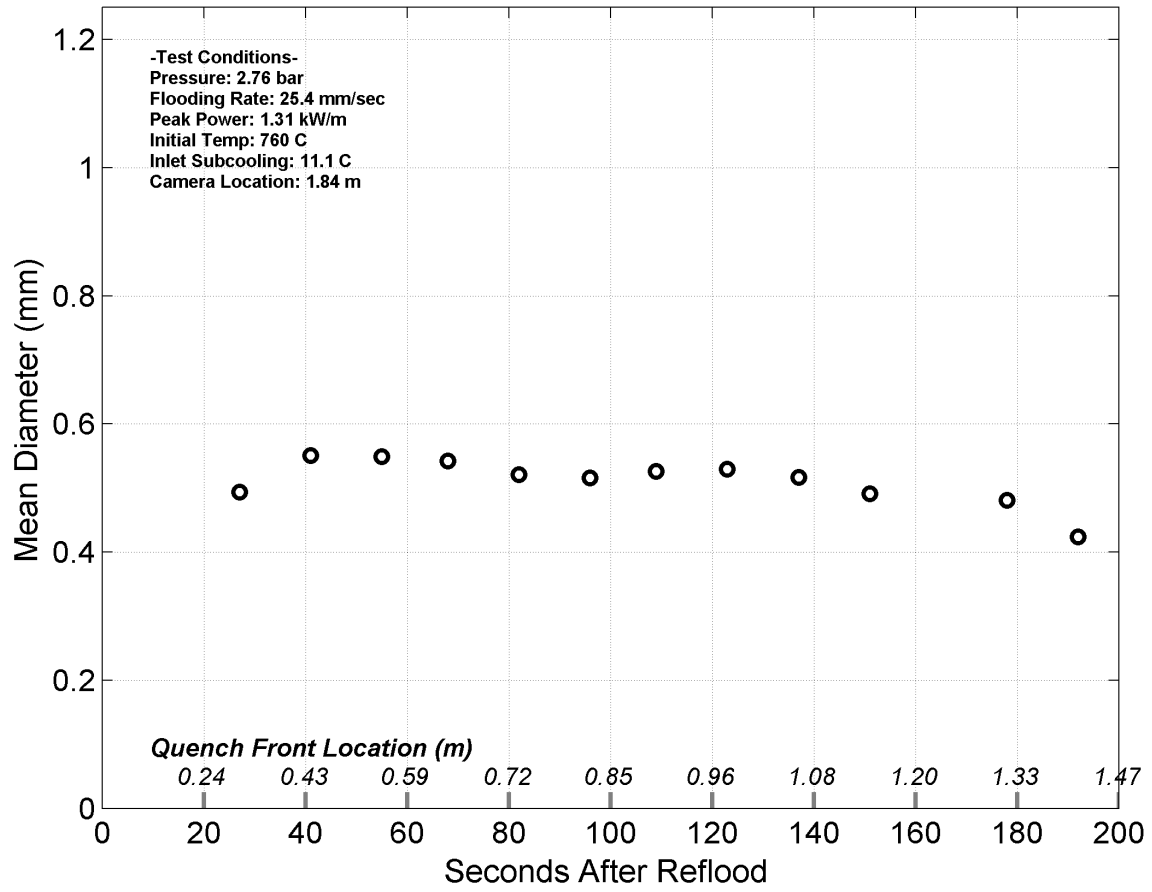
Quench Data, RBHT Exp. 1319



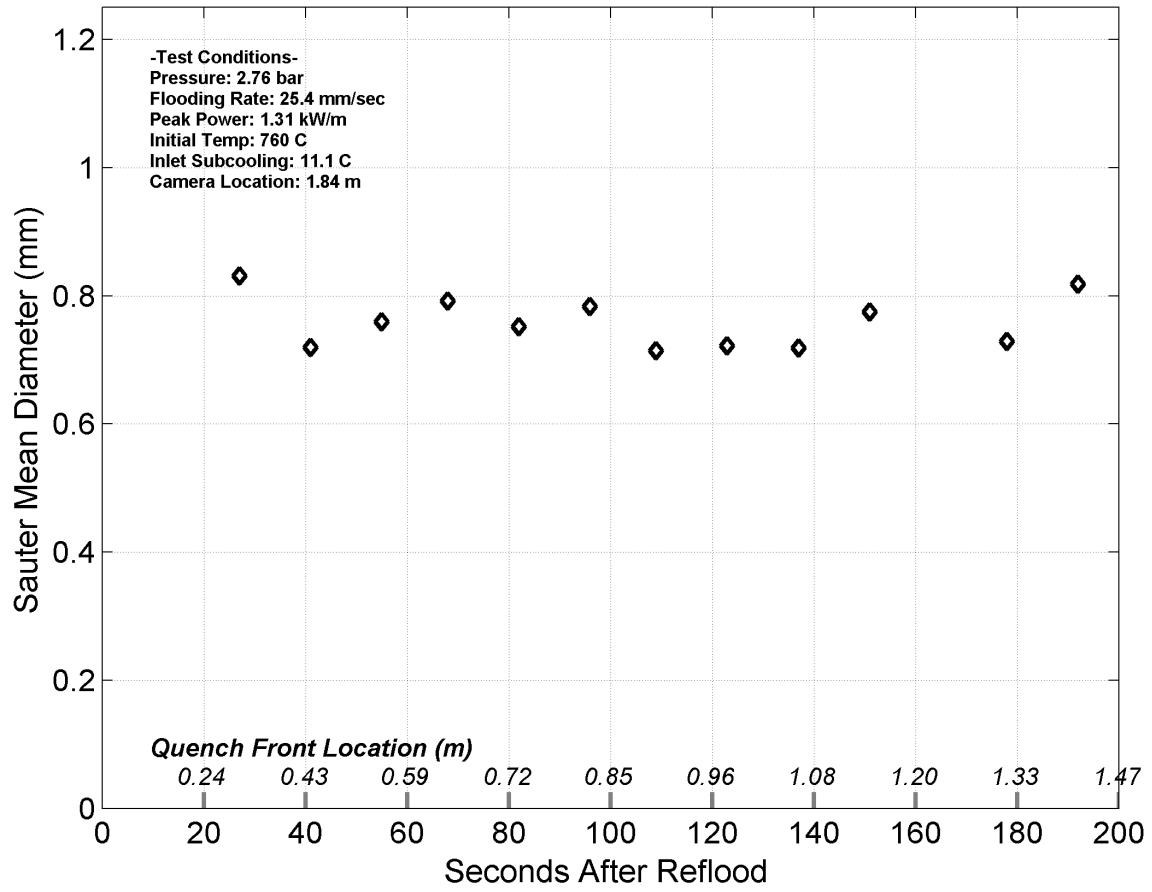
Droplet Counts - Exp. 1319



Mean Droplet Diameter - Exp. 1319



Droplet Sauter Mean Diameter - Exp. 1319



RBHT - REFLOOD TESTS

SUMMARY SHEET

RUN NO: **1383**

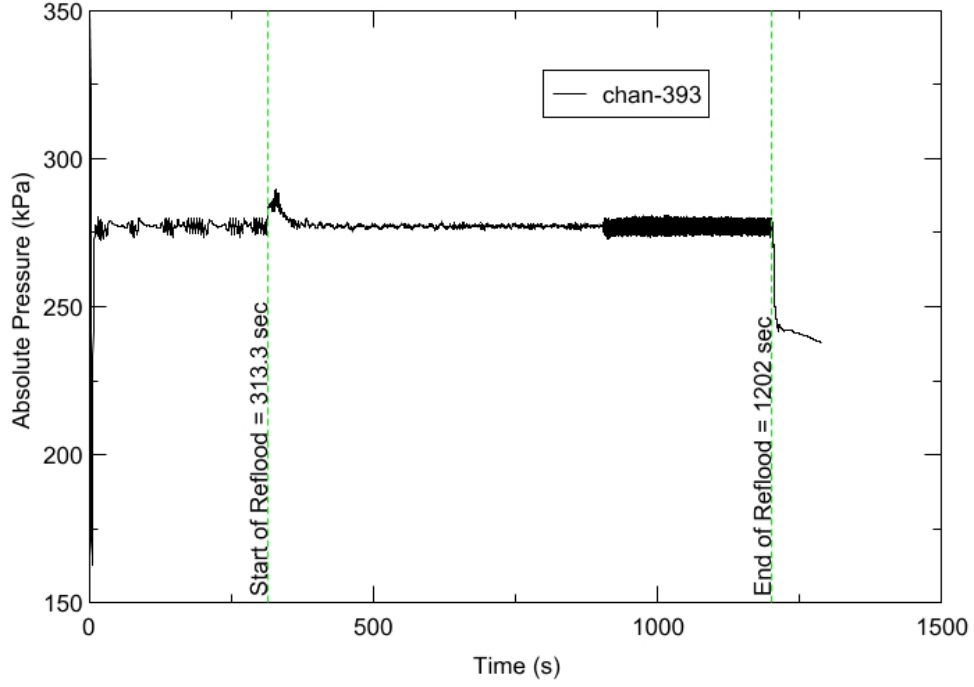
RUN CONDITIONS

Upper Plenum Pressure:	276 kPa (40 psia)
Initial Peak Clad Temperature:	1033 degrees K (1400 degrees F)
Rod Peak Power:	1.31 kW/m (0.4 kW/ft)
Flooding Rate:	0.0254 m/s (1 in/s)
Inlet Subcooling:	11 degrees K (20 degrees F)
Start of Reflood:	313.2 s
End of Reflood:	1202 s
Test Date:	8/23/2002
Comments:	

Rod_Elevation	Channel Number	Temperature at Reflood (K)	Temperature at Reflood (°F)	Turnaround Time (sec.)	Turnaround Temperature (K)	Turnaround Temperature (°F)	Quench Time (sec.)	Quench Temperature (K)	Quench Temperature (°F)
B6 0.592m	148	722.19	840.26	10.55	741.9	875.72	59.05	585.62	594.43
B6 0.744m	149	757.21	903.3	12.55	780.09	944.48	78.05	568.54	563.68
B6 0.846m	150	786.23	955.52	12.55	811.52	1001.04	89.55	587.81	598.37
B6 0.897m	151	796.59	974.18	13.05	822.67	1021.12	95.05	603.11	625.91
C6 1.04m	137	842.34	1056.52	17.55	871.93	1109.79	111.55	646.63	704.24
D5 1.27m	217	896.04	1153.18	14.05	927.35	1209.54	143.55	649.31	709.06
C6 1.34m	138	882.6	1128.99	18.55	917.48	1191.78	159.55	656.95	722.81
D5 1.37m	218	913.57	1184.75	19.55	948.77	1248.1	163.05	675.58	756.36
C6 1.39m	139	888.21	1139.09	18.05	923.97	1203.45	171.55	655.96	721.04
D5 1.45m	219	923.69	1202.95	29.05	960.76	1269.68	178.55	683.43	770.49
C6 1.47m	140	898.08	1156.85	30.05	937.24	1227.34	188.55	674.88	755.1
D5 1.52m	220	933.2	1220.08	41.05	976.73	1298.42	197.05	700.48	801.18
C6 1.62m	141	911.12	1180.33	67.05	971.08	1288.25	230.55	695.4	792.03
D5 1.68m	221	944.92	1241.17	62.55	1009.37	1357.18	241.55	723.01	841.72
D5 1.78m	222	939.84	1232.02	14.05	973.36	1292.36	271.05	623.99	663.49
D5 1.85m	223	956.14	1261.36	62.05	1004.17	1347.83	287.05	685.59	774.37
C6 1.87m	142	934.38	1222.19	40.55	984.8	1312.96	299.55	671.38	748.79
D5 1.90m	224	963.42	1274.46	67.05	1023.33	1382.31	303.05	707.3	813.45
C6 1.95m	144	944.99	1241.29	67.05	1008.49	1355.59	327.55	681.29	766.63
C3 2.17m	178	974.68	1294.73	14.55	1017.29	1371.43	420.05	643.95	699.43
D4 2.24m	241	1017.48	1371.78	16.05	1058.72	1446	444.55	635.02	683.36
D4 2.32m	242	1025.09	1385.48	25.05	1073.12	1471.92	462.05	693.17	788.02
C3 2.35m	180	1016.83	1370.6	61.05	1072.82	1471.4	462.05	706.03	811.16
D4 2.37m	243	1030.42	1395.07	25.05	1079.11	1482.71	480.05	690.37	782.98
C3 2.40m	181	1018.82	1374.19	61.55	1070.56	1467.32	484.05	680.77	765.7
D4 2.54m	245	1045.46	1422.13	67.05	1115.95	1549.03	560.55	680.64	765.46
D6 2.62m	129	1023.7	1382.97	91.05	1112.41	1542.65	566.05	717.08	831.06
D6 2.69m	130	1009.52	1357.45	102.55	1119.06	1554.62	596.05	689.51	781.44
C3 2.76m	183	1009.28	1357.01	206.05	1133.85	1581.24	662.05	634.36	682.16
D4 2.79m	247	994.99	1331.3	234.05	1065.5	1458.21	691.55	595.22	611.72
D6 2.87m	131	949.57	1249.54	17.05	996.35	1333.74	671.55	640.23	692.73
D6 2.92m	132	932.93	1219.59	68.05	997.4	1335.63	684.05	683.64	770.86
D6 2.97m	133	917.66	1192.1	304.05	1000.42	1341.07	704.05	676.28	757.62
D6 3.07m	134	899.12	1158.72	304.05	1004.54	1348.49	727.55	675.16	755.59
E3 3.12m	197	907.53	1173.87	344.05	1010.64	1359.47	763.05	655.36	719.96
D6 3.17m	135	876.93	1118.78	344.05	1001.02	1342.15	752.05	667	740.92
D6 3.27m	136	840.04	1052.38	344.05	987.83	1318.41	775.05	648.08	706.85
D4 3.61m	248	642.66	697.1	103.05	773.35	932.34	835.55	569.2	564.87

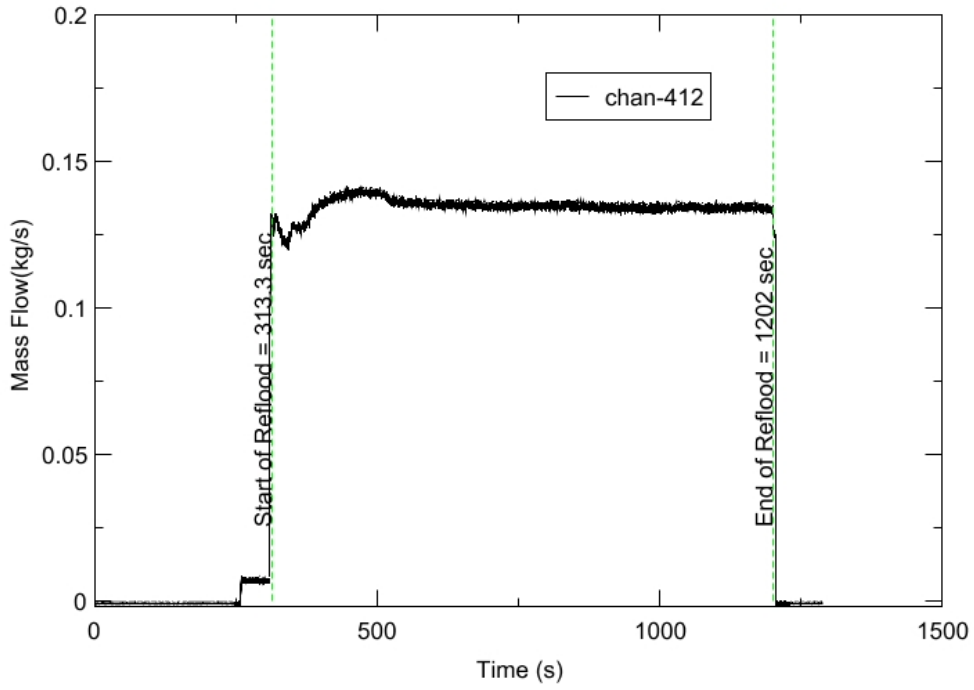
RBHT - TEST FACILITY

Upper Plenum Pressure vs. Time, Exp 1383



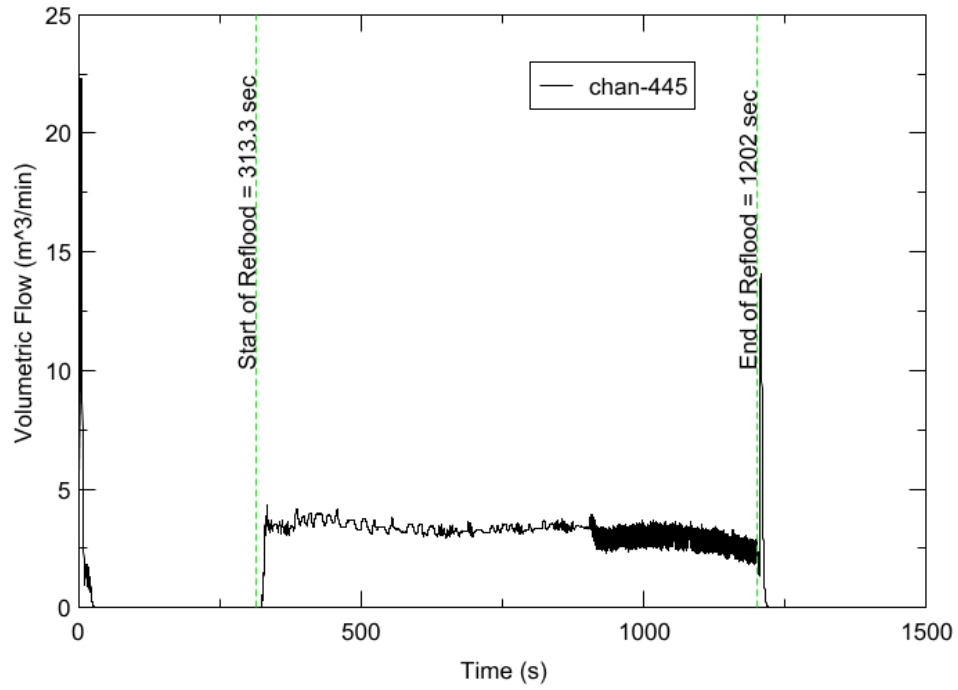
RBHT - TEST FACILITY

Inlet Flow vs. Time, Exp 1383



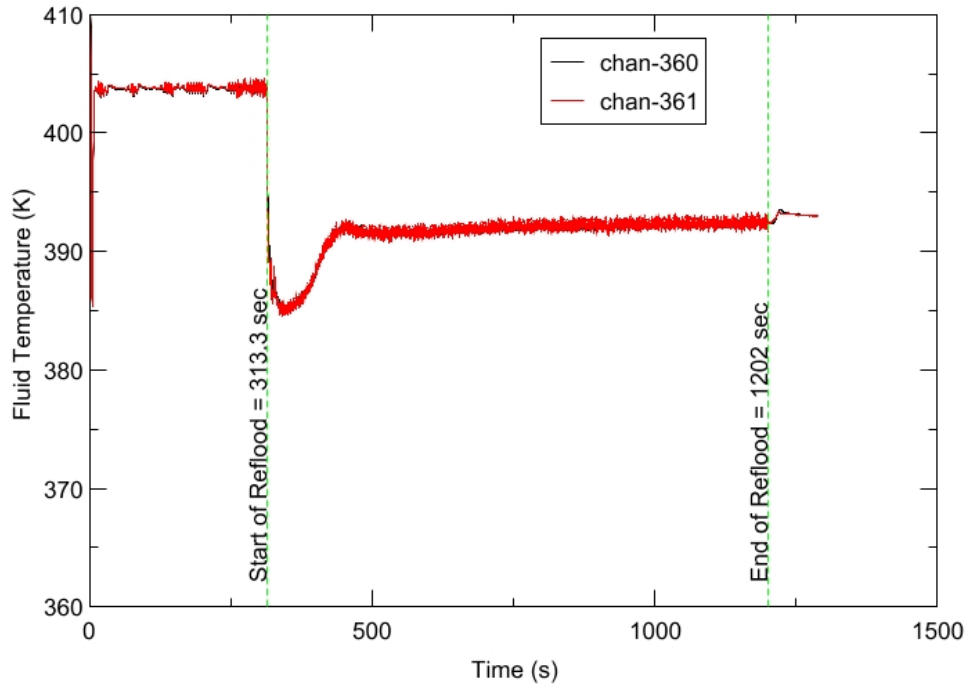
RBHT - TEST FACILITY

Steam Exhaust Flow vs. Time, Exp 1383



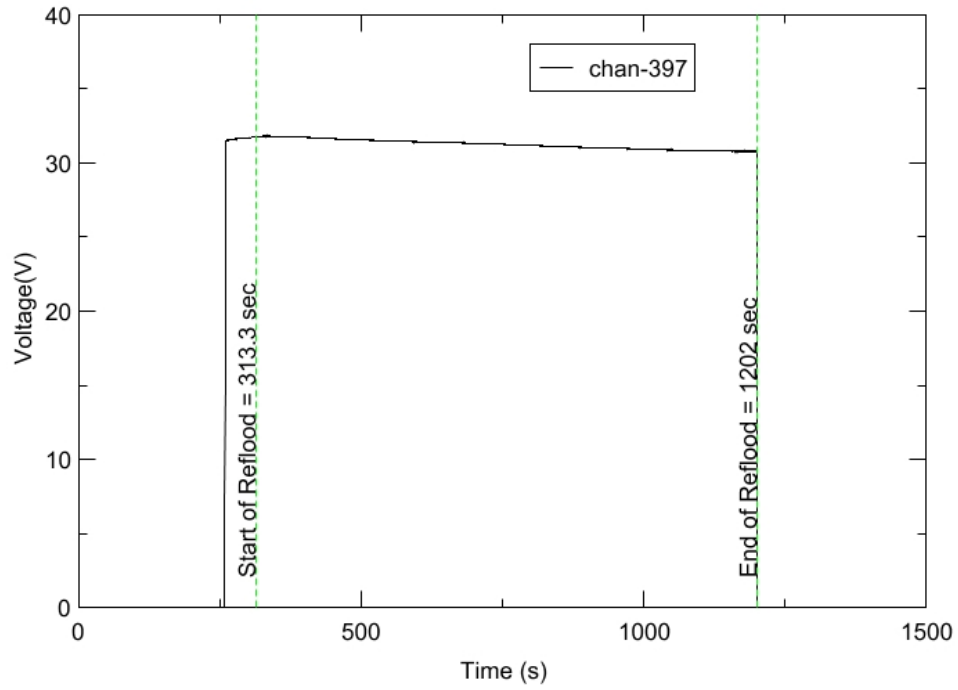
RBHT - TEST FACILITY

Inlet Flow Temperature vs. Time, Exp 1383



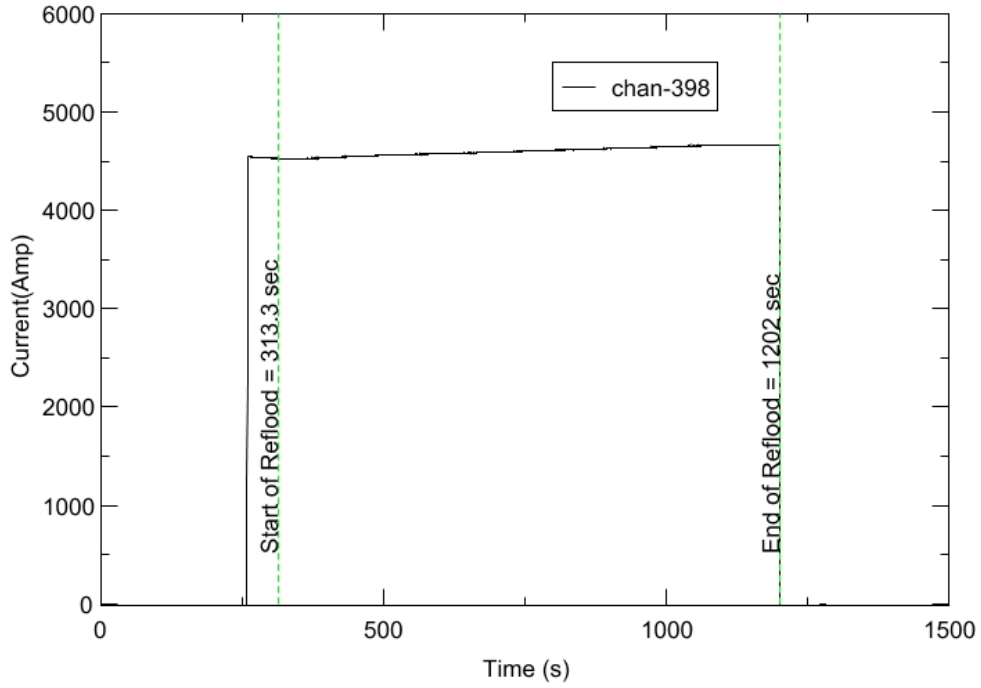
RBHT - TEST FACILITY

Test Section Voltage vs. Time, Exp 1383

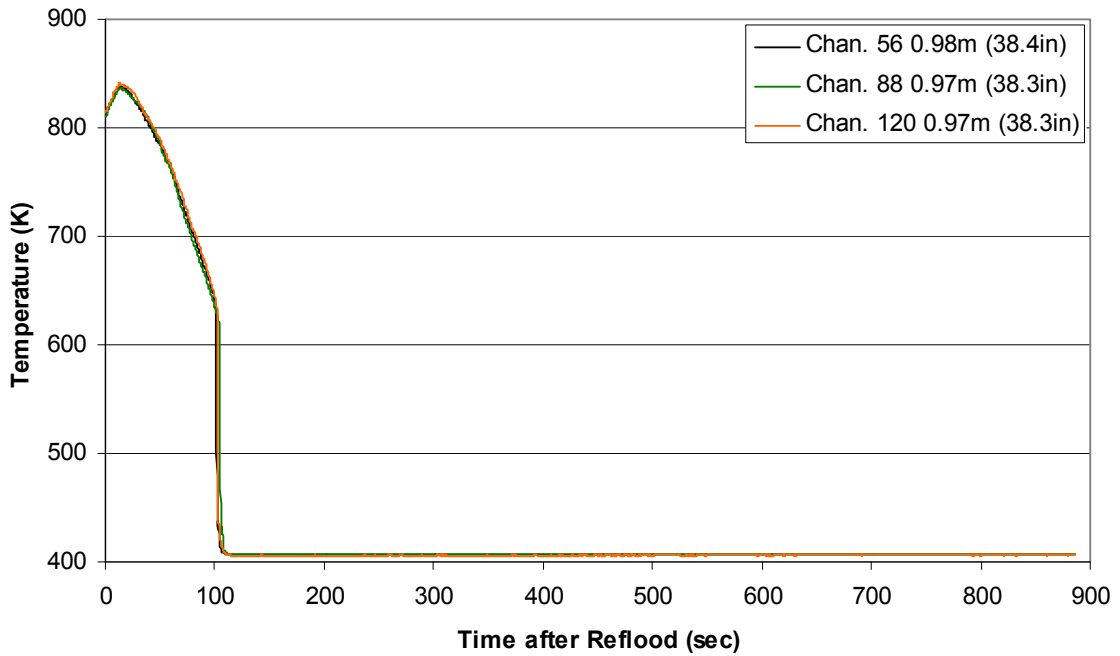


RBHT - TEST FACILITY

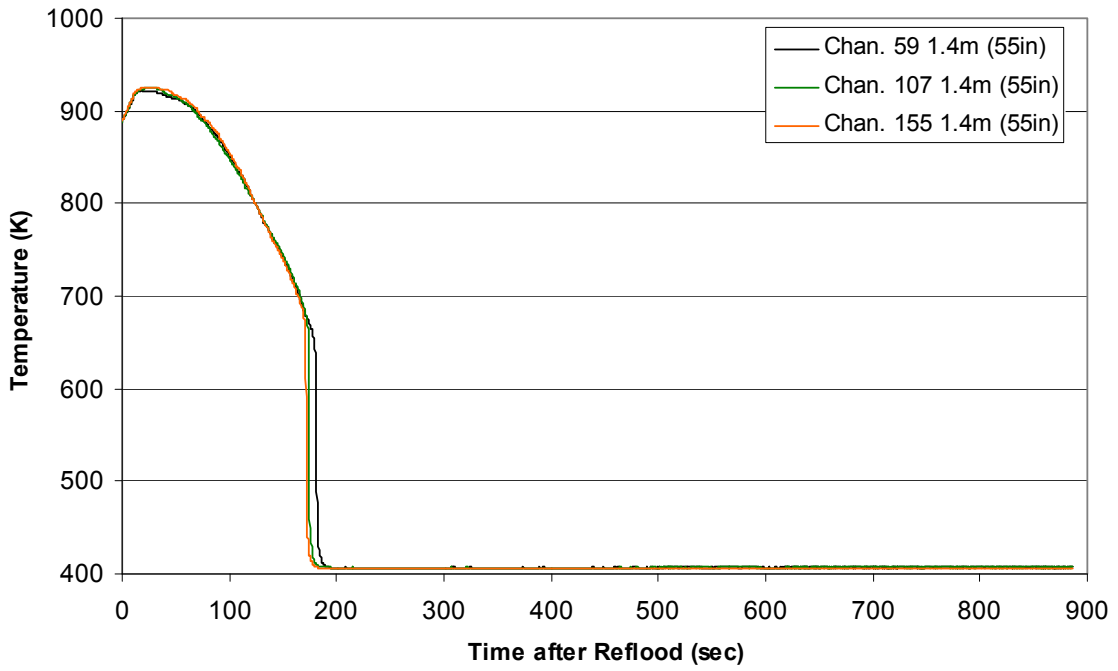
Test Section Current vs. Time, Exp 1383



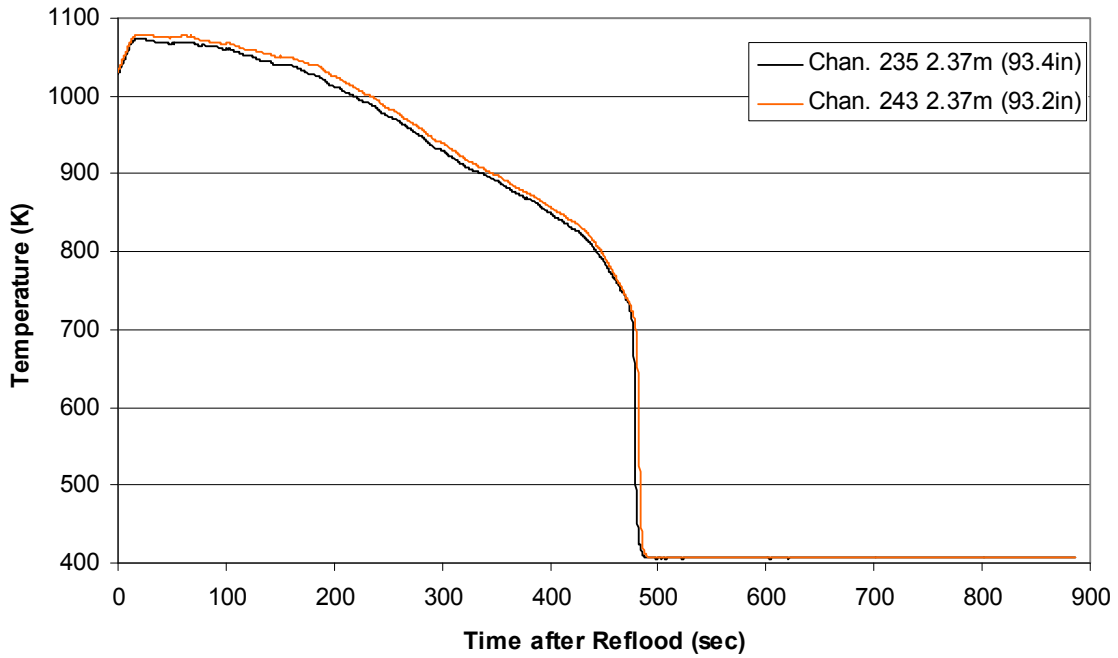
Heater Rod Temperature during Reflood RBHT Exp. 1383



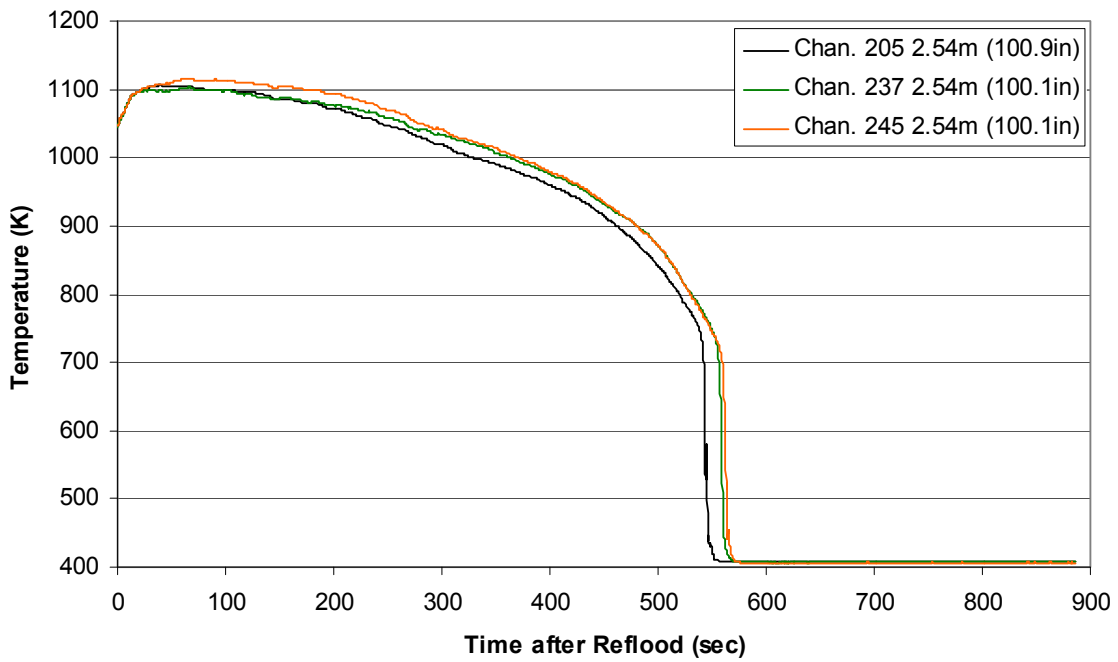
Heater Rod Temperature during Reflood
RBHT Exp. 1383



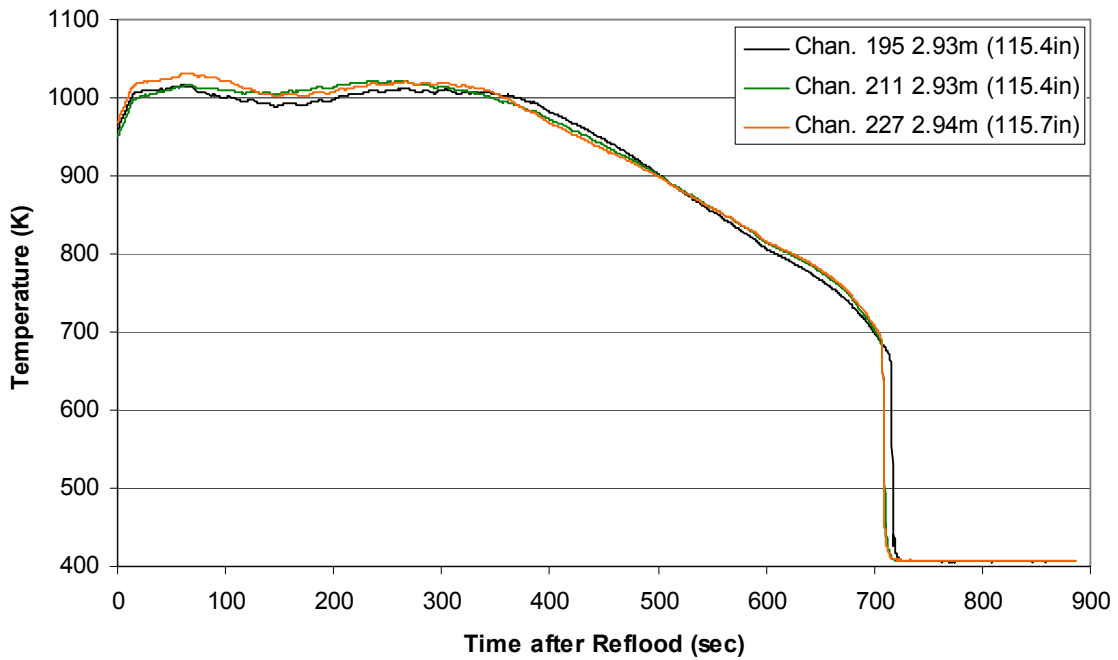
Heater Rod Temperature during Reflood
RBHT Exp. 1383



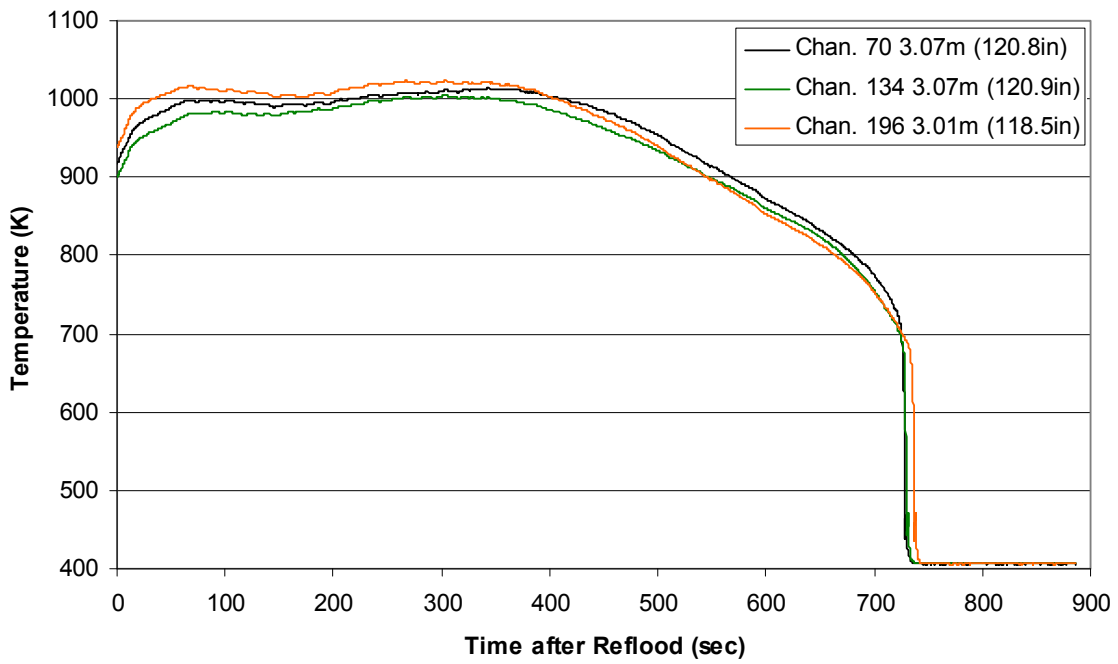
**Heater Rod Temperature during Reflood
RBHT Exp. 1383**



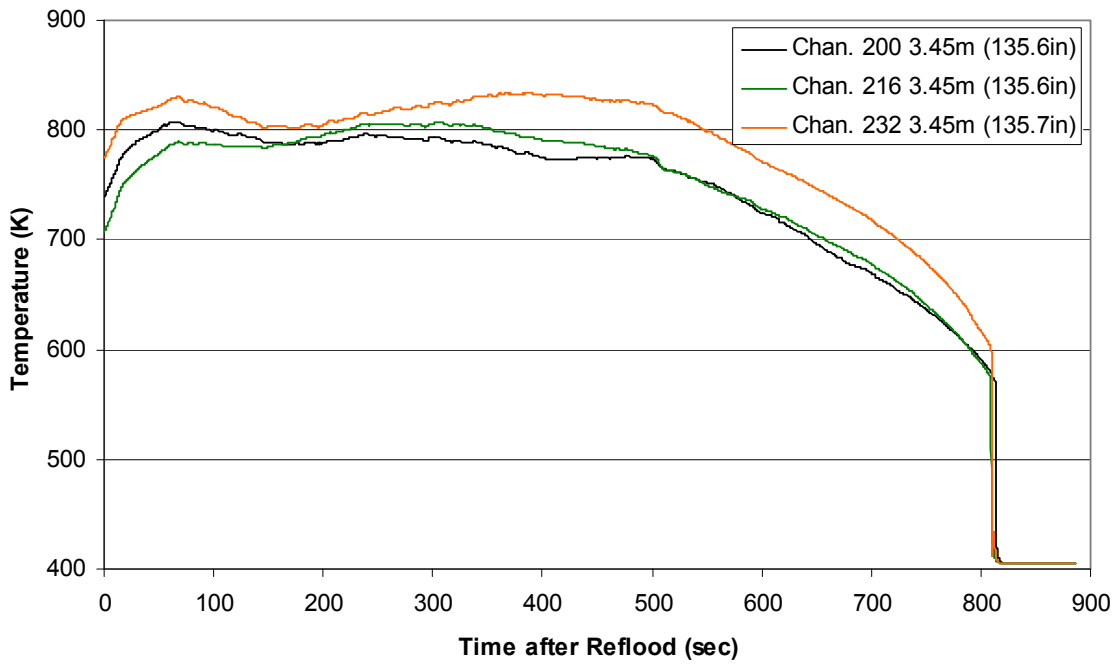
**Heater Rod Temperature during Reflood
RBHT Exp. 1383**



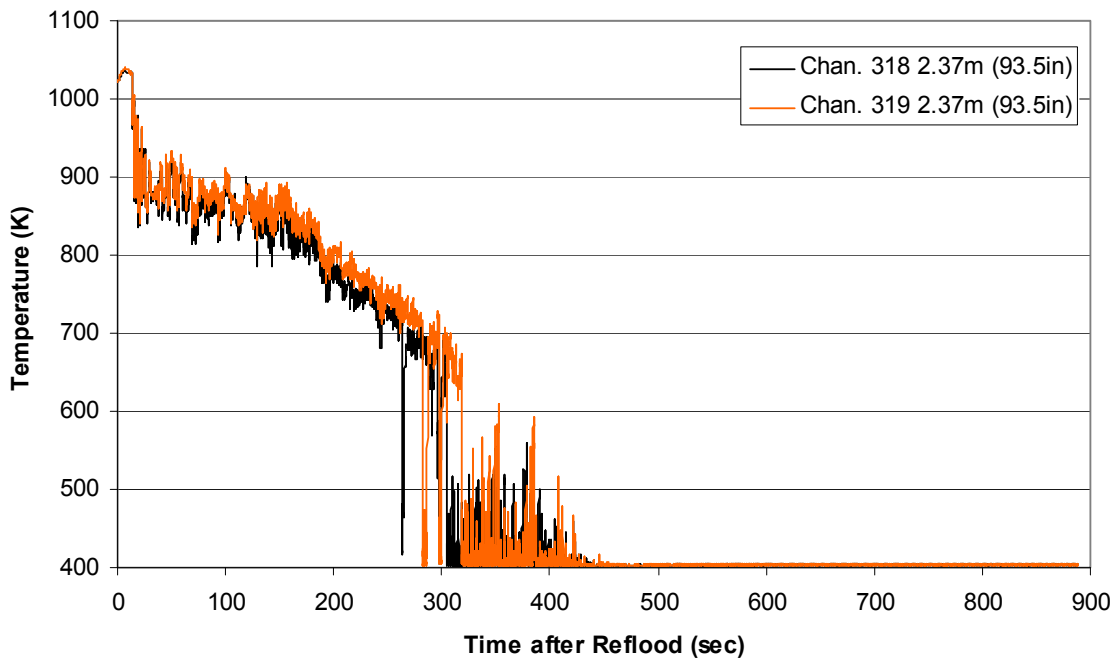
**Heater Rod Temperature during Reflood
RBHT Exp. 1383**



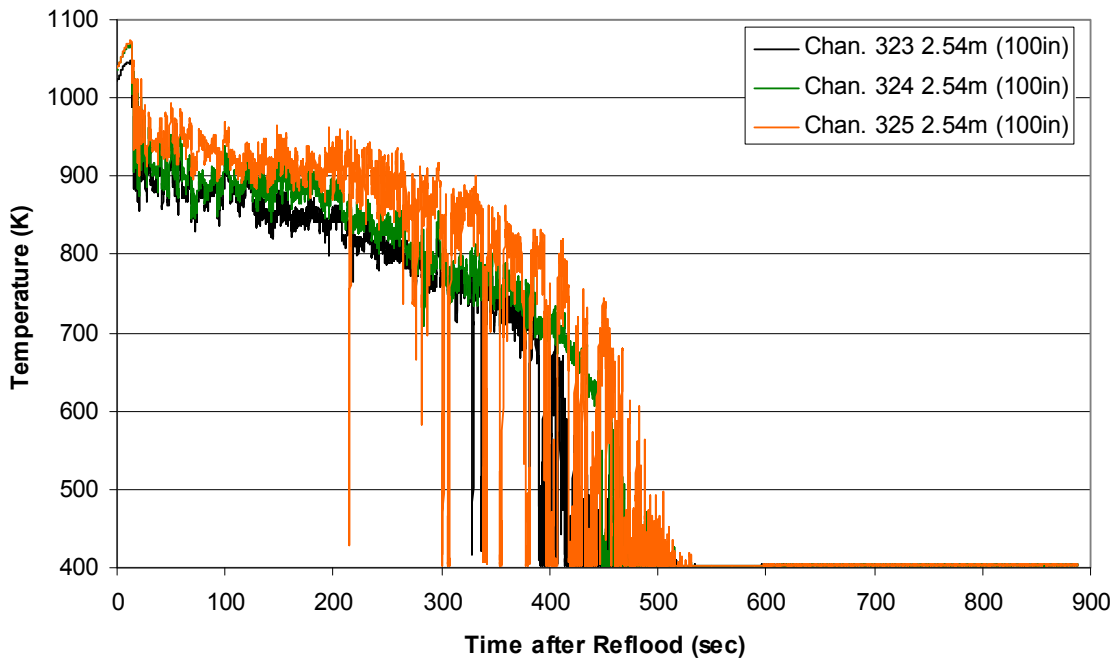
**Heater Rod Temperature during Reflood
RBHT Exp. 1383**



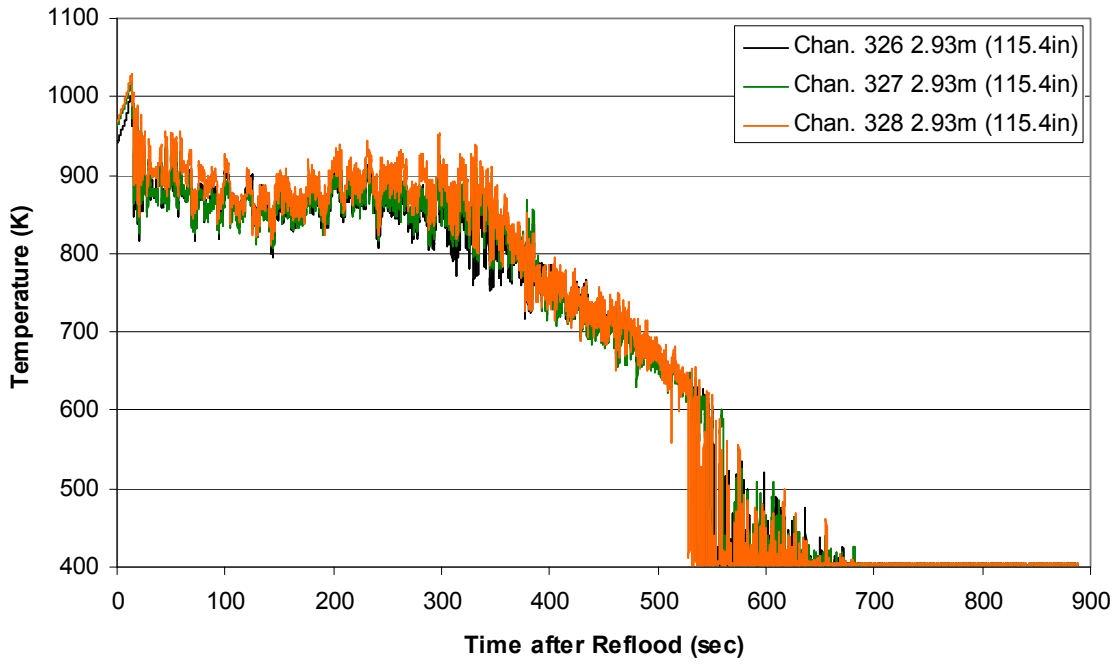
Steam Probe Temperature during Reflood
RBHT Exp. 1383



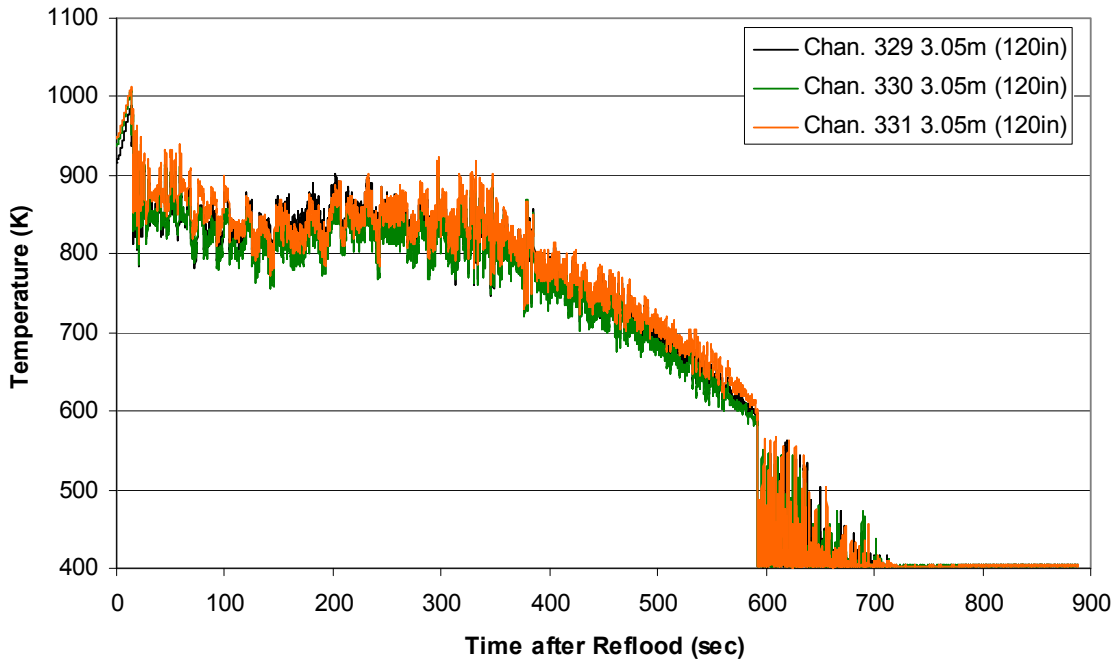
Steam Probe Temperature during Reflood
RBHT Exp. 1383



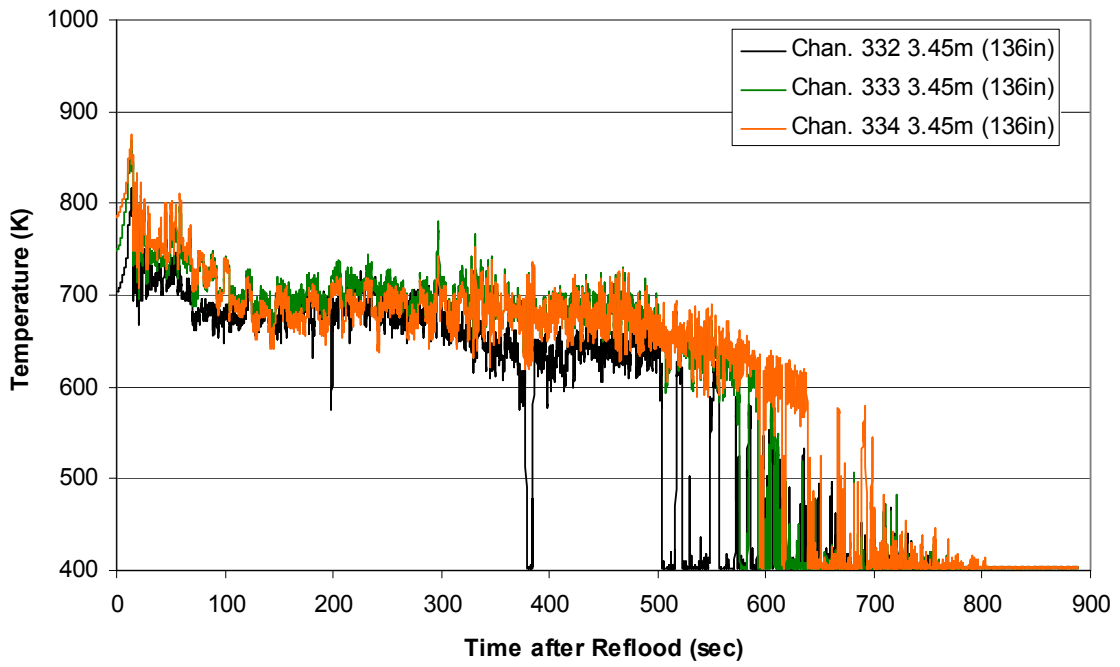
Steam Probe Temperature during Reflood
RBHT Exp. 1383



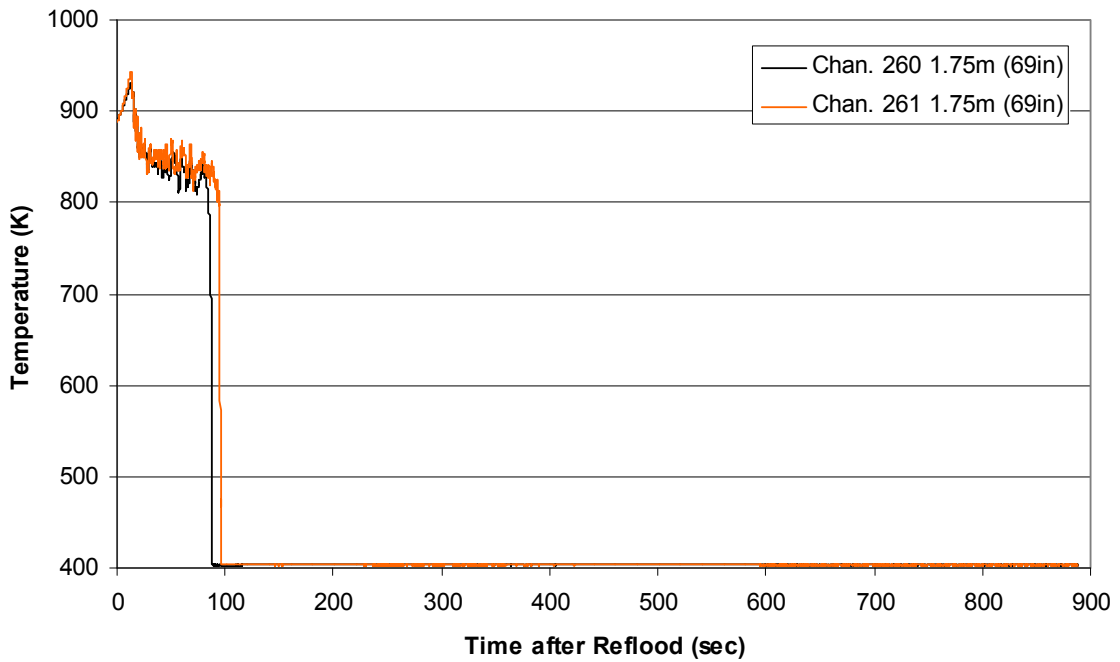
Steam Probe Temperature during Reflood
RBHT Exp. 1383



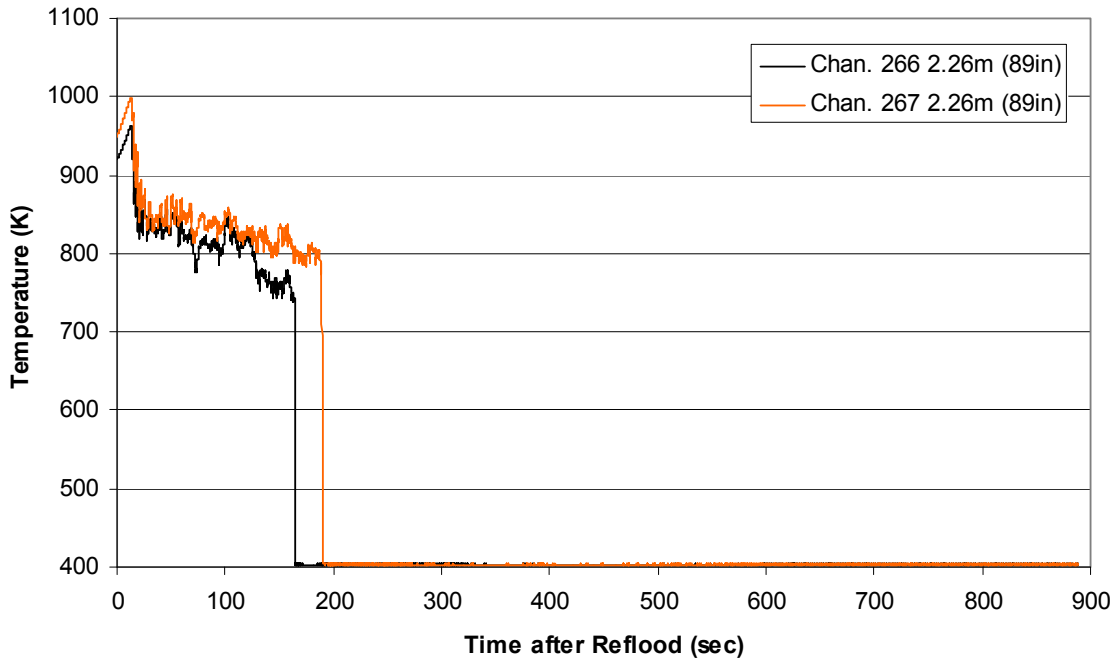
Steam Probe Temperature during Reflood RBHT Exp. 1383



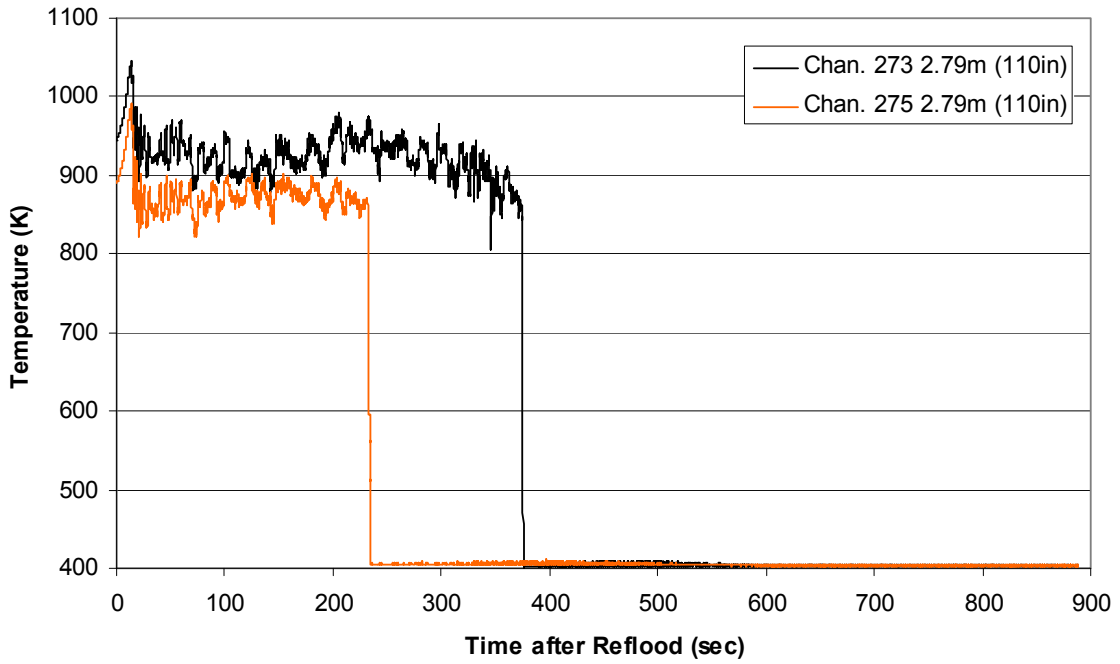
Spacer Grid Temperature during Reflood RBHT Exp. 1383



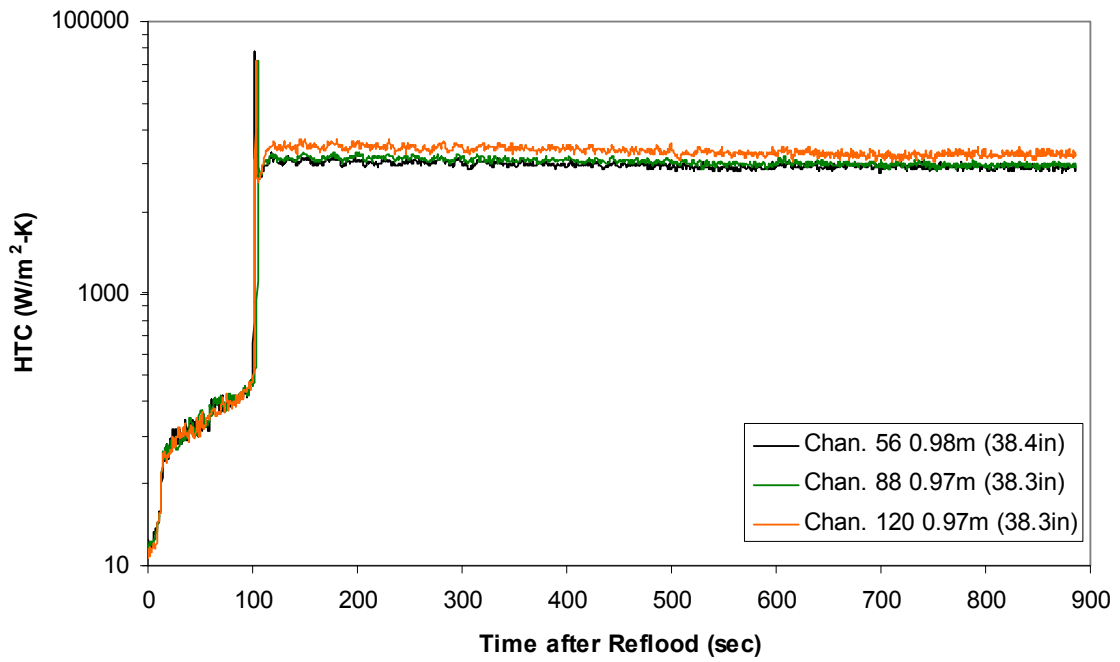
Spacer Grid Temperature during Reflood
RBHT Exp. 1383



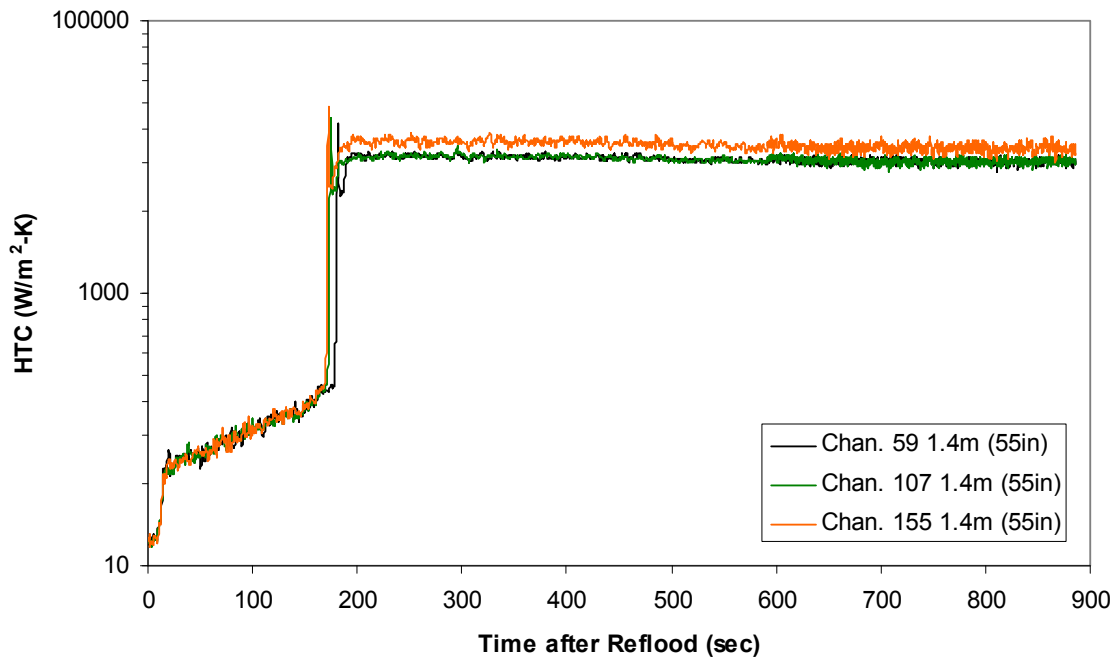
Spacer Grid Temperature during Reflood
RBHT Exp. 1383



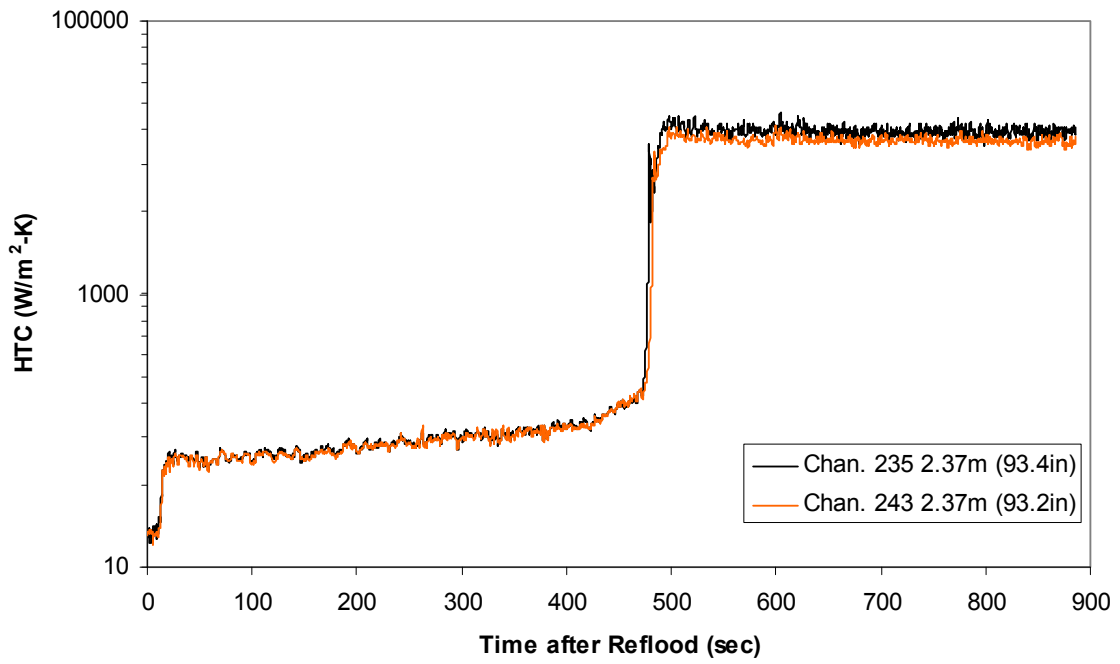
Heat Transfer Coefficient during Reflood
RBHT Exp. 1383



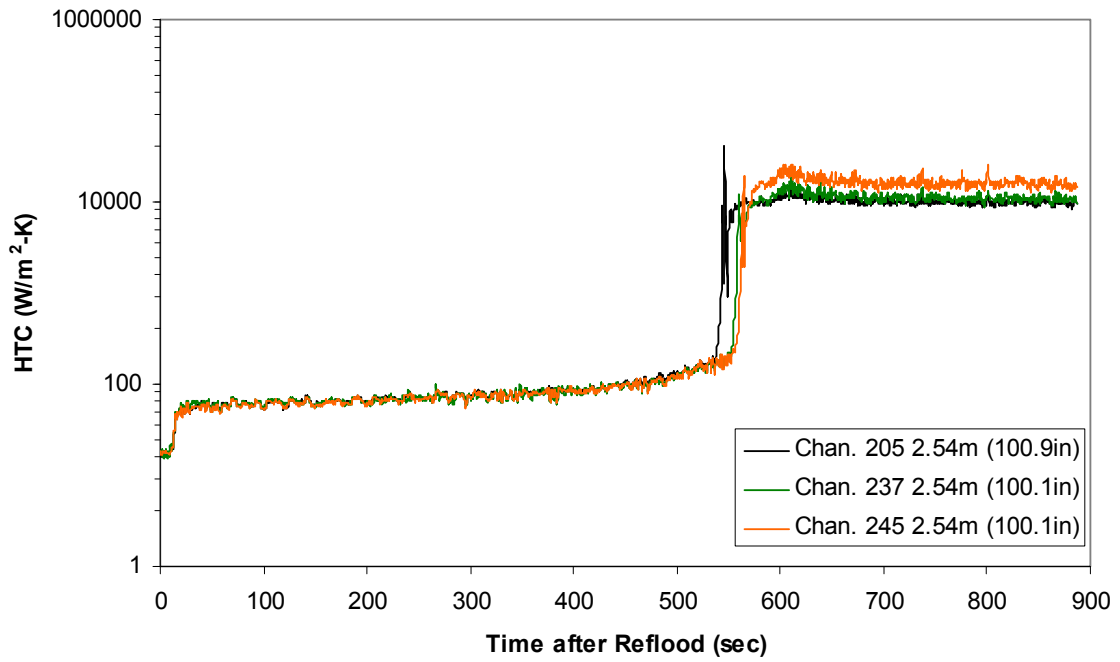
Heat Transfer Coefficient during Reflood
RBHT Exp. 1383



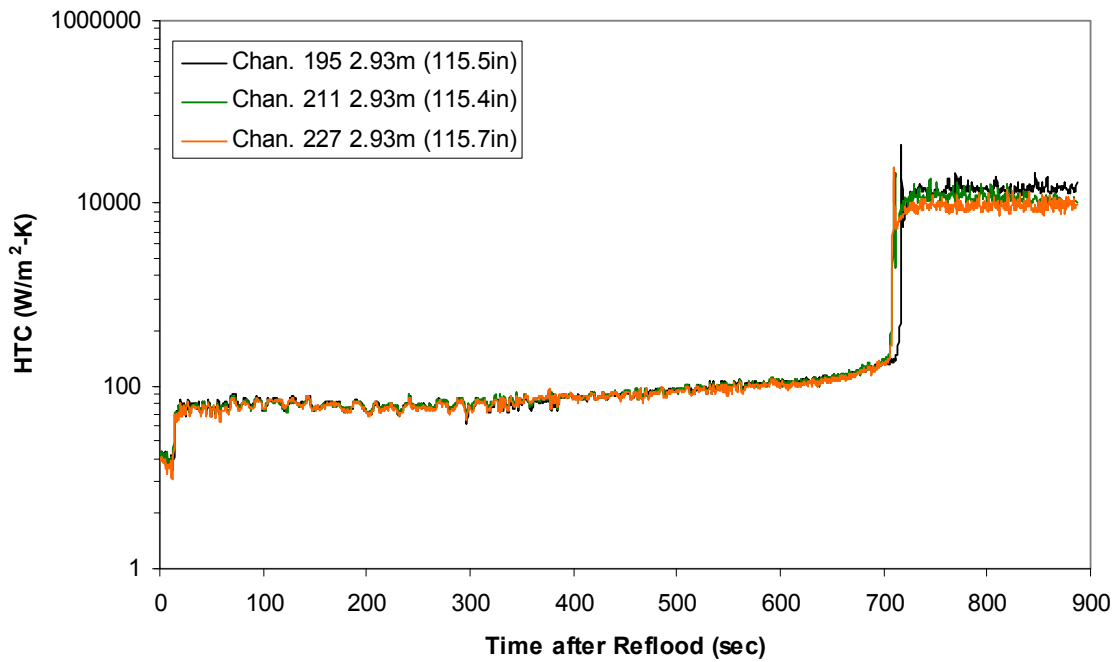
Heat Transfer Coefficient during Reflood RBHT Exp. 1383



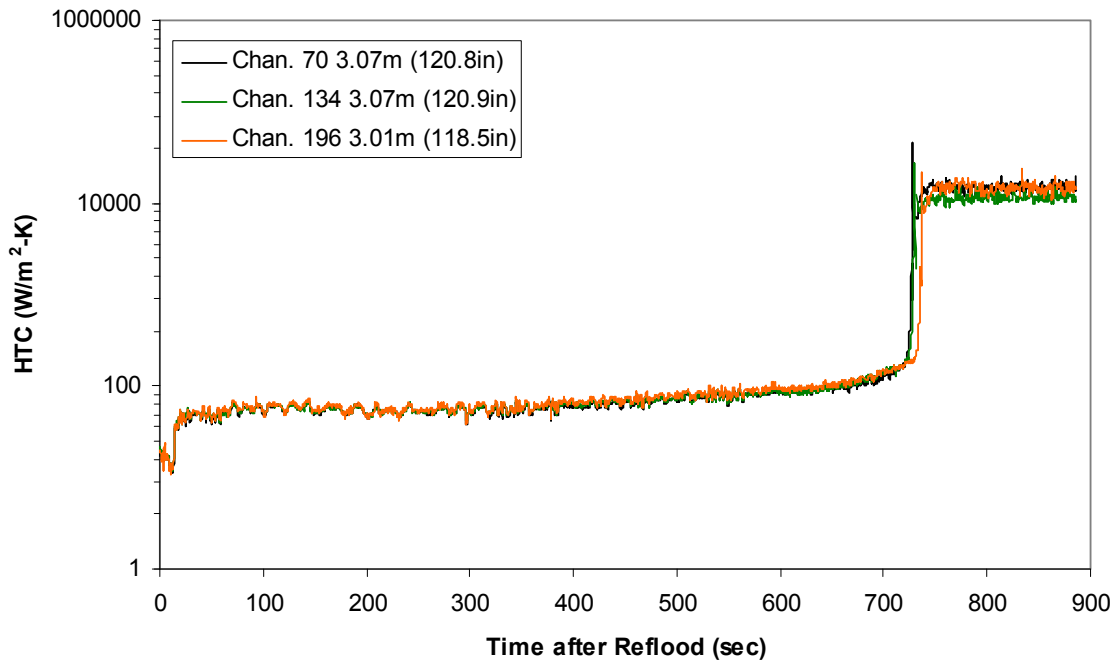
Heat Transfer Coefficient during Reflood RBHT Exp. 1383



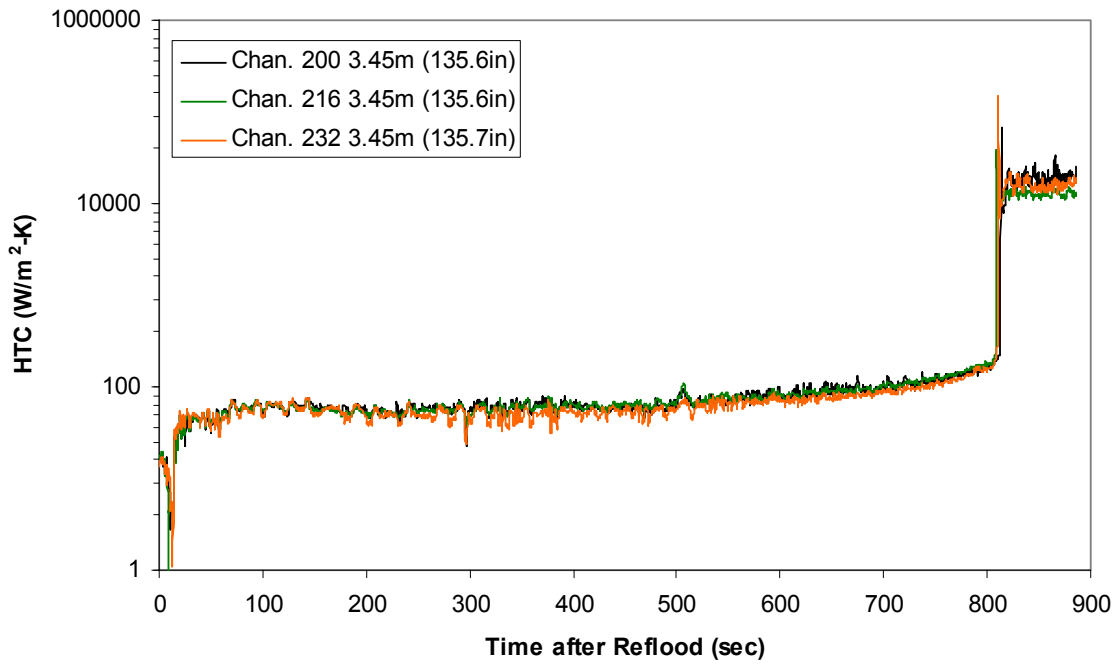
Heat Transfer Coefficient during Reflood RBHT Exp. 1383



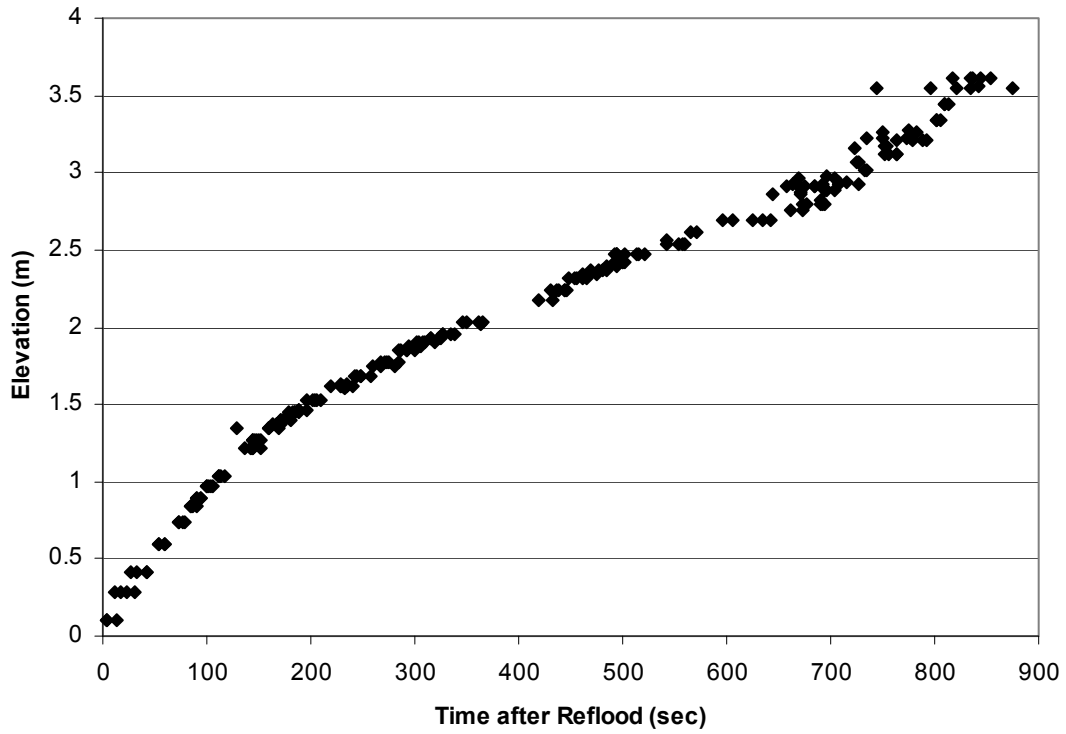
Heat Transfer Coefficient during Reflood RBHT Exp. 1383

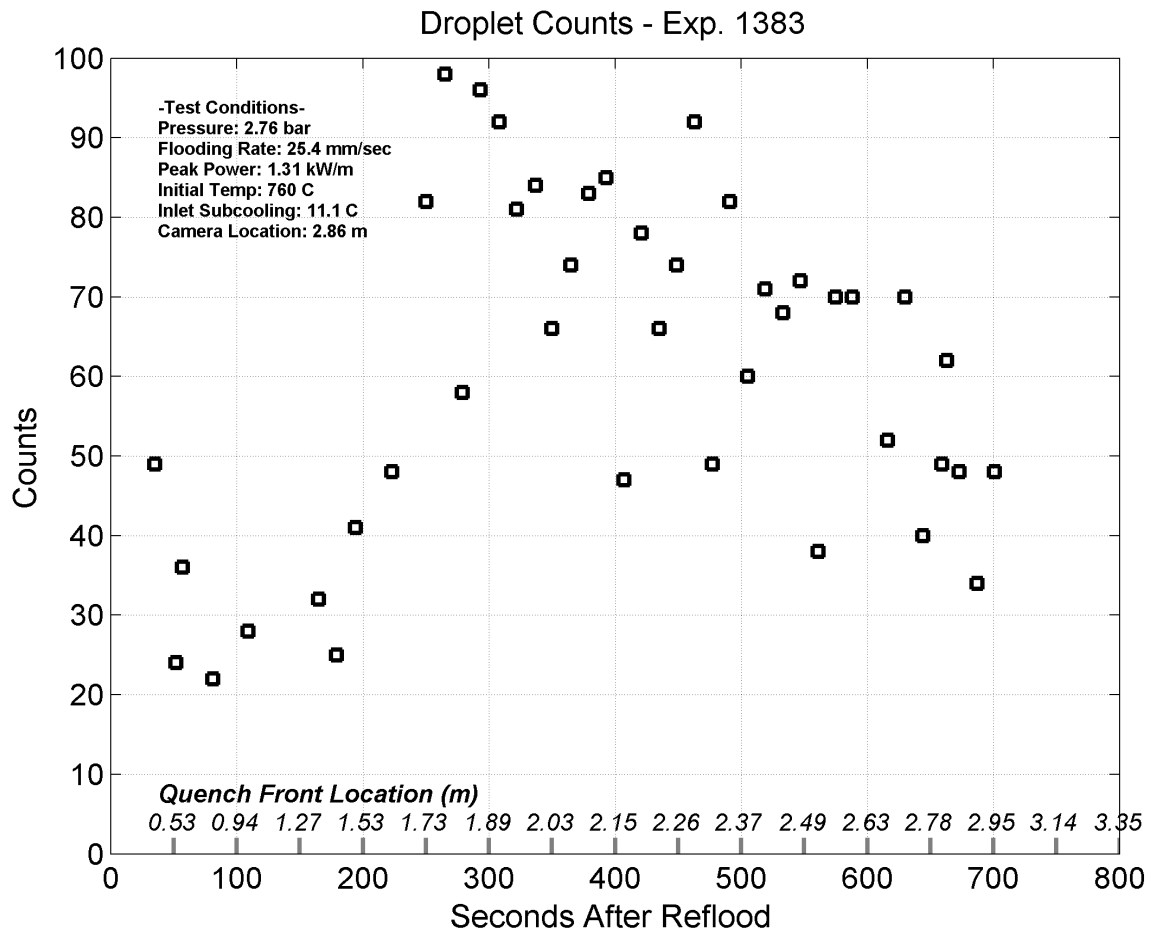


Heat Transfer Coefficient during Reflood RBHT Exp. 1383

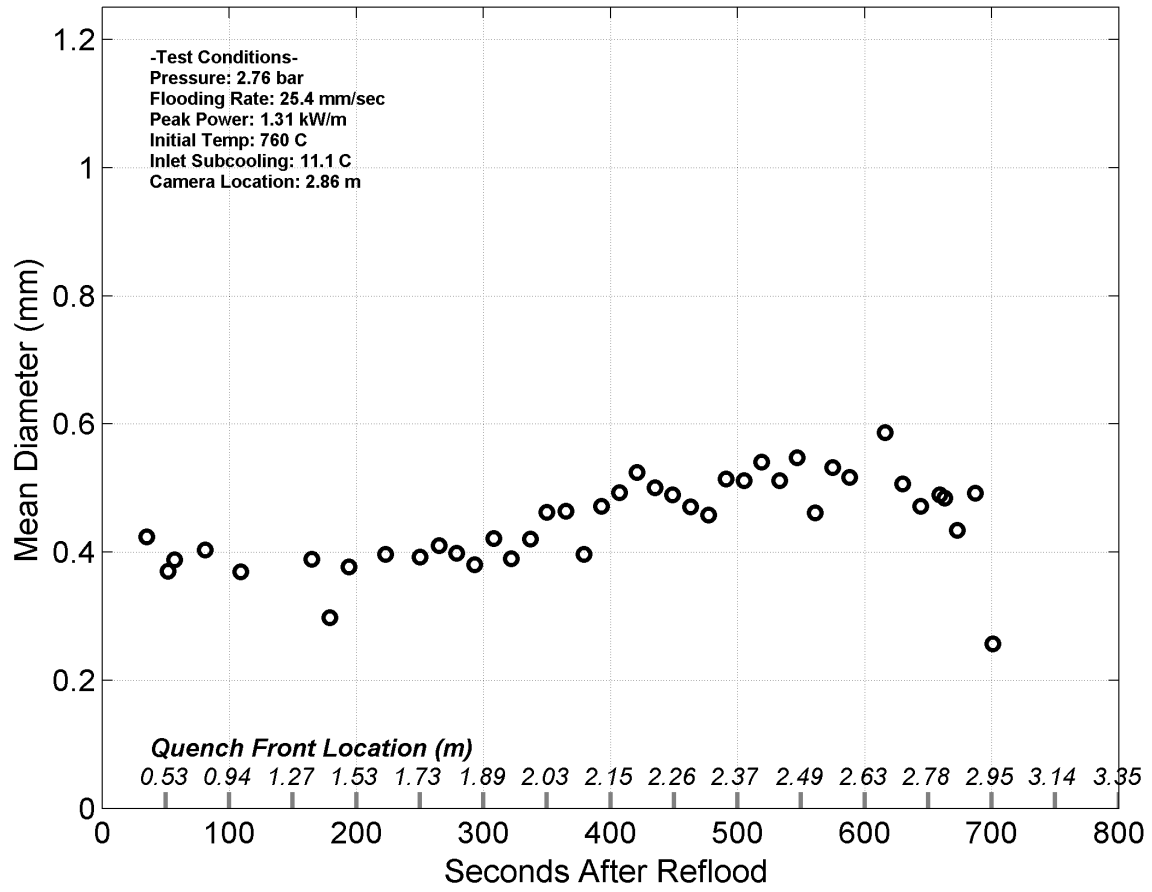


Quench Data, RBHT Exp. 1383

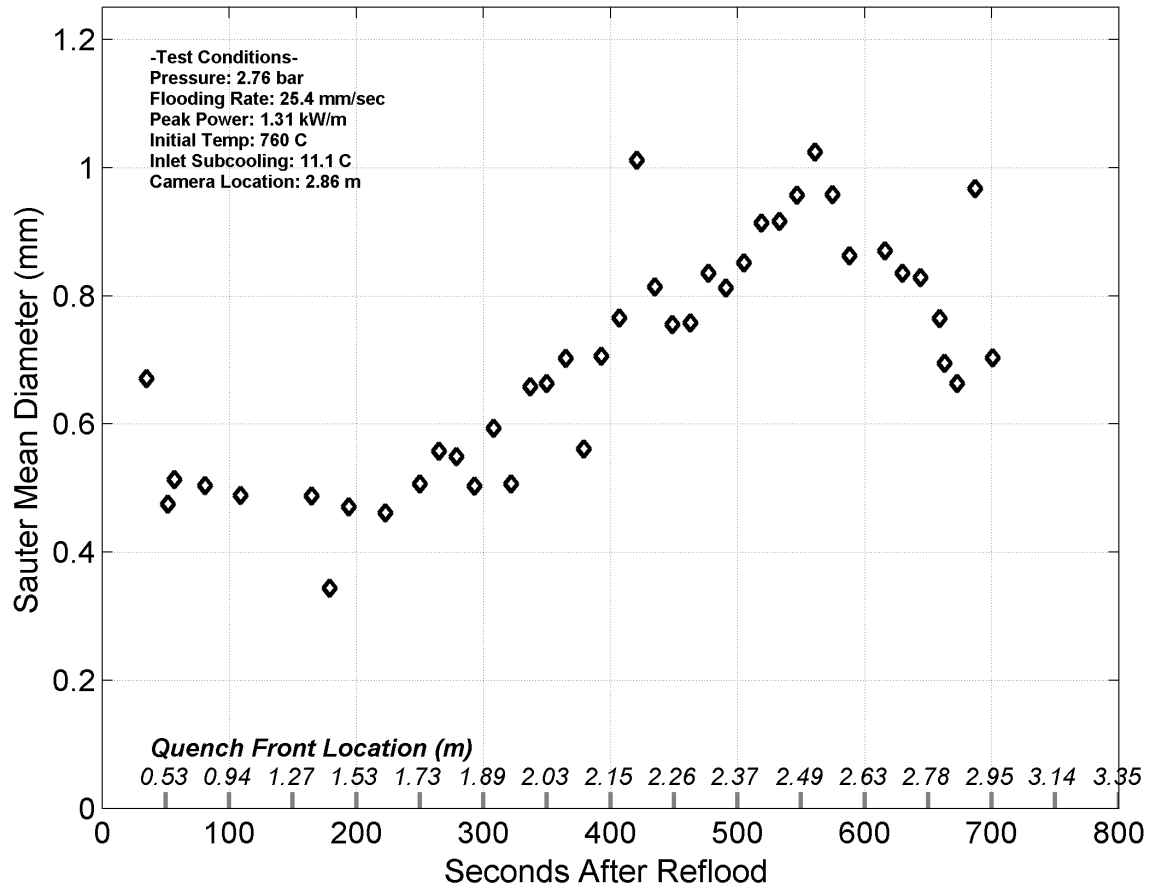




Mean Droplet Diameter - Exp. 1383



Droplet Sauter Mean Diameter - Exp. 1383



RBHT - REFLOOD TESTS

SUMMARY SHEET

RUN NO: **1389**

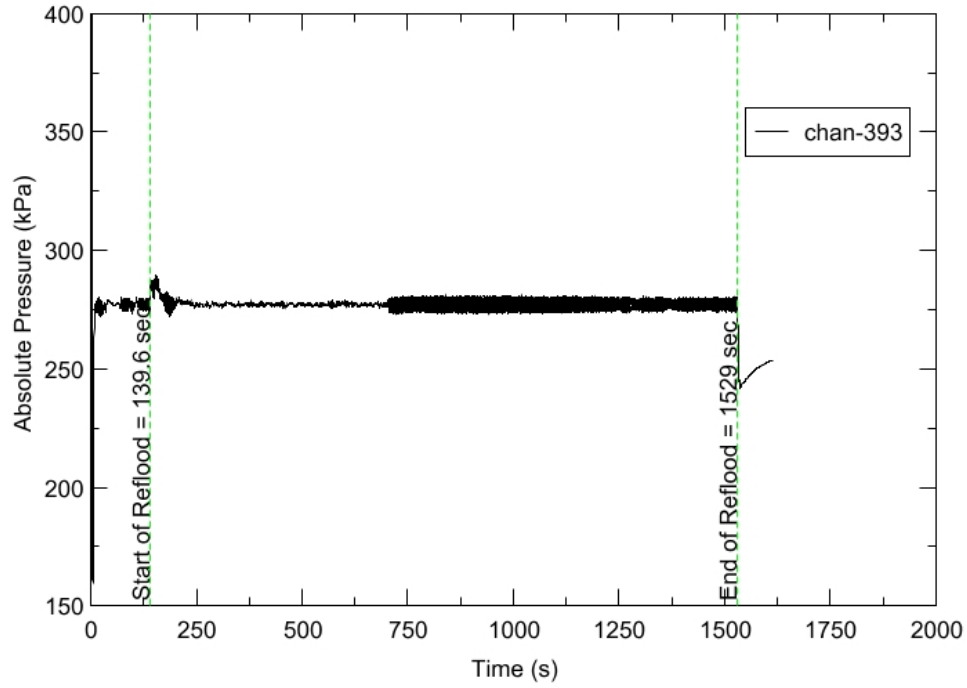
RUN CONDITIONS

Upper Plenum Pressure:	276 kPa (40 psia)
Initial Peak Clad Temperature:	1033 degrees K (1400 degrees F)
Rod Peak Power:	1.31 kW/m (0.4 kW/ft)
Flooding Rate:	0.0254 m/s (1 in/s)
Inlet Subcooling:	11 degrees K (20 degrees F)
Start of Reflood:	139.6 s
End of Reflood:	1529 s
Test Date:	8/26/2002
Comments:	

Rod_Elevation	Channel Number	Temperature at Reflood (K)	Temperature at Reflood (°F)	Tumaround Time (sec.)	Tumaround Temperature (K)	Tumaround Temperature (°F)	Quench Time (sec.)	Quench Temperature (K)	Quench Temperature (°F)
B6 0.592m	148	666.54	740.09	9.15	685.06	773.43	52.15	565.42	558.07
B6 0.744m	149	681.68	767.33	10.65	702.36	804.56	67.15	547.91	526.55
B6 0.846m	150	703.79	807.13	11.15	726.89	848.71	76.15	573.44	572.5
B6 0.897m	151	712.14	822.16	12.65	736.75	866.46	81.15	586.7	596.37
C6 1.04m	137	747.74	886.24	15.65	776.18	937.44	97.65	611.06	640.22
D5 1.27m	217	793.06	967.81	15.65	824.81	1024.97	126.15	610.58	639.36
C6 1.34m	138	787.46	957.75	19.15	820.65	1017.48	138.65	621.11	658.31
D5 1.37m	218	813.7	1004.97	19.15	848.28	1067.22	141.65	642.9	697.53
C6 1.39m	139	794.7	970.77	55.15	832.11	1038.11	147.65	637.63	688.04
D5 1.45m	219	826.38	1027.8	57.15	869.38	1105.19	154.65	650.69	711.55
C6 1.47m	140	806.36	991.76	57.15	854.29	1078.04	163.65	642.4	696.63
D5 1.52m	220	839.27	1051	60.65	893.5	1148.62	172.65	662.3	732.46
C6 1.62m	141	828.62	1031.83	63.65	898.45	1157.52	200.65	658.89	726.31
D5 1.68m	221	864.36	1096.17	63.65	937.9	1228.54	212.15	691.8	785.55
D5 1.78m	222	872.62	1111.02	12.15	901.27	1162.59	240.65	605.5	630.2
D5 1.85m	223	897.05	1155	25.65	934.78	1222.91	257.65	667	740.91
C6 1.87m	142	877.42	1119.67	63.65	926.69	1208.35	271.15	650.99	712.09
D5 1.90m	224	912.6	1182.99	59.65	958.77	1266.09	275.65	662.18	732.24
C6 1.95m	144	900.71	1161.59	63.65	957.18	1263.23	303.15	608.64	635.87
C3 2.17m	178	952.72	1255.21	64.15	991.48	1324.97	394.15	630.48	675.18
D4 2.24m	241	995.22	1331.71	14.15	1031.08	1396.25	416.15	642.89	697.51
D4 2.32m	242	1004.96	1349.25	63.65	1071.22	1468.51	443.15	622.93	661.58
C3 2.35m	180	996.46	1333.93	68.15	1067.32	1461.49	448.65	655.61	720.41
D4 2.37m	243	1012.23	1362.33	79.65	1079.77	1483.89	463.65	651.13	712.34
C3 2.40m	181	1000.67	1341.53	68.15	1068.24	1463.14	470.15	660.43	729.09
D4 2.54m	245	1033.09	1399.87	145.15	1124.8	1564.95	551.15	653.87	717.28
D6 2.62m	129	1013.03	1363.76	148.15	1114.53	1546.47	557.65	690.33	782.91
D6 2.69m	130	1009.11	1356.71	177.15	1136.22	1585.51	601.65	694.51	790.44
C3 2.76m	183	1008.92	1356.37	178.65	1157.35	1623.54	666.15	663.47	734.56
D4 2.79m	247	997.33	1335.51	219.65	1103.01	1525.73	702.15	620.18	656.64
D6 2.87m	131	957.29	1263.43	219.15	1017.35	1371.54	681.15	656.04	721.18
D6 2.92m	132	937.02	1226.95	221.15	1036.75	1406.46	700.15	647.63	706.05
D6 2.97m	133	913.02	1183.75	221.15	1039.4	1411.23	725.15	650.76	711.69
D6 3.07m	134	882.91	1129.54	275.65	1038.49	1409.59	753.15	663.28	734.22
E3 3.12m	197	875.65	1116.48	331.15	1056.5	1442.01	797.15	651.39	712.82
D6 3.17m	135	853.38	1076.4	331.15	1033.48	1400.58	779.15	670.33	746.91
D6 3.27m	136	813.24	1004.14	352.65	1021.36	1378.76	803.15	673.89	753.31
D4 3.61m	248	611.29	640.64	487.15	860.32	1088.89	892.65	598.55	617.71

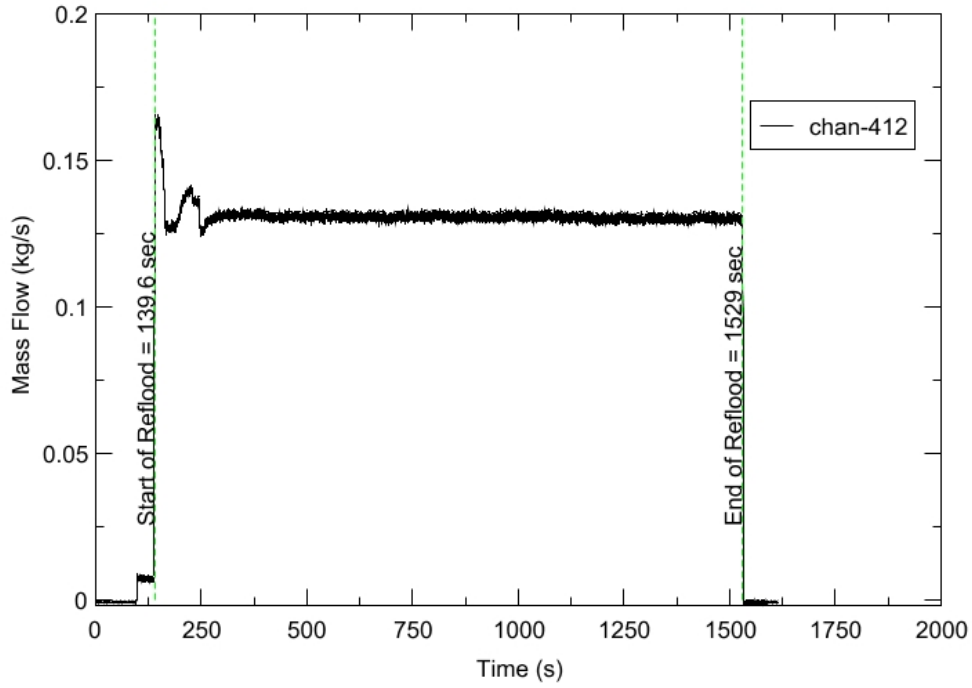
RBHT - TEST FACILITY

Upper Plenum Pressure vs. Time, Exp 1389



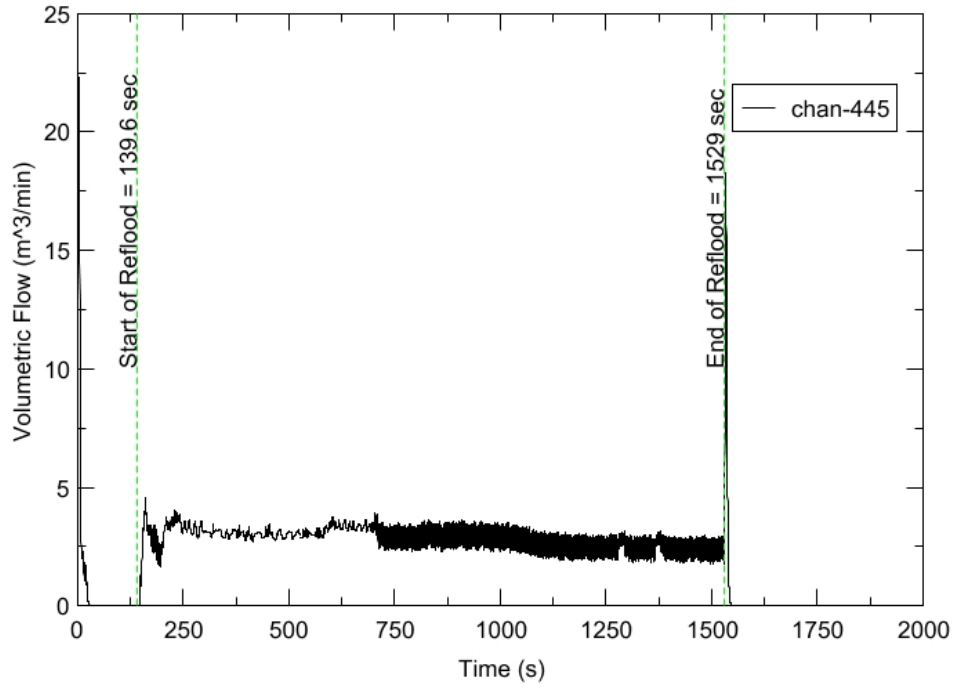
RBHT - TEST FACILITY

Inlet Flow vs. Time, Exp 1389



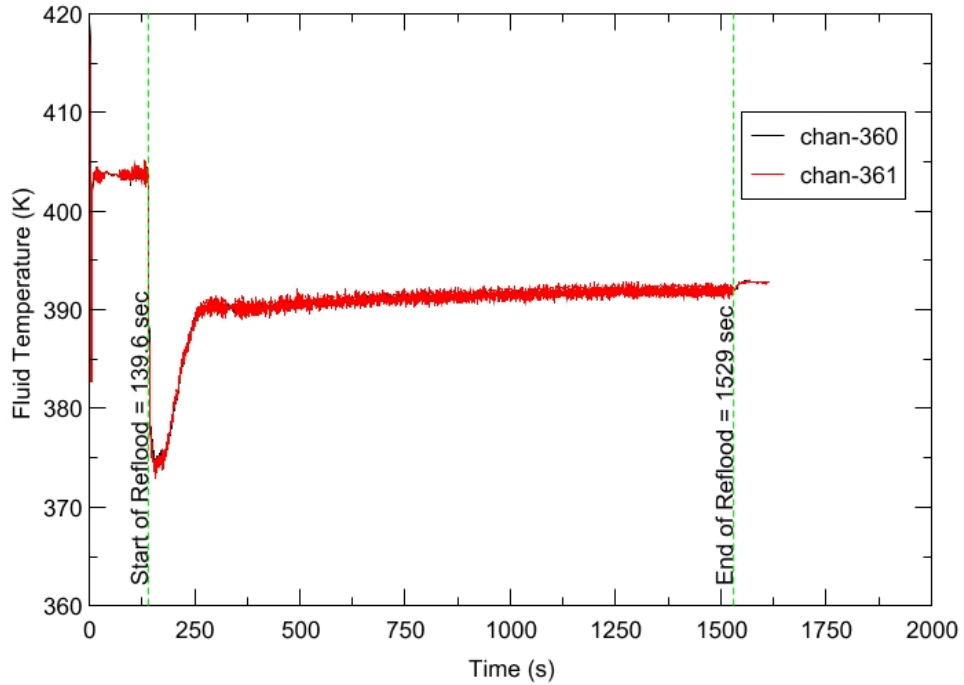
RBHT - TEST FACILITY

Steam Exhaust Flow vs. Time, Exp 1389



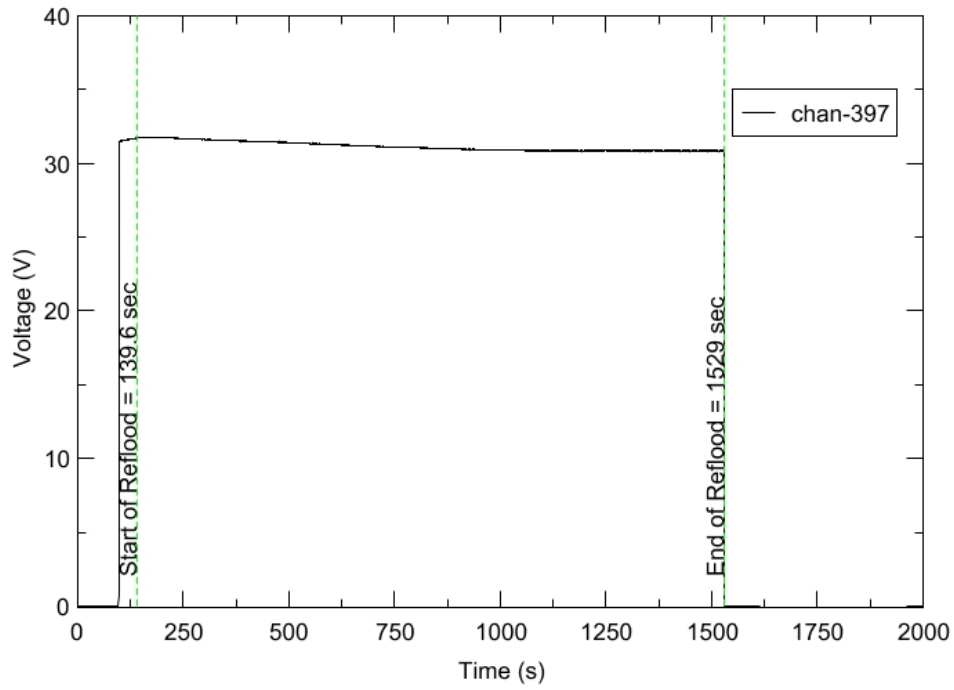
RBHT - TEST FACILITY

Inlet Flow Temperature vs. Time, Exp 1389



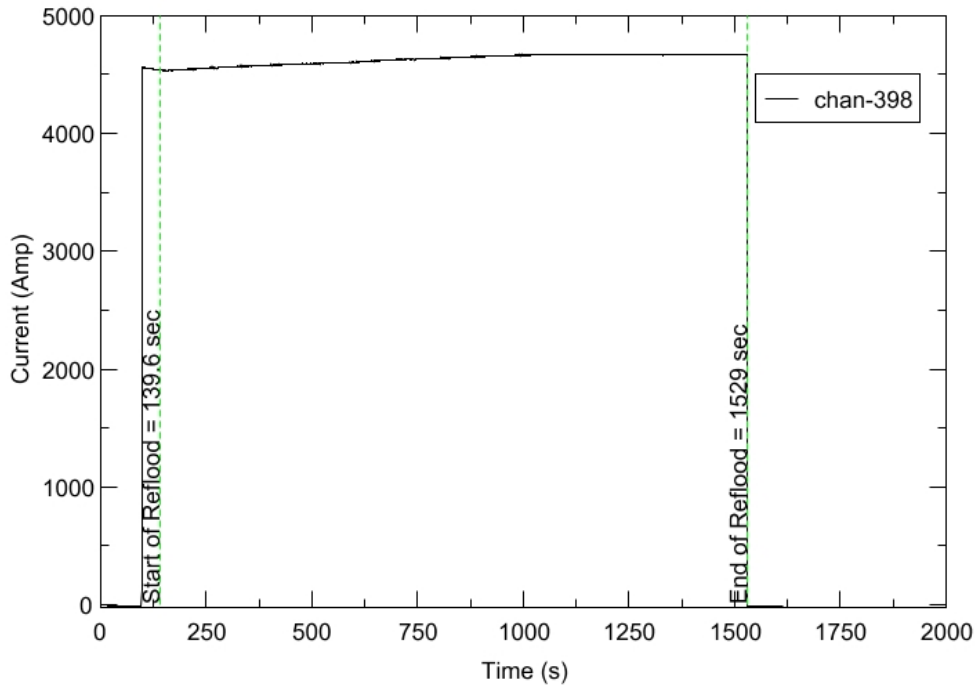
RBHT - TEST FACILITY

Test Section Voltage vs. Time, Exp 1389

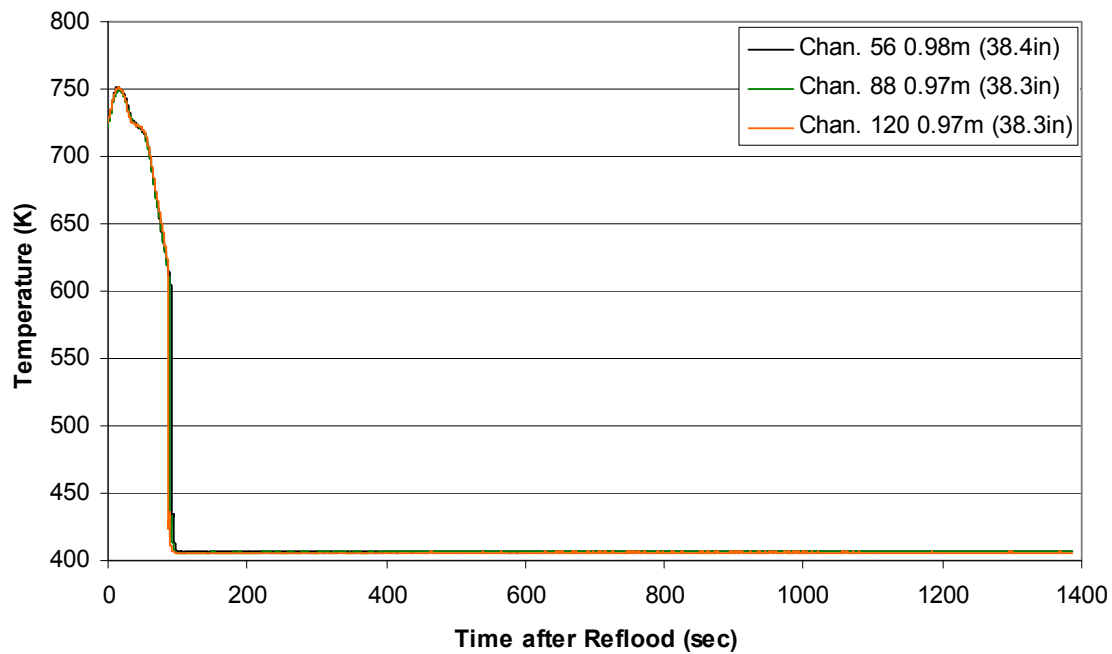


RBHT - TEST FACILITY

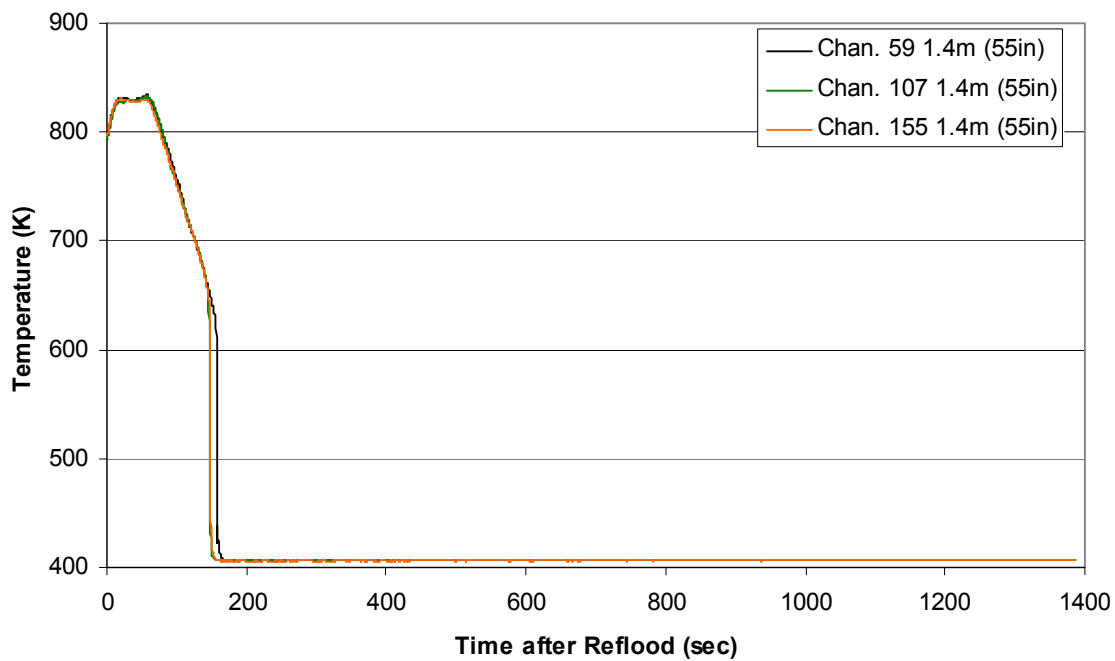
Test Section Current vs. Time, Exp 1389



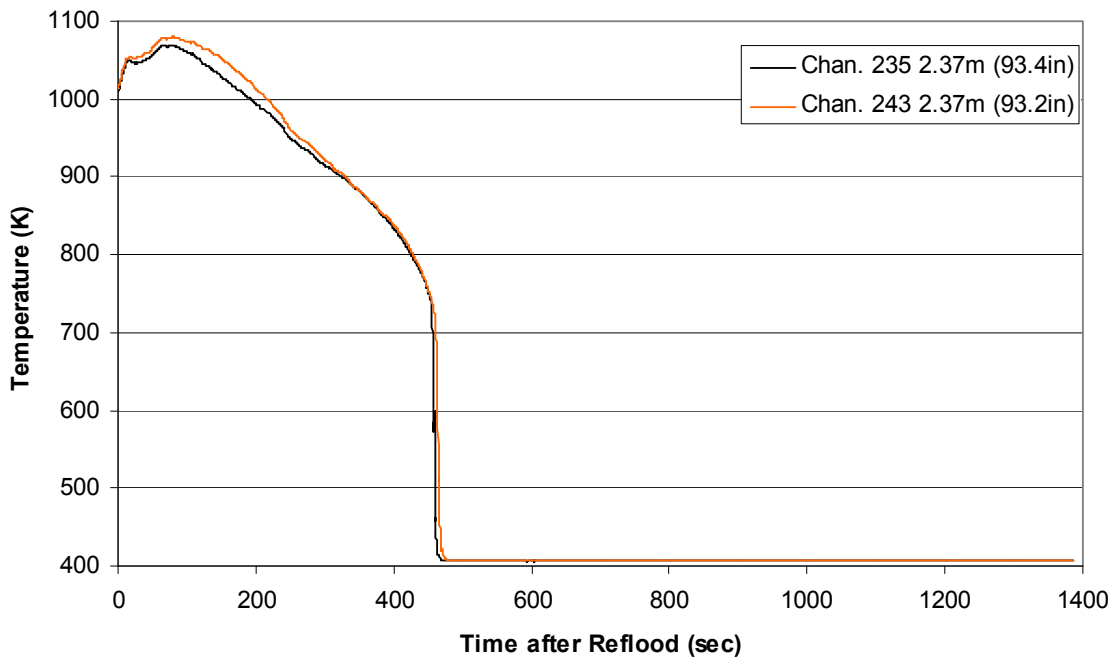
Heater Rod Temperature during Reflood
RBHT Exp. 1389



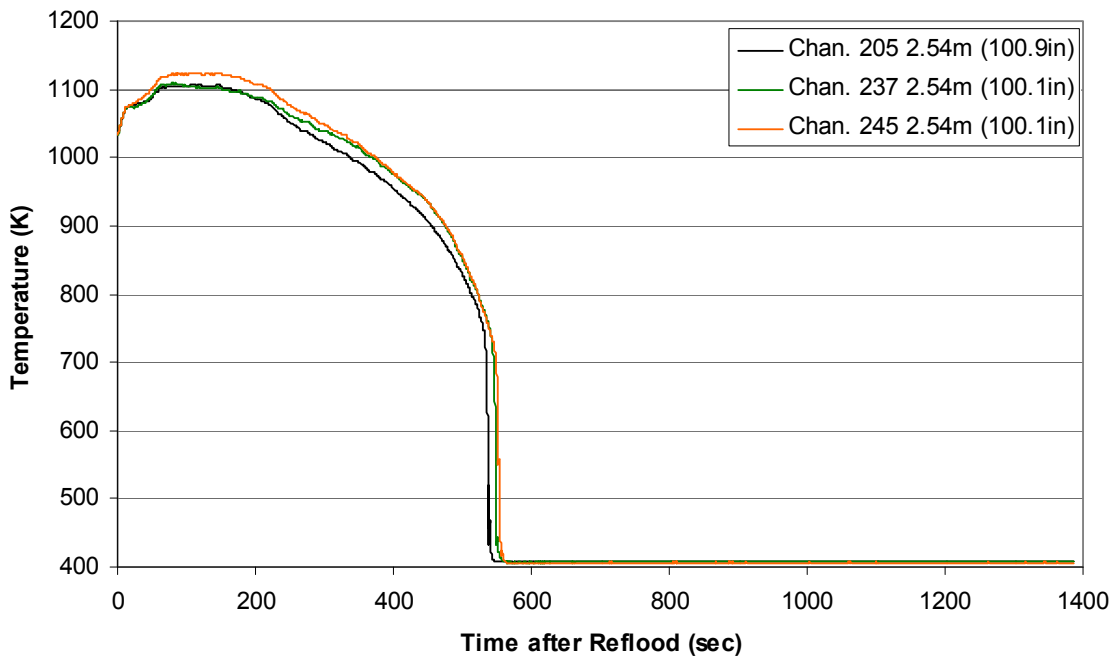
Heater Rod Temperature during Reflood
RBHT Exp. 1389



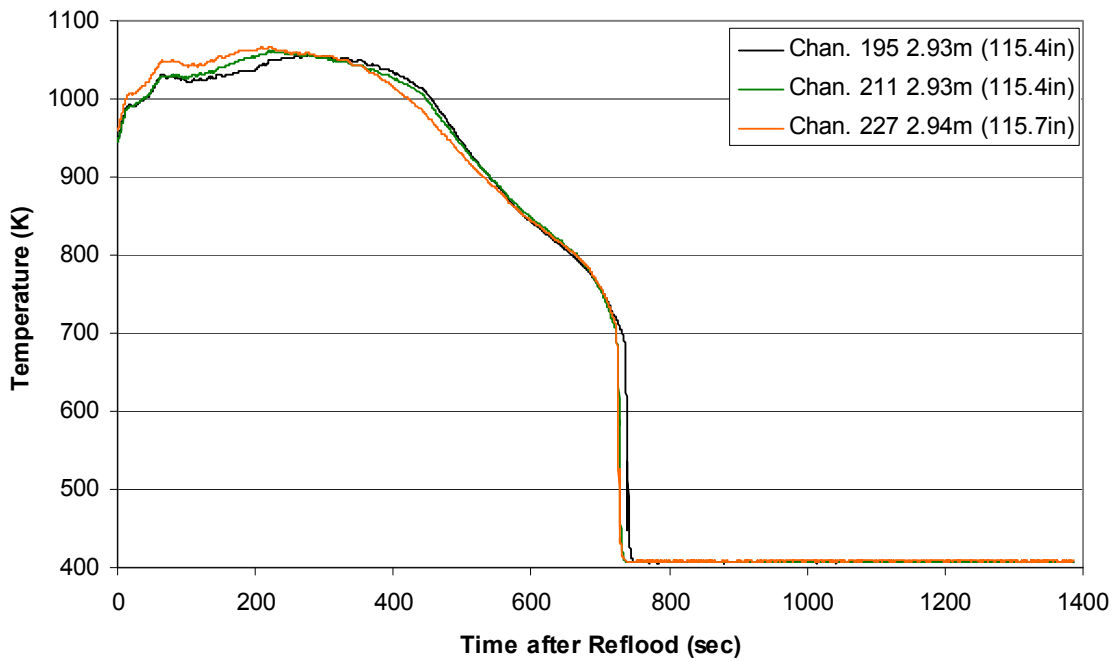
Heater Rod Temperature during Reflood
RBHT Exp. 1389



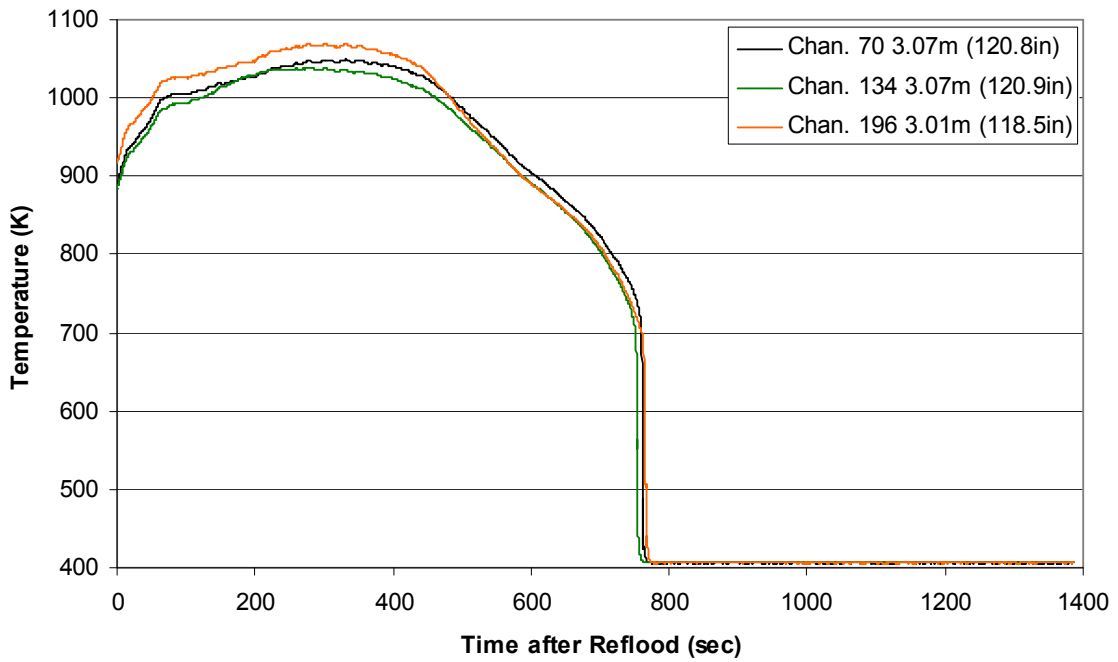
Heater Rod Temperature during Reflood
RBHT Exp. 1389



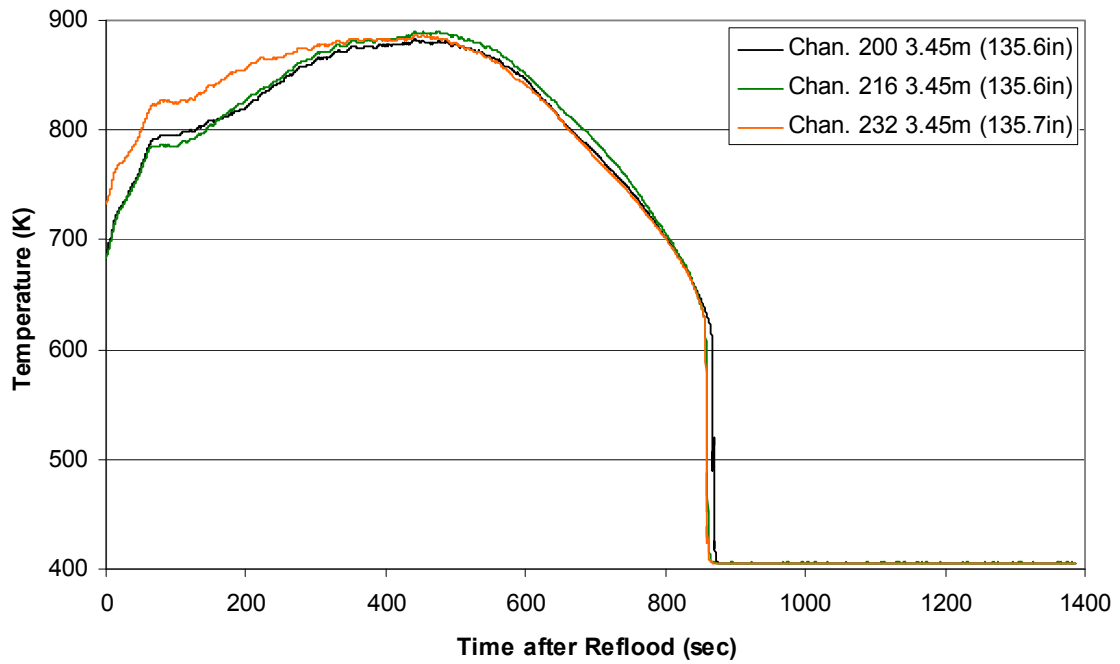
Heater Rod Temperature during Reflood
RBHT Exp. 1389



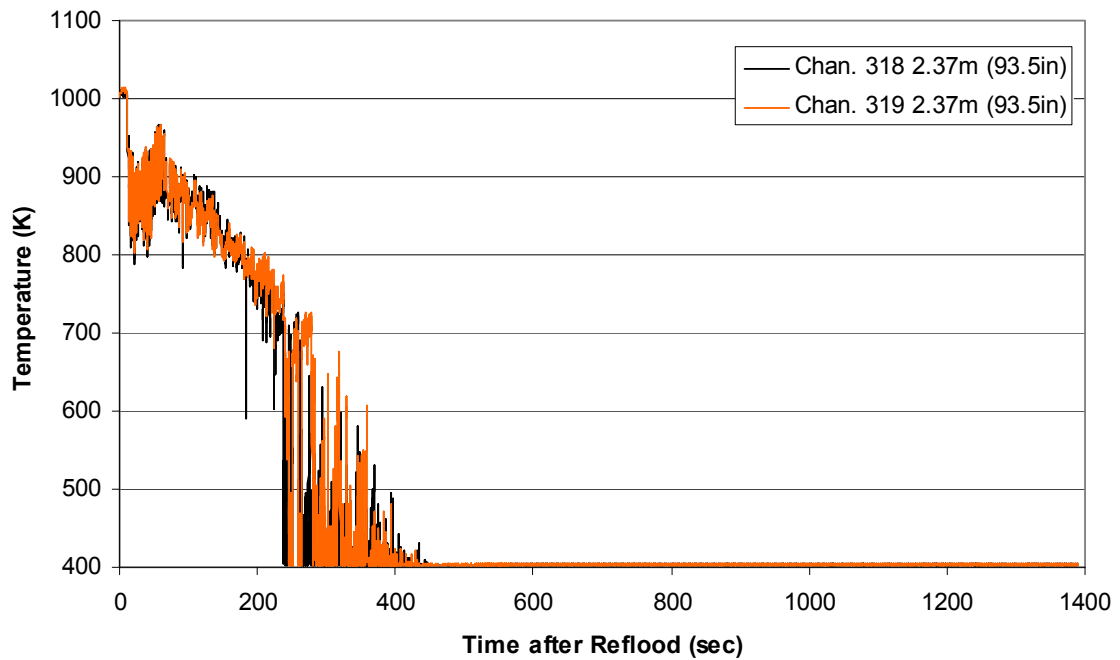
Heater Rod Temperature during Reflood
RBHT Exp. 1389



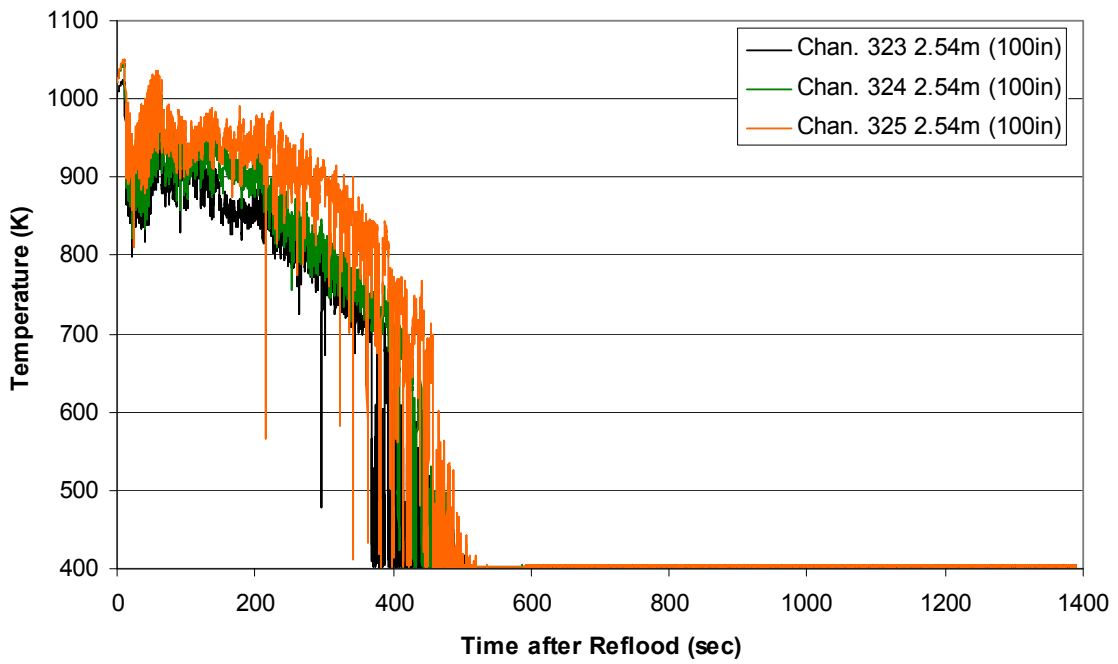
Heater Rod Temperature during Reflood RBHT Exp. 1389



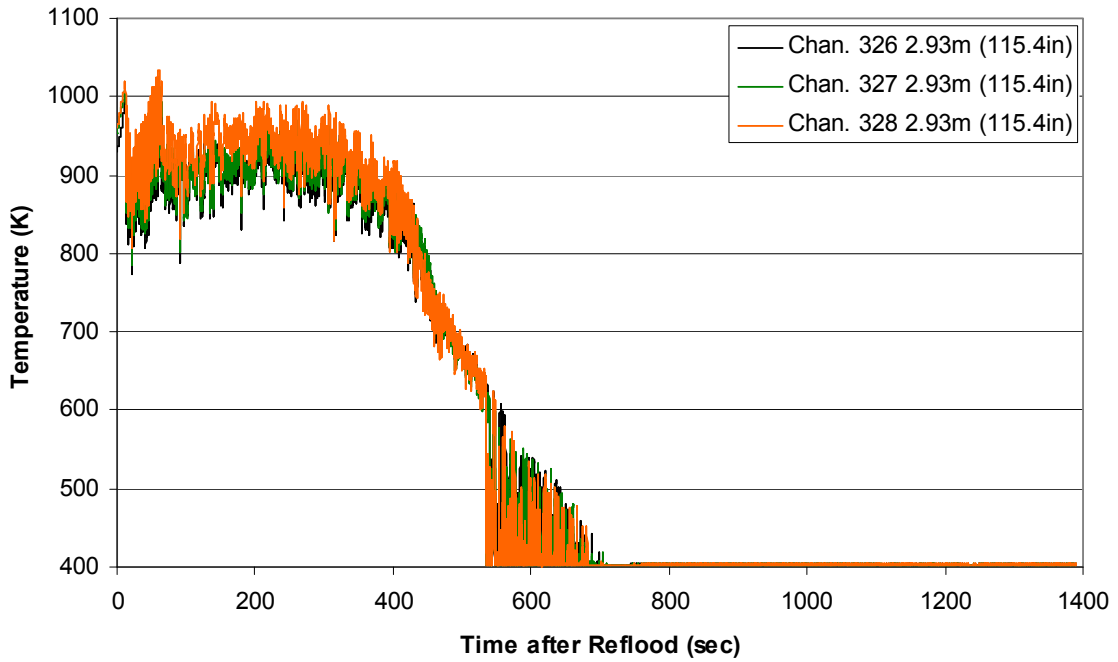
Steam Probe Temperature during Reflood RBHT Exp. 1389



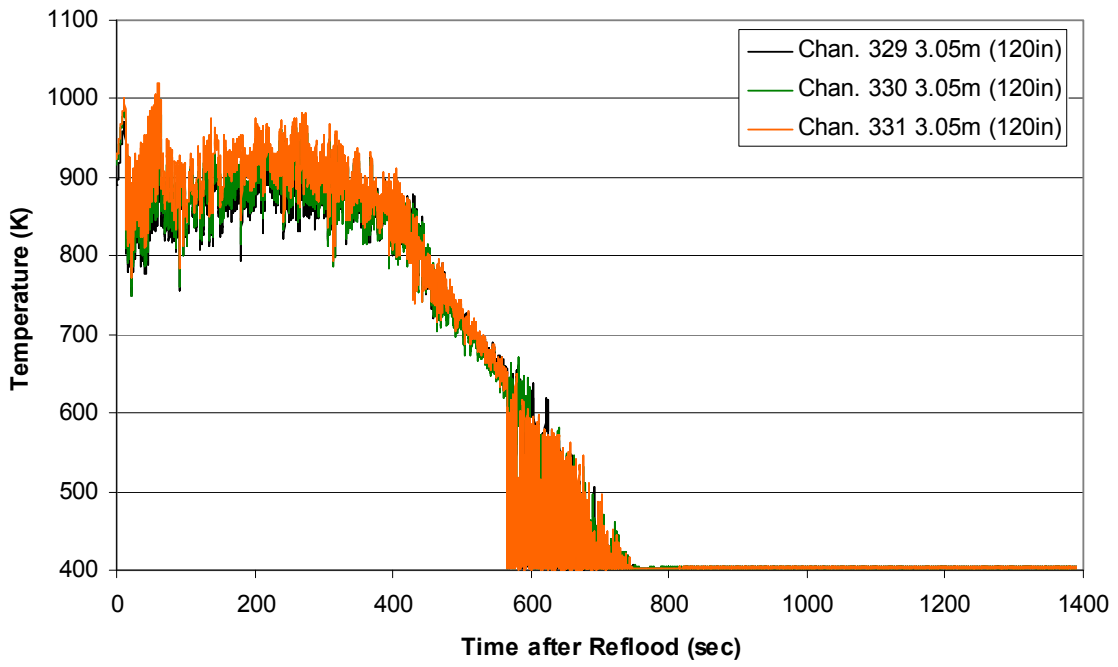
Steam Probe Temperature during Reflood
RBHT Exp. 1389



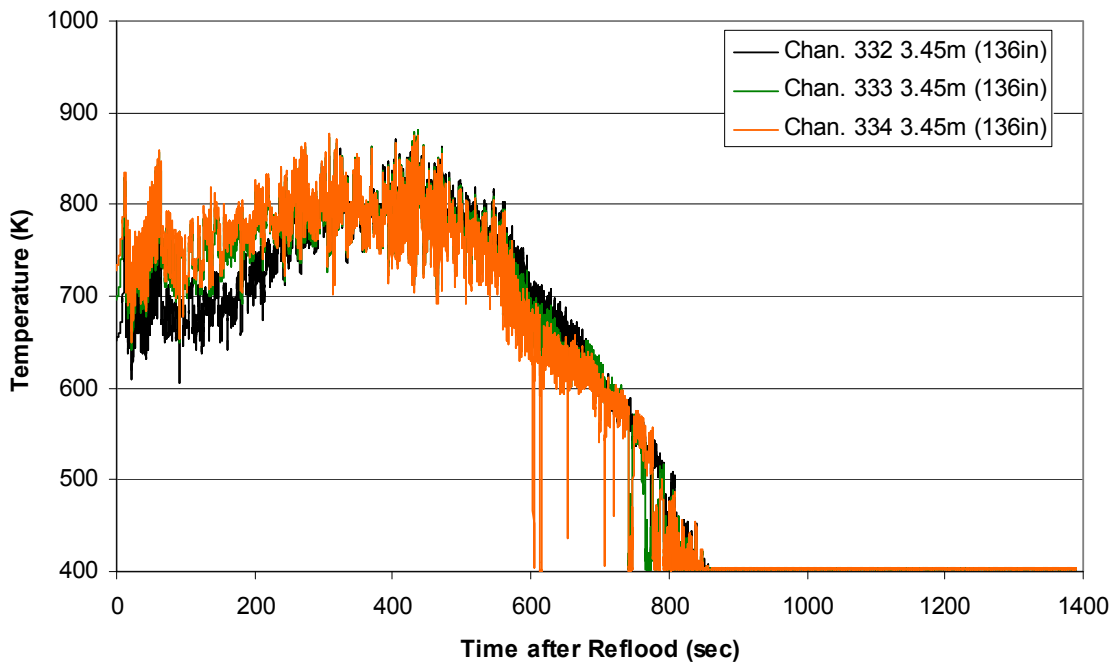
Steam Probe Temperature during Reflood
RBHT Exp. 1389



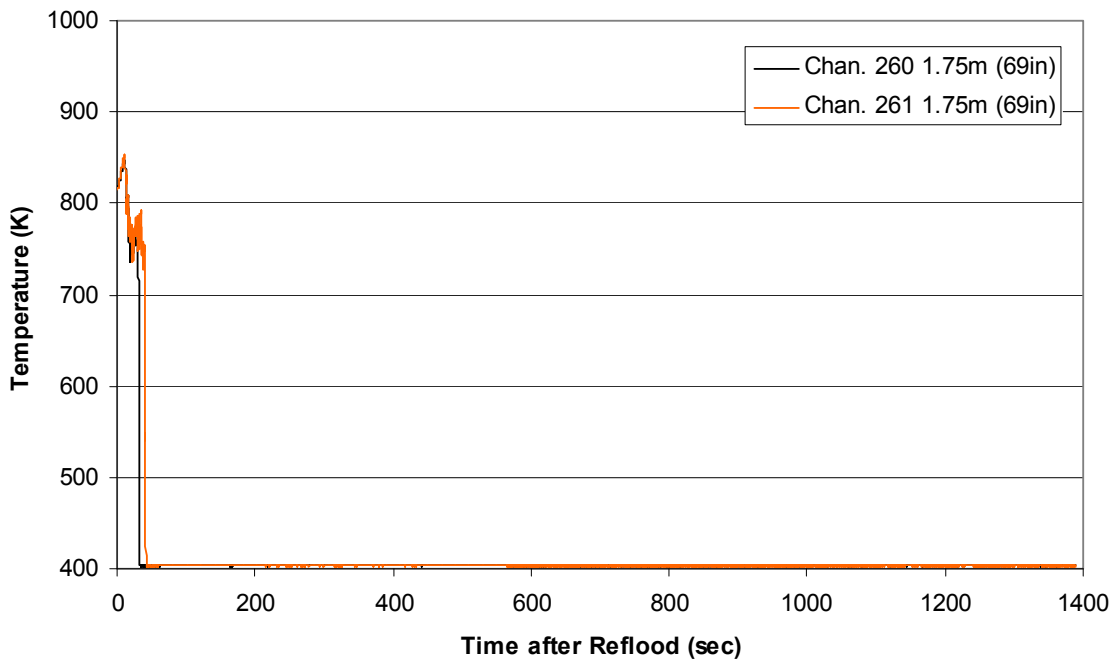
Steam Probe Temperature during Reflood
RBHT Exp. 1389



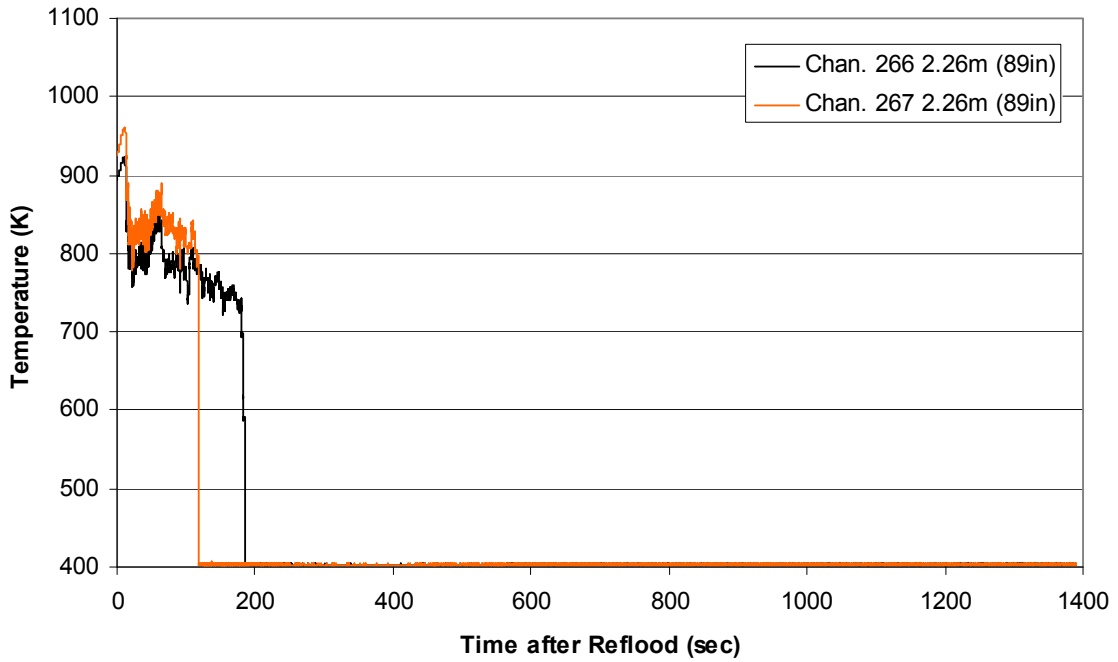
Steam Probe Temperature during Reflood
RBHT Exp. 1389



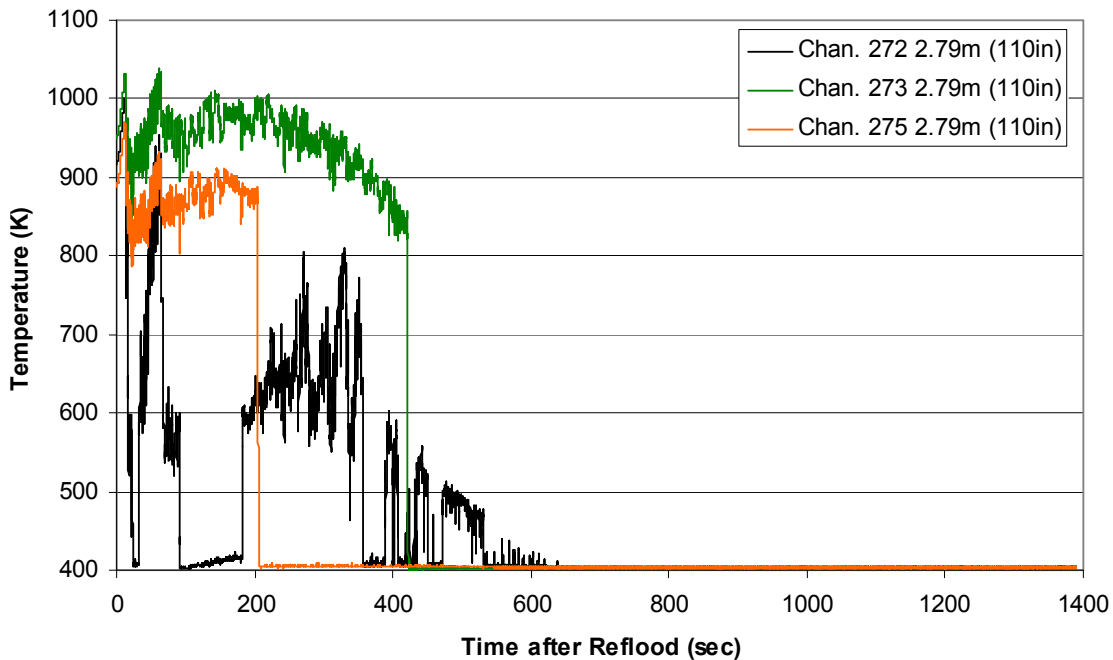
Spacer Grid Temperature during Reflood
RBHT Exp. 1389



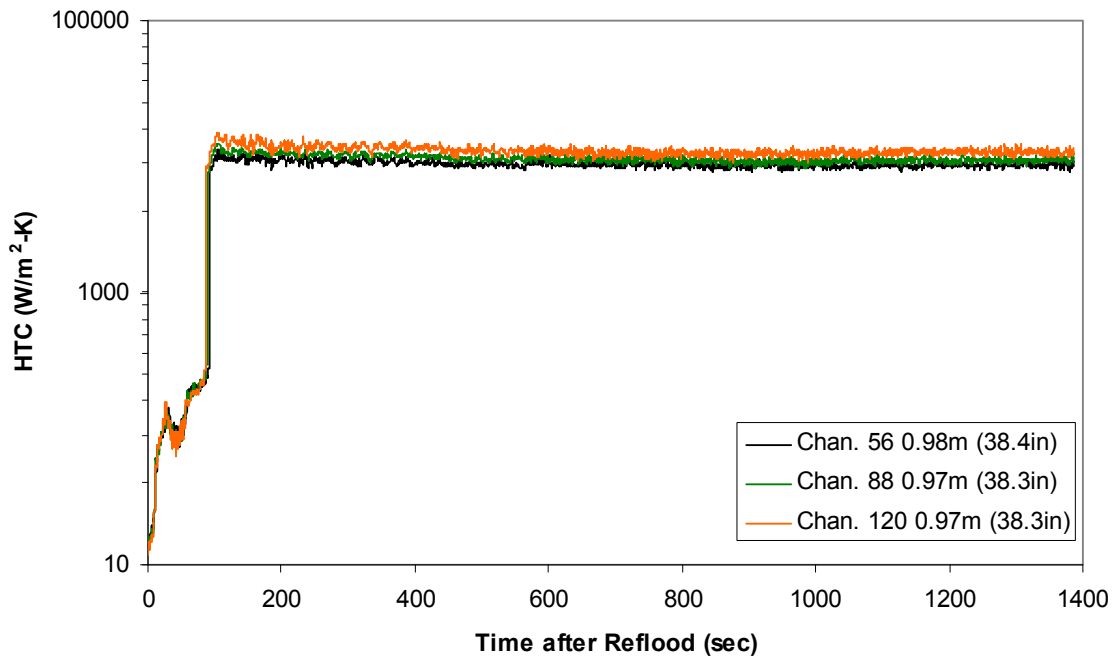
Spacer Grid Temperature during Reflood
RBHT Exp. 1389



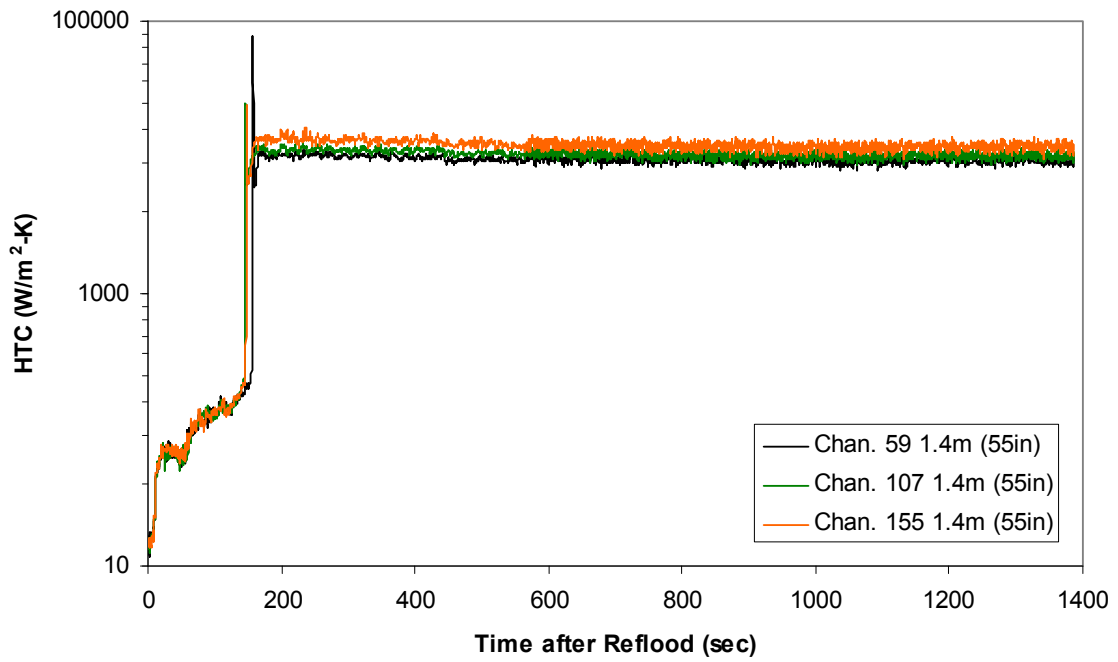
Spacer Grid Temperature during Reflood RBHT Exp. 1389



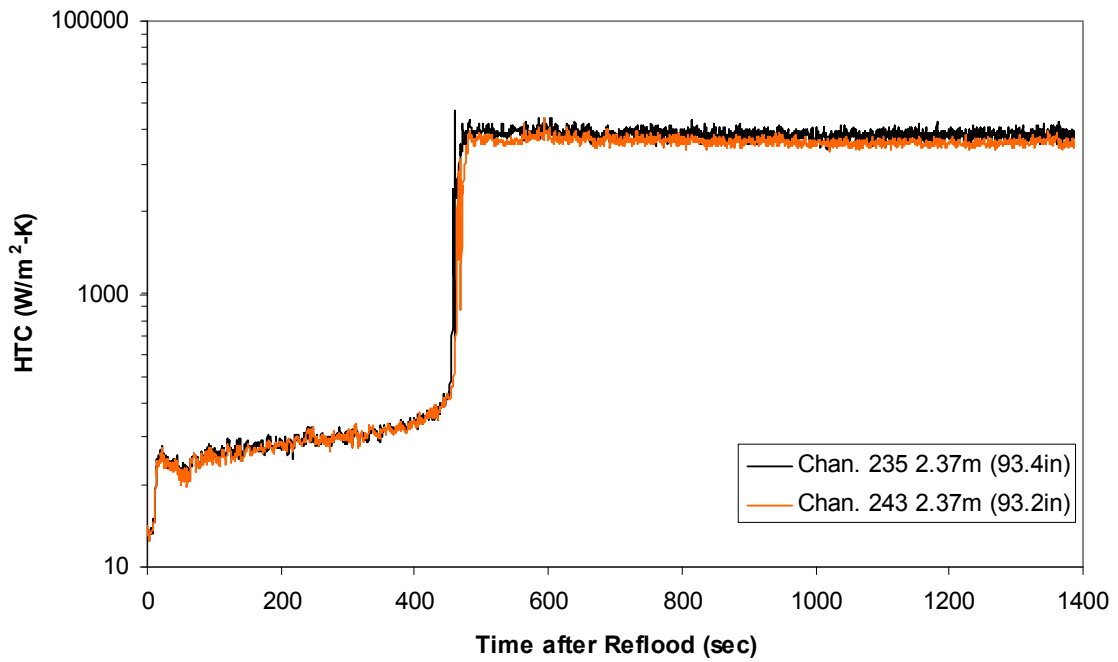
Heat Transfer Coefficient during Reflood RBHT Exp. 1389



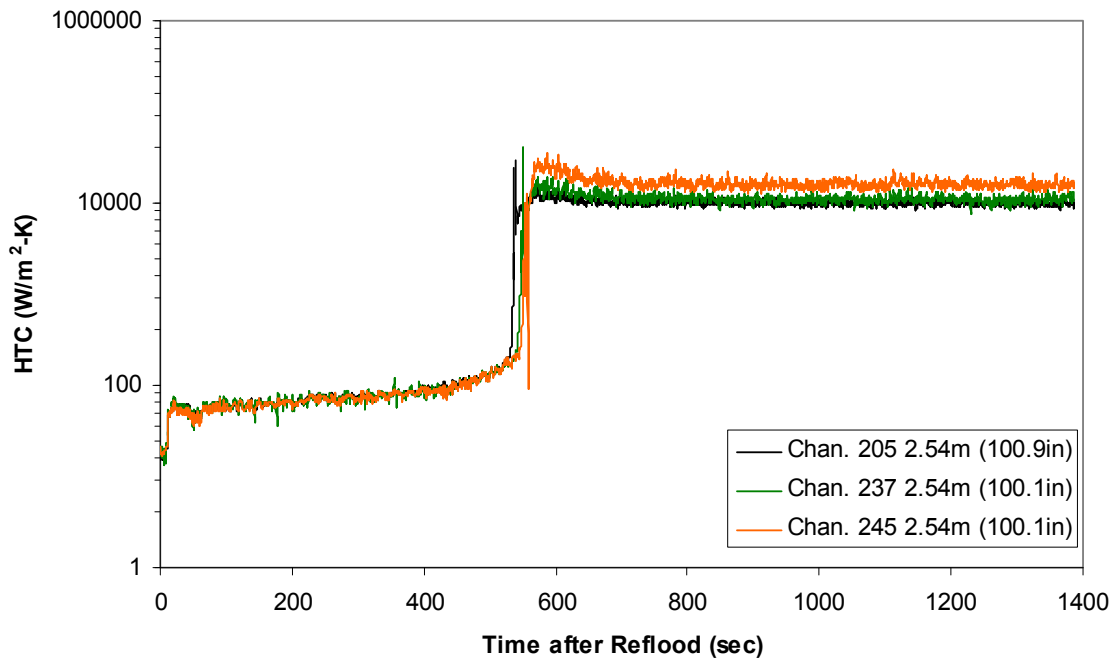
Heat Transfer Coefficient during Reflood
RBHT Exp. 1389



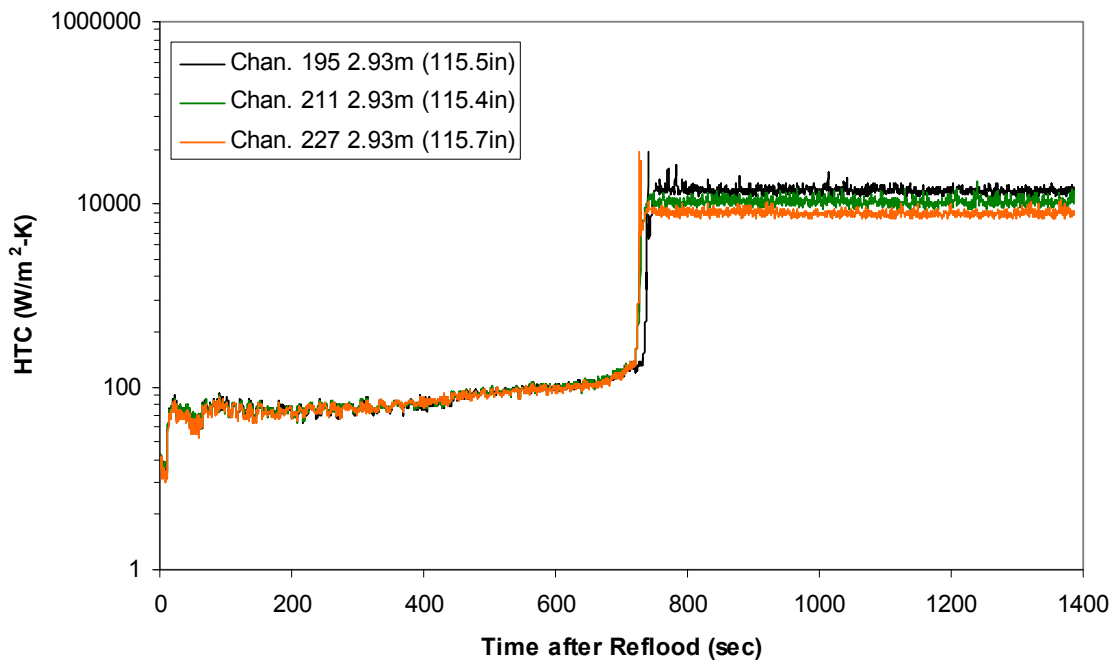
Heat Transfer Coefficient during Reflood
RBHT Exp. 1389



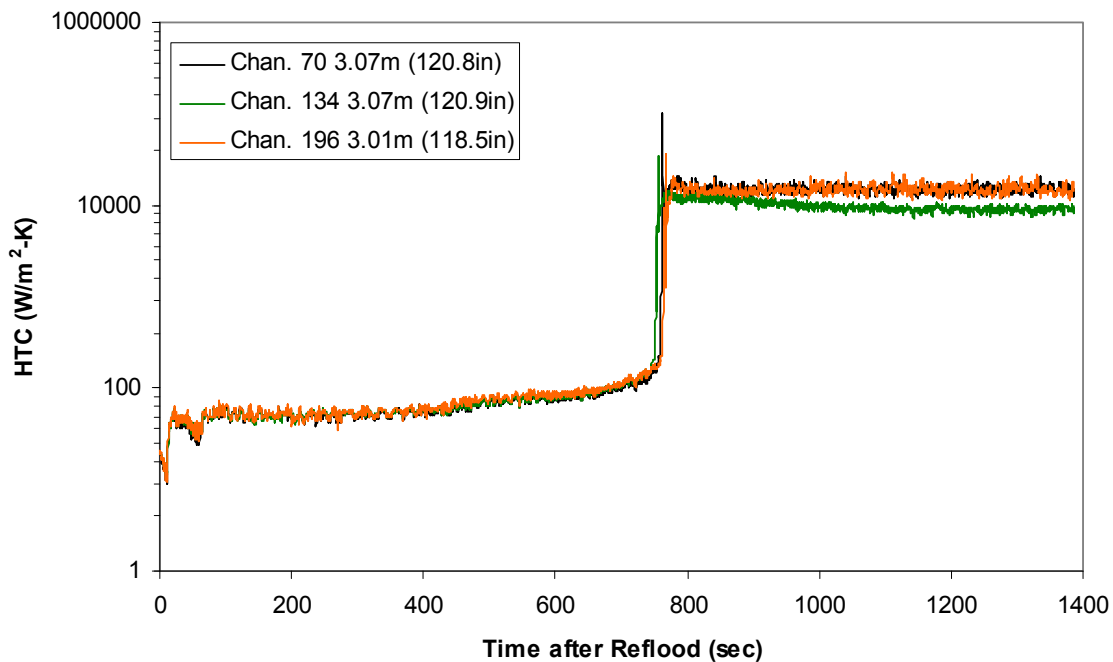
Heat Transfer Coefficient during Reflood RBHT Exp. 1389



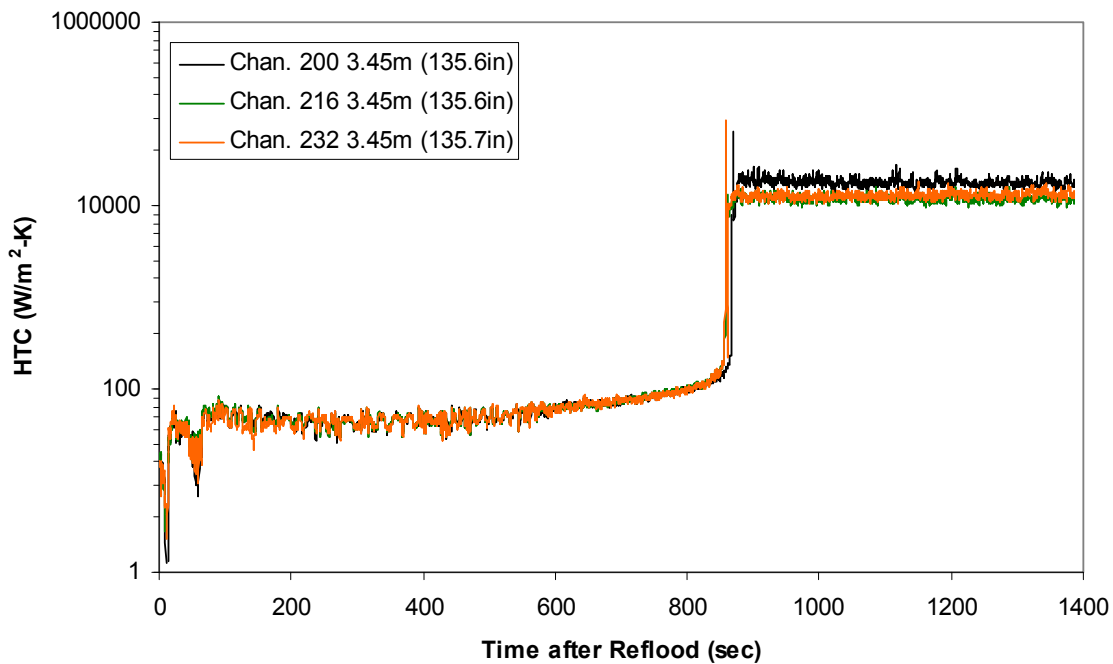
Heat Transfer Coefficient during Reflood RBHT Exp. 1389



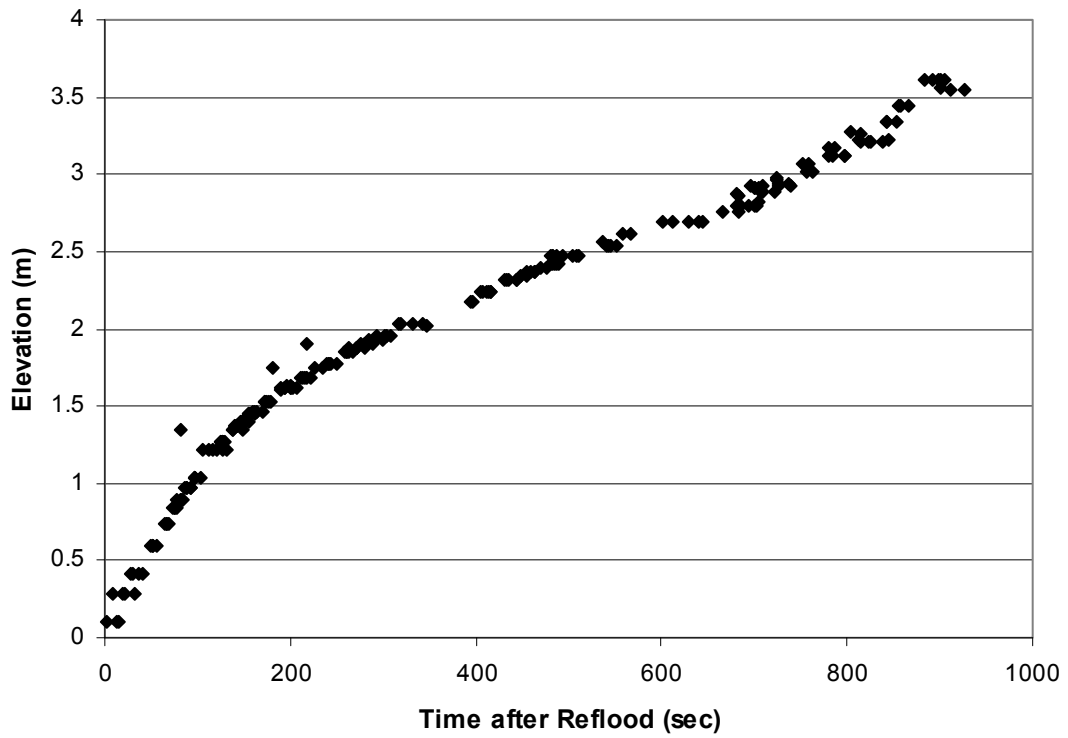
Heat Transfer Coefficient during Reflood RBHT Exp. 1389



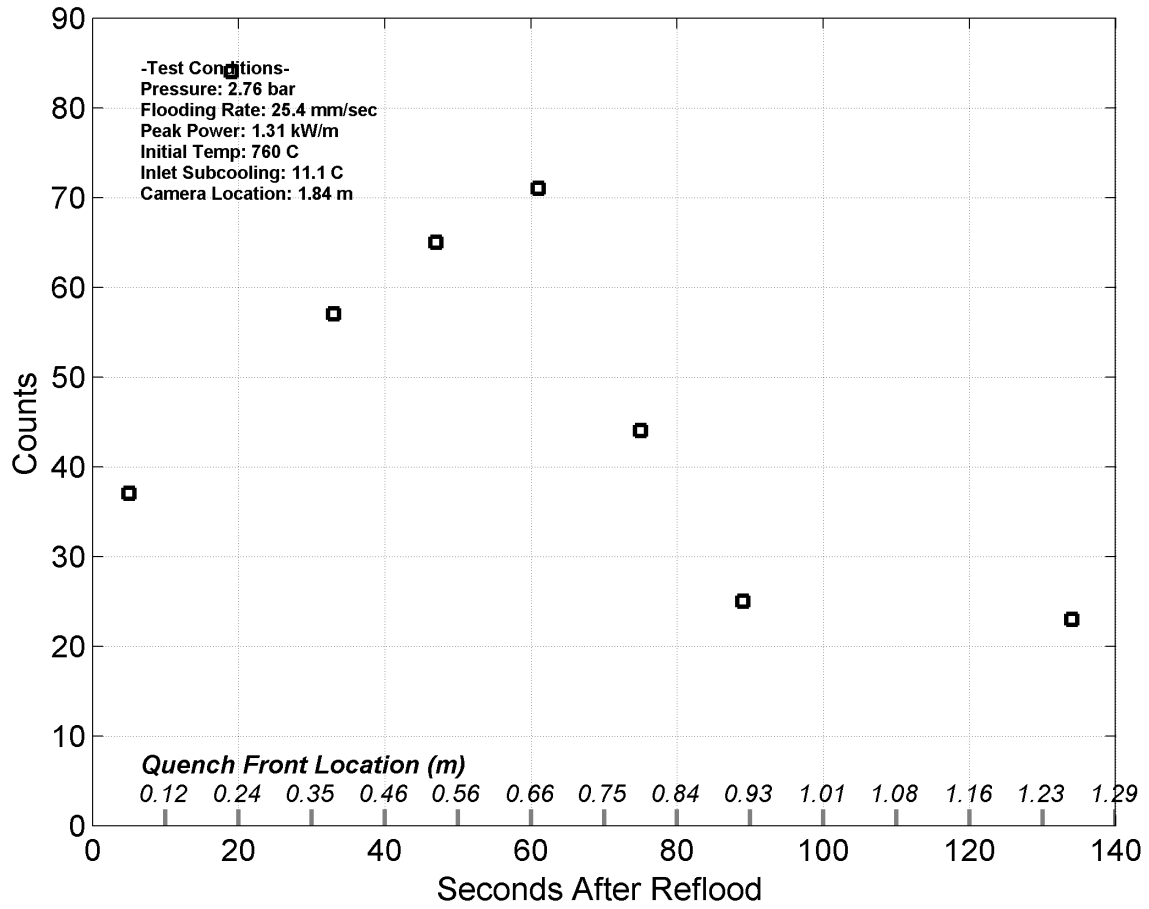
Heat Transfer Coefficient during Reflood RBHT Exp. 1389



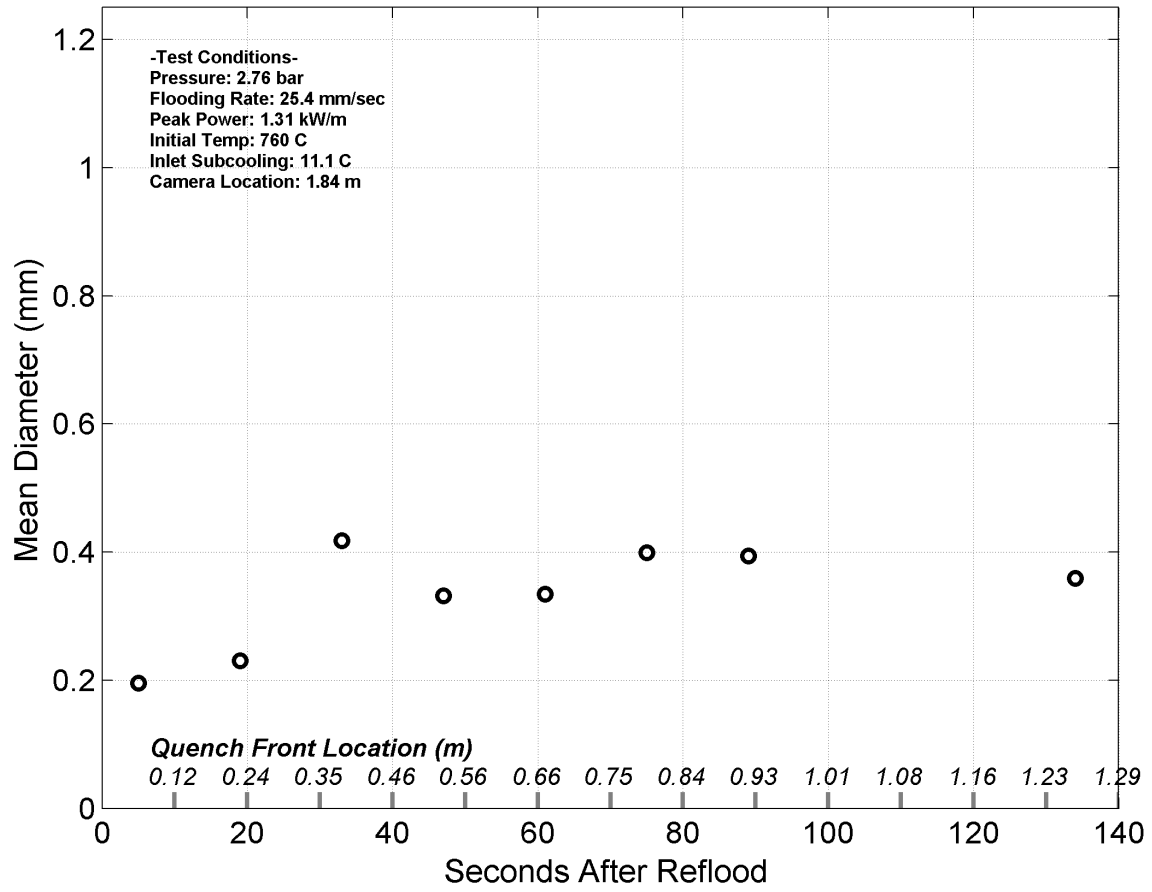
Quench Data, RBHT Exp. 1389



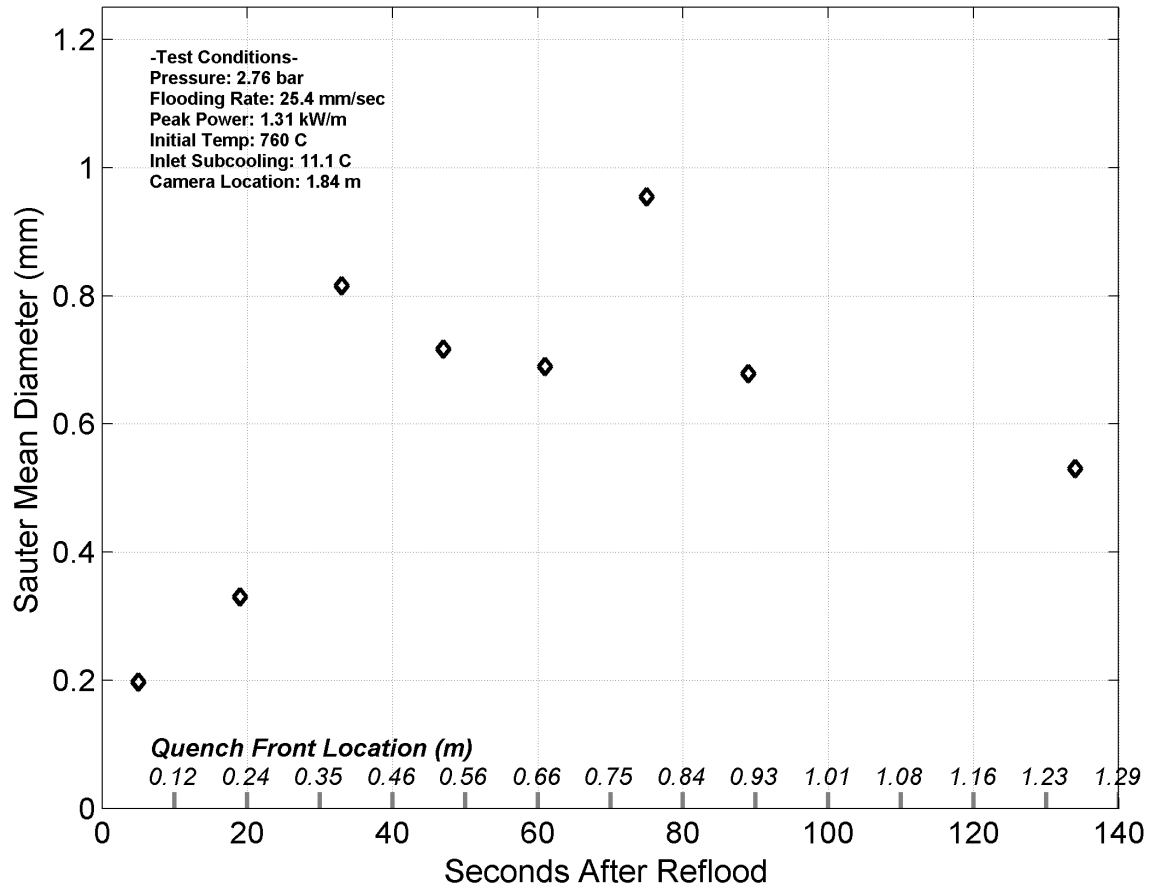
Droplet Counts - Exp. 1389



Mean Droplet Diameter - Exp. 1389



Droplet Sauter Mean Diameter - Exp. 1389



RBHT - REFLOOD TESTS

SUMMARY SHEET

RUN NO: **1402**

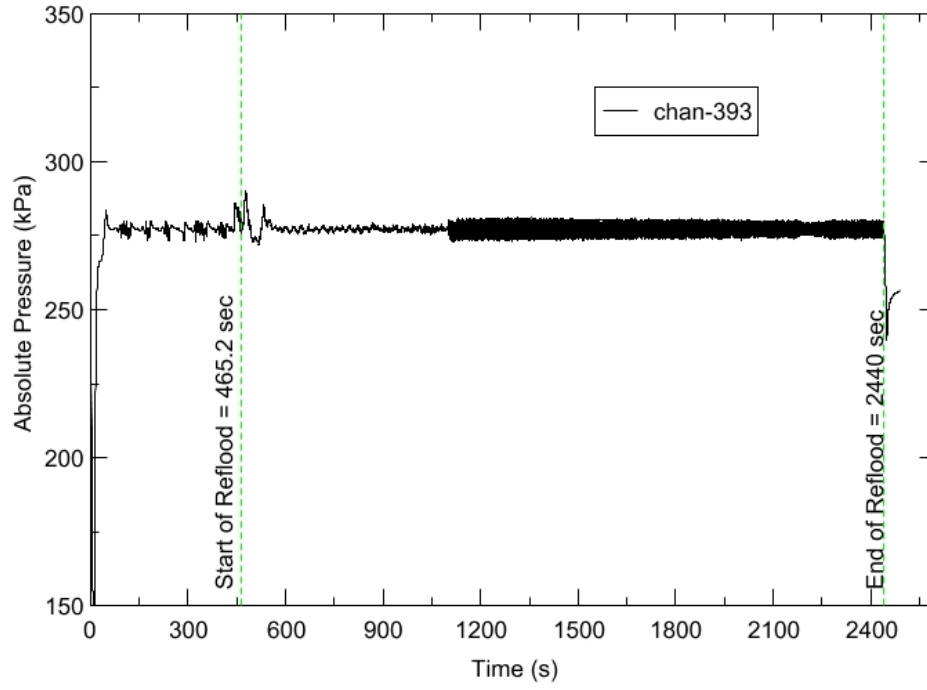
RUN CONDITIONS

Upper Plenum Pressure:	276 kPa (40 psia)
Initial Peak Clad Temperature:	1033 degrees K (1400 degrees F)
Rod Peak Power:	1.31 kW/m (0.4 kW/ft)
Flooding Rate:	0.0254 m/s (1 in/s)
Inlet Subcooling:	11 degrees K (20 degrees F)
Start of Reflood:	465.2 s
End of Reflood:	2440 s
Test Date:	8/26/2002
Comments:	

Rod_Elevation	Channel Number	Temperature at Reflood (K)	Temperature at Reflood (°F)	Turnaround Time (sec.)	Turnaround Temperature (K)	Turnaround Temperature (°F)	Quench Time (sec.)	Quench Temperature (K)	Quench Temperature (°F)
B6_0.592m	148	742.45	876.72	6.55	753.93	897.39	75.05	572.72	571.2
B6_0.744m	149	791.15	964.39	7.05	803.24	986.15	97.05	566.29	559.63
B6_0.846m	150	822.23	1020.32	7.55	835.79	1044.73	110.55	590.34	602.92
B6_0.897m	151	832.91	1039.56	7.55	847.08	1065.05	118.05	606.78	632.51
C6_1.04m	137	872.31	1110.48	8.05	888.36	1139.36	143.55	653.99	717.49
D5_1.27m	217	932.84	1219.42	8.55	949.95	1250.23	188.05	646.16	703.39
C6_1.34m	138	923.02	1201.75	63.05	951.59	1253.18	206.05	668.85	744.24
D5_1.37m	218	955.81	1260.78	63.05	992.36	1326.56	213.55	687.27	777.4
C6_1.39m	139	930.73	1215.62	63.05	967.16	1281.19	221.55	673.29	752.24
D5_1.45m	219	969.61	1285.61	63.05	1016.02	1369.15	235.55	701.89	803.71
C6_1.47m	140	945.74	1242.65	64.05	990.81	1323.77	245.05	686.03	775.16
D5_1.52m	220	980.92	1305.97	63.05	1038.2	1409.07	260.05	689.73	781.83
C6_1.62m	141	959.71	1267.79	64.55	1028.93	1392.39	300.05	646.17	703.41
D5_1.68m	221	987.3	1317.46	65.05	1070.87	1467.88	319.55	688.84	780.23
D5_1.78m	222	981.5	1307.01	64.55	1018.63	1373.84	350.05	623.94	663.41
D5_1.85m	223	1010.13	1358.55	65.05	1065.62	1458.44	371.55	661.4	730.84
C6_1.87m	142	994.58	1330.56	65.55	1057.25	1443.36	384.55	665.24	737.74
D5_1.90m	224	1020.35	1376.94	64.55	1087.49	1497.79	395.05	678.63	761.85
C6_1.95m	144	1005.64	1350.46	65.55	1078.78	1482.11	420.55	684.22	771.9
C3_2.17m	178	1014.36	1366.17	64.55	1089.42	1501.28	529.55	612.65	643.08
D4_2.24m	241	1066.3	1459.65	65.05	1101.62	1523.23	551.55	649.5	709.42
D4_2.32m	242	1081.3	1486.64	65.05	1143.77	1599.11	574.55	670.55	747.31
C3_2.35m	180	1077.18	1479.24	65.55	1141.33	1594.7	581.55	675.33	755.9
D4_2.37m	243	1089.82	1501.99	65.05	1156.93	1622.78	600.55	658.74	726.05
C3_2.40m	181	1081.43	1486.89	65.05	1146.46	1603.94	607.55	676.98	758.87
D4_2.54m	245	1116.29	1549.63	64.55	1197.16	1695.2	723.05	598.53	617.66
D6_2.62m	129	1104.69	1528.75	64.55	1192.61	1687.02	733.55	623.34	662.33
D6_2.69m	130	1099.62	1519.63	64.55	1199.62	1699.63	777.05	670.12	746.52
C3_2.76m	183	1085.31	1493.88	81.55	1199.73	1699.83	836.55	665.37	737.97
D4_2.79m	247	1058.58	1445.76	64.05	1162.63	1633.05	882.55	620.14	656.57
D6_2.87m	131	1049.29	1429.03	64.05	1095.88	1512.89	858.05	658.46	725.54
D6_2.92m	132	1032.96	1399.64	65.55	1099.47	1519.35	877.05	665.35	737.93
D6_2.97m	133	1009.19	1356.85	65.55	1085.2	1493.67	902.55	666.08	739.26
D6_3.07m	134	976.79	1298.53	65.55	1062.46	1452.74	931.55	667.49	741.79
E3_3.12m	197	972.77	1291.3	402.55	1073.57	1472.73	981.55	644.11	699.71
D6_3.17m	135	935.63	1224.45	402.55	1050.86	1431.86	961.55	668.44	743.5
D6_3.27m	136	874.01	1113.52	463.05	1038.15	1408.99	988.05	652.89	715.51
D4_3.61m	248	661.67	731.31	493.55	881.08	1126.26	1085.55	577.7	580.18

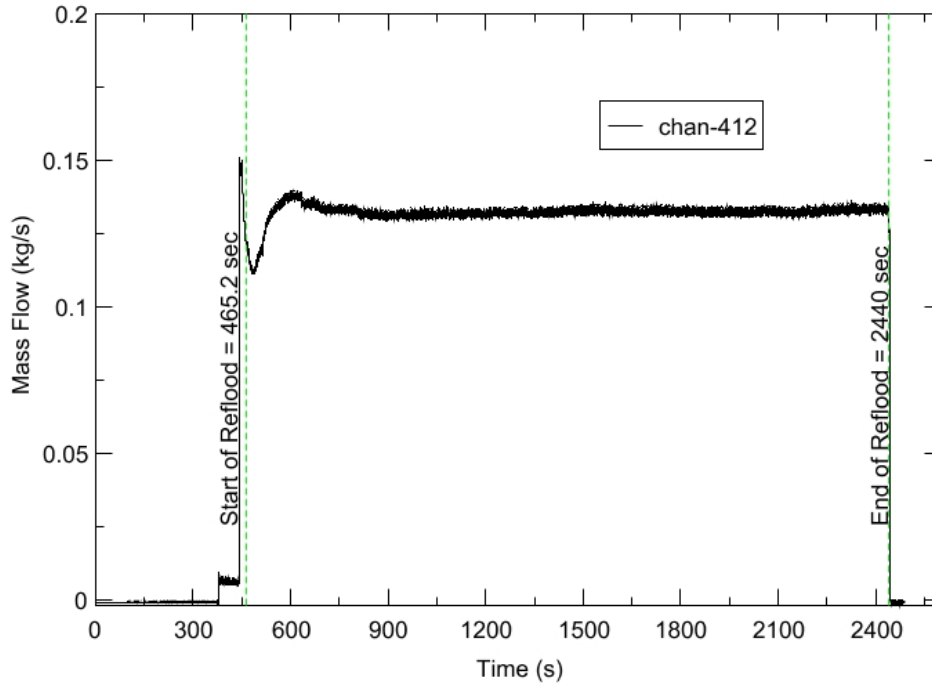
RBHT - TEST FACILITY

Upper Plenum Pressure vs. Time, Exp 1402



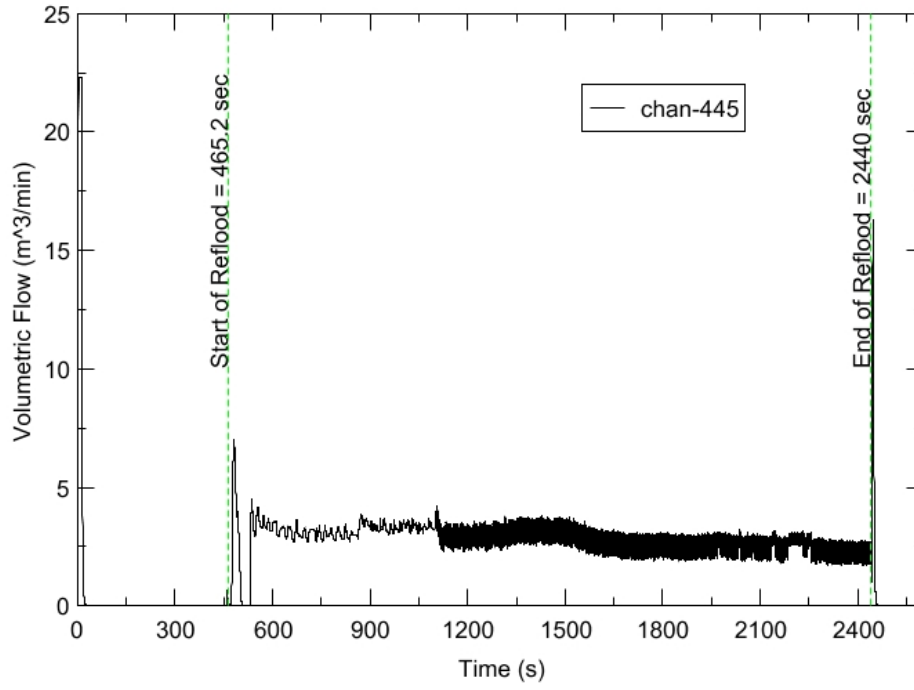
RBHT - TEST FACILITY

Inlet Flow vs. Time, Exp 1402



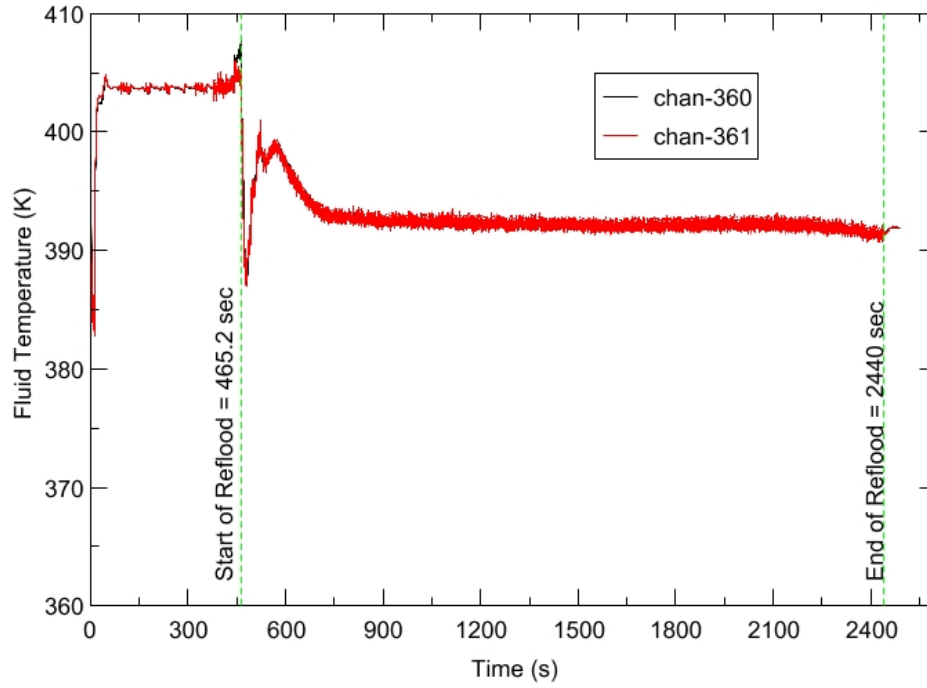
RBHT - TEST FACILITY

Steam Exhaust Flow vs. Time, Exp 1402



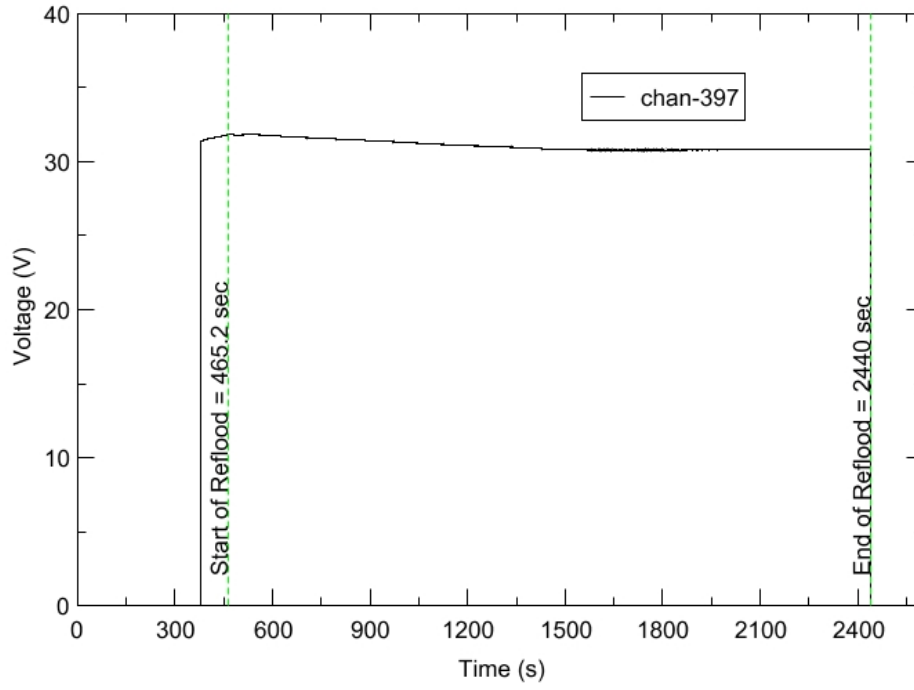
RBHT - TEST FACILITY

Inlet Flow Temperature vs. Time, Exp 1402



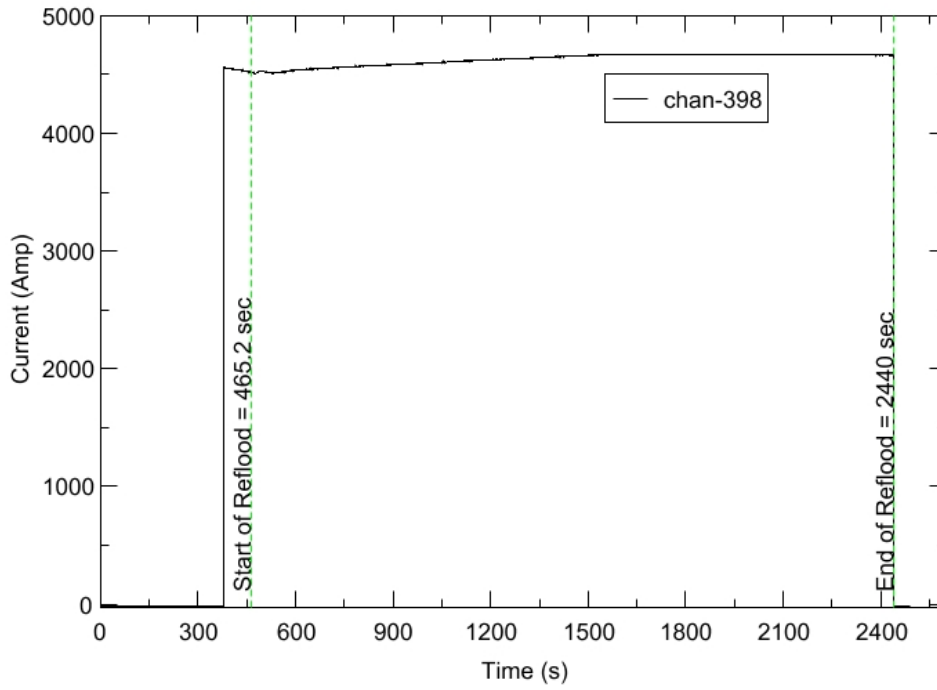
RBHT - TEST FACILITY

Test Section Voltage vs. Time, Exp 1402

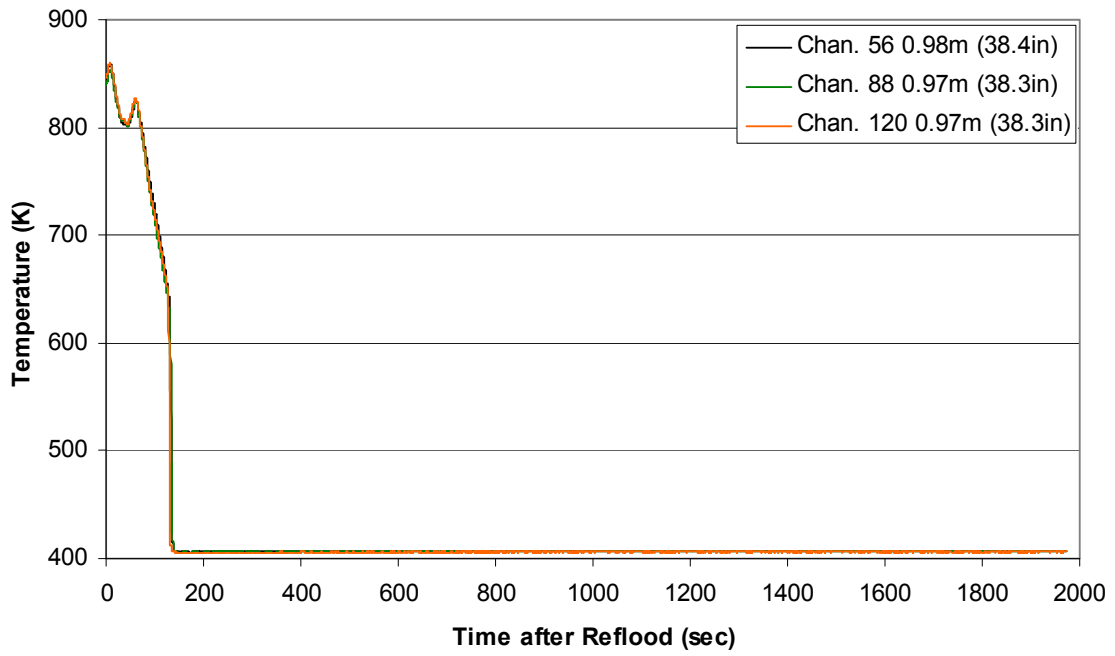


RBHT - TEST FACILITY

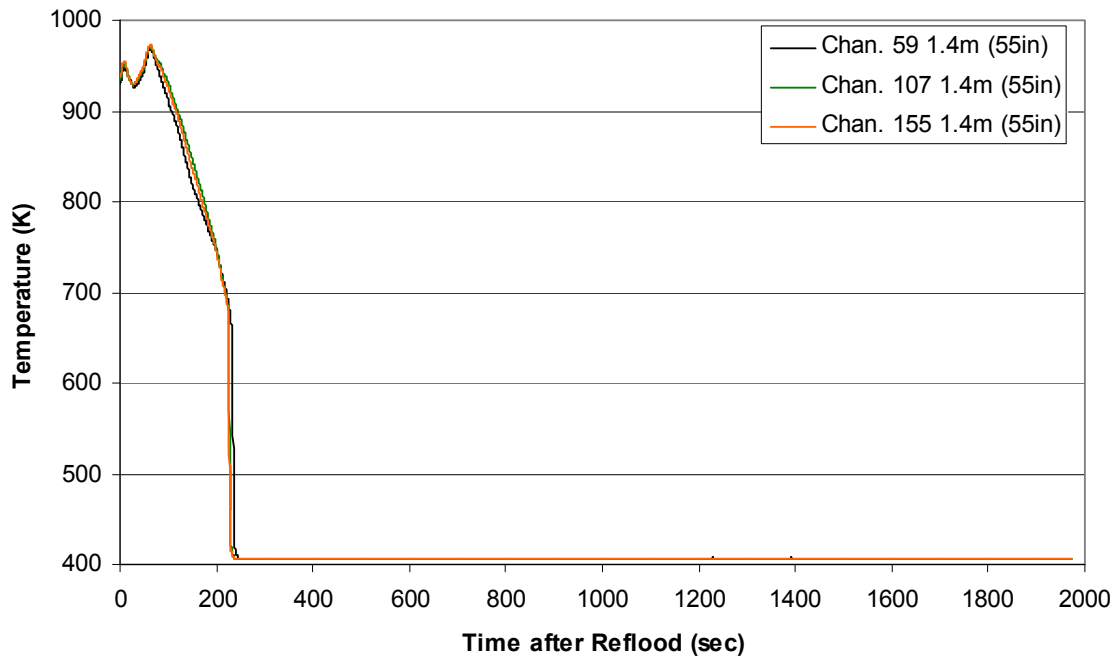
Test Section Current vs. Time, Exp 1402



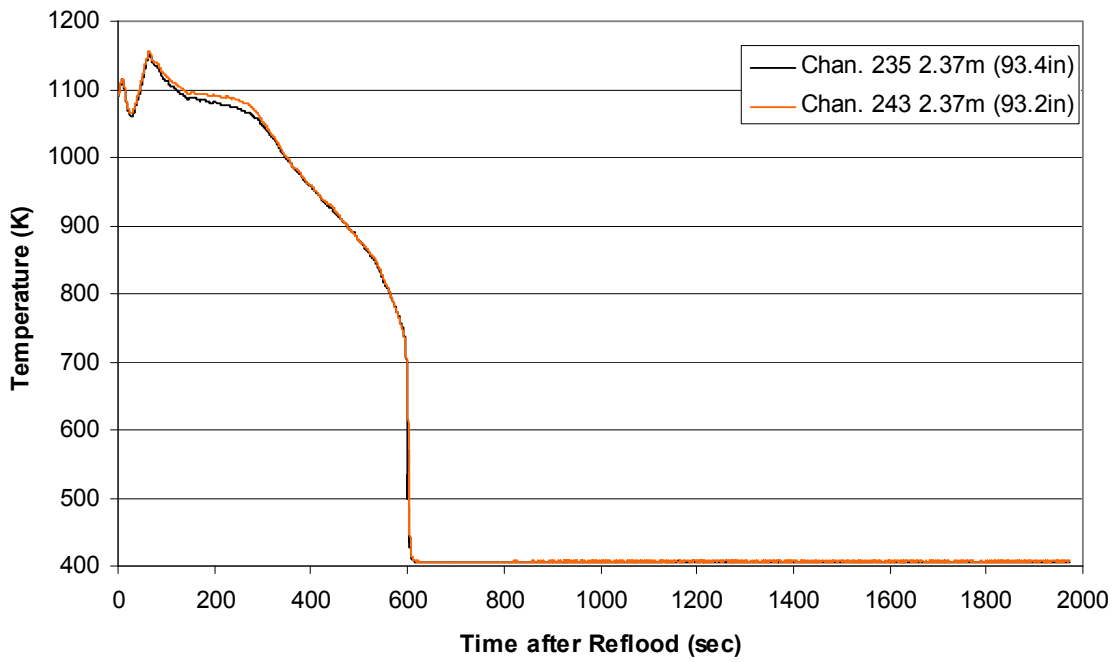
Heater Rod Temperature during Reflood RBHT Exp. 1402



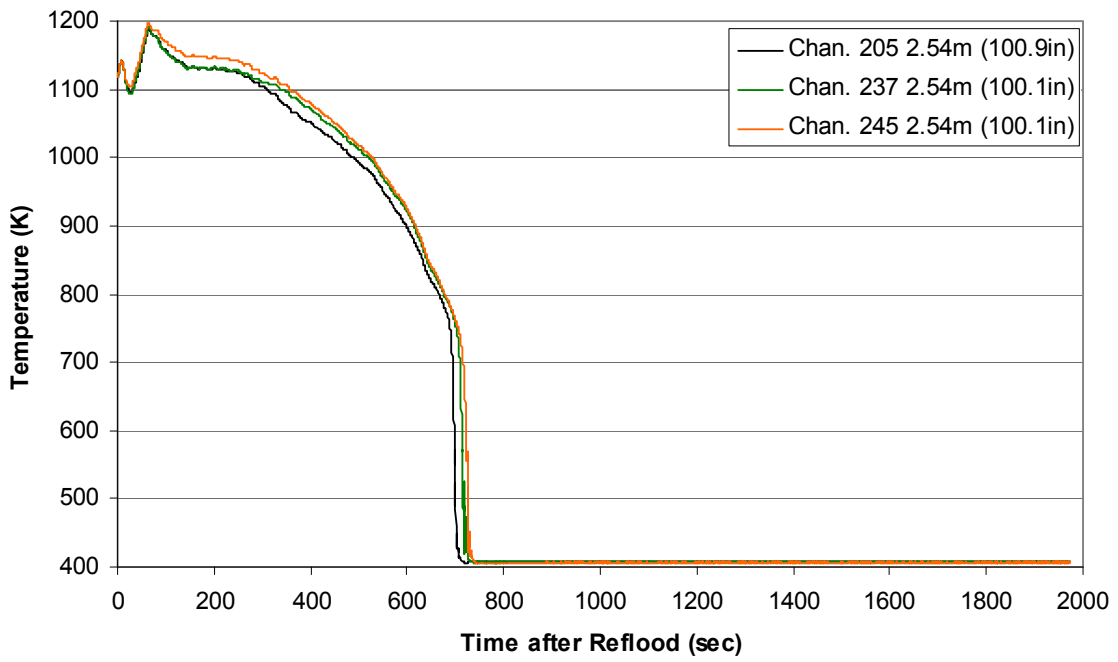
Heater Rod Temperature during Reflood RBHT Exp. 1402



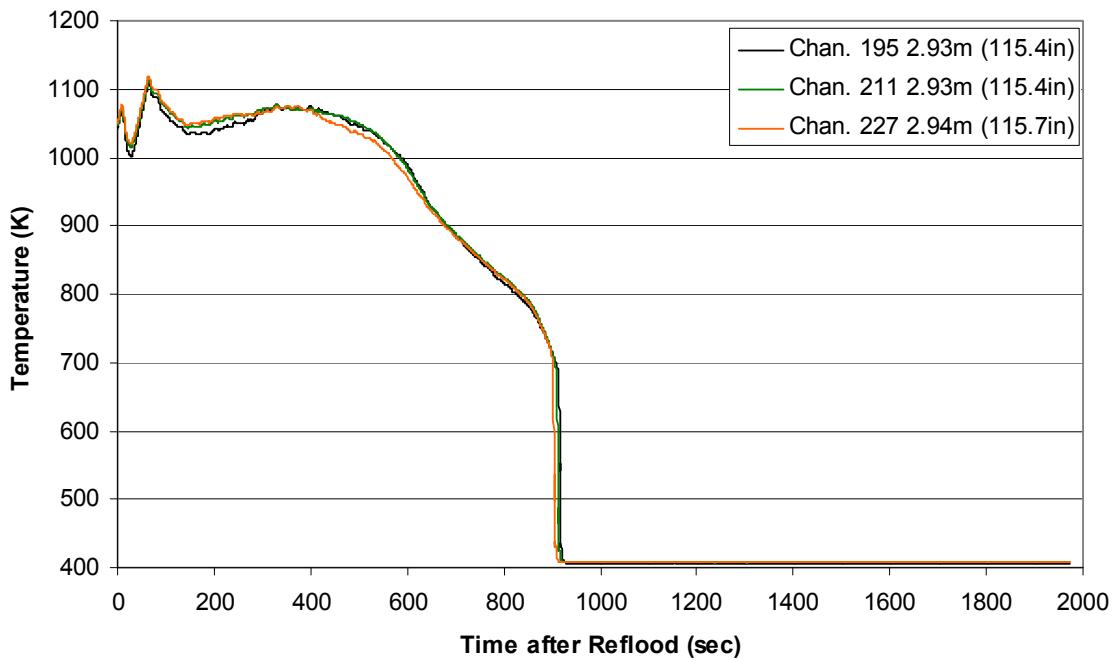
**Heater Rod Temperature during Reflood
RBHT Exp. 1402**



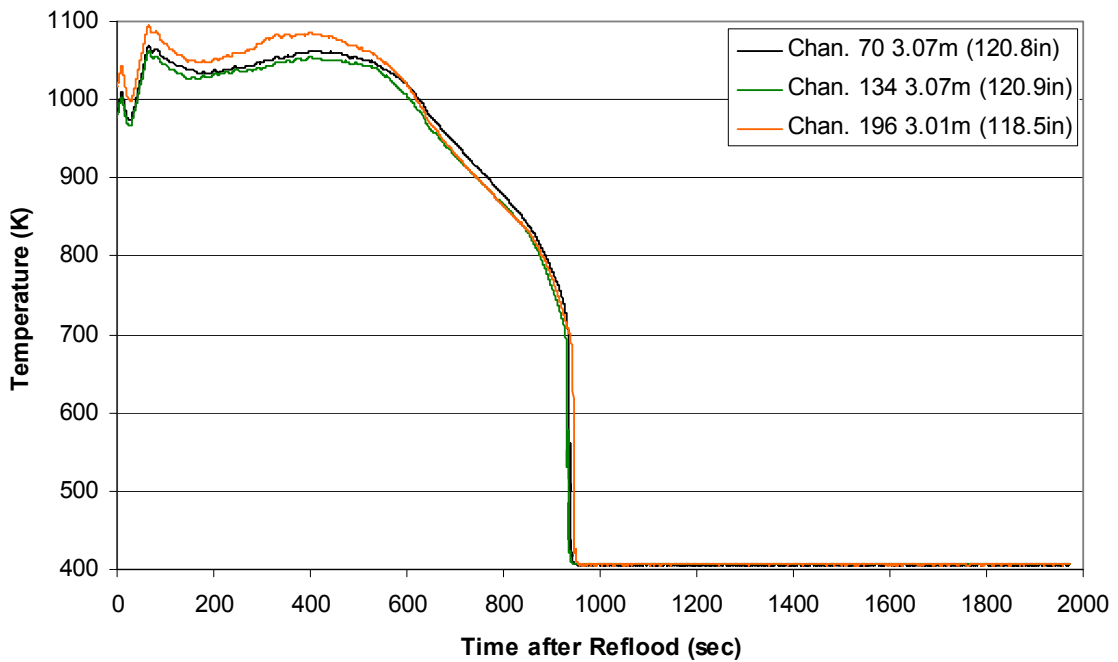
**Heater Rod Temperature during Reflood
RBHT Exp. 1402**



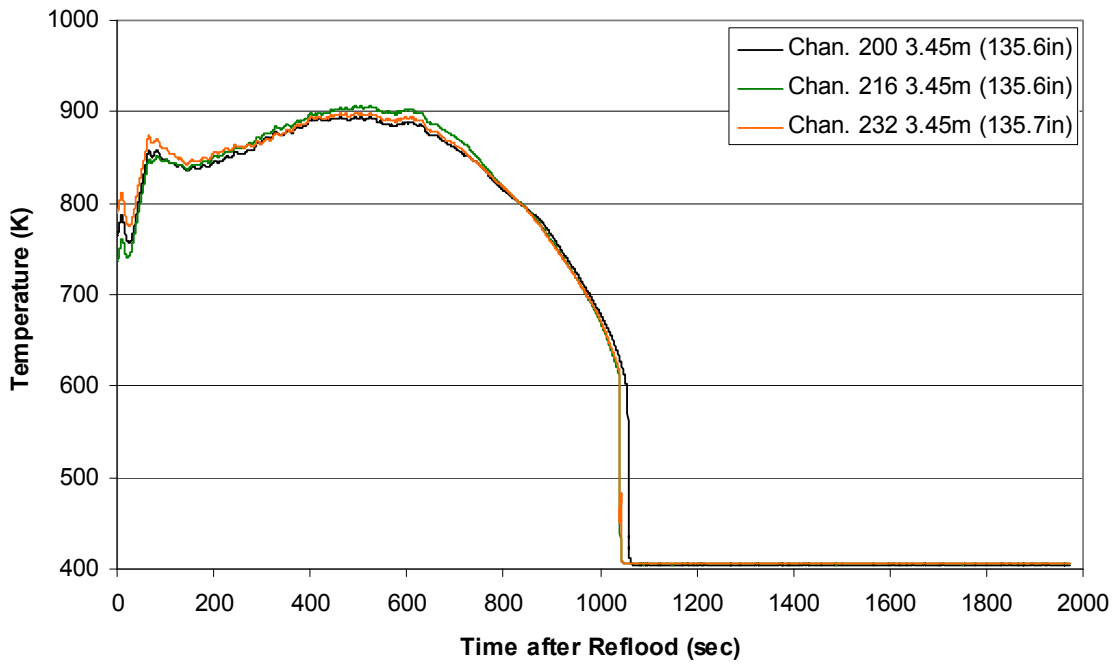
Heater Rod Temperature during Reflood
RBHT Exp. 1402



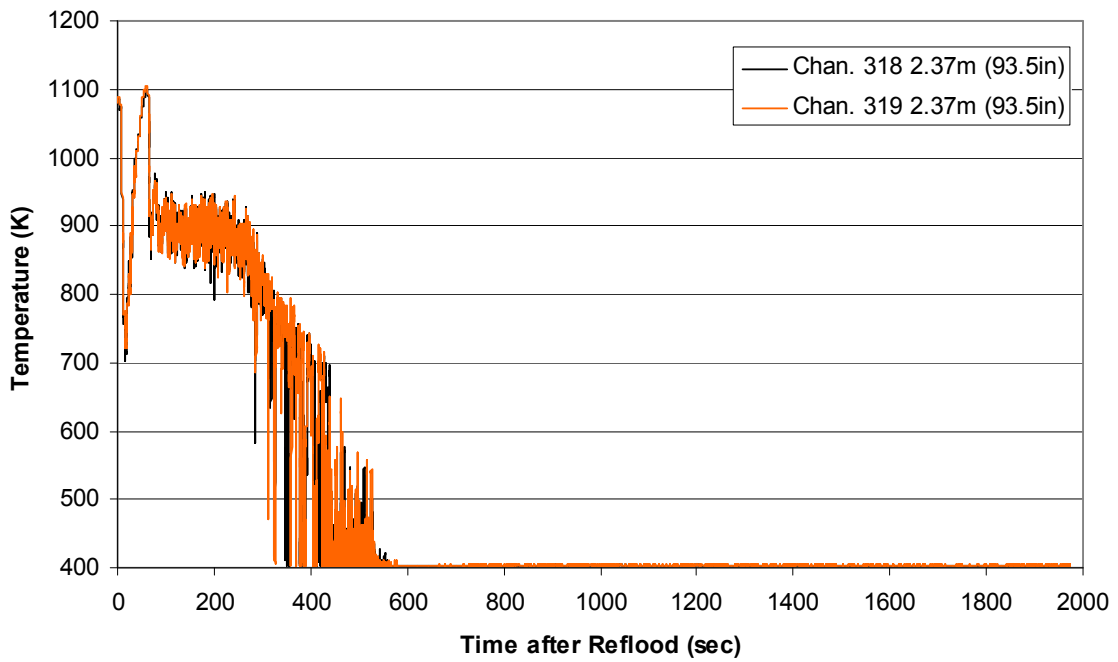
Heater Rod Temperature during Reflood
RBHT Exp. 1402



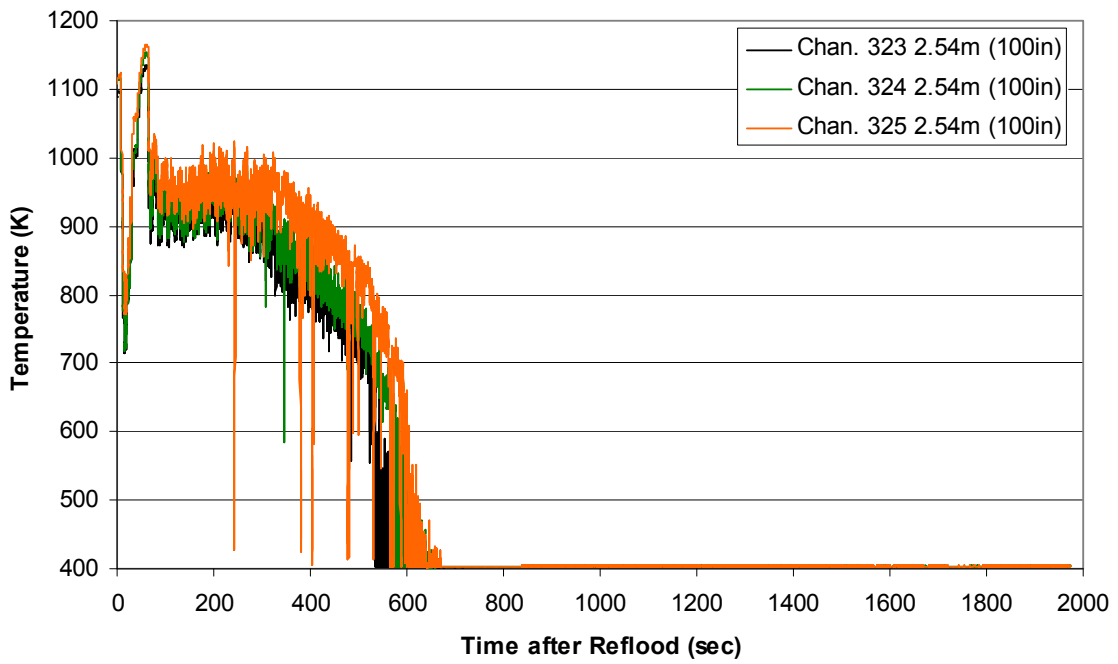
Heater Rod Temperature during Reflood RBHT Exp. 1402



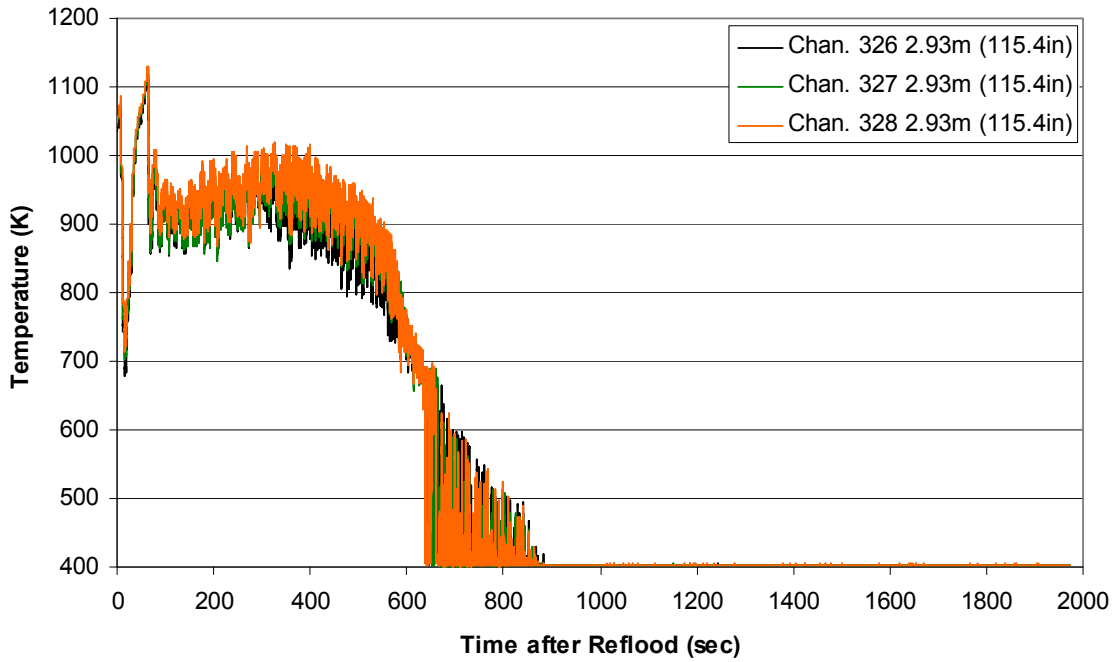
Steam Probe Temperature during Reflood RBHT Exp. 1402



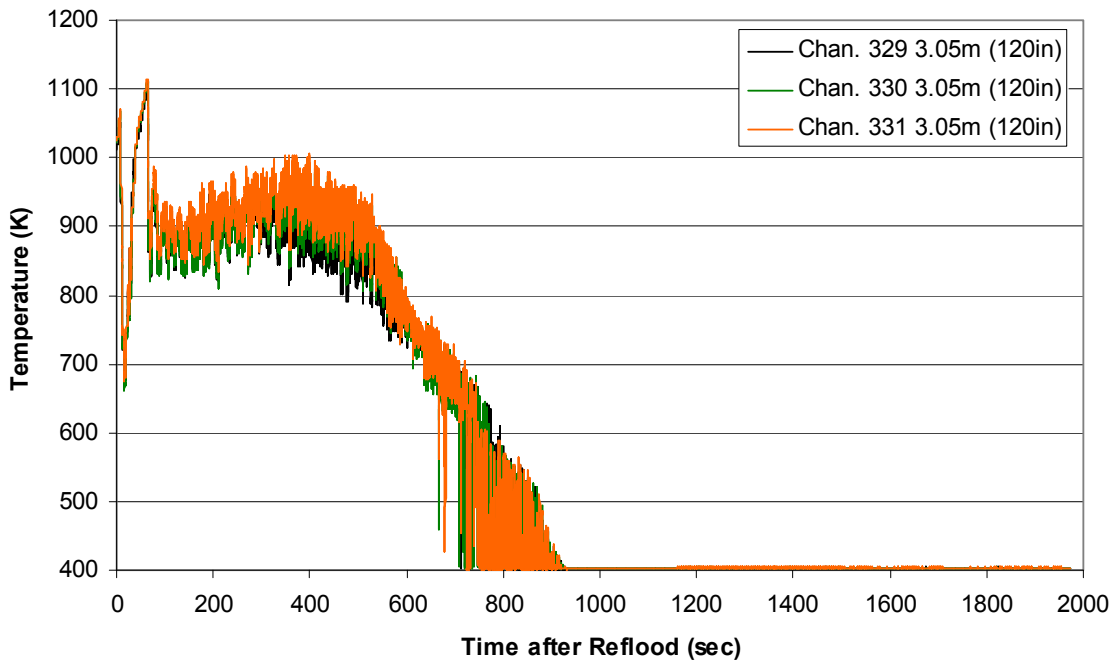
Steam Probe Temperature during Reflood
RBHT Exp. 1402



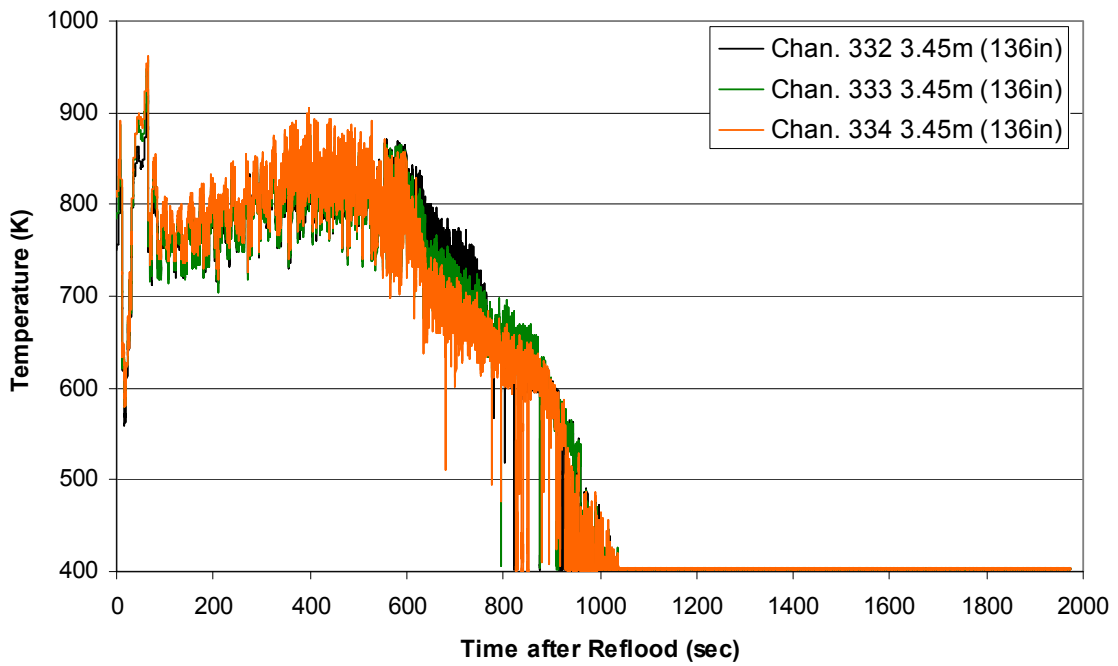
Steam Probe Temperature during Reflood
RBHT Exp. 1402



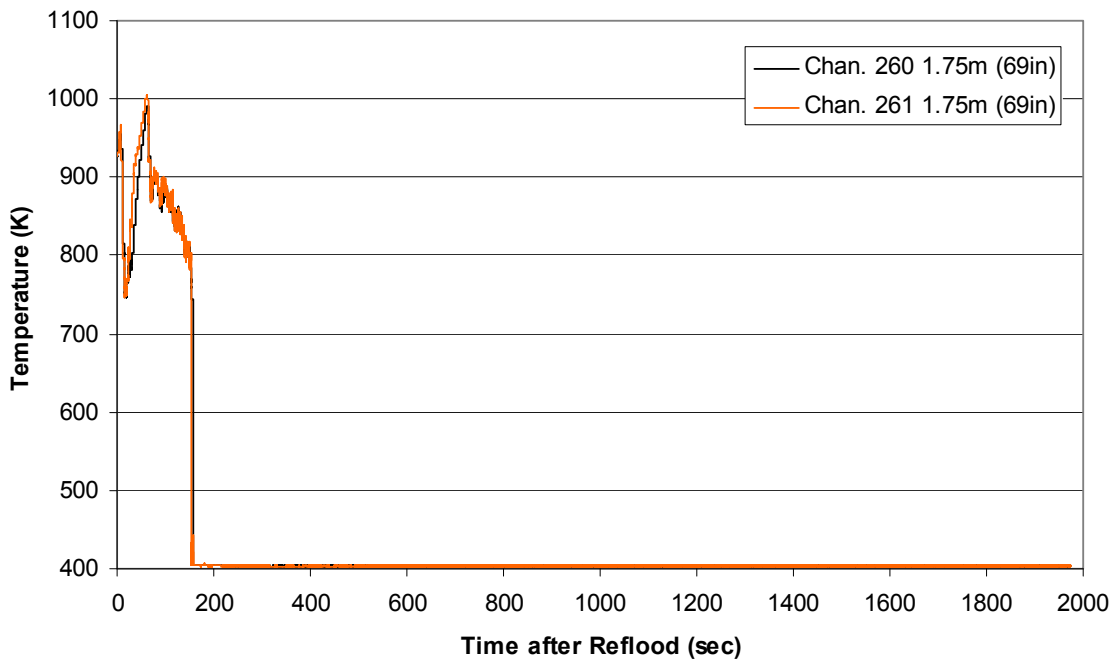
Steam Probe Temperature during Reflood
RBHT Exp. 1402



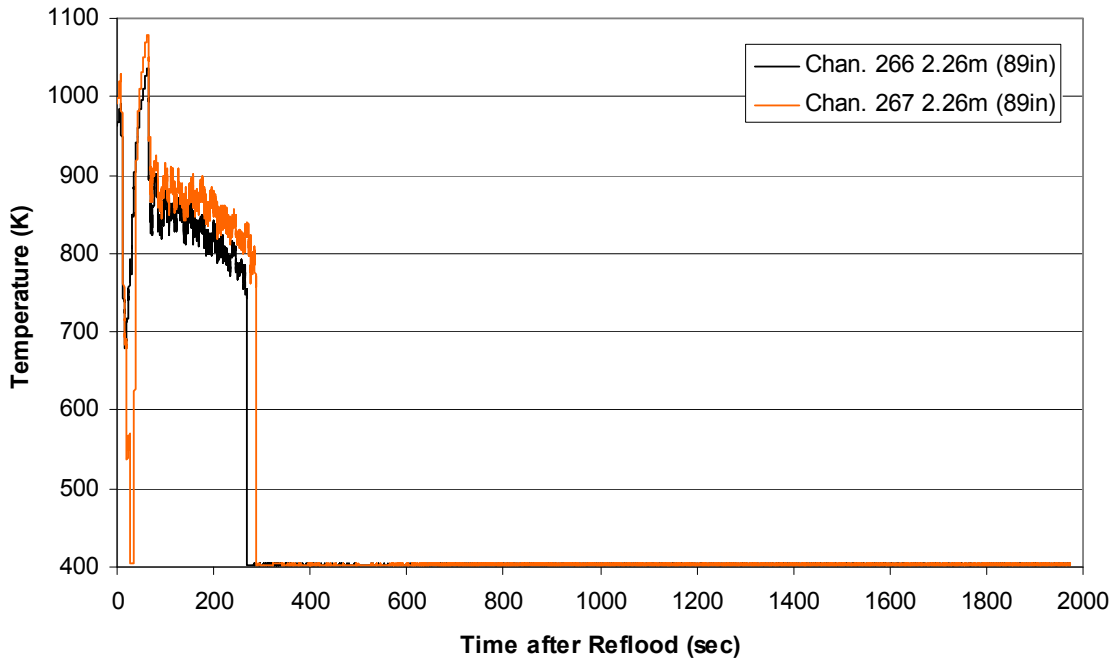
Steam Probe Temperature during Reflood
RBHT Exp. 1402



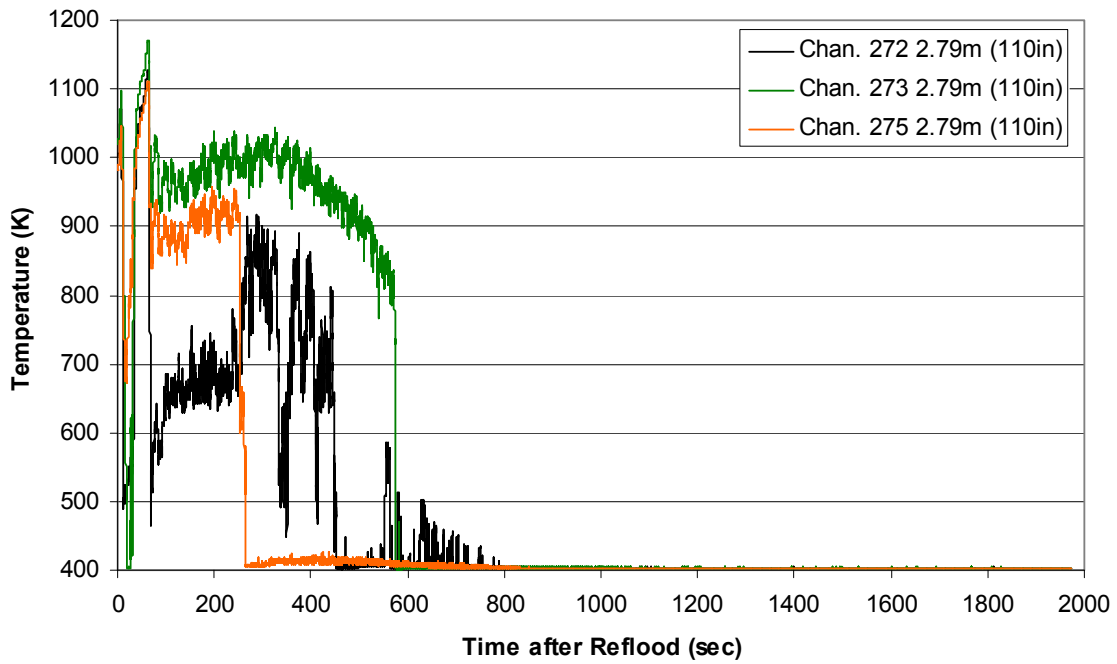
Spacer Grid Temperature during Reflood
RBHT Exp. 1402



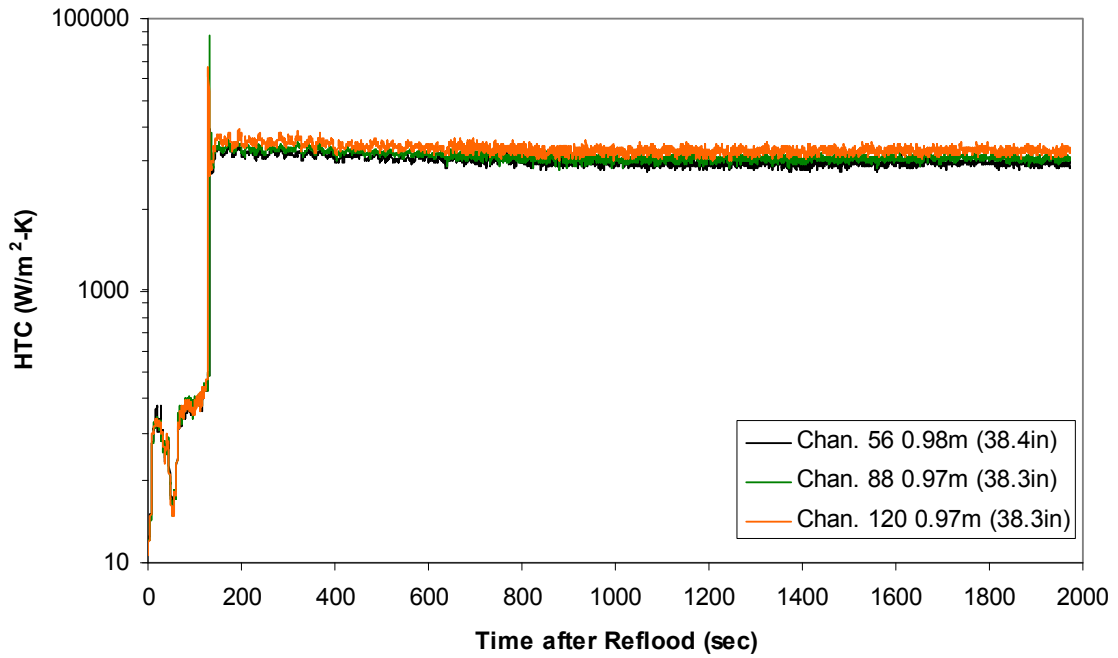
Spacer Grid Temperature during Reflood
RBHT Exp. 1402



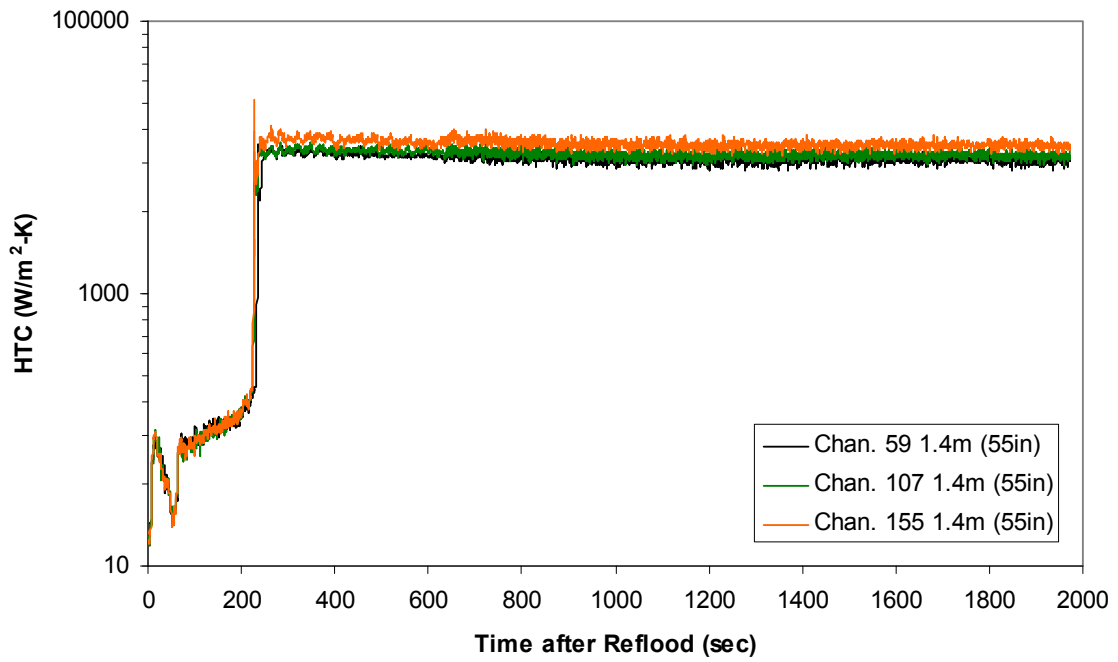
Spacer Grid Temperature during Reflood RBHT Exp. 1402



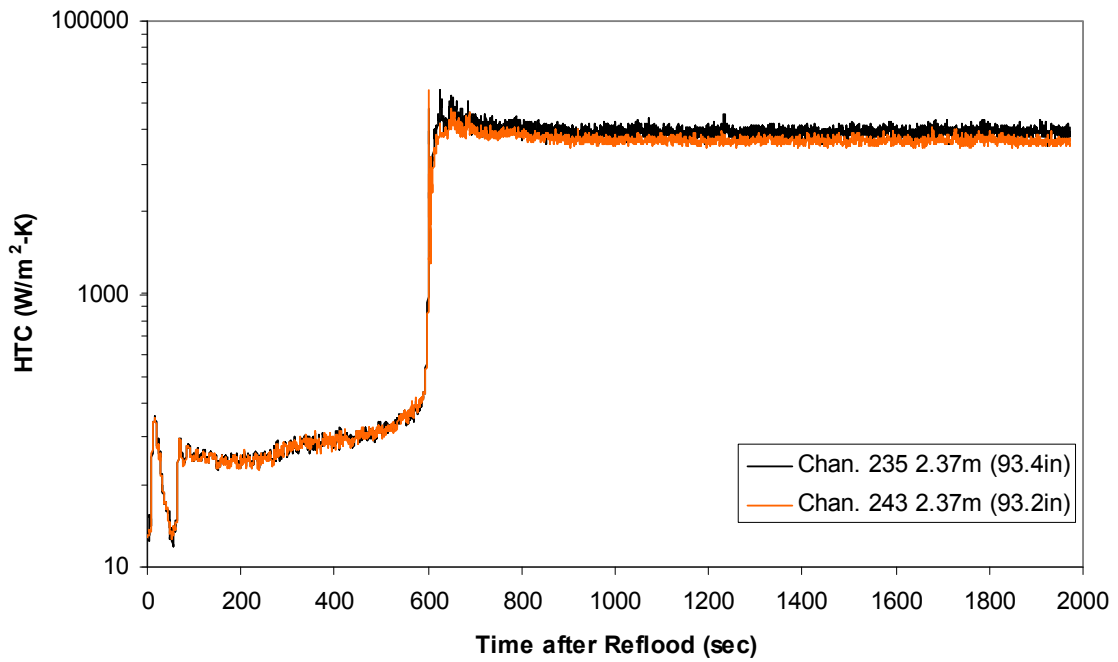
Heat Transfer Coefficient during Reflood RBHT Exp. 1402



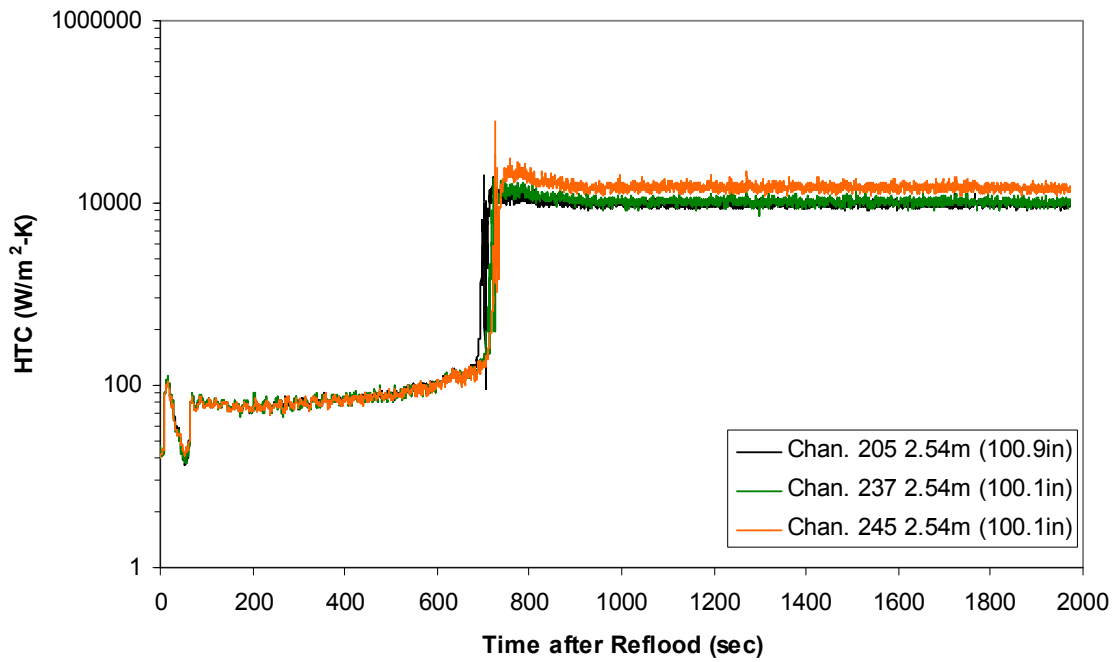
Heat Transfer Coefficient during Reflood
RBHT Exp. 1402



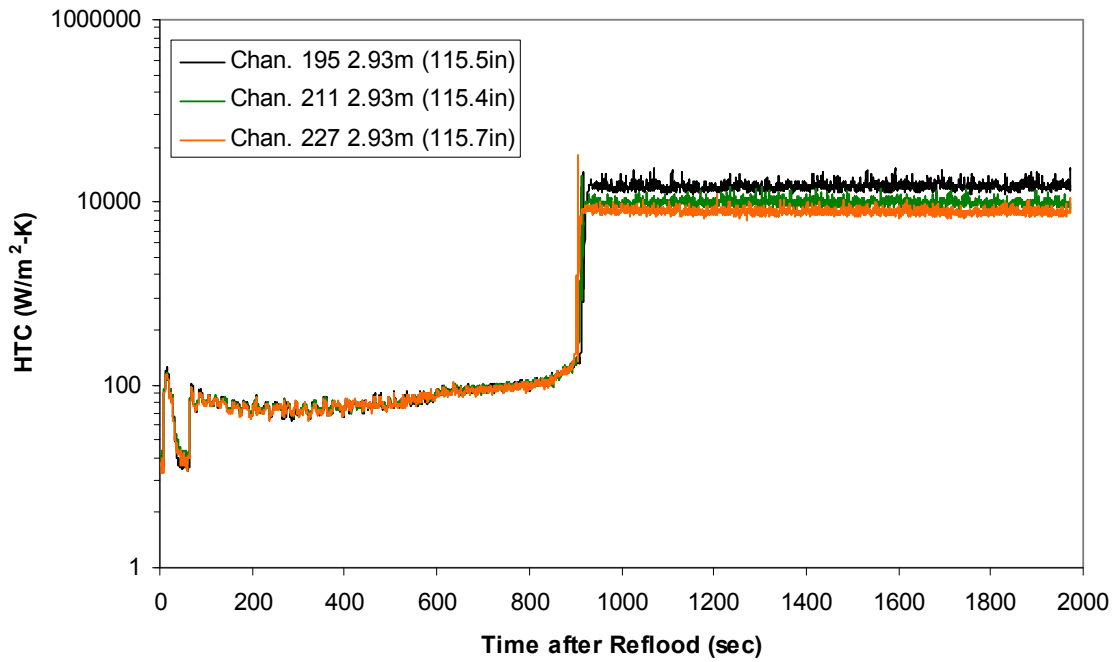
Heat Transfer Coefficient during Reflood
RBHT Exp. 1402



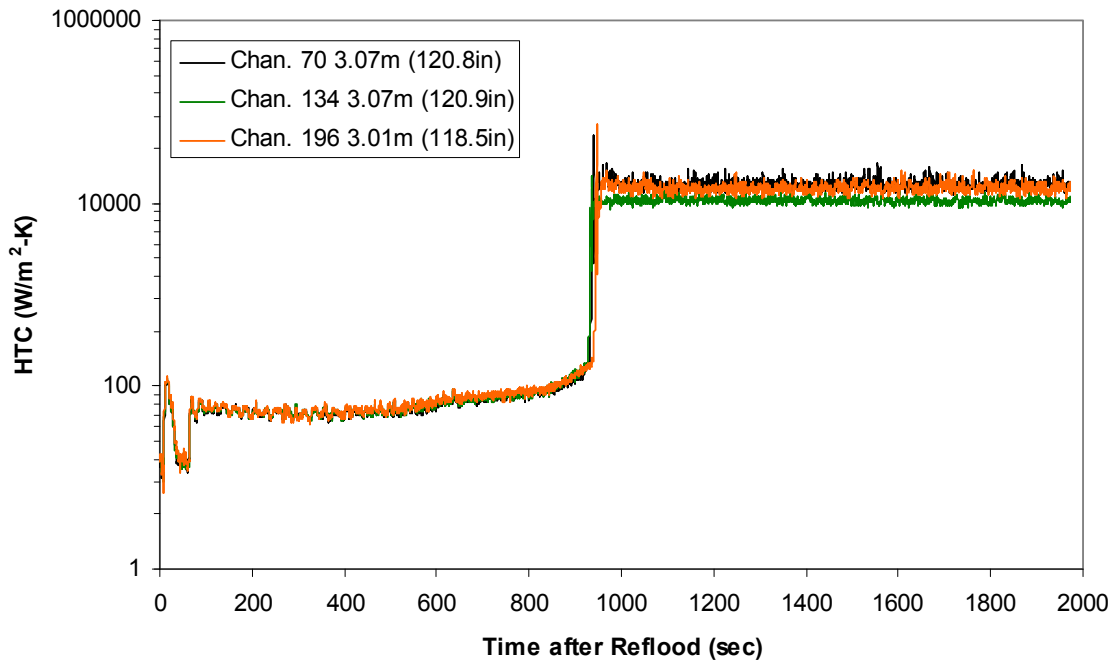
Heat Transfer Coefficient during Reflood RBHT Exp. 1402



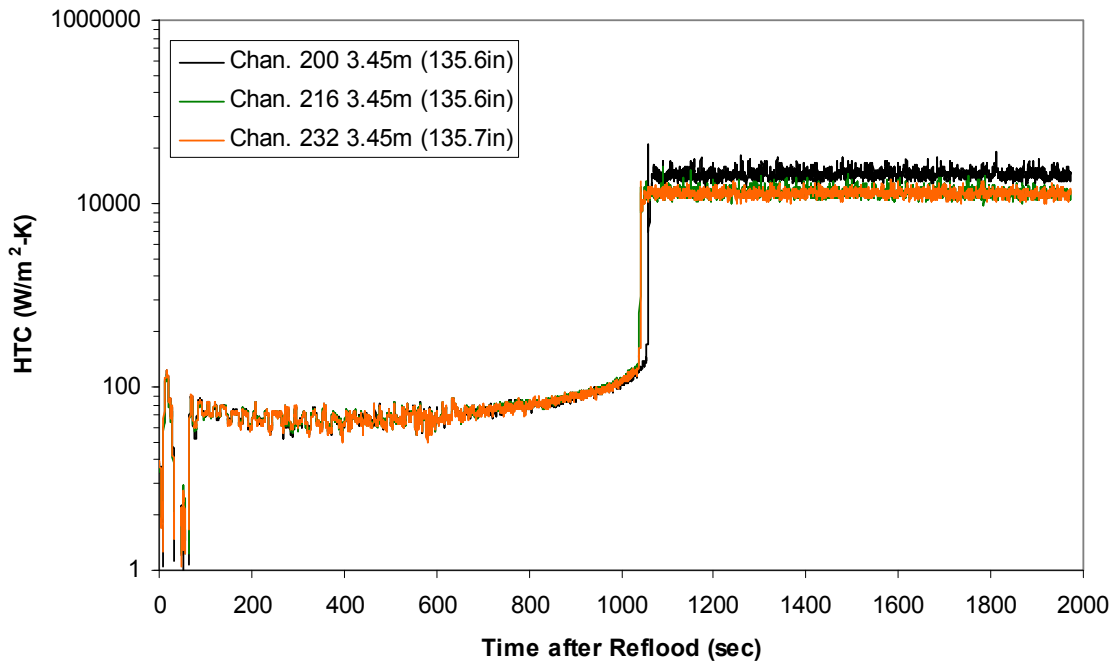
Heat Transfer Coefficient during Reflood RBHT Exp. 1402



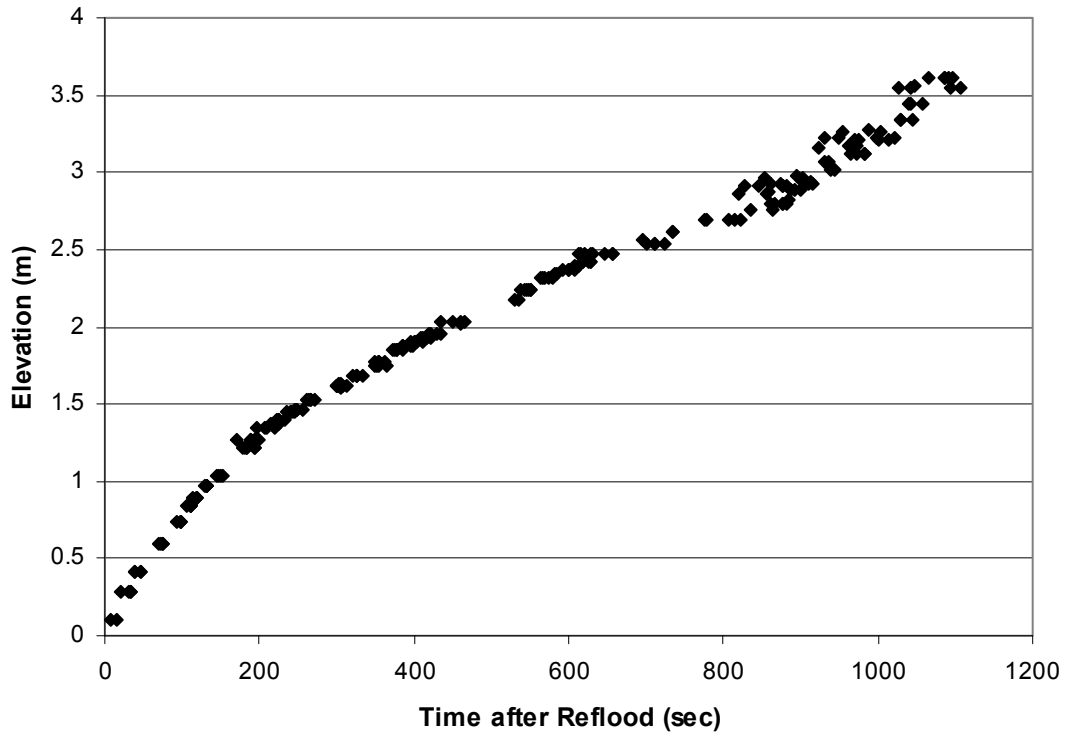
Heat Transfer Coefficient during Reflood RBHT Exp. 1402



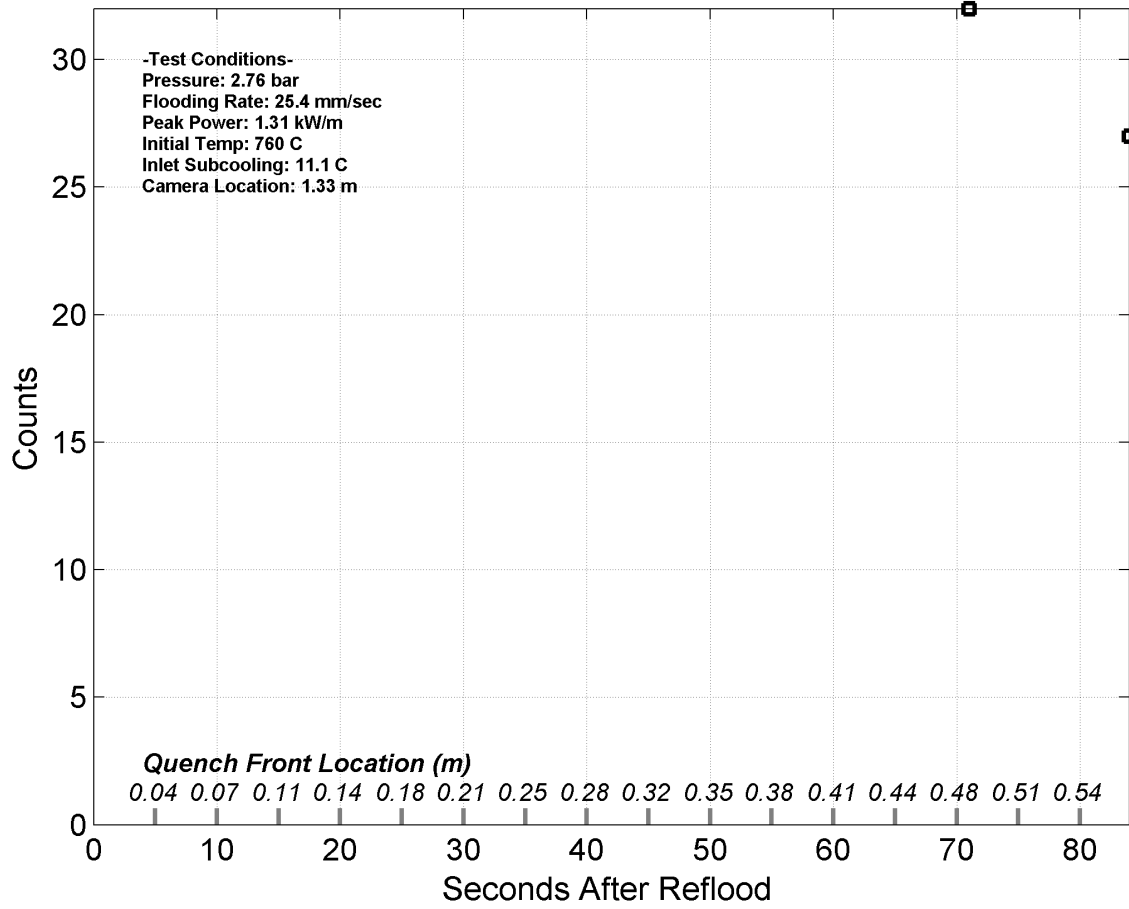
Heat Transfer Coefficient during Reflood RBHT Exp. 1402



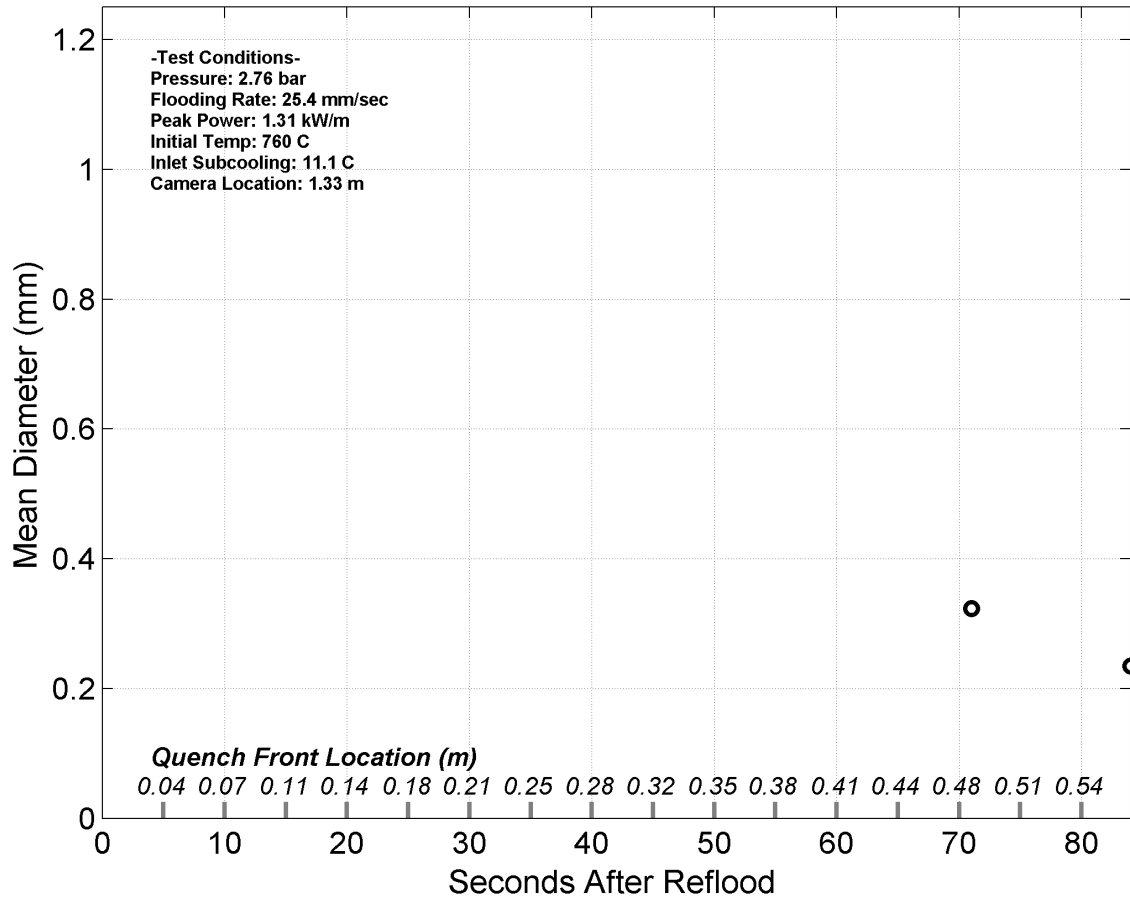
Quench Data, RBHT Exp. 1402



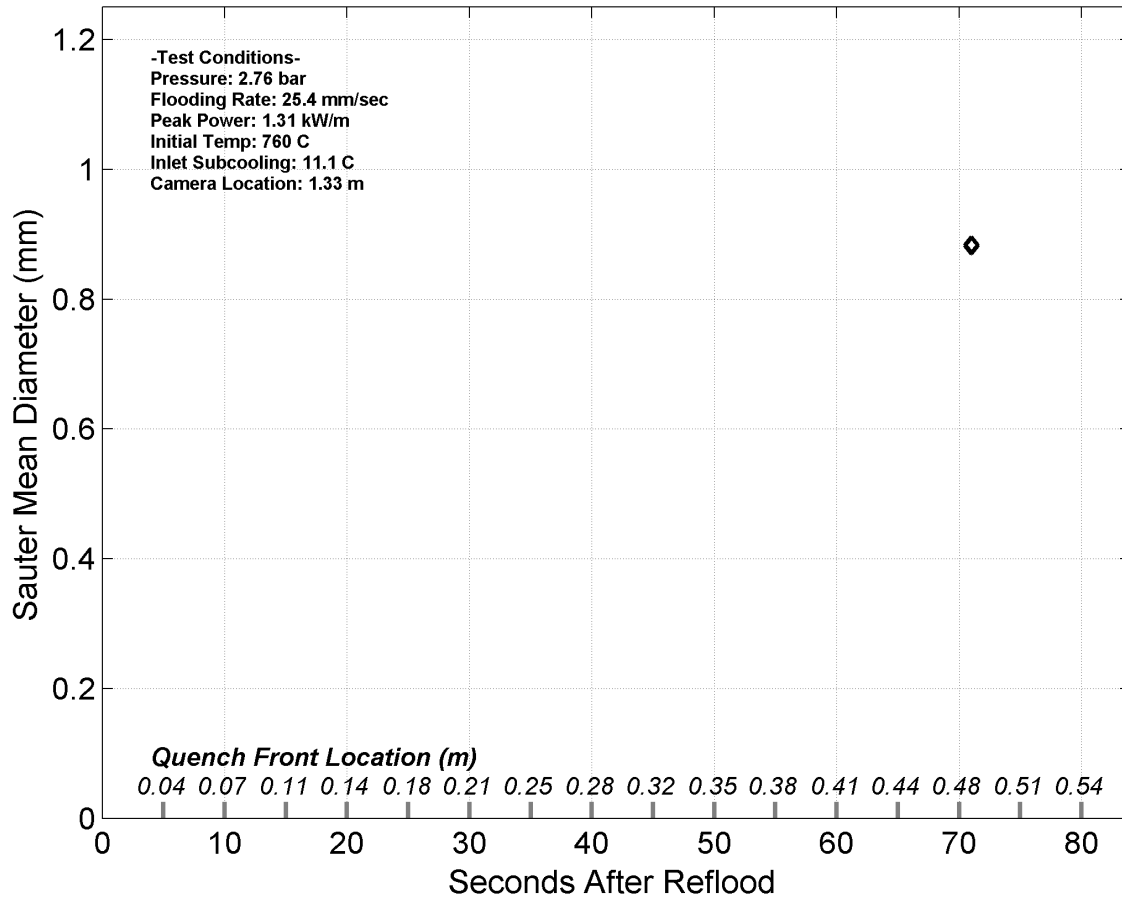
Droplet Counts - Exp. 1402



Mean Droplet Diameter - Exp. 1402



Droplet Sauter Mean Diameter - Exp. 1402



RBHT - REFLOOD TESTS

SUMMARY SHEET

RUN NO: **1407**

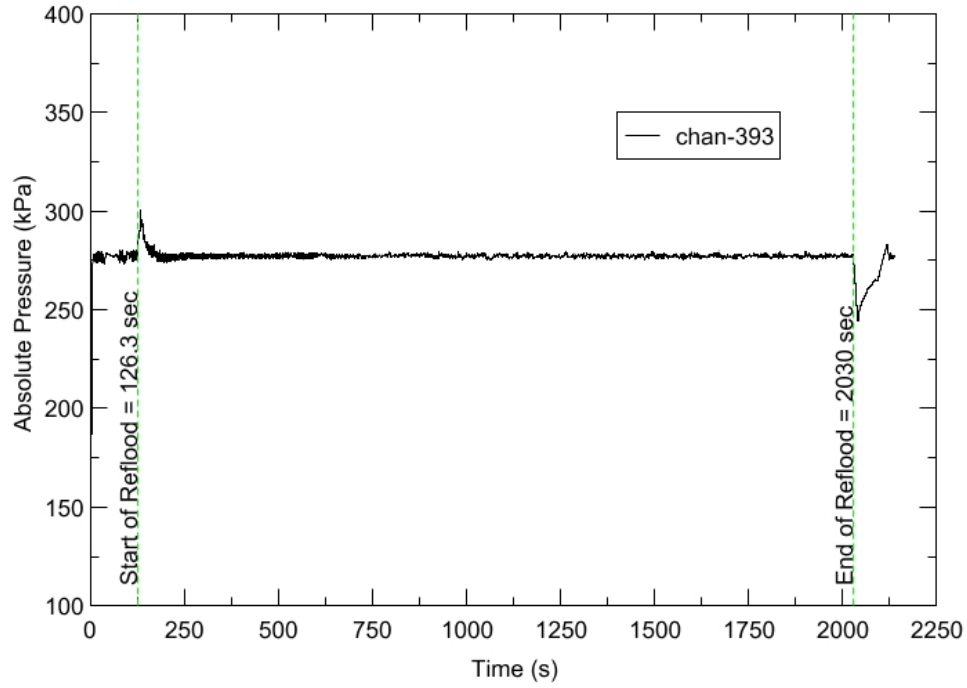
RUN CONDITIONS

Upper Plenum Pressure:	276 kPa (40 psia)
Initial Peak Clad Temperature:	1144 degrees K (1600 degrees F)
Rod Peak Power:	2.3 kW/m (0.7 kW/ft)
Flooding Rate:	0.0762 m/s (3 in/s)
Inlet Subcooling:	23 degrees K (41 degrees F)
Start of Reflood:	126.3 s
End of Reflood:	2030 s
Test Date:	8/29/2002
Comments:	

Rod_Elevation	Channel Number	Temperature at Reflood (K)	Temperature at Reflood (°F)	Turnaround Time (sec.)	Turnaround Temperature (K)	Turnaround Temperature (°F)	Quench Time (sec.)	Quench Temperature (K)	Quench Temperature (°F)
B6 0.592m	148	753.92	897.38	3.95	764.92	917.17	48.95	587.54	597.89
B6 0.744m	149	768.57	923.74	4.45	81.34	946.72	67.95	583.36	590.35
B6 0.846m	150	793.83	969.21	4.45	808.58	995.76	77.45	604.92	629.18
B6 0.897m	151	803.72	987.01	4.45	819.13	1014.74	82.45	609.58	637.56
C6 1.04m	137	847.36	1065.56	5.45	864.84	1097.02	93.95	660.1	728.49
D5 1.27m	217	899.16	1158.79	5.95	918	1192.71	122.95	685.23	773.73
C6 1.34m	138	896.02	1153.15	5.95	916.49	1190	135.45	697.92	796.56
D5 1.37m	218	922.22	1200.31	5.95	942.85	1237.45	138.95	712.93	823.58
C6 1.39m	139	903.17	1166.02	5.95	923.81	1203.16	144.45	704.59	808.57
D5 1.45m	219	937.78	1228.31	5.95	959.13	1266.74	150.95	721.97	839.86
C6 1.47m	140	918.46	1193.54	5.95	940.05	1232.4	157.95	720.38	836.99
D5 1.52m	220	953.24	1256.15	5.95	975.01	1295.34	165.45	742.89	877.52
C6 1.62m	141	947.4	1245.63	16.95	972.32	1290.48	188.95	757.48	903.78
D5 1.68m	221	984.14	1311.76	17.95	1009.6	1357.59	197.95	778.3	941.25
D5 1.78m	222	986.29	1315.63	4.95	1004.39	1348.21	219.95	682.03	767.97
D5 1.85m	223	1014.52	1366.45	5.95	1036.73	1406.43	233.95	762.51	912.84
C6 1.87m	142	999.42	1339.26	5.95	1023.57	1382.74	243.45	767.06	921.02
D5 1.90m	224	1026.67	1388.33	5.45	1049.92	1430.17	245.95	781.44	946.9
C6 1.95m	144	1015.23	1367.72	5.95	1039.76	1411.88	262.95	774.28	934.02
C3 2.17m	178	1044.24	1419.95	5.45	1068.87	1464.28	316.45	727.21	849.3
D4 2.24m	241	1098.38	1517.4	4.95	1121.51	1559.03	355.45	699.42	799.27
D4 2.32m	242	1107.52	1533.85	5.45	1133.4	1580.44	374.95	732.43	858.68
C3 2.35m	180	1102.29	1524.43	5.95	1130.1	1574.49	350.95	794.05	969.6
D4 2.37m	243	1114.68	1546.74	5.45	1141.12	1594.32	388.45	737.76	868.28
C3 2.40m	181	1105.27	1529.79	5.45	1132.96	1579.65	362.45	807.57	993.94
D4 2.54m	245	1141.2	1594.47	4.95	1165.63	1638.45	441.95	726.92	848.78
D6 2.62m	129	1130.07	1574.44	4.95	1155.36	1619.95	434.45	758.32	905.29
D6 2.69m	130	1121.06	1558.21	5.45	1147.57	1605.94	450.95	769.65	925.68
C3 2.76m	183	1118.56	1553.73	5.45	1145.42	1602.08	451.95	796.1	973.29
D4 2.79m	247	1089.99	1502.29	4.45	1115.22	1547.7	501.95	698.54	797.69
D6 2.87m	131	1061.16	1450.39	4.45	1083.88	1491.3	483.45	716.01	829.13
D6 2.92m	132	1039.46	1411.35	5.95	1067.87	1462.47	492.95	738.46	869.53
D6 2.97m	133	1021.06	1378.21	5.95	1048.24	1427.15	503.95	723.4	842.43
D6 3.07m	134	995.41	1332.05	5.95	1020.72	1377.61	516.95	710.01	818.33
E3 3.12m	197	997.13	1335.14	5.45	1022.53	1380.86	538.95	714.07	825.65
D6 3.17m	135	958.98	1266.48	5.95	983.4	1310.44	530.45	691.84	785.63
D6 3.27m	136	905.56	1170.33	5.95	930.12	1214.53	541.95	684.99	773.29
D4 3.61m	248	690.79	783.74	5.95	720.06	836.41	602.95	578.68	581.93

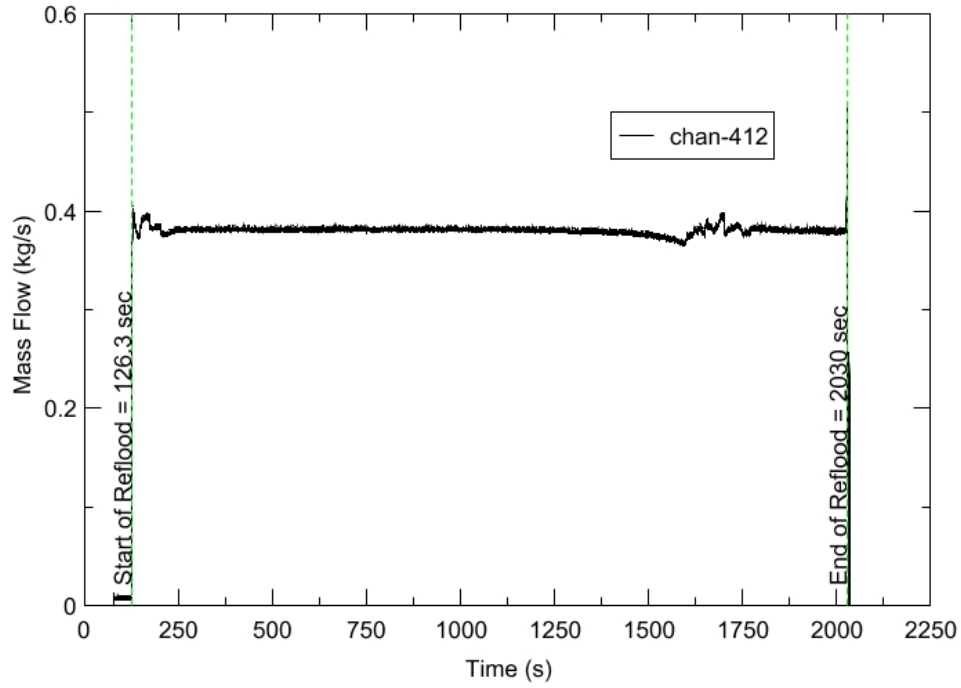
RBHT - TEST FACILITY

Upper Plenum Pressure vs. Time, Exp 1407



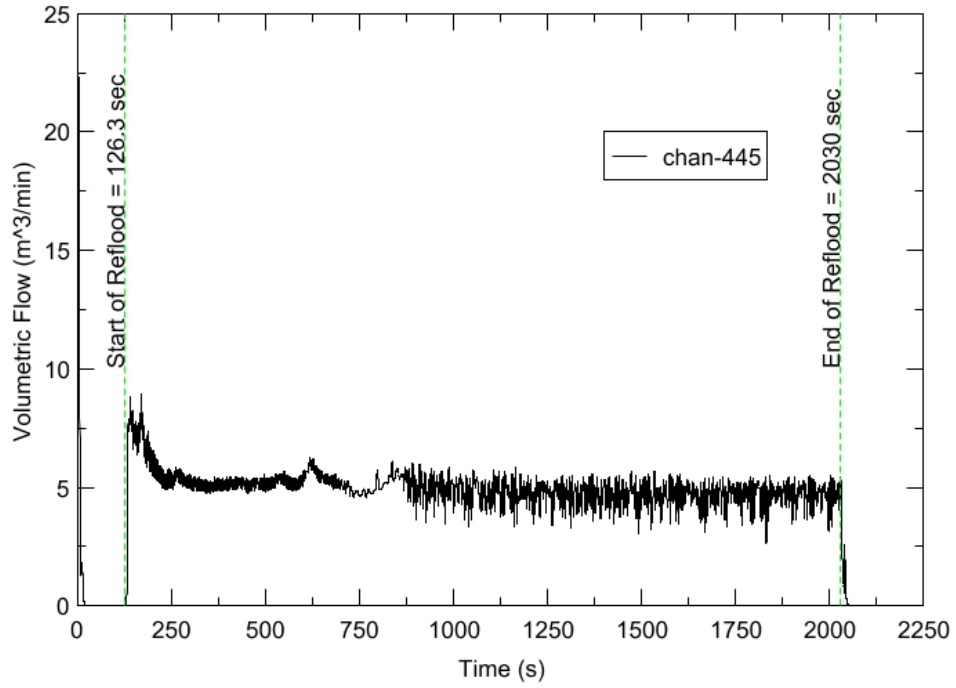
RBHT - TEST FACILITY

Inlet Flow vs. Time, Exp 1407



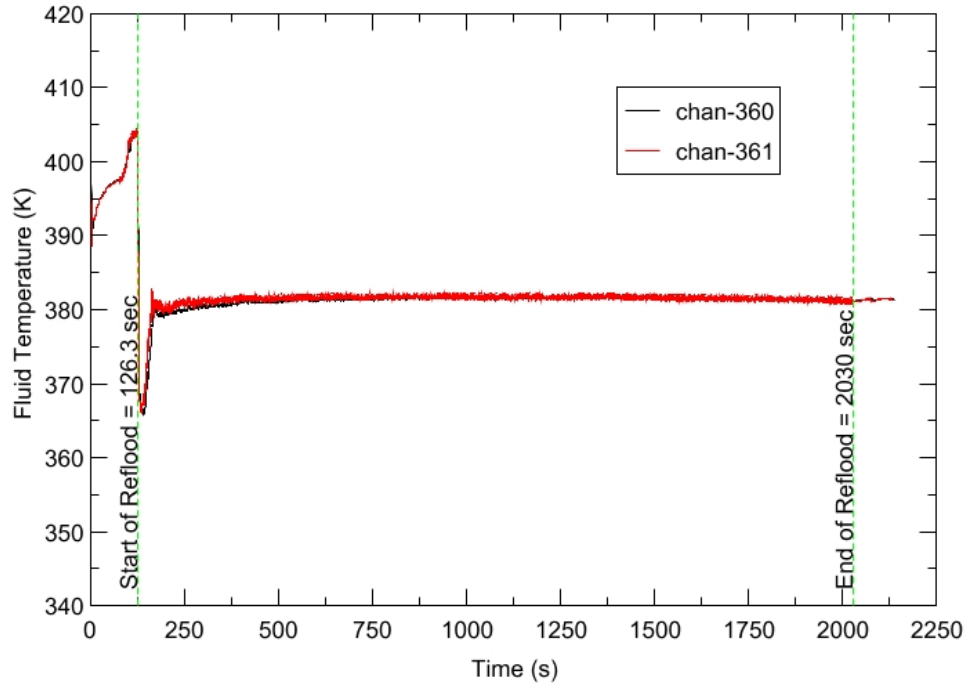
RBHT - TEST FACILITY

Steam Exhaust Flow vs. Time, Exp 1407



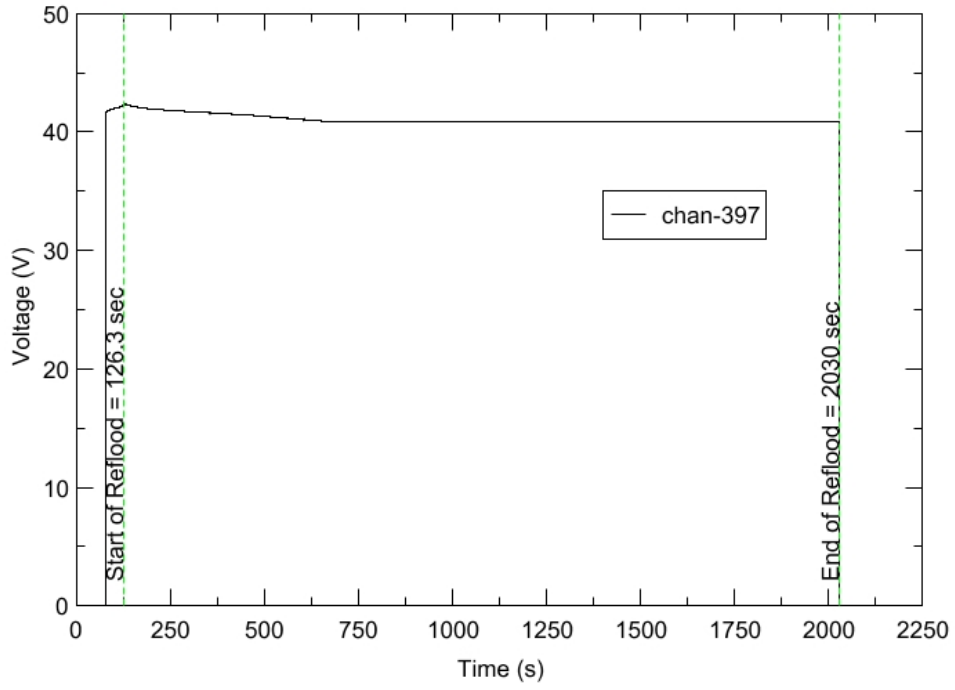
RBHT - TEST FACILITY

Inlet Flow Temperature vs. Time, Exp 1407



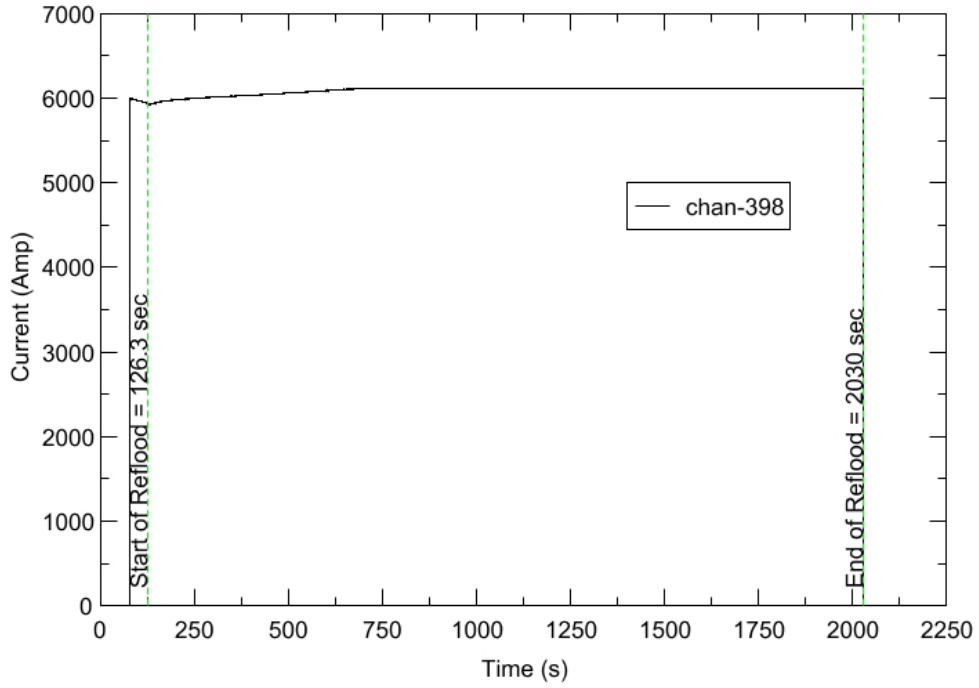
RBHT - TEST FACILITY

Test Section Voltage vs. Time, Exp 1407

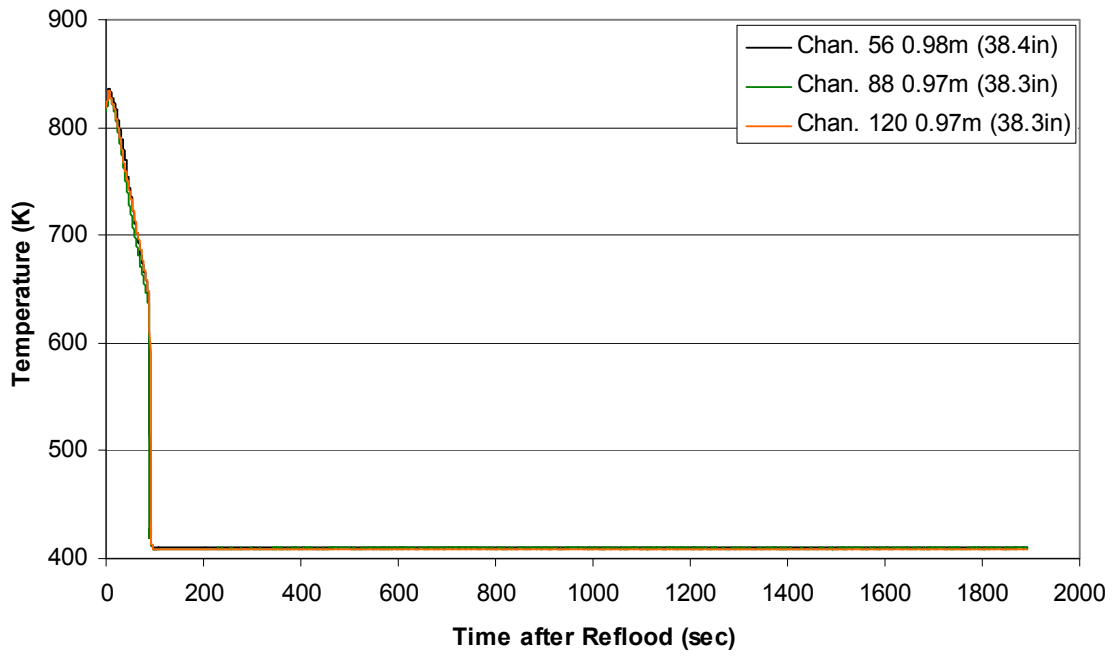


RBHT - TEST FACILITY

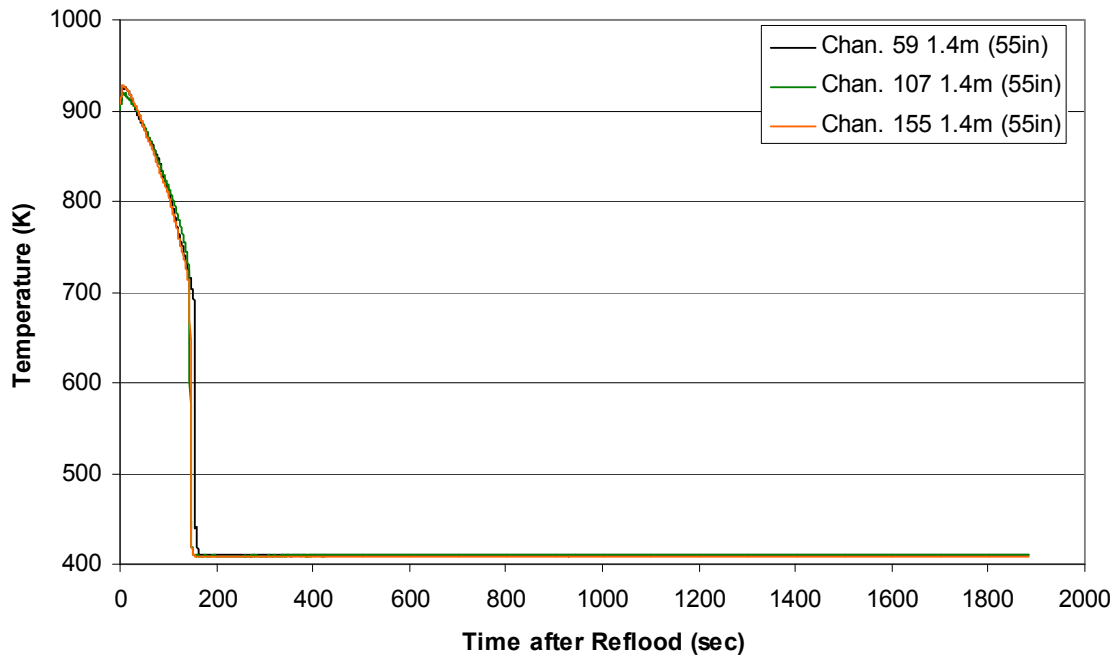
Test Section Current vs. Time, Exp 1407



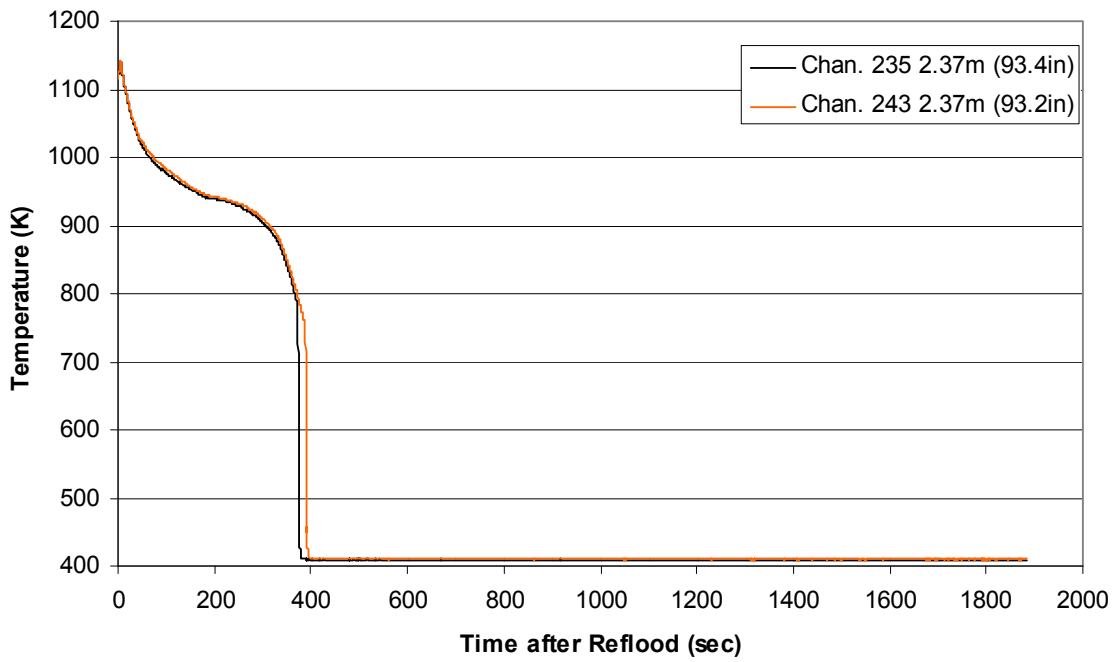
Heater Rod Temperature during Reflood RBHT Exp. 1407



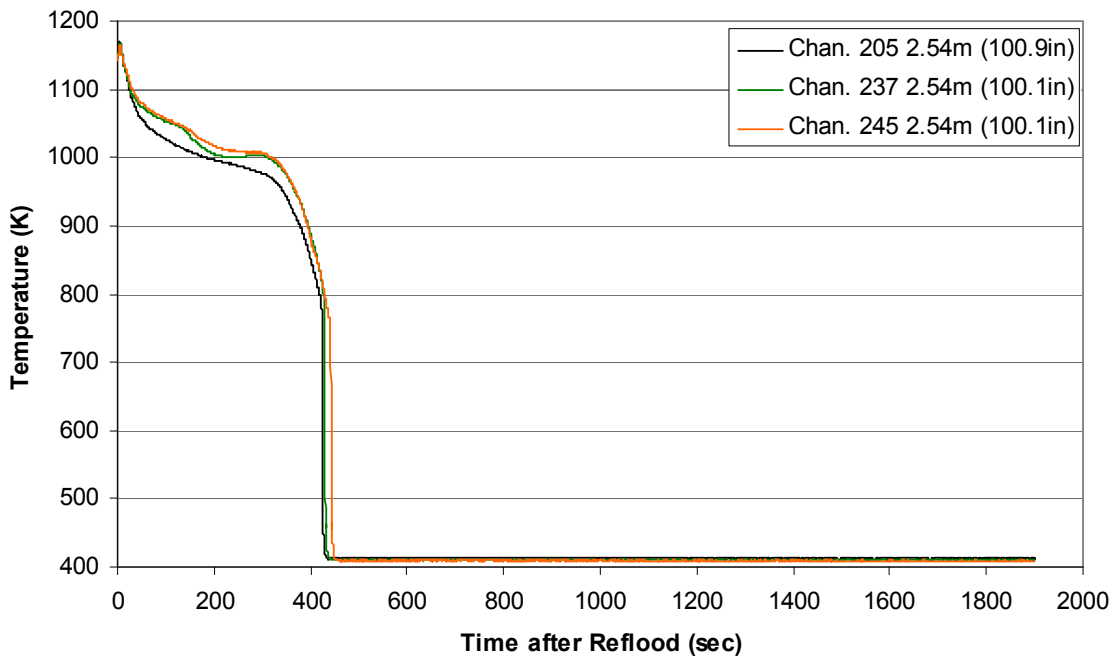
Heater Rod Temperature during Reflood RBHT Exp. 1407



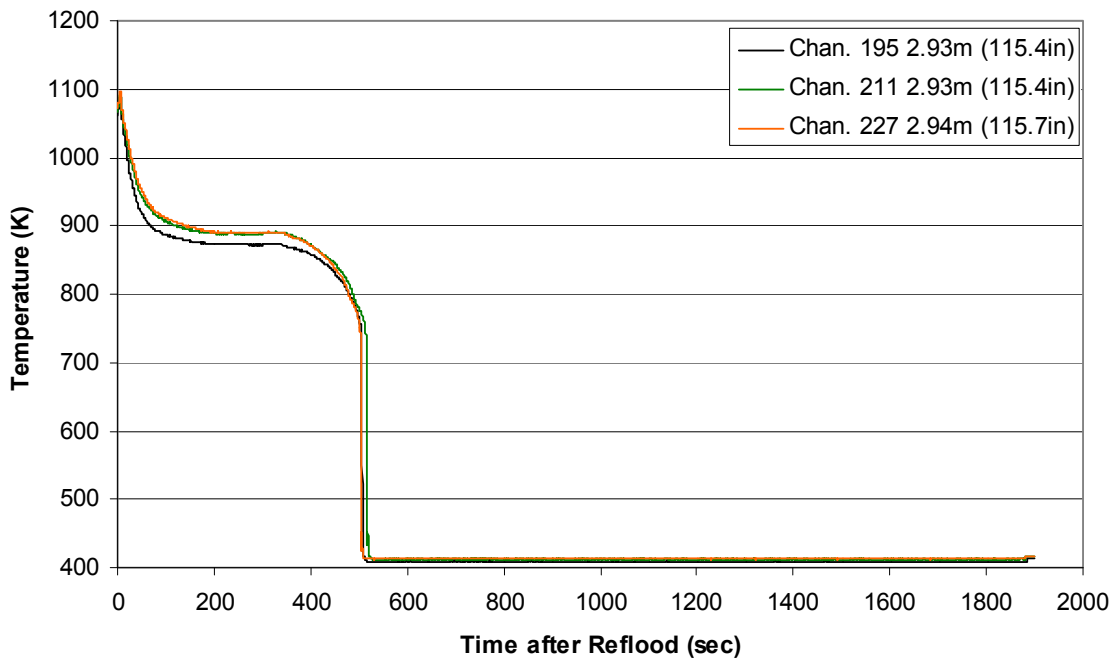
**Heater Rod Temperature during Reflood
RBHT Exp. 1407**



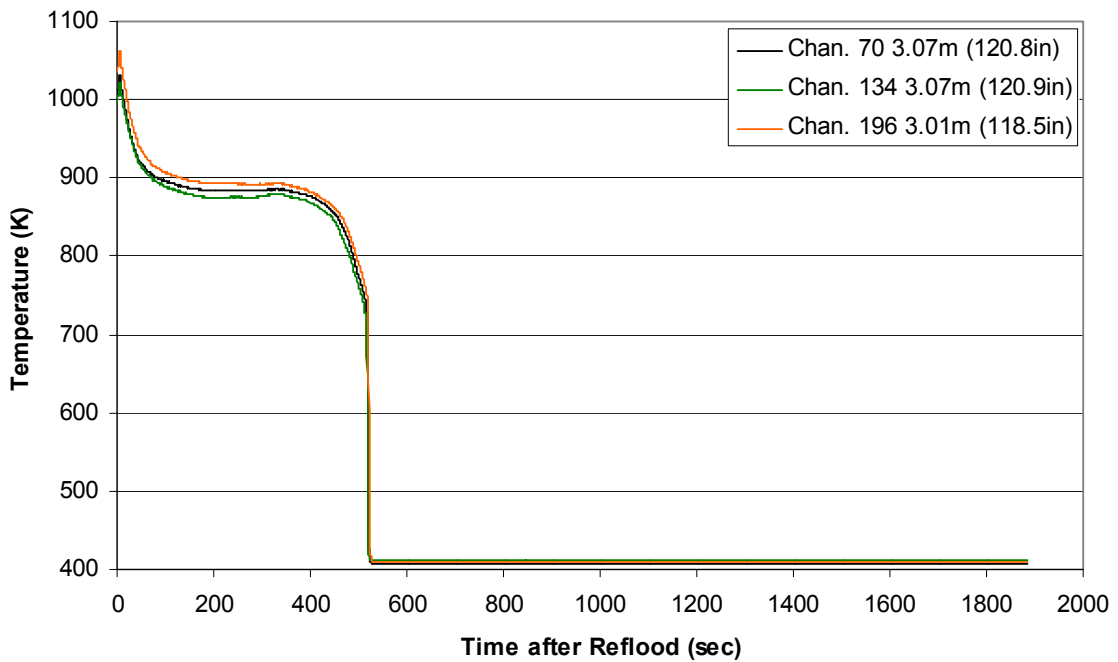
**Heater Rod Temperature during Reflood
RBHT Exp. 1407**



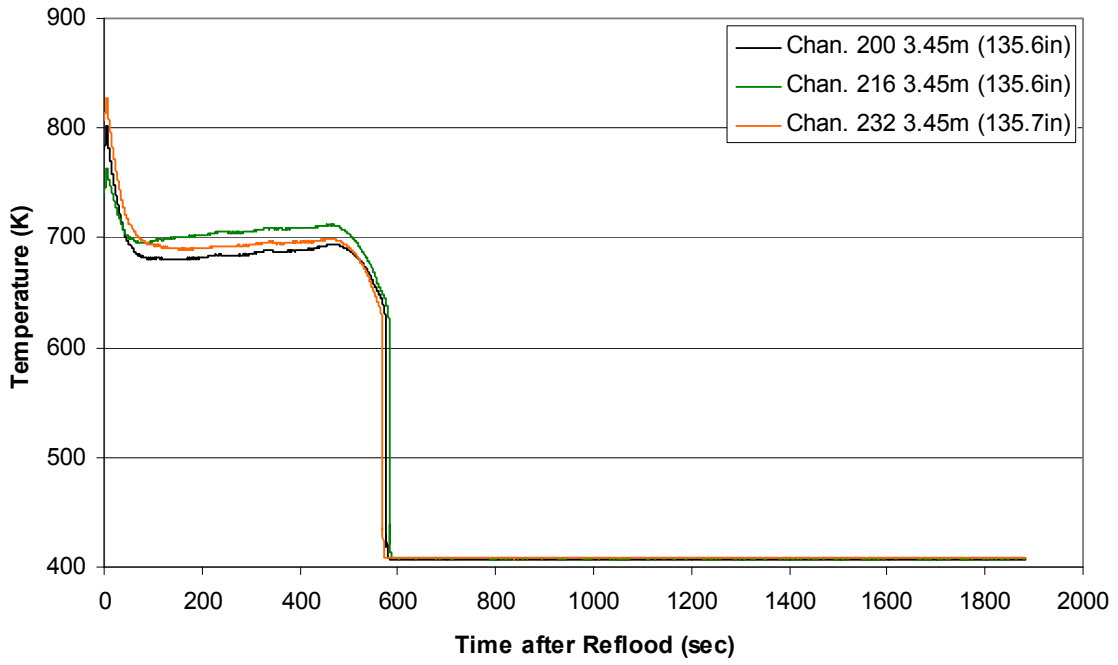
Heater Rod Temperature during Reflood
RBHT Exp. 1407



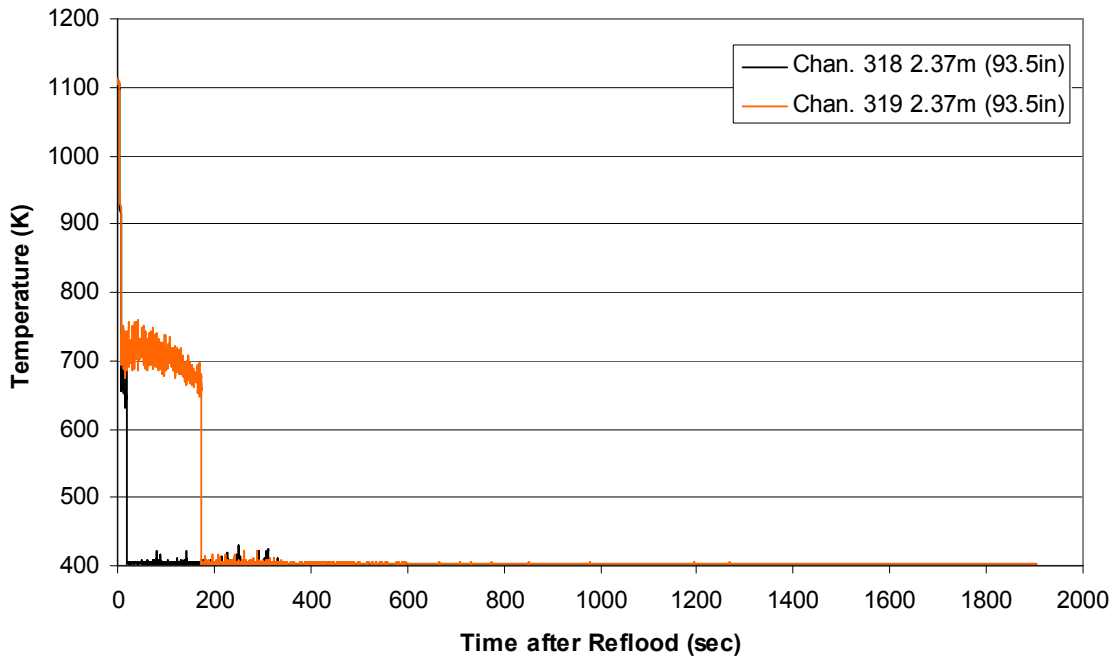
Heater Rod Temperature during Reflood
RBHT Exp. 1407



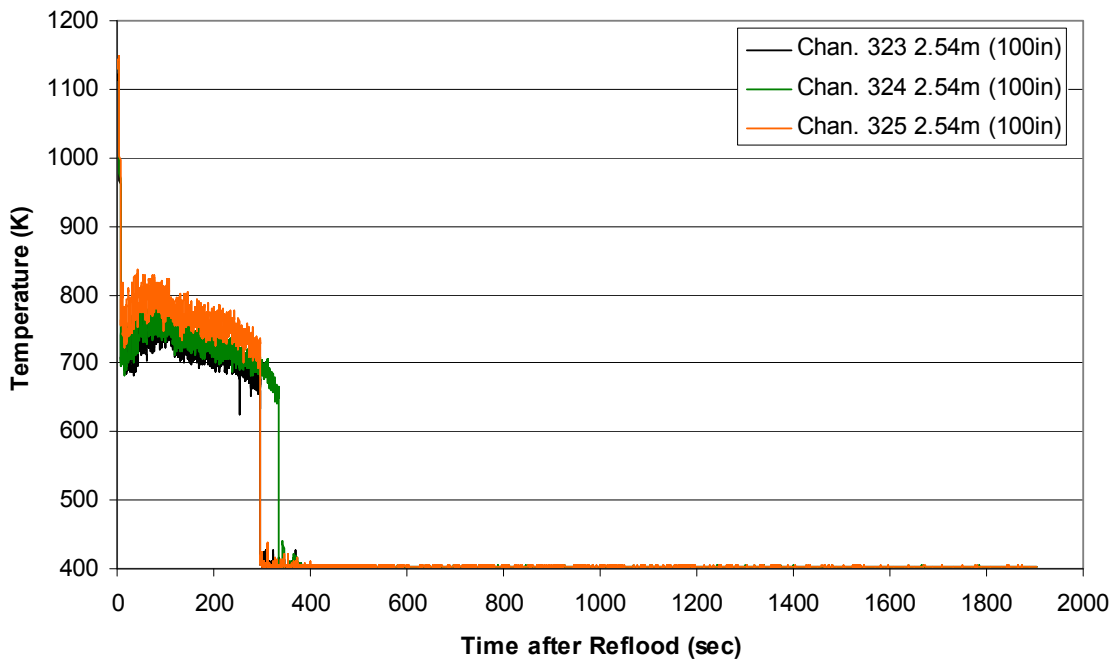
Heater Rod Temperature during Reflood RBHT Exp. 1407



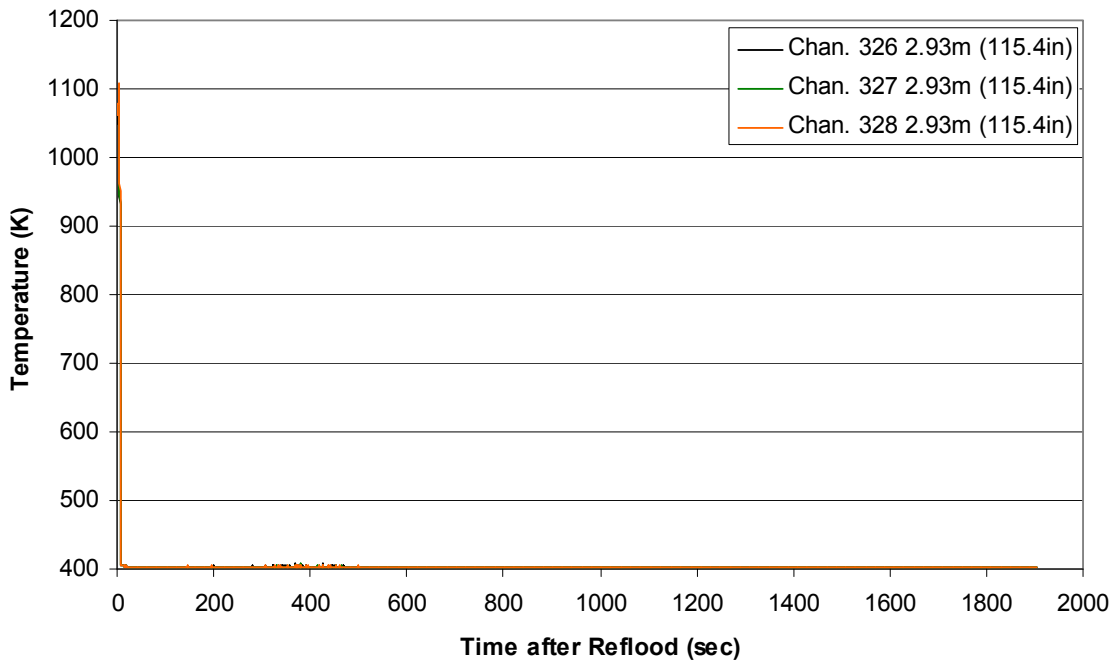
Steam Probe Temperature during Reflood RBHT Exp. 1407



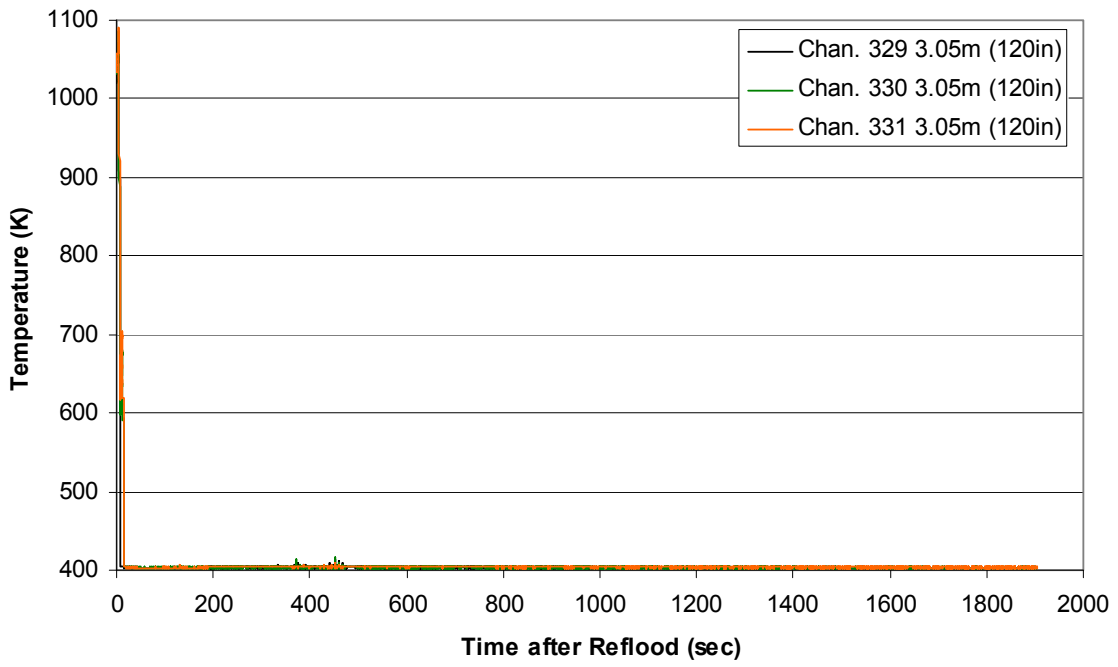
Steam Probe Temperature during Reflood RBHT Exp. 1407



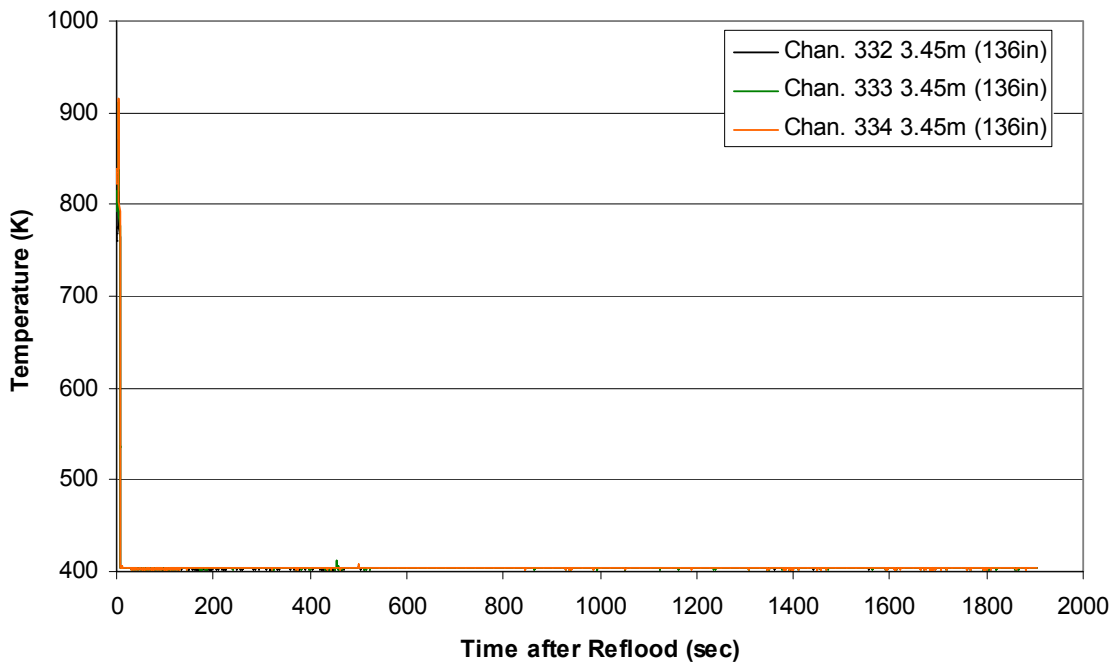
Steam Probe Temperature during Reflood RBHT Exp. 1407



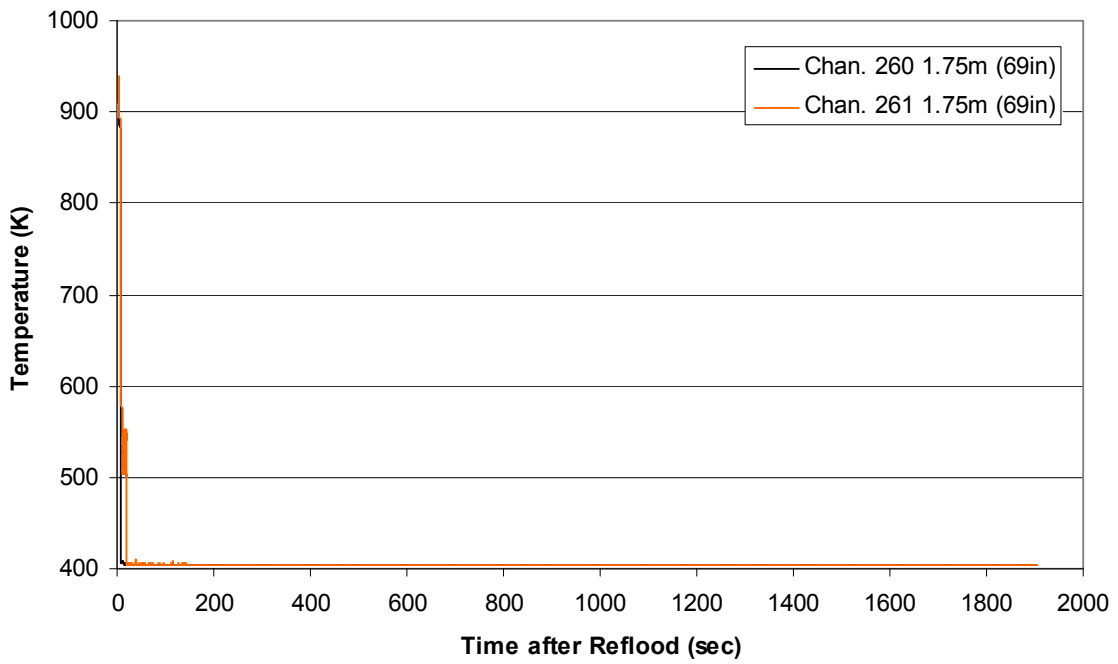
Steam Probe Temperature during Reflood RBHT Exp. 1407



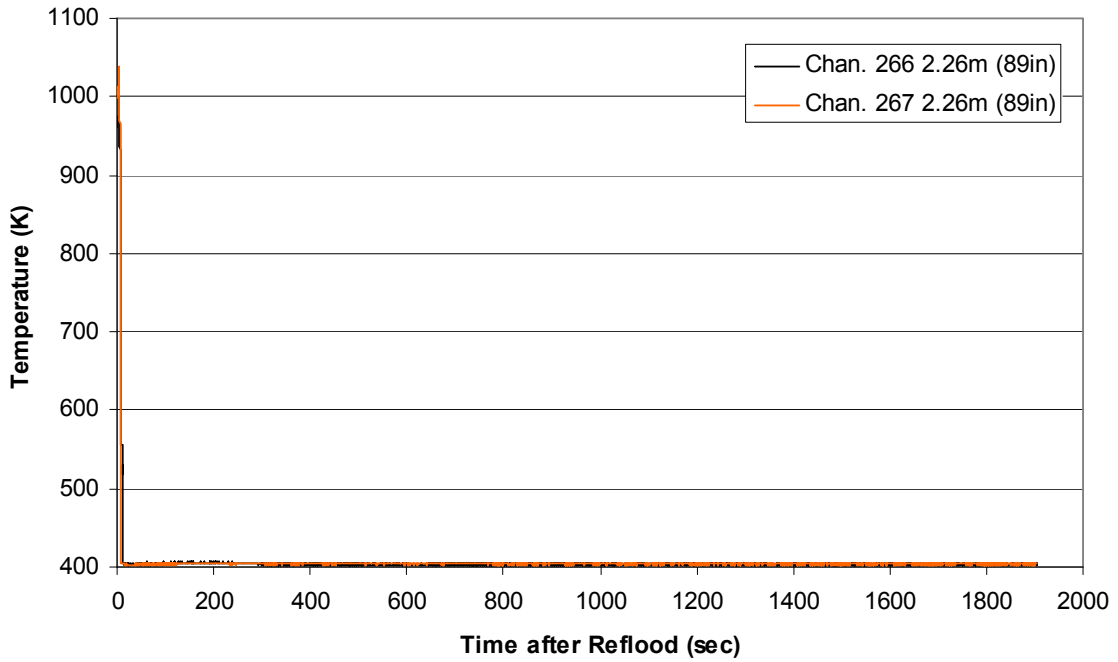
Steam Probe Temperature during Reflood RBHT Exp. 1407



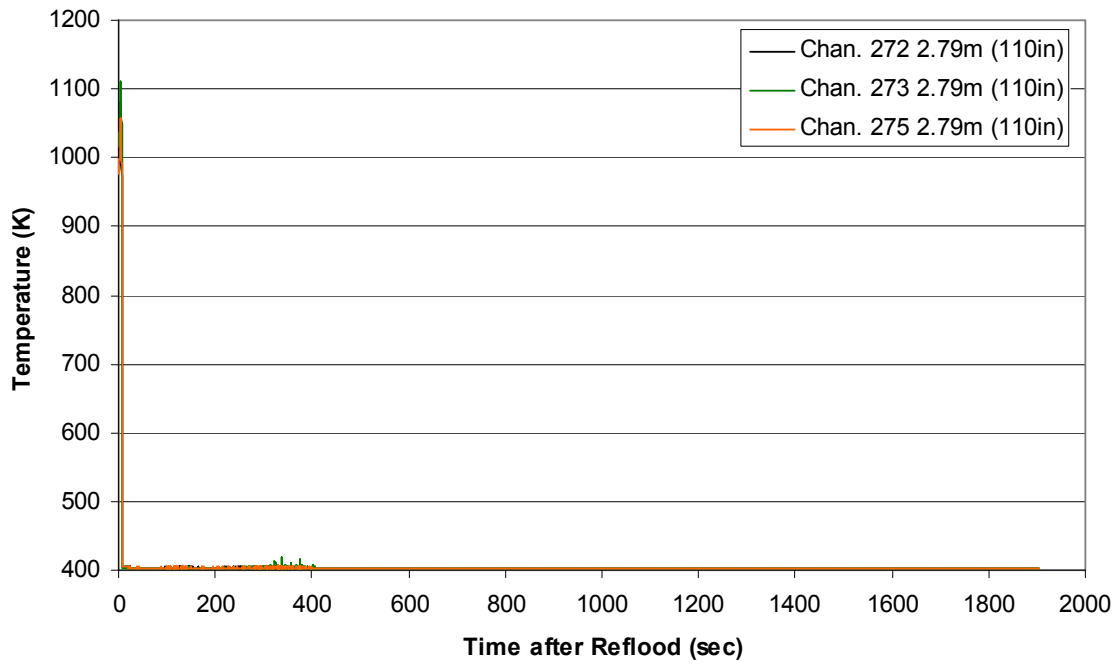
Spacer Grid Temperature during Reflood RBHT Exp. 1407



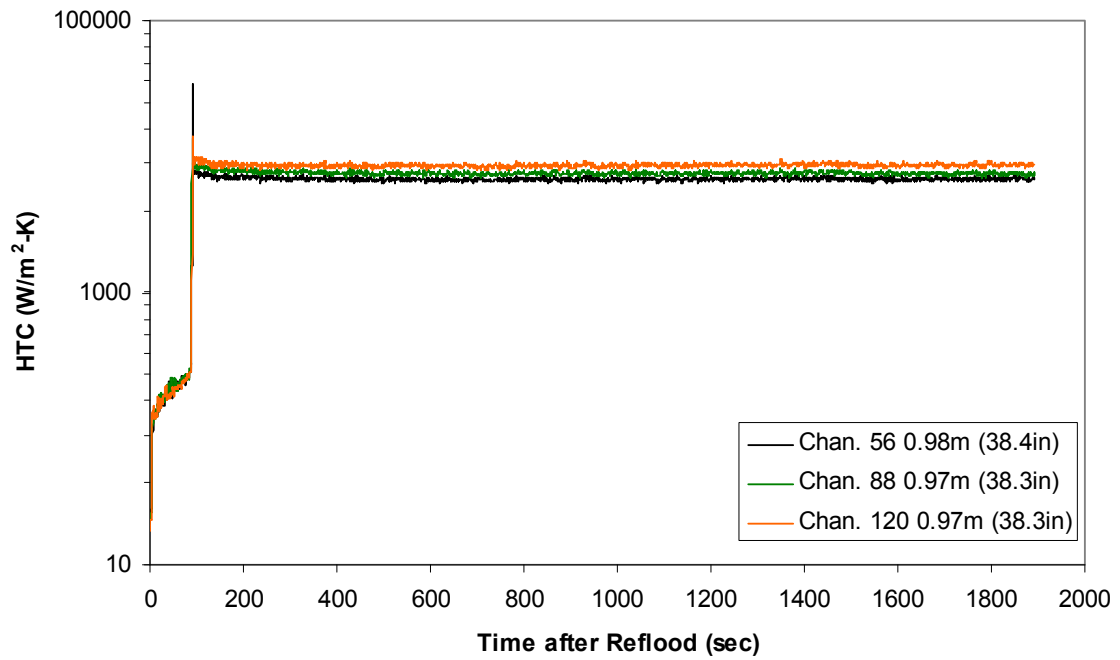
Spacer Grid Temperature during Reflood RBHT Exp. 1407



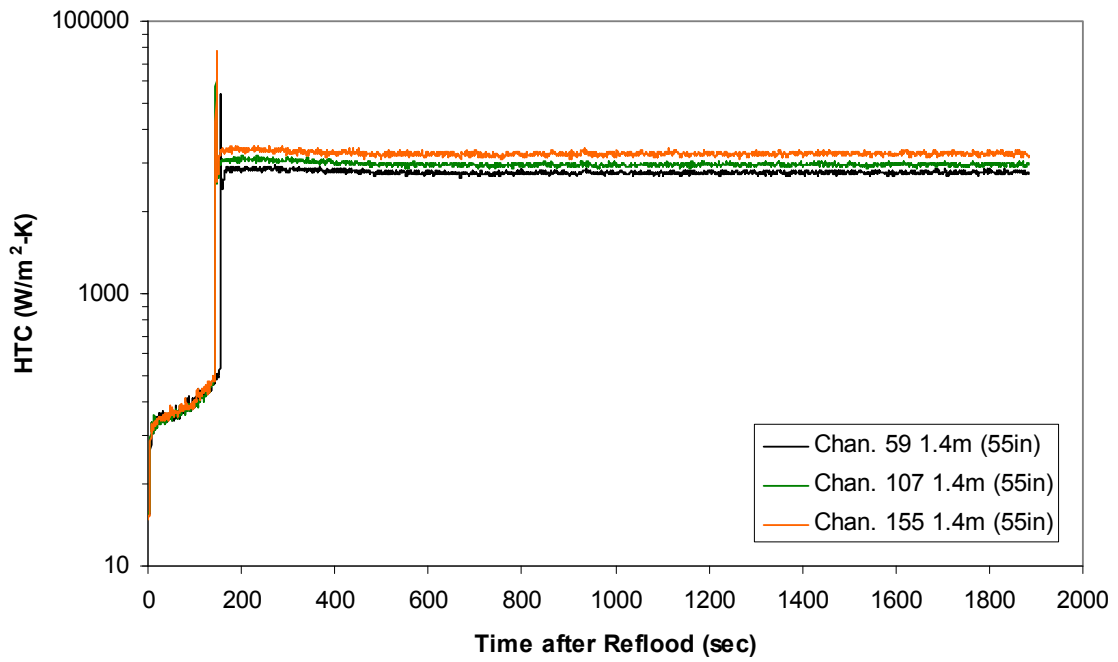
Spacer Grid Temperature during Reflood RBHT Exp. 1407



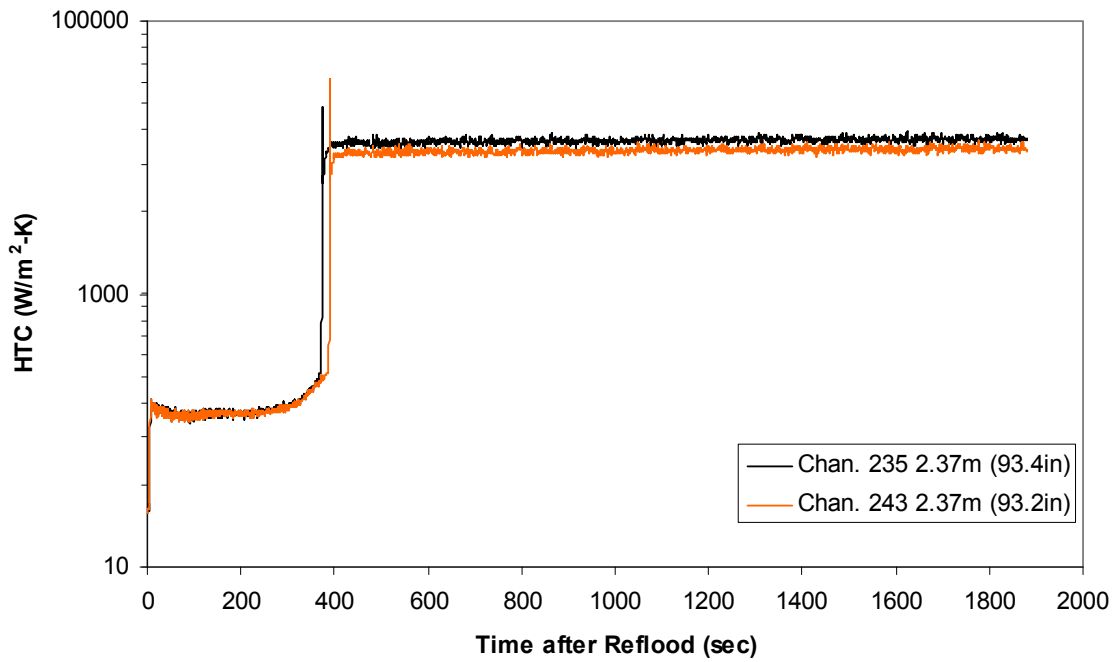
Heat Transfer Coefficient during Reflood RBHT Exp. 1407



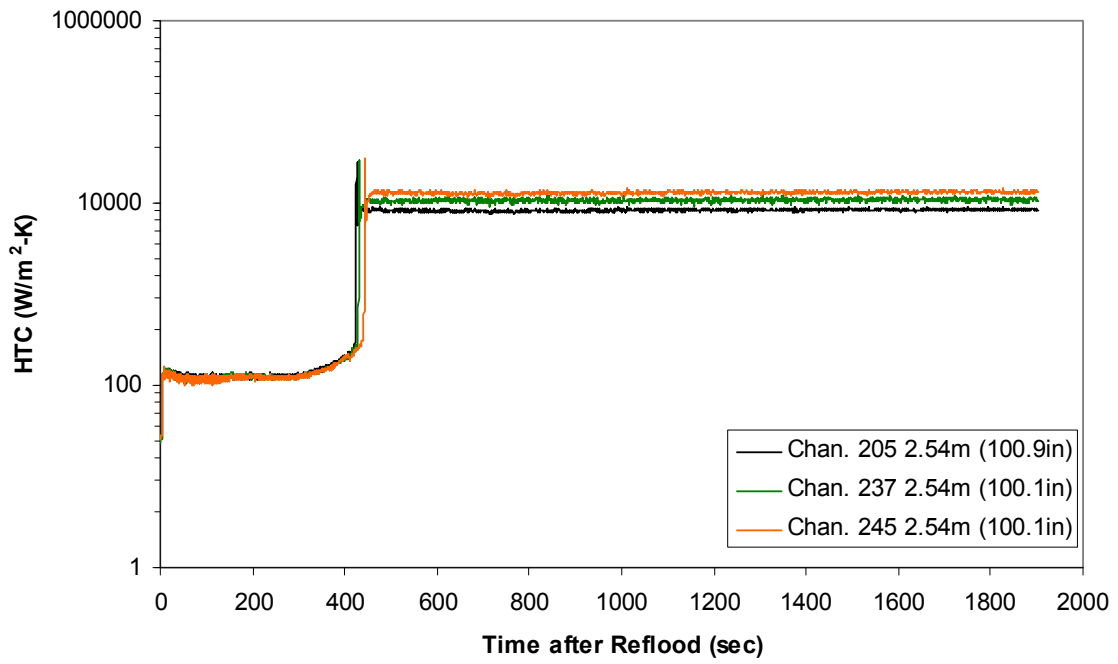
Heat Transfer Coefficient during Reflood
RBHT Exp. 1407



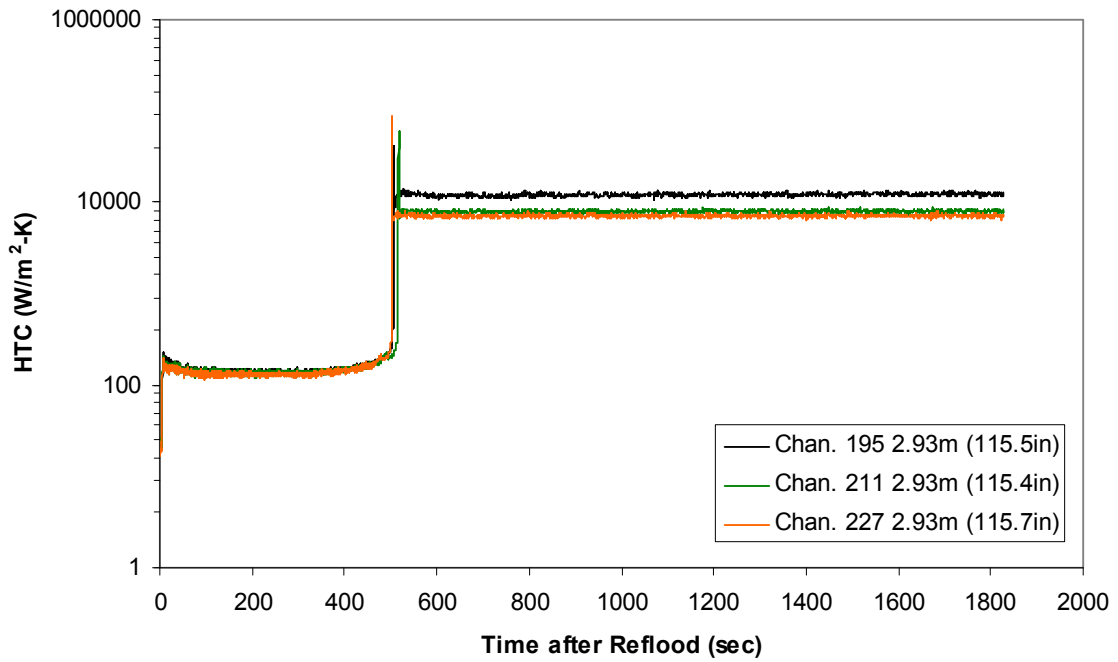
Heat Transfer Coefficient during Reflood
RBHT Exp. 1407



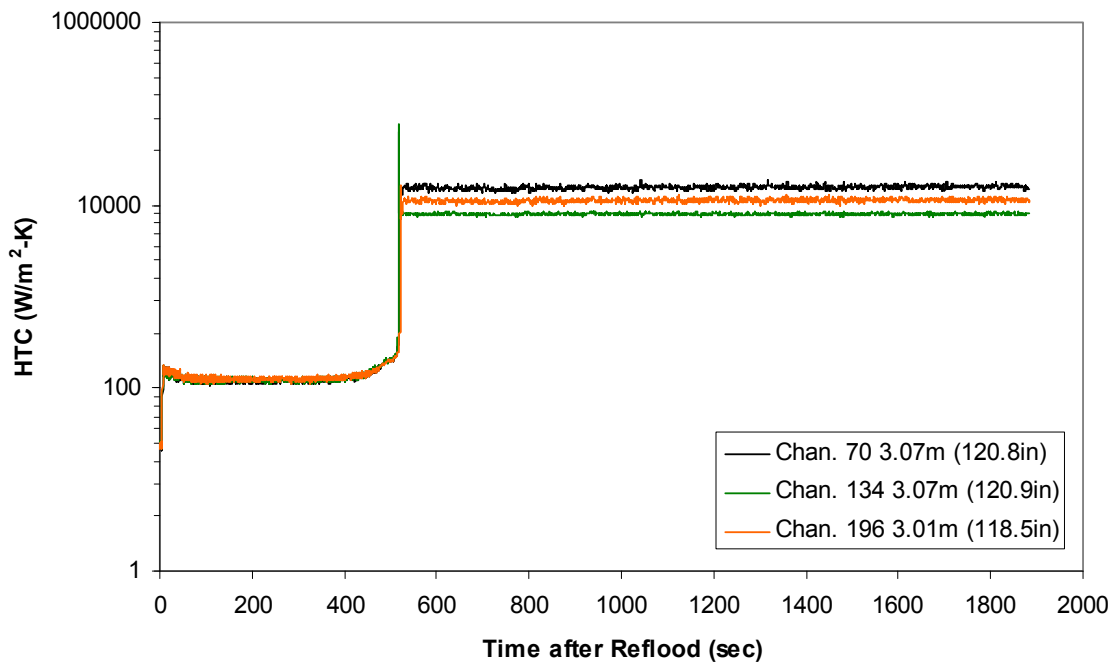
Heat Transfer Coefficient during Reflood RBHT Exp. 1407



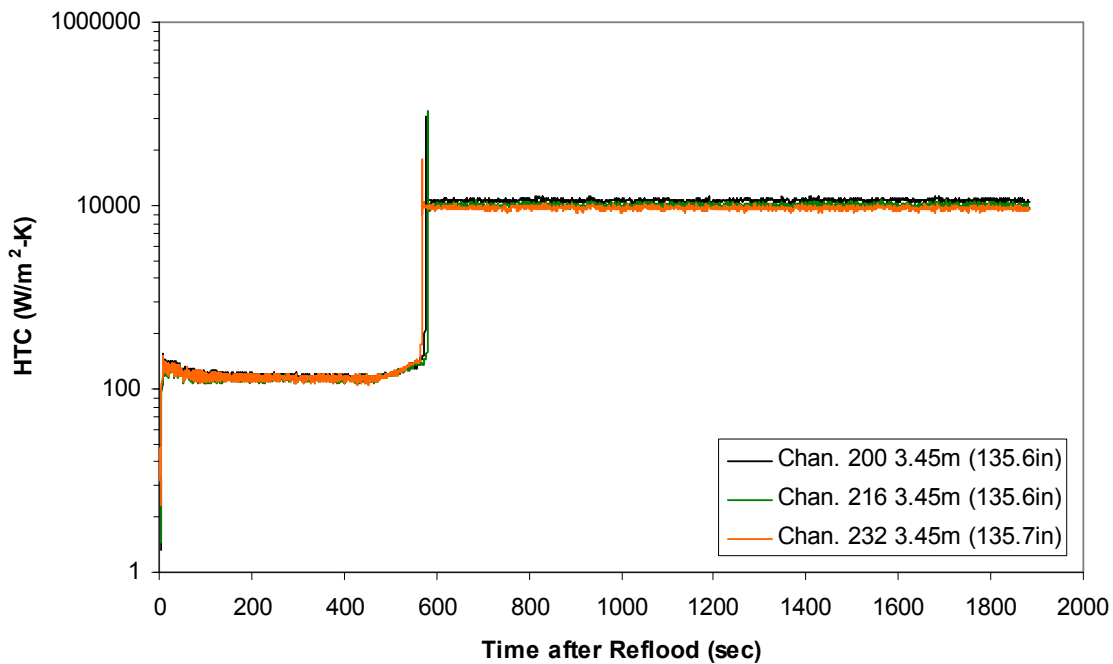
Heat Transfer Coefficient during Reflood RBHT Exp. 1407



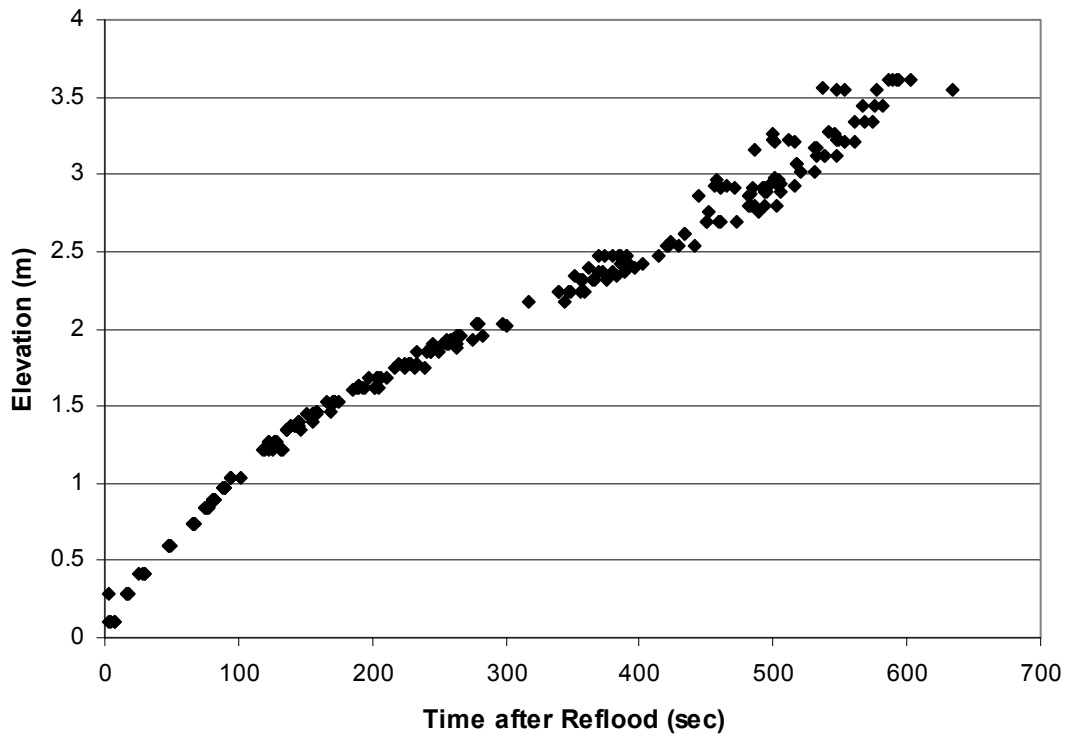
Heat Transfer Coefficient during Reflood
RBHT Exp. 1407



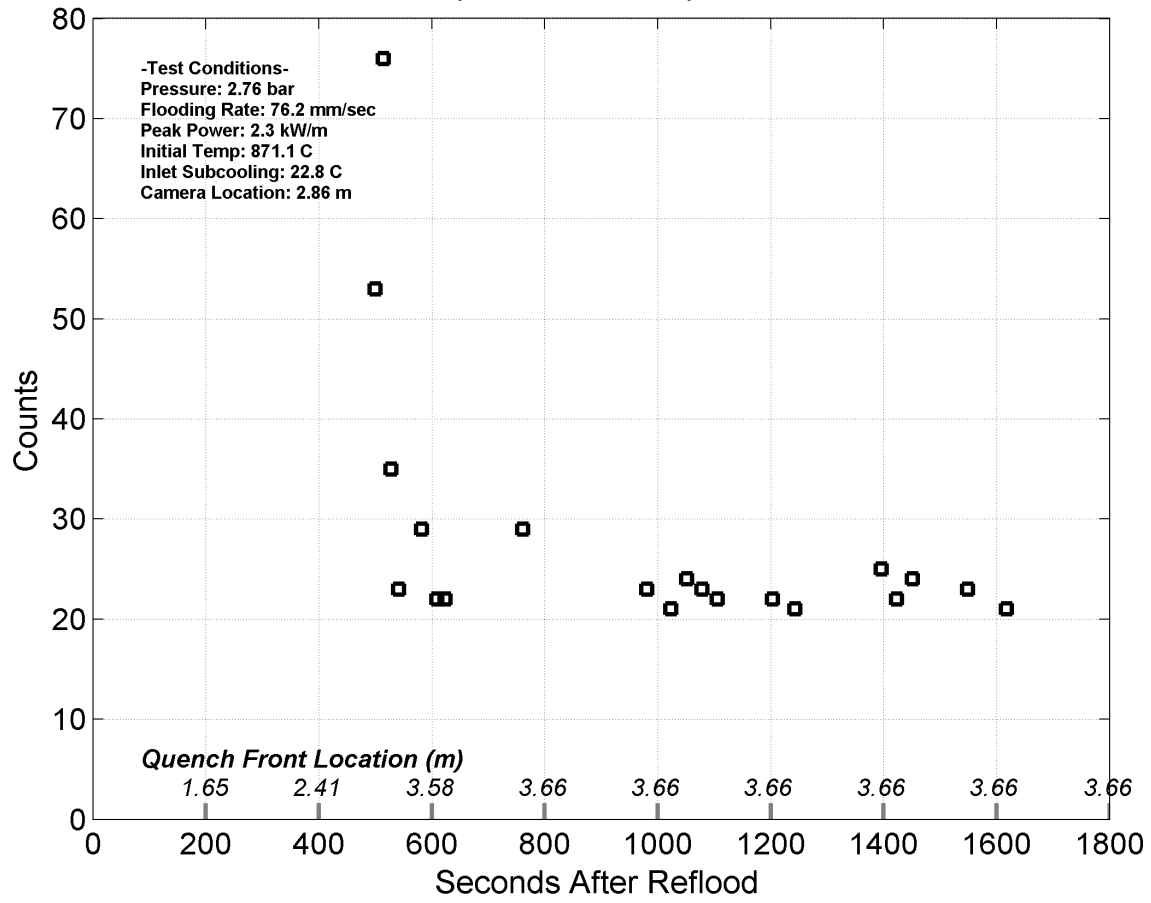
Heat Transfer Coefficient during Reflood
RBHT Exp. 1407



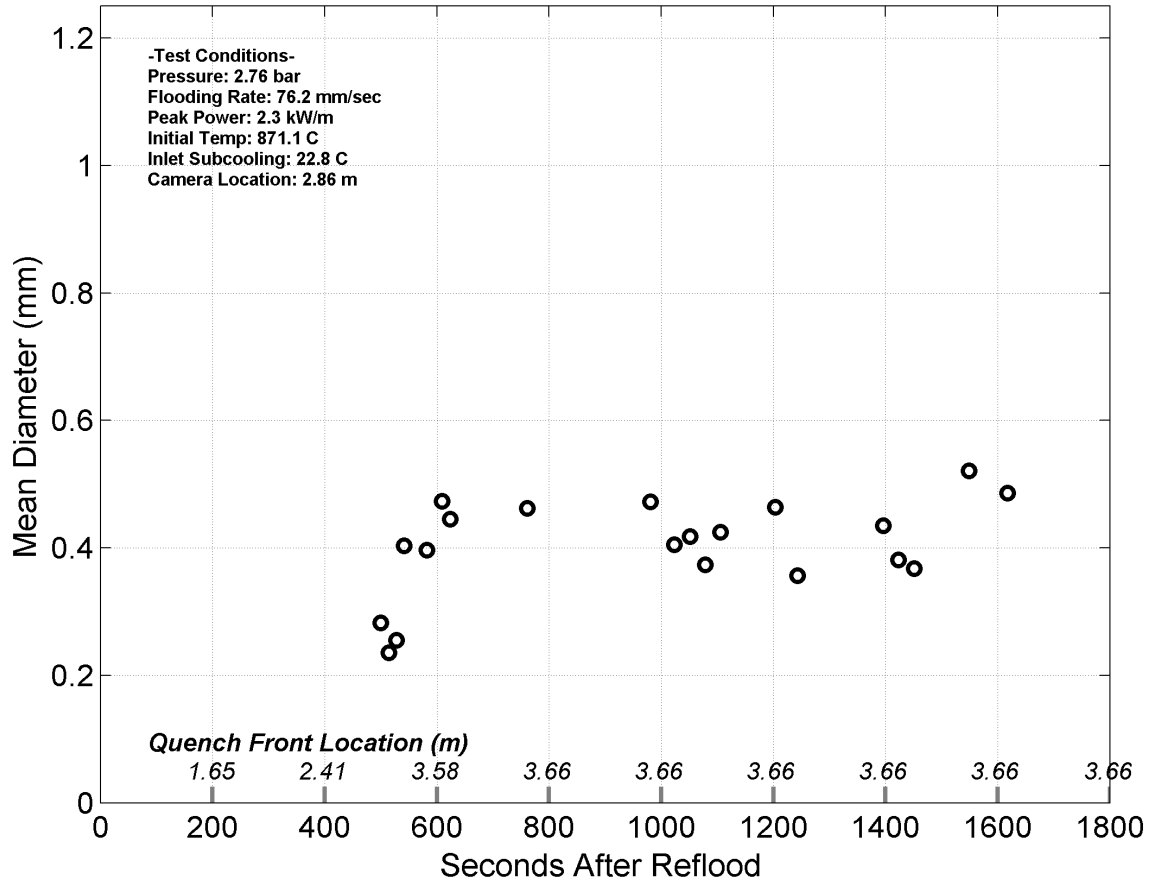
Quench Data, RBHT Exp. 1407



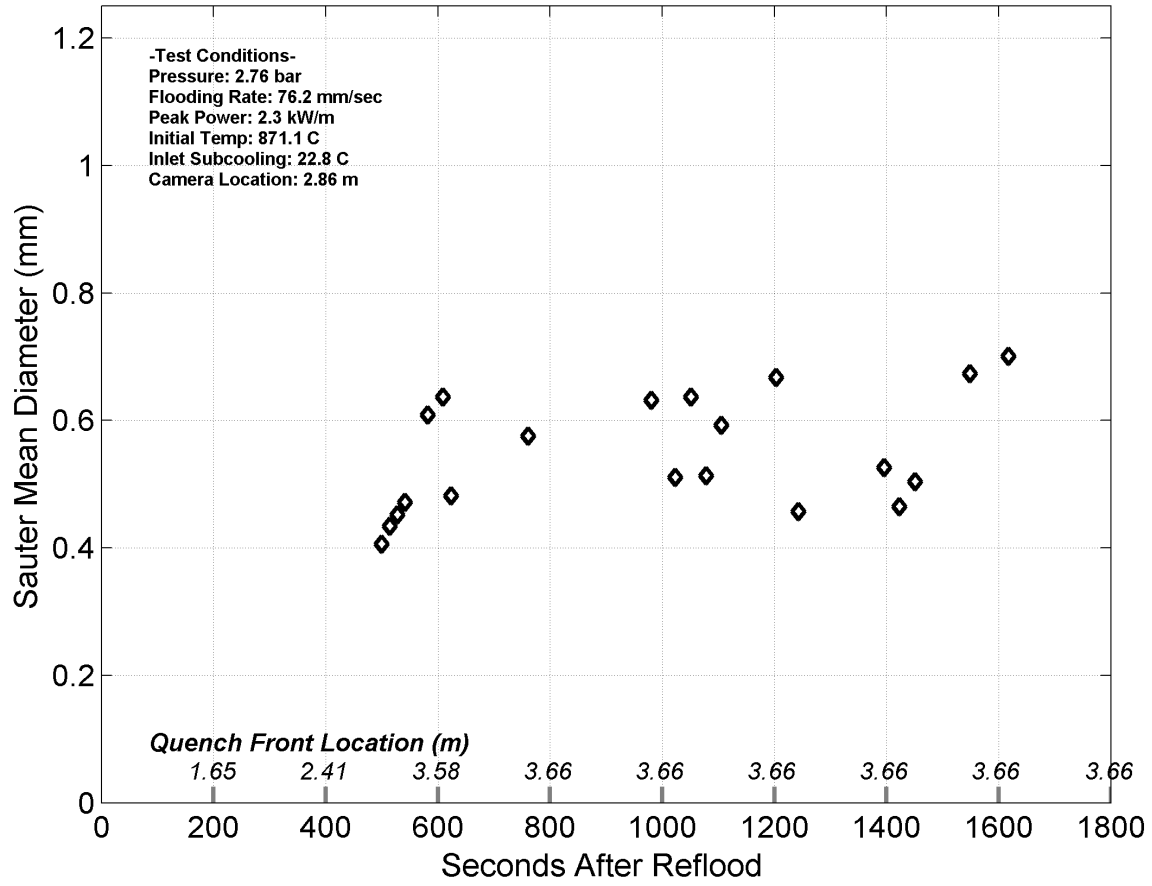
Droplet Counts - Exp. 1407



Mean Droplet Diameter - Exp. 1407



Droplet Sauter Mean Diameter - Exp. 1407



APPENDIX B. UNCERTAINTIES

This appendix describes the measurement errors in the calculations performed for the analysis. The first section contains the error analysis for temperature, pressure and flow measurements. The second section describes the uncertainty analysis for the heat transfer coefficient calculations.

B.1 Measurement Errors

The instrumentation error associated with the data from RBHT test series can be derived either from equipment manufacturers' specifications or system calibration data. Component calibrations are performed to verify that the manufacturers' specifications are met, and these manufacturers' specifications are used to compute the error estimate for the data path. System calibrations are performed when component calibrations are not expedient or when an accuracy improvement could be accomplished with a system calibration. The system calibration data are used to compute an estimate of error for the system response, and calibration data points. The total system error from a system calibration is a function of both system response error and calibration data error.

In all cases of error estimate, the standard deviation has been computed and presented as the most probable error. The manufacturer-specified error is the maximum possible error. The standard deviation error is calculated from the maximum error by the following:

$$\rho^2 = \sum_{i=1}^n \left(\frac{E_i^2}{n} \right) \quad (\text{B-1})$$

where

ρ^2 data path standard deviation

E_i^2 component i maximum error

n number of sources of error

When a system calibration is performed, the standard deviation from the calibration data and that from the calibration equipment can be combined by the following equation to produce the best estimate of error:

$$\rho = \sqrt{E_d^2 + E_c^2} \quad (\text{B-2})$$

where

E_d calibration data standard deviation

E_c calibration equipment standard deviation

The calibration data standard deviation is a measure of the error involved in fitting the calibration data. That is,

$$E_d = \left[\frac{\sum_{i=1}^n (Y_i - Y_f)^2}{n} \right]^{1/2} \quad (\text{B-3})$$

where

Y_i calibration point
 Y_f predicted output from the calibrations curve
 n number of calibration points

The calibration equipment standard deviation is a measure of the absolute error of the calibration point. If the calibration point in the above equation is calculated from an equation of the form

$$Y = x_1 \cdot x_2 \cdot x_3 \quad (\text{B-4})$$

then

$$\left(\frac{\sigma_y}{y} \right)^2 = \sum_{i=1}^n \left(\frac{\sigma_{x_i}}{x} \right)^2 \quad (\text{B-5})$$

and

$$E_c = \sqrt{\sigma_y^2} \quad (\text{B-6})$$

The data path has been broken down into three parts called sensor, conditioner, and readout. The sensor is the device whose electrical output is proportional to a physical quantity (temperature, pressure, flow, power). The conditioner is a device which matches the electrical output of the sensor to the input requirements of the readout device. The readout device measures and records the electrical value of the signal from the conditioner. This recorded electrical value is subsequently used to compute the physical quantity it represents. The errors due to the transmission wire errors are very small (± 0.001 percent) in comparison to the element errors and are considered negligible.

The error values for sensor, conditioning, and readout are the manufacturers' specifications in engineering units. These numbers are used to compute the most probable error, as previously described. Where systems calibrations are performed, the equipment calibration data provide the standard deviation and maximum error as computed from the calibration data points in fitting the points to a first-order polynomial. The calibration point standard deviation is computed using the method described above. The calibration point maximum error occurs simultaneously in each component of the calibration equation. The overall system standard deviation may then be calculated using Equation (B-2).

The calculated Total Probable Errors using Equation (B-2) for each instrumentation channel are shown in the following tables:

- Table B.1 Temperature measurements including the heater rods, grid fluid, grid walls, support rods, steam probe rakes, flow housing walls, flow housing insulation, vessel and piping walls, and quartz windows thermocouples.
- Table B.2 Differential pressure cells (DP's), static pressure transducers (P's), and vessels liquid level transducers.
- Table B.3 Inlet Mass and exhaust steam flow transmitters (FM).
- Table B.4 Steam probe rakes linear position transmitter.
- Table B.5 Heater Rod Bundle input voltage (V), amperage (Amps), and Power (W) measurements.

Table B.1 Error in Temperature Measurement

CHANNEL NO.	INPUT SENSOR	RANGE	INSTRUMENT		DATA ACQUISITION SYSTEM					
			ERROR ± 1.11°C	± °C	SCP	AUTO- RANGING ± 0.02% TEMPERATURE RE RANGE	REF JCTN MEAS	ISO REF GRADIENT	TEMP RANGE FOR ERROR NUMBERS	
	TYPE K TC	°C	± °C	± °C	± °C	± °C	± °C	± °C	± °C	°C
1-96, 98-183, 185-248, 311-313	HEATER ROD'S	10 - 1371 °C	1.11	± °C	0.20	0.08	0.01	0.20	0.20	0 TO 375
249-276, 278-279	GRID WALL & FLUID	10 - 1371 °C	1.11	± °C	0.25	0.16	0.01	0.20	0.20	375 TO 800
					0.40	0.27	0.01	0.20	0.20	800 TO 1371
280 THRU 295	SUPPORT RODS	10 - 1371 °C	1.11	± °C	0.20	0.08	0.01	0.20	0.20	0 TO 375
296-310, 314-334, 493-495	ST. PROBE RAKES	10 - 1371 °C	1.11	± °C	0.25	0.16	0.01	0.20	0.20	375 TO 800
335 THRU 359, & 496	FLOW HOUSING WALL	10 - 1371 °C	1.11	± °C	0.25	0.16	0.01	0.20	0.20	800 TO 1371
97, 184, 277, 400	INSULATION	10 - 1371 °C	1.11	± °C	0.40	0.27	0.01	0.20	0.20	0 TO 375
386 THRU 388	L. PLEN. FL & WALL	10 - 1371 °C	1.11	± °C	0.20	0.08	0.01	0.20	0.20	0 TO 375
389, 391, 392	U. PLEN. FL & WALL	10 - 1371 °C	1.11	± °C	0.20	0.08	0.01	0.20	0.20	0 TO 375
399, 401	SUPPLY TANK FLUID	10 - 1371 °C	1.11	± °C	0.20	0.08	0.01	0.20	0.20	0 TO 375
407 THRU 410	SUP LINE FL. & WALL	10 - 1371 °C	1.11	± °C	0.20	0.08	0.01	0.20	0.20	0 TO 375
418 THRU 424	(SM, LG) CARRYOVER TANKS FL. & WALL	10 - 1371 °C	1.11	± °C	0.20	0.08	0.01	0.20	0.20	0 TO 375
385, 404, 435, 436, 437	PRESS. OSC. DAMP TANK FL. & WALL	10 - 1371 °C	1.11	± °C	0.20	0.08	0.01	0.20	0.20	0 TO 375
440 THRU 443	EXHAUST LINE	10 - 1371 °C	1.11	± °C	0.20	0.08	0.01	0.20	0.20	0 TO 375
360, 361	ROD BUNDLE INLET	10 - 1371 °C	1.11	± °C	0.20	0.08	0.01	0.20	0.20	0 TO 375
414-415	STM SUP FL & WALL	10 - 1371 °C	1.11	± °C	0.20	0.08	0.01	0.20	0.20	0 TO 375
403, 428-432	STEAM SEP	10 - 1371 °C	1.11	± °C	0.20	0.08	0.01	0.20	0.20	0 TO 375
446-457	QUARTZ WINDOWS	10 - 1371 °C	1.11	± °C	0.20	0.08	0.01	0.200	0.200	0 TO 375
					0.25	0.160	0.01	0.200	0.200	375 TO 800
CHANNEL NO.	TERMISTOR TYPE 5000	°C	± °C	± °C	± °C	± °C	± °C	± °C	± °C	°C
497-512	TERM PNL REF THERMISTORS	-10 - 85 °C	0.01	± °C	± °C	± °C	± °C	± °C	± °C	-10 TO 65

Table B.2 Error in Differential Pressure Cells (DP's), Static Pressure Transducers (P's), and Vessels Liquid Label Transducers

SPAN (CALIBRATION)	ACCURACY ± 0.075% SPAN ± mm H ₂ O	PERFORMANC E ± 0.15% SPAN ± mm H ₂ O	SCP LINEARITY ± 0.01% VOLTAGE RANGE ± mm H ₂ O	AUTO- RANGING ± 0.02% VOLTAGE RANGE ± mm H ₂ O	SCP OFFSET ERROR ± mm H ₂ O	NOISE ± mm H ₂ O	VOLTAGE RANGE FOR ERROR NUMBERS ± Volts	TOTAL PROBABLE ERROR ± mm H ₂ O
0 TO 76.2 mm H2O	0.06	0.11	0.003	0.005	0.001	0.002	0.25	0.13
0 TO 101.6 mm H2O	0.08	0.15	0.010	0.021	0.003	0.007	1.00	0.13
0 TO 127 mm H2O	0.10	0.19	0.003	0.007	0.001	0.003	0.25	0.17
0 TO 152.4 mm H2O	0.11	0.23	0.014	0.027	0.004	0.009	1.00	0.17
0 TO 177.8 mm H2O	0.13	0.27	0.004	0.009	0.001	0.004	0.25	0.21
0 TO 203.2 mm H2O	0.15	0.30	0.017	0.034	0.005	0.011	1.00	0.22
0 TO 279.4 mm H2O	0.21	0.42	0.005	0.010	0.002	0.005	0.25	0.26
0 TO 304.8 mm H2O	0.23	0.46	0.021	0.041	0.006	0.013	1.00	0.26
0 TO 330.2 mm H2O	0.25	0.50	0.006	0.012	0.002	0.006	0.25	0.30
0 TO 365.7 mm H2O	0.27	0.30	0.024	0.048	0.007	0.015	1.00	0.30
0 TO 279.4 mm H2O	0.21	0.42	0.007	0.014	0.002	0.006	0.25	0.34
0 TO 304.8 mm H2O	0.23	0.46	0.027	0.055	0.009	0.018	1.00	0.35
0 TO 330.2 mm H2O	0.25	0.50	0.009	0.019	0.003	0.009	0.25	0.47
0 TO 365.7 mm H2O	0.27	0.30	0.038	0.075	0.012	0.024	1.00	0.48
0 TO 311.15 mm H2O	0.23	0.47	0.010	0.021	0.003	0.009	0.25	0.51
0 TO 127 mm H2O	0.10	0.19	0.041	0.082	0.013	0.026	1.00	0.52
0 TO 155.575 mm H2O	0.12	0.23	0.011	0.022	0.004	0.010	0.25	0.55
0 TO 6350 mm H2O	4.76	9.53	0.045	0.089	0.014	0.029	1.00	0.56
0 TO 3022.6 mm H2O	2.27	4.53	0.123	0.247	0.039	0.114	0.25	6.14
0 TO 1574.8 mm H2O	1.18	2.36	0.494	0.987	0.153	0.316	1.00	6.24
0 TO 895.35 mm H2O	0.67	1.34	0.011	0.021	0.003	0.010	0.25	0.53
0 TO 1663.7 mm H2O	1.25	2.50	0.042	0.084	0.013	0.027	1.00	0.52
			0.004	0.009	0.001	0.004	0.25	0.21
			0.017	0.034	0.005	0.011	1.00	0.22
			0.005	0.011	0.002	0.005	0.25	0.26
			0.021	0.042	0.007	0.013	1.00	0.27
			0.214	0.429	0.069	0.197	0.25	10.66
			0.857	1.714	0.266	0.549	1.00	10.84
			0.102	0.204	0.033	0.094	0.25	5.08
			0.408	0.816	0.126	0.261	1.00	5.16
			0.053	0.106	0.017	0.049	0.25	2.64
			0.213	0.425	0.066	0.136	1.00	2.69
			0.030	0.060	0.010	0.028	0.25	1.50
			0.121	0.242	0.037	0.077	1.00	1.53
			0.056	0.112	0.018	0.052	0.25	2.79
			0.225	0.449	0.070	0.144	1.00	2.84
kPa	± kPa	± kPa	± kPa	± kPa	± kPa	± kPa	± Volts	± kPa
0 TO 413.7 kPa	0.31	0.62	0.014	0.028	0.004	0.013	0.25	0.69
0 TO 689.5 kPa	0.52	1.03	0.056	0.112	0.017	0.036	1.00	0.71
0 TO 344.7 kPa	0.26	0.52	0.023	0.047	0.007	0.021	0.25	1.16
0 TO 34.5 kPa	0.03	0.05	0.093	0.186	0.029	0.060	1.00	1.18
			0.012	0.023	0.004	0.011	0.25	0.58
			0.047	0.093	0.014	0.030	1.00	0.59
			0.001	0.002	0.000	0.001	0.25	0.06
			0.005	0.009	0.001	0.003	1.00	0.06

Table B.3 Error in Inlet Mass and Exhaust Steam Flow Transmitters (FM)

INPUT SENSOR	INSTRUMENT		DATA ACQUISITION SYSTEM				TOTAL	
	SPAN (CALIBRATION)	ACCURACY ¹ ± 0.11% SPAN	SCP LINEARITY ± 0.01% VOLTAGE RANGE	AUTO-RANGING ± 0.02% VOLTAGE RANGE	SCP OFFSET ERROR	NOISE		VOLTAGE RANGE FOR ERROR NUMBERS
MASS FLOW TRANSDUCER	g/sec	± g/sec	± g/sec	± g/sec	± g/sec	± g/sec	± Volts	± g/sec
SUPPLY LINE FM	0 TO 1247 g/sec	0.00137	0.042	0.084	0.013	0.039	0.25	0.103
DROP INJ FM	0 TO 45 g/sec	0.00005	0.168	0.337	0.052	0.108	1.00	0.395
			0.002	0.003	0.000	0.001	0.25	0.004
			0.006	0.012	0.002	0.004	1.00	0.014

INPUT SENSOR	INSTRUMENT		DATA ACQUISITION SYSTEM				TOTAL	
	SPAN (CALIBRATION)	ACCURACY ¹ ± 1.35% SPAN	PERFORMANC E ± 0.173% SPAN	SCP LINEARITY ± 0.01% VOLTAGE RANGE	AUTO-RANGING ± 0.02% VOLTAGE RANGE	SCP OFFSET ERROR		NOISE
VOLUME FLOW TRANSDUCER	m ³ /min	± m ³ /min	± m ³ /min	± m ³ /min	± m ³ /min	± m ³ /min	± Volts	± m ³ /min
STM SUPPLY FM	0 TO 7.1 m ³ /min	0.096	0.012	0.000	0.000	0.000	0.25	0.096
EXH PIPE FM	0 TO 12.7 m ³ /min	0.172	0.022	0.001	0.000	0.000	1.00	0.096
				0.002	0.003	0.001	0.25	0.172
						0.001	1.00	0.172

Table B.4 Error in Steam Probe Rakes Linear Position Transmitter

CHANNEL NO.	INPUT SENSOR	INSTRUMENT		DATA ACQUISITION SYSTEM				
		SPAN (CALIBRATION)	ACCURACY ± 1.0% SPAN	SCP LINEARITY ± 0.01% VOLTAGE RANGE	AUTO-RANGING ± 0.02% VOLTAGE RANGE	SCP OFFSET ERROR	NOISE	VOLTAGE RANGE FOR ERROR NUMBERS
482-489	POSITION TRANSDUCER	mm	± mm	± mm	± mm	± mm	± mm	± Volts
	RAKE POSITION	0 TO 88.9 mm	0.889	0.003	0.006	0.001	0.003	0.25
				0.012	0.024	0.004	0.008	1.00

Table B.5 Error in Heater Rod Bundle Input Voltage (V), Amperage (Amps), and Power (W) Measurements

		INSTRUMENT			DATA ACQUISITION SYSTEM				
CHANNEL NO.	INPUT SENSOR	SPAN (CALIBRATION)	ISOLATOR ACCURACY ± 0.1% SPAN		SCP LINEARITY ± 0.01% VOLTAGE RANGE	AUTO-RANGING ± 0.02% VOLTAGE RANGE	SCP OFFSET ERROR	NOISE	VOLTAGE RANGE FOR ERROR NUMBERS
397	VOLTAGE TRANSDUCER	Volts	± V		± mV	± mV	± uV	± uV	± Volts
	ELECTRICAL SYSTEM	0 TO 10 Volts	0.01		0.27 1.08	0.67 2.70	107.99 418.47	310.48 863.93	0.25 1.00
INSTRUMENT									
DATA ACQUISITION SYSTEM									
CHANNEL NO.	INPUT SENSOR	SPAN (CALIBRATION)	SHUNT ACCURACY ± 0.1% SPAN	ISOLATOR ACCURACY ± 0.1% SPAN	SCP LINEARITY ± 0.01% VOLTAGE RANGE	AUTO-RANGING ± 0.02% VOLTAGE RANGE	SCP OFFSET ERROR	NOISE	VOLTAGE RANGE FOR ERROR NUMBERS
398	CURRENT TRANSDUCER	Amps	± A	± A	± A	± A	± A	± A	± Volts
	ELECTRICAL SYSTEM	0 TO 15000 Amps	15	15	0.40 1.62	1.01 4.05	0.16 0.63	0.47 1.30	0.25 1.00
INSTRUMENT									
DATA ACQUISITION SYSTEM									
CHANNEL NO.	INPUT SENSOR	SPAN (CALIBRATION)	DAS VOLTS ACCURACY ± 0.1% SPAN	DAS AMPS ACCURACY ± 0.14% SPAN					
397 * 398	DERIVED POWER (V*A)	kWatts	± W	± W					
	ELECTRICAL SYSTEM	0 TO 750 kWatts	750	1050					

B.2 Heat Transfer Coefficient Uncertainty Analysis

The purpose of this uncertainty analysis was to estimate the confidence limits in the heat transfer coefficients calculated for heater rods in the RBHT Test Facility bundle test series using the uncertainty analysis using performed on the FLECHT-SEASET heater rods. It is believed that the uncertainty geometry analysis performed on the FLECHT-SEASET heater rods is applicable to the RBHT heater rods since the construction and materials are the same or very similar.

The uncertainty analysis used the FLECHT-SEASET heat transfer coefficients calculated from test data, using DATARH. The sensitivity of the heat transfer coefficient to variations in the test data and heater rod design was also calculated by the code. This code solves an inverse heat conduction problem using a finite-difference technique.

The uncertainty analysis used standard statistical treatment of independent uncertainty components to establish 1σ (70 percent) and 2σ (95 percent) confidence intervals on the total uncertainty in the heat transfer coefficient. Individual uncertainty components were obtained from heater rod inspection data, physical information, or professional experience and judgment. Each component of the total uncertainty was assumed to be independent, and of known variance.

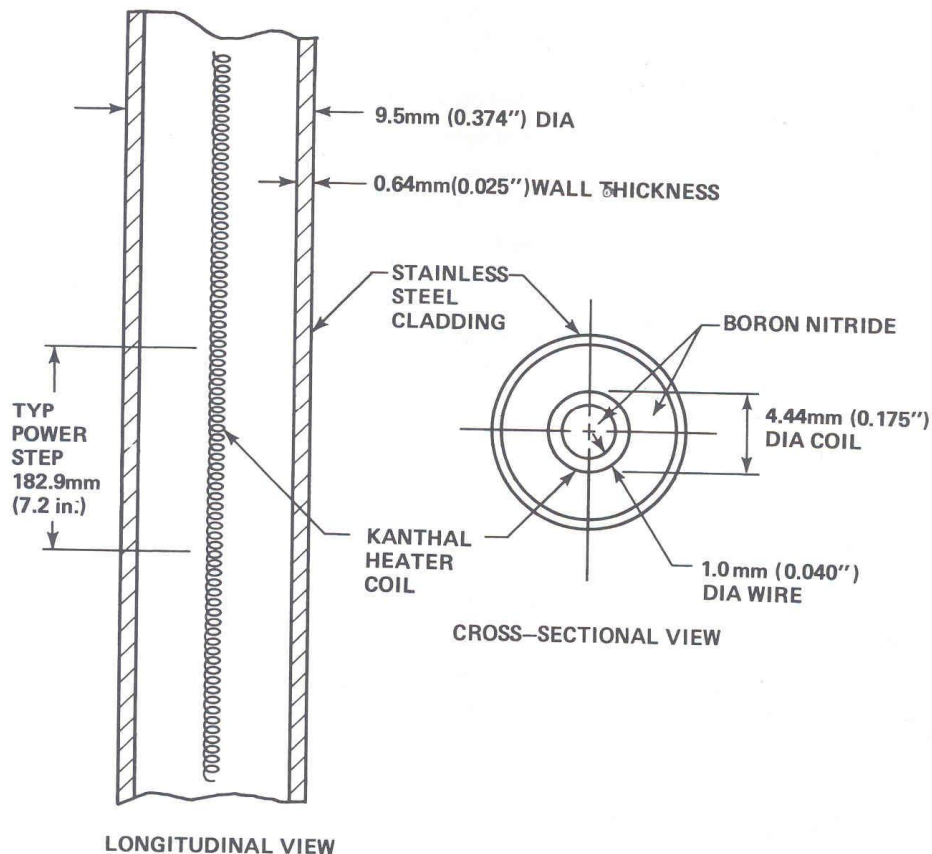


Figure B.1 Heater Rod Design.

The FLECHT SEASET unblocked bundle test series utilized stainless steel clad, boron nitride filled heater rods with coiled Kanthal wire heating elements (Figure B.1). For the RBHT test bundle the cladding was Inconel and not stainless steel but the remaining of the heater rod design was the same. The other properties were the same. In the instrumented heated rods, thermocouples were located at several different axial locations on the inside wall of the cladding. The thermocouple output was used in the DATARH code to compute the heat transfer coefficient. The code input requires density, specific heat, and thermal conductivity for the heater rod materials and geometric details of the heater coil.

The heater rod geometric input included clad inside and outside diameters and thermocouple radial location. Code input from the FLECHT SEASET bundle test instruments included thermocouple temperature, bundle pressure, and SCR power output.

The heat transfer coefficient may be expressed as

$$h = h[x_1, x_2, \dots, x_n] \quad (\text{B-7})$$

where x_i ($i = 1, 2, \dots, n$) are the individual parameters that affect the heat transfer coefficient h . The statistical variation of calculated h about its expected value may be expressed by expanding the function $h[x_1, x_2, \dots, x_n]$ in a multivariable Taylor series.

Including only first-order terms, the result is

$$h[x_1, x_2, \dots, x_n] - E[h] = \sum_{i=1}^n \left(\frac{\partial h}{\partial x_i} \right)_{\bar{x}} \{x_i - E[x_i]\} \quad (\text{B-8})$$

or

$$\Delta h = \sum_{i=1}^n \left(\frac{\partial h}{\partial x_i} \right)_{\bar{x}} \Delta x_i \quad (\text{B-9})$$

where the derivatives are evaluated using the means of all the random variables x_i (denoted by \bar{x}). $E[h]$ is the expected or mean value of the function h ; that is, h evaluated at the means of the random variables x_i . Each $(\partial h / \partial x_i)_{\bar{x}} \Delta x_i$ term also is a random variable with a mean of zero and a variance given by

$$\text{var} \left(\frac{\partial h}{\partial x_i} \right)_{\bar{x}} \Delta x_i = \left(\frac{\partial h}{\partial x_i} \right)_{\bar{x}}^2 \sigma_{x_i}^2 = \sigma_{\Delta h_i}^2 \quad (\text{B-10})$$

where $(\partial h / \partial x_i)_{\bar{x}}$ is constant for given \bar{x} .

Assuming the $(\partial h / \partial x_i)_{\bar{x}} \Delta x_i$ terms are independent, the mean of h becomes

$$E[\Delta h] = \sum_{i=1}^n \left(\frac{\partial h}{\partial x_i} \right)_{\bar{x}} E[\Delta x_i] = 0 \quad (\text{B-11})$$

and the variance of h is

$$\sigma_{\Delta h}^2 = \sum_{i=1}^n \sigma_{\Delta h_i}^2 = \sum_{i=1}^n \left(\frac{\partial h}{\partial x_i} \right)_{\bar{x}}^2 \sigma_{x_i}^2 \quad (\text{B-12})$$

Approximating the $(\partial h / \partial x_i)_x$ terms by $(\Delta h / \Delta x_i)_x$, the variance becomes

$$\sigma_{\Delta h}^2 = \sum_{i=1}^n \left(\frac{\Delta h_i}{\Delta x_i} \right)_{\bar{x}}^2 \sigma_{x_i}^2 \quad (\text{B-13})$$

A consequence of the central limit theorem in statistics is that the distribution of the uncertainty calculated above approaches a normal distribution. With a known distribution function, the confidence interval of the uncertainty can be calculated from the variance. The 1σ (70 percent) and 2σ (95 percent) confidence intervals are reported in this evaluation.

These values were obtained by individually perturbing each parameter x_i from its expected value by its estimated standard deviation in numerous runs of the DATARH code. Each perturbation resulted in a new value of calculated h , from which the nominal or expected value was subtracted to provide h_i . Since in these perturbations x_i was assumed to be equal to σ_{x_i} , the variance can be evaluated by simply summing the squares of the resultant h_i terms:

$$\sigma_{\Delta h}^2 = \sum_{i=1}^n \Delta_{h_i}^2 \quad (\text{B-14})$$

Positive and negative h_i terms ($\Delta h_i^+, \Delta h_i^-$) were obtained by perturbing each x_i both above and below its expected value. They are indicative of the heat transfer coefficient's sensitivity to uncertainty in each parameter, and were statistically combined to provide both upper and lower uncertainty bands on calculated h . Differences in the and for each Δh_i^+ and Δh_i^- are due to nonlinearities in the function $h [x_1, x_2, \dots, x_n]$.

Uncertainty in the heat transfer coefficient, h , calculated by the DATARH code stems from the following factors:

- Uncertainty in the measured test parameters input to the program
- Uncertainty due to manufacturing tolerances on heater rod dimensions and instrumentation location
- Material property uncertainties

Measured test parameters that are input to DATARH are bundle power, pressure, and clad inside temperature.

The uncertainty in the measured parameters is combined with other sources of uncertainty by summing the variance of each uncertainty component. For the test instruments, the instrument uncertainty was assumed to be uniformly distributed over the uncertainty interval. The variance of a uniformly distributed random variable over the interval $-\infty < x < \infty$ is $\frac{2}{3}$. The total instrument uncertainty consists of uncertainty in the sensor, in signal conditioning equipment, and in recording the signal. The variance of each of these components was calculated as described above and summed to get the total variance of the instrument uncertainty. Transducer uncertainty is normally dominant, and thus total uncertainty and transducer uncertainty will be very similar.

The standard deviation (that is, the positive square root of the variance) and maximum uncertainty for each data path are shown in Tables B.1 through B.5. The maximum uncertainty was calculated by summing the maximum uncertainty of all contributors to the total instrument uncertainty.

Manufacturing tolerances on rod dimensions and instrumentation location also contribute to uncertainty in the calculated heat transfer coefficient h . Heater coil dimensions, clad inside and outside diameters, and thermocouple locations are incorporated in the DATARH geometric heater rod model, because they are possible contributors to uncertainty in h . Uncertainty in the thermocouple radial location was estimated from X-ray inspection of actual heater rods. Clad outside diameter uncertainty was obtained from the rod inspection data. Uncertainty in clad inside diameter was estimated by combining the uncertainty in clad outside diameter with the uncertainty in clad thickness.

Axial power is also a factor. In FLECHT SEASET heater rods, the number of heater coil turns per in (coil spacing) is variable (Figure B.1); this changes the length of heater wire per unit length of heater rod. From the X-ray radiographs of the heater rods, the geometry of the axial power steps was determined. Similar approach has been used for the RBHT heater rods.

The rod inspection data do not reflect any variation in the diameter of the Kanthal heater wire. The wire diameter was nominally 0.10 cm (0.040 in), and small variations in diameter were beyond the resolution of the radiograph. To estimate the uncertainty due to wire diameter variation, the assumption was made that the local variation in wire resistance due to the wire cross-sectional area variation could be approximated from the variation in heater rod resistance between rods.

Uncertainty in the physical properties of the material in the heater rods was based largely on engineering judgment. The boron nitride density uncertainty was based on a sample of five measurements from sections of heater rods that were destructively analyzed.

The input parameters for power factor ($P_{\text{local}}/P_{\text{average}}$) determination are local step length, total heated length, local step length coil resistance, and total heated length coil resistance. An analysis identical to that discussed was performed for this calculation, varying the input parameters by the estimated standard deviations. Estimated power factor parameter uncertainties are shown in Table B.6, and the power factor uncertainty analysis in Table B.7.

Table B.6 Uncertainty of Power

ESTIMATED UNCERTAINTY OF POWER
FACTOR CALCULATION

Parameter	Estimated Uncertainty ^(a)	Best-Estimated Value	Reference/ Comments
Step length	± 0.06 in.	14.52 in.	Rod inspection data
Step resistance	$\pm 0.03\%$	3.595 Ω	Rod inspection data
Total length	± 0.06 in.	144.48 in.	Rod inspection data
Total resistance	$\pm 0.03\%$	21.60 Ω	Rod inspection data

a. All uncertainties are listed at the 1σ level.

Table B.7 summarizes the certainties of all the parameters used by DATARH to calculate the FLECHT SEASET heat transfer coefficient. These uncertainties were evaluated at the 1σ (70 percent confidence) level. The uncertainties in Table B.8 for the heater rod material properties are expected to be similar as the same uncertainties used for the RBHT heater rods since the design and materials are similar.

Other sources of uncertainties that could lead to increased uncertainty in the value of h were reviewed; however, for the most part, they were of relatively minor importance and their absence in this analysis would not be significant. Those other factors were as follows:

- Induction and skin effects - These effects of high-frequency components of the chopped ac power were neglected.
- Wire effective length - Analytically, the effective length for a tightly coiled wire is less than the length based on the helix mean radius (which is used in DATARH). However, this source of uncertainty is the same for each wire and will cancel out in the relative power calculation. Therefore, such a correction was not required.
- Electrical resistivity variation with temperature at rod quench - Changes in rod temperature distribution will affect the local P/P_{avg} . For example, if half the rod is quenched, resistivity in the upper half could be as much as four percent greater than that in the lower half, and power would be redistributed within the rod. Since there was no method by which this could be accounted for proportionately, this effect was ignored.
- Kanthal heater helix position - The heater coil may be slightly off center in the rod. This effect was analyzed by varying the coil diameter; however, no coil displacement was examined.

- Thermocouple axial location - The thermocouples were located at different positions along the length of the rod. Any axial conduction in the heater rod in the vicinity of the thermocouples was assumed to be small since the axial profile is linear and the rate of change of power over the bottom 2.74 m (9 ft) of the heater rod is also small.

Table B.7 Thermocouple Power Factor Uncertainty Analysis

THERMOCOUPLE POWER FACTOR UNCERTAINTY ANALYSIS

Parameter	Calculated P/P_{avg} (a)	$\Delta(P/P_{avg})^{+(b)}$	$\Delta(P/P_{avg})^{-}$
Nominal case	1.6561		
Step length + 0.06 in.	1.6493		-0.0068
Step length - 0.06 in.	1.6630	0.0069	
Step resistance + 0.03%	1.6566	0.0005	
Step resistance - 0.03%	1.6556		-0.0005
Total length + 0.06 in.	1.6568	0.0007	
Total length - 0.06 in.	1.6554		-0.0007
Total resistance + 0.03%	1.6556		-0.0005
Total resistance - 0.03%	1.6566	0.0005	
Using values for $\Delta(P/P_{avg})^{+}$: $\sigma_{P/P_{avg}} = (0.0069^2 + 0.0005^2 + 0.0007^2 + 0.0005^2)^{1/2} = 0.0070$ (absolute) $= 0.42$ (%)			
Using values for $\Delta(P/P_{avg})^{-}$: $\sigma_{P/P_{avg}} = (0.0068^2 + 0.0005^2 + 0.0007^2 + 0.0005^2)^{1/2} = 0.0069$ (absolute) $= 0.42$ (%)			

a.
$$\frac{P}{P_{avg}} = \left(\frac{\text{step resistance}}{\text{step length}} \right) \left(\frac{\text{total length}}{\text{total resistance}} \right)$$

b.
$$\Delta(P/P_{avg}) = P/P_{avg} - (P/P_{avg})_{\text{nominal}}$$

Table B.8 Uncertainties Affecting the Heat Transfer Coefficient Calculations

ESTIMATED UNCERTAINTY OF PARAMETERS AFFECTING CALCULATED
HEAT TRANSFER COEFFICIENT

Parameter	Estimated Uncertainty(σ) ^(a)	Reference/Comments
Measured power	± 2.14 kw	Table B-5
Measured temperature	At $T < 277^{\circ}\text{C}$ (530°F), $\pm 1.39^{\circ}\text{C}$ ($\pm 2.51^{\circ}\text{F}$) At $277^{\circ}\text{C} < T < 1316^{\circ}\text{C}$ ($530^{\circ}\text{F} < T < 2400^{\circ}\text{F}$), $\pm [1.539 + (0.00217T)^2]^{1/2}$ $^{\circ}\text{C}$ $\{ \pm [4.986 + (0.00217T)^2]^{1/2}$ $^{\circ}\text{F}$ }	Table B-1 $\sigma_{\text{temp}}^2 = 1/3 (\sigma_{\text{sensor}}^2 + \sigma_{\text{cond}}^2 + \sigma_{\text{readout}}^2)$
Measured pressure	± 2.66 kPa (± 0.386 psi)	Table B-2
Thermocouple radial location	-0.05 mm (-0.002 in.)	X-ray inspection data. T/C location assumed at clad inside surface. Radial position can only be in boron nitride; thus there is only negative uncertainty.
Rod OD	± 0.012 mm (± 0.00049 in.)	Heater rod inspection data
Clad ID	± 0.012 mm (± 0.00049 in.)	Estimate based on rod OD and clad thickness inspection data

a. All errors or uncertainties are listed at the 1 σ level.

Table B.8 Uncertainties Affecting the Heat Transfer Coefficient Calculations (Continued)

ESTIMATED UNCERTAINTY OF PARAMETERS AFFECTING CALCULATED
HEAT TRANSFER COEFFICIENT

Parameter	Estimated Uncertainty(σ) ^(a)	Reference/Comments
Power step factor	$\pm 0.42\%$	Table B -5
Boron nitride properties		
Density	$\pm 3\%$	Heater rod inspection data
Thermal conductivity	$\pm 10\%$	Watlow Electric estimate
Specific heat	$\pm 5\%$	Touloukian, ^(b) engineering judgment
Kanthal properties		
Density	$\pm 2\%$	Engineering estimate
Thermal conductivity	$\pm 5\%$	Engineering estimate
Specific heat	$\pm 5\%$	Engineering estimate
Stainless steel 347 properties		
Density	$\pm 1\%$	Touloukian, ^(b) engineering judgment
Thermal conductivity	$\pm 3\%$	
Specific heat	$\pm 3\%$	

a. All errors or uncertainties are listed at the 1σ level.

b. Touloukian, Y. S., Thermophysical Properties of High Temperature Solid Materials, Macmillan, New York, 1967.

The uncertainty analysis was performed for FLECHT-SEASET test 31504 with the following nominal initial conditions:

Pressure	0.28 MPa (40 psia)
Initial Clad Temperature	871 degrees C (1600 degrees F)
Rod Peak Power	2.3 kW/m (0.7 kW/ft)
Flooding Rate	25 mm/s (1.0 in/s)
Inlet Subcooling	60 degrees C (140 degrees F)
Radial Power	Uniform
Housing Temperature	T_{sat}

These test conditions are similar to the low flooding rate RBHT tests.

The analysis was performed on the heat transfer coefficient calculated for the hot rod 8K at the 1.98 m (78 in) elevation. The calculated value of the heat transfer coefficient from rod 8K was obtained with the best-estimate values of all the parameters in Table B-8. Both positive and negative values of h_i were obtained from subsequent DATARH calculations for which the parameters given in Table B.8 were varied. The calculated positive and negative values of h_i are listed in Table B.9 as a function of time. They are indicative of the heat transfer coefficient sensitivity for each parameter. The various values of Δh_i^+ and Δh_i^- are statistically combined in Table B.10 and the resulting calculated h values with the estimated 95 percent confidence bands (2σ) are shown in Table B.11.

Examination of the h_i values in Table B.9 shows that the measured power, rod outside diameter, clad thickness, and power step factor had the largest effects on the calculated heat transfer coefficient. Other parameters such as the rod properties (except the boron nitride density), rod temperature, and system pressure clearly had second-order effects on the accuracy of the calculated heat transfer.

The method used in this analysis presupposes that the process is linear; higher-order terms in the Taylor series expansion [Equation (B-6)] were neglected. If the method is linear, then the h_i values would be of equal magnitude but opposite sign. However, as the h_i values listed in Table B.9 indicate, the inverse conduction scheme is not a linear equation and h_i values can have different magnitudes if the deviation is taken in either the positive or negative direction from the normal value. Therefore, when the upper and lower bands are calculated as in Table B.10, these bands will not have the same magnitude. One method of compensating for the effect of nonlinearity is to simply average each deviation, both positive and negative values, and obtain an averaged deviation at each time step. This will result in a centered confidence band about the estimated heat transfer coefficient data. The calculations for this approach are given in Table B.12.

Figure B.2, which shows the calculated heat transfer coefficient (h) with the 95 percent confidence limits, indicates that the largest uncertainty in h is early in the transient, particularly at the beginning of reflood. Figure B.3 shows the relative uncertainty for the upper 95 percent confidence band as plotted from Table B.10. This indicates that the relative uncertainty quickly decreased to approximately 10 percent by 30 s for this test.

Table B.9 Parameter Sensitivities
PARAMETER SENSITIVITIES^(a)

Time (sec)	Base Case	Measured Power ± 2.14		Measured Temperature		Measured Pressure		Thermocouple Radial Location		Rod OD	
		Δh_1^+	Δh_1^-	Δh_2^+	Δh_2^-	Δh_3^+	Δh_3^-	Δh_4^+	Δh_4^-	Δh_5^+	Δh_5^-
0	1.3773	0.1603	-0.1602	0.0424	-0.0415	0.0007	-0.0006	0.0000	-0.0201	0.0594	-0.0592
1	0.9133	0.1585	-0.1584	0.0380	-0.0372	0.0004	-0.0004	0.0000	-0.0105	0.0585	-0.0584
2	1.0165	0.1568	-0.1568	0.0376	-0.0368	0.0005	-0.0005	0.0000	-0.0087	0.0575	-0.0574
3	1.1095	0.1553	-0.1553	0.0373	-0.0367	0.0005	-0.0005	0.0000	-0.0093	0.0567	-0.0567
4	1.2058	0.1538	-0.1537	0.0406	-0.0428	0.0006	-0.0005	0.0000	-0.0101	0.0561	-0.0559
5	1.1835	0.1525	-0.1522	0.0444	-0.0480	0.0006	-0.0005	0.0000	-0.0098	0.0554	-0.0552
10	1.3702	0.1450	-0.1450	0.0615	-0.0633	0.0006	-0.0006	0.0000	-0.0084	0.0516	-0.0515
20	3.5014	0.1340	-0.1339	0.0680	-0.0670	0.0014	-0.0013	0.0000	-0.0024	0.0413	-0.0412
30	4.7009	0.1276	-0.1268	0.0648	-0.0641	0.0017	-0.0018	0.0000	-0.0056	0.0354	-0.0353
40	7.1790	0.1219	-0.1219	0.0667	-0.0659	0.0026	-0.0025	0.0000	-0.0035	0.0278	-0.0277
50	7.1358	0.1183	-0.1182	0.0631	-0.0622	0.0025	-0.0024	0.0000	-0.0048	0.0258	-0.0257
60	8.0461	0.1157	-0.1154	0.0626	-0.0617	0.0028	-0.0026	0.0000	-0.0049	0.0225	-0.0222
70	7.9255	0.1133	-0.1133	0.0600	-0.0592	0.0026	-0.0026	0.0000	-0.0022	0.0209	-0.0209
80	8.0829	0.1116	-0.1115	0.0584	-0.0576	0.0027	-0.0026	0.0000	-0.0058	0.0198	-0.0196
90	8.2738	0.1100	-0.1100	0.0571	-0.0564	0.0027	-0.0027	0.0000	-0.0047	0.0180	-0.0180
100	9.0284	0.1091	-0.1089	0.0576	-0.0567	0.0030	-0.0028	0.0000	-0.0025	0.0156	-0.0154
120	9.9713	0.1085	-0.1084	0.0580	-0.0571	0.0032	-0.0031	0.0000	-0.0034	0.0126	-0.0124
140	10.9637	0.1091	-0.1088	0.0595	-0.0585	0.0036	-0.0034	0.0000	-0.0011	0.0097	-0.0094
160	11.8892	0.1116	-0.1116	0.0622	-0.0615	0.0039	-0.0039	0.0000	-0.0040	0.0080	-0.0080
180	15.2355	0.1165	-0.1164	0.0724	-0.0714	0.0052	-0.0052	0.0000	-0.0010	0.0020	-0.0018
200	15.5146	0.1235	-0.1233	0.0775	-0.0765	0.0057	-0.0055	0.0000	-0.0018	0.0029	-0.0026
220	17.2969	0.1318	-0.1317	0.0875	-0.0875	0.0067	-0.0039	0.0000	-0.0008	0.0009	-0.0008
240	18.8704	0.143	-0.1427	0.1001	-0.0985	0.0080	-0.0078	0.0000	-0.0033	0.0006	-0.0003
260	21.1816	0.1573	-0.1571	0.1400	-0.1378	0.0098	-0.0097	0.0000	-0.0029	0.0005	-0.0002
280	22.9392	0.1755	-0.1751	0.1558	-0.1577	0.0119	-0.0116	0.0006	0.0000	0.0011	-0.0006
300	28.0444	0.2007	-0.2005	0.1576	-0.1546	0.0164	-0.0164	0.0000	0.0000	0.0038	-0.0036
320	49.1724	0.2500	-0.2500	0.3565	-0.3495	0.0364	-0.0366	0.0000	0.0000	0.0516	-0.0515
325	812.0703	2.3737	-2.3609	26.5086	-22.8027	7.4468	-7.2825	6.3471	0.0000	3.6697	-3.6360

a. $\Delta h_i = \left(\frac{\partial h}{\partial x_i} \right) \sigma_{x_i}$

b. Values of h are given in Btu/hr-ft²-°F. To convert to w/m²-°C, multiply by 5.678.

Table B.9 Parameter Sensitivities (Continued)

PARAMETER SENSITIVITIES^(a)

Time (sec)	Clad ID		Power Step Factor Axial Power		Boron Nitride Density		Boron Nitride Specific Heat		Boron Nitride Thermal Conductivity		Kanthal Density	
	Δh_6^+	Δh_6^-	Δh_7^+	Δh_7^-	Δh_8^+	Δh_8^-	Δh_9^+	Δh_9^-	Δh_{10}^+	Δh_{10}^-	Δh_{11}^+	Δh_{11}^-
0	0.0138	-0.0137	0.0810	-0.0842	0.3231	-0.3228	0.5440	-0.5436	0.0128	-0.0112	0.0389	-0.0380
1	0.0127	-0.0126	0.0798	-0.0830	0.3359	-0.3295	0.5550	-0.5247	0.0064	-0.0052	0.0390	-0.0382
2	0.0122	-0.0122	0.0786	-0.0818	0.3240	-0.3239	0.5456	-0.5454	0.0048	-0.0039	0.0373	-0.0364
3	0.0121	-0.0122	0.0774	-0.0807	0.3182	-0.3182	0.5358	-0.5358	0.0050	-0.0042	0.0354	-0.0347
4	0.0121	-0.0120	0.0763	-0.0794	0.3123	-0.3122	0.5258	-0.5256	0.0051	-0.0041	0.0337	-0.0329
5	0.0120	-0.0119	0.0752	-0.0782	0.3084	-0.3083	0.5192	-0.5191	0.0044	-0.0036	0.0326	-0.0318
10	0.0111	-0.0111	0.0699	-0.0727	0.2840	-0.2840	0.4782	-0.4782	0.0017	-0.0013	0.0274	-0.0268
20	0.0079	-0.0078	0.0619	-0.0644	0.2114	-0.2114	0.3559	-0.3560	0.0033	-0.0040	0.0204	-0.0199
30	0.0066	-0.0067	0.0566	-0.0590	0.1647	-0.1648	0.2774	-0.2774	0.0009	-0.0007	0.0156	-0.0153
40	0.0040	-0.0040	0.0530	-0.0552	0.1044	-0.1044	0.1757	-0.1757	0.0007	-0.0008	0.0100	-0.0098
50	0.0038	-0.0037	0.0501	-0.0521	0.0918	-0.0918	0.1546	-0.1545	0.0006	-0.0004	0.0088	-0.0085
60	0.0029	-0.0027	0.0481	-0.0498	0.0657	-0.0654	0.1105	-0.1103	0.0018	-0.0012	0.0063	-0.0060
70	0.0022	-0.0022	0.0461	-0.0480	0.0602	-0.0602	0.1013	-0.1014	0.0007	-0.0007	0.0059	-0.0057
80	0.0023	-0.0022	0.0445	-0.0462	0.0491	-0.0490	0.0827	-0.0825	0.0029	-0.0023	0.0046	-0.0044
90	0.0017	-0.0017	0.0430	-0.0447	0.0395	-0.0395	0.0666	-0.0665	0.0017	-0.0014	0.0038	-0.0036
100	0.0007	-0.0005	0.0420	-0.0435	0.0217	-0.0215	0.0364	-0.0363	0.0002	-0.0000	0.0022	-0.0020
120	0.0004	-0.0003	0.0404	-0.0419	0.0028	-0.0026	0.0046	-0.0045	0.0016	-0.0012	0.0003	-0.0001
140	0.0018	-0.0015	0.0395	-0.0408	0.0243	-0.0241	0.0408	-0.0406	0.0004	-0.0000	0.0023	-0.0020
160	0.0020	-0.0020	0.0393	-0.0409	0.0418	-0.0418	0.0704	-0.0704	0.0030	-0.0026	0.0039	-0.0040
180	0.0049	-0.0048	0.0402	-0.0372	0.0982	-0.0981	0.1652	-0.1652	0.0013	-0.0011	0.0090	-0.0091
200	0.0047	-0.0044	0.0418	-0.0433	0.0973	-0.0971	0.1638	-0.1635	0.0038	-0.0028	0.0091	-0.0091
220	0.0056	-0.0055	0.0436	-0.0453	0.1210	-0.1209	0.2036	-0.2036	0.0017	-0.0014	0.0112	-0.0113
240	0.0059	-0.0056	0.0466	-0.0482	0.1382	-0.1379	0.2325	-0.2322	0.0051	-0.0040	0.0130	-0.0130
260	0.0066	-0.0065	0.0504	-0.0523	0.1618	-0.1616	0.2724	-0.2721	0.0044	-0.0035	0.0174	-0.0176
280	0.0074	-0.0070	0.0554	-0.0573	0.1660	-0.1656	0.2794	-0.2790	0.0025	-0.0017	0.0238	-0.0240
300	0.0095	-0.0094	0.0624	-0.0648	0.2317	-0.2315	0.3901	-0.3899	0.0142	-0.0116	0.0288	-0.0292
320	0.0457	-0.0457	0.0765	-0.0797	0.5322	-0.5330	0.8957	-0.8979	0.0619	-0.0694	0.0464	-0.0475
325	2.3341	-2.3172	0.7236	-0.7473	22.1188	-21.5054	37.6067	-35.8766	24.5470	-16.6868	2.7891	-2.8425

Table B.9 Parameter Sensitivities (Continued)
PARAMETER SENSITIVITIES^(a)

Time (sec)	Kanthal Thermal Conductivity		Kanthal Specific Heat		Stainless Steel Density		Stainless Steel Thermal Conductivity		Stainless Steel Specific Heat	
	Δh_{12}^+	Δh_{12}^-	Δh_{13}^+	Δh_{13}^-	Δh_{14}^+	Δh_{14}^-	Δh_{15}^+	Δh_{15}^-	Δh_{16}^+	Δh_{16}^-
0	0.0006	-0.0004	0.0975	-0.0974	0.0541	-0.0540	0.0006	-0.0006	0.1635	-0.1634
1	0.0004	-0.0003	0.0978	-0.0979	0.0541	-0.0541	0.0001	0.0000	0.1635	-0.1634
2	0.0004	-0.0003	0.0934	-0.0934	0.0530	-0.0530	0.0002	-0.0001	0.1602	-0.1602
3	0.0000	-0.0003	0.0887	-0.0888	0.0521	-0.0522	0.0001	-0.0001	0.1576	-0.1577
4	0.0004	-0.0003	0.0844	-0.0844	0.0514	-0.0513	0.0000	0.0000	0.1552	-0.1552
5	0.0003	-0.0002	0.0816	-0.0815	0.0508	-0.0507	0.0000	0.0000	0.1535	-0.1534
10	0.0002	-0.0001	0.0687	-0.0687	0.0470	-0.0469	0.0001	0.0000	0.1419	-0.1418
20	0.0001	0.0000	0.0510	-0.0510	0.0348	-0.0347	0.0003	-0.0003	0.1049	-0.1049
30	0.0000	-0.0001	0.0395	-0.0393	0.0276	-0.0276	0.0002	-0.0001	0.0834	-0.0834
40	0.0000	0.0000	0.0251	-0.0251	0.0174	-0.0174	0.0003	-0.0002	0.0526	-0.0525
50	0.0001	0.0000	0.0219	-0.0219	0.0156	-0.0155	0.0002	-0.0001	0.0469	-0.0469
60	0.0002	0.0000	0.0157	-0.0155	0.0113	-0.0111	0.0002	-0.0001	0.0339	-0.0337
70	0.0000	0.0000	0.0146	-0.0146	0.0100	-0.0100	0.0003	-0.0003	0.0302	-0.0302
80	0.0002	0.0000	0.0116	-0.0114	0.0086	-0.0085	0.0002	0.0000	0.0259	-0.0258
90	0.0001	0.0000	0.0094	-0.0094	0.0068	-0.0068	0.0002	-0.0001	0.0206	-0.0206
100	0.0001	0.0000	0.0055	-0.0052	0.0036	-0.0034	0.0003	-0.0002	0.0108	-0.0105
120	0.0001	0.0000	0.0006	-0.0005	0.0006	-0.0005	0.0003	-0.0002	0.0017	-0.0015
140	0.0002	0.0000	0.0056	-0.0053	0.0046	-0.0043	0.0005	-0.0003	0.0136	-0.0133
160	0.0001	-0.0001	0.0100	-0.0100	0.0071	-0.0071	0.0003	-0.0002	0.0215	-0.0215
180	0.0001	0.0000	0.0231	-0.0230	0.0170	-0.0169	0.0007	-0.0005	0.0512	-0.0511
200	0.0002	0.0000	0.0232	-0.0229	0.0166	-0.0164	0.0007	-0.0006	0.0499	-0.0497
220	0.0001	0.0000	0.0285	-0.0284	0.0205	-0.0204	0.0009	-0.0007	0.0618	-0.0617
240	0.0002	0.0000	0.0332	-0.0329	0.0229	-0.0226	0.0009	-0.0006	0.0688	-0.0686
260	0.0001	0.0000	0.0444	-0.0442	0.0264	-0.0262	0.0012	-0.0010	0.0796	-0.0814
280	0.0003	0.0000	0.0608	-0.0604	0.0274	-0.0270	0.0018	-0.0014	0.0824	-0.0820
300	0.0005	-0.0003	0.0736	-0.0734	0.0377	-0.0375	0.0027	-0.0025	0.1136	-0.1135
320	0.0022	-0.0023	0.1188	-0.1191	0.1024	-0.1024	0.0260	-0.0244	0.3095	-0.3093
325	0.3265	-0.3061	7.1965	-7.0988	2.1869	-2.1797	8.3582	-7.6746	6.6077	-6.5858

Table B.10 Standard Deviations

UPPER, LOWER, AND AVERAGE STANDARD DEVIATIONS ON CALCULATED HEAT TRANSFER COEFFICIENTS^(a)

Time (sec)	σ_h^+	$2\sigma_h^+$	σ_h^-	$2\sigma_h^-$	$(\sigma_h)_{avg}$
0	0.6921	1.3842	0.6921	1.3842	0.6921
1	0.7034	1.4068	0.7029	1.4058	0.7031
2	0.6906	1.3812	0.6907	1.3814	0.6906
3	0.6781	1.3562	0.6845	1.3690	0.6813
4	0.6659	1.3318	0.6662	1.3324	0.6660
5	0.6577	1.3154	0.6581	1.3162	0.6579
10	0.6080	1.2160	0.6085	1.2170	0.6082
20	0.4634	0.9268	0.4637	0.9274	0.4635
30	0.3720	0.7440	0.3723	0.7446	0.3721
40	0.2617	0.5234	0.2619	0.5238	0.2618
50	0.2377	0.4754	0.2378	0.4756	0.2377
60	0.1955	0.3910	0.1952	0.3904	0.1953
70	0.1848	0.3696	0.1851	0.3702	0.1849
80	0.1685	0.3370	0.1686	0.3372	0.1685
90	0.1553	0.3106	0.1555	0.3110	0.1554
100	0.1386	0.2772	0.1384	0.2768	0.1385
120	0.1303	0.2606	0.1303	0.2606	0.1303
140	0.1400	0.2800	0.1396	0.2796	0.1398
160	0.1590	0.3180	0.1592	0.3184	0.1591
180	0.2469	0.4938	0.2460	0.4920	0.2464
200	0.2505	0.5010	0.2499	0.4998	0.2502
220	0.2971	0.5942	0.2969	0.5938	0.2970
240	0.3353	0.6706	0.3346	0.6692	0.3349
260	0.3959	0.7918	0.3954	0.7908	0.3956
280	0.4193	0.8386	0.4195	0.8390	0.4194
300	0.5441	1.0882	0.5431	1.0862	0.5436
320	1.2007	2.4014	1.1897	2.3794	1.1952
325	58.0459	116.0918	52.8334	105.6668	55.439

$$a. \sigma_h^+ = \left[\sum_i (\Delta h_i^+)^2 \right]^{1/2}$$

$$\sigma_h^- = \left[\sum_i (\Delta h_i^-)^2 \right]^{1/2}$$

$$(\sigma_h)_{avg} = \frac{\sigma_h^+ + \sigma_h^-}{2}$$

Table B.11 Calculated h and 95 Percent Confidence Limits Versus Time

Time (Sec)	Calculated $h^{(a)}$	Upper 95% Confidence Limit ^(a)		Lower 95% Confident Limit	
		Absolute	Percent Error	Absolute	Percent Error
		$(h + 2\sigma_h^+)$	$\left(\frac{2\sigma_h^+}{h} \times 100\right)$	$(h - 2\sigma_h^-)$	$\left(\frac{2\sigma_h^-}{h} \times 100\right)$
0	1.3773	2.7615	100.50	-0.0069	100.50
1	0.9133	2.3201	154.03	-0.4925	153.93
2	1.0165	2.3977	135.88	-0.3649	135.90
3	1.1095	2.4657	122.24	-0.2595	123.39
4	1.2058	2.5376	110.45	-0.1260	110.50
5	1.1835	2.3670	111.14	-0.1309	111.21
10	1.3702	2.5862	88.75	0.1532	88.82
20	3.5014	4.4282	26.47	2.5740	26.49
30	4.7009	4.8393	2.94	4.5616	2.96
40	7.1790	7.7024	7.29	6.6552	7.29
50	7.1358	7.6112	6.50	6.6602	6.66
60	8.0461	8.4371	4.86	7.6557	4.85
70	7.9255	8.2951	4.66	7.5553	4.67
80	8.0829	8.4199	4.17	7.7457	4.17
90	8.2738	8.5844	3.75	7.9628	3.75
100	9.0284	9.3056	3.07	8.7516	3.06
120	9.9713	10.2319	2.61	9.7107	2.61
140	10.9637	11.2437	2.55	10.6841	2.55
160	11.8892	12.2072	2.67	11.5708	2.68
180	15.2355	15.7293	3.24	14.7435	3.23
200	15.5146	16.0156	3.23	15.0148	3.22
220	17.2969	17.8911	3.44	16.7031	3.43
240	18.8704	19.5410	3.55	18.2012	3.54
260	21.1816	21.9734	3.74	20.3908	3.73
280	22.9392	23.7778	3.66	22.1002	3.66
300	28.0440	29.1322	3.88	26.9578	3.87
320	49.1724	51.5738	4.88	46.7930	4.84
325	812.0703	928.0901	14.29	706.4035	13.01

a. Values of h are given in Btu/hr-ft²-°F. To convert to w/m²-°C, multiply by 5.678.

Table B.12 Calculated h and 95 Percent Confidence Limits Versus Time Using $(\sigma_h)_{avg}$ Values

CALCULATED h AND 95-PERCENT CONFIDENCE LIMITS VERSUS TIME
USING $(\sigma_h)_{avg}$ VALUES

Time (sec)	Calculated h ^(a)	$(\sigma_h)_{avg}$	$2(\sigma_h)_{avg}$	Upper 95% Confidence Limit $h + 2(\sigma_h)_{avg}$	Lower 95% Confidence Limit $h - 2(\sigma_h)_{avg}$	Percent Error $\frac{2(\sigma_h)_{avg}}{h} \times 100$
0	1.3773	0.6921	1.3842	2.7615	-0.0069	100.5009
1	0.9133	1.4063	2.8126	3.7259	-1.8993	307.9601
2	1.0165	1.3813	2.7626	3.7791	-1.7461	271.7757
3	1.1095	1.3626	2.7252	3.8347	-1.6157	245.6241
4	1.2058	1.3321	2.6642	3.8700	-1.4584	220.9487
5	1.1835	1.3158	2.6316	3.8151	-1.4481	222.3574
10	1.3702	1.2165	2.4330	3.8032	-1.0628	177.5653
20	3.5014	0.9271	1.8542	5.3556	1.6490	52.9560
30	4.7009	0.1389	0.2778	4.9787	4.4231	5.9095
40	7.1790	0.5236	1.0472	8.2262	6.1318	14.5870
50	7.1358	0.4755	0.9510	8.0868	6.1848	13.3271
60	8.0461	0.3907	0.7814	8.8275	7.2647	9.7115
70	7.9255	0.3699	0.7398	8.6653	7.1867	9.3344
80	8.0829	0.3371	0.6742	8.7571	7.4087	8.3410
90	8.2738	0.3108	0.6216	8.8954	7.6522	7.5129
100	9.0284	0.2770	0.5540	9.5824	8.4744	6.1362
120	9.9713	0.2606	0.5212	10.4925	9.4501	5.2270
140	10.9637	0.2798	0.5596	11.5233	10.4041	5.1041
160	11.8892	0.3182	0.6364	12.5256	11.2528	5.3528
180	15.2355	0.4929	0.9858	16.2213	14.2497	6.4704
200	15.5146	0.5004	1.0008	16.5154	14.5138	6.4507
220	17.2969	0.5940	1.1880	18.4849	16.1089	6.8683
240	18.8704	0.6699	1.3398	20.2102	17.5306	7.1000
260	21.1816	0.7913	1.5826	22.7642	19.5990	7.4716
280	22.9392	0.8388	1.6776	24.6168	21.2616	7.3132
300	28.0440	1.0872	2.1744	30.2184	25.8696	7.7535
320	49.1724	2.3904	4.7808	53.9532	44.3916	9.7225
325	812.0703	110.8433	221.6866	1033.7569	590.3837	27.2989

a. Values of h are given in Btu/hr-ft²-°F. To convert to w/m²-°C, multiply by 5.678.

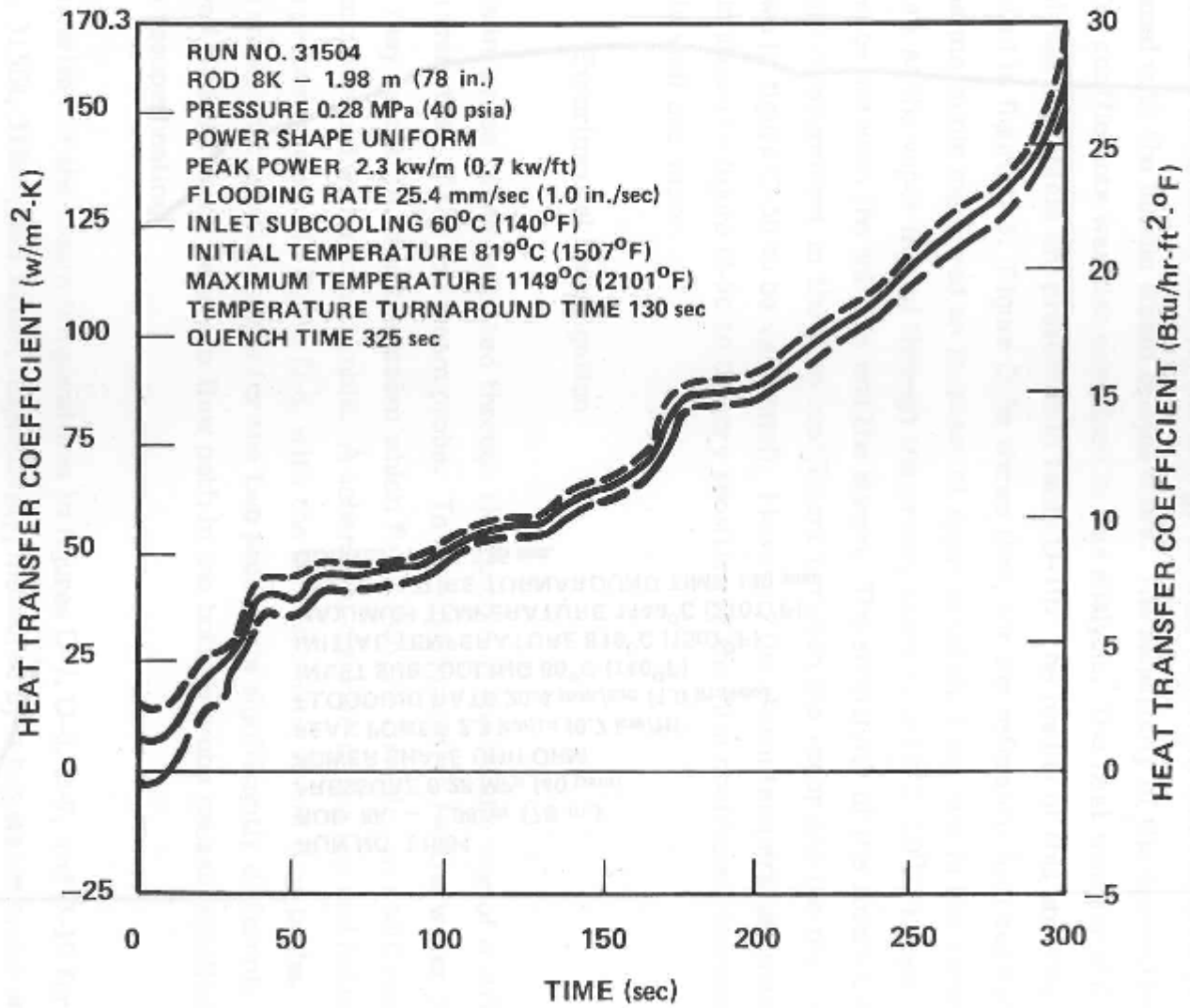


Figure B.2 Rod Heat Transfer Coefficient as a Function of Time (95 Percent Confidence Limits).

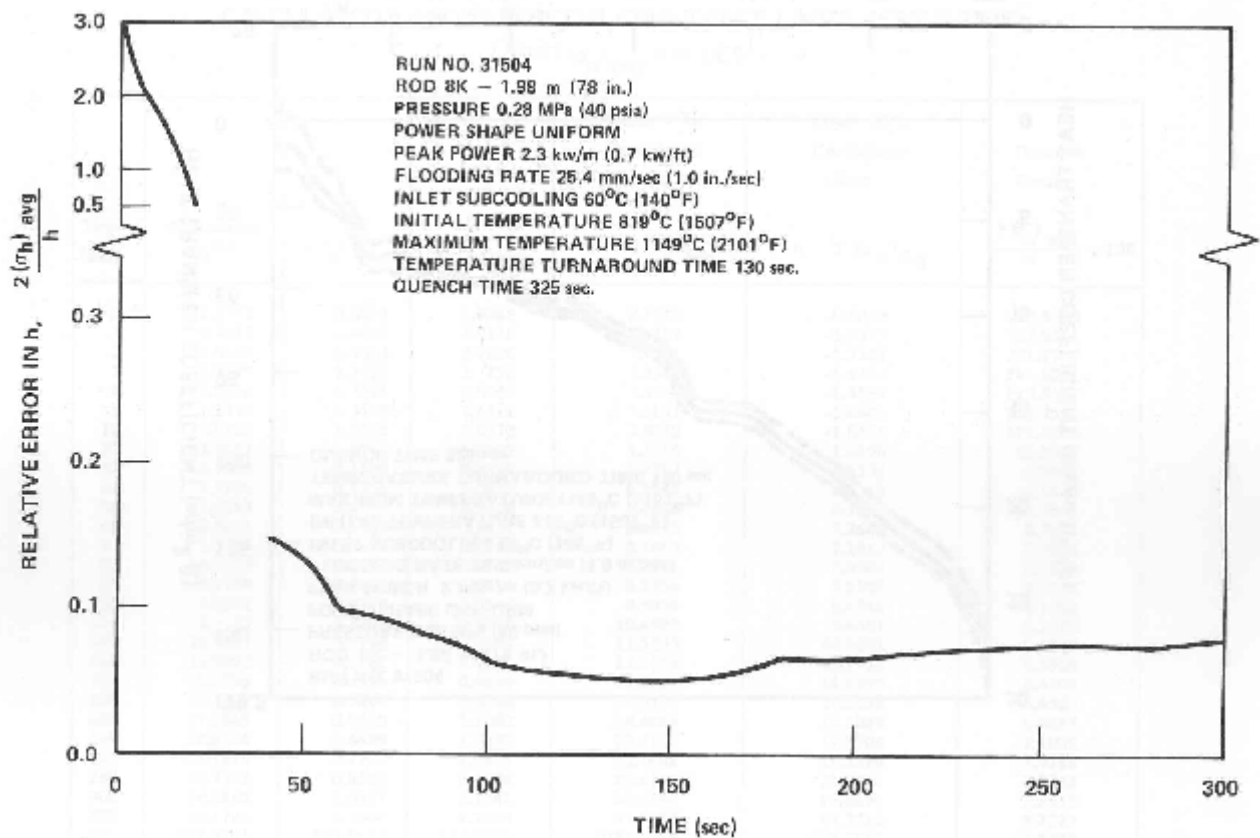


Figure B.3 Relative Uncertainty in Heat Transfer Coefficient as a Function of Time.

B.3 References

1. Loftus, M. J., Hochreiter, L. E., Conwig, C. E., Dodge, C., Tong, A., Rosal, E. R., Valkovic, M. M., and Wong, S., "PWR FLECHT-SEASET Unblocked Bundle, Forced and Gravity Reflood Task Data Report," NUREG/CR-1532, Volume 1, June 1980.

BIBLIOGRAPHIC DATA SHEET

(See instructions on the reverse)

NUREG/CR-6980

2. TITLE AND SUBTITLE

RBHT Reflood Heat Transfer Experiments Data and Analysis

3. DATE REPORT PUBLISHED

MONTH

YEAR

April

2012

4. FIN OR GRANT NUMBER

N6154

5. AUTHOR(S)

L.E. Hochreiter, F-B. Cheung, T.F. Lin, S. Ergun, A. Sridharan, A. Ireland, E.R. Rosal

6. TYPE OF REPORT

Technical

7. PERIOD COVERED (Inclusive Dates)

Nov 1997 - Feb 2003

8. PERFORMING ORGANIZATION - NAME AND ADDRESS (If NRC, provide Division, Office or Region, U.S. Nuclear Regulatory Commission, and mailing address; if contractor, provide name and mailing address.)

The Pennsylvania State University
University Park, PA 16802

9. SPONSORING ORGANIZATION - NAME AND ADDRESS (If NRC, type "Same as above"; if contractor, provide NRC Division, Office or Region, U.S. Nuclear Regulatory Commission, and mailing address.)

Division of Systems Analysis
Office of Nuclear Regulatory Research
U.S. Nuclear Regulatory Commission
Washington, DC 20555-0001

10. SUPPLEMENTARY NOTES

K. Tien, NRC Project Manager

11. ABSTRACT (200 words or less)

A total of 25 valid bottom reflood heat transfer experiments have been performed in the Pennsylvania State University/U.S. Nuclear Regulatory Commission Rod Bundle Heat Transfer (RBHT) Test Facility to examine the effects of both dispersed flow film boiling and inverted annular film boiling in a rod bundle geometry. The RBHT Test Facility has a full length, 3.66 m (12 ft), 7x7 rod array with typical pressurized water reactor rod diameters of 9.49 mm (0.374 in) and a rod pitch of 12.59 mm (0.496 in). The heater rods had a top skewed power shape with a peak to average power of 1.5 at the 2.77 m (9.08 ft) elevation. The ranges of conditions for the experiments were pressures from 137.9 to 413.7 kPa (20 to 60 psia), flooding rates from 0.0147 to 0.1524 m/s (0.58 to 6 in/s), and initial temperatures from 760 to 871 degrees C (1400 to 1600 degrees F), inlet subcooling from 11.1 to 83.33 degrees C (20 to 150 degrees F), and peak powers of 1.32 to 2.31 kW/m (0.4 to 0.7 kW/ft). The experiments were performed using a constant power rather than simulating the reactor decay power. The use of constant bundle power extended the reflood transient several hundred seconds and resulted in quasi-steady film boiling over the majority of the bundle length.

12. KEY WORDS/DESCRIPTORS (List words or phrases that will assist researchers in locating the report.)

dispersed flow film boiling, heat transfer enhancement, mixing vane, quench front progression, reactor safety, reactor systems codes, reflood heat transfer, rod bundle, spacer grid, thermal hydraulics

13. AVAILABILITY STATEMENT

unlimited

14. SECURITY CLASSIFICATION

(This Page)

unclassified

(This Report)

unclassified

15. NUMBER OF PAGES

16. PRICE



Federal Recycling Program



**UNITED STATES
NUCLEAR REGULATORY COMMISSION**
WASHINGTON, DC 20555-0001

OFFICIAL BUSINESS

NUREG/CR-6980

RBHT Reflood Heat Transfer Experiments Data and Analysis

April 2012